VOLUME 27 / NUMBER 23
DECEMBER 8, 1989
ACC. NOS. N89-28485 TO N89-29302

STAR

AN ABSTRACT JOURNAL

Scientific and Technical Aerospace Reports

PRODUCED BY THE
SCIENTIFIC AND TECHNICAL
INFORMATION
DIVISION

NASA

NATIONAL AERONAUTICS AND SPACE ADMINISTRATION

WHAT YOU CAN DO FOR *STAR*

All users of this abstract service are urged to forward reports to be considered for announcement in *STAR*. This will aid NASA in its efforts to provide the fullest possible coverage of all scientific and technical publications that might support aeronautics and space research and development. If you have prepared relevant reports (other than those that you will transmit to NASA, DoD, or DOE through the usual contract- or grant-reporting channels), please send them for consideration to the NASA Scientific and Technical Information Facility, P.O. Box 8757, BWI Airport, Maryland 21240.

Reprints of journal articles, book chapters, and conference papers are also welcome. These will be considered for announcement in *STAR's* companion journal, *International Aerospace Abstracts*.

You may specify a particular source to be included in a report announcement if you wish; otherwise the report will be placed on public sale at the National Technical Information Service. Copyrighted publications will be announced but not distributed or sold.

PURCHASE OF *STAR*

The semimonthly issues are available to registered users on annual subscription for $99.00 from the NASA Scientific and Technical Information Facility, ATTN: Registration Services, P.O. Box 8757, BWI Airport, MD 21240. *STAR* is publically available on annual subscription for $99.00 from the Superintendent of Documents, U.S. Government Printing Office, Washington, DC 20402.

PUBLISHED BY:

UNITED STATES GOVERNMENT
NATIONAL AERONAUTICS AND SPACE ADMINISTRATION
SCIENTIFIC AND TECHNICAL INFORMATION DIVISION
Scientific and Technical Aerospace Reports, Volume 27, is prepared by the NASA Scientific and Technical Information Facility operated for the National Aeronautics and Space Administration by RMS Associates.

The Administrator of the National Aeronautics and Space Administration has determined that the publication of this periodical is necessary in the transaction of the public business required by law of this Agency. Use of funds for printing this periodical has been approved by the Director of the Office of Management and Budget through March 22, 1990.

US ISSN 0036-8741

INTRODUCTION

Scientific and Technical Aerospace Reports (STAR) is a major component of a comprehensive National Aeronautics and Space Administration information system covering aeronautics, space, and supporting disciplines. *STAR* is issued on the 8th and 23rd of each month and announces current publications of the following types:

- NASA, NASA contractor, and NASA grantee reports
- Reports issued by other U.S. Government Agencies, domestic and foreign institutions, universities, and private firms
- Translations in report form
- NASA-owned patents and patent applications
- Other U.S. Government Agency and foreign patents and patent applications
- Domestic and foreign dissertations and theses

Journal, book, and conference literature, cover-to-cover journal translations, and certain foreign dissertations are announced in a companion journal, *International Aerospace Abstracts (IAA),* available on subscription from the American Institute of Aeronautics and Astronautics, Technical Information Service, 555 West 57th Street, 12th Floor, New York, New York 10019.

SUBJECT SCOPE

Subject scope of *STAR,* and *IAA* includes all aspects of aeronautics and space research and development, supporting basic and applied research, and applications. Aerospace aspects of earth resources, energy development, conservation, oceanography, environmental protection, urban transportation, and other topics of high national priority are also covered.

OTHER NASA PUBLICATIONS

Other NASA publications and information services are described in the publication, *The NASA Scientific and Technical Information System ... and How to Use It,* available without charge from the NASA Scientific and Technical Information Facility, P.O. Box 8757, BWI Airport, Maryland 21240.

HOW TO USE *STAR* SUBJECT CATEGORIES

STAR is categorized by 10 major subject divisions divided into 76 specific subject categories and one general category/division. The major subject divisions are listed in the Table of Contents, together with a note for each that defines its scope and provides any cross-references. For example:

AERONAUTICS

Includes aeronautics (general); aerodynamics; air transportation and safety; aircraft communications and navigation; aircraft design, testing and performance; aircraft instrumentation; aircraft propulsion and power; aircraft stability and control; and research and support facilities (air).

For related information see also *Astronautics.*

Each major division is further divided into as many as nine specific categories, which are identified by category numbers.

Abstracts in *STAR* are grouped by specific category, the categories appearing in sequential order. Category breaks in the abstract section are identified by the category number and title, and a scope note. Cross-references to other categories are provided as appropriate. For example:

02 AERODYNAMICS

Includes aerodynamics of bodies, combinations, wings, rotors, and control surfaces; and internal flow in ducts and turbomachinery.

For related information see also *34 Fluid Mechanics and Heat Transfer.*

CROSS-REFERENCES

Individual *STAR* abstracts are not ordinarily cross-referenced, except for certain conference reports or book translations that have had separate abstracts written for their component papers or chapters. Citations and abstracts of the components follow immediately after those of the parent document. When the subject content of a component differs sufficiently from the general content of the parent, a cross-reference citation also is printed at the end of the category to which it normally would have been assigned if it were independent.

DOCUMENTS ON MICROFICHE

Documents on microfiche[1] are designated by a pound sign (#) following the accession number. The pound sign is used without regard to the source or quality of the microfiche.

AVAILABILITIES

One or more sources from which a document announced in *STAR* is available to the public is given in each citation. The most commonly indicated sources and their acronyms or abbreviations are listed below. If the publication is available from a source other than those listed, the publisher and his address will be displayed on the availability line or in combination with the corporate source line.

Avail: NTIS. Sold by the National Technical Information Service. Prices for hard copy (HC) and microfiche (MF) are indicated by a price code following the letters HC or MF in the *STAR* citation. Current values for the price codes are given in the tables on page vii.

Initially distributed microfiche under the NTIS SRIM (Selected Research in Microfiche) is available at greatly reduced unit prices. For this service and for information concerning subscription to NASA printed reports, consult the NTIS Subscription Section, Springfield, Va. 22161.

NOTE ON ORDERING DOCUMENTS: When ordering NASA publications (those followed by the * symbol), use the N accession number. NASA patent applications (only the specifications are offered) should be ordered by the US-Patent-Appl-SN number. Non-NASA publications (no asterisk) should be ordered by the AD, PB, or other *report number* shown on the last line of the citation, not by the N accession number. It is also advisable to cite the title and other bibliographic identification.

Avail: SOD (or GPO). Sold by the Superintendent of Documents, U.S. Government Printing Office, in hard copy. The current price and order number are given following the availability line. (NTIS will fill microfiche requests, as indicated above, for those documents identified by a # symbol.)

(1) A microfiche is a transparent sheet of film, 105 by 148 mm in size, containing as many as 60 to 98 pages of information reduced to micro images (not to exceed 26:1 reduction).

Avail: BLL (formerly NLL): British Library Lending Division, Boston Spa, Wetherby, Yorkshire, England. Photocopies available from this organization at the price shown. (If none is given, inquiry should be addressed to the BLL.)

Avail: DOE Depository Libraries. Organizations in U.S. cities and abroad that maintain collections of Department of Energy reports, usually in microfiche form, are listed in *Energy Research Abstracts.* Services available from the DOE and its depositories are described in a booklet, *DOE Technical Information Center - Its Functions and Services* (TID-4660), which may be obtained without charge from the DOE Technical Information Center.

Avail: ESDU. Pricing information on specific data, computer programs, and details on ESDU topic categories can be obtained from ESDU International Ltd. Requesters in North America should use the Virginia address while all other requesters should use the London address, both of which are on page vi.

Avail: Fachinformationszentrum, Karlsruhe. Sold by the Fachinformationszentrum Energie, Physik, Mathematik GMBH, Eggenstein Leopoldshafen, Federal Republic of Germany, at the price shown in deutschmarks (DM).

Avail: HMSO. Publications of Her Majesty's Stationery Office are sold in the U.S. by Pendragon House, Inc. (PHI), Redwood City, California. The U.S. price (including a service and mailing charge) is given, or a conversion table may be obtained from PHI.

Avail: NASA Public Document Rooms. Documents so indicated may be examined at or purchased from the National Aeronautics and Space Administration, Public Documents Room (Room 126), 600 Independence Ave., S.W., Washington, D.C. 20546, or public document rooms located at each of the NASA research centers, the NASA Space Technology Laboratories, and the NASA Pasadena Office at the Jet Propulsion Laboratory.

Avail: Univ. Microfilms. Documents so indicated are dissertations selected from *Dissertation Abstracts* and are sold by University Microfilms as xerographic copy (HC) and microfilm. All requests should cite the author and the Order Number as they appear in the citation.

Avail: US Patent and Trademark Office. Sold by Commissioner of Patents and Trademarks, U.S. Patent and Trademark Office, at the standard price of $1.50 each, postage free. (See discussion of NASA patents and patent applications below.)

Avail: (US Sales Only). These foreign documents are available to users within the United States from the National Technical Information Service (NTIS). They are available to users outside the United States through the International Nuclear Information Service (INIS) representative in their country, or by applying directly to the issuing organization.

Avail: USGS. Originals of many reports from the U.S. Geological Survey, which may contain color illustrations, or otherwise may not have the quality of illustrations preserved in the microfiche or facsimile reproduction, may be examined by the public at the libraries of the USGS field offices whose addresses are listed in this Introduction. The libraries may be queried concerning the availability of specific documents and the possible utilization of local copying services, such as color reproduction.

Avail: Issuing Activity, or Corporate Author, or no indication of availability. Inquiries as to the availability of these documents should be addressed to the organization shown in the citation as the corporate author of the document.

NASA PATENTS AND PATENT APPLICATIONS

Patents and patent applications owned by NASA are announced in *STAR* under appropriate subject categories and are referenced in the *STAR* indexes. In the Report/Accession Number Index, patents are indexed by the NASA Case Number (which appears in lieu of the report number in other indexes), the U.S. Patent Number, the U.S. Patent Application Serial Number, and the U.S. Patent Class. Patent applications for which patents have not yet been issued are indexed by the NASA Case Number and the U.S. Patent Application Serial Number.

NASA *patent application specifications* are sold in paper copy by the National Technical Information Service at price code A02. Microfiche are sold at price code A01. The US-Patent-Appl-SN- number should be used in ordering either paper copy or microfiche from NTIS. Printed copies of *patents* (which are not microfiched) are available for purchase at $1.50 per copy from:

Commissioner of Patents and Trademarks
U.S. Patent and Trademark Office
Washington, D.C. 20231

When ordering patents, the U.S. Patent Number should be used, and payment must be remitted in advance, preferably by money order or check payable to the Commissioner of Patents and Trademarks. Prepaid purchase coupons for ordering are also available from the Patent and Trademark Office. The patents and patent applications announced in *STAR* are owned by NASA and are available for royalty-free licensing. Requests for licensing terms and further information should be addressed to:

Associate General Counsel for Intellectual Property/Code GP
National Aeronautics and Space Administration
Washington, D.C. 20546

ELIGIBILITY AND REGISTRATION FOR NASA INFORMATION PRODUCTS AND SERVICES

A variety of services is available to organizations of the following types that have registered with NASA to receive specific services or products:

1. NASA offices, research centers, contractors, subcontractors, grantees, and consultants;
2. Other U.S. Government agencies and their contractors;
3. Libraries in the United States that have arrangements with NASA to maintain collections of NASA documents for public reference;
4. Other organizations in the United States having a need for NASA documents in work related to aeronautics and space research;
5. Organizations abroad that have established reciprocal document exchange arrangements with NASA.

Only the central service points or central points of document acquisition and control within qualified organizations are eligible to register for NASA products and services. Domestic organizations that may be eligible to receive various classes of NASA publications and services should address their requests for registration or for further information to:

NASA Scientific and Technical Information Facility
ATTN: Registration Services
Post Office Box 8757
BWI Airport, Maryland 21240

Organizations abroad should direct requests to Manager, International STI Activities, NTT, NASA Headquarters, Washington, D.C. 20546.

AVAILABILITY OF *STAR* ABSTRACTS ON MICROFICHE

Microfiche of the abstract sections of this issue and other issues of *STAR* are available on annual subscription from NTIS as PB89-911300, Attn: Subscriptions, 5285 Port Royal Road, Springfield, Virginia 22161. Annual subscription rates are $70.00 North America; $140.00 foreign. Abstract sections for previous years retroactive to 1964 are available at the current rates. Microfiche for individual *STAR* issue abstract sections are not available.

PUBLIC COLLECTIONS OF NASA DOCUMENTS

DOMESTIC: NASA and NASA-sponsored documents and a large number of aerospace publications are available to the public for reference purposes at the library maintained by the American Institute of Aeronautics and Astronautics, Technical Information Service, 555 West 57th Street, 12th Floor, New York, New York 10019

EUROPEAN: An extensive collection of NASA and NASA-sponsored publications is maintained by the British Library Lending Division, Boston Spa, Wetherby, Yorkshire, England for public access. The British Library Lending Division also has available many of the non-NASA publications cited in *STAR*. European requesters may purchase facsimile copy or microfiche of NASA and NASA-sponsored documents, those identified by both the symbols # and * from ESA - Information Retrieval Service European Space Agency, 8-10 rue Mario-Nikis, 75738 Paris CEDEX 15, France.

FEDERAL DEPOSITORY LIBRARY PROGRAM

In order to provide the general public with greater access to U.S. Government publications, Congress established the Federal Depository Library Program under the Government Printing Office (GPO), with 50 regional depositories responsible for permanent retention of material, inter-library loan, and reference services. At least one copy of nearly every NASA and NASA-sponsored publication, either in printed or microfiche format, is received and retained by the 50 regional depositories. A list of the regional GPO libraries, arranged alphabetically by state, appears on the inside back cover. These libraries are *not* sales outlets. A local library can contact a Regional Depository to help locate specific reports, or direct contact may be made by an individual.

ADDRESSES OF ORGANIZATIONS

American Institute of Aeronautics and Astronautics
Technical Information Service
555 West 57th Street, 12th Floor
New York, New York 10019

British Library Lending Division,
Boston Spa, Wetherby, Yorkshire,
England

Commissioner of Patents and Trademarks
U.S. Patent and Trademark Office
Washington, D.C. 20231

Department of Energy
Technical Information Center
P.O. Box 62
Oak Ridge, Tennessee 37830

ESA-Information Retrieval Service
ESRIN
Via Galileo Galilei
00044 Frascati (Rome) Italy

ESDU International
P.O. Box 1633
Manassas, Virginia 22110

ESDU International, Ltd.
251-259 Regent Street
London, W1R 7AD, England

Fachinformationszentrum Energie, Physik, Mathematik GMBH
7514 Eggenstein Leopoldshafen
Federal Republic of Germany

Her Majesty's Stationery Office
P.O. Box 569, S.E. 1
London, England

NASA Scientific and Technical Information Facility
P.O. Box 8757
B.W.I. Airport, Maryland 21240

National Aeronautics and Space Administration
Scientific and Technical Information Division (NTT)
Washington, D.C. 20546

National Technical Information Service
5285 Port Royal Road
Springfield, Virginia 22161

Pendragon House, Inc.
899 Broadway Avenue
Redwood City, California 94063

Superintendent of Documents
U.S. Government Printing Office
Washington, D.C. 20402

University Microfilms
A Xerox Company
300 North Zeeb Road
Ann Arbor, Michigan 48106

University Microfilms, Ltd.
Tylers Green
London, England

U.S. Geological Survey Library
National Center - MS 950
12201 Sunrise Valley Drive
Reston, Virginia 22092

U.S. Geological Survey Library
2255 North Gemini Drive
Flagstaff, Arizona 86001

U.S. Geological Survey
345 Middlefield Road
Menlo Park, California 94025

U.S. Geological Survey Library
Box 25046
Denver Federal Center, MS914
Denver, Colorado 80225

NTIS PRICE SCHEDULES

(Effective January 1, 1989)

Schedule A
STANDARD PRICE DOCUMENTS AND MICROFICHE

PRICE CODE	NORTH AMERICAN PRICE	FOREIGN PRICE
A01	$ 6.95	$13.90
A02	10.95	21.90
A03	13.95	27.90
A04-A05	15.95	31.90
A06-A09	21.95	43.90
A10-A13	28.95	57.90
A14-A17	36.95	73.90
A18-A21	42.95	85.90
A22-A25	49.95	99.90
A99	*	*
NO1	55.00	70.00
NO2	55.00	80.00

Schedule E
EXCEPTION PRICE DOCUMENTS AND MICROFICHE

PRICE CODE	NORTH AMERICAN PRICE	FOREIGN PRICE
E01	$ 9.00	18.00
E02	11.50	23.00
E03	13.00	26.00
E04	15.50	31.00
E05	17.50	35.00
E06	20.50	41.00
E07	23.00	46.00
E08	25.50	51.00
E09	28.00	56.00
E10	31.00	62.00
E11	33.50	67.00
E12	36.50	73.00
E13	39.00	78.00
E14	42.50	85.00
E15	46.00	92.00
E16	50.50	101.00
E17	54.50	109.00
E18	59.00	118.00
E19	65.50	131.00
E20	76.00	152.00
E99	*	*

*Contact NTIS for price quote.

IMPORTANT NOTICE

NTIS Shipping and Handling Charges

U.S., Canada, Mexico — ADD $3.00 per TOTAL ORDER

All Other Countries — ADD $4.00 per TOTAL ORDER

Exceptions — Does NOT apply to:

ORDERS REQUESTING NTIS RUSH HANDLING
ORDERS FOR SUBSCRIPTION OR STANDING ORDER PRODUCTS *ONLY*

NOTE: Each additional delivery address on an order requires a separate shipping and handling charge.

VOLUME 27 NUMBER 23 / DECEMBER 8, 1989

TABLE OF CONTENTS

AERONAUTICS

Includes aeronautics (general); aerodynamics; air transportation and safety; aircraft communications and navigation; aircraft design, testing and performance; aircraft instrumentation; aircraft propulsion and power; aircraft stability and control; and research and support facilities (air).

For related information see also *Astronautics.*

01 AERONAUTICS (GENERAL) 3243

02 AERODYNAMICS 3243

Includes aerodynamics of bodies, combinations, wings, rotors, and control surfaces; and internal flow in ducts and turbomachinery.

For related information see also *34 Fluid Mechanics and Heat Transfer*

03 AIR TRANSPORTATION AND SAFETY 3246

Includes passenger and cargo air transport operations; and aircraft accidents.

For related information see also *16 Space Transportation* and *85 Urban Technology and Transportation.*

04 AIRCRAFT COMMUNICATIONS AND NAVIGATION 3247

Includes digital and voice communication with aircraft; air navigation systems (satellite and ground based); and air traffic control.

For related information see also *17 Space Communications, Spacecraft Communications, Command and Tracking* and *32 Communications and Radar.*

05 AIRCRAFT DESIGN, TESTING AND PERFORMANCE 3247

Includes aircraft simulation technology.

For related information see also *18 Spacecraft Design, Testing and Performance* and *39 Structural Mechanics.* For land transportation vehicles see *85 Urban Technology and Transportation.*

06 AIRCRAFT INSTRUMENTATION 3248

Includes cockpit and cabin display devices; and flight instruments.

For related information see also *19 Spacecraft Instrumentation* and *35 Instrumentation and Photography.*

07 AIRCRAFT PROPULSION AND POWER 3248

Includes prime propulsion systems and systems components, e.g., gas turbine engines and compressors; and onboard auxiliary power plants for aircraft.

For related information see also *20 Spacecraft Propulsion and Power, 28 Propellants and Fuels,* and *44 Energy Production and Conversion.*

08 AIRCRAFT STABILITY AND CONTROL 3249

Includes aircraft handling qualities; piloting; flight controls; and autopilots.

For related information see also *05 Aircraft Design, Testing and Performance.*

09 RESEARCH AND SUPPORT FACILITIES (AIR) 3249

Includes airports, hangars and runways; aircraft repair and overhaul facilities; wind tunnels; shock tubes; and aircraft engine test stands.

For related information see also *14 Ground Support Systems and Facilities (Space).*

ASTRONAUTICS

Includes astronautics (general); astrodynamics; ground support systems and facilities (space); launch vehicles and space vehicles; space transportation; space communications, spacecraft communications, command and tracking; spacecraft design, testing and performance; spacecraft instrumentation; and spacecraft propulsion and power.

For related information see also *Aeronautics*

12 ASTRONAUTICS (GENERAL) 3250

For extraterrestrial exploration see *91 Lunar and Planetary Exploration.*

13 ASTRODYNAMICS 3251

Includes powered and free-flight trajectories; and orbital and launching dynamics.

14 GROUND SUPPORT SYSTEMS AND FACILITIES (SPACE) 3252

Includes launch complexes, research and production facilities; ground support equipment, e.g., mobile transporters; and simulators.

For related information see also *09 Research and Support Facilities (Air).*

15 LAUNCH VEHICLES AND SPACE VEHICLES 3253

Includes boosters; operating problems of launch/space vehicle systems; and reusable vehicles.

For related information see also *20 Spacecraft Propulsion and Power.*

16 SPACE TRANSPORTATION N.A.

Includes passenger and cargo space transportation, e.g., shuttle operations; and space rescue techniques.

For related information see also *03 Air Transportation and Safety* and *18 Spacecraft Design, Testing and Performance.* For space suits see *54 Man/System Technology and Life Support.*

17 SPACE COMMUNICATIONS, SPACECRAFT COMMUNICATIONS, COMMAND AND TRACKING N.A.

Includes telemetry; space communications networks; astronavigation and guidance; and radio blackout.

For related information see also *04 Aircraft Communications and Navigation* and *32 Communications and Radar.*

18 SPACECRAFT DESIGN, TESTING AND PERFORMANCE 3254

Includes satellites; space platforms; space stations; spacecraft systems and components such as thermal and environmental controls; and attitude controls.

For life support systems see *54 Man/System Technology and Life Support.* For related information see also *05 Aircraft Design, Testing and Performance, 39 Structural Mechanics,* and *16 Space Transportation.*

19 SPACECRAFT INSTRUMENTATION 3256

For related information see also *06 Aircraft Instrumentation* and *35 Instrumentation and Photography.*

20 SPACECRAFT PROPULSION AND POWER 3256

Includes main propulsion systems and components, e.g. rocket engines; and spacecraft auxiliary power sources.

For related information see also *07 Aircraft Propulsion and Power, 28 Propellants and Fuels, 44 Energy Production and Conversion,* and *15 Launch Vehicles and Space Vehicles.*

CHEMISTRY AND MATERIALS

Includes chemistry and materials (general); composite materials; inorganic and physical chemistry; metallic materials; nonmetallic materials; propellants and fuels; and materials processing.

23 CHEMISTRY AND MATERIALS (GENERAL) 3258

24 COMPOSITE MATERIALS 3258

Includes physical, chemical, and mechanical properties of laminates and other composite materials.

For ceramic materials see *27 Nonmetallic Materials.*

25 INORGANIC AND PHYSICAL CHEMISTRY 3260

Includes chemical analysis, e.g., chromatography; combustion theory; electrochemistry; and photochemistry.

For related information see also *77 Thermodynamics and Statistical Physics.*

26 METALLIC MATERIALS 3265

Includes physical, chemical, and mechanical properties of metals, e.g., corrosion; and metallurgy.

27 NONMETALLIC MATERIALS 3268

Includes physical, chemical, and mechanical properties of plastics, elastomers, lubricants, polymers, textiles, adhesives, and ceramic materials.

For composite materials see *24 Composite Materials.*

28 PROPELLANTS AND FUELS 3271

Includes rocket propellants, igniters and oxidizers; their storage and handling procedures; and aircraft fuels.

For related information see also *07 Aircraft Propulsion and Power, 20 Spacecraft Propulsion and Power,* and *44 Energy Production and Conversion.*

29 MATERIALS PROCESSING 3273

Includes space-based development of products and processes for commercial application.

For biological materials see *55 Space Biology.*

ENGINEERING

Includes engineering (general); communications and radar; electronics and electrical engineering; fluid mechanics and heat transfer; instrumentation and photography; lasers and masers; mechanical engineering; quality assurance and reliability; and structural mechanics.

For related information see also *Physics.*

31 ENGINEERING (GENERAL) 3273

Includes vacuum technology; control engineering; display engineering; cryogenics; and fire prevention.

32 COMMUNICATIONS AND RADAR 3274

Includes radar; land and global communications; communications theory; and optical communications.

For related information see also *04 Aircraft Communications and Navigation* and *17 Space Communications, Spacecraft Communications, Command and Tracking.* For search and rescue see *03 Air Transportation and Safety,* and *16 Space Transportation.*

33 ELECTRONICS AND ELECTRICAL ENGINEERING 3279

Includes test equipment and maintainability; components, e.g., tunnel diodes and transistors; microminiaturization; and integrated circuitry.

For related information see also *60 Computer Operations and Hardware* and *76 Solid-State Physics.*

34 FLUID MECHANICS AND HEAT TRANSFER 3284

Includes boundary layers; hydrodynamics; fluidics; mass transfer and ablation cooling.

For related information see also *02 Aerodynamics* and *77 Thermodynamics and Statistical Physics.*

35 INSTRUMENTATION AND PHOTOGRAPHY 3293

Includes remote sensors; measuring instruments and gages; detectors; cameras and photographic supplies; and holography.

For aerial photography see *43 Earth Resources and Remote Sensing.* For related information see also *06 Aircraft Instrumentation* and *19 Spacecraft Instrumentation.*

36 LASERS AND MASERS 3297

Includes parametric amplifiers.

For related information see also *76 Solid-State Physics.*

37 MECHANICAL ENGINEERING 3300

Includes auxiliary systems (nonpower); machine elements and processes; and mechanical equipment.

38 QUALITY ASSURANCE AND RELIABILITY 3304

Includes product sampling procedures and techniques; and quality control.

39 STRUCTURAL MECHANICS 3305

Includes structural element design and weight analysis; fatigue; and thermal stress.

For applications see *05 Aircraft Design, Testing and Performance* and *18 Spacecraft Design, Testing and Performance.*

GEOSCIENCES

Includes geosciences (general); earth resources and remote sensing; energy production and conversion; environment pollution; geophysics; meteorology and climatology; and oceanography.

For related information see also *Space Sciences.*

42 GEOSCIENCES (GENERAL) **N.A.**

43 EARTH RESOURCES AND REMOTE SENSING **3308**

Includes remote sensing of earth resources by aircraft and spacecraft; photogrammetry; and aerial photography.

For instrumentation see *35 Instrumentation and Photography.*

44 ENERGY PRODUCTION AND CONVERSION **3320**

Includes specific energy conversion systems, e.g., fuel cells; global sources of energy; geophysical conversion; and windpower.

For related information see also *07 Aircraft Propulsion and Power, 20 Spacecraft Propulsion and Power,* and *28 Propellants and Fuels.*

45 ENVIRONMENT POLLUTION **3323**

Includes atmospheric, noise, thermal, and water pollution.

46 GEOPHYSICS **3324**

Includes aeronomy; upper and lower atmosphere studies; ionospheric and magnetospheric physics; and geomagnetism.

For space radiation see *93 Space Radiation.*

47 METEOROLOGY AND CLIMATOLOGY **3327**

Includes weather forecasting and modification.

48 OCEANOGRAPHY **3329**

Includes biological, dynamic, and physical oceanography; and marine resources.

For related information see also *43 Earth Resources and Remote Sensing.*

LIFE SCIENCES

Includes life sciences (general); aerospace medicine; behavioral sciences; man/system technology and life support; and space biology.

51 LIFE SCIENCES (GENERAL) **N.A.**

52 AEROSPACE MEDICINE **3330**

Includes physiological factors; biological effects of radiation; and effects of weightlessness on man and animals.

53 BEHAVIORAL SCIENCES **3333**

Includes psychological factors; individual and group behavior; crew training and evaluation; and psychiatric research.

54 MAN/SYSTEM TECHNOLOGY AND LIFE SUPPORT **3334**

Includes human engineering; biotechnology; and space suits and protective clothing.

For related information see also *16 Space Transportation.*

55 SPACE BIOLOGY **N.A.**

Includes exobiology; planetary biology; and extraterrestrial life.

MATHEMATICAL AND COMPUTER SCIENCES

Includes mathematical and computer sciences (general); computer operations and hardware; computer programming and software; computer systems; cybernetics; numerical analysis; statistics and probability; systems analysis; and theoretical mathematics.

59 MATHEMATICAL AND COMPUTER SCIENCES (GENERAL) **3335**

60 COMPUTER OPERATIONS AND HARDWARE **3335**

Includes hardware for computer graphics, firmware, and data processing.

For components see *33 Electronics and Electrical Engineering.*

61 COMPUTER PROGRAMMING AND SOFTWARE **3337**

Includes computer programs, routines, algorithms, and specific applications, e.g., CAD/CAM.

62 COMPUTER SYSTEMS **3343**

Includes computer networks and special application computer systems.

63 CYBERNETICS **3345**

Includes feedback and control theory, artificial intelligence, robotics and expert systems.

For related information see also *54 Man/System Technology and Life Support.*

64 NUMERICAL ANALYSIS **3347**

Includes iteration, difference equations, and numerical approximation.

65 STATISTICS AND PROBABILITY **3352**

Includes data sampling and smoothing; Monte Carlo method; and stochastic processes.

66 SYSTEMS ANALYSIS **3352**

Includes mathematical modeling; network analysis; and operations research.

67 THEORETICAL MATHEMATICS **3353**

Includes topology and number theory.

PHYSICS

Includes physics (general); acoustics; atomic and molecular physics; nuclear and high-energy physics; optics; plasma physics; solid-state physics; and thermodynamics and statistical physics.

For related information see also *Engineering.*

70 PHYSICS (GENERAL) **3353**

For precision time and time interval (PTTI) see *35 Instrumentation and Photography;* for geophysics, astrophysics or solar physics see *46 Geophysics, 90 Astrophysics,* or *92 Solar Physics.*

71 ACOUSTICS 3354
Includes sound generation, transmission, and attenuation.
For noise pollution see *45 Environment Pollution.*

72 ATOMIC AND MOLECULAR PHYSICS 3355
Includes atomic structure, electron properties, and molecular spectra.

73 NUCLEAR AND HIGH-ENERGY PHYSICS 3358
Includes elementary and nuclear particles; and reactor theory.
For space radiation see *93 Space Radiation.*

74 OPTICS 3359
Includes light phenomena and optical devices.
For lasers see *36 Lasers and Masers.*

75 PLASMA PHYSICS 3361
Includes magnetohydrodynamics and plasma fusion.
For ionospheric plasmas see *46 Geophysics.* For space plasmas see *90 Astrophysics.*

76 SOLID-STATE PHYSICS 3364
Includes superconductivity.
For related information see also *33 Electronics and Electrical Engineering* and *36 Lasers and Masers.*

77 THERMODYNAMICS AND STATISTICAL PHYSICS 3370
Includes quantum mechanics; theoretical physics; and Bose and Fermi statistics.
For related information see also *25 Inorganic and Physical Chemistry* and *34 Fluid Mechanics and Heat Transfer.*

SOCIAL SCIENCES

Includes social sciences (general); administration and management; documentation and information science; economics and cost analysis; law, political science, and space policy; and urban technology and transportation.

80 SOCIAL SCIENCES (GENERAL) N.A.
Includes educational matters.

81 ADMINISTRATION AND MANAGEMENT 3371
Includes management planning and research.

82 DOCUMENTATION AND INFORMATION SCIENCE 3372
Includes information management; information storage and retrieval technology; technical writing; graphic arts; and micrography.
For computer documentation see *61 Computer Programming and Software.*

83 ECONOMICS AND COST ANALYSIS N.A.
Includes cost effectiveness studies.

84 LAW, POLITICAL SCIENCE AND SPACE POLICY 3373
Includes NASA appropriation hearings; aviation law; space law and policy; international law; international cooperation; and patent policy.

85 URBAN TECHNOLOGY AND TRANSPORTATION 3374
Includes applications of space technology to urban problems; technology transfer; technology assessment; and surface and mass transportation.
For related information see *03 Air Transportation and Safety, 16 Space Transportation,* and *44 Energy Production and Conversion.*

SPACE SCIENCES

Includes space sciences (general); astronomy; astrophysics; lunar and planetary exploration; solar physics; and space radiation.
For related information see also *Geosciences.*

88 SPACE SCIENCES (GENERAL) 3374

89 ASTRONOMY 3374
Includes radio, gamma-ray, and infrared astronomy; and astrometry.

90 ASTROPHYSICS 3375
Includes cosmology; celestial mechanics; space plasmas; and interstellar and interplanetary gases and dust.
For related information see also *75 Plasma Physics.*

91 LUNAR AND PLANETARY EXPLORATION 3377
Includes planetology; and manned and unmanned flights.
For spacecraft design or space stations see *18 Spacecraft Design, Testing and Performance.*

92 SOLAR PHYSICS 3377
Includes solar activity, solar flares, solar radiation and sunspots.
For related information see *93 Space Radiation.*

93 SPACE RADIATION 3377
Includes cosmic radiation; and inner and outer earth's radiation belts.
For biological effects of radiation see *52 Aerospace Medicine.* For theory see *73 Nuclear and High-Energy Physics.*

GENERAL

Includes aeronautical, astronautical, and space science related histories, biographies, and pertinent reports too broad for categorization; histories or broad overviews of NASA programs.

99 GENERAL 3378

Note: N.A. means that no abstracts were assigned to this category for this issue.

SUBJECT INDEX I-1
PERSONAL AUTHOR INDEX I-59
CORPORATE SOURCE INDEX I-67
CONTRACT NUMBER INDEX I-79
REPORT/ACCESSION NUMBER INDEX I-81

TYPICAL CITATION AND ABSTRACT

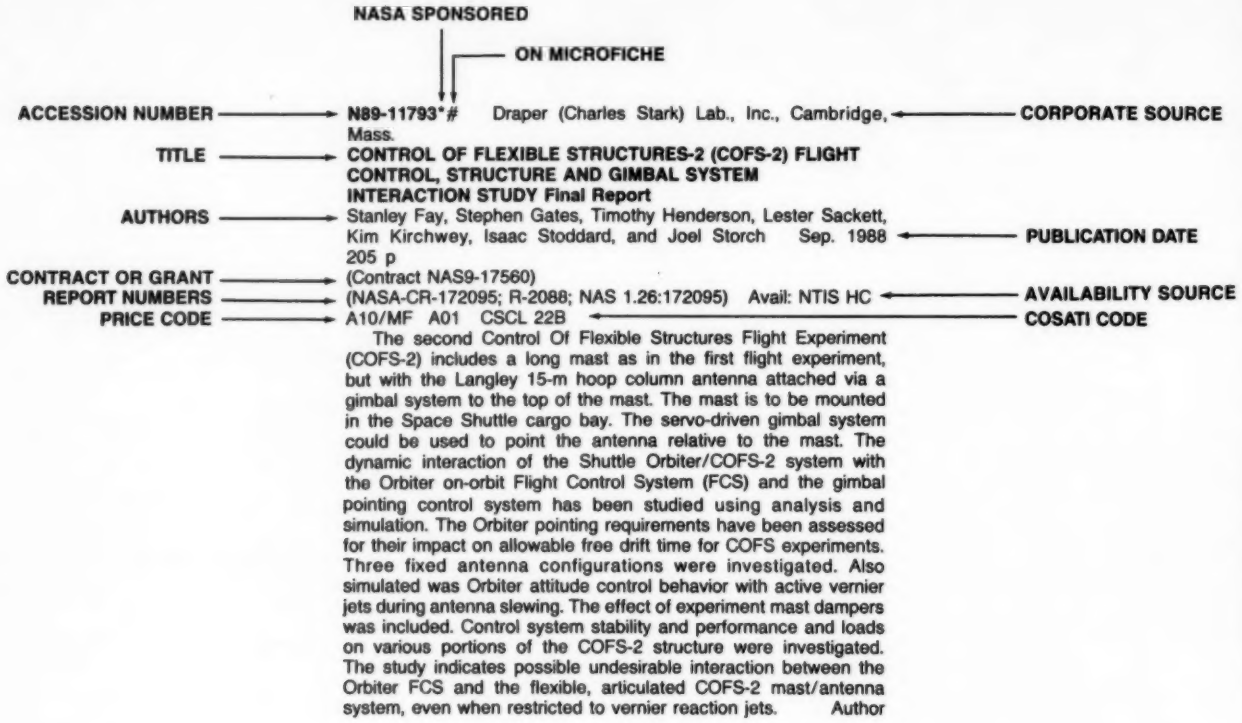
NASA SPONSORED
ON MICROFICHE
ACCESSION NUMBER
N89-11793*# Draper (Charles Stark) Lab., Inc., Cambridge, Mass.
CORPORATE SOURCE
TITLE
CONTROL OF FLEXIBLE STRUCTURES-2 (COFS-2) FLIGHT CONTROL, STRUCTURE AND GIMBAL SYSTEM INTERACTION STUDY Final Report
AUTHORS
Stanley Fay, Stephen Gates, Timothy Henderson, Lester Sackett, Kim Kirchwey, Isaac Stoddard, and Joel Storch
Sep. 1988
PUBLICATION DATE
205 p
CONTRACT OR GRANT
(Contract NAS9-17560)
REPORT NUMBERS
(NASA-CR-172095; R-2088; NAS 1.26:172095) Avail: NTIS HC
AVAILABILITY SOURCE
PRICE CODE
A10/MF A01 CSCL 22B
COSATI CODE
The second Control Of Flexible Structures Flight Experiment (COFS-2) includes a long mast as in the first flight experiment, but with the Langley 15-m hoop column antenna attached via a gimbal system to the top of the mast. The mast is to be mounted in the Space Shuttle cargo bay. The servo-driven gimbal system could be used to point the antenna relative to the mast. The dynamic interaction of the Shuttle Orbiter/COFS-2 system with the Orbiter on-orbit Flight Control System (FCS) and the gimbal pointing control system has been studied using analysis and simulation. The Orbiter pointing requirements have been assessed for their impact on allowable free drift time for COFS experiments. Three fixed antenna configurations were investigated. Also simulated was Orbiter attitude control behavior with active vernier jets during antenna slewing. The effect of experiment mast dampers was included. Control system stability and performance and loads on various portions of the COFS-2 structure were investigated. The study indicates possible undesirable interaction between the Orbiter FCS and the flexible, articulated COFS-2 mast/antenna system, even when restricted to vernier reaction jets. Author

VOLUME 27 NUMBER 23 / DECEMBER 8, 1989

Scientific and Technical Aerospace Reports

A Semimonthly Publication of the National Aeronautics and Space Administration

01 AERONAUTICS (GENERAL)

N89-28485# Deutsche Forschungs- und Versuchsanstalt fuer Luft- und Raumfahrt, Cologne (Germany, F.R.).
[ACTIVITIES REPORT IN AEROSPACE RESEARCH IN GERMANY, F.R.] Annual Report, 1987
Sep. 1988 101 p In GERMAN Previously announced in IAA as A89-32775 Report contains color illustrations
(ISSN-0070-3966; ETN-89-94382) Avail: NTIS HC A06/MF A01

The activities of the FRG aerospace research organization DFVLR for 1987 are reported. In the research field of aeronautics, investigations were performed on Compas (a planning and decision aid for air traffic controllers) and on a delta wing (a contribution to the International Vortex Flow Experiment). Space-related activities were the German Front Experiment 1987 (an example for the mesoscale probing of the atmosphere) and wind tunnel testing of reentry bodies in the hypersonic range. In the field of energy technology, renewable energy sources for Baden-Wuerttemberg were investigated. Photographs, drawings, and diagrams are provided, and an English summary is given for each section. ESA

02 AERODYNAMICS

Includes aerodynamics of bodies, combinations, wings, rotors, and control surfaces; and internal flow in ducts and turbomachinery.

For related information see also *34 Fluid Mechanics and Heat Transfer.*

N89-28486* National Aeronautics and Space Administration. Langley Research Center, Hampton, VA.
LOW-SPEED STATIC AND DYNAMIC FORCE TESTS OF A GENERIC SUPERSONIC CRUISE FIGHTER CONFIGURATION
David E. Hahne Washington Oct. 1989 35 p
(NASA-TM-4138; L-16599; NAS 1.15:4138) Avail: NTIS HC A03/MF A01 CSCL 01A

Static and dynamic force tests of a generic fighter configuration designed for sustained supersonic flight were conducted in the Langley 30- by 60-foot tunnel. The baseline configuration had a 65 deg arrow wing, twin wing mounted vertical tails and a canard. Results showed that control was available up to C sub L,max (maximum lift coefficient) from aerodynamic controls about all axes but control in the pitch and yaw axes decreased rapidly in the post-stall angle-of-attack region. The baseline configuration showed stable lateral-directional characteristics at low angles of attack but directional stability occurred near alpha = 25 deg as the wing shielded the vertical tails. The configuration showed positive effective dihedral throughout the test angle-of-attack range. Forced oscillation tests indicated that the baseline configuration had stable damping characteristics about the lateral-directional axes. Author

N89-28487# Midwest Research Inst., Golden, CO. Solar Energy Research Inst.
THREE-DIMENSIONAL AIRFOIL PERFORMANCE MEASUREMENTS ON A ROTATING WING
C. P. Butterfield Jun. 1989 6 p Presented at the European Wind Energy Conference and Exhibition, Glasgow, Scotland, 10 Jul. 1989
(Contract DE-AC02-83CH-10093)
(DE89-009443; SERI/TP-217-3505; CONF-890717-2) Avail: NTIS HC A02/MF A01

The objective of this comprehensive research program was to study the effects of Horizontal Axis Wind Turbine (HAWT) blade rotation on aerodynamic behavior below, near, and beyond stall. The flow angle sensor used to measure Angle Of Attack (AOA) is described along with how the sensor was calibrated, and results are given of pressure integrations on the blade. Aerodynamic, load, flow visualization, and inflow measurements were made on a 10-m, three-bladed, downwind HAWT. A video camera was mounted on the rotor to record video images of tufts attached to the low pressure side of a constant-chord, zero-twist blade. Load measurements were made using strain gages mounted every 10 percent of the blade's span. Pressure taps were located at 32 chordwise positions and revealed pressure distributions comparable with wind tunnel data. Inflow was measured using a vertical plane array of eight propvane and five triaxial (U-V-W) prop-type anemometers located 10 m upwind in the predominant wind direction. Results show evidence of stall hysteresis and unsteadiness at high AOA. Correlations with analytical predictions and wind tunnel tests show good agreement at low AOA and poor agreement at high AOA. DOE

N89-28488# General Dynamics Corp., Fort Worth, TX.
SMALL SCALE MODEL TESTS IN SMALL WIND AND WATER TUNNELS AT HIGH INCIDENCE AND PITCH RATES. VOLUME 1: TEST PROGRAM AND DISCUSSION OF RESULTS Final Report, Sep. 1985 - Sep. 1988
Atlee M. Cunningham, Jr., Todd Bushlow, John R. Mercer, Tim A. Wilson, and Steve N. Schwoerke Apr. 1989 144 p
(Contract N00014-85-C-0419)
(AD-A208647) Avail: NTIS HC A07/MF A01 CSCL 01/1

Volume 1 presents the test program, correlations with other data, and discussions of the specific objectives of this investigation. In general it was shown that the small scale wind tunnel and water tunnel test techniques do provide reasonable dynamic force and moment data for a wide variety of planforms and conditions. The force testing of small-scale models in either a small wind tunnel or a water tunnel was investigated as an inexpensive and quick means to obtain meaningful dynamic force and moment data representative of rapidly maneuvering full-scale aircraft. Force tests of flat-plate semi-span models were conducted in the General Dynamics Aerodynamic Development Facility (ADF) which is a small 14x14 in. low speed wind tunnel. Oscillatory model motions up to 48 deg (peak to peak) amplitude were tested at frequencies of 1 to 3 Hz. Force tests of flat and three-dimensional full span models were conducted in the General Dynamics Hydroflow Facility (HFF) which is a horizontal flow water tunnel with a 24x24 in. test section. Pitch/pulse model motions were tested for conditions similar to those tested in the ADF. GRA

N89-28489# Aeronautical Research Labs., Melbourne (Australia).
COMPARISON OF FLOW-VISUALISED VORTICES WITH COMPUTED GEOMETRY OVER THIN DELTA WINGS

L. D. MacLaren Feb. 1989 6 p
(AD-A209083; ARL-FLIGHT-MECH-TM-409) Avail: NTIS HC A02/MF A01 CSCL 01/1

The vortex flow patterns over thin delta wings were photographed during experiments in a vertical water tunnel making use of appropriate flow visualization techniques. The flow geometry for these wings was also calculated using the VORSBA vortex flow computer program. A comparison is made between the calculated and experimental results and discrepancies between them are discussed. GRA

N89-28490# Air Force Inst. of Tech., Wright-Patterson AFB, OH. School of Engineering.
GLIDER GROUND EFFECT INVESTIGATION M.S. Thesis
Nathan H. Jones May 1989 131 p
(AD-A209152; AFIT/GAE/ENY/89J-2) Avail: NTIS HC A07/MF A01 CSCL 01/3

This research used glider flight tests and optimized glider simulations to evaluate the aerodynamics of ground effect and to determine the optimum flight profile for maximum gliding range in gliders. A series of 122 sorties were flown in the Grob G-103 Twin II and the Let L-13 Blanik gliders on a specially designed very low altitude speed course. Radar tracking data were used to determine the glider position and velocity, and a 3 degree of freedom glider performance simulation was used to determine the glider parasite and induced drag coefficients in ground effect. Lifting line derived predictions of ground effect induced drag reduction developed by Dr. Sighard Hoerner were found to be accurate at altitudes above 20 percent wingspan but were up to 16 percent too optimistic at low altitudes. A revised prediction of ground effect induced drag reduction was developed based on the flight test data, and this revised prediction was used along with a turbulent boundary layer wind model in two optimization algorithms to develop the optimum flight profiles for maximum range gliding flight. GRA

N89-28491# Air Force Geophysics Lab., Hanscom AFB, MA.
THE FIRST LARGE BALLOON LAUNCH FROM ANTARCTICA Final Scientific Report
John Ground, Kenneth Dallas, Ralph Cowie, and Willard F. Thorn 26 Sep. 1988 103 p
(AD-A207735; AFGL-TR-88-0265; AFGL-ERP-1015) Avail: NTIS HC A06/MF A01 CSCL 01/3

This collection of five papers discusses the many practical problems, logistics, metrological planning, flight history and recovery operations for the first very large (11.6M cu ft) stratospheric balloon launched from Antarctica. The on-board Gamma Ray Advanced Detector (GRAD) was flown successfully to detect gamma ray emissions from Supernova 1987A. The 2500-lb payload was recovered from a 12,500-ft plateau by LC-130 aircraft. The instrumentation for command-control and telemetry, payload integration and testing, and the telemetry station installed aboard an LC-130 aircraft are described. An overview of the performance of the ARGOS satellite tracking and data-recovery system on this flight is included. GRA

N89-28492# National Aerospace Lab., Tokyo (Japan). Structural Mechanics Div.
SOME COMPUTATIONS OF UNSTEADY NAVIER-STOKES FLOW AROUND OSCILLATING AIRFOIL/WING
Jiro Nakamichi Oct. 1988 25 p
(NAL-TR-1004T; ISSN-0389-4010) Avail: NTIS HC A03/MF A01

Unsteady Navier-Stokes calculations around an airfoil/wing are demonstrated. 2D transonic flutter simulations are performed about the NACA 64A010 airfoil using not only a diagonal form of a Beam-Warming scheme but also a non-diagonal form. The effects of time accuracy of the algorithms on the flutter boundaries are checked by comparing two results. 3D unsteady computations around an oscillating wing in elastic motions are also carried out and the obtained results are compared with experimental data. It is found that the diagonal form of a Beam-Warming scheme is efficient in predicting the flutter boundaries of airfoils where the flow is not separated. It is also demonstrated that the present 3D code gives results in agreement with experimental data and it can be used for 3D flutter simulation programs in a similar manner to 2D programs. Author

N89-28493*# California Polytechnic State Univ., San Luis Obispo.
ANALYSIS OF LEADING EDGE SEPARATION USING A LOW ORDER PANEL METHOD Final Report
Doral R. Sandlin Sep. 1989 26 p
(Contract NCC2-226)
(NASA-CR-185892; NAS 1.26:185892) Avail: NTIS HC A03/MF A01

An examination of the potential flow computer code VSAERO to model leading edge separation over a delta wing is examined. Recent improvements to the code suggest that it may be capable of predicting pressure coefficients on the body. Investigation showed that although that code does predict the vortex roll-up, the pressure coefficients have significant error. The program is currently unsatisfactory, but with some additional development it may become a useful tool for this application. Author

N89-28494# Institut Franco-Allemand de Recherches, Saint-Louis (France).
STUDY OF THE WING-VORTEX INTERACTION IN THREE DIMENSIONAL FLOWS (INCOMPRESSIBLE INVISCID FLOW) [ETUDE DE L'INTERACTION AILE/TOURBILLON EN TRIDIMENSIONNEL (ECOULEMENT INCOMPRESSIBLE SANS VISCOSITE)]
M. Schaffar 16 Aug. 1987 45 p In FRENCH Original contains color illustrations
(ISL-R-123/87; ETN-89-94856) Avail: NTIS HC A03/MF A01

The use of horseshoe vortices on the wing and of a turbulent network for the wake, permitted treatment in three dimensions of the case of a thin wing for steady flow and unsteady flow (incident wing with upstream vortex). For steady flow and large spans the calculated lift is close to the two dimensional value. For the unsteady case the variations in lift along the path of the vortex are described. ESA

N89-28495# Institut Franco-Allemand de Recherches, Saint-Louis (France).
PROFILE-VORTEX INTERACTIONS [INTERACTION PROFIL/TOURBILLON]
J. Haertig, Ch. Johe, and M. Schaffar 3 Nov. 1987 49 p In FRENCH
(Contract DRET-85-031)
(ISL-R-125/87; ETN-89-94858) Avail: NTIS HC A03/MF A01

The time evolution of the lift coefficient of a profile exposed to incident vortices is calculated by a perfect fluid two dimensional method and compared to experimental results obtained in a hydrodynamic channel. The unsteady turbulent field is analyzed using laser anemometry. The results are in good agreement with the theoretical model adopted, except for the case when the vortex path is too close to the profile. ESA

N89-28496# National Aeronautical Lab., Bangalore (India). Computational and Theoretical Fluid Dynamics Div.
ROLE OF SUPERCOMPUTER IN COMPUTATIONAL AERODYNAMICS
N. R. Subramanian and Anand Kumar Jun. 1989 20 p
(PD-CF-8925) Avail: NTIS HC A03/MF A01

An overview is given of the computational requirement for solving CFD problems. Also described are two examples, typical of two different types of approximation of Navier-Stokes equations, carried out on a Supercomputer. The first problem deals with the full potential transonic flow computations around a wing in a body fitted coordinate system, while the second deals with vortex flow computation on a low aspect ratio wing based on Euler equations using finite volume and Runge-Kutta time stepping approaches. Author

N89-28497# National Aeronautical Lab., Bangalore (India). Computational and Theoretical Fluid Dynamics Div.
FLOW CALCULATION OVER A DELTA-WING USING THE THIN-LAYER NAVIER-STOKES EQUATIONS
Anand Kumar Jun. 1989 9 p Presented at the International Symposion on CFD, Nagoya (Japan), 28-31 Aug. 1989
(PD-CF-8924) Avail: NTIS HC A02/MF A01

A 3D laminar thin-layer Navier-Stokes solver is developed which employs finite volume spatial discretisation and Runge-Kutta time integration. The code is applied to compute vortex flow over a round leading edge delta wing, and the results are compared with experiment and an Euler simulation. Author

N89-28498*# National Aeronautics and Space Administration. Ames Research Center, Moffett Field, CA.
CORRELATION OF PUMA AIRLOADS: EVALUATION OF CFD PREDICTION METHODS
Roger C. Strawn, Andre Desopper, Judith Miller, and Alan Jones (Royal Aerospace Establishment, Farnborough, England) Aug. 1989 22 p
(NASA-TM-102226; A-89223; NAS 1.15:102226; USAAVSCOM-TM-89-A-001) Avail: NTIS HC A03/MF A01 CSCL 01A

A cooperative program was undertaken by research organizations in England, France, Australia and the U.S. to study the capabilities of computational fluid dynamics codes (CFD) to predict the aerodynamic loading on helicopter rotor blades. The program goal is to compare predictions with experimental data for flight tests of a research Puma helicopter with rectangular and swept tip blades. Two topics are studied. First, computed results from three CFD codes are compared for flight test cases where all three codes use the same partial inflow-angle boundary conditions. Second, one of the CFD codes (FPR) is iteratively coupled with the CAMRAD/JA helicopter performance code. These results are compared with experimental data and with an uncoupled CAMRAD/JA solution. The influence of flow field unsteadiness is found to play an important role in the blade aerodynamics. Alternate boundary conditions are suggested in order to properly model this unsteadiness in the CFD codes. Author

N89-28499# Technische Univ., Delft (Netherlands). Inst. for Wind Energy.
THE ANGLES OF THE KOLIBRIE ROTOR TIPVANES ON THE RODS AND ON THE BLADES
A. Bruining Delft University Press Oct. 1988 24 p Sponsored by the Netherlands Ministry of Economic Affairs
(IW-R515; ISBN-90-627-5496-1; ETN-89-95428) Copyright Avail: NTIS HC A03/MF A01

The data of the adjusted angles of the tipvanes used on the Kolibrie rotor blades and rods, are reported. Two measuring methods are applied: one method is based on determining the chord vector and the span wise vector of the tipvane. The other method is based on the angles of the mounting parts of the tipvanes. The theoretical background and the measurement procedure are not included. Due to the unreliability of the position of the chord vector and the span wise vector the results from the first method are not used. Calculations are carried out with the data from the second method, based on the angles of the mounting parts of the tipvanes. ESA

N89-28500# Aeronautical Research Inst. of Sweden, Stockholm. Aerodynamics Dept.
WIND TUNNEL TESTS OF 16 PERCENT THICK AIRFOIL WITH 30 PERCENT TRAILING EDGE FLAP AT HIGH ANGLES OF ATTACK AND WITH FLAP ANGLES
Sven-Olof Ridder Dec. 1988 45 p Sponsored by the Swedish National Energy Administration
(FFA-TN-1985-58; ETN-89-94312) Avail: NTIS HC A03/MF A01

Wind tunnel tests are carried out at low speeds. The test program includes high negative flap angles and an angle of attack range of 180 deg. The test Reynolds number is 2,200,000. The test results indicate that it is impossible to overcome the strong driving tangential force of the basic section by means of any of the trailing edge devices investigated. ESA

N89-28501 British Aerospace Public Ltd. Co., Preston (England). Military Aircraft Div.
A DETAILED SURVEY OF THE FLOW PASSING THROUGH AN ASYMMETRIC CONTRACTION AND PARALLEL DUCT
M. T. Stickland 16 Nov. 1988 44 p
(BAe-WWT-RP-RES-AXR-000194-Pt-A; ETN-89-94958) Avail: British Aerospace Public Ltd. Co., Preston Lancs PR4 1AX, United Kingdom

A research program was undertaken to reduce or remove an undesirable flow effect in a transonic wind tunnel. The effect is a four lobe swirl appearing in the working section. An experimental study was carried out in the wind tunnel using a model of the contraction and square duct, and existing software was used to numerically simulate the phenomena. The physical simulation was quite successful in reproducing the flow perturbation, while the numerical simulation failed. The flow anomaly is found not to be a problem with the normal types of test work carried out in the tunnel, but it casts serious doubts on the tunnel value in duct code validation work. ESA

N89-28502 British Aerospace Public Ltd. Co., Preston (England). Military Aircraft Div.
A DETAILED SURVEY OF THE FLOW PASSING THROUGH AN ASYMMETRIC CONTRACTION AND PARALLEL DUCT
M. T. Stickland 16 Nov. 1988 179 p
(BAe-WWT-RP-RES-AXR-000194-Pt-B; ETN-89-94959) Avail: British Aerospace Public Ltd., Preston Lancs, PR4 1AX, United Kingdon

A research program was undertaken to reduce or remove an undesirable flow effect in a transonic wind tunnel. The effect is a four lobe swirl appearing in the working section. An experimental study was carried out in the wind tunnel using a model of the contraction and square duct, and existing software was used to numerically simulate the phenomena. The physical simulation was quite successful in reproducing the flow perturbation, while the numerical simulation failed. The flow anomaly is found not to be a problem with the normal types of test work carried out in the tunnel, but it casts serious doubts on the tunnel value in duct code validation work. ESA

N89-28503# Naples Univ. (Italy). Istituto di Aerodinamica.
HERMES PREPARATORY PROGRAM. FLUID DYNAMICS AND NUMERICAL ANALYSIS. THEORETICAL MODELING OF HIGH TEMPERATURE HYPERSONIC FLOWS Progress Report
Luigi G. Napolitano 1987 33 p
(ANE-13/87; ETN-89-95199) Avail: NTIS HC A03/MF A01

The activities performed, up to March 1988, on theoretical modeling of high temperature hypersonic flows, are reported. The phases of the research program are related to: the critical analysis of the thermo-fluid dynamics modeling of hypersonic flows; the formulation in dyadic form of the full set of field equations in a parallel surface curvilinear system; the linear phenomendogical one-fluid theory; the formulation of nonlinear phenomenological relations and nondimensional field equations; the order of magnitude analysis for steady states; the failure of the linear phenomenology and identification of the proper physical necessary modeling for hypersonic flows; and the formulation of the closed set of field equations for the case of a reacting gas mixture in nonequilibrium with respect to an arbitrary number of internal exchanges of mass and energy. Single fluid and linear irreversible thermodynamics are considered. Interaction between mass and electromagnetic energy is supposed negligible. ESA

N89-28504# Deutsche Forschungs- und Versuchsanstalt fuer Luft- und Raumfahrt, Goettingen (Germany, F.R.). Abteilung fuer Numerische Stroemungsmechanik.
THREE-DIMENSIONAL VISCOUS HYPERSONIC FLOW OVER BLUNG BODIES
Stefan Riedelbauch, Bernhard Mueller, and Dietrich Rues 9 Mar.

1989 75 p Sponsored in part by the Deutsche Forschungsgemeinschaft, Bonn
(DFVLR-FB-89-09; ISSN-0171-1342; ETN-89-95306) Avail: NTIS HC A04/MF A01; DFVLR, VB-PL-DO, Postfach 90 60 58, 5000 Cologne, Fed. Republic of Germany, 25.50 DM

Three-dimensional laminar hypersonic flows of perfect gas over blunt bodies are investigated numerically. The thin-layer Navier-Stokes equations are solved for the steady state using a semi-implicit finite-difference scheme. The robustness of the bow shock fitting routine has been improved for interactions with captured embedded shocks. Hypersonic flows over a spacecraft nose and a double ellipsoid are considered. Separated flow, shock-shock and shock-boundary layer interactions are simulated. Skin-friction lines and heat-flux distributions agree qualitatively with oil flow and thermographic pictures. The extension of the code to consider high-temperature effects and the problem of code validation difficulties due to lack of suitable experimental data are discussed. ESA

N89-28505# Deutsche Forschungs- und Versuchsanstalt fuer Luft- und Raumfahrt, Goettingen (Germany, F.R.). Abteilung Messphysik.
EVALUATION OF LDA 3-COMPONENT VELOCITY DATA ON A 65 DEG DELTA WING AT M = 0.85 AND FIRST RESULTS OF AN ANALYSIS
S. N. Seshadri and Karl-Aloys Buetefisch Mar. 1989 67 p
(DFVLR-FB-89-19; ISSN-0171-1342; ETN-89-95314) Avail: NTIS HC A04/MF A01; DFVLR, VB-PL-DO, Postfach 90 60 58, 5000 Cologne, Fed. Republic of Germany, 21 DM

The laser Doppler anenometry (LDA) three-component velocity data obtained for a 65 deg sweptback, cropped delta wing at a free stream Mach number of 0.85 is analyzed with the aid of a menu driven computer program. The program was developed to process the LDA data employing a linear or a weighted quadratic interpolation technique to compute velocities in the vortex core or at any other field point where no measurement data is available. Basic results obtained using the two techniques to compute velocities in the vortex core or at any other field point polation scheme are presented. Limited analysis related to the structure of the vortex and the development of the leeside flow field is made. A good correlation of LDA results with surface results obtained through oil flow/static pressure is found. Existence of a shock wave located above the vortex core is indicated. The weighted quadratic interpolation theory is concluded to give preferable results to these produced by linear technique. ESA

N89-28736# Princeton Univ., NJ. Dept. of Mechanical and Aerospace Engineering.
LARGE SCALE MOTIONS IN SUPERSONIC TURBULENT BOUNDARY LAYERS (Computer Diskette Supplement)
A. J. Smits and J. H. Watmuff *In* AGARD, A Survey of Measurements and Measuring Techniques in Rapidly Distorted Compressible Turbulent Boundary Layers May 1989 14 p Computer diskette supplement (data file): IBM compatible DS HD 5.25-inch formatted 1.2 MB using MS DOS 3.20 (For primary document see N89-28734 23-34)
Avail: NTIS HC A11/MF A01; set of 5 computer diskettes available from NASA Scientific and Technical Information Facility, BWI Airport, MD at $13.00/set

N89-28738# Princeton Univ., NJ. Dept. of Mechanical and Aerospace Engineering.
HOT-WIRE ANEMOMETRY IN SUPERSONIC FLOW (Computer Diskette Supplement)
A. J. Smits and J. P. Dussauge (Aix-Marseilles Univ., France) *In* AGARD, A Survey of Measurements and Measuring Techniques in Rapidly Distorted Compressible Turbulent Boundary Layers May 1989 14 p Sponsored in part by CNRS, France Computer diskette supplement (data file): IBM compatible DS HD 5.25-inch formatted 1.2 MB using MS DOS 3.20 (For primary document see N89-28734 23-34)
Avail: NTIS HC A11/MF A01; set of 5 computer diskettes available from NASA Scientific and Technical Information Facility, BWI Airport, MD at $13.00/set

N89-28740# Aix-Marseilles Univ. (France). Inst. de Mecanique Statistique de la Turbulence.
LASER DOPPLER ANEMOMETRY IN SUPERSONIC FLOWS: PROBLEMS OF SEEDING AND ANGULAR BIAS (Computer Diskette Supplement)
M. Elena *In* AGARD, A Survey of Measurements and Measuring Techniques in Rapidly Distorted Compressible Turbulent Boundary Layers May 1989 6 p Computer diskette supplement (data file): IBM compatible DS HD 5.25-inch formatted 1.2 MB using MS DOS 3.20 (For primary document see N89-28734 23-34)
Avail: NTIS HC A11/MF A01; set of 5 computer diskettes available from NASA Scientific and Technical Information Facility, BWI Airport, MD at $13.00/set

03 AIR TRANSPORTATION AND SAFETY

Includes passenger and cargo air transport operations; and aircraft accidents.

For related information see also *16 Space Transportation* and *85 Urban Technology and Transportation.*

N89-28506# Systems Control Technology, Inc., Arlington, VA.
RISK MANAGEMENT FOR AIR AMBULANCE HELICOPTERS OPERATORS Final Report
Rich Adams and Jack Thompson Jun. 1989 57 p Prepared in cooperation with Advanced Aviation Concepts, Jupiter, FL
(Contract DTFA01-87-C-0014)
(DOT/FAA/DS-88/7) Avail: NTIS HC A04/MF A01

This manual is intended to provide an easy reference for dealing with the operating pitfalls, the human frailties, and the risks in managing an air ambulance operation. It is not designed to give the operator step-by-step instructions. Rather, the manual describes techniques and tools that can be used to balance the demands of running a business with the need for maintaining safety. It provides pilot selection and training guidelines, as well as a review of a risk assessment technique that has proven successful. In addition, the manual recommends a workable format for establishing standard operating procedures to reduce risks. Finally, it highlights the key concerns that should be carefully considered from a risk management viewpoint. This operators manual is one of an integrated set of five Aeronautical Decision Making (ADM) manuals developed by the Federal Aviation Administration in a concerted effort to reduce the number of human factor related helicopter accidents. It can be used as one element of a comprehensive program for improving safety, reducing risk and, hopefully, the high cost of helicopter hull and liability insurance. The other four documents of the set are: (1) ADM for Helicopter Pilots (DOT/FAA/PM-86/45); (2) ADM for EMS Helicopter Pilots - Learning from Past Mistakes (DOT/FAA/DS-88/5); (3) ADM for EMS Helicopter Pilots - Situational Awareness Exercises (DOT/FAA/DS-88/6); and (4) ADM for Air Ambulance Hospital Administrators (DOT/FAA/DS-88/8). Author

N89-28507# National Transportation Safety Board, Washington, DC. Bureau of Field Operations.
AIRCRAFT ACCIDENT/INCIDENT SUMMARY REPORTS: BELLEVILLE, ILLINOIS, AUGUST 22, 1987; PENSACOLA, FLORIDA, DECEMBER 27, 1987
30 Jun. 1989 25 p
(PB89-910405; NTSB/AAR-89/02/Sum) Avail: NTIS HC A03/MF A01 CSCL 01C

Two separate aircraft accidents investigated by the National Transportation Safety Board are compiled. The accident locations and their dates are as follows: Belleville, Illinois, August 22, 1987; and Pensacola, Florida, December 27, 1987. Author

N89-28508# Technische Univ., Berlin (Germany, F.R.). Wirtschaftswissenschaftliche Dokumentation.
COMPETITION AND SAFETY IN AIR TRAFFIC Thesis [WETTBEWERB UND SICHERHEIT IM LUFTVERKEHR]
Matthias-Wolfgang Stoetzer 1988 50 p In GERMAN; ENGLISH summary
(TUB-Diss-Paper-128; ETN-89-94421) Avail: NTIS HC A04/MF A01

The relations between competition and safety in the air transportion market are investigated. The allegation that competition in the air transportion market necessarily results in a deterioration of flight safety is examined on theoretical grounds. Existing studies of the relationship of safety and competition in flight transportation are summarized. The development of flight safety in the USA before and after the Airline Deregulation Act of 1978 is analyzed. Theoretical reasoning and the empirical confirmation lead to the conclusion that economic regulation is not inevitable in order to secure a high level of safety in air transportion. The maintaining or the regulation of technical standards is advised. ESA

04 AIRCRAFT COMMUNICATIONS AND NAVIGATION

Includes digital and voice communication with aircraft; air navigation systems (satellite and ground based); and air traffic control.

For related information see also *17 Space Communications, Spacecraft Communications, Command and Tracking* and *Communications and Radar.*

N89-28509# Mitre Corp., McLean, VA.
COLLISION AVOIDANCE OPERATIONAL CONCEPT Final Report
Meera Sharma Jun. 1989 33 p
(Contract DTFA01-89-C-00001)
(WP-88W00418; NAS-SR-1325; DOT/FAA/DS-89/27) Avail: NTIS HC A03/MF A01

An operational concept is presented for collision avoidance services which will be in place upon implementation of the Federal Aviation Administration (FAA) National Airspace System (NAS) Plan. This operational concept only discusses the ground-base portion of how the Air Traffic Control System (ATCS) provides flight safety by maintaining adequate aircraft separation. This concept discusses the aircraft separation assurance per the National Airspace System Requirement Specification (NASSRS). The objective is to describe the relationship among subsystems, facilities, information, and operators/users involved in the collision avoidance service. In addition, the elements and operations of the NAS Plan are mapped into the collision avoidance requirements stated in the NASSRS, NAS-SR-1000. Several types of block diagrams are used to illusrate systems connectively and operational flow. Scenarios are also derived to describe the collision avoidance process from a user's perspective. Author

N89-28510# Technische Univ., Delft (Netherlands). Faculteit der Geodesie.
KINEMATIC VERTICAL POSITIONING USING THE GLOBAL POSITIONING SYSTEM [KINEMATISCHE HOOGTEBEPALING MET HET GLOBAL POSITIONING SYSTEM]
J. J. M. Lammerts Aug. 1988 84 p In DUTCH; ENGLISH summary
(ETN-89-94804) Avail: NTIS HC A05/MF A01

The accuracy of static and kinematic vertical positioning using the global positioning system is studied both theoretically and by the analysis of measured data, with a view to depth measurements in open sea. The hitherto used kinematic model, which is of the type pseudo-range/phase, is rearranged in such a way that the position drift of the static baselines is eliminated. The influence of an error in the satellite position on the unknowns is analyzed; the linear relation between such an error and the positioning is derived by simulation. Simulations show that for a precise vertical positioning at least one satellite has to be in or near the zenith, and the others should be equally spaced around the zenith. The precision reached with the improved kinematic model is on the order of 1 cm; it decreases from 1 cm, using zero baselines, to 3 cm, using static baselines. A precision of 7 cm in horizontal positioning and 4 cm in vertical positioning is obtained with the model, using kinematic baselines. ESA

05 AIRCRAFT DESIGN, TESTING AND PERFORMANCE

Includes aircraft simulation technology.

For related information see also *18 Spacecraft Design, Testing and Performance* and *39 Structural Mechanics.* For land transportation vehicles see *85 Urban Technology and Transportation.*

N89-28511# Aerospace Medical Research Labs., Wright-Patterson AFB, OH.
SPECIFICATIONS AND MEASUREMENT PROCEDURES AND AIRCRAFT TRANSPARENCIES Final Report, Dec. 1987 - Jun. 1988
Peter T. LaPuma and John C. Bridenbaugh Sep. 1988 56 p
(AD-A209396; AAMRL-TR-88-058) Avail: NTIS HC A04/MF A01 CSCL 01/3

This report is a summary of the specification requirements for optical quality for several military aircraft transparencies. It is intended to provide the design engineer with an easy reference to a majority of the accumulated historical information concerning optical quality. GRA

N89-28512# Army Lab. Command, Watertown, MA. Material Technology Lab.
COMPARATIVE ANALYSIS OF ULTRASONIC INSPECTION PROCEDURES FOR KAMAN K747 ROOT END FITTINGS Final Report
Walter N. Roy, Philip G. Bennett, and Bradley M. Taber, III Apr. 1989 68 p
(AD-A207762; MTL-TR-89-27) Avail: NTIS HC A04/MF A01 CSCL 14/2

This report provides a comparative analysis of two ultrasonic inspection procedures for Kaman Aerospace Corporation's K747 root end fittings. The procedure currently being used was originally developed by Truton under contract through Kaman Aerospace, the fabricator of the root end fitting. The other procedure is a revision of the existing Truton procedure which was prepared by the U.S. Army Materials Technology Laboratory (MTL). Both procedures were compared against a sample of ten previously rejected root end fittings. GRA

N89-28513# Office of the Secretary of Defense, Washington, DC.
OPERATIONAL TEST PLAN CONCEPT FOR EVALUATION OF CLOSE AIR SUPPORT ALTERNATIVE AIRCRAFT Summary Report
31 Mar. 1989 130 p
(AD-A208185) Avail: NTIS HC A07/MF A01 CSCL 15/6

The FY 1989 Defense Authorization Amendments and Base Closure and Realignment Act, Public Law 100-526, required the Director, Operational Test and Evaluation (DOT&E) to prepare an operational test plan to conduct a competitive fly-off of alternative aircraft for the Close Air Support (CAS) mission and to complete the test plan. The Act also directed the Secretary of Defense to conduct an independent assessment of ongoing studies and analyses related to selection of an aircraft for the CAS mission and to examine the feasibility of transferring the CAS mission from the Air Force to the Army. The Army and Air Force have jointly developed a list of requirements for a CAS aircraft. In addition, a Mission Need Statement (MNS) for a fixed wing aircraft has been developed and approved by the Joint Requirements Oversight Council, Office of the Chairman, Joint Chiefs of Staff. These requirements can be grouped into three principal categories:

effectiveness in killing assigned targets, survivability and responsiveness. The USAF has proposed to replace the A-10 Thunderbolt, which is currently its primary CAS aircraft. Air Force assessments have concluded that the A-10, even with an engine modification, cannot survive on current and future battlefields while faster aircraft have significantly greater survivability. The Air Force has recommended that the A-10 be replaced by a modified version of the F-16, which has been designated the A-16. GRA

N89-28514# National Aerospace Lab., Tokyo (Japan).
AN EXPERIMENTAL OPTICAL COUPLING DEVICE FOR AN AIRBORNE DIGITAL REDUNDANT SYSTEM
Akira Watanabe and Kaoru Wakairo 1988 41 p In JAPANESE; ENGLISH summary
(NAL-TR-1003; ISSN-0389-4010) Avail: NTIS HC A03/MF A01

A new optical coupling device for an airborne digital redundant system is described. For an onboard system, it is very important to increase reliability and safety, so a redundant system is applied. In a redundant system, in order to verify whether each operation is correct, it is necessary to compare it with the same time data from other systems. A new characteristic coupling device was developed and its features verified experimentally. This system has the following characteristics: (1) It has a simple hardware architecture in order to increase reliability and safety; (2) Synchronization and data exchange are separated in time, so this system utilizes the same hardware for these tasks; (3) To increase transfer speed, a broadcast method is used and the number of receivers is (redundancy-1); thus each system can transmit and receive simultaneously; and (4) An optical signal is used in order to increase transfer speed and this is effective for electric separation among systems. Finally, a discussion is presented of how to recognize the end of transfer without an interrupt signal in a digital computer. Author

06 AIRCRAFT INSTRUMENTATION

Includes cockpit and cabin display devices; and flight instruments.

For related information see also *19 Spacecraft Instrumentation* and *35 Instrumentation and Photography.*

N89-28515# School of Aerospace Medicine, Brooks AFB, TX.
TOWARDS A PHYSIOLOGICALLY BASED HUD (HEAD-UP DISPLAY) SYMBOLOGY Final Report, Jul. 1987 - Jun. 1988
Fred H. Previc Jan. 1989 22 p
(AD-A207748; USAFSAM-TR-88-25) Avail: NTIS HC A03/MF A01 CSCL 01/4

New concepts in HUD symbology, based on an understanding of the physiological mechanisms and ecological origins of the human visual system are described which may enable future HUD displays to serve as primary flight directors in addition to their current roles. The four key elements of this new symbology are: (1) prioritization of space according to the three-dimensional structure of visual attention, (2) an attitude display in the form of a global percept; (3) effective preattentive attitude cueing based on an ecologically valid simulation of the visual terrain during flight ; and (4) visual reference framing which depicts the roll of the aircraft relative to a stable horizon. Prototypes which illustrate the physiological HUD concept are presented. The specific advantage of the proposed symbology may be to allow the pilot to maintain effective attitude control while directing his attention towards the out-the-window environment. GRA

07 AIRCRAFT PROPULSION AND POWER

Includes prime propulsion systems and systems components, e.g., gas turbine engines and compressors; and onboard auxilliary power plants for aircraft.

For related information see also *20 Spacecraft Propulsion and Power, 28 Propellants and Fuels,* and *44 Energy Production and Conversion.*

N89-28516# Naval Air Propulsion Test Center, Trenton, NJ.
STATISTICS ON AIRCRAFT GAS TURBINE ENGINE ROTOR FAILURES THAT OCCURRED IN US COMMERCIAL AVIATION DURING 1984 Final Report
R. A. DeLucia, J. T. Salvino, and B. C. Fenton (Federal Aviation Administration, Atlantic City, NJ.) Jun. 1989 26 p
(Contract DOT/FA71NA-AP98)
(NAPC-PE-185; DOT/FAA/CT-89/6) Avail: NTIS HC A03/MF A01

Presented here is statistical information relating to gas turbine engine rotor failures which occurred during 1984 in commercial aviation service use. Two hundred and six failures occurred in 1984. Rotor fragments were generated in 114 of the failures and, of these, 18 were uncontained. The predominant failure involved blade fragments, 90.3 percent of which were contained. Seven disk failures occurred and all were uncontained. Seventy percent of the 206 failures occurred during the takeoff and climb stages of flight. This service data analysis is prepared on a calendar year basis and published yearly. The data are useful in support of flight safety analyses, proposed regulatory actions, certification standards, and cost benefit analyses. Author

N89-28517# Naval Air Propulsion Test Center, Trenton, NJ.
STATISTICS ON AIRCRAFT GAS TURBINE ENGINE ROTOR FAILURES THAT OCCURRED IN US COMMERCIAL AVIATION DURING 1985 Final Report
R. A. DeLucia, J. T. Salvino, and B. C. Fenton (Federal Aviation Administration, Atlantic City, NJ.) Jul. 1989 28 p
(Contract DOT/FA71NA-AP98)
(NAPC-PE-188; DOT/FAA/CT-89/7) Avail: NTIS HC A03/MF A01

Statistics relating to gas turbine engine rotor failures which occurred during 1985 in U.S. commercial aviation service use are given. Two hundred and seventy-three failures occurred in 1985. Rotor fragments were generated in 150 of the failures, and of these 14 were uncontained. The predominant failure involved blade fragments, 94.4 percent of which were contained. Six disk failures occurred and all were uncontained. Fifty-seven percent of the 273 failures occurred during the takeoff and climb stages of flight. This service data analysis is prepared on a calendar year basis and published yearly. The data support flight safety analyses, proposed regulatory actions, certification standards, and cost benefit analyses. Author

N89-28518# Aeronautical Research Labs., Melbourne (Australia).
AERODYNAMIC MODEL TESTS OF EXHAUST AUGMENTORS FOR F/A-18 ENGINE RUN-UP FACILITY AT RAAF WILLIAMTOWN Summary Report
S. A. Fisher and A. M. Abdel-Fattah Dec. 1988 29 p
(AD-A208110; ARL-AERO-PROP-TM-458; AR-005-583) Avail: NTIS HC A03/MF A01 CSCL 21/5

Model tests of the air cooled exhaust augmentors proposed for the F/A-18 engine ground run-up facilities at RAAF Williamtown were undertaken, to confirm satisfactory aerodynamic behavior of the augmentor designs and to provide data for optimizing certain aspects of the designs. The tests were carried out on 1/45 scale models, using an unheated air jet to represent the engine exhaust. Geometric features were identified which had important influence on augmentor duct flow symmetry and the cooling flow augmentation ratio. GRA

N89-28519# Institut Franco-Allemand de Recherches, Saint-Louis (France).
MEASUREMENTS OF MEAN-FLOW AND TURBULENCE CHARACTERISTICS IN A TURBOJET EXHAUST USING A LASER VELOCIMETER
H. J. Schaefer 13 Sep. 1988 16 p Presented at the 11th Symposium on Turbulence, Rolla, MO, 17-19 Oct. 1988
(ISL-CO-226/88; ETN-89-95033) Avail: NTIS HC A03/MF A01

Mean-flow and turbulence characteristics are measured in a high-temperature axisymmetric jet exhausting from an aero engine. The effects of exit Mach number and temperature on the jet flow field are studied. A laser Doppler velocimeter is used to map the flow characteristics over a range of Mach numbers from 0.46 to 0.84. Radial distributions of the mean axial velocity and the root mean square of the corresponding fluctuations are obtained at different axial stations in the flow. The various distributions are found to collapse when plotted in appropriate coordinates. The collapsed data can be approximated by a universal profile. The radial mean-velocity scans at various axial stations exhibit a strong similarity when compared in reduced lateral coordinates. The spread of the mixing layer decreases with increasing exit Mach number and temperature. ESA

08 AIRCRAFT STABILITY AND CONTROL

Includes aircraft handling qualities; piloting; flight controls; and autopilots.

For related information see also *05 Aircraft Design, Testing and Performance.*

N89-28520# Naval Postgraduate School, Monterey, CA.
THE EFFECT OF AUTOPILOT CONFIGURATION ON MISSILE RESPONSE M.S. Thesis
Kenneth E. Cockerham Mar. 1989 75 p
(AD-A207822) Avail: NTIS HC A04/MF A01 CSCL 16/4

A comparison of two different autopilot configurations and their effect on missile response is presented. The comparison includes the steps taken in determining missile parameters from wind tunnel data and flight condition data. The missile parameters are coupled with two different autopilot configurations to determine any significant advantage of one configuration over the other. Pole placement is used in determining required autopilot feedback and feed forward gains. Simulations of each autopilot are conducted and the responses are compared. GRA

N89-28521# National Aeronautical Lab., Bangalore (India). Systems Engineering Div.
MODEL SIMPLIFICATION BASED ON THE CONCEPT OF EQUIVALENT DEAD TIME
Shaik Ismail Dec. 1988 38 p
(NAL-TM-SE-8802) Avail: NTIS HC A03/MF A01

The concept of equivalent dead time and its use in the simplification of s-domain and z-domain higher order transfer functions (HOTF) is examined. A preliminary lower order transfer function (LOTF) is obtained by retaining a few dominant poles and zeros of the HOTF. This lower order model is then enhanced by including a pure time delay element. This element is related to the difference between equivalent dead times of HOTF and the preliminary LOTF. FORTRAN routines are developed for this procedure and several examples are given to illustrate the procedure. Author

N89-28522# Technische Univ., Berlin (Germany, F.R.). Inst. fuer Luft- und Raumfahrt.
STATUS AND DEVELOPMENT POTENTIAL OF THE FLY BY LIGHT TECHNOLOGY IN CIVIL AIRCRAFT [STAND UND ENTWICKLUNGSPOTENTIAL DER FLY-BY-LIGHT TECHNOLOGIE IN ZIVILEN LUFTFAHRZEUGEN]
Heinrich Menson and Ralph Schuette Apr. 1988 142 p In GERMAN
(ILR-Mitt-212; ETN-89-94562) Avail: NTIS HC A07/MF A01

Fiber optics communication techniques and their applicability in flight control are reviewed. The design of an optical digital system (communication principle, emitting sources, optical waveguides, receiver element, optical coupling) is outlined. The fundamentals of data communication systems aboard aircrafts, the technical requirements and operational behavior of optical components, and existing fly by light concepts are presented. Fly by light technology is compared with conventional technology. Further application of fiber optics elements in aircrafts are discussed. ESA

09 RESEARCH AND SUPPORT FACILITIES (AIR)

Includes airports, hangars and runways; aircraft repair and overhaul facilities; wind tunnels; shock tubes; and aircraft engine test stands.

For related information see also *14 Ground Support Systems and Facilities (Space).*

N89-28523# Naval Civil Engineering Lab., Port Hueneme, CA.
JOINT SEALANTS FOR AIRPORT PAVEMENTS. PHASE 1: LABORATORY AND FIELD INVESTIGATIONS Final Report, Jul. 1986 - Dec. 1988
C. M. Inaba, M. C. Hironaka, and T. Novinson Dec. 1988 63 p
(Contract DTFA01-86-1-02015)
(DOT/FAA/DS-89/2-Phase-1) Avail: NTIS HC A04/MF A01

The objectives were to determine the essential characteristics of sealants for joints in Portland cement concrete (PCC) airport pavements that should be incorporated in specifications and select best candidate sealants for field evaluation. Laboratory and field investigations of sealants were performed for data needed to meet these objectives. Major factors that sealants must be resistant to are: chemicals (jet fuel, hydraulic fluid, lubricating oil), physical (elongation, compression, intrusion), and environmental (thermal, sunlight, weathering). In laboratory specification conformance tests, only 3 of 18 (17 percent) of the sealants passed the tests. In field inspection of sealants and discussions with airport personnel, there was no one clearly outstanding performing seal that was identified; however, several airports favored the Dow Corning 888 silicone seal. There is a strong indication of material of specification (or both) deficiencies. Sealants selected for evaluation in Phase 2 have the following material compositions: silicone, polyurethane, coal tar/polyvinyl chloride, and chloroprene. Author

N89-28524# Mitre Corp., McLean, VA.
DIRECT USER ACCESS TERMINAL (DUAT) OPERATIONAL CONCEPT Final Report
A. L. Springen Jun. 1989 36 p
(Contract DTFA01-89-C-00001)
(WP-88W00075; NAS-SR-DUAT; DOT/FAA/DS-89/28) Avail: NTIS HC A03/MF A01

This concept of operations is one of a set that in total describes the operation of the National Airspace System (NAS) when the projected upgrades are completed. The Direct User Access Terminal (DUAT) is a Federal Aviation Administration (FAA) program that enables pilots to obtain self-briefings and submit flight plans, much as they receive these services from Flight Service Stations (FSSs) and Automated FSSs (AFSSs) today; however, DUAT is provided by the private sector. DUAT Service capabilities and interactions between the user, the DUAT Service, and NAS subsystems are described. It is intended to provide a common perspective for personnel engaged in DUAT-related activities. Author

N89-28525# Mainz Univ. (Germany, F.R.).
THE SCAVENGING OF ATMOSPHERIC POLLUTANTS BY CLOUDS AND PRECIPITATION USING A VERTICAL WIND TUNNEL, PHASE 1 Final Report, 31 Jan. 1987
H. R. Pruppacher 1 Apr. 1988 80 p In GERMAN; ENGLISH summary

(Contract BMFT-FKZ-070-4580-6)
(BPT-9/88; ISSN-0176-0777; ETN-89-94423) Copyright Avail: NTIS HC A05/MF A01

The design and performance characteristics of a vertical wind tunnel, adapted for research in cloud physics and atmospheric chemistry, are described. The Prandtl type wind tunnel is driven by suction of air into vacuum through a sonic valve which, together with a screen, honeycomb, and contration section provides a positive air flow velocity control and a laminar flow of extremely low turbulence. This air stream quality allows the free suspension of water drops, ice crystals, snow flakes, and hailstones. An air conditioning system allows the simulation of a wide range of physical conditions in atmospheric clouds. Preliminary experiments show the feasibility of quantitative studies of, the rates at which atmosphere pollutants become incorporated by cloud drops, rain drops and ice particles, of the mechanisms controlling this incorporation, of the chemical reactions inside these particles, of the desorption of trace gases from these particles, of the drop-to-particle conversion, and of numerous other basic microphysical processes in atmospheric clouds. ESA

N89-28526# National Aerospace Lab., Amsterdam (Netherlands). Informatics Div.
AIRPORT NOISE MEASURING DATA COLLCTION SYSTEM
M. H. J. B. Versteeg 19 Jan. 1987 12 p Presented at the VMEbus Application Seminar, Antwerp, Belgium, 25 Feb. 1987
(NLR-MP-87006-U; ETN-89-95410) Avail: NTIS HC A03/MF A01

The technical aspects of the central unit of the permanent noise measuring system, are discussed. The measured noise data values are obtained from a set of noise monitoring terminals located near a military airbase on Dutch territory. These values are collected together with time tags, stored on magnetic tape and processed. The central unit of this system is built using versa module eurocard technology, and the controlling software is developed using micro concurrent PASCAL language, whose compiler performs extensive type checking and identifies development errors. The most time consuming part of the software development is the development of the links of the system hardware. The central unit of the noise measuring system is built in such a way as to be fault tolerant. Missing data samples, lost connections or erroneous collected data should not disrupt the operation of the system. ESA

12 ASTRONAUTICS (GENERAL)

For extraterrestrial exploration see *91 Lunar and Planetary Exploration.*

N89-28527# Joint Publications Research Service, Arlington, VA.
JPRS REPORT: SCIENCE AND TECHNOLOGY. USSR REPORT: LIFE SCIENCES
15 Mar. 1989 77 p Transl. into ENGLISH from various Russian articles
(JPRS-USP-89-005) Avail: NTIS HC A05/MF A01

Topics addressed in these translated Russian articles include: (1) manned mission highlights (preparations, research program and launch of the Soviet-French Mission to Mir); (2) aerospace sciences; (3) aerospace engineering; (4) space technology applications; and (5) Soviet space policy and administration. Over 50 articles from various Russian publications are included. For individual titles, see N89-28528 through N89-28532.

N89-28528# Joint Publications Research Service, Arlington, VA.
THE ORBITAL SPACE OBSERVATORY GAMMA **c18**
V. G. Kirillov-Ugryumov *In its* JPRS Report: Science and Technology. USSR Report: Life Sciences 15 Mar. 1989 p 14-23 Transl. into ENGLISH from Zemlya i Vselennaya (Moscow, USSR), no. 5, Sep.-Oct. 1988 p 5-13 (For primary document see N89-28527 23-12)
Avail: NTIS HC A05/MF A01

The approaching launch of the Soviet space observatory, Gamma, into near-Earth orbit is discussed. Although the energy of gamma quanta is great, their flux near Earth is negligible. Gamma astronomy outside the atmosphere has the potential for looking even farther than radioastronomy and seeing still earlier epochs of development of the Universe. Instrumentation of the Gamma observatory which includes three telescopes, is discussed.
Author

N89-28529# Joint Publications Research Service, Arlington, VA.
BURAN FLIGHT TESTING, CAPABILITIES DISCUSSED **c16**
In its JPRS Report: Science and Technology. USSR Report: Life Sciences 15 Mar. 1989 p 36-37 Transl. into ENGLISH from Tass (Moscow, USSR) 1923 GMT, 25 Jan. 1989 (For primary document see N89-28527 23-12)
Avail: NTIS HC A05/MF A01

The flight testing capabilities of the unmanned reusable Soviet orbiter, Buran, are described. Aspects of the spacecraft's landing are briefly discussed. K.C.D.

N89-28530# Joint Publications Research Service, Arlington, VA.
DESIGNERS' COMMENTARY ON BURAN FLIGHT CONTROL SYSTEM **c16**
G. Gromov *In its* JPRS Report: Science and Technology. USSR Report: Life Sciences 15 Mar. 1989 p 39-40 Transl. into ENGLISH from Pravda (Moscow, USSR), 6 Dec. 1988 p 3 (For primary document see N89-28527 23-12)
Avail: NTIS HC A05/MF A01

The automated landing control system of the Soviet unmanned reusable spacecraft, Buran, is described. The electronic systems developed for this purpose were integrated into a unified navigation, traffic control and landing system named Vympel. It included the instrumental and electronic systems that made up the ground and on-board equipment. K.C.D.

N89-28531# Joint Publications Research Service, Arlington, VA.
DEVELOPMENT, TESTING PROCEDURES FOR BURAN SHUTTLE **c16**
Andrey Tarasov *In its* JPRS Report: Science and Technology. USSR Report: Life Sciences 15 Mar. 1989 p 40-49 Transl. into ENGLISH from Pravda (Moscow, USSR), 2 Jan. 1989 p 4 (For primary document see N89-28527 23-12)
Avail: NTIS HC A05/MF A01

A brief description of the planning that went into the development of the Soviet reusable spacecraft, Buran, is given. Opinions about the shuttle by its main designers are reviewed. K.C.D.

N89-28532# Joint Publications Research Service, Arlington, VA.
METHOD FOR RESEARCH ON PLANET VENUS USING FLOATING BALLOON STATIONS: MATHEMATICAL MODEL **c91**
V. A. Vorontsov, V. A. Deryugin, V. P. Karyagin, R. S. Kremnev, V. V. Kuznetsov, V. M. Linkin, K. M. Pichkhadze, G. N. Rogovskiy, and A. V. Terterashvili *In its* JPRS Report: Science and Technology. USSR Report: Life Sciences 15 Mar. 1989 p 49-50 Transl. into ENGLISH from Kosmicheskiye Issledovaniya (Moscow, USSR), v. 26 no. 3, May-Jun. 1988 p 430-433 (For primary document see N89-28527 23-12)
Avail: NTIS HC A05/MF A01

A mathematical model of balloon probes such as those used in the Vega project of 1985 was formulated for understanding the nature of the drift process and correct interpretation of the experimentally collected data. The model describes both the characteristic and perturbed motion of a balloon during drift.
Author

N89-28533# Los Alamos National Lab., NM. Chemical and Laser Sciences Div.
LABORATORY INVESTIGATIONS: LOW EARTH ORBIT ENVIRONMENT CHEMISTRY WITH SPACECRAFT SURFACES
Jon B. Cross 1989 8 p Presented at the Space Operations Automation and Robotics Workshop, Houston, TX, 25-27 Jul. 1989

(Contract W-7405-eng-36)
(DE89-014280; LA-UR-89-2168; CONF-890799-1) Avail: NTIS HC A02/MF A01

Long-term space operations that require exposure of material to the low earth orbit (LEO) environment must take into account the effects of this highly oxidative atmosphere on material properties and the possible contamination of the spacecraft surroundings. Ground-based laboratory experiments at Los Alamos using a newly developed hyperthermal atomic oxygen (AO) source have shown that not only are hydrocarbon based materials effected but that inorganic materials such as MoS2 are also oxidized and that thin (750A) protective coatings such as Al2O3 can be breached, producing oxidation of the underlying substrate material. Gas-phase reaction products, such as SO2 from oxidation of MoS2 and CO and CO2 from hydrocarbon materials, have been detected and have consequences in terms of spacecraft contamination. Energy loss through gas-surface collisions causing spacecraft drag has been measured for a few select surfaces and has been found to be highly dependent on the surface reactivity. DOE

N89-28534# Army War Coll., Carlisle Barracks, PA.
US ARMY ROLE IN SPACE Study Project
Joseph R. Nowland 12 Apr. 1989 36 p
(AD-A209178) Avail: NTIS HC A03/MF A01 CSCL 22/1

The future battlefield has been described as non-linear, chaotic, intense and highly lethal. To fight and win in this environment, the Army has developed the AirLand Battle Doctrine, which relies heavily on the fundamental tenets of initiative, agility, depth, and synchronization as it fights the close, deep and rear battle. Our current terrestrial intelligence and communications systems alone do not provide the sufficiency of connectivity, reliability and capacity to meet the demands of this new doctrine. These systems also suffer from electronic jamming, frequency detection and coverage limitations. New battlefield surveillance and communications systems offer increased day/night, all-weather capability to see deep behind enemy lines, but will be limited because of stand-off positioning limitations and air platform flight-time restrictions. Space-based systems cannot totally replace terrestrial and airborne systems but offer enhanced capabilities that provide timely, reliable information in a ready-to-use form necessary to fight the deep-attack doctrine. This paper will review current military uses of space and suggest several roles and missions for the Army in space as it moves into the 21st century and attempts to meet the demands of the AirLand Battle 2004 Doctrine. GRA

N89-28535*# National Aeronautics and Space Administration. Lewis Research Center, Cleveland, OH.
COLD-SAT: CRYOGENIC ON-ORBIT LIQUID DEPOT-STORAGE, ACQUISITION AND TRANSFER
Jul. 1989 14 p Original contains color illustrations
(NASA-TM-102308; E-4997; NAS 1.15:102308) Avail: NTIS HC A03/MF A01 CSCL 22A

NASA is entering an era of expanded space activity. Space-based transportation systems will carry cargo and humans from low earth orbit to geosynchronous orbit, to lunar bases, and to the Martian surface. Support of these future missions will require new, long lived, on-orbit systems using subcritical cryogens for propellants and life support systems. Such on-orbit systems present low gravity fluid management challenges of long term storage and efficient fluid transfer and supply techniques. Development of these cryogenic systems requires on-orbit experimentation to demonstrate the capability of performing these fluid management tasks and to obtain the engineering data base required to correlate analytical tools used for system design. Author

N89-28536# Technische Univ., Berlin (Germany, F.R.). Inst. fuer Luft- und Raumfart.
[ACTIVITIES REPORT OF THE INSTITUTE OF SPACE RESEARCH] Annual Report, 1986-1987 [JAHRESBEREICHT 1986/87]
K. Knothe, H. H. Koelle, and Prochnow 1988 73 p In GERMAN
(ILR-1986/87; ETN-89-94420) Avail: NTIS HC A04/MF A01

The teaching tasks of the institute and the services offered to the students are outlined. Research activities are listed, but research results are not shown. ESA

N89-28537*# Alabama Univ., Huntsville. Dept. of Mechanical Engineering.
COORDINATION OF ADVANCED SOLAR OBSERVATORY (ASO) SCIENCE WORKING GROUP (SWG) FOR THE STUDY OF INSTRUMENT ACCOMMODATION AND OPERATIONAL REQUIREMENTS ON SPACE STATION Final Report, 1 Aug. 1987 - 30 Apr. 1989
S. T. Wu Oct. 1989 127 p
(Grant NAG8-682)
(NASA-CR-185371; NAS 1.26:185371) Avail: NTIS HC A07/MF A01 CSCL 22A

The objectives are to coordinate the activities of the Science Working Group (SWG) of the Advanced Solar Observatory (ASO) for the study of instruments accommodation and operation requirements on board space station. In order to facilitate the progress of the objective, two conferences were organized, together with two small group discussions. Author

13 ASTRODYNAMICS

Includes powered and free-flight trajectories; and orbital and launching dynamics.

N89-28538# Air Force Inst. of Tech., Wright-Patterson AFB, OH. School of Engineering.
NUMERICAL DETERMINATION OF THE LOCATION OF CRITICAL INCLINATIONS FOR LONG TERM HIGH ECCENTRICITY ORBITS ABOUT MARS M.S. Thesis
Denis F. Durand Jun. 1989 107 p
(AD-A209200; AFIT/GA/ENY/89J-2) Avail: NTIS HC A06/MF A01 CSCL 03/3

The purpose of this study is to locate critical inclinations in long term high eccentricity orbits about Mars using numerical methods. A critical inclination is defined as the inclination at orbit insertion which produces a local maximum in the amplitude of the variation of eccentricity or inclination. The perturbation model consists of the first non-zero zonal harmonic of the Mars gravity potential and the Sun as a point mass third body. The search range consists of inclinations from 0.25 to 90.0 degrees, eccentricities from 0.40 to 0.90, periapse radii from 4000 km to 7000 km, and orbit lifetimes of 10 earth years. The numerical search comprises the following procedure: (1) A time history of eccentricity and inclination is produced for each combination of orbit insertion initial conditions by numerically propagating Lagrange's Planetary Equations. (2) Each time history is fit, in the least squares sense, to a linear function. The standard deviation of the residuals for each fit is employed as the search parameter. (3) A three-dimensional surface plot of the standard deviation in eccentricity and the standard deviation in inclination versus eccentricity and inclination is produced for each value of periapse radius considered. (4) The three-dimensional surfaces are then reduced to two dimensions by plotting inclination versus eccentricity for the local maximums in standard deviation. GRA

N89-28539# Air Force Inst. of Tech., Wright-Patterson AFB, OH. School of Engineering.
ORBITS CONTAINING ARCS OF MINIMUM ALTITUDE VARIATION M.S. Thesis
Christina L. Cain Jun. 1989 123 p
(AD-A209206; AFIT/GA/ENY/89J-1) Avail: NTIS HC A06/MF A01 CSCL 22/3

This thesis identifies the mean orbital elements which produce arcs of minimum altitude variation over an oblate planet with an axi-symmetric gravitational field. Such orbits are useful for surveillance or scientific study missions using optics with fixed focal lengths. Both Earth and Mars are considered and the optimum eccentricity is found as a function of argument of periapsis and inclination for two values of semi-major axis for each planet. The

results are curve fitted to develop a single equation which identifies the eccentricity needed to produce an arc of minimum altitude variation given the argument of periapsis, inclination, semi-major axis, ellipticity of the planet, equatorial radius, and the zonal J2. Once arcs with minimum altitude variations are identified, the properties of the arcs are considered. The mid-latitude, altitude, duration, and latitude range of the arcs are found as a function of argument of periapsis and inclination for various planet and semi-major axis combinations. The secular change in mean orbital elements will determine the most stable orbits. Secular changes in orbital elements due to the geopotential, drag, and third body effects are considered. GRA

N89-28540# Air Force Inst. of Tech., Wright-Patterson AFB, OH. School of Engineering.
ORBIT DETERMINATION OF SUNLIGHT ILLUMINATED OBJECTS DETECTED BY OVERHEAD PLATFORMS M.S. Thesis
Richard P. Osedacz Jun. 1989 79 p
(AD-A209227; AFIT/GA/ENY/89J-3) Avail: NTIS HC A05/MF A01 CSCL 22/3

A technique for determining the orbital element set of a sunlight-illuminated object detected by an overhead platform (when passing through the sensor's field of view) is developed. The technique uses a Gauss orbit determination technique to find an initial target state estimate and then the estimate is refined via a batch weighted least squares estimation routine. A six element state vector consisting of three position and three velocity components describe the state at epoch. It was found that the Gaussian method produced reasonable initial orbits when the data bias was sufficiently zero. Each analyst-supplied slant range fit the data equally well, indicating that orbit determination is impossible with a single set of data. A unique series of events where the same object was tracked four consecutive days was fit using the developed algorithm, producing favorable results. The results of two single data set events and one multiple collection events are presented. GRA

14 GROUND SUPPORT SYSTEMS AND FACILITIES (SPACE)

Includes launch complexes, research and production facilities; ground support equipment, e.g., mobile transporters; and simulators.

For related information see also *09 Research and Support Facilities (Air).*

N89-28541*# Houston Univ., TX. Space Vacuum Epitaxy Center.
[PRIMARY RESEARCH EFFORTS ON EXPLORING THE COMMERCIAL POSSIBILITIES OF THIN FILM GROWTH AND MATERIALS PURIFICATION IN SPACE] Annual Report, 1987-1988
1989 16 p
(NASA-CR-184913; NAS 1.26:184913) Avail: NTIS HC A03/MF A01 CSCL 09B

The progress made on research programs in the 1987 to 1988 year is reported. The research is aimed at producing thin film semiconductors and superconductor materials in space. Sophisticated vacuum chambers and equipment were attained for the epitaxial thin film growth of semiconductors, metals and superconductors. In order to grow the best possible epitaxial films at the lowest possible temperatures on earth, materials are being isoelectronically doped during growth. It was found that isoelectrically doped film shows the highest mobility in comparison with films grown at optimal temperatures. Success was also attained in growing epitaxial films of InSb on sapphire which show promise for infrared sensitive devices in the III-V semiconductor system. E.R.

N89-28542# Los Alamos National Lab., NM.
PROTOTYPE TESTING FOR A HYBRID GAS-GUN/RAILGUN DEVICE
Jerald V. Parker 1989 20 p Presented at the 5th International Conference on Megagauss Magnetic Field Generation and Related Topics, Novosibirsk, USSR, 3-7 Jul. 1989
(Contract W-7405-eng-36)
(DE89-014294; LA-UR-89-2138; CONF-890710-11) Avail: NTIS HC A03/MF A01

In 1984 Los Alamos began the design of the Lethality Test System (LTS), a facility to be used for the study of impact physics at velocities up to 15 km/s. The key component of LTS was an electromagnetic launcher capable of accelerating a 30 gram mass to 15 km/s. By the time of the preliminary design review (July 1985) it was known from laboratory experiments that a conventional railgun was incapable of reaching 15 km/s starting at low velocity (approx. 1 km/s) and a hybrid design was adopted for the LTS launcher. The hybrid launcher consisted of a two-stage hydrogen gun that preaccelerated the test mass to 6.5 km/s and an electromagnetic launcher for the final acceleration from 6.5 to 15 km/s. Design calculations predicted that injection into the railgun at 6.5 km/s would reduce ablation sufficiently to permit operation at 12 km/s with reasonable probability of achieving 15 km/s. The hybrid launcher design adopted for LTS presents some unique mechanical and electrical issues. In particular, the hybrid design requires that the plasma armature be established in a high pressure gas environment behind the projectile. To address this issue, as well as to evaluate the mechanical and electrical design, an 1.83 meter long prototype of the electromagnetic launcher barrel was built and tested. This paper describes the prototype launcher tests and the performance achieved. In addition, testing of a plasma initiator operating in a high pressure gas environment is discussed. DOE

N89-28543# Sandia National Labs., Albuquerque, NM. Plasma Theory Div.
REGGIE RESULTS FOR THE NUNNALLY MASS LAUNCHER
John R. Freeman Jun. 1989 13 p
(Contract DE-AC04-76DP-00789)
(DE89-014377; SAND-89-0927) Avail: NTIS HC A03/MF A01

Preliminary analyses are presented for the Nunnally mass launcher. The Nunnally launcher is much like ones described in U.S. Patents 1,370,200; 1,421,435; and 1,422,427 which were issued to A.L.O. Fauchon-Villeplee in the period 1917 to 1922. A discussion of why a high conductivity projectile impulsively accelerated in a uniform transverse B-field does not experience a drag force, even for very large magnetic Reynolds numbers (R sub m = 10(2)-10(4) is also presented. DOE

N89-28544# Range Commanders Council, White Sands Missile Range, NM. Range Safety Group.
DESIGN, PERFORMANCE AND TEST STANDARDS FOR FLIGHT TERMINATION RECEIVER/DECODERS. VOLUME 1: DESIGN AND PERFORMANCE REQUIREMENTS Final Report
Jun. 1989 34 p
(AD-A209644; RCC/RSG-313-89-Vol-1) Avail: NTIS HC A03/MF A01 CSCL 20/14

This standard consists of three volumes: volume 1, Design and Performance Requirements, specifies the engineering design, performance and test standards: volume 2, Inspection and Test Methods; and volume 3, Automatic Test Procedures. Receiver/decoders submitted for acceptance which are intended for use in range safety applications shall, as a minimum, pass the tests and inspections specified. The receiver/decoders submitted for acceptance shall be compatible with existing range transmitting systems. Since specific missile systems and range requirements vary, this document should be used in conjunction with other related publications to develop a program test document for new systems. Any exceptions, deletions or additions to test requirements imposed by this document for new range safety receiver/decoders should be presented to the lead range for review and approval. GRA

N89-28545*# National Aeronautics and Space Administration. Lewis Research Center, Cleveland, OH.
DIGITALLY MODULATED BIT ERROR RATE MEASUREMENT SYSTEM FOR MICROWAVE COMPONENT EVALUATION
Mary Jo W. Shalkhauser and James M. Budinger Washington Jul. 1989 20 p
(NASA-TP-2912; E-4456; NAS 1.60:2912) Avail: NTIS HC A03/MF A01 CSCL 14B

The NASA Lewis Research Center has developed a unique capability for evaluation of the microwave components of a digital communication system. This digitally modulated bit-error-rate (BER) measurement system (DMBERMS) features a continuous data digital BER test set, a data processor, a serial minimum shift keying (SMSK) modem, noise generation, and computer automation. Application of the DMBERMS has provided useful information for the evaluation of existing microwave components and of design goals for future components. The design and applications of this system for digitally modulated BER measurements are discussed. Author

N89-28546*# National Aeronautics and Space Administration. Marshall Space Flight Center, Huntsville, AL.
O-RING GASKET TEST FIXTURE Patent Application
James Eric Turner, inventor (to NASA) and D. Scott McCluney, inventor (to NASA) 5 Jun. 1989 14 p
(NASA-Case-MFS-28376-1; NAS 1.71:MFS-28376-1; US-Patent-Appl-SN-361479) Avail: NTIS HC A03/MF A01 CSCL 14B

An apparatus is presented for testing O-ring gaskets under a variety of temperature, pressure, and dynamic loading conditions. Specifically, this apparatus has the ability to simulate a dynamic loading condition where the sealing surface in contact with the O-ring moves both away from and axially along the face of the O-ring. NASA

N89-28547*# National Aeronautics and Space Administration. Langley Research Center, Hampton, VA.
A TORSIONAL SUSPENSION SYSTEM FOR TESTING SPACE STRUCTURES Patent Application
Wilmer H. Reed, III, inventor (to NASA) and Ronald R. Gold, inventor (to NASA) (Dynamic Engineering, Inc., Newport News, VA.) 26 May 1989 12 p
(NASA-Case-LAR-14149-1-SB; NAS 1.71:LAR-14149-1-SB; US-Patent-Appl-SN-357757) Avail: NTIS HC A03/MF A01 CSCL 14B

A low frequency torsional suspension system for testing a space structure uses a plurality of suspension stations attached to the space structure along the length thereof in order to suspend the space structure from an overhead support. Each suspension station includes a disk pivotally mounted to the overhead support, and two cables which have upper ends connected to the disk and lower ends connected to the space structure. The two cables define a parallelogram with the center of gravity of the space structure being vertically beneath the pivot axis of the disk. The vertical distance between the points of attachment of the cables to the disk and the pivot axis of the disk is adjusted to lower the frequency of the suspension system to a level which does not interfere with frequency levels of the space structure, thereby enabling accurate measurement. NASA

N89-28548# Ballistic Research Labs., Aberdeen Proving Ground, MD.
PLASMA PROPERTIES OF A LARGE-BORE, ARC-ARMATURE RAILGUN
Keith A. Jamison, Henry S. Burden, and John D. Powell Jul. 1989 66 p
(AD-A209550; AD-E900860; BRL-TR-3014) Avail: NTIS HC A04/MF A01 CSCL 20/3

Diagnostic measurements on the plasma armature of the large-bore railgun, CHECMATE, have been made for four separate firings. These measurements include time-dependent values of the current, light output, and breech and muzzle voltages. In addition, signals obtained from B-dot data are used to infer the armature induction field, current-density profile, and arc length. The measured results are then employed in conjunction with a one-dimensional, steady-state model to calculate properties of the arc which cannot be measured directly. Among the quantities calculated are the armature mass and the temperature and ionization state as a function of position in the arc. As a result of this analysis, it is concluded that the armature remains nearly constant and that the arc temperature is somewhat lower than had been expected previously. Both these factors lend some credence to the use of plasma armatures for a wide variety of applications. GRA

N89-28549*# National Aeronautics and Space Administration. Lewis Research Center, Cleveland, OH.
FURNACE FOR TENSILE/FATIGUE TESTING Patent Application
Pamela K. Brindley, inventor (to NASA) 21 Jul. 1989 11 p
(NASA-Case-LEW-14848-1; NAS 1.71:LEW-14848-1; US-Patent-Appl-SN-382885) Avail: NTIS HC A03/MF A01 CSCL 14B

Mechanical properties of short test specimens are tested in tension and fatigue using an improved electrical resistance heating furnace having a short length that mounts between the grips of a typical testing machine. The furnace includes a ceramic inner liner having an oval cross-section to reduce heat loss at the ends. The furnace is divided into a plurality of individually controlled heating zones. Provision is made to supply an inert gas to the volume around the specimen in the center of the furnace. NASA

15 LAUNCH VEHICLES AND SPACE VEHICLES

Includes boosters; operating problems of launch/space vehicle systems; and reusable vehicles.

For related information see also *20 Spacecraft Propulsion and Power.*

N89-28550*# National Aeronautics and Space Administration. Langley Research Center, Hampton, VA.
NEAR-FIELD TESTING OF THE 15-METER HOOP-COLUMN ANTENNA
Lyle C. Schroeder, Richard R. Adams, M. C. Bailey, W. Keith Belvin, David H. Butler, and Thomas G. Campbell Aug. 1989 131 p
(NASA-TM-4073; L-16410; NAS 1.15:4073) Avail: NTIS HC A07/MF A01 CSCL 20N

A 15-m-diameter antenna was tested to verify that dimensional tolerances for acceptable performance could be achieved and to verify structural, electromagnetic, and mechanical performance predictions. This antenna utilized the hoop column structure, a gold plated molybdenum mesh reflector, and 96 control cables to adjust the reflector conformance with a paraboloid. The dimensional conformance of the antenna structure and surface was measured with metric camera and theodolites. Near field pattern data were used to assess the electromagnetic performance at five frequencies from 2.225 to 11.6 GHz. The reflector surface was adjusted to greatly improve electromagnetic performance with a finite element model and the surface measurements. Measurement results show that antenna surface figure and adjustments and electromagnetic patterns agree well with predictions. Author

N89-28551*# National Aeronautics and Space Administration. Marshall Space Flight Center, Huntsville, AL.
WIND MODELS FOR THE NSTS ASCENT TRAJECTORY BIASING FOR WIND LOAD ALLEVIATION
O. E. Smith, S. I. Adelfang, G. W. Batts, and C. K. Hill Aug. 1989 55 p
(NASA-TM-100375; NAS 1.15:100375) Avail: NTIS HC A04/MF A01 CSCL 22A

New concepts are presented for aerospace vehicle ascent wind profile biasing. The purpose for wind biasing the ascent trajectory is to provide ascent wind loads relief and thus decrease the probability for launch delays due to wind loads exceeding critical

limits. Wind biasing trajectories to the profile of monthly mean winds have been widely used for this purpose. The wind profile models presented give additional alternatives for wind biased trajectories. They are derived from the properties of the bivariate normal probability function using the available wind statistical parameters for the launch site. The analytical expressions are presented to permit generalizations. Specific examples are given to illustrate the procedures. The wind profile models can be used to establish the ascent trajectory steering commands to guide the vehicle through the first stage. For the National Space Transportation System (NSTS) program these steering commands are called I-loads. Author

16 SPACE TRANSPORTATION

Includes passenger and cargo space transportation, e.g., shuttle operations; and space rescue techniques.

For related information see also *03 Air Transportation and Safety* and *18 Spacecraft Design, Testing and Performance.* For space suits see *54 Man/System Technology and Life Support.*

N89-28529# Joint Publications Research Service, Arlington, VA.
BURAN FLIGHT TESTING, CAPABILITIES DISCUSSED
In its JPRS Report: Science and Technology. USSR Report: Life Sciences 15 Mar. 1989 p 36-37 Transl. into ENGLISH from Tass (Moscow, USSR) 1923 GMT, 25 Jan. 1989 (For primary document see N89-28527 23-12)
Avail: NTIS HC A05/MF A01

N89-28530# Joint Publications Research Service, Arlington, VA.
DESIGNERS' COMMENTARY ON BURAN FLIGHT CONTROL SYSTEM
G. Gromov *In its* JPRS Report: Science and Technology. USSR Report: Life Sciences 15 Mar. 1989 p 39-40 Transl. into ENGLISH from Pravda (Moscow, USSR), 6 Dec. 1988 p 3 (For primary document see N89-28527 23-12)
Avail: NTIS HC A05/MF A01

N89-28531# Joint Publications Research Service, Arlington, VA.
DEVELOPMENT, TESTING PROCEDURES FOR BURAN SHUTTLE
Andrey Tarasov *In its* JPRS Report: Science and Technology. USSR Report: Life Sciences 15 Mar. 1989 p 40-49 Transl. into ENGLISH from Pravda (Moscow, USSR), 2 Jan. 1989 p 4 (For primary document see N89-28527 23-12)
Avail: NTIS HC A05/MF A01

17 SPACE COMM., SPACECRAFT COMM., COMMAND & TRACKING

Includes telemetry; space communications networks; astronavigation and guidance; and radio blackout.

For related information see also *04 Aircraft Communications and Navigation* and *32 Communications and Radar.*

No abstracts in this category.

18 SPACECRAFT DESIGN, TESTING AND PERFORMANCE

Includes satellites; space platforms; space stations; spacecraft systems and components such as thermal and environmental controls; and attitude controls.

For life support systems see *54 Man/System Technology and Life Support.* For related information see also *05 Aircraft Design, Testing and Performance, 39 Structural Mechanics,* and *16 Space Transportation.*

N89-28552*# National Aeronautics and Space Administration. Lyndon B. Johnson Space Center, Houston, TX.
DOCKING MECHANISM FOR SPACECRAFT Patent Application
Gregory A. Lange, inventor (to NASA), John P. McManamen, inventor (to NASA), and John A. Schliesing, inventor (to NASA) 30 Dec. 1988 24 p
(NASA-Case-MSC-21386-1; NAS 1.71:MSC-21386-1; US-Patent-Appl-SN-292123) Avail: NTIS HC A03/MF A01 CSCL 22B

A system is presented for docking a space vehicle to a space station where a connecting tunnel for in-flight transfer of personnel is required. Cooperable coupling mechanisms include docking rings on the space vehicle and space station. The space station is provided with a tunnel structure, a retraction mechanism, and a docking ring. The vehicle coupling mechanism is designed to capture the station coupling mechanism, arrest relative spacecraft motions while limiting loads to acceptable levels, and then realign the spacecraft for final docking and tunnel interconnection. The docking ring of the space vehicle coupling mechanism is supported by linear attentuator actuator devices, each of which is controlled by a control system which receives loading information signals and attenuator stroke information signals from each device and supplies output signals for controlling its linear actuation to attenuate impact loading or to realign the spacecraft for final docking and tunnel interconnection. The retraction mechanism is used to draw the spacecraft together after initial contact and coupling. Tunnel trunnions, cooperative with the latches on the space vehicle constitute the primary structural tie between the spacecraft in final docked configuration. NASA

N89-28553* National Aeronautics and Space Administration. Lyndon B. Johnson Space Center, Houston, TX.
SPACE MODULE ASSEMBLY APPARATUS WITH DOCKING ALIGNMENT FLEXIBILITY AND RESTRAINT Patent
Willie D. Whitaker, inventor (to NASA) (McDonnell-Douglas Corp., Long Beach, CA.) 7 Mar. 1989 9 p Filed 8 Oct. 1987
(NASA-Case-MSC-21211-1; US-Patent-4,809,936; US-Patent-Appl-SN-105841; US-Patent-Class-244-161; US-Patent-Class-244-159; US-Patent-Class-403-51; US-Patent-Class-285-226) Avail: U.S. Patent and Trademark Office CSCL 22B

A berthing mechanism especially for use in berthing and compliant air-tight securing between manned space vehicle and modules is disclosed. The interface is provided by a pair of annular rings, one of which is typically, mechanically attached to the vehicle and the other to the module to which it is to be docked and secured. One of the two rings is attached to a base by resilient bellows. The facing surface of one annular ring is joined to a base by a cable laced through alternating pulleys attached circumferentially so that the interface surface of that ring may be tilted to accommodate angular misalignment as the annular rings are brought into docking (berthing) contact. Interleaving guide flanges with chambered sides provide at least some rotational mialignmnet correction. A plurality of electromechanical actuator/attenuator units provide means for extending one annular ring toward the other in the final stages of docking, for absorbing the initial docking shock and for drawing the annular rings into tight interface contact. Locking hooks provide for securing the interfaces.
Official Gazette of the U.S. Patent and Trademark Office

N89-28554*# National Aeronautics and Space Administration. Lyndon B. Johnson Space Center, Houston, TX.
EXPANDABLE PALLET FOR SPACE STATION INTERFACE ATTACHMENTS Patent
Clarence J. Wesselski, inventor (to NASA) 21 Feb. 1989 11 p Filed 21 Apr. 1988 Division of US-Patent-Appl-SN-929875, filed 13 Nov. 1986
(NASA-Case-MSC-21117-2; US-Patent-4,805,368; US-Patent-Appl-SN-184233; US-Patent-Appl-SN-929875; US-Patent-Class-52-573; US-Patent-Class-403-4; US-Patent-Class-403-30; US-Patent-Class-248-DIG-1; US-Patent-Class-52-648) Avail: U.S. Patent and Trademark Office CSCL 22B

A foldable expandable pallet having a basic square configuration is disclosed. Each pallet is comprised of a plurality of struts, joined together by node point fittings to make a rigid structure. Some of the struts have hinge fittings and are spring loaded to permit collapse of the module for stowage and transport to a space station. Dimensions of the pallet are selected to provide convenient, closely spaced attachment points between the relatively widely spaced trusses of a space station platform. A pallet is attached to a truss at four points; one close fitting hole; two oversize holes; and a slot; to allow for thermal expansion/contraction and for manufacturing tolerances. Applications of the pallet include its use in rotary or angular joints; servicing of splints; with gridded plates; as an instrument mounting bases; and as a roadbed for a Mobile Service Center (MSC).

Official Gazette of the U.S. Patent and Trademark Office

N89-28555# Los Alamos National Lab., NM.
RELIABILITY ESTIMATES FOR LARGE SATELLITE MEMORIES IN LOW EARTH ORBITS
E. P. Evans, S. B. Roeske, J. S. Browning, D. B. Holtkamp, and G. B. Stoddard (Dense-Pac Microsystems, Inc., Garden Grove, NM.) 1989 5 p Presented at the 26th Annual Conference on Nuclear and Space Radiation Effects, Marco Island, FL, 24-28 Jul. 1989
(Contract W-7405-eng-36)
(DE89-007764; LA-UR-89-489; CONF-890723-6) Avail: NTIS HC A02

Los Alamos and Sandia National Laboratories are building an ultrasoft X-ray space telescope experiment, designed to be flown on a cheap-sat. Reliability estimates for the combined total dose and single event environments are given for the onboard memories as large as 1 gigabit. DOE

N89-28556*# National Aeronautics and Space Administration. Marshall Space Flight Center, Huntsville, AL.
SPACECRAFT COMPONENT HEATER CONTROL SYSTEM Patent Application
Frederick D. Bachtel, inventor (to NASA) and James W. Owen, inventor (to NASA) 5 Jun. 1989 16 p
(NASA-Case-MFS-28327-1; NAS 1.71:MFS-28327-1; US-Patent-Appl-SN-361200) Avail: NTIS HC A03/MF A01 CSCL 22B

A heater control circuit is disclosed as being constructed in a single integrated circuit, with the integrated circuit conveniently mounted proximate to a spacecraft component requiring temperature control. Redundant heater controllers control power applied to strip heaters disposed to provide heat to a component responsive to sensed temperature from temperature sensors. Signals from these sensors are digitized and compared with a dead band temperature and set point temperature stored in memory to generate an error signal if the sensed temperature is outside the parameter stored in the memory. This error signal is utilized by a microprocessor to selectively instruct the heater controllers to apply power to the strip heaters. If necessary, the spacecraft central processor may access or interrogate the microprocessor in order to alter the set point temperature and dead band temperature range to obtain operational data relating to the operation of an integrated circuit for relaying to the ground control, or to switch off faulty components. NASA

N89-28557# Naval Postgraduate School, Monterey, CA.
CONSIDERATION OF GRAVITY GRADIENT STABILIZATION FOR ORION M.S. Thesis
Frank W. Boyd Mar. 1989 98 p
(AD-A207845) Avail: NTIS HC A05/MF A01 CSCL 22/2

Certain ORION missions may require three axis stabilization. Since ORION's physical size severely limits its onboard fuel storage capability, passive stabilization techniques warrant investigation. The development of linearized equations of motion and regions of stability are shown with respect to gravity gradient stabilization. Gravity gradient stabilization by itself provides little yaw restoring torque; therefore, additional torque generating devices are necessary to augment the gravity gradient effect. Control moment gyros, reaction wheels, and magnetic torquers are investigated as to their suitability for ORION. GRA

N89-28558# Naval Postgraduate School, Monterey, CA.
ACTIVE DAMPING OF VIBRATION IN LARGE SPACE STRUCTURES USING A KARHUNEN-LOEVE REDUCED ORDER MODEL M.S. Thesis
Terence M. Grogan Mar. 1989 72 p
(AD-A208183) Avail: NTIS HC A04/MF A01 CSCL 22/2

Large space structures are difficult to control because of the high order of their mathematical models. The high order mathematical model makes the use of a reduced order model to control the structure desirable. The Karhunen-Loeve expansion along with Galerkin's method is used to generate a reduced order model. A control algorithm is achieved by applying linear quadratic regulator theory to the reduced order model. The Karhunen-Loeve basis functions or mode shapes must first be found to identify the reduced order model. Previous results have shown that in the limit as the structural damping approaches zero the Karhunen-Loeve mode shapes and natural mode shapes converge. Numerical techniques are applied to evaluate the structural damping required for convergence. Once the Karhunen-Loeve mode shapes are determined, the reduced order control model is applied to the full order system. The performance of various Karhunen-Loeve models is compared by measuring the modal energies in the controlled and uncontrolled modes. GRA

N89-28559# Naval Postgraduate School, Monterey, CA.
DESIGN OF A RELIABLE COMPUTING SYSTEM FOR THE PETITE AMATEUR NAVY SATELLITE (PANSAT) M.S. Thesis
James K. Hiser Mar. 1989 96 p
(AD-A208194) Avail: NTIS HC A05/MF A01 CSCL 12/7

This thesis proposes a processor design for the Petite Amateur Navy Satellite (PANSAT). The missions of PANSAT are considered. It compares the design of three previous satellites with similar missions and determines the processor functions required to support PANSAT missions. Particular attention is given to the store and forward message system. A reliable processor design that implements these functions is developed. The reliability of the proposed design is examined. Minimum software requirements for the resulting design are listed. GRA

N89-28560# Naples Univ. (Italy). Istituto di Aerodinamica.
PHYSICAL PHENOMENOLOGY AND MATHEMATICAL MODELS OF HYPERSONIC MOTION Ph.D. Thesis [FENOMENOLOGIA FISICA E MODELLISTICA MATEMATICA DEI MOTI IPERSONICI]
Raffaele Savino 1988 161 p In ITALIAN
(ETN-89-95201) Avail: NTIS HC A08/MF A01

The hypersonic reentry problem is analyzed in relation to the Hermes vehicle design. The equilibrium properties of the high atmosphere and the molecular energy distribution are discussed. A mathematical description of the aerothermodynamic flow is presented. A multi zone approach is used, solving, independently, the Euler or Navier-Stokes flow equations of the different flow regions. The illustrations give detailed results concerning aerothermodynamic characteristics and reentry parameters. ESA

N89-28561# Messerschmitt-Boelkow-Blohm G.m.b.H., Bremen (Germany, F.R.).
KEY STRUCTURES MECHANICAL ISSUES OF THE EUROPEAN SPACE STATION AND PLATFORM PROGRAM COLUMBUS
S. Gazey and E. Winkelhoff 1988 10 p Presented at the Spacecraft Structures and Mechanical Testing Conference, Noordwijk, Netherlands, 19-21 Oct. 1988
(MBB-UD-0041-88-PUB; OTN-010456; ETN-89-95334) Avail: NTIS HC A02/MF A01

The main technical features of the Columbus space segment are discussed. The attached pressurized module (APM), integrated into NASA's Space Station Freedom; the man tended free flyer (MTFF) - Europe's first step into autonomy in space; and the polar platform (PPF), are described. The requirements for long life in orbit operation are considered: more realistic APM design loads must be determined to define maximum allowable launch mass; Columbus flight configuration responses to in-orbit operation loads must be determined by advanced nonlinear analysis tools; protection of the crew and subsystems against meteoroids and space debris are necessary, as well as analytical tools and test facilities to verify the required probability of nonpenetration of the modules; and repair procedures and maintenance tools have to be developed to ensure in-orbit structural integrity. ESA

N89-28528# Joint Publications Research Service, Arlington, VA.
THE ORBITAL SPACE OBSERVATORY GAMMA
V. G. Kirillov-Ugryumov *In its* JPRS Report: Science and Technology. USSR Report: Life Sciences 15 Mar. 1989 p 14-23 Transl. into ENGLISH from Zemlya i Vselennaya (Moscow, USSR), no. 5, Sep.-Oct. 1988 p 5-13 (For primary document see N89-28527 23-12)
Avail: NTIS HC A05/MF A01

19 SPACECRAFT INSTRUMENTATION

For related information see also *06 Aircraft Instrumentation* and *35 Instrumentation and Photography.*

N89-28562*# Texas A&M Univ., College Station.
INTELLIGENT MULTI-SENSOR INTEGRATIONS Final Report
Richard A. Volz, Ramesh Jain, and Terry Weymouth 3 Aug. 1989 32 p
(Contract NAG2-350; JPL-958086)
(NASA-CR-185846; NAS 1.26:185846) Avail: NTIS HC A03/MF A01 CSCL 14B

Growth in the intelligence of space systems requires the use and integration of data from multiple sensors. Generic tools are being developed for extracting and integrating information obtained from multiple sources. The full spectrum is addressed for issues ranging from data acquisition, to characterization of sensor data, to adaptive systems for utilizing the data. In particular, there are three major aspects to the project, multisensor processing, an adaptive approach to object recognition, and distributed sensor system integration. Author

N89-28563# Sira Inst. Ltd., Chislehurst (England).
A MEDIUM RESOLUTION IMAGING SPECTROMETER FOR THE EUROPEAN POLAR ORBITING PLATFORM
M. A. Cutter, D. R. Lobb, Y. Ramon, G. Ratier, and J. L. Bezy (European Space Agency. European Space Research and Technology Center, ESTEC, Noordwijk, Netherlands) 1989 10 p
(ETN-89-95235) Avail: NTIS HC A02/MF A01

The design for the Medium Resolution Imaging Spectrometer (MERIS), proposed as a candidate core instrument for the European polar platform scheduled for launch in 1997, is described. The instrument has a spectral range of 400 to 1050 nm, a swath width of 1500 km, spectral resolution of 1.25 nm, and spatial resolution of 260 m. Spectral bands, and spectral and spatial resolution, can be reprogrammed in orbit. The instrument has applications in the fields of marine, land and atmospheric research. MERIS provides high radiometric performance at medium spatial resolution, which is appropriate primarily for oceanographic measurements. The instrument also offers the capability of monitoring high albedo targets which are of value in remote sensing of ice, land and coastal regions. ESA

N89-28564# Messerschmitt-Boelkow-Blohm G.m.b.H., Ottobrunn (Germany, F.R.).
PROPOSED CONCEPTS FOR A ADVANCED OPTICAL PAYLOAD FOR SECOND GENERATION METEOSAT
B. Kunkel, F. Blechinger, J. L. Bezy, G. Ratier, D. R. Lobb, M. A. Cutter, E. Hettlage, E. OMongain, A. F. J. Morgownik, and B. C. Taylor (British Aerospace Public Ltd. Co., Bristol, England) 1989 15 p
(ETN-89-95236) Avail: NTIS HC A03/MF A01

The technical concepts of a visible/infrared imaging radiometer and an infrared vertical sounder (payloads of the Meteosat second generation) are described. All instruments are assumed to be operated on a 3-axis stabilized satellite, while the current system is a spin stabilized satellite. The imaging radiometer has 2 visible and 6 infrared channels for cloud tracking and sea surface/cloud top temperature measurements (compared to currently 3), partly split channels at reduced bandwith and 2 km instantaneous field-of-view (angular resolution). The proposed solution of a hybrid scan system, involving 2-axis mechanical scan combined with a north/south fine scan (by means of short detector arrays), is presented. The infrared sounder is required to scan the Earth disc in 16 km instantaneous field-of-view (angular resolution) intervals and 18 channels for water vapor and temperature profiling. The proposed technical concept uses a spectrometer for spectral channel multiplexing rather than a filter wheel as the standard principle for such instruments. It is also foreseen for the GOES-Next. Both instruments provide promising performance data. Imager can be used in the fields of oceanography, vegetation mapping, radiation budget determination for climatology and environmental monitoring. ESA

20 SPACECRAFT PROPULSION AND POWER

Includes main propulsion systems and components, e.g., rocket engines; and spacecraft auxilliary power sources.

For related information see also *07 Aircraft Propulsion and Power, 28 Propellants and Fuels, 44 Energy Production and Conversion,* and *15 Launch Vehicles and Space Vehicles.*

N89-28565*# National Academy of Sciences - National Research Council, Washington, DC.
ADVANCED POWER SOURCES FOR SPACE MISSIONS
Joseph G. Gavin, Jr., Tommy R. Burkes, Robert E. English, Nicholas J. Grant, Gerald L. Kulcinski, Jerome P. Mullin, K. Lee Peddicord, Carolyn K. Purvis, W. James Sarjeant, and J. Pace Vandevender (Sandia National Labs., Albuquerque, NM.) et al Washington NAS-NRC 1989 152 p
(Contract F49620-85-C-107)
(NASA-TM-101811; NAS 1.15:101811; LC-88-63907; ISBN-0-309-03999-1) Copyright Avail: NTIS HC A08/MF A01 CSCL 10B

Approaches to satisfying the power requirements of space-based Strategic Defense Initiative (SDI) missions are studied. The power requirements for non-SDI military space missions and for civil space missions of the National Aeronautics and Space Administration (NASA) are also considered. The more demanding SDI power requirements appear to encompass many, if not all, of the power requirements for those missions. Study results indicate that practical fulfillment of SDI requirements will necessitate substantial advances in the state of the art of power technology. SDI goals include the capability to operate space-based beam weapons, sometimes referred to as directed-energy weapons. Such weapons pose unprecedented power requirements, both during preparation for battle and during battle conditions. The power

regimes for these two sets of applications are referred to as alert mode and burst mode, respectively. Alert-mode power requirements are presently stated to range from about 100 kW to a few megawatts for cumulative durations of about a year or more. Burst-mode power requirements are roughly estimated to range from tens to hundreds of megawatts for durations of a few hundred to a few thousand seconds. There are two likely energy sources, chemical and nuclear, for powering SDI directed-energy weapons during the alert and burst modes. The choice between chemical and nuclear space power systems depends in large part on the total duration during which power must be provided. Complete study findings, conclusions, and eight recommendations are reported. Author

N89-28566*# Morton Thiokol, Brigham City, UT. Space Div.
IGNITER HEATER EMI TRANSIENT TEST Final Report
M. Cook 9 Jun. 1989 16 p
(Contract NAS8-30490)
(NASA-CR-183743; NAS 1.26:183743; TWR-18915) Avail: NTIS HC A03/MF A01 CSCL 21H

Testing to evaluate Redesigned Solid Rocket Motor igniter heater electromagnetic interference (EMI) effects on the Safe and Arm (S and A) device was completed. It was suspected that EMI generated by the igniter heater and its associated electromechanical relay could cause a premature firing of the NASA Standard Initiators (NSIs) inside the S and A. The maximum voltage induced into the NSI fire lines was 1/4 of the NASA specified no-fire limit of one volt (SKB 26100066). As a result, the igniter heaters are not expected to have any adverse EMI effects on the NSIs. The results did show, however, that power switching causes occasional high transients within the igniter heater power cable. These transients could affect the sensitive equipment inside the forward skirt. It is therefore recommended that the electromechanical igniter heater relays be replaced with zero crossing solid state relays. If the solid state relays are installed, it is also recommended that they be tested for EMI transient effects. Author

N89-28567*# Thiokol Corp., Brigham City, UT. Space Operations.
TECHNICAL EVALUATION MOTOR 3 (TEM-3) Final Test Report
Diane Garecht Jul. 1989 227 p
(Contract NAS8-30490)
(NASA-CR-183740; NAS 1.26:183740; TWR-17639; DR-5-3; WBS-HQ601-20-10; ECS-SS-1858) Avail: NTIS HC A11/MF A01 CSCL 21H

A primary objective of the technical evaluation motor program is to recover the case, igniter and nozzle hardware for use on the redesigned solid rocket motor flight program. Two qualification objectives were addressed and met on TEM-3. The Nylok thread locking device of the 1U100269-03 leak check port plug and the 1U52295-04 safe and arm utilizing Krytox grease on the barrier-booster shaft O-rings were both certified. All inspection and instrumentation data indicate that the TEM-3 static test firing conducted 23 May 1989 was successful. The test was conducted at ambient conditions with the exception of the field joints (set point of 121 F, with a minimum of 87 F at the sensors), igniter joint (set point at 122 F with a minimum of 87 F at sensors) and case-to-nozzle joint (set point at 114 F with a minimum of 87 F at sensors). Ballistics performance values were within specification requirements. Nozzle performance was nominal with typical erosion. The nozzle and the case joint temperatures were maintained at the heaters controlling set points while electrical power was supplied. The water and the CO2 quench systems prevented damage to the metal hardware. All other test equipment performed as planned, contributing to a successful motor firing. All indications are that the test was a success, and all expected hardware will be refurbished for the RSRM program. Author

N89-28568*# National Aeronautics and Space Administration. Marshall Space Flight Center, Huntsville, AL.
STATIC AND DYNAMIC DEFLECTION STUDIES OF THE SRM AFT CASE-NOZZLE JOINT
David C. Christian, Lawrence D. Kos, and Isaias Torres Aug. 1989 37 p
(NASA-TM-100373; NAS 1.15:100373) Avail: NTIS HC A03/MF A01 CSCL 21H

The redesign of the joints on the solid rocket motor (SRM) has prompted the need for analyzing the behavior of the joints using several different types of analyses. The types of analyses performed include modal analysis, static analysis, transient response analysis, and base driving response analysis. The forces used in these analyses to drive the mathematical model include SRM internal chamber pressure, nozzle blowout and side forces, shuttle vehicle lift-off dynamics, SRM pressure transient rise curve, gimbal forces and moments, actuator gimbal loads, and vertical and radial bolt preloads. The math model represented the SRM from the aft base tangent point (1,823.95 in) all the way back to the nozzle, where a simplified, tuned nozzle model was attached. The new design used the radial bolts as an additional feature to reduce the gap opening at the aft dome/nozzle fixed housing interface. Author

N89-28569# Pisa Univ. (Italy). Facolta di Ingegneria.
ANALYSIS OF THE REGENERATIVE COOLING OF A ROCKET MOTOR FED WITH MONOMETHYLHYDRAZINE AND NITROGEN TETROXIDE Ph.D. Thesis [ANALISI SUL RAFFREDDAMENTO RIGENERATIVO DI UN MOTORE A RAZZO ALIMENTATO CON MONOMETILIDRAZINA E TETROSSIDO DI AZOTO]
Niccola Kutufa 1988 224 p In ITALIAN
(ETN-89-94976) Avail: NTIS HC A10/MF A01

The thermal exchange, gas side and total, of a rocket motor using regenerative cooling is studied. The combustion and dissociation chemical reactions are characterized. The NASA calculation program Gordon McBride was employed to identify the transport and thermodynamic properties of the combustion products. Motor configurations are studied and the global thermal flow is determined. The geometrical parameters of the cooling channels and its thermodynamical constraints are identified. ESA

N89-28570*# National Aeronautics and Space Administration. Lewis Research Center, Cleveland, OH.
EVOLUTIONARY GROWTH FOR SPACE STATION FREEDOM ELECTRICAL POWER SYSTEM
Matthew F. Marshall, Kerry L. McLallin, and Michael J. Zernic 1989 8 p Presented at the 24th Intersociety Energy Conversion Engineering Conference, Washington, DC, 6-11 Aug. 1989; cosponsored by IEEE, AIAA, ANS, ASME, SAE, ACS, and AIChE
(NASA-TM-102339; E-5047; NAS 1.15:102339) Avail: NTIS HC A02/MF A01 CSCL 22B

Over an operational lifetime of at least 30 yr, Space Station Freedom will encounter increased space station user requirements and advancing technologies. The space station electrical power system is designed with the flexibility to accommodate these emerging technologies and expert systems and is being designed with the necessary software hooks and hardware scars to accommodate increased growth demand. The electrical power system is planned to grow from the initial 75 kW up to 300 kW. The Phase 1 station will utilize photovoltaic arrays to produce the electrical power; however, for growth to 300 kW, solar dynamic power modules will be utilized. Pairs of 25 kW solar dynamic power modules will be added to the station to reach the power growth level. The addition of solar dynamic power in the growth phase places constraints in the initial space station systems such as guidance navigation and control, external thermal, truss structural stiffness, computational capabilities and storage which must be planned-in in order to facilitate the addition of the solar dynamic modules. Author

N89-28571*# National Aeronautics and Space Administration. Lewis Research Center, Cleveland, OH.
ION OPTICS FOR HIGH POWER 50-cm-DIAM ION THRUSTERS
Vincent K. Rawlin and Marc G. Millis Sep. 1989 23 p Presented at the 25th Joint Propulsion Conference, Monterey, CA, 10-12 Jul. 1989; cosponsored by AIAA, ASME, SAE, and ASEE Previously announced in IAA as A89-47040
(NASA-TM-102143; E-4938; NAS 1.15:102143; AIAA-89-2717)
Avail: NTIS HC A03/MF A01 CSCL 21C

The process used at the NASA-Lewis to fabricate 30 and 50-cm-diameter ion optics is described. The ion extraction capabilities of the 30 and 50-cm diameter ion optics were evaluated on divergent field and ring-cusp discharge chambers and compared. Perveance was found to be sensitive to the effects of the type and power of the discharge chamber and to the accelerator electrode hole diameter. Levels of up to 0.64 N and 20 kW for thrust and input power, respectively, were demonstrated with the divergent-field discharge chamber. Thruster efficiencies and specific impulse values up to 79 percent and 5000 sec., respectively, were achieved with the ring-cusp discharge chamber. E.R.

23 CHEMISTRY AND MATERIALS (GENERAL)

N89-28572# Computer Sciences Corp., Research Triangle Park, NC.
MATERIALS AEROMETRIC DATABASE FOR USE IN DEVELOPING MATERIALS DAMAGE FUNCTIONS
Ruen-Tai Tang, P. Michael Barlow, and Paul Waldruff Apr. 1989 29 p
(Contract EPA-68-01-7365)
(PB89-181259; EPA/600/3-89/031) Avail: NTIS HC A03/MF A01 CSCL 07D

Meteorological and air quality data acquired at field exposure sites were accessed into the Materials Aerometric Database (MAD). The National Acid Precipitation Assessment Program (NAPAP) will use the MAD to develop damage functions for materials exposed at the sites; these functions then will be used in preparing NAPAP integrated assessment reports to Congress. The MAD data cover as many as six and a half years at five materials exposure sites in the eastern United States. Conservative techniques based on secondary-site data, regression predictions, and other information were applied to the MAD to enhance the quality and usability of the database. Author

24 COMPOSITE MATERIALS

Includes physical, chemical, and mechanical properties of laminates and other composite materials.
For ceramic materials see *27 Nonmetallic Materials*.

N89-28573# Rockwell International Corp., Golden, CO.
A COMPREHENSIVE GUIDE TO THE LITERATURE ON ACOUSTIC EMISSION FROM COMPOSITES, SUPPLEMENT 2
Thomas F. Drouillard 25 Apr. 1989 22 p Presented at the 3rd International Symposium on Acoustic Emission From Reinforced Composites, Paris, France, 17-21 Jul. 1989 Submitted for publication
(Contract DE-AC04-76DP-03533)
(DE89-013524; RFP-4297-Supp-2; CONF-890789-1-Supp-2)
Avail: NTIS HC A03/MF A01

Comprehensive bibliographies on the subject of Acoustic Emission (AE) from composites were compiled for the First and Second International Symposiums on Acoustic Emission from Reinforced Composites. The current bibliography is the third in the series. It presents 212 references of new material. The material is presented in the same format as previously used, which consists of a bibliographic section, an author index, and a subject index. Although not all-inclusive, this series of bibliographies presents a compilation of the bulk of world literature published on the subject of acoustic emission from composites. DOE

N89-28574# Naval Postgraduate School, Monterey, CA. Dept. of Mechanical Engineering.
COMPOSITE MATERIAL REPAIR AND RELIABILITY M.S. Thesis
Shmuel Maman Mar. 1989 160 p
(AD-A209150) Avail: NTIS HC A08/MF A01 CSCL 11/4

Composite structure repair methodology has been developed to specific applications (typically in small area and limited to secondary structure) and is being extended to Large Area Composite Structure Repair (with target extension to primary structures). Therefore, the repair becomes more critical because we get redistribution of stresses that can also affect the zones outside of the repair area. For this reason, an analytic evaluation of the repair's reliability has to be performed to define a parameter which reflects on the effectiveness of the repair. In this work, we establish a principal guideline to evaluate the redundancy and compare the reliability of the repair to the reliability of the parent structure (i.e., the structure in the undamaged state). The approach adopted is to utilize structural finite element analysis to compute the state and of the candidate repaired state. The reliability of these two spatially non-uniform stresses is computed by a probabilistic failure criterion. Thus, we can optimize the repair configuration by varying the strength and the stiffness of any element in the repair site by varying the lamination angles, and selectively using hybrid materials. GRA

N89-28575# Massachusetts Inst. of Tech., Cambridge. Dept. of Civil Engineering.
OPTIMUM DESIGN METHODS FOR STRUCTURAL SANDWICH PANELS Final Technical Report, 1 Jan. - 31 Dec. 1988
Lorna J. Gibson Feb. 1989 68 p
(Contract DAAL03-87-K-0005)
(AD-A209427; ARO-24620.18-EG-UIR) Avail: NTIS HC A04/MF A01 CSCL 13/3

A software program is presented for the optimum design of sandwich panels. This program calculates the minimum weight design of sandwich beams and plates subject to stiffness and/or strength constraints. The program was designed to run on an IBM PC compatible computer. The analysis performed by the program is described together with a complete listing of program. The program is available on diskette. GRA

N89-28576# Connecticut Univ., Storrs. Inst. of Materials Science.
A NEW METHOD FOR MONITORING CURE AND MOBILITY IN EPOXY MATRIX AND FIBER/EPOXY INTERPHASES Final Report
C. S. P. Sung 28 Mar. 1989 3 p
(Contract DAAG29-85-K-0055)
(AD-A209428; ARO-22303.8-MS) Avail: NTIS HC A02/MF A01 CSCL 11/9

The objective of this contract was to develop a new method based on reactive labelling technique for monitoring cure and mobility in epoxy matrix and fiber/epoxy interphases. These reactive labels were chosen to exhibit spectral changes in the region of UV-visible and fluorescence spectra where the polymerizing matrix has little absorption or emission. In this method, advantage was taken of the magnified effects of the substituent changes in the para and para (prime) positions of conjugated aromatic reactive labels on the UV-visible and fluorescence spectra. This method was applied to characterize the kinetics and mechanisms of the cure in epoxy networks and in polyurethanes, the imidization process in polyimides, and the acylation in polyamides. One particular advantage of this method is that one can often distinguish between several cure species in some polymers. This advantage makes it possible to follow cure composition throughout the cure process and to analyze the kinetics and the mechanisms of several consecutive polymerization steps in some polymers. GRA

N89-28577# Ohio State Univ., Columbus. Dept. of Metallurgical Engineering and Materials Science.
EXPLANATORY RESEARCH ON THE PROTECTION OF CARBON-CARBON COMPOSITES AGAINST OXIDATION AT VERY HIGH TEMPERATURES (GREATER THAN 3000 F) WITH ENGEL-BREWER AND OTHER INTERMETALLIC COMPOUNDS Final Report
George StPierre Jun. 1988 205 p
(Contract N00014-86-K-0130; RF7-65208)
(AD-A207907) Avail: NTIS HC A10/MF A01 CSCL 11/3

Iridium-based coatings have been proposed for the protection of carbon/carbon composites against oxidation at temperatures greater than 1600 C. However, Ir exposed to an oxidizing atmosphere at such high temperatures reacts with oxygen to form volatile oxides. Alloying Ir with a reactive element that forms a protective scale was proposed as a method to prevent the evaporation of Iridium base coatings. Hafnium and Zr were suggested as possible alloying elements. Investigations of the Ir-Hf and the Pt-Zr systems, however, have shown that Hf and Zr are only moderately protective. In both systems the reactive element, Hf and Zr, did not form a highly protective oxide scale. Aluminum is another possible alloying addition for the prevention of evaporation of the noble metal suboxides. Samples of C/C composite would be coated with HfC and then a layer of Iridium would be applied. It was demonstrated that an adherent layer of Ir3Hf can be grown between these coatings. The surface of the Ir would be impregnated with Al and Cr. GRA

N89-28578# Ceramic Process Systems Corp., Cambridge, MA.
HIGHLY ORIENTED FIBER REINFORCED CERAMIC COMPOSITES Final Report, 1 Aug. 1988 - 31 Jan. 1989
Ran-Rong Lee, James D. Hodge, Wen-Cheng J. Wei, John Halloran, and Frances Schutzberg 31 Mar. 1989 79 p
(Contract F49620-88-C-0104; AF Proj. 3005)
(AD-A208119; CPS-89-004; AFOSR-89-0531TR) Avail: NTIS HC A05/MF A01 CSCL 11/4

Highly dense SiC-AlN alloys having unique microstructures and a fracture toughness up to 6 MPam 1/2 were successfully produced by pressureless sintering of commercially available SiC and AlN powders. Appropriate sintering aids, sintering temperatures, sintering period and sintering conditions were identified. The sintered SiC-AlN alloys can achieve a single phase solid solution after an appropriate thermal treatment. The lattice constants of the solid solution varied linearly with SiC/AlN ratio. Optimized annealing yielded decomposition of the solid solution and formed a unique microstructure, which was composed of equiaxed grains with modulated features, heavily faulted elongated grains and very clean grain boundaries. GRA

N89-28579*# National Aeronautics and Space Administration. Langley Research Center, Hampton, VA.
FIVE YEAR GROUND EXPOSURE OF COMPOSITE MATERIALS USED ON THE BELL MODEL 206L FLIGHT SERVICE EVALUATION
Donald J. Baker (Army Aviation Research and Development Command, Hampton, VA.) Jul. 1989 93 p
(NASA-TM-101645; NAS 1.15:101645; AVSCOM-TM-89-B-007)
Avail: NTIS HC A05/MF A01 CSCL 11D

Part of the results of a U.S. Army/NASA-Langley sponsored research program to establish the long term-term effects of realistic ground based exposure on advanced composite materials is presented. Residual strengths and moisture absorption as a function of exposure time and exposure location are reported for four different composite material systems that were exposed for five years on the North American Continent. Author

N89-28580# Aeronautical Research Labs., Melbourne (Australia).
ANALYSIS AND REPAIR OF IMPACT DAMAGED COMPOSITES
J. Paul and R. Jones Jan. 1989 44 p
(ARL-Struct-R-435; AR-005-570) Copyright Avail: NTIS HC A03/MF A01

The repair of impact damaged graphite/epoxy composite laminates is discussed. The behavior of delamination damage under both uniaxial and biaxial compressive loading is examined and the predictive capabilities of several fracture parameters are investigated. Based upon the results of this analysis a simple repair methodology is proposed and compared with experimental test results. Author

N89-28581 Staatliches Forschungsinstitut fuer Geochemie, Bamberg (Germany, F.R.).
DETERMINATION OF MOISTURE DIFFUSION IN CARBON FIBER REINFORCED EPOXY COMPOSITES BY MEANS OF RADIOISOTOPE TRACER TECHNIQUE Final Report, Feb. 1984
H. Meier, D. Boesche, G. Zeitler, W. Hecker, E. Zimmerhackl, and W. Albrecht Feb. 1984 123 p In GERMAN; ENGLISH summary
(Contract BMVg-T/RF52/80025/81524)
(BMVg-FBWT-88-2; BMVg-RUFO-5(ALT); ETN-89-94412)
Copyright Avail: Dokumentations- und Fachinformationzentrum der Bundeswehr, Friedrich-Ebert-Allee 34, 5300 Bonn 1, Fed. Republic of Germany, 60 DM

Moisture diffusion into graphite-epoxy composites is studied using a radiotracer technique. Diffusion parameters and maximum moisture content of the carbon fiber reinforced plastic samples are measured. Tritiated water tracer, profile sectioning technique and liquid scintillation counting are applied. The diffusion coefficients, activation energies and frequency factors are determined for the composites fibredux 913C and 914C and fiberite 1076, as well as the maximum moisture content for different relative humidities and absorption constants. The results can be used to calculate moisture absorption/desorption curves, as a function of time, for various relative humidities and temperatures. General rules for diffusion and moisture absorption of both composites are deduced. Neutron induced autoradiography measurements show a high concentration of diffused water at the carbon fiber-resin interface. ESA

N89-28582# Paris VI Univ. (France). Lab. d'Acoustique et Mecanique.
COMPOSITE DAMAGING: METHODOLOGICAL APPROACH Final Report [ENDOMMAGEMENT DES COMPOSITES: APPROCHE METHODOLOGIQUE]
H. Dumontet, A. Guiraud, A. Thionnet, and Y. Xu Sep. 1988 100 p In FRENCH Prepared in cooperation with Aerospatiale Usines de Toulouse, France
(Contract DRET-87-34-325-00-470-7501)
(ETN-89-94866) Avail: NTIS HC A05/MF A01

A calculation method for constraints is presented, based on a two scale asymptotic development technique associated to a boundary layer theory and expressed in terms of displacement. The numerical implementation and algorithms are described. The results of computerized simulations are detailed for carbon-epoxy specimens with varying plys and orientation. The influence of structural factors on the results are discussed. ESA

N89-28583 National Physical Lab., Teddington (England). Div. of Materials Applications.
MEASUREMENT OF MODE 1 AND MODE 2 STRAIN ENERGY RELEASE RATES: A VAMAS ROUND ROBIN PROJECT ON DELAMINATION OF COMPOSITE MATERIALS
M. W. Money Mar. 1989 78 p
(NPL-DMA(A)-178; ISSN-0143-7313; ETN-89-95146) Copyright Avail: National Physical Laboratory, Teddington, Middlesex, TW11 0LW, United Kingdom

The study of delamination in composite materials, performed at the National Physical Laboratory to determine G sub C values for a variety of test geometries in fracture modes 1 and 2 is reported. Materials studied include aligned carbon fiber/epoxy, aligned glass fiber/epoxy and woven glass fiber/epoxy. The glass reinforced materials are considered in both 3 mm and 20 mm thickness. The test methods and the different analytical techniques used to evaluate the fracture parameter are discussed. ESA

N89-28584 National Physical Lab., Teddington (England). Div. of Materials Applications.
A SUMMARY OF THE UK RESULTS FOR A VAMAS ROUND ROBIN PROJECT ON DELAMINATION OF COMPOSITE MATERIALS
M. W. Money Apr. 1989 27 p
(NPL-DMA(A)-179; ISSN-0143-7313; ETN-89-95255) Copyright Avail: National Physical Laboratory, Teddington, Middlesex, TW11 0LW, United Kingdom

The study of delamination in composite materials (especially the contributions made by the British participants in this program) is reported. Values of G(C) (compliance geometry) were determined for a variety of test geometries in fracture modes 1 and 2. Materials studied included aligned carbon fiber/epoxy, aligned glass fiber/epoxy and woven glass fiber/epoxy. The glass reinforced materials are considered in 3 mm and 20 mm thickness. The experimental results show that the values of G(C)1 are greater than G(C)2 for both materials; that for mode 1 and mode 2 the thicker glass fiber/epoxy samples have lower values of the fracture parameter than thin specimens (G(C) value is greater for the woven glass fiber/epoxy than for the aligned glass fiber/epoxy); and that G(C)1 and G(C)2 for the carbon fiber/epoxy is lower than for the glass fiber/epoxy material. ESA

N89-28585 National Physical Lab., Teddington (England). Div. of Materials Applications.
A VAMAS ROUND ROBIN ON FATIGUE TEST METHODS FOR POLYMER MATRIX COMPOSITES. PART 1: TENSILE AND FLEXURAL TESTS OF UNIDIRECTIONAL MATERIAL
G. D. Sims Apr. 1989 51 p
(NPL-DMA(A)-180-Pt-1; ISSN-0143-7313; ETN-89-95256) Copyright Avail: National Physical Laboratory, Teddington, Middlesex, TW11 0LW, United Kingdom

A program on tensile and flexural fatigue test methods for advanced polymer matrix composites is outlined. The initial survey of test methods in use, the results of the pre-program and the development of the full program are also discussed. The particular requirements of fatigue tests for high volume fraction polymer matrix composites are outlined. Strong interest is expressed in further aspects including multi-directional specimens, compression testing and fully reversed loading. The concentration of the current program on the test geometry and specimen geometry reflects the incomplete development of static versions of these test methods. ESA

N89-28586*# National Aeronautics and Space Administration. Langley Research Center, Hampton, VA.
DELAMINATION TEST APPARATUS AND METHOD Patent Application
John H. Crews, Jr., inventor (to NASA) and James R. Reeder, inventor (to NASA) 28 Jul. 1989 16 p
(NASA-Case-LAR-13985-1; NAS 1.71:LAR-13985-1; US-Patent-Appl-SN-386172) Avail: NTIS HC A03/MF A01 CSCL 11D

A delamination test apparatus and method uses a single beam to simultaneously apply opening and shear stresses to a test specimen. A fulcrum extending downwardly from the beam produces shear stress in the specimen by downward movement, and opening stress by pivotal upward movement of the beam, which results by virtue of the fact that the applied load is on one side of the fulcrum while the test specimen is connected to the beam on the opposite side of the fulcrum. NASA

25 INORGANIC AND PHYSICAL CHEMISTRY

Includes chemical analysis, e.g., chromatography; combustion theory; electrochemistry; and photochemistry.

For related information see also *77 Thermodynamics and Statistical Physics.*.

N89-28587# Fluor Technology, Inc., Irvine, CA.
HIGEE TECHNOLOGY DEVELOPMENT PROGRAM, PHASE 1 Topical Report, Jan. - Aug. 1988
S. C. Smelser, R. W. Bucklin, R. V. Ramanathan, D. G. Lamprecht, and R. Fowler (Glitsch, Inc., Dallas, TX.) Jan. 1989 139 p
(Contract GRI-5084-222-1063)
(PB89-161434; GRI-89/0002) Avail: NTIS HC A07/MF A01 CSCL 07D

Phase 1 results are generated for the Higee Development program which is organized to bring the high gravity (Higee) centrifugal separator for selective H2S absorption and stripping to commercial readiness. First pass designs and cost estimates for a conventional amine treating unit and for conservative and optimistic Higee units were prepared along with designs and cost estimates for sulfur recovery. With only a conservative improvement, Higee could penetrate the high pressure natural gas treating market based on reduced treating costs; however, this penetration will likely be limited. Results suggest that Higee technology for selective H2S removal will have broad application if the optimistic improvement in performance is achieved. GRA

N89-28588# Bailey Controls Co., Wickliffe, OH.
ENGINE COMBUSTION OPTIMIZATION BY EXHAUST ANALYSIS Final Report, Dec. 1986 - Jul. 1988
R. K. Jahn, D. J. Lee, S. P. Cremean, and R. A. Bayless (Columbia Gas System Service Corp., Columbus, OH.) Jan. 1989 186 p
(Contract GRI-5083-231-0956)
(PB89-195788; GRI-88/0312) Avail: NTIS HC A09/MF A01 CSCL 21B

The application of an air/fuel ratio analyzer and trim control system to a two-cycle turbocharged compressor engine is documented. The trim control strategy is based upon both oxygen and combustibles in the exhaust gases. The use of exhaust gas analysis demonstrated that an improvement in combustion efficiency on two-cycle turbocharged engines is possible. However, the prevention of detonation must be demonstrated with further testing before these controls can be satisfactorily applied to turbocharged engines. The application of the controls on naturally aspirated engines is thought to be more feasible at this time. The potential benefits justify the continuation of work to develop fully operational systems for both turbocharged and naturally aspirated engines. GRA

N89-28589# Indiana Univ., Bloomington.
HIGH RESOLUTION ELECTRON ENERGY LOSS STUDIES OF SURFACE VIBRATIONS Progress Report, 1 Jul. 1988 - 20 Jun. 1989
L. L. Kesmodel Jun. 1989 7 p
(Contract DE-FG02-84ER-45147)
(DE89-013964; DOE/ER-45147/4) Avail: NTIS HC A02/MF A01

New experimental investigations of surface vibrational properties of materials with high-resolution Electron Energy Loss Spectroscopy (EELS) are reported. The effort has focused on surface phonon dispersion measurements for copper (111) and ultrathin epitaxial films of nickel and cobalt grown on a copper (001) substrate. Data and analysis of several surface modes and resonances on Cu (111) is consistent with a modest (15 percent) softening of the intraplanar force constant between surface atoms. For epitaxial thin films of a few monolayers thickness of nickel on Cu (001), new film modes are identified experimentally and correspond to vibrational motion localized primarily in the film. Measurements for epitaxial films of cobalt on a Cu (001) substrate exhibit substantial flattening of the Rayleigh phonon dispersion, suggestive of surface stress in the films. DOE

N89-28590# Northwestern Univ., Evanston, IL. Dept. of Engineering Science and Applied Mathematics.
BIFURCATION AND PATTERN FORMATION IN COMBUSTION
A. Bayliss, B. J. Matkowsky, and M. Minkoff (Argonne National Lab., IL.) 1988 61 p Presented at the 10th Dundee Conference on Differential Equations, Dundee, UK, 4 Jul. 1988
(Contracts W-31-109-eng-38; DE-FG02-87ER-25027; NSF DMS-87-01543)
(DE89-013629; CONF-8807172-1) Avail: NTIS HC A04/MF A01

A combination of analytical and numerical methods is employed to determine the behavior of solutions of combustion problems. Specifically, highly nonlinear time dependent systems of partial differential equations are considered which model the behavior of both solid and gaseous fuel combustion. In gaseous fuel combustion, particular interest is shown in the transition from laminar to turbulent combustion, including a description of the intermediate stages of this transition. An adaptive pseudo-spectral method which is both very accurate and very efficient is developed. The algorithm allows the description of a solution on bifurcation branches, well beyond the region where analytical methods work well. Advantage was taken of the analytical results that was first obtained to aid in choosing appropriate parameter values and initial conditions for the numerical computations. In addition the analytical results serve as benchmarks for the computations. The computations reveal new and interesting behavior, not otherwise obtainable. Two problems are discussed involving solid snd gaseous fuel combustion. DOE

N89-28591# Argonne National Lab., IL. Chemical Technology Div.
CHEMICAL TECHNOLOGY DIVISION Annual Technical Report, 1988
May 1989 212 p
(Contract W-31-109-eng-38)
(DE89-013917; ANL-89/15) Avail: NTIS HC A10/MF A01

Highlights of the Chemical Technology (CMT) Divisions's activities during 1988 are presented. In this period, CMT conducted research and development in the following areas: (1) high-performance batteries (mainly lithium alloy/metal sulfide, sodium/metal chloride, and sodium/sulfur); (2) aqueous batteries (lead-acid, nickel/iron, etc.); (3) advanced fuel cells with molten carbonate or solid oxide electrolytes; (4) coal utilization, including the heat and seed recovery technology for coal-fired magnetohydrodynamics plants and the technology for fluidized-bed combustion; (5) methods for recovery of energy from municipal waste and techniques for treatment of hazardous chemical water; (6) nuclear technology related to a process for separating and recovering transuranic elements from nuclear waste and for producing Mo-99 from low-enriched uranium targets, the recovery processes for discharged fuel and the uranium blanket in a sodium-cooled fast reactor, and waste management; and (7) physical chemistry of selected materials in environments simulating those of fission and fusion energy systems. The Division also has a program in basic chemistry research in the areas of fluid catalysis for converting small molecules to desired products; materials chemistry for superconducting oxides and associated and ordered solutions at high temperatures; interfacial processes of importance to corrosion science, high-temperature superconductivity, and catalysis; and the geochemical processes responsible for trace-element migration within the earth's crust. The Division continued to be the major user of the technical support provided by the Analytical Chemistry Laboratory at ANL. DOE

N89-28592# Pacific Northwest Labs., Richland, WA. Chemical Methods and Separations Group.
CAPILLARY ZONE ELECTROPHORESIS-MASS SPECTROMETRY OF PEPTIDES AND PROTEINS
Joseph A. Loo, Harold R. Udseth, and Richard D. Smith May 1989 3 p Presented at the 37th American Society for Mass Spectroscopy Annual Symposium, Miami Beach, FL, 22-26 May 1989
(Contract DE-AC06-76RL-01830)
(DE89-014466; PNL-SA-16622; CONF-8905166-3) Avail: NTIS HC A02/MF A01

Capillary zone electrophoresis (CZE) is attracting extensive attention as a fast, high resolution analytical and micro-preparative separations technique for systems of biological interest. In zone electrophoresis, a column is filled with a single electrolyte having a specific conductivity. The mixture of substances to be separated is applied as a narrow band to the head of a buffer filled column in a band whose width is much less than the length of the column and at a concentration too low to affect the buffer conductivity. An electric field is then applied across the length of the column and the individual substances migrate and separate according to their net electrophoretic velocities. Zone electrophoresis carried out in small diameter (less than 100 micron) fused silica capillaries is a relatively new approach to the high resolution separation of aqueous samples. Very small volume samples (picoliter range) with separation efficiencies on the order of 10(6) theoretical plates for amino acids have been achieved. The method can be further enhanced by the dynamic combination of detection sensitivity and selectivity offered by mass spectrometry (MS). The on-line marriage of mass spectrometry to CZE is accomplished by an atmospheric pressure electrospray ionization source interface. Our research efforts have demonstrated that proteins with MW's greater than 100 kDa can be analyzed using a conventional quadrupole mass spectrometer with an upper m/z limit of only 1700. DOE

N89-28593# Brown Univ., Providence, RI. Dept. of Chemistry.
PREPARATION OF COMPOUNDS WITH THE TETRAHEDRAL STRUCTURE WHICH TRANSMIT IN THE FAR INFRARED
Y. M. Gao, P. W. Kershaw, K. Dwight, and A. Wold 30 May 1989 7 p Submitted for publication
(Contract N00014-85-C-0177)
(AD-A208697; TR-10) Avail: NTIS HC A02/MF A01 CSCL 20/12

A number of chalcogenides and phosphides crystallize with the tetrahedral structure in which the cations and anions are in tetrahedral positions. The 2 to 6 compounds such as ZnS, ZnSe, Cds and CdSe are known to transmit in the far infrared. However, they are soft and decompose in air at relatively low temperatures. Efforts have been made at Brown University to improve the properties of these compounds, either by alloying them with 3 to 5 semiconductors, or by substituting transition metals such as nickel for the divalent specie. GRA

N89-28594# Harvard Univ., Cambridge, MA. Dept. of Chemistry.
FORMATION OF MONOLAYERS BY THE COADSORPTION OF THIOLS ON GOLD: VARIATION IN THE LENGTH OF THE HEAD GROUP, TAIL GROUP AND SOLVENT Interim Technical Report
Colin D. Bain, Joe Evall, and George M. Whitesides May 1989 65 p Submitted for publication
(Contract N00014-85-K-0898)
(AD-A208919; TR-19) Avail: NTIS HC A04/MF A01 CSCL 07/4

Long-chain alkanethiols, HS(CH2) (n)X, adsorb from solution onto gold and form oriented, ordered monolayers. Although alkyl chains terminated by other functional groups (e.g., trialkylphosphines, dialkyl disulfides and dialkyl sulfides) also form monolayers on gold that are stable at room temperature, thiols are adsorbed preferentially from solutions containing mixtures of a thiol and one of these other adsorbates. Surfaces containing more than one functional group can be generated by coadsorption of two or more thiols from solution. In general, the ratio of the concentrations of the two components in a mixed monolayer is not the same as in solution but reflects the relative solubilities of the components in solution and interactions between the tail groups, X, in the monolayer. Multi-component monolayers do not phase-segregate into single-component domains large enough to influence the contact angle (a few tens of angstroms across), but also do not act as ideal two-dimensional solutions. From dilute solutions in alkanes, adsorption of HS(CH2)10CH2OH is strongly

preferred over HS(CH2)10CH3, probably due to the stabilization afforded by intra-monolayer hydrogen bonds between the hydroxyl tail groups. The wettability of mixed monolayers is not linear in the composition of the surface. GRA

N89-28595# Pennsylvania State Univ., University Park. Dept. of Chemistry.
THE AGGREGATED STATE OF MATTER: ELUCIDATING TRANSITIONS FROM THE GAS TO THE CONDENSED PHASE AND THE FORMATION OF AEROCOLLOIDS Final Report, 15 Aug. 1985 - 14 Feb. 1989
A. Welford Castleman, Jr. 21 Apr. 1989 39 p
(Contract DAAG29-85-K-0215)
(AD-A209080; ARO-23040.27-CH) Avail: NTIS HC A03/MF A01 CSCL 07/4

Understanding the behavior of matter in a highly dispersed state whose properties are influenced by the finite dimensions of the system--aerosols or aerocolloidal media in the gas phase, fine particles, clusters or thin films at the surface, and colloids dispersed in liquids--is of considerable fundamental scientific interest, and at the same time bears on a number of applied areas of technological importance. From a scientific point of view, a number of challenging problems were addressed with the prospect of advancing knowledge in the field of phase transformations, condensed matter and surfaces, and aerosol science. In terms of application to programs of interest to the U.S. Army, the research bears on problems of interest in the field of detection, obscuration by both natural and intentional methods of particle generation, the dispersal of agents, mechanisms of reactions that are involved in combustion and fast reactions in energetic materials, the formation and growth of small clusters and their optical properties that are of value in the area of propulsion and missile signatures, as well as reactions within and on small particles that bear on the areas of decontamination and even the dispersal of agents. Research was undertaken on a number of major projects including studies of the formation and growth of clusters, photodissociation and energy transfer, and investigations to deduce the thermochemistry of clusters. GRA

N89-28596# Air Force Inst. of Tech., Wright-Patterson AFB, OH. School of Engineering.
INVESTIGATION OF LASER-INDUCED FLUORESCENCE DETECTION OF BORON OXIDES IN FLAMES M.S. Thesis
Jong W. Cha Jun. 1989 90 p
(AD-A209154; AFIT/GEO/ENP/89J-1) Avail: NTIS HC A05/MF A01 CSCL 20/10

The purpose of this project was to demonstrate the feasibility of a laser-induced fluorescence (LIF) technique for determining the concentration of boron compounds in an atmospheric-pressure, boron seeded flame. Such a demonstration would provide a useful tool to investigate the detailed combustion chemistry of boron fuels. The two radical species which are thought to be the most important reaction intermediates in the boron combustion process, BO and BO2, were sought. A tunable pulsed dye laser which was pumped by an excimer laser was used to match the absorption bands of BO and BO2. Although a rather extensive search for LIF signal of BO was conducted, no LIF signal attributable to BO was detected. The most possible reason for this negative result was thought to be a heavy quenching under a high-pressure environment. GRA

N89-28597# Northwestern Univ., Evanston, IL. Dept. of Chemistry.
REACTION KINETICS AND MECHANISM OF CHAIN REACTIONS AND EXPLOSIONS VIA TRANSIENT SPECTROSCOPY Final Report, Apr. 1986 - Apr. 1989
Eric Weitz 16 May 1989 7 p
(Contract DAAL03-86-G-0036)
(AD-A209169; ARO-23783.1-CH-F) Avail: NTIS HC A02/MF A01 CSCL 07/5

This is the final technical report for an Army Research Office Science and Technology Fellowship. The Fellow was Robert Ryther, a graduate student in the Department of Chemistry at Northwestern University. He worked under the direction of Professor Eric Weitz. His work involved the use of transient infrared diode laser spectroscopy to follow the reaction kinetics, photophysics and photochemistry of radicals and coordinatively unsaturated organometallic species. GRA

N89-28598# California Univ., Davis. Dept. of Chemistry.
MODELLING THE IN SITU INFRARED REFLECTION-ABSORPTION SPECTRA OF THE DIFFUSE LAYER
P. W. Faguyr, S. McCullough, and W. Ronald Fawcett 1 May 1989 4 p Presented at the Electrochemical Society Meeting, Los Angeles, CA, May 1989
(Contract N00014-87-K-0541)
(AD-A209347; TR-10) Avail: NTIS HC A02/MF A01 CSCL 07/4

Using a stratified medium model for the electrochemical interface and Gouy-Chapman-Stern theory of the double layer, a method to model infrared reflection-absorption spectra of the diffuse layer is developed. This method is applied to spectra obtained in the double layer region for aprotic, organic electrolytes on gold electrodes. GRA

N89-28599# Texas Univ., Austin. Dept. of Mechanical Engineering.
OXYGEN STORAGE ON ZEOLITES Final Report, Aug. 1986 - Jun. 1988
Joseph J. Beaman Jan. 1989 80 p
(Contract F33615-83-D-0603)
(AD-A209352; USAFSAM-TR-88-26) Avail: NTIS HC A05/MF A01 CSCL 23/5

In an effort to eliminate hazards associated with high pressure and liquid oxygen reserve systems, the United States Air Force has supported studies at the University of Texas to determine the feasibility of using zeolite filled cylinders of oxygen storage. Because of the adsorptive capacity of the zeolite, more oxygen can be contained in a zeolite filled cylinder than in an unpacked cylinder, depending on the pressure. However, this study has revealed that differences in adsorptive capacity between charge and exhaust pressures determine the deliverable amount of gas in a bed. Using this criterion (instead of merely comparing isotherm capacities to unpacked cylinder capacities), the advantage of zeolite filled cylinders over unpacked cylinders is diminished. Parameters have been measured to allow calculation of estimated bed size for a 200 liter (NPT) reserve oxygen system. Assuming an exhaust pressure of 8.82 psia (0.6 atm), the required size of the system for an unpacked cylinder operating at OBOGS pressure (40 psig) is approximately 64.2 liters. The same system filled with zeolite is 16.8 liters (zeolite mass is 13.2kg). While the improvement using the zeolite is impressive, the cylinder size does not compare favorably with the 1 liter size of an unpacked cylinder operating at 3000 psig. GRA

N89-28600# California Univ., Davis. Dept. of Chemistry.
SOLVENT EFFECTS ON SIMPLE ELECTRON TRANSFER REACTIONS. A COMPARISON OF RESULTS FOR HOMOGENEOUS AND HETEROGENEOUS SYSTEMS
W. Ronald Fawcett and Colby A. Foss, Jr. 1 May 1989 31 p
(Contract N00014-87-K-0541)
(AD-A209381; TR-9) Avail: NTIS HC A03/MF A01 CSCL 07/4

Solvents effects on the rate constants for both homogeneous and heterogeneous electron transfer reactions have been analyzed on the basis of current models which consider the role of dynamic relaxation processes in determining the magnitude of the pre-exponential factor. A statistical method for separating the effects of the solvent longitudinal relaxation time tau sub L from those of the solvent permittivity parameter gamma is described and applied to 15 sets of experimental data for which results are available in at least four solvents. The degree to which the explained variation in the logarithm of the rate constant could be attributed to either of these effects varied all the way from 0 to 100 percent depending on the degree of reaction adiabaticity and

the relative sizes of the inner and outer sphere components of the free energy of activation. Data for the limiting cases in which there is no tau sub L dependence in the pre-exponential factor or in which the pre-exponential factor is proportional to 1/tau sub L were analyzed further to obtain the size-distance parameter and the components of the pre-exponential factor relevant to the encounter pre-equilibrium model. These parameters have been discussed with respect to current developments in electron transfer theory. Problems in estimating the longitudinal relaxation time in the solvent, required for the analysis, are also considered. GRA

N89-28601# California Univ., Los Angeles. Dept. of Physics.
ELECTRONIC-STRUCTURE STUDY OF THE Ni-Ga AND Ni-In INTERMETALLIC COMPOUNDS USING X-RAY PHOTOEMISSION SPECTROSCOPY
Lishing Hsu, Barakat Alavi, David K. Shuh, and R. Stanley Williams 1 Jul. 1989 28 p Submitted for publication
(Contract N00014-87-K-0014)
(AD-A209696; TR-17) Avail: NTIS HC A03/MF A01 CSCL 07/2

Polycrystalline Ni-Ga and Ni-In intermetallic compounds of various stoichiometric compositions have been examined by X-ray photoemission spectroscopy. The observed valence-band spectra for all the compounds are very similar to those for elemental Ni. Those for Ni3Ga and NiIn agree rather well with the band-structure calculations of Kubo and others (J. Phys., F17, 397 (1987)) and Collinet and others (Z. Metallkd. 77, 798 (1986), respectively. Only a partial filling of the empty Ni 3d states occurs on forming compounds with gallium or indium. GRA

N89-28602# California Univ., Davis. Dept. of Chemistry.
THE ANALYSIS OF SOLVENT EFFECTS ON THE KINETICS OF SIMPLE HETEROGENEOUS ELECTRON TRANSFER REACTIONS
W. Ronald Fawcett and C. A. Foss, Jr. 12 Aug. 1988 23 p
(Contract N00014-87-K-0541)
(AD-A210078; TR-6) Avail: NTIS HC A03/MF A01 CSCL 07/4

A method for separating the solvent dependence of the pre-exponential factor from that in the free energy of activation is described for adiabatic electron transfer reactions in which the inner sphere contribution to the activation energy is much less than the outer sphere contribution. The analysis is applied to data published in the literature in which the heterogeneous electron transfer rate constant was measured in at least 4 different solvents. The resulting kinetic parameters are discussed with respect to current theory. GRA

N89-28603*# National Aeronautics and Space Administration. Marshall Space Flight Center, Huntsville, AL.
CONTROLLED METHOD OF REDUCING ELECTROPHORETIC MOBILITY OF VARIOUS SUBSTANCES Patent Application
James M. VanAlstine, inventor (to NASA) (Universities Space Research Association, Huntsville, AL.) 7 Jul. 1989 20 p
(NASA-Case-MFS-26049-1-NP; NAS 1.71:MFS-26049-1-NP; US-Patent-Appl-SN-376487) Avail: NTIS HC A03/MF A01 CSCL 07D

A method of reducing electrophoretic mobility of macromolecules, particles, cells, and the like is provided. The method comprises interacting the particles or cells with a polymer-linked affinity compound composed of: a hydrophilic neutral polymer such as polyethylene glycol, and an affinity component consisting of a hydrophobic compound such as a fatty acid ester, an immunocompound such as an antibody or active fragment thereof or simular macromolecule, or other ligands. The reduction of electrophoretic mobility achieved is directly proportional to the concentration of the polymer-linked affinity compound employed, and the mobility reduction obtainable is up to 100 percent for particular particles and cells. The present invention is advantageous in that analytical electrophoretic separation can not be achieved for macromolecules, particles, and cells whose native surface charge structure had prevented them from being separated by normal electrophoretic means. Depending on the affinity component utilized, separation can be achieved on the basis of specific/irreversible, specific/reversible, semi-specific/reversible, relatively nonspecific/reversible, or relatively nonspecific/irreversible ligand-substance interactions. The present method is also advantageous in that it can be used in a variety of standard laboratory electrophoresis equipment. NASA

N89-28604# Massachusetts Inst. of Tech., Cambridge. Dept. of Chemistry.
USE OF MICROELECTRODE ARRAYS TO DIRECTLY MEASURE DIFFUSION OF IONS IN SOLID ELECTROLYTES: PROOF OF CONCEPT EXPERIMENTS INVOLVING Ag+ IN A SOLID POLYMER ELECTROLYTE Interim Technical Report No. 30, 1 Jun. 1988 - 1 Jun. 1989
Vince Cammarata, Daniel R. Talham, Richard M. Crooks, and Mark S. Wrighton 21 Jun. 1989 32 p
(Contract N00014-84-K-0553)
(AD-A209536) Avail: NTIS HC A03/MF A01 CSCL 07/4

Proof of concept experiments is provided, demonstrating a new methodology for direct measurement of molecular or ionic species in electrolyte media. A microelectrode array of closely spaced Platinum microelectrodes allows direct measurement of the movement of Silver cations in aqueous electrolyte and in the solid polymer electrolytes, LICF3SO3/MEEP (MEEP = poly (bis(2-(2-methoxyethoxy) ethoxy)phosphazene) at 298 K with a molar ratio of LiCF3SO3 to polymer repeat unit of 1 to 4 and LiCF3SO3/PEO (PEO = poly(ethylene oxide)) at 352 K and a molar ratio of LiCF3SO3 to polymer repeat unit of 1 to 8. The crucial experiments involve anodically stripping Ag from a Ag-coated Pt microelectrode (generator) and electrochemically detecting the resulting Ag(+) at nearby Pt electrodes (collectors) by reducing the Ag(+) back to Ag. The time dependence of the collector current corresponding to Ag(+) to Ag reduction after the generation step allows evaluation of the diffusion coefficient, D, for the Ag(+) in the various media and conditions used. GRA

N89-28605# Colorado State Univ., Fort Collins. Dept. of Chemistry.
VIBRATIONAL DYNAMICS OF ANILINE (Ar)1 AND ANILINE (CH4)1 CLUSTERS
M. R. Nimlos, M. A. Young, E. R. Bernstein, and D. F. Kelley 1 Jun. 1989 37 p Submitted for publication
(Contract N00014-79-C-0647)
(AD-A209560; AD-E900860; TR-56) Avail: NTIS HC A03/MF A01 CSCL 07/4

The first excited electronic state (S1) vibrational dynamics of aniline(Ar)1 and aniline(CH4)1 van der Waals (vdW) clusters have been studied using molecular jet and time resolved emission spectroscopic techniques. The rates of intramolecular vibrational energy redistribution (IVR) and Vibrational Predissociation (VP) as a function of excess vibrational energy are reported for both clusters. For vibrational energy in excess of the cluster binding energy, both clusters are observed to dissociate. The dispersed emission spectra of these clusters demonstrate that aniline(Ar)1 dissociates to all energetically accessible bare molecule states and that aniline(CH4)1 dissociates selectively to only the bare molecule vibrationless state. The emission kinetics show that in the aniline(AR)1 case, the initially excited states have nanosecond lifetimes, and intermediate cluster states have very short lifetimes. In contrast, the initially excited aniline(CH4)1 states and other vibrationally excited cluster states are very short lived (less than 100 ps), and the intermediate cluster zeroth order state is observed. GRA

N89-28606# Cornell Univ., Ithaca, NY. School of Chemical Engineering.
MULTICOMPONENT E-BEAM RESISTS CONTAINING ORGANOMETALLIC COMPOUNDS AND REACTIVE MONOMERS
Y. M. N. Namaste, B. C. Dems, S. Malhotra, L. M. Vane, S. K. Obendorf, and F. Rodriguez 12 May 1989 14 p Presented at the Regional Technical Conference on Photopolymers of the Society of Plastic Engineers, Ellenville, NY, 3 Oct. - 2 Nov. 1988

Sponsored in part by NSF
(Contract N00014-85-K-0474)
(AD-A207716; TR-11) Avail: NTIS HC A02/MF A01 CSCL 07/6

Negative working resists with combined e-beam sensitivity and oxygen etch resistance have been formulated by combining a host polymer for dimensional stability during radiation processing, an unsaturated, non-volatile monomeric component for control of sensitivity, and, an organometallic compound to contribute Reactive Ion Etching (RIE) resistance in an oxygen plasma. We have incorporated these three components into blends by three methods. GRA

N89-28607# Ballistic Research Labs., Aberdeen Proving Ground, MD.
COLLISIONAL TRANSFER BETWEEN AND QUENCHING OF THE 3p 3p AND 5p STATES OF THE OXYGEN ATOM Final Report, Oct. 1987 - Sep. 1988
Brad E. Forch, Andrzej W. Miziolek, and Paul J. Dagdigian May 1989 31 p
(AD-A207759; BRL-TR-2998) Avail: NTIS HC A03/MF A01 CSCL 07/2

Collisional quenching and excitation transfer between the oxygen atom 3p 3p and 5p states have been investigated in a discharge flow apparatus with O2 and N2 collisional partners. The 3P state was excited by two photon excitation at 225.6 nm from the 2p4 3P ground state, and temporal profiles of the 3p 3S and 5P 5S emission at 844.7 and 777.5 nm, respectively, to the lower 3s manifold were recorded. GRA

N89-28608# State Univ. of New York, Buffalo. Dept. of Chemistry.
ION-MOLECULE CHEMISTRY WITHIN DOUBLY CHARGED AMMONIA CLUSTERS Technical Report No. 1
M. T. Coolbaugh, William R. Peifer, and James F. Garvey 1989 14 p
(Contract N00014-88-K-0493)
(AD-A207764; SUNY/DC/TR-1) Avail: NTIS HC A03/MF A01 CSCL 07/4

We present in this paper the observation of intramolecular ion-molecule reactions within doubly charged clusters produced via electron impacts ionization of neat beams of ammonia molecules. The fragmentation pattern strongly suggests that reactions occurring within these doubly charged clusters are similar to those observed for singly charged ammonia clusters. This behavior implies that these cluster ions consist of two separate, singly charged ammonia cations which act separately within the bulk neutral cluster. That is, either one, both, or neither of the ammonia cations may react with the neutrals solvating them within the doubly charged cluster. GRA

N89-28609# State Univ. of New York, Buffalo. Dept. of Chemistry.
ION-MOLECULE CHEMISTRY WITHIN TRIPLY CHARGED AMMONIA CLUSTERS Technical Report No. 3
M. T. Coolbaugh, William R. Peifer, and James F. Garvey 1989 17 p
(Contract N00014-88-K-0493)
(AD-A207766; SUNY/DC/TR-3) Avail: NTIS HC A03/MF A01 CSCL 07/4

We present in this communication the first observation of intramolecular ion-molecule reactions within triply charged clusters produced via electron impact ionization of neat beams of ammonia molecules. The fragmentation pattern strongly suggests that reactions occurring within these triply charged clusters are similar to those previously observed for singly and doubly charged ammonia clusters. This behavior implies that these cluster ions consist of three singly charged ammonia cations which react separately within the bulk neutral cluster. That is either one, two, three or none of the ammonia cations may react with the solvating neutrals within the cluster. We also report for singly charged ammonia clusters the observation that extensive fragmentation can occur within the cluster producing ions with the empirical formulas of (NH3) n-1 (N+) and (NH3) n-1 (NH+). GRA

N89-28610# Deutsche Forschungs- und Versuchsanstalt fuer Luft- und Raumfahrt, Cologne (Germany, F.R.). Inst. fuer Antriebstechnik.
SUPERSONIC COMBUSTION AT THE DFVLR: RESULTS AND EXPERIENCES [UEBERSCHALLVERBRENNUNG IN DER DFVLR. ERGEBNISSE UND ERFAHRUNGEN]
G. Winterfeld 1988 11 p In GERMAN
(DFVLR-88-044; ETN-89-94381) Avail: NTIS HC A03/MF A01

The research activities of the DFVLR Institute of Jet Engines in the field of supersonic combustion are reviewed. The ignition and stabilization of hydrogen-air diffusion flames are investigated. Many qualitative and quantitative results on the essential effects on thermal self ignition are obtained, which together with the obtained reaction-kinetics data allow a satisfactory calculation of induction lengths during parallel injection of H2. The possibilies of improving thermal self-ignition by catalytic effects or precombustion, as well as the self-ignition characteristics of several hydrocarbons are studied. With a view to flame stabilization by recirculation domains in the supersonic flow at low temperatures, quantitative data on the characteristic test time at the boundary of the recirculation domain are obtained. The importance of interactions between supersonic flow and local subsonic domains in combustion zones is demonstrated. ESA

N89-28611# Gesamthochschule, Kassel (Germany, F.R.). Fachbereich Physik.
SIMULTANEOUS SECONDARY ION AND AUGER ELECTRON ANALYSIS, ILLUSTRATED BY EXAMPLES FROM MICROELECTRONICS RESEARCH AND TECHNOLOGY Ph.D. Thesis [SIMULTANE SEKUNDAERIONEN- UND AUGERELEKTRONEN-ANALYTIK AN BEISPIELEN AUS FORSCHUNG UND TECHNOLOGIE DER MIKROELEKTRONIK]
Klaus Masseli Nov. 1987 151 p In GERMAN
(ETN-89-94431) Avail: NTIS HC A08/MF A01

Problems in the fields of modern microelectronics research, development and technology were studied using surface analysis methods. The combination of the two most important methods, secondary ion mass spectrometry (SIMS) and Auger electron spectroscopy (AES), allows the solving of complex problems, especially mechanisms in the interface region of SiO2/InP. The direct determination of the chemical composition of oxide layers, the control of diffusion steps, and the analysis of contaminations from dry etching processes are possible. The optimization of the depth resolution of SIMS in abrupt doping transition was also investigated. ESA

N89-28612 National Physical Lab., Teddington (England). Div. of Materials Applications.
STANDARD REFERENCE MATERIAL FOR HIGH TEMPERATURE VISCOSITY MEASUREMENTS: RESULTS OF INTERLABORATORY COMPARISON PROGRAMME
K. C. Mills Mar. 1989 92 p
(NPL-DMA(A)-175; ISSN-0143-7313; ETN-89-95254) Copyright Avail: National Physical Laboratory, Teddington, Middlesex, TW11 0LW, United Kingdom

Viscosity measurements were carried out on the standard reference material (SRM) issued by Community Bureau of Reference (BCR) at ten different laboratories. The SMR's composition is 19.46 percent Li2O, 14.06 percent Al2O3 and 65.68 percent SiO2. The rotating crucible, the rotating cylinder and the oscillating plate techniques are applied. The results show appreciable scatter. The dispersion in the results is probably due to small changes in the chemical composition of the SRM, which occurred during the measurement sequence. A program of further measurements is proposed to reduce the experimental scatter and provide a set of recommended viscosity data. ESA

N89-28613# Helsinki Univ. of Technology, Espoo (Finland). Lab. of Inorganic and Analytical Chemistry.
THE ATOMIC LAYER EPITAXY GROWTH AND CHARACTERIZATION OF ZINC SULFIDE AND ALKALINE EARTH SULFIDE THIN FILMS FOR ELECTROLUMINESCENCE APPLICATIONS Ph.D. Thesis
Markku Tammenmaa 1988 19 p Sponsored by the Academy of Finland, the Technology Development Center and the Emil Aaltonen Founda tion
(ISBN-952-90014-6-0; ETN-89-95179) Avail: NTIS HC A03/MF A01

A review, nine publications, and the results, on the preparation and characterization of thin films for electroluminescent (EL) applications, are discussed. Atomic layer epitaxy (ALE) is used to grow the ZnS, CaS, SrS, and BaS films and to dope them with divalent manganese (ZnS) and trivalent rare earths. The starting materials for the thin film growth are zinc chloride or acetate, alkaline earth and rare earth complexes of 2,2,6,6-tetramethyl 3,5-heptanedione and hydrogen sulfide. The films are characterized by measuring their photoluminescence spectra, X-ray diffraction patterns, and activator concentrations using methods based on X-ray fluorescence. In addition, electroreflectance, ellipsometric, Auger, secondary-ion mass spectrometry measurements and chemical analysis are used. The results indicate that good quality EL thin films can be grown by the ALE process. For the growth of zinc sulfide films from zinc acetate, the growth rates are relatively low. ESA

N89-28614 Technische Univ., Delft (Netherlands).
MULTIVARIATE ANALYSIS OF UV-SPECTRAL DATA FOR SOLUTE TRACKING IN HPLC Ph.D. Thesis
Joost Karel Strasters Delft University Press 1989 146 p
(ISBN-90-6275-535-6; ETN-89-95460) Copyright Avail: Delft Univ. Press, Stevinweg 1, 2628 CN Delft, Netherlands

Some aspects related to peak tracking or peak recognition in high performance liquid chromatography (HPLC) are investigated. A number of possible alternative techniques, such as relative peak areas, dual wavelength ratios, and comparison of complete spectra, are applied. These applications indicate that a coelution of two or more components in a peak cluster presents one of the main problems. The use of peak tracking in early stages of the chromatographic optimization process, (characterizing components as basic, acidic, or neutral), allows for an efficient selection of optimization parameters. The number of actual experiments required during the optimization process is thus reduced. ESA

26 METALLIC MATERIALS

Includes physical, chemical, and mechanical properties of metals, e.g., corrosion; and metallurgy.

N89-28615# National Inst. of Standards and Technology, Gaithersburg, MD. Metallurgy Div.
METALLURGICAL EVALUATION OF 17-4 PH STAINLESS STEEL CASTINGS
George E. Hicho and John H. Smith May 1989 35 p Sponsored by Naval Ordnance Station, Indian Head, MD
(PB89-193262; NISTIR-89/4075) Avail: NTIS HC A03/MF A01 CSCL 11F

A metallurgical evaluation was conducted to determine if selected castings of 17-4 PH stainless steel used in head caps on missile weapon systems had been properly heat treated as required by SAE specification AMS-5355D. Optical metallographic analysis and hardness measurements were made on four samples of as-received castings and on selected samples that were homogenized, solution annealed and aged at various temperatures. Metallographic and hardness results indicate that the head caps identified as 5066, 5441, NIST 1, and 20 were not heat treated according to AMS specification 5355D, in particular to condition H1000, which refers to the aging temperature (1000 F). GRA

N89-28616# California Univ., Berkeley. Lawrence Berkeley Lab. Materials and Chemical Sciences Div.
OXIDATIVE ADDITION OF C-H BONDS IN ORGANIC MOLECULES TO TRANSITION METAL CENTERS
Robert G. Bergman (California Univ., Berkeley.) Apr. 1989 10 p Presented at the Annual Chemical Congress, Hull, United Kingdom, 4 Apr. 1989 Sponsored by American Chemical Society and Chevron Research Co.
(Contract DE-AC03-76SF-00098)
(DE89-012991; LBL-27164; CONF-8904236-1; CONF-8906152-1) Avail: NTIS HC A02/MF A01

Alkanes are among the most chemically inert organic molecules. They are reactive toward a limited range of reagents, such as highly energetic free radicals and strongly electrophilic and oxidizing species. This low reactivity is a consequence of the C-H bond energies in most saturated hydrocarbons. These values range from 90 to 98 kcal/mole for primary and secondary C-H bonds; in methane, the main constituent of natural gas, the C-H bond energy is 104 kcal/mole. This makes methane one of the most common but least reactive organic molecules in nature. This report briefly discusses the search for metal complexes capable of undergoing the C-H oxidative addition process allowing alkane chemistry to be more selective than that available using free radical reagents. DOE

N89-28617# Oak Ridge National Lab., TN. Metals and Ceramics Div.
SULFIDATION/OXIDATION PROPERTIES OF IRON-BASED ALLOYS CONTAINING NIOBIUM AND ALUMINUM
J. H. DeVan, H. S. Hsu, and M. Howell May 1989 38 p
(Contract DE-AC05-84OR-21400)
(DE89-013766; ORNL/TM-11176) Avail: NTIS HC A03/MF A01

Compatibility with mixed gases containing S, O, and Cl is a critical requirement for high temperature alloys used in coal conversion and combustion applications. Comparative corrosion tests of Fe-25Cr-20Ni, Fe-18Cr-6Al, and Fe-9Cr-9Nb-6Al (wt percent) at 700 to 800 C in a simulated coal gasification environment led to the development of Fe-Nb-Al alloys and testing of both Fe-Nb-Al and Fe3Al alloys. The niobium and aluminum content in the latter alloys ranged from 8 to 18 and 6 to 16 wt percent, respectively. The niobium addition was intended as a selective refractory sulfide former. Testing was carried out at 700 to 800 C in H2S-H2-H2O gas mixtures with relatively low oxygen activities (less than or equal to 10(-22) atm) and high sulfur activities (greater than or equal to 10(-6) atm). Metallographic and chemical analyses of the corrosion product scales and the underlying alloy were performed to determine the role of the respective metallic elements on sulfidation/oxidation processes. DOE

N89-28618# Massachusetts Inst. of Tech., Cambridge. Dept. of Materials Science and Engineering.
THEORETICAL ANALYSIS OF PHASE TRANSFORMATIONS IN Fe-Ni INVAR-TYPE ALLOYS
Kenneth C. Russell and F. A. Garner (Pacific Northwest Labs., Richland, WA.) Feb. 1989 33 p Presented at the Symposium on Physical Metallurgy of Controlled Expansion Invar-Type Alloys, Las Vegas, NV, 28 Feb. 1989 Submitted for publication
(Contract DE-AC06-76RL-01830)
(DE89-014454; PNL-SA-16211; CONF-8902117-1) Avail: NTIS HC A03/MF A01

Many studies have suggested that Fe-Ni and Fe-Ni-Cr alloys of ca. 35 at. percent Ni are susceptible to decomposition into two FCC (face centered cubic) phases. We herein model the kinetics and thermodynamics of spinodal decomposition, nucleation, growth, and coarsening of these alloys. Prediction of the scale of a microstructure formed by growth or coarsening may be done with some confidence. The absence of a model for surface energy and gradient energy in systems with negative departure from ideality reduce us to little more than guesses for the kinetics of nucleation and of spinodal decomposition. We combine our calculations with those of others and studies of terrestrial and celestial

decomposition to suggest a miscibility gap for Fe-Ni alloys. The gap is very narrow at high temperatures but is broadened at low temperatures by magnetic effects. DOE

N89-28619# California Univ., Berkeley. Lawrence Berkeley Lab. National Center for Electron Microscopy.
FUNDAMENTAL STUDIES OF GRAIN BOUNDARY STRUCTURE AND PROPERTIES IN ICB ALUMINUM
K. H. Westmacott and U. Dahmen May 1989 18 p Presented at the 12th Symposium on Ion Sources and Ion-Assisted Technology, Tokyo, Japan, 5 Jun. 1989
(Contract DE-AC03-76SF-00098)
(DE89-014884; LBL-27187; CONF-8906157-2) Avail: NTIS HC A03/MF A01

Thin films prepared by the Ionized-Cluster-Beam (ICB) technique, pioneered at Kyoto University, are of great interest for both their fundamental structure and properties and their potential for practical applications. At Berkeley, a research program was initiated, in collaboration with professor Yamada and his colleagues at Kyoto University, to investigate a different aspect of ICB films. The unique bicrystal microstructure that forms with some thin film/substrate combinations are exploited to conduct a fundamental investigation of grain boundary structure and properties. Initially, the studies are being carried out on aluminum bicrystal films formed by deposition on a 100-silicon single crystal substrate. Two types of Transmission Electron Microscopy (TEM) experiments are reported. High resolution imaging of specific grain boundary segments is performed on a second HVEM capable of resolving the position of atom columns in the core regions of a grain boundary. Complementary information obtained by the two techniques helps the understanding of the structure and properties of grain boundaries as well as learn more about ICB thin films. The results of preliminary high resolution observations of silver clusters dispersed on a carbon grid are given. DOE

N89-28620# Pacific Northwest Labs., Richland, WA.
FREEZE-DRIED TUNGSTEN HEAVY ALLOYS
G. D. White and W. E. Gurwell Mar. 1989 19 p Presented at the Powder Metallurgy Conference, San Diego, CA, 11-14 Jun. 1989
(Contract DE-AC06-76RL-01830)
(DE89-014933; PNL-SA-16378; CONF-8906119-2) Avail: NTIS HC A03/MF A01

Tungsten heavy alloy powders were produced from freeze-dried aqueous solutions of ammonium metatungstate and, primarily, sulfates of Ni and Fe. The freeze-dried salts were calcined and hydrogen reduced to form very fine, homogenous, low-density, W heavy alloy powders having a coral-like structure with elements of approximately 0.1 micrometer in diameter. The powders yield high green strength and sinterability. Tungsten heavy alloy powders of 70, 90, and 97 percent W were prepared by freeze drying, compacted, and solid-state (SS) sintered to full density at temperatures as low as 1200 C and also at conventional liquid-phase (LP) sintering temperatures. Solid-state sintered microstructures contained polygonal W grains with high contiguity; the matrix did not coat and separate the W grains to form low-contiguity, high-ductility structures. Liquid-phase sintered microstructures were very conventional in appearance, having W spheroids of low contiguity. All of these materials were found to be brittle. High levels of residual S accompanied by segregation of the S to all the microstructural interfaces are principally responsible for the brittleness; problems with S could be eliminated by using Fe and Ni nitrates rather than the sulfates. Unusually high hardness, approaching 48 HRC, was obtained from sintering at 1130 C. As-sintered hardness decreases as grain size increases with sintering temperature during SS sintering and with time during LP sintering. DOE

N89-28621* National Aeronautics and Space Administration. Langley Research Center, Hampton, VA.
ALUMINUM ALLOY Patent
Linda B. Blackburn, inventor (to NASA) and Edgar A. Starke, Jr., inventor (to NASA) (Virginia Univ., Charlottesville.) 11 Apr. 1989 5 p Filed 23 Mar. 1988 Supersedes N88-24753 (26 - 18, p 2487)
(NASA-Case-LAR-13924-1-CU; US-Patent-4,820,488; US-Patent-Appl-SN-172102; US-Patent-Class-420-529; US-Patent-Class-148-159; US-Patent-Class-148-416; US-Patent-Class-148-417; US-Patent-Class-420-533) Avail: U.S. Patent and Trademark Office CSCL 11F

This invention relates to aluminum alloys, particularly to aluminum-copper-lithium alloys containing at least about 0.1 percent by weight of indium as an essential component, which are suitable for applications in aircraft and aerospace vehicles. At least about 0.1 percent by weight of indium is added as an essential component to an alloy which precipitates a T1 phase (Al2CuLi). This addition enhances the nucleation of the precipitate T1 phase, producing a microstructure which provides excellent strength as indicated by Rockwell hardness values and confirmed by standard tensile tests. Official Gazette of the U.S. Patent and Trademark Office

N89-28622# Army Lab. Command, Watertown, MA. Material Technology Lab.
OXIDATION AND HOT CORROSION OF SOME ADVANCED SUPERALLOYS AT 1300F TO 2000F (740C TO 1093C) Final Report
Milton Levy, Robert M. Huie, and Fred Pettit (Pittsburgh Univ., PA.) Apr. 1989 27 p
(DA Proj. 1L1-62105-AH-84)
(AD-A209353; MTL-TR-89-26) Avail: NTIS HC A03/MF A01 CSCL 11/6

The cyclic oxidation resistance and the hot corrosion resistance of three single crystal nickel-base superalloys and DS MAR M 200 are compared. The comparison is made by using burner rig oxidation tests at 2000 F (1093 C), and tube furnace oxidation and hot corrosion tests at 2000 F (1093 C), 1650 F (900 C), and 1300 F (704 C). The rig tests and the tube furnace tests produce similar results with the single crystal alloys being more oxidation resistant than DS MAR M 200. A significant difference between the hot corrosion resistance of these alloys was not observed. All four alloys were extremely susceptible to hot corrosion induced by a liquid deposit. GRA

N89-28623# Army Lab. Command, Watertown, MA. Material Technology Lab.
THE BAUSCHINGER EFFECT IN 6-6-2 TITANIUM ALLOY AND ITS INFLUENCE ON ADVANCED ARTILLERY PROJECTILES Final Report
Hemen Ray Apr. 1989 40 p
(AD-A209355; MTL-TR-89-39) Avail: NTIS HC A03/MF A01 CSCL 11/6

The Bauschinger effect may be defined as a phenomenon by which plastic deformation of a polycrystalline material causes a reduction in yield strength upon reloading in a direction opposite to the original direction. This characteristic of plastic flow results from the inhomogeneity of plastic flow on the microscopic level. In this report, the Bauschinger effect in 6-6-2 titanium alloy is evaluated and an illustration is given to demonstrate its importance in the design and reliability of the Army's advanced artillery projectiles. The tension-compression specimens, fabricated from the recovered projectiles, are loaded to compression to a specified plastic range, followed by tension after unloading. The experimental results indicate that the original yield strength of the material is greatly reduced due to reverse loading. GRA

N89-28624# Army Lab. Command, White Sands Missile Range, NM. Material Technology Lab.
AN INVESTIGATION OF THE WORKABILITY OF Al-8.5 PERCENT Mg ALLOYS Final Report
Marietta R. Cappucci Apr. 1989 18 p
(AD-A209451; MTL-TR-89-33) Avail: NTIS HC A03/MF A01 CSCL 11/6

Aluminum-magnesium alloys containing greater than 5 wt percent magnesium are high strength, lightweight alloys which show potential to be utilized by the Army in armor applications. A problem encountered thus far with these high strength alloys is some

difficulty in achieving necessary cold work levels to provide the alloys with optimum mechanical properties. The results are detailed of an investigation of the hot and cold workability of three Al-8.5 wt percent Mg alloys with variations in Mn and Cr additions.
GRA

N89-28625# Iowa State Univ. of Science and Technology, Ames. Dept. of Materials Science and Engineering.
SYNTHESIS AND HOT PRESSING OF ZnS POWDERS
Mufit Akinc and Ahmet Celikkaya 30 Mar. 1989 10 p Submitted for publication
(Contract N00014-87-K-0738)
(AD-A209602; TR-3) Avail: NTIS HC A02/MF A01 CSCL 11/2

A comprehensive investigation into the processing of ZnS, which involve synthesis and characterization of submicron powders and their processing at elevated temperature to produce dense ceramic parts, was the main objective of this investigation. Thermomechanical characterization of the dense polycrystalline ceramics is also an integral part of such a study, and is underway. Zinc sulfide powders with submicron particle size were prepared by homogeneous precipitation from acidic zinc solutions by aging with thioacetamide at elevated temperatures. Monosize, polycrystalline particles having 0.35 micrometer diameter were obtained. Sulfide ion generation rate in solution depended on temperature, pH and initial thioacetamide concentration. The rate of sulfide ion generation, in turn, influenced precipitation kinetics and particle morphology. The types of supporting anions in solution also influenced the morphology of the particles produced. Monosize powders were hot pressed for various time, temperature and pressure combinations. Compacts achieved near-theoretical density in less than 30 minutes at temperatures 850 to 900 C and applied pressures of about 70 to 105 MPa. The dominant densification mechanisms were identified at various stages of the process.
GRA

N89-28626# Air Force Wright Aeronautical Labs., Wright-Patterson AFB, OH.
FATIGUE CRACK GROWTH-MICROSTRUCTURAL RELATIONSHIP OF Ti-6Al-4V Final Report, Sep. 1987 - Jun. 1988
Steven R. Thompson Nov. 1988 31 p
(AD-A208107; AFWAL-TR-88-4254) Avail: NTIS HC A03/MF A01 CSCL 11/6

In a previous effort the fatigue crack growth rate characteristics of Ti-6A-4V were obtained from two forgings and compared to reference data in the literature. Both the test data and the reference data were from forgings identified as being in the beta-quenched condition but the fatigue crack growth rates were different. An understanding is provided of the cause of the difference of examining the microstructure and developing additional fatigue crack growth rate (FCGR) data for the six inch thick forgings used to develop the test data. The reference data was developed on two inch thick forgings.
GRA

N89-28627*# National Aeronautics and Space Administration. Lewis Research Center, Cleveland, OH.
THE INTERFACE IN TUNGSTEN FIBER REINFORCED NIOBIUM METAL-MATRIX COMPOSITES Final Report Ph.D. Thesis - Case Western Reserve Univ., Cleveland, OH
Toni L. Grobstein Sep. 1989 81 p
(Contract DE-AI03-86SF-16310)
(NASA-TM-102122; E-4754; DOE/NASA/16310-10; NAS 1.15:102122) Avail: NTIS HC A05/MF A01 CSCL 11F

The creep resistance of tungsten fiber reinforced niobium metal-matrix composites was evaluated. The interface region between the fiber and matrix was characterized by microhardness and electron probe microanalysis measurements which indicated that its properties were between those of fiber and matrix. However, the measured properties of the composite exceeded those calculated by the rule of mixtures even when the interface zone was assumed to retain all the strength of the fiber. The composite structure appeared to enhance the strengths of both the fibers and the matrix above what they exhibited in stand-alone tests. The effect of fiber orientation and matrix alloy composition on the fiber/matrix interface were also evaluated. Small alloying additions of zirconium and tungsten to the niobium matrix affected the creep resistance of the composites only slightly. A decrease in the creep resistance of the composite with increasing zirconium content in the matrix was ascribed to an increase in the diffusion rate of the fiber/matrix interdiffusion reaction, and a slight increase in the creep resistance of the composite was observed with an addition of 9 w percent tungsten to the matrix. In addition, Kirkendall void formation was observed at the fiber/matrix interface; the void distribution differed depending on the fiber orientation relative to the stress axis.
Author

N89-28628# National Aeronautical Lab., Bangalore (India). Materials Science Div.
PRESSURE INDUCED ANOMALY AT Tc IN Fe78 Mo2 B20
V. Shubha and T. G. Ramesh Dec. 1988 14 p
(NAL-TM-MT-8806) Avail: NTIS HC A03/MF A01

The effect of pressure on the nature of the anomaly near the curie temperature (T sub c) in the amorphous ferromagnetic metallic glass Fe78Mo2B20 was investigated. The continuous variation in resistivity near T sub c at ambient pressure changes into a discontinuous type of transition at higher pressures. Thermoelectric Power exhibits a marked anomaly near T sub c at ambient pressure.
Author

N89-28629# Ecole Nationale Superieure des Arts et Metiers, Bordeaux (France). Lab. Arts et Metiers d'Etude de la Fatigue.
STEEL FATIGUE UNDER COMBINED LOADS [FATIGUE DES ACIERS SOUS SOLLICITATIONS COMBINEES. APPLICATION A L'ACIER 30 NCD 16]
Catherine Froustey and Serge Lasserre Oct. 1988 42 p In FRENCH
(Contract DRET-87-115)
(ETN-89-94864) Avail: NTIS HC A03/MF A01

Multiaxial fatigue tests done on 30NCD16 steel for aircraft structures are described. Combined flexion and torsion loads were applied at variable frequencies and cycles. It is concluded that the Dang Van model is the best fitted to the results obtained. It is also shown that the phase difference between types of loading has no effect on the yield limits. A design method based on the described results is presented.
ESA

N89-28630 British Aerospace Public Ltd. Co., Preston (England). Aircraft Group Warton Div.
IN-SITU ANODISING OF ALUMINIUM ALLOYS
C. Brindle Aug. 1988 19 p
(BAe/WMD/AR/GEN/00666; ETN-89-95221) Avail: British Aerospace Public Ltd. Co., Preston Lancs PR4 1AX, United Kingdom

The results of the work on aluminium alloys, for the assessment of local anodizing process or treatment, are reported. The comparison between the brush processes with and without chromic acid pickle, is made. The investigation of brush anodizing for 7000 series of aluminum alloys shows that the selectrons Alorode process provides corrosion protection as good as a conventional chromic acid anodizing. The extention of this process for use on other alloys indicates that process improvement is needed.
ESA

N89-28631 National Physical Lab., Teddington (England). Div. of Materials Applications.
EFFECT OF TEMPERATURE AND H2S CONTENT ON THE CRACKING RESISTANCE OF A 13 PERCENT CHROMIUM MARTENSITIC STAINLESS STEEL IN ACIDIFIED NaCl
A. Turnbull and A. T. May Dec. 1988 18 p
(NPL-DMA(A)-173; ISSN-0143-7313; ETN-89-95253) Copyright Avail: National Physical Laboratory, Teddington, Middlesex, TW11 0LW, United Kingdom

The cracking resistance of a 13 percent chromium martensitic steel (used for oil production tubing) was determined, applying the slow strain rate technique, as a function of the temperature (23 C to 80 C) and H2S content of acidified NaCl. It is observed

that a temperature increase of the solution leads to an increase in time-to-failure (for H2S concentrations less than 100 parts per million). For constant sub-surface hydrogen content an increase in time to failure, associated with reduced occupancy of reversible traps at high temperatures, is revealed. The predominant factor determining cracking is shown to be the fractional occupancy of reversible trap sites. A correlation was identified between relative time-to-failure and fractional occupancy of traps irrespective of whether the latter is obtained by varying temperature, H2S content or pH (less than or equal to 3.6). ESA

N89-28632# Helsinki Univ. of Technology, Espoo (Finland). Lab. of Metal Working and Heat Treatment.
THE INFLUENCE OF STRUCTURE AND ALLOYING ON THE COLD-FORMABILITY OF FERRITIC STEELS AND THE UTILITY OF UNIAXIAL TENSILE TESTING IN ITS ASSESSMENT Ph.D. Thesis
Vesa Ollilainen 1988 104 p Sponsored by the Academy of Finland and the Ovako Steel Oy Ab
(ISBN-952-90044-3-5; ETN-89-95180) Avail: NTIS HC A06/MF A01

The dependence of the cold-formability of ferritic steels on their structure and alloying is studied. The assessment of cold-formability is based on material parameters. Attention is paid to the effects of chromium on the yield stress. The applicability of material parameters describing stress-strain relationship, especially strain-hardening, and those predicting ductility in terms of formability maps, is evaluated. The utility of the uniaxial tensile testing in the assessment of cold-formability is discused. It is shown that: chromium affects the yield stress of ferritic irons through three mechanisms; double eta behavior is favored by a coarse grain size and by a fine distribution of a non-deformable NbC particles; the use of eta value as a measure of the rate of strain hardening is misleading; an entire formability map for ferritic sheet steels may be predicted from parameters determined in a uniaxial tensile test; and that by lowering the yield and flow stress, chromium alloying and a coarse grain size the cold-formability of ferritic steels, is improved. ESA

27 NONMETALLIC MATERIALS

Includes physical, chemical, and mechanical properties of plastics, elastomers, lubricants, polymers, textiles, adhesives, and ceramic materials.

For composite materials see *24 Composite Materials.*

N89-28633# Massachusetts Inst. of Tech., Cambridge.
THE MIT/MARINE INDUSTRY COLLEGIUM: NOVEL APPLICATIONS OF MARINE BIOPOLYMERS
John Moore, Jr., ed. 13 Apr. 1989 26 p Workshop held in Cambridge, MA, 13 Apr. 1989
(Grant NA86AA-D-SG089; MIT Proj. A-1)
(PB89-182950; MITSG-89-7; OPPORTUNITY-BRIEF-54) Avail: NTIS HC A03/MF A01 CSCL 11C

Polymers produced by marine plants and animals have been long valued as food and industrial ingredients. Recent developments in biotechnology, enzyme technology, and food and biochemical engineering have lead to new applications for these marine biopolymers. In the biomedical field, research is under way to develop a process for the encapsulation of mammalian cells prior to a transplantation operation. Within the food industry, marine biopolymers have always played an important role, such as stabilizers, and gelling ingredients, etc. Several research projects were undertaken to devise new applications for marine biopolymers in the food industry. These include: chitosan fibers, films and globules; encapsulation of biologicals with chitosan; fluorescence sensor for food and oil deterioration; stabilization of alcohol oxidase by entrapment in alginate beads; complex marine biopolymer coacervate capsules in plant technology; and, microencapsulated liposomes (the use of alginates for drug delivery systems). GRA

N89-28634# Lehigh Univ., Bethlehem, PA. Dept. of Chemistry.
INFRARED STUDY OF CARBON DEPOSITS ON CATALYSTS
R. P. Eischens 1989 10 p Presented at the Worldwide Catalysis Seminar: Successful Design of Catalysts, Philadelphia, PA, 5 Jul. 1989
(Contract DE-FG02-86ER-13612)
(DE89-013310; CONF-890792-1) Avail: NTIS HC A02/MF A01

The deposition of carbon on alumina and on catalysts, in which alumina was the support for platinum and rhenium, was followed by simultaneously weighing the total deposit and observing the infrared spectra. At total carbon deposit levels of 1 percent or less, produced by exposure to acetylene at 525 K or ethylene at 625 K, bands were observed near 1580 and 1470 cm sup minus 1. Isotopic labeling with oxygen-18 and deuterium shows that these bands are attributable to the asymmetric and symmetric stretching vibrations of a carbon-oxygen species similar to a carboxylate ion. This species involves about one-sixth of the total carbon in deposits on alumina. Platinum does not markedly affect the total carbon or the fraction that is carboxylate. Rhenium does not affect the total carbon but it significantly lowers the carbon-oxygen species. Pretreatment of desulfurization catalysts with ammonia reduces the total carbon by about one-half and almost eliminates carboxylate formation. Carboxylates are not found in carbon deposits on silica. DOE

N89-28635# Tulsa Univ., OK.
METALLIC BONDING TO HIGH-TEMPERATURE SUPERCONDUCTING CERAMICS
Douglas C. Hague, V. A. Maroni, and John H. Meiser (Argonne National Lab., IL.) 1989 6 p Presented at the 3rd National Conference on Undergraduate Research, San Antonio, TX, 27-29 Apr. 1989 Submitted for publication
(Contract W-31-109-eng-38)
(DE89-014668; CONF-8904238-1) Avail: NTIS HC A02/MF A01

Yttrium-barium-copper-oxide (123) superconducting ceramic pellets where obtained from J. P. Singh and K. C. Goretta at Argonne National Laboratory (ANL). The pellets were prepared in accordance with established methods. The pellets were then thermocompressively bonded by the methods of Meiser, et al. The resistivities of the samples were determined using a Keithley 181 Nanovoltmeter and a Keithley 227 Current Source. The resistances were taken over a range of 0.1 amp to 1 amp and were converted to interfacial resistivities. A simple tensile test was also applied to the samples to determine bond strengths. DOE

N89-28636# Oak Ridge National Lab., TN.
MICROWAVE SINTERING OF CERAMICS
W. B. Snyder 1989 5 p Presented at the International Congress on Technology and Technology Exchange, New York, NY, 28 Jun. 1989
(Contract DE-AC05-84OR-21400)
(DE89-014769; CONF-8906135-2) Avail: NTIS HC A02/MF A01

Successful adaptation of microwave heating to the densification of ceramic materials require a marriage of microwave and materials technologies. Using an interdisciplinary team of microwave and materials engineers, the ability to density ceramic materials over a wide range of temperatures was successfully demonstrated. Microstructural evolution during microwave sintering was found to be significantly different from that observed in conventional sintering. The results and those of others indicate that microwave sintering has the potential to fabricate components to near net shape with mechanical properties equivalent to hot pressed or hot isostatically pressed material. DOE

N89-28637# Harvard Univ., Cambridge, MA. Dept. of Chemistry.
MONOLAYERS OF 11-TRICHLOROSILYLUNDECYL THIOACETATE: A SYSTEM THAT PROMOTES ADHESION BETWEEN SILICON DIOXIDE AND EVAPORATED GOLD Interim Technical Report

Stephen R. Wasserman, Hans Biebuyck, and George M. Whitesides May 1989 46 p Submitted for publication
(Contract N00014-85-K-0898; NR Proj. 356-856)
(AD-A208266; TR-16) Avail: NTIS HC A03/MF A01 CSCL 07/4

This chapter describes the use of sulfur-containing organic monolayers to improve the adhesion of gold to silicon substrates having a native silicon dioxide surface layer. Gold adheres to clean silicon, but not to silicon dioxide. The affinity of gold toward silicon dioxide can be improved by coating with chromium or titanium films or by adding interlayers containing fluoride salts. Bombardment of gold-covered silicon dioxide with electrons or heavy ions also enhances adhesion. Thin covalently-bonded alkylsiloxane films containing amines or epoxides improve the adherence of gold to glass. Here we demonstrate that covering a Silicon/Silicon dioxide substrate with a covalently attached organic monolayer film containing thiol groups (and possibly disulfides derived from them) or thioacetate groups improves the adhesion of gold to the substrate. GRA

N89-28638# Missouri Univ., Rolla. Dept. of Chemistry.
CHARACTERIZATION OF SUBSTITUTED PHENOL-FORMALDEHYDE RESINS USING SOLID-STATE CARBON-13 NMR Interim Report, Apr. 1988 - 22 May 1989
Frank D. Blum, Brijnaresh R. Sinha, and Daniel OConnor (Cardolite Corp., Newark, NJ.) 22 May 1989 15 p Revised Submitted for publication
(Contract N00014-88-K-0109; NSF DMR-86-16789)
(AD-A208745; UMR-FDB-9) Avail: NTIS HC A02/MF A01 CSCL 07/6

Crosslinked substituted phenol formaldehyde resins were synthesized from cashew nut shell liquid, 3-n-pentadecylphenol and phenol with formaldehyde. The resulting resins were crosslinked and then investigated using carbon-13 NMR in the solid state using cross-polarization, magic angle spinning, and dipolar decoupling. Comparisons were made between the spectra of pure phenol-formaldehyde and modified phenol-formaldehyde resins and it was shown possible to distinguish between the resins. It was also shown that the proton-dephased spectrum gave better spectral resolution for the substituted compounds. In addition the solid carbon-13 technique verified that the degradation of the substituted phenolic resins occurs first with the degradation of the side chain in agreement with suggestions from earlier work. GRA

N89-28639# Stanford Univ., CA. Dept. of Chemical Engineering.
LITHOGRAPHY AND SPECTROSCOPY OF ULTRATHIN LANGMUIR-BLODGETT POLYMER FILMS Technical Report No. 16, 1 Jun. 1988 - 31 May 1989
S. W. Kuan, P. S. Martin, L. L. Kosbar, C. W. Frank, and R. F. Pease 30 May 1989 23 p Submitted for publication
(Contract N00014-87-K-0426)
(AD-A208970) Avail: NTIS HC A03/MF A01 CSCL 20/12

Ultrathin (0.9 to 15.3 nm) poly (methyl methacrylate) (PMMA) and (30 to 40 nm) novolac/diazoquinone films prepared by the Langmuir-Blodgett (LB) technique were explored as high resolution electron beam resists and photoresists, respectively. One-eighth micron lines-and-spaces patterns were achieved in PMMA using the Perkin Elmer MEBES I pattern generation system as the exposure tool. The etch resistance of PMMA films with thicknesses greater than 4.5 nm is sufficient to allow patterning of chromium film suitable for photomask fabrication. One micron lines-and-spaces patterns were fabricated by optical lithography in 30 nm thick novolac/diazoquinone films, and etched into 50 nm of chromium. Monolayer PMMA films containing 5 mol percent pyrenedodecanoic acid (PDA) is a probe were prepared by transfer to a quartz substrate at different surface pressures and characterized by fluorescence spectroscopy. The ratio of excimer to monomer emission intensity (Ie/Im) has a maximum value at 10 dyn/cm, which is suggestive of a structural rearrangement occurring in the Langmuir film at the surface pressure. GRA

N89-28640# Connecticut Univ., Storrs.
MICROCELLULAR FOAMS FROM RIGID-ROD POLYMERS IN SOLUTIONS: EFFECT OF AGGREGATION CHARACTERISTICS ON FOAM PROPERTIES Final Report, Mar. 1986 - Feb. 1989
M. T. Shaw and C. L. Jackson 30 Apr. 1989 5 p
(Contract DAAL03-86-G-0061)
(AD-A209024; ARO-23793.3-MS) Avail: NTIS HC A02/MF A01 CSCL 11/1

Upon cooling, solutions of rigid-rod macromolecules often form gels . These can be further processed to form microcellular materials with very regular structure. A two-stage melting of the precursor gels has been tentatively associated with a bimodal structure found in the microcellular materials. GRA

N89-28641# Northwestern Univ., Evanston, IL.
RADIOTHERMOLUMINESCENCE STUDIES OF POLYMER SOLIDS Final Report, 1 Aug. 1985 - 31 Jul. 1988
Crist Buckley, Jr. 1 Apr. 1989 36 p
(Contract DAAG29-85-K-0203)
(AD-A209036; ARO-22743.1-MS) Avail: NTIS HC A03/MF A01 CSCL 07/6

Radiothermoluminescence (RTL) involves irradiating a solid at low temperature (77K) with ionizing radiation and observing luminescence when heating the sample at a constant rate (10 K/min). Glow peaks are observed at characteristic temperatures which, for polymers, are diagnostic of the onset of thermally activated molecular motions. A scanning electron microscope (SEM) was modified to irradiate polymer samples with medium energy (5 to 30 keV) electrons. This SEM-RTL device is more convenient and reliable than other techniques which utilize remote radiation sources though information is confined to the near surface regions of the sample. In particular, the oxygen-free environment of the SEM-RTL experiment permitted observation of high temperature relaxations (up to 150 C or 423 K) for the first time in a number of thermoplastics. GRA

N89-28642# Dayton Univ., OH. Research Inst.
DAMPING PROPERTIES OF VARIOUS MATERIALS Final Report, Sep. 1985 - Oct. 1988
Michael L. Drake Mar. 1989 289 p
(Contract F33615-85-C-5040)
(AD-A209071; UDR-TR-88-122; AFWAL-TR-88-4248) Avail: NTIS HC A13/MF A01 CSCL 11/2

Complex modulus data is presented for a total of 44 materials. The material types include polymers, enamels, and structural adhesives. The complex modulus data was obtained using the ASTM E-756 standard test. The complex modulus data set for each material given contains the following information: a full page reduced frequency nomogram (FRN), a half page RFN with a list of the modulus, loss factor, and alpha sub T equations and equation parameters used to fit the data. A plot of test frequency versus test temperature. A plot of material modulus versus test temperature. GRA

N89-28643# Hughes Aircraft Co., El Segundo, CA. Electro-Optical and Data Systems Group.
HIGH TEMPERATURE ADHESIVE SYSTEMS Final Report, 25 Sep. 1985 - 24 Apr. 1989
E. H. Catsiff, T. K. Dougherty, W. E. Elias, D. J. Vachon, G. Angsten, R. W. Seibold, W. G. Knauss, S. Shimabukuro, and K. M. Liechti (Texas Univ., Austin.) Apr. 1989 224 p
(Contract N00014-85-C-0881)
(AD-A209166; HAC-REF-F7896-F) Avail: NTIS HC A10/MF A01 CSCL 11/1

Projected requirements for future high-performance jet engine, missile, and fighter aircraft structures will necessitate extensive use of high temperature structural adhesives. For example, many advanced jet engine and tactical aircraft components will need to perform for hundreds of hours at 700 F (371 C) and above. For advanced air-to-air tactical missiles and air-launched stand-off missiles, composite airframe structures capable of maintaining strength for short periods (minutes) at 1000 F (538 C) and above will be needed. Other needs for adhesives capable of performing

at high temperatures include bonding of structures for extended range cruise missiles, bonding of specialty materials for stealth applications, and, potentially, joining of aerospace plane structures. Under this program, a comprehensive technical effort was undertaken with the goal of developing high-temperature adhesive systems with inherent processibility and toughness. The approach was to perform a multidisciplinary integrated research effort involving a combination of polymer chemistry, moisture diffusion analysis, and fracture mechanics to tailor, characterize, and qualify tough adhesive systems for bonding to titanium and ferrous alloys. GRA

N89-28644# Implant Sciences Corp., Danvers, MA.
ION IMPLANTATION OF CERAMIC BEARINGS Final Report, 1 Sep. 1988 - 1 Mar. 1989
A. J. Armini and S. N. Bunker Jun. 1989 34 p
(Contract F33615-88-C-2857)
(AD-A209770; WRDC-TR-89-2088) Avail: NTIS HC A03/MF A01 CSCL 11/8

This report explores the use of ion implantation techniques to form solid lubricating surfaces on all ceramic (silicon nitride) and hybrid ball bearings. Techniques were developed to implant and/or coat silicon nitride and 52100 bearing steel with MoS2, boron, and tin ion beams. A friction/wear tester was also developed to evaluate these coatings in both air and dry nitrogen atmospheres. Friction test results have yielded durable films on both silicon nitride and 52100 steel that exhibit friction coefficients less than 0.1 in a dry state. Oil lubricated controls in a hybrid bearing also show 0.1. Other dry film processes developed have exhibited ultra-low friction (0.02 to 0.05), but these films had limited lifetime. The dry films are fairly durable and adherent but more work is needed to further improve the durability and adapt the coating process to coating complicated shapes such as balls and rings. GRA

N89-28645# Cornell Univ., Ithaca, NY. School of Chemical Engineering.
REACTIVE ION ETCHING OF POLYMER FILMS
B. C. Dems, F. Rodriguez, C. M. Solbrig, Y. M. N. Namaste, and S. K. Obendorf 12 May 1989 25 p Submitted for publication Sponsored in part by NSF
(Contract N00014-85-K-0474)
(AD-A207674; TR-10) Avail: NTIS HC A02/MF A01 CSCL 07/2

The need for nanometer sized features in integrated circuits calls for the use of dry etching techniques using glow discharge plasmas. The reactive ion etching, RIE, mode in which there is a large difference in potential between the gas phase and the solid surface yields particularly desirable, straight walled etched structures. The design of processes and materials for RIE requires a knowledge of the effects of operating variables on various parameters. In the present work, the parameter emphasized is the etch rate. A novel aspect of the apparatus used incorporates a laser interferometer for in situ measurements of etch rate. GRA

N89-28646# Naval Research Lab., Washington, DC.
ACOUSTO-OPTIC AND LINEAR ELECTRO-OPTIC PROPERTIES OF ORGANIC POLYMERIC MATERIALS
Michael E. Boyle and Robert F. Cozzens 27 Apr. 1989 35 p
(AD-A207974; NRL-MR-6454) Avail: NTIS HC A03/MF A01 CSCL 07/6

The potential of organic polymeric materials for use in acoustooptic and electrooptic devices operating at GHz frequencies is examined. This is accomplished by identifying and briefly discussing the important molecular properties for enhanced acoustooptic and electrooptic effects and then relating these to current polymeric materials. GRA

N89-28647# Akron Univ., OH. Inst. of Polymer Science.
PULL-OUT AND PUSH-OUT TESTS FOR RUBBER-TO-METAL ADHESION
A. N. Gent and S. Y. Kaang May 1989 28 p
(Contract N00014-85-K-0222)
(AD-A208100; TR-18) Avail: NTIS HC A03/MF A01 CSCL 14/2

A steel rod embedded in a rubber block can be debonded either by pulling it out or by pushing it out. A comparison is made between the two failure forces. It is shown that friction, aggravated by the tendency of rubber to undergo Poissonian contraction as the block is stretched, makes the pull-out force much higher for rods of large diameter, deeply embedded in the block. On the other hand, the push-out experiment is difficult to carry out because of the inherent instability of tall blocks in compression. Thus, pull-out is still the preferred way of measuring adhesion, but the product aL, where a is the rod radius and L the depth of embedment, should be made much smaller than the cross-sectional area of the block in order to minimize frictional contributions to failure force. GRA

N89-28648# Akron Univ., OH. Inst. of Polymer Science.
PLASTIC YIELDING OF PARTIALLY-CRYSTALLINE POLYMERS
A. N. Gent and S. Madan May 1989 39 p
(Contract N00014-85-K-0222)
(AD-A208101; TR-20) Avail: NTIS HC A03/MF A01 CSCL 07/6

Measurements are described of characteristic stress strain properties in tension for several representative partially crystalline polymers, prepared by cooling from the melt. Striking differences were found in the natural draw ratio, ranging from 2X to 11X. They are interpreted in terms of a simple molecular model of the yielding process in which polymer chains, folded to different degrees in the crystallites, are pulled taut. Values of yield and draw stress were found to be of the same order as the free energy Um of melting, suggesting that yielding and drawing take place by stress-induced disruption of crystallites, analogous to melting. The mechanical work of drawing was similar to, but generally larger than, that required for melting, ranging from Um to about 4Um. The difference is attributed to strain energy of drawn material and possible recrystallization during drawing. GRA

N89-28649# Northrop Corp., Hawthorne, CA. Aircraft Div.
EMERGING RESIN CHARACTERIZATION Interim Report, 29 Jul. 1987 - 29 Jul. 1988
Paul J. Dynes 30 Apr. 1989 28 p Prepared in cooperation with University of Dayton Research Inst
(Contract F33615-87-C-5223)
(AD-A208173; WRDC-TR-89-4016) Avail: NTIS HC A03/MF A01 CSCL 07/3

The synthesis of a bisbenzocyclobutene (BCB) -terminated aromatic imide oligomer has been completed. This BCB oligomer resin was prepared from the condensation reaction of two moles of 2,2-bis (4-pthalic anhydrido)- hexafluoropropane, one mole of m-phenylenediamine and two moles of 4-aminobenzocyclobutene. The 4-aminobenzocyclobutene was prepared from the nitration and subsequent hydrogen reduction of benzocyclobutene obtained from Dow Chemical. Approximately 1,200 grams of the BCB oligomer resin have been prepared. Preliminary High Performance Liquid Chromatography (HPLC) and Differential Scanning Calorimetry (DSC) analyses indicated this material to be equivalent to BCB oligomer resin previously synthesized by the materials laboratory. GRA

N89-28650# Societe Nationale Elf Acquitaine, Paris (France).
TGMDA/DDS TYPE IMPREGNATING RESINS STRUCTURAL STUDY Final Report [ETUDE STRUCTURALE DES RESINES D'IMPREGNATION TYPE TGMDA-DDS]
P. Horny Jan. 1988 108 p In FRENCH
(Contract DRET-86-443)
(SNEA-9595; ETN-89-94865) Avail: NTIS HC A06/MF A01

Liquid chromatography was used to isolate the main constituants of the Lopox B 3302 resin and one of the main impurities. The TGMDA/DDS systems were cross-linked and measured using

differential scanning calorimetry, water absorption, and solvent extraction. The detailed results are given. ESA

N89-28651*# National Aeronautics and Space Administration. Lewis Research Center, Cleveland, OH.
ARC-TEXTURED HIGH EMITTANCE RADIATOR SURFACES Patent Application
Bruce A. Banks, inventor (to NASA) 18 Jul. 1989 11 p
(NASA-Case-LEW-14679-1; NAS 1.71:LEW-14679-1; US-Patent-Appl-SN-381240) Avail: NTIS HC A03/MF A01 CSCL 11C

High emittance radiator surfaces are produced by arc-texturing. This process produces such a surface on a metal by scanning it with a low voltage electric arc from a carbon electrode in an inert environment. NASA

N89-28652# Southampton Univ. (England). Inst. of Sound and Vibration Research.
DEVELOPMENT OF DAMPING TREATMENT SUITABLE FOR HIGH TEMPERATURE ENVIRONMENT
L. C. Chow and R. J. Pinnington Jan. 1989 131 p Sponsored by the Central Electricity Generating Board, United Kingdom
(ISVR-TR-174; ETN-89-94962) Avail: NTIS HC A07/MF A01

Attempts to find damping techniques and materials suitable for high temperature damping applications are described. The experimental work and the attempted modelling are outlined. Materials such as ceramic fiber materials polymer and enamel coating materials have been tested for their damping effectiveness at temperatures between 200 and 650 C. The design of test rigs for high temperature damping tests is described. Results obtained using such rigs are compared to those obtained using a dynamic mechanical thermal analyzer. ESA

N89-28653# Kernforschungsanlage, Juelich (Germany, F.R.). Projedktleitung Material- und Rohstofforschung.
SURVEY OF TEST PROCEDURES FOR HIGH PERFORMANCE CERAMIC MATERIALS AND THEIR FUNDAMENTALS [PRUEFVERFAHEN KERAMISCHER HOCHLEISTUNGSWERKSTOFFE UND DEREN GRUNDLAGEN: EINE UEBERSICHT]
Wolfgang Kollenberg Oct. 1988 73 p In GERMAN
(JUEL-Spez-470; ISSN-0343-7639; ETN-89-94596) Avail: NTIS HC A04/MF A01

The status of known test procedures for high performance ceramics is outlined, and their characteristics are discussed. For the description of the bending strength two fully developed methods, the four point tending test and the double ring test, are available; the tensile test is not yet fully developed. For the testing of cracking and fracture toughness many methods are used, but they give different, noncomparable results; a standard procedure is required here. For the determination of the hardness and the thermal properties the existing method (e.g. for testing of glass) can be modified and applied to ceramics. ESA

N89-28654# Universiteit Twente, Enschede (Netherlands). Faculty of Applied Mathematics.
A GRAPH-THEORETICAL APPROACH TO BLOCK-CO-POLYMER COMPLEXES. PART 1: STARS
Bernard J. Geurts and Ruud vanDamme Dec. 1988 10 p
(Memo-757-Pt-1; ISSN-0169-2690; ETN-89-95122) Avail: NTIS HC A02/MF A01

In a sequence of three articles, of which this is the first, rheological properties of block-co-polymers in solution are examined. A configuration sum of such systems, using a graph theoretical approach is attempted. Block-co-polymers consisting of a small molecule in a poor solvent and a long flexible polymer in a good solvent are investigated, where the small molecule parts cluster together forming star molecules containing a certain number of block-co-polymers. The statistical properties of these star molecules are derived for the cases of disregarded and included topological hindrance effects using the methods of equilibrium statistical physics. The increase in the viscosity of this system as a function of the block-co-polymer density, called the density dependence of the viscosity, is derived, under the assumption that the star molecules can be treated as uniform porous spheres, in order to gain insight into the size of the star molecule. The configuration sum of this system is derived and the relation between the viscosity and the size distribution of the star molecules is shown. Cases where the arms of the stars have no mutual non-self interaction and in which excluded volume interaction are accounted are considered. ESA

N89-28655# Universiteit Twente, Enschede (Netherlands). Faculty of Applied Mathematics.
A GRAPH-THEORETICAL APPROACH TO BLOCK-CO-POLYMER COMPLEXES. PART 2: TREE APPROXIMATION
Bernard J. Geurts and Ruud vanDamme Dec. 1988 32 p
(Memo-758-Pt-2; ISSN-0169-2690; ETN-89-95123) Avail: NTIS HC A03/MF A01

In a sequence of three articles, of which this is the second, rheological properties of block copolymers in solution are examined. A configuration sum of such systems, using a graph theoretical approach is attempted. The statistical physics of a system of linear, two-component block copolymers in solution are determined assuming these complexes have the topological structure of a tree or a line-dressed tree. The tree structure system is shown to undergo a gelation transition at sufficiently high polymer concentration and the transition is shown to be absent for the line-dressed tree structure system. From these results, the influence of the assumption of the topological structure is shown to be relevant for the statistical properties of the system. The average size of the complexes is determined and the viscosity of the system is calculated assuming that the complexes can be geometrically treated as porous spheres. Predictions for the viscosity of the two cases considered are compared. ESA

N89-28656# Technische Univ., Delft (Netherlands). Engineering Design Section.
A STUDY OF THE ULTRAVIOLET DEGRADATION EMBRITTLEMENT OF POLYPROPYLENE POLYMER Ph.D. Thesis
G. E. Schoolenberg 1988 216 p
(ISBN-90-9002498-0; ETN-89-95458) Avail: NTIS HC A10/MF A01

The effects of weathering on the mechanical reliability of plastic products is investigated. Weathering under outdoor conditions, due mainly to UV-light and only secondarily to heat and humidity is studied. A method, which uses mechanical concepts for the prediction of the reliability of plastic products exposed to outdoor conditions is developed. The use of this method in helping to establish design parameters, such as the type of polymer user for a certain purpose, its dimensions and geometry, and predictions of its load bearing abilities over a projected life-time, is outlined. The method developed does not allow for the prediction of loadability of plastic products, but the relationship between chemical effects and the mechanical loadability is established. ESA

28 PROPELLANTS AND FUELS

Includes rocket propellants, igniters, and oxidizers; their storage and handling procedures; and aircraft fuels.

For related information see also *07 Aircraft Propulsion and Power, 20 Spacecraft Propulsion and Power,* and *44 Energy Production and Conversion.*

N89-28657# Midwest Research Inst., Golden, CO. Solar Energy Research Inst.
FUELS FROM MICROALGAE
Jun. 1989 42 p
(Contract DE-AC02-83CH-10093)
(DE88-001192; SERI/SP-320-3396) Avail: NTIS HC A03/MF A01

Many species of aquatic plants can provide a source of renewable energy. Some species of microalgae, in particular,

produce lipids (oils) that can be extracted and converted to a diesel fuel substitute or to gasoline. Since 1979 the Aquatic Species Program element of the Biofuels Program, has supported fundamental and applied research to develop the technology for using this renewable energy resource. This document, produced by the Solar Technical Information Program, provides an overview of the DOE/SERI Aquatic Species Program element. Chapter 1 is an introduction to the program and to the microalgae. Chapter 2 is an overview of the general principles involved in making fuels from microalgae. It also outlines the technical challenges to producing economic, high-energy transportation fuels. Chapter 3 provides an overview of the Algal Production and Economic Model (APEM). This model was developed by researchers within the program to identify aspects of the process critical to performance with the greatest potential to reduce costs. The analysis using this model has helped direct research sponsored by the program. Finally, Chapter 4 provides an overview of the Aquatic Species Program and describes current research. DOE

N89-28658# Midwest Research Inst., Golden, CO. Solar Energy Research Inst.
BIOFUELS TECHNICAL INFORMATION GUIDE
Apr. 1989 202 p
(Contract DE-AC02-83CH-10093)
(DE89-000894; SERI/SP-220-3366) Avail: NTIS HC A10/MF A01

This guide combines an overview of the biofuels technologies with extensive references to useful information sources. A brief history and overview of biomass applications in the United States and offers relevant information resources is presented in chapter 1. Also included are descriptions of Federal programs that address biofuels. Although the primary focus of the guide is on U.S. applications and research, Chapter 1 also reviews activities around the world. The biomass resources in the United States is surveyed in chapter 2, while chapter 3 describes technologies for producing a number of liquid and gaseous fuels. Several environmental and economic aspects of biofuels are discussed in Chapter 4. Chapters 2 through 4 focus primarily on the technologies being pursued by the U.S. Department of Energy (DOE) through the Biofuels and Municipal Waste Technology (BMWT) Division. Although this approach does not address all potential applications of biomass and wastes, it covers the majority of current U.S. research on liquid and gaseous fuels. Chapter 5 is a directory of U.S. agencies, companies, and laboratories involved in biofuels research. Each entry includes a description of the organization's activities, the address, and names of key contacts. Finally, Chapter 6 lists a variety of research tools, including bibliographies, data bases, directories, periodicals, and software. DOE

N89-28659# Pittsburgh Energy Technology Center, PA. Engineering Research Div.
STRUCTURAL DEFINITION OF SYNTHETIC FUELS: WILSONVILLE 1
M. B. Perry, C. E. Schmidt, and C. M. White May 1989 74 p
(DE89-013627; DOE/PETC-TR/89/6) Avail: NTIS HC A04/MF A01

The results of an in-depth characterization of products formed from Wilsonville Run 245 is summarized. Specifically, the Thermal Hydrocracker, Catalytic Hydrotreater, and Thermal Hydrocracker vacuum still bottom products were further distilled into well defined, narrow boiling range distillates. The physical, chemical, and thermodynamic properties of these distillates were measured, including specific gravity, refractive index, boiling point, elemental composition, viscosity, number-average molecular weight, and others. These results were then empirically correlated with one another. DOE

N89-28660# Los Alamos National Lab., NM.
NUMERICAL SIMULATION OF THE SIMULTANEOUS DETONATION OF TWO IDENTICAL, FULLY CONTAINED EXPLOSIONS
Bruce C. Trent Jul. 1989 81 p
(Contract W-7405-eng-36)
(DE89-014844; LA-11294-MS) Avail: NTIS HC A05/MF A01

It has been proposed that a multiburst environment may have certain advantages over a single burst for driving a stress wave with given characteristics to a particular depth. This report describes a numerical study performed with the SHALE code to look at the simultaneous detonation of two fully contained, identical 500-kt bursts. Calculations are presented that show the distance a given peak stress is propagated in a low-porosity, saturated limestone and how this distance is enhanced if the stress waves from two bursts, with known separation, are allowed to interact. DOE

N89-28661# Southwest Research Inst., San Antonio, TX. Fuels and Lubricants Research Facility.
A SURVEY OF JP-8 AND JP-5 PROPERTIES Interim Report, Oct. 1987 - Sep. 1988
J. N. Bowden, S. R. Westbrook, and M. E. LePera (Army Research and Development Lab., Fort Belvoir, VA.) Sep. 1988 111 p
(Contract DAAK70-87-C-0043; DA Proj. 1L2-63001-D-150)
(AD-A207721; BFLRF-253) Avail: NTIS HC A06/MF A01
CSCL 21/4

With the help of the Defense Fuel Supply Center, JP-8, Jet A-1, and JP-5 samples from worldwide sources, representing tenders of products destined for Department of Defense bases, have been received at Belvoir Fuels and Lubricants Research Facility at Southwest Research Institute for evaluation. Inspection data for each sample on DD Form 250 or other data reporting form were also received and entered into a data base. The evaluation of these samples consisted of a few inspection tests for comparison with the data provided by the supplier, and tests related to the use of these fuels in diesel engines, which were measured cetane number, calculated cetane indices by two methods, net heat of combustion, and kinematic viscosity measurements at 40 and 70 C. GRA

N89-28662# Pennsylvania State Univ., University Park. Dept. of Mechanical Engineering.
MODELING OF HOT FRAGMENT CONDUCTIVE IGNITION OF SOLID PROPELLANTS WITH APPLICATION TO MELTING AND EVAPORATION OF SOLIDS Final Report
K. K. Kuo, W. H. Hsieh, and K. C. Hsieh Dec. 1988 94 p
Presented at the 24th JANNAF Combustion Meeting, Monterey, CA, 5-9 Oct. 1987 and the 10th International Symposium on Ballistics, San Francisco, CA, 27-29 Oct. 1987 Submitted for publication
(Contract DAAK11-83-C-0015)
(AD-A207727; BRL-CR-607) Avail: NTIS HC A05/MF A01
CSCL 19/1

A comprehensive theoretical model has been formulated for studying the degree of vulnerability of various solid propellants being heated by hot spall fragments. The model simulates the hot fragment conductive ignition (HFCI) processes caused by direct contact of hot inert particles with solid propellant samples. The model describes the heat transfer and displacement of the hot particle, the generation of the melt (or foam) layer caused by the liquefaction, pyrolysis, and decompression of the propellant, and the regression of the propellant as well as the time variation of its temperature distributions. To partially validate the theoretical model in the absence of the necessary chemical kinetic data, an ice-melting and evaporation experiment was designed and conducted. These experiments provide features of the conductive heating, melting, and evaporating process. Calculated results compare well with experimental data in temperature-time traces, spall particles-sinking velocity, and displacement. GRA

N89-28663# Ballistic Research Labs., Aberdeen Proving Ground, MD.
EFFECT OF HYDRAULIC FLUID ON HYDROXYLAMMONIUM NITRATE BASED LIQUID PROPELLANT FORMULATIONS
Madelyn M. Decker and Cris A. Watson Apr. 1989 24 p
(AD-A208061; BRL-TR-2986) Avail: NTIS HC A03/MF A01
CSCL 21/9

Seven hydrocarbon based hydraulic fluids were evaluated for

compatibility with hydroxylammonium nitrate based liquid propellants, LGP 1846 and LGP 1845. The results did not indicate changes in the oxidizer-to-fuel ration or nitric acid concentration due to the presence of hydraulic fluid contamination. Discoloration of the liquid propellant and several hydraulic fluids was observed and ascribed to leeching of dye from the hydraulic fluid and not decomposition. The effect of hydraulic fluid contamination on the ignition and combustion of the HAN-based liquid propellant LGP 1845 was also investigated using a closed bomb. The results did not indicate significant differences in the pressure rise rate or the ignition energy for most of the fluid/propellant combinations. However, slight decreases in the pressure rise rate were noted for two of the hydraulic fluid propellant combinations. The fluid Brayco 783, chosen for the liquid propellant 155-mm program, did not effect the ignition and low pressure combustion of the propellant LGP 1845. GRA

N89-28664# Lyon-1 Univ., Villeurbanne (France).
SYNTHESIS OF MONOMETHYLHYDRAZINE Final Report [SYNTHESE DE LA MONOMETHYLHYDRAZINE]
M. Giudice, M. Ferriol, and M. T. SaugierCohen-Adad Jan. 1989 87 p In FRENCH
(Contract DRET-84-062)
(ETN-89-94863) Avail: NTIS HC A05/MF A01

A fundamental study of the chemical reactions of monomethylhydrazine was carried on, a pilot unit was built to verify the feasibility of the method, and a separation procedure was defined. The results presented were obtained at atmospheric pressure. An industrial procedure would require higher operating pressure. It is shown that the difficulties of synthesis and separation are comparable to those of dimethylhydrazine. ESA

29 MATERIALS PROCESSING

Includes space-based development of products and processes for commercial applications.
For biological materials see *55 Space Biology*.

N89-28665*# National Aeronautics and Space Administration. Lewis Research Center, Cleveland, OH.
MICROGRAVITY COMBUSTION SCIENCE: A PROGRAM OVERVIEW
Jan. 1989 20 p
(NASA-TM-101424; E-4524; NAS 1.15:101424) Avail: NTIS HC A03/MF A01 CSCL 12A

The promise of microgravity combustion research is introduced by way of a brief survey of results, the available set of reduced gravity facilities, and plans for experimental capabilities in the Space Station era. The study of fundamental combustion processes in a microgravity environment is a relatively new scientific endeavor. A few simple, precursor experiments were conducted in the early 1970's. Today the advent of the U.S. space shuttle and the anticipation of the Space Station Freedom provide for scientists and engineers a special opportunity, in the form of long duration microgravity laboratories, and need, in the form of spacecraft fire safety and a variety of terrestrial applications, to pursue fresh insight into the basic physics of combustion. The microgravity environment enables a new range of experiments to be performed since buoyancy-induced flows are nearly eliminated, normally obscured forces and flows may be isolated, gravitational settling or sedimentation is nearly eliminated, and larger time or length scales in experiments become permissible. The range of experiments completed to date was not broad, but is growing. Unexpected phenomena have been observed often in microgravity combustion experiments, raising questions about the degree of accuracy and completion of our classical understanding and our ability to estimate spacecraft fire hazards. Because of the field's relative immaturity, instrumentation has been restricted primarily to high-speed photography. To better explain these findings, more sophisticated diagnostic instrumentation, similar to that evolving in terrestrial laboratories, is being developed for use on Space Station Freedom and, along the way, in existing microgravity facilities. Author

N89-28666*# National Aeronautics and Space Administration. Lewis Research Center, Cleveland, OH.
NUMERICAL STUDIES OF CONVECTIVE HEAT TRANSFER IN AN INCLINED SEMIANNULAR ENCLOSURE
Lin-Wen Wang, Chain-Nan Yung, An-Ti Chai, and Nasser Rashidnia (Sverdrup Technology, Inc., Cleveland, OH.) Aug. 1989 9 p Presented at the National Heat Transfer Conference, Philadelphia, PA, 6-9 Aug. 1989; sponsored in part by ASME
(NASA-TM-102011; E-4723; NAS 1.15:102011) Avail: NTIS HC A02/MF A01 CSCL 22A

Natural convection heat transfer in a two-dimensional differentially heated semiannular enclosure is studied. The enclosure is isothermally heated and cooled at the inner and outer walls, respectively. A commercial software based on the SIMPLER algorithm was used to simulate the velocity and temperature profiles. Various parameters that affect the momentum and heat transfer processes were examined. These parameters include the Rayleigh number, Prandtl number, radius ratio, and the angle of inclination. A flow regime extending from conduction-dominated to convection-dominated flow was examined. The computed results of heat transfer are presented as a function of flow parameter and geometric factors. It is found that the heat transfer rate attains a minimum when the enclosure is tilted about +50 deg with respect to the gravitational direction. Author

N89-28667# Techno System Developments, Naples (Italy).
TOLERABLE g-LEVEL FOR FLUID SCIENCE EXPERIMENTS Final Report
Apr. 1987 85 p
(Contract ESA-R-66-525)
(TS-7-87; ETN-89-95197) Avail: NTIS HC A05/MF A01

The tolerable gravity levels for fluid and material science experiments, concerning space platforms, are investigated. The definition of the scenario of the gravity disturbances (topology and levels), the evaluation of the effects of the gravity disturbances on typical material and fluid science experiments, and the actions to be taken in order to reduce the spoiling effects of the gravity disturbances, are discussed. It is shown that the gravity level criteria, for orbiting microgravity platforms, is based on an oversimplification of the effects of the on-board gravity disturbances. Actions and recommendations for future activities are given. ESA

31 ENGINEERING (GENERAL)

Includes vacuum technology; control engineering; display engineering; cryogenics; and fire prevention.

N89-28668# Oregon State Univ., Corvallis. Dept. of Civil Engineering.
EFFECT OF ENVIRONMENTAL FACTORS ON PAVEMENT DETERIORATION. VOLUME 1: BACKGROUND AND METHODOLOGY
Gustavo Ordonez and Ted S. Vinson Nov. 1988 76 p Sponsored by in part by Oregon Dept. of Transportation, Salem
(Contract HPR-5263)
(PB89-182109; TRI-88-12-Vol-1; FHWA-OR-RD-89-04A-Vol-1)
Avail: NTIS HC A05/MF A01 CSCL 13B

A computerized model for the determination of pavement deterioration responsibilities due to load and non-load related factors was developed. The model is based on predicted pavement performance and the relationship of pavement field performance to a quantification of level of routine maintenance. Predicted performance provides the basis to quantify total pavement deterioration due to load-related factors. Field performance measurements and a quantification of level of routine maintenance are used to quantify total pavement deterioration due to load and non-load related factors. Proportionality assumptions are made to determine pavement deterioration responsibilities based on these

relationships. Volume 1 describes the performance based approach, the theoretical basis for the model, and the methodology applied to create the computer model. Volume 2 presents the software user's manual and the BASIC source code of the computer model. GRA

N89-28669# Bureau of Mines, Pittsburgh, PA. Research Center.
HAZARDS OF EXPLOSIVES DUSTS
1989 109 p
(Contract DE-AI01-88EH-79050)
(DE89-014554; DOE/EH-79050/T1) Avail: NTIS HC A06/MF A01

The Bureau of Mines has investigated the hazards of military explosives dispersed as dust clouds in a 20-L test chamber. For purposes of personnel safety, the spark ignitability of the explosives in the form of unconfined dust layers was also studied. The 20-L data show that most of the explosive dusts were capable of sustaining explosions as dust clouds dispersed in air and some dusts were even capable of sustaining explosions when dispersed in nitrogen. The finest sizes of explosive dusts were less reactive than the larger sizes; this is opposite to the particle size effect observed previously for the pure fuel dusts. The data for the explosive dusts were compared to those for pure fuel dusts. DOE

N89-28670# Alabama Cryogenic Engineering, Inc., Huntsville.
A CRYOCOOLER FOR HIGH ACCELERATION APPLICATIONS Quarterly Report No. 3, 15 Mar. - 14 Jun. 1989
Michael L. Dingus 23 Jun. 1989 4 p
(Contract N00014-88-C-0571)
(AD-A210075) Avail: NTIS HC A02/MF A01 CSCL 13/1

A decision was made to use stainless steel spacers and copper plates in the construction of the cryocooler. Calculations indicate a better design for a heat exchanger using stainless steel spacers and copper plates rather than niobium plates and glass ceramic spacers as originally planned. Feasibility of bonding copper plates to stainless steel spacers was demonstrated. Equipment for the contractor-owned heat exchanger manufacturing facility is now complete. The Leybold-Heraus sputtering system was installed and tested. All designs for the basic support hardware (gas panel, dewar supports and mounting plates) were finished. Designs for the test cryostat hardware are nearing completion. Construction of the gas handling panel for the system is complete. Mounts and supports for the dewar are complete and in place. The contractor owned Gifford-McMahon cryocooler was mounted in a suitable dewar and was tested. K.C.D.

32 COMMUNICATIONS AND RADAR

Includes radar; land and global communications; communications theory; and optical communications.

For related information see also *04 Aircraft Communications and Navigation* and *17 Space Communications, Spacecraft Communications, Command and Tracking.* For search and rescue see *03 Air Transportation and Safety,* and *16 Space Transportation.*

N89-28671# Helsinki Univ. of Technology, Espoo (Finland). Electroomagnetics Lab.
EXACT IMAGE THEORY FOR UNIAXIALLY ANISOTROPIC DIELECTRIC HALF SPACE
Ismo V. Lindell, Ari J. Viitanen, and Ari H. Sihvola Nov. 1988 26 p
(PB89-146450; ISBN-951-754-692-0; Rept-35) Avail: NTIS HC A03/MF A01 CSCL 20N

Applying TE/TM decomposition of the problem, the exact image theory, previously derived for problems involving isotropic half spaces is extended to allow uniaxial anisotropy for one of the half spaces with an axis perpendicular to the planar interface. The image functions are seen to be generalizations of the isotropic case. As an application, image functions corresponding to sea ice parameters, calculated from a mixing formula, are presented. Author

N89-28672* National Aeronautics and Space Administration. Langley Research Center, Hampton, VA.
ALMOND TEST BODY Patent
Allen K. Dominek, inventor (to NASA) (Ohio State Univ., Columbus.), Richard M. Wood, inventor (to NASA), and Melvin C. Gilreath, inventor (to NASA) 28 Feb. 1989 4 p Filed 23 May 1988 Supersedes N88-24845 (26 - 18, p 2502)
(NASA-Case-LAR-13747-1-CU; US-Patent-4,809,003; US-Patent-Appl-SN-197191; US-Patent-Class-342-165; US-Patent-Class-342-1; US-Patent-Class-342-5) Avail: U.S. Patent and Trademark Office CSCL 20N

The invention is an almond shaped test body for use in measuring the performance characteristics of microwave anechoic chambers and for use as a support for components undergoing radar cross-section measurements. The novel aspect of this invention is its shape, which produces a large dynamic scattered field over large angular regions making the almond valuable for verifying the performance of microwave anechoic chambers. As a component mount, the almond exhibits a low return that does not perturb the measurement of the component and it simulates the backscatter characteristics of the component as if over an infinite ground plane. Official Gazette of the U.S. Patent and Trademark Office

N89-28673# National Inst. of Standards and Technology, Boulder, CO. Electromagnetic Fields Div.
BIBLIOGRAPHY OF THE NIST (NATIONAL INSTITUTE OF STANDARDS AND TECHNOLOGY) ELECTROMAGNETIC FIELDS DIVISION PUBLICATIONS
Anne M. Reidy, ed. and Kathryn A. Gibson, ed. Sep. 1988 112 p
(PB89-189211; NISTIR-88/3900) Avail: NTIS HC A06/MF A01 CSCL 20N

The bibliography lists the publications by the staff of the Electromagnetic Fields Division of the National Institute of Standards and Technology for the period January 1970 through August 1988. Selected earlier publications from the Division's predecessor organizations are included. Author

N89-28674# Colorado Univ., Boulder. Optoelectronic Computing Systems Center.
PHOTONIC ARCHITECTURES FOR PERFORMING PERFECT SHUFFLE ON A TIME-DIVISION MULTIPLEXED SIGNAL
Srinivasan Ramanan and Harry F. Jordan Jan. 1989 96 p Prepared in cooperation with Colorado State Univ., Fort Collins
(Grant NSF CDR-86-22236)
(PB89-184352; OCS-TR-89-03) Avail: NTIS HC A05/MF A01 CSCL 17B

A time-slot interchange with specific reference to performing perfect shuffle within the frames of a time-division multiplexed photonic signal is ana lyzed. Different parameters for measurement based on time-slot shift are presented and used in analyzing the interchange problem and studying the power and limitation of a 2x2 photonic directional coupler. Important classes of architectures using directional couplers are developed for performing perfect shuffle on odd and even-sized frames of different lengths. Finally the basic relationship between ternary base and the 2x2 switch used in the feedback mode are brought out and used to develop minimum switch architectures. GRA

N89-28675# Naval Research Lab., Washington, DC. Plasma Theory Branch.
AN X-RAY SOURCE FOR LITHOGRAPHY BASED ON A QUASI-OPTICAL MASER UNDULATOR Interim Report
P. Sprangle, B. Hafizi, and F. Mako (FM Technologies, Inc., Alexandria, VA.) 9 May 1989 46 p
(AD-A208522; NRL-MR-6274) Avail: NTIS HC A03/MF A01 CSCL 09/3

The use of electromagnetic waves is proposed as an undulator

in order to generate X-rays in the wavelength range required for fabrication of integrated circuits. The configuration consists of a quasi optical maser cavity through which a beam of relativistic electrons is made to propagate, spontaneously emitting X-rays of the desired energy. For 5 inch silicon wafers covered with a sensitive resist such as PBS, this translates into a throughput of 26 wafers/hr using an aggressive stepper. The scaling of X-ray power with wavelength indicates that the throughput can be increased substantially using resist which are sensitive to shorter wavelength X-rays. GRA

N89-28676* National Aeronautics and Space Administration. Pasadena Office, CA.

TELEVISION MONITOR FIELD SHIFTER AND AN OPTO-ELECTRONIC METHOD FOR OBTAINING A STEREO IMAGE OF OPTIMAL DEPTH RESOLUTION AND REDUCED DEPTH DISTORTION ON A SINGLE SCREEN Patent

Daniel B. Diner, inventor (to NASA) (Jet Propulsion Lab., California Inst. of Tech., Pasadena.) 4 Apr. 1989 19 p Filed 25 Nov. 1987

(Contract NAS7-918)

(NASA-Case-NPO-17249-1-CU; US-Patent-4,819,064; US-Patent-Appl-SN-125666; US-Patent-Class-358-88; US-Patent-Class-358-91; US-Patent-Class-358-92) Avail: U.S. Patent and Trademark Office CSCL 17B

A method and apparatus is developed for obtaining a stereo image with reduced depth distortion and optimum depth resolution. Static and dynamic depth distortion and depth resolution tradeoff is provided. Cameras obtaining the images for a stereo view are converged at a convergence point behind the object to be presented in the image, and the collection-surface-to-object distance, the camera separation distance, and the focal lengths of zoom lenses for the cameras are all increased. Doubling the distances cuts the static depth distortion in half while maintaining image size and depth resolution. Dynamic depth distortion is minimized by panning a stereo view-collecting camera system about a circle which passes through the convergence point and the camera's first nodal points. Horizontal field shifting of the television fields on a television monitor brings both the monitor and the stereo views within the viewer's limit of binocular fusion.

Official Gazette of the U.S. Patent and Trademark Office

N89-28677# Naval Research Lab., Washington, DC.

RECIPROCAL PERFECT AND ASYMPTOTICALLY PERFECT PERIODIC RADAR WAVEFORMS AND THEIR APERIODIC PROPERTIES

Karl Gerlach and Frank F. Kretschmer, Jr. 24 May 1989 23 p

(AD-A208938; NRL-9059) Avail: NTIS HC A03/MF A01 CSCL 17/9

Digitally coded radar waveforms can be employed to obtain large time-bandwidth products (pulse compression ratios). A perfect periodic code is defined to be a periodic code whose autocorrelation function has zero sidelobes and whose amplitude is uniform (maximum power efficiency = 1). An asymptotically perfect periodic code has the property that as the number of elements in the code goes to infinity the code's autocorrelation function has zero sidelobes and its power efficiency is one. A new class of radar wave forms are introduced that are either perfect of asymptotically perfect codes. They are called reciprocal codes because they can be derived through a linear transformation of the known codes. The reciprocal code's aperiodic performance is examined. This is motivated by the tendency of good periodic codes to yield good aperiodic codes, and hence high pulse compression ratios with low sidelobe responses are attainable. GRA

N89-28678# Massachusetts Inst. of Tech., Lexington. Lincoln Lab.

ADAPTIVE DETECTION AND PARAMETER ESTIMATION FOR MULTIDIMENSIONAL SIGNAL MODELS

E. J. Kelly and K. M. Forsythe 19 Apr. 1989 243 p

(Contract F19628-85-C-0002)

(AD-A208971; TR-848; ESD-TR-88-333) Avail: NTIS HC A11/MF A01 CSCL 17/1

The problem of target detection and signal parameter estimation in a background of unknown interference is studied, using a multidimensional generalization of the signal models usually employed for radar, sonar, and similar applications. The required techniques of multivariate statistical analysis are developed and extensively used throughout the study, and the necessary mathematical background is provided in Appendices. Target detection performance is shown to be governed by a form of the Wilks' Lambda statistic, and a new method for its numerical evaluation is given which applies to the probability of false alarm of the detector. Signal parameter estimation is shown to be directly related to known techniques of adaptive nulling, and several new results relevant to adaptive nulling performance are obtained. GRA

N89-28679# Air Force Inst. of Tech., Wright-Patterson AFB, OH.

A METHODOLOGY FOR MODELING RADAR DETECTION RANGE IN AIR COMBAT SIMULATION M.S. Thesis

Damon Neal Lum Mar. 1989 70 p

(AD-A209153; AFIT/GST/ENS/89M-12) Avail: NTIS HC A04/MF A01 CSCL 17/9

The purpose of this thesis is to develop a methodology for modeling fighter aircraft radar detection range performance. Response surface methodology is used to form a meta-model of the TAC BRAWLER Air Combat Model. Using experimental design theory, detection range data was collected using TAC BRAWLER and regressed to develop an equation for predicting radar detection range. The resulting equation is valid for specific ranges of the target's radar cross section, altitude, and airspeed and the attacker's altitude and airspeed. GRA

N89-28680# Harry Diamond Labs., Adelphi, MD.

HEMP (HIGH-ALTITUDE ELECTROMAGNETIC PULSE) VALIDATION OF FAA (FEDERAL AVIATION ADMINISTRATION) RADIO FACILITY Final Report, Apr. - May 1987

Stephen C. Sanders May 1989 28 p

(HDL Proj. E247E4)

(AD-A209187; HDL-TM-89-5) Avail: NTIS HC A03/MF A01 CSCL 09/7

The Harry Diamond Lab. provided high-altitude electromagnetic pulse (HEMP) and partial lightning hardness verification testing to a high-frequency radio facility for the FAA. The facility consisted of a shielded enclosure with antennas and cables connected through protective devices at the shield to dummy loads within the shield. It was exposed to low-level radiation with measurements of internal fields extrapolated to threat levels and compared to specific criteria. Each typical penetration was injected with a simulated lightning source, and internal measurements were compared to specific criteria. Although criteria were not always met, it was judged with confidence that the facility would protect radio equipment. It was noted that the ac power spark gap would remain shorted until ac power shut down, resulting in system upset. GRA

N89-28681# Delaware Univ., Newark. Dept. of Mathematical Sciences.

THE INVERSE SCATTERING PROBLEM FOR ACOUSTIC AND ELECTROMAGNETIC WAVES Final Report, 1 Jun. 1986 - 31 May 1989

David Colton, Peter Monk, and R. L. Ochs 31 May 1989 6 p

(Grant AF-AFOSR-0087-86; AF Proj. 2304)

(AD-A209202; AFOSR-89-0608TR) Avail: NTIS HC A02/MF A01 CSCL 20/1

This research project was concerned with the problem of determining the physical and geometric properties of an obstacle by probing with time harmonic acoustic or electromagnetic waves. A new method has been developed to solve problems of this type based on the theory of Herglotz wave functions and complete sets of solutions to the Helmholtz and Maxwell equations. Numerical examples have been given for the case of acoustic waves. GRA

N89-28682# Air Force Inst. of Tech., Wright-Patterson AFB, OH. School of Engineering.

EVALUATION OF THE BISTATIC EQUIVALENCE THEOREM FOR THE NEAR AND FAR-FIELD RADAR CROSS SECTION OF COMPLEX TARGETS M.S. Thesis

Charles G. Walls Jun. 1989 165 p

(AD-A209228; AFIT/GE/ENG/89J-1) Avail: NTIS HC A08/MF A01 CSCL 17/9

This research examined the applicability of the monostatic-bistatic equivalence theorem (MBET) and associated extensions in determining the extent to which correlation exists between monostatic and bistatic data for both the near and far-field. A secondary objective was to determine whether reliable bistatic near-field radar cross section (RCS) data could be collected on a range originally designed to take monostatic far-field measurements. Dr. David Falconer developed two extensions of the MBET in an effort to estimate the bistatic RCS pattern in both the near and far-field by measuring the monostatic RCS pattern at one-half the bistatic angle, at a reduced frequency, and, for the near-field case, at an adjusted target-to-receiver separation range. The pattern representation and accuracy of these two extensions were examined by measuring the RCS of an ogive, a circular flat plate, and two circular cylinders of different lengths. GRA

N89-28683# Naval Postgraduate School, Monterey, CA. Dept. of Electrical and Computer Engineering.

NEC (NUMERICAL ELECTROMAGNETICS CODE), NECGS (NUMERICAL ELECTROMAGNETICS CODE-GROUND SCREEN), AND MININEC (MINI-NUMERICAL ELECTROMAGNETICS CODE) NUMERICAL MODELS OF LF TOP-HAT MONOPOLE ANTENNAS M.S. Thesis

Slamet Suharsa Padmosutoyo Mar. 1989 59 p

(AD-A209230) Avail: NTIS HC A04/MF A01 CSCL 09/1

The U.S. Navy needs to increase the power handling capability of its current VLF and LF top-hat monopole antennas. This is most efficiently studied via numerical analysis of candidate antennas. Previous computer models based on the Numerical Electromagnetics Code (NEC-3) were shown to be unacceptable. The reasons for the inaccuracies were discovered to be NEC's inability to accurately model the effects of step changes of radius on adjacent portions of the structure. This thesis investigates two additional numerical models. The first uses the MININEC SYSTEM which has been shown to be accurate for stepped-radius antennas, and the second approximates a top-hat monopole antennas by a wire-cage structure. The latter employs NECGS, a special version of NEC-3 which efficiently uses radial symmetry. The performance parameters of interest which were calculated are static capacitance, resonant frequency, effective height, and radiation resistance. The results of these new models are compared to scale-model measurements and to the numerical results of the earlier NEC-3 study. The MININEC SYSTEM product acceptable values but is limited in the number of unknowns used to describe the model. NECGS results indicate that an acceptable wire-cage equivalency to a top-hat monopole may not exist. GRA

N89-28684*# National Aeronautics and Space Administration. Pasadena Office, CA.

DIGITAL CARRIER DEMODULATOR EMPLOYING COMPONENTS WORKING BEYOND NORMAL LIMITS Patent Application

William J. Hurd, inventor (to NASA) and Ramin Sadr, inventor (to NASA) (Jet Propulsion Lab., California Inst. of Tech., Pasadena.) 12 May 1987 10 p

(Contract NAS7-918)

(NASA-Case-NPO-17628-1-CU; NAS 1.71:NPO-17628-1-CU; US-Patent-Appl-SN-350813) Avail: NTIS HC A02/MF A01 CSCL 17B

In a digital device, having an input comprised of a digital sample stream at a frequency F, a method is disclosed for employing a component designed to work at a frequency less than F. The method, in general, is comprised of the following steps: dividing the digital sample stream into odd and even digital samples streams each at a frequency of F/2; passing one of the digital sample streams through the component designed to work at a frequency less than F where the component responds only to the odd or even digital samples in one of the digital sample streams; delaying the other digital sample streams for the time it takes the digital sample stream to pass through the component; and adding the one digital sample stream after passing through the component with the other delayed digital sample streams. In the specific example, the component is a finitie impulse response filter of the order ((N + 1)/2) and the delaying step comprised passing the other digital sample streams through a shift register for a time (in sampling periods) of ((N + 1)/2) + r, where r is a pipline delay through the finite impulse response filter. NASA

N89-28685# Naval Postgraduate School, Monterey, CA.

ELECTROMAGNETIC SCATTERING FROM TWO DIMENSIONAL OBJECTS USING THE FIELD FEEDBACK FORMULATION M.S. Thesis

Thaddeus B. Welch, III Mar. 1989 150 p

(AD-A209563; AD-E900860) Avail: NTIS HC A07/MF A01 CSCL 20/14

Integral equations (IE's) are widely utilized to calculate induced currents on antennas and scatters, but they are seriously restricted in their ability to handle inhomogeneous penetrable structures having multiwavelength dimensions. The utilization of finite element (FE) techniques has not been as pervasive as the use of IE's. The IE representation matrix is full, containing few, if any, zero valued elements. The techniques for operating on these large sized full matrices require undesirable amounts of processor time. FE techniques produce sparse matrices due to the strictly local interactions between discrete unknowns. The application of FE's to unbounded problems, however, requires supplementary enforcement of the far field radiation conditions. The Field Feedback Formulation (FFF) circumvents the full-matrix computational bottleneck by allowing FE based numerical methods to be employed. Even though the resultant spare matrices may be larger than the full matrices discussed earlier, most elements have a value of zero. Numerical procedures exist to optimize operations with these sparse matrices. Calculational speeds can be orders of magnitude faster. Computer technique to implement and validate this new technique are examined. Excellent agreement with classical results are demonstrated. GRA

N89-28686# Naval Weapons Center, China Lake, CA.

SCATTERING REPRESENTATION OF WAVEGUIDE/CAVITY DISCONTINUITIES USING MODE-MATCHING AND THE LEAST-SQUARES BOUNDARY RESIDUAL Final Report, 1986-88

P. L. Overfelt Oct. 1988 54 p

(AD-A209571; AD-E900860; NWC-TP-6941) Avail: NTIS HC A04/MF A01 CSCL 20/14

In this report, a scattering matrix representation of waveguide discontinuities using mode-matching and the least-squares boundary residual is developed. GRA

N89-28687# Army Missile Command, Redstone Arsenal, AL. Directed Energy Directorate.

DESIGN OF A COMMAND, COMMUNICATIONS, AND CONTROL VAN (SURROGATE) Final Technical Report, Jun. - Nov. 1988

J. Darryl Holder and Jerome Fishback 24 Mar. 1989 28 p

(AD-A207652; AD-E951351; AMSMI/TR-RD-DE-89-1) Avail: NTIS HC A03/MF A01 CSCL 25/5

This report describes the design, construction, and checkout of a radio and telephone multi-mode communications hub. This unit is to serve as a surrogate for a command, control, and communications van which is to be used in support of a special series of testing at a remote site. This unit is assembled in a military four-wheel van and has a crew of a commander and three operators. Radio communications monitoring can be performed in all popular modes of transmission from 50 KHz to 2 GHz and transmission can be performed on selected frequencies in the

40-meter, 6-meter, and 2-meter bands. Both voice and digital (teletype, packet, facsimile, etc.) communications are supported. GRA

N89-28688# Army Construction Engineering Research Lab., Champaign, IL.
THE RELATIONSHIP BETWEEN GROUND PERMITTIVITY AND THE INPUT IMPEDANCE OF A HORIZONTAL DIPOLE NEAR GROUND Final Report
John H. Spears Apr. 1989 80 p
(AD-A207746; CERL-TM-M-89/05) Avail: NTIS HC A05/MF A01 CSCL 20/14

Transmitting antennas located near the earth have a problem with electromagnetic scattering caused by the ground. Researchers suggest that the inverse of this problem may be used to determine the complex permittivity of the ground. That application is the goal of this thesis. The solution of the half-space problem was originally formulated in 1909 by Arnold Sommerfeld. Unfortunately, his formulation was written in terms of a set of integrals that tend to have a slow rate of convergence. Since then, researchers have sought faster methods of computing fields in the presence of an arbitrary infinite half space by making approximations to Sommerfeld's integrals to increase their convergence rate. Others have replaced the ground with an equivalent image current. GRA

N89-28689# Georgia Inst. of Tech., Atlanta. School of Electrical Engineering.
TWO-DIMENSIONAL SIGNAL PROCESSING AND STORAGE AND THEORY AND APPLICATIONS OF ELECTROMAGNETIC MEASUREMENTS Annual Report, 1 Jan. - 31 Dec. 1988
R. W. Schafer and D. T. Paris 1 Jan. 1989 44 p
(Contract DAAL03-87-K-0059)
(AD-A207827) Avail: NTIS HC A03/MF A01 CSCL 17/5

This is an annual report on research conducted under the auspices of the Joint Services Electronics Program. Specific topics covered are: digital signal processing, parallel processing architectures, two-dimensional optical storage and processing, hybrid optical/digital signal processing, electromagnetic measurements in the time domain, and automatic radiation measurements for near-field and far-field transformation. GRA

N89-28690# Naval Ocean Systems Center, San Diego, CA.
QUALITY FACTOR AND STATISTICS FOR RADIATION PATTERNS OF SHIPBOARD HF ANTENNAS Final Report, Feb. 1987 - Sep. 1988
E. A. Thowless and S. T. Li Sep. 1988 30 p
(AD-A207931; NOSC/TD-1453) Avail: NTIS HC A03/MF A01 CSCL 20/14

The characteristics of various statistical entities of radiation patterns are reviewed in an effort to: improve the technical representation and definition of a figure-of-merit quality factor for antenna patterns; improve understanding of the distribution of pattern gain values; determine requirements for antenna patterns; improve understanding of the distribution of pattern gain values; determine requirements for antenna pattern statistical data for various applications; develop an improved antenna pattern statistical summary that employs the fewest numbers to provide a statistical characterization of radiation patterns. GRA

N89-28691# IIT Research Inst., Chicago, IL.
ELF (EXTREMELY LOW FREQUENCY) COMMUNICATIONS SYSTEM ECOLOGICAL MONITORING PROGRAM Progress Report, 1 Jan. - 31 Dec. 1987
John E. Zapotosky Apr. 1989 85 p
(Contract N00039-88-C-0065)
(AD-A208198; IIT-E06595-3) Avail: NTIS HC A05/MF A01 CSCL 20/14

A long-term Ecological Monitoring Program is being conducted to monitor for possible effects from the operation of the U.S. Navy's ELF Communications System to resident biota and their ecological relationships. Monitoring studies were selected through a peer reviewed, competitive bidding process in mid-1982, and work on most studies began in late summer of that year. Preliminary activities of the program consisted of site selection, characterization of critical study aspects, and validation of assumptions made in original proposals. Subsequently, increasing emphasis has been placed on the collection of preoperational and operational databases at the Michigan and Wisconsin Transmitting Facilities. The databases are being used to make proposed spatial and/or temporal comparisons of biological and ecological variables. This report summarizes the progress of the Ecological Monitoring Program during 1987. GRA

N89-28692# National Telecommunications and Information Administration, Annapolis, MD.
METEOR BURST SYSTEM COMMUNICATIONS COMPATIBILITY
David Cohen, William Grant, and Francis Steele Mar. 1989 113 p
(PB89-191167; NTIA-TR-89-241) Avail: NTIS HC A06/MF A01 CSCL 17B

The technical and operating characteristics of meteor burst systems of importance for spectrum management applications are identified. A technical assessment is included which identifies the most appropriate frequency subbands within the VHF spectrum to support meteor burst systems. The electromagnetic compatibility of meteor burst systems with other equipments in the VHF spectrum is determined using computerized analysis methods for both ionospheric and ground wave propagation modes. It is shown that meteor burst equipments can cause and are susceptible to ground wave interference from other VHF equipments. Included are tables of geographical distance separations between meteor burst and other VHF equipments which satisfy interference threshold criteria. Author

N89-28693# Nationaal Inst. voor Kernfysica en Hoge Energiefysica, Amsterdam (Netherlands).
THE BEAM VIEWER [DE BEAMVIEWER]
G. J. vanVliet and H. Nieuwenkamp 5 Oct. 1988 13 p In DUTCH
(LINO-160; ETN-89-94920) Avail: NTIS HC A03/MF A01

The beam viewer and all the related apparatus such as camera, control, drive, illumination and wiring are considered. The beam viewer is an optical control system which checks position, form, and charge distribution, of the electron beam. It consists of a hard aluminum housing mounted in the beam line. In the housing there is a fluorescent plate (the TV target) which can be moved into the beam by a set of levers. When hit by electrons, the plate emits visible radiation which is detected by a camera. The degree of lightening of the plate is a measure of the beam charge density. ESA

N89-28694# Nationaal Inst. voor Kernfysica en Hoge Energiefysica, Amsterdam (Netherlands).
VIDEO PROCESSING USING THE MSX COMPUTER [VIDEOBEWERKING MET DE MSX-COMPUTER]
G. J. vanVliet 18 Nov. 1988 17 p In DUTCH
(LINO-163; ETN-89-94921) Avail: NTIS HC A03/MF A01

The processing of video images using the Philips MSX-2 computer is considered, with a view to the processing of video signals of beam viewers and the creation of an extra control function for the beam. The structure of the video signal is outlined. The control function is realized by the mixing of video signals with an ideal computer video plate. The MSX manual and the important commands are described. ESA

N89-28695 British Aerospace Public Ltd. Co., Preston (England).
ANTENNA FUNDAMENTALS: A TUTORIAL PAPER
J. C. Robertson 7 Jan. 1988 44 p
(BAe-WAA-R-GEN-RAD-533; TNAAS-439; ETN-89-95222) Avail: British Aerospace Public Ltd. Co., Preston Lancs PR4 1AX, United Kingdom

The principles and characteristics of antennas, operating in the radio frequency band, are examined. A descriptive approach with the minimum of mathematical derivation is given. The antenna

and radiation definitions, and terms are considered. The characteristics and applications of linear, aperture and specialized antennas are emphasized. The techniques discussed can be adapted and modified to tackle and evaluate whatever new antenna types the future will offer. A list of the leading parameters of the more common, contemporary antenna types, is given. ESA

N89-28696 British Aerospace Public Ltd. Co., Preston (England).
THE AIRBORNE PULSE DOPPLER RADAR: AN INTRODUCTION TO THE BASIC PRINCIPLES
J. C. Robertson 4 Jul. 1988 50 p
(BAe-WAA-RP-GEN-RAD-584; ETN-89-95223) Avail: British Aerospace Public Ltd. Co., Preston Lancs PR4 1AX, United Kingdom

The basic principles of the airborne pulse Doppler radar are examined, to provide a foundation for the following studies on practical realizations of the pulse Doppler principle. The exploitation of the Doppler phenomenon offers the means, of discriminating among low level radar echoes from airborne targets and unwanted, strong swamping returns from such features (terrain background). It is demonstrated that the realization of the various types of practical pulse Doppler radars depends on parallel progress in the field of solid state, electronic, digital, signal processing hardware and on the development of processing algorithms. This dependency becomes vital with the demand for more versatility and multi-function capability from the compact, tactical pulse Doppler radar. It can be considered as a transducer/processor assembly to emphasize the equivalent status of the signal processing element vis a vis the front-end hardware. ESA

N89-28697 British Aerospace Public Ltd. Co., Preston (England).
AIRBORNE PULSE DOPPLER RADAR. PART 3: PERFORMANCE ESTIMATION
J. C. Robertson 20 Apr. 1989 52 p
(BAe-WAA-RP-GEN-RAD-645-Pt-3; TNAAS-445-Pt-3; ETN-89-95225) Avail: British Aerospace Public Ltd. Co., Preston Lancs PR4 1AX, United Kingdom

Techniques and methods which can be used to obtain an indication of the performance capabilities of a pulse Doppler radar, are analyzed. The effects of target fluctuation, clutter characteristics, detailed radar parameters and radar-target encounter geometry, are discussed. The basic detection theory, the analysis of signal-to-noise ratio, the determination of the target detectability, the applications of the radar equation, and the operating limitations (other than thermal noise), are outlined. It is concluded that the prediction of radar maximum range performance can never be guaranteed to be accurate in the exact sense, and precise agreement between prediction and the results of limited experimental measurement is not to be expected. ESA

N89-28698# Deutsche Forschungs- und Versuchsanstalt fuer Luft- und Raumfahrt, Oberpfaffenhofen (West Germany). Abteilung HF-Systeme.
POLARIMETRIC CALIBRATION USING PASSIVE CORNER REFLECTORS
Maurice Borgeaud Mar. 1989 29 p
(DFVLR-FB-89-21; ISSN-0171-1342; ETN-89-95316) Avail: NTIS HC A03/MF A01; DFVLR, VB-PL-DO, Postfach 90 60 58, 5000 Cologne, Fed. Republic of Germany, 12.50 DM

Polarization impurities, losses and gains in the receiver or transmitter of a radar system are taken into account using a polarimetric calibration procedure. Using only passive elements, the polarimetric calibration is carried out using one trihedral and two dihedral corner reflectors whose seams are rotated 45 degrees with respect to each other. Mathematically the procedure is equivalent to solving a nonlinear system of twelve equations with eleven unknowns. The detailed solution is presented and computer simulations are shown. ESA

N89-28699# Technische Univ., Delft (Netherlands).
DEVELOPMENT OF AN INTEGRATED AM SHORTWAVE UPCONVERSION RECEIVER FRONT-END Ph.D. Thesis
Johannes Wilhelmus T Eikenbroek 1989 166 p Sponsored by the Netherlands Foundation for Technical Sciences
(ETN-89-95455) Avail: NTIS HC A08/MF A01

Receivers in general, and the up conversion type in particular, are discussed. Noise optimization of the amplifier to the antenna is discussed. This optimization is a first requirement for maximum sensitivity of the receiver. A thorough analysis of the frequency dependent distortion performance of a differential pair used as either an automatic gain control stage or a switching mixer is presented. The design of surface acoustic wave resonators on the piezoelectric substrate material quartz is discussed. ESA

N89-28700# Swedish Inst. of Space Physics, Uppsala.
ELECTROMAGNETIC PULSE PROPAGATION THROUGH A STRATIFIED IONOSPHERE
Bengt Lundborg et al 29 Mar. 1989 56 p Sponsored by the Swedish Defence Research Establishment and the Swedish Defence Material Administration
(IRF-SR-199; ISSN-0284-1703; ETN-89-95162) Avail: NTIS HC A04/MF A01

The single path propagation of pulses or wave packets through a smooth horizontally stratified ionospheric plasma is studied. The derivation of the ray tracing equations, are obtained and the usual expressions for the group path and pulse delay time is reviewed. The ionospheric transfer function involving the rise time is obtained. The rise time is shown to be larger for the high ray and for low frequencies on the low ray, and the most favorable communication over a few hundred kilometers is shown to be obtained with the low ray. Rise times are shown to be higher for profiles with scale lengths of an ordinary ionospheric layer, and typically in the range 1 to 10 microsecond; the lower value pertaining to a steeper profile. ESA

N89-28701# Technische Univ., Delft (Netherlands).
SEGMENTATION OF NOISY IMAGES Ph.D. Thesis
Jan Jacob Gerbrands 1988 173 p
(ETN-89-95461) Avail: NTIS HC A08/MF A01

Techniques for carrying out the segmentation of images which are severely contaminated by noise are discussed. Attempts to improve performance by exploiting the spatial context and by incorporating generic a priori knoledge are described. Since accurate delineation of object regions is a priority, the research concentrates on edge-oriented methods. A sequential boundary detection method on the basis of dynamic programming is elucidated. The restricted-search dynamic programming boundary detection method is concluded to be a robust and useful tool, especially suited for application in image measurement systems. ESA

N89-28702# Office National d'Etudes et de Recherches Aerospatiales, Paris (France).
MULTITARGET TRACKING BY SINGLE SENSOR ANALYSIS OF THE MAIN APPROACHES DEVELOPED IN THIS AREA
Jean Dezert 1988 159 p In FRENCH; ENGLISH summary Original report will also be announced as translation (ESA-TT-1171)
(ONERA-NT-1988-10; ISSN-0078-3781; ETN-89-95292) Avail: NTIS HC A08/MF A01

The most important multitarget trackig methods using a single sensor system are analyzed, based on a bibliographical review. Two basic approaches are proposed: the Bayes decision rule approach, and the maximum likelihood approach. The methods using the Bayes decision rule approach are superseding those based on the maximum likelihood theory and special attention is therefore devoted to them in this analysis. ESA

N89-28703# Office National d'Etudes et de Recherches Aerospatiales, Paris (France).
A METHOD FOR ASSISTING IN DECISION-MAKING FOR MULTILAYER RADAR ABSORBENT COVERINGS Ph.D. Thesis - Paris VI Univ.
Annie Bastiere 1989 250 p In FRENCH; ENGLISH summary Original report will also be announced as translation

(ESA-TT-1173)
(ONERA-NT-1989-2; ISSN-0078-3781; ETN-89-95294) Avail: NTIS HC A12/MF A01

A multicriteria optimization method for multi-layer radar absorbent coverings destined for use with existing aircraft is presented. This technique first uses an optimization procedure with nonlinear constraints, specifically the generalized projected gradient method. Next, the application of a modified multi-criteria decision theory fuses several design criteria and provides decision assistance to the designer. The method permits the use of three fusion laws, one based on the Dempster-Shafer theory of evidence, and two based on fuzzy set theory. Experimental results of the proposed method are presented. They concern materials of the same class configured with three layers, as well as materials of different classes configured with one to five layers. ESA

N89-28878# Joint Publications Research Service, Arlington, VA.
A BISTATIC PARASITICAL RADAR (BIPAR)
Philipp Hartl and Hans Martin Braun *In its* JPRS Report: Science and Technology. USSR: Space. 16th International Congress of the International Society for Photogrammetry and Remote Sensing, Volume 1 30 Jan. 1989 p 11-19 Transl. into ENGLISH from International Archives of Photogrammetry and Remote Sensing (Kyoto, Japan), v. 27, 1988 p 45-53 (For primary document see N89-28876 23-43)
Avail: NTIS HC A12/MF A01

N89-28882# Joint Publications Research Service, Arlington, VA.
KRAS: A DANISH HIGH RESOLUTION AIRBORNE SAR
Soren Norvang Madsen, Erik Lintz Christensen, and Niels Skou *In its* JPRS Report: Science and Technology. USSR: Space. 16th International Congress of the International Society for Photogrammetry and Remote Sensing, Volume 1 30 Jan. 1989 p 48-57 Transl. into ENGLISH from International Archives of Photogrammetry and Remote Sensing (Kyoto, Japan), v. 27, 1988 p 90-97 (For primary document see N89-28876 23-43)
Avail: NTIS HC A12/MF A01

N89-28887# Joint Publications Research Service, Arlington, VA.
SAR ACTIVITIES AT DORNIER
Hans Martin Braun and Gerhard Hans Rausch *In its* JPRS Report: Science and Technology. USSR: Space. 16th International Congress of the International Society for Photogrammetry and Remote Sensing, Volume 1 30 Jan. 1989 p 98-104 Transl. into ENGLISH from International Archives of Photogrammetry and Remote Sensing (Kyoto, Japan), v. 27, 1988 p 44-50 (For primary document see N89-28876 23-43)
Avail: NTIS HC A12/MF A01

N89-28913# Joint Publications Research Service, Arlington, VA.
NOISE REDUCTION FROM SYNTHETIC APERTURE RADAR IMAGERY
Olli Sirkia *In its* JPRS Report: Science and Technology. USSR: Space. 16th International Congress of the International Society for Photogrammetry and Remote Sensing, Volume 2 31 Jan. 1989 p 96-101 Transl. into ENGLISH from International Archives of Photogrammetry and Remote Sensing (Kyoto, Japan), v. 27, pt. B9, 1988 p 329-336 (For primary document see N89-28903 23-43)
Avail: NTIS HC A09/MF A01

33 ELECTRONICS AND ELECTRICAL ENGINEERING

Includes test equipment and maintainability; components, e.g., tunnel diodes and transistors; microminiaturization; and integrated circuitry.

For related information see also *60 Computer Operations and Hardware* and *76 Solid-State Physics.*

N89-28704# Helsinki Univ. of Technology, Espoo (Finland). Electronic Circuit Design Lab.
HIGHER ORDER BASE DYNAMICS OF A BIPOLAR TRANSISTOR WITH NONUNIFORM DOPING
Markku Sipila Jan. 1989 22 p
(PB89-155451; Rept-6; ISBN-951-754-726-9) Avail: NTIS HC A03/MF A01 CSCL 09A

The modeling of bipolar transistors is studied in the case when the quasi-static assumption does not hold, i.e., the base and collector currents follow the controlling voltages not at once, but with certain time delays. In the case of nonuniform base doping, the magnitudes of these delays are calculated by first solving numerically the minority carrier distribution in the base region. A simple but realistic model for the doping density is presented. A higher order carrier distribution is then found, enabling one to obtain the time delays. They are found to be slightly larger but in the same order of magnitude compared to the base transit time as in the case of constant base doping, although the transit time is greatly diminished due to the base doping gradient. Author

N89-28705# Department of the Army, Washington, DC.
OPTICAL GAIN CONTROL OF GaAs MICROWAVE MONOLITHIC INTEGRATED CIRCUIT DISTRIBUTED AMPLIFIER Patent Application
Arthur Paolella, inventor (to Army) and Peter R. Herczfeld, inventor (to Army) 27 Feb. 1989 19 p
(AD-D013969; US-Patent-Appl-SN-316358) Avail: NTIS HC A03/MF A01 CSCL 09/5

An optical gain control circuit for controlling the gain of a GaAs MMIC distributed amplifier having a dc gain control is provided. Variable intensity light from a controlled LED is directed to the surface of a GaAs multi-finger FET by means of an optical fiber. The FET is gate biased to a point near pinch-off to maximize its light sensitivity and the drain and source of the FET are serially connected with a fixed resistance in a dc voltage divider circuit so that the output of the voltage divider circuit changes as a function of the change in light intensity of the LED. A MMIC operational amplifier connected in an inverter mode is coupled between the output of the voltage divider circuit and the dc gain control of the distributed amplifier to control the gain of that amplifier. GRA

N89-28706# National Inst. of Standards and Technology, Gaithersburg, MD. Center for Electronics and Electrical Engineering.
CENTER FOR ELECTRONICS AND ELECTRICAL ENGINEERING TECHNICAL PUBLICATION ANNOUNCEMENTS: COVERING CENTER PROGRAMS, JULY - SEPTEMBER 1988, WITH 1989 CEEE EVENTS CALENDAR
E. J. Walters, comp. Mar. 1989 24 p
(PB89-189302; NISTIR-89/4067) Avail: NTIS HC A03/MF A01 CSCL 09C

The 18th issue is presented of a quarterly publication providing information on the technical work of the National Institute of Standards and Technology (formerly the National Bureau of Standards) Center for Electronics and Electrical Engineering. The issue of the Center for Electronics and Electrical Engineering Technical Publication Announcements covers the third quarter of calendar year 1988. Author

N89-28707# National Inst. of Standards and Technology, Boulder, CO. Electromagnetic Fields Div.
PERFORMANCE EVALUATION OF RADIOFREQUENCY, MICROWAVE, AND MILLIMETER WAVE POWER METERS

Eleanor M. Livingston and Robert T. Adair Dec. 1988 149 p (PB89-193916; NIST/TN-1310) Avail: NTIS HC A07/MF A01; SOD HC $8.50 as 003-003-02931-9 CSCL 09A

Measurement techniques are described for the evaluation of the electrical performance of commercially available radiofrequency (rf), microwave (mw), and millimeter wave (mmw) power meters which use bolometric power sensors and typically operate from 10 MHz to 26.5 GHz for an average power range of 10 microW to 10 mW with appropriate attenuation for higher power ranges. Techniques are described for analysis of: ranges of frequency and power, operating temperature, stability, response time, calibration factor, extended power measurement, overload protection, and characteristics of the internal power reference source. Some automated methods are discussed. Block diagrams of test setups are presented. Sources of uncertainty in the bolometric method are analyzed. Author

N89-28708# Sandia National Labs., Albuquerque, NM.
COMPOUND-LENS DIODE FOR HERMES 3
T. W. L. Sanford, J. A. Halbleib, J. W. Poukey, T. Sheridan, D. Muirhead, C. E. Yagow, K. A. Mikkelson, R. Mock, P. W. Spence, and V. L. Bailey (Pulse Sciences, Inc., San Leandro, CA.) et al 1989 5 p Presented at the 7th Institute of Electrical and Electronics Engineers Pulsed Power Conference, Monterey, CA, 12 Jun. 1989
(Contract DE-AC04-76DP-00789)
(DE89-013065; SAND-88-3360C; CONF-890665-25) Avail: NTIS HC A02/MF A01

Significantly improved spatial uniformity of bremsstrahlung radiation, relative to a diode with a planar anode, is predicted for the HERMES 3 accelerator when a compound-lens diode is used to actively control the high-power electron beam at the exit of a coaxial, magnetically-insulated transmission line. Electron flow within the diode and subsequent radiation output is characterized as a function of diode parameters. The results of these calculations are applicable to coaxial geometries where active control of high-energy, high-current, upsilon/gamma approximately greater than greater than or equal to 1 beams is desired. DOE

N89-28709# Los Alamos National Lab., NM.
EXPLODING METALLIC FOILS AND FUSES: A COMPUTATIONAL MODELING UPDATE
Irvin R. Lindemuth and Robert E. Reinovsky 1989 17 p Presented at the 7th IEEE Pulsed Power Conference, Monterey, CA, 11-14 Jun. 1989 Submitted for publication
(Contract W-7405-eng-36)
(DE89-014033; LA-UR-89-1990; CONF-890665-27) Avail: NTIS HC A03/MF A01

The Los Alamos computational model of exploding metallic foil behavior was used to analyze and design a wide range of experiments in which exploding metallic foils were driven by the output current of capacitor banks and magnetic flux compression generators. Currents in the experiments ranged from 1 kA-16 MA and foil conduction times ranged from 200 ns-300 ms. The successes and limitations of the computational models are surveyed. DOE

N89-28710# Argonne National Lab., IL.
ACCELERATED LIFE EVALUATION OF VALVE-REGULATED LEAD-ACID BATTERIES
W. H. DeLuca and J. F. Miller 1989 9 p Presented at the International Lead-Acid Zinc Research Seminar, Orlando, FL, 4 May 1989
(Contract W-31-109-eng-38)
(DE89-012429; CONF-8905175-1) Avail: NTIS HC A02/MF A01

Valve-regulated lead-acid (VRLA) batteries are primarily used in standby and uninterruptable power source applications at present. Manufacturers expect these and/or similar VRLA batteries to provide a life of 1000 to 1500 cycles with deep discharging at operating temperatures of approximately 25 C. However, insufficient data are available to determine their suitability and life in such repetitive cycling applications. Argonne National Laboratory (ANL) has developed and initiated an accelerated life evaluation of VRLA batteries to acquire this data. The objectives of the ANL accelerated life evaluation are: (1) to use accelerated testing techniques to obtain supporting evidence within 6 months that VRLA batteries have an expected life of more than 500 cycles in deep-discharge applications, and (2) to determine VRLA battery life within a 2 to 3 year time period under conditions (temperature and depth-of-discharge) that simulate those encountered in a utility operating environment. DOE

N89-28711# Los Alamos National Lab., NM.
HIGH-BRIGHTNESS ELECTRON INJECTORS: A REVIEW
Richard L. Sheffield 1989 6 p Presented at the 13th Particle Accelerator Conference, Chicago, IL, 20-23 Mar. 1989
(Contract W-7405-eng-36)
(DE89-014244; LA-UR-89-965; CONF-890335-215) Avail: NTIS HC A02/MF A01

The last decade has seen increased emphasis on the development of high-brightness electron beams because of rigorous requirements of the new generation of colliders and the advent of free-electron lasers. The approaches now being explored for attaining intense, bright electron beams are described. The methods for producing bright electron beams include photocathode-based, short-pulse injectors, direct current electrostatic accelerator sources; long-pulse beams, which are then compressed in time using subharmonic bunching; combining first and third harmonics in an accelerator to attain the equivalent of high-gradient dc fields; and LaB6 radio frequency guns. For several of the approaches, the temporal length of the electron pulse is decreased after acceleration to relativistic energies by impressing an energy spread on the electron bunch and using a nonisochronous beam-transport system to increase the peak current. DOE

N89-28712# Los Alamos National Lab., NM.
THE MARK 101 FLUX COMPRESSION GENERATOR: DEVELOPMENT PROGRESS
B. L. Freeman, C. M. Fowler, D. G. Rickel, and M. L. Hodgdon 1989 9 p Presented at the 5th International Conference on Megagauss Magnetic Field Generation and Related Topics, Novosibirsk, USSR, 3-7 Jul. 1989
(Contract W-7405-eng-36)
(DE89-014298; LA-UR-89-2080; CONF-890710-10) Avail: NTIS HC A02/MF A01

The Mark 101 explosive flux compression generator is a line-initiated, helical generator that offers the possibility of a theoretical dL/dt greater than or equal to 0.5 ohm. Subsequent to early results, which demonstrated current gains of only approx. 1.2:1, the generator design was modified and now includes a low-density foam staging layer between the PBX 9501 explosive and the aluminum armature and a vinyl coating on the stator winding. This redesigned Mark 101 has an initial working inductance of 5.36 micro H and a load inductance of 0.60 micro H. The lossless current gain of this unit is 9.9:1, and the estimated practical gain is approx. 5.5. Experiments were performed using SF6 and vacuum as the insulating media between the armature and stator. Measured current gains of approx. 5.0:1 were achieved. The maximum measured dI/dt of approx. 1.2 x 10(11) amps/sec and V of approx. 62 kV were significantly less than expected during high-current tests. However, a case motion experiment showed that the armature is probably disintegrating during the last few microseconds of the armature run. Thus, the configuration of the staging layer between the explosive and the armature was the subject of study. The results of the generator tests are presented. DOE

N89-28713* National Aeronautics and Space Administration. Pasadena Office, CA.
SYSTOLIC VLSI ARRAY FOR IMPLEMENTING THE KALMAN FILTER ALGORITHM Patent
Jaw J. Chang, inventor (to NASA) (Jet Propulsion Lab., California Inst. of Tech., Pasadena.) and Hen-Geul Yeh, inventor (to NASA) 18 Apr. 1989 12 p Filed 1 Apr. 1987

(Contract NAS7-918)
(NASA-Case-NPO-17108-1-CU; US-Patent-4,823,299; US-Patent-Appl-SN-032819; US-Patent-Class-364-735; US-Patent-Class-364-754; US-Patent-Class-364-724.01; US-Patent-Class-364-724.05) Avail: U.S. Patent and Trademark Office CSCL 09A

A method and apparatus for processing signals representative of a complex matrix/vector equation is disclosed and claimed. More particularly, signals representing an orderly sequence of the combined matrix and vector equation, known as a Kalman filter algorithm, is processed in real-time in accordance with the principles of this invention. The Kalman filter algorithm is converted into a Faddeev algorithm, which is a matrix-only algorithm. The Faddeev algorithm is modified to represent both the matrix and vector portions of the Kalman filter algorithm. The modified Faddeev algorithm is embodied into electrical signals which are applied as inputs to a systolic array processor, which performs triangulation and nullification on the input signals, and delivers an output signal to a real-time utilization circuit.

Official Gazette of the U.S. Patent and Trademark Office

N89-28714# Rome Air Development Center, Griffiss AFB, NY.
ELECTRICAL CHARACTERIZATION OF SIGNAL PROCESSING MICROCIRCUIT Report, Oct. 1982 - Sep. 1986
Daniel F. Fayette and Nancy A. Koziarz Apr. 1989 246 p
(AD-A209078; RADC-TR-89-122) Avail: NTIS HC A11/MF A01 CSCL 09/1

The objective of this effort is to conduct characterization efforts for analog integrated circuit device types for inclusion into the MIL-M-38510 specification system (General Specification for Microcircuits). The effort includes determination of a devices's parameters and its limits as well as static and dynamic test circuits to verify these limits. All of the characterization and specification efforts performed are guided by the fundamental objectives of MIL-M-38510 specification system which are to achieve quality, reliability, interchangeability, and standardization of microcircuits procured for use in military systems. The scope of the effort includes electrical characterization of the following device types: (1) AD534, AD532, 4213VM analog multipliers, (2) 180 J-FET analog switch series, (3) 200, 300, 5040 CMOS analog switch series, (4) 506-509, 506A-509A CMOS multiplexer series, (5) 2000 darlington transistor array series, (6) 1524, 1525, 1526, 1527 regulating pulse width modulators, and (7) TL431 shunt regulating reference. GRA

N89-28715# North Carolina Univ., Chapel Hill. Dept. of Physics and Astronomy.
EXPERIMENTAL AND THEORETICAL STUDY OF TRANSIENT BEHAVIOR OF VARISTORS Final Report, 11 Jan. 1988 - 10 Jan. 1989
Sang-il Choi and Marvin Silver 25 Apr. 1989 11 p
(Contract DAAL03-88-K-0028)
(AD-A209081; ARO-25495.2-PH) Avail: NTIS HC A03/MF A01 CSCL 09/1

Transient currents below and above the breakdown voltage were studied for metal oxide (zinc oxide) varistors. Above the breakdown voltage the voltage overshoot phenomenon effectively lengthens the turn-on time making the turn-off time smaller than the effective turn-on time. Below the breakdown voltage, slow decaying currents following the capacitance charging peak/discharging peak are found to show a power law temporal behavior, 1/t to the nth power where n is very close to unity, over a time ranging from one microsecond to thousands of seconds after the beginning/end of the applied voltage pulse. Activation energies of these transient currents were found to be approx. 10 meV and approx. 160 meV. A theoretical explanation is provided of this time dependence: tunneling from deep donors into the conduction band as the Fermi level is shifted down across the donor levels by the applied bias. A preliminary effort was made to relate the cause of the voltage overshoot to the time needed for the depletion layer narrowing and hole creation. GRA

N89-28716# California Univ., Los Angeles. Solid State Science Center.
THERMODYNAMICALLY STABLE CONDUCTING FILMS OF INTERMETALLIC PtGa2 ON GALLIUM ARSENIDE Technical Report, 1988 - 1989
Larry P. Sadwick, Kang L. Wang, David K. Shuh, Young K. Kim, and R. Stanley Williams 1 Jul. 1989 9 p Submitted for publication
(Contract N00014-87-K-0014)
(AD-A210077; TR-16) Avail: NTIS HC A02/MF A01 CSCL 09/1

The first epitaxial platinum gallium two (PtGa2) films have been grown on gallium arsenide (GaAs)(100) by co-evaporation of the elements under ultra-high vacuum conditions. An electron-beam evaporator and a Knudsen cell were used to produce the platinum and gallium beams, respectively. The resulting films and bulk PtGa2 have been characterized by X-ray diffraction, Auger electron spectroscopy, and X-ray photoelectron spectroscopy. The data confirm the PtGa2 stoichiometry and crystal structure of the films, and demonstrate their chemical stability on GaAs(100). This study supports the contention that PtGa2 can be a suitable, temperature-stable contact material on GaAs substrates. GRA

N89-28717# Air Force Occupational and Environmental Health Lab., Kelly AFB, TX.
ACOUSTIC TESTS ON A NEW MOTOR GENERATOR SYSTEM FOR THE MINUTEMAN LAUNCH CONTROL CENTERS IN HILL ENGINEERING TEST FACILITIES 1 AND 2, HILL AFB, UTAH Final Report
Terry M. Fairman Apr. 1989 186 p
(AD-A209598; AFOEHL-89-033EH0086DNA) Avail: NTIS HC A09/MF A01 CSCL 16/1

Post critical design review acoustic tests were performed in Hill Engineering Test Facilities 1 and 2 (HETF) on a proposed new motor generator system for the Minuteman Launch Control Centers (LCC). A performance noise criteria equivalent to a preferred noise criterion (PNC-50) curve was established as the standard by which to judge the effectiveness of the new motor generator. Measurements were obtained at both the commander's console and the deputy commander's console. Results indicated the noise from the motor generator as configured in HETF 1 (the small LCC) exceeded the PNC-50 criteria primarily in the 63 hertz (Hz) octave band by 10 decibels (dB) when operated in both the ac and dc modes. The motor generator as configured in HETF 2 (the large LCC) exceeded the PNC-50 criteria by 3 dB in the 125 Hz octave band only at the deputy commander's console when operated in the ac mode. Acoustic intensity measurements were obtained to isolate specific noise sources and determine the transmission loss of the floor panels. Vibration measurements were also made on and near the motor generator to determine paths of structure-borne vibration energy. Specific recommendations for improving the acoustic environment in the LCC's are presented. GRA

N89-28718# Columbia Univ., New York, NY. Dept. of Electrical Engineering.
VLSI INTEGRATED CIRCUIT CONTACT RELIABILITY BY INTERFACE SPECTROSCOPY Final Report, Nov. 1985 - Jun. 1988
E. S. Yang and H. Evans Jan. 1989 99 p
(Contract F30602-85-C-0072; AF Proj. 2306)
(AD-A207666; RADC-TR-88-284) Avail: NTIS HC A05/MF A01 CSCL 09/1

Metal semiconductor contacts comprise one of the most important interfaces in modern microelectronics. However, the underlying physical mechanisms which lead to their gross electrical characteristics are not well understood. The thrust of our work has been to explore the microscopic origins of the energy barrier present at the metal semiconductor interface. We feel that only with such an understanding can the degradation and reliability of ohmic and rectifying contracts be understood and hence better controlled. First, we developed and utilized forward bias capacitance techniques for determining the interface state

distribution in silicon Schottky diodes. These techniques were applied to as deposited and annealed palladium silicon diodes as well as epitaxial and non-epitaxial nickel silicide structures. GRA

N89-28719# Cornell Univ., Ithaca, NY. School of Chemical Engineering.
MOLECULAR WEIGHT DEPENDENCE OF e-BEAM RESIST SENSITIVITY
Y. M. N. Namaste, S. K. Obendorf, B. C. Dems, F. Rodriguez, and A. A. Krasnopoler 12 May 1989 33 p Presented at the ACS Division of Polymeric Materials: Science and Engineering International Symposium on Radiation Curing of Polymeric Material, Dallas, TX, 9-14 Apr. 1989
(Contract N00014-85-K-0474)
(AD-A207835; TR-13) Avail: NTIS HC A03/MF A01 CSCL 09/1

Any measure of lithographic sensitivity must take into account both the events during exposure (latent image formation) and their subsequent conversion into an etch-resistant stencil (real image formation) by selective dissolution. Poly(methyl methacrylate), a popular positive chain-scissioning resist, is developed by dissolving exposed areas. Poly(chloromethyl styrene), a negative resist, crosslinks on exposure and is developed by dissolving the unexposed polymer. In each case the equations relating primary exposure events to parameters such as molecular weight need to be coupled with the dissolution characteristics to define sensitivity. The reconcilation of lithographic sensitivity (and resolution) with conventional radiation measurements also requires an understanding of important secondary phenomena. Some, like microporosity and gel-swelling, may also depend on the initial molecular weight and molecular weight distribution of the polymer. GRA

N89-28720# Northern Telecom Electronics Ltd., Ottawa (Ontario).
MEASUREMENTS AND MODELLING OF THIN SILICON DIOXIDE FILMS ON SILICON Interim Technical Report
A. Kalnitsky, S. P. Tay, J. P. Ellul, J. W. Andrews, E. A. Irene, and S. Chongsawangvirod (North Carolina Univ., Chapel Hill.) 9 May 1989 27 p Submitted for publication
(Contract N00014-89-J-1178)
(AD-A207853; TR-26) Avail: NTIS HC A03/MF A01 CSCL 09/1

The ellipsometric measurement of refractive indices for films less than 50 nm thick is of dubious quality due to the significance of the size of random errors relative to the accuracy required to extract reliable index values from the measurements. The various errors are quantitatively assessed as a function of the film thickness, and then compared with experimental data obtained from differently prepared silicon dioxide films on silicon. The new results confirm previous work that shows higher refractive indices for thinner films. Transmission electron microscopy results confirm the results and graded and discreet layer models are compared. GRA

N89-28721# Naval Research Lab., Washington, DC. Airborne EW Systems Branch.
SLOTTED-WAVEGUIDE AMPLIFIERS FOR MILLIMETER WAVES Memorandum Report, Oct. 1986 - Oct. 1988
S. T. Smith 10 May 1989 25 p
(AD-A207932; NRL-MR-6423) Avail: NTIS HC A03/MF A01 CSCL 09/1

Slotted waveguides and ribbon electron beams are studied as electron-beam interaction circuits instead of the usual circular-beam devices. The slotted waveguide and ribbon beam can be many wavelengths long, and therefore the effective beam cross-sectional area is greatly increased over that of the circular beam helix, coupled-cavity or kylstron tubes. This increased beam area results in more beam current, more beam power, and less stringent requirements on cathode current density and focusing fields. The slotted waveguides are made by milling either grooves or threads into a slab of metal, and are therefore rugged and self-aligning. Both theory and experiments are described. GRA

N89-28722# Naval Research Lab., Washington, DC. Applied Optics Branch.
ACOUSTO-OPTICAL VECTOR MATRIX PRODUCT PROCESSOR: IMPLEMENTATION ISSUES
Eugene P. Mosca (Naval Academy, Annapolis, MD.), Frank P. Pursel, Richard D. Griffin, and John N. Lee 25 Apr. 1989 26 p
(AD-A207933; NRL-MR-6372) Avail: NTIS HC A03/MF A01 CSCL 09/6

An Acousto-Optic Technique is used to design and construct a prototype of a processor capable of multiplying a 128 x 128 element matrix by a 128 element vector. The elements of the matrix and the vectors are complex numbers. The device is specified to execute 100,000 vector/matrix products per second with 8-bit accuracy. The performance of each component of the prototype was evaluated as was the impact of component performance on system performance. GRA

N89-28723# Utah Univ., Salt Lake City. Dept. of Materials Science and Engineering.
STOCHASTIC PROCESSES IN CHEMFETS
Jiri Janata 9 May 1989 8 p
(Contract N00014-87-K-0060)
(AD-A207977) Avail: NTIS HC A02/MF A01 CSCL 09/1

The fluctuation analysis was extended to study of liquid/liquid interface and of phospholipid bilayer membranes. These studies were done with a discrete amplifier as opposed to FETs used before. This technique allows to carry out impedance measurements approximately one decade below that normally used in ac impedance analysis. The representation of power spectra on logarithmic scale of frequencies without distortion was developed. This is a new approach to digital filtering. Preliminary investigation of chemical modulation of work function of synthetic metals was initiated. It was shown that a rigorous control of electropolymerization conditions can produce materials of widely different work function. GRA

N89-28724# Michigan Univ., Ann Arbor. Dept. of Chemical Engineering.
METAL/METALLION SYSTEM IN LOW TEMPERATURE MOLTEN SALTS Final Report, 1987 - 1988
Francis M. Donahue, Leif Simonsen, Russell Moy, and Sara Mancini 24 Mar. 1989 19 p
(Grant AF-AFOSR-0079-88; AF Proj. 2303)
(AD-A208025; AFOSR-89-0623TR) Avail: NTIS HC A03/MF A01 CSCL 09/1

Potential arrests on open circuit following passivation of aluminum electrodes and cathodic stripping immediately following passivation were studied in acidic low temperature molten salt solutions (1-methyl-3-ethylimidazolium chloride, MEIC, and aluminum chloride binaries). A model of classes of charge transfer processes which could be responsible for the processes occurring during open circuit decay and cathodic stripping were proposed. GRA

N89-28725# Utah Univ., Salt Lake City. Dept. of Materials Science and Engineering.
STOCHASTIC PROCESSES IN CHEMFETs Final Report, 1 Oct. 1986 - 1 Jun. 1989
Jiri Janata 1 Jun. 1989 6 p
(Contract N00014-87-K-0060)
(AD-A208092) Avail: NTIS HC A02/MF A01 CSCL 09/1

It was shown that equilibrium fluctuation analysis offers a fundamentally different approach to characterizations of dynamic properties of various electrochemical systems ranging from fast redox couples, to liquid/liquid interface, bilayer membranes and even insulator/solution interface. These measurements can be extended to frequencies approximately one decade below those normally used in ac impedance analysis . The representation of power spectra on logarithmic scale of frequencies without distortion was developed. Chemical modulation of work function was identified as an important factor which has to be considered in application of materials such as synthetic metals. The preliminary study shows

that a rigorous control of electropolymerization conditions can produce materials of widely different work function. GRA

N89-28726# Polytechnic Univ., Farmingdale, NY.
BASIC RESEARCH IN ELECTRONICS (JSEP) Annual Report, 4 Jan. - 31 Dec. 1988
Erich E. Kunhardt 31 Dec. 1988 60 p
(Contract F49620-88-C-0075)
(AD-A208181; POLY-WRI-1554-89) Avail: NTIS HC A04/MF A01 CSCL 09/1

This report presents a summary of the scientific progress and accomplishments on research projects in the Joint Services Electronics Program (JSEP) for the contract period from 1 April 1988 through 31 December 1988. It also includes work accomplished under Contract No. F49620-85-C-0078 from 1 January 1988 to 31 March 1988. The Joint Services Electronics Program at Polytechnic University is the core of interdisciplinary research in electronics encompassing programs in the Department of Electrical Engineering, Physics, and Chemistry under the aegis of the Weber Research Institute. The research encompassed by this program is grouped under two broad categories: Interactions of Wide-Band Electromagnetic Radiation with Complex Macro- and Micro-structures (EM) and Field-Particle Interactions in Matter: Single Particle, Collective and Cooperative Phenomena (FP). The detailed projects (research units) comprising the complete program are listed in the Table of Contents. GRA

N89-28727# Technische Univ., Brunswick (Germany, F.R.). Fakultaet fuer Maschinenbau und Elektrotechnik.
A MODEL FOR THE SIMULATION OF THE DC AND SMALL-SIGNAL BEHAVIOR OF THE BIPOLAR TRANSISTOR Ph.D. Thesis [EIN MODELL ZUR SIMULATION VON GLEICHSTROM- UND KLEINSIGNALVERHALTEN DES BIPOLARTRANSISTORS]
Christian Maier 1988 165 p In GERMAN
(ETN-89-94442) Avail: NTIS HC A08/MF A01

A transistor model which can be used for the DC and AC analysis of electronic circuits is presented. It is based on a basic concept for a one-dimensional arrangement. Numerical calculations on a one-dimensional transistor structure show that the Kirk effect clearly affects the behavior of the component at high currents. Therefore, the Kirk effect was also DC modeled, as well as the avalanche effect. The frequency behavior of the small-signal parameters was obtained with better accuracy than in previous models. A simple procedure for the determination of the model parameters was developed; examples demonstrate the accuracy of the procedure. It is concluded that the presented model describes the behavior of real transistors with sufficient accuracy. ESA

N89-28728 Max-Planck-Inst. fuer Plasmaphysik, Garching (Germany, F.R.).
ANALYTICAL SOLUTIONS FOR THE FIELD, CURRENT DENSITY, FORCE FORCE DENSITY AND MECHANICAL STRESS DISTRIBUTION IN TOROIDAL COIL SYSTEMS [ANALYTISCHE LOESUNGEN FUER DIE FELD-, STROMDICHTE-, KRAFTDICHTE- UND DIE MECHANISCHE SPANNUNGSVERTEILUNG IN TOROIDALEN SPULENSYSTEMEN]
E. Harmeyer May 1989 37 p In GERMAN; ENGLISH summary
(IPP-2/294; ETN-89-94608) Copyright Avail: Fachinformationszentrum Karlsruhe, 7514 Eggenstein-Leopoldsshafen 2, Fed. Republic of Germany

The Magnetic field distribution and the current density distribution, and hence the force densities, the resulting forces, and the mechanical stress distribution, in a thin, current carrying toroidal shell are calculated as a function of geometric parameters using analytical methods. The calculations are based on the model of the ideal torus with finite wall thickness, i.e., a toroidal shell. The magnetic field distribution was obtained for a toroidal shell of finite wall thickness subject to a given current distribution. This allows the derivation of the stored magnetic energy of the system, and the distributions of the force density and the mechanical stresses in the shell. The mechanical stresses are also determined for a constant force density distribution and a distribution inversely proportional to the radius. The virial theorem was applied to the configurations and compared with the analytical solutions. ESA

N89-28729# Technische Univ., Munich (Germany, F.R.). Fakultaet fuer Chemie, Biologie und Geowissenschaften.
CORROSION PREVENTION OF LITHIUM-ALLOY ANODES IN ACCUMULATORS WITH ORGANIC ELECTROLYTIC SOLUTIONS Ph.D. Thesis [KORROSIONSSCHUTZ VON LITHIUM-LEGIERUNGSANODEN IN STROMSPEICHERN MIT ORGANISCHEN ELEKTROLYTLOESUNGEN]
Peter Komenda 1987 137 p In GERMAN
(ETN-89-94652) Avail: NTIS HC A07/MF A01

Methods for protection against corrosion of lithium-rich alloy electrodes in organic electrolytic solutions are developed. Phase-sensitive ac polarography showed that long-chain as well as cyclic hydrocarbons can be absorbed at the electrode surface. Tests with beta-LiIn electrodes show that their durability in organic electrolytes at room temperature is enhanced. Cyclic tests with Cu-AlLi electrodes show that the morphology of this ternary alloy remains largely unchanged, but contact and isolation problems occur due to the reaction with organic electrolytes. ESA

N89-28730# Universiteit Twente, Enschede (Netherlands). Dept. of Computer Science.
A PARTITIONING AND REDUNDANCY MODEL FOR WAFER SCALE INTEGRATED CIRCUITS
Martin Beusekamp Apr. 1989 21 p
(MEMO-INF-88-65; ISSN-0923-1714; ETN-89-95424) Avail: NTIS HC A03/MF A01

A general, architecture-independent model is presented which calculates the required amount of redundancy and the necessary degree or partitioning of any desired circuit to achieve a maximum efficiency. The model takes several technological parameters into account. It is shown that in practical cases, the efficiency curve round the maximum is relatively flat, and that the model can be adapted to any specific architecture by the adjustment of technological parameters and the limiting of possible solutions to restricted, architecture-dependent values. A specific critical circuit size is shown to exist for every technological environment above which the implementation of partitioning and redundancy is necessary to achieve an optimal efficiency. ESA

N89-28731 Technische Univ., Delft (Netherlands).
ROUTING CHANNELS IN VLSI LAYOUT Ph.D. Thesis
Hong Cai Delft University Press 1989 143 p
(ISBN-90-6275-535-4; ETN-89-95462) Copyright Avail: Delft Univ. Press, Stevineg 1, 2628 CN Delft, Netherlands

A number of algorithms for the automatic routing of interconnections in Very Large Scale Integration (VLSI) building-block layouts are presented. Algorithms for the topological definition of channels, the global routing and the geometrical definition of channels are presented. In contrast to traditional approaches the definition and ordering of the channels is done after the global routing. This approach has the advantage that global routing information can be taken into account to select the optimal channel structure. A polynomial algorithm for the channel definition and ordering problem is presented. The existence of a conflict-free channel structure is guaranteed by enforcing a sliceable placement. Algorithms for finding the shortest connection path are described. A separate algorithm is developed for the power net routing, because the two power nets must be planarly routed with variable wire width. An integrated placement and routing system for generating building-block layout is briefly described. Some experimental results and design experiences in using the system are also presented. Very good results are obtained. ESA

N89-28732# Technische Univ., Delft (Netherlands).
ACCURATE AND EFFICIENT MODELING OF GLOBAL CIRCUIT BEHAVIOR IN VSLI LAYOUTS Ph.D. Thesis

Zhen-Qiu Ning 1989 180 p
(ESPRIT Proj. 991)
(ETN-89-95459) Avail: NTIS HC A09/MF A01

A boundary finite element method for the accurate and efficient modeling of global circuit behavior in VLSI (Very Large Scale Integration) layout is presented. This method consists of three important parts: the determination of Green's function, the use of boundary finite elements, and approximate Schur inversion. Different methods of reducing the Green's function integral equation to a discrete problem are presented. Various geometries are studied using this boundary finite method and the derivation of accurate heuristics leading to a faster extraction method is proposed. A more general method for the global modeling in VLSI layouts, in which capacitive (and resistive) effects in the interconnects are combined with detailed behavior at the transistor level is discussed. ESA

N89-28733# Technische Univ., Eindhoven (Netherlands).
FUNDAMENTAL ASPECTS OF REACTIONS IN TITANIUM-SILICON THIN FILMS FOR INTEGRATED CIRCUITS Ph.D. Thesis
Ivo Johannes Mechtil Raaijmakers 1988 158 p
(ETN-89-95466) Avail: NTIS HC A08/MF A01

The formation mechanisms and electrical properties of titanium silicide are described. Titanium silicide (TiSi2) fitting in the process flow of integrated circuits by two different preparation methods is described. The first involves heat treating a co-sputtered amorphous alloy of Ti and Si which causes a crystallization reaction to occur. The second method involves heat treating a Ti-Si diffusion couple which causes compound growth by chemical inter-diffusion. In situ studies of the Ti-Si binary amorphous alloys by transmission electron microscope are described. ESA

34 FLUID MECHANICS AND HEAT TRANSFER

Includes boundary layers; hydrodynamics; fluidics; mass transfer; and ablation cooling.

For related information see also *02 Aerodynamics* and *77 Thermodynamics and Statistical Physics.*

N89-28734# Advisory Group for Aerospace Research and Development, Neuilly-Sur-Seine (France). Fluid Dynamics Panel.
A SURVEY OF MEASUREMENTS AND MEASURING TECHNIQUES IN RAPIDLY DISTORTED COMPRESSIBLE TURBULENT BOUNDARY LAYERS (Computer Diskette Supplement)
H. H. Fernholz, P. J. Finley, J. P. Dussauge, A. J. Smits, and E. Reshotko, ed. (Case Western Reserve Univ., Cleveland, OH.) May 1989 246 p Computer diskette supplement (data file): IBM compatible DS HD 5.25-inch formatted 1.2 MB using MS DOS 3.20
(AGARD-AG-315; ISBN-92-835-0506-9; NONP-Suppl-DK-89-223860) Copyright Avail: NTIS HC A11/MF A01; set of 5 computer diskettes available from NASA Scientific and Technical Information Facility, BWI Airport, MD at $13.00/set

A wide range of recent work on compressible turbulent boundary layers is described. Special attention was paid to flows with rapid changes in pressure including flows with shock waves, curved walls, and expansions. The application of rapid distortion theory to flows transversing expansion and shock waves is reviewed. This is followed by an account of experiments aimed at elucidating the large scale structures present in supersonic boundary layers. The current status of laser-Doppler and hot-wire anemometry in supersonic flow is discussed, and a new interferometric technique for the determination of wall-stress is described. The use of small pressure transducers to deduce information about the structure of zero pressure-gradient and severely perturbed boundary layers is investigated. Finally, there is an extension of the data presentation of AGARDographs 223, 253 and 263 to cover rapidly distorted boundary layers. For individual titles, see N89-28735 through N89-28745.

N89-28735# Aix-Marseilles Univ. (France). Inst. de Mecanique Statistique de la Turbulence.
RAPIDLY DISTORTED COMPRESSIBLE BOUNDARY-LAYERS (Computer Diskette Supplement)
J. P. Dussauge, J. F. Debieve, and A. J. Smits (Princeton Univ., NJ.) *In* AGARD, A Survey of Measurements and Measuring Techniques in Rapidly Distorted Compressible Turbulent Boundary Layers May 1989 11 p Computer diskette supplement (data file): IBM compatible DS HD 5.25-inch formatted 1.2 MB using MS DOS 3.20 (For primary document see N89-28734 23-34)
Avail: NTIS HC A11/MF A01; set of 5 computer diskettes available from NASA Scientific and Technical Information Facility, BWI Airport, MD at $13.00/set

The theoretical work in rapidly distorted compressible flows can be classed into three distinct groups: analyses based on formal linearizations of the equations of motion (rapid distortion theory, RDT), analyses based on the Rankine-Hugoniot jump relations to study shock/turbulence interactions (RDT and rapid distortion approximation, RDA), and approximations to the Reynolds stress transport equations to obtain second order closure (RDA). These three groups are considered. An attempt is made to classify the currently available analyses in terms of restrictions placed on the mean and fluctuating fields, and on the boundary conditions. Finally, the application of rapid distortion methods to supersonic flows is considered, and the limits of applicability are discussed. M.G.

N89-28736# Princeton Univ., NJ. Dept. of Mechanical and Aerospace Engineering.
LARGE SCALE MOTIONS IN SUPERSONIC TURBULENT BOUNDARY LAYERS (Computer Diskette Supplement) **c02**
A. J. Smits and J. H. Watmuff *In* AGARD, A Survey of Measurements and Measuring Techniques in Rapidly Distorted Compressible Turbulent Boundary Layers May 1989 14 p Computer diskette supplement (data file): IBM compatible DS HD 5.25-inch formatted 1.2 MB using MS DOS 3.20 (For primary document see N89-28734 23-34)
Avail: NTIS HC A11/MF A01; set of 5 computer diskettes available from NASA Scientific and Technical Information Facility, BWI Airport, MD at $13.00/set

The results from a number of experiments are summarized. The experiments encompassed zero pressure gradient and adverse pressure gradient flat-plate boundary layers, flows over concavely curved walls, and shock-wave/boundary layer interactions. The Reynolds-averaged turbulent stresses and the corresponding mean-flow data were obtained along with a large number of other measurements taken in an attempt to describe the time-dependent behavior of the turbulent field. Observations on large-scale structures are discussed. The suitability of various conditional sampling techniques is examined with particular attention being given to the limitations of the VITA method of Blackewlder and Kaplan (1976). M.G.

N89-28737*# Pennsylvania State Univ., University Park. Dept. of Mechanical Engineering.
SKIN-FRICTION MEASUREMENTS BY LASER INTERFEROMETRY (Computer Diskette Supplement)
K.-S. Kim and G. S. Settles *In* AGARD, A Survey of Measurements and Measuring Techniques in Rapidly Distorted Compressible Turbulent Boundary Layers May 1989 8 p Computer diskette supplement (data file): IBM compatible DS HD 5.25-inch formatted 1.2 MB using MS DOS 3.20 (For primary document see N89-28734 23-34)
(Grant NAG3-527)
Copyright Avail: NTIS HC A11/MF A01; set of 5 computer diskettes available from NASA Scientific and Technical Information Facility, BWI Airport, MD at $13.00/set CSCL 20D

The measurement of skin friction in rapidly distorted compressible flows is difficult, and very few reliable techniques are available. A recent development, the laser interferometer skin

friction (LISF) meter, promises to be useful for this purpose. This technique interferometrically measures the time rate of thinning of an oil film applied to an aerodynamic surface. Under the proper conditions the wall shear stress may thus be found directly, without reference to flow properties. The applicability of the LISF meter to supersonic boundary layers is examined experimentally. Its accuracy and repeatability are assessed, and conditions required for its successful application are considered. Author

N89-28738# Princeton Univ., NJ. Dept. of Mechanical and Aerospace Engineering.
HOT-WIRE ANEMOMETRY IN SUPERSONIC FLOW (Computer Diskette Supplement) **c02**
A. J. Smits and J. P. Dussauge (Aix-Marseilles Univ., France) *In* AGARD, A Survey of Measurements and Measuring Techniques in Rapidly Distorted Compressible Turbulent Boundary Layers May 1989 14 p Sponsored in part by CNRS, France Computer diskette supplement (data file): IBM compatible DS HD 5.25-inch formatted 1.2 MB using MS DOS 3.20 (For primary document see N89-28734 23-34)
Avail: NTIS HC A11/MF A01; set of 5 computer diskettes available from NASA Scientific and Technical Information Facility, BWI Airport, MD at $13.00/set

The theory and practice of both the constant current and constant temperature modes of hot-wire anemometry are summarized, and the advantages and disadvantages are discussed. Probe designs suitable for supersonic flow are considered first. Next, the behavior of a single wire placed normal to the flow direction is examined, including its quasi-static response and its dynamic response. The behavior of inclined and crossed-wire probes is discussed. The effects of low Mach and Reynolds numbers are considered. Finally, two examples illustrating the uncertainties in measurements are given and discussed. Author

N89-28739*# National Aeronautics and Space Administration. Ames Research Center, Moffett Field, CA.
LASER DOPPLER ANEMOMETRY (Computer Diskette Supplement)
Dennis A. Johnson *In* AGARD, A Survey of Measurements and Measuring Techniques in Rapidly Distorted Compressible Turbulent Boundary Layers May 1989 10 p Computer diskette supplement (data file): IBM compatible DS HD 5.25-inch formatted 1.2 MB using MS DOS 3.20 (For primary document see N89-28734 23-34)
Copyright Avail: NTIS HC A11/MF A01; set of 5 computer diskettes available from NASA Scientific and Technical Information Facility, BWI Airport, MD at $13.00/set CSCL 20D

The application of laser Doppler anemometry (LDA) to compressible flows is discussed. Specifically, burst-counter and dual-beam LDA systems are addressed. Much has been accomplished with LDA in compressible flows despite the difficulties posed by the high speeds and additionally by the rapid spatial changes in speed or flow direction. The successful application of the technique is difficult because the signal to noise ratios (SNRs) are fairly low even under the best of conditions and highly variable because of variations in particle size and particle location with the sensing volume. The available signal processing is not very effective in discarding signals that are too noisy to provide an accurate velocity measurement. The temptation is to work with particles which are too large to adequately follow the flow but which provide cleaner signals due to increased scattering intensities. For the data to have credibility, some check on the particle response must be made for a given facility and LDA system. The capability, if developed, of being able to determine the size of each particle upon which a measurement is based and the SNR of the corresponding signal burst would be extremely valuable in reducing much of the uncertainty now present in LDA compressible flow measurements. Author

N89-28740# Aix-Marseilles Univ. (France). Inst. de Mecanique Statistique de la Turbulence.
LASER DOPPLER ANEMOMETRY IN SUPERSONIC FLOWS: PROBLEMS OF SEEDING AND ANGULAR BIAS (Computer Diskette Supplement) **c02**
M. Elena *In* AGARD, A Survey of Measurements and Measuring Techniques in Rapidly Distorted Compressible Turbulent Boundary Layers May 1989 6 p Computer diskette supplement (data file): IBM compatible DS HD 5.25-inch formatted 1.2 MB using MS DOS 3.20 (For primary document see N89-28734 23-34)
Avail: NTIS HC A11/MF A01; set of 5 computer diskettes available from NASA Scientific and Technical Information Facility, BWI Airport, MD at $13.00/set

The application of laser Doppler anemometry in supersonic flows is examined with particular attention being given to the problems associated with seeding and angular bias. The response of seed particles to abrupt changes in flow condition is discussed along with the effects of injection methodology. The mechanism underlying the measurement distortions caused by angular bias is described. The use of Bragg cells to reduce the effect of angular bias is also briefly discussed. B.G.

N89-28741*# Texas Univ., Austin. Dept. of Aerospace Engineering and Engineering Mechanics.
FLUCTUATING WALL-PRESSURE MEASUREMENTS (Computer Diskette Supplement)
D. S. Dolling and J. P. Dussauge (Aix-Marseilles Univ., France) *In* AGARD, A Survey of Measurements and Measuring Techniques in Rapidly Distorted Compressible Turbulent Boundary Layers May 1989 18 p Sponsored in part by NASA, Washington, DC and ONR, Washington, DC Computer diskette supplement (data file): IBM compatible DS HD 5.25-inch formatted 1.2 MB using MS DOS 3.20 (For primary document see N89-28734 23-34)
(Grant AF-AFOSR-0112-86)
Copyright Avail: NTIS HC A11/MF A01; set of 5 computer diskettes available from NASA Scientific and Technical Information Facility, BWI Airport, MD at $13.00/set CSCL 20D

The wall pressure fluctuations under zero pressure gradient and perturbed compressible turbulent boundary layers are studied. The method of measurement, common sources of error, and calibration methods are discussed. Analysis of the published data in zero pressure gradient shows that due largely to poor spatial resolution there are few, if any, really reliable measurements. Within the accuracy of the measurements, it does not appear that the structure of turbulence in equilibrium supersonic boundary layers is not significantly altered by compressibility. In perturbed flows most of the data are in shock/boundary layer interactions. Attention is focussed on the separation process which is characterized by large amplitude, low frequency shock-induced pressure fluctuations, on the separated flow, and on the outgoing boundary layer. Results are presented for two- and three-dimensional flows. Author

N89-28742# Imperial Coll. of Science and Technology, London (England). Dept. of Aeronautics.
GENERAL COMMENTS ON THE INTERPRETATION OF DATA (Computer Diskette Supplement)
P. J. Finley and H. H. Fernholz (Technische Univ., Berlin, Germany, F.R.) *In* AGARD, A Survey of Measurements and Measuring Techniques in Rapidly Distorted Compressible Turbulent Boundary Layers May 1989 12 p Computer diskette supplement (data file): IBM compatible DS HD 5.25-inch formatted 1.2 MB using MS DOS 3.20 (For primary document see N89-28734 23-34)
Avail: NTIS HC A11/MF A01; set of 5 computer diskettes available from NASA Scientific and Technical Information Facility, BWI Airport, MD at $13.00/set

Mean flow for a number of rapidly distorted turbulent boundary layers is discussed. A majority of the problems arising in the interpretation of mean flow data for such boundary layers are related to the effects of normal pressure gradients. The most serious intractable problem is the determination of wall shear-stress. The flows in question include regions in which a Preston tube can never be expected to give a valid result, though it may be possible to extend the range of validity if calibrations are based

on pure wall-law similarity. It is also shown that the Van Driest transformation should not be used for data affected by normal pressure gradients, and profile-derived wall shear-stress values deduced from such profiles can not be trusted. Finally, it is pointed out that the direction of the mean flow may change significantly in a short distance so that it is necessary to take special measures to ensure that probes sensitive to misalignment, in particular static probes and oblique wires, are correctly oriented. M.G.

N89-28743# Technische Univ., Berlin (Germany, F.R.). Inst. fuer Thermo und Fluiddynamik.
REVIEW OF MEAN FLOW DATA (Computer Diskette Supplement)
H. H. Fernholz and P. J. Finley (Imperial Coll. of Science and Technology, London, England) *In* AGARD, A Survey of Measurements and Measuring Techniques in Rapidly Distorted Compressible Turbulent Boundary Layers May 1989 16 p Computer diskette supplement (data file): IBM compatible DS HD 5.25-inch formatted 1.2 MB using MS DOS 3.20 (For primary document see N89-28734 23-34)
Avail: NTIS HC A11/MF A01; set of 5 computer diskettes available from NASA Scientific and Technical Information Facility, BWI Airport, MD at $13.00/set

Mean flow data for three compressible boundary layers are discussed. First, the zero-pressure gradient flow (ZPG) of Spina and Smits (1987, CAT8603T) is addressed followed by the reflected wave case, Fernando and Smits (1986, CAT8601T), providing an adverse pressure gradient (APG) of the same order of magnitude as those in the concavely curved surface flows of Taylor (1984, CAT8401T). The latter flows have appreciable normal pressure gradients as has the expansion flow of Dussauge (1987, CAT8602T). The remaining ten cases are shock/boundary layer interactions which are dealt with in two groups, quasi-normal shock interactions and compression corner flows. Comparisons between measurements and the logarithmic law of the wall on the one hand and the outer law on the other hand were made for all cases in this survey using the van Driest transformation with allowance for the recovery factor. M.G.

N89-28744# Technische Univ., Berlin (Germany, F.R.). Inst. fuer Thermo und Fluiddynamik.
REVIEW OF TURBULENCE DATA (Computer Diskette Supplement)
H. H. Fernholz and P. J. Finley (Imperial Coll. of Science and Technology, London, England) *In* AGARD, A Survey of Measurements and Measuring Techniques in Rapidly Distorted Compressible Turbulent Boundary Layers May 1989 19 p Computer diskette supplement (data file): IBM compatible DS HD 5.25-inch formatted 1.2 MB using MS DOS 3.20 (For primary document see N89-28734 23-34)
Avail: NTIS HC A11/MF A01; set of 5 computer diskettes available from NASA Scientific and Technical Information Facility, BWI Airport, MD at $13.00/set

The physical interpretation of the turbulence data for compressible boundary layers is presented. A listing is provided of investigations in which measurements of fluctuating components were performed. Zero, adverse, and favorable pressure gradient flows are discussed and the behavior of Reynolds normal stresses is examined for the zero and adverse cases. The influence of curved ramp flows is also addressed. Shock/boundary layer interactions are dealt with in two groups, quasi-normal shock interactions and compression corner flows. Finally, measurements of Reynolds shear stress are discussed. M.G.

N89-28745# Technische Univ., Berlin (Germany, F.R.). Inst. fuer Thermo und Fluiddynamik.
THE ENTRIES (Computer Diskette Supplement)
H. H. Fernholz and P. J. Finley (Imperial Coll. of Science and Technology, London, England) *In* AGARD, A Survey of Measurements and Measuring Techniques in Rapidly Distorted Compressible Turbulent Boundary Layers May 1989 102 p Computer diskette supplement (data file): IBM compatible DS HD 5.25-inch formatted 1.2 MB using MS DOS 3.20 (For primary document see N89-28734 23-34)
Avail: NTIS HC A11/MF A01; set of 5 computer diskettes available from NASA Scientific and Technical Information Facility, BWI Airport, MD at $13.00/set

Mean flow and turbulence data from 12 studies investigating rapidly-distorted turbulent compressible boundary layers are presented. Only a selection of the available profile data is given for each study (complete profile listings are available on computer diskettes). Each of the 12 entries includes a description of the experiment, tables of principle boundary conditions and derived quantities, mean-profile data, and a miscellany of supplementary data. Only a partial presentation of turbulence data is provided. M.G.

N89-28746# Argonne National Lab., IL. Multiphase Flow Research Inst.
TIME- AND VOLUME-AVERAGED CONSERVATION EQUATIONS FOR MULTIPHASE FLOW
W. T. Sha, B. T. Chao, and S. L. Soo (Illinois Univ., Urbana.) 1989 20 p Presented at the 2nd International Symposium on Multiphase Flow and Heat Transfer, Xian, China, 22 Jun. 1989 Sponsored in part by Nuclear Regulatory Commission
(Contract W-31-109-eng-38)
(DE89-012418; CONF-8906131-1) Avail: NTIS HC A03/MF A01

Governing equations for multiphase flow were rigorously derived via local volume averaging of single phase conservation equations of mass, momentum, and energy, followed by time averaging. This averaging procedure leads to a set of differential-integral equations in which the area integrals represent interfacial transport. The spatial averaging theorems are subject to the length scale restriction d much less than l less than or equal to L, where d, l, and L are, respectively, the characteristic length of the dispersed phase, the averaging volume, and the physical system. The equations presented are appropriate for dispersed systems. DOE

N89-28747*# Wright State Univ., Dayton, OH.
MATHEMATICAL MODELING AND ANALYSIS OF HEAT PIPE START-UP FROM THE FROZEN STATE Final Report
Jong Hoon Jang, Amir Faghri, Won Soon Chang, and Edward T. Mahefkey (Aeronautical Systems Div., Wright-Patterson AFB, OH.) Aug. 1989 12 p Prepared for presentation at the Annual Winter Meeting of the American Society of Mechanical Engineers, San Francisco, CA, 10-15 Dec. 1989 Sponsored in part by NASA. Lewis Research Center
(Contract F33615-88-C-2820)
(NASA-CR-185132; E-5028; NAS 1.26:185132) Avail: NTIS HC A03/MF A01 CSCL 20D

The start-up process of a frozen heat pipe is described and a complete mathematical model for the start-up of the frozen heat pipe is developed based on the existing experimental data, which is simplified and solved numerically. The two-dimensional transient model for the wall and wick is coupled with the one-dimensional transient model for the vapor flow when vaporization and condensation occur at the interface. A parametric study is performed to examine the effect of the boundary specification at the surface of the outer wall on the successful start-up from the frozen state. For successful start-up, the boundary specification at the outer wall surface must melt the working substance in the condenser before dry-out takes place in the evaporator. Author

N89-28748*# National Aeronautics and Space Administration. Lewis Research Center, Cleveland, OH.
THE UPPER-BRANCH STABILITY OF COMPRESSIBLE BOUNDARY LAYER FLOWS
J. S. B. Gajjar and J. W. Cole (Iowa State Univ. of Science and Technology, Ames.) Aug. 1989 36 p Prepared in cooperation with Exeter Univ. (England)
(NASA-TM-102128; ICOMP-89-15; E-4916; NAS 1.15:102128)
Avail: NTIS HC A03/MF A01 CSCL 20D

The upper-branch linear and nonlinear stability of compressible boundary layer flows is studied using the approach of Smith and

Bodonyi (1982) for a similar incompressible problem. Both pressure gradient boundary layers and Blasius flow are considered with and without heat transfer, and the neutral eigenrelations incorporating compressibility effects are obtained explicitly. The compressible nonlinear viscous critical layer equations are derived and solved numerically and the results indicate some solutions with positive phase shift across the critical layer. Various limiting cases are investigated including the case of much larger disturbance amplitudes and this indicates the structure for the strongly nonlinear critical layer of the Benney-Bergeon (1969) type. It is also shown how a match with the inviscid neutral inflexional modes arising from the generalized inflexion point criterion, is achieved. Author

N89-28749*# National Aeronautics and Space Administration. Lewis Research Center, Cleveland, OH.

CALCULATION OF REATTACHING SHEAR LAYERS IN DIVERGENT CHANNEL WITH A MULTIPLE-TIME-SCALE TURBULENCE MODEL

S.-W. Kim Aug. 1989 27 p

(NASA Order C-99066-G)

(NASA-TM-102293; ICOMP-89-18; E-4965; NAS 1.15:102293) Avail: NTIS HC A03/MF A01 CSCL 20D

Numerical calculations of turbulent reattaching shear layers in a divergent channel are presented. The turbulence is described by a multiple-time-scale turbulence model. The turbulent flow equations are solved by a control-volume based finite difference method. The computational results are compared with those obtained using k-epsilon turbulence models and algebraic Reynolds stress turbulence models. It is shown that the multiple-time-scale turbulence model yields significantly improved computational results than the other turbulence models in the region where the turbulence is in a strongly inequilibrium state. Author

N89-28750# Lawrence Livermore National Lab., CA.

DYNAMICS OF COLLOIDAL DISPERSIONS VIA LATTICE-GAS MODELS OF AN INCOMPRESSIBLE FLUID

Anthony J. C. Ladd and Daan Frenkel (FOM-Inst. voor Atoom- en Molecuulfysica, Amsterdam, Netherlands) May 1989 6 p Presented at the Cellular Automata and Modeling of Complex Physical Systems, Les Houches, France, 21 Feb. - 2 Mar. 1989 Submitted for publication

(Contract W-7405-eng-48)

(DE89-013146; UCRL-100997; CONF-8902113-1) Avail: NTIS HC A02/MF A01

Progress in applying lattice-gas models to the simulation of colloidal dispersions is described. A new set of collision rules for the four-dimensional face-centered-hypercubic lattice, which lead to an exactly isotropic viscosity and which can be implemented with a small table lookup, have been developed. However, they are only suitable for low Reynolds number flows. A new implementation of a constant-velocity boundary condition for lattice-gas models is described. DOE

N89-28751# Argonne National Lab., IL. Materials and Components Technology Div.

PRESSURE DROP AND HEAT TRANSFER CHARACTERISTICS OF NEARLY NEUTRALLY BUOYANT PARTICULATE SLURRY FOR ADVANCED ENERGY TRANSMISSION FLUIDS

K. V. Liu, U. S. Choi, and K. E. Kasza 1988 25 p Presented at the 3rd International Symposium on Liquid-Solid Flows, Chicago, IL, 28 Nov. - 2 Dec. 1988

(Contract W-31-109-eng-38)

(DE89-013645; CONF-881123-4) Avail: NTIS HC A03/MF A01

Under sponsorship of the U.S. Department of Energy, Argonne National Laboratory (ANL) is developing high-performance energy transmission fluids that have the potential to substantially reduce frictional losses and improve heat transfer in a variety of thermal systems, allowing the use of smaller piping, pumps, heat exchangers, and storage tanks. This paper presents experimental results and discusses the pressure drop and heat transfer characteristics of non-melting slurry flows. The experimental data obtained in this study improve the fundamental understanding of slurry fluid mechanics and heat transfer, and provide support for the use of slurries as advanced energy transmission fluids in thermal system applications. DOE

N89-28752# Argonne National Lab., IL. Energy and Environmental Systems Div.

ANALYSIS OF FLOW BOILING OF AMMONIA AND R-114 IN A MATRIX HEAT EXCHANGER

C. B. Panchal 1989 28 p Presented at the ASME/AIChE National Heat Transfer Conference, Philadelphia, PA, 6-8 Aug. 1989 Submitted for publication

(Contract W-31-109-eng-38)

(DE89-012427; CONF-890819-15) Avail: NTIS HC A03/MF A01

An analysis is carried out for flow boiling in a vertical matrix aluminum heat exchanger. The prediction model, developed for thin film evaporation in a previous study, is extended to include heat transfer in the slug-flow regime that exists at low mass qualities. Appropriate criteria is used to switch from slug-flow to thin-film annular-flow analysis. The two-phase-flow convective heat transfer enhancement for the slug-flow is correlated with inclusion of fluid Reynolds and Prandtl numbers in addition to commonly used Martinelli parameter. This approach reflects transient nature of heat transfer in the slug-flow regime. The thin-film annular-flow analysis developed in the previous study is refined with inclusion of a reliable two-phase friction factor correlation. The experimentally measured pressure drop is used to validate the friction factor correlation. The resulting prediction method is used to predict exit mass qualities for ammonia and R-114. The experimental analysis includes flow boiling of ammonia and R-114 in a vertical brazed-aluminum matrix heat exchanger. The test unit has straight perforated fins on the fluid side and extruded rectangular channels on the single-phase (water) heating-media side. Only two parameters are adjusted to validate the analytical prediction method, the constant in the friction factor correlation, and the constant in the slug-flow heat transfer correlation. The results show that the combination of slug-flow and thin-film annular-flow model gives better prediction of the overall performance of the matrix heat exchanger than a single model applied for the whole range of mass qualities. DOE

N89-28753# Sandia National Labs., Albuquerque, NM. Process Research Div.

EXACT SOLUTIONS FOR SYMMETRIC DEFORMATIONS OF HOLLOW BODIES OF IDEAL FLUIDS WITH APPLICATION TO INERTIAL STABILITY

Stephen L. Passman and Dennis E. Grady May 1989 36 p

(Contract DE-AC04-76DP-00789)

(DE89-014374; SAND-88-3383) Avail: NTIS HC A03/MF A01

Solutions are presented for the problems of radial motion of spherical and cyclindrical bodies of an incompressible inviscid fluid, with an initial kinetic energy, and subjected to pressure on the outer (or equivalently, inner) boundary. These solutions have bearing on the inertial stability of ejecta in hypervelocity impact and of explosively compressed shells. DOE

N89-28754# Scientific Research Associates, Inc., Glastonbury, CT.

HYPERSONIC VEHICLE ENVIRONMENT SIMULATION, PHASE 1 Final Report, 1 Aug. 1988 - 31 Mar. 1989

F. J. DeJong, J. S. Sabnis, and H. McDonald May 1989 41 p

(Contract DAAL03-88-C-0028)

(AD-A209030; ARO-26239.1-EG-SBI) Avail: NTIS HC A03/MF A01 CSCL 20/4

The hypersonic, viscous, chemically reacting flow around a vehicle in the upper layers of the atmosphere influences vehicle performance, thermal environment, and sensor visibility. Under the Phase 1 effort, a unique hybrid Navier-Stokes/Monte Carlo method has been successfully developed for the simulation of said hypersonic flows. This method combines a continuum description of the gas mixture with a statistical (or particle) description of the species transport and the chemical reactions, thereby allowing easy use of available chemical kinetics data. As such, the hybrid

approach is capable of exploiting both the efficiency of a continuum approach for the fluid dynamic calculations and the benefits in physical modeling of the Monte Carlo approach for chemical reactions. The viability of this hybrid approach for practical hypersonic flow calculations has been demonstrated in the Phase 1 effort via the calculation of the chemically reacting flow field over an axisymmetric cone. A proposed Phase 2 effort would continue the development of this method by improving the numerical efficiency of the particle transport scheme, and by incorporating physical models for catalytic walls, recombination reactions, and ionization. In addition, radiation would be included via a radiation transport model. GRA

N89-28755# Air Force Inst. of Tech., Wright-Patterson AFB, OH. School of Engineering.

WAKE DISSIPATION AND TOTAL PRESSURE LOSS IN A TWO-DIMENSIONAL COMPRESSOR CASCADE WITH CRENULATED TRAILING EDGES M.S. Thesis

Janet Lyle Veesart Jun. 1989 92 p
(AD-A209176; AFIT/GAE/ENY/89J-3) Avail: NTIS HC A05/MF A01 CSCL 20/4

Wake dissipation and total pressure loss in a two-dimensional, subsonic, compressor cascade with crenulated trailing edges were investigated in the Cascade Test Facility. Three blade configurations, a baseline NACA 64-905 airfoil and two crenulated edge patterns were used. Hot wire anemometry and a total pressure rake were used to collect the flow data. The smaller crenulation configuration exhibited the greatest turning angle and the least total pressure losses. The most rapid wake dissipation was generated by the larger crenulations' counterrotating vortices accompanied by slightly higher pressure losses than those created by the small crenulations. Both crenulated blade configurations had better wake dissipation, increased turning angles, and smaller pressure loss coefficients than the uncrenulated baseline blade. GRA

N89-28756# Naval Ship Research and Development Center, Bethesda, MD.

THEORETICAL MODEL OF GRAVITATIONAL PERTURBATION OF CURRENT COLLECTOR AXISYMMETRIC FLOW FIELD

John S. Walker, Samuel H. Brown, and Neal A. Sondergaard Mar. 1989 44 p Prepared in cooperation with Illinois Univ., Urbana
(AD-A209499; DTRC-89/004) Avail: NTIS HC A03/MF A01 CSCL 20/4

Some designs of liquid metal collectors in homopolar motors and generators are essentially rotating liquid metal fluids in cylindrical channels with free surfaces and will, at critical rotational speeds, become unstable. The role of gravity in modifying this ejection instability is investigated. Some gravitational effects can be theoretically treated by perturbation techniques on the axisymmetric base flow of the liquid metal. This leads to a modification of previously calculated critical current collector ejection values neglecting gravity effects. The derivation of the mathematical model which determines the perturbation of the liquid metal base flow due to gravitational effects is documented. Since gravity is a small force compared with the centrifugal effects, the base flow solutions can be expanded in inverse powers of the Froude number and modified liquid flow profiles can be determined as a function of the azimuthal angle. This model will be used in later work to theoretically study the effects of gravity on the ejection point of the current collector. A rederivation of the hydrodynamic instability threshold of a liquid metal current collector is presented. GRA

N89-28757# Army Engineer Waterways Experiment Station, Vicksburg, MS. Hydraulics Lab.

DEVELOPMENT OF AN EFFICIENT SOLUTION SCHEME FOR INCOMPRESSIBLE STEADY-STATE FLOW Ph.D. Thesis - Colorado State Univ. Final Report

Jeffrey P. Holland Apr. 1989 193 p
(AD-A207726; WES/TR/HL-89-8) Avail: NTIS HC A09/MF A01 CSCL 20/4

The understanding of numerical simulation of steady state, incompressible flows is advanced through development of a new solution method for two dimensional Navier-Stokes equations. Details are presented of a numerical scheme formulated specifically to simulate flows generally observed in the approaches to hydraulic structures. An explicit predictor-corrector finite volume relaxation scheme is coupled with pseudo-compressibility method to integrate the governing equations of motion and continuity. Use of the pseudo-compressibility concept negates the need for solving a Poisson equation relating the pressure and flux fields. Results from the simulations of four model case studies show the efficacy of the relaxation scheme. To accelerate the convergence of the basic relaxation scheme, a multigrid algorithm is coupled with the predictor-corrector. Results from additional simulation of the four model case studies conclusively show the validity and attractiveness of employing the multigrid approach in simulating incompressible, steady state flows. The flow fields numerically generated through inclusion of the multigrid algorithm are just as accurate as those computed with the basic relaxation scheme alone. The model test case results obtained with the multigrid algorithm are also generally from 3 to 12 times more efficient in reaching a predefined convergence tolerance than their relaxation scheme-only counterparts based on computer resource usage. The optimal multigrid setup was that which uses the maximum number of total grids allowable given the resolution on the finest grid. GRA

N89-28758# Ballistic Research Labs., Aberdeen Proving Ground, MD.

APPLICATION OF COMPUTATIONAL FLUID DYNAMICS TO THE ANALYSIS OF THE AERODYNAMICS OF A RAILGUN PROJECTILE

Paul Weinacht Mar. 1989 29 p
(AD-A207758; BRL-MR-3742) Avail: NTIS HC A03/MF A01 CSCL 20/4

An existing computational capability has been applied to assess the aerodynamic performance of a novel railgun projectile currently being investigated. The viscous flow field over the railgun configuration has been computed using a Parabolized Navier-Stokes computations technique. The configuration has been determined. Using the computed pitch-plane aerodynamic coefficients, it was concluded that the proposed design is aerodynamically stable. GRA

N89-28759# Arizona Univ., Tucson. Dept. of Aerospace and Mechanical Engineering.

EXPERIMENTAL AND NUMERICAL INVESTIGATION OF COHERENT STRUCTURES IN TURBULENT WAKE FLOWS Final Scientific Report, 6 Feb. 1985 - 5 Aug. 1988

Frank H. Champagne 25 Apr. 1989 70 p
(Grant AF-AFOSR-0146-85; AF Proj. 2307)
(AD-A207866; AFOSR-89-0568TR) Avail: NTIS HC A04/MF A01 CSCL 20/4

Large scale coherent structures were observed in two-dimensional wakes behind bluff bodies as well as non-vortex shedding bodies. There is a strong indication that these large scale structures are related to the two-dimensional instability modes of the slowly diverging mean wake flow. The Orr-Sommerfeld equation admits two solution modes for the two-dimensional plane wake. These are the sinuous mode with antisymmetric streamwise fluctuations and the varicose mode with symmetric streamwise fluctuations. The wake response to controlled sinuous and varicose types of disturbance waves was investigated. Sinuous disturbances at several amplitudes and frequencies were introduced to the wake of a flat plate by oscillating a small trailing edge flap. The Strouhal numbers of the disturbance waves were specially chosen so that the downstream location of the neutral point was well within the range of measurements. The streamwise variation of the half width of the wake an the centerline deficit was dependent on the amplitude level and showed dramatic deviations, starting near the neutral point, at large forcing levels from the well known square root behavior of the unforced case. The measured coherent Reynolds stresses were observed to change sign in the

neighborhood of the neutral point as predicted from linear stability theory. The extent of the validity of linear stability theory was investigated. GRA

N89-28760# Dayton Univ., OH. Research Inst.
FAST-ALGORITHM DEVELOPMENT FOR LARGE-EDDY SIMULATION OF CIRCULAR-JET TURBULENCE Final Report, 1 Jan. - 31 Dec. 1988
L. Krishnamurthy Mar. 1989 91 p
(Contract F49620-88-C-0040)
(AD-A207928; UDR-TR-89-29; AFOSR-89-0591TR) Avail: NTIS HC A05/MF A01 CSCL 20/4

The research reported herein addresses a theoretical investigation of a free, turbulent round jet issuing into a quiescent ambient, and deals with asymptotic analysis for farfield development and subgrid-scale turbulence modeling and with computational considerations for a large-eddy simulation. Higher-order asymptotic analysis of the fully developed downstream region has uncovered new information for the stress- and pressure-function solutions in the exterior region. The analytical predictions of the centerline decay of the mean axial velocity and those of the radial distributions of the axial and radial mean-velocity components and the shear- and normal - stress components compare well with available experimental data and provide the needed farfield boundary conditions for the large-eddy computations. The numerical considerations for the latter examine the construction of hybrid-difference methods that preserve weak but persistent unsteady features, the two-dimensional jet, and dual-variable algorithm for simulating incompressible three-dimensional flows. GRA

N89-28761# Air Force Wright Aeronautical Labs., Wright-Patterson AFB, OH.
HEAT-TRANSFER AND FRICTION FACTOR DESIGN DATA FOR ALL-METAL COMPACT HEAT EXCHANGERS Summary Report, Jan. 1985 - Nov. 1987
Christina L. Cain Mar. 1989 111 p
(AD-A208108; AFWAL-TR-88-3102) Avail: NTIS HC A06/MF A01 CSCL 20/13

To improve system life, an effort was undertaken to develop all-metal compact heat exchangers to replace existing heat exchangers which contain organic materials. Eliminating organic materials increases system life because outgassing organics can contaminate the helium working fluid and reduce system life. Perforated plate heat exchangers were found to have inherently low axial conduction and are therefore excellent candidates for cryogenic applications where an all-metal design is required. A total of 11 plate cores were tested; 2 were chemically etched, 1 was mechanically punched, and 8 were manufactured using electron beam drilling. Hole size, percent open area, and plate thickness parameters were varied among the plates. Experimental results were compared to analytical projections and found to differ significantly. The single-blow transient test technique was used to determine the heat transfer coefficients and the isothermal pressure drop test was used to determine friction factors, as a function of Reynolds number. GRA

N89-28762*# National Aeronautics and Space Administration. Langley Research Center, Hampton, VA.
DISCUSSION OF THE POTENTIAL AND LIMITATIONS OF DIRECT AND LARGE-EDDY SIMULATIONS Final Report
M. Y. Hussaini, Charles G. Speziale (Institute for Computer Applications in Science and Engineering, Hampton, VA.), and Thomas A. Zang Aug. 1989 18 p Submitted for publication
(Contract NAS1-18605)
(NASA-CR-181892; NAS 1.26:181892; ICASE-89-61) Avail: NTIS HC A03/MF A01 CSCL 20D

The full text of the discussion paper presented at the Whither Turbulence Workshop on the potential and limitations of direct and large-eddy simulations is provided. Particular emphasis is placed on discussing the role of numerics and mathematical theory in direct simulations of both compressible and incompressible flows. A variety of unresolved issues with large-eddy simulations such as their implementation in high-order finite difference codes, problems with defiltering, and modifications to accommodate integrations to solid boundaries are elaborated on. These as well as other points are discussed in detail along with the authors' views concerning the prospects for future research. Author

N89-28763*# National Aeronautics and Space Administration. Langley Research Center, Hampton, VA.
ON THE LARGE-EDDY SIMULATION OF TRANSITIONAL WALL-BOUNDED FLOWS Final Report
Ugo Piomelli, Thomas A. Zang, Charles G. Speziale, and M. Y. Hussaini (Institute for Computer Applications in Science and Engineering, Hampton, VA.) Aug. 1989 29 p Submitted for publication
(Contract NAS1-18605)
(NASA-CR-181883; NAS 1.26:181883; ICASE-89-55) Avail: NTIS HC A03/MF A01 CSCL 20D

The structure of the subgrid scale fields in plane channel flow has been studied at various stages of the transition process to turbulence. The residual stress and subgrid scale dissipation calculated using velocity fields generated by direct numerical simulations of the Navier-Stokes equations are significantly different from their counterparts in turbulent flows. The subgrid scale dissipation changes sign over extended areas of the channel, indicating energy flow from the small scales to the large scales. This reversed energy cascade becomes less pronounced at the later stages of transition. Standard residual stress models of the Smagorinsky type are excessively dissipative. Rescaling the model constant improves the prediction of the total (integrated) subgrid scale dissipation, but not that of the local one. Despite the somewhat excessive dissipation of the rescaled Smagorinsky model, the results of a large eddy simulation of transition on a flat-plate boundary layer compare quite well with those of a direct simulation, and require only a small fraction of the computational effort. The inclusion of non-dissipative models, which could lead to further improvements, is proposed. Author

N89-28764*# Institute for Computer Applications in Science and Engineering, Hampton, VA.
A PRELIMINARY COMPRESSIBLE SECOND-ORDER CLOSURE MODEL FOR HIGH SPEED FLOWS Final Report
Charles G. Speziale and Sutanu Sarkar Jul. 1989 9 p
(Contract NAS1-18605)
(NASA-CR-181875; NAS 1.26:181875; ICASE-IR-8) Avail: NTIS HC A02/MF A01 CSCL 20D

A preliminary version of a compressible second-order closure model that was developed in connection with the National Aero-Space Plane Project is presented. The model requires the solution of transport equations for the Favre-averaged Reynolds stress tensor and dissipation rate. Gradient transport hypotheses are used for the Reynolds heat flux, mass flux, and turbulent diffusion terms. Some brief remarks are made about the direction of future research to generalize the model. Author

N89-28765# National Aerospace Lab., Tokyo (Japan). V/STOL Aircraft Research Group.
FINITE ELEMENT ANALYSIS OF INCOMPRESSIBLE VISCOUS FLOWS AROUND SINGLE AND MULTI-ELEMENT AEROFOILS IN HIGH REYNOLDS NUMBER REGION
Masashi Shigemi Dec. 1988 18 p
(NAL-TR-1010T; ISSN-0389-4010) Avail: NTIS HC A03/MF A01

Incompressible viscous flows around aerofoils are solved by a finite element method. This finite element method makes use of the penalty function method as well as the streamline-upwind Petrov-Galerkin (SUPG) method and, therefore, it can be applied to the computations of the flow at a high Reynolds number. In unsteady formulations, pressure distributions are evaluated by solving Poisson's equation with regard to pressure, rather than by direct application of the penalty function equation, since the latter tends to introduce violent oscillations in the solution. Though the present computation assumes that the flows are laminar, good agreement is obtained with experimentally measured results,

particularly when the flow shows laminar separation. It is shown that this method can be applied to problems of flow around complicated geometries, and it is stated that the extension of the method to three-dimensional problems is promising. Author

N89-28766*# Institute for Computer Applications in Science and Engineering, Hampton, VA.
A NONLINEAR INVESTIGATION OF THE STATIONARY MODES OF INSTABILITY OF THE THREE-DIMENSIONAL COMPRESSIBLE BOUNDARY LAYER DUE TO A ROTATING DISC Final Report
Sharon O. Seddougui Jul. 1989 31 p Submitted for publication
(Contract NAS1-18605)
(NASA-CR-181901; NAS 1.26:181901; ICASE-89-50) Avail: NTIS HC A03/MF A01 CSCL 20D

The effects of compressibility on a stationary mode of instability of the 3-D boundary layer due to a rotating disc are investigated. The aim is to determine whether this mode will be important in the finite amplitude destabilization of the boundary layer. This stationary mode is characterized by the effective velocity profile having zero shear stress at the wall. Triple-deck solutions are presented for an adiabatic wall and an isothermal wall. It is found that this stationary mode is only possible over a finite range of Mach numbers. Asymptotic solutions are obtained which describe the structure of the wavenumber and the orientation of these modes as functions of the local Mach number. The effects of nonlinearity are investigated allowing the finite amplitude growth of a disturbance close to the neutral location to be described. Author

N89-28767# North Carolina State Univ., Raleigh. Dept. of Mechanical and Aerospace Engineering.
A SPACE MARCHING ALGORITHM FOR THE THIN-LAYER NAVIER-STOKES EQUATIONS M.S. Thesis
Francis A. Greene 1989 71 p
Avail: NTIS HC A04/MF A01

An implicit upwind code which globally iterates the thin-layer Navier-Stokes equations for a laminar perfect gas is converted into an implicit space marching code. The base code is the previously developed Langley Aerothermodynamic Upwind Relaxation Algorithm (LAURA), and is used to generate the starting solution for the newly developed space marching version. Since the two algorithms differ only in the computation of the streamwise flux, an added degree of consistency between the starting code and the marching code is achieved. The modified streamwise flux is formulated to be 1st or 2nd order accurate, using upwind or Symmetric Total Variation Diminishing (STVD) differencing, respectively. Each crossflow plane is locally iterated in time until converged, then marched in space to the next station. This procedure gives a complete solution in a single pass over the body. The new scheme solves the thin-layer Navier-Stokes equations and is a fully conservative, second order accurate, finite volume scheme, which yields solutions equivalent to Parabolized Navier-Stokes (PNS) solutions, and is subject to the same flow restrictions. The algorithm is tested on a sphere-cone geometry and a geometry which models the windward side of the Space Shuttle Orbiter. Computational results for surface heating are compared to ground based experimental results. In addition, space marching solutions for surface pressure, heating, and computational times are compared to the base algorithm. Author

N89-28768# California Univ., Los Angeles. Dept. of Mechanical, Aerospace and Nuclear Engineering.
ENHANCEMENT OF FORCED CONVECTION HEAT TRANSFER IN TUBES USING STAGED TANGENTIAL FLOW INJECTION Annual Report, Jun. 1987 - Sep. 1988
V. X. Tung, V. K. Dhir, F. Chang, A. R. Karagozian, and F. Zhou Mar. 1989 68 p
(Contract GRI-5087-260-1535)
(PB89-204598; GRI-89/0020) Avail: NTIS HC A04/MF A01 CSCL 20D

Experiments using air as the test fluid were carried out to study enhancement in heat transfer in tangential injection induced swirl flows. In the experiments, an electrically heated tube 25.4 mm in inside diameter and 3.05 m in length was used. Tangential injection of fluid was accomplished through four injectors placed around the tube periphery. The flow rate through the injectors was varied parametrically. Tangential injection is found to enhance heat transfer significantly. A two-fold increase in average heat transfer coefficient over a 70 hydraulic diameters long tube is observed when all of the fluid is injected tangentially through four 5.08 mm diameter injectors. The average heat transfer coefficient increases weakly with Reynolds number but decreases with Prandtl number. It is calculated that on a constant pumping power basis, as much as 45 percent enhancement can occur with single stage injection. With multiple injection, higher enhancements are possible. Both analytical and numerical modeling of the process was attempted. Author

N89-28769# Technische Univ., Clausthal-Zellerfeld (Germany, F.R.). Fakultaet fuer Bergbau, Huettenwesen und Maschinenwesen.
NUMERICAL DETERMINATION OF GUARANTEED RAYLEIGH NUMBERS AND THE PERTAINING FLOW FORMS IN STEADY, AXISYMMETRIC CONVECTION IN CYLINDERS Ph.D. Thesis [NUMERISCHE BESTIMMUNG GESICHERTER RAYLEIGH-ZAHLEN UND ZUGEHOERIGER STROEMUNGSFORMEN BEI STATIONAERER, ROTATIONSSYMMETRISCHER KONVEKTION IN ZYLINDERN]
Erich Buergel 1988 122 p In GERMAN
(ETN-89-94432) Avail: NTIS HC A06/MF A01

The determination of guaranteed Rayleigh numbers and the pertaining flow forms for steady axisymmetric (natural) convection in closed and open-at-the-top, vertical circular cylinders was investigated. The condition of adhesion to the wall is fulfilled. The starting equations for the disturbance variables are the Boussinesq-approximated equations. The eigenvalues for the steady, axisymmetric case were determined using the Ritz method for the upper limits, and the generalized Lehmann-Maehly method of Goerisch for the lower limits. The calculations show that for slender cylinders the eigenvalue curves converge for higher height-to-radius ratios whereby the Rayleigh numbers change only imperceptibly. For compact, closed cylinders the flow forms pertaining to low Rayleigh numbers show a pure radially subdivided cellular structure. ESA

N89-28770# Karlsruhe Univ. (Germany, F.R.). Fakultaet fuer Chemieingenieurwesen.
EXPERIMENTAL INVESTIGATIONS OF FLOW FORCES EXERTED ON SPHERES IN REST AND IN MOTION, IN A PLANE POISEVILLE FLOW Ph.D. Thesis [EXPERIMENTELLE UNTERSUCHUNGEN UEBER STROEMUNGSKRAEFTE AUF RUHENDE UND BEWEGTE KUGELN IN EINER EBENEN POISEUILLE-STROEMUNG]
Eugen-Walter Buechner 1987 155 p In GERMAN Sponsored by the Deutsche Forschungsgemeinschaft, Bonn, Fed. Republic of Germany
(ETN-89-94433) Avail: NTIS HC A08/MF A01

Flow forces were measured on a sphere at rest and on moving, non-rotatable spheres in a plane Poiseuille flow, as well as on a moving sphere in a medium at rest. It is shown that walls increase the drag force on spheres and produce a force perpendicular to the flow direction. For low inflow Reynolds (Re) numbers the drag force depends linearly on Re, the lift force approximately quadratically. For higher Re the drag force has a quadratic part and the lift force dependence becomes more linear. The influence of the Reynolds number of the Poiseuille flow is weak. It is shown that for moving spheres in a plane Poiseuille flow forces directed towards the wall can exist; besides those directed away from the wall. The measurements show the existence of a velocity slip whose behavior as a function of the sphere-wall distance is similar to that of the drag force. The torque on spheres could not be measured. The results can approximately be applied to free-flowing, rotatable spheres. ESA

N89-28771# Technische Univ., Berlin (Germany, F.R.). Fachbereich Physik.

THE ANISOTROPY OF THE FRICTION PRESSURE OF DIPOLAR FLUIDS Ph.D. Thesis [ZUR ANISOTROPIE DES REIBUNGSDRUCKES DIPOLARER FLUESSIGKEITEN]

Josef Friedrich Schwarzl 1988 147 p In GERMAN
(ETN-89-94438) Avail: NTIS HC A07/MF A01

The behavior of anisotropic fluids under the influence of a plane Couette flow was investigated. A model fluid where components are parallel dipoles in a strong magnetic field is considered. A simple relaxation assumption for the pair correlation function under shear was used, for the calculation of the linear contribution of the potential part of the friction pressure tensor to shear rate. This assumption is shown to be valid for sufficiently weak dipole moments. The results are consistent with a known assumption for the linear viscosity, that is almost exclusively based on general symmetry considerations. A molecular dynamics program was adapted to the model fluid for the verification of the theoretically predicted relations between the friction pressure components. The simulations are in agreement with theory. ESA

N89-28772# Technische Univ., Brunswick (Germany, F.R.). Fakultaet fuer Maschinenbau und Elektrotechnik.

HEAT TRANSFER IN FREE CONVECTION AND FORCED, LAMINAR FLOW IN VERTICAL TUBES, CONSIDERING TEMPERATURE DEPENDENT MEDIUM CHARACTERISTICS Ph.D. Thesis [DER WAERMEUEBERGANG BEI FREIER KONVEKTION UND ERZWUNGENER, LAMINARER STROEMUNG IN SENKRECHTEN ROHREN UNTER BERUECKSICHTIGUNG TEMPERATURABHAENGIGER STOFFWERTE]

Hans-Jochen Kessler 1988 165 p In GERMAN
(ETN-89-94441) Avail: NTIS HC A08/MF A01

The local and average heat transfer coefficients in the laminar flow in vertical tubes, which are significantly better than in the case of horizontal flow, were calculated. The numerical calculation was performed for a heated upward flow and a cooled downward flow. Navier-Stokes equations, energy equation, continuity equation, medium characteristics functions and the simplified equation system with boundary conditions are deduced. The similarity theory was applied to obtain the required set of characteristic values. The numerical method and the Runge-Kutta-Fehlberg time integration are outlined. The correlations of the analytical boundary solutions concord with other analytical solutions and with experimental data. The systematic, but acceptable errors are partly due to insufficient discretization. ESA

N89-28773# Technische Univ., Munich (Germany, F.R.). Fakultaet fuer Maschinenwesen.

HEAT TRANSFER AND FILM COOLING IN COMPRESSIBLE NOZZLE FLOW Ph.D. Thesis [WAERMEUEBERGANG UND FILMKUEHLUNG IN KOMPRESSIBLER DUESENSTROEMUNG]

Joachim Stoll 1987 228 p In GERMAN
(ETN-89-94653) Avail: NTIS HC A11/MF A01

Heat transfer and film cooling in convergent-divergent nozzles were experimentally and theoretically investigated. Tests with adiabatic wall and with coding film injection show an almost linear increase of the coding film efficiency with injection flow for relatively low flows; to obtain higher efficiencies more than a proportional injection is required. The optimum injection speed ratios, and the significant effects of free flow turbulence degree and wall coding on the film coding efficiency were determined. An improved computer program developed for a compressible, turbulent boundary layer allowed to demonstrate the efficiency and compatibility of different turbulence models using experimental results. An efficient method for the computation of transonic nozzle flow, taking into account the boundary layer, was developed. A simple procedure for the calculation of heat transfer and film cooling efficiency, in accelerated flows, is presented. ESA

N89-28774# Institut Franco-Allemand de Recherches, Saint-Louis (France).

LASER VELOCIMETRY IN THE CLOSE WAKE OF AN AXISYMMETRIC REAR BODY [MESURES DE VELOCIMETRIE LASER DANS LE SILLAGE PROCHE D'ARRIERE-CORPS A SYMETRIE DE REVOLUTION]

C. Berner, V. Petitdamage, and J. P. Duperoux 24 Jun. 1987 48 p In FRENCH
(ISL-R-114/87; ETN-89-94855) Avail: NTIS HC A03/MF A01

Experimental data were obtained with axisymmetric specimens placed in a cold jet for Mach number = 0.35. The velocimeter is a two dimensional argon laser (two colors, three beams, 5W). The analysis of the average velocity and turbulent fluctuations show strong variations with the geometry of the body with strong velocity gradients and large shear stress causing turbulent flow in the mixing zone. The Reynolds tensions are 30 percent lower than indicated in the literature. ESA

N89-28775# Centre d'Etudes et de Recherches, Toulouse (France). Dept. Informatique.

SOLUTION OF EULER EQUATIONS BY A DISCONTINUOUS GALERKIN METHOD OBTAINED FROM A VARIATIONAL FORMULATION OF ENTROPY Final Report [RESOLUTION DES EQUATIONS D'EULER PAR UNE METHODE DE GALERKIN DISCONTINUE, ISSUE D'UNE FORMULATION VARIATIONELLE EN ENTROPIE]

F. Bourdel and P.-A. Mazet Jan. 1989 58 p In FRENCH
(Contract DRET-88-002-11)
(CERT-1/332400/DERI; ETN-89-94867) Avail: NTIS HC A04/MF A01

The flow splitting method is generalized to nonlinear system with the restriction that they must be interpreted as averages of a linear scalar equation called system Boltzmann equation. The numerical results for two dimensional applications are presented. A self adaptive space-time networking strategy specific to the method is described. It is shown that the procedure is robust, and that the results do not show parasitic oscillations. ESA

N89-28776# Universiteit Twente, Enschede (Netherlands). Faculty of Applied Mathematics.

ON THE CLASSIFICATION OF PLANE GRAPHS REPRESENTING STRUCTURALLY STABLE RATIONAL NEWTON-FLOWS

H. Th. Jongen, P. Jonker, and F. Twilt Nov. 1988 22 p Revised
(Memo-750-Rev; Memo-645-Rev; ISSN-0169-2690;
ETN-89-95117) Avail: NTIS HC A03/MF A01

Certain plane graphs, called Newton-graphs, are studied, which represent a special class of dynamical systems which are closely related to Newton's iteration method for finding zeros of rational functions defined on the complex plane. These Newton-graphs are defined in terms of nonvanishing angles between edges at the same vertex. Necessary and sufficient conditions of a purely combinatorial nature are derived for an arbitrary plane graph in order to be topologically equivalent with a Newton-graph. The structure of Newton-graphs is analyzed and the existence of a polynomial algorithm to recognize such graphs is proved. ESA

N89-28777# National Aerospace Lab., Amsterdam (Netherlands). Informatics Div.

NUMERICAL GRID GENERATION IN 3D EULER-FLOW SIMULATION

J. W. Boerstoel 26 Apr. 1988 28 p Presented at the Conference on Numerical Methods for Fluid Dynamics, Oxford, United Kingdom, 21-24 Mar. 1988 Submitted for publication Prepared in cooperation with Aeritalia S.p.A., Naples, Italy and Fokker B.B., Amsterdam, Netherlands
(Contract NIVR-0604N)
(NLR-MP-88013-U; ETN-89-95416) Avail: NTIS HC A03/MF A01

The technical problems with grid generation are analyzed and an overview of proposed solutions is given. The usefulness of grid-generation techniques, for the numerical simulation of Euler

(and Navier-Stokes) flows around complex three-dimensional aerodynamic configurations, is illustrated. It is shown that the core of the grid-generation problem is a topology problem. The following remarks are sketched: grid generation is a subtask in a numerical simulation of a flow in industrial and research environments; the design requirements of a grid generation concern the geometrical imput, the desired grid as output, the technical means to control grid resolution and quality and turnaround time performance; the construction of a blocked grid can be subdivided in a block-decomposition task and a grid-point distribution task. A technique for using connectivity relations to define conventions about local coordinate systems in edges, faces and blocks is presented. Experiences are reported and an example concerning a 96-blocked grid around a complex aerodynamic configuration is given. Concepts for improvements in the presented technique are discussed. ESA

N89-28778# Cambridge Univ. (England). Dept. of Engineering.
A COMPRESSIBLE INVERSE DESIGN METHOD BASED ON AN ANALYTICAL APPROACH
M. Zangeneh 1989 62 p
(CUED/A-Turbo/TR-125; ISSN-0309-6521) Avail: NTIS HC A04/MF A01

A method of designing highly loaded blades in compressible flow is presented. The method is based on a recently developed, versatile 3-D design method, in which the blades are represented by sheets of vorticity whose strength is obtained from a specified distribution of swirl velocity. In the present application, the flow is assumed subsonic and inviscid and the blades are assumed to have negligible thickness. The blade shape is computed iteratively, by first assuming an initial blade shape and then computing the corresponding flow field, from which a new estimate of the blade shape is obtained by requiring the blades to be tangential to the velocity at the blade. The flow field is computed by using a kinematic approach in which the Clebsch formulation of steady rotational flow and the continuity equation are used to find an equation for the unknown potential function. In order to investigate the effect of different approximations of the compressible flow problem on the accuracy of the method, it is here applied to the design of 2-D rectilinear cascades, whose simple geometry makes an analytical solution possible. The effect of neglecting the pitchwide variation of density on the method was investigated by deriving analytical expressions for the error terms and then calculating these terms for different blade profiles, Mach numbers and swirl distributions. The results indicate that, in most cases, the magnitude of the error terms are quite small and that, in subsonic flow, the magnitude of the largest error terms are proportional to the derivative of the blade loading. Therefore, it is shown that the approximate form of the continuity equation (average density approach), which simplifies the problem significantly, can be used in the 3-D version of the design method without loss of accuracy. Author

N89-28779# Universiteit Twente, Enschede (Netherlands). Faculty of Applied Mathematics.
GRADIENT NEWTON-FLOWS FOR COMPLEX POLYNOMIALS
F. Twilt, P. Jonker, and M. Streng Jan. 1989 22 p
(Memo-764; ISSN-0169-2690; ETN-89-95059) Avail: NTIS HC A03/MF A01

Gradient Newton-flows for a class of functions closely related to the complex polynomials are studied. Concepts of Gradient and Rational Newton-flows are summarized and properties including structural stability and global convergence are investigated. Results on the global qualitative behavior of certains types of Newton-flows are derived from the studies of these properties. For the special case of third degree polynomials a complete description of the local and global features of the involved phase-portraits is given. ESA

N89-28780 Technische Univ., Delft (Netherlands). Faculty of Mechanical Engineerng and Marine Engineering.
COMPACT HEAT AND MASS EXCHANGERS OF THE PLATE FIN TYPE IN THERMAL SORPTION SYSTEMS: APPLICATION IN AN ABSORPTION HEAT PUMP WITH THE WORKING PAIR CH3OH-LiBr/ZnBr2 Ph.D. Thesis
Harry Becker 1989 118 p
(ISBN-90-370-0022-3; ETN-89-95453) Copyright Avail: Technische Univ. Delft, Mechanical Engineering Dept., 1 Stevinweg 1, 2628 CN Delft, Netherlands

The possible application of Compact Heat and Mass Exchangers (CHME) in a gas fired Absorption Heat Pump (AHP) for domestic heating is studied. The above mentioned heat and mass exchangers are of the plate type. The space between the parallel and plain plates is filled up with corrugated plates of a certain height. The plain and finned plates are stacked and welded together. This gives a heat and mass exchanger which is very compact, expressed by a high area density (m2/m3). This leads to heat and mass transfer processes with small temperature and concentration differences. For testing purposes a pilot plant was built using the above type of components in order to test their heat and/or mass transfer performance. Only the generator is of the Shell And Tube (SAT) type. As the working pair, CH3OH - LiBr/ ZnBr2 was chosen, with the alcohol as the solvent and the salt mixture as the absorbent. This leads to sub atmospheric working pressures with only solvent in the vapor phase. Three series of experiments have been carried out, during which the input parameters were varied over a certain range. It is concluded that the plate fin CHMES are very suitable for application in an AHP for domestic heating purposes. ESA

N89-28781# Office National d'Etudes et de Recherches Aerospatiales, Paris (France).
LA RECHERCHE AEROSPATIALE, BIMONTLY BULLETIN, NUMBER 1988-3
ESA Jan. 1989 77 p Transl. into ENGLISH of La Recherche Aerospatiale, Bulletin Bimestriel (Paris, France, ONERA), no. 1988-3 p 1-77
(ESA-TT-1137; ETN-89-94446) Avail: NTIS HC A05/MF A01

The titles include, prediction of separated flow past airfoil using viscous-inviscid interaction technique, interaction of diffusion and premixed flames with a vortex, modeling of beam or tube damage under torsional stress, recent progress in wall interference calculations for industrial wind tunnels, and experimental analysis of turbulent separation on an ablate ellipsoid cylinder. ESA

N89-28782# Universiteit Twente, Enschede (Netherlands). Faculty of Applied Mathematics.
A DYNAMIC VARIATION PRINCIPLE FOR ELASTIC-FLUID CONTACTS, APPLIED TO ELASTOHYDRODYNAMIC LUBRICATION THEORY
E. vanGroesen and R. Verstappen Nov. 1988 28 p
(Memo-746; ISSN-0169-2690; ETN-89-95114) Avail: NTIS HC A03/MF A01

The variational structure underlying elastohydrodynamic lubrication theory is investigated by the study of the variational structure of the line contact problem between an elastic medium and a fluid. Equations for the deformation in the elastic material, and the flow of viscous fluid are determined from an elastic energy and power functional, and a variational formula given for the combined system. Equations expressing the balance of forces on the separating boundary, and equations in the interior of both media, are obtained. Time dependent deformations are considered, where the velocity in the elastic medium vanishes, and the particle acceleration on both sides of the common boundary is equal. The result is applied to a typical problem from elastohydrodynamic theory and resulting expressions are simplified by imposing a common restriction to small deformations and exploiting the characteristic length scales of the problem. The formulation of the approximated system is shown to be a genuine variational principle and to correctly produce the differential expressions. A natural way of generating efficient numerical methods to calculate

the deformation of, and the pressure at, the free boundary, if the time variable is descretized, is achieved. ESA

N89-28783# Naples Univ. (Italy). Istituto di Aerodinamica.
EFFECTS OF REAL GAS IN HYPERSONIC EXPANSION Ph.D. Thesis [EFFETTI DEI GAS REALI NELLE ESPANSIONI IPERSONICHE]
Edmondo Bassano 1988 195 p In ITALIAN
(ETN-89-95200) Avail: NTIS HC A09/MF A01

The irreversible processes related to chemical and vibratory relaxation phenomena are described, and used to develop a generalization of Crocco theorem for equilibrium states. The equations are expressed in polar coordinates and the Prandtl-Meyer hypothesis is introduced. The characteristic parameters of the field equations are identified. Exact solutions and a small perturbation theory are derived. Approximations obtained by two methods are compared to the exact solutions and findings discussed. ESA

35 INSTRUMENTATION AND PHOTOGRAPHY

Includes remote sensors; measuring instruments and gages; detectors; cameras and photographic supplies; and holography.

For aerial photography see *43 Earth Resources and Remote Sensing*. For related information see also *06 Aircraft Instrumentation*, and *19 Spacecraft Instrumentation*.

N89-28784# Sandia National Labs., Albuquerque, NM.
A METHOD FOR EVALUATING STRUCTURAL TRANSDUCERS USED IN TYPE B PACKAGE TESTING
Marcella M. Madsen, William L. Uncapher, David R. Bronowski, and Duane R. Stenberg (Southwest Engineering Associates, El Paso, TX.) 1989 9 p Presented at the International Symposium on Packaging and Transporting of Radioactive Materials, Washington, DC, 11 Jun. 1989
(Contract DE-AC04-76DP-00789)
(DE89-013591; SAND-89-0560C; CONF-890631-14) Avail: NTIS HC A02/MF A01

As a result of an agreement between DOE and the Nuclear Regulatory Commission (NRC), each transport cask must be certified by the NRC. To meet these requirements, OCRWM is undertaking a program to design, test, certify, and fabricate a variety of cask systems. Design verification tests will be performed by the cask contractor to demonstrate design safety and to aid in cask certification by the NRC. During Type B packaging design verification testing designers may verify analytical calculations with instrumentation data. Many packagings are tested with accelerometers and strain gages, collectively known as transducers, that measure structural response. Accelerometers measure acceleration and strain gages measure surface strain at the mounted location. This paper describes a method developed for OCRWM to evaluate various transducers of these two types that have been suggested for use in design verification testing. Typically transducers are characterized by the manufacturer under laboratory conditions. In this program ruggedness, failure frequency, repeatability, and manufacturer's data under field and laboratory conditions were investigated. Specific cask model test require transducers with specific ranges; transducers of the selected types were procured with ranges appropriate for this test. DOE

N89-28785# National Inst. of Standards and Technology, Gaithersburg, MD. Office of Physical Measurement Services.
NIST (NATIONAL INSTITUTE OF STANDARDS AND TECHNOLOGY) CALIBRATION SERVICES USERS GUIDE, 1989 EDITION
Joe D. Simmons, ed. Jan. 1989 212 p Revised Original contains color illustrations
(PB89-200216; NIST/SP-250) Avail: NTIS HC A10/MF A01; SOD HC $11.00 as 003-003-02909-2 CSCL 14B

The National Institute of Standards and Technology (NIST) Calibration Services Users Guide provides detailed descriptions of currently available NIST calibration services, measurement assurance programs, and special test services. The following measurement areas are covered: (1) dimensional; (2) mechanical, including flow, accoustic, and ultrasonic; (3) thermodynamic; (4) optical radiation; (5) ionizing radiation; and (6) electromagnetic, including dc, ac, rf, and microwave. A separate Fee Schedule is issued as required, providing current prices for the services offered, updates on points-of-contact, and information on measurement seminars. Author

N89-28786# Sandia National Labs., Albuquerque, NM.
A FULLY AUTOMATED, SINGLE-CONNECTION TESTER FOR T/R MODULES
George R. Sloan and James M. Simons 1989 10 p Presented at the Automatic RF Technologies Group Meeting, Long Beach, CA, 15 Jun. 1989
(Contract DE-AC04-76DP-00789)
(DE89-013155; SAND-89-1192C; CONF-8906132-1) Avail: NTIS HC A02/MF A01

An inherent aspect of active array radars is the use of large numbers, typically hundreds, of transmit/receive (T/R) modules. The implementation of this technology at Sandia has created new challenges for the tester designer. Foremost among these challenges is the need to design T/R module testers which can accommodate such large numbers of Devices-Under-Test (DUTs). This task is complicated by the fact that state-of-the-art T/R modules are extremely sophisticated and require a broad spectrum of tests for adequate evaluation. The Sandia T/R module operates in Ku band and consists of a transmitter, receiver, programmable phase shifter, programmable attenuator, modulator, switched limiter, and gate-array controller. The programmable phase shifter is common to both the transmitter and receiver, but the attenuator is unique to the receiver. The instruments required for the tests include a network analyzer, a spectrum analyzer, a noise figure meter, a peak power meter, and an automated tuner system. The key to a successful tester is in integrating all of the above instruments such that the desired measurements can all be performed from a single, two-port, tester-to-DUT connection. The natural consequence of such a design is that some measurements will have to be de-embedded from the integrated test setup. DOE

N89-28787# EG and G Energy Measurements, Inc., Las Vegas, NV.
IN SEARCH OF MORE OUTPUT: TWO STRAIN GAGE BRIDGE CIRCUITS REVISITED
Roger P. Noyes and John Kalinowski (EG and G Energy Measurements, Inc., Pleasanton, CA.) 1989 7 p Presented at the 15th Transducer Workshop, Cocoa Beach, FL, 20 Jun. 1989
(Contract DE-AC08-88NV-10617)
(DE89-014039; EGG-10617-1033; CONF-8906133-2) Avail: NTIS HC A02/MF A01

The emplacement of large loads via drill pipe is common in Nevada. EG and G Energy Measurements, Inc. is involved in instrumentation. The loading of the drill pipe is of interest and is often measured with strain gages. Sometimes the amount of loading is small relative to the size of the pipe and only produces strain level on the order of 500 to 1000 microstrain. These circumstances have led to implementation of practical methods of measuring these strain levels. The original measurements were made utilizing piezoresistive strain gages with gage factors on the order of 55. Although having large outputs, these gages posed other problems. As a need for more reliable measurements arose, more stable gages were used. These gages have lower output, on the order of 2; therefore, techniques were investigated to gain more output. These techniques used proven circuits and were investigated for the best practical use under our particular circumstances and environments. The results of these investigations will be reported, and conclusions given, in the summary of this presentation. DOE

N89-28788# California Univ., Berkeley. Lawrence Berkeley Lab. Center for X-ray Optics.
AN X-RAY MICROPROBE USING FOCUSSING OPTICS WITH A SYNCHROTRON RADIATION SOURCE
A. C. Thompson, J. H. Underwood, Y. Wu, and R. D. Giauque Jan. 1989 16 p Presented at the 3rd International Conference on Synchrotron Radiation Instrumentation, Tsukuba, Japan, 29 Aug. 1988
(Contract DE-AC03-76SF-00098)
(DE89-013425; LBL-26862; CONF-8808141-13) Avail: NTIS HC A03/MF A01

An X-ray microprobe can be used to produce maps of the concentration of elements in a sample. Synchrotron radiation provides X-ray beams with enough intensity and collimation to make possible elemental images with femtogram sensitivity. The use of focussing X-ray mirrors made from synthetic multilayers with a synchrotron X-ray beam allows beam spot sizes of less than 10 micrometers x 10 micrometers to be produced. Since minimal sample preparation is required and a vacuum environment is not necessary, there will be a wide variety of applications for such microprobes. DOE

N89-28789# Los Alamos National Lab., NM.
THE LOS ALAMOS FOURIER-TRANSFORM SPECTROMETER: APPLICATIONS TO MOLECULAR SPECTROSCOPY
Byron A. Palmer and Robin S. McDowell 1989 7 p Presented at the 7th International Conference on Fourier Transform Spectroscopy, Fairfax, VA, 19-23 Jun. 1989 Submitted for publication
(Contract W-7405-eng-36)
(DE89-014258; LA-UR-89-1951; CONF-890674-3) Avail: NTIS HC A02

The design considerations and operating characteristics are outlined for the Los Alamos Fourier transform spectrometer, a state-of-the-art instrument operating from 200 nm to 20 micrometer with a resolution of 0.0026/cm and very high wave number and intensity accuracy. Recent work in molecular spectroscopy carried out with this instrument is discussed, including N2(+) spectra obtained in inductively-coupled plasmas; high-temperature spectra of diatomic molecules of astrophysical interest; high-resolution rovibrational fine structure; and Fourier transform Raman spectroscopy of species in expansion-cooled gases. DOE

N89-28790# Sandia National Labs., Albuquerque, NM.
THE PVF2 PIEZOELECTRIC POLYMER SHOCK STRESS SENSOR: SYSTEM CHARACTERIZATION FOR APPLICATION UNDER FIELD TEST CONDITIONS
R. P. Reed and J. I. Greenwoll 1989 24 p Presented at the 15th Transducer Workshop, Cocoa Beach, FL, 20-22 Jun. 1989
(Contract DE-AC04-76DP-00789)
(DE89-014629; SAND-89-1594C; CONF-8906133-3) Avail: NTIS HC A03/MF A01

The piezoelectric polymer, polyvinylidene di-fluoride (PVDF or PVF2), properly processed by the proprietary Bauer technique, is a material for a transducing element that can be used for a wide variety of stress, pressure, or temperature related measurements. Its versatility as a sensor requires especially careful attention to the special requirements for associated gauge packaging, installation, signal conditioning, recording, and analysis that are imposed by the particular diverse test conditions. Most applications reported to date were for tests performed under laboratory conditions. But, the PVDF sensor was also successfully used for stress wave measurement under adverse and often hostile field test conditions that require the use of lengthy transmission lines and allow only limited recording capability. One crucial aspect of field application is discussed, measuring system characterization, and correction of signals distorted by systems of marginal frequency capability. DOE

N89-28791# Brookhaven National Lab., Upton, NY. Dept. of Chemistry.
POSITIONING ERROR INDUCED BY AXIAL SAMPLING IN POSITRON EMISSION TOMOGRAPHY
Bernard Bendriem, Stephen L. Dewey, and David J. Schlyer 1989 11 p Presented at the International Congress on Optical Science and Engineering, Paris, France, 24 Apr. 1989
(Contract DE-AC02-76CH-00016)
(DE89-014519; BNL-42829; CONF-8904242-1) Avail: NTIS HC A03/MF A01

A multi-slice Positron Camera organizes data as a set of parallel slices whose thickness is defined by the Axial Response Function (ARF) of the tomograph. This ARF is usually not uniform and the sensitivity is maximum for a point source located at the center of the slice. As a consequence, the partial volume effect (quantitation loss for structures that are smaller than two to three times the FWHM resolution) will be dependent not only on the size of the structure but also on its relative position with regard to the ARF. A computer simulation was developed to analyze this effect. Objects of different size and shape are examined and it is shown that on a system with a 6 mm axial resolution (FWHM), a shift of 3 mm can introduce more than 10 percent variation on the final measurement. The simulation is confirmed by experimental results on a high resolution PET. It was concluded that positioning and repositioning must be handled with great care in order to make reproducible measurements and allow accurate partial volume corrections. DOE

N89-28792# Georgia Inst. of Tech., Atlanta. School of Electrical Engineering.
HOLOGRAPHIC MODULATOR ARRAYS Final Report, Apr. - Dec. 1987
H. J. Caulfield May 1989 27 p
(Contract F30602-81-C-0185)
(AD-A209387; RADC-TR-89-53) Avail: NTIS HC A03/MF A01
CSCL 25/3

The report contains an assessment of the performance of a spatial light modulator concept known as double phase conjugate mirrors using a barium titanate crystal as the conjugating medium. It was concluded that these crystals are inaccurate for this application because of their low efficiency and speed. More research is necessary on new materials such as non-linear optical polymers to provide materials with the necessary response times to be useful in this application. It also contains an assessment of a method to write complex microwave antenna information onto laser beams in analog format. It was concluded that the performance of spatial light modulators that are currently available makes them unacceptable for this application. GRA

N89-28793*# National Aeronautics and Space Administration. Marshall Space Flight Center, Huntsville, AL.
HOLLOW FIBER CLINOSTAT: TECHNICAL ABSTRACT Patent Application
Percy H. Rhodes, inventor (to NASA), Teresa Y. Miller, inventor (to NASA), and Robert S. Snyder, inventor (to NASA) 28 Jul. 1989 13 p
(NASA-Case-MFS-28370-1; NAS 1.71:MFS-28370-1;
US-Patent-Appl-SN-386175) Avail: NTIS HC A03/MF A01
CSCL 14B

A clinostat for simulating microgravity on cell systems carried in a fiber fixedly mounted in a rotatable culture vessel is disclosed. The clinostat is rotated horizontally along its longitudinal axis to simulate microgravity or vertically as a control response. Cells are injected into the fiber and the ends of the fiber are sealed and secured to spaced end pieces of a fiber holder assembly which consists of the end pieces, a hollow fiber, a culture vessel, and a tension spring with three alignment pins. The tension spring is positioned around the culture vessel with its ends abutting the end pieces for alignment of the spring. After the fiber is secured, the spring is decompressed to maintain tension on the fiber while it is being rotated. This assures that the fiber remains aligned along the axis of rotation. The fiber assembly is placed in the culture vessel and culture medium is added. The culture vessel is then inserted into the rotatable portion of the clinostat and subjected to rotate at selected rpms. The internal diameter of the hollow fiber determines the distance the cells are from the axis of rotation. NASA

N89-28794*# National Aeronautics and Space Administration. Pasadena Office, CA.
APPARATUS AND METHOD FOR CHARACTERIZING THE TRANSMISSION EFFICIENCY OF A MASS SPECTROMETER Patent Application
Santash Srivasytava, inventor (to NASA) (Jet Propulsion Lab., California Inst. of Tech., Pasadena.) 26 May 1989 19 p
(Contract NAS7-918)
(NASA-Case-NPO-16989-1-CU; NAS 1.71:NPO-16989-1-CU; US-Patent-Appl-SN-358027) Avail: NTIS HC A03/MF A01
CSCL 14B

An electron/ion coincidence technique is employed to characterize the absolute mass dependent transmission efficiency of mass spectrometers. The technique is not dependent upon the partial pressure of the sample beam or the ionization cross sections of calibrant gases. NASA

N89-28795*# National Aeronautics and Space Administration. Pasadena Office, CA.
REVERSAL ELECTRON ATTACHMENT IONIZER FOR DETECTION OF TRACE SPECIES Patent Application
Mark T. Bernius, inventor (to NASA) and Ara Chutjian, inventor (to NASA) (Jet Propulsion Lab., California Inst. of Tech., Pasadena.) 5 Jun. 1989 34 p
(Contract NAS7-918)
(NASA-Case-NPO-17596-1-CU; NAS 1.71:NPO-17596-1-CU; US-Patent-Appl-SN-361531) Avail: NTIS HC A03/MF A01
CSCL 14B

An in-line reversal electron, high-current ionizer capable of focusing a beam of electrons to a reversal region and executing a reversal of the electrons, such that the electrons possess zero kinetic energy at the point of reversal, may be used to produce both negative and positive ions. A sample gas is introduced at the point of electron reversal for low energy electron-(sample gas) molecule attachment with high efficiency. The attachment process produces negative ions from the sample gas, which includes species present in trace (minute) amounts. These ions are extracted efficiently and directed to a mass analyzer where they may be detected and identified. The generation and detection of positive ions is accomplished in a similar fashion with minimal adjustment to potentials applied to the apparatus. NASA

N89-28796*# National Aeronautics and Space Administration. Pasadena Office, CA.
FIELD INDUCED GAP INFRARED DETECTOR Patent Application
C. Thomas Elliott, inventor (to NASA) (Jet Propulsion Lab., California Inst. of Tech., Pasadena.) 21 Jun. 1989 27 p
(Contract NAS7-918)
(NASA-Case-NPO-17526-1-CU; NAS 1.71:NPO-17526-1-CU; US-Patent-Appl-SN-369403) Avail: NTIS HC A03/MF A01
CSCL 14B

A tunable infrared detector which employs a vanishing band gap semi-metal material provided with an induced band gap by a magnetic field to allow intrinsic semiconductor type infrared detection capabilities is disclosed. The semi-metal material may thus operate as a semiconductor type detector with a wavelength sensitivity corresponding to the induced band gap in a preferred embodiment of a diode structure. Preferred semi-metal materials include Hg(1-x)Cd(x)Te, x is less than 0.15, HgCdSe, BiSb, alpha-Sn, HgMgTe, HgMnTe, HgZnTe, HgMnSe, HgMgSe, and HgZnSe. The magnetic field induces a band gap in the semi-metal material proportional to the strength of the magnetic field allowing tunable detection cutoff wavelengths. For an applied magnetic field from 5 to 10 tesla, the wavelength detection cutoff will be in the range of 20 to 50 micrometers for Hg(1-x)Cd(x)Te alloys with x about 0.15. A similar approach may also be employed to generate infrared energy in a desired band gap and then operating the structure in a light emitting diode or semiconductor laser type of configuration. NASA

N89-28797# North Carolina Univ., Chapel Hill. Dept. of Computer Science.
EXPLORING VIRTUAL WORLDS WITH HEAD-MOUNTED DISPLAYS
James C. Chung, Mark R. Harris, F. P. Brooks, Henry Fuchs, and Michael T. Kelley Feb. 1989 12 p
(Contracts N00014-86-K-0680; PHS-RR-02170-05)
(AD-A208088; TR89-009) Avail: NTIS HC A03/MF A01
CSCL 12/5

Research has been conducted in the use of simple head mounted displays in real world applications. Such units provide the user with non-holographic true 3-D information, since the kinetic depth effect, stereoscopy, and other visual cues combine to immerse the user in a virtual world which behaves like the real world in some respects. UNC's head mounted display was built inexpensively from commercially available off-the-shelf components. Tracking of the user's head position and orientation is performed by a Polhemus Navigation Sciences' 3SPACE tracker. The host computer uses the tracking information to generate updated images corresponding to the user's new left eye and right eye views. The images are broadcast to two liquid crystal television screens (220x320 pixels) mounted on a horizontal shelf at the user's forehead. The user views these color screens through half-silvered mirrors, enabling the computer generated image to be superimposed upon the user's real physical environment. The head mounted display was incorporated into existing molecular and architectural applications being developed at UNC. In molecular structure studies, chemists are presented with a room sized molecule with which they can interact in a manner more intuitive than that provided by conventional 2-D displays and dial boxes. Walking around and through the large molecule may provide quicker understanding of its structure, and such problems as drug enzyme docking may be approached with greater insight. GRA

N89-28798# Max-Planck-Inst. fuer Physik und Astrophysik, Munich (Germany, F.R.). Werner-Heisenberg Inst. fuer Physik.
DEVELOPMENT OF A NOVEL SILICON DETECTOR WITH INTERNAL AMPLIFICATION Thesis - Tech. Univ. Munich [ENTWICKLUNG EINES NEUARTIGEN SILIZIUMDETEKTORS MIT INTERNER VERSTAERKUNG]
Karl-Friedrich Schuster Nov. 1988 66 p In GERMAN
(MPI-PAE/Exp.El-197; ETN-89-94389) Copyright Avail: NTIS HC A04/MF A01

The first test versions of a new high-purity silicon radiation detector were designed and produced. The detector operation principle was aimed at applying an internal gate for a combination of a MOS field effect transistor and lateral depletion. This principle was confirmed by the tests. The energy resolution of the detectors at 300 K and 6keV is shown to be a halfwidth of 520eV and significantly better than that of the conventional uncooled detectors. The detector principle allows the realization of an addressable two-dimensional detector matrix with nondestructive readout possibility. The measured signal-to-noise ratio of the single detector is better than 400 for minimum ionizing particles. Novel fast readout procedures with good spatial resolution (about 50 micron) in high energy physics are then allowed. ESA

N89-28799# Cologne Univ. (Germany, F.R.). Inst. fuer Geophysik und Meteorologie.
OPTICAL PROPERTIES AND ERROR SOURCES OF AN AIRBORNE RADIOMETER [OPTISCHE EIGENSCHAFTEN UND FEHLERQUELLEN EINES FLUGZEUGGETRAGENEN RADIOMETERS]
Bernd Bauche, A. Ebel, ed., M. Neubauer, ed., E. Raschke, ed., and P. Peth, ed. 1988 138 p In GERMAN; ENGLISH summary
(Contract BMFT-01-QS-1138)
(Mitt-60; ISSN-0069-5882; ETN-89-94415) Avail: NTIS HC A07/MF A01

The spectral and spatial response functions of the AVCSR (Airborne Version of the Conical Scan Radiometer) were analyzed. An appropriate signal processing procedure was developed, allowing the achievement of rotational symmetry of the point spread

function. Instrumental errors produced by internal sampling processes, the instrument noise and the calibration uncertainties were investigated. Aliasing is shown to be reduced by about a factor of ten due to the telescope aberrations which act as a low pass filter and to special demodulation algorithms that virtually double the sampling frequency of the optical chopper. The instrument noise can be reduced to the level of the detector noise using an improved compensation technique. The calibration accuracy in the solar channels is limited by the uncertainties of the calibration lamp. The dominant error sources in the thermal infrared channels are probably temperature fluctuations of blackbodies and baffles. ESA

N89-28800# Technische Univ., Berlin (Germany, F.R.). Inst. fuer Luft- und Raumfahrt.

PIEZOELECTRIC FOILS AS SENSORS IN EXPERIMENTAL FLOW MECHANICS Final Report [PIEZOELEKTRISCHE FOLIEN ALS SENSOR IN DER EXPERIMENTELLEN STROEMUNGSMECHANIK]

Wolfgang Nitsche Oct. 1988 23 p In GERMAN
(ILR-Mitt-214; FIP-12/10; ETN-89-94563) Avail: NTIS HC A03/MF A01

The use of piezoelectric foils as sensors for the analysis of complex aerodynamic flow fields is discussed. The sensors consist of a thin (9 to 100 micrometer) and highly elastic thermoplastic film. It can be mounted, trouble-free, on the surface of very complex flow configurations, and is thus a completely covering array of sensors, allowing large-scale surface force determination. The piezofoil is an active signal source which only requires a suitable amplifier. Wind tunnel tests on wing profiles show that flow instabilities and the characteristics of laminar-turbulent boundary layer transition can be determined. These results were confirmed by free flight tests, which also demonstrate the possibility of on-line data evaluation. Examples of the use of piezoelectric matrix, and taster sensors for the recognition of global flow structures, are given. ESA

N89-28801# Institut Franco-Allemand de Recherches, Saint-Louis (France).

ON STRAIN GAGES USING THE PVF2 PIEZOELECTRIC POLYMER Progress Report [ETAT DES RECHERCHES SUR LES JAUGES DE CONTRAINTE EN POLYMERE PIEZOELECTRIQUE PVF2]

F. Bauer, R. A. Graham, L. M. Lee (Ktech Corp., Albuquerque, NM.), and G. Samara (Sandia Natl. Labs, Albuquerque, NM.) 17 May 1988 12 p In FRENCH; ENGLISH summary Presented at the 2nd Congres International sur le Comportement Mecanique et Physique des Materiaux sous Sollicitations Dynamiques, Ajaccio, France, 19-23 Sep. 1988
(Contract DRET-85-193)
(ISL-CO-210/88; ETN-89-94850) Avail: NTIS HC A03/MF A01

The frequency, temperature, and hydrostatic pressure dependences of the dielectric properties, molecular relaxation, and phase transition in PVF2 (polyvinyl fluoride) and a copolymer with 30 percent trifluorethylene are presented. The dynamic melting temperature shows a large increase with pressure. The electrical response of film shock gages with various degrees of polarization are studied under shock loading (35 GPa). The observed response shows good fidelity until 30 GPa. The value of the remanent polarization has a significant influence on nonlinearity and probably affects the maximum useful stress for shock gage applications. ESA

N89-28802# Institut Franco-Allemand de Recherches, Saint-Louis (France).

THE COPY OF SINGLE BEAM HOLOGRAMS [LA COPIE DES HOLOGRAMMES A FAISCEAU UNIQUE]

H. Royer 2 Jun. 1988 8 p In FRENCH Presented at the OPTO 88 Colloquium, Paris, France, May 1988
(ISL-CO-212/88; ETN-89-94851) Avail: NTIS HC A02/MF A01

A theory and an experimental procedure for the duplication of single beam holograms are presented. The optimum recording conditions for the original hologram and for the copies are described. The applications are discussed including quality enhancement, automatic exploitation of particle images, multiple exposures, and restitution of submicron particle images. ESA

N89-28803# Centre d'Etudes et de Recherches, Toulouse (France). Dept. d'Etudes et de Recherches en Mecanique et Energetique des Systemes.

EXPERIMENTING CAVITATION MEASURING INSTRUMENTS Final Report [EXPERIMENTATION DE DISPOSITIFS DE MESURE DE POCHE DE CAVITATION]

G. Toulouse Sep. 1988 63 p In FRENCH
(Contract DRET-87-002-16)
(CERT-2305; ETN-89-94868) Avail: NTIS HC A04/MF A01

A calibrating method for measuring the volume of cavitation bubbles is presented and the results of open air experiments are given. The bubbles appearing on the surface of a marine rotating propeller are measured using CCD cameras and optical procedures. Square bubble section first approximations is used. The performance of cameras equipped with light amplifiers is studied in order to use them for real bubble cross section measurements. ESA

N89-28804# Institut Franco-Allemand de Recherches, Saint-Louis (France).

THE PROBLEM OF VERY HIGH MAGNIFICATIONS IN HOLOGRAPHY

H. Royer 22 Jun. 1988 17 p Presented at Optics-ECOOSA 88, Birmingham, United Kingdom, 24 Mar. 1988
(ISL-CO-218/88; ETN-89-95031) Avail: NTIS HC A03/MF A01

The problem of high magnification in holography is discussed. The study is focused on problems concerning the image magnification, the in-line system for Gabor's two step processes, the recording in parallel light, the gain of resolution, and the off-axis system. It is concluded that three steps processes are required to obtain optimum results : the recording at a specific wave length (lambda), the magnification (g) of the hologram itself, and the reconstruction (at lambda prime = to g multiplied by lambda). The fringes must be larger than the intermolecular distance of the recording material. ESA

N89-28805# Danish Space Research Inst., Lyngby.

THE FLUXGATE RINGCORE SENSOR DEMAGNETISING FACTOR AND NOISE

F. Primdahl, B. Hernando, O. V. Nielsen, and J. R. Petersen (Technical Univ. of Denmark, Lyngby.) 1989 22 p
(ORI-1-89; ISSN-0109-6605) Avail: NTIS HC A03/MF A01

A method for measuring the demagnetization of fluxgate sensors is introduced and used to evaluate the demagnetizing factors for 4 ringcore sensors having 5, 10, 15, and 20 wraps of magnetic core ribbon. The demagnetizing factor is proportional to the number of wraps, and the noise is also proportional to the number of wraps except for the more noisy 5 wrap core. The estimated internal core noise was 1 pT RMS taking into consideration the demagnetizing factor and the relative permeability of the core material. Author

N89-28806*# National Aeronautics and Space Administration. Lewis Research Center, Cleveland, OH.

FATIGUE TESTING APPARATUS Patent Application

Robert J. Buzzard, inventor (to NASA) 21 Aug. 1989 14 p
(NASA-Case-LEW-14124-1; NAS 1.71:LEW-14124-1;
US-Patent-Appl-SN-396263) Avail: NTIS HC A03/MF A01
CSCL 14B

An apparatus is provided for obtaining a single crack in fatigue loading which emanates from a predetermined starting notch in a test specimen. This crack propagates in a direction in line with that of the applied Mode 2 load. The loading may be performed either monotonically or in a cyclic fatigue. NASA

N89-28807# Southampton Univ. (England). Inst. of Sound and Vibration Research.

NEARFIELD ACOUSTIC HOLOGRAPHY: REVIEW AND PERSPECTIVES

A. E. Perezmatzumoto, F. J. Fahy, and S. J. Elliott Jul. 1989 107 p
(ISVR-TR-179; ETN-89-95532) Avail: NTIS HC A06/MF A01

The development of the Nearfield Acoustic Holography technique (NAH) for planar arrays is reported. A critical review shows that this technique represents an improvement over standard Acoustic Holography (AH) only for reconstructions of sources radiating at low frequencies. The possible reasons for a bad source reconstruction in NAH are investigated. The sensitive parameters for producing this distortion in a given system are detected. It is shown that the aliasing of the signal requires a formal approach or research. This formal approach is necessary for generalizing the technique, and for avoiding the subjectivity in choosing a good reconstruction. The results lead to the conclusion that prior knowledge of the source under study is required, making NAH a case-by-case method. The choosing of the true solution appears to be a time consuming technique from just a mathematical approach, or a highly subjective technique if there is not a formal approach. At the present state of development, NAH can only work in some cases. A system for industrial applications does not seem a real possibility at the present time. ESA

N89-28877# Joint Publications Research Service, Arlington, VA.
A NEW HOLOGRAPHIC INVERSE FILTERING METHOD AND ITS APPLICATION TO RESTORATION OF DEGRADED REMOTE SENSING IMAGES
Haisheng Cao and Xiangqian Chang *In its* JPRS Report: Science and Technology. USSR: Space. 16th International Congress of the International Society for Photogrammetry and Remote Sensing, Volume 1 30 Jan. 1989 p 1-10 Transl. into ENGLISH from International Archives of Photogrammetry and Remote Sensing (Kyoto, Japan), v. 27, 1988 p 37-44 (For primary document see N89-28876 23-43)
Avail: NTIS HC A12/MF A01

36 LASERS AND MASERS

Includes parametric amplifiers.
For related information see also *76 Solid-State Physics*.

N89-28808# Oak Ridge National Lab., TN.
NON-LINEAR SURFACE FITTING OF LASER RANGE IMAGES USING A HYPERCUBE CONCURRENT COMPUTER
Michael Finley (Transylvania Univ., Lexington, KY.) Jun. 1989 16 p
(Contract DE-AC05-84OR-21400)
(DE89-013720; ORNL/TM-11198; CESAR-89/24) Avail: NTIS HC A03/MF A01

Segmentation and non-linear surface fitting with laser range images are attempted on a hypercube concurrent processor. Low-level software acquires range images onto the hypercube. A substantially modified existing range image edge detector works in the hypercube image analysis environment to accomplish segmentation. The Levenberg-Marquardt algorithm implements the non-linear least squares fitting of the surfaces. Problems were found with each part of the approach. The edge detection algorithm is unnecessarily complex and yields an all too cluttered edge map. The fitting routine is limited by hardware in the number of surfaces that it can process. Finally, the fitting approach requires input estimates of the parameters which do not appear to be generalized for any image, thus keeping the process from being totally automated. Other research in surface fitting on serial computers has yielded results which may be helpful additions to solve the problems of automation. DOE

N89-28809# National Bureau of Standards, Boulder, CO. Time and Frequency Div.
THE 12C16O LASER FREQUENCY TABLES FOR THE 34.2 TO 62.3 THz (1139 TO 2079 cm-1) REGION
M. Schneider, K. M. Evenson, M. D. Vanek, D. A. Jennings, J. S. Wells, A. Stahn, and W. Urban (Bonn Univ., Germany, F.R.) Aug. 1988 27 p
(PB89-193908; NBS/TN-1321) Avail: NTIS HC A03/MF A01; SOD HC $1.75 as 003-003-02933-5 CSCL 20E

Frequencies for C(12)O(16) laser transitionsd are tabulated for the spectral range from 34.2 to 62.3 THz (1139 to 2079/cm). The transition frequencies were calculated using molecular constants which were derived by heterodyne frequency measurements on the C(12)O(16) laser. Author

N89-28810# Los Alamos National Lab., NM.
AN IMPROVED HIBACHI SUPPORT STRUCTURE FOR ELECTRON-BEAM DIODE FOILS
M. Kang, B. Weinstein, and E. A. Rose 1989 15 p Presented at the 7th IEEE Pulsed Power Conference, Monterey, CA, 11-14 Jun. 1989
(Contract W-7405-eng-36)
(DE89-014023; LA-UR-89-1932; CONF-890665-30) Avail: NTIS HC A03

AURORA is a KrF laser system at Los Alamos designed to demonstrate the feasibility of optical multiplexing for KrF lasers. The first two amplifiers in the amplifier chain are the Small Aperture Module (SAM) and the Pre-Amplifier (PA). The engineering design of replacement hibachis for the SAM and PA as part of a general upgrade to increase e-beam pumping is described. Hibachi shading loss mechanisms are briefly discussed. A simple model that calculates relative shading losses between hibachis for the axial-field-free case is presented. Based on modeling results, sample hibachi slots were fabricated and foils tested to destruction to verify standard membrane stress equation. Test results were used in the design and fabrication of hibachis that were installed on the amplifiers. Relative energy deposition measurements using capacitive manometers are presented. DOE

N89-28811# Los Alamos National Lab., NM. Chemical and Laser Sciences Div.
CHEMICAL AND LASER SCIENCES DIVISION Annual Report, 1988
Jun. 1989 117 p
(Contract W-7405-eng-36)
(DE89-014385; LA-11600-PR) Avail: NTIS HC A06/MF A01

This annual report from the Chemical and Laser Sciences Division at Los Alamos contains both programmatic and technical information on the following research: KrF lasers for inertial confinement fusion; free electron lasers; neutral particle beam sensing; chemical sensing; mass spectroscopy; orbit simulations; high temperature kinetics; and microwave absorption spectrometers. DOE

N89-28812# Lawrence Livermore National Lab., CA.
LINEAR THEORY OF UNCOMPENSATED THERMAL BLOOMING IN TURBULENCE
D. H. Chambers, T. J. Karr, J. R. Morris, P. G. Cramer, J. A. Viecelli, and A. K. Gautesen (Iowa State Univ. of Science and Technology, Ames.) Feb. 1989 34 p
(Contract W-7405-eng-48)
(DE89-014604; UCID-21696) Avail: NTIS HC A03/MF A01

A linearized theory of small perturbations in thermal blooming gives a surprisingly accurate description of the initial evolution of a plane wave propagating through an absorbing fluid medium. In the case of constant absorption and fluid velocity, a sinusoidal perturbation of the optical field grows quasi-exponentially at a rate determined by its Fresnel number and the accumulated OPD due to blooming. Perturbations with small transverse length scales grow more rapidly than those with large length scales. The evolution of the optical spectrum and Strehl ratio in the presence of optical turbulence is accurately described. The growth of the small scale fluctuations eventually leads to a drop in Strehl. More complicated cases with varying absorption and velocity profiles can be formally analyzed using a WKB approximation. Numerical simulations show growth suppression when the velocity varies along the optical path. These predictions from the linearized theory agree well with results from numerical simulations of the full nonlinear system and thus

provides a standard for comparing different numerical codes. DOE

N89-28813# Mound Lab., Miamisburg, OH.
INVESTIGATION OF AMBIENT AND HIGH TEMPERATURE AGING OF PETN (PENTAERYTHRITOL TETRANITRATE) BY LASER INDUCED FLUORESCENCE AND ULTRAVIOLET ABSORPTION SPECTROSCOPIES
Larry R. Dosser and Carl J. Seliskar 23 Jun. 1989 20 p
(Contract DE-AC04-88DP-43495)
(DE89-013740; MLM-3590) Avail: NTIS HC A03/MF A01

The chemical aging of pentaerythritol tetranitrate (PETN) was and continues to be an important problem in producing and maintaining high energy compounds and components. The work done to date has identified several key concerns in evaluating the chemical and physical aging processes of PETN. These include the manner in which a particular type of PETN is prepared, the sample preparation procedure insofar as it can influence the adsorbed species on the solid PETN, and the methods of measurement and their influence on the quantitative determination on the gaseous decomposition products. In the work reported here, two noninvasive spectroscopic methods of measurement were chosen: laser induced fluorescence, which was used to monitor NO2, and ultraviolet spectroscopy, which was used to monitor NO. A unique sample vessel design permitted both measurements to be made on the sample, and these two species could readily be measured in the presence of one another. Adsorbed NO2, and its subsequent reaction to yield NO, was detected. Three types of PETN samples were aged at elevated temperatures, and varying amounts of NO and NO2 were detected, depending on the sample and the method of preparation. The results indicate that an in situ experiment is necessary to further investigate PETN aging. DOE

N89-28814# Lawrence Livermore National Lab., CA.
ON THE USE OF THE FEL TO PRODUCE HIGH TRANSIENT SPACE-CHARGE POTENTIALS IN A MAGNETIZED PLASMA
R. F. Post 26 Jun. 1989 14 p
(Contract W-7405-eng-48)
(DE89-014325; UCID-21734) Avail: NTIS HC A03/MF A01

A recently developed approximate theory is used to estimate the magnitude of the space-charge potentials and electric fields that could be produced within a plasma column exposed to the focussed microwave beam from the Livermore free-electron laser (FEL). The plasma, composed of electrons and singly charged high mass ions, is assumed immersed in a solenoidal magnetic field with a strong longitudinal gradient. Cyclotron resonance of the electrons in the magnetic field leads to rapid heating and an associated strong axial expelling force resulting from the interaction of the electrons' magnetic moment with the magnetic field gradient. Ion inertia, together with the quasineutrality constraint, leads to the development of a flat-bottomed potential well, thereby forcing the electron loss rate to equal the inertia-dominated rate of the ions. This phenomenon, first observed experimentally in the 1960's, is made much more effective by the high power levels of the FEL. At present FEL power levels (2 GW), positive potentials of 4 MV and associated sheath electric fields approaching 1 GV/meter are predicted, with column-averaged fields of order 50 MV/meter. At projected FEL power levels, potentials of 15 MV, and sheath fields of 1.6 GV/meter are predicted. These figures are much higher than the corresponding figures for conventional RF or induction-type ion accelerators. Plasma parameters appropriate for a proof-of-principle experiment are given. DOE

N89-28815# Naval Research Lab., Washington, DC.
HIGH-POWER FREE-ELECTRON LASERS DRIVEN BY RF LINEAR ACCELERATORS Interim Memorandum Report
T. F. Godlove (FM Technologies, Inc., Alexandria, VA.) and P. Sprangle 16 May 1989 50 p
(AD-A209740; NRL-MR-6463) Avail: NTIS HC A03/MF A01 CSCL 09/3

The free electron laser (FEL) has been developed to the point where projections of its high-power capability have made it an important component of the directed-energy research program within the Strategic Defense Initiative. To achieve the desired near-visible wavelength and high intensity, stringent demands are placed on the electron beam that drives the FEL. Typical requirements are high peak current (0.2 to 2 kA) at a kinetic energy of 100 to 150 MeV, small energy spread (less than 1 percent), small diameter (less than 3mm), and low divergence (less than 0.1 mrad). Either an induction linear accelerator (linac) or an RF linac may be a suitable candidate to provide the electron beam. The technical issues and technology needed to achieve a visible light FEL driven by an RF linac are described. A recently installed RF linac at Boeing Aerospace is used as the principal illustrative example. GRA

N89-28816*# National Aeronautics and Space Administration. Langley Research Center, Hampton, VA.
METHOD AND CIRCUIT FOR CONTROLLING THE EVOLUTION TIME INTERVAL OF A LASER OUTPUT PULSE
Norman P. Barnes, inventor (to NASA) 31 May 1989 13 p
(NASA-Case-LAR-13772-1; NAS 1.71:LAR-13772-1; US-Patent-Appl-SN-359460) Avail: NTIS HC A03/MF A01 CSCL 20E

The invention is a method and circuit for controlling the evolution time interval of a laser output pulse used for making precise spectral measurements. It comprises the means for pumping a laser medium in a resonator that includes a Q-switch and polarizer that act in combination to control the loss in the resonator. A photodiode senses the resulting fluorescence which is applied to a two level Q-switch and polarizer from high to intermediate to substantially zero loss states to control the evolution time interval of the resulting laser output pulse. NASA

N89-28817*# National Aeronautics and Space Administration. Langley Research Center, Hampton, VA.
METHOD AND CIRCUIT FOR SHAPING LASER OUTPUT PULSES Patent Application
Norman P. Barnes, inventor (to NASA) 31 May 1989 9 p
(NASA-Case-LAR-14203-1; NAS 1.71:LAR-14203-1; US-Patent-Appl-SN-359459) Avail: NTIS HC A02/MF A01 CSCL 20E

The invention is a method and circuit for shaping laser output pulses from a laser resonator. A Q-switch and polarizer act in combination to control the loss to the resonator and provide the laser output representative of such loss. An optical diode senses the level of the output pulse and provides an output signal that when amplified is used to control voltage from a supply to provide a control signal which is applied to the Q-switch to control the shape of the output pulse by adjusting its length. NASA

N89-28818# Massachusetts Inst. of Tech., Lexington. Lincoln Lab.
LASER-INDUCED DIODE LINKING FOR WAFER-SCALE INTEGRATION
S. S. Cohen, P. W. Wyatt, G. H. Chapman, and J. M. Canter 16 Mar. 1989 195 p
(Contract F19628-85-C-0002)
(AD-A207921; TR-820; ESD-TR-88-224) Avail: NTIS HC A09/MF A01 CSCL 13/8

The use of laser beam melting of silicon for the purpose of forming electrical links between two adjacent diodes is studied. The diodes, which are formed by ion implantation and diffusion in a conventional CMOS process, are positioned such that when desired they may be used to obtain an electrical link between two otherwise separated sections of the integrated circuit. Electrical connections so obtained enable the realization of wafer-scale ICs, as demonstrated in recent applications. The theory of laser beam application to silicon is discussed, and the various beam and substrate parameters are shown to affect the properties of the diode links. Particular attention is paid to the important issue of the reflectivity from the composite system. Careful analytical examinations of the resulting molten zone properties were performed in order to fully qualify the use of laser radiation in this technology. Both scanning electron microscopy and secondary-ion

mass spectrometry were used to examine such parameters as the lateral and in-depth extension of the molten zone. In addition, electrical measurements were carried out. The results for the various observables compare well with the theoretical predictions. GRA

N89-28819# Texas Univ. at Dallas, Richardson. Center for Quantum Electronics.
PROOF OF THE FEASIBILITY OF COHERENT AND INCOHERENT SCHEMES FOR PUMPING A GAMMA-RAY LASER Quarterly Technical Progress Report, 1 Jan. - 31 Mar. 1989
Carl B. Collins Apr. 1989 69 p
(Contract N00014-86-C-2488)
(AD-A208071; GRL/8804) Avail: NTIS HC A04/MF A01 CSCL 09/3

Recent approaches to the problem of the gamma-ray laser have focused upon upconversion techniques in which metastable nuclei are pumped with long wave length radiation. At the nuclear level the storage of energy can approach tera-Joules 10 to the 12th power per liter for thousands of years. An approach to the gamma-ray laser that depends upon incoherent pumping is examined. This nuclear analog of the ruby laser embodies the simplest concept for a gamma-ray laser and it is not surprising that the greatest rate of achievement toward a sub-Angstrom laser has continued in this direction. Emphasis has remained upon the giant pumping resonances that enabled the dumping of populations of the only available sample of the 29 candidates, Ta 180 sub m, through a cross section that was 10,000 times more favorable than even the most optimistic estimates. The lessons taught by that major milestone were extended throughout the region of mass-180 nuclides. Reported is the success in pumping of only two of the candidates that are accidentally available, together with 17 other comparison isomers with the bremsstrahlung X-rays from a MeV linac. Previous excitations of the giant resonances pumping these materials had been made with a continum of photon energies reaching to 6 MeV and concern had lingered that the full 6 MeV of energy might have been actually needed. At such values the density of nuclear states is high and the onset of evaporation of particles from nuclei is near. Either would make the resonances useless to laser development. GRA

N89-28820*# David Sarnoff Research Center, Princeton, NJ.
AlGaAs PHASED ARRAY LASER FOR OPTICAL COMMUNICATIONS Final Report, 6 Aug. 1987 - 9 Jun. 1989
N. W. Carlson Sep. 1989 57 p
(Contract NAS1-18525)
(NASA-CR-181869; NAS 1.26:181869) Avail: NTIS HC A04/MF A01 CSCL 20E

Phased locked arrays of multiple AlGaAs diode laser emitters were investigated both in edge emitting and surface emitting configurations. CSP edge emitter structures, coupled by either evanescent waves or Y-guides, could not achieve the required powers (greater than or similar to 500 mW) while maintaining a diffraction limited, single lobed output beam. Indeed, although the diffraction limit was achieved in this type of device, it was at low powers and in the double lobed radiation pattern characteristic of out-of-phase coupling. Grating surface emitting (GSE) arrays were, therefore, investigated with more promising results. The incorporation of second order gratings in distribute Bragg reflector (DBR) structures allows surface emission, and can be configured to allow injection locking and lateral coupling to populate 2-D arrays that should be able to reach power levels commensurate with the needs of high performance, free space optical communications levels. Also, a new amplitude modulation scheme was developed for GSE array operation. Author

N89-28821*# David Sarnoff Research Center, Princeton, NJ.
MONOLITHIC NARROW-LINEWIDTH InGaAsP SEMICONDUCTOR LASER FOR COHERENT OPTICAL COMMUNICATIONS Final Report, 6 Aug. 1987 - 9 Jun. 1989
S. L. Palfrey, R. E. Enstrom, and P. A. Longeway Sep. 1989 59 p
(Contract NAS1-18539)
(NASA-CR-181870; NAS 1.26:181870) Avail: NTIS HC A04/MF A01 CSCL 20E

A design for a monolithic narrow-linewidth InGaAsP diode laser has been developed using a multiple-quantum-well (MQW) extended-passive-cavity distributed-Bragg-reflector (DBR) laser design. Theoretical results indicate that this structure has the potential for a linewidth of 100 kHz or less. To realize this device, a number of the fabrication techniques required to integrate low-loss passive waveguides with active regions have been developed using a DBR laser structure. In addition, the MOCVD growth of InGaAs MQW laser structures has been developed, and threshold current densities as low as 1.6 kA/sq cm have been obtained from broad-stripe InGaAs/InGaAsP separate-confinement-heterostructure MQW lasers. Author

N89-28822# Heraeus (W. C.) G.m.b.H., Hanau (Germany, F.R.). Produktbereich Original Hanau.
IMPROVEMENTS OF THE EFFICIENCY OF SOLID STATE LASERS BY SPECTRAL CONVERSION OF THE EXCITATION LAMP'S OUTPUT Final Report, Sep. 1987
Horst Kremmling Sep. 1987 14 p In GERMAN; ENGLISH summary
(Contract BMFT-13-EU-0027/0)
(ETN-89-94425) Avail: NTIS HC A03/MF A01

The improvement of the efficiency of solid state was investigated, with emphasis on the method of the spectral adaptation of the lamp emission to the absorption band of the laser medium (Nd:YAG). Measurements to determine the technical limits of excitation lamps, taking into account their lifetime, are shown to be unsuccessful due to the production related differences in the lamp behavior. Theoretical studies and experimental tests show the realizability of metal-halide-doped excitation lamps with high brightness and long lifetime. The conversion of radiation by means of a fluorescent layer is shown to be unrealistic at the required power densities. ESA

N89-28823 Technische Univ., Hanover (Germany, F.R.). Fachbereich Physik.
QUANTITATIVE INVESTIGATION OF THE KINETICS OF A LASER-PUMPED BARIUM VAPOR Ph.D. Thesis [QUANTITATIVE UNTERSUCHUNG ZUR KINETIK EINES LASERGEPUMPTEN BARIUMDAMPFES]
Arne Kallenbach 1988 136 p In GERMAN
(ETN-89-94434) Avail: Universitaet Hannover, Welfengarten 1, D-3000 Hannover 1, Federal Republic of Germany

A numerical model was developed for the description of a barium vapor which is nearly resonantly excited by a laser. The atomic constants, required for the model, were experimentally elaborated since they are not at all or very inaccurately known in the literature. The data of the most important elementary processes were experimentally obtained by a systematic variation of the parameters. The adaptation of the model calculations to the measured values gives a complete set of cross sections and transition probabilities, resulting in the quantitative understanding of the essential phenomena in the vapor. The time evolution of the excitation of eleven real states, several radiation processes, and the ionization of barium were calculated, in good agreement with the experiments. ESA

N89-28824 Technische Univ., Hanover (Germany, F.R.). Fachbereich Physik.
INCREASE OF THE DAMAGE THRESHOLDS OF DIELECTRIC LAYER SYSTEMS FOR THE Nd LASER Ph.D. Thesis [ERHOEHUNG DER ZERSTOERSCHWELLEN DIELEKTRISCHER SCHICHTSYSTEME FUER DEN-ND-LASER]
Detlev Ristau 1988 181 p In GERMAN
(ETN-89-94436) Avail: Universiteit Hannover, Welfengarten 1, D-3000 Hannover 1, Federal Republic of Germany

High power layer systems were developed and optimized using the electron beam vapor deposition technique, with emphasis on the determination of the parameters which influence the interaction between dielectric layers and intense layer radiation. The

measurement of these quantities allowed a theoretically well-founded classification of the damage mechanism in single layers of TiO2, Ta2O5, HfO2, ZrO2, AL2O3, and SiO2. The transition in layer systems are shown to contribute essentially to the damage process. The optimization of antireflection coatings and highly reflecting mirrors for gradual systems increase the damage threshold by 20 percent in comparison with conventional designs up to 50j/sq cm. Ninety-degree phase-active mirrors were designed and realized with a damage threshold up to 30j/sq cm. ESA

N89-28825 National Physical Lab., Teddington (England). Div. of Mechanical and Optical Metrology.
ACHIEVEMENT OF THE OPTIMUM PERFORMANCE FROM LASER INTERFEROMETER SYSTEMS WHEN APPLIED TO PRECISION LENGTH MEASUREMENT IN THE FREE ATMOSPHERE
M. J. Downs Apr. 1989 21 p
(NPL-MOM-92; ISSN-0309-3069; ETN-89-94966) Copyright
Avail: National Physical Laboratory, Teddington, Middlesex, TW11 0LW, United Kingdom

The limitations to the accuracy and resolution achievable by interferometry in the precision measurement of length in the free atmosphere are described and a number of aspects of the physics of these systems, when used in this particular application, are discussed. The calibrated frequencies of the helium-neon laser radiation sources used in these instruments typically change by only 1 or 2 parts in 100 million in the lifetime of the laser tube, and providing the correct optical and mechanical alignment procedures are employed then an absolute measurement accuracy of better than 1 part in 10 million can be achieved from these systems in a thermally controlled enclosure. When these optical systems are used on length measurement applications in the free atmosphere, corrections for the atmosphere wavelength variations can be made in two ways: firstly by measuring the parameters of pressure, temperature and humidity and calculating the refractive index of the air using the Edlen's equation with a modification to the water term; and secondly by measuring the refractive index directly using an interference refractometer. An absolute accuracy of better than 1 part in 10 million in the measurement of length can be achieved by these systems in the free atmosphere, with nanometric resolution in certain applications through the use of fringe fractioning electronics. ESA

N89-28826# Institut Franco-Allemand de Recherches, Saint-Louis (France).
THE USE OF HIGH-FREQUENCY PULSED LASER DIODES IN FRINGE TYPE LASER DOPPLER ANEMOMETRY
D. Dopheide, H. J. Pfeifer, M. Faber, and G. Taux (Physikalisch-Technische Bundesanstalt, Brunswick, Germany, F.R.) 28 Sep. 1988 14 p Presented at the International Congress on Applications of Lasers and Electrooptics, Santa Clara, CA, 30 Oct. - 4 Nov. 1988
(ISL-CO-230/88; ETN-89-95034) Avail: NTIS HC A03/MF A01

The benefits obtained by using pulsed laser diodes with repetition rates much higher than the Doppler frequency are described. The advantages over coherent wave (CW) pulse and long-pulse operation are shown. In pulsed mode the time average number of photons may be higher than in CW mode. For some of the laser Doppler anemometry data acquisition systems the laser pulses can be synchronized with the sampling process of the acquisition systems. In multiple-component systems the phases of the laser pulses, in the emitter parts, can be shifted with respect to each other. It is shown that one single receiver part is sufficient for all components and an identical wavelength can be used for all components. The feasibility of these conceptions are proved. ESA

N89-28827 Santiago Univ., Compostela (Spain).
THE MANUFACTURE OF BLAZED OBLIQUE ZONE PLATES FOR USE AT 10.6 MICRONS
V. MorenodelaCuevas and M. C. Hutley 1989 33 p
(NPL-MOM-91; ISSN-0309-3069; ETN-89-95144) Copyright
Avail: National Physical Laboratory, Teddington, Middlesex, TW11 0LW, United Kingdom

The manufacture of blazed zone plates, which are designed to reflect a beam of CO2 laser radiation through 90 degrees and to bring it to a focus, is reported. The pattern of zones is first drawn on a phototypesetter under computer control and each zone is plotted with an increasing density from one side to the other. The pattern is reduced to the appropriate size by photographing onto 35 mm film. This is then contact printed into photoresist in such a way that the variation of density is recorded as a variation of depth and zones with a triangular sawtooth profile are produced. Efficiencies of over 70 percent are recorded and measurements of the form of the diffracted wavefront indicate focussing properties which are close to the diffraction limit. The virtue of the present method is its simplicity and its low cost. ESA

N89-28828 National Physical Lab., Teddington (England). Div. of Mechanical and Optical Metrology.
AN EVALUATION OF BLAZED ZONE PLATES FOR USE IN THE 10 MICRON SPECTRAL REGION
M. C. Hutley, R. F. Stevens, and S. J. Wilson 1989 21 p
(NPL-MOM-93; ISSN-0309-3069; ETN-89-95145) Copyright
Avail: National Physical Laboratory, Teddington, Middlesex, TW11 0LW, United Kingdom

The feasibility and the advantages of applying blazed zone plates in the design of infrared optics is analyzed. The zone plate offers the possibility of combining the high transmission of a Fresnel lens with the imaging quality performance of a conventional lens. The zone plate is generated by photographing the narrow circular fringes transmitted by a Fabry-Perot interferometer. A sawtooth profile is generated by recording a series of exposure patterns as the fringes are scanned radially by varying the spacing of the mirrors. The fringes are recorded in photoresist and the pattern is scanned across one fringe order under computer control. The exposure varies linearly from one side of the zone to the other. When the resist is developed, grooves are generated with a triangular, blazed cross-section. A germanium zone plate, with a diffraction efficiency of 82 percent, is produced. The method presents the advantage of saving material and lowering the cost of production. ESA

37 MECHANICAL ENGINEERING

Includes auxiliary systems (nonpower); machine elements and processes; and mechanical equipment.

N89-28829*# National Aeronautics and Space Administration. Lyndon B. Johnson Space Center, Houston, TX.
VIBRATION ANALYZER Patent Application
Richard J. Bozeman, Jr., inventor (to NASA) 31 Jan. 1989 17 p
(NASA-Case-MSC-21408-1; NAS 1.71:MSC-21408-1; US-Patent-Appl-SN-304154) Avail: NTIS HC A03/MF A01 CSCL 13I

The invention relates to monitoring circuitry for the real time detection of vibrations of a predetermined frequency and which are greater than a predetermined magnitude. The circuitry produces an instability signal in response to such detection. The circuitry is particularly adapted for detecting instabilities in rocket thrusters, but may find application with other machines such as expensive rotating machinery, or turbines. The monitoring circuitry identifies when vibration signals are present having a predetermined frequency of a multi-frequency vibration signal which has an RMS energy level greater than a predetermined magnitude. It generates an instability signal only if such a vibration signal is identified. The circuitry includes a delay circuit which responds with an alarm signal only if the instability signal continues for a predetermined time period. When used with a rocket thruster, the alarm signal may be use to cut off the thruster if such thruster is being used in flight. If the circuitry is monitoring tests of the thruster, it generates

signals to change the thruster operation, for example, from pulse mode to continuous firing to determine if the instability of the thruster is sustained once it is detected. NASA

N89-28830*# National Aeronautics and Space Administration. Lewis Research Center, Cleveland, OH.
HIGH TEMPERATURE FLEXIBLE SEAL Patent Application
Bruce M. Steinetz, inventor (to NASA) and Paul J. Sirocky, inventor (to NASA) 30 Dec. 1988 14 p
(NASA-Case-LEW-14695-1; NAS 1.71:LEW-14695-1; US-Patent-Appl-SN-292146) Avail: NTIS HC A03/MF A01 CSCL 11A

This device is concerned with sealing the sliding interfaces between structural panels that are roughly perpendicular to each other or whose edges are butted against one another. The gap which the seal element must seal in not uniform along the seal length requiring significant seal flexibility. The seal is mounted in a rectangular groove in a moveable structural panel. The seal comprises a plurality of rectangular shaped wafers stacked next to one another and preloaded in the axial direction to minimize leakage between wafers. The wafers are laterally preloaded to maintain sealing contact along the wafer faces which engage the adjacent wall of a sidewall using one of several approaches, such as the pressurized linear bellows. The seal accommodates distortions in the adjacent panel by relative sliding between adjacent wafers. Leakage between wafers is further minimized with good wafer surface finishes. Leakage between the seal nose and the adjacent structural panel is minimized when sealing against a distorted sidewall with relatively thin wafers and suitable seal preload apparatus. Leakage behind the seal is minimized with good groove tolerances and good sealing contact between the preload system and the back of the peripheral edge of the wafers. NASA

N89-28831* National Aeronautics and Space Administration. Marshall Space Flight Center, Huntsville, AL.
UNIVERSAL PRECISION SINE BAR ATTACHMENT Patent
Franklin D. Mann, inventor (to NASA) 7 Mar. 1989 9 p Filed 9 Mar. 1988 Supersedes N88-24971 (26 - 18, p 2523
(NASA-Case-MFS-28253-1; US-Patent-4,809,441; US-Patent-Appl-SN-165943; US-Patent-Class-33-536) Avail: U.S. Patent and Trademark Office CSCL 13I

This invention relates to an attachment for a sine bar which can be used to perform measurements during lathe operations or other types of machining operations. The attachment can be used for setting precision angles on vises, dividing heads, rotary tables and angle plates. It can also be used in the inspection of machined parts, when close tolerances are required, and in the layout of precision hardware. The novelty of the invention is believed to reside in a specific versatile sine bar attachment for measuring a variety of angles on a number of different types of equipment.
Official Gazette of the U.S. Patent and Trademark Office

N89-28832# Lawrence Livermore National Lab., CA.
A PROPOSAL OF MORE EXPEDIENT METHODS OF TESTING MACHINE TOOLS
Herman W. Hauschildt 10 May 1989 11 p Presented at the IMOG Maintenance Subgroup, Denver, CO, 17-18 May 1989 Submitted for publication
(Contract W-7405-eng-48)
(DE89-013033; UCRL-101051; CONF-8905158-1) Avail: NTIS HC A03/MF A01

In the continuing search for more efficient means of testing machine tools, there are some recent experiences that should be shared. This report will discuss techniques, some old, some new, that are worthwhile evaluating for application as part of a machine tool maintenance function. DOE

N89-28833# Sandia National Labs., Albuquerque, NM. Intelligent Machine Principles Div.
ROBOTIC GRASPING OF UNKNOWN OBJECTS: A KNOWLEDGE-BASED APPROACH
S. A. Stansfield Jun. 1989 46 p
(Contract DE-AC04-76DP-00789)
(DE89-013875; SAND-89-1087) Avail: NTIS HC A03/MF A01

A general purpose robotic grasping system for use in unstructured enviroments is demonstrated. Using computer vision and a compact set of heuristics, the system automatically generates the robot arm and hand motions required for grasping an unmodeled object. The utility of such a system is most evident in environments where the robot will have to grasp and manipulate a variety of unknown objects, but where many of the manipulation tasks may be relatively simple. Examples of such domains are planetary exploration and astronaut assistance, undersea salvage and rescue, and nuclear waste site clean-up. A two-stage model of grasping is implemented: stage one is an orientation of the hand and wrist and a ballistic reach toward the object; and stage two is hand preshaping and adjustment. Visual features are first extracted from the unmodeled object. These features and their relations are used by an expert system to generate a set of valid reach/grasps for the object. These grasps are then used in driving the robot hand and arm to bring the fingers into contact with the object in the desired configuration. Experimental results are presented to illustrate the functioning of the system. DOE

N89-28834# Massachusetts Inst. of Tech., Cambridge. Dept. of Ocean Engineering.
PRELIMINARY DESIGN OF A CONSULTATION KNOWLEDGE-BASED SYSTEM FOR THE MINIMIZATION OF DISTORTION IN WELDED STRUCTURES M.S. Thesis
Patrick Jean Regis Feb. 1989 144 p
(Contract N00228-85-G-3262)
(AD-A208842) Avail: NTIS HC A07/MF A01 CSCL 12/5

The problem of distortion due to welding has been the subject of continuous research since the early days of ship construction. The control of distortion in welded structures through preventive and corrective procedures is generally well established. However, there are rules of thumb knowledge, or heuristics, which streamline the design process and enhance the performance of the final product. Those rules of thumb are usually known to a few experts who, through their own personal involvement and experience over the years, have accumulated considerable knowledge in their field. This thesis proposes to demonstrate the feasibility of implementing such knowledge in a knowledge-based environment. The preliminary design of such a system for the minimization of distortion in welded structures is presented through its development phases. The specific areas of out of plane and bucking distortions are considered. The report consists of three major parts: (1) describes the distortion problem, the selected tools for its analysis and the current procedures for its prevention and correction; (2) introduces the concepts inherent in knowledge-based systems and their applications in the fields of structural design and welding; and (3) presents the preliminary design of DISCON (for DIStortion CONtrol) which includes the derivation of functional specifications as well as a suitable architecture for implementation. Author

N89-28835# Dayton Univ., OH. Research Inst.
LUBRICANT EVALUATION AND PERFORMANCE Final Technical Report, Jan. 1987 - Jun. 1988
Costandy S. Saba, Hoover A. Smith, Michael A. Keller, Robert E. Kauffman, and Vinod K. Jain Apr. 1989 553 p
(Contract F33615-85-C-2507)
(AD-A208925; UDR-TR-88-95; AFWAL-TR-89-2008) Avail: NTIS HC A24/MF A01 CSCL 11/8

The development of improved methods for defining and measuring turbine engine lubricant performance is examined along with the development of improved techniques for lubricant monitoring, lubrication system health monitoring, investigating antiwear characteristics and load carrying capacities of lubricants. Arrhenius plots were developed for describing the effective life of MIL-L-7808, MIL-L-23699 and 4 cSt viscosity candidate lubricants as a function of time and temperature for selected limiting values of changes in physical and chemical properties. Significant improvement in AE spectrometer sensitivity for analyzing wear metal particles was achieved when using a cup-tip electrode with

the reversible polarity pin stand. The COBRA, a dielectric constant (DC) tester and a dielectric breakdown strength device were evaluated as lubricant monitoring devices. An assessment of the literature on lubricant load carrying capacity (LCC) test methods was made. A software system was developed and implemented on the Zenith Z-100 microcomputer for storage, retrieval and correlation of MIL-L-7808 lubricant qualification data. Finally, the remaining useful life of a lubricant evaluation rig (RULLER) was developed for MIL-L-7808 and MIL-L-23699 type lubricants and was based on reductive cyclic voltammetry. GRA

N89-28836# Rensselaer Polytechnic Inst., Troy, NY. Dept. of Mechanical Engineering.
SOLID LUBRICATION STUDIED BY OPTICAL MEANS Final Report, 1 Mar. 1986 - 28 Feb. 1989
James L. Lauer 31 Mar. 1989 22 p
(Contract DAAL03-86-G-0042)
(AD-A209008; ARO-23760.2-EG-F) Avail: NTIS HC A03/MF A01 CSCL 11/8

The well-known and unwelcome phenomenon of the formation of carbon or coke on the surfaces of some clay and clay-supported transition metal cracking and dehydrogenation catalysts used in petroleum refining was applied to develop a process for the lubrication of tribo-surfaces at high temperatures by continuously regenerated surface carbon derived from flow of ethylene gas. Measurements with a pin-on-disc tribometer showed an immediate reduction of friction (from as high as 0.6 to as low as 0.05) and wear for nickel, palladium, and ceramics coated with these metals and for bare silicon carbide and nitride at temperatures between 400 and 650 C and 0.2 MPa average Hertzian pressures, as soon as ethylene was introduced into the conjunction region. The environment could be air under ambient conditions. The carbon deposits were analyzed by Auger and Raman spectroscopy and ellipsometry and found to be generally about 400 A thick and microcrystalline graphite or vitreous. GRA

N89-28837# Massachusetts Inst. of Tech., Cambridge. Lab. for Mfg. and Productivity.
THE TRIBOLOGY OF UNDULATED SURFACES Final Report, 1 Feb. 1986 - 31 Jan. 1989
Nannaji Saka, Hong Tian, Turker Oktay, and Dew E. Kim 30 May 1989 122 p
(Contract N00014-86-K-0269)
(AD-A209275) Avail: NTIS HC A06/MF A01 CSCL 20/11

The objective of this research has been to investigate the friction, wear and lubrication characteristics of undulating metallic surfaces. Both dry and lubricated sliding experiments have been conducted to evaluate the tribological behavior of metallic surfaces. In addition, analytical studies have been carried out on the friction and wear behavior of the undulated surfaces, and practical applications of the undulated surfaces have also been explored. GRA

N89-28838# Advanced Mechanical Technology, Inc., Newton, MA.
HIGH TEMPERATURE TRIBOMETER, PHASE 1 Final Report, 8 Sep. 1988 - 7 Mar. 1989
Forest J. Carignan and Bruce H. Knoth Jun. 1989 81 p
(Contract F33615-88-C-2871)
(AD-A209356; AMTI-2236-1; WRDC-TR-89-2095) Avail: NTIS HC A05/MF A01 CSCL 14/2

Tribological research has become more important due to the awareness that friction and wear accounts for a large portion of our nation's energy and raw material usage. A machine is available that performs pin-on-disk friction and wear tests at temperatures up to 1200 C. Software to control the machine and acquire test data using IBM-PC compatible computers was designed and developed and initial tests of the software were conducted. A commercial software package, Labtech Notebook, was used as the basis for the system, although unique data-acquisition and graphics modules were also developed. A piston type liquid lubricant feed pump was chosen for accurately dispensing small quantities of test lubricant. A prototype of a solid powder feed system was built and functioned well with granular material but unsatisfactorily with the two very fine powders. GRA

N89-28839# Creare, Inc., Hanover, NH.
SUPERCONDUCTING MEISSNER EFFECT BEARINGS FOR CRYOGENIC TURBOMACHINES, PHASE 1 Final Report, Sep. 1988 - Mar. 1989
Victor Iannello, Jeffrey S. Marshall, and W. D. Stacy May 1989 52 p
(Contract F49620-88-C-0137)
(AD-A209875; CREARE-TM-1352; AFOSR-89-0825TR) Avail: NTIS HC A04/MF A01 CSCL 20/3

State of the art miniature expansion turbines and centrifugal compressors used in spaceborne sensor cryocoolers employ self-acting gas bearings to achieve high reliability and long operating life. Because these bearings must run at room temperature to achieve adequate stiffness and stability, they result in an avoidable source of heat leak to the process gas, thereby lowering overall cycle efficiency and increasing the system launch weight. This report shows that the gas bearings can be replaced by Meissner effect bearings fabricated from high temperature superconducting materials. Analyses are presented to predict Meissner bearing performance, and a preliminary design of a miniature expansion incorporating Meissner bearings is conceptualized. Because these bearings operate at cryogenic temperatures, a substantial reduction in heat leak to the process gas can be achieved. For a typical cryocooler providing 1 watt of cooling at 10 K, a 40 percent reduction in input cycle power can be achieved by replacing the self-acting gas bearings by Meissner bearings in the cold expansion turbine. GRA

N89-28840# National Academy of Sciences - National Research Council, Washington, DC. Air Force Studies Board.
ADVANCED ROBOTICS FOR AIR FORCE OPERATIONS Final Report, Feb. 1987 - Nov. 1988
Jun. 1989 158 p
(AD-A210098) Avail: NTIS HC A08/MF A01 CSCL 12/9

While robots are gaining widespread use in industry, application of robotic technology has not progressed as quickly within the military. However, projected manpower shortages, shorter weapon response times, and the severe environmental conditions anticipated in combat make the use of robots more attractive. To help the Air Force assess the potential for operational use of robots, this study reviews the component technologies, infrastructure, data base systems, and management structure required to support the next generation of maintenance, repair, supply, and distribution systems in the field and at the depots as they pertain to robotics. The committee: (1) evaluated current and potential uses of advanced robotic systems to support Air Force systems; (2) recommended the most effective applications of advanced robotics; (3) identified high payoff areas for research and development, particularly at the component level; and (4) assessed the potential effects robots will have on acquisition, logistics, and manpower considerations, such as education and training. GRA

N89-28841*# National Aeronautics and Space Administration. Marshall Space Flight Center, Huntsville, AL.
TURBOMACHINERY ROTOR SUPPORT WITH DAMPING Patent Application
George L. vonPragenau, inventor (to NASA) 26 May 1989 19 p
(NASA-Case-MFS-28345-1; NAS 1.71:MFS-28345-1;
US-Patent-Appl-SN-364743) Avail: NTIS HC A03/MF A01 CSCL 13I

Damping seals, damping bearings, and a support sleeve are presented for the ball bearings of a high speed rotor. The ball bearings consist of a duplex set having the outer races packaged tightly within the sleeve while the sleeve provides a gap with a support member so that the bearings may float with the sleeve. The sleeve has a web extending radially between the pair of out races and acts in conjunction with one or more springs to apply

an axial preload to the outer races. The sleeves have a series of slits which provide the sleeve with a spring-like quality so that the spring acts to center the rotor upon which the bearings are mounted during start up and shut down. A damping seal or a damping bearing may be used in conjunction with the ball bearings and supporting sleeve, the damping seal and damping bearing having rotor portions including rigid outer surfaces mounted within the bore of a stator protion having triangular shaped pockets on the surface facing the rotor. Axial gates are provided between adjacent pockets in sections of the stator permitting fluid to flow with less resistance axially relative to the flow of fluids circumferentially between the rotor and the stator. NASA

N89-28842*# National Aeronautics and Space Administration. Marshall Space Flight Center, Huntsville, AL.
TURBOMACHINERY SHAFT INSERT Patent Application
George L. vonPragenau, inventor (to NASA) 26 May 1989 12 p
(NASA-Case-MFS-28345-2; NAS 1.71:MFS-28345-2; US-Patent-Appl-SN-358028) Avail: NTIS HC A03/MF A01 CSCL 13I

An insert is presented for a hollow rotatable shaft on the end of which an impeller is mounted, the insert having a first cylindrical portion receivable within the end of the shaft. The insert includes a radially extending portion adjacent the end of the shaft having an annular wall including radially inner and outer surfaces for engaging tightly similar surfaces in a recess formed in the impeller to provide inner and outer pilot surfaces. The insert also includes a tubular extension which is received within a bore in the impeller, the tubular extension having spaced longitudinally extending slits for permitting the extension together with radially extending hook-like tongues thereon to be received within radial slots in the bore of the impeller to lock the impeller to the insert. NASA

N89-28843# Naval Postgraduate School, Monterey, CA.
A STUDY OF THE THERMAL PROFILES DURING AUTOGENOUS ARC WELDING M.S. Thesis
Robert L. Ule Mar. 1989 163 p
(AD-A209440) Avail: NTIS HC A08/MF A01 CSCL 11/6

The 3-D transient temperature variations during autogenous Gas Tungsten Arc Welding are determined. The model employs a combination of unequally spaced moving meshes to minimize the total number of nodes. Finite differencing is used for the spatial terms. The resulting ordinary differential equations for the transient evolution of thermal transport are solved using 4th order Runge-Kutta technique. The temperature dependent properties and latent heats of phase transformations are accounted for. Computations are carried out for a rectangular parallelepiped, with convective and radiative surface thermal conditions. Results are presented for the evolution of thermal profiles during ideal welding conditions. These are next compared with variations obtained due to defects such as weld track misalignment and inclusions. A study of the startup and shutdown transients makes it possible to control the cooling rate during these transients. The potential use of this model in the development of an expert welding system using infrared imagery is indicated. In addition, a low cost infrared detector using an indium arsenide diode is prototyped to determine its feasibility for production welding control. GRA

N89-28844 Forschungsinstitut fuer Hochfrequenzphysik, Werthhoven (Germany, F.R.).
AN APPROXIMATION FORMULA TO EVALUATE THE COEFFICIENT UPDATE RATE OF PARTIALLY ADAPTIVE ANTENNAS
J. Worms Jul. 1988 46 p In GERMAN; ENGLISH summary
(Contract BMVg-T/RF-31E-0020/E-1317)
(Rept-5-88; Lfd-274; ETN-89-94400) Copyright Avail: Forschungsinstitut fuer Hochfrequenzphysik, Wachtberg-Werthhoven, Fed. Republic of Germany

The prediction of the necessary update rate of the filter coefficients of a partially adaptive antenna, consisting of a rotating main antenna and a fixed auxiliary group, is investigated. The misadjustment noise of a partially adaptive array is analyzed. The stationary case and the convergence rate of the sample-matrix-inversion method, which is applied to the rotating main antenna, are approximated. The covariance matrix and the correlation vector are estimated by the moving average method and by the Wiener extrapolation method. The influence of the target signals on the convergence rate are quantified. Using the obtained approximation formulas, the coefficient update rate can be estimated. ESA

N89-28845# Universiteit Twente, Enschede (Netherlands). Faculty of Applied Mathematics.
MODEL REDUCTION OF LINEAR CONSERVATIVE MECHANICAL SYSTEMS
A. J. vanderSchaft and J. E. Oeloff Dec. 1988 17 p
(Memo-752; ISSN-0169-2690; ETN-89-95118) Avail: NTIS HC A03/MF A01

An approach for model reduction of linear conservative or weakly dissipative mechanical systems based on the balancing of an associated gradient system is proposed. The case of collocated sensors and actuators is considered. Gyroscopic forces are not taken into account. Numerical examples are shown to be promising. Questions raised by this approach are considered and future investigations discussed. ESA

N89-28846*# National Aeronautics and Space Administration. Pasadena Office, CA.
ROBUST HIGH-PERFORMANCE CONTROL FOR ROBOTIC MANIPULATORS Patent Application
Homayoun Seraji, inventor (to NASA) (Jet Propulsion Lab., California Inst. of Tech., Pasadena.) 17 May 1989 60 p
(NASA-Case-NPO-17785-1-CU; NAS 1.71:NPO-17785-1-CU; US-Patent-Appl-SN-353411) Avail: NTIS HC A04/MF A01 CSCL 13I

Model-based and performance-based control techniques are combined for an electrical robotic control system. Thus, two distinct and separate design philosophies were merged into a single control system having a control law formulation including two distinct and separate components, each of which yields a respective signal componet that is combined into a total command signal for the system. Those two separate system components include a feedforward controller and feedback controller. The feedforward controller is model-based and contains any known part of the manipulator dynamics that can be used for on-line control to produce a nominal feedforward component of the system's control signal. The feedback controller is performance-based and consists of a simple adaptive PID controller which generates an adaptive control signal to complement the nomical feedforward signal. NASA

N89-28847# Deutsche Forschungs- und Versuchsanstalt fuer Luft- und Raumfahrt, Oberpfaffenhofen (West Germany). Abteilung Regelung.
FORMULATION AND NUMERICAL SOLUTION OF THE EQUATIONS OF CONSTRAINED MECHANICAL MOTION
Claus Fuehrer and Benedict Leimkuhler Mar. 1989 35 p
(DFVLR-FB-89-08; ISSN-0171-1342; ETN-89-95305) Avail: NTIS HC A03/MF A01; DFVLR, VB-L-DO, Postfach 90 60 58, 5000 Cologne, Federal Republic of Germany, 14 deutsche marks

Two alternative formulations are proposed for the simulation of constrained mechanical motion. They lie somewhere between the classical state-space which is based on a restatement of the problem in the form of an ordinary differential equation, and the descriptor form which results in a high-index system of differential algebraic equations. How the two alternative formulations are mathematically related is shown. Some techniques for their efficient solution and an illustration of the results obtained with a numerical example are demonstrated. ESA

N89-28848# Oxford Univ. (England). Dept. of Engineering Science.
DEVELOPMENT AND IMPLEMENTATION OF AN ON-LINE MULTIVARIABLE CONTROL ALGORITHM FOR THE FORCE CONTROL OF AN INDUSTRIAL ROBOT

Paul Elosegui 1988 68 p Sponsored by the Basque Government
(OUEL-1748/88; ETN-89-95536) Avail: NTIS HC A04/MF A01

The design of a multivariable force control algorithm is presented. The algorithm is part of the active force controller implemented in a industrial robot project. The aim of the project is to demonstrate the feasibility of direct joint torque feedback to achieve fine force and motion control of an instrumented industrial robot. The first three joints of the robot are instrumented for strain and an end-effector force/torque sensor is incorporated to permit torque sensing in all six joints. The original controller is replaced by a sophisticated transputer based controller. The multivariable control design requires a mathematical model of the plant. This model depends on the joint level servo used in the system. The results of the first stages of the control system design are shown. The sequence of tasks remaining for the implementation of the designed algorithm are outlined. A program of the time allocated to each task is included. The reason for the lack of constructive criticism that attempts to classify, compare and characterize proposed algorithms is the absence of adequate implementation results. The design process described yields conclusive results on the performance, robustness and ultimate validity of many proposed control law designs. ESA

N89-28849# Oxford Univ. (England). Robotics Research Group.
TACTILE SENSING AND THE PHOTOELASTIC TACTILE SENSOR
Alec Cameron, Ron Daniel, and Hugh Durrant-Whyte 1989 40 p
(OUEL-1758/89; ETN-89-95537) Avail: NTIS HC A03/MF A01

The research performed in the field of tactile sensing for robotics applications is discussed. The developed photoelastic tactile sensor is described. Its ability to be cast readily into any desirable shape is proposed as being useful in attempting to develop sensors which can be mounted on robot actuators, and there provide data for use in manipulation operations. The mathematical models to describe the mechanisms of the photoelastic tactile sensor are included. In determining that no mathematical solution exists to reconstruct completely the sensed surface from the sensory data, limitations are down regarding the abilities of tactile sensors, and parallels are drawn with human touch. The use of motion by human touch is seen as essential in providing the additional information necessary to obtain useful information about the sensed object. ESA

N89-28850# Universiteit Twente, Enschede (Netherlands). Faculty of Applied Mathematics.
A SIMPLE NUMERICAL ALGORITHM FOR ELASTOHYDRODYNAMIC LUBRICATION, BASED ON A DYNAMIC VARIATION PRINCIPLE
R. Verstappen Jan. 1989 40 p
(Memo-761; ISSN-0169-2690; ETN-89-95126) Avail: NTIS HC A03/MF A01

An efficient numerical method for the fully lubricated line contact between a rotating, deformable cylinder and a rigid surface is described. By exploiting the dynamic variation structure of this nonlinear problem the deformation of, and the pressure at, the free contact boundary are calculated. The dynamic formulation leads in a natural way to an interative procedure, where the evolution from one iterate to a subsequent one is governed by a minimization problem. The application of the Euler-Lagrange equation which expresses the fact that the mass has to be conserved avoids the occurrence of mass flux deflects suffered in earlier solutions. The proposed dynamic algorithm starts with the calculation of the lubricated contact between a rigid cylinder and the rigid surface. The stiffness of the cylinder is lessened until the desired value is reached, whereàfter the loading on the cylinder is increased by moving it towards the rigid surface. Calculations needed for one time-step are significantly reduced by preconditioning, where the discretized Euler-Lagrange equation is multiplied by an approximation of the inverse of the global operator governing the deflection of the cylinder. Solutions that are comparable to large-time (or super-) computer computations are shown to be calculable on a PC, using only a few gridpoints and a small amount of run-time. ESA

38 QUALITY ASSURANCE AND RELIABILITY

Includes product sampling procedures and techniques; and quality control.

N89-28851*# National Aeronautics and Space Administration. Lewis Research Center, Cleveland, OH.
NON-UNIFORM TRANSITION CONDUCTIVITY OF SUPERCONDUCTING CERAMIC
Edward R. Generazio, Don J. Roth, and Aloysius F. Hepp Jul. 1989 9 p Presented at the 16th Annual Review of Progress in Quantitative Nondestructive Evaluation, Brunswick, ME, 23-28 Jul. 1989; sponsored in part by DOE, AFWAL, ONR and ASNT
(NASA-TM-102133; E-4928; NAS 1.15:102133) Avail: NTIS HC A02/MF A01 CSCL 14D

The effects of microstructural variations on the superconducting properties of SmBa2Cu3Ox are investigated. A scanning eddy current probe revealed the onset and growth of a normal conducting region. Resistance versus temperature measurements taken at different regions of the sample support the concept of a physically mixed state system. Regional variations in porosity and grain size distributions affect the observed superconducting transition. Author

N89-28852# Oak Ridge National Lab., TN. Development Div.
NONFILM RADIOGRAPHY AT THE OAK RIDGE Y-12 PLANT
Bruce B. Marshall, Zane W. Bell, and Thomas J. Sworski 17 Mar. 1989 19 p
(Contract DE-AC05-84OR-21400)
(DE89-014523; Y/DW-783/R1) Avail: NTIS HC A03/MF A01

Nonfilm, real time radiography is being developed in a form applicable to U-6-Nb wt percent alloy parts. A development facility is in operation for use in prototyping the equipment and methods to be used, and equipment for the production facility has been procured and is being installed. The production facility is scheduled to be transferred to production in FY 1990. Fully automated data acquisition and analysis methods were developed and demonstrated on the development system. The software was translated onto the production computer system and individually tested. A statistical comparison of nonfilm radiography, using the development facility, was completed in FY 1986. Results of this study indicate that the nonfilm method exhibits superior precision and accuracy but slightly poorer resolution than the normal film radiography. The nonfilm system also yielded a small number of false alarms apparently associated with the camera system. The size of the false alarms were less than the resolution limits of the system. A second statistical comparison of nonfilm radiography with conventional film radiography using actual production parts and the production facility is scheduled for FY 1990. DOE

N89-28853*# National Aeronautics and Space Administration. Lewis Research Center, Cleveland, OH.
ULTRASONIC IMAGING OF TEXTURED ALUMINA
David B. Stang (Sverdrup Technology, Inc., Cleveland, OH.), Jonathan A. Salem, and Edward R. Generazio May 1989 11 p
(NASA-TM-101478; E-4600; NAS 1.15:101478) Avail: NTIS HC A03/MF A01 CSCL 14D

Ultrasonic images representing the bulk attenuation and velocity of a set of alumina samples were obtained by a pulse-echo contact scanning technique. The samples were taken from larger bodies that were chemically similar but were processed by extrusion or isostatic processing. The crack growth resistance and fracture toughness of the larger bodies were found to vary with processing method and test orientation. The results presented here demonstrate that differences in texture that contribute to variations in structural performance can be revealed by analytic ultrasonic techniques. Author

N89-28854# Etablissement Technique Central de l'Armement, Arcueil (France). Dept. Physique des Surfaces.
NONDESTRUCTIVE CHARACTERIZATION OF SIMPLE INTERFACES USING VOLUME SOUND WAVES [CARACTERISATION NON DESTRUCTIVE DES INTERFACES SIMPLES A L'AIDE DES ONDES ULTRASONORES DE VOLUME]
J. Y. Chatellier and P. Fraisse 2 Feb. 1989 95 p In FRENCH
(Contract DRET/ETCA/CREA-048-329)
(ETCA-89-R-015; ETN-89-94862) Avail: NTIS HC A05/MF A01

The technique is used to characterize adhesive bonded joints and the substrate/adhesive interface. The resonance technique consists of creating a stationary wave system in the thickness of the bond. The observations with acoustic microscopy show that it is possible to observe the interfaces for thickness of tens of microns. The potential of this procedure is discussed. ESA

N89-28855# Technical Research Centre of Finland, Espoo. Lab. of Electrical and Automation Engineering.
ESTIMATION OF SOME STOCHASTIC MODELS USED IN RELIABILITY ENGINEERING
Tapio Huovinen Apr. 1989 149 p Sponsored by the Finnish Ministry of Trade and Industry and the Nordic Liasion Committee for Atomic Energy
(VTT-RR-598; ISBN-951-38-3332-1; ISSN-0358-5077; ETN-89-95183) Copyright Avail: NTIS HC A07/MF A01; Government Printing Center, Mail Orders, P.O. 516, SF-00101 Helsinki, Finland, 84 Finnish marks

The estimation of some stochastic models used in reliability engineering is presented. In reliability engineering continuous probability distributions have been used as models for the lifetime of technical components. The following distributions are considered: exponential, two-mixture exponential, conditional exponential, Weibull, lognormal and gamma. Maximum likelihood method is used to estimate distributions from observed data which may be either complete or censored. Models based on homogeneous Poisson process such as gamma-poisson and lognormal-poisson models for analysis of failure intensity are considered. A beta-binomial model for analysis of failure probability is studied. The estimators of the parameters for three models are estimated by the matching moments method and in the case of gamma-poisson and beta-binomial models also by maximum likelihood method. Statistical analysis of non-homogeneous Poisson processes are used to describe the failing phenomena of a set of components with a Weibull intensity function. We use the method of maximum likelihood to estimate the parameters of the Weibull model. A common cause failure can seriously reduce the reliability of a system. A binomial failure rate model is used as an application of the marked point processes for modelling common cause failure in a system. The parameters of the binomial failure rate model are estimated with the maximum likelihood method. ESA

39 STRUCTURAL MECHANICS

Includes structural element design and weight analysis; fatigue; and thermal stress.

For applications see *05 Aircraft Design, Testing and Performance* and *18 Spacecraft Design, Testing and Performance.*

N89-28856*# Maryland Univ., College Park. Dept. of Mechanical Engineering.
THE STRUCTURAL RESPONSE OF UNSYMMETRICALLY LAMINATED COMPOSITE CYLINDERS
T. A. Butler and M. W. Hyer Aug. 1989 152 p
(Grant NAG1-665)
(NASA-CR-185834; NAS 1.26:185834; UM-TR-89-2) Avail: NTIS HC A08/MF A01 CSCL 20K

The responses of an unsymmetrically laminated fiber-reinforced composite cylinder to an axial compressive load, a torsional load, and the temperature change associated with cooling from the processing temperature to the service temperature are investigated. These problems are considered axisymmetric and the response is studied in the context of linear elastic material behavior and geometrically linear kinematics. Four different laminates are studied: a general unsymmetric laminate; two unsymmetric but more conventional laminates; and a conventional quasi-isotropic symmetric laminate. The responses based on closed-form solutions for different boundary conditions are computed and studied in detail. Particular emphasis is directed at understanding the influence of elastic couplings in the laminates. The influence of coupling decreased from a large effect in the general unsymmetric laminate, to practically no effect in the quasi-isotropic laminate. For example, the torsional loading of the general unsymmetric laminate resulted in a radial displacement. The temperature change also caused a significant radial displacement to occur near the ends of the cylinder. On the other hand, the more conventional unsymmetric laminate and the quasi-isotropic cylinder did not deform radially when subjected to a torsional load. From the results obtained, it is clear the degree of elastic coupling can be controlled and indeed designed into a cylinder, the degree and character of the coupling being dictated by the application. Author

N89-28857# Queensland Univ., Brisbane (Australia). Dept. of Civil Engineering.
OUT-OF-PLANE BUCKLING FORMULAE FOR BEAM-COLUMNS/TIE BEAMS
S. Kitipornchai and C. M. Wang (National Univ. of Singapore.) Oct. 1988 33 p
(Grant ARGS-510)
(PB89-191613; RR-CE92; ISBN-0-86776-312-4) Avail: NTIS HC A03/MF A01 CSCL 20K

It is shown that the closed form expression for the elastic out-of-plane buckling of doubly symmetric beam-columns under uniform moment can be expressed in the familiar form for beams by introducing a beam-column parameter, eta = 4r(2)/h(2) in which r is the radius of gyration about the centroid and h is the distance between flange centroids. The closed form solution is equally applicable to tie-beams. For beam-column/tie-beams under other loading conditions, accurate solutions are determined using the Rayleigh-Ritz energy approach. Approximate formulae to predict the out-of-plane buckling capabilities of beam-columns/tie-beams under moment gradient, uniformly distributed load and central concentrated load are presented. GRA

N89-28858# Queensland Univ., Brisbane (Australia). Dept. of Civil Engineering.
NEW SET OF BUCKLING PARAMETERS FOR MONOSYMMETRIC BEAM-COLUMNS/TIE BEAMS
C. M. Wang and S. Kitipornchai (Asian Inst. of Tech., Bangkok, Thailand) Nov. 1988 37 p
(PB89-191639; RR-CE94; ISBN-0-86776-311-6) Avail: NTIS HC A03/MF A01 CSCL 20K

The elastic out-of-plane buckling of monosymmetric beam-columns/tie-beams under uniform moment or eccentric axial loads is discussed. A new set of parameters is introduced to describe the buckling behavior of such members. These easily calculated parameters can represent any general monosymmetrical-section and enable the designers to visualize the form of the cross section. The exact buckling solution, normally presented in a complicated transcendental form, can now be expressed explicitly and compactly using these parameters. GRA

N89-28859# Queensland Univ., Brisbane (Australia). Dept. of Civil Engineering.
FLEXURAL-TORSIONAL BUCKLING OF MONOSYMMETRIC BEAM-COLUMNS/TIE BEAMS
S. Kitipornchai and C. M. Wang (National Univ. of Singapore.) Nov. 1988 33 p
(PB89-191654; RR-CE96; ISBN-0-86776-314-0) Avail: NTIS HC A03/MF A01 CSCL 20K

Recent research developments on elastic flexural-torsional buckling of monosymmetric I-beams, and of doubly- and

monosymmetric beam-columns/tie-beams are reviewed. The developments include the introduction of a new set of nondimensional parameters, which illuminates the buckling behavior of these types of members and facilitates the derivation of simple design formulae for predicting the buckling capacities. More importantly, the recent work is extended to monosymmetric beam-columns/tie-beams under non-uniform moment load cases including double curvature bending. Approximate out-of-plane buckling formulae describing the stability criteria for such members under common in-plane loading conditions are derived. GRA

N89-28860# Sandia National Labs., Albuquerque, NM.
A TEST SYSTEM FOR THERMOMECHANICAL FATIGUE OF SOLDER JOINTS
D. T. Schmale and D. R. Frear Jun. 1989 23 p
(Contract DE-AC04-76DP-00789)
(DE89-013886; SAND-89-0521) Avail: NTIS HC A03/MF A01

The thermomechanical fatigue behavior of solder joints is a critical reliability issue in electronic packaging. A need exists for a thorough metallurgical understanding of solder joints in conditions of thermal fatigue. A method is presented to test solder joints under conditions of thermomechanical fatigue. This method involves simultaneous imposition of temperature and strain cycles on discrete solder joints in a shear orientation. The stress, microstructure, and number of cycles to failure are monitored. Cycles to failure are determined by a continuous electrical resistance detection method. 60Sn-40Pb and 40Sn-40In-20Pb solder joints were tested using this new method at 20 percent shear strain. DOE

N89-28861# Pacific Northwest Labs., Richland, WA.
ACOUSTIC EMISSION TECHNOLOGY FOR SPACE APPLICATIONS
M. A. Friesel, D. K. Lemon, J. R. Skorpik, and P. H. Hutton May 1989 13 p Presented at the 6th NASA Nondestructive Evaluation Workshop, Houston, TX, 23 May 1989
(Contract DE-AC06-76RL-01830)
(DE89-014449; PNL-SA-16952; CONF-8905178-2) Avail: NTIS HC A03/MF A01

Clearly the structural and functional integrity of space station components is a primary requirement. The combinations of advanced materials, new designs, and an unusual environment increase the need for inservice monitoring to help assure component integrity. Continuous monitoring of the components using Acoustic Emission (AE) methods can provide early indication of structural or functional distress, thus allowing time to plan remedial action. The term AE refers to energy impulses propagated from a growing crack in a solid material or from a leak in a pressurized pipe or tube. In addition to detecting a crack or leak, AE methods can provide information on the location of the defect and an estimate of crack growth rate and leak rate. DOE

N89-28862# CSA Engineering, Inc., Palo Alto, CA.
OPTIMIZATION OF STRUCTURES WITH PASSIVE DAMPING AND ACTIVE CONTROLS Final Report, May - Nov. 1988
Warren C. Gibson Feb. 1989 53 p
(Contract F33615-88-C-5451)
(AD-A208937; CSA-88-11-03; AFWAL-TR-88-4253) Avail: NTIS HC A04/MF A01 CSCL 13/13

Vibration suppression may be approached in three ways: by optimal distribution of structural mass, by viscoelastic damping treatments, and by active feedback control systems. Software design tools that address all three approaches are needed for SDI structures so that each approach can be exploited with minimal weight penalties. This report documents development in structural optimization under dynamic loads, both steady-state and transient. New methods for these problems are derived and demonstrated on small-scale structural models. The methods address minimization of structural mass subject to constraints on peak responses in either domain, together with frequency constraints and side constraints on member sizes. The methods are exercised with and without active control systems. GRA

N89-28863# Stanford Univ., CA. Physics Lab.
PICOSECOND ELECTROOPTIC INVESTIGATIONS OF INTEGRATED CIRCUITS Final Report, 12 Sep. 1986 - 11 Dec. 1987
B. A. Auld, D. M. Bloom, J. L. Freeman, R. Majidi-Ahy, M. J. W. Rodwell, and K. J. Weingarten Jan. 1989 289 p
(Contract F33615-86-C-1126)
(AD-A209134; AFWAL-TR-88-1071) Avail: NTIS HC A13/MF A01 CSCL 09/3

The continuing development of integrated electronic circuits operating to 110 GHz, and the development of digital circuits with toggle rates above 20 GHz, has given rise to commensurate need for instrumentation capable of diagnosing the internal operation of these circuits. These analog microwave and millimeter-wave integrated circuits are critical to the development of compact, low-cost, and frequency agile radar and communication systems for military applications, while the ultrafast digital technologies address the need in military electronic systems to rapidly acquire, digitize, and process very large amounts of data. However, current electronic instrumentation falls far short of the need for internal, high-frequency probing capability without severely disturbing circuit operation. Direct electrooptic sampling provides extremely high bandwidth while permitting non-invasive examination of internal node voltages of both digital and microwave GaAs integrated circuits. Characterization of this probe in terms of accuracy, repeatability, and invasiveness, as well as extension of its probing capability to the millimeter regime, is critical to its continued viability as a powerful diagnostic tool. GRA

N89-28864# Carnegie-Mellon Univ., Pittsburgh, PA. Dept. of Mechanical Engineering.
THE EFFECT OF TRANSIENTS ON CRACK TIP STRESS FIELDS DURING THERMAL FATIGUE LOADING Final Report, 1 Apr. 1986 - 31 Mar. 1989
J. H. Griffin and S. E. Cunningham 25 Apr. 1989 129 p
(Grant AF-AFOSR-0142-86; AF Proj. 2302)
(AD-A210084; AFOSR-89-0684TR) Avail: NTIS HC A07/MF A01 CSCL 11/6

A method is developed for evaluating the effect of cyclic thermal loading on crack tip stress fields. Advantage is taken of the periodic nature of fatigue loading and only harmonic loadings are considered. Formulating the problem in this way permits the extraction of time as an explicit variable and replaces its role with a dependence on the frequency of the thermal loading. The means for evaluating the effect of thermal transients on crack tip stress fields is the stress intensity factor which is calculated from numerically defined stress and displacement fields using a path independent integral. Results obtained indicate that stress intensity factors of cracked components exposed to thermal fatigue conditions have a significant dependence on the frequency of the thermal cycle and the crack geometry. Numerical estimates for Mode 1 thermal stress intensity were obtained for the case of a titanium alloy that was heated using intense light sources. GRA

N89-28865# Wisconsin Univ., Madison. Dept. of Mathematics.
MODELLING, INFORMATION, PROCESSING, AND CONTROL Final Scientific Report, 30 Sep. 1985 - 29 Sep. 1988
David L. Russell 15 Jan. 1989 118 p
(Grant AF-AFOSR-0263-85; AF Proj. 2304)
(AD-A207810; AFOSR-89-0527TR) Avail: NTIS HC A06/MF A01 CSCL 20/11

Research was conducted in identification and control of distributed parameter systems, particularly damping mechanisms in distributed elastic systems, modeling of flexible structures, control of systems with nonlinear behavior and control of systems with solitary waves. A thorough analysis of damping mechanisms in elastic systems was carried out, including common classical forms of damping, which led to a new model of damping (spatial hysteresis) which correctly models observed asymptotic behavior in the frequency domain. More recent work focused on transfer function methods for infinite dimensional linear systems. Papers included some remarks on transfer function methods for infinite

dimensional linear systems; spectral and asymptotic properties of linear elastic systems with internal damping; and frequency/period estimation and adaptive rejection of periodic disturbances. GRA

N89-28866# Massachusetts Inst. of Tech., Cambridge. Artificial Intelligence Lab.
RESIDUAL VIBRATION REDUCTION IN COMPUTER CONTROLLED MACHINES Ph.D. Thesis
Neil C. Singer Feb. 1989 241 p
(Contracts N00014-86-K-0685; N00014-85-K-0124)
(AD-A208074; AI-TR-1030) Avail: NTIS HC A11/MF A01 CSCL 13/9

Control of machines that exhibit flexibility becomes important when designers attempt to push the state of the art with faster, lighter machines. Three steps are necessary for the control of a flexible plant. First, a good model of the plant must exist. Second, a good controller must be designed. Third, inputs to the controller must be constructed using knowledge of the system dynamic response. There is a great deal of literature pertaining to modeling and control but little dealing with the shaping of system inputs. Two input shaping techniques based on frequency domain analysis are examined. The first involves the use of the first derivative of a gaussian exponential as a driving function template. The second, a causal filtering, involves removal of energy from the driving functions at the resonant frequencies of the system. A linear programming technique for generating vibration reducing driving functions for systems is presented. The results of the previous chapter by developing a direct solution are extended to the new class of driving functions. A detailed analysis of the new technique is presented from five different perspectives and several extensions are presented. The theories of the previous two chapters with hardware experiments are verified. Because the new technique resembles common signal filtering, the new approach is compared to eleven standard filters. The new technique are shown to result in less residual vibration, have better robustness to system parameter uncertainty, and require less computation than other currently used input shaping techniques. GRA

N89-28867# Akron Univ., OH. Inst. of Polymer Science.
COMPARISON OF PEEL AND LAP SHEAR BOND STRENGTHS FOR ELASTIC JOINTS WITH AND WITHOUT RESIDUAL STRESSES
A. N. Gent and C. W. Lin May 1989 32 p
(Contract N00014-85-K-0222)
(AD-A208102; TR-19) Avail: NTIS HC A03/MF A01 CSCL 20/11

Fracture energies were calculated from peel and lap shear experiments on rubber strips bonded together with a pressure sensitive acrylic adhesive layer. In some cases, one strip was held stretched during bonding, to create joints with built in stresses. Good agreement was obtained in all cases, provided that elastic strain energy was taken into account, the work of detachment being about 180 J/sq. m. For thick rubber layers, about 3 to 4 mm. or greater, the strain induced by peel or shear forces was rather small and the assumption of linear elastic behavior was found to be satisfactory. Good agreement was then obtained with the relations derived by Kendall. GRA

N89-28868# Ballistic Research Labs., Aberdeen Proving Ground, MD.
ADIABATIC SHEAR BANDS IN ONE DIMENSION
Thomas W. Wright and John W. Walter May 1989 24 p
(AD-A208105; BRL-MR-3759) Avail: NTIS HC A03/MF A01 CSCL 20/11

The progress is summarized which was made at the Ballistic Research Laboratory to date in analyzing and understanding the dynamical processes that cause the formation of adiabatic shear bands and the influence of various physical parameters on their formation. GRA

N89-28869# Cornell Univ., Ithaca, NY. Coll. of Engineering.
NONLINEAR DYNAMICS AND CONTROL OF FLEXIBLE STRUCTURES Annual Report, 1 Oct. 1987 - 30 Sep. 1988
Francis C. Moon, Peter Gergely, James S. Thorp, and John F. Abel 30 Mar. 1989 81 p
(Contract F49620-87-C-0011)
(AD-A208120; AFOSR-89-0595TR) Avail: NTIS HC A05/MF A01 CSCL 20/11

Chaotic vibrations were demonstrated in pinjointed truss structure and various factors involved, such as prestress (tension cables), member buckling, joint free-play and friction were investigated. Modeling techniques were developed through integration of finite and optimal controls, application of group theoretic concepts, and effective usage of computer graphics. GRA

N89-28870*# National Aeronautics and Space Administration. Ames Research Center, Moffett Field, CA.
ONE-DEGREE-OF-FREEDOM MOTION INDUCED BY MODELED VORTEX SHEDDING
L. A. Yates, A. Unal (Army Aviation Research and Development Command, Moffett Field, CA.), M. Szady, and G. T. Chapman Jul. 1989 50 p
(NASA-TM-101038; A-88302; NAS 1.15:101038) Avail: NTIS HC A03/MF A01 CSCL 20K

The motion of an elastically supported cylinder forced by a nonlinear, quasi-static, aerodynamic model with the unusual feature of a motion-dependent forcing frequency was studied. Numerical solutions for the motion and the Lyapunov exponents are presented for three forcing amplitudes and two frequencies (1.0 and 1.1 times the Strouhal frequency). Initially, positive Lyapunov exponents occur and the motion can appear chaotic. After thousands of characteristic times, the motion changes to a motion (verified analytically) that is periodic and damped. This periodic, damped motion was not observed experimentally, thus raising questions concerning the modeling. Author

N89-28871# Aeronautical Research Labs., Melbourne (Australia).
STRESSES AND STRAINS IN A COLD-WORKED ANNULUS
G. S. Jost Sep. 1988 52 p
(AR-005-548; ARL-Struc-R-434) Copyright Avail: NTIS HC A04/MF A01

Analytically-derived plane strain stresses and strains in an annulus pressurized sufficiently to cause plastic flow are given. Unloading giving rise to reyielding around the bore is then examined, along with the effect of reaming. Cold-working is then included in the analysis in terms of interference between mandrel and hole. Finally, comparisons of stress and strain predictions are made with those from a finite element analysis. Author

N89-28872# Technische Univ., Berlin (Germany, F.R.). Fachbereich Elektrotechnik.
CONTRIBUTION TO THE GENERATION OF CIRCULAR POLARIZATION OF HIGH PURITY USING PLANAR WIRE ANTENNA STRUCTURES Ph.D. Thesis [EIN BEITRAG ZUR ERZEUGUNG VON ZIRKULARPOLARISATION HOHER REINHEIT MITTELS PLANARER DRAHTANTENNENSTRUKTUREN]
Ulrich Ralf Kraft 1988 157 p In GERMAN
(ETN-89-94659) Avail: NTIS HC A08/MF A01

Circular polarization criteria for the antenna shape and the realization using a wire antenna structure were investigated. The formulation of the polarization problem of spherical waves is presented. Perfect circular polarization for the defined radiation main direction can be realized under idealized conditions using symmetric multiple-arm antennas; theoretical multiple arangements are given. The characteristics of wire antenna structures which can be realized in practice were analyzed. The stability and the sensitivity of the desired polarization state with respect to errors in the antenna feed are quantitatively determined using a newly defined characteristic: the polarization stability factor. The polarization stability of spiral structures is phenomenologically explained, and topical values of the stability factor are numerically obtained. Experimental results are in good agreement with simulations. ESA

N89-28873# Institut Franco-Allemand de Recherches, Saint-Louis (France).
COMPRESSION TESTS USING HOPKINSON BARS: NUMERICAL SIMULATION AND EXPERIMENTAL STUDY [ESSAIS DE COMPRESSION SUR BARRES D'HOPKINSON: SIMULATION NUMERIQUE ET ETUDE EXPERIMENTALE]
A. Lichtenberger, G. Gazeaud, and E. Lach 2 May 1988 11 p In FRENCH Presented at the 2nd Congres International sur le Comportement Mecanique et Physique des Materiaux sous Sollicitations Dynamiques, Ajaccio, France, 19-23 Sep. 1988
(ISL-C-208/88; ETN-89-94848) Avail: NTIS HC A03/MF A01

The limits of the compression test method are discussed as well as the rules for the choice of specimen geometries. The numerical simulations carried on with the Lagrangian hydrodynamic HEMP code allow the method error to be quantified. ESA

N89-28874# Technische Univ., Delft (Netherlands).
COHESION AND INTERPARTICLE FORCES Ph.D. Thesis
Erik Floor Hobbel 1988 287 p
(ETN-89-95454) Avail: NTIS HC A13/MF A01

A number of properties connected with the cohesive behavior of a powder have been analyzed and related to the interparticle forces. The tensile strength and cohesion of compacted systems, and the cohesion of an aerated system, have been studied experimentally. The mechanisms which give rise to the behavior observed have been clarified and suitable models suggested. These models are based on the idea that all the interparticle interactions are dispersely distributed. Assuming a Gamma distribution of the interparticle forces, it is shown that the maximum force measured in a tensile test does not coincide with the breakage force, but can be substantially lower. The fracturing of a powder cake is analyzed in detail and a crack propagation theory is adapted for powders to explain the phenomena quantitatively. ESA

N89-28875# Universiteit Twente, Enschede (Netherlands). Faculty of Applied Mathematics.
SMOOTH PIECEWISE POLYNOMIALS AS CONFORMING FINITE ELEMENTS FOR PLATE BENDING PROBLEMS
R. H. J. GmeligMeyling Nov. 1988 33 p
(Memo-747; ISSN-0169-2690; ETN-89-95115) Avail: NTIS HC A03/MF A01

A computational method is presented for constructing smooth piecewise polynomials with respect to a triangular mesh. The aim is to obtain different conforming finite elements of lowest possible degree for the numerical solution of the biharmonic equation. This equation describes the deformation of a thin elastic plate subject to perpendicular forces. The elements considered are all C-one-smooth and either polynomial or piecewise polynomial per triangle. The Bezier-Bernstein representation is employed as a convenient form to describe piecewise polynomial functions which are constrained by smoothness conditions. A comparison is made between three specific conforming elements for the biharmonic equation with elements based on triangles and either polynomial or piecewise polynomial per triangle. Numerical examples illustrating the performance of these elements in practical circumstances are presented, and a convergence of the approximants towards the exact solution is shown to occur when the mesh size is reduced. Increasing the degree of the piecewise polynomial is found to greatly improve the accuracy. The computational costs of the different elements are discussed and the global cubic element is suggested as the most efficient. The quadratic C-one-smooth element is found to facilitate the construction of accurate and visually pleasing contour maps. ESA

42 GEOSCIENCES (GENERAL)

No abstracts in this category.

43 EARTH RESOURCES AND REMOTE SENSING

Includes remote sensing of earth resources by aircraft and spacecraft; photogrammetry; and aerial photography.

For instrumentation see *35 Instrumentation and Photography.*

N89-28876# Joint Publications Research Service, Arlington, VA.
JPRS REPORT: SCIENCE AND TECHNOLOGY. USSR: SPACE. 16TH INTERNATIONAL CONGRESS OF THE INTERNATIONAL SOCIETY FOR PHOTOGRAMMETRY AND REMOTE SENSING, VOLUME 1
30 Jan. 1989 252 p Transl. into ENGLISH from International Archives of Photogrammetry and Remote Sensing (Kyoto, Japan), v. 27, pt. B1, B2, B4, B5, B6 and B7, 1988 Congress held in Kyoto, Japan, 1988
(JPRS-USP-89-002-Vol-1) Avail: NTIS HC A12/MF A01

Space application topics addressed include: holography, remote sensing, satellite observation, synthetic aperture radar, expert systems, software engineering, satellite imagery, image processing, photogrammetry, and sea surface temperature. For individual titles, see N89-28877 through N89-28902.

N89-28877# Joint Publications Research Service, Arlington, VA.
A NEW HOLOGRAPHIC INVERSE FILTERING METHOD AND ITS APPLICATION TO RESTORATION OF DEGRADED REMOTE SENSING IMAGES **c35**
Haisheng Cao and Xiangqian Chang *In its* JPRS Report: Science and Technology. USSR: Space. 16th International Congress of the International Society for Photogrammetry and Remote Sensing, Volume 1 30 Jan. 1989 p 1-10 Transl. into ENGLISH from International Archives of Photogrammetry and Remote Sensing (Kyoto, Japan), v. 27, 1988 p 37-44 (For primary document see N89-28876 23-43)
Avail: NTIS HC A12/MF A01

An anti-noise inverse filtering system is presented. In this system the diffraction gratings are superposed on the point spread function (PSF) and blurred images to be restored on the input plane respectively. Then the multi-channel inverse filtering process is done on the Fourier spectrum plane. The signal to noise ratio of N-channel processing system is increased by N times that of a single one. In addition, the filter (1/H) is made in the back of an absorptive mask (1/abs(H)), and then the reference beam need not be too low, the modulation of the interference fringes of the filter is increased. Therefore, the filter with high efficiency and extended dynamic range can be achieved. The above mentioned advantages were verified by the theoretical analysis and the experimental results. Author

N89-28878# Joint Publications Research Service, Arlington, VA.
A BISTATIC PARASITICAL RADAR (BIPAR) **c32**
Philipp Hartl and Hans Martin Braun *In its* JPRS Report: Science and Technology. USSR: Space. 16th International Congress of the International Society for Photogrammetry and Remote Sensing, Volume 1 30 Jan. 1989 p 11-19 Transl. into ENGLISH from International Archives of Photogrammetry and Remote Sensing (Kyoto, Japan), v. 27, 1988 p 45-53 (For primary document see N89-28876 23-43)
Avail: NTIS HC A12/MF A01

After decades of remote sensing from aircraft and satellites with cameras and other optical sensors, earth observation by imaging radars becomes more and more suitable because of their night and day and all weather operations capability and their information content being complementary to those of optical sensors. The major problem with microwave sensors (radars) is that there are not enough of them presently in operation and therefore not enough data available for effective radar signature research for civil applications. It is shown that airborne bistatic real aperture radar receivers can be operated with spaceborne transmitters of opportunity. Famous candidates for those systems are high power communications or direct TV satellites illuminating the earth surface with a power denisty of more than 10(-12) Watt/sq

meter. The high sophisticated status of signal processing technology today allows the realization of receivers correlating the received direct path signal from a communications satellite with its avoidable reflection on the ground. Coherent integration can improve the signal to noise ratio up to values where the radiometric resolution can satisfy users needs. The development of such parasitic radar receivers could even provide a cost effective way to open up new frequency bands for radar signature research. Advantages of these quiet systems for the purpose of classical radar reconnaissance are evident. Author

N89-28879# Joint Publications Research Service, Arlington, VA.
A PRACTICAL METHOD OF REMOTELY SENSED DIGITAL IMAGE'S RESOLVING POWER
Izumi Kamiya *In its* JPRS Report: Science and Technology. USSR: Space. 16th International Congress of the International Society for Photogrammetry and Remote Sensing, Volume 1 30 Jan. 1989 p 20-29 Transl. into ENGLISH from International Archives of Photogrammetry and Remote Sensing (Kyoto, Japan), v. 27, 1988 p 64-72 (For primary document see N89-28876 23-43)
Avail: NTIS HC A12/MF A01

A method which decides the resolving power of a digital remote sensor in a field experiment was developed. It was applied to the MOS-1 airborne verification experiment and predicted a resolving power of the Multispectral Electric Self-Scanning Radiometer (MESSR) on the MOS-1 satellite. An outline of this method is presented. An airphoto signal, reflectance of which is like a step function, is laid slightly obliquely to the perpendicular to the flying direction and observed. It is equivalent to observing an object, the radiance of which changes like a step function, in various phases. A calculation method of the point spread function (PSF) and MTS from the data was developed. Author

N89-28880# Joint Publications Research Service, Arlington, VA.
A CONCEPTUAL STUDY OF OPTICAL EARTH OBSERVATION FROM GEOSYNCHRONOUS ORBIT
Hajime Koshiishi and Kohzo Homma *In its* JPRS Report: Science and Technology. USSR: Space. 16th International Congress of the International Society for Photogrammetry and Remote Sensing, Volume 1 30 Jan. 1989 p 30-38 Transl. into ENGLISH from International Archives of Photogrammetry and Remote Sensing (Kyoto, Japan), v. 27, 1988 p 73-81 (For primary document see N89-28876 23-43)
Avail: NTIS HC A12/MF A01

At first it was assumed that requisitions of earth observation from geosynchronous orbit are 100 m spatial resolution at 1.1 micrometer wavelength. Then the design of the telescope system was done with the Schmidt type telescope. The optical parameters of the resulting design are 5 m focal length and 1 m aperture. Then a new scanning scheme was introduced: conical scan on an image plane. Analytical calculation by wave optics was done and it became clear that the 100 m spatial resolution can have a very high OTF with this conical scheme. Author

N89-28881# Joint Publications Research Service, Arlington, VA.
MODELLING ORIENTATION PARAMETERS OF SENSOR PLATFORMS
Joachim Lindenberger *In its* JPRS Report: Science and Technology. USSR: Space. 16th International Congress of the International Society for Photogrammetry and Remote Sensing, Volume 1 30 Jan. 1989 p 39-47 Transl. into ENGLISH from International Archives of Photogrammetry and Remote Sensing (Kyoto, Japan), v. 27, 1988 p 82-89 (For primary document see N89-28876 23-43)
Avail: NTIS HC A12/MF A01

Autoregressive integrated (ARI) stochastic processes are introduced for modeling the dynamic characteristics of the exterior orientation parameters of a sensor platform. The ARI model in combination with a variance component estimation enables the entire functional and stochastical description of the orientation parameters. The main advantages of this model are the easy handling, the low number of necessary ARI process parameters and the dispensation of any a-priori information concerning the stochastic model. The successful application of the ARI model to very different kinds of sensor orientation parameters improves the power of the concept. Comparisons to other methods for accuracy estimation demonstrate that the obtained results are realistic. Author

N89-28882# Joint Publications Research Service, Arlington, VA.
KRAS: A DANISH HIGH RESOLUTION AIRBORNE SAR c32
Soren Norvang Madsen, Erik Lintz Christensen, and Niels Skou *In its* JPRS Report: Science and Technology. USSR: Space. 16th International Congress of the International Society for Photogrammetry and Remote Sensing, Volume 1 30 Jan. 1989 p 48-57 Transl. into ENGLISH from International Archives of Photogrammetry and Remote Sensing (Kyoto, Japan), v. 27, 1988 p 90-97 (For primary document see N89-28876 23-43)
Avail: NTIS HC A12/MF A01

A C-band high resolution airborne synthetic aperture radar (SAR) is presently being constructed. The main purpose of the project, which is called KRAS, is to develop the knowledge base required to build advanced coherent radars. The design rationale is presented. The design of the radar is based on digital technology to the largest possible degree. This results in a very flexible radar system, with most of the system parameters being software controlled. Variable waveforms of bandwidths larger than 100 MHz and durations up to 20 microsec can be generated. Calibration of the system was also given much consideration, and design principles usually applied in radiometers were implemented. The significant flexibility and the calibration is of major importance since the system is intended for applications ranging from medium resolution wide swath mapping, i.e., sea ice mapping or oil pollution surveillance, to high resolution narrow swath mapping for cartography or reconnaissance. Author

N89-28883# Joint Publications Research Service, Arlington, VA.
OUTLINE OF MOS-1 VERIFICATION PROGRAM (MVP)
Korehiro Maeda, Hiroyuki Wakabayashi, Kazuyuki Tasaki, Masanobu Shimada, and Hideo Sato *In its* JPRS Report: Science and Technology. USSR: Space. 16th International Congress of the International Society for Photogrammetry and Remote Sensing, Volume 1 30 Jan. 1989 p 58-68 Transl. into ENGLISH from International Archives of Photogrammetry and Remote Sensing (Kyoto, Japan), v. 27, 1988 p 98-108 (For primary document see N89-28876 23-43)
Avail: NTIS HC A12/MF A01

The Marine Observation Satellite-1 (MOS-1) was successfully launched from Tanegashima Space Center, by an N-2 launch vehicle at 10:23 JST on February 19, 1987. The MOS-1 has 4 mission instruments: multispectral electronic self-scanning radiometer (MESSR), visible and thermal infrared radiometer (VTIR), microwave scanning radiometer (MSR), and data collection system transponder (DCST). All mission instruments were found to be satisfactory during the mission check period (three months after the launch) though there was an interference problem in the DCS due to the outer radio interference source which was resolved by changing the frequency of the data collection platform (DCP). The MOS-1 Verification Program (MVP) was planned and initiated to evaluate the MOS-1 observation system since March, 1987. As a part of the MVP, airborne experiments in summer and winter were conducted in several tests sites in FY-87 in Japan on passing days of MOS-1, and summer airborne experiments will be conducted in FY-88. The outline of the MVP is described and some initial results of the MVP are presented. Author

N89-28884# Joint Publications Research Service, Arlington, VA.
INVESTIGATION OF THE EFFECTIVENESS AND APPLICATIONS OF JAPANESE ERS-1 STEREOSCOPIC IMAGES
Nobuhiko Mori, Hidetoshi Takaoka, Kunishige Tonoike, Jiro Komai, and Shunji Murai *In its* JPRS Report: Science and Technology. USSR: Space. 16th International Congress of the International Society for Photogrammetry and Remote Sensing, Volume 1 30 Jan. 1989 p 69-79 Transl. into ENGLISH from International

Archives of Photogrammetry and Remote Sensing (Kyoto, Japan), v. 27, 1988 p 109-119 (For primary document see N89-28876 23-43)
Avail: NTIS HC A12/MF A01

A remote sensing satellite named the Japanese Earth Resources Satellite-1 (JERS-1) is scheduled to be launched in 1992 in Japan. The satellite will be able to take stereoscopic images continuously by two linear array sensors. A system was developed to make JERS-1 simulation stereoscopic images by computer, and then using this system, stereoscopic images were produced from a large format camera (LFC) photograph taken from the Space Shuttle. The quality and the usefulness of the JERS-1 stereoscopic images was investigated using these simulation images. The work results in high quality stereoscopic vision to explore Earth resources from JERS-1 stereoscopic images which have about 20 m ground resolution and 0.3 base-to-height ratio. Author

N89-28885# Joint Publications Research Service, Arlington, VA.
A SATELLITE ASSISTED-TRACKING SYSTEM WITH REAL-TIME ACCOMMODATION FOR MAXIMAL POINTING
Jose Luiz deBarros Aguirre and Valder Matos deMedeiros *In its* JPRS Report: Science and Technology. USSR: Space. 16th International Congress of the International Society for Photogrammetry and Remote Sensing, Volume 1 30 Jan. 1989 p 80-89 Transl. into ENGLISH from International Archives of Photogrammetry and Remote Sensing (Kyoto, Japan), v. 27, 1988 p 1-10 (For primary document see N89-28876 23-43)
Avail: NTIS HC A12/MF A01

An operational difficulty of ground receiving stations is to reacquire a satellite in high elevation after a loss due to a zenithal pass (when employing an El-over-Az antenna), a receiving chain malfunction, or another cause that breaks reception. Traditional recovery schemes employ rate memory or precalculated pointing data (programmed tracking) to command the antenna movement after a tracking loss. The system described was implemented at the Brazilian LANDSAT receiving station. It does not require a fast computer and takes very little memory, yet has proven extremely effective, with significant advantages over previously available systems. Extensions to the method, to be employed for the upcoming Brazilian satellites, are discussed. Author

N89-28886# Joint Publications Research Service, Arlington, VA.
LOCAL AREA NETWORK AND DATA NETWORK FOR THE ADVANCED EARTH OBSERVING SATELLITE, ADEOS SYSTEM
Kohei Arai *In its* JPRS Report: Science and Technology. USSR: Space. 16th International Congress of the International Society for Photogrammetry and Remote Sensing, Volume 1 30 Jan. 1989 p 90-97 Transl. into ENGLISH from International Archives of Photogrammetry and Remote Sensing (Kyoto, Japan), v. 27, 1988 p 11-19 (For primary document see N89-28876 23-43)
Avail: NTIS HC A12/MF A01

NASDA is planning the next generation of earth observation satellites, following MOS-1, MOS-1b, and JERS-1, called the Advanced Earth Observing Satellite (ADEOS). ADEOS will carry an ocean color and temperature scanner (OCTS), advanced visible and near infrared radiometer (AVNIR), and announcement opportunity sensors (AO) and will require a quick data distribution. Not only direct broadcasting, but also data distribution through a network are useful for the dissemination of such data. Therefore, a data network which users can access a quicklook image data base in a quasi real-time basis is now considered. In order for the preoperational data handling, a local area network (LAN) is taken into account for an ADEOS ground facility. The processed data are sent to the film recorder through the LAN together with the histograms for the generation of look up table for the gamma correction. Key items of the processed data are also transmitted to the information retrieveal subsystem for the registration. The acquired quidk look data are transmitted to not only the film recorder but also quick look image data base and the information retrieval subsystem in a real time basis. The idea and concept for the development of the ADEOS ground facility is described. Author

N89-28887# Joint Publications Research Service, Arlington, VA.
SAR ACTIVITIES AT DORNIER **c32**
Hans Martin Braun and Gerhard Hans Rausch *In its* JPRS Report: Science and Technology. USSR: Space. 16th International Congress of the International Society for Photogrammetry and Remote Sensing, Volume 1 30 Jan. 1989 p 98-104 Transl. into ENGLISH from International Archives of Photogrammetry and Remote Sensing (Kyoto, Japan), v. 27, 1988 p 44-50 (For primary document see N89-28876 23-43)
Avail: NTIS HC A12/MF A01

Radar remote sensing from space was a key element in the German and the European Earth Observation Programs for more than a decade now. From the beginning, the Dornier-System was involved in these activities. Supported by the German Ministry of Research and Technology (BMFT) and by the Forschungs- und Versuchsanstalt for Luft- und Raumfahrt (DFVLR), Dornier-System has developed important key technologies and extensive system design tools for many spaceborne radars with special emphasis on radars with synthetic aperture (SAR). The main space SAR activities in which Dornier was involved are briefly presented, and it is indicated that these demanding programs again need a creative engagement of innovative industries in the future. Author

N89-28888# Joint Publications Research Service, Arlington, VA.
ERS-1 SAR PROCESSING WITH CESAR
Einar-Arne Herland *In its* JPRS Report: Science and Technology. USSR: Space. 16th International Congress of the International Society for Photogrammetry and Remote Sensing, Volume 1 30 Jan. 1989 p 105-113 Transl. into ENGLISH from International Archives of Photogrammetry and Remote Sensing (Kyoto, Japan), v. 27, 1988 p 191-199 (For primary document see N89-28876 23-43)
Avail: NTIS HC A12/MF A01

A vector processor called Computer for Experimental Synthetic Aperture Radar (CESAR), is now in the final stage of development. It is connected to a supermini computer, and has a maximum performance of 320 Megaflops. This is achieved through parallelism and pipelining, and the processor is fully programmable. The architecture of CESAR and the implementation of a set of algorithms for processing of images from the ERS-1 synthetic aperture radar are described. Author

N89-28889# Joint Publications Research Service, Arlington, VA.
EXPERIENCES IN IMPLEMENTING AN EXPERT SYSTEM SUPPORTED MAN-MACHINE-INTERFACE FOR THE CONFIGURATION OF THE INTELLIGENT SAR PROCESSOR
W. Noack, A. Popella, and R. Konjack *In its* JPRS Report: Science and Technology. USSR: Space. 16th International Congress of the International Society for Photogrammetry and Remote Sensing, Volume 1 30 Jan. 1989 p 120-131 Transl. into ENGLISH from International Archives of Photogrammetry and Remote Sensing (Kyoto, Japan), v. 27, 1988 p 344-356 (For primary document see N89-28876 23-43)
Avail: NTIS HC A12/MF A01

In view of ERS-1 and X-SAR, DFVLR is establishing a high throughput Processing and Archiving Facility (PAF) for high precision synthetic aperture radar (SAR) products. Concerning the requirements throughput and product quality, it was realized that the SAR processing task needs a distributed and dedicated computer system to be controlled by an expert system. The solution is called the Intelligent SAR (ISAR) processor. During the first development phase, a prototype of the man-machine interface was implemented. It is the task of this interface to monitor, control, and debug the whole processing system. Especially, the configuration capability of this expert system controlled man-maching interface was investigated with relation to SAR processing. The experiences gathered during the development are presented with emphasis on structuring the knowledge domains and the realization of facts and rules applying frame based

methods. Additionally it will demonstrate the use of an expert system shell for software engineering. Recommendations for future work are also given. Author

N89-28890# Joint Publications Research Service, Arlington, VA.
EXAS: EXPERIMENT ON AUTONOMOUS SAR PROCESSOR CALIBRATION
H. Runge, A. Popella, and W. Noack *In its* JPRS Report: Science and Technology. USSR: Space. 16th International Congress of the International Society for Photogrammetry and Remote Sensing, Volume 1 30 Jan. 1989 p 132-140 Transl. into ENGLISH from International Archives of Photogrammetry and Remote Sensing (Kyoto, Japan), v. 27, 1988 p 369-377 (For primary document see N89-28876 23-43)
Avail: NTIS HC A12/MF A01

Future synthetic aperture radar (SAR) missions like the SIR-C with the German X-band radar will acquire multifrequency and multipolarization data with various incidence angles. In order to exploit the mission's full scientific potential DFVLR is going to calibrate both its Intelligent SAR Processor (ISAR) and the final image products. The idea of the EXAS proposal is to use the extra data gained from an independent Doppler measurement. These data will be gathered at a geolocated receiver in order to tune and finally calibrate the ISAR processor. The receiver will be adjusted to the sensor carrier frequency, the signals will be mixed down to baseband, be digitalized and transferred to the ISAR hardware system. This can be performed in parallel for three frequencies with two different polarizations. Immediately after the fly-over the data will be analyzed. The azimuth antenna pattern will be computed and fed back into the processing chain. The replica of the chirps radiated by the sensor will be recorded by the ground receiver. Therefore, the exact range reference function is known and can be used for the processing. The calibrated processor will produce images with a very accurate absolute pixel location. In order to verify this, a cluster of geolocated point reflectors shall be positioned over the swath and the SAR image will be compared with a cartographic map. The experiment plan and the contributions of the three institutes are described.
Author

N89-28891# Joint Publications Research Service, Arlington, VA.
ZEISS DIGITAL MAPPING: A NEW HARDWARE AND SOFTWARE SYSTEM CONCEPT FROM KOMBINAT VEB CARL ZEISS JENA
Wolfgang Wallwitz *In its* JPRS Report: Science and Technology. USSR: Space. 16th International Congress of the International Society for Photogrammetry and Remote Sensing, Volume 1 30 Jan. 1989 p 141-147 Transl. into ENGLISH from International Archives of Photogrammetry and Remote Sensing (Kyoto, Japan), v. 27, 1988 p 441-449 (For primary document see N89-28876 23-43)
Avail: NTIS HC A12/MF A01

Mapping and map production as the main tasks of geodesy/photogrammetry as well as of remote sensing are characterized by rapid advances, which are essentially aimed at the generation of digital maps. These advances were made possible, on the one hand, by the development of computer hardware including the most sophisticated firmware and the resulting possibilities of efficient software solutions, but on the other hand also by revolutionary solutions in the equipment systems. Zeiss JENA has made its contribution to this trend with the LMK aerial camera, the first commercially available camera with forward motion compensation (1982) as well as with the efficient plotting machines STEREOMETROGRAPH, TOPOCART, and STEREOPLOT, of which the two last-mentioned systems will also in the era of analytical plotters have a strong foothold for a long period in the field of stereoplotting because of their favorable price/performance ratio. A system is presented which is characterized by its capability of being connected with existing equipment and by its high utility value in all its parts and which radically changes the traditional process of map production and map use. Author

N89-28892# Joint Publications Research Service, Arlington, VA.
HIGH RESOLUTION SOVIET SPACE PHOTOGRAPHS FOR TOPOGRAPHIC MAPPING
Romuald Kaczynski and Jan Konieczny *In its* JPRS Report: Science and Technology. USSR: Space. 16th International Congress of the International Society for Photogrammetry and Remote Sensing, Volume 1 30 Jan. 1989 p 148-153 Transl. into ENGLISH from International Archives of Photogrammetry and Remote Sensing (Kyoto, Japan), v. 27, 1988 p 501-505 (For primary document see N89-28876 23-43)
Avail: NTIS HC A12/MF A01

The results of the evaluation of high resolution panchromatic photographs acquired from the Cosmos satellite and multispectral space photographs taken by the MKF-6 camera installed on the Salyut space station are discussed. High resolution space photographs taken from 220 km orbit were evaluated on analytical plotters and orthophotoprojectors. The achieved accuracy is satisfactory for topographic mapping in the scale 1:50,000 and map revision up to the scale 1:25,000. Author

N89-28893# Joint Publications Research Service, Arlington, VA.
MAP PRODUCTION AND REVISION WITH SATELLITE PHOTOGRAPHS TAKEN BY THE MKF-6 CAMERA AND BY THE CAMERAS KATE-140, KATE-200, AND KFA-1000
Joachim Kraemer *In its* JPRS Report: Science and Technology. USSR: Space. 16th International Congress of the International Society for Photogrammetry and Remote Sensing, Volume 1 30 Jan. 1989 p 154-162 Transl. into ENGLISH from International Archives of Photogrammetry and Remote Sensing (Kyoto, Japan), v. 27, 1988 p 506-512 (For primary document see N89-28876 23-43)
Avail: NTIS HC A12/MF A01

In the practical work done so far with space photographs in this country, it was proved that for many problems, in principle, the equipment and methods commonly used in photogrammetry can be employed. The methods are partial enlargement or rectification, graphic photogrammetric stereoplotting, and digital photogrammetric restitution. Photogrammetry and remote sensing viewed as related sciences very often provide a definitive photogrammetric or cartographic final-product. These are map products as photomaps or in vector format, thematic, or topographic maps. Thematic maps between 1:50,000 scale and 1:500,000 scale and smaller produced from space photographs are mainly used for special purposes such as geological exploration, for agriculture, forestry, ecological, or local planning purposes. Until recently, considering the fact, that the resolution of satellite image data was inadequate for mapping or revision of topographic maps at a scale of 1:25,000. Since 1987 high resolution Soviet space photographs taken with the KFA-1000 camera, which were the subject of various theoretical and practical studies in photogrammetry are available. Since 1976 photomaps were produced from space photographs taken with the MKF-6 multispectral camera and taken with the USSR-cameras made in the last years. Author

N89-28894# Joint Publications Research Service, Arlington, VA.
AN EXPERT SYSTEM FOR SATELLITE IMAGE INTERPRETATION AND G.I.S. BASED PROBLEM SOLVING
J. Desachy, P. Debord, and S. Castan *In its* JPRS Report: Science and Technology. USSR: Space. 16th International Congress of the International Society for Photogrammetry and Remote Sensing, Volume 1 30 Jan. 1989 p 163-175 Transl. into ENGLISH from International Archives of Photogrammetry and Remote Sensing (Kyoto, Japan), v. 27, 1988 p 518-528 (For primary document see N89-28876 23-43)
Avail: NTIS HC A12/MF A01

An expert system is described for satellite image interpretation and thematic mapping. The thematician knowledge is kept in a data base as a set of production rules with certainty factors. The facts data base for a given problem is composed of the image to be interpreted and the associated geographic information system. The system can handle two kinds of reasoning depending on the nature of the given problem: data-driven reasoning for classification

problems; and goal-driven reasoning for object possible location mapping. In addition, a learning process is included in the expert system. Author

N89-28895# Joint Publications Research Service, Arlington, VA.
NATIONAL REPORT OF POLISH SOCIETY OF PHOTOGRAMMETRY AND REMOTE SENSING Report, Jan. 1980 - Dec. 1987
Ryszard Florek, Jozef Jachimski, Romuald Kaczynski, Wladyslaw Mierzwa, Stefan Papiernik, Ryszard Preuss, Zbigniew Sitek, Andrzej Swiatkiewicz, and Jacek Uchanski *In its* JPRS Report: Science and Technology. USSR: Space. 16th International Congress of the International Society for Photogrammetry and Remote Sensing, Volume 1 30 Jan. 1989 p 183-192 Transl. into ENGLISH from International Archives of Photogrammetry and Remote Sensing (Kyoto, Japan), v. 27, 1988 p 52-59 (For primary document see N89-28876 23-43)
Avail: NTIS HC A12/MF A01

Topographic operations in Poland; non-topographic applications of photogrammetry methods; remote sensing activities; and research and development are described. Also covered were education; publications; professional organizations; and addresses of organizations other than education and research. B.G.

N89-28896# Joint Publications Research Service, Arlington, VA.
A COMPARISON BETWEEN THE VARIABILITY STRUCTURE OF THE REMOTELY SENSED SEA-SURFACE TEMPERATURE AND PIGMENT DISTRIBUTIONS
Mati Kahru *In its* JPRS Report: Science and Technology. USSR: Space. 16th International Congress of the International Society for Photogrammetry and Remote Sensing, Volume 1 30 Jan. 1989 p 193-202 Transl. into ENGLISH from International Archives of Photogrammetry and Remote Sensing (Kyoto, Japan), v. 27, 1988 p 252-260 (For primary document see N89-28876 23-43)
Avail: NTIS HC A12/MF A01

The spatial variance spectra of the near-surface pigment concentrations (from the coastal zone color scanner) and the sea surface temperature (from the advanced very high resolution radiometer) are analyzed. Most of the images originate from the California Current area, and a few from the North and Baltic Seas. Author

N89-28897# Joint Publications Research Service, Arlington, VA.
A STUDY ON INFORMATION ANALYSIS AIDS FOR SEA SURFACE TEMPERATURE IMAGE DATA
Hajime Koshiishi, Masao Naka, Hiromichi Yamamoto, Kohtaro Matsumoto, Kohzo Homma, Satsuki Matsumura, Hideo Takahashi, Yoshihiro Okada, Ken-ichi Okamoto, and Hideo Tameishi *In its* JPRS Report: Science and Technology. USSR: Space. 16th International Congress of the International Society for Photogrammetry and Remote Sensing, Volume 1 30 Jan. 1989 p 203-208 Transl. into ENGLISH from International Archives of Photogrammetry and Remote Sensing (Kyoto, Japan), v. 27, 1988 p 288-293 (For primary document see N89-28876 23-43)
Avail: NTIS HC A12/MF A01

Sea surface temperature (SST) charts obtained from a satellite includes various oceanic conditions such as fronts, ocean currents, and eddies. In extracting these oceanic conditions, simplified processing and high accuracy of the processed results are important. Technology of knowledge based processing is applicable to these problems. A feasibility study on information analysis aids for SST image data using this technology were performed. Implementation of the prototype knowledge based system is also described. Author

N89-28898# Joint Publications Research Service, Arlington, VA.
INTERPRETATION OF REMOTE SENSING DATA FROM EASTERN AREAS OF THE BALTIC SEA
J. Lokk, V. Pelevin, and V. Solomakha *In its* JPRS Report: Science and Technology. USSR: Space. 16th International Congress of the International Society for Photogrammetry and Remote Sensing, Volume 1 30 Jan. 1989 p 209-214 Transl. into ENGLISH from International Archives of Photogrammetry and Remote Sensing (Kyoto, Japan), v. 27, 1988 p 360-365 (For primary document see N89-28876 23-43)
Avail: NTIS HC A12/MF A01

A method for the determination of concentrations of optically active substances (phytopigments, suspended and yellow matter) in waters with high concentrations and unequal indices of optically active substances is suggested. The method was worked out relying on the Baltic Sea phenomenon but it can be applied to other water bodies of similar parameters. Possible ways of applying remote sensing to the admixture concentration determination in the eastern Baltic waters are considered. Author

N89-28899# Joint Publications Research Service, Arlington, VA.
DEVELOPMENT OF BOREHOLE SCANNER FOR UNDERGROUND GEOLOGICAL SURVEY
Shunji Murai, Chikaosa Tanimoto, Yoshitaka Matsumoto, and Koji Nagata *In its* JPRS Report: Science and Technology. USSR: Space. 16th International Congress of the International Society for Photogrammetry and Remote Sensing, Volume 1 30 Jan. 1989 p 215-219 Transl. into ENGLISH from International Archives of Photogrammetry and Remote Sensing (Kyoto, Japan), v. 27, 1988 p 391-395 (For primary document see N89-28876 23-43)
Avail: NTIS HC A12/MF A01

The borehole scanner was developed to obtain digital imagery of the inner wall of a borehole for geological survey. As compared with the existing borehole TV camera system, the following significant advantages were obtained. Continuous color image of the inner wall of the whole borehole can be obtained in digital form, while the TV camera system produces only a partial image in analog form. The speed of the data acquisition is very high, 36 m/hour, while the TV system is only 2 m/hour. Digital image analysis can be effectively applied to extract useful information. Author

N89-28900# Joint Publications Research Service, Arlington, VA.
AN IMPROVING MULTISPECTRAL RECORDING SET ANALYSIS METHOD
Nicolae Oprescu and Constantin Borduselu *In its* JPRS Report: Science and Technology. USSR: Space. 16th International Congress of the International Society for Photogrammetry and Remote Sensing, Volume 1 30 Jan. 1989 p 220-230 Transl. into ENGLISH from International Archives of Photogrammetry and Remote Sensing (Kyoto, Japan), v. 27, 1988 p 406-415 (For primary document see N89-28876 23-43)
Avail: NTIS HC A12/MF A01

An analytical method to select the best combination out of a multispectral image set is presented, starting from the spectral signature of a certain class of the study. Parameters established analytically are then used in an analogical process using the MSP-4C multispectral projector to obtain the best resolution of an involved spectral class. Author

N89-28901# Joint Publications Research Service, Arlington, VA.
DEVELOPMENT OF A FIELD RADIOMETER AS A GROUND TRUTH EQUIPMENT FOR THE JAPANESE ERS-1
Yasushi Yamaguchi and Isao Sato *In its* JPRS Report: Science and Technology. USSR: Space. 16th International Congress of the International Society for Photogrammetry and Remote Sensing, Volume 1 30 Jan. 1989 p 231-238 Transl. into ENGLISH from International Archives of Photogrammetry and Remote Sensing (Kyoto, Japan), v. 27, 1988 p 718-727 (For primary document see N89-28876 23-43)
Avail: NTIS HC A12/MF A01

A new field radiometer was developed to provide ground truth data for the optical sensor of the Japanese Earth Resources Satellite-1 (ERS-1), which is scheduled to be launched in 1992. This radiometer has two motor-driven filter wheels, each of which can contain up to eight filters and corresponds to the silicon and lead-sulphide detectors respectively. The same field of view exactly is guaranteed to all the spectral bands, because only one aperature is used to observe a target. It takes approximately twenty seconds

to perform one continuous measurement for the seven spectral bands equivalent to the ERS-1 sensor. A portable lap-top computer controls the radiometer and records measured results on a floppy disc. An officially-calibrated lamp and a standard reflection plate mounted on an optical bench were also prepared for the purpose of absolute energy calibration of the radiometer. Preliminary investigation has shown that this newly developed radiometer can provide reliable spectral data. Author

N89-28902# Joint Publications Research Service, Arlington, VA.
APPLICATION OF AERIAL SIDE-LOOKING RADAR IMAGERY IN CHINA
Pinghe Yang and Lianke Wang *In its* JPRS Report: Science and Technology. USSR: Space. 16th International Congress of the International Society for Photogrammetry and Remote Sensing, Volume 1 30 Jan. 1989 p 239-247 Transl. into ENGLISH from International Archives of Photogrammetry and Remote Sensing (Kyoto, Japan), v. 27, 1988 p 728-736 (For primary document see N89-28876 23-43)
Avail: NTIS HC A12/MF A01

A brief history of the side-looking radar in China is presented. Applications in geological surveys; mi revision and compilation; food control and disaster relief; and forestry investigations are discussed. B.G.

N89-28903# Joint Publications Research Service, Arlington, VA.
JPRS REPORT: SCIENCE AND TECHNOLOGY. USSR: SPACE. 16TH INTERNATIONAL CONGRESS OF THE INTERNATIONAL SOCIETY FOR PHOTOGRAMMETRY AND REMOTE SENSING, VOLUME 2
31 Jan. 1989 197 p Transl. into ENGLISH from International Archives of Photogrammetry and Remote Sensing (Kyoto, Japan), v. 27, pt. B8, B9, B10 and B11, 1988 Congress held in Kyoto, Japan, 1988
(JPRS-USP-89-003-Vol-2) Avail: NTIS HC A09/MF A01

Space application topics addressed include: synthetic aperture radar, remote sensing, remote sensing data systems, lidar measurements of sea surface waves, radar imagery, image processing, geocoding system, SPOT imagery, image reconstruction, and noise reduction. For individual titles, see N89-28904 through N89-28921.

N89-28904# Joint Publications Research Service, Arlington, VA.
PERFORMANCE EVALUATION OF ERS-1 SYNTHETIC APERTURE RADAR FAST DELIVERY PROCESSOR
J. P. Guignard and P. Hasan *In its* JPRS Report: Science and Technology. USSR: Space. 16th International Congress of the International Society for Photogrammetry and Remote Sensing, Volume 2 31 Jan. 1989 p 1-7 Transl. into ENGLISH from International Archives of Photogrammetry and Remote Sensing (Kyoto, Japan), v. 27, pt. B8, 1988 p 1-7 (For primary document see N89-28903 23-43)
Avail: NTIS HC A09/MF A01

The factory acceptance test (FAT) of ESA's ERS-1 synthetic aperture radar fast delivery processor (SAR FDP) took place recently at MacDonald Dettwiler in Vancouver, Canada. The process will eventually be installed in the principal ERS-1 ground station in Kiruna, Sweden. The comprehensive set of tests performed during the FAT are described. The focus is on the tests and measurements of: image quality parameters; throughput for both image and wave mode product generation; and operational aspects of the processor demonstrating its ability to run in an operational environment. The SAR FDP shows a significant improvement in throughput compared to previous SEASAT processors, while preserving the integrity of the image quality. Author

N89-28905# Joint Publications Research Service, Arlington, VA.
THE BRAZILIAN EXPERIENCE IN HANDLING 15 YEARS OF REMOTE SENSING SATELLITE DATA
Marcio Nogueira Barbosa and Sergio dePaula Pereira *In its* JPRS Report: Science and Technology. USSR: Space. 16th International Congress of the International Society for Photogrammetry and Remote Sensing, Volume 2 31 Jan. 1989 p 8-23 Transl. into ENGLISH from International Archives of Photogrammetry and Remote Sensing (Kyoto, Japan), v. 27, pt. B8, 1988 p 15-29 (For primary document see N89-28903 23-43)
Avail: NTIS HC A09/MF A01

The Brazilian experience in acquiring, storing, processing, and disseminating remote sensing data collected from satellites since the first LANDSAT in 1973 to SPOT 1 in 1987/1988 is described. INPE's role in operating, upgrading, specifying, designing, and integrating the related systems are covered, giving an evolution history which can be useful to other developing countries in the field of remote sensing. Author

N89-28906# Joint Publications Research Service, Arlington, VA.
ESA'S ACTIVITIES AND PLANS FOR REMOTE SENSING DATA SYSTEMS
Livio Marelli *In its* JPRS Report: Science and Technology. USSR: Space. 16th International Congress of the International Society for Photogrammetry and Remote Sensing, Volume 2 31 Jan. 1989 p 24-34 Transl. into ENGLISH from International Archives of Photogrammetry and Remote Sensing (Kyoto, Japan), v. 27, pt. B8, 1988 p 84-94 (For primary document see N89-28903 23-43)
Avail: NTIS HC A09/MF A01

Remote sensing systems seem to change generation every 5 to 6 years: LANDSAT-1 in 1972; LANDSAT-3 Seasat, Nimbus, HSMM in 1978; LANDSAT-5/SPOT in 1984/64; ERS, JERS, TOPEX in 1990-2; and PFFs in 1995-97. Within such a time span two major aspects evolve: user requirements and technology available. An attempt was made to describe how in Europe the transition from experimental to pre-operational space remote sensing system is taking place, and its impact on data systems. The technology evolution is obviously playing an equally important role but unfortunately, each generatcn of remote sensing systems operates approximately with the technology prevailing during the previous generation and little can be done to modify this pattern. So far the most glamorous evolution in remote sensing payload data handling is in the area of available computing power and on-line storage. Author

N89-28907# Joint Publications Research Service, Arlington, VA.
THE POSSIBILITIES OF APPLICATION OF SATELLITE DATA FOR MONITORING ICE CONDITION IN THE ANTARCTIC REGION
N. N. Shvyrkov *In its* JPRS Report: Science and Technology. USSR: Space. 16th International Congress of the International Society for Photogrammetry and Remote Sensing, Volume 2 31 Jan. 1989 p 35-40 Transl. into ENGLISH from International Archives of Photogrammetry and Remote Sensing (Kyoto, Japan), v. 27, pt. B8, 1988 p 1-6 (For primary document see N89-28903 23-43)
Avail: NTIS HC A09/MF A01

Based on satellite observation in visible and microwave ranges the possibility of investigation of ice formation process and ice melting in high latitude zones of the World Ocean is considered. The modern methods of data acquisition of the borders of drift ice, size of ice fields, age of ice formations are analyzed. The methods of construction of weekly ice charts of the Arctic and Antarctic regions resulting from satellites, aircraft, and vessel observations are considered. The analysis of ice distribution in the Antarctic region in the light period of 1980 to 1984 seasons is made. Annual and seasonal dynamics of ice cover is estimated. The results obtained are of practical and theoretical interest for ecological studies and for the investigations of possibilities of exploitation of live resources of the Antarctic region. The data available can be used for the development of some methods for prediction of ice conditions in the South Ocean. Author

N89-28908# Joint Publications Research Service, Arlington, VA.
SEA SPECTRA AS DETERMINED FROM LOW-ALTITUDE SLAR IMAGES
Konstantin Voliak *In its* JPRS Report: Science and Technology.

USSR: Space. 16th International Congress of the International Society for Photogrammetry and Remote Sensing, Volume 2 31 Jan. 1989 p 41-54 Transl. into ENGLISH from International Archives of Photogrammetry and Remote Sensing (Kyoto, Japan), v. 27, pt. B8, 1988 p 58-67 (For primary document see N89-28903 23-43)
Avail: NTIS HC A09/MF A01

The analytic composite theory for the surface of Gaussian slope statistics has revealed that backscattering of vertically (V) polarized microwaves from the sea at large angles of incidence might have an azimuthal characteristic, which corresponds to the angular dependence of the small-scale Bragg spectrum, with an accuracy to within the slope variance of the long waves. For horizontally (H) polarized radiowaves, the model relates the image speckles to the statistics of spikes in a random surface-wave field. Fourier analysis and photometering of radioimages taken over various seas have allowed the estimation of the spectra of large- and small-scale sea surface waves as well as to study other phenomena imprinted on surface waves. Author

N89-28909# Joint Publications Research Service, Arlington, VA.
LIDAR MEASUREMENTS OF SEA SURFACE WAVES
K. I. Voliak and M. V. Solntsev *In its* JPRS Report: Science and Technology. USSR: Space. 16th International Congress of the International Society for Photogrammetry and Remote Sensing, Volume 2 31 Jan. 1989 p 55-65 Transl. into ENGLISH from International Archives of Photogrammetry and Remote Sensing (Kyoto, Japan), v. 27, pt. B8, 1988 p 68-77 (For primary document see N89-28903 23-43)
Avail: NTIS HC A09/MF A01

A lidar method is developed to measure the sea wave spectrum and other sea characteristics by using a narrow amplitude-modulated beam. Some techniques are suggested for determining the slope and curvature variance from a backscatterer (reflected) power. The model field experiment was carried out at an oceanographic platform. The experimental data demonstrate that the introduced method is highly effective. Author

N89-28910# Joint Publications Research Service, Arlington, VA.
NATIONAL PROGRAM FOR HANDLING LARGE VOLUMES OF SATELLITE DATA
B. L. Deekshatulu *In its* JPRS Report: Science and Technology. USSR: Space. 16th International Congress of the International Society for Photogrammetry and Remote Sensing, Volume 2 31 Jan. 1989 p 66-74 Transl. into ENGLISH from International Archives of Photogrammetry and Remote Sensing (Kyoto, Japan), v. 27, pt. B9, 1988 p 119-126 (For primary document see N89-28903 23-43)
Avail: NTIS HC A09/MF A01

With the completion of the activities relating to the augmentation program the data products supply is expected to be streamlined and will have a turn around time (TAT) of within 7 days for 50 percent of the products and within 21 days for the balance. It will also be possible to cater to increase in use demand for any other type of sensor products with the corresponding decrease in any other sensor products. It will also ensure guaranteed supply of products in case of emergency and the data products quality is also better. While, going through this program it will also be ensured that future expansion can be done easily. Until a couple of years ago, the facilities available for digital analysis of remote sensing data were practically non-existent in this country. To overcome this situation, 5 Regional Remote Sensing Service Centers along with two Associate Centers which can perform high throughput digital analysis were established. It is likely that in the next few years the digital analysis of satellite data will increase manifoldly and remote sensing will be used in an operational mode regularly. Author

N89-28911# Joint Publications Research Service, Arlington, VA.
REAL TIME SAR PROCESSING TECHNIQUES
Roland Schotter *In its* JPRS Report: Science and Technology. USSR: Space. 16th International Congress of the International Society for Photogrammetry and Remote Sensing, Volume 2 31 Jan. 1989 p 75-82 Transl. into ENGLISH from International Archives of Photogrammetry and Remote Sensing (Kyoto, Japan), v. 27, pt. B9, 1988 p 184-190 (For primary document see N89-28903 23-43)
Avail: NTIS HC A09/MF A01

Spaceborne synthetic aperture radar (SAR) systems provide raw radar data information at high data rates of 10 Mwords per second. Real time SAR processors, therefore, must perform more than 1 giga-operations (multiplications, additions) per second in order to generate images from the raw data. Since conventional computer systems are not able to cope with these requirements Dornier has developed real time SAR processors on the basis of a modular pipeline concept. The processing pipeline is built up to standardized hardware modules which are required for digital signal processing of two-dimensional data. These modules show identical electrical and mechanical interfaces so that each hardware module can be used in any place of the pipelines. The basic principles are presented for the real time modular pipeline concept and its processing rate requirements for real time SAR processing applications. The implementation of some of the most important modules like Fast Fourier Transformation, correlation, interpolation, and data memory is described. Finally, a short outlook on further applications of the pipeline processing concept is given. Author

N89-28912# Joint Publications Research Service, Arlington, VA.
SIMULATION OF ERS-1/OPS BY THE USE OF AIRBORNE SPECTRORADIOMETER
H. Watanabe and T. Osanai *In its* JPRS Report: Science and Technology. USSR: Space. 16th International Congress of the International Society for Photogrammetry and Remote Sensing, Volume 2 31 Jan. 1989 p 83-95 Transl. into ENGLISH from International Archives of Photogrammetry and Remote Sensing (Kyoto, Japan), v. 27, pt. B9, 1988 p 277-286 (For primary document see N89-28903 23-43)
Avail: NTIS HC A09/MF A01

Several sets of optical sensor (OPS) bands to be mounted on the Japanese Earth Resources Satellite-1 (ERS-1) were simulated and evaluated. Simulated data were produced by the use of airborne spectroradiometer (ASR) of the Geophysical Environmental Research, Inc., U.S.A. Data acquisition was conducted in Death Valley, California and in Comb Ridge, Utah. Evaluation of these simulated data contributes to the finalization of OPS specification. Ground truth using field spectrometer IRIS was also conducted to check ASR data. Author

N89-28913# Joint Publications Research Service, Arlington, VA.
NOISE REDUCTION FROM SYNTHETIC APERTURE RADAR IMAGERY **c32**
Olli Sirkia *In its* JPRS Report: Science and Technology. USSR: Space. 16th International Congress of the International Society for Photogrammetry and Remote Sensing, Volume 2 31 Jan. 1989 p 96-101 Transl. into ENGLISH from International Archives of Photogrammetry and Remote Sensing (Kyoto, Japan), v. 27, pt. B9, 1988 p 329-336 (For primary document see N89-28903 23-43)
Avail: NTIS HC A09/MF A01

The characteristic of the noise in synthetic aperture radar (SAR) images differs very much from that of more conventional digital spaceborne or airborne images. Removal of such usually high-amplitude speckle noise without losing too much high-frequency information requires at least some kind of adaptiveness from the filter. Some adaptive spatial filters are described and results of their use compared. Author

N89-28914# Joint Publications Research Service, Arlington, VA.
THE NEW GENERATION SPOT SATELLITES SPOT 4 AND 5
Michel Arnaud and Marc Leroy *In its* JPRS Report: Science and Technology. USSR: Space. 16th International Congress of the International Society for Photogrammetry and Remote Sensing, Volume 2 31 Jan. 1989 p 102-114 Transl. into ENGLISH from International Archives of Photogrammetry and Remote Sensing (Kyoto, Japan), v. 27, pt. B10, 1988 p 113-123 (For

primary document see N89-28903 23-43)
Avail: NTIS HC A09/MF A01

The main characteristics of the new generation SPOT 4 and 5 satellites, the improved version of a series of high resolution imaging remote sensing satellites constituting the SPOT family are presented. The main objective of the SPOT 4/5 mission concern: the continuity of the SPOT 1/2/3 services and products; the extension of the high resolution mission, in particular, the addition of a new band in the middle infrared region; the development of a new optical instrument called Vegetation, characterized by a wide field of view and a high radiometric resolution for the purposes of agricultural forecasts and environmental studies; the extension of the satellite life duration; the capability to offer an embarkment to new passengers; and the reorganization and development of the ground segment.
Author

N89-28915# Joint Publications Research Service, Arlington, VA.
DESIGN ASPECTS OF A SYSTEM FOR GEOCODING SATELLITE SAR IMAGES
G. Schreier, D. Kosmann, and A. Roth *In its* JPRS Report: Science and Technology. USSR: Space. 16th International Congress of the International Society for Photogrammetry and Remote Sensing, Volume 2 31 Jan. 1989 p 115-128 Transl. into ENGLISH from International Archives of Photogrammetry and Remote Sensing (Kyoto, Japan), v. 27, pt. B10, 1988 p 135-143 (For primary document see N89-28903 23-43)
Avail: NTIS HC A09/MF A01

The concepts in algorithmic design and operational use of the German Processing and Archiving Facility Geocoding System for ERS-1 are presented. The system will produce non-terrain corrected and terrain corrected products. The latter require complex algorithms in terrain height consideration and ground control pointing. This geocoding system will be implemented on UNIX workstations and programmed within an image processing system. To guarantee operational throughput and flexibility, new software tools will be implemented.
Author

N89-28916# Joint Publications Research Service, Arlington, VA.
A SURVEY OF AERIAL IMAGE QUALITY ASSESSMENT METHODS
Anders Boberg *In its* JPRS Report: Science and Technology. USSR: Space. 16th International Congress of the International Society for Photogrammetry and Remote Sensing, Volume 2 31 Jan. 1989 p 129-141 Transl. into ENGLISH from International Archives of Photogrammetry and Remote Sensing (Kyoto, Japan), v. 27, pt. B10, 1988 p 144-154 (For primary document see N89-28903 23-43)
Avail: NTIS HC A09/MF A01

The accuracy of photogrammetric mapping, as well as the reliability of image interpretation, strongly depend upon the quality of the images used. It is therefore important to assess or describe image quality. Different areas of application and various methods of evaluation imply quality demands that differ considerably. An investigation into the nature of these demands and into the differences between them is necessary as a basis for further investigations of image quality criteria. Image quality measures must be revelant with respect to subjectively experience image quality or image usefulness. At the same time the measures should be based on objective measurements of image properties. In this survey, subjective as well as objective image quality criteria are studied. Methods for evaluation of image information are investigated from an image quality point of view. Special emphasis is put on the adjustment of objective assessment methods to subjectively experience image quality with respect to certain applications.
Author

N89-28917# Joint Publications Research Service, Arlington, VA.
THE PROCESSING OF SPOT IMAGERY IN BRAZIL
Machado eSilva, Antonio Jose Ferreir dAlge, Jollo Cesar Lima Bezerra, Paulo Cesar Rego Barbosa, and Osvaldo Caldas *In its* JPRS Report: Science and Technology. USSR: Space. 16th International Congress of the International Society for Photogrammetry and Remote Sensing, Volume 2 31 Jan. 1989 p 142-150 Transl. into ENGLISH from International Archives of Photogrammetry and Remote Sensing (Kyoto, Japan), v. 27, pt. B10, 1988 p 300-307 (For primary document see N89-28903 23-43)
Avail: NTIS HC A09/MF A01

The present situation of the Brazilian SPOT Direct Receiving Station, involving both the SPOT Receiving and Recording Station and the SPOT Image Processing Center is shown. One of the main functions of the Processing Center is to perform the radiometric and geometric treatments in order to eliminate system distortions inherent to the HRV-SPOT image generation process. Nowadays, the station is capable of processing images in the 1A and 1B levels, in both digital and analog domains. In addition, new developments are being carried out for the generation of HRV-SPOT images in the levels 2A, 2, and 3, where extra information obtained from ground control points and digital terrain elevation models are used to refine the geometric system corrections.
Author

N89-28918# Joint Publications Research Service, Arlington, VA.
DATA PROCESSING AND CALIBRATION OF SAR DATA IN JAPAN
Korehiro Maeda and Hideo Sato *In its* JPRS Report: Science and Technology. USSR: Space. 16th International Congress of the International Society for Photogrammetry and Remote Sensing, Volume 2 31 Jan. 1989 p 151-163 Transl. into ENGLISH from International Archives of Photogrammetry and Remote Sensing (Kyoto, Japan), v. 27, pt. B11, 1988 p 232-241 (For primary document see N89-28903 23-43)
Avail: NTIS HC A09/MF A01

Japanese Earth Resources Satellite-1 (JERS-1) will be launched from Tanegashima Space Center, National Space Development Agency of Japan (NASDA) by an H-I rocket in February 1992. The JERS-1 has two observation systems: the synthetic aperture radar (SAR) and the optical sensor (OPS) which consists of visible, near-infrared, and short-wave infrared radiometers. In order to evaluate parameters of SAR, to develop processing and calibration methods, and to evaluate the utility of SAR data in various fields of applications, NASDA conducted the SAR-850 experiment by using variable parameter SAR mounted on Convair 580 owned by Canada Center for Remote Sensing (CCRS) during October and November, 1983 in collaboration with many research organizations. As a part of this experiment, NASDA conducted a calibration experiment in Tsukuba where several corner reflectors were set up. NASDA processed about 100 scenes of SAR-580 by newly developed autofocusing method and evaluated SAR data from various points of view. Moreover, Communications Research Laboratory (CRL) participated in the SIR-B experiment planned and conducted by JPL in collaboration with several agencies including NASDA. The outline of data processing and calibration for SAR data in Japan is presented.
Author

N89-28919# Joint Publications Research Service, Arlington, VA.
STUDIES ON OBJECT RECONSTRUCTION FROM SPACE USING THREE LINE SCANNER IMAGERY
Heinrich Ebner, Franz Muller, and Zhang Senlin *In its* JPRS Report: Science and Technology. USSR: Space. 16th International Congress of the International Society for Photogrammetry and Remote Sensing, Volume 2 31 Jan. 1989 p 164-174 Transl. into ENGLISH from International Archives of Photogrammetry and Remote Sensing (Kyoto, Japan), v. 27, pt. B11, 1988 p 242-249 (For primary document see N89-28903 23-43)
Avail: NTIS HC A09/MF A01

The capability of object reconstruction from space is investigated for two specific projects. Both of them are based on the use of three line scanner systems allowing for simultaneous digital image recording from three different angles. An efficient model for combined point determination is proposed, considering the digital image data as well as orbit information, GPS and INS observations. The resulting accuracy is estimated from project

oriented simulations. Finally the possibilities for DTM generation, orthophoto production, and stereo compilation from three line scanner imagery are discussed. Author

N89-28920# Joint Publications Research Service, Arlington, VA.
EARTH OBSERVATION PROGRAMS IN JAPAN
Tomifumi Godai *In its* JPRS Report: Science and Technology. USSR: Space. 16th International Congress of the International Society for Photogrammetry and Remote Sensing, Volume 2 31 Jan. 1989 p 175-185 Transl. into ENGLISH from International Archives of Photogrammetry and Remote Sensing (Kyoto, Japan), v. 27, pt. B11, 1988 p 434-442 (For primary document see N89-28903 23-43)
Avail: NTIS HC A09/MF A01

The history of Japanese remote sensing involvement is discussed from the initial steps through the role in the upcoming Space Station polar platform. B.G.

N89-28921# Joint Publications Research Service, Arlington, VA.
ESTIMATION OF THE SIMULATED JERS-1 DATA
T. Takemura, I. Kohno, I. Kakimoto, Kohei Arai, and Kunishige Tonoike *In its* JPRS Report: Science and Technology. USSR: Space. 16th International Congress of the International Society for Photogrammetry and Remote Sensing, Volume 2 31 Jan. 1989 p 186-193 Transl. into ENGLISH from International Archives of Photogrammetry and Remote Sensing (Kyoto, Japan), v. 27, pt. B11, 1988 p 770-777 (For primary document see N89-28903 23-43)
Avail: NTIS HC A09/MF A01

The optical sensors (OPS) borne in the Japanese Earth Resources Satellite-1 (JERS-1), which will be launched in 1992, is being watched by the world, because it has four bands in the short wave infrared region. The JERS-1 data were simulated by using the Geophysical Environmental Research Corporation (GER) 64 channel airborne imaging spectrometer (AIS) data and evaluated as a mineral exploration tool. The area studied is Goldfield, Nevada, U.S.A. Author

N89-28922# Analytic Sciences Corp., Reading, MA.
STUDY OF AN ADVANCED CIVIL EARTH REMOTE SENSING SYSTEM: EXECUTIVE SUMMARY
Arthur Bass, Steven Berner, Allen Coburn, Al. Gargiulo, Brad Meslin, Mark Oderman, and Marc Vaucher 12 Aug. 1988 22 p
(Contract MANE-8-4002)
(PB89-163208; TR-5629-1-ES; NOAA-NESDIS-89/01) Avail: NTIS HC A03/MF A01 CSCL 08B

The present and foreseeable trends in the domestic and international markets for earth remotely sensed data and value-added information products were examined. Other topics studied were 1990's technology projections for spacecraft, sensors, data management, and communications and options for substantial private investment. Two study elements examined were Market Survey and Data Processing Technology. The goal was to evaluate technical, financial and organizational options which could maximize the role of the private sector in all aspects of the development and operation of a Civil Earth Remote Sensing System (CERSS), while progressively minimizing Government support. Author

N89-28923# Oak Ridge National Lab., TN.
HIGH RESOLUTION SUBSURFACE IMAGING WITH GEOPHYSICAL DIFFRACTION TOMOGRAPHY
W. Chris King (Army Environmental Hygiene Activity, Aurora, CO.) and Alan J. Witten 1989 15 p Presented at the 3rd National Water Well Association Outdoor Action Conference, Orlando, FL, 22 May 1989
(Contract DE-AC05-84OR-21400)
(DE89-013615; CONF-8905127-4) Avail: NTIS HC A03/MF A01

This paper describes the evolution of a promising new technique for subsurface remote sensing, geophysical diffraction tomography, from its theoretical formalism to its current state as a proven field technique capable of high resolution imaging of natural and buried subsurface features. The paper begins with a brief introduction of the concept of diffraction tomography and a review of the theoretical development of a scheme for implementing diffraction tomography in a geophysical imaging technique. Next, the field procedure is described. The final topic for this paper, and its primary objective, is to present results of three recent field tests of the system. DOE

N89-28924# Washington State Univ., Pullman. Dept. of Geology.
THREE-DIMENSIONAL COMPUTER ANALYSIS AND MODELLING OF REMOTE SENSING-STRUCTURAL GEOLOGIC PROBLEMS
Richard L. Thiessen, Jay R. Eliason (Geologic Analysis and Consulting Services, Deary, ID.), and Eric R. Rieken 1989 5 p Presented at the International Geoscience and Remote Sensing Symposium, Vancouver, British Columbia, 10 Jul. 1989
(Contract DE-FG06-87ER-13796)
(DE89-010875; DOE/ER-13796/2; CONF-890768-2) Avail: NTIS HC A02/MF A01

Fault and fracture plane orientations and locations are vital for energy resource exploration and assessment, site stability evaluations, mineral exploration, earthquake hazard assessment, groundwater modelling, and basic geologic mapping. A package of Geologic Spatial Analysis (GSA) computer programs designed to determine crustal fracture geometries is being generated. Crustal structures are determined from analysis of digital data bases developed from topography, lineaments from satellite imagery and radar data bases, faults and joints observed in the field, earthquake foci, gravity, magnetics, and borehole data. The unique power of the GSA techniques being developed are their three-dimensionality; older techniques looked at orientations of structures or their surface traces, but rarely both. DOE

N89-28925# Instituto de Pesquisas Espaciais, Sao Jose dos Campos (Brazil).
IDENTIFICATION OF IRRIGATED AREAS IN THE SAO FRANCISCO VALLEY THROUGH REMOTE SENSING DATA. PILOT AREA: PETROLINA-JUAZEIRO
Sergio dosAnjos Ferr Pinto, Jose Ernesto Telles Ferrante, Mario Valerio Filho, and Francisco Bezerra Siqueira (Companhia de Desenvolvimento do Vale, Sao Francisco, Brazil) Apr. 1989 55 p In PORTUGUESE; ENGLISH summary Presented at the Technical Convention between INPE and CODEVASF
(INPE-4800-RPE/587) Avail: NTIS HC A04/MF A01

The objective was to identify, monitor and map irrigated crops using LANDSAT/Thematic Mapper (TM) data. The selected area for this study was Petrolina-Juazeiro region (northeastern Brazil). Digital and analogic products of TM data were analyzed using multispectral and multitemporal approaches. Three LANDSAT overpasses (26 July, 14 October, and 15 November 1987) were analyzed using multispectral color composites images. From this TM data evaluation, a map of distribution of irrigated croplands (to the scale 1:50,000) was obtained. Using the ground truth information, the classification accuracy estimation of the thematic map was obtained. At the significance level of 0.5 the overall map accuracy was estimated to be over 93 percent. Since only two classes are present in the thematic map (irrigated crops and non-irrigated areas), it can be assumed that this classification performance is directly related to the identification of the irrigated crops. It was concluded that the utilized methodology is adequate for the derivation of reliable thematic mapping of the irrigated crops from TM data, except for some limitations due to local context. Author

N89-28926# Los Alamos National Lab., NM. Electronics Research Group.
SIGNIFICANT IMPROVEMENT IN IR SURFACE-TEMPERATURE MEASUREMENTS
Scott D. Briles, Gloria A. Bennett, Timothy H. Larkin, and Peter Worcester (Edo Corp., Shelton, CT.) Jun. 1989 30 p
(Contract W-7405-eng-36)
(DE89-014808; LA-11525-MS) Avail: NTIS HC A03/MF A01

Obtaining infrared (IR) surface-temperature measurements of

miniature square targets on the order of 1.6 mm with a spatial resolution of 15 microns has recently become possible using the Barnes Engineering Computherm System, but the accuracy and precision of the measurements have been limited. The objective of this work is to provide a calibration procedure that will improve by a factor of 8 the accuracy and precision of the two-dimensional temperature measurement. The IR microscope detects energy emitted by the target and displays it as a radiance image. Heating the target to two known temperatures permits calculation of the target emissivity using the radiances at each pixel in the two-dimensional field. An error is induced in the emissivity calculation by substituting the thermal-well temperature for the known target surface temperature. At the same time, the radiance image is distorted by two functions that affect the measurement accuracy. The precision of the instrument is altered by a random noise field function. The noise functions were investigated to determine whether they were added to or multiplied by the radiance equation. A plot of image-radiance means shows the same trends as the added noise functions suggested by the prediction. Correction of the induced distortions improves the accuracy noticeably. Further improvement in the accuracy is accomplished by using a syringe thermocouple to measure the actual surface temperatures used for the emissivity calculations. Investigation of the random noise field shows that it is zero-mean and Gaussian in nature. We can therefore average images over time to improve the precision. DOE

N89-28927# Scripps Institution of Oceanography, La Jolla, CA.
OCEAN REMOTE SENSING AND MODELING Semiannual Progress Report No. 5, 15 Sep. 1988 - 15 Mar. 1989
James J. Simpson, Geoffrey K. Vallis, and Warren B. White 18 May 1989 14 p
(Contract N00014-86-K-0752)
(AD-A208406) Avail: NTIS HC A03/MF A01 CSCL 08/3

The performance period of 15 September 1988-15 March 1989 is covered. A set of unedited technical statements prepared by individual scientists is presented. The statements are arranged by alphabetical order and separated by index tabs. Author

N89-28928# Arkansas Univ., Fayetteville. Dept. of Geology.
MILITARY HYDROLOGY: ASSESSMENT OF SHUTTLE IMAGING RADAR AND LANDSAT IMAGERY FOR GROUND-WATER EXPLORATION IN ARID ENVIRONMENTS
Harold C. MacDonald, Brent C. Clark, Doug S. Taylor, Gregory L. Rainwater, Verne H. Kaupp, and William P. Waite Jun. 1989 89 p
(Contract DACA39-85-C-0013; DA Proj. 4A7-62719-AT-40)
(AD-A209527; WES/MP/EL-79-6-16) Avail: NTIS HC A05/MF A01 CSCL 08/8

This report provides: (1) an evaluation of suitability of LANDSAT imagery to bridge the gap between shuttle radar flight lines; (2) a discussion of the circumstances under which either remote sensor may be superior for detecting relict drainage systems; and (3) an assessment of the value of imaging radar for ground-water exploration in arid regions. The investigation indicates that relict fluvial channels initially inferred on shuttle imagery can be extended and mapped on a regional basis if the LANDSAT imagery data base is properly selected and processed. Success of military operations in such desert areas depends on the location of sufficient quantities of water to sustain the force. The utility of Shuttle Imaging Radar (SIR) and LANDSAT imagery for mapping relict fluvial channels in arid regions is therefore important to the military, particularly with the attention currently being directed toward Southwest Asia. GRA

N89-28929# Naval Postgraduate School, Monterey, CA.
DETERMINING THE LOCATION OF AN OBSERVER WITH RESPECT TO AERIAL PHOTOGRAPHS M.S. Thesis
Jill D. Wolfe Dec. 1988 81 p
(AD-A207791) Avail: NTIS HC A05/MF A01 CSCL 17/5

In this study, the possibility of using a computer to detect the motion of an observer by comparing two successive aerial photographs is examined. The purpose of the study was to experiment with a technique for finding a point common to both images. The technique presented uses only sharp boundary lines and their distribution in the images to produce the primal sketches of the image. Once the primal sketches are made, the original images are not referred to again. A point common to both images is identified by comparing the number of cells with strong gradient magnitudes and their distribution in 3-pixel by 3-pixel blocks. The technique produces excellent results in analyzing simulated successive photographs, suggesting good results with photographs that are taken in succession by a moving observer. Compared with other work on image correlation and object identification, the technique uses fewer features (only two) in its primal sketches, and it does not need any human intervention. Possible applications are photo interpretation, high-altitude navigation, and underwater station-keeping. GRA

N89-28930# Pacific Missile Test Center, Point Mugu, CA. Geophysics Div.
SATELLITE-DERIVED MOISTURE-BOGUSING PROFILES FOR THE NORTH ATLANTIC OCEAN Final Report, Jan. - Dec. 1988
Lee W. Eddington May 1989 34 p
(AD-A207829; PMTC/GSTN-145; NEPRF-CR-89-03) Avail: NTIS HC A03/MF A01 CSCL 04/2

Due to the lack of observational data over oceans, a technique was created which uses meteorological satellite image analysis to better assess the spatial distribution of moisture in the atmosphere. The technique, called moisture bogusing, has been used since the early 1970's by the National Meteorological Center (NMC) to improve their model initialization. The technique is used by assigning one of a number of previously computed vertical moisture profiles to different areas on a satellite image, gridding the analysis, and incorporating these profiles into model initialization. A set of 12 vertical profiles of relative humidity for use in satellite bogusing of moisture into numerical weather prediction model initial analysis is presented for the North Atlantic Ocean Region. The profiles are based on a satellite image cloud classification scheme applied to a concurrent data set of satellite images and upper-air soundings. Relative humidity profile composites and statistical significance tests are presented for each cloud category. Sources of error in the compositing process are discussed, and possible improvements are suggested. GRA

N89-28931# Cologne Univ. (Germany, F.R.). Inst. fuer Geophysik und Meteorologie.
ERRORS IN THE SCENE IDENTIFICATION FROM SATELLITE DATA. EFFECTS ON THE DETERMINATION OF RADIATION BUDGET PARAMETERS [FEHLER IN DER SZENENIDENTIFIKATION AUS SATELLITENDATEN - AUSWIRKUNGEN AUF DIE BESTIMMUNG VON STRAHLUNGSHAUSHALTSPARAMETERN]
Frank-Juergen Diekmann, A. Ebel, ed., F. M. Neubauer, ed., E. Raschke, ed., and P. Speth, ed. 1988 114 p In GERMAN; ENGLISH summary
(Mitt-59; ISSN-0069-5882; ETN-89-94414) Avail: NTIS HC A06/MF A01

Scene identification probability matrices were studied in order to evaluate the effects of scene identification errors on the resulting radiant fluxes. Empirical evaluations of these matrices were made by comparing results from the ERBE (Earth Radiation Budget Experiment) scene identification algorithm with AVHRR (Advanced Very High Resolution Radiometer) data. This comparison demonstrates some of the advantages and the problems of the ERBE algorithm. Estimates of the radiant flux errors due to scene misidentification show the strong dependence on the probability matrices. An approximation of the second error part due to instrument noise and uncertainties in the bidirectional and filter functions in the radiance-to-flux inversion process is given, allowing first estimates of radiant flux errors of discrete measurements. ESA

N89-28932# Technical Research Centre of Finland, Espoo. Instrument Lab.
METHODS FOR ANALYZING SAR IMAGES

Yrjo Rauste May 1989 102 p
(VTT-RR-612; ISBN-951-38-3434-4; ISSN-0358-5077;
ETN-89-95185) Copyright Avail: NTIS HC A06/MF A01;
Government Research Center, Mail Orders, P.O. 516, SF-00101
Helsinki, Finland, 62 Finnish marks

Methods for Synthetic Aperture Radar (SAR) image analysis were studied. A Seasat SAR image of a test site in northern Sweden near Arjeplog was analyzed together with a LANDSAT thematic mapper image of the same area. The SAR image was rectified using a polynomial rectification method with a digital elevation model. A backscatter anomaly map was produced. Quantitative analysis of topography-induced variation in SAR images was carried out. The separability of four land cover classes in Seasat data was studied. It is shown that the polynomial rectification using digital elevation data is well suited for applications where SAR data is merged with images from other sensors. Terrain topography can explain more than 65 percent of the total variation of SAR image in land areas. The separability of land cover classes improved with increasing incidence angle and increasing amount of speckle reduction. ESA

N89-28933# National Aerospace Lab., Amsterdam (Netherlands). Space Div.

INTEGRATING SATELLITE DATA WITH INFORMATION FROM TOPOGRAPHIC MAPS: METHOD AND APPLICATIONS

F. B. vanderLaan 12 May 1987 21 p Presented at the EARSeL General Assembly and Symposium, Noordwijkerhout, Netherlands, 4-8 May 1987 Original contains color illustrations
(NLR-MP-87035-U; ETN-89-95412) Avail: NTIS HC A03/MF A01

The capabilities of keeping topographic maps up to date, by using information from LANDSAT thematic mapper, SPOT panchromatic and SPOT MSS imagery (from 1986), are investigated. A method, for combining topographic information with satellite information, is developed. The optimum product is useful for visual updating of topographic maps of scale 1:50,000. Line information from the topographic map dating from 1977 is used. The method promises to be capable of improving the accuracy of extracting information from satellite imagery. The use of topographic information as a mask for stratification of a region, in preparation for a classification procedure, can help to improve the accuracy (at present 70 to 80 percent on the average) to over 95 percent. Remote sensing information is potentially acceptable for practical use. ESA

N89-28934# National Aerospace Lab., Amsterdam (Netherlands). Informatics Div.

THE USE OF EXPERT SYSTEMS FOR PREPROCESSING IMAGE DATA

B. v.d.Moezel and T. P. Zijsling 1 Jan. 1988 10 p Presented at the SPIE Symposium on Applications of Artificial Intelligence, Orlando, FL, 4-6 Apr. 1988
(NLR-MP-88009-U; ETN-89-95415) Avail: NTIS HC A02/MF A01

The expert system to assist users in selecting the best signal processing algorithms (with respect to sensor and uses of the data under consideration) is discussed. The first experiences with this system are shown. The results lead to the conclusion that it is necessary to combine human and technical resources, in solving problems related to the development and application of a multitude of sensors. The combination in this case concerns airplane operation, electronics design, remote sensing expertises and aspects of informatics. The complexity of such systems requires the application of artificial intelligence techniques. The development of the prototype shows the feasibility to build intelligent user interfaces, by using an expert system tool to combine expertise from a number of disciplines with other programming tools. ESA

N89-28935# National Aerospace Lab., Amsterdam (Netherlands). Space Div.

IMPROVEMENT OF CLASSIFICATION RESULTS OF SATELLITE IMAGERY USING CONTEXT INFORMATION FROM A TOPOGRAPHIC MAP

F. B. vanderLaan 11 Apr. 1988 20 p Presented at the International Society of Photogrammetry and Remote Sensing Conference, Kyoto, Japan, Jul. 1988 Original contains color illustrations
(NLR-MP-88020-U; ETN-89-95417) Avail: NTIS HC A03/MF A01

The possibilities of using LANDSAT thematic mapper images, for updating land use information on topographic maps, are described. The results provide a forecast of landscape dynamics based on the map and satellite information. The reliability of the information obtained (in 1986) from satellite images is improved by over 95 percent, by using the topographic information from 1980 as a point-by-point reference. The method allows the identification of a large number of additional classes and provides quantitative insight into the dynamics of landscape change. Remote sensing information can be applied in physical planning, wherever topographic maps permit the extraction of land-use information. The next step of the study is the verification of the results on the basis of aerial photographs. ESA

N89-28936# National Aerospace Lab., Amsterdam (Netherlands). Space Div.

UPDATING LAND-USE INFORMATION ON TOPOGRAPHIC MAPS USING SATELLITE IMAGERY: COMBINING THE ADVANTAGES OF TWO ACCESSIBLE SOURCES OF GEOGRAPHIC INFORMATION

F. B. vanderLaan and P. G. Meijer 11 May 1988 9 p Presented at the IGARSS 88 Conference on Remote Sensing: Moving Towards the 21st Century, Edinburgh, Scotland, 12-16 Sep. 1988 Previously announced as N89-18897
(NLR-MP-88030-U; ETN-89-95420) Avail: NTIS HC A02/MF A01

The possibilities of using LANDSAT thematic mapper images, for updating land use information on topographic maps, are examined. The reliability (40 to 90 percent) of the satellite images is improved, by using digitized land use information from a topographic map as a source of contest information. Verification using 1:18,000 scale aerial photographs and field data showed the results to have a reliability of over 95 percent. It can be expected that whereever topographic maps permit the extraction of land use information in a similar way as described, remote sensing information meets operational accuracy requirements for application in physical planning, map updating, and land-use planning. The method allowed the identification of a large number of additional classes and provided quantitative insight into the dynamics of landscape change. ESA

N89-28937# International Inst. for Aerial Survey and Earth Sciences, Enschede (Netherlands).

MONITORING AND MEASURING HUMAN SETTLEMENT CHANGES BY REMOTE SENSING METHODS

V. F. L. Polle, M. Juppenlatz, T. Lukman Aziz, Bobby SantosoD., Ishak H. Ismullah, D. Muhally Hakim, Irawan Sumarto, Saptomo HandoroM., Bambang Edhi Leksono, and Hassan Poerbo (Bandung Inst. of Tech., Indonesia) et al Dec. 1988 63 p Sponsored by Beleidcommissie Remote Sensing, Delft, Netherlands Original contains color illustrations
(BCRS-88-16C; ETN-89-95475) Avail: NTIS HC A04/MF A01

The results of the research done with SPOT images, from the city of Bandung in Indonesia, are reported. Sirphoto coverage of Bandung was also avaiable. Two typical new urban developments are studied: one residential area and one industrial area. Experiments with 18 interpreters are carried out to interpret the urban boundary. This study of a SPOT false color composite image scale 1:50,000 is supported by a reconnaissance fieldwork in Baundung. The identification of expansion of the urban area is good enough to make possible the planning of small format aerial photographic missions for map updating. Further research on the interpretation techniques, with the materials already collected, is proposed. Research on delineating the urban area of Bandung started in the second half of January 1988. ESA

N89-28938# Beleidscommie Remote Sensing, Delft (Netherlands).
TRAINING COURSE FOR TROPICAL EARTH RESOURCES SATELLITE (EARS) BRIDGING PHASE Final Report
Dec. 1988 93 p Course held in Bandar, Lampung, Indonesia, 7-12 Dec. 1987 Prepared in cooperation with EUROCONSULT, B.V., Arnhem, Netherlands Original contains color illustrations
(Contract BCRS-Proj-4533/TO-3.13)
(BCRS-88-16D; ETN-89-95476) Avail: NTIS HC A05/MF A01

A training course, held by Euroconsult in Indonesia, for the counterparts of the Rawa Sragi project, is reported. This project is part of the Tropical Earth Resources Satellite (TERS) bridging phase. The objective of the course was to train these counterparts in remote sensing techniques in order to awaken a latent demand for satellite imagery of the TERS type. The majority of the participiants are connected to the regional planning bureau and data center of the regional planning office. For simulation of TERS imagery, multispectral SPOT scenes of the project are acquired. The course was held from 7 to 12 December 1987 in Bandar, Lampung. The course included lectures on remote sensing techniques, and on the interpretation of satellite images for which purpose field studies were included. It was concluded that without the use of remote sensing, a survey covering the same area would take much more time and produce less accurate results. The best option for remote sensing is LANDSAT imagery with a resolution that matched the mapping scale of the project. The most cost-effective way of processing multispectral satellite imagery is the Diazo method. Remote sensing imagery has a higher interpretation potential in lowlands than in uplands. ESA

N89-28939# Beleidscommie Remote Sensing, Delft (Netherlands).
MARKETING AND CASE STUDY OF SATELLITE THEMATIC MAPS AND OTHER PRODUCTS OF SATELLITE REMOTE SENSING Final Report
Cendekia Jasa Ihe Dec. 1988 27 p Prepared in cooperation with DHV Raadgevend Ingenieurs Bureau B.V., Amersfoot, Netherlands Original contains color illustrations
(Contract BCRS-Proj-4533/TO-3.13)
(BCRS-55-16E; ETN-89-95477) Avail: NITS HC A03/MF A01

The project of marketing for satellite thematic maps in Indonesia is presented. The interest in high resolution satellite data arises from the feeling that traditional data collection systems, which are partly based on ground observations and partly on aerial photographs, are no longer satisfactory. Conclusions on the commercial and technical prospects for products derived from Tropical Earth Resources Satellite (TERS) data, are drawn. The study of the Cirebon area of West Java is reported. It was concluded that basic information on land use is lacking. It also became clear that there is limited experience and expertise in high resolution sateliite image interpretation in Indonesia. The cost effectiveness of this type of mapping depends in part on the extent to which the requirements of the user are met. An efficient procedure for land use mapping may be found in a combination of satellite data, existing aerial photography and additional data collection on the ground. Not all land use information that is required by the different potential users can be obtained exclusively from remote sensing imagery. ESA

N89-28940# Technische Univ., Delft (Netherlands). Faculty of Aerospace Engineering.
RESULTS OF SEASAT ALTIMETER DATA PROCESSING FOR THE NORTHEAST ATLANTIC Final Report
G. H. M. vanGeldorp, D. Oskam, and K. F. Wakker May 1989 75 p Original contains color illustrations
(Contract BCRS-Proj-3104/TO-1.4)
(BCRS-89-05; ETN-89-95486) Avail: NTIS HC A04/MF A01

The processing of satellite altimeter data for the determination of the mean sea surface and the detection of mesoscale sea surface variability is analyzed. The study is performed with data collected from September 1986 to August 1988. The analysis of the spectrum of satellite radial orbit errors and the development of optimal computational techniques for the processing of global altimeter data from two or more satellites simultaneously, is considered. The technique of measuring the mean sea surface variability, by processing altimeter data acquired along collinear tracks is discussed. The results of the application of the crossover difference residuals minimization concept to all Seasat altimeter data, taken over a 750 km by 770 km area in northeast Atlantic, are given. The techniques described are capable of measuring the marine geoid and of detecting variabilities of the mean sea surface, despite relatively large errors in the satellite orbit. It is shown that tide model errors seriously hamper the application of these techniques close to land areas. The major goal of satellite altimetry (the detection of the global ocean circulation) cannot yet be realized due to the relatively large errors in the available marine geoid models. ESA

N89-28941# Technische Univ., Delft (Netherlands). Faculty of Electrical Engineering, Telecommunication and Remote Sensing Technology.
ATMOSPHERIC INFLUENCE ON MICROWAVE REMOTE SENSING AT DIFFERENT FREQUENCIES: RESULTS OF THE 1ST SEPTEMBER 1987 DUSCAT FLIGHT Final Report
L. Krul, P. Snoeij, and P. J. F. Swart May 1989 19 p
(Contract BCRS-Proj-4451/TE-1.8)
(BCRS-89-07; ETN-89-95487) Avail: NTIS HC A03/MF A01

The results of a scatterometer flight held on 1 September 1987 during the Agriscatt-87 campaign are discussed. An experimental verification and extension of knowledge concerning the atmospheric influence on the propagation of microwave signals at different frequencies is reported. The comparison of data from the three different flights using normalized radar cross section values is included. The absolute calibration of these values using a passive corner reflector set-up is shown. The results do not have the required accuracy to extract the atmospheric induced differences. The flight requirements for this external calibration are not compatible with the atmospheric measurement requirements. The acquisition of external calibration data is useful and enables comparison with other (Agriscatt-87) experiment results. The inherent shortcoming of absolute calibration accuracy comparison is based on relative calibration only. Due to uncertainties in the internal calibration accuracy of the DUTSCAT instrument it was decided after the first flight to hold up the project. To date, the lack of sufficient internal calibration accuracy is recognized and improvements are studied and implemented. ESA

N89-28942# Deutsche Forschungs- und Versuchsanstalt fuer Luft- und Raumfahrt, Oberpfaffenhofen (West Germany). Abteilung Hochfrequenzsysteme.
THE ARCHIMEDES 2a EXPERIMENT ON OIL SLICK DECTION OVER THE NORTH SEA, APRIL 1988: MEASUREMENT RESULTS OBTAINED BY THE E-SAR SYSTEM OF THE AEROSPACE RESEARCH ESTABLISHMENT
Ralf Horn and Alberto Moreira Feb. 1989 46 p
(DFVLR-MITT-89-08; ISSN-0176-7739; ETN-89-95299) Avail: NTIS HC A03/MF A01; DFVLR, VB-PL-DO, Postfach 90 60 58, 5000 Cologne, Fed. Republic of Germany, 18.50 DM

The results of the Archimedes 2a experiment on oil slick detection over the North Sea obtained by the experimental airborne SAR System E-SAR (synthetic aperture radar) are presented. This system is part of the research program at the Institute for Radio Frequency Technology of the German Aerospace Research Establishment. During the experiment carried out on 21 April 1988 the system was operated in L-band at 1.29 GHz. The report discusses briefly some problems with oil slick detection by SAR. It gives an overview of the E-SAR system configuration and system performance. SAR data and image processing procedures are described as well. SAR images of an oil slick of 5 cubic meters of crude oil and corresponding image analysis results are presented. ESA

N89-28943# Deutsche Forschungs- und Versuchsanstalt fuer Luft- und Raumfahrt, Oberpfaffenhofen (West Germany). Abteilung Planetare Erkundung.
MODELING OF SHORT ARC ORBITAL CONSTRAINTS FOR INCORPORATION INTO PHOTOGRAMMETRIC ADJUSTMENT OF MEOSS DATA
Hiroshi Masaharu Feb. 1989 52 p
(DFVLR-FB-89-14; ISSN-0171-1342; ETN-89-95310) Avail: NTIS HC A04/MF A01; DFVLR, VB-PL-DO, Postfach 90 60 58, 5000 Cologne, Fed. Republic of Germany, 19 DM

Two kinds of models were studied by least square fitting method to simulate satellite position and velocity data of the MEOSS/SROSS mission (circular orbit of 450 km height over Hyderabad, India). In the first model, the time variations of instantaneous Keplerian elements (osculating Keplerian elements) are expressed as polynomials of time. In the second model, the differences of geocentric coordinates from a nominal orbit are treated as polynomials of time. Both methods have shown enough accuracy by second or third order polynomials. The root means square errors of position for an orbit arc of 600 s/4600 km length were well below 50 m, the pixel size of the MEOSS image. The second method is recommended for orbital constraints of photogrammetric adjustment because of its simplicity and numerical stability. The fitting test results are summarized. The selection between an Earth co-rotating or inertial space coordinate system is discussed. Related problems concernig photogrammetric adjustment of spaceborne imagery is outlined. ESA

44 ENERGY PRODUCTION AND CONVERSION

Includes specific energy conversion systems, e.g., fuel cells; global sources of energy; geophysical conversion; and windpower.

For related information see also *07 Aircraft Propulsion and Power, 20 Spacecraft Propulsion and Power,* and *28 Propellants and Fuels.*

N89-28944# Delaware Univ., Newark. Inst. of Energy Conversion.
MATERIALS ANALYSIS AND DEVICE OPTIMIZATION OF CuInSe2 SOLAR CELLS Annual Report, 16 Jan. 1987 - 15 Jan. 1988
R. W. Birkmire, J. E. Phillips, and W. N. Shafarman Jun. 1989 75 p Prepared for Midwest Research Inst., Golden, CO
(Contracts DE-AC02-83CH-10093; XL-7-06031-5)
(DE89-009434; SERI/STR-211-3523) Avail: NTIS HC A04/MF A01

This report presents results and conclusions from the first year of research on CuInSe sub 2 thin-film solar cells. The research was carried out in two tasks: materials preparation and analysis and high-efficiency solar cell fabrication and analysis. CuInSe sub 2 thin films were prepared by vacuum evaporation of elemental Cu, In, and Se onto heated substrates. Systematic studies of the effects of incident flux and substrate temperature on CuInSe sub 2 film composition and morphology are presented. Mirror-smooth CuInSe sub 2 films were prepared using a newly developed aqueous bromine solution as chemical polishing etch. Heterojunctions photovoltaic devices with (CdZn)S, ITO/(CdZn)S, ZnO, and ZnO/(CdZn)S window layers were fabricated and analyzed. The dominant recombination mechanism in high-efficiency CuInSe sub 2 devices was found to be space-charge recombination in the CuInSe sub 2. Optimized one-square-centimeter CuInSe sub 2/(CdZn)S solar cells with efficiencies greater than 10 percent were fabricated. DOE

N89-28945# Ametek, Inc., Harleysville, PA.
POLYCRYSTALLINE CADMIUM TELLURIDE 3N-I-P SOLAR CELL Annual Report, 1 Jun. 1987 - 31 Aug. 1988
P. V. Meyers Jun. 1989 67 p Prepared for Midwest Research Inst., Golden, CO
(Contract DE-AC02-83CH-10093)
(DE89-009437; SERI/STR-211-3519) Avail: NTIS HC A04/MF A01

The CdS/CdTe/ZnTe n-i-p solar cell and its ternary relatives have the potential to meet Department of Energy cost, efficiency, and stability goals. This report describes results of a continuing program to achieve these goals. A record-breaking efficiency of 11 percent has been demonstrated and verified at the Solar Energy Research Institute (SERI). Stability testing for 3000 hours indicates that the n-i-p structure is stable. Improving the short-circuit current by substituting Cd/sub x/Zn/sub 1-x/S for CdS has been successful and has produced 8 plus percent efficient cells with 2.6 eV windows using improved pyrolysis equipment. Transparent n-i-p devices have been produced with a SERI-verified efficiency of 9.4 percent . Collaborations with researchers at the Georgia Institute of Technology, the Institute of Energy Conversion, and Jet Propulsion Laboratory have resulted in jointly produced n-i-p cells. Cells produced by molecular beam epitaxy and metal organic chemical vapor deposition had efficiencies greater than 9 percent; cells produced by thermal vacuum evaporation had efficiencies greater than 7 percent. DOE

N89-28946# Chronar Corp., Princeton, NJ.
RESEARCH ON STABLE, HIGH-EFFICIENCY, LARGE-AREA, AMORPHOUS-SILICON-BASED SUBMODULES, TASK B Semiannual Report, 16 Mar. 1988 - 15 Sep. 1988
A. E. Delahoy and F. J. Kampas Jun. 1989 59 p Prepared for Midwest Research Inst., Golden, CO
(Contracts DE-AC02-83CH-10093; ZB-7-06003-1)
(DE89-009439; SERI/STR-211-3528-Task-B) Avail: NTIS HC A04/MF A01

This research concerns the improvement of the efficiency and stability of large-area amorphous silicon photovoltaic submodules, based on both single- and tandem-junction device structures. For the improvement of cell efficiency, carbon-graded a-Si(x)C(1-x):H p-layers, ITO/Ag back reflectors, alternate SnO2 substrates, and TiO(x) recombination layers at the n/p interface of tandem cells are described. Significant contributions to the study of transport and defect states in a-Si:H were made using the steady-state photocarrier grating technique, charge collection in thick p-i-n structures, thermally stimulated currents, and current DLTS. An extensive study of the deposition of SiO2 barrier layers on soda lime glass to improve SnO2:F conductivity is reported. Submodule research includes laser isolation, active scribe tracking, post-fabrication defect removal, and a new interconnect scheme employing two levels of metallization. Power output and aperture area efficiency for single junction submodules were 5.9W (7.0 percent) for 1 x 1 sq. ft. and 17.7W (6.9 percent) for 1 x 3 sq. ft. Outdoor stability tests on glass-glass encapsulated tandem submodules are also described. DOE

N89-28947# Midwest Research Inst., Golden, CO. Solar Energy Research Inst.
SOLAR THERMAL PROGRAM SUMMARY. VOLUME 2: RESEARCH SUMMARIES, FISCAL YEAR 1988
May 1989 84 p
(Contract DE-AC02-83CH-10093)
(DE89-000861; DOE/CH-10093/46) Avail: NTIS HC A04/MF A01

The Solar Thermal Program Summary for Fiscal Year 1988 is a two-volume reference set describing the technological advances and future research and development (R and D) direction of the Solar Thermal Technology Program. Volume 1 contains capsule descriptions of the various activities undertaken in the year, a brief history of the program, and the significant accomplishments realized. It also describes the management framework for the program and sets forth the FY-88 budget. Volume 2 consists mainly of a compilation of detailed descriptions of the various research and development activities performed by the national laboratories and their subcontractors from industry, academia, and nonprofit research institutions. It also contains a bibliography of the various publications produced under the program in recent years. DOE

N89-28948# Midwest Research Inst., Golden, CO. Solar Energy Research Inst.
PHOTOVOLTAICS ADVANCED RESEARCH AND DEVELOPMENT
1989 135 p Presented at the 9th SERI Review Meeting, Lakewood, CO, 24 May 1989
(Contract DE-AC02-83CH-10093)
(DE89-000895; SERI/CP-213-3495; CONF-890533-Absts) Avail: NTIS HC A07/MF A01

A list of abstracts of papers presented at the conference is presented. Topics covered include: thin film technology; fundamental research; and measurement and characterization techniques. DOE

N89-28949# San Diego State Univ., CA. Dept. of Physics.
DEVELOPMENT OF A CARBONACEOUS SELECTIVE ABSORBER FOR SOLAR THERMAL ENERGY COLLECTION AND PROCESS FOR ITS FORMATION Final Report
John D. Garrison 25 Feb. 1989 23 p
(Contract DE-FG01-86CE-15289)
(DE89-008587; DOE/CE-15289/T1) Avail: NTIS HC A03/MF A01

The main goal of the US Department of Energy supported part of this project is to develop information about controlling the complicated chemical processes involved in the formation of a carbonaceous selective absorber and learn what equipment will allow production of this absorber commercially. The work necessary to accomplish this goal is not yet complete. Formation of the carbonaceous selective absorber in the conveyor oven tried so far has been unsatisfactory, because the proper conditions for applying the carbonaceous coating in each conveyor oven fabricated, either have been difficult to obtain, or have been difficult to maintain over an extended period of time. A new conveyor oven is nearing completion which is expected to allow formation of the carbonaceous selective absorber on absorber tubes in a continuous operation over many days without the necessity of cleaning the conveyor oven or changing the thickness of the electroplated nickel catalyst to compensate for changes in the coating environment in the oven. Work under this project concerned with forming and sealing glass panels to test ideas on evacuated glass solar collector designs and production have been generally quite satisfactory. Delays in completion of the selective absorber work, has caused postponement of the fabrication of a small prototype evacuated glass solar collector panel. Preliminary cost estimates of the selective absorber and solar collector panel indicate that this collector system should be lower in cost than evacuated solar collectors now on the market. DOE

N89-28950# Midwest Research Inst., Golden, CO. Solar Energy Research Inst.
TWO-TERMINAL CuInSe-BASED CASCADE CELLS Annual Subcontract Report, 16 Jan. 1987 - 15 Jan. 1988
R. W. Birkmire, B. E. McCandless, and J. E. Phillips (Delaware Univ., Newark.) May 1989 37 p
(Contract DE-AC02-83CH-10093)
(DE89-009422; SERI/STR-211-3511) Avail: NTIS HC A03/MF A01

Results and conclusions from the first year of a two year research program on multijunction thin film solar cells utilizing a CuInSe2 heterojunction for the low band gap (E sub g = 1.8 eV) or a CdTe (E sub g = 1.5 eV) heterojunction for the high band gap component in a monolithic two terminal cascade structure are reported. Physical vapor deposition with extrinsic doping was studied as a preparation technique for depositing low resistivity p-type CdTe on transparent ohmic contact materials at low temperature (T less than 300 C). Photochemical vapor deposition was used to deposit a-Si cells. The presence of a CuInSe2/(CdZn)S cell in the a-Si deposition reactor did not introduce contaminants or adversely affect the performance of conventional p-i-n cells. Procedures for fabricating monolithic cascade structures devices having the configuration ITO/a-Si(n-i-p)/ZnO (CdZn)S/CuInSe2/Mo/glass were developed. A prototype two terminal cascade structure had an open circuit voltage over 1 volt. DOE

N89-28951# California Univ., Berkeley. Lawrence Berkeley Lab. Applied Science Div.
FUEL CELL TECHNOLOGY IN THE UNITED STATES
Kim Kinoshita Apr. 1989 31 p Presented at the Seminar At Paul Scherrer Institute, Wurenlingen, Switzerland, 29 May 1989
(Contract DE-AC03-76SF-00098)
(DE89-013430; LBL-27082; CONF-8905164-1) Avail: NTIS HC A03/MF A01

Fuel cells provide a new and exciting option for the efficient conversion of fossil fuels to electricity. Development of fuel- cell technology was underway in the United States (U.S.) for over 20 years, with the initial focus on space application (i.e., Gemini, Apollo). More recently, commercialization of fuel cells for utility power generation and transportation applications has received considerable attention in the U.S. The status of fuel-cell technology is summarized for the U.S., where development of five major fuel cell systems are underway. DOE

N89-28952# Sandia National Labs., Albuquerque, NM.
DAMAGE PREDICTIONS FOR WIND TURBINE COMPONENTS USING THE LIFE2 COMPUTER CODE
Herbert J. Sutherland 1989 6 p Presented at the European Wind Energy Conference and Exhibition, Glasgow, Scotland, 10 Jul. 1989
(Contract DE-AC04-76DP-00789)
(DE89-013813; SAND-88-3057C; CONF-890717-1) Avail: NTIS HC A02/MF A01

The LIFE2 computer code is a fatigue/fracture analysis code that is specialized to the analysis of wind turbine components. It is a PC-compatible FORTRAN code that is written in a top-down modular format. The service lifetime of a component can be divided into three phases: crack initiation, growth and coalescence of micro-cracks and growth of a macro-crack. In the LIFE2 formulation, a S-n fatigue analysis is used to describe the first two phases and a linear, da/dn fracture analysis is used to describe the third phase. The code is divided into five main sections. The first four describe the wind resource, the constitutive properties of the turbine material, the stress state in which the turbine operates and operational parameters for the turbine system. The fifth uses the data files written by the first four sections to calculate the service lifetime of a turbine component. In addition to the main sections, auxiliary sections are included to permit the storage of data and code calculations and to permit the plotting of results. This report describes the computational framework used in the LIFE2 code to evaluate the damage rules cited above. An example problem is presented here to illustrate the capabilities of the code. DOE

N89-28953# Science Applications International Corp., San Diego, CA. Energy Projects Div.
AN IMPROVED DESIGN FOR STRETCHED-MEMBRANE HELIOSTATS
Kelly Beninga, Barry Butler, Jeff Sandubrae, and Kerry Walcott Jun. 1989 184 p
(Contracts DE-AC04-76DP-00789; SAND-33-1226)
(DE89-013872; SAND-89-7027) Avail: NTIS HC A09/MF A01

Science Applications International Corporation (SAIC) has developed an improved stretched-membrane heliostat mirror module under contract to Sandia National Laboratories, Albuquerque, New Mexico. Both a 150 sq. meter commercial mirror module and a 50 sq. meter prototype mirror module have been designed. The prototype mirror module has been fabricated and is being tested at the Central Receiver Test Facility (CRTF) in Albuquerque. Two .0762-mm (.003-in) thick stainless steel membranes are stressed to approximately 90 MPa (13,000 psi) and welded to either side of a carbon steel, rectangular cross-section ring, which is compressed to approximately one-tenth of its yield strength. The ring is supported by five trusses, which radiate from a central hub. The mirror module is mounted on a conventional pedestal drive system for sun-tracking purposes. The mirror module is air-tight, and focusing is achieved by modulating

the position of the back membrane. The ring stiffness and tolerance achievable by conventional manufacturing methods dictate the ring distortions prior to installation of the mirror module. Once the mirror module is installed, wind loads on the heliostat exert additional out-of-plane loads. A comprehensive finite-element computer model of the mirror module was used for the structural design of the ring/membrane system and truss supports. DOE

N89-28954# Lawrence Livermore National Lab., CA.
ENERGY AND TECHNOLOGY REVIEW
Andrew J. Poggio, ed. and Brian H. Mayall, ed. Apr. 1989 32 p
(Contract W-7405-eng-48)
(DE89-013919; UCRL-52000-89-4) Avail: NTIS HC A03/MF A01

The Lawrence Livermore National Laboratory (LLNL) is an acknowledged world center for analytical cytology. This leadership was recognized by the Regents of the University of California (UC), who in 1982 established and funded the Program for Analytical Cytology to facilitate the transfer of this technology from scientists at LLNL to their University colleagues, primarily through innovative collaborative research. This issue of Energy and Technology Review describes three of the forty projects that have been funded in this way, chosen to illustrate the potential medical application of the research. Analytical cytology is a relatively new field of biomedical research that is increasingly being applied in clinical medicine. It has been particularly important in unraveling the complexities of the human immune system and in quantifying the pathobiology of malignancy. Defined as the characterization and measurement of cells and cellular constituents for biological and medical purposes, analytical cytology bridges the gap between the quantitative discipline of molecular biology and the more qualitative disciplines of anatomy and pathology. It is itself multidisciplinary in nature. Two major approaches to analytical cytology are flow cytometry and image cytometry. In each of these research techniques, cells are measured one at a time in an automated device. In flow instruments, the cells are dispersed in fluid suspension and pass in single file through a beam of laser light to generate optical signals that are measured. In image cytometry, cells are dispersed on a slide and are imaged through a microscope onto an electronic imaging and analysis system that processes the cell image to extract measurements of interest. DOE

N89-28955# Oak Ridge National Lab., TN.
ENERGY TECHNOLOGY R AND D: WHAT COULD MAKE A DIFFERENCE. A STUDY BY THE STAFF OF THE OAK RIDGE NATIONAL LABORATORY. PART 1: SYNTHESIS REPORT, VOLUME 1
William Fulkerson, Stanley I. Auerbach, Alan T. Crane, Don E. Kash (Oklahoma Univ., Norman.), Alfred M. Bud Perry, David B. Reister, and Charles W. Hagan, Jr., ed. May 1989 184 p
(Contract DE-AC05-84OR-21400)
(DE89-014568; ORNL-6541/V1-Pt-1) Avail: NTIS HC A09/MF A01

Both energy technologies and crosscutting areas of science and technology were surveyed in order to identify important R and D needs and opportunities in the context of the US and world energy situations. The imperative for R and D was judged against its potential for fixing current energy system problems; for providing a robust set of options for coping with, taking advantage of, or encouraging future energy circumstances; and for creating unanticipated opportunities. DOE

N89-28956# Midwest Research Inst., Golden, CO. Solar Energy Research Inst.
THIN FILM PHOTOVOLTAICS
K. Zweibel and H. S. Ullal May 1989 9 p Presented at the 24th Intersociety Energy Conversion Engineering Conference, Washington, DC, 6-11 Aug. 1989
(Contract DE-AC02-83CH-10093)
(DE89-009425; SERI/TP-211-3501; CONF-890815-4) Avail: NTIS HC A02/MF A01

Thin films are considered a potentially attractive technological approach to making cost effective electricity by photovoltaics. Over the last 20 years, many have been investigated and some (cadmium telluride, copper indium diselenide, amorphous silicon) have become leading candidates for future large scale commercialization. The past development of these key thin films are surveyed and their status and future prospects are given. In all cases, significant progress toward cost effective PV electricity has been made. If this progress continues, it appears that thin film PV could provide electricity that is competitive for summer daytime peaking power requirements by the middle of the 1990s; and electricity in a range that is competitive with fossil fuel costs (i.e., 6 cents/kw-hr) should be available from PV around the turn of the century. DOE

N89-28957# Argonne National Lab., IL.
MATERIAL AND FABRICATION CHALLENGES IN THE DEVELOPMENT OF MONOLITHIC SOLID OXIDE FUEL CELLS
U. Balachandran, S. E. Dorris, J. J. Picciolo, R. B. Poeppel, C. C. McPheeters, and N. Q. Minh (Allied-Signal Aerospace Co., Torrance, CA.) 1989 26 p Presented at the 24th Intersociety Energy Conversion Engineering Conference, Washington, DC, 6-11 Aug. 1989 Submitted for publication Sponsored in part by Gas Research Inst.
(Contract W-31-109-eng-38)
(DE89-012422; CONF-890815-5) Avail: NTIS HC A03/MF A01

Monolithic solid oxide fuel cells (MSOFCs) are presently under development for a variety of practical applications (e.g., advanced space and aerospace power systems, electric utility power generation). The MSOFC is composed of a honeycomb of very small cells of 1 to 2 mm in diameter. The walls of the honeycomb are formed from thin (25 to 100 mm) ceramic layers of cell components: cathode (Sr-doped LaMnO3), anode (Ni/Y2O3-ZrO2 cermet), electrolyte (Y2O3-stabilized ZrO2), and interconnect (doped LaCrO3) materials. These walls form the passages for fuel and oxidant gases. The MSOFC will convert hydrogen or hydrocarbon fuels to dc power at more than 50 percent efficiency and can achieve considerably higher energy densities than many other technologies. Successful fabrication of an MSOFC depends on incorporating the materials into a self-supporting structure at a higher sintering temperature. A fabrication scheme for the MSOFC must incorporate each material such that no conditions of any fabrication step will destroy desired material characteristics of any of the component layers. Material characteristics and processing parameters must be tailored and controlled to fabricate the MSOFC with desired properties. Material properties, material requirements, and fabrication issues in the development of the MSOFC are discussed. DOE

N89-28958# Sandia National Labs., Albuquerque, NM.
FIELD TESTS OF A NOVEL INVERTER FOR PHOTOVOLTAIC POWER CONDITIONING
Art Dickerson, Ward Bower, and Frank Schalles (EG and G Washington Analytical Services Center, Inc., Albuquerque, NM.) May 1989 61 p
(Contract DE-AC04-76DP-00789)
(DE89-014322; SAND-88-2974) Avail: NTIS HC A04/MF A01

The Dickerson inverter synthesizes a sinewave current from a photovoltaic array that is segmented into a number of subarrays. These subarrays are switched among the ac phases so that the current from a given subarray is continuous, and each phase is connected at all times to one or more subarrays. The control scheme assures a near-unity power factor current with real-time phase adjustment to power-system disturbances. A prototype inverter was operated into a three-phase power system, with the dc supplied by a photovoltaic array at Sandia National Laboratories. The results of these tests under normal, abnormal and fault conditions are reported. Inversion efficiencies up to 99 percent were achieved with 0.97 power factor. A simple filter reduced current harmonics from 18 to 5 percent. The performance for the inverter was projected for a 480-V, three-phase system at the 50-kVA level. An analysis of filtering costs indicates that harmonic reduction to 5 percent can be achieved at under $0.003 per watt for typical central-station applications. The intended power range

for these inverters is 50-250 kVA. The cost to produce the inverter at the 50-kVA level in quantities of 1000 units is estimated to be $0.05 per watt, which is less than the projected cost of other 50-kVA inverters. DOE

N89-28959# Aeronautical Research Inst. of Sweden, Stockholm. Aerodynamics Dept.
COMPARISON BETWEEN TWO DIFFERENT TECHNIQUES OF COMPUTING THE AXIAL INDUCTION FOR HORIZONTAL AXIS WIND TURBINES IN A LOCALLY DEFORMED FLOW FIELD
Goeran Ronsten Nov. 1988 81 p Sponsored by the Swedish National Energy Administration
(FFA-TN-1986-56; ETN-89-94943) Avail: NTIS HC A05/MF A01

A comparison between a fast two dimensional method and lengthy three dimensional methods is presented. The analysis results in correction functions to be applied to the former method. The time and cost advantage of the simple method is retained and at the same time three dimensional effects are accounted for. ESA

45 ENVIRONMENT POLLUTION

Includes atmospheric, noise, thermal, and water pollution.

N89-28960# California State Air Resources Board, Sacramento. Technical Support Div.
OZONE TRENDS WITHIN A LARGE METROPOLITAN AREA: THE LOS ANGELES BASIN
Terry McGuire May 1988 20 p
(PB89-145965; ARB/TSD-88-008) Avail: NTIS HC A03/MF A01 CSCL 13B

Trends are reviewed in ambient ozone concentrations in the Los Angeles Basin from 1955. Most emphasis is placed on data acquired since 1973. Temperature adjustment is used as a tool to reduce year-to-year ozone fluctuations. Trends of emissions of hydrocarbons and nitrogen oxides are also examined. In general, the trend in ambient ozone concentrations have been improving, but some periods during the record and some locations in the basin have experienced increases. Decided differences in ozone concentrations and trends are evident for different geographic parts of the basin. Author

N89-28961*# State Univ. of New York, Albany. Atmospheric Sciences Research Center.
DAYTIME TURBULENT EXCHANGE BETWEEN THE AMAZON FOREST AND THE ATMOSPHERE
David R. Fitzjarrald, Kathleen E. Moore, Osvaldo M. R. Cabral, Jose Scolar, Antonio O. Manzi, and Leonardo D. deAbreuSa (Instituto de Pesquisas Espaciais, Sao Jose dos Campos, Brazil) 19 May 1989 99 p
(Grant NAG1-692)
(NASA-CR-185487; NAS 1.26:185487) Avail: NTIS HC A05/MF A01 CSCL 13B

Detailed observations of turbulence just above and below the crown of the Amazon rain forest during the wet season are presented. The forest canopy is shown to remove high frequency turbulent fluctuations while passing lower frequencies. Filter characteristics of turbulent transfer into the Amazon rain forest canopy are quantified. Simple empirical relations that relate observed turbulent heat fluxes to horizontal wind variance are presented. Changes in the amount of turbulent coupling between the forest and the boundary layer associated with deep convective clouds are presented both as statistical averages and as a series of case studies. These convective processes during the rainy season are shown to alter the diurnal course of turbulent fluxes. In wake of giant coastal systems, no significant heat or moisture fluxes occur for up to a day after the event. Radar data is used to demonstrate that even small raining clouds are capable of evacuating the canopy of substances normally trapped by persistent static stability near the forest floor. Recovery from these events can take more than an hour, even during mid-day. In spite of the ubiquitous presence of clouds and frequent rain during this season, the average horizontal wind speed spectrum is well described by dry CBL similarity hypotheses originally found to apply in flat terrain. Author

N89-28962# Oak Ridge National Lab., TN.
ADEQUACY OF FORESTRY DATA IN ASSESSING THE IMPACT OF OZONE: A NATIONAL PERSPECTIVE
David S. Shriner and Dean E. Carpenter (NSI Technology Services Corp., Research Triangle Park, NC.) 1989 15 p Presented at the 82nd Annual Air and Waste Management Association Meeting and Exhibition, Anaheim, CA, 25 Jun. 1989
(Contract DE-AC05-84OR-21400)
(DE89-012359; CONF-890692-9) Avail: NTIS HC A03/MF A01

Regional-scale assessment of the effects of ozone on forest ecosystems involves a diffuse array of sources distributed across tens of thousands of square kilometers. Exposure characteristics have short-term dynamics (hours or days), but effects may be manifest only after years of exposure. Discussion of the adequacy of forestry data for assessing the impact of ozone on forests from the national perspective requires first a discussion of the process by which such an assessment might be done, and secondly, discussion of the other types of data necessary to permit differentiation of forest impacts. This paper addresses a variety of approaches to assessment of forest impacts, discusses the basic data requirements necessary for an assessment of ozone impacts on forests, and provides an assessment of data availability on a national scale. DOE

N89-28963# Environmental Protection Agency, Research Triangle Park, NC. Atmospheric Research and Exposure Assessment Lab.
USER'S GUIDE TO THE COMPLEX TERRAIN DISPERSION MODEL PLUS ALGORITHMS FOR UNSTABLE SITUATIONS (CTDMPLUS). VOLUME 1: MODEL DESCRIPTION AND USER INSTRUCTIONS
Steven G. Perry, Donna J. Burns, Lucy H. Adams, Robert J. Paine, Michael G. Dennis, Michael Te. Mills, David G. Strimaitis, Robert J. Yamartino, and Elizabeth M. Insley (Sigma Research, Inc., Lexington, MA.) Mar. 1989 211 p
(PB89-181424; EPA/600/8-89/041-Vol-1) Avail: NTIS HC A10/MF A01 CSCL 13B

The Complex Terrain Dispersion Model Plus Algorithms for Unstable Situations (CTDMPLUS) is a refined air quality model for use in all stability conditions for complex terrain applications. It contains the technology of the original Complex Terrain Dispersion Model (CTDM) for stable and neutral conditions, but also models daytime, unstable conditions. The model makes use of considerable detail in the terrain and meteorological data (as compared to current EPA regulatory models) and requires the parameterization of individual terrain features, thus considering the 3-D nature of the interaction of the plume and terrain. The user's manual describes, in detail, the basis of the model and instructions for its use. Author

N89-28964# Environmental Protection Agency, Research Triangle Park, NC. Atmospheric Research and Exposure Assessment Lab.
ATMOSPHERIC PROCESSES AND EFFECTS ON MATERIALS
J. J. Bufalini and E. O. Edney 1989 22 p
(PB89-173215; EPA/600/D-89/001) Avail: NTIS HC A03/MF A01 CSCL 13B

The effects expected from the depletion of stratospheric ozone by the presence of CFCs are summarized. The two areas considered are materials damage and atmospheric processes. Increased UV can affect materials in the following ways: (1) corrosion of metals is expected to increase because of increased acid deposition; (2) stone deterioration is expected to increase again because of increased acid deposition; (3) dyes are expected to fade more quickly; (4) polymers are expected to breakdown more rapidly; and (5) paints will weather faster. In the area of atmospheric processes, increased UV is expected to: (1) increase

photochemical reations in cities and more ozone is expected; (2) sulfur dioxide is expected to oxidize to sulfate more quickly; and (3) gas particle reaction rates are expected to increase. Author

N89-28965# Brookhaven National Lab., Upton, NY.
CHARACTERIZATION OF PAINTED SURFACES IN THE UNITED STATES FROM THE PERSPECTIVE OF POTENTIAL DAMAGE FROM ACIDIC DEPOSITION
F. W. Lipfert Mar. 1989 53 p Prepared for Syracuse Research Corpt., NY
(Contract DE-AC02-76CH-00016)
(DE89-014264; BNL-42768) Avail: NTIS HC A04/MF A01

Data on the types and applications of exterior paints used in the United States are reviewed from the perspective of potential damage by air pollution or acidic deposition. The data show that residential buildings are the most economically important subset of the painted structures in the U.S. for painting costs. The trends for new construction suggest that this ranking is likely to continue in the future. Although both new construction and maintenance painting are economically important, the more difficult conditions involved in painting over existing finishes make this an important class of situations for research. Consumer surveys show that the most important mode of paint failure is peeling and flaking which, in its various manifestations, accounts for about half of residential paint problems. Such problems often occur within two to three years after painting. Color changes (deterioration) are next in importance. Although chalking and erosion were observed their roles in decisions to repaint are less apparent. The trends in paint usage and performance are generally supportive of (or not inconsistent with) the hypothesis that air pollution or acid rain may be having some adverse effects, although such data are by no means conclusive. It is recommended that selections of coatings and substrate for acid deposition research include those combinations that are widely used (latex over wood and over previous paint) and those that are sensitive to acid deposition (paints containing CaCO3; alkyd paint over steel). DOE

N89-28966# Ballistic Research Labs., Aberdeen Proving Ground, MD.
DENSE HEAVY METAL AEROSOL MONITORING BY DIRECT X-RAY FLUORESCENCE
George M. Thomson Jun. 1989 47 p
(AD-A209077; BRL-TR-3003) Avail: NTIS HC A03/MF A01
CSCL 19/1

Dense aerosols are widely found as active ingredients or byproducts in pyrotechnics, explosives, obscurants, antipersonnel munitions, and rocket engines. The Ballistic Research Laboratory (BRL) is applying a state-of-the-art microanalytical tool, X-ray fluorescence, to a new task of monitoring the mass concentrations of dense aerosols containing metals. The results obtained promise a solution for a long-standing problem in metal aerosol work - the necessity of extracting particles out of the air prior to assessment in a fashion that gives samples that are truly representative of the aerosol. The new method works directly on the dispersed aerosol and provides noninvasive concentration measurements rapidly, simply, and reliably for most materials with atomic number above 24. The potential of the direct X-ray fluorescence method has been evaluated in tests targeting a two dimensional simulant iron aerosol. The results show that, in a minute or less, one can assess aerosol concentrations from a few milligrams up to several grams per cubic meter. Higher sensitivities can be readily realized if increased X-ray doses can be tolerated. Based on these findings, developing a more advanced instrument appears worthwhile. GRA

N89-28967*# National Aeronautics and Space Administration. John C. Stennis Space Center, Bay Saint Louis, MS.
A COMBINED AIR AND WATER POLLUTION CONTROL SYSTEM Patent Application
Billy C. Wolverton, inventor (to NASA) and Lamont Jarrell, inventor (to NASA) 26 May 1989 15 p
(NASA-Case-NST-00007-1; NAS 1.71:NST-00007-1; US-Patent-Appl-SN-357938) Avail: NTIS HC A03/MF A01
CSCL 13B

A bioaquatic air pollution control system for controlling both water and atmospheric pollution is disclosed. The pollution control system includes an exhaust for directing polluted gases out of a furnace and a fluid circulating system which circulates fluid, such as waste water, from a source, past the furnace where the fluid flow entrains the pollutants from the furnace. The combined fluid and pollutants are then directed through a rock/plant/microbial filtering system. A suction pump pumps the treated waste water from the filter system past the exhaust to again entrain more pollutants form the furnace where they are combined with the fluid (waste water) and directed to the filter system. NASA

N89-28968 Institut d'Aeronomie Spatiale de Belgique, Brussels.
ABSORPTION CROSS SECTION OF ALTERNATIVE CHLOROFLUOROETHANES AND POTENTIAL EFFECTS ON THE OZONE LAYER
Didier Gillotay, Paul C. Simon, and Guy Brasseur 1989 12 p Submitted for publication
(Aeronomica-Acta-A-340-1989; ISSN-0065-3713; ETN-89-95189)
Avail: Institut d'Aeronomie Spatiale de Belgique, 3 Avenue Circulaire, B-1180 Brussels, Belgium

The measurements of the chlorofluoroethanes ultraviolet absorption cross sections are reported. Three compounds are considered (CH3-CF2Cl - HCFC 142b, CH3-CFCl2 - HCFC 141b and CF3-CHCL2 - HCFC 123) and uncertainties of two percent are measured. These compounds are photodissociated in the stratosphere. It is shown that a substantial fraction of these molecules is destroyed in the troposphere by hydroxyl radicals. As a consequence, the lifetime and the ozone depletion potential of these chlorofluoroethanes are significantly lower than those of the used chlorofluorocarbons 11 and 12. ESA

46 GEOPHYSICS

Includes aeronomy; upper and lower atmosphere studies; ionospheric and magnetospheric physics; and geomagnetism.

For space radiation see *93 Space Radiation.*

N89-28969*# Jet Propulsion Lab., California Inst. of Tech., Pasadena.
A HIGH-RESOLUTION ATLAS OF THE INFRARED SPECTRUM OF THE SUN AND THE EARTH ATMOSPHERE FROM SPACE. A COMPILATION OF ATMOS SPECTRA OF THE REGION FROM 650 TO 4800 cm-1 (2.3 TO 16 MICRONS). VOLUME 2: STRATOSPHERE AND MESOSPHERE, 650 TO 3350 cm-1
Crofton B. Farmer and Robert H. Norton Washington 1989 688 p
(Contract NAS7-918)
(NASA-RP-1224-Vol-2; JPL-400-370-Vol-2; NAS 1.61:1224-Vol-2; LC-89-600203) Avail: NTIS HC A99/MF E03 CSCL 04A

During the period April 29 to May 2, 1985, the Atmospheric Trace Molecule Spectroscopy (ATMOS) experiment was operated for the first time, as part of the Spacelab-3 payload of the shuttle Challenger. The principal purpose of this experiment was to study the distributions of the atmosphere's minor and trace molecular constituents. The instrument, a modified Michelson interferometer covering the frequency range from 600 to 5000/cm-1 at a spectral resolution of 0.01/cm-1, recorded infrared absorption spectra of the sun and of the earth's atmosphere at times close to entry into and exit from occultation by the earth's limb. Spectra were obtained that are free from absorptions due to constituents of the atmosphere (i.e., they are pure solar spectra), as well as spectra of the atmosphere itself, covering line-of-sight tangent altitudes that span the range from the lower thermosphere to the bottom of the troposphere. This atlas presents a compilation of these spectra arranged in a hardcopy format suitable for quick-look reference purposes. Volume 2 covers the stratosphere and mesosphere (i.e., tangent altitudes from 20 to 80 km) for frequencies from 650 to 3350/cm-1. Author

N89-28970# Los Alamos National Lab., NM.
PARALLEL ELECTRIC FIELDS IN A SIMULATION OF MAGNETOTAIL RECONNECTION AND PLASMOID EVOLUTION
Michael Hesse and Joachim Birn 1989 26 p Presented at the Chapman Conference on the Physics of Magnetic Flux Ropes, Hamilton, Bermuda, 27-31 Mar. 1989 Sponsored by NASA
(Contract W-7405-eng-36)
(DE89-012622; LA-UR-89-1592; CONF-8903131-1) Avail: NTIS HC A03/MF A01

Properties of the electric field component parallel to the magnetic field (E sub parallel) in a three-dimensional MHD simulation of plasmoid formation and evolution in the magnetotail in the presence of a net dawn-dusk magnetic field component were observed. Particularly emphasized was the spatial location of E(sub parallel), the concept of a diffusion zone and the role of E(sub parallel) in accelerating electrons. A localization of the region of enhanced E(sub parallel) in all space directions with a strong concentration in the z direction was found. This region was identified as the diffusion zone, which plays a crucial role in reconnection theory through the local break-down of magnetic flux conservation. The presence of B(sub y) implies a north-south asymmetry of the injection of accelerated particles into the near-earth region, if the net B(sub y) field is strong enough to force particles to follow field lines through the diffusion region. It is estimated that for a typical net B(sub y) field this should affect the injection of electrons into the near-earth dawn region, so that precipitation into the Northern (Southern) Hemisphere should dominate for duskward (dawnward) net B(sub y). In addition, a spatial clottiness of the expected injection of adiabatic particles which could be related to the appearance bright spots in auroras was observed. DOE

N89-28971# New Mexico State Univ., Las Cruces. Physical Science Lab.
ENGINEERING AND INSTRUMENTATION SUPPORT OF THE AFGL (AIR FORCE GEOPHYSICS LABORATORY) RESEARCH BALLOON PROGRAM Final Report, 7 Mar. 1984 - 30 Nov. 1987
Squire B. Seagraves 9 Dec. 1988 16 p
(Contract F19628-84-C-0039)
(AD-A209107; AFGL-TR-89-0089) Avail: NTIS HC A03/MF A01 CSCL 01/3

The direct pre-flight and flight support of 24 free balloon and 7 tether balloon missions at Holloman AFB and various remote locations are examined. Extensive effort was also made in upgrading the Building 850 Control Center configuration for a more efficient operation while also generating up-to-data documentation. The telemetry room computer equipment was reconfigured with major changes in both hardware and software systems. The telemetry van computer system was also upgraded to the same level of support as the telemetry room system. A continuing effort was made to improve the quality of support given to Air Force Geophysics Laboratory and to the other agencies and users involved in the balloon operations as well as to enhance the utilization of the equipment and facilities at AFGL and Holloman AFB. GRA

N89-28972# Naval Ocean Systems Center, San Diego, CA.
IONOSPHERIC VARIABILITY Final Report, Oct. 1985 - Oct. 1988
Adolf K. Paul Mar. 1989 13 p
(AD-A209251; NOSC/TR-1277) Avail: NTIS HC A02/MF A01 CSCL 04/1

The results are summarized of a study of short term variations of the ionosphere. The digital ionograms used in this analysis were recorded at Brighton, Colorado, many of them at a high rate of 12 ionograms per hour and faster. The results show that oscillations of the electron density distribution take place in the F region with varying amplitudes and with periods of a fraction of an hour. The oscillations are coupled with varying tilts. Rapid changes, mainly of the electron density, are also observed at E layer heights and many records indicate that the echoes come from tilted sporadic-E patches with relatively small dimensions. GRA

N89-28973# McDonnell-Douglas Astronautics Co., Huntington Beach, CA.
ELECTRIC FIELDS IN EARTH ORBITAL SPACE Final Report
K. A. Pfitzer May 1989 30 p
(Contract N00014-80-C-0796)
(AD-A209542; AD-E900860) Avail: NTIS HC A03/MF A01 CSCL 04/1

During the last few years we have worked on the entry of solar wind into the magnetosphere and on the control the interplanetary magnetic field (IMF) has on the magnetosphere. Correlative data conclusively prove that both the solar wind and the IMF exert considerable influence on magnetospheric processes, and the magnetospheric substorm in particular. Our work on this subject may be roughly divided into two parts, particle entry and representation of the interaction of the IMF with the magnetosphere. We discuss particle entry first. We have quantitatively determined where on the magnetopause that low energy (solar wind) charged particles can gain entry to the magnetosphere. GRA

N89-28974# Spectral Sciences, Inc., Burlington, MA.
THE STRATEGIC HIGH-ALTITUDE ATMOSPHERIC RADIATION CODE (SHARC) USER INSTRUCTIONS Technical Report, Sep. 1987 - Jan. 1989
R. L. Sundberg, J. W. Duff, L. S. Bernstein, P. K. Acharya, J. H. Gruninger, and D. C. Robertson 3 Feb. 1989 175 p
(Contract F19628-87-C-0130)
(AD-A207667; SSI-TR-152; AFGL-TR-89-0062; SR-3) Avail: NTIS HC A08/MF A01 CSCL 04/1

This report describes how to implement and use the Strategic High-Altitude Radiance Code (SHARC). SHARC calculates atmospheric radiation for paths from 60 to 300 km altitude in the 2 to 40 micron spectral region. It models radiation due to NLTE (Non-Local Thermodynamic Equilibrium) molecular emissions which are the dominant sources at these altitudes. This initial version of SHARC includes the five strongest IR radiators, CO2, NO, O3, H2O, and CO. The code is available on magnetic tape and can be obtained by written request to AFGL/OPB. GRA

N89-28975# Washington Univ., Seattle. Dept. of Atmospheric Sciences.
APPLICATION OF SPECIAL SENSOR MICROWAVE/IMAGER DATA FOR ANALYSIS OF CYCLONIC STORMS IN MIDLATITUDES OVER THE SEA Annual Report, Aug. 1987 - Nov. 1988
Kristina B. Katsaros, Grant W. Petty, Iftekhar Bhatti, and Douglas Miller Mar. 1989 42 p
(Contract N00014-86-K-0453; NR Proj. R35-82)
(AD-A207675; NEPRF-CR-89-02) Avail: NTIS HC A03/MF A01 CSCL 04/1

Previously we developed algorithms and criteria for identifying fronts in cyclonic weather systems with data on atmospheric water vapor and rain obtained with microwave sensors in space. Using data from the 18, 21 and 37 GHz channels of the Scanning Multichannel Microwave Radiometer (SMMR) on the SEASAT and NIMBUS-7 satellites, we calculated fields of these variables in cyclonic storms. This report is concerned with currently operating microwave radiometer, the Special Sensor Microwave/Imager (SSM/I) on the F8 satellite in the Defense Meteorological Satellite Program (DMSP). This sensor employs three frequencies with similar characteristics as the ones giving atmospheric water data on SMMR, but not at exactly the same frequencies. For this reason we needed to test the algorithms for identifying fronts with data from this new sensor. In addition, the SSM/I has two channels at 85 GHz which are sensitive to scattering caused by large ice particles and graupel in the clouds. We found that an index of this scattering gives a unique view of the deep clouds in frontal zones. We also tested cloud liquid water and wind algorithms developed for SSM/I, and found good qualitative agreement with

conventional data. Several cyclones occurring in the fall of 1987 were examined in some detail. GRA

N89-28976# SRI International Corp., Menlo Park, CA.
COLLISION DYNAMICS AND TRANSITION PROBABILITIES FOR VIBRATIONALLY EXCITED OH Final Report, 1 Jun. 1987 - 31 Dec. 1988
Richard A. Copeland Jan. 1989 59 p
(Contract F19628-87-K-0043)
(AD-A207856; AFGL-TR-89-0072) Avail: NTIS HC A04/MF A01 CSCL 04/1

Vibrationally excited OH is a significant source of infrared emission in the upper atmosphere. Modeling the nonequilibrium processes responsible for the emission between vibrational levels in the ground state (called the Meinel bands) requires values for absolute transition probabilities and vibrational energy transfer rate constants for OH. However, the accuracy of currently available information is questionable. Most experimental studies have used the Meinel band emission itself to measure these quantities, with limited success. The development of a new laser induced fluorescence method for detecting high lying vibrational levels of OH is described. GRA

N89-28977# Cologne Univ. (Germany, F.R.). Inst. fuer Geophysik und Meteorologie.
PARAMETERIZATION OF ICE AND WATER CLOUDS AND THEIR RADIATION TRANSPORT CHARACTERISTICS FOR LARGE SCALE ATMOSPHERIC MODELS [PARAMETRISIERUNG VON EIS- UND WASSERWOLKEN UND IHRER STRAHLUNGSTRANSPORTEIGENSCHAFTEN FUER GROSSRAEUMIGE ATMOSPHAERENMODELLE]
Burkhardt Rockel, A. Ebel, ed., F. M. Neubauer, ed., E. Raschke, ed., and P. Speth, ed. 1988 112 p In GERMAN
(Contract BMFT-07-KF-111)
(Mitt-58; ISSN-0069-5882; ETN-89-94413) Avail: NTIS HC A06/MF A01

A cloud and radiation transport model, for large-scale atmospheric models, which takes into account the ice as well as the water phase of clouds, is presented. An existing radiation model was extended for the parameterization of radiation transport in ice clouds. Calculations of the cloud coverage are in agreement with METEOSAT pictures. A sensitivity study shows a strong dependence of the coverage degree on changes in the relative humidity. The radiation transport model reacts sensitively to variations of coverage degree and ice content. Taking into account ice clouds it leads, on the average, to an increase of the lower cloudiness and to a decrease of the medium, high and convective cloudiness, as well as to a temperature rise. ESA

N89-28978 Karlsruhe Univ. (Germany, F.R.). Inst. fuer Meteorologie und Klimaforschung.
ANALYSIS OF TURBULENT TRANSPORT PHENOMENA IN THE MARITIME ATMOSPHERIC BOUNDARY LAYER Thesis [ANALYSE TURBULENTER BEWEGUNGSVORGAENGE IN DER MARITIMEN ATMOSPHAERISCHEN GRENZSCHICHT]
Ulrich Corsmeier May 1988 199 p In GERMAN
(WISS-BER-10; ISSN-0179-5619; ETN-89-94418) Avail: Fachinformationszentrum Karlsruhe, 7514
Eggenstein-Lepoldshafen 2, Fed. Republic of Germany

Turbulent transport phenomena in the atmospheric boundary layer are investigated using the statistical methods for turbulence structures and single structure analysis. The atmospheric flows characteristics are outlined. The status of knowledge about turbulent structures in the boundary layer is presented. The analysis of the turbulence data set of JASIN (Joint Air Sea Interaction Experiments) using moment analysis methods, correlation calculations, spectral calculation and optical analysis is performed. It leads to different statements concerning turbulent structures in the flow field as a function of the boundary conditions of the large scale wind field. The analysis of JASIN data provides new knowledge concerning the turbulence structure in the mainly neutral to light unstable, layered medium and upper maritime atmospheric boundary layer (Ekman layer). ESA

N89-28979 Karlsruhe Univ. (Germany, F.R.). Inst. fuer Meteorologie und Klimaforschung.
APPLICATION OF SIMILARITY METHODS TO THE TURBULENT DIFFUSION IN THE CONVECTIVE AND STABLE BOUNDARY LAYER Thesis [ANWENDUNG VON AEHNLICHKEITSVERFAHREN AUF DIE TURBULENTE DIFFUSION IN DER KONVEKTIVEN UND STABILEN GRENZSCHICHT]
Gervasio Annes Degrazia Jan. 1989 100 p In GERMAN Sponsored by the Deutscher Akademischer Austauschdienst and the Comissao de Aperfeicoamento de Pessoal de Ensino Superior
(WISS-BER-12; ISSN-0179-5619; ETN-89-94603) Avail: Fachinformationszentrum Karlsruhe, 7514
Eggenstein-Leopoldshafen 2, Fed. Republic of Germany

Spectral equations are deduced to describe measured turbulent velocity spectra, based on experimental results allowing a simple extension of the similarity theory in regions above the convective and stable Prandtl layer. The spectra of the turbulent velocity components in the convective boundary layer are calculated. A model for the case of turbulent diffusion is developed. The diffusion of pollutants, emitted by high-lying sources in the convective boundary layer is studied. Local similarity and spectra of the turbulent velocity components in the stable boundary layer are discussed. The turbulent diffusion in the convective and stable boundary layer is numerically simulated. The simultaneous measurement of air pollutants concentration and several parameters allows a good simulation of the diffusion processes. ESA

N89-28980 Institut d'Aeronomie Spatiale de Belgique, Brussels.
AERONOMIC PROBLEMS OF MOLECULAR OXYGEN PHOTODISSOCIATION. 5: PREDISSOCIATION IN THE SCHUMMAN-RUNGE BANDS OF OXYGEN
Marcel Nicolet, S. Cieslik, and Robert Kennes 1989 74 p Submitted for publication Sponsored by the Commission of the European Communities, Directorate General for Science, Research and Development, Environment Research Program and the ONR
(Contract FC-85-563)
(Aeronomica-Acta-A-341-1989-5; ISSN-0065-3713; ETN-89-95190) Avail: Institut d'Aeronomie Spatiale de Belgique, 3 Avenue Circulaire, B-1180 Brussels, Belgium

The new independent sets of laboratory absorption data for molecular oxygen are analyzed. They provide sufficient spectral resolution in the Schumann-Runge region to yield linewidths of the rotational lines. The determination of the absorption cross sections as a function of wavelength and temperature is possible. The analysis of these results to prepare a parameterization is made. It is adapted to 500/cm intervals for atmospheric conditions between 170 and 270 K in the mesosphere and stratosphere. ESA

N89-28981 Institut d'Aeronomie Spatiale de Belgique, Brussels.
AERONOMIC PROBLEMS OF MOLECULAR OXYGEN PHOTODISSOCIATION. 6: PHOTODISSOCIATION FREQUENCY AND TRANSMITTANCE IN THE SPECTRAL RANGE OF THE SCHUMMAN-RUNGE BANDS
Marcel Nicolet and Robert Kennes 1989 64 p Submitted for publication
(Contract FC-86-621)
(Aeronomica-Acta-A-342-1989-6; ISSN-0065-3713; ETN-89-95191) Avail: Institut d'Aeronomie Spatiale de Belgique, 3 Avenue Circulaire, B-1180 Brussels, Belgium

The relative photodissociation frequency and direct transmittance of O2 are investigated. They are derived from parametric formulas for 500/cm intervals in the 175 to 202 nm spectral region that corresponds to the domain of the bands of the Schumann-Runge system. The parameterization is obtained by comparison of calculations (0.1/cm intervals from 115 km to 15 km) with formulas that depend on the solar zenith angle and the O2 column abundances. Similarity between the results of the detailed calculations and of the parameterization, is obtained. It is

shown that the set of transmission functions and relative photodissociation rates for O2 is appropriate for atmospheric modeling in the mesosphere and stratosphere. ESA

N89-28982# Technische Univ., Eindhoven (Netherlands).
THE BOUNDARY LAYER WIND REGIME OF A REPRESENTATIVE TROPICAL AFRICAN REGION, CENTRAL SUDAN Ph.D. Thesis
Eiman Hassan AbuBakr 1988 163 p Sponsored by the Netherlands Organization for the Advancement of Scientific Research Prepared in cooperation with the Royal Netherlands Meteorological Inst., De Bilt
(KNMI-WR-88-04; ETN-89-95467) Avail: NTIS HC A08/MF A01

An assessment technique for wind energy potential in tropical African countries is presented. The insufficient number of meteorological stations in many African countries calls for the development of models to interpolate horizontally between the few available stations with surface wind and/or upper wind data. Such a model is developed for the Sudanese area using unprocessed meteorological data collected from eight stations. The results of the study are included and indicate the need for a more elaborate data base in order to understand certain aspects of local and mesoscale circulation. ESA

47 METEOROLOGY AND CLIMATOLOGY

Includes weather forecasting and modification.

N89-28983*# National Aeronautics and Space Administration. Goddard Space Flight Center, Greenbelt, MD.
THE 1988 ANTARCTIC OZONE MONITORING NIMBUS-7 TOMS DATA ATLAS
Arlin J. Krueger, Lanning M. Penn, David E. Larko, Scott D. Doiron, and Patricia T. Guimaraes (ST Systems Corp., Vienna, VA.) Aug. 1989 153 p
(Contract NAS5-29375)
(NASA-RP-1225; Rept-89B00176; NAS 1.61:1225) Avail: NTIS HC A08/MF A01 CSCL 04B

Because of the great environmental significance of ozone and to support continuing research at McMurdo, Syowa, and other Southern Hemisphere stations, the development of the 1988 ozone hole was monitored using data from the Nimbus-7 Total Ozone Mapping Spectrometer (TOMS) instrument, produced in near-real-time. This Atlas provides a complete set of daily polar orthographic projections of the TOMS total ozone measurements over the Southern Hemisphere for the period August 1 through November 17, 1988. Although total ozone in mini-holes briefly dropped below 150 DU in late August, the main ozone hole is seen to be much less pronounced than in 1987. Minimum values, observed in late September and early October 1988, were seldom less than 175 DU. Compared with the same period in 1987, when a pronounced ozone hole whose minimum value of 109 Dobson Units (DU) was the lowest total ozone ever observed, the 1988 ozone hole is displaced from the South Pole, opposing a persistent maximum with values consistently above 500 DU. Daily ozone values above selected Southern Hemisphere stations are presented, along with comparisons of the 1988 ozone distribution to that of other years. Author

N89-28984# Brookhaven National Lab., Upton, NY. Environmental Chemistry Div.
CLIMATE REGULATION BY MARINE PHYTOPLANKTON: A TEST BY ANTHROPOGENIC SO2 EMISSIONS
Stephen E. Schwartz May 1989 7 p Presented at the 28th Liege International Astrophysical Colloqiuim on our Changing Atmosphere, Liege, Belgium, 26-30 Jun. 1989
(Contract DE-AC02-76CH-00016)
(DE89-014708; BNL-42744; CONF-8906154-1) Avail: NTIS HC A02/MF A01

The potential sensitivity of global mean albedo and temperature to N prompted a novel suggestion consistent with the Gaia hypothesis for regulation of global climate by marine phytoplankton. Certain species of coccolithophores excrete dimethylsulfide (DMS), and this DMS is arguably the principal source of reduced sulfur gases in the global atmosphere and, in the absence of anthropogenic SO2, the principal source of atmospheric gaseous sulfur species. Such gaseous sulfur species are oxidized in the atmosphere to form sulfuric acid, which rapidly forms an aerosol. Since sulfate-containing AP are highly efficient CCN, it is argued that an increase in DMS production by marine phytoplankton would yield increased concentrations of CCN, resulting in increased cloud albedo, decreased surface insolation, and decreased planetary temperature. It is further hypothesized that such decreased insolation or temperature might result in decreased production of DMS by marine phytoplankton, i.e., that the process might constitute a negative feedback loop for regulation of planetary climate by marine microorganisms. DOE

N89-28985# Air Force Environmental Technical Applications Center, Scott AFB, IL.
EUROPEAN CROSSWIND FREQUENCIES
Gary H. Tryon Feb. 1989 430 p
(AF Proj. 80402)
(AD-A209137; USAFETAC/PR-89/001) Avail: NTIS HC A19/MF A01 CSCL 04/2

This report documents the results of a study to determine percent occurrence frequency of crosswinds at 39 selected European bases. It provides percent frequency of occurrence tables for crosswinds greater than or equal to 10, 15, 20, and 25 knots under various weather conditions such as precipitation and below-freezing temperature. Sixteen tables are provided for each base, and each set is followed by a number of actual cases table. The study should help forecasters, planners, and engineers in estimating crosswind possibilities at various speed thresholds, and should further help in estimating those during rain, snow, and below-freezing conditions. GRA

N89-28986# Massachusetts Inst. of Tech., Lexington. Lincoln Lab.
STORM MODELS FOR END-TO-END TDWR (TERMINAL DOPPLER WEATHER RADAR) SIGNAL PROCESSING SIMULATION TESTS
J. E. Evans 1 May 1989 47 p
(Contracts DTFA01-83-C-10579; F19628-85-C-0002)
(AD-A209384; ATC-155; DOT/FAA/PM-87/37) Avail: NTIS HC A03/MF A01 CSCL 17/9

End-to-end qualification testing of the Terminal Doppler Weather Radar (TDWR) contractor signal processing system will be accomplished by a signal processing simulation test. Government furnished storm models will be used to provide inputs to the signal processor. The corresponding hazardous weather product results will be compared to the results determined by the detection algorithm developers. This report examines the role of the end-to-end tests in the context of overall TDWR qualification testing and concludes that the signal waveform/velocity ambiguity resolution should be the principal focus of the signal processing simulation testing. Salient characteristics of the initial pair of storm models (a high reflectivity microburst observed in Huntsville, AL, and a series of low-to-moderate reflectivity microburst storms observed in Denver, CO) are described as well as desirable characteristics of additional storm models to be provided later. GRA

N89-28987# Atmospheric and Environmental Research, Inc., Cambridge, MA.
SATELLITE ENHANCED NUMERICAL WEATHER PREDICTION Final Report, Jul. 1986 - Feb. 1989
R. N. Hoffman, R. Isaacs, J. F. Louis, T. Nehrkorn, and M. Mickelson 11 Apr. 1989 118 p
(Contract F19628-86-C-0141)
(AD-A210108; AFGL-TR-89-0099) Avail: NTIS HC A06/MF A01 CSCL 04/2

We have made substantial progress in areas related to improving Numerical Weather Prediction (NWP), especially the

analysis and forecast of moisture and cloudiness, through spaceborne observing systems. We have: developed, implemented and evaluated techniques for retrieving geophysical parameters from satellite observations for use in NWP; tested the impact of these data and data from other sources in a series of Observing System Experiments (OSEs); developed and applied a comprehensive data simulation methodology; and conducted a series of observing system simulation experiments to evaluate the impact of new observing systems. Work in techniques development focused on retrieving relative humidity profiles from 3 distinct sources: the civilian infrared sounder (TOVS), the operational nephanalysis (3DNEPH) and the DMSP microwave sounder (SSM/T-1,2). The real data sources, TOVS and 3DNEPH, provided only marginally useful data, while in simulation, the SSM/T retrievals were significantly useful. A series of real data OSEs was conducted to measure the impact of retrieved humidity profile data as well as the impact of other satellite data. Two data denial experiments examined the effect of using limited surface-based data and of using satellite observations only. Such data systems are clearly inferior to the full operational system. However, for the first few days of data denial such a system may be adequate. GRA

N89-28988# Israel Oceanographic and Limnological Research Ltd., Haifa.

THE SENSITIVITY OF MIDDLE EAST PRECIPITATION AND CLOUD FORECASTS TO CHANGES IN EASTERN MEDITERRANEAN SEA SURFACE TEMPERATURES Final Report, 1 Oct. 1986 - 31 Dec. 1988

Stephen Brenner 1 Mar. 1989 40 p
(Grant AF-AFOSR-0066-87; AF Proj. 2301)
(AD-A207864; GL-TR-89-0106) Avail: NTIS HC A03/MF A01 CSCL 04/2

The unimolecular decomposition dynamics of Silicon Hydride were investigated using classical trajectory methods on a global potential-energy surface fitted to the results of a ab-initio calculations and the available experimental data. The required phase-space averages are computed using metropolis sampling techniques. It is found that unless the parameters of the Markov walk are adjusted for each different type of atom present, extremely long Markov walks are required to adequately cover the phase space of the system. The most important dissociation channel over this energy range is three-center elimination of molecular hydrogen leading to H2Si=Si. At energies below 7.0 eV, the other channels are, in order of importance, Si-Si bond rupture, four-center H2 elimination, and simple Si-H bond rupture. At or above 8.0 eV, four-center H2 elimination replaces Si-Si bond rupture as the second most important decomposition channel. GRA

N89-28989# Northwest Research Associates, Inc., Bellevue, WA.

PROPAGATION AND SATURATION OF NONLINEAR INERTIA-GRAVITY WAVES IN THE ATMOSPHERE Final Report, 15 Feb. 1986 - 14 Feb. 1989

Timothy J. Dunkerton 14 Apr. 1989 29 p
(Contract F49620-86-C-0026)
(AD-A207871; NWRA-CR-89-R044; AFOSR-89-0626TR) Avail: NTIS HC A03/MF A01 CSCL 04/2

Inertia gravity waves play a significant role in the transport of momentum, heat, and constituents in the terrestrial atmosphere. This transport process is subgrid scale in general circulation models and must be parameterized. A generalized parameterization scheme is developed in which a gravity wave is subject to localized breaking that creates turbulent mixing and retards amplitude growth. The effect of turbulence localization on turbulent viscosity, diffusivity and mean flow acceleration is described for the convectively unstable case. Possible generalizations to Kelvin-Helmholtz breaking are suggested. Numerical simulations at high resolution illustrate the evolution to small scales characteristic of convective instability. GRA

N89-28990*# California Univ., Los Angeles. Dept. of Electrical Engineering.

WIND PROFILE ESTIMATION FROM POINT TO POINT LASER DISTORTION DATA

Robert Leland 1 Aug. 1989 16 p
(Contract NCC2-374)
(NASA-CR-185891; NAS 1.26:185891) Avail: NTIS HC A03/MF A01 CSCL 04B

The author's results on the problem of using laser distortion data to estimate the wind profile along the path of the beam are presented. A new model for the dynamics of the index of refraction in a non-constant wind is developed. The model agrees qualitatively with theoretical predictions for the index of refraction statistics in linear wind shear, and is approximated by the predictions of Taylor's hypothesis in constant wind. A framework for a potential in-flight experiment is presented, and the estimation problem is discussed in a maximum likelihood context. Author

N89-28991 Karlsruhe Univ. (Germany, F.R.). Inst. fuer Meteorologie und Klimaforschung.

DIFFERENCE TECHNIQUES FOR SOLVING THE ADVECTION EQUATION [DIFFERENZENVERFAHREN ZUR BEHANDLUNG DER ADVEKTION]

C. P. Hugelmann Feb. 1988 78 p In GERMAN
(WISS-BER-8; ISSN-0179-5619; ETN-89-94416) Avail: Fachinformationszentrum Karlsruhe, 7514
Eggenstein-Leopoldshafen 2, Fed. Republic of Germany

The development of difference schemes (high resolution schemes) for the numerical solution of hyperbolic differential equations, applied to the advection equation, is described. The dominant role in these schemes is played by stability related to the total variation. The fundamental concepts of the difference techniques are outlined. The derivation of schemes via the method of flux corrections is explained. The efficiency of the schemes is illustrated and evaluated. ESA

N89-28992 Karlsruhe Univ. (Germany, F.R.). Inst. fuer Meteorologie und Klimaforschung.

EXPERIMENTAL INVESTIGATION OF THE PRESSURE DRAG IN THE ALPS Thesis [EXPERIMENTELLE UNTERSUCHUNG ZUM DRUCKWIDERSTAND DER ALPEN]

Thomas Hafner Apr. 1988 234 p In GERMAN
(WISS-BER-9; ISSN-0179-5619; ETN-89-94417) Avail: Fachinformationszentrum Karlsruhe, 7514
Eggenstein-Leopoldshafen 2, Fed. Republic of Germany

A comprehensive representation of the pressure drag on mountains, based on experimental investigations in the Alps is given. The horizontal 2-D pressure drag vectors were calculated for three height layers and time resolution of three hours; the short time fluctuations are substantially larger than presently accepted. The pressure drag component perpendicular to the main ridge was determined using a microbarograph chain. The contribution of the wave drag was determined foot turbulent crossflow, propagating and resonance waves, using high resolution wind data (1H2) from aircraft measurements. Further experimental and theoretical studies are required for a comprehensive theoretical description of the drag problem. ESA

N89-28993*# National Aeronautics and Space Administration. Langley Research Center, Hampton, VA.

ISCCP CX OBSERVATIONS DURING THE FIRE/SRB WISCONSIN EXPERIMENT FROM OCTOBER 14 THROUGH NOVEMBER 2, 1986

Charles H. Whitlock, Stuart R. LeCroy, William B. Rossow, and Ken L. Bell (National Aeronautics and Space Administration. Goddard Inst. for Space Studies, New York, NY.) Sep. 1989 120 p
(NASA-TM-101653; NAS 1.15:101653) Avail: NTIS HC A06/MF A01 CSCL 04B

Maps and tables are presented which show 45 satellite derived physical, radiation, or cloud parameters from ISCCP CX tapes during the FIRE/SRB Wisconsin experiment region from October 14 through November 2, 1986. Pixel locations selected for

presentation are for an area which coincided with a 100 x 100 km array of evenly spaced ground truth sites. Area-averaged parameters derived from the ISSCP data should be consistent with area averages from the groundtruth stations. Author

N89-28994# World Meteorological Organization, Geneva (Switzerland).
THE WMO LONG-TERM PLAN OVERALL POLICY AND STRATEGY 1988-1997: SECOND WMO LONG-TERM PLAN, PART 1
1987 102 p
(WMO-690-Pt-1; ISBN-92-63-10690-8; ETN-89-94929) Copyright Avail: NTIS MF A01; print copy available from World Meteorological Organization, Case Postale No. 5, CH-1211 Geneva 20, Switzerland

The members of the World Meteorological Organization (WMO) define the overall policy and strategy of the organization and outline the main long term objectives of WMO programs for the coming decade, including, world weather watch, world climate, applications of meteorology, hydrology and water resources, education and training, and technical cooperation. ESA

N89-28995# World Meteorological Organization, Geneva (Switzerland).
THE WORLD WEATHER WATCH PROGRAM 1988-1997: SECOND WMO LONG-TERM PLAN, PART 2, VOLUME 1
1987 240 p
(WMO-691-Pt-2-Vol-1; ISBN-92-63-10691-6; ETN-89-94930) Copyright Avail: NTIS MF A01; print copy available from World Meteorological Organization, Case Postale No.5, CH-1211 Geneva 20, Switzerland

The members of the World Meteorological Organization (WMO) define the overall policy and strategy of the organization and outline the main long term objectives of WMO programs for the coming decade. Details of the world weather watch program are given, including descriptions of the global data processing system, the global observing system, the global telecommunication system, data management, support activities, and coordination. ESA

N89-28996# World Meteorological Organization, Geneva (Switzerland).
THE WORLD CLIMATE PROGRAM 1988-1997: SECOND WMO LONG-TERM PLAN, PART 2, VOLUME 2
1987 83 p
(WMO-692-Pt-2-Vol-2; ISBN-92-63-10692-4; ETN-89-94931) Copyright Avail: NTIS MF A01; print copy available from World Meteorological Organization, Case Postale No. 5, CH-1211 Geneva 20, Switzerland

The members of the World Meteorological Organization (WMO) define the overall policy and strategy of the organization and outline the main long term objectives of WMO programs for the coming decade. Details of the world climate program are given, including descriptions of the objectives, the climate applications program, the climate impact studies program and the world climate research program. ESA

N89-28997# World Meteorological Organization, Geneva (Switzerland).
THE WMO RESEARCH AND DEVELOPMENT PROGRAM 1988-1997: SECOND WMO LONG-TERM PLAN, PART 2, VOLUME 3
1987 51 p
(WMO-693-Pt-2-Vol-3; ISBN-92-63-10693-2; ETN-89-94932) Copyright Avail: NTIS MF A01; print copy available from World Meteorological Organization, Case Postale No. 5, CH-1211 Geneva 20, Switzerland

The member of the World Meteorological Organization (WMO) define the overall policy and strategy of the organization and outline the main long term objectives of WMO programs for the coming decade. Details of research and development program are given, including descriptions of specific programs on weather prediction research, long range forecasting, tropical meteorology research, environmental pollution and cloud physics. ESA

N89-28998# World Meteorological Organization, Geneva (Switzerland).
THE WMO APPLICATIONS OF METEOROLOGY PROGRAM 1988-1997: SECOND WMO LONG-TERM PLAN, PART 2, VOLUME 4
1987 115 p
(WMO-694-Pt-2-Vol-4; ISBN-92-63-10694-0; ETN-89-94933) Copyright Avail: NTIS MF A01; print copy available from World Meteorological Organization, Case Postale No. 5, CH-1211 Geneva 20, Switzerland

The members of the World Meteorological Organization (WMO) define the overall policy and strategy of the organization and outline the main long term objectives of WMO programs for the coming decade. The detailed plans for applications of meteorology programs are presented, including the agricultural meteorology program, the aeronautical program, and the marine meteorology and associated oceanographic programs. ESA

N89-28999# International Meteorological Inst., Stockholm (Sweden).
[ACTIVITIES REPORT IN METEOROLOGY IN SWEDEN] Annual Report, Jul. 1987 - Jun. 1988
Dec. 1988 52 p
(AR-87-88; ISSN-0349-0068; ETN-89-94939) Avail: NTIS HC A04/MF A01

Research activities at the International Meteorological Institute in Stockholm are reported. The work is organized into four sections: (1) dynamic meteorology and geophysical fluid dynamics; (2) chemical meteorology and biogeochemistry; (3) atmospheric physics; and (4) atmospheric aerosol science. ESA

N89-29000# Office National d'Etudes et de Recherches Aerospatiales, Paris (France).
ANALYSIS OF THE VHF-UHF ELECTROMAGNETIC RADIATION OF LIGHTNING: APPLICATION TO A MODEL OF THE NEGATIVE STEPPED-LEADER PROPAGATION Ph.D. Thesis - Paris VI Univ.
Isabelle Taudiere 1989 165 p In FRENCH; ENGLISH summary Original report will also be announced as translation (ESA-TT-1172)
(ONERA-NT-1989-1; ISSN-0078-3781; ETN-89-95293) Avail: NTIS HC A08/MF A01

The space and time characteristics of the VHF-UHF radiation of lightning is analyzed on the basis of the 300 MHz emission sources, localized in three dimensions by interferometric measurements. The main phases that contribute to the development of intra-cloud lightning are examined in detail, also using the electric field measurements at a lower frequency. This research is complemented by an experimental and theoretical analysis of long-discharge (8 m) radio emissions generated in both polarities in the laboratory. These investigations have revealed that the VHF radiation is associated with the channel reillumination phase accompanying each step in the negative spark. This research resulted in the creation of a simple model of the negative leader propagation. The current and the field radiated during this phase of the discharge are computed according to an electrical representation using the physical laws of variation of resistance. The extrapolation of these results to the stepped leader of natural lightning are discussed. ESA

48 OCEANOGRAPHY

Includes biological, dynamic, and physical oceanography; and marine resources.

For related information see also *43 Earth Resources and Remote Sensing.*

N89-29001# Delaware Univ., Newark. Dept. of Mathematical Sciences.
PROPAGATION PROBLEM AND FAR-FIELD PATTERNS IN A STRATIFIED FINITE DEPTH OCEAN
R. P. Gilbert and Yongzhi Xu Feb. 1989 21 p

(Grant NA86AA-D-SG040)
(PB89-180707; DEL-SG-06-89) Avail: NTIS HC A03/MF A01 CSCL 08C

The direct, or propagation, problem associated with the scattering of a plane wave off of a submerged body is investigated. It assumes that the body is contained in an ocean of finite, constant depth. The index of refraction is assumed to be dependent only on the depth. Author

N89-29002# Naval Postgraduate School, Monterey, CA. Dept. of Oceanography.
A NUMERICAL STUDY OF A MESOSCALE EDDY INTERACTION WITH AN OCEAN FRONT IN THE MARGINAL ICE ZONE M.S. Thesis
Rutledge P. Lumpkin Mar. 1989 97 p
(AD-A209192) Avail: NTIS HC A05/MF A01 CSCL 08/12

The East Greenland Current and its associated marginal ice zone is a region of intense dynamic activity. A two layer, primitive equation, numerical model is used to simulate an eddy-jet interaction in the East Greenland marginal ice zone region. The effects of wind direction, topography, and sense of eddy rotation on the eddy-jet interaction are examined to determine the seaward ice transport, icebanding, and dipole formation. It is determined that an anticyclone (15 cm/s) interacting with a jet (30 cm/s) will develop a dipole that advects ice away from the ice edge. The dipole formation and ice advection away from the ice edge is not seen for a cyclone-jet interaction. It is also seen that a jet with no winds flowing parallel to the ice edge will create an iceband due to the cross ice edge Ekman transport. The interaction of both the cyclone and anticyclone with the jet creates downstream perturbations in the jet leading to a sinuous ice edge. Winds greater that 10 m/s dominate the ice dynamics over that induced by the ocean flow fields. GRA

N89-29003# Planning Systems, Inc., McLean, VA.
PRELIMINARY NEURAL NETWORK DETECTION OF A GULF STREAM IN IMAGES OF SEA SURFACE TEMPERATURE GRADIENTS, PHASE 1 Final Report, 30 Sep. 1988 - 30 Mar. 1989
Eugene J. Molinelli and Michael J. Flanigan 28 Apr. 1989 38 p Prepared for Office of Naval Research, Arlington, VA
(AD-A207801; PSI-TR-477421) Avail: NTIS HC A03/MF A01 CSCL 08/3

A concept is tested for automatically identifying Gulf Stream surface temperature gradients among the myriad fronts discernable as edges in satellite infrared imagery. The concept is to use the techniques of neural networks in concert with a principal component climatology of Gulf Stream axes. Sample neural networks were constructed that successfully produced mode coefficients for the first three components for a large set of well defined Gulf Streams. One network, operating on a jumble of edges from a real composite sea surface temperature image, produced a 3-mode Gulf Stream sufficiently close to the actual Gulf Stream edges as to hold promise for identifying the Gulf Stream's gradients automatically. GRA

N89-29004# Coastal Engineering Research Center, Vicksburg, MS.
HURRICANE HINDCAST METHODOLOGY AND WAVE STATISTICS FOR ATLANTIC AND GULF HURRICANES FROM 1956 - 1975 Final Report
Charles E. Abel, Barbara A. Tracy, C. L. Vincent, and Robert A. Jensen Apr. 1989 85 p
(AD-A207849; CERC-WIS-19) Avail: NTIS HC A05/MF A01 CSCL 08/3

Ocean wave conditions at locations along the U.S. Atlantic and Gulf of Mexico coastlines are hindcast during hurricanes occurring between 1956 and 1975. A total of 68 hurricanes occurred in the period, 43 affecting the Atlantic coast and 25 the gulf coast. The hindcast method is discussed and verification presented for storms where observations are available. Results are presented as the highest wave occuring at each location and significant wave height versus return period for each location. GRA

N89-29005# Woods Hole Oceanographic Institution, MA.
ENTRAINMENT AND HOMOGENIZATION OF A PASSIVE TRACER IN A NUMERICAL MODEL GYRE
Robert S. Pickart 15 Jun. 1988 15 p Submitted for publication
(Contracts N00014-76-C-0197; N00014-84-C-0132; N00014-82-C-0019; N00014-85-C-0001)
(AD-A208020; WHOI-CONTRIB-6517) Avail: NTIS HC A03/MF A01 CSCL 08/3

The mechanism by which tracer is entrained into a spatially decaying gyre from an external source is examined, as well as the homogenization which subsequently occurs. A simple advective-diffuse numerical model is used whose streamlines consist of a elongated gyre situated beside a distinct boundary current, which inputs tracer into the domain. This is meant to represent the deep cyclonic recirculation of the Gulf Stream and adjacent deep western boundary current. A shear flow analysis shows that two parameters indicate the manner in which a tracer penetrates across streamlines of the gyre: a peclet number and a parameter which measures the strength of the cross-stream shear. The large values of these parameters cause a plume of tracer to spiral inward toward the center of the gyre. At steady state the tracer which has accumulated in the gyre becomes homogenized. The size of this uniform area is related to the extent to which the spiral penetrated the gyre and decreases with increasing diffusivity, as several examples illustrate. GRA

N89-29006# Technische Univ., Delft (Netherlands). Faculty of Geodesy.
SEA GRAVIMETRY AND EOTVOS CORRECTION
J. H. M. Smit May 1988 77 p
(Rept-88.3; ETN-89-95429) Avail: NTIS HC A05/MF A01

A physical model for sea gravimetry, which includes the Eotvos effect, is derived. An error model for sea gravimetry, which includes Eotvos correction errors, cross coupling errors and off level errors is shown. The possibilities of obtaining ship velocity estimates with high accuracy by using the Global Positioning System (GPS) pseudorange code measurements and carrier phase measurements are investigated. An analysis of Eotvos corrections computer from velocity measurements is given. Data collected at the North Sea in the period from April 21 to May 13, 1986 is considered. The comparison of Eotvos corrections compound with ship velocity estimates from GPS pseudorange measurements, Doppler smoothed pseudorange measurements, carrier phase measurements and Syledis and Hyperfix positions shows no discrepancies. Best results are obtained from the GPS Doppler smoothed pseudorange method and show that the GPS is a promising development for sea gravimetry. ESA

51 LIFE SCIENCES (GENERAL)

No abstracts in this category.

52 AEROSPACE MEDICINE

Includes physiological factors; biological effects of radiation; and effects of weightlessness on man and animals.

N89-29007# Los Alamos National Lab., NM. Neuromagnetism Lab.
MONTE CARLO ANALYSIS OF LOCALIZATION ERRORS IN MAGNETOENCEPHALOGRAPHY
Patricia A. Medvick, Paul S. Lewis, Cheryl Aine, and Edward R. Flynn 1989 5 p Presented at the 7th International Conference on Biomagnetism, New York, NY, 14-18 Aug. 1989
(Contract W-7405-eng-36)

(DE89-013221; LA-UR-89-1579; CONF-890849-2) Avail: NTIS HC A02/MF A01

In magnetoencephalography (MEG), the magnetic fields created by electrical activity in the brain are measured on the surface of the skull. To determine the location of the activity, the measured field is fit to an assumed source generator model, such as a current dipole, by minimizing chi-square. For current dipoles and other nonlinear source models, the fit is performed by an iterative least squares procedure such as the Levenberg-Marquardt algorithm. Once the fit has been computed, analysis of the resulting value of chi-square can determine whether the assumed source model is adequate to account for the measurements. If the source model is adequate, then the effect of measurement error on the fitted model parameters must be analyzed. Although these kinds of simulation studies can provide a rough idea of the effect that measurement error can be expected to have on source localization, they cannot provide detailed enough information to determine the effects that the errors in a particular measurement situation will produce. In this work, we introduce and describe the use of Monte Carlo-based techniques to analyze model fitting errors for real data. Given the details of the measurement setup and a statistical description of the measurement errors, these techniques determine the effects the errors have on the fitted model parameters. The effects can then be summarized in various ways such as parameter variances/covariances or multidimensional confidence regions. DOE

N89-29008# Los Alamos National Lab., NM. Life Sciences Div.
TRANSIENT VISUAL EVOKED NEUROMAGNETIC RESPONSES: IDENTIFICATION OF MULTIPLE SOURCES
Cheryl Aine, J. George, Patricia A. Medvick, E. Flynn, I. Bodis-Wollner, and S. Supek 1989 5 p Presented at the 7th International Conference on Biomagnetism, New York, NY, 14-18 Aug. 1989
(Contract W-7405-eng-36)
(DE89-013438; LA-UR-89-1729; CONF-890849-1) Avail: NTIS HC A02/MF A01

Neuromagnetic measurements and associated modeling procedures must be able to resolve multiple sources in order to localize and accurately characterize the generators of visual evoked neuromagnetic activity. Workers have identified at least 11 areas in the macaque, throughout occipital, parietal, and temporal cortex, which are primarily or entirely visual in function. The surface area of the human occipital lobe is estimated to be 150 to 250 cm. Primary visual cortex covers approximately 26 sq cm while secondary visual areas comprise the remaining area. For evoked response amplitudes typical of human MEG data, one report estimates that a two-dipole field may be statistically distinguishable from that of a single dipole when the separation is greater than 1 to 2 cm. Given the estimated expanse of cortex devoted to visual processes, along with this estimate of resolution limits it is likely that MEG can resolve sources associated with activity in multiple visual areas. Researchers have noted evidence for the existence of multiple sources when presenting visual stimuli in a half field; however, they did not attempt to localize them. Numerous human MEG field patterns were examined resulting from different visual field placements of a small sinusoidal grating which suggest the existence of multiple sources. The analyses utilized for resolving multiple sources in these studies differ depending on whether there was evidence of: (1) synchronous activation of two spatially discrete sources, or (2) two discrete asynchronous sources. In some cases observed field patterns were observed which appear to be adequately explained by a single source changing its orientation and location across time. DOE

N89-29009# Army Research Inst. of Environmental Medicine, Natick, MA.
THERMOREGULATORY COMPETENCE DURING EXERCISE TRANSIENTS IN A GROUP OF HEAT-ACCLIMATED YOUNG AND MIDDLE-AGED MEN IS INFLUENCED MORE DISTINCTLY BY MAXIMAL AEROBIC POWER THAN AGE
Richard R. Gonzalez and Kent B. Pandolf May 1989 7 p
(AD-A209753; USARIEM-M48-89) Avail: NTIS HC A02/MF A01 CSCL 06/10

A fundamental change that occurs with advancing age is a diminishing maximal aerobic power (VO2 max). In sedentary individuals the rate of decline in VO2 max as a function of age is estimated at 10 percent per ten years after age 20 but becomes more gradual in endurance-trained individuals regardless of gender, approaching about 5 percent with each ten year span. It is thought that reduced sweating and vasomotor responses to heat stress indicate deterioration in thermoregulatory function. A scrutiny of thermoregulatory mechanisms in the aging process is necessary because other quantitative studies of actual efferent thermoregulatory drive point to a maintenance of thermoregulatory competence well into the sixth decade of life provided a level of aerobic fitness is sustained. Pandolf and others studied a group of nine young and nine middle-aged men having parallel body weights, skin surface areas, percent body fat and maximal aerobic power. These groups displayed almost equivalent thermoregulatory responses to comparable exercise and heat stress conditions following 10-days of heat acclimation. The present paper is an examination of the above study's thermoregulatory responses during exercise transients. Transient analysis to specific exercise/heat stress provocation provides a clearer understanding of the influence of age and aerobic fitness on thermoregulatory control of sweating than steady-state analysis. GRA

N89-29010# Vision Sciences Research Corp., San Ramon, CA.
SUPRATHRESHOLD CONTRAST SENSITIVITY VISION TEST CHART Annual Progress Report
Arthur P. Ginsburg 15 Jun. 1989 26 p
(Contract F49620-88-C-0083)
(AD-A209915) Avail: NTIS HC A03/MF A01 CSCL 06/4

This research period concentrated on the further design and development of a suprathreshoid contrast sensitivity test chart with which to create a family of contrast matching functions. Three different chart configurations were developed and tested for suitability. Preliminary test-retest, subject instruction, and chart configuration experiments were completed. The results show good test-retest reliability. Individual differences in contrast matching using previously developed suprathreshold contrast sensitivity charts are also evident in these new data. Different subject instructions having the subjects either make the contrast judgements using global or local contrast analysis resulted in similar results. The spatial positioning of grating test patches appears to bias the contrast matches and warrants further investigation. Future research will finalize the suprathreshold contrast sensitivity chart configuration and compare the resulting contrast matching data to that obtained using a computer-video system and continuous contrast test increments. The final chart will be used for large population, clinical and performance testing. GRA

N89-29011# Harvard Univ., Cambridge, MA.
COMPONENTS OF HIGH-LEVEL VISION: A COGNITIVE NEUROSCIENCE ANALYSIS AND ACCOUNTS OF NEUROLOGICAL SYNDROMES Annual Report, Dec. 1987 - Dec. 1988
Stephen M. Kosslyn 28 Feb. 1989 89 p
(Grant AF-AFOSR-0012-88; AF Proj. 2313)
(AD-A207848; TR-89-1; AFOSR-89-0628TR) Avail: NTIS HC A05/MF A01 CSCL 12/9

High level visual processes make use of stored information, and are invoked during object identification, navigation, tracking, and visual mental imagery. A theory of the component processing subsystems used in high level vision is examined. This theory was developed by considering neuroanatomical, neurophysiological, and computational constraints. The theory has led to three kinds of empirical work: First, specific claims associated with individual processing subsystems were tested. For example, the analysis of the representation of spatial relations led to the prediction that two subsystems are used to encode this information, and a set of experiments was conducted that provided support for this distinction. Second, predictions from the theory as a whole were formulated, and some of these predictions are now being tested.

And third, the subsystems were implemented in a running computer simulation model, which was used to generate predictions about specific neurological syndromes. The model can be damaged in a variety of ways, and its performance on a set of tasks then observed. The experiments conducted to data and predictions from the computer model are summarized. In addition, the most common dysfunctions of vision following brain damage are reviewed, and accounts are offered by reference to the simulation model. GRA

N89-29012# Letterman Army Inst. of Research, San Francisco, CA.
TRANSIENT VISUAL EFFECTS OF PROLONGED SMALL SPOT FOVEAL LASER EXPOSURE Report, Jan. - Mar. 1989
Harry Zwick, David O. Robins, and Nawim Magsood Mar. 1989 19 p
(AD-A207945; LAIR-373) Avail: NTIS HC A03/MF A01 CSCL 06/7

In recent experiments, the effects were evaluated of acute, threshold damage levels of small spot foveal laser exposure. These experiments revealed transient changes in acuity and contrast sensitivity lasting from 10 to 15 minutes postexposure. Following recovery from such effects, normal acuity and contrast sensitivity are not necessarily degraded, although continuous exposure at these levels does result in parafoveal compensation for foveal damage and eventual deficit in fine visual acuity. Development of a test of foveal function during and after small spot foveal exposure was the primary objective of this investigation. This objective was accomplished. At retinal damage levels, only a small focal foveal lesion was observed indicating the ability to utilize the fovea during such exposure. Postexposure recovery effects analyzed for target size and contrast conditions suggest retinal and possibly cortical saturation processes. GRA

N89-29013# Army Command and General Staff Coll., Fort Leavenworth, Kansas. School of Advanced Military Studies.
SLEEP DEPRIVATION AND ITS EFFECT ON COMBAT EFFECTIVENESS Report, 1988 - 1989
Clinton T. Anderson 26 Nov. 1988 46 p
(AD-A207970) Avail: NTIS HC A03/MF A01 CSCL 06/10

The effects of sleep loss on the combat effectiveness of the US Army's leaders and soldiers were examined. It begins with an examination of U.S. and Soviet doctrine for conducting continuous operations. This section discusses the doctrinal methods and procedures that both major powers employ to maintain continuous pressure on their opponent. After laying the theoretical groundwork, it then examines the changes that have occurred in tactical force design since World War 2 to determine what was done to enhance or degrade the ability to execute that doctrine. After this discussion on the mechanical aspect of combat, the paper discusses the effects of sleep loss on units and the individual soldier. It concludes that the U.S. Army currently has no doctrine for the conduct of combat over an extended period of time. Adequate doctrine was provided for the conduct of operations in periods of both limited and unlimited visibility, but the doctrine necessary to transition to continuous operations is not available. Furthermore, recent changes in the force structure of combat units (primarily Armor and Mechanized Infantry) have significantly reduced the redundancy and robustness in those units that is necessary to conduct continuous operations. During continuous operations, the units will be effected by loss of sleep. Sleep deprivation affects the cognitive skills of the leaders greater than the physical skills of the soldiers. GRA

N89-29014# Brigham and Women's Hospital, Boston, MA.
A PROGRAM FOR THE STUDY OF SKELETAL MUSCLE CATABOLISM FOLLOWING PHYSICAL TRAUMA Annual Report, 21 Feb. 1988 - 20 Feb. 1989
Douglas W. Wilmore 15 Mar. 1989 10 p
(Contract DAMD17-86-C-6157; DA Proj. 351-62772-A-874)
(AD-A207983; AD-E951354) Avail: NTIS HC A02/MF A01 CSCL 06/5

Following injury or infection there is accelerated net breakdown of skeletal muscle protein associated with negative nitrogen balance. A variety of factors influence this response, including food intake, inactivity and the hormonal environment. In studies that control for food intake and exercise, infusion of the catabolic hormones causes negative nitrogen balance but does not account for the accelerated proteolysis that occurs following moderate to severe injury. The recent recognition that injured tissue or invasive infection stimulates the production of a variety of cytokines has caused a variety of investigators to hypothesize that these mediators may serve as the signal to accelerate skeletal muscle proteolysis. Some of the initial in vitro studies have suggested that increased skeletal muscle protein breakdown may be simulated by activation of the cyclooxygenase pathway. Others have presented data which demonstrates that proteolysis may continue even when prostinoid mechanisms are not activated. Infusion of Prostaglandin E2 (PGE2) into the single hind leg of the dog failed to stimulate the increased release of amino acids. Additional animals underwent lumbar sympathectomy and then sympathetic nerve stimulation. Following sympathectomy, leg blood flow increased, and with stimulation leg blood flow returned toward control values. Glucose Flux did not change in either leg throughout the study and was similar in both hind limbs. Amino acid analysis is presently in process. GRA

N89-29015# Defence and Civil Inst. of Environmental Medicine, Downsview (Ontario).
CANADIAN FORCES AIRCREW EJECTION, DESCENT, AND LANDING INJURIES, 1 JANUARY 1975 - 31 DECEMBER 1987
Wayne R. Sturgeon Jan. 1989 21 p
(AD-A208116; DCIEM-88-RR-56) Avail: NTIS HC A03/MF A01 CSCL 06/10

During the 13 year period from January 1975 through December 1987, there were 78 attempted ejections from Canadian Forces (CF) aircraft of which 67 were successful. Fifty-eight of these ejectees received injuries from four main causative mechanisms: harness (restraint and parachute), body contact with cockpit surroundings during ejection, windblast force, and ejection acceleration force. Nineteen individuals (28.3 percent) received major injuries (dislocations, fractures, connective tissue injury, and organ contusion) from ejection jolt, windblast flail, collision with the seat structure, and landing. Fourteen of these individuals (20.9 percent) suffered fractured vertebrae, six (8.7 percent) during ejection and eight (12.2 percent) during landing. Minor injuries were primarily superficial abrasions, contusions, and lacerations. The majority of these were caused by the harness system (ballistic inertia reel yoke and parachute saddle), followed by windblast pressure on the helmet and oxygen mask, and lastly, contact with cockpit surroundings during ejection. Aircrew factors that contributed to injury were: improper position on ejection, loose restraint system and parachute harness, loose oxygen mask and helmet, and failure to release the seat pack prior to landing. GRA

N89-29016*# National Aeronautics and Space Administration. Ames Research Center, Moffett Field, CA.
MUSCLE CHANGES WITH ECCENTRIC EXERCISE: IMPLICATIONS ON EARTH AND IN SPACE
Alan R. Hargens, Scott Parazynski, Michael Aratow, and Jan Friden (Umea Univ., Sweden) Aug. 1989 17 p Presented at the International Society for Myochemistry Meeting, Nice, France, 12-14 Oct. 1989 Sponsored by Swedish Medical Research Council; Tore Nilsson Foundation; Swedish Sports Research Council
(Contract NIH-AM-25501)
(NASA-TM-102227; A-89224; NAS 1.15:102227) Avail: NTIS HC A03/MF A01 CSCL 06P

Recent investigations of fluid pressure, morpholo gy, and enzyme activities of skeletal muscle exercised eccentrically or concentrically in normal human subjects are reviewed. Intramuscular pressures were measured before, during, and after submaximal exercise and correlated with subjective muscle soreness, fiber size, water content, and blood indices of muscle enzymes. High intensity eccentric exercise is characterized by post exercise pain, elevated intramuscular pressures, and swelling of both type 1 and 2 fibers as compared to concentric exercise.

Thus, long periods of unaccustomed, high level eccentric contraction may cause muscle injury, fiber swelling, fluid accumulation, elevated intramuscular pressure, and delayed muscle soreness. Training regimens of progressively increasing eccentric exercise, however, cause less soreness and are extremely efficacious in increasing muscle mass and strength. It is proposed that on Earth, postural muscles are uniquely adapted to low levels of prolonged eccentric contraction that are absent during weightlessness. The almost complete absence of eccentric exercise in space may be an important contributor to muscle atrophy and therefore equipment should be designed to integrate eccentric contractions into exercise protocols for long-term spaceflight. Author

N89-29017*# National Aeronautics and Space Administration. Lyndon B. Johnson Space Center, Houston, TX.
VISUAL SUPPRESSION OF THE VESTIBULO-OCULAR REFLEX DURING SPACE FLIGHT
John J. Uri, William E. Thornton, Thomas P. Moore (Methodist Hospital, Indianapolis, IN.), and Sam L. Pool Aug. 1989 14 p
(NASA-TM-102157; S-598; NAS 1.15:102157) Avail: NTIS HC A03/MF A01 CSCL 06P

Visual suppression of the vestibulo-ocular reflex was studied in 16 subjects on 4 Space Shuttle missions. Eye movements were recorded by electro-oculography while subjects fixated a head mounted target during active sinusoidal head oscillation at 0.3 Hz. Adequacy of suppression was evaluated by the number of nystagmus beats, the mean amplitude of each beat, and the cumulative amplitude of nystagmus during two head oscillation cycles. Vestibulo-ocular reflex suppression was unaffected by space flight. Subjects with space motion sickness during flight had significantly more nystagmus beats than unaffected individuals. These susceptible subjects also tended to have more nystagmus beats before flight. Author

N89-29018# Southampton Univ. (England). Inst. of Sound and Vibrational Research.
A STUDY OF THE EFFECT OF STIMULUS UPON THE REFLEX RESPONSE AS ELICITED AND RECORDED BY THE TYMPANIC MEMBRANE DISPLACEMENT MEASUREMENT DEVICE
S. M. Moss, R. J. Marchbanks, and A. M. Martin Mar. 1989 71 p Sponsored by the Action Research for the Crippled Child and the Medical Research Council, United Kingdom
(ISVR-TR-177; ETN-89-95531) Avail: NTIS HC A04/MF A01

The possibility of using a ramp stimulus to obtain the reflex response as measured by the Tympanic Membrane Displacement (TMD) technique is investigated. Three reflex growth functions produced from three stimuli used upon the same individual are constructed. The first growth function is constructed using three intensities of the routinely used stimulus. The second using just the response to the routinely used stimulus at 115 decibels sound pressure level, and the third an intensity ramp stimulus. The ramp stimulus is repeated, and two analysis techniques are used upon both results. The study leads to the conclusion that the decision as to whether a ramp stimulus can be used to elicit the reflex depends on the experience of the tester to interpret the reflex response. If the test is to be performed by inexperienced operators, then it is better that three separate reflex responses are obtained. ESA

53 BEHAVIORAL SCIENCES

Includes psychological factors; individual and group behavior; crew training and evaluation; and psychiatric research.

N89-29019# Air Force Human Resources Lab., Brooks AFB, TX.
PREVENTION, REDUCTION, AND MEASUREMENT OF COMBAT STRESS REACTIONS: A BIBLIOGRAPHY Interim Paper May 1986 - Nov. 1988
Cheryl L. Batchelor Jun. 1989 17 p
(AD-A209375; AFHRL-TP-88-61) Avail: NTIS HC A03/MF A01 CSCL 05/8

The Combat Logistics Branch of the Air Force Human Resources Laboratory's Logistics and Human Factors Division is tasked with developing programs and methods which will enhance aircraft maintenance performance in peacetime as well as in combat environments. This focus on aircraft maintenance is the real lifeline of the Air Force because without effective and efficient aircraft maintenance, the routine maintenance tasks, as well as troubleshooting repairs, would not be accomplished. If routine maintenance and troubleshooting repairs were not accomplished, the required combat sortie generation rate would not be achieved. If the required combat sortie generation rate were not achieved, then U.S. air superiority could not be attained. This bibliography lists source documents relevant to combat stress. While this list is certainly not all-inclusive, the documents listed served as a basis for current research efforts in the area of combat stress. Other areas are also important, but these areas have been studied extensively. Aircraft maintenance personnel are tasked to repair the aircraft and let someone else take care of the enemy. A similar situation exists for other support personnel as well. As this bibliography illustrates, there is very little information available on the peacetime stresses of aircraft maintenance personnel. Information about their reactions in combat is even scarcer. GRA

N89-29020*# Massachusetts Inst. of Tech., Cambridge. Space Systems Lab.
SPACECRAFT FLIGHT SIMULATION: A HUMAN FACTORS INVESTIGATION INTO THE MAN-MACHINE INTERFACE BETWEEN AN ASTRONAUT AND A SPACECRAFT PERFORMING DOCKING MANEUVERS AND OTHER PROXIMITY OPERATIONS
Adam R. Brody Sep. 1988 97 p
(Grant NAGw-21)
(NASA-CR-177502; NAS 1.26:177502) Avail: NTIS HC A05/MF A01 CSCL 05I

The anticipated increase in rendezvous and docking activities in the various space programs in the Space Station era necessitates a renewed interest in manual docking procedures. Ten test subjects participated in computer simulated docking missions in which the influence of initial velocity was examined. All missions started from a resting position of 304.8 meters (1000 feet) along the space station's +V-bar axis. Test subjects controlled their vehicle with a translational hand controller and digital auto pilot which are both virtually identical to their space shuttle counterparts. While the 0.1 percent rule (range rate is equal to 0.1 percent of the range) used by space shuttle pilots is comfortably safe, it is revealed to be extremely inefficient in terms of time and not justifiable in terms of marginal safety. Time is worth money, not only because of training and launch costs, but because the sooner a pilot and spacecraft return from a mission, the sooner they can begin the next one. Inexperienced test subjects reduced the costs of simulated docking by close to a factor of 2 and achieved safe dockings in less than 4 percent of the time the baseline approach would entail. This reduction in time can be used to save lives in the event of an accident on orbit, and can tremendously reduce docking costs if fuel is produced from waste water on orbit. Author

54 MAN/SYSTEM TECHNOLOGY AND LIFE SUPPORT

Includes human engineering; biotechnology; and space suits and protective clothing.

For related information see also *16 Space Transportation.*

N89-29021# Human Engineering Labs., Aberdeen Proving Ground, MD.
CHOICE AND PERCEIVED CONTROL: IMPLICATIONS FOR THE DESIGN OF DISPLAYS Final Report
Richard A. Monty and Lawrence C. Perlmuter (Veterans Administration Learning and Memory Center, Boston, MA.) Apr. 1989 21 p
(AD-A208400; HEL-TN-5-89) Avail: NTIS HC A03/MF A01 CSCL 23/2

This report summarizes several years of research on how offering subjects a choice of task parameters leads to a perception of control over their environment, which in turn can lead to improved task performance. The development of a theoretical explanation of the phenomenon is traced, and implications for the design of displays are deduced and illustrated with hypothetical examples. GRA

N89-29022# Aerospace Medical Research Labs., Wright-Patterson AFB, OH.
INVESTIGATION OF A LINEAR SYSTEMS MODEL FOR HUMAN VISUAL DETECTION AND SPATIAL FREQUENCY DISCRIMINATION Final Report, Oct. 1986 - Dec. 1988
Harold S. Merkel Dec. 1988 55 p
(AD-A209397; AAMRL-TR-88-061) Avail: NTIS HC A04/MF A01 CSCL 06/4

This research investigated the application of a linear systems model to two parameters of vision: the contrast threshold and the spatial frequency difference threshold. The contrast threshold is the contrast of a target when an observer is just able to detect its presence. The spatial frequency difference threshold is the smallest difference in spatial frequency that permits two grating targets to be distinguished. The model investigated was for observation with a fixed visual field size of one-dimensional, time-invariant sinusoidal grating targets. A mathematical development indicated that a linear model could be used to represent the human spatial frequency difference threshold function. The model was implemented using an electro-optical hardware system which consisted of a charge-coupled device video camera, a frame grabber, and a personal computer. Because of its similarities to the structure of the eye, linear response, and ability to acquire digital image data, a charge coupled device array video camera and frame grabber were used to simulate the eye. The action of the neural pathways and visual cortex was simulated by Fourier transform computations on the camera and frame grabber output. The experimental data from the electro-optical hardware system agreed with the theoretical models for both parameters. GRA

N89-29023# Naval Postgraduate School, Monterey, CA.
HUMAN FACTORS EVALUATION OF COLOR USE IN THE TARGET DATA PROCESSOR RELEASE 10 (TDP R10) M.S. Thesis
Claudia J. Schmidly Mar. 1989 64 p
(AD-A209438) Avail: NTIS HC A04/MF A01 CSCL 09/5

Color is provided as guidelines for static military CRT display formats. A total of 13 guidelines are discussed, relating to color as a coding dimension, the quantity of colors to include, selection of colors to use, ambient luminesce, display legibility and readability, human color deficiencies, and operator fatigue. Guidelines are then applied to the operator-machine interface of the U.S. Navy's Target Data Processor Release 10 (TDP R10), a tactical computer workstation for use in the Integrated Undersea Surveillance System. Specific color related design recommendations are included for the TDP R10 alphanumeric and geographic display screens with the goal of enhancing user performance. Since the TDP R10 is being developed using an iterative design process (design, test, redesign, etc.), test and evaluation considerations also are discussed at length. Various types of user self-support techniques are discussed, along with user performance testing, sample sizes, and data analysis procedures. GRA

N89-29024# Army Cold Regions Research and Engineering Lab., Hanover, NH.
PRELIMINARY DESIGN GUIDE FOR ARCTIC EQUIPMENT
Michael R. Walsh and James S. Morse May 1989 38 p
(AD-A209455; CRREL-SR-89-13) Avail: NTIS HC A03/MF A01 CSCL 08/12

Designing equipment for arctic environments requires special considerations from the design engineer. Low temperatures and harsh environments place special demands on equipment and components. Many materials in common use will experience drastic changes in physical properties, resulting in catastrophic failure of the systems in which they are incorporated. Components may no longer meet original specifications, and instrumentation may not work properly. This design guide should familiarize the design engineer with the factors that must be considered when designing for the Arctic environment. A list of environmental factors and how they may affect a design is first presented. Then, a general design procedure is presented and a detailed analysis of problems and solutions for materials, components and systems follows. GRA

N89-29025# Anthropology Research Project, Yellow Springs, OH. Science and Advanced Technology Directorate.
ANTHROPOMETRIC SURVEY OF US ARMY PERSONNEL: SUMMARY STATISTICS Interim Technical Report, 1987 - 1988
Claire C. Gordon, Thomas Churchill, Charles E. Clauser, Bruce Bradtmiller, John T. McConville, Ilse Tebbets, and Robert A. Walker Mar. 1989 336 p
(Contract DAAK60-86-C-0128)
(AD-A209600; NATICK-TR-89/027) Avail: NTIS HC A15/MF A01 CSCL 05/9

Results of the 1987 to 1988 anthropometric survey of Army personnel are presented in the form of summary statistics and percentile data. These anthropometric data are presented for a subset of personnel (1774 men and 2208 women) sampled to match the proportions of age categories and racial/ethnic groups found in the active duty Army of June, 1988. Dimensions included in this report include 132 standard measurements made in the course of the survey, 60 derived dimensions calculated largely by adding and subtracting standard measurement data, and 48 head and face dimensions reported in traditional linear terms but collected by means of an automated headboard designed to obtain three-dimensional data. Measurement descriptions, visual indices, and a glossary of terms are included to help identify and locate dimensions. GRA

N89-29026# Massachusetts Inst. of Tech., Cambridge. Artificial Intelligence Lab.
A ROBOT THAT WALKS: EMERGENT BEHAVIORS FROM A CAREFULLY EVOLVED NETWORK
Rodney A. Brooks Feb. 1989 15 p
(Contracts N00014-86-K-0685; N00014-85-K-0124)
(AD-A207958; AI-M-1091) Avail: NTIS HC A03/MF A01 CSCL 12/9

Most animals have significant behavioral expertise built in without having to explicitly learn it all from scratch. This expertise is a product of evolution of the organisms; it can be viewed as a very long term form of learning which provides a structured system within which individuals might learn more specialized skills or abilities. This paper suggests one possible mechanism for analogous robot evolution by describing a carefully designed series of networks, each one being a strict augmentation of the previous one, which control a six legged walking machine capable of walking over rough terrain and following a person passively sensed in the infrared spectrum. As the completely decentralized networks are augmented, the robot's performance and behavior repertoire demonstrably improve. The rationale for such demonstrations is

that they may provide a hint as to the requirements for automatically building massive networks to carry out complex sensory-motor tasks. The experiments with an actual robot ensure that an essence of reality is maintained and that no critical disabling problems have been ignored. GRA

N89-29027*# National Aeronautics and Space Administration. Lyndon B. Johnson Space Center, Houston, TX.
METHOD AND APPARATUS FOR BIO-REGENERATIVE LIFE SUPPORT SYSTEM Patent Application
Hatice S. Cullingford, inventor (to NASA) 11 Jul. 1989 34 p
(NASA-Case-MSC-21629-1; NAS 1.71:MSC-21629-1; US-Patent-Appl-SN-378548) Avail: NTIS HC A03/MF A01 CSCL 06K

A life support system is disclosed for human habitation (cabin) which has a bioregenerative capability through the use of a plant habitat (greenhouse) whereby oxygen-rich air from the greenhouse is processed and used in the cabin and carbon dioxide-rich air from the cabin is used in the greenhouse. Moisture from the air of both cabin and greenhouse is processed and reused in both. Wash water from the cabin is processed and reused in the cabin as hygiene water, and urine from the cabin is processed and used in the greenhouse. Spent water from the greenhouse is processed and reused in the greenhouse. Portions of the processing cycles are separated between cabin and greenhouse in order to reduce to a minimum cross contamination of the two habitat systems. Other portions of the processing cycles are common to both cabin and greenhouse. The use of bioregenerative techniques permits a substantial reduction of the total consumables used by the life support system. NASA

55 SPACE BIOLOGY

Includes exobiology; planetary biology; and extraterrestrial life.

No abstracts in this category.

59 MATHEMATICAL AND COMPUTER SCIENCES (GENERAL)

N89-29028*# Institute for Computer Applications in Science and Engineering, Hampton, VA.
VARIATIONAL FORMULATION FOR A NONLINEAR ELLIPTIC EQUATION IN A THREE-DIMENSIONAL EXTERIOR DOMAIN Final Report
Christine Bernardi, Vivette Girault, and Laurence Halpern (Paris Univ., France) Jul. 1989 16 p Submitted for publication
(Contract NAS1-18605)
(NASA-CR-181885; NAS 1.26:181885; ICASE-89-48) Avail: NTIS HC A03/MF A01 CSCL 12A

An existence result was obtained for a nonlinear second-order equation in an exterior domain of IR(3). The proof relies on a variational formulation in weighted Sobolev spaces. Author

60 COMPUTER OPERATIONS AND HARDWARE

Includes hardware for computer graphics, firmware, and data processing.

For components see *33 Electronics and Electrical Engineering.*

N89-29029# Defence Research Establishment Pacific, Victoria (British Columbia).
A COMPAQ-286 MICRO-PROCESSOR BASED HIGH-SPEED HIGH-DENSITY DIGITAL DATA-ACQUISITION AND RECORDING SYSTEM. VOLUME 1: SYSTEM OVERVIEW
K. B. Ashcroft, P. M. Holtham, and K. M. Kobewka (Barrodale Computing Services Ltd., Victoria, British Columbia) Jan. 1989 33 p
(AD-A207429; DREP-TM-88-23-Vol-1) Avail: NTIS HC A03/MF A01 CSCL 12/6

A design is presented for a state-of-the-art high-speed high-density data-acquisition system based on a commercially available COMPAQ-286 microcomputer. The system utilizes an in house developed A/D board, capable of sampling 31 channels (expandable to 62) with 16-bit resolution, and with an aggregate sample rate of 100 kbytes/sec. Data are logged on a Hewlett Packard 9144 digital cassette drive that uses 68 megabyte formatted cassettes. To achieve the required throughput, the software, written in 286-assembler, is interrupt-driven and uses direct memory access on output. The data-acquisition system is described in two volumes, the first giving a system overview, and the second providing sufficient software and hardware for the system to be reproduced. GRA

N89-29030# Colorado Univ., Boulder. Optoelectronic Computing Systems Center.
DIGITAL OPTICAL COMPUTING WITH FIBERS AND DIRECTIONAL COUPLERS
Harry F. Jordan Jan. 1989 8 p Prepared in cooperation with Colorado State Univ., Fort Collins
(Grant NSF CDR-86-22236)
(PB89-184378; OCS-TR-89-01) Avail: NTIS HC A02/MF A01 CSCL 09B

The goal of the Digital Optical Computing program of the Center for Optoelectronic Computing Systems is to design and demonstrate a prototype of a stored program optical computer using the knowledge base developed in connection with electronic digital computers. The target architecture is to be all-optical. This means that components with only optical inputs and outputs (except perhaps for power) are the basis of the architecture. The devices making up these components may have significant electronic parts which mediate the optical switching. The emphasis is thus on optical architecture, the architecture of a machine in which all information is carried between logic elements by optical signals, and in which the role of electronics interior to switching elements is minimized to the extent which is realizable. GRA

N89-29031# Colorado Univ., Boulder. Optoelectronic Computing Systems Center.
THE MOCK COUNTER: A HYBRID OPTICAL-ELECTRONIC COUNTER USING FIBER DELAY LINE MEMORY
Ann B. Yadlowsky Sep. 1988 34 p Prepared in cooperation with Colorado State Univ., Fort Collins
(Grant NSF CDR-86-22236)
(PB89-184410; OCS-TR-88-04) Avail: NTIS HC A03/MF A01 CSCL 09B

The principle of operation of a bit serial counter with lithium niobate (LiNbO3) directional coupler switches as the active logic elements and fiber delay lines as the memory is discussed. A preliminary version of the counter was built using mock switches consisting of PIN diode receivers, ECL switching logic, and LED transmitters. By building the counter with mock components, problems with high speed electronics and synchronization of the system could by dealt with without dealing with all of the non-idealities of the LiNbO3 directional couplers. The results of

the project are applied to issues that will arise in the construction of digital optical circuits using actual LiNbO3 directional couplers. GRA

N89-29032*# National Aeronautics and Space Administration. Lewis Research Center, Cleveland, OH.
A REAL TIME MICROCOMPUTER IMPLEMENTATION OF SENSOR FAILURE DETECTION FOR TURBOFAN ENGINES
John C. DeLaat and Walter C. Merrill Aug. 1989 27 p
(NASA-TM-102327; E-5029; NAS 1.15:102327) Avail: NTIS HC A03/MF A01 CSCL 09B

An algorithm was developed which detects, isolates, and accommodates sensor failures using analytical redundancy. The performance of this algorithm was demonstrated on a full-scale F100 turbofan engine. The algorithm was implemented in real-time on a microprocessor-based controls computer which includes parallel processing and high order language programming. Parallel processing was used to achieve the required computational power for the real-time implementation. High order language programming was used in order to reduce the programming and maintenance costs of the algorithm implementation software. The sensor failure algorithm was combined with an existing multivariable control algorithm to give a complete control implementation with sensor analytical redundancy. The real-time microprocessor implementation of the algorithm which resulted in the successful completion of the algorithm engine demonstration, is described. Author

N89-29033# Naval Postgraduate School, Monterey, CA. Dept. of Administrative Sciences.
PC TO MAINFRAME CONNECTION: IBM PC 3270 EMULATION M.S. Thesis
John D. Mann Mar. 1989 70 p
(AD-A209204) Avail: NTIS HC A04/MF A01 CSCL 12/6

The purpose of this thesis is to provide nontechnical information concerning microcomputer to mainframe connectivity utilizing terminal emulation. The focus is on IBM, and IBM compatible, microcomputers and on IBM 3270 Terminal Emulation. An appendix to this thesis is a User's Manual for the IBM PC 3270 Emulation Program, version 3.00. This manual is intended for use in the Administrative Sciences Department microcomputer labs of the Naval Postgraduate School. GRA

N89-29034# Alphatech, Inc., Burlington, MA.
FAULT-TOLERANT COMPUTER ARCHITECTURE MODELING AND ANALYSIS Final Technical Report, Aug. 1985 - Aug. 1988
M. P. Kastner, S. R. Dunham, Krishna R. Pattipati, J. M. Stueve, L. C. Kramer, and J. C. Deckert Feb. 1989 313 p
(Contract F30602-85-C-0261)
(AD-A209364; RADC-TR-88-299) Avail: NTIS HC A14/MF A01 CSCL 12/7

This document is the final report. It describes a three-year research effort to develop an engineering tool capable of supporting design and analysis of large-scale, parallel, fault-tolerant computer architectures (FTCAs). The tool, a software package called Computer-Aided Performance and Reliability Evaluation System (CAPRES), allows an FTCA designer or FTCA-design evaluator to predict, by analytical means, the performance, reliability, and performability of candidate computer architectures executing candidate workloads, rather than requiring costly simulation or prototype testing for such prediction, as is currently the case. The analytic capability of CAPRES will make its most important contribution early in the system engineering cycle, when many candidate designs may appear feasible and the best is far from clear. Designers using CAPRES will be able to examine in a matter of hours or days alternatives that today take weeks or months to assess using conventional methods. GRA

N89-29035# Massachusetts Inst. of Tech., Cambridge. Mirosystems Research Center.
CRITICAL PROBLEMS IN VERY LARGE SCALE COMPUTER SYSTEMS Semiannual Technical Report, 1 Oct. 1988 - 31 Mar. 1989
Paul Penfield, Jr., Anant Agarwal, William J. Dally, Srinivas. Devadas, Thomas F. Knight, Jr., F. Thomson Leighton, Charles E. Leiserson, Jacob K. White, and John L. Wyatt, Jr. 31 Mar. 1989 68 p
(Contract N00014-87-K-0825)
(AD-A208070) Avail: NTIS HC A04/MF A01 CSCL 12/7

The research vehicle for this contract is the largest possible computer that could be conceived for the mid to late 1990s. The technical challenges of such a machine serve as the guiding stimulus for the research. It is imagined that this machine will occupy a 14-story building, to cost upwards of $1,000,000,000 and to be so colossal that the nation could only afford one or two of them. The available chip technology and machine size are consistent with a million billion FLOPS (that's 10 to 15th) and a million billion Bytes of memory. It will dissipate 50 megawatts of power using CMOS technology. Communication across the machine will be much slower than computation at a node. The architecture, software, interconnect technology, packaging, and operating system are unknown. Hardware technology, software techniques, programming algorithms, communications, processing elements, and applications are examined. The plausibility (not feasibility) is determined of such a machine. Progress in these various areas are highlighted in the individual sections. GRA

N89-29036# North Carolina Univ., Chapel Hill. Dept. of Computer Science.
A MICROPROGRAMMING SUPPORT TOOL FOR PIPELINED ARCHITECTURES
Steven Molnar and Mark C. Surles Dec. 1988 3 p
(Contract N00014-86-K-0680; NSF MIP-86-01552; DARPA Order 6090)
(AD-A208090) Avail: NTIS HC A02/MF A01 CSCL 12/5

A software tool is described which aids the development of microcode for horizontal, pipelined architectures. The tool is a preprocessor for microcode source that allows the programmer full flexibility to optimize code, but removes many of the tedious and error-prone aspects of micro-programming. It automatically allocates floating point registers, expands complex instructions, and analyzes code for pipeline-related errors. A working version of the tool was written for the Weitek XL-8032 floating point chip set, a horizontal architecture with pipelined sequencer and floating point datapaths. Although the tool was designed for the XL architecture, the algorithms used are applicable to other parallel/pipelined architectures. The need for such tools is expressed, the algorithms needed to analyze control are summarized along with data flow in the presence of pipelining, and characterizes the tool's performance based on nine microcoded routines written for a real time 3-D graphics system. GRA

N89-29037# Universiteit Twente, Enschede (Netherlands). Dept. of Computer Science.
FAULT-TOLERANT COMPUTER SYSTEMS: A SURVEY OF SOME METHODS AND TECHNIQUES [FOUT-TOLERANTE COMPUTERSYSTEM EEN OVERZICHT VAN ENKELE METHODEN EN TECHNIEKEN]
L. J. M. Nieuwenhuis Apr. 1988 37 p In DUTCH
(MEMO-INF-88-15; ISBN-90-365-0153-9; ETN-89-94750) Avail: NTIS HC A03/MF A01

A global survey of methods and techniques for the realization of fault tolerance using multiprocessor systems is given. The reliability of systems, the profits and costs, error detection and error recovery, redundancy in a system, and repairable and non-repairable models for the calculation of the reliability and performance of a system, are presented. The Byzantine Generals Problem is outlined. Examples of realized fault-tolerant systems are given. Some considerations concerning future developments are given. ESA

N89-29038 Technische Univ., Delft (Netherlands).
INVESTIGATIONS OF NONLINEAR STREAMCIPHER SYSTEMS: CONSTRUCTION AND EVALUATION METHODS Ph.D. Thesis
Cornelis Johannes Ad Jansen 1989 214 p
(ETN-89-95456) Copyright Avail: Technische Univ. Delft, Cees J. A. Jansen, 1 Stevinweg, 2628 CN Delft, Netherlands

Nonlinear aspects of streamcipher systems are discussed. Construction methods are proposed and evaluation methods are presented. The mixer is identified as the important part of streamcipher systems when the protection against active eavesdropping is considered. This mixer is usually depicted as a simple linear device without memory. Efficient nonlinear mixers are proposed, based on the use of JK-flipflops. For blockciphers various new modes of use are presented and analyzed with respect to their protection against active eavesdropping. The best mode uses simple nonlinear operations on the plaintext and is very effective and easy to implement. It is concluded that keystream generators should be able to generate an ensemble of sequences, from which a particular one is chosen at random, governed by a secret key. The initial phase, however, should be chosen at random, but should not be regarded as secret key information. ESA

61 COMPUTER PROGRAMMING AND SOFTWARE

Includes computer programs, routines, alogorithms, and specific applications, e.g., CAD/CAM.

N89-29039# Minerals Management Service, Anchorage, AK.
WINDROSE: A PROGRAM FOR IBM-COMPATIBLE PERSONAL COMPUTERS, DOCUMENTATION
Kyle Monkelien and Thomas L. Murrell May 1988 40 p
(PB89-167423; OCS/MMS-88/0043; DOI/SW/DK-89/005A)
Avail: NTIS HC A03/MF A01 CSCL 09B

A printout of the WINDROSE program and instructions for its use are presented. The WINDROSE program was developed to read wind-speed and wind-direction data from an American Standard Code for Information Interchange (ASCII) file, to perform a statistical analysis of the data, and to present the results in the form of a table or a windrose. Included on a separate WINDROSE diskette is a WINDDATA program which can be used to manually input data to create the initial ASCII file. (Other programs can also be used.) GRA

N89-29040# Oak Ridge National Lab., TN. Engineering Physics and Mathematics Div.
CHAOTIC BEHAVIOR IN A NEW CLASS OF PARALLEL OPTIMIZATION ALGORITHMS
J. C. Culioli, V. Protopopescu, and R. C. Mann 1989 11 p
Presented at the 7th Symposium on Energy Engineering Sciences, Argonne, IL, 19-21 Jun. 1989 Sponsored in part by Martin Marietta Energy Systems, Inc.
(Contracts DE-AC05-84OR-21400; DOE-1570-1579-A1)
(DE89-014069; CONF-8906112-1) Avail: NTIS HC A03/MF A01

A new class of optimization algorithms for linear and nonlinear problems is proposed. The algorithms are based on sigmoidic updatings and can be looked upon as nonlinear multidimensional maps. The bifurcation and chaotic regimes of these maps are analyzed and their possible application to optimization problems are indicated. DOE

N89-29041# Army Cold Regions Research and Engineering Lab., Hanover, NH.
QUICKDRAW DATA STRUCTURES FOR IMAGE PROCESSING
Perry J. LaPotin (Dartmouth Coll., Hanover, NH.) and Harlan L. McKim Apr. 1989 22 p
(AD-A208945; CRREL-SP-89-8) Avail: NTIS HC A03/MF A01 CSCL 12/5

Standard binary data formats are currently used to import and export satellite images to geographic information-and image-processing systems. These data structures provide a standard sequential method to read and write large volumes of information in a semicompressed format. While the binary structure is adequate for strict import of image data, it is poorly adapted to fast image-processing at the microcomputer level. In this study, new data structures are investigated that use operating codes to quickly convert raster binary image data and vector overlay files into a high-speed graphical language for efficient display and processing. Binary data is converted into picture handles of variable size and resolution using 2-byte operating codes to symbolize the graphical process. As a result, images are drawn as objects that may be coupled as independent vector components in multiple bit planes. The bit planes may be specified for each pixel to support 24- and 32-bit color of both raster and vector data. The efficiency of these structures allows the user to display 1024 x 1024 scenes in multiple overlapping windows using simple Cut/Copy/Paste commands. In addition, the use of operating codes allows an analyst to quickly store and retrieve archived images in their compressed form using simple scrap manager techniques. GRA

N89-29042# Software Architecture and Engineering, Inc., Arlington, VA.
SOFTWARE TECHNOLOGY TO SUPPORT REAL-TIME EMBEDDED ARTIFICIAL INTELLIGENCE-BASED APPLICATIONS, PHASE 1 Final Report, 1 Oct. 1988 - 31 Mar. 1989
Thomas E. Shields 4 May 1989 25 p
(Contract DAAL03-88-C-0033)
(AD-A209133; ARO-25998.1-EL-SBI-Phase-1) Avail: NTIS HC A02/MF A01 CSCL 12/5

Current-generation KB systems run-time implementations are too abstract and non-deterministic for use in real time systems. The real time applications designer just cannot deal with systems that are non-deterministic and do not provide explicit control. The proposed research ideas were either abandoned or were not developed much beyond their initial conception. However, the fundamental conclusion, herein, is that the proposed ideas were really attempting to tackle the wrong problems. GRA

N89-29043# Defence Research Establishment, Ottawa (Ontario). Communications Electronic Warfare Section.
BIT RATE RECOVERY USING DIGITAL LADDER NETWORKS Technical Note
Brian W. Kozminchuk and Lawrence E. Kuhl Dec. 1988 38 p
(AD-A209865; DREO-TN-89-1) Avail: NTIS HC A03/MF A01 CSCL 12/5

An algorithm that estimates the bit rate of Phase Shift Keying (PSK) and Frequency Shift Keying (FSK) signals has been developed and its performance simulated. The basis of the algorithms stems from a Digital Ladder Network to detect bit changes in intercepted signals. Random bit changes are reflected in large values of the ladder's so-called likelihood parameter. The characteristics and trends of this parameter are observed and documented. The bit rate is obtained from an estimate of the likelihood parameter's power spectrum. Simulation results show that the algorithm produces a distinct spectral line at the bit rate for signal-to-noise ratios as low as -1 dB. GRA

N89-29044# Cornell Univ., Ithaca, NY. Dept. of Computer Science.
AN EXPLICIT SEPARATION OF RELATIVISED RANDOM POLYNOMIAL TIME AND RELATIVISED DETERMINISTIC POLYNOMIAL TIME
Richard Zippel Feb. 1989 10 p
(Contracts N00014-88-K-0591; N00014-86-K-0281; NSF DMS-86-17355)
(AD-A210103; CU-CSD-TR-89-965) Avail: NTIS HC A02/MF A01 CSCL 12/1

This note demonstrates that a certain class of naturally occuring problems involving an oracle are solvable in random polynomial time, but not in deterministic polynomial time. This class of problems

is especially interesting because a very slight change in the parameters of the problem yields one that does have a polynomial solution. GRA

N89-29045# Cornell Univ., Ithaca, NY. Dept. of Computer Science.
AN EFFICIENTLY COMPUTABLE METRIC FOR COMPARING POLYGONAL SHAPES
Esther M. Arkin, L. P. Chew, Daniel P. Huttenlocher, Klara Kedem, and Joseph S. Mitchell May 1989 22 p
(Contracts N00014-88-K-0591; N00014-86-K-0281; NSF IRI-87-10858; NSF ECSE-88-57642)
(AD-A210105; CU-CSD-TR-89-1007) Avail: NTIS HC A03/MF A01 CSCL 12/9

Model-based recognition is concerned with comparing a shape A, which is stored as a model for some particular object, with a shape B, which is found to exist in an image. If A and B are close to being the same shape, then a vision system should report a match and return a measure of how good that match is. To be useful this measure should satisfy a number of properties, including: (1) it should be a metric, (2) it should be invariant under translation, rotation, and change-of-scale, (3) it should be reasonably easy to compute, and (4) it should match our intuition (i.e., answers should be similar to those that a person might give). We develop a method for comparing polygons that has these properties. The method works for both convex and nonconvex polygons and runs in time O(mn log mn) where m is the number of vertices in one polygon and n is the number of vertices in the other. Some examples are presented that show the method produces answers that are intuitively reasonable. GRA

N89-29046# Cornell Univ., Ithaca, NY. Dept. of Computer Science.
ON PLANAR POINT MATCHING UNDER AFFINE TRANSFORMATION
John E. Hopcroft and Daniel P. Huttenlocher Apr. 1989 15 p
(Contracts N00014-88-K-0591; N00014-86-K-0281; NSF DCM-86-17355)
(AD-A210106; CU-CSD-TR-89-986) Avail: NTIS HC A03/MF A01 CSCL 12/9

An important geometric matching problem in machine vision and robotics is to determine whether there exists an affine transformation (a general linear transformation and a translation) that maps each point of a set A onto a corresponding point of a set B. In the case of matched cardinality point sets, we have developed an optimal theta (n log n) algorithm for determining the existence of such a transformation. The method makes use of the fact that an affine transformation preserves the center gravity of a point set, as well as the ratios of triangle areas. If the absolute value of A is less than the absolute value of B, then there can be O(n to the 3rd power) affine transformations from A to B. In general the number of transformations will be much smaller, so we have developed an output sensitive algorithm that runs in time O(n to the 2nd power (log n) + tm log n), where m = the absolute value of A, n = the absolute value of B, and t depends on the number of transformations. The method relies on the affine properties that intersection points and length ratios along a line are preserved. GRA

N89-29047*# National Aeronautics and Space Administration. Langley Research Center, Hampton, VA.
FREQ: A COMPUTATIONAL PACKAGE FOR MULTIVARIABLE SYSTEM LOOP-SHAPING PROCEDURES
Daniel P. Giesy (PRC Kentron, Inc., Hampton, VA.) and Ernest S. Armstrong Sep. 1989 107 p
(NASA-TM-4127; L-16566; NAS 1.15:4127) Avail: NTIS HC A06/MF A01 CSCL 09B

Many approaches in the field of linear, multivariable time-invariant systems analysis and controller synthesis employ loop-sharing procedures wherein design parameters are chosen to shape frequency-response singular value plots of selected transfer matrices. A software package, FREQ, is documented for computing within on unified framework many of the most used multivariable transfer matrices for both continuous and discrete systems. The matrices are evaluated at user-selected frequency-response values, and singular values against frequency. Example computations are presented to demonstrate the use of the FREQ code. Author

N89-29048# Naval Postgraduate School, Monterey, CA.
DESIGN AND DEVELOPMENT OF A USER INTERFACE AND USER MANUAL FOR A SYSTEM DYNAMICS MODEL OF SOFTWARE MANAGEMENT M.S. Thesis
Daniel W. Swindell Mar. 1989 152 p
(AD-A209486) Avail: NTIS HC A08/MF A01 CSCL 12/5

Simulation models typically possess primitive user interfaces. Users must spend substantial amounts of time learning the model before they gain proficiency in using the model. A versatile, user-friendly interface reduces the time and frustration involved in learning a new system. A user friendly interface is designed for the System Dynamics Model of Software Management. The interface is written in a batch programming language, compatible with the IBM personal microcomputer. The interface is a product of the prototype design approach. A sophisticated batch language provides the self-generating menu structures, advanced string handling capabilities, and color enhancements. GRA

N89-29049# Air Force Weapons Lab., Kirtland AFB, NM.
A MODEL OF PARALLEL PERFORMANCE Final Report, Jul. - Dec. 1988
Edward A. Carmona and Michael D. Rice Apr. 1989 50 p
(AD-A207792; AFWL-TR-89-01) Avail: NTIS HC A03/MF A01 CSCL 12/5

This report introduces a general model of parallel performance. With the goal of developing conceptual and empirical methods for characterizing and understanding parallel algorithms, new definitions of speedup and efficiency have been formulated. These definitions take into account the effects that problem size and the number of processors have on efficiency and speedup, and provide a natural and quantifiable measure of parallel performance. The terms introduced in the definitions provide new and improved interpretations of the serial and parallel fraction parameters commonly used in the literature (i.e., Amdahl's Law) to explain the behavior of parallel algorithms. The model provides a more complete characterization of parallel algorithm behavior and is used to correct apparent deficiencies in the formulation of speedup as expressed by Amdahl's Law. Reviewed are the basic definitions of speedup and efficiency. New definitions of these quantities are discussed in terms of work units. Two illustrative examples are given. The two formulations of speedup and efficiency are based on the notion of serial and parallel fractions and present an apparent dichotomy which must be resolved. Then, the serial and parallel fractions are expressed terms of the new work quantities. GRA

N89-29050# Naval Postgraduate School, Monterey, CA.
A CONCEPTUAL LEVEL DESIGN OF A DESIGN DATABASE FOR THE COMPUTER-AIDED PROTOTYPING SYSTEM M.S. Thesis
Bryant S. Douglas Mar. 1989 98 p
(AD-A207808) Avail: NTIS HC A05/MF A01 CSCL 12/5

Vast amounts of evolving data are created in the design of hard real-time software systems. This data must be managed so that it can be stored and retrieved according to the needs of design engineers. In the Computer-Aided Prototyping System (CAPS), a Design Database (DDB) must manage the storage and retrieval of the entire Prototype System Description Language (PSDL) program. This thesis presents a conceptual design and initial implementation of a Design Database (DDB) for CAPS. GRA

N89-29051# Massachusetts Inst. of Tech., Cambridge. Lab. for Computer Science.
A PROGRAMMING LANGUAGE SUPPORTING FIRST-CLASS PARALLEL ENVIRONMENTS
Suresh Jagannathan Jan. 1989 210 p

(Contract N00014-84-K-0099)
(AD-A207833; MIT/LCS/TR-434) Avail: NTIS HC A10/MF A01 CSCL 12/5

This thesis presents a new programming model called the symmetric model in which the representation of programs is identical to the representation of data: to specify a computation, one defines a data structure. This data structure possesses the semantics of a first-class naming environment. It defines a scope and can be used to affect the evaluation environment of other expressions. We present a new programming language called Symmetric Lisp based on the symmetric model. Program structures in Symmetric Lisp are considered non-strict: a program's components may be examined even as its other elements continue to evaluate. The first part of the thesis investigates the interaction of non-strictness with first-class naming environments. The second part of the thesis discuss the compilation and implementation of Symmetric Lisp. We present an extended type-inference system for first-class environments that can be used to infer the proper evaluation environment of identifiers found within the scope of environment-yielding expressions. We also present a translation of Symmetric Lisp into a high-level data flow language. GRA

N89-29052# Connecticut Univ., Storrs. Dept. of Electrical and Systems Engineering.

BM/C(3) ALGORITHM MAPPING ONTO CONCURRENT PROCESSORS Final Report, May - Dec. 1987

Krishna R. Pattipati, Peter B. Luh, Rong-Tay Lee, Samir Shah, and Somanth Deb Mar. 1989 98 p
(Contract F30602-81-C-0169)
(AD-A207877; UCT/DESE-TR-88-3; RADC-TR-88-147) Avail: NTIS HC A05/MF A01 CSCL 12/5

This report is concerned with the mapping of large scale resource allocation algorithms onto parallel computing architectures. The mapping problem is viewed as one of assigning the nodes of a finite, directed, acylic task graph (representing the logical and data dependencies among the tasks constituting the algorithm) onto the nodes of a finite, undirected processor graph (denoting the parallel computing architecture). The objective is to minimize the completion time of the algorithm such that the redundancy, processor memory and security constraints are satisfied. The delays introduced by task queueing, message transmission, message collision and precedence constraints are explicitly modeled. Four algorithms are presented to solve the mapping problem. GRA

N89-29053# Naval Research Lab., Washington, DC. Lab. for Computational Physics and Fluid Dynamics.

NEAR-NEIGHBOR ALGORITHMS FOR PROCESSING BEARING DATA

J. M. Picone, J. P. Boris, S. G. Lambrakos, J. Uhlmann, and M. Zuniga (Science Applications International Corp., McLean, VA.) 10 May 1989 45 p
(AD-A207935; NRL-MR-6456) Avail: NTIS HC A03/MF A01 CSCL 17/1

The authors discuss the use of near-neighbor algorithms for correlating sets of tracks and sensor data on large numbers of rapidly moving objects. By investigating the scaling of such algorithms with the numbers of elements in the data sets, one finds that near-neighbor algorithms need not be universally more cost-effective than brute force methods. While the data access time of near-neighbor techniques scales with the number of objects N better than brute force, the cost of setting up the data structure could scale worse than brute force by a multiplicative factor of log N in an extreme case. For cases in which near-neighbor algorithms are advantageous, the authors describe how such techniques could be used to correlate three-dimensional tracks with bearing data recorded as two angles (theta, phi) from a single sensor. The paper then presents a high-speed algorithm for fusing bearing data from three or more sensors with overlapping fields of view in order to obtain the three-dimensional positions of the objects being observed. The algorithm permits the use of near-neighbor techniques, reducing the scaling of the problem from N to the m power to N lnN, where N is the number of objects in the common domain of observation, and m is the number of sensors involved. Numerical tests indicate the relative efficiencies of typical near-neighbor techniques in solving the multisensor angle-to-position fusion problem. GRA

N89-29054# Naval Research Lab., Washington, DC. Information Technology Div.

PACKET-ERROR PROBABILITY ANALYSIS FOR UNSLOTTED FH-CDMA (FREQUENCY HOPPED-CODE DIVISION MULTIPLE-ACCESS) SYSTEMS WITH ERROR CONTROL CODING Interim Report

J. A. Tarr, J. E. Wieselthier, and A. Ephremides 28 Apr. 1989 19 p
(AD-A207964; NRL-9192) Avail: NTIS HC A03/MF A01 CSCL 25/5

In unslotted Frequency-Hopped (FH) Code-Division Multiple-Access (CDMA) systems, a number of users can simultaneously transmit their packets by using quasi-orthogonal FH patterns (codes). The number of interfering users varies throughout the packet duration; thus, the symbol error probability is not constant throughout the transmission, and symbol errors with the packet are not independent. In this report we present an exact analysis of such systems that use Reed-Solomon error-control coding. The computational task for the evaluation of the performance is enormous; thus, bounds and approximations are derived that are easier to compute and that prove to be very close to the exact results for the cases in which the exact results are computable. The results of this study confirm our observation, made also elsewhere, that the widely used threshold-based model of other-user interference is not an accurate one. GRA

N89-29055# Army Missile Command, Redstone Arsenal, AL. Research, Development and Engineering Center.

MAXIMUM-LIKELIHOOD PARAMETER ESTIMATION OF A GENERALIZED GUMBEL DISTRIBUTION Final Technical Report, May 1988 - Feb. 1989

Charles E. Hall, Jr., Siegfried H. Lehnigk, and Guttalu R. Viswanath 24 Mar. 1989 52 p
(AD-A207994; AD-E951354; AMSMI/TR-RD-RE-89-5) Avail: NTIS HC A04/MF A01 CSCL 12/3

A microcomputer-based algorithm for estimation of the three parameters of a generalized Gumbel (extreme value type 1) distribution class is presented. The parameters are shift, scale, and shape. The classical Gumbel distribution results if the shape parameter is equal to unity. Three-parameter as well as two-parameter (shape equal to unity) estimation can be performed for given histogram data. Parameter estimation is accomplished by means of the maximum-likelihood principle. The derivative equations which result from the associated logarithmic likelihood function are used. A more comprehensive presentation of generalized Gumbel distribution estimation which also allows treatment of population data and which includes moment estimates and maximum-likelihood estimates by direct optimization of the logarithmic likelihood function will be presented elsewhere. GRA

N89-29056# Massachusetts Inst. of Tech., Cambridge. Artificial Intelligence Lab.

AN OBJECT-ORIENTED SOFTWARE REUSE TOOL

Michael D. Monegan Apr. 1989 93 p
(Contract N00014-88-K-0487; NSF IRI-86-16644)
(AD-A208018; AI-M-1118) Avail: NTIS HC A05/MF A01 CSCL 12/5

The Object oriented Reuse Tool (ORT) provides support for the reuse of object oriented software by maintaining a library of reusable classes, recording information about reusability, allowing easy exploration of library entries, and providing an extensible approach to facilitating reuse in a software development environment. ORT takes advantage of opportunities provided by the object oriented style of programming that are unavailable in reuse schemes for conventional programming languages. It also records information useful in assessing the reusability of library entries and in relating these entries to each other. In the early design phases of object oriented development, ORT facilitates

reuse by providing a flexible way to navigate the classes recorded in library and the information associated with them. It thereby aids in the process of refining a design to maximally reuse existing classes. The implementation of ORT is extensible. A collection of other useful tools were identified. These tools can be directly implemented within the existing architecture and would compose the remainder of a practical system useful in increasing the amount of reuse in an objected oriented software development environment. GRA

N89-29057# North Carolina Univ., Chapel Hill. Dept. of Computer Science.
WALKTHROUGH-EXPLORING VIRTUAL WORLDS Annual Report, No. 2
John M. Airey and F. P. Brooks 16 Feb. 1989 7 p
(Contract N00014-86-K-0680; NSF CCR-86-09588)
(AD-A208087; TR89-012) Avail: NTIS HC A02/MF A01 CSCL 12/5

A virtual world system is a computer graphics system allowing natural real time interaction with a 3-d model world. Walkthrough is a virtual world system for architectures and their clients to explore buildings before they are built, so as to iteratively refine their specifications. Much of our virtual world research at Chapel Hill has involved molecules or human anatomy. In neither of these applications does one know exactly how the virtual world should seem to the explorer. In Walkthrough, on the other hand, the researcher can easily tell how closely the virtual world matches the real in the ways that matter. Any virtual world research project must continually improve in four aspects. The videotape, part 2, shows the progress to date, and gives short previews of some of the advances not yet integrated into the system. GRA

N89-29058# North Carolina Univ., Chapel Hill. Dept. of Computer Science.
A HETEROGENEOUS MULTIPROCESSOR GRAPHICS SYSTEM USING PROCESSOR-ENHANCED MEMORIES
Henry Fuchs, John Poulton, John Eyles, Trey Greer, Jack Goldfeather (Carleton Coll., Northfield, MN.), David Ellsworth, Steven Molnar, Greg Turk, Brice Tebbs, and Laura Israel Feb. 1989 23 p
(Contract N00014-86-K-0680; NSF DCI-86-01152; DARPA Order 6090)
(AD-A208089; TR89-005) Avail: NTIS HC A03/MF A01 CSCL 12/5

The architecture and initial algorithms are introduced for Pixel-planes 5, a heterogeneous multi-computer designed both for high speed polygon and sphere rendering (1M Phong-shaded triangles/second) and for supporting algorithm and application research in interactive 3D graphics. Techniques are described for volume rendering at multiple frames per second, font generation directly from conic, spline descriptions, and rapid calculation of radiosity form factors. The hardware consists of up to 32 math-oriented processors, up to 16 rendering units, and a conventional 1280 x 1024-pixel frame buffer, interconnected by a 5 gigabit ring network. Each rendering unit consists of a 128 x 128-pixel array of processors-with-memory with parallel quadratic expression evaluation. Implemented on fast custom CMOS chips, this array has 208 bits/pixel on-chip and is connected to a video RAM memory system that provides 4,096 bits of off-chip memory. Rendering units can be independently reassigned to any part of the screen or to non-screen-oriented computation. A message-passing operating system encourages algorithms to mix and match capabilities of the massively parallel rendering units with those of the math-oriented processors. As of January 1989, both hardware and software are still under construction, with initial system operation scheduled for summer 1989. GRA

N89-29059# Naval Postgraduate School, Monterey, CA.
A PROTOTYPE FOR CONVERTING LINEAR PROGRAMMING (LP) MODELS TO STRUCTURED MODELING GRAPHS M.S. Thesis
David S. Hill Mar. 1989 144 p
(AD-A208166) Avail: NTIS HC A07/MF A01 CSCL 12/4

Geoffrion's structured modeling provides a very promising framework for the development of future Model Management Systems (MMS). This thesis presents a prototype that converts a mathematical representation of simple LP models to Geoffrion's structured modeling representations. The general procedures presented could be extended to convert an LP model represented in any precisely defined mathematical language. This would allow the development of integrated modeling environments based upon the structured modeling framework which could accept input in a number of common LP language formats. GRA

N89-29060# Naval Postgraduate School, Monterey, CA.
SOFTWARE ENGINEERING WITH DATABASE MANAGEMENT SYSTEMS M.S. Thesis
Labros G. Karatasios Mar. 1989 189 p
(AD-A208167) Avail: NTIS HC A09/MF A01 CSCL 12/5

The purpose of this thesis is to communicate a general knowledge of software engineering principles that can be applied to the development of a software system. Fundamental software engineering concepts are first discussed and then applied to a personnel database management system which is featured throughout the thesis. The individual tools and techniques that are used in each phase of the system development are widely known in the computer science community and each has been employed successfully in certain situations. GRA

N89-29061*# Institute for Computer Applications in Science and Engineering, Hampton, VA.
PARALLEL LANGUAGE CONSTRUCTS FOR TENSOR PRODUCT COMPUTATIONS ON LOOSELY COUPLED ARCHITECTURES Final Report
Piyush Mehrotra (Purdue Univ., West Lafayette, IN.) and John VanRosendale Sep. 1989 32 p Submitted for publication
(Contracts NAS1-18605; N00014-88-M-0108; IDA-10-00008)
(NASA-CR-181900; NAS 1.26:181900; ICASE-89-41) Avail: NTIS HC A03/MF A01 CSCL 09B

Distributed memory architectures offer high levels of performance and flexibility, but have proven awkard to program. Current languages for nonshared memory architectures provide a relatively low level programming environment, and are poorly suited to modular programming, and to the construction of libraries. A set of language primitives designed to allow the specification of parallel numerical algorithms at a higher level is described. Tensor product array computations are focused on along with a simple but important class of numerical algorithms. The problem of programming 1-D kernal routines is focused on first, such as parallel tridiagonal solvers, and then how such parallel kernels can be combined to form parallel tensor product algorithms is examined. Author

N89-29062# Universiteit Twente, Enschede (Netherlands). Dept. of Computer Science.
APL CONVERSION SOFTWARE [APL CONVERSIE PROGRAMMATUR]
H. G. Posthuma May 1988 30 p In DUTCH
(MEMO-INF-88-21; ETN-89-94753) Avail: NTIS HC A03/MF A01

The APL conversion software and changes implemented therein are presented. The functions of the conversion program are explained. The structure of the sequential access inventory ASCII is outlined. The different APL programs are presented. The changes made in the software (changes to workspace Write and changes to workspace Qreaddec) are explained. Advice concerning the different subjects is given. The most important computer programs and some basic explanations are included. ESA

N89-29063# Office National d'Etudes et de Recherches Aerospatiales, Paris (France).
GENERALIZED PROJECTED GRADIENT-TYPE ITERATIVE METHOD FOR PARAMETRIC AND FUNCTIONAL OPTIMIZATION OF DYNAMICAL SYSTEMS SUBJECT TO CONSTRAINTS
Claude Aumasson and Philippe Landiech 1988 95 p In

FRENCH; ENGLISH summary
(ONERA-NT-1988-9; ISSN-0078-3781; ETN-89-94860) Avail: NTIS HC A05/MF A01

The theoretical aspects of the method are described, including the calculations of the cost and constraint sensitivities to variations in the control laws and parameters, a choice of objectives in constraint adjustments at each iteration, and the termination of the corresponding optimum control laws and parameters variations. An example of trajectory optimization is given, for which the analytical solution is known. It is shown that the software that implements the method works correctly. ESA

N89-29064# Laboratoire d'Automatique et d'Analyse des Systemes, Toulouse (France).
ON THE COMPOSITION OF INTERCONNECTED SYSTEMS BY NONSERIAL DYNAMIC PROGRAMMING: APPLICATION TO POWER SYSTEMS Ph.D. Thesis - Toulouse Univ.
Jose Luis Gimenez 1989 157 p In FRENCH; ENGLISH summary Sponsored by CONICIT, Brazil; CEFI and Centre International des Etudiants et Stagiaires
(LAAS-89.096; ETN-89-94871) Avail: NTIS HC A08/MF A01

A decomposition method based on dynamic programming principles is presented. Due to embedding and parametrization procedures, the technique works by arranging interconnected subsystems into a sequence and applying the principle of optimality across subsystems in the same manner as it is applied across stages in classical dynamic programming. The optimal design of an electric distribution network (static case) and the optimal short-term operation of a multireservoir power system are studied. ESA

N89-29065# Centro Studi e Laboratori Telecomunicazioni, Turin (Italy).
THE DESIGN OF VLSI CIRCUITS [LA PROGETTAZIONE DI CIRCUITI INTEGRATI VLSI]
Muccini Sep. 1987 16 p In ITALIAN Presented at the Convegno IRI Ricerca e Tecnologia: Nuove Frontiere per il Mezzogiorno, Bari, Italy, 15 Sep. 1987
(ETN-89-94968) Avail: NTIS HC A03/MF A01

The characteristics and manufacturing processes of VLSI are presented. The examples given include vocal synthetizer, commutation processor, modems, memories, and communication modules. The automatic design software is described. Technological trends are discussed. ESA

N89-29066# Universiteit Twente, Enschede (Netherlands). Faculty of Applied Mathematics.
AN ALGORITHM FOR SMOOTH INTERPOLATION TO SCATTERED DATA IN R2
P. R. Pfluger (Amsterdam Univ., Netherlands) and R. H. J. GmeligMeyling Nov. 1988 15 p
(Memo-748; ISSN-0169-2690; ETN-89-95116) Avail: NTIS HC A03/MF A01

An algorithm which determines a smooth piecewise polynomial interpolant to scattered data in the plane is presented. An appropriate triangulation is chosen and the interpolant is determined in the splinespace with a high degree of polynomial precision. Numerical experiments using the interpolant method are presented. Tests performed on cardinal interpolation show the almost local behavior of the interpolant method. Five tests on different triangulations are used and results include confirmation of third order convergence. ESA

N89-29067# National Aerospace Lab., Amsterdam (Netherlands). Informatics Div.
TOOLS FOR THE DEVELOPMENT AND USAGE OF INDUSTRIAL MATHEMATICAL SOFTWARE
F. J. Heerema, W. Loeve, and J. J. P. vanHulzen 17 Mar. 1987 30 p Presented at the 1st International Conference on Industrial and Applied Mathematics, Paris, France, 29 Jun. - 3 Jul. 1987
(NLR-MP-87020-U; ETN-89-95411) Avail: NTIS HC A03/MF A01

An infrastructure for information processing, comprising hardware and software, is discussed. This infrastructure can be applied to support research and engineering activities of the industry. A computer, a terminal network, and a supercomputer for fast computations are developed. The network allows access from outside to software, information from experiments, and digital simulations. The kernel of the software infrastructure consists of an engineering data management system with 4th generation characteristics. A standardized command language system (COLAS) for user interaction, and a method base system (MEBAS), which supports the management, assemblage and use of software components, are created. The main components of the infrastructure are facilities for data management, method management, and user interfaces, all implemented on a computer and terminal network. ESA

N89-29068# Universiteit Twente, Enschede (Netherlands). Dept. of Computer Science.
A LOGIC QUERY LANGUAGE AND ITS ALGEBRAIC OPTIMIZATION FOR A MULTIPROCESSOR DATABASE MACHINE
Maurice A. W. Houtsma, Hendricus J. A. vanKuijk, Jan Flokstra, Peter M. G. Apers, and Martin L. Kersten Dec. 1988 32 p Sponsored in part by the Stimuleringsprojectteam Informaticaonderzoek Nederland Prepared in cooperation with Philips Research Labs., Eindhoven, Netherlands
(MEMO-INF-88-52; ISBN-90-265-236-5; ETN-89-95421) Avail: NTIS HC A03/MF A01

A logic query language, called PRISMAlog, is introduced. The language is one of the interfaces of a multiprocessor, main-memory database machine, called PRISMA. It is a language with a purely declarative semantics; the meaning of a program is given by its least fixed-point. PRISMAlog allows recursive rules, and supports operations like negation, arithmetic, aggregates, and group-by. Optimization of PRISMAlog programs is completely algebraic, and focusses on the use of distributed database techniques to introduce parallelism. Optimization criterion is minimization of response time. Techniques used to optimize PRISMAlog programs and to produce parallel schedules are illustrated. ESA

N89-29069# Universiteit Twente, Enschede (Netherlands). Dept. of Computer Science.
A METHOD OF SOFTWARE DEVELOPMENT USING FUNCTIONAL PROGRAMMING
S. M. M. Joosten 15 Dec. 1988 34 p
(MEMO-INF-88-64; ISBN-90-365-0239-X; ETN-89-95423) Avail: NTIS HC A03/MF A01

A software development method which aims to be both formal and practical is presented. The attention is focused on the problem solving part of software development found in the very early stages of design. A format specification is developed and prototypes are implemented. A functional programming approach is used, which allows prototypes to be built that are very close to specification. External aspects, including manageability and maintainability, are improved, which considerably enhance the overall quality of software. The method does not require the use of any specific design language. The design is formalized in logic and mathematics to make it accessible to designers who do not want to learn new formalisms. An example of software development is given in which a non-trivial problem is solved. The entire development route is followed, from the formal specification to an imperative realization. ESA

N89-29070# Universiteit Twente, Enschede (Netherlands). Dept. of Computer Science.
A CODE OPTIMIZATION PACKAGE FOR REDUCE
J. A. vanHulzen, B. J. A. Hulshof, B. L. Gates (RAND Corp., Santa Monica, CA.), and M. C. vanHeerwaarden Apr. 1989 19 p Presented at the 1988 International Symposium on Symbolic and Algebraic Computation, Portland, OR, 17-19 Jul. 1989 Submitted for publication
(Grant NSF ASC-85-16384)
(MEMO-INF-89-29; ISSN-0923-1714; ETN-89-95427) Avail: NTIS HC A03/MF A01

A survey of the strategy behind and the facilities of a code optimization package for REDUCE are given. A straight forward use of an Optimizer is discussed and illustrated. Declaration facilities and different file-handling possibilities are discussed. Detailed discussion of the underlying algorithms is avoided and the capabilities of the package are surveyed in general terms. Examples of straightforward and more advanced usage are shown. Conclusions are summarized and indications of future work are given. ESA

N89-29071# National Aeronautical Lab., Bangalore (India). Systems Engineering Div.
PHOTOETCHED DOUBLE SPIRAL DEVICE
B. S. Dasannacharya Jun. 1989 8 p
(PD-SE-8911) Avail: NTIS HC A02/MF A01

The computer graphic generation of a master drawing of a double spiral design is described along with the mask fabrication and the fabrication of the end product, the free filament resistance element of a 200 micron Manganin (Cu, Ni, Mn) foil. A listing of a program for generation of concentric circles is also listed. Author

N89-29072# Universiteit Twente, Enschede (Netherlands). Faculty of Applied Mathematics.
A SURVEY OF SELF-CONSISTENCY PROPERTIES IN COOPERATIVE GAME THEORY
Theo S. H. Driessen Jan. 1989 39 p
(Memo-763; ISSN-0169-2690; ETN-89-95058) Avail: NTIS HC A03/MF A01

The use of reduced games in the study of cooperative games is reviewed in characteristic function form. The axiomatic characterizations of the Shapley value, the prekernel, the prenucleolus and the core are reviewed by means of an investigation into a self-consistency property in terms of the reduced games. The reduced game property for solutions and the reduced game property for a class of games are considered. From the proof of reduced game property for a class of games, including the class of convex games, conclusions are drawn concerning the solutions on the relevant class of games. The reduced game property is applied to a bankruptcy problem. Results and proofs are given. ESA

N89-29073# Universiteit Twente, Enschede (Netherlands). Faculty of Applied Mathematics.
METHODS OF COMBINATORIAL OPTIMIZATION AND THEIR RANGE OF APPLICABILITY [VERFAHREN DER KOMBINATORISCHEN OPTIMIERUNG UND IHRE GUELTIGKEITSBEREICH]
W. Kern Feb. 1989 46 p In GERMAN; ENGLISH summary
(Memo-766; ISSN-0169-2690; ETN-89-95061) Avail: NTIS HC A03/MF A01

The basic techniques and methods of combinatorial optimization are outlined, and their range of applicability are investigated (i.e. a characterization of general classes of problems allowing a successful application of the methods). The matroid theory is introduced, and matroids are treated in connection with a number of combinatorial problems. The simplest method of combinatorial optimization, the Greedy algorithm, is presented, and a class of linear optimization problems which can be solved by the Greedy strategy is characterized. The simplex algorithm for solving linear programs is described. Linear programming relaxation is presented as a basic strategy for solving integral (nonlinear programming complete) optimization problems. An heuristic method (simulated annealing) for solving nonlinear-programming-complete problems is outlined. ESA

N89-29074# Universiteit Twente, Enschede (Netherlands). Faculty of Applied Mathematics.
SOLUTION OF A TINNED IRON PURCHASING PROBLEM BY LAGRANGIAN RELAXATION
B. Dorhout Sep. 1988 19 p
(Memo-735; ISSN-0169-2690; ETN-89-95112) Avail: NTIS HC A03/MF A01

The problem in minimizing total purchase cost of tinned iron sheets, for a tin factory with a fixed production program, and the exploitation of the price structure by the formulation of a combinatorial optimization problem are described. A combinatorial programming model of the problem is formulated and solutions to this model are obtained by Lagrangean relaxation and subgradient techniques. The principles of these methods are described and a computer program, written in TURBO PASCAL, was executed on a microcomputer, to implement them for the specific problem. Extensions, modifications, and other possible applications of the model are formulated including reduction of computation time and the purchase of arbitrary goods from various sellers on the basis of value order discounts. Technical details on the solving of knapsack problems, and the transformation of infeasible solutions to feasible, are included. ESA

N89-29075# Universiteit Twente, Enschede (Netherlands). Faculty of Applied Mathematics.
LANGUAGE CONSTRUCTS AND A SEARCH PROCEDURE TO MODEL AND SOLVE COMBINATORIAL PROBLEMS
J. J. Bisschop and T. W. Smits Dec. 1988 33 p
(Memo-753; ISSN-0169-2690; ETN-89-95119) Avail: NTIS HC A03/MF A01

Language constructs to model combinatorial problems, intended as an integrated part of an existing modeling language, are introduced. To use these constructs, the problem is stated, and an algorithm defined to solve it, which allows the construction of more exact and efficient algorithms describing heuristics that are derived from the character of the problem and are expressed in terms of problem components. The underlying algorithm chosen for solving the combinatorial problems is basically a depth-first search procedure. The language constructs are used to specify and control the search procedure and in this way to narrow down the search space. A major advantage of the search model is the ease of model modification. The proposed language constructs allow for the separation of the model into problem description and algorithm directives. Recommendations for improvements to the constructs are given. ESA

N89-29076# Universiteit Twente, Enschede (Netherlands). Faculty of Applied Mathematics.
THREE DIMENSIONAL RECONSTRUCTION FROM SERIAL CROSS SECTIONS BY SET VALUED INTERPOLATION
R. H. J. GmeligMeyling Dec. 1988 33 p
(Memo-754; ISSN-0169-2690; ETN-89-95120) Avail: NTIS HC A03/MF A01

The problems of three dimensional reconstruction are addressed, and a computer aided reconstruction algorithm, based on the concept of set valued interpolation as proposed by Levin (1986), is described. The method is completely automatic and requires no human intervention. A set valued and shape preserving interpolation scheme is shown to greatly facilitate the detection of the boundary surface and allow the accurate reconstruction of closed three dimensional objects of abitrary shape. The use of low degree piecewise polynomials (splines), which are flexible and highly efficient, to solve the associated univariate interpolation problems, is shown to significantly improve the computational properties of the method. The use of a parallel computer architecture is shown to eliminate the potential drawback of high computational costs. The method is proposed to have practical importance in the medical field. ESA

N89-29077# Technische Univ., Delft (Netherlands).
PARALLEL ALGORITHMS FOR SOLVING SYSTEMS OF LINEAR EQUATIONS AND THEIR MAPPING ON SYSTOLIC ARRAYS Ph.D. Thesis
K. Jainandunsing 1989 195 p
(ETN-89-95457) Avail: NTIS HC A09/MF A01

Algorithms for solving systems of linear equations with a maximum degree of parallelism and pipelining are presented. Partitioning strategies for the design of systolic arrays with the number of processor elements independent of the size of the problem are developed. The synthesis of a concrete systolic array

with a fixed number of processor elements for the algorithms is developed. It is concluded that the feed forward direct methods developed, thanks to their high degree of parallelism and pipelining, allow for fast execution of systolic arrays. ESA

N89-29078# Universiteit Twente, Enschede (Netherlands). Dept. of Computer Science.
A STATIC LOAD DISTRIBUTION STRATEGY FOR PROCESSOR TOOLS
E. G. Zondag Dec. 1988 20 p
(Memo-INF-88-43; ISBN-90-365-0242-X; ETN-89-95064) Avail: NTIS HC A03/MF A01

In order to avoid costly process migration which might restrict realtime behaviour in the TUMULT multi-processor system, a search for a static load determination process to optimize system throughput was initiated. A load distribution strategy for static assignment of processes in a processor pool is presented under the assumption that processes cannot migrate. A resource allocation is attempled that (nearly) optimizes the execution progress of the set or processes. A simple and a more complex, cost function, which take into account execution related process and processor attributes are defined. Methods for the calculation of a proper assignment using these functions, including a simulated annealing algorithm, are described. The strategy relies on the behavior histories of processes and processors. Problems concerning the general applicability of this strategy, its reliance on behavior stability, and its simple approach to task or machine learning, are outlined as future topics for consideration. ESA

N89-29079# Universiteit Twente, Enschede (Netherlands). Dept. of Computer Science.
THE APPLICATION OF CONSTRAINTS IN QUERY OPTIMIZATION
Hendricus J. A. vanKuijk 1988 84 p
(Memo-INF-88-55; ISSN-0923-1714; ETN-89-95065) Avail: NTIS HC A05/MF A01

A hierarchy of static constraints is demonstrated to be at the foundation of a framework unifying the solution to a number of existing and new problems encountered during the overall process of (semantic) query optimization in (distributed) database systems. Domain constraints, attribute constraints, and tuple constraints are applied to explicitly represent knowledge inherent to the application being modeled. The context of the theory presented is found in the knowledge-based approach to semantic query optimization in a distributed environment and the explicit representation of query optimization knowledge of various sources so that it can be manged (added, deleted, modified). Constraints are used, to represent and apply semantic knowledge (including the so-called if-then rules known from literature), to augment selection and join predicate formulas to arrive at more efficient schedules for these operations, to define and apply horizontal fragmentation knowledge in case of distributed database systems, and to estimate more accurately the parameters of profiles of the relations resulting from relational operations. Given the individual constraints on relations, a mechanism is provided to derive the constraints on the relations resulting from relational operations. Conclusions are considered, including the power of this approach by virtue of its flexibity, and related to passible future discussion. ESA

N89-29080# Universiteit Twente, Enschede (Netherlands). Dept. of Computer Science.
BACKWARD ANALYSIS
M. Ramaer 1989 45 p
(Memo-INF-89-14; ETN-89-95066) Avail: NTIS HC A03/MF A01

An analysis technique for functional languages called backward analysis and its application for strictness analysis are described. Backward analysis is favored over forward analysis for its superior time complexity and ability to detect more strictness for example in datastructures. The workings of the analysis are shown by the application to a very simple first order language. The language is extended gradually with tuples, recursive functions, lists and other recursive algebraic types, and finally higher order functions. The first three extensions are shown to be handled more or less straight forwardly and necessary design decisions are illustrated for the user defined (recursive) algebraic data types. The large amount of extra work required for the higher order functions is shown to necessitate a change in the analysis technique. An acceptable level is achieved by the division of the analysis into two parts and subsequent independent handling. ESA

62 COMPUTER SYSTEMS

Includes computer networks and special application computer systems.

N89-29081# Colorado Univ., Boulder. Optoelectronic Computing Systems Center.
AN OPTOELECTRONIC MULTI-Gb/s PACKET SWITCHING NETWORK
J. R. Sauer (Bell Telephone Labs., Inc., Murray Hill, NJ.) Feb. 1989 35 p Prepared in cooperation with Colorado State Univ., Fort Collins
(Grant NSF CDR-86-22236)
(PB89-184345; OCS-TR-89-06) Avail: NTIS HC A03/MF A01 CSCL 09B

An optoelectronic network architecture is proposed that would provide multi-Gb/s data for electronic users at the network access points. Constructed with current technology, the network transports short packets through multiple switching nodes optically. It is based on three interlocking concepts that exploit the advantages of optics: a simple interconnection topology supporting high connectivity and concurrency, a lean self-routing flow-through protocol permitting an optical implementation, and large-scale optical packet time compression/decompression to/from the electronic format of the users. GRA

N89-29082# Massachusetts Inst. of Tech., Cambridge. Dept. of Electrical Engineering and Computer Science.
A RECONFIGURABLE ARITHMETIC PROCESSOR M.S. Thesis
James Alexander Stua Fiske Apr. 1989 72 p Sponsored in cooperation with Fonds pour la Formation de Chercheurs et l'Aide a la Recherche, NSF, GE Corp., and IBM Corp.
(Contracts N00014-88-K-0738; N00014-87-K-0825; N00014-85-K-0124)
(AD-A208323; VLSI-Memo-89-521) Copyright Avail: NTIS HC A04/MF A01 CSCL 12/6

Achieving high rates of floating-point computation is one of the primary goals of many computer designs. Many high speed floating-point datapaths have been designed in order to address this problem. However, conventional designs often neglect the real problem in achieving high performance floating-point: providing the necessary I/O bandwidth to keep the high speed datapaths busy. The Reconfigurable Arithmetic Processor (RAP) is an arithmetic processing node for a message-passing, MIMD concurrent computer. Its datapath is designed to sustain high rates of floating-point operations, while requiring only a fraction of the I/O bandwidth required by a conventional floating-point datapath. The RAP incorporates on one chip eight 4-bit serial, 64 bit floating-point arithmetic units connected by a switching network. By sequencing the switch through different patterns, the RAP chip calculates complete arithmetic formulas. By chaining together its arithmetic units the RAP eliminates the I/O bandwidth associated with storing and retrieving intermediate results, and reduces the amount of off chip data transfer. This thesis describes and evaluates the RAP architecture. It presents two important aspects of the chip design: the control logic design, and the schematic level design of the RAP datapath. GRA

N89-29083# Aerospace Corp., El Segundo, CA. Computer Science Lab.
GAUGE: ITS PHILOSOPHY AND DESIGN
M. M. Gorlick, C. F. Kesselman, and D. S. Parker 22 May 1989 27 p

(Contract F04701-85-C-0086)
(AD-A208944; TR-0086A(2920-05)-2; SD-TR-89-33) Avail: NTIS HC A03/MF A01 CSCL 12/5

Gauge is a workbench for gaining understanding of the performance of large parallel logic programs. A Gauge user is provided with a variety of interactive tools for analyzing the execution of programs. This report describes the philosophy, design, and implementation of Gauge and its use in analyzing parallel systems. GRA

N89-29084# Massachusetts Inst. of Tech., Cambridge. Lab. for Computer Science.
CHAPTER ON DISTRIBUTED COMPUTING
Leslie Lamport and Nancy Lynch Feb. 1989 71 p
(Contracts N00014-85-K-0168; N00014-83-K-0125)
(AD-A208996; MIT/LCS/TM-384) Avail: NTIS HC A04/MF A01 CSCL 12/7

Rigorous analysis starts with a precise model of a distributed system; the most popular models, differing in how they represent interprocess communication, are message passing, shared variables, and synchronous communication. The properties satisfied by an algorithm must be precisely stated and carefully proved; the most successful approach is based on assertional reasoning. Algorithms for solving particular problems in a distributed system can then be designed and analyzed. Typical of the problems that were addressed are: concurrently accessing shared data, achieving consensus, analyzing network topology, obtaining consistent global information, and controlling database transactions. GRA

N89-29085# Naval Ocean Systems Center, San Diego, CA.
THE NOSC (NAVAL OCEAN SYSTEMS CENTER) CODE 911 DIGITAL DYNAMICS PROCESSOR (DDP): A MILDLY COUPLED DISTRIBUTED-COMPUTING SYSTEM Interim Report, Jul. 1984 - Apr. 1989
S. P. Murphy May 1989 14 p
(AD-A210148; NOSC/TD-1538) Avail: NTIS HC A03/MF A01 CSCL 12/6

The Naval Ocean Systems Center (NOSC), Code 911 Digital Dynamics Processor (DDP) is described. The DDP is a multiprocessor system designed for high speed numerical calculation. This system implements a new variation of common memory in order to allow a far greater number of processors than found currently on a TCDS. The conceptual design of the DDP was done in mid and late 1984 by Jack Zyphur. A variation of this design was implemented in hardware by Mitchell (1989) in early 1985. The first prototype was only two processor slaves, a repeater slave, and a master. Since the original goal of the DDP was to replace an EAI 8800 Analog computer, the first attempt at software for the DDP was a simulation language consisting of assembly language modules that would do the favor of direct equation implementation using a C cross-compiler that run on the master. In early 1987 Murphy programmed in a quaternion algorithm and the DDP proved operational in the NOSC Hybrid-Simulator. The DDP has since been up graded to six processor slaves running MC68030 CPUs at 25 MHz. GRA

N89-29086# Stanford Univ., CA. Dept. of Computer Science.
MULTICAST COMMUNICATION IN MULTIPROCESSOR SYSTEMS
Gregory T. Byrd, Nakul P. Saraiya, and Bruce A. Delagi (Digital Equipment Corp., Palo Alto, CA.) Jan. 1989 20 p
(Contract F30602-85-C-0012)
(AD-A209606; SU-STAN-CS-89-1246; KSL-88-81) Avail: NTIS HC A03/MF A01 CSCL 25/5

Recent high-performance multiprocessors exploit cut-through routing, with packets routed as their first bytes arrive. Hardware-supported multicast can benefit the many parallel programs in which producers provide each value to multiple consumers. We describe several cut-through multicast protocols, including a restrictive (yet adaptive) routing scheme for deadlock avoidance. Simulations using synthetic and application-driven loads show it has significantly better performance than either multicast emulation or deadlock detection and resolution. The scheme provides cut-through multicast without requiring dedicated storage in the communication facilities for a full packet. We thus extend ideas considered for efficient cut-through routing in multiprocessor systems to include multicast. GRA

N89-29087# Johns Hopkins Univ., Baltimore, MD. Dept. of Mathematical Sciences.
LARGE SCALE FUNCTION MINIMIZATION Final Scientific Report, 15 Jul. 1985 - 14 Oct. 1988
Stephen G. Nash 14 Oct. 1988 5 p
(Grant AF-AFOSR-0222-85; AF Proj. 2304)
(AD-A207718; AFOSR-89-0532TR) Avail: NTIS HC A02/MF A01 CSCL 12/2

Several new optimization techniques suitable for parallel computers have been developed and have been tested on an Intel hypercube. On a number of nonlinear problems, the algorithms tested have demonstrated dramatic speed-ups over their sequential counterparts. The fact that these speedups are better than can be attributed to parallelism suggests that they may lead to improved sequential methods. GRA

N89-29088# Stanford Univ., CA. Dept. of Computer Science.
INFORMATION REQUIREMENTS AND THE IMPLICATIONS FOR PARALLEL COMPUTATION Ph.D. Thesis
Patrick H. Worley Jun. 1988 149 p
(Contracts N00014-75-C-1132; DE-AC05-84OR-21400)
(AD-A207802; SU-STAN-CS-88-1212) Avail: NTIS HC A07/MF A01 CSCL 12/1

The best serial algorithms for numerically approximating the solution of a linear partial differential equation (PDE) exploit knowledge of the solution operator. This dissertation describes how the solution operator also influences the behavior of parallel algorithms. Approximating the solution at a single location in the problem domain is considered. A lower bound on the error in the approximation is derived that is a function of the amount of data used and the smoothness of the data functions. From this one can derive a lower bound on the parallel complexity of algorithms that approximate the solution. The lower bound is a linear function of log 1/epsilon, where epsilon is an upper bound on the error. Thus the parallel complexity increases as epsilon decreases, independent of the number of processors used. An algorithm is also constructed whose parallel complexity is of this form, proving that the form of the bound is the best possible. The execution time of parallel algorithms is a function of both the communication costs and the parallel complexity. We describe bounds on the communication cost of parallel algorithms that are functions of the distance between collaborating processors. GRA

N89-29089# Stanford Univ., CA. Computer Systems Lab.
ANALYSIS OF CACHE INVALIDATION PATTERNS IN MULTIPROCESSORS
Wolf-Dietrich Weber and Anoop Gupta 1989 20 p
(Contract N00014-87-K-0828)
(AD-A207820) Avail: NTIS HC A03/MF A01 CSCL 12/5

To make shared-memory multiprocessors scalable, researchers are now exploring cache coherence protocols that do not rely on broadcast, but instead send invalidation messages to individual caches that contain stale data. The feasibility of such directory-based protocols is highly sensitive to the cache invalidation patterns that parallel programs exhibit. In this paper, we analyze the cache invalidation patterns caused by several parallel applications and investigate the effect of these patterns on a directory-based protocol. Our results are based on multiprocessor traces with 4, 8 and 16 processors. To get insight into what the invalidation patterns would look like beyond 16 processors, we propose a classification scheme for data objects found in parallel applications and link the invalidation traffic patterns observed in the traces back to these high-level objects. Our results show that synchronization objects have very different invalidation patterns from those of other data objects. A write reference to a synchronization object usually causes invalidations in many more caches. We point out situations where restructuring the application seems appropriate to reduce the invalidation traffic, and others

where hardware support is more appropriate. Our results also show that it should be possible to scale well-written parallel programs to a large number of processors without an explosion in invalidation traffic. GRA

N89-29090# Universiteit Twente, Enschede (Netherlands). Dept. of Computer Science.
TWENTENET CHIP DESIGN
B. G. M. OldeHampsink and D. B. deVries Nov. 1988 22 p In DUTCH; ENGLISH summary
(MEMO-INF-88-49; ETN-89-94767) Avail: NTIS HC A03/MF A01

The different aspects of very large scale integration chip design during the implementation of the TWENTENET chip are examined. This chip is part of the Data Link Layer of the TWENTENET Local Area Network according to the ISO-OSI/RM for open systems interconnection. The floorplanning for the global estimation of the required silicon surface, the simulation for the control of the correct operation of the chip, the layout, the processing of the chip, the structural and functional tests, and the error verification are discussed. The design of a chip, starting from formal specifications, is concluded to be more difficult than is claimed in the literature. ESA

N89-29091# Swedish Defence Research Establishment, Linkoeping. Dept. of Information Technology.
TIME: TIME AND MEMORY EFFICIENT DISTANCE TRANSFORMATIONS FOR PARALLEL AND PYRAMID MACHINES
Gunilla Borgefors May 1989 23 p
(FOA-C-30531-3.4; ISSN-0347-3708; ETN-89-95194) Avail: NTIS HC A03/MF A01; Swedish Defence Research Establishment, Box 1165, S-581 11, Linkoeping, Sweden, 50 Swedish crowns

An algorithm that computes weighted distance transforms on parallel machines, is presented. It can also be adapted to the city block and chessboard distances. The algorithm is fast, of order O(M), where M is the longest side of the image, and uses no arithmetic. Distances are propagated by checking if any of each pixel's neighbors have a certain value. If the distance transform is computed in a resolution pyramid, then the pyramid structure can be used to reduce the memory requirement for each pixel. Only four bits are necessary to measure distances of arbitrary size in the 3 to 4 weighted distance transform; and only two bits are necessary for the chessboard distance. ESA

N89-29092 National Physical Lab., Teddington (England). Div. of Information Technology and Computing.
APPRAISAL OF SECURITY OF DATA HANDLING SYSTEMS AND PRODUCTS: A TUTORIAL AND DISCUSSION DOCUMENT
W. L. Price Mar. 1989 18 p
(NPL-DITC-141/89; ETN-89-95251) Copyright Avail: National Physical Laboratory, Teddington, Middlesex, TW11 0LW, United Kingdom

Technical aspects of appraisal of security of data handling systems and products, in the civil domain, are discussed. The behavior of security personnel is not considered. The points of view of the U.S. Department of Defense (DOD) Orange and Red books and the UK Department of Trade and Industry (DTI) Commercial Computer Security Center are discussed. Products claiming conformance to particular International Standard Organization (ISO), or other organizations, security standards and the methods avaiable for testing the claimed conformance, are analyzed. The essential features of security analysis are outlined, but further studies on the subject are required. ESA

63 CYBERNETICS

Includes feedback and control theory, artificial intelligence, robotics and expert systems.

For related information see also *54 Man/System Technology and Life Support.*

N89-29093# Stanford Linear Accelerator Center, CA.
REAL-TIME APPLICATIONS OF NEURAL NETS
J. E. Spencer May 1989 5 p Presented at the 6th Conference on Real-Time Computer Applications in Nuclear, Particle and Plasma Physics, Williamsburg, VA, 15 May 1989
(Contract DE-AC03-76SF-00515)
(DE89-014400; SU-SLAC-PUB-4963; CONF-890545-6) Avail: NTIS HC A02/MF A01

Producing, accelerating and colliding very high power, low emittance beams for long periods is a formidable problem in real time control. As energy has grown exponentially in time so has the complexity of the machines and their control systems. Similar growth rates have occurred in many areas, e.g., improved integrated circuits have been paid for with comparable increases in complexity. However, in this case, reliability, capability and cost have improved due to reduced size, high production and increased integration which allow various kinds of feedback. In contrast, most Large Complex Systems (LCS) are perceived to lack such possibilities because only one copy is made. Neural nets, as a metaphor for LCS, suggest ways to circumvent such limitations. It is argued that they are logically equivalent to multi-loop feedback/forward control of faulty systems. While complimentary to AI, they mesh nicely with characteristics desired for real time systems. Such issues are considered, examples given and possibilities discussed. DOE

N89-29094# Syracuse Univ., NY.
NORTHEAST ARTIFICIAL INTELLIGENCE CONSORTIUM. VOLUME 1: EXECUTIVE SUMMARY Annual Report, Dec. 1986 - Dec. 1987
Volker Weiss and James F. Brule Mar. 1989 38 p Prepared in cooperation with the Northeast Artificial Intelligence Consortium, Syracuse, NY
(Contract F30602-85-C-0008)
(AD-A209395; RADC-TR-88-324-Vol-1) Avail: NTIS HC A03/MF A01 CSCL 12/9

The Northeast Artificial Intelligence Consortium (NAIC) purpose is to conduct pertinent research in artificial intelligence and to perform activities ancillary to this research. The topics covered in general are: versatile expert system for equipment maintenance, distributed AI for communications system control, automatic photo interpretation, time-oriented problem solving, speech understanding systems, knowledge base maintenance, hardware architectures for very large systems, knowledge-based reasoning and planning, parallel structural, and optimal techniques in vision, and a knowledge acquisition, assistance, and explanation system. GRA

N89-29095# Syracuse Univ., NY.
NORTHEAST ARTIFICIAL INTELLIGENCE CONSORTIUM ANNUAL REPORT 1987. VOLUME 8: KNOWLEDGE BASE MAINTENANCE USING LOGIC PROGRAMMING METHODOLOGIES Interim Report, Dec. 1986 - Dec. 1987
Kenneth A. Bowen Mar. 1989 50 p Prepared in cooperation with the Northeast Artificial Intelligence Consortium, Syracuse, NY
(Contract F30602-85-C-0008)
(AD-A209453; RADC-TR-88-324-Vol-8) Avail: NTIS HC A03/MF A01 CSCL 12/9

The Northeast Artificial Intelligence Consortium (NAIC) purpose is to conduct pertinent research in artificial intelligence and to perform activities ancillary to this research. The progress is described that was made in the 3rd year of the existence of the NAIC. The topics covered in general are: versatile expert system for equipment maintenance, distributed AI for communications system control, automatic photo interpretation, time oriented problem solving, speech understanding systems, knowledge base maintenance, hardware architectures for very large systems, knowledge-based reasoning and planning, and a knowledge

acquisition, assistance, and explanation system. The specific topic for this volume is the use of logic programming methodologies for knowledge base maintenance. GRA

N89-29096# Syracuse Univ., NY.
NORTHEAST ARTIFICIAL INTELLIGENCE CONSORTIUM ANNUAL REPORT 1987. VOLUME 9: COMPUTER ARCHITECTURES FOR VERY LARGE KNOWLEDGE BASES Interim Report, Dec. 1986 - Dec. 1987
P. Bruce Berra Mar. 1989 216 p Prepared in cooperation with the Northeast Artificial Intelligence Consortium, Syracuse, NY (Contract F30602-85-C-0008)
(AD-A209454; RADC-TR-88-324-Vol-9) Avail: NTIS HC A10/MF A01 CSCL 12/9

The Northeast Artificial Intelligence Consortium (NAIC) purpose is to conduct pertinent research in artificial intelligence and to perform ancillary activities. Progress made is described. The topics covered in general are: versatile expert system for equipment maintenance, distributed AI for communications system control, automatic photo interpretation, time-oriented problem solving, speech understanding systems, knowledge base maintenance, hardware architectures for very large systems, knowledge based reasoning and planning, and a knowledge acquisition, assistance, and explanation system. The specific topic for this volume is the development of architectures for very large knowledge bases, especially in light of real time requests, parallelism, and the advent of optical computing. GRA

N89-29097# Massachusetts Inst. of Tech., Cambridge. Artificial Intelligence Lab.
THE PERFORMANCE OF A MECHANICAL DESIGN COMPILER
Allen C. Ward and Warren P. Seering Jan. 1989 13 p
(Contract N00014-86-K-0685)
(AD-A209540; AD-E900860; AIM-1084) Avail: NTIS HC A03/MF A01 CSCL 12/5

Among the research goals is the development of mechanical design compilers; that is, programs which take as input a schematic (or other high-level description) of a mechanical design, plus specifications and a cost function, and return a description of the optimal implementation of the design, sufficiently detailed to support manufacture. Such programs should decrease design time and cost, increase design quality, and allow designers to explore more alternatives in greater depth. The domain of mechanical and hydraulic power transmission systems built from cataloged components is examined. For this domain, the goals were mostly accomplished; the evidence is presented for that success, and its limitations are discussed. After mentioning some related work, a very brief overview is provided of the compiler, intended only to allow the reader to understand the performance evaluation. GRA

N89-29098# Texas A&M Univ., College Station. Dept. of Mathematics.
COMPUTATIONS OF OPTIMAL CONTROLS AND DESIGNS FOR DISTRIBUTED SYSTEMS IN OPTICS AND ELASTICITY Final Project Report, 1 Jan. - 31 Dec. 1988
Goong Chen and Jianxin Zhou 24 Mar. 1989 12 p
(Grant AF-AFOSR-0091-88; AF Proj. 2304)
(AD-A207924; AFOSR-89-0593TR) Avail: NTIS HC A03/MF A01 CSCL 12/2

The boundary element methods are studied for a variety of partial differential equations in optics and elasticity, including the Helmholtz equation on an exterior domain, the eigenvalue problem for the Laplacian, the elastostatic Timoshenko plate and 3-D elastostatic solid mechanics. Numerical software was accumulated and computer graphics was successfully developed. GRA

N89-29099# Naval Postgraduate School, Monterey, CA.
COMPUTER IMPLEMENTATION AND SIMULATION OF SOME NEURAL NETWORKS USED IN PATTERN RECOGNITION AND CLASSIFICATION M.S. Thesis
Mohamed H. Khaidar Mar. 1989 131 p
(AD-A208112) Avail: NTIS HC A07/MF A01 CSCL 12/9

Searchers and scientists have been studying neural networks for many years hoping to achieve human-like performance in the fields of speech and pattern recognition and classification. An introduction is made to the field of artificial neural networks, then some of the neural nets used in the pattern recognition and classification are described. A computer simulation program from an algorithmic approach for each one of these networks is constructed and used to implement the operation of the net. Its ability is demonstrated in differentiating between different patterns and even correcting a noisy pattern and recognizing it. The Hopfield network, the Hamming network and the Carpenter/Grossberg network is individually utilized in developing an algorithm for pattern recognition and classification. The maximum likelihood sequence estimation function is mapped onto a neural network structure. The application of this structure computations for data detection in digital communications receivers is described. A computer simulation program is constructed and used to show that neural networks offer attractive implementation alternatives for MLSE. GRA

N89-29100# Kensal Consulting, Tucson, AZ.
THREE DIMENSIONAL CELLULAR AUTOMATA FOR SUBPIXEL TARGET DETECTION Final Technical Progress Report, No. 6, 1 Oct. 1988 - 28 Feb. 1989
Kendall Preston, Jr. 15 Mar. 1989 69 p
(Contract N00014-88-C-0717)
(AD-A208163; KSC-TR-88-006) Avail: NTIS HC A04/MF A01 CSCL 09/1

This project on subpixel target detection relates to research in the optimization of three-dimensional computing structures for use in target detection and to research in the reduction of an optimum computing to an efficiently-designed silicon chip. The work reported here has led to this final report which is divided into three sections: (1) presentation of the mathematical analysis which treats multiply-redundant massively-parallel processors for target detection, (2) a report on VLSI implementation of the target-detection processor as presented by our subcontractor Visual Information Technologies, (Plano, Texas), and (3) a description of the Macintosh-based three-dimensional, target-detection software emulator designed during the course of this study for use in Phase 2 to predict target miss rates and target false alarm rates using three-dimensional logical processing. GRA

N89-29101# Laboratoire d'Automatique et d'Analyse des Systemes, Toulouse (France).
ON CONSTRAINED MULTIVARIABLE ADAPTIVE CONTROL Ph.D. Thesis - Toulouse Univ.
Jean-Paul Beziat 1989 134 p In FRENCH; ENGLISH summary
(LAAS-89.093; ETN-89-94870) Avail: NTIS HC A07/MF A01

A first approach to adaptive control is based on the optimization of a predictive criterion under quadratic input constraints. Optimality conditions are obtained from the Lagrangean formulation of the problem. The second approach uses the positive invariance concept applied to discrete-time linear systems. The adaptive control law is obtained by a recursive estimation of the model's parameters and by the resolution of a linear programming problem. Simulation results illustrate the performance of the method. ESA

N89-29102# Universiteit Twente, Enschede (Netherlands). Faculty of Applied Mathematics.
THE COMMUNICATION COMPLEXITY OF INTERVAL ORDERS
Ulrich Faigle, Rainer Schrader, and Gyorgy Turan (Chicago Univ., IL.) Oct. 1988 18 p
(Memo-745; ISSN-0169-2690; ETN-89-95113) Avail: NTIS HC A03/MF A01

The communication complexity of interval orders is studied within a model where two players choose two elements, X and Y, and attempt to determine whether X is less than Y holds, by the exchange of the least bits of information. An optimal one-way protocol is shown to exist by the initial establishment of a rank optimality result for a subclass of generalized interval orders obtained by the generalization of the results of Faigle and Schrader

(1987). Analysis based on the studies of Gierz and Poguntke (1983), prove that deterministic and nondeterministic communication complexities coincide for generalized interval orders. The analogous statement for the complementary relation is shown to be true for interval orders in the strict sense and shown to not necessarily hold for generalized interval orders. ESA

N89-29103# Universiteit Twente, Enschede (Netherlands). Faculty of Applied Mathematics.
HAMILTONIAN CONTROL SYSTEMS: DECOMPOSITION AND CLAMPED DYNAMICS
A. J. vanderSchaft Jan. 1989 22 p Submitted for publication
(Memo-759; ISSN-0169-2690; ETN-89-95124) Avail: NTIS HC A03/MF A01

The decomposition and clamped dynamics of Hamiltonian control systems are investigated. The definitions of Hamiltonian and Poisson control systems are surveyed. A Hamiltonian control system is shown under some regularity assumptions, to admit a local canonical decomposition which reflects its controllability and observability properties. A natural Poisson mapping from this system onto a Poisson control system of lower dimension and the same input-output behavior is thereby defined. The clamped dynamics of a Hamiltonian system is shown, under extra assumptions, to be Hamiltonian, and a conjecture is formulated for the general case. ESA

N89-29104# Universiteit Twente, Enschede (Netherlands). Faculty of Applied Mathematics.
APPLICATION OF OPTIMAL CONTROL THEORY FOR SELECTIVE VIBRATIONAL EXCITATION IN MOLECULES MODELED AS HARMONIC SYSTEMS
J. G. B. Beumee and H. Rabitz (Princeton Univ., NJ.) Dec. 1988 32 p
(Memo-755; ISSN-0169-2690; ETN-89-95121) Avail: NTIS HC A03/MF A01

The design of optimal electromagnetic fields producing selective vibrational excitation in molecules modeled as harmonic physical systems is shown to be equivalent to minimizing a quadratic cost functional, balancing the energy distribution in the molecule and the fluence of the input. In the control problem two approaches are employed to insure that the final excitation is attained. One method uses a control strategy which employs a terminal constraint and in the other approach the cost functional is augmented with a terminal cost. The asymptotic form of the state and costate are investigated for both strategies in the limit that the final time approaches infinity and some mathematical results on the form of the Lagrange parameter are presented for the first type of controller. These two results are used to discuss an appropriate choice of practical design constants. For the example of a linear chain molecule an approximation for the eigenvalues of the Hamiltonian matrix is derived for the limiting case where the weighting on the fluence of the optical field in the cost functional increases to infinity. Also for the linear chain it is shown that the eigenvalues are bounded and that this bound does not depend on the length of the chain. ESA

64 NUMERICAL ANALYSIS

Includes iteration, difference equations, and numerical approximation.

N89-29105# Technische Univ., Delft (Netherlands). Faculty of Technical Mathematics and Informatics.
ROW-ORIENTED DIRECT SOLVING OF LINEAR ALGEBRAIC EQUATIONS: ROW ORTHOGONALIZATION METHOD
L. Dekker and E. Dekker 1988 8 p
(Rept-88-82; ISSN-0922-5641; ETN-89-94911) Copyright Avail: NTIS HC A02/MF A01

Serial and parallel algorithms were derived from a direct row-oriented solution method for linear algebraic equations. The row orthogonalization method are discussed. As in the inverse projection method, no elimination of unknowns is applied. The matrix equation is considered to be a set of inner product equations. For the row orthogonalization method the set of inner product equations is transformed into one with orthogonal row vectors by applying orthogonalization techniques to the original row vectors. The resulting equations can be solved independently. The transforming and solving process require extensive inner product calculus. Pipeline as well as parallel processing can be applied, resulting in parallel algorithms with a large speed-up which can easily and efficiently be implemented onto MIMD supercomputers provided with local memories and designed to perform both parallel and pipelined processing. In the case of structural sparse matrices the structural characteristics can be exploited resulting in a considerable speed improvement. ESA

N89-29106# California Univ., Berkeley. Lawrence Berkeley Lab. Accelerator Fusion Research Div.
CANONICAL INTEGRATION AND ANALYSIS OF PERIODIC MAPS USING NON-STANDARD ANALYSIS AND LIE METHODS
Etienne Forest and Martin Berz (Universities Research Association, Inc., Berkeley, CA.) Jun. 1988 24 p Presented at the 2nd Workshop on Lie Methods in Optics, Morelos, Mexico, 19-22 Jul. 1988
(Contract DE-AC03-76SF-00098)
(DE89-013369; LBL-25609; CONF-8807177-1; ESG-46) Avail: NTIS HC A03/MF A01

A method and a way of thinking which is ideally s uited for the study of systems represented by canonical integrators is described. Starting with the continuous description provided by the Hamiltonians, it is replaced by a succession of preferably canonical maps. The power series representation of these maps can be extracted with a computer implementation of the tools of Non-Standard Analysis and analyzed by the same tools. For a nearly integrable system, a Floquet ring is described in a way consistent with the needs. Using the finite time maps, the Floquet ring is defined only at the locations where one perturbs or observes the phase space. At most the total number of locations is equal to the total number of steps of the integrator. Pseudo-Hamiltonians which describe the motion induced by these maps are also produced. DOE

N89-29107# International Centre for Theoretical Physics, Trieste (Italy).
ON THE RIEMANNIAN CURVATURE OF A TWISTOR SPACE
Johann Davidov and Oleg Muskarov Dec. 1988 22 p Submitted for publication
(DE89-611897; IC-88/414) Avail: NTIS (US Sales Only) HC A03/MF A01

Coordinate free formulas for the sectional curvatures of a family of pseudo-Riemannian metrics on a twistor space are obtained in terms of the curvature of the base four manifold. The respective Ricci curvatures and the holomorphic sectional curvatures of two natural almost complex structures are also discussed. DOE

N89-29108# Argonne National Lab., IL. High Energy Physics Div.
NEW INFINITE-DIMENSIONAL ALGEBRAS, SINE BRACKETS, AND SU (INFINITY)
C. K. Zachos and D. B. Fairlie (Durham Univ., England) 1989 10 p Presented at the Strings 1989 Conference, College Station, TX, 13 Mar. 1989
(Contract W-31-109-eng-38)
(DE89-013178; ANL-HEP-CP-89-36; CONF-8903130-1) Avail: NTIS HC A02/MF A01

The infinite dimensional algebras previously introduced, which involve trigonometric functions in their structure constants, are investigated. A realization was found for them which provides a basis-independent formulation, identified with the algebra of sine brackets. A special family of them, the cyclotomic ones, contain SU(N) as invariant subalgebras. In this basis, it is evident by inspection that the algebra of SU(infinity) is equivalent to the centerless algebra of SDiff(0) on two-dimensional manifolds. Gauge theories of SU(infinity) are thus simply reformulated in terms of

surface (sheet) coordinates. Spacetime-independent configurations of their gauge fields describe strings through the quadratic Schild action. DOE

N89-29109# California Inst. of Tech., Pasadena. Dept. of Applied Mathematics.
DIFFERENTIAL EQUATIONS AND CONTINUUM MECHANICS Final Report
Donald S. Cohen 2 May 1989 6 p
(Grant AF-AFOSR-0270-87; AF Proj. 2304)
(AD-A208637; AFOSR-89-0703TR) Avail: NTIS HC A02/MF A01 CSCL 07/6

Recent advances in materials science and synthetic chemistry have led to the development and design of new classes of polymeric materials with desirable and beneficial properties. These are of enormous importance in many industrial and military situations. Most of these materials have features not well understood scientifically and not explainable with current standard equations of motion. The authors looked at several classes of these polymers with the intent of developing the nonlinear models for the study of transport by and through them. The models are then applied to specific new technological problems necessitating the development of new asymptotic, perturbation and numerical techniques for their solutions. GRA

N89-29110# Air Force Inst. of Tech., Wright-Patterson AFB, OH. School of Engineering.
SIGNED-DIGIT HIGH SPEED TRANSCENDENTAL FUNCTION PROCESSOR ARCHITECTURE M.S. Thesis
Robert Alan Peterson Jun. 1989 159 p
(AD-A209199; AFIT/GCE/ENG/89J-1) Avail: NTIS HC A08/MF A01 CSCL 12/7

In support of the computation requirements of complex equations, a processor which can compute elementary transcendental functions with high throughput is becoming a hard requirement for many systems. In particular, the computation of components of the Vector Wave Equation are becoming bottlenecked by the reduced speed of the processor when computing the required elementary functions. To speed up the computation of these type of functions, a pipelined processor with high throughput is developed. This processor will compute Sine, Cosine, Tangent, Cotangent, Arctangent, Exponential, Natural Logarithm and Division as a minimum. The accuracy of the computations will be greater than IEEE double precision. The majority of the approximation algorithms are derived from Chebyshev Polynomials, due to their error characteristics and compatability with a pipelined processor. The only approximation algorithm not derived from Chebyshev Polynomials is the division algorithm. GRA

N89-29111# Illinois Univ., Urbana. Dept. of Mechanical and Industrial Engineering.
TOTAL LAGRANGIAN FORMULATION FOR LARGE-DISPLACEMENT ANALYSIS OF THE TRIANGULAR FINITE ELEMENTS
A. A. Shabana and S. K. Niamathullah 1989 6 p
(Contract DAAL03-87-K-0124)
(AD-A209378; ARO-25170.11-EG) Avail: NTIS HC A02/MF A01 CSCL 12/1

In this reprint a total Lagrangian dynamic finite element formulation is developed for the six degree of freedom constant-strain triangular element. In the formulation developed in this paper, the element may undergo large translational and rotational displacements. The formulation presented can be of use in many applications related to multibody dynamics wherein systems are assumed to consist of interconnected deformable bodies each of which may undergo large translational and rotational displacements. For convenience of describing the relative motion between interconnected bodies, two sets of generalized coordinates are employed in order to identify the configuration of the constant-strain triangular element used in the finite element discretization of the deformable bodies. These two sets are the reference and elastic coordinates. The reference coordinates define the location and orientation of a selected deformable body reference, while the elastic coordinates are the nodal coordinates that describe the displacement of selected nodal points in the finite element discretization. GRA

N89-29112# Utah Univ., Salt Lake City. Dept. of Chemistry.
APPLICATION OF CHOLESKY-LIKE MATRIX DECOMPOSITION METHODS TO THE EVALUATION OF ATOMIC ORBITAL INTEGRALS AND INTEGRAL DERIVATIVES Technical Report No. 1, Jan. - Jun. 1989
Douglas W. ONeal and Jack Simons 28 Jun. 1989 33 p Submitted for publication
(Contract N00014-89-J-1497)
(AD-A209682) Avail: NTIS HC A03/MF A01 CSCL 07/4

When viewed as a square two-indexed matrix, the array of atomic orbital based, two-electron integrals (ij/kl) is a positive semidefinite array. Beebe and Linderberg showed, in 1977, that actual or near linear dependencies often exist within the types of atomic orbital basis sets employed in conventional quantum chemical calculations. In fact, large (i.e., higher quality) bases were shown to be substantially more redundant than smaller or more spatially separated bases. In situations where these exists significant basis near redundancy, the rank (r) of the (ij/kl) = V(sub I,J) matrix of integrals will be significantly smaller than the matrix dimension M. GRA

N89-29113# Florida Univ., Gainesville.
PROBABILISTIC ANALYSIS OF SEMILINEAR PARTIAL DIFFERENTIAL EQUATIONS Final Report, 30 Sep. 1985 - 29 Mar. 1989
Joseph Glover and Kai Lai Chung 28 May 1989 6 p
(Grant AF-AFOSR-0330-85; AF Proj. 2304)
(AD-A209903; AFOSR-89-0806TR) Avail: NTIS HC A02/MF A01 CSCL 12/1

A major thrust of the original proposal was to find new probabilistic methods for dealing with semilinear partial differential equations. Mathematicians are currently devoting more of their attention to studying nonlinear partial differential equations since they recognize that descriptions of physical phenomena must incorporate nonlinear behavior. The author succeeded in finding a method for solving systems of semilinear elliptic equations by a new procedure which does not need the old hypotheses of quasi-monotone systems. It combines probability, analysis and a transfinite induction scheme to solve equations of a certain form on a domain E in R to the d power subject to boundary conditions u sub 1 = u sub 2 = ... u sub n =0 on the boundary of E. GRA

N89-29114# Cornell Univ., Ithaca, NY. Dept. of Computer Science.
INTERPOLATING POLYNOMIALS FROM THEIR VALUES
Richard Zippel Jan. 1989 31 p
(Contracts N00014-88-K-0591; N00014-86-K-0281; NSF DMS-86-17355)
(AD-A210102; CU-CSD-TR-89-963) Avail: NTIS HC A03/MF A01 CSCL 12/1

A fundamental technique used by many algorithms in computer-algebra is interpolating polynomials from their values. This paper discusses two algorithms for solving this problem for sparse multivariate polynomials, an updated version of a probabilistic one and a new deterministic technique that uses some ideas due to Ben-Or and Tiwari (1988). In addition algorithms are presented for quickly finding points that are not zeroes of sparse multivariate polynomials-the zero avoidance problem. GRA

N89-29115# Cornell Univ., Ithaca, NY. Dept. of Computer Science.
PLACING THE LARGEST SIMILAR COPY OF A CONVEX POLYGON AMONG POLYGONAL OBSTACLES
L. P. Chew and Klara Kedem Jan. 1989 21 p
(Contracts N00014-88-K-0591; N00014-86-K-0281; NSF DMS-86-17355)

(AD-A210104; CU-CSD-TR-89-964) Avail: NTIS HC A03/MF A01 CSCL 12/2

Given a convex polygon P and an environment consisting of polygonal obstacles, we find the largest similar copy of P that does not intersect any of the obstacles. Allowing translation, rotation, and change-of-size, our method combines a new notion of Delaunay triangulation for points and edges with the well-known functions based on Davenport-Schinzel sequences producing an almost quadratic algorithm for the problem. Namely, if P is a convex k-gon and if Q has n corners and edges then we can find the placement of the largest similar copy of P in the environment Q in time O(k to the 4th power (n) lambda sub 4 (kn) log n), where (lambda sub 4) is one of the almost-linear functions related to Davenport-Schinzel sequences. If the environment consists only of points then we can find the placement of the largest similar copy of P in time O (k to the 2nd power (n) lambda sub 3 (kn) log n). GRA

N89-29116# Maryland Univ., College Park. Inst. for Physical Science and Technology.

THE P-VERSION OF THE FINITE ELEMENT METHOD FOR DOMAINS WITH CORNERS AND FOR INFINITE DOMAINS Final Report

Ivo Babuska and Hae-Soo Oh (North Carolina Univ., Charlotte.) Nov. 1988 42 p

(Contract N00014-85-K-0169; NSF DMS-85-16191)

(AD-A207797; BN-1091) Avail: NTIS HC A03/MF A01 CSCL 12/2

A special approach to deal with elliptic problems with singularities is introduced. It is shown that this approach, to be called the auxiliary mapping technique, in the frame of the p-version of the finite element method yields an exponential rate of convergence at virtually no extra cost. From the view-point of implementation it is the easiest and the cheapest method of all. It is also shown that this technique can be used for elliptic problems on unbounded domains in R-sq as well. GRA

N89-29117# Maryland Univ., College Park. Inst. for Physical Science and Technology.

THE PROBLEM OF SELECTING THE SHAPE FUNCTIONS FOR A P-TYPE FINITE ELEMENT Final Report

Ivo Babuska, M. Griebel (Technische Univ., Munich, Germany, F.R.), and J. Pitkaranta Nov. 1988 40 p Prepared in cooperation with Helsinki Univ. of Technology, Espoo (Finland) Sponsored in part by Univ. of Maryland, and by Finnish Academy

(Contract N00014-85-K-0169)

(AD-A207798; BN-1090; MD88-36-IB-MG-JP; TR-88-36) Avail: NTIS HC A03/MF A01 CSCL 12/1

The paper addresses the question of the optimal selection of the shape functions for p-type finite elements and discusses the effectivity of the conjugate gradient and multilevel iteration method for solving the corresponding linear system. The selection of the shape functions is of major importance for the performance of the solver based on iterative methods. Neither the theory nor practice of the optimal selection of the shape functions is available yet. We have seen that the condensation approach which has obvious advantages from the point of parallel computations is a very effective tool for keeping the condition number under the control and is especially advantageous for the conjugate gradient method. GRA

N89-29118# Maryland Univ., College Park. Inst. for Physical Science and Technology.

IMPLEMENTATION OF NONHOMOGENEOUS DIRICHLET BOUNDARY CONDITIONS IN THE p-VERSION OF THE FINITE ELEMENT METHOD

Ivo Babuska, B. Guo, and Manil Suri (Maryland Univ., Baltimore.) Sep. 1988 42 p

(Contract N00014-85-K-0169; AF-AFOSR-0322-85; NSF DMS-85-16191)

(AD-A207799; BN-1089; MD88-32-IB; TR-88-32) Avail: NTIS HC A03/MF A01 CSCL 12/1

Various methods for treating nonhomogeneous Dirichlet boundary conditions for the p-version of the finite element method are presented. These methods are theoretically and computationally analyzed. Numerical experimentations are given. They clearly illustrate the importance of the right treatment of the nonhomogeneous Dirichlet boundary conditions. GRA

N89-29119# Iowa State Univ. of Science and Technology, Ames. Dept. of Mathematics.

NUMERICAL SOLUTION OF ILL POSED PROBLEMS IN PARTIAL DIFFERENTIAL EQUATIONS Final Technical Report, 1 Oct. 1984 - 30 Jun. 1988

Howard A. Levine 30 Jun. 1988 26 p

(Grant AF-AFOSR-0252-84; AF Proj. 2304)

(AD-A207852; AFOSR-89-0607TR) Avail: NTIS HC A03/MF A01 CSCL 12/1

This project is concerned with several questions conerning the existence, uniqueness, continuous data dependence and numerical computation of solutions of various ill posed problems in partial differential equations. Several problems involving reaction diffusion equations with and without convection terms present were studied. In the latter case the ability of finite element approximate solutions to reproduce the continuous time dynamics was investigated. In the former case, a convective diffusion equation with a semilinear source in the boundary conditions was analyzed. A fairly complete picture of the dynamics was obtained. With the source term in the equation, computations revealed a rich structure which has been partially analyzed theoretically. Several problems for reaction diffusion equations in unbounded regimes were also investigated. It was shown that under certain conditions in the rate law all nonzero solutions blow up in finite time, while for other conditions in the rate law, solutions damp out. It was shown that a potential well theory is possible for certain hyperbolic problems in which a nonlinear boundary condition is prescribed and not possible in certain cases when forcing term in the differential equation is singular. Numerical experiments performed on the wave equation with a singular forcing term have down that when quenching occurs, the time and exact derivatives blow up in finite time. The nature of the blowup was studied computationally. GRA

N89-29120# Illinois Univ., Chicago. Biometric Lab.

CONDITIONAL DEPENDENCE Final Report, 1 Aug. 1985 - 1 Aug. 1988

Robert D. Gibbons, R. Darrell Bock, and Donald Hedeker 15 Mar. 1989 33 p Submitted for publication

(Contract N00014-85-K-0586)

(AD-A207881; Rept-89-1) Avail: NTIS HC A03/MF A01 CSCL 12/1

The probability of m correlated random variables drawn from a multivariate normal distribution being non-negative is given. Exact results for this probability integral are unavailable for m is larger than 3. Approximations for higher dimensional problems have generally yielded poor results for special cases, such as compound symmetry, which is of limited value in practice. The purpose is to present a general approximation of this probability integral. The algorithm developed is computationally tractable for m equals 50 and accurate for very general correlational structures. The performance of this algorithm is compared to results based on Clark's (1961) original approximation, Gaussian quadrature formulae, and Monte Carlo simulation methods. Application of this approximation to problems of conditional dependence in IRT estimation problems is discussed. GRA

N89-29121# Naval Research Lab., Washington, DC. Atmospheric Physics Branch.

A USER'S GUIDE TO THE SEVP (STABILIZED ERROR VECTOR PROPAGATION) SOLVER: AN EFFICIENT DIRECT SOLVER FOR ELLIPTIC PARTIAL DIFFERENTIAL EQUATIONS

Keith D. Sashegyi (Science Applications International Corp., McLean, VA.) and Rangarao V. Madala 13 Apr. 1989 41 p

(AD-A208117; NRL-MR-6450) Avail: NTIS HC A03/MF A01 CSCL 12/5

How to use the Stabilized Error Propagation (SEVP) FORTRAN

subroutines, which were developed at the Naval Research Laboratory, to solve an elliptic partial differential equation using finite difference methods is described. The SEVP method is an efficient direct method which can be used for separable and non-separable elliptic equations. The derivation of the finite difference equations and the use of Dirichlet, Neumann and periodic boundary conditions are demonstrated. The method and a test example are also described. GRA

N89-29122*# Institute for Computer Applications in Science and Engineering, Hampton, VA.
A HYBRID PERTURBATION-GALERKIN METHOD FOR DIFFERENTIAL EQUATIONS CONTAINING A PARAMETER Final Report
James F. Geer and Carl M. Andersen (College of William and Mary, Williamsburg, VA.) Jun. 1989 28 p Submitted for publication
(Contract NAS1-18605)
(NASA-CR-181891; NAS 1.26:181891; ICASE-89-49) Avail: NTIS HC A03/MF A01 CSCL 12A

A two-step hybrid perturbation-Galerkin method to solve a variety of differential equations which involve a parameter is presented and discussed. The method consists of: (1) the use of a perturbation method to determine the asymptotic expansion of the solution about one or more values of the parameter; and (2) the use of some of the perturbation coefficient functions as trial functions in the classical Bubnov-Galerkin method. This hybrid method has the potential of overcoming some of the drawbacks of the perturbation method and the Bubnov-Galerkin method when they are applied by themselves, while combining some of the good features of both. The proposed method is illustrated first with a simple linear two-point boundary value problem and is then applied to a nonlinear two-point boundary value problem in lubrication theory. The results obtained from the hybrid method are compared with approximate solutions obtained by purely numerical methods. Some general features of the method, as well as some special tips for its implementation, are discussed. A survey of some current research application areas is presented and its degree of applicability to broader problem areas is discussed. Author

N89-29123*# Institute for Computer Applications in Science and Engineering, Hampton, VA.
SOLUTION OF THE HYDRODYNAMIC DEVICE MODEL USING HIGH-ORDER NON-OSCILLATORY SHOCK CAPTURING ALGORITHMS Final Report
Emad Fatemi, Joseph Jerome, and Stanley Osher Jul. 1989 62 p Submitted for publication
(Contract NAS1-18605)
(NASA-CR-181886; ICASE-89-52; NAS 1.26:181886) Avail: NTIS HC A04/MF A01 CSCL 12A

A micron n+ - n - n+ silicon diode is simulated via the hydrodynamic model for carrier transport. The numerical algorithms employed are for the non-steady case, and a limiting process is used to reach steady state. The simulation employs shock capturing algorithms, and indeed shocks, or very rapid transition regimes, are observed in the transient case for the coupled system, consisting of the potential equation and the conservation equations describing charge, momentum, and energy transfer for the electron carriers. These algorithms, termed essentially non-oscillatory, were successfully applied in other contexts to model the flow in gas dynamics, magnetohydrodynamics, and other physical situations involving the conservation laws in fluid mechanics. The method here is first order in time, but the use of small time steps allows for good accuracy. Runge-Kutta methods allow one to achieve higher accuracy in time if desired. The spatial accuracy is of high order in regions of smoothness. Author

N89-29124*# Institute for Computer Applications in Science and Engineering, Hampton, VA.
OPTIMAL ERROR ANALYSIS OF SPECTRAL METHODS WITH EMPHASIS ON NON-CONSTANT COEFFICIENTS AND DEFORMED GEOMETRIES Final Report
Yvon Maday and Einar M. Ronquist (Massachusetts Inst. of Tech., Cambridge.) Sep. 1989 24 p Submitted for publication
(Contract NAS1-18605)
(NASA-CR-181902; NAS 1.26:181902; ICASE-89-56) Avail: NTIS HC A03/MF A01 CSCL 12A

The numerical analysis of spectral methods when non-constant coefficients appear in the equation, either due to the original statement of the equations or to take into account the deformed geometry, is presented. Particular attention is devoted to the optimality of the discretization even for low values of the discretization parameter. The effect of some overintegration is also addressed, in order to possibly improve the accuracy of the discretization. Author

N89-29125 National Physical Lab., Teddington (England). Div. of Information Technology and Computing.
LEAST-SQUARES BEST-FIT GEOMETRIC ELEMENTS
Alistair B. Forbes Apr. 1989 34 p
(NPL-DITC-140/89; ISSN-0262-5369; ETN-89-95250) Copyright Avail: National Physical Laboratory, Teddington, Middlesex, TW11 0LW, United Kingdom

Algorithms for computing least-squares best-fit geometric elements to data are described. The elements considered are lines, planes, circles, spheres, cylinders and cones. The algorithms employ stable parameterizations of the elements and are based on sound mathematical and numerical principles. These algorithms should be of value to the manufacturers and users of coordinate measurement systems. ESA

N89-29126 National Physical Lab., Teddington (England). Div. of Information Technology and Computing.
LINEAR ALGEBRA SUPPORT MODULES FOR APPROXIMATION AND OTHER SOFTWARE
M. G. Cox Apr. 1989 25 p Presented at the NPL/RMCS Symposium on Scientific Software and Systems, Shrivenham, England, 11 Jul. 1988
(NPL-DITC-142/89; ISSN-0262-5369; ETN-89-95252) Copyright Avail: National Physical Laboratory, Teddington, Middlesex, TW11 0LW, United Kingdom

A suite of linear algebra modules applied to the solution of problems in least-squares data approximation and modeling of discrete processes is shown. This suite of modules forms the core of a number of computer packages including the National Physical Laboratory's Data Approximation Subroutine Library. The suite consists of routines that treat three types of structured linear systems: those with banded, bordered and block-angular matrices, in addition to conventional systems with full matrices. The design of the suite is discussed, and the coverage of the suite indicated. Particular attention is given to the use of the suite in solving rank-deficient least-squares problems. ESA

N89-29127# Leiden Univ. (Netherlands). Div. of Applied Mathematics.
THE STABILITY OF THE THETA-METHODS IN THE NUMERICAL SOLUTION OF DELAY DIFFERENTIAL EQUATIONS
M. Z. Liu and M. N. Spijker Sep. 1988 24 p
(TW-88-08; ETN-89-95394) Avail: NTIS HC A03/MF A01

The stability analysis of numerical methods for the solution of delay differential equations is studied. The behavior of the one-leg theta-method and the linear theta-method in the solution of a linear test equation are examined. The stability regions for both methods are determined and compared, and are shown to be equal when theta = 0 or theta = 1. ESA

N89-29128# Leiden Univ. (Netherlands). Div. of Applied Mathematics.
A GENERALIZATION OF THE NUMERICAL RANGE OF A MATRIX
H. W. J. Lenferink and M. N. Spijker 1988 18 p Sponsored by the Netherlands Organization for Scientific Research
(TW-88-09; ETN-89-95395) Avail: NTIS HC A03/MF A01

A generalization of the classical numerical range of a matrix is

presented. Various properties and basic characterizations of this generalized numerical range are established. A resolvent inequality for a discretized version of the differential operator (second derivative) is proved, using one of these characteristics. ESA

N89-29129# Leiden Univ. (Netherlands). Div. of Applied Mathematics.
A NECESSARY CONDITION FOR B-CONVERGENCE OF RUNGE-KUTTA METHODS
J. Schneid (Technische Univ., Vienna, Austria) 1989 8 p Sponsored by the Netherlands Organization for Scientific Research and the Fonds zur Forderung der Wissenschafilichen Forschung
(TW-89-01; ETN-89-95397) Avail: NTIS HC A02/MF A01

Algebraic stability as a property necessary for B-convergence of a Runge-Kutta method is investigated. A weaker property is established which turns into algebraic stability. Lobatto Three A methods with more than two stages, and two commonly used three-stage semi-implicit methods, are shown not to be B-convergent. ESA

N89-29130# Universiteit Twente, Enschede (Netherlands). Faculty of Applied Mathematics.
SOME RECENT RESULTS ON LONG CYCLES IN TOUGH GRAPHS
D. Bauer, E. Schmeichel, and H. J. Veldman Feb. 1989 16 p
(Memo-765; ISSN-0169-2690; ETN-89-95060) Avail: NTIS HC A03/MF A01

Recent results concerning the relationship between the toughness of a graph and the maximum length of a cycle in a graph are surveyed. Finite undirected graphs without loops or multiple edges are investigated. The problems of recognizing tough graphs and Hamiltonian cycles in graphs is addressed. No proofs are given but statements of theorems and their validity are presented. ESA

N89-29131# Universiteit Twente, Enschede (Netherlands). Faculty of Applied Mathematics.
A NOTE ON THE COMMUNICATION COMPLEXITY OF TOTALLY UNIMODULAR MATRICES
Ulrich Faigle and W. Kern Feb. 1989 13 p
(Memo-768; ISSN-0169-2690; ETN-89-95063) Avail: NTIS HC A03/MF A01

The communication complexity of matrices in the context of distributed computing is addressed. A lower bound on the communication complexity of a matrix is described and an upper bound is proven for a unimodular matrix, based on Seymour's (1980) decomposition theory for totally unimodular matrices. ESA

N89-29132# Deutsche Forschungs- und Versuchsanstalt fuer Luft- und Raumfahrt, Brunswick (Germany, F.R.). Abteilung Unterschall-Entwurfsverfahren.
GRID GENERATION USING ELLIPTIC PARTIAL DIFFERENTIAL EQUATIONS
Thomas Sonar Mar. 1989 125 p
(DFVLR-FB-89-15; ISSN-0171-1342; ETN-89-95311) Avail: NTIS HC A06/MF A01; DFVLR, VB-PL-DO, Postfach 90 60 58, 5000 Cologne, Fed. Republic of Germany, 41 DM

A rigorous mathematical treatment of the properties of elliptic grid generation systems is described. Such a treatment is necessary to understand the underlying ideas. The classical general approach to source term control based on ideas of Thompson, and several particular methods often used in practice are explained. It is made clear that all these methods are unstable if the solution process of the generating system is viewed as an iterative procedure to solve a multi-dimensional operator equation. A perturbation theorem concerning this iterative process is shown. Based on this perturbation theorem a unified treatment of all source term control methods is possible, and it is shown that all of these methods become stable when using a new approach to grid generation. The possibilities of dynamically adaptive grids using the elliptic system approach are outlined. ESA

N89-29133# Technische Univ., Eindhoven (Netherlands).
ON THE SHAPE OF MATHEMATICAL ARGUMENTS Ph.D. Thesis
Antonetta Johanna Ma vanGasteren 1988 187 p Sponsored by British Petroleum International Ltd.
(ETN-89-95465) Avail: NTIS HC A09/MF A01

Ways in which computing scientists can make their proofs more effective are outlined. The historical need for such proof making techniques is presented. The recommended approach involves a combination of completeness and brevity of argument. A series of rules guiding clarity of exposition, naming, and the use of formalism are outlined. Proof rules for guarded-command programs are also included. Experimental results are provided. ESA

N89-29134# Universitaet der Bundeswehr, Neubiberg (Germany, F.R.). Forschungsschwerpunkt Simulation und Optimierung Deterministischer und Stochastischer Dyn. Systeme.
ON THE SOLVING OF STOCHASTIC ITO DIFFERENTIAL EQUATIONS BY SIMULATION [BERICHT UEBER DIE LOESUNG STOCHASTISCHER ITO-DIFFERENTIALGLEICHUNGEN DURCH SIMULATION]
Franz Schenkel Sep. 1988 197 p In GERMAN
(ETN-89-94610) Avail: NTIS HC A09/MF A01

The simulation of the stochastic Ito differential equation is described. The extent of sampling tests of the simulation, taking into account the moments up to the second order, is calculated. The step size of the integration in the simulation is calculated. The simulation of the solution of a stochastic Ito differential equation is described. The construction of a nonlinear, stochastic Ito differential equation is given as an example. The simulation is compared with the method using Markov chains. ESA

N89-29135*# Universiteit Twente, Enschede (Netherlands). Faculty of Applied Mathematics.
A TORUS BIFURCATION THEOREM WITH SYMMETRY
S. A. vanGils and M. Golubitsky (Houston Univ., TX.) Jan. 1989 44 p
(Grants NAG2-432; NSF DMS-87-00897)
(NASA-CR-185907; NAS 1.26:185907; Memo-760; ISSN-0169-2690; ETN-89-95125) Avail: NTIS HC A03/MF A01 CSCL 12A

Hopf bifurcation in the presence of symmetry, in situations where the normal form equations decouple into phase/amplitude equations is described. A theorem showing that in general such degeneracies are expected to lead to secondary torus bifurcations is proved. By applying this theorem to the case of degenerate Hopf bifurcation with triangular symmetry it is proved that in codimension two there exist regions of parameter space where two branches of asymptotically stable two-tori coexist but where no stable periodic solutions are present. Although a theory was not derived for degenerate Hopf bifurcations in the presence of symmetry, examples are presented that would have to be accounted for by any such general theory. ESA

N89-29136# Technical Research Centre of Finland, Espoo. Telecommunications Lab.
MINIMIZATION OF BOOLEAN SUM OF PRODUCTS WITH APPLICATIONS TO THE COMPUTATION OF RELIABILITY OF GENERAL NETWORKS
Seppo J. Nevalainen Nov. 1988 94 p
(VTT-RR-571; ISBN-951-38-3298-8; ISSN-0358-5077; ETN-89-95182) Copyright Avail: NTIS HC A05/MF A01; Government Printing Center, Mail Orders, P.O. 516, SF-00101 Helsinki, Finland, 76 Finnish marks

A new binary vector method is presented for the computerized search of minimum ties of a general network. The resolved minimum ties are utilized in generating a network's probability space, i.e. set of points of success and points of failure. The data file of these points is interpreted as the network's Boolean system function. It provides basic information for the new minimization algorithm of the Boolean SOP (sum of products) expression which is discussed in detail. In addition to these computer algorithms a short reliability calculation program is presented for the verification

of the former results. The developed methods are each, in turn, applied to several sample networks, and the results are compared and studied to ascertain the new algorithms. ESA

65 STATISTICS AND PROBABILITY

Includes data sampling and smoothing; Monte Carlo method; and stochastic processes.

N89-29137# Naval Research Lab., Washington, DC. Target Characteristics Branch.
STEIN'S LEMMA: A LARGE DEVIATIONS APPROACH Interim Report
R. Sowers 21 Mar. 1989 14 p
(AD-A209090; NRL-9185) Avail: NTIS HC A02/MF A01
CSCL 12/3

Stein's Lemma is proven by using a Large Deviations principle. The proof is general, direct, and intuitive. The log-likelihood ratio used to test between the two hypotheses on the basis of the first n observations as a sample mean of i.i.d. observations is presented. Led by the Strong Law of Large Numbers, a series of hypothesis that bound the true Neyman-Pearson tests is formulated. The asymptotic behavior of these tests is determined by using arguments from the proof of Cramer's Theorem. The conclusion of Stein's Lemma is given. GRA

N89-29138# Stanford Univ., CA. Computer Systems Lab.
CHARACTERIZATION OF PARALLELISM AND DEADLOCKS IN DISTRIBUTED DIGITAL LOGIC SIMULATION
Larry Soule and Anoop Gupta 3 Nov. 1988 15 p
(Contract N00014-87-K-0828)
(AD-A207842) Avail: NTIS HC A03/MF A01 CSCL 12/5

This paper explores the suitability of the Chandy-Misra algorithm for digital logic simulation. We use four realistic circuits as benchmarks for our analysis, with one of them being the vector-unit controller for the Titan supercomputer from Ardent. Our results show that the average number of logic elements available for concurrent execution ranges from 6.2 to 92 for the four circuits, with an overall average of 50. Although this is twice as much parallelism as that obtained by traditional event-driven algorithms, we feel it is still too low. One major factor limiting concurrency is the large number of global synchronization points- deadlocks in the Chandy-Misra terminology-that occur during execution. Towards the goal of reducing the number of deadlocks, the paper presents a classification of the types of deadlocks that occur during digital logic simulation. Four different types are identified and described both intuitively in terms of circuit structure and formally with equations. Using domain specific knowledge, the paper proposes methods for reducing these deadlock occurrences. For one of the benchmark circuits, the use of the proposed techniques eliminated all deadlocks and increased the average parallelism from 40 to 160. GRA

N89-29139# Leiden Univ. (Netherlands). Div. of Applied Mathematics.
ARE LIMITS OF ALPHA-DISCOUNTED OPTIMAL POLICIES BLACKWELL OPTIMAL: A COUNTEREXAMPLE
Arie Hordijk and Flos Spieksma 1988 15 p Sponsored by the Netherlands Organization for Scientific Research
(TW-88-10; ETN-89-95396) Avail: NTIS HC A03/MF A01

The Blackwell optimal limit of alpha-discounted optimal policies, for alpha tending to 1, in Markov Decision Chains (MDC's) with a finite state space and finite action sets are described. The conjecture, by Cavazos-Cadena and Lasserre, that this property of limiting policies also holds for Unichain MDC's is investigated. The conjecture is disproved by the construction of a non-Blackwell limiting policy in a unichain MDC with finitely many states and compact action sets. ESA

N89-29140# Grenoble-1 Univ. (France). Lab. Techniques de l'Informatique, Mathematiques, Microelectronique et Microscopie Quatitative.
AN A PRIORI APPROACH TO THE EVALUATION OF SIGNATURE ANALYSIS EFFICIENCY
P. Caspi, J. Piotrowski, and R. Velazco Oct. 1988 14 p
(IMAG-RR-746-I; ETN-89-95489) Avail: NTIS HC A03/MF A01

An evaluation of signature analysis efficiency which does not rely on assumptions about the distribution of the analyzed error sequences is presented. The use of an a priori randomization technique, which leads to choosing LFSRs (linear feedback signature registers) corresponding to randomly chosen prime polynomials of a given degree is outlined. The technique takes into account the length of the analyzed sequence. It is shown to be valuable when the efficiency of signature analysis has to be guaranteed, for example in highly dependable applications. In this case LFSRs of length 32 seem to be a practical choice, with respect to both the maximum length of the analyzed sequences and the aliasing error probability. ESA

66 SYSTEMS ANALYSIS

Includes mathematical modeling; network analysis; and operations research.

N89-29141# Army War Coll., Carlisle Barracks, PA.
SDI (STRATEGIC DEFENSE INITIATIVE): SHIELD OR SWORD?
Charles S. Butler and George R. Spiczak 15 May 1989 37 p
(AD-A209777; AD-E951363) Avail: NTIS HC A03/MF A01
CSCL 15/6

The paper attempts to answer the fundamental question, Is SDI an adjunct to a first strike strategy. As its criteria, it discusses Soviet and U.S. opposing views on SDI, an historical application of Mutual Assured Destruction strategy, and a discussion of Soviet and U.S. thinking on first strike capability. President Reagan's March 1983 address on SDI is used as the backdrop to set the stage for the discussion. It is the objective of the authors to evaluate and analyze the potential impact of SDI on first strike. GRA

N89-29142# Institute for Defense Analyses, Alexandria, VA.
SDS (STRATEGIC DEFENSE SYSTEM) SOFTWARE TESTING AND EVALUATION: A REVIEW OF THE STATE-OF-THE-ART IN SOFTWARE TESTING AND EVALUATION WITH RECOMMENDED R AND D TASKS Final Report
Christine Youngblut, Bill R. Brykczynski, John Salasin, Karen D. Gordon, and Reginald N. Meeson Feb. 1989 166 p
(Contract MDA903-84-C-0031)
(AD-A209447; AD-E501119; IDA-P-2132; IDA/HQ-88-33599)
Avail: NTIS HC A08/MF A01 CSCL 15/3

The technology required for effective and efficient testing and evaluation of Strategic Defense System (SDS) software is identified. An overview is provided of current testing and evaluation technology, a mapping of available technology against SDS needs, and recommendations to close critical gaps in technology. GRA

N89-29143# Army Stategic Defense Command, Huntsville, AL.
GROUND-BASED RADAR (GBR): ENVIRONMENTAL ASSESSMENT Final Report
Mar. 1989 131 p
(AD-A207654) Avail: NTIS HC A07/MF A01 CSCL 17/9

The President's Strategic Defense Initiative (SDI), announced on March 23, 1983, initiated an extensive research program to determine the feasibility of developing an effective ballistic missile defense system. The technological progress that has been made on the SDI research program since 1983 has advanced at an unexpectedly fast pace and is still accelerating. Recognizing that no strategic defense system could be deployed all at once, the Strategic Defense Initiative Organization is using an evolutionary approach to strategic concept, addressing the question of how to deploy or deploy. In September 1987, some technologies were advanced from the Concept Exploration phase of the material

acquisition process to the Concept Demonstration and Validation phase under this approach, because they were judged to be mature enough in concept definition to warrant further evaluation. GRA

N89-29144# Institute for Defense Analyses, Alexandria, VA.
A COMPARISON AND ANALYSIS OF STRATEGIC DEFENSE TRANSITION STABILITY MODELS Final Report
Ivan Oelrich and Jerome Bracken Dec. 1988 102 p
(AD-A208033; AD-E501099; IDA-P-2145; IDA/HQ-88-33716)
Avail: NTIS HC A06/MF A01 CSCL 15/3

The nature and causes of strategic stability and instability, how defenses affect the stability equation, problems of partial defenses and various attempts to model stability during the transition to effective defense are discussed. All of the models reviewed demonstrate that there is some stable path from no defenses to near perfect (99 percent effective) defenses, and an integrated theory is presented that shows the common nature of all of the stable paths. It is demonstrated that the results of the various transition stability differ not in numerical results but in the measures of stability used. Recommendations for future transition stability studies are included, based on the review of the various models. The appendices contain detailed descriptions of models used in the various transition stability studies reviewed. GRA

N89-29145# Institute for Defense Analyses, Alexandria, VA.
STRATEGIC DEFENSE SYSTEM DISTRIBUTED OPERATING SYSTEM R AND D REVIEW AND RECOMMENDATIONS Final Report
Karen D. Gordon and Cathy J. Linn Apr. 1989 66 p
(Contract MDA903-84-C-0031)
(AD-A208034; AD-E501102; IDA-P-2142; IDA/HQ-88-33701)
Avail: NTIS HC A04/MF A01 CSCL 15/3

The Strategic Defense System (SDS) imposes a set of requirements on distributed operating systems that is not met by state-of-the-art systems. The key requirements are identified as being real time support, reliability/fault tolerance, and security. The extent to which these requirements are being addressed by current distributed operating system research is discussed. The three distributed operating system projects that are currently receiving SDIO funds; Alpha, Cronus, and Mach; are reviewed. A fourth project, the V distributed system project of Stanford University, is also highlighted, because of its unique potential for meeting certain SDS needs. Recommendations on the directions in which the SDIO should pursue each of these projects are made. The Office of Naval Research (ONR) Real Time Computing Initiative, which is addressing some issues critical to the development of the SDS, is described. It is recommended that the SDIO seek to coordinate with the ONR in this effort. The appendix provides detailed descriptions of the Alpha, Cronus, Mach, and V distributed operating system projects, as well as three other projects noted: Amoeba, Clouds, and the Heterogeneous Computer Systems (HCS) Project. GRA

67 THEORETICAL MATHEMATICS

Includes topology and number theory.

N89-29146# Universiteit Twente, Enschede (Netherlands). Faculty of Applied Mathematics.
ON ADJOINTS AND DUAL MATROIDS
M. Alfter, W. Kern, and A. Wanka Feb. 1989 11 p
(Memo-767; ISSN-0169-2690; ETN-89-95062) Avail: NTIS HC A03/MF A01

The set-theoretical version of duality among matroids, and lattice-theoretical concepts, are investigated. Based on the generalization that matroids may fail to have duals in the lattice-theoretical sense, the question is addressed as to the existence of a dual in the set-theoretical dual of a matroid which does have a dual in the lattice-theoretical sense. A counterexample is presented which proves the answer to be negative. ESA

70 PHYSICS (GENERAL)

For precision time and time interval (PTTI) see *35 Instrumentation and Photography;* for geophysics, astrophysics or solar physics see *46 Geophysics, 90 Astrophysics,* or *92 Solar Physics.*

N89-29147# Pacific Northwest Labs., Richland, WA.
ENERGY AND ANGULAR DISTRIBUTIONS OF ELECTRONS EMITTED FROM GASES AND THIN FOILS DURING LIGHT ION BOMBARDMENT
L. H. Toburen May 1989 67 p Presented at the 8th Pfefferkorn Conference on Fundamental Beam Interactions with Solids for Microscopy, Microanalysis and Microlithography, Park City, UTH, 7-12 May 1989
(Contract DE-AC06-76RL-01830)
(DE89-014445; PNL-SA-16890; CONF-8905179-1) Avail: NTIS HC A04/MF A01

The energy and angular distributions of electrons ejected by fast charged particles in ionizing collisions provide detailed information regarding the effects of atomic, molecular, and condensed-phase structure on the energy loss process. The cross sections for electron production by light ions will be reviewed with emphasis on the effects of projectile and target structure on the magnitude and spectral properties of the energy and angular distributions of ejected electrons. Analysis of the wide range of available data has lead to several general conclusions. For ionization of atomic and molecular targets by protons having energies above a few hundred keV, the cross sections for electron production have been found to scale as the number of loosely bound target electrons. DOE

N89-29148# Dayton Univ., OH. Dept. of Electrical Engineering.
STUDY OF SINTERED MAGNETS OF THE Nd-Fe-B TYPE Final Report, Sep. 1984 - Sep. 1987
Karl J. Strnat and Herbert F. Mildrum Feb. 1989 92 p
(Contract DAAK20-84-K-0458; DA Proj. 1L1-61102-H-4702)
(AD-A209185; SLCET-TR-84-0458-F) Avail: NTIS HC A05/MF A01 CSCL 20/3

This is the final report of a 3 1/2-year effort to assess the utility and limitations of Nd-Fe-B based sintered magnets for microwave devices such as traveling wave tubes. In these devices, the magnetic properties at elevated temperatures are of importance, as is the flux stability during thermal cycling and long-term exposure. The experimental work described here involved several tasks: (1) the characterization of magnets from industrial research and development laboratories and from early pilot production; (2) development of our own techniques and the capabilities for preparing Nd-Fe-B alloys and sintered magnets from them; (3) modification of the alloy compositions and heat treatments in order to improve the elevated temperature magnetic properties, making the magnets more suitable for applications in the 100 to 200 C range at low operating permeance values; and (4) the attempt to better understand the magnetization reversal behavior and the relationship between coercivity and microstructure. GRA

N89-29149# Harry Diamond Labs., Adelphi, MD.
THE POTENTIAL AND ELECTRIC FIELDS OF A CONDUCTING SPHERE IN THE PRESENCE OF A CHARGED CONDUCTING PLANE Summary Report, Aug. - Nov. 1988
Clyde A. Morrison Jun. 1989 29 p
(AD-A209498; HDL-TR-2161) Avail: NTIS HC A03/MF A01 CSCL 20/3

The solution is given to Laplace's equation for a conducting sphere above a ground plane. The solution includes the presence of a uniform electric field perpendicular to the ground plane. The arbitrary constants in the solution are determined by applying the boundary conditions on the plane and on the sphere. Formulas are given for the evaluation of the potential and electric fields at an arbitrary field point. All the resulting formulas are expressed in a style for computation. GRA

N89-29150# Hebrew Univ., Jerusalem (Israel). Dept. of Atmospheric Sciences.
THE COAGULATION AND DISPERSION OF NONSPHERICAL, AEROSOL PARTICLES IN A TURBULENT ATMOSPHERE Final Report, Sep. 1986 - Nov. 1988
Isaiah Gallily and F. Gauze 7 May 1989 32 p
(Contract DAJA45-86-C-0041; DA Proj. 1L1-61102-BW-57)
(AD-A208064; R/D-5293-EN-01) Avail: NTIS HC A03/MF A01 CSCL 07/4

A numerical model was constructed for the simulation of dispersion and coagulation of a cloud of non spherical aerosol particles in turbulent conditions. Coagulation was observed in the early stages of the dispersion of the cloud. It appears from the calculations that, in a small cloud, dispersion is the dominant process from the early stages of the formation of cloud and coagulation stops after a short time. Nevertheless, at the time coagulation occurred it exhibited a behavior similar to what is expected from existing theories but modified by the strong dispersion of the cloud. The intention of the chief investigator was to perform numerical simulations with a much larger number of particles, to examine the behavior of the system with particles of different aspect ratios and to take account of the particle-particle hydrodynamic interaction. Due to the death of Prof. Gallily these additional goals were not achieved. GRA

N89-29151# Nationaal Inst. voor Kernfysica en Hoge Energiefysica, Amsterdam (Netherlands).
SOME ASPECTS OF A LATTICE FORMULATION OF CHIRAL GAUGE THEORIES
Jan Smit Nov. 1988 5 p Presented at the Symposium on Lattice Field Theory, Batavia, IL, 22-25 Sep. 1988 Submitted for publication Sponsored by Stichting voor Fundamenteel Onderzoek der Materie, Amsterdam, Netherlands
(NIKHEF-ITFA-88-51; ETN-89-95403) Avail: NTIS HC A02/MF A01

The spectrum of the lattice Dirac operation is discussed. The calculations on approximate mean field and hopping expansion are presented. It is shown that Higgs field must have long range correlations if lattice artifacts in the spectrum of the Dirac operator are to disappear. The fermion-Higgs system is studied. Prospects are favorable in the broken phase, as the correlations have infinite range three. The unbroken phase is difficult to analyze and it is not clear if the approximation is qualitatively reliable. Fermion doubler masses of the order of the cutoff are gotten. Triviality does not seem to be important. Anomalies do not influence the calculations in four dimensions. ESA

71 ACOUSTICS

Includes sound generation, transmission and attenuation. For noise pollution see *45 Environmental Pollution.*

N89-29152*# United Technologies Research Center, East Hartford, CT.
NOISE PRODUCED BY TURBULENT FLOW INTO A ROTOR: USERS MANUAL FOR NOISE CALCULATION Final Report
R. K. Amiet, C. G. Egolf, and J. C. Simonich Jun. 1989 38 p
(Contract NAS1-17763)
(NASA-CR-181790; NAS 1.26:181790) Avail: NTIS HC A03/MF A01 CSCL 20A

A users manual for a computer program for the calculation of noise produced by turbulent flow into a helicopter rotor is presented. These inputs to the program are obtained from the atmospheric turbulence model and mean flow distortion calculation, described in another volume of this set of reports. Descriptions of the various program modules and subroutines, their function, programming structure, and the required input and output variables are included. This routine is incorporated as one module of NASA's ROTONET helicopter noise prediction program. Author

N89-29153# Sandia Labs., Albuquerque, NM.
ULTRASONIC SYSTEMS AND SYSTEM DEVELOPMENT AT SNL ALBUQUERQUE
William W. Shurtleff 1989 12 p Presented at the 31st Weapons Agencies Nondestructive Testing Organization, Kansas City, MO, 5 Jun. 1989
(Contract DE-AC04-76DP-00789)
(DE89-013164; SAND-89-1406C; CONF-8906139-1) Avail: NTIS HC A03/MF A01

With completion of the High Precision Ultrasonic Scanning System (HPUSS) and purchase of the Olympus acoustic microscope, the SNL Albuquerque NDE divisions now have the capability to ultrasonically scan almost any size and shape of test object. The general purpose ultrasonic scanning system, the high precision ultrasonic scanning system, and the acoustic microscope cover a wide resolution and magnification range. The rest of this paper describes the three systems in more detail and talks about future ultrasonic system development at Sandia. DOE

N89-29154*# United Technologies Research Center, East Hartford, CT.
NOISE PRODUCED BY TURBULENT FLOW INTO A ROTOR: USERS MANUAL FOR ATMOSPHERIC TURBULENCE PREDICTION AND MEAN FLOW AND TURBULENCE CONTRACTION PREDICTION Final Report
J. C. Simonich and B. Caplin Jun. 1989 43 p
(Contract NAS1-17763)
(NASA-CR-181791; NAS 1.26:181791) Avail: NTIS HC A03/MF A01 CSCL 20A

A users manual for a computer program for predicting atmospheric turbulence and mean flow and turbulence contraction as part of a noise prediction scheme for nonisotropic turbulence ingestion noise in helicopters is described. Included are descriptions of the various program modules and subroutines, their function, programming structure, and the required input and output variables. This routine is incorporated as one module of NASA's ROTONET helicopter noise prediction program. Author

N89-29155*# Southwest Research Inst., San Antonio, TX.
AIRCRAFT PROPELLER INDUCED STRUCTURE-BORNE NOISE
James F. Unruh Washington Oct. 1989 113 p
(Contract NAS1-17921)
(NASA-CR-4255; NAS 1.26:4255; SRI-04-8542-1) Avail: NTIS HC A06/MF A01 CSCL 20A

A laboratory-based test apparatus employing components typical of aircraft construction was developed that would allow the study of structure-borne noise transmission due to propeller induced wake/vortex excitation of in-wake structural appendages. The test apparatus was employed to evaluate several aircraft installation effects (power plant placement, engine/nacelle mass loading, and wing/fuselage attachment methods) and several structural response modifications for structure-borne noise control (the use of wing blocking mass/fuel, wing damping treaments, and tuned mechanical dampers). Most important was the development of in-flight structure-borne noise transmission detection techniques using a combination of ground-based frequency response function testing and in-flight structural response measurement. Propeller wake/vortex excitation simulation techniques for improved ground-based testing were also developed to support the in-flight structure-borne noise transmission detection development. Author

N89-29156 Forschungsinstitut fuer Hochfrequenzphysik, Werthhoven (Germany, F.R.).
ACOUSTICAL TRACKING OF FAST MANEUVERING AIRCRAFT BY DISTRIBUTED SENSORS
F. Dommermuth Aug. 1988 41 p In GERMAN; ENGLISH summary
(Contract BMVg-T/RF-31/G-0022/G-1312)
(Rept-6-88; Lfd-275; ETN-89-94401) Copyright Avail: Forschungsinstitut fuer Hochfrequenzphysik, Wachtberg-Werthhoven, Fed. Republic of Germany

A method for the aeroacoustic tracking of nearly arbitrarily maneuvering subsonic sound sources is presented. With the proposed procedure, the target position can be determined at any instant, if the measured data of at least two acoustical sensors (consisting of three or four microphones each) are available. The pertaining error covariance matrix is given. The application to simulated data shows that even very fast maneuvering targets can be tracked reliably. A data update rate of 5 Hz allows a near real time tracking, including the extensive measuring data treatment of four sensors. The application to real data is shown to have good results. ESA

N89-29157# Southampton Univ. (England). Inst. of Sound and Vibration Research.
THE MEASUREMENT OF SEA LOSS FACTORS ON A FULLY ASSEMBLED STRUCTURE
N. Lalor Aug. 1987 8 p
(ISVR-TR-150; ETN-89-94960) Avail: NTIS HC A02/MF A01

The use of Statistical Energy Analysis (SEA) as a vibro-acoustic tool is outlined. Possible sources of error involving the use of the SEA method are described. These include: inaccurate measurement of modal density and the fact that the internal loss factor for each sub structure may not be the same attached as it is measured detached. Several other sources of measurement error are reviewed. The theory behind the SEA loss Factor measurement is described. ESA

N89-29158# Southampton Univ. (England). Inst. of Sound and Vibration Research.
THE ACOUSTIC CALIBRATION OF AIRCRAFT FUSELAGE STRUCTURES, PART 1
J. M. Mason and F. J. Fahy 23 Jan. 1989 35 p Sponsored by the Department of Trade and Industry, London, United Kingdom
(ISVR-TR-169-Pt-1; ETN-89-94961) Avail: NTIS HC A03/MF A01

A new technique for calibrating a fuselage as a transducer of pressure from the external surface to the interior is described. The data generated may be combined with any impinging sound field to obtain a prediction of cabin sound pressure level. As a preliminary to tests on scale model fuselage structures, the technique is validated for sound transmission through flat panels attached to a rigid walled box. The results of these tests are described. ESA

72 ATOMIC AND MOLECULAR PHYSICS

Includes atomic structure, electron properties, and molecular spectra.

N89-29159*# Washington State Univ., Pullman. Dept. of Physics.
PHOTONUCLEAR ABSORPTION CROSS SECTIONS Final Report
John W. Norbury 15 Aug. 1989 142 p
(Grant NAG1-797)
(NASA-CR-185488; NAS 1.26:185488) Avail: NTIS HC A07/MF A01 CSCL 20H

Neutron multiplicity in photonuclear reactions; invariance of classical electromagnetism; momentum transfer models in ion collisions; cosmic ray electromagnetic interactions; quadrupole excitations in nucleus-nucleus collisons and Y-89 interactions with relativistic nuclei; and the Weizsacker-Williams theory for nucleon emission via electromagnetic excitations in nucleus-nucleus collisions are discussed. For individual titles, see N89-29160 through N89-29166.

N89-29160*# National Aeronautics and Space Administration. Langley Research Center, Hampton, VA.
CALCULATION OF TWO-NEUTRON MULTIPLICITY IN PHOTONUCLEAR REACTIONS
John W. Norbury (Rider Coll., Lawrenceville, NJ.) and Lawrence W. Townsend *In* Washington State Univ., Photonuclear Absorption Cross Sections 15 Aug. 1989 p 1-27 Presented at Conference (For primary document see N89-29159 23-72)
Avail: NTIS HC A07/MF A01 CSCL 20H

The most important particle emission processes for electromagnetic excitations in nucleus-nucleus collisions are the ejection of single neutrons and protons and also pairs of neutrons and protons. Methods are presented for calculating two-neutron emission cross sections in photonuclear reactions. The results are in a form suitable for application to nucleus-nucleus reactions. Author

N89-29161*# Washington State Univ., Pullman. Dept. of Physics.
THE INVARIANCE OF CLASSICAL ELECTROMAGNETISM UNDER CHARGE-CONJUGATION, PARITY AND TIME-REVERSAL (CPT) TRANSFORMATIONS
John W. Norbury *In its* Photonuclear Absorption Cross Sections 14 p(SEE N89-29159 23-72) 15 Aug. 1989 Submitted for publication (For primary document see N89-29159 23-72)
Avail: NTIS HC A07/MF A01 CSCL 20H

The invariance of classical electromagnetism under charge-conjugation, parity, and time-reversal (CPT) is studied by considering the motion of a charged particle in electric and magnetic fields. Upon applying CPT transformations to various physical quantities and noting that the motion still behaves physically demonstrates invariance. Author

N89-29162*# National Aeronautics and Space Administration. Langley Research Center, Hampton, VA.
AN OPTICAL MODEL DESCRIPTION OF MOMENTUM TRANSFER IN HEAVY ION COLLISIONS
F. Khan, G. S. Khandelwal, Lawrence W. Townsend, J. W. Wilson, and John W. Norbury (Rider Coll., Lawrenceville, NJ.) *In* Washington State Univ., Photonuclear Absorption Cross Sections 15 Aug. 1989 21 p Submitted for publication (For primary document see N89-29159 23-72)
Avail: NTIS HC A07/MF A01 CSCL 20H

An optical model description of momentum transfer in relativistic heavy ion collisions, based upon composite particle multiple scattering theory, is presented. The imaginary component of the complex momentum transfer, which comes from the absorptive part of the optical potential, is identified as the longitudinal momentum downshift of the projectile. Predictions of fragment momentum distribution observables are made and compared with experimental data. Use of the model as a tool for estimating collision impact parameters is discussed. Author

N89-29163*# Washington State Univ., Pullman. Dept. of Physics.
ELECTROMAGNETIC INTERACTIONS OF COSMIC RAYS WITH NUCLEI **c93**
John W. Norbury *In its* Photonuclear Absorption Cross Sections 22 p(SEE N89-29159 23-72) 15 Aug. 1989 Submitted for publication (For primary document see N89-29159 23-72)
Avail: NTIS HC A07/MF A01 CSCL 03B

Parameterizations of single nucleon emission from the electromagnetic interactions of cosmic rays with nuclei are presented. These parameterizations are based upon the most accurate theoretical calculations available today. When coupled with Strong interaction parameterizations, they should be very suitable for use in cosmic ray propagation through intersteller space, the Earth's atmosphere, lunar samples, meteorites and spacecraft walls. Author

N89-29164*# Washington State Univ., Pullman. Dept. of Physics.
ELECTRIC QUADRUPOLE EXCITATIONS IN RELATIVISTIC NUCLEUS-NUCLEUS COLLISIONS
John W. Norbury *In its* Photonuclear Absorption Cross Sections 16 p(SEE N89-29159 23-72) 15 Aug. 1989 Submitted for publication (For primary document see N89-29159 23-72)
Avail: NTIS HC A07/MF A01 CSCL 20H

Calculations are presented for electric quadrupole excitations in relativistic nucleus-nucleus collisions. The theoretical results are compared to an extensive data set and it is found that electric quadrupole effects provide substantial corrections to cross sections, especially for heavier nuclei. Author

N89-29165*# Rider Coll., Lawrenceville, NJ. Dept. of Mathematics and Physics.
ELECTRIC QUADRUPOLE EXCITATIONS IN THE INTERACTIONS OF Y-89 WITH RELATIVISTIC NUCLEI
John W. Norbury *In* Washington State Univ., Photonuclear Absorption Cross Sections 15 Aug. 1989 7 p Submitted for publication Prepared in cooperation with Washington State Univ., Pullman (For primary document see N89-29159 23-72)
Avail: NTIS HC A07/MF A01 CSCL 20H

The first complete calculations of electric quadrupole excitations in relativistic nucleus-nucleus collisions are presented herein. Neutron emission from Y-89 is studied and quadrupole effects are found to be a significant fraction of the cross section. Author

N89-29166*# Washington State Univ., Pullman. Dept. of Physics.
NUCLEON EMISSION VIA ELECTROMAGNETIC EXCITATION IN RELATIVISTIC NUCLEUS-NUCLEUS COLLISIONS: RE-ANALYSIS OF THE WEIZSACKER-WILLIAMS METHOD
John W. Norbury *In its* Photonuclear Absorption Cross Sections 24 p(SEE N89-29159 23-72) 15 Aug. 1989 Submitted for publication (For primary document see N89-29159 23-72)
Avail: NTIS HC A07/MF A01 CSCL 20H

Previous analyses of the comparison of Weizsacker-Williams (WW) theory to experiment for nucleon emission via electromagnetic (EM) excitations in nucleus-nucleus collisions were not definitive because of different assumptions concerning the value of the minimum impact parameter. This situation is corrected by providing criteria that allows definitive statements to be made concerning agreement or disagreement between WW theory and experiment. Author

N89-29167# Los Alamos National Lab., NM.
PARTICLE PRODUCTION RESULTS FROM HELIOS
Barbara Jacak 1989 9 p Presented at the 3rd Conference on Intersections Between Particle and Nuclear Physics, Rockport, ME, 14-19 May 1989
(Contract W-7405-eng-36)
(DE89-013454; LA-UR-89-1649; CONF-8905163-1) Avail: NTIS HC A02/MF A01

It is shown that global variables such as transverse energy and multiplicity can be used to characterize events according to impact parameter. E(sub t) and multiplicity show a linear relationship, indicating that higher E(sub t) arises from production of more particles rather than a large change in the particle spectra. The shapes of the distributions can be explained by superposition of nucleon-nucleon scattering. There is no large difference among the observed charged particle spectra from p + W, O + W, and S + W. No sharp rise was observed in /p sub t/ (derived from the measured spectra by correcting the mean value in the range 0.4 is less than p sub t is less than 2.0 GeV/c under the assumption of an exponential spectrum) vs E(sub t), but it must be noted that the detected p sub t spectrum is affected by the hadronization process and reflects conditions at the time of freezeout of hadrons. Also, an increase in the cross section for large pt is expected from hard scattering of partons and does not necessarily indicate more exotic processes. DOE

N89-29168# Louisiana State Univ., Baton Rouge. Dept. of Physics and Astronomy.
MEASUREMENT OF SOLAR PROTON-PROTON FUSION NEUTRINOS WITH A SOVIET-AMERICAN GALLIUM EXPERIMENT Technical Progress Report
M. L. Cherry Jun. 1989 6 p
(Contract DE-FG05-88ER-40481)
(DE89-014563; DOE/ER-40481/2) Avail: NTIS HC A02/MF A01

A gallium solar neutrino detector is sensitive to low-energy proton-proton fusion neutrinos. A flux of 70 SNU is expected in a gallium detector from the p-p reaction independent of solar model calculations. If, however, neutrino oscillations in the solar interior are responsible for the suppressed (8)B flux measured by the Homestake (37)Cl experiment, then a comparison of the gallium and chlorine results may make possible a determination of the neutrino mass difference and mixing angle. A 60-ton gallium detector is currently being constructed in the Baksan Laboratory in the Soviet Union, and should be taking data by the end of 1989. DOE

N89-29169* National Aeronautics and Space Administration. Pasadena Office, CA.
TROCHOIDAL ANALYSIS OF SCATTERED ELECTRONS IN A MERGED ELECTRON-ION BEAM GEOMETRY Patent
Ara Chutjian, inventor (to NASA) (Jet Propulsion Lab., California Inst. of Tech., Pasadena.) 4 Apr. 1989 10 p Filed 11 Feb. 1988 Supersedes N88-25281 (26 - 18, p 2573)
(Contract NAS7-918)
(NASA-Case-NPO-16789-1-CU; US-Patent-4,818,868; US-Patent-Appl-SN-154713; US-Patent-Class-250-252; US-Patent-Class-250-397) Avail: U.S. Patent and Trademark Office CSCL 20H

The method and apparatus of this invention provides a plurality of measurements indicative of the absolute cross section for excitation of an ion beam. The ion beam is merged for excitation by specific energies of electrons in an electron beam. Both beams are merged in an evacuated enclosure having a longitudinal magnetic field and a crossed uniform electric field. The ions and electrons interact over a known merged longitudinal length in a merged beam area. After collision, the electron and ion beams are demerged. Forward and backward-scattered electrons are collected and position-detected by a pair of microchannel plate arrays located at opposite ends of said longitudinal beam-merging area. A series of electron and ion primary current measurements are taken at full ion and electron beam strength. Measurements are also taken at greatly reduced beam strength to obtain a beam overlap profile.
Official Gazette of the U.S. Patent and Trademark Office

N89-29170# Air Force Systems Command, Edwards AFB, CA. Astronautics Lab.
PROCEEDINGS OF THE ANTIPROTON TECHNOLOGY WORKSHOP HELD IN UPTON, NEW YORK ON 10 MAY 1989
Gerald D. Nordley, ed. May 1989 247 p Workshop held in Upton, NY, 10 May 1989
(AD-A210045; AL-CP-89-001) Avail: NTIS HC A11/MF A01 CSCL 20/8

Titles of presentations included: Stopping Power of MeV Proton and Antiproton Beams; Recent Simulation Results of ASTER; Pbar Testing of Hydrogen Effects in Sealed Carbon-Carbon Composites; Potential for Antiprotons in Radiation Oncology; Prospects for a Commercial Antiproton Source; Prospects for Exciting Extreme States in Nuclear Matter with Intense Antiproton Beams; Status of AL Studies Relating to Condensed Antimatter; Electromagnetic Traps for Atomic Antihydrogen; Antihydrogen Production; Headquarters DoE Antiproton Activities; Antiproton Catalyzed Fusion; Antiproton Induced Fusion Reaction; Options for a Laboratory Microfusion Facility; Modeling Antiproton-Plasma Interactions; Concepts for Experimental Determination of Radiation Shielding and Metal Clad Pellet Performance; Introduction to CP Violation Studies with Pbars; Search for CP Violation in Pbar-P to J/psi; Studies of Rare Models of Pbar-P Annihilation; and Antiproton Production Calculation by the Multistring Model VENUS Computer Code. GRA

N89-29171# Colorado State Univ., Fort Collins. Dept. of Chemistry.
A STUDY OF NON-RIGID AROMATIC MOLECULES BY SUPERSONIC MOLECULAR JET SPECTROSCOPY: OBSERVATION AND SPECTROSCOPIC ANALYSIS OF THE STABLE CONFORMATIONS OF VARIOUS ALKYLBENZENES

J. I. Seeman, H. V. Secor, P. J. Breen, V. H. Grassian, and E. R. Bernstein 1 Jun. 1989 23 p Submitted for publication
(Contract N00014-79-C-0647)
(AD-A209561; AD-E900860; TR-50) Avail: NTIS HC A03/MF A01 CSCL 07/3

The technique of supersonic molecular jet laser spectroscopy was used to determine the stable conformations of a series of alkylbenzenes. This study demonstrates, for the first time, the sensitivity of molecular jet spectroscopy in determining both the number of stable conformation as well as the geometry of various ethyl, propyl, and butyl substituents relative to the aromatic ring. Different rotamers with low barriers to interconversion, greater than 5 kcal/mol. can be isolated in the supersonic jet expansion. Each observed conformation exhibits its own spectroscopic origin (Si yields So reverse transition) in a two color Time-Of-Flight Mass Spectrum (TOFMS). The number of stable conformations is then used to determine the minimum energy geometries of the substituent group. Previous identification of individual molecular conformations for such low barriers to interconversion has not been attainable with conventional techniques such as variable-temperature NMR. GRA

N89-29172# RAND Corp., Santa Monica, CA.
PROCEEDINGS OF A RAND WORKSHOP ON ANTIPROTON SCIENCE AND TECHNOLOGY Interim Report
Bruno W. Augenstein Oct. 1988 39 p Workshop held in Santa Monica, CA, 6-9 Oct. 1987
(Contract F49620-86-C-0030)
(AD-A208168; RAND/N-2763-AF) Avail: NTIS HC A03/MF A01 CSCL 20/8

This Note describes a conference held in October 1987 to review the critical issues surrounding the establishment of a comprehensive U.S. antiproton research program and to help formulate its research goals. The conference was organized around three major themes: (1) basic machine, facility, and scale-up review--antiproton production and collection; (2) a basic physics program for a low-energy antiproton source in North America; and (3) near-term and precursor applications using an initial low-energy antiproton source. Among the major conclusions were the following: The United States can construct an intense source of low-energy antiprotons in three to four years, and develop portable antiproton storage devices (rings and ion traps). A dozen classes of key low-energy antiproton experiments can be conducted on questions ranging from charge parity violation to condensed matter. A number of near-term important applications are possible using the source and portable storage devices. GRA

N89-29173# Max-Planck-Inst. fuer Physik und Astrophysik, Munich (Germany, F.R.). Werner-Heisenberg-Inst. fuer Physik.
MEASUREMENT OF ELECTROWEAK EFFECTS AND TOPOLOGICAL BRANCHING CONDITIONS IN THE REACTION E(+)E(-) YIELDS TAU(+)TAU(-) IN THE STORAGE RING PETRA Thesis - Tech. Univ. Munich [MESSUNG ELEKTROSCHWACHER EFFEKTE UND TOPOLOGISCHER VERZWEIGUNGSVERHAELTNISSE IN DER REAKTION E(+)E(-) YIELDS TAU(+)TAU(-) AM SPEICHERRING PETRA]
Werner Wiedenmann Oct. 1988 208 p In GERMAN
(MPI-PAE/Exp.El-195; ETN-89-94388) Copyright Avail: NTIS HC A10/MF A01

The detection of the electroweak interference in the production of tau-lepton-pairs at the highest obtainable energies in e(+)e(-) storage rings was investigated. Using the detector CELLO and Monte Carlo simulations, total cross section and charge asymmetry, for the production of tau-pairs are obtained. The measured cross sections are in agreement with theoretical expectations, from quantum electrodynamics and the Glashow-Salam-Weinberg (GSW) theory. The observed electroweak effects, leading to a charge asymmetry in the differential cross sections concord with GSW-expectations, and with the axial vector coupling constants of the tau-lepton. The tau-coupling constants agree with those of the electrons and muons, supporting the hypothesis of the universal coupling of leptons to the weak current. The measurement of the topological branching conditions of the tau-lepton is improved and previous measurements are confirmed. ESA

N89-29174# Max-Planck-Inst. fuer Kernphysik, Heidelberg (Germany, F.R.).
[ACTIVITIES REPORT OF THE MAX-PLANCK INSTITUTE OF NUCLEAR PHYSICS] Annual Report, 1987 [JAHRESBERICHT 1987]
H. V. Klapdor and E. K. Jessberger 1988 203 p In GERMAN Original contains color illustrations
(ETN-89-94398) Avail: NTIS HC A10/MF A01

The research work in the field of nuclear physics comprises: (1) technical developments on tandem accelerators, the Heidelberg Heavy ion postaccelerator, the Heildelberg Heavy ion test storage ring, and a source for polarized alkali ions; (2) experimental work on, the development of detectors and experimental set-ups, solids and microstructures, giant resonances and continuum excitations, nuclear spectroscopy, mechanisms of nuclear reactions, fusion and fission, atomic physics and interaction of charged particles with matter, and medium and high energy physics; and (3) theoretical work on a statistical model of nuclei, reactions and solids, nuclear reactions at high energies, many-particles, quantum chromo-dynamics, and nuclear beta and double beta decay. In the field of cosmophysics, research activities were performed on meteorites and lunar rocks, the gallium solar neutrino experiment, comets, the PHOBOS project, interplanetary and interstellar dust, planetary atmospheres, interstellar medium and cosmic rays, molecular collisions, nuclear geology and geochemistry, and archaeometry. ESA

N89-29175 Technische Univ., Hanover (Germany, F.R.). Fachbereich Physik.
PHOTON-ION ANGULAR CORRELATION MEASUREMENTS ON THE SYSTEM He(+) + Ne: DETERMINATION OF THE SPIN INVERSION Ph.D. Thesis [PHOTON-ION-WINKELKORRELATIONSMESSUNGEN AM SYSTEM HE(+) + NE: BESTIMMUNG DER SPININVERSION]
Helmut Pfeiffer 1987 138 p In GERMAN
(ETN-89-94435) Avail: Universitaet Hannover, Welfengarten 1, D-3000 Hannover 1, Federal Republic of Germany

The angular distributions of the resonance light of Ne*(2p53s) atoms, excited by collisions with He(+) ions were measured in coincidence with the scattered He(+) ions, in order to get information about the angle and energy dependences of the density matrix elements. The calibration of the photon detection channeltrons with two different methods gave consistent results. The theoretically required strict image symmetry of the experimental data was found. The density matrix elements, determined at constant collision energy show no oscillations. When the energy was varied at constant reduced scattering angle, the density matrix elements show oscillations, whose phase agrees with that of the integral scattering cross section, and in addition a structure for energies between 100 and 120 eV. Simple models could not explain the measurements. ESA

N89-29176# Technische Univ., Delft (Netherlands).
DEEPLY BOUND ORBITS IN PIONIC ATOMS AND THE OPTICAL POTENTIAL Ph.D. Thesis
Arie Taal 1989 109 p Sponsored by the Stichting voor Fundamenteel Onderzoek der Materie, Amsterdam, Netherlands; the Netherlands Organization for the Advancement of Scientific Research; the Swiss National Foundation and others
(ETN-89-95463) Avail: NTIS HC A06/MF A01

The study of the pion-nucleus interaction is studied by means of the measurement and the analysis of X-ray transitions in pionic atoms. For the 3d-levels of these heavy pionic atoms, the data extended almost up to the end of the stable isotopes of the periodic system. For the pionic 2p to 1s X-ray transition in the isotopes 24Mg, 27Al and 28Si, the yield is rather low. Only a few percent of the captured pions manage to reach the 1s-orbit due to the large absorption probability in higher orbits. Therefore, these transitions occur as broad low intensity peaks in the recorded energy spectra. In order to measure these transitions in a way

suitable for a reliable analysis, special spectroscopic techniques were applied. All experiments were performed by using the very intense, high-duty factor pion beam at the meson factory of the Paul Scherrer Institute (formerly Schweizerisches Institut fuer Nucklearforschung). This was especially necessary to obtain satisfactory counting statistics for these low intensity pionic transitions within a reasonable measuring period. The calculations according to the optical potential parameter sets are found to agree with the pionic strong interaction. ESA

N89-29177# Amsterdam Univ. (Netherlands).
THE INFLUENCE OF THE SHELL CLOSURE ON THE MICROSCOPIC STRUCTURE OF EVEN-EVEN Hg ISOTOPES: A STUDY WITH ELECTRON AND MUON BEAMS Ph.D. Thesis
Andreas Jef Cornelis Burghardt 1989 142 p Sponsored by the National Inst. voor Kernfysica en Hoge Energiefysica and Stichting voor Fundamenteel Onderzoek der Materize, Amsterdam, Netherlands and Netherlands Organization for the Advancement of Pure Scientific Research
(ETN-89-95464) Avail: NTIS HC A07/MF A01

Eleven of the many excitations observed in the spectra of 204 Hg are investigated in detail. The level scheme of 204 Hg is compared to three shell-model calculations. The transition charge distributions of six of the eleven analyzed states are described by the shell-model calculation of Poppelier. The lack of predicted strength at the nuclear surface indicates that core-polarization effects should be taken into account. ESA

N89-29178# Max-Planck-Institut fuer Stroemungsforschung, Goettingen (Germany, F.R.).
MOLECULAR BEAM EXPERIMENT FOR THE DETERMINATION OF DIFFERENTIAL CROSS SECTIONS OF THE REACTION OF DEUTERIUM ATOMS WITH VIBRATIONALLY EXCITED HYDROGEN MOLECULES Thesis
[MOLEKULARSTRAHLEXPERIMENT ZUR BESTIMMUNG DIFFERENTIELLER STREUQUERSCHNITTE DER REAKTION VON DEUTERIUMATOMEN MIT SCHWINGUNGSANGEREGTEN WASSERSTOFFMOLEKUELEN]
M. Vodegel Jun. 1988 199 p In GERMAN
(MPIS-10/1988; ISSN-0436-1199; ETN-89-94567) Avail: NTIS HC A09/MF A01; Max-Planck Inst. fuer Stroemungsforschung, Boettinger Strasse 6-8, 3400 Goettinghen, Fed. Republic of Germany, 40 DM

The vibrationally excited reaction D + h2 is investigated in a molecular beam experiment at a most probable collision energy of 0.33 eV. Vacuum system, primary beam, secondary beam (D-atomic beam source), and detection system are described. Doubly differential cross sections are measured in the form of angle-and product velocity distributions. After the calibration of the apparatus the absolute integral reactive cross section is determined. The comparison with theoretical calculations shows good agreement if the dependence of the cross section on the initial rotational state is taken into account. Also the angle at time-of-flight distributions can be well fitted with models based on classical trajectories. Quantum-mechanical calculations give a much higher branching ratio of the vibrationally adiabatic to the nonadiabatic channel than classical calculations. The resolution of the experiment does not allow a verification of this discrepancy. ESA

N89-29179# Laboratoire d'Automatique et d'Analyse des Systemes, Toulouse (France).
STUDY AND SIMULATION OF AN E-BEAM MICROLITHOGRAPHY PROCESS ON A MULTILAYER RESIN STRUCTURE. RESEARCH OF AN OPTIMIZATION Ph.D. Thesis - Inst. National des Sciences Appliquees, Toulouse, France
Emmanuelle Petit-Bourdelle 1989 191 p In FRENCH; ENGLISH summary
(LAAS-89.012; ETN-89-95257) Avail: NTIS HC A09/MF A01

The metal type and metal thickness parameters in three layer microlithography systems are studied by statistical computation of the electron scattering in a material using a Monte Carlo technique and are confirmed by an experimental study. The computational program employed gives dissipated energy in the resist versus the lateral distance to the incident beam at a given depth. In order to realize a good theoretical approach a simple relationship for the energy deposition function is proposed. This relationship is shown to be an improvement on the classical relationships which use Gaussian functions. ESA

73 NUCLEAR AND HIGH-ENERGY PHYSICS

Includes elementary and nuclear particles; and reactor theory.

For space radiation see *93 Space Radiation.*

N89-29180# Los Alamos National Lab., NM.
GENERAL-PURPOSE HEAT SOURCE DEVELOPMENT: EXTENDED SERIES TEST PROGRAM SRB FRAGMENT/FUSELAGE TESTS
Theresa A. Cull Jun. 1989 17 p
(Contract W-7405-eng-36)
(DE89-014389; LA-11574) Avail: NTIS HC A03/MF A01

General-Purpose Heat Source radioisotope thermoelectric generators (GPHS-RTGs) will provide electrical power for the NASA Galileo and European Space Agency (ESA) Ulysses missions. Each GPHS-RTG comprises two major components: GPHS modules, which provide thermal energy, and a thermoelectric converter, which converts the thermal energy into electrical power. Each of the 18 GPHS modules in a GPHS-RTG contains four Pu-238O2-fueled capsules. LANL conducted a series of safety verification tests on the GPHS-RTG before the scheduled May 1986 launch of the Galileo spacecraft to assess the ability of the GPHS modules to contain plutonia in potential accident environments. As a result of the Challenger 51-L accident in January 1986, NASA postponed the launch of Galileo; the spacecraft launch vehicle was reconfigured and the spacecraft trajectory modified. These actions prompted NASA to reevaluate potential mission accidents and the extended series safety test program was initiated. This program included a series of solid rocket booster (SRB) fragment/fuselage tests that simulated the interaction of SRB fragments generated in an SRB motor case rupture (or resulting from a range safety officer SRB destruct action) with sections of the Shuttle Orbiter. The test data helped verify and refine the analytical models of the SRB fragment/fuselage interaction. The results showed that the fragment velocity decreased significantly (up to 40 percent) after penetrating the Orbiter section(s). The interactions also reduced, and in some cases eliminated, the original fragment rotational rate and direction and initiated rotation in other directions. DOE

N89-29181# Massachusetts Inst. of Tech., Cambridge. Research Lab. of Electronics.
MICROWAVE EMISSION FROM RELATIVISTIC ELECTRON BEAMS Final Report, 1 Nov. 1983 - 31 Oct. 1988
George Bekefi Mar. 1989 40 p
(Grant AF-AFOSR-0026-84; AF Proj. 2301)
(AD-A209653; AFOSR-89-0787TR) Avail: NTIS HC A03/MF A01 CSCL 09/3

Profile modification by optical guiding in a Raman Free Electron Laser (FEL) operating at microwave frequencies was studied experimentally. A cyclotron autoresonance maser (CARM) amplifier was designed, built, and tested. This CARM operates at 35 GHz with a power output of 10 MW and an efficiency of three percent. We report measurements of the spatial distribution of the RF electric field intensities and phases induced in a free electron laser amplifier operating in the collective (Raman) regime. The studies are carried out at a microwave frequency of about 10 GHz in a FEL using a mildly relativistic electron beam of about 200 keV energy and 1 - 4 A current. The probing of the ponderomotive (space charge) and the electromagnetic waves is accomplished by means of small movable electric dipole antennas inserted into the interaction region. A 35 GHz Cyclotron Autoresonance Maser Amplifier is discussed. Measurements are

carried out at a frequency of 35 GHz using a mildly relativistic electron beam (1.5 MeV, 260 A) generated by a field emission electron gun followed by an emittance selector that removes the outer, hot electrons. GRA

N89-29182# Nationaal Inst. voor Kernfysica en Hoge Energiefysica, Amsterdam (Netherlands).
NEW LAYOUT OF AMSTERDAM PULSE STRETCHER
R. Maas and Y. Y. Wu Aug. 1988 8 p Revised
(NIKHEF-K/APS/88-01A-Rev; ETN-89-95398) Avail: NTIS HC A02/MF A01

The modifications of the Amsterdam pulse stretcher layout are reported. These changes concern the elevation of the ring level, the displacement of the internal target hall, the allocation of more space for monitors and orbit corrections, the new dimensions for the straight section, the physical dimensions of quadrupoles and sextupoles, the orbit correction scheme, the beam injection/extraction procedures, the beam handling system and the results of the dynamic aperture studies. ESA

N89-29183# Nationaal Inst. voor Kernfysica en Hoge Energiefysica, Amsterdam (Netherlands).
APERTURES OF RING QUADRUPOLES AND SEXTUPOLES
R. Maas and Y. Y. Wu Dec. 1988 12 p
(NIKHEF-K/APS/88-03; ETN-89-95399) Avail: NTIS HC A03/MF A01

The required mechanical dimensions (apertures and lengths) of the Amsterdam electron accelerator quadrupoles and sextupoles are analyzed. The stretcher mode operation and the storage mode conditions are discussed. The beam excursions due to misalignments are indicated. The chosen quadrupoles parameters are, at the curved section, l (yoke) = 18.0 or 17.78 cm, l (eff) = 21.2 or 21.0 cm, aperture = 7.5 or 7.62 cm; and at the straight section, l (yoke) = 25.0 cm, l (eff) = 29.7 cm, aperture = L1 cm. For the sextupoles the suggested lengths are l (eff) = 20.1 or 19.9 cm. ESA

N89-29184# Nationaal Inst. voor Kernfysica en Hoge Energiefysica, Amsterdam (Netherlands).
ORBIT CORRECTION SCHEME FOR THE NEW RING
Y. Y. Wu Aug. 1988 9 p
(NIKHEF-K/APS/88-04; ETN-89-95400) Avail: NTIS HC A02/MF A01

The orbit correction scheme of the optical design of the Amsterdam pulse stretcher is reported. The scheme is verified both for the stretcher mode and storage mode operation of the ring. Misalignments, incorrect field settings and field inhomogeneities are taken into account for orbit correction. Computerized simulation of the proposed orbit correction scheme shows a reduction of the deviation from 3.0 mm root mean square without correction to about 0.3 mm root mean square with correction, assuming realistic alignment and magnetic field errors of the optical elements. Thirty-two pairs of orbit correctors are installed along the ring. Among them 16 horizontal orbit correctors are combined with bending magnets in the curve. In the straight section all the orbit correctors used for horizontal and vertical plane are combined as one set. Thirty-two position monitors are used in the ring. In all cases orbit correction scheme works well. The strength of those orbit correctors used in the ring for two different modes remains lower than 1.0 milliradian (at E sub max = 900 MeV). ESA

N89-29185# Nationaal Inst. voor Kernfysica en Hoge Energiefysica, Amsterdam (Netherlands).
UPDATED OC SCHEME
Y. Y. Wu Sep. 1988 3 p
(NIKHEF-K/APS/88-04A; ETN-89-95401) Avail: NTIS HC A02/MF A01

The scheme of the orbit correction (OC) unit, in the curved section of the Amsterdam electron accelerator, is described. Comparison between the original scheme and the proposed one is effectuated. The positions of the injector kickers are checked. The results of the kickers effect to the local orbit bump are shown. ESA

74 OPTICS

Includes light phenomena; and optical devices.
For lasers see *36 Lasers and Masers.*

N89-29186# Lawrence Livermore National Lab., CA.
REALTIME TRACKING SYSTEM FOR THE WIDE-FIELD-OF-VIEW TELESCOPE PROJECT
Hye-Sook Park, Timothy S. Axelrod, Nicholas J. Colella, Michael E. Colvin, and Arno G. Ledebuhr May 1989 9 p Presented at the Society of Photo-Optical Instrumentation Engineers Conference on Applications of Artificial Intelligence, Orlando, FL, 28 Mar. 1989
(Contract W-7405-eng-48)
(DE89-013787; UCRL-99801; CONF-890358-5) Avail: NTIS HC A02/MF A01

A wide-field-of-view (WFOV) telescope system is being developed for military, commercial and scientific purposes. The systems will have smart focal plane processors to recognize and track moving objects. Candidate algorithms intended for these processors which are currently implemented on a commercial image processing system interfaced to the prototype WFOV telescope are described. DOE

N89-29187# Army Cold Regions Research and Engineering Lab., Hanover, NH.
RADIATIVE TRANSFER IN FALLING SNOW: A TWO-STREAM APPROXIMATION
Gary Koh Apr. 1989 15 p
(AD-A208960; CRREL-89-6) Avail: NTIS HC A03/MF A01 CSCL 20/6

Light transmission measurements through falling snow have produced results unexplainable by single scattering arguments. A two-stream approximation to radiative transfer is used to derive an analytical expression that describes the effects of multiple scattering as a function of the snow optical depth and the snow asymmetry parameter. The approximate solution is simple and it may be as accurate as the exact solution for describing the transmission measurements within the limits of experimental uncertainties. GRA

N89-29188# Boeing Aerospace Co., Seattle, WA. SRAM-A Support Program.
HELIUM BOTTLE PRESSURE MEASUREMENT BY PORTABLE ULTRASONIC TECHNIQUE Final Engineering Report, 15 Jan. 1987 - 7 Feb. 1989
Alden Olson 7 Feb. 1989 129 p
(Contracts F34601-84-C-1068; F34601-88-D-0987)
(AD-A208994; SRAM-A-EA-87-7-1-12) Avail: NTIS HC A07/MF A01 CSCL 14/2

The report details the application of a portable ultrasonic method to accurately check the pressure in a helium bottle. The subject helium bottle provides an initial launch boost to the Short Range Attack Missile's (SRAM-A, or AGM-69A) hydraulic flight control system. The method described would apply to any pressure vessel, with minor variations from those procedures and equipment detailed in the report. A series of tests was conducted at the Boeing Aerospace facility in Kent, Washington on a SRAM-A helium gas bottle, to determine the feasibility of measuring gas pressure within the helium bottle by ultrasonic technique. The method, based on measurement of the speed of ultrasonic waves transmitted through a medium at constant pressure and temperature, provides the ability to determine bottle pressure without the necessity of removing the bottle from the missile. This bottle had previously been used for pressurizing the Flight Control Actuation System. The ultrasonic waves were introduced into the bottle by a transducer attached to one side of the gas bottle and received by a transducer attached 180 directly opposite the input transducer.

The amplitude of the ultrasonic signal decreased with decreasing pressure, proving that the method was feasible. GRA

N89-29189# Naval Ocean Systems Center, San Diego, CA.
AIRBORNE FLIR (FORWARD LOOKING INFRARED) DETECTION OF SURFACE TARGETS Interim Report
H. G. Hughes Feb. 1989 24 p
(AD-A209250; NOSC/TR-1275) Avail: NTIS HC A02/MF A01 CSCL 17/5

An algorithm is presented for predicting the detection ranges of a surface target by an airborne Forward Looking Infrared system. The total infrared background radiance scene under cloud-free skies is modeled to include the atmospheric path emissions between the target and sensor and the effects of a wind ruffled sea on the surface emissions and sky radiance reflections. A model is also introduced of the average temperature of a ship based upon the solar heating effects throughout a specified course, the ambient meteorological conditions, and the viewing angle. Together, these two models allow the range to be determined where the difference between the apparent ship's temperature (i.e., the actual ship temperature degraded by the atmospheric transmittance) and the effective background temperature of the sea surface as viewed from the sensor altitude is equal to the minimum detectable temperature difference of the FLIR. A case study is presented to demonstrate the vulnerability of a frigate class ship to detection by an airborne FLIR during a 5 hour period where the ship's course changed allowing solar heating of different sides of the ship. Study results show considerable increases in predicted detection ranges with altitude using the present algorithm over those based on a fixed temperature difference between the target and its background. GRA

N89-29190# Cornell Univ., Ithaca, NY. Dept. of Computer Science.
AN IMPROVED ALGORITHM FOR LABELING CONNECTED COMPONENTS IN A BINARY IMAGE
Xue D. Yang Mar. 1989 20 p
(Contracts N00014-88-K-0591; N00014-86-K-0281; N00014-87-K-0129; NSF DMS-86-17355)
(AD-A210100; CU-CSD-TR-89-981) Avail: NTIS HC A03/MF A01 CSCL 20/6

In this note, we present an improved algorithm to Schwartz, Sharir and Siegel's algorithm for labeling the connected components of a binary image. Our algorithm uses the same bracket marking mechanisms as is used in the original algorithm to associate equivalent groups. The main improvement of our algorithm is that it reduces the three scans on each line required by the original algorithm in its first pass into only one scan by using a recursive group-boundary dynamic tracking technique, while maintaining the computation on each pixel during scan still a constant time. This algorithm is fast enough to handle images in real time and simple enough to allow an easy and very economical hardware implementation. GRA

N89-29191*# National Aeronautics and Space Administration. Pasadena Office, CA.
FIBER OPTIC FREQUENCY TRANSFER LINK Patent Application
Lori Primas, inventor (to NASA), Richard Sydnor, inventor (to NASA), and George Lutes, inventor (to NASA) (Jet Propulsion Lab., California Inst. of Tech., Pasadena.) 31 May 1989 22 p
(Contract NAS7-918)
(NASA-Case-NPO-17703-1-CU; NAS 1.71:NPO-17703-1-CU; US-Patent-Appl-SN-359801) Avail: NTIS HC A03/MF A01 CSCL 20F

A reference frequency distribution system is disclosed for transmitting a reference frequency from a reference unit to a remote unit while keeping the reference frequency at the reference unit and the remote unit in phase. A fiber optic cable connects the reference unit to the remote unit. A frequency source at the reference unit produces a reference frequency having an adjustable phase. A fiber optic transmitter at the reference unit modulates a light beam with the reference frequency and transmits the light beam into the fiber optic cable. A 50/50 reflector at the remote unit reflects a first portion of the light beam from the reference unit back into the fiber optic cable to the reference unit. A first fiber optic receiver disposed at the remote unit receives a second portion of the light beam and demodulates the reference frequency to be used at the remote unit. A second fiber optic receiver disposed at the reference unit receives the first portion of the light beam and demodulates a reference frequency component. A phase conjugator is connected to the frequency source for comparing the phase of the reference frequency component to the phase of the reference frequency modulating the light beam being transmitted from the reference unit to maintain a conjugate (anti-symmetric) relationship between the reference frequency component and the reference frequency modulating the light beam where virtually no phase difference exists between the phase of the reference frequency component and the phase of the reference frequency modulating the light beam. NASA

N89-29192# Colorado School of Mines, Golden. Center for Wave Phenomena.
APPROXIMATION METHODS FOR SCATTERING FROM ROUGH SURFACES Final Report, 1 Feb. 1986 - 31 Jan. 1989
John A. DeSanto 30 Mar. 1989 13 p
(Contract DAAL03-86-K-0031)
(AD-A209482; CWP-089; ARO-22971.3-GS) Avail: NTIS HC A03/MF A01 CSCL 20/6

Rigorous analytical methods in rough surface scattering lead to integral equations. In coordinate space these integral equations are written on the surface value of the field, the surface value of the normal derivative of the field or coupled equations on both (interface or penetrable surface or dielectric problem). An additional integration is necessary to find the scattered or transmitted field. In Fourier transform space the corresponding equations are on the scattering and/or transmission amplitudes with a direct interpretation as scattered or transmitted fields as a function of angle. GRA

N89-29193# Dayton Univ., OH. Research Inst.
DISPLAY CHARACTERISTICS OF EXAMPLE LIGHT-VALVE PROJECTORS Final Technical Report, Mar. 1987 - Feb. 1989
Celeste M. Howard Jun. 1989 78 p
(Contracts F33615-84-C-0066; F33615-87-C-0012)
(AD-A209580; UDR-TR-88-124; AFHRL-TR-88-44) Avail: NTIS HC A05/MF A01 CSCL 20/6

Quantitative data is provided on performance characteristics of light valve projectors in simulator displays as well as in optimal laboratory conditions. Two types of light valve projectors are discussed: a single light-valve projector (also called Talaria) and a multiple light-valve projector. The data show that: (1) these projectors do not achieve brightnesses above the mesopic level in large screen simulator displays, (2) color output includes a dark-field haze which must be dealt with like ambient illumination, and (3) light/dark ratios (L/D) above 5:1 are obtainable only when the light region is white or yellow-green. GRA

N89-29194# Naval Postgraduate School, Monterey, CA.
OPTICAL LASER TECHNOLOGY AND ITS APPLICATION TO DEFENSE MANPOWER DATA CENTER'S (DMDC) QUERRY FACSIMILE (QFAX) DATA BASE SYSTEM M.S. Thesis
Mark K. Brown Mar. 1989 120 p
(AD-A207832) Avail: NTIS HC A06/MF A01 CSCL 12/6

Optical storage technology holds the capability to increase the amount of data stored on a single 5 1/4-inch disc from 1.2 Megabytes (Mb) to 640 Mb. The three basic types of optical disks, Compact Disk-Read Only Memory (CD-ROM), Write Once, Read Many (WORM), and erasable optical, each has its own application niche. For this reason, it is critical for managers to analyze present systems carefully prior to seeking optical storage solutions. An in-depth evaluation of performance and interfacing requirements of currently marketed optical systems was performed. That evaluation was used in the process of determining if Defense Manpower Data Center's (DMDC) Querry Facsimile (QFAX) System, a system of nine databases currently stored on a Direct Access

Storage Device (DASD), was a candidate for an optical storage application. Additional consideration was given to industry standards for optical devices. A detailed analysis of the current system configuration and end-users requirements was made to determine acceptability of optical systems interfaces and associated capabilities. GRA

N89-29195# Gesamthochschule, Kassel (Germany, F.R.). Fachbereich Physik.
A NEW SCATTERING FORMULA FOR DEPTH-RESOLVING X-RAY DIFFRACTOMETRY BASED ON A KINEMATIC THEORY Ph.D. Thesis [EINE NEUE STREUFORMEL FUER DIE TIEFENAUFLOESENDE ROENTGENSTRAHLDIFFRAKTOMETRIE NACH DER KINEMATISCHEN THEORIE]
Thomas Wieder 1988 97 p In GERMAN
(ETN-89-94430) Avail: NTIS HC A05/MF A01

A new X-ray scattering formula was deduced for depth-resolving X-ray structural analysis. The theoretical fundamentals of the present depth-resolving X-ray diffractometry are shown. The new scattering formula for the calculation of the X-ray reflection from a polycrystalline solid sample whose lattice plane distances are depth-dependent, is deduced. Differential intensities are calculated. The formula is also suited for lattices with ideal periodicity. Tests with thin titanium layers with an oxygen diffusion profile are in agreement with calculations using the new scattering formula; calculations based on the old formula lead to less satisfactory results. ESA

N89-29196# Technische Univ., Berlin (Germany, F.R.). Fachbereich Elektrotechnik.
THEORETICAL INVESTIGATIONS OF AN INTEGRATED OPTICS SWITCHING ELEMENT WITH ASYMMETRIC DIRECTIONAL COUPLERS FOR SWITCHING MATRICES Ph.D. Thesis [THEORETISCHE UNTERSUCHUNG ZU EINEM INTEGRIERT-OPTISCHEN SCHALTELEMENT MIT ASYMMETRISCHEN RICHTKOPPLERN FUER SCHALTMATRIZEN]
Henning Buelow 1988 167 p In GERMAN Sponsored by Siemens AG, Fed. Republic of Germany
(ETN-89-94439) Avail: NTIS HC A08/MF A01

An electro-optical switchable integrated-optics directional coupler and a switching element with a coupler pair are presented. In contrast with conventional directional couplers, this coupler has an imprinted switching state and hence a cross state which is less sensitive to parameter variations. The local mode theory was used for the calculation and optimization of the asymmetric coupler. Coupling coefficients and cross talk (describing parameter sensitivity) are connected by the Fourier transformation. An electrode voltage that compensates detuning, brings the switch into the parallel state. The systems mode amplitudes in switched directional couplers can be illustrated as the rotation of a point of the Poincare sphere. The intrinsic detuning of a structure with Ti:LiNbO3 waveguides can be realized by waveguides of different width. ESA

N89-29197# Technische Univ., Brunswick (Germany, F.R.). Fakultaet fuer Maschinenbau und Elektrotechnik.
CHARACTERIZATION, OPTIMIZATION AND DESIGN OF SINGLE-MODE MULTISTEP FIBERS Ph.D. Thesis [CHARAKTERISIERUNG OPTIMIERUNG UND ENTWURF EINWELLIGER MEHRSTUFENFASERN]
Risheng Yang 1988 149 p In GERMAN
(ETN-89-94440) Avail: NTIS HC A07/MF A01

The dispersion and damping in single-mode fibers, as well as their design and optimization are treated. The basic damping by absorption and scattering, and the losses by microcurvature and macrobending are discussed. The dispersion in multistop fibers was calculated using the scalar approximation. The design and optimization procedures are outlined for the following single-mode multistep fibers: fibers with dispersion compensation and low curvature losses; fibers with lowered refraction number in the inner mantle; and low-loss fibers with reduced refraction number in the middle mantle. ESA

N89-29198# Etablissement Technique Central de l'Armement, Arcueil (France). Dept. Systeme de Perception.
DETECTION OF TARGET FORMATIONS IN INFRARED IMAGERY Final Report [RECONNAISSANCE DE CIBLES EN FORMATION EN IMAGERIE INFRAROUGE]
B. Hoeltzener-Douarin 20 Jul. 1988 60 p In FRENCH
(Contract ETCA/CREA/SP-CI-47475)
(ETCA-88-R-070; ETN-89-94861) Avail: NTIS HC A04/MF A01

Automatic identification algorithms are described. Space pattern recognition is discussed (linear, H, or W). Initial data are sequences of low space and time resolution infrared imagery. The design and adoption of adaptive filters produce an almost point to point target representation. Structural analysis techniques are used to recognize the formation types. ESA

N89-29199# Physikalisch-Technische Bundesanstalt, Brunswick (Germany, F.R.). Abteilung Fertigungsmesstechnik.
INVESTIGATION OF OPTOELECTRONIC ANGLE MEASURING SYSTEMS AND THEIR USE IN A DIFFRACTION-OPTICAL STRAIN MEASUREMENT AND A PHOTOELECTRIC TWO-COORDINATE AUTOCOLLIMATOR Ph.D. Thesis - Tech. Hochschule Aachen [UNTERSUCHUNG VON OPTOELEKTRONISCHEN WINKELMESSSYSTEMEN UND DEREN EINSATZ IN EINER BEUGUNGSOPTISCHEN DEHNUNGSMESSUNG UND IN EINEM PHOTOELEKTRISCHEN 2-KOORDINATEN-AKF]
Rolf Krueger Mar. 1989 128 p In GERMAN
(PTB-F-5; ISBN-3-88314-867-9; ISSN-0179-0609; ETN-89-94986)
Avail: NTIS HC A07/MF A01

Angle-sensitive optoelectronic measuring systems are investigated with a view to their suitability for developed measuring systems: a diffraction-optical strain measurement and a photoelectric two-coordinate autocollimator. The optoelectronic measurement of small angles is outlined. The electrodynamic slaving system is used in the diffraction-optical measurement, resulting in on accuracy of one order of magnitude larger than that of speckle and holographic methods, and a real time strain measurement. The electrodynamic slaving system is also used in an autocollimator telescope, resulting in a compact and simple construction and an accuracy which is comparable with the more complicated and more expensive interferometric comparative measuring system ESA

75 PLASMA PHYSICS

Includes magnetohydrodynamics and plasma fusion.
For ionospheric plasmas see *46 Geophysics*. For space plasmas see *90 Astrophysics*.

N89-29200# Technische Univ., Eindhoven (Netherlands). Faculty of Electrical Engineering.
STABILITY OF A TAYLOR-RELAXED CYLINDRICAL PLASMA SEPARATED FROM THE WALL BY A VACUUM LAYER
W. Schuurmann and M. P. H. Weenink Nov. 1988 48 p Sponsored by the Stichting voor Fundamenteel Onderzoek der Materie, Amsterdam, Netherlands; the Netherlands Organization for the Advancement of Pure Research, Amsterdam and Euratom
(EUT-88-E-207; ISBN-90-6144-207-9; ISSN-0167-9708;
ETN-89-94795) Avail: NTIS HC A03/MF A01

The minimum energy principle of Taylor is extended to the case where a vaccum layer is situated between the weakly resistive plasma and the perfectly conducting wall. The second variation is investigated for periodic perturbations (m and/or k not 0) as well as for symmetric perturbations (m=k=0). A necessary and sufficient criterion for stability is derived by means of the Rayleigh ratio method and turns out to be identical with the results of the resistive mode analysis. Stability diagrams lambda vs k are presented. An instability region at m=1 is found at negative values

of k, already present when lambda is small. The symmetric mode becomes more unstable as the vacuum layer grows thicker.
ESA

N89-29201# Nagoya Univ. (Japan). Inst. of Plasma Physics.
ECH PLASMA FOR DIFFERENT MAGNETIC AXIS POSITIONS AND INITIAL ICRF PLASMA PRODUCTION EXPERIMENTS IN CHS
S. Okamura, M. Fujiwara, M. Hosokawa, K. Ida, H. Idei, H. Iguchi, S. Kubo, K. Masai, K. Matsuoka, and S. Morita et al Apr. 1989 25 p Presented at the 16th European Conference on Controlled Fusion and Plasma Physics Revised
(IPPJ-907) Avail: NTIS HC A03/MF A01

Electron cyclotron heating (ECH) experiments were performed in the Compact Helical System (CHS) for three typical magnetic field configurations which correspond to different magnetic axis positions. The obtained electron temperatures are different for these configurations as well as the shapes of temperature and density profiles. The inward shifted configuration was better in that both the central temperature and the total energy are higher than the outward shifted case. ICRF heating with the Type-3 antenna and/or the poloidal antenna produced a plasma for wide range of magnetic field strength. Author

N89-29202# Los Alamos National Lab., NM. Center for Nonlinear Studies.
CAVITON DYNAMICS IN STRONG LANGMUIR TURBULENCE
Don DuBois, Harvey A. Rose, and David Russell 1989 63 p Presented at the International Centre for Theoretical Physics Conference, Trieste, Italy, 22-26 May 1989 Sponsored in part by ONR and Inst. for Geophysics and Planetary Physics
(Contract W-7405-eng-36)
(DE89-012635; LA-UR-89-1848; CONF-8905156-1) Avail: NTIS HC A04/MF A01

Recent studies based on long time computer simulations of Langmuir turbulence as described by Zakharov's model will be reviewed. These show that for strong to moderate ion sound samping the turbulent energy is dominantly in nonlinear caviton excitations which are localized in space and time. A local caviton model will be presented which accounts for the nucleation collapse burnout cycles of individual cavitons as well as their space-time correlations. This model is in detailed agreement with many features of the electron density fluctuation spectra in the ionosphere modified by powerful HF waves as measured by incoherent scatter radar. Recently such observations have verified a prediction of the theory that free Langmuir waves are emitted in the caviton collapse process. These observations and theoretical considerations also strongly imply that cavitons in the heated ionosphere, under certain conditions, evolve to states in which they are ordered in space and time. The sensitivity of the high frequency Langmuir field dynamics to the low frequency ion density fluctuations and the related caviton nucleation process will be discussed. DOE

N89-29203# California Univ., Berkeley.
NONLINEAR STABILITY IN FLUID AND PLASMA DYNAMICS Final Technical Report
Jerrold E. Marsden 28 Feb. 1989 17 p
(Contract F49620-87-C-0118; AF Proj. 2304)
(AD-A207715; AFOSR-89-0533TR) Avail: NTIS HC A02/MF A01 CSCL 20/11

This report presents a block diagonalization theorem which is designed to study the stability and bifurcation of rotating systems, or more generally, of relative equilibria. The context of the discussion is the energy-momentum method of mechanical systems with symmetry. Crucial special cases of the block diagonalization theorem for uniformly rotating system, including general nonlinear elasticity and geometrically exact rods are discussed. The purpose here is to abstract these examples and prove a general geometric theorem. These general results will be important for rotating gravitational fluid masses as well. GRA

N89-29204# Stanford Univ., CA. High Temperature Gasdynamics Lab.
FUNDAMENTAL PROCESSES IN PARTIALLY IONIZED PLASMAS Final Report, 1 Aug. 1986 - 31 Jul. 1988
C. H. Kruger Aug. 1988 11 p
(Grant AF-AFOSR-0225-86; AF Proj. 2917)
(AD-A207910; AFOSR-89-0613TR) Avail: NTIS HC A03/MF A01 CSCL 20/9

The purpose of this program has been to provide modern plasma sources and data acquisition capability for the ongoing research program on Fundamental Processes in Partially Ionized Plasmas. Under this Grant, Stanford has acquired, installed, and characterized a 50kW induction plasma torch system and associated diagnostic, and has modernized the data acquisition capability through micro-computer systems. This new equipment has had a very favorable effect on the experimental capability and has already contributed to the research output. GRA

N89-29205# Naval Research Lab., Washington, DC. Geophysical and Plasma Dynamics Branch.
EFFECTS OF MAGNETIC AND COLLISIONAL VISCOSITY ON THE E X B GRADIENT DRIFT INSTABILITY
S. T. Zalesak, J. D. Huba, and P. Satyanarayana (Science Applications International Corp., McLean, VA.) 27 Apr. 1989 43 p
(Contract MIPR-88-526)
(AD-A207975; NRL-MR-6438) Avail: NTIS HC A03/MF A01 CSCL 20/9

The role of magnetic viscosity (i.e., Larmor radius effects) and collisional viscosity on the Ex B gradient drift instability is investigated in both the collisional and inertial regimes. The equations describing the time evolution of small perturbations to an equilibrium two dimensional (x,y) magnetized plasma are derived where the equilibrium electron density is an arbitrary function of y. The equations are then solved iteratively in time to obtain the growth rate of the fastest growing eigenmode for a given Fourier wavenumber k in the x direction. We compare our results for appropriate profiles with two asymptotic results: the long wavelength limit, valid for kL is dominated by 1, and the short wavelength or local limit, valid for kL is much greater than 1, where L is the gradient scale length of the equilibrium profile. It is found that although the long and short wavelength limits do indeed provide accurate growth rates for kL is dominated by 1 and kL is much greater than 1, respectively, neither provides reliable growth rates for kL approx. 1. In comparing these results to the long wavelength limit, in addition to affecting gamma in an absolute sense, increasing L to a finite value decreases k sub max, the value of k for which gamma(k) maximizes, and also affects the sharpness of the peak of gamma(k) about k sub max. Both of these phenomena have large effects on freezing models. GRA

N89-29206# Minnesota Univ., Minneapolis. Dept. of Electrical Engineering.
STUDIES OF THE VOLUME AND PLASMA SHEATH PROPERTIES OF RADIO FREQUENCY DISCHARGES Final Report, 1 Jun. 1983 - 28 Feb. 1987
D. W. Ernie and H. J. Oskam Nov. 1988 109 p
(Contract F33615-83-K-2340)
(AD-A207980; AFWAL-TR-88-2103) Avail: NTIS HC A06/MF A01 CSCL 20/3

Radio frequency discharges currently play a major role in the fabrication of microelectronic devices. This manuscript reports on theoretical and experimental studies undertaken in an effort to develop a better understanding of the underlying gas discharge physics occuring in these discharges. An equivalent circuit model was developed for a planar rf reactor based on the physical properties of the plasma sheath. This model shows that the waveforms of the potentials across the plasma sheaths are highly nonlinear and agree with previously reported measurements. These waveforms were subsequently incorporated into a model for the energy distribution of ions bombarding the electrode surfaces in low pressure rf reactors. Numerical calculations based on this model show the ion bombardment energy distribution is bimodal

and skewed toward lower impact energies. Experimental measurements were also performed on the ion bombardment energy distribution in a planar rf reactor. The results of these measurements agree with the model predictions at low pressure and give information at higher pressures about the effects of collisions on the distribution, which agree with previous studies. The importance of negative ions in a discharge through an electronegative gas was investigated by the development of a collisionless plasma sheath model for such a discharge. A sheath criterion was derived and used to determine the effects of negative ions on the sheath properties. GRA

N89-29207# Nagoya Univ. (Japan). Inst. of Plasma Physics.
SOLID-VAPOR DIFFERENCES OF ELECTRONIC STOPPING POWERS FOR PROTONS
Toshiaki Kaneko (Okayama Univ. of Science, Japan) Mar. 1989 25 p Sponsored in part by Ministry of Education, Science, and Culture, Japan
(IPPJ-901) Avail: NTIS HC A03/MF A01

By applying the recently-developed wave packet theory and the Lindhard-Winther (LW) theory to estimation of the stopping powers of bound electrons and conduction electrons, respectively, the solid-vapor differences in the electronic stopping of target materials for protons are estimated quantitatively over the energy range from 1 keV/amu to 10 MeV/amu. Here, comparison was made of current theoretical predictions with each other. The wave packet theory shows that the solid-vapor difference of stopping cross sections are enhanced for low-energy protons because of the binding effect. Author

N89-29208# Nagoya Univ. (Japan). Inst. of Plasma Physics.
UNLIMITED ACCELERATION OF PARTICLES BY A SYSTEM OF MULTI-LASER BEAMS
Ryo Sugihara Mar. 1989 20 p
(IPPJ-902) Avail: NTIS HC A03/MF A01

A scheme of particle acceleration is proposed in which an electron (or a positron) can coherently interact with a system of multi-laser beams. The system can trap and accelerate the particle obliquely to the direction of the beams, the principle being analogous to the V sub p XB or the cross field acceleration. It is demonstrated that if the electric field of an individual laser beam is 10(12)V/cm a 1 TeV electron with a 2m long device is obtained in a static magnetic field less than 20 tesla. Author

N89-29209# Nagoya Univ. (Japan). Inst. of Plasma Physics.
HIGH POWER ICRF HEATING EXPERIMENTS ON THE JIPP T-IIU TOKAMAK
Y. Ogawa, K. Masai, T. Watari, R. Akiyama, R. Ando, J. Fujita, Y. Hamada, S. Hirokura, K. Ida, and K. Kadota et al Mar. 1989 42 p
(IPPJ-903) Avail: NTIS HC A03/MF A01

In the JIPP T-IIU tokamak, a high power ICRF heating experiment was conducted up to an extremely high power density (similar to 2MW/m(3)) with a total RF power of P sub RF = 2 MW. Much attention was paid initially to the problem of impurities, and it was found that the adoption of low-Z materials for the limiter, in situ carbon coating (i.e., carbonization), and adequate gas-puffing synchronized to the RF pulse are very effective in suppressing radiation loss. In combination with these methods, a remarkable reduction in metal impurities (especially in iron impurity) was achieved, suppressing the total radiation loss to less than 30 similar to 40 percent of the input power. In these reduced-radiation-loss plasmas, characteristics of ICRF-heated plasmas were intensively studied. With an increase in the ICRF heating power, the deterioration of the energy confinement time is observed, indicating quantitative agreement with Kaye-Goldston L-mode scaling. It is shown that the so-called profile consistency, which is the leading feature in NBI-heated plasmas, holds also in the ICRF-heated plasma. It has been observed that the electron temperature profile responds only to the safety factor q(a), and is not changed by the deposition profile controlled by tailoring the k(parallel) spectrum. Author

N89-29210# Nagoya Univ. (Japan). Inst. of Plasma Physics.
A THREE-DIMENSIONAL RESISTIVE MHD SIMULATION ANALYSIS OF FIELD REVERSAL CONTROL IN THE REVERSED FIELD PINCH
A. Nagata, H. Ashida (Electrotechnical Lab., Ibaraki, Japan), S. Koide, K. I. Sato, and T. Amano Mar. 1989 39 p
(IPPJ-904) Avail: NTIS HC A03/MF A01

A 3-D resistive magnetohydrodynamic simulation code under the compressibility condition is applied to analysis of the field reversal control in the reversed field pinch (RFP). Simulation results show that a loss of the field reversal at the wall leads to increase of q-value on the axis and broad one of the q-profile, and also to the rapid increase of the fluctuating magnetic energy due to nonlinear tearing modes with the m=1 and m=2 modes. By deepening the field reversal at the wall, the reversal surface moves inside the plasma, and the q-profile becomes narrow. As a result, a rapid growth and saturation of these tearing modes is suppressed by the field reversal control. Author

N89-29211# Nagoya Univ. (Japan). Inst. of Plasma Physics.
CAOTIC MAGNETIC FIELD LINE IN TOROIDAL PLASMAS
Tadatsugu Hatori, Haruyuki Irie (Nihon Univ., Tokyo, Japan), Yoshihiko Abe, and Kazuhiro Urata May 1989 64 p
(IPPJ-911) Avail: NTIS HC A04/MF A01

This is an introductory review of chaotic magnetic field line in plasmas, together with some new results, with emphasis on the long-time tail and the fractional Brownian motion of the magnetic field line. The chaotic magnetic field line in toroidal plasmas is a typical chaotic phenomena in the Hamiltonian dynamical systems. The onset of stochasticity induced by a major magnetic perturbation is thought to cause a macroscopic rapid phenomena called the current disruption in the tokamak discharges. Numerical simulations on the basis of magnetohydrodynamics reveal in fact the disruptive phenomena. Some dynamical models which include the area-preserving mapping such as the standard mapping, and the two-wave Hamiltonian system can model the stochastic magnetic field. Theoretical results with use of the functional integral representation are given regarding the long-time tail on the basis of the radial twist mapping. It is shown that application of renormalization group technique to chaotic orbit in the two-wave Hamiltonian system proves decay of the velocity autocorrelation function with the power law. Some new numerical results are presented which supports these theoretical results. Author

N89-29212# Nagoya Univ. (Japan). Inst. of Plasma Physics.
FULL CONSISTENT ANALYSIS OF HIGH BETA STEADY STATE TOKAMAKS SUSTAINED BY BEAM DRIVEN AND BOOTSTRAP CURRENTS
K. Okano, Y. Ogawa, and H. Naitou (Yamaguchi Univ., Japan) May 1989 46 p
(IPPJ-912; ISSN-0469-4732) Avail: NTIS HC A03/MF A01

Beam driven steady state tokamaks of moderate size (R sub o = 4.55 m) was analyzed by a full consistent beam current drive analysis code, which consistently includes MHD equilibrium, kink and ballooning stability analysis, bootstrap current, power balance and momentum balance calculations. It was found that this moderate size is sufficient to demonstrate the feasibility of steady state operation by the neutral beam current drive. The maximum Q value attains Q = 7 to approx. 9 with the fusion power P sub f = 500 to approx. 800 MW and L-mode confinement is sufficient to sustain self consistent equilibria. The Q value is nearly doubled due to the bootstrap current and the T sub i greater than T sub e feature of beam driven tokamaks. The optimum beam energy is 1.0 to approx. 1.2 MeV and the toroidal rotation effects were negligible. Author

N89-29213# Nagoya Univ. (Japan). Inst. of Plasma Physics.
IMPROVED CONFINEMENT IN HIGH DENSITY OHMIC DISCHARGE
Y. Hamada, K. Sakamoto, K. N. Sato, K. Masai, K. Toi, K. Ida, K. Kawahata, K. Adati, A. Ando, and S. Hidekuma et al May 1989 13 p
(IPPJ-913; ISSN-0469-4732) Avail: NTIS HC A03/MF A01

The improvement of the confinement of the ohmic plasma with limiter configuration, similar to the Improved Ohmic Confinement (IOC) mode of ASDEX, is observed in JIPP T-IIU. The features of the IOC mode are summarized in the following way: the circular limiter-plasma instead of the divertor plasma; very high density threshold for IOC in contrast to the ASDEX IOC mode; and no enhanced radiation due to impurity accumulation. The preliminary experimental results are discussed. Author

N89-29214# Nagoya Univ. (Japan). Inst. of Plasma Physics.
EFFECT OF A CONVERTER ELECTRODE IN A MULTICUSP NEGATIVE ION SOURCE
Henry J. Ramos, Mamiko Sasao, Hitoshi Yamaoka, and Motoi Wada (Doshisha Univ., Kyoto, Japan) May 1989 18 p Sponsored in part by Japan Society for the Promotion of Science
(IPPJ-914; ISSN-0469-4732) Avail: NTIS HC A03/MF A01

The electron temperature of a negative ion source has to be low so as not to destroy produced negative ions by electron impact processes. The bulk plasma characteristics of a multicusp negative ion source with a converter electrode are examined by a probe data acquisition system for two cases; converter with cesium and converter without cesium. The effects of the converter bias on bulk plasma parameters were observed when cesium is not introduced. Under cesiated discharge condition, the converter bias effects are obscure. The addition of cesium into a helium discharge decreases the high energy electron component, which is unfavorable from a view point of negative ion extraction, and hence lowers the electron temperature. Author

N89-29215# Nagoya Univ. (Japan). Inst. of Plasma Physics.
A NEW METHOD OF TESTING NUCLEAR FUSION IN METALS
Noriaki Itoh May 1989 6 p
(IPPJ-915; ISSN-0469-4732) Avail: NTIS HC A02/MF A01

A new crucial test for nuclear fusion in palladium or titanium metal is suggested. This method is capable to heat a deuterium-metal mixture to a given temperature, and hence is expected to yield detailed information on fusion reactions in metallic environments. Author

N89-29216# Royal Inst. of Tech., Stockholm (Sweden). Dept. of Plasma Physics.
EXPERIMENTS ON THE MAGNETIC FIELD AND NEUTRAL DENSITY LIMITS ON CIV INTERACTION
I. Axnas and Nils Brenning Oct. 1988 11 p Presented at the COSPAR Conference, Espoo, Finland, 1988 Sponsored by the Swedish Natural Science Research Council
(TRITA-EPP-88-08; ISSN-0348-7539; ETN-89-95147) Avail: NTIS HC A03/MF A01

Experiments on the critical ionization velocity (CIV) interaction in the impact configuration are reported. Different values of the plasma density, the neutral density, and the magnetic field strength are used. A combination of microwave interferometry and spectroscopy is used to measure the plasma density and to study the electron energy distribution. The efficiency of the CIV process is evaluated as a function of the ratio between the Alfven velocity and the plasma stream velocity. The ratio between the ionization frequency and the ion gyro frequency is obtained. In the parameter range studied so far, efficient electron heating is found only when both these parameters exceed unity. ESA

N89-29217# Royal Inst. of Tech., Stockholm (Sweden). Dept. of Plasma Physics.
ON THE SPOKE STRUCTURE IN CRITICAL VELOCITY ROTATING PLASMAS
Nils Brenning Jan. 1989 13 p Sponsored by the Swedish Natural Science Research Council
(TRITA-EPP-89-01; ISSN-0348-7539; ETN-89-95150) Avail: NTIS HC A03/MF A01

The ionizing front model for the current spokes in homopolar experiments on the critical ionization velocity phenomenon is briefly reviewed, and the main predictions are compared to experimental observations. The proposed mechanism of localized electron heating at the leading edges of the spokes is well supported by the observations. A discrepancy about the sheath thickness, and about the location of the observed high frequency emission in relation to the space charge structure is detected. The observed spokes have a thickness which exceeds the limit of applicability of the ionizing front model by typically a factor of ten. The azimuthal electric field is found to be closely proportional to (n sub e - n sub e average density). This relation holds on both sides of the density spokes, and also between the spokes, in spite of the fact that the electron temperature, current density, and high frequency emission are all strongly peaked about the leading spoke edge. This indicates that the mechanism which maintains the space charge structure depends mainly on the plasma density, and only indirectly on the ionization rate. It is proposed that a density-related partial blocking of the azimuthal Hall current could give the observed correlation between azimuthal electric field and plasma density. ESA

76 SOLID-STATE PHYSICS

Includes superconductivity.

For related information, see also *33 Electronics and Electrical Engineering* and *36 Lasers and Masers.*

N89-29218# Helsinki Univ. of Technology, Espoo (Finland). Low Temperature Lab.
MEASUREMENTS OF THE DIPOLAR VELOCITY OF SUPERFLUID 3 He-B
K. K. Nummila, P. J. Hakonen, and O. V. Magradze (Akademiya Nauk Gruzinskoi SSR, Tiflis.) Jan. 1989 16 p
(PB89-155444; TKK-F-A636; ISBN-951-754-665-3) Avail: NTIS HC A03/MF A01 CSCL 20L

The frequency shift of the counterflow-induced peak was measured in the NMR spectrum of the flare-out texture in rotating 3He in a vortex-free state. From a comparison with the calculated shifts, the temperature dependence of the dipolar velocity at P=5.0 and 29.3 bars was deduced. The results are in good agreement with theoretical predictions. Author

N89-29219# Department of the Army, Washington, DC.
METHOD OF MASS PRODUCING SUPERCONDUCTING PERSISTENT CURRENT RINGS Patent Application
Herbert A. Leupold, inventor (to Army) 13 Mar. 1989 9 p
(AD-D013968; US-Patent-Appl-SN-322381) Avail: NTIS HC A02/MF A01 CSCL 20/3

Superconducting persistent current rings are mass produced by passing each superconducting ring through a tapered magnetic field that is tapered in strength so that when each ring passes through the maximum magnetic field of the tapered magnetic field which, is above the critical field of the tapered magnetic field, the superconducting ring becomes normal thereby admitting all of the flux to which its cross section is exposed. When the ring is passed to a region of field lower in strength than the critical field, the ring becomes superconducting again and traps the flux to which its cross section is exposed. GRA

N89-29220# Therma-Wave, Inc., Freemont, CA.
THERMAL CONDUCTIVITY ANISOTROPY IN SINGLE CRYSTAL YBa2Cu3O7-x
Allan Rosencwaig, Jon Opsal, D. L. Willenborg, and H. Coufal (International Business Machines Corp., San Jose, CA.) 1989 3 p Presented at the 6th International Topical Meeting on Photoacoustic and Photothermal Phenomena, Baltimore, MD, 31 Jul. - 3 Aug. 1989
(Contract DE-AC03-88ER-80652)
(DE89-009643; CONF-890754-1) Avail: NTIS HC A02/MF A01

We have used the modulated reflectance thermal wave technique to measure the crystallographic anisotropy in the room temperature thermal conductivity of single crystals of YBa sub 2 Cu sub 3 O sub 7-x. DOE

N89-29221# Associacao Latino-Americana de Metalurgia e Materiais, Rio de Janeiro (Brazil).
PLASTIC DEFORMATION OF YBa2Cu3O7-x SUPERCONDUCTOR COMPOUND
Gabriel TorresVillasenor and Jose E. Moreno 1988 7 p In PORTUGUESE; ENGLISH summary Presented at the 3rd Latin-American Colloquium about Fatigue and Fracture of Materials, Rio de Janeiro, Brazil, 27 Nov. 1988
(DE89-613395; INIS-BR-1531; CONF-8811214) Avail: NTIS (US Sales Only) HC A02/MF A01

The high temperature superconductor YBa sub 2 Cu sub 3 O sub 7-x shown a brittle behavior when deformed under ambient conditions. If a hydrostatic state of stress is imposed with a metal matrix, it is possible to induce exttended plastic deformations as a great as 200 percent were achieved using this method without loosing the superconductivity in the ceramic. The observed deformations mechanisms are similar to those observed in the superplastic metals and the boundary ceramic metal matrix was found to be highly coherent. This method opens a new technique that can be apllied in the manufacture of superconductor wire.
DOE

N89-29222# Associacao Latino-Americana de Metalurgia e Materiais, Rio de Janeiro (Brazil).
FACTORS AFFECTING STRESS DISTRIBUTION AND DISPLACEMENTS IN CRYSTALS 3-5 GROWN BY CZOCHRALSKI METHOD WITH LIQUID ENCAPSULATION
C. E. Schvezov, I. Samarasekera, and F. Weinberg 1988 20 p In SPANISH; ENGLISH summary Presented at the 3rd Latin-American Colloquium about Fatigue and Fracture of Materials, Rio de Janeiro, Brazil, 27 Nov. 1988
(DE89-613396; INIS-BR-1533; CONF-8811214) Avail: NTIS (US Sales Only) HC A03/MF A01

A mathematical model based on the finite element method for calculating temperature and shear stress distributions in 3 to 5 crystals grown by LEC technique was developed. The calculated temperature are in good agreements with the experimental measurements. The shear stress distribution was calculated for several environmental conditions. The results showed that the magnitude and the distribution of shear stresses are highly sensitive to the crystal environment, including thickness and temperature distribution in boron oxides and the gas. The shear stress is also strongly influenced by interface curvature and cystals radius.
DOE

N89-29223# Lowell Univ., MA. Dept. of Chemistry.
COGNITION AND ORDER IN LANGMUIR-BLODGETT FILMS OF A 3-HEXADECYL PYRROLE AND FERROCENE-DERIVATIZED PYRROLE MIXED MONOLAYER SYSTEM
L. Samuelson, A. K. M. Rahman, G. P. Puglia, S. Clough, S. Tripathy, T. Inagaki, b0661237, X. Q. Yang, T. A. Skotheim, and Y. Okamoto (Polytechnic Univ., Brooklyn, NY.) 1989 10 p Presented at the International Conference on Intelligent Materials, Tsukuba, Japan, 1 Mar. 1989 Sponsored in part by ONR
(Contract DE-AC02-76CH-00016)
(DE89-012974; BNL-42655; CONF-8903128-1) Avail: NTIS HC A02/MF A01

Novel, self-assembled materials were designed and produced from first principle to possess unique structural hierarchy and electronic and optical properties. The Langmuir-Blodgett technique was used to study the molecular organization of a mixed 3-hexadecyl pyrrole (3HDP) and ferrocene-derivatized pyrrole (Fc-Py) surfactant system. The pyrrole moiety was chosen for its' well established electronic and optical properties when polymerized, while ferrocene, it is theorized, if properly oriented into a Langmuir-Blodgett monolayer film may show a layered array of transition metals which would be extremely valuable as a model for 2-D magnets. The ferrocene group may also provide the possibility of charge coupling between neutral ferrocene and oxidized ferricenium which could be controlled electrochemically or photochemically. It has been determined that stable monolayer films of the mixed system could be formed at the air-water interface. The growth and assembly process led to polypyrrole 2-D lattices with heretofore unsurpassed order. In fact, the process of template polymerization leads to a new crystal phase for the polypyrrole component of the thin film structure. Various monolayer and multilayer films were prepared on platinum coated substrates for surface spectroscopic characterization using synchrotron radiation. Near Edge X-Ray Absorption Fine Structure studies revealed that highly ordered multilayer structures are being formed.
DOE

N89-29224# Lawrence Livermore National Lab., CA. Nonlinear Optical Materials Group.
CHIRAL ORGANIC CRYSTALS FOR HIGH POWER FREQUENCY CONVERSION
Laura E. Davis, Stephan P. Velsko, and David Eimerl May 1989 8 p Presented at the Sessions on Materials Processing in Space, Chicago, IL, 25 Sep. 1988
(Contract W-7405-eng-48)
(DE89-013791; UCRL-101023; CONF-8809364-1) Avail: NTIS HC A02/MF A01

Water soluble organic salts comprise a class of crystalline materials containing many efficient harmonic generators for high power lasers. Statistical studies of the simple chiral salts reveal that approximately ten percent have nonlinearities similar to or better than potassium dihydrogen phosphate, the material most commonly used for high power frequency conversion. Furthermore, high damage thresholds (greater than 40 J/sq cm at 1.06 microns) have been demonstrated in 1-arginine phosphate which is a representative crystal from this class. Simple chiral salts have ultraviolet cutoff wavelengths of 200 to 500 nm, and this, together with the fact that many are very birefringent, implies that phasematching over a wide range of wavelengths should be possible. In particular, this class of materials may be expected to contain efficient harmonic generators of blue and ultraviolet light. Finally, very large single crystals (greater than 1000 cm) of many of these water soluble materials can be grown, making the fabrication of large aperture frequency conversion devices possible.
DOE

N89-29225# Oak Ridge National Lab., TN. Solid State Div.
ION BEAM DEPOSITION OF EPITAXIAL GERMANIUM AND GALLIUM ARSENIDE LAYERS
T. E. Haynes, R. A. Zuhr, S. J. Pennycook, and B. C. Larson May 1989 11 p Presented at the 12th Symposium on Ion Sources and Ion-Assisted Technology, Tokyo, Japan, 5-7 Jun. 1989 Submitted for publication
(Contract DE-AC05-84OR-21400)
(DE89-014044; CONF-8906157-1) Avail: NTIS HC A03/MF A01

Low-energy, mass-separated ion beams of Ge, Ga, and As at 30 and 40 eV were used to deposit isotopically pure, epitaxial layers of Ge-76 and Ge-70 on GaAs(100) and of Ga(69)As and Ga(71)As on Ge(100). Epitaxial growth of Ge and GaAs layers was achieved at temperatures as low as 250 C. Growth of the compound GaAs was accomplished by repetitive magnetic switching between the Ga(+) and As(+) ion beams obtained simultaneously from a single ion source. The structure of the deposited layers is characterized by ion channeling, transmission electron microscopy, and X-ray diffraction.
DOE

N89-29226# Oak Ridge National Lab., TN. Matals and Ceramics Div.
THE AMORPHOUS TO GAMMA TRANSFORMATION IN ION IMPLANTED Al2O3
P. S. Sklad, J. C. McCallum, C. J. McHargue, and C. W. White 1989 14 p Presented at the Radiation Effects in Insulators-5: Crystalline Oxides and Ceramics Session, Hamilton, Ontario, 19 Jun. 1989
(Contract DE-AC05-84OR-21400)
(DE89-014797; CONF-8906155-1) Avail: NTIS HC A03/MF A01

Amorphous surface layers, free of implanted impurities, were produced on single crystal alpha--Al2O3 substrates by implantation at -185 C with 2 x 10(16)^{a} Al/sq cm at 90 keV and 3 x 10(16)C/sq

cm at 55 keV. The response of these amorphous layers to post-implantation annealing in the temperature range from 700 C to 800 C was investigated by in situ Transmission Electron Microscopy (TEM) and conventional TEM of specimens annealed in bulk form. It was found that the amorphous Al2O3 transformed to the transitional gamma phase along an irregular front. The recrystallized material is columnar with the individual columns or domains irregular in size and shape. The alpha-Al2O3 is composed of two variants which are twin related and have the following orientation relationship with the substrate: <110> gamma <10 bar 1 0> alpha and 111 gamma 0001 alpha . The temperature dependence velocity of the amorphous-to-gamma transformation front was measured by in situ TEM. Assuming a thermally activated process, the activation energy has been determined from an Arrhenius plot of velocity versus T(-1). These results are discussed in terms of possible rate controlling processes of the transformation. DOE

N89-29227# California Univ., Berkeley. Dept. of Materials Science and Mineral Engineering.
STATES OF OXYGEN ORDERING IN YBa2Cu3Oz
D. deFontaine May 1989 15 p Presented at the Conference on Oxygen Disorder Effects in High Tc Superconductors, Trieste, Italy, 18 Apr. 1989 Prepared in cooperation with California Univ., Berkeley. Lawrence Berkeley Lab.
(Contract DE-AC03-76SF-00098)
(DE89-014893; LBL-27267; CONF-890480-1) Avail: NTIS HC A03/MF A01

The compound YBa2Cu3O(x) (1-2-3) was the first one whose superconducting transition temperature exceeded the technologically important temperature of 77K. Actually, the 1-2-3 compound at close to oxygen stoichiometry z = 7 became superconducting at about T sub c = 90K, with T sub c dropping by increments as z decreased from the value 7. In the 90K superconducting phase, occupied sites form O-Cu-O chains, and the resulting 3-D structure has orthorhombic symmetry. When available sites in the mirror plane are occupied statistically by O ions, the resulting structure has tetragonal symmetry and the material is nonsuperconducting. It thus appears that the tetragonal to orthorhombic transition in the 1-2-3 compound can be modeled by an order-disorder transition in the mirror plane. The properties of this transition are reviewed and appropriate phase diagrams pertaining to oxygen ordering in the plane are derived. Much pertinent information concerning oxygen ordering in 1-2-3 is reviewed in a recent paper by Beyers and Shaw. DOE

N89-29228# California Univ., Berkeley. Lawrence Berkeley Lab. Center for Advanced Materials.
VERTICAL GRADIENT FREEZE GaAs: GROWTH AND ELECTRICAL PROPERTIES Ph.D. Thesis
Maria Lucie Galiano May 1989 66 p Prepared in cooperation with California Univ., Berkeley
(Contract DE-AC03-76SF-00098)
(DE89-014894; LBL-27271) Avail: NTIS HC A04/MF A01

The influence of silicon contamination prevention methods on the electrical properties of GaAs grown by the Vertical Gradient Freeze (VGF) technique was investigated. The effectiveness, is reported, of these methods for GaAs crystals grown from two different starting materials: n-type with resistivities in the range of 10(-1) to 10(3) omega-cm and semi-insulating (SI) with a resistivity of 10(8) omega-cm. It was found that the impurities in the starting materials, specifically boron, carbon and silicon, have an effect on the ability to control silicon contamination with methods that have been reported previously in the literature. The attainment is reported of SI crystals using a PBN crucible, a SI charge and B2O3 encapsulation. DOE

N89-29229# Los Alamos National Lab., NM.
HIGH-TEMPERATURE SUPERCONDUCTOR MATERIALS PROCESSING: DEVELOPMENT OF ENVIRONMENTALLY ACCEPTABLE PROCESSING TECHNOLOGIES
E. J. Peterson, L. E. Wangen, K. C. Ott, K. M. Hargis, T. E. Hakonsen, T. W. Whaley, and W. J. Parkinson Jul. 1989 16 p
(Contract W-7405-eng-36)
(DE89-014391; LA-11613-MS) Avail: NTIS HC A03/MF A01

The Los Alamos National Laboratory, as a national scientific resource, should be a major participant in the development of new technologies and the improvement of existing technologies that will enhance the nation's industrial competitiveness. Because the Laboratory is a national resource the broadest view of technology development and technology transfer must be taken. As the basic research is converted into useable technologies that can be transferred to the industrial sector, it must be recognized that the job remains incomplete when the product engineering phase is accomplished. A technology or product application that industry cannot implement because of health and environmental constraints will not contribute to our industrial competitiveness. Similarly, a sophisticated technology not accompanied by the appropriate expert knowledge base and process control strategies when technology transfer is attempted will be of marginal use to industry. Thus, it is essential for the Laboratory to take a multidimensional approach to technology development and technology transfer to the industrial sector. The superconducting ceramic oxide materials processing effort of the Exploratory Research and Development Center at Los Alamos provides an excellent opportunity to develop strategies that will address these issues. DOE

N89-29230# Sandia National Labs., Albuquerque, NM.
EFFECTIVE MASSES AND G FACTORS FOR 2-D LIGHT HOLES IN InSb
J. E. Schirber, C. P. Tigges, L. R. Dawson, H. P. Hjalmarson, and I. J. Fritz 1989 7 p Presented at the International Conference on Narrow-gap Semiconductors and Related Materials, Gaithersburg, MD, 12 Jun. 1989
(Contract DE-AC04-76DP-00789)
(DE89-014899; SAND-89-0324C; CONF-890621-1) Avail: NTIS HC A02/MF A01

The light holes in InSb are characterized using a Shubnikov-de Haas technique by exploiting the Type 2 band offset of an InAs(.15)SB(.85)InSb strained layer superlattice. The data are analyzed to determine the effective masses and g factors as a function of carrier concentration. DOE

N89-29231# Ohio State Univ., Columbus. Dept. of Physics.
ULTRASONIC ATTENUATION IN HEAVY FERMION SUPERCONDUCTORS
Liam Coffey, N. E. Phillips, ed., R. N. Shelton, ed., and W. A. Harrison, ed. 1989 2 p Presented at the International Conference on Materials and Mechanisms of Superconductivity - High-Temperature Superconductors, Stanford, CA, 23-24 Jul. 1989 Submitted for publication
(Contract DE-FG02-88ER-45347)
(DE89-014937; DOE/ER-45347/13; CONF-890718-7) Avail: NTIS HC A02/MF A01

The large effective electron mass in the heavy fermion superconductors UPt3 and UBe13 can produce peaks and other features in the temperature and magnetic field dependent sound attenuation. DOE

N89-29232# Massachusetts Inst. of Tech., Cambridge. Microsystems Research Center.
A MANUFACTURING SCHEDULER'S PERSPECTIVE ON SEMICONDUCTOR FABRICATION
X. Bai and S. B. Gershwin Apr. 1989 33 p
(Contracts N00014-85-K-0213; MDA972-88-K-0008)
(AD-A208372; VLSI-Memo-89-518; LMP-88-004) Copyright Avail: NTIS HC A03/MF A01 CSCL 09/1

In this paper, we describe the phenomena in semiconductor fabrication which are important for production scheduling. We focus our attention on collecting and understanding events, and describing related concepts, such as fabrication processes, operation sets, production machines, support machines, accessories, operation workers, support technicians, activities,

objectives, etc. We do not suggest scheduling policies here; instead the goal is to characterize all the events that must be considered in developing such a policy. GRA

N89-29233# Washington Univ., Seattle.
MULTILAYERED ELECTRONIC MATERIALS AND DEVICES BASED ON 3-5 COMPOUNDS Final Report, 1 Oct. 1986 - 30 Sep. 1988
Larry C. Olsen Dec. 1988 13 p
(Grant AF-AFOSR-0034-87; AF Proj. 2917)
(AD-A208861; AFOSR-89-0732TR) Avail: NTIS HC A03/MF A01 CSCL 20/12

The objectives of this program were to purchase and install a Metal Organic Chemical Vapor Deposition (MOCVD) system in the Electronic Materials Laboratory at the Tri-Cities University Center of the University of Washington. This system would be used to grow films of 3 to 5 compounds. This reactor will be used to grow layered structures based on Gallium Arsenide, AlxGa1-xAs, InyGa(1-y)As or GaAsxP1-x. Prior to shipping the MOCVD system, Spire personnel grew GaAs films on GaAs substrates with the TUC 500XT reactor. Excellent results were obtained. Films grown on two-inch wafers exhibited a thickness uniformity of better than 2 percent and a doping uniformity better than 4.5 percent. With three-inch wafers, films were characterized by a thickness uniformity of 4 percent and doping uniformity of 8 percent. They also found that the Aluminum Gallium Arsenide composition uniformity was better than 2 percent for AlGaAs films grown on two-inch waters. Finally, the background doping in epitaxial GaAs films grown with the TUC reactor was determined to be less than 1.5x10 to the 14th power/CC. These performance figures represent a significant improvement in GaAs epitaxial film growth. GRA

N89-29234# Brown Univ., Providence, RI. Dept. of Chemistry.
REDETERMINATION OF CRYSTAL STRUCTURE OF ZINC THIOGALLATE
G. B. Carpenter, P. Wu, Y. M. Gao, and A. Wold 30 May 1989 8 p Submitted for publication
(Contract N00014-85-C-0177)
(AD-A208931; TR-12) Avail: NTIS HC A02/MF A01 CSCL 07/2

Zinc thiogallate crystallizes in a tetragonal space group. In this space group zinc and gallium are disordered in the 4(d) sites. Most of the AGa2x4 compounds crystallize with the defect chalcopyrite, space group I4 where the A and Ga ions are ordered and half of the A-sites are vacant. The result of this work indicates that disordering of Zn and Ga ions can occur and result in a structure with higher symmetry. All of these compounds transmit in the far infrared and are potential infrared window materials. GRA

N89-29235# EIC, Inc., Norwood, MA.
MORPHOLOGY CONTROL OF PHOTOELECTROCHEMICALLY ETCHED PROFILES IN n-GaAs
Jianguo Li, Michael M. Carrabba, and R. D. Rauh Jun. 1989 4 p Presented at the Fall Meeting of the Electrochemical Society, Inc., Hollywood, FL, 15-20 Oct. 1989
(Contract N00014-87-C-0408)
(AD-A208991; TR-5) Avail: NTIS HC A02/MF A01 CSCL 20/12

Photoelectromechanical etching of (100) n-gallium arsenide along the (011) crystallographic direction produces V-grooves. It was determined that the groove angle and rate of undercutting of the photoresist mask was dependent on electrolyte composition, light intensity and bias potential. Grating structures could be produced in neutral aqueous electrolytes containing KCL, with angles varying from 80 to 120 degrees as the KCL concentration was varied from 0.01M to 4M. The angles could also be controlled with applied bias and with light intensity. The V-grooves are formed due to the exposure of Ga-rich faces, their composition and angle probably depending on the extent of adsorption of Chloride(-). Non-adsorbing electrolytes such as Fluoride(-) and Sulfate(-) generally gave rougher morphologies and/or passivation. GRA

N89-29236# EIC, Inc., Norwood, MA.
PHOTOELECTROCHEMICAL FABRICATION OF GRATINGS IN SiC
Michael M. Carrabba, Jianguo Li, John P. Hachey, R. D. Rauh, and Y. Wang (North Carolina State Univ., Raleigh.) Jun. 1989 6 p Presented at the Fall Meeting of the Electrochemical Society, Inc., Hollywood, FL, 15-20 Oct. 1989
(Contract N00014-87-C-0408)
(AD-A208992; TR-4) Avail: NTIS HC A02/MF A01 CSCL 20/12

Photochemical etching has been demonstrated as a means for generating high resolution patterns in silicon carbide. Both chemical vapor deposition (CVD) and epitaxial (on Si) SiC were used. Liquid electrolytes containing either fluoride or ethylene diamine were found to promote smooth photoanodic dissolution, without passivation. Very low anodic dark currents permitted the highest degree of spatial selectivity in the epitaxial material, although patterned photoetching of CVD-SiC could be achieved under high light intensity. Diffraction gratings were demonstrated by defining the grating structure in photoresist on the electrode surface, then photoetching the spaces exposed to the electrolyte. SiC has considerable significance as a substrate for gratings in the vacuum ultraviolet and X-ray wavelengths due to its high reflectance in these regions. Additionally, it has a high degree of stability against thermal degradation and radiation damage, making it a choice material for high power laser optics. Because of the extreme hardness of SiC, it is difficult to fabricate gratings by ruling. The photoelectrochemical method demonstrated here is a simple one-step technique that should be adaptable to large area CVD epitaxial SiC substrates that are available commercially. GRA

N89-29237# Aerospace Corp., El Segundo, CA. Electronics Research Lab.
APPLIED FIELD AND TOTAL DOSE DEPENDENCE OF TRAPPED CHARGE BUILDUP IN MOS DEVICES
R. J. Krantz, L. W. Aukerman, and T. C. Zeitlow 26 Apr. 1989 26 p
(Contract F04701-88-C-0089)
(AD-A209064; TR-0089(4925-07)-4; SD-TR-89-34) Avail: NTIS HC A03/MF A01 CSCL 20/12

A rate equation for charge buildup which includes carrier sweep out, geminate recombination, hole/electron trapping, and effects of internal fields is developed. The first moment of the resulting charge distribution is calculated to yield the midgap voltage shift as a function of irradiation time. The initial midgap voltage shift per dose and the maximum midgap voltage shift are derived. The field dependence of these quantities is shown to be a consequence of the field dependence of the hole/electron capture cross sections and geminate recombination escape probability. The results of this formulation show that the E to the 1/2 power decrease in the midgap shift per dose with increasing applied field. The theory is validated by comparison with experimental results obtained on 225 A thermal oxide on p-type silicon test capacitors irradiated under bias at room temperature. GRA

N89-29238# Spire Corp., Bedford, MA.
SELECTIVE AREA EPITAXY OF GALLIUM ARSENIDE ON SILICON, PHASE 1 Final Report, 15 Jul. 1988 - 14 Jan. 1989
N. H. Karam Feb. 1989 37 p
(Contract DAAL03-88-C-0015)
(AD-A209079; FR-60112; ARO-26204.1-EL-SBI) Avail: NTIS HC A03/MF A01 CSCL 20/12

The research program was to investigate selective-area epitaxy of Gallium Arsenide-on-Silicon by Metal Organic Chemical Vapor Deposition (MOCVD) as a means of reducing the thermal expansion mismatch effects, hence, improving the deposited film quality, wafer bow, and eliminating film cracking. This has been achieved by MOCVD of GaAs through openings patterned in the silicon dioxide coated wafers. The object of this research program was to develop the technology that will yield device quality GaAs-on-Si and a process applicable for monolithic integration of the high speed and/or optical communication capabilities of GaAs with the

sophistication of the Si very large scale integration (VLSI) technology. The feasibility of this approach has been clearly demonstrated in the Phase 1 research effort, in which successful selective deposition of GaAs films on patterned Si wafers was achieved and the deposited films were characterized by a number of techniques. Preliminary results clearly indicate the effectiveness of this approach to eliminate wafer bow, minimize film cracking, and improve the quality of the heteroepitaxial films. A new deposition technique for GaAs-on-Si by Atomic Layer Epitaxy (ALE) has been introduced which has the potential of producing superior quality GaAs-on-Si films. GRA

N89-29239# Measurement Concepts Corp., Colts Neck, NJ.
DIGITAL REFRACTOMETRY OF PIEZOELECTRIC CRYSTALLINE MEDIA Interim Report No. 1, Aug. 1987 - Oct. 1988
Edward Collett Nov. 1988 25 p
(Contract DAAL01-87-C-0727)
(AD-A209362; SLCET-TR-87-0727-1) Avail: NTIS HC A03/MF A01 CSCL 20/2

The contractual objectives of this program are as follows: (1) Perform a theoretical analysis of the measurement of piezoelectric crystals using Dual-Beam Digital Refractometry, (2) Set up the laboratory configuration to determine the refractive indices of piezoelectric crystals using a HeNe Laser source, (3) Determine the refractive indices of various piezoelectric crystals, (4) Expand the measurements to the ultraviolet and infrared regions, and (5) Analyze the requirements for applying Dual-Beam Digital Refractometry to the millimeter and the microwave regions. Contract objective 1 has been completed and is now being written up as a publication. Contract objective 2 was completed by the end of August, 1988. Measurements are now being performed on various samples and the first results will be submitted by the end of February, 1989. Contract objectives 3, 4, and 5 will be completed at the end of the contract, February, 1990. GRA

N89-29240# Army Lab. Command, Watertown, MA. Material Technology Lab.
CRYSTAL CHEMISTRY, MAGNETIC AND ELECTRICAL PROPERTIES OF La(SUB2-x)Ba(SUBx)NiO4 M.S. Thesis - Massachusetts Inst. of Technology
Amy Beth Austin (Massachusetts Inst. of Tech., Cambridge.) Feb. 1989 83 p
(DA Proj. 1L1-61102-AH-42)
(AD-A209376; MTL-TR-89-10) Avail: NTIS HC A05/MF A01 CSCL 20/2

The series of compositions La(2-X)BaXNiO4 (0 less than or = x less than or = 1.0) was prepared by standard ceramic techniques. All members of the system crystalized with the tetragonal K2NiF4 structure. The ratio of lattice parameters, c/a, reached a maximum in the range x = 0.5 to 0.6; c increased up to this point while a decreased, and this trend reversed after the maximum was reached. Increase in c/a is attributed to a weak Jahn-Teller distortion due to octahedral site low-spin Ni(3+) ions. Magnetic susceptibilities measured in the temperature range 6 to 300 K and room temperature resistivity measurements showed that with addition of any barium into the system, a significant change was seen in both magnetic and electrical properties. An anomaly in the magnetic susceptibility was seen at 110 K in La2NiO4. This anomaly disappeared and magnetic susceptibility dropped by a factor of at least one-third with addition of barium. With further increases in barium, the susceptibility value did not differ significantly in all Ba-substituted compounds. Room temperature resistivity dropped from 0.14 Ohm-cm for La2NiO4 to 0.05 Ohm-cm for La(1.8)Ba(.2)NiO4 and decreased only slightly thereafter with increasing barium. Semiconducting behavior was observed for all the compounds. Oxygen stoichiometry is suspected to play a critical role in explaining these behaviors. GRA

N89-29241# California Univ., Los Angeles. Dept. of Chemistry and Biochemistry.
A STUDY OF THERMODYNAMIC PHASE STABILITY OF INTERMETALLIC THIN FILMS OF Pt2Ga, PtGa AND PtGa2 ON GALLIUM ARSENIDE Technical Report, 1988 - 1989
Young K. Kim, David K. Shuh, R. Stanley Williams, Larry P. Sadwick, and Kang L. Wang 1 Jul. 1989 9 p Submitted for publication
(Contract N00014-87-K-0014)
(AD-A209698; TR-20) Avail: NTIS HC A02/MF A01 CSCL 09/1

Epitaxial thin films of three different Pt-Ga intermetallic compounds have been grown on gallium arsenide by molecular beam epitaxy (MBE). The resultant films have been annealed at various temperatures and then examined using X-ray two-theta diffraction. Both PtGa2 and PtGa thin films are chemically stable on GaAs under 1 atmosphere of N2 up to 450 C and 600 C, respectively. Thin films of Pt2Ga react with GaAs at temperatures as low as 200 C to form phases with higher Gallium concentration. GRA

N89-29242# California Univ., Los Angeles. Solid State Science Center.
A BOLT-ON DEPOSITION SOURCE FOR ULTRA-HIGH-VACUUM GROWTH OF INTERMETALLIC COMPOUND FILMS
David K. Shuh, Young K. Kim, and R. Stanley Williams 1 Jul. 1989 11 p Submitted for publication
(Contract N00014-87-K-0014)
(AD-A209699; TR-19) Avail: NTIS HC A02/MF A01 CSCL 09/1

An eight-inch ConFlat flange assembly with both an electron-beam evaporator and a Knudsen cell has been constructed to deposit intermetallic compounds containing transition and group-3 metals with specific phase composition. Initial depositions of thin films using this design have shown excellent epitaxy with the desired compound stoichiometry. GRA

N89-29243# California Univ., Los Angeles. Dept. of Chemistry and Biochemistry.
LINESHAPE AND LIFETIME STUDIES OF EXCITON LUMINESCENCE FROM CONFINED CuCl THIN FILMS Technical Report, 1988 - 1989
David K. Shuh, R. Stanley Williams, Yusaburo Segawa, Jun-ichi Kusano, Yoshinobu Aoyagi, and Susumu Namba (Institute of Physical and Chemical Research, Saitama, Japan) 1 Jul. 1989 25 p
(Contract N00014-87-K-0014)
(AD-A209750; TR-21) Avail: NTIS HC A03/MF A01 CSCL 20/12

Photoluminescence studies have been performed on structures, grown by molecular beam epitaxy, with thin films of copper chloride (30 to 1200A) confined between layers of calcium fluoride. Excitons were formed by irradiation of these systems with UV frequencies above the CuCl bandgap, and the spectral and temporal dependences of the recombination radiation were compared to those of a bulk CuCl single crystal. We suggest a kinetic model to explain why the photoluminescence lineshapes of the free excitons in the films were characteristic of a much hotter exciton temperature and the radiative lifetimes were much shorter (less than 40 ps) than those of the bulk CuCl crystal. The photoluminescence from excitons created by hot electrons and holes that combine after above-bandgap excitation in confined CuCl thin films has been investigated. The lifetime of the free-exciton photoluminescence from films with thicknesses of 1200A and less was shorter than the 40-ps resolution of the instrumentation used, whereas the measured lifetime of that in a 1.5 microns-thick CuCl single crystal was 850 ps. This dramatic decrease of the lifetime has been attributed mainly to a decrease of the radiative lifetime of the excitons in the thin films. By examining the lineshape of the free-exciton photoluminescence, an effective temperature of the excitons at the time of decay could be determined. This temperature was increased both by decreasing

the thickness of the region available to the excitons and increasing the exciton density. GRA

N89-29244# California Univ., Santa Barbara. Dept. of Physics.
EFFECT OF AN ELECTRIC FIELD ON A SPLIT BLOCH BAND
Qian Niu 21 Jun. 1989 47 p Submitted for publication
(Contract N00014-84-K-0548; NSF DMR-87-03434; NR Proj. 372-160)
(AD-A209857; TR-22) Avail: NTIS HC A03/MF A01 CSCL 20/5

The effect of a constant and uniform electric field on a split Bloch band is studied through a tight binding model. The Wannier-Stark ladders of the parent band are modified by a potential in addition to that of the crystal. It is shown how the frequency spectrum behaves as the field strength varies from weak to strong. In the case that the parent band is split into a finite number of sub-bands, there exists a set of subspaces to which the states return periodically in time, and that the constituent states of each subspace are localized around a given unit cell. A theoretical framework is developed which naturally exploits the symmetries of the system, and which allows for easy and clean numerical calculations. GRA

N89-29245# California Univ., Los Angeles. Dept. of Chemistry and Biochemistry.
INITIAL STAGES OF METAL/SEMICONDUCTOR INTERFACE FORMATION: Au AND AgON Si(111) Technical Report, 1988 - 1989
R. Stanley Williams, Richard S. Daley, Judy H. Huang, and Robert M. Charatan 20 Jun. 1989 17 p
(Contract N00014-87-K-0014)
(AD-A209490; TR-18) Avail: NTIS HC A03/MF A01 CSCL 20/12

The atomic structure formed by monolayer coverages of Au and Ag on the Si(111) surface was studied using primarily the technique of Impact-Collision Ion Scattering Spectroscopy (ICISS). For the case of Au films annealed at 700 C, three different types of LEED patterns are formed depending on the fractional monolayer coverage: 5x1, sq. root of 3 x sq. root of 3, and 6x6. The ICISS data reveal that all the three surfaces are structurally similar: the Au atoms reside above the Si(111) plane, most likely in threefold-hollow sites, and the different surfaces appear to be characterized by rows (5x1) or a honeycomb network (sq. root of 3 x sq. root of 3 and 6x6). In contrast, the Ag films deposited at elevated substrate temperature (480 C) display only a sq. root of 3 x sq. root of 3 LEED pattern for coverages ranging from 0.25 to 35 monolayers. A trimer model appears to be more consistent with the low coverage Ag ICISS data rather than a honeycomb arrangement of the Ag atoms. GRA

N89-29246# Pittsburgh Univ., PA. School of Engineering.
A STUDY OF THE T(1) TRANSITION OF POLY(BIS(TRIFLUOROETHOXY)PHOSPHAZENE) (PBFP) USING SOLID-STATE NUCLEAR MAGNETIC RESONANCE SPECTROSCOPY Report, 1985
Scott G. Young and Joseph H. Magill 4 May 1989 17 p Submitted for publication Sponsored in part by NSF
(Contract N00014-85-K-0358)
(AD-A207719; ONR-11) Avail: NTIS HC A02/MF A01 CSCL 20/5

In situ solid state variable temperature NMR measurements have been made on Poly(bis(trifluoroethoxy)phosphazene above and below the first order thermotropic transition, T(1). A single mobile ordered 2D phase exists above T(1). Below T(1) and at room temperature there is a 3D phase in agreement with other physical property measurements. The OCH2CF3 side chains exhibit similar mobility on either side of the 2D in equilibrium with 3D transition. The activation energies associated with the CH2 and CF3 side groups are E sub CH2 about 17.3 kJ/mole and E sub CF3 about 13.7 kJ/mole. The spin lattice relaxation measurements for these same groups are 1.75s. and 3.55s. respectively. The crystallinity ascertained from solid state NMR results is strongly dependent upon annealing conditions and temperature of measurement. GRA

N89-29247# Aerospace Corp., El Segundo, CA. Chemistry and Physics Lab.
CHEMICAL EFFECTS OF Ne(+) BOMBARDMENT ON THE MoS2(0001) SURFACE STUDIED BY HIGH-RESOLUTION PHOTOELECTRON SPECTROSCOPY
Jeffrey R. Lince, Thomas B. Stewart, Malina M. Hills, Paul D. Fleischauer, Jory A. Yarmoff, and Amina Taleb-Ibrahimi (IBM Watson Research Center, Yorktown Heights, NY.) 28 Mar. 1989 36 p Prepared in cooperation with Brookhaven National Lab., Upton, NY
(Contracts F04701-85-C-0086; DE-AC02-76CH-00016)
(AD-A207734; TR-0088(3945-03)-2; SD-TR-89-28) Avail: NTIS HC A03/MF A01 CSCL 07/4

The effect of 1-keV Neon cation bombardment on the clean Molybdenum disulfide (0001) - 1 x 1 surface with fluences between 4 x 10 to the 14th power Ne(+)/sq cm was studied using high-resolution photoelectron spectroscopy excited with synchrotron radiation. Spectra of the Mo-3d and S-2p core levels were measured with photon energies that ensured that the kinetic energy of their photoelectrons was the same, resulting in the same depth being probed for both core levels. For lower fluences, S vacancy defect formation occurs in the MoS2 lattice, with the concurrent formation of a small amount (less than 10 percent) of dispersed elemental molybdenum Mo(0). For fluences greater than approx. 1 x 10 to the 16th power Ne(+)/sq cm, the Mo(0) is the predominant species in the surface region, while the remaining species consists of amorphous MoS(2-x) and polysulfide species. Valence band spectra taken with photon energies of 152 eV and 225 eV were consistent with the core level results. The movement of the valence band maximum toward the Fermi level indicated the formation of a metallic surface region. A qualitative depth distribution of the chemical species present after Ne(+) bombardment was determined. GRA

N89-29248# Cornell Univ., Ithaca, NY. School of Chemical Engineering.
QUANTITATIVE ANALYSIS OF LASER INTERFEROMETER WAVEFORMS OBTAINED DURING OXYGEN REACTIVE-ION ETCHING OF THIN POLYMER FILMS
B. C. Dems, F. Rodriguez, and P. D. Krasicky 12 May 1989 23 p Presented at the ACS Division of Polymeric Materials, Science and Engineering Symposium on Polymers in Microlithography, Dallas, TX, 9-14 Apr. 1989
(Contract N00014-85-K-0474)
(AD-A207836; TR-14) Avail: NTIS HC A03/MF A01 CSCL 20/12

Continuous laser interferometry, especially of inorganic materials, during reactive ion etching often has been used as an end-point detection method. However, the detailed patterns obtained during etching of thin organic polymer films have not been fully exploited. The sinusoidal oscillations in reflected light intensity often exhibit almost uniform amplitudes. In addition to variations in the rate of etching with time or depth, a rigorous analysis of the waveform yields an in situ measure of the refractive index of the film. A reduction factor for the medium/polymer interface Fresnel coefficient is used to account for the diffuseness arising from roughening of the film. Ion bombardment causes the roughening and necessitates the correction which is not usually the case when interferometry is used in solvent dissolution studies. The analysis, an iterative procedure for its use, and the application to oxygen/RIE of several polymers will be described. GRA

N89-29249# Utah Univ., Salt Lake City. Dept. of Physics.
FLUXONS AND ORDER IN LONG JOSEPHSON JUNCTIONS Final Report, 15 Nov. 1985 - 14 Nov. 1988
Orest G. Symko 24 Feb. 1989 50 p
(Grant AF-AFOSR-0020-86)
(AD-A207925; AFOSR-89-0604TR) Avail: NTIS HC A03/MF A01 CSCL 20/12

Studies were made of fluxon dynamics, instabilities, and noise

in long overlap type Josephson junctions made out of Niobium Nitride and Niobium. Noise and fluctuations measurements were performed in the voltage state of the junctions biased in a magnetic field. Telegraph noise due to fluxon fluctuations between two energy states determined by the geometry of the junction and the external magnetic field bias were observed. The studies covered life-times of these states, metastability, thermal and quantum mechanical tunneling, and effects of dissipation. At certain bias points of the junction, chaotic behavior which was found was preceded by period doubling bifurcation. Also negative resistance regions were observed; they can be used for amplification. These observations were supported by computer modeling using a perturbed sine-Gordon equation. Fluxon motion in long Josephson junctions provides an excellent system for studies of non-linear phenomena and it has a variety of applications to superconducting electronics. GRA

N89-29250# Wisconsin Univ., Madison. Dept. of Electrical and Computer Engineering.
VORTICES IN LONG JOSEPHSON JUNCTIONS Final Report, 15 Nov. 1985 - 14 Nov. 1988
James E. Nordman and James B. Beyer 5 Feb. 1989 13 p
(Grant AF-AFOSR-0025-86; AF Proj. 2305)
(AD-A207936; AFOSR-89-0422TR) Avail: NTIS HC A03/MF A01 CSCL 20/12

The properties of long Josephson junction structures are studied along with the electronic device possibilities suggested by these structures. A large part of the work involved fabrication and modeling. A particular effort was made to build and to understand the basic operating mechanisms of a type of superconducting transistor, the vortex flow transistor. The thin film fabrication techniques were developed using niobium and lead superconductors. GRA

N89-29251 Technische Univ., Hanover (Germany, F.R.). Fachbereich Physik.
INVESTIGATIONS OF STEP DISTRIBUTIONS AT Si/SiO2 INTERFACES USING HR-SPA-LEED Ph.D. Thesis [UNTERSUCHUNGEN VON STUFENVERTEILUNGEN AN DER Si/SiO2-GRENZFLAECHE MIT HR-SPA-LEED]
Peter Marienhoff 1988 86 p In GERMAN Sponsored by the European Research Office, U.S.
(ETN-89-94437) Avail: Universitaet Hannover, Welfengarten 1, D-3000 Hannover 1, Federal Republic of Germany

The roughness of interfaces of industrially produced thermal SiO2 on silicon, was experimentally and theoretically investigated. The roughness was analyzed on the basis of the diffraction of slow electrons on single crystal surface using LEED (low energy electron diffraction) reflection and the kinematic diffraction theory. Several models for terrace lateral distributions on linear lattice chains of scatterers are presented; the Markov chains proved to be especially useful. The measured data on two-dimensional surfaces allow an extrapolation to linear chains of atoms. The method was applied to the interface Si/SiO2 of several industrially produced samples with oxide layer thicknesses between 10 and 50 nm. The results show average step distances between 3 and 19 nm and roughness depths between 0.15 and 0.2 nm. Annealing leads to substantially larger step distances. The measured roughnesses are comparable with mobility and transmission electron microscope results. ESA

N89-29252# Technische Univ., Munich (Germany, F.R.). Fakultaet fuer Elektrotechnik und Informationstechnik.
MICROWAVE DETECTION USING JOSEPHSON ELEMENTS Ph.D. Thesis [MIKROWELLEN-DETEKTION MIT JOSEPHSON-ELEMENTEN]
Martin Rieger 1988 150 p In GERMAN
(ETN-89-94650) Avail: NTIS HC A07/MF A01

Models and design methods for microwave detectors with Josephson elements were elaborated. The equivalent electric circuit of the Josephson element is presented. These methods for solving the differential equation system for of circuit containing a Josephson element are outlined: numerical integration, Fokker-Planck method and analog simulation. Microwave detectors with Josephson elements for 40 GHz are optimized for maximum voltage sensitivity and minimum noise equivalent power using the Fokker-Planck method. The experimental results are in agreement with the detector characteristics calculated in the design. The validity of the modeling of Josephson element and detector circuit is confirmed. It is shown that sensitive detection at 485 GHz is also possible. ESA

N89-29253# Office National d'Etudes et de Recherches Aerospatiales, Paris (France).
WEAK BEAM ELECTRON MICROSCOPY OF DISLOCATION SPLITTING IN TiAl: RELATIONSHIP WITH PLASTICITY Ph.D. Thesis - Paris-Sud Univ.
Gilles Hug 1988 158 p In FRENCH; ENGLISH summary
(ONERA-NT-1988-3; ISSN-0078-3781; ETN-89-94815) Avail: NTIS HC A08/MF A01

A weak beam dark field transmission electron study was carried out in order to characterize the dislocation together with their fine structure as a function of the deformation temperature. The nature of the Burgers vectors encountered in TiAl depend upon the temperature of the deformation test. As far as the Burgers of superdislocations is concerned four domains are found around room temperature, 600 C, 800 C, and 1000 C. A glissile-sessile core transition explains the flow stress anomaly that appear as the consequence of the loss of mobility of the superdislocations. ESA

77 THERMODYNAMICS AND STATISTICAL PHYSICS

Includes quantum mechanics; theoretical physics; and Bose and Fermi statistics.

For related information see also *25 Inorganic and Physical Chemistry* and *34 Fluid Mechanics and Heat Transfer.*

N89-29254# Universidade Estadual de Campinas (Brazil). Inst. de Matematica, Estatistica e Ciencia da Computacao.
FIFTH FORCE, SIXTH FORCE AND ALL THAT: A THEORETICAL (CLASSICAL) COMMENT
Erasmo Recami and Vilson Tonin-Zanchin 1988 10 p
(DE89-611971; UNICAMP-IMECC-RT-22/88) Avail: NTIS (US Sales Only) HC A02/MF A01

In the recent literature, a few claims appeared about possible deviations from the ordinary gravitational laws (both at the terrestrial and at galactic level). The experimental evidence does not seem to be conclusive; nor it is clear if new forces are showing up, or if actual deviations must be accepted from Newton or Einstein gravitation (in the latter case, the validity of the very Equivalence Principle might be on the stage). The problem within the classical realm, by exploring whether the possible new effects can be accounted for through minimal modifications of the standard formulation of General Relativity, in particular, through exploitation and extension of the role of the cosmological constant, is approached. DOE

N89-29255# Brown Univ., Providence, RI.
RESEARCH PROGRAM IN COMPUTATIONAL PHYSICS Progress Report
G. S. Guralnik 1989 4 p
(Contract DE-AC02-76ER-03130)
(DE89-013952; DOE/ER-03130/3) Avail: NTIS HC A02/MF A01

This work has been going on for several years and has encompassed many aspects of the field, including algorithms, machines, theoretical studies and large scale simulations. This last year we made progress in the following areas: studies of QCD including the effects of dynamical fermions, large scale simulations (in particular the calculation of matrix elements for hadronic weak interactions), and in new algorithms. We describe these in this paper. DOE

N89-29256# State Univ. of New York, Buffalo. Dept. of Chemistry.
ELECTRON ENERGY LEVELS IN A QUANTUM WELL WITHIN AN IN-PLANE MAGNETIC FIELD
H. R. Lee, H. G. Oh, Thomas F. George, and C. I. Um Jun. 1989 23 p Submitted for publication
(Contract N00014-86-K-0043)
(AD-A209351; UBUFFALO/DC/89/TR-101) Avail: NTIS HC A03/MF A01 CSCL 20/5

The exact eigenenergy spectrum of an electron is calculated in a quantum well within an in-plane magnetic field. The numerical solutions for the excited energy states as well as the ground state energy are found for various quantum-well widths and barrier heights. The cyclotron orbits are considerably affected by the quantum well. The energy levels higher than the potential height of the quantum well and the energy levels lower than the potential height of the quantum well show quite different behaviors. These are explained with the properties of the combined potential and the wave function inherent to the system. GRA

N89-29257# Universitaet der Bundeswehr, Neubiberg (Germany, F.R.). Fachbereich Maschinenbau.
EVAPORATION THERMODYNAMICS OF MONOTELLURIDES OF SELECTED RARE EARTH AND ALKALINE EARTH ELEMENTS, AND AN ATTEMPT TO SYSTEMATIC CORRELATION BETWEEN THE STANDARD ENTHALPIES OF FORMATION Ph.D. Thesis [UEBER DIE VERDAMPFUNGSTHERMODYNAMIK VON MONOTELLURIDEN AUSGEWAEHLTER SELTENERD- UND ERDALKALIELEMENTE SOWTE EINEN VERSUCH ZUR SYSTEMATISCHEN KORRELATION DER STANDARDBILDUNGSENTHALPIEN]
Johannes Ludwigs 1988 223 p In GERMAN
(ETN-89-94655) Avail: NTIS HC A11/MF A01

A contribution was made to improve the knowledge of the thermochemical characteristics of monotellurides (especially the binary lanthanoide monotelluride) by the determination of the enthalpies of formation, as well as to improve the production and analysis method of these compounds. The fundamentals for the thermodynamical quantities determination of rare earth and alkaline earth elements are reviewed. The determination of the evaporation thermodynamical quantities and the enthalpy of formation of CaTe, SrTe, BaTe, SmTe, YbTe and TmTe 1,30 is outlined. The measurement and thermodynamical interpretation of the dissociation pressure as well as the determination of standard enthalpy of formation using the Knudsen effusion method are presented. The experimentally obtained enthalpies of formation are compared with thermodynamical data calculated from refined, prediction methods. ESA

80 SOCIAL SCIENCES (GENERAL)

Includes educational matters.

No abstracts in this category.

81 ADMINISTRATION AND MANAGEMENT

Includes management planning and research.

N89-29258# Massachusetts Inst. of Tech., Cambridge. Lab. for Information and Decision Systems.
EVALUATION OF FUNCTIONALITY IN DISTRIBUTED SYSTEMS M.S. Thesis
Francois Rene Henri Valraud May 1989 155 p Revised
(Contract N00014-85-K-0782)
(AD-A209167; LIDS-R-1868) Avail: NTIS HC A08/MF A01 CSCL 25/5

A new quantitative methodology is presented for identifying and evaluating the shortfalls and the overlaps between the desired functionality of a distributed decision making system, as characterized by the design requirements, and the functionality of a proposed or implemented distributed system. First, compatible Petri Net models of both the requirements and the system are presented. Second, a correspondence is established between structural properties of the Petri Net representation of the system and the functions it performs. On the performance side, a functionality is defined as a set of coordinated functions that a system must be able to carry out in order to accomplish a task. On the structural side, simple and complete information flow paths, i.e., sub-nets of a Petri Net, are defined. Thus a particular functionality is identified as a sub-net of the Petri Net representation of the system. Algorithms are presented to determine the various simple and complete information flow paths in the nets representing both the system and the requirements. This is accomplished through extensive use of the invariant theory of Petri Nets. The next step is the comparison of the two sets of flow paths to determine shortfall and overlaps. GRA

N89-29259# Universal Energy Systems, Inc., Dayton, OH.
UNITED STATES AIR FORCE RESEARCH INITIATION PROGRAM FOR 1987, VOLUME 2 Interim Report
Rodney C. Darrah Apr. 1989 583 p
(Contract F49620-85-C-0013)
(AD-A209727; AFOSR-89-0830TR-Vol-2) Avail: NTIS HC A25/MF A01 CSCL 05/1

The U.S. Air Force Research Initiaion Program has sponsored studies in many different areas. This volume is the 2nd of 4 volumes. Titles of reports in this volume include: The Omnidirectional Torquer - Experimental Prototype Model 1; Calculation of Nonlinear Optical Properties; Modelling and Prediction in a Nonlocal Turbulence Model; CO2 (001) Vibrational Temperatures and Limb-View Infrared Radiance Under Terminator Conditions in the 60 to 100 Altitude Range; Comparison of SSM/I Rainrates and Surface Winds with the Corresponding Conventional Data in the North West Pacific Typhoons; Development of a System for the Measurement of Electron Excitation Cross Sections of Atoms and Molecules in the Near Infrared; Superconductor Testing; A Form and Function Knowledge Representation for Reasoning about Classes and Instances of Objects; Development and Evaluation of a Bayesian Test for System Testability; Crystalline Silicon Electro-Optic Waveguides; Measurements of a Slot Antenna Fed by Coplanar Waveguide and Solution of an Infinite Phased Array of Slots Fed by Coplanar Waveguide Over a Dielectric Half-Space; A New Measure of Maintainability/Reliability and Its Estimation; Signed-Digit Number System for Optical Adaptive Processing; Implementation of Iterative Algorithms for an Optical Signal Processor; Experimental Evaluation of Imaging Correlography; Interaction of Lasers with Superconductors; and Three Dimensional Thermal Conduction Effects in High Power CW Laser Target Plates. GRA

N89-29260# Institute for Defense Analyses, Alexandria, VA.
COMPUTER-AIDED GROUP PROBLEM SOLVING FOR UNIFIED LIFE CYCLE ENGINEERING (ULCE) Final Report, Apr. - Sep. 1988
David A. Dierolf and Karen J. Richter Feb. 1989 80 p
(Contract MDA903-84-C-0031)
(AD-A209446; AD-E501121; IDA-P-2149; IDA/HQ-88-33815)
Avail: NTIS HC A05/MF A01 CSCL 05/1

Unified Life Cycle Engineering (ULCE) is a design engineering environment in which the quality of a product is improved by integrating the consideration of the design attributes of producibility and supportability with the design attributes of performance, cost, and schedule. The ULCE program has traditionally focused on developing tools and techniques for a single designer to use to accomplish this integration. The goals of the ULCE program, however, are congruent with the goals of the current simultaneous engineering programs in industry, and industry uses multi-functional design teams to accomplish these goals. It is asserted that the application of computer aided group problem solving technology

to engineering design represents an unexploited opportunity to enhance the effectiveness of simultaneous engineering design teams. Thus, it is recommended that the ULCE program broaden its focus to include research in computer-aided group problem solving techniques and tools to be used by design teams. To support the findings and recommendations, a survey is included of both industry design team practices and computer aided group problem solving methodologies and terminology. GRA

N89-29261# Advisory Group for Aerospace Research and Development, Neuilly-Sur-Seine (France).
CALENDAR OF SELECTED AERONAUTICAL AND SPACE MEETINGS
Jun. 1989 152 p In FRENCH and ENGLISH
(AGARD-CAL-89/2; ISBN-92-835-0520-4) Copyright Avail: NTIS HC A08/MF A01

Three kinds of events are covered by this calendar: technical meetings, conferences, and symposia; exhibitions and technical displays; and educational courses. For each meeting, exhibition, or course, the following information is given: reference number, data, location, title and sponsor, keywords indicating main topics covered, and contact code for inquiries. A subject index in the form of keywords is given, each keyword being followed by reference numbers of all the meetings relevant to that particular keyword. Author

82 DOCUMENTATION AND INFORMATION SCIENCE

Includes information management; information storage and retrieval technology; technical writing; graphic arts; and micrography.

For computer documentation see *61 Computer Programming and Software.*

N89-29262*# National Aeronautics and Space Administration, Washington, DC.
NASA THESAURUS SUPPLEMENT. A FOUR PART CUMULATIVE SUPPLEMENT TO THE 1988 EDITION OF THE NASA THESAURUS Semiannual Report
Mar. 1989 16 p
(NASA-SP-7064-Suppl-1; NAS 1.21:7064-Suppl-1) Avail: NTIS HC A03 CSCL 05B

The four-part cumulative supplement to the 1988 edition of the NASA Thesaurus includes the Hierarchical Listing (Part 1), Access Vocabulary (Part 2), Definitions (Part 3), and Changes (Part 4). The semiannual supplement gives complete hierarchies and accepted upper/lowercase forms for new terms. Author

N89-29263# Oak Ridge National Lab., TN. Environmental Sciences Div.
NEW DIMENSIONS FROM STATISTICAL GRAPHICS FOR GIS (GEOGRAPHIC INFORMATION SYSTEM) ANALYSIS AND INTERPRETATION
R. A. McCord and R. J. Olson 1988 10 p Presented at the 8th ESRI Annual User Conference, Palm Springs, CA, 21 Mar. 1988
(Contract DE-AC05-84OR-21400)
(DE89-012339; CONF-880385-2) Avail: NTIS HC A02/MF A01

Environmental research and assessment activities at Oak Ridge National Laboratory (ORNL) include the analysis of spatial and temporal patterns of ecosystem response at a landscape scale. Analysis through use of Geographic Information System (GIS) involves an interaction between the user and thematic data sets frequently expressed as maps. A portion of GIS analysis has a mathematical or statistical aspect, especially for the analysis of temporal patterns. ARC/INFO is an excellent tool for manipulating GIS data and producing the appropriate map graphics. INFO also has some limited ability to produce statistical tabulation. ORNL's capabilities were extended by graphically interfacing ARC/INFO and SAS/GRAPH to provide a combined mapping and statistical graphics environment. With the data management, statistical, and graphics capabilities of SAS added to ARC/INFO, the analytical and graphical dimensions of the GIS environment were extended. Pie or bar charts, frequency curves, hydrographs, or scatter plots as produced by SAS can be added to maps from attribute data associated with ARC/INFO coverages. Numerous, small, simplified graphs can also become a source of complex map symbols. These additions extend the dimensions of GIS graphics to include time, details of the thematic composition, distribution, and interrelationships. DOE

N89-29264* National Aeronautics and Space Administration, Washington, DC.
PATENT ABSTRACTS BIBLIOGRAPHY: A CONTINUING BIBLIOGRAPHY. SECTION 2: INDEXES (SUPPLEMENT 35)
Jan. 1989 512 p
(NASA-SP-7039(35)-Sect-2; NAS 1.21:7039(35)-Sect-2) Avail: NTIS HC A22; NTIS standing order as PB89-911100, $29.00 domestic, $58.00 foreign CSCL 05B

A subject index is provided for over 4600 patents and patent applications for the period May 1969 through June 1989. Additional indexes list personal authors, corporate authors, contract numbers, NASA case numbers, U.S. patent class numbers, U.S. patent numbers, and NASA accession numbers. Author

N89-29265# Naval Postgraduate School, Monterey, CA.
IMPLEMENTATION OF A DISTRIBUTED OBJECT-ORIENTED DATABASE MANAGEMENT SYSTEM M.S. Thesis
Lynn A. Wyrick Mar. 1989 121 p
(AD-A209437) Avail: NTIS HC A06/MF A01 CSCL 12/7

Distributed database management systems provide for more flexible and efficient processing. Research in object oriented database management systems is revealing an abundance of additional benefits that cannot be provided by more traditional database management systems. The Naval Military Personnel Command (NMPC) is used as a case study to evaluate the requirements of transitioning from a centralized to a distributed database management system. Features and characteristics of both distributed and object oriented database management systems are used to determine the appropriate configuration for different application environments. The distributed and object oriented concepts are evaluated in detail in order to allow an organization to appropriately select the type of system to meet their needs. Transition requirements for NMPC, in particular, are identified and a suggested plan of action is presented. GRA

N89-29266# Naval Postgraduate School, Monterey, CA.
CONVERSION OF HARD-COPY DOCUMENTS TO DIGITAL FORMAT UTILIZING OPTICAL SCANNERS AND OPTICAL STORAGE MEDIA M.S. Thesis
Robert R. Taylor Mar. 1989 120 p
(AD-A209473) Avail: NTIS HC A06/MF A01 CSCL 14/3

Storage of hard copy archival paper documents requires vast amount of storage space and time to search and retrieve. Technology exists today to convert hard copy texts using optical scanners and storing in a digital formal on optical disks. An indepth current technology research is conducted of optical scanners, optical storage mediums, and optical information systems. Utilizing the thesis documents presently stored in the library aboard Naval Postgraduate School, as a statistical base, the requirements to convert the thesis documents to digital format is analyzed. It is concluded that an image optical information system is a viable alternate to storing hard copy documents and recommends follow-on research to build an in-house optical information system. GRA

N89-29267# Naval Postgraduate School, Monterey, CA.
THE USE OF A UNIX-BASED WORKSTATION IN THE INFORMATION SYSTEMS LABORATORY M.S. Thesis
Charlotte V. Smith Mar. 1989 78 p
(AD-A209485) Avail: NTIS HC A05/MF A01 CSCL 12/5

The Information Systems laboratory of the Department of Administrative Sciences has installed a UNIX-based workstation for student use. The UNIX operating system is an attempt to

provide a powerful operating system that is largely machine-independent. The capabilities and limitations are examined of the UNIX operating system as it pertains to the Information Systems student. A user's manual is also provided for the students, thus, allowing them to gain a working knowledge of the system and prepare them to take advantage of its capabilities. It is concluded that, with proper administration, the use of UNIX workstations can be very valuable to the Information Systems student. GRA

N89-29268# Naval Postgraduate School, Monterey, CA.
MOVING OPTICAL TECHNOLOGY IN-HOUSE M.S. Thesis
Bruce E. France, Sr. Mar. 1989 37 p
(AD-A207850) Avail: NTIS HC A03/MF A01 CSCL 05/2

The Navy, through a series of projects and programs, is identifying a considerable number of uses for optical technology. Key commands and Navy projects using optical technology are identified and reviewed. Currently, the Navy has no production capability for this medium nor does an optical production facility exist for classified data. The issue is whether the Navy should develop an optical technology production facility to avoid the use of outside contractors. Current costs for producing compact disk-read only memory and what cost savings might be incurred through the in-house use of this technology is examined. And if the technology were developed internally, questions such as who should manage this program and how should it be managed need to be addressed. The impact and benefits and barriers to developing an optical technology in-house capability in the Navy are summarized. GRA

N89-29269*# National Aeronautics and Space Administration, Washington, DC.
NASA THESAURUS SUPPLEMENT: A FOUR PART CUMULATIVE SUPPLEMENT TO THE 1988 EDITION (SUPPLEMENT 2)
Sep. 1989 22 p
(NASA-SP-7064-Suppl-2; NAS 1.21:7064-Suppl-2) Avail: NTIS HC A03/MF A01 CSCL 05B

The four-part cumulative supplement to the 1988 edition of the NASA Thesaurus includes the Hierarchical Listing (Part 1), Access Vocabulary (Part 2), Definitions (Part 3), and Changes (Part 4). The semiannual supplement gives complete hierarchies and accepted upper/lowercase forms for new terms. Author

N89-29270# National Aeronautical Lab., Bangalore (India). Computer Centre.
TRANSFER OF FILES BETWEEN IE-32C PC/AT CAD SYSTEM AND AUTOTROL AD/380 GRAPHICS SYSTEM
Uma R. Murthy, D. Ranganathan, N. Kumar, and S. Janardhan Apr. 1989 20 p
(NAL Proj. CC-9-000)
(PD-CC-8903) Avail: NTIS HC A03/MF A01

GS-1000 on Autotrol AD/380 provides a 2 1/2D data base whereas MicroCADDS on IE-32C offers a true 3D data base. These two databases have different data structures necessitating the development of software for transfer of drawings between them. These have the following advantages: (1) a MicroCADDS drawing can be plotted on AD/380 Flatbed plotter; (2) autotrol drawing can be shaded and 3D analysis can be performed after transfer to IE-32C; and (3) plotting operations can be switched to the working plotter in case of breakdown of any plotter. Author

N89-29271# National Aerospace Lab., Amsterdam (Netherlands). Informatics Div.
METHOD BASES: A NEW TOOL FOR APPLIED INFORMATION SYSTEM DESIGN
J. J. P. vanHulzen and J. J. Schuurman 14 Jan. 1988 10 p Presented at the 1st European Conference on Information Technology for Organizational Systems, Athens, Greece, May 1988
(NLR-MP-88002-U; ETN-89-95414) Avail: NTIS HC A02/MF A01

The method base system (MEBAS), for applications on information processing needed in the industry, is described. This version of MEBAS supports the definition and mantainance of the information describing the methods and the composition of new methods out of existing methods. The use of MEBAS in projects implemeting flow calculation algorithms based on the Euler and Navier-Stokes equations is considered. An evaluation of the facilities currently available in MEBAS shows the soundness of the approach and stresses the identified need to further hide the implementation aspects of software components from the user. ESA

N89-29272# Universiteit Twente, Enschede (Netherlands). Dept. of Computer Science.
GENERALIZED GRID FILES: DESCRIPTION AND PERFORMANCE ASPECTS
Henk Blanken and Bert vandenAkker Dec. 1988 32 p
(MEMO-INF-88-63; ISSN-0923-1714; ETN-89-95422) Avail: NTIS HC A03/MF A01

The generalized grid file (GGF), offering fast single attribute access, is described. The GGF is compared with implementations of the multi-attribute access grid file (GF). The internal and external memory occupation of the GGF directory is shown to be confined and modest for non-uniform data distributions. Assessment of the application of the GGF is given, including the conclusion that the problem of exploding directories, observed for grid files, does not occur. ESA

83 ECONOMICS AND COST ANALYSIS

Includes cost effectiveness studies.

No abstracts in this category.

84 LAW, POLITICAL SCIENCE AND SPACE POLICY

Includes NASA appropriation hearings; aviation law; space law and policy; international law; international cooperation; and patent policy.

N89-29273# Committee on Appropriations (U.S. House).
DEPARTMENTS OF VETERANS AFFAIRS AND HOUSING AND URBAN DEVELOPMENT AND INDEPENDENT AGENCIES APPROPRIATIONS FOR 1990. PART 6: NATIONAL AERONAUTICS AND SPACE ADMINISTRATION
1989 169 p Hearings before a Subcommittee of the Committee on Appropriations, 101st Congress, 1st Session, 25 Apr. 1989
(GPO-99-598) Avail: Subcommittee of the Committee on Appropriations, House of Representatives, Washington, D.C. 20510 HC free; SOD HC $31.00

Hearings before a subcommittee of the House Committee on Appropriations are presented along with budget estimates for the National Aeronautics and Space Administration for the fiscal year 1990. All written testimony and submittals for the record are also included. The budget estimates provide a detailed outline of budgetary information and justifications for research and development, construction of facilities, space flight and communications, and research and program management. B.G.

85 URBAN TECHNOLOGY AND TRANSPORTATION

Includes applications of space technology to urban problems; technology transfer; technology assessment; and surface and mass transportation.

For related information see also *03 Air Transportation and Safety, 16 Space Transportation,* and *44 Energy Production and Conversion.*

N89-29274# Army War Coll., Carlisle Barracks, PA.
INTERNATIONAL TECHNOLOGY TRANSFER AS PRACTICED BY THE U.S.S.R.: IMPLICATIONS FOR US NATIONAL SECURITY
Marvin D. Redd, Sr. 12 Feb. 1989 28 p
(AD-A208010) Avail: NTIS HC A03/MF A01 CSCL 05/1

In its broadest sense, technology transfer encompasses the collection, documentation and dissemination of scientific and technical information, including data on the performance and costs of using the technology; the transformation of research and technology into processes, products, and services that can be applied to public or private needs; and the secondary application of research or technology developed for a particular mission that fills a need in another environment. The above perspective of technology transfer is a benign one; one which takes place among and between amicable and cooperating sociopolitical, cultural and/or national friends. The following paper examines the more notorious side of the technology transfer issue, with especial emphasis on its practice by the Soviet Union, who through copying, espionage, and blatant thievery, sooner or later acquire western technology for themselves and Warsaw Pact nations. Forms of technology transfer are scrutinized through the use of several case studies and finally the efforts used by the U.S. at deterring this leaching away of one of the bulwarks of western-nation national security are surveyed. GRA

N89-29275# Technische Univ., Eindhoven (Netherlands).
ENTREPRENEURSHIP AND INNOVATION: THE DUTCH SUGAR BEET INDUSTRY (1858-1919) Ph.D. Thesis [ONDERNEMERSCHAP EN VERNIEUWING DE NEDERLANDSE BIETSUIKERINDUSTRIE 1858-1919]
Martijn Steven Coen Bakker 1989 319 p In DUTCH
(ISBN-90-71617-11-4; ETN-89-94873) Avail: NTIS HC A14/MF A01

The historical evolutions of entrepreneurship and evolution in the Dutch sugar beet industry, in the period 1858 to 1919, are studied. The growth of this entirely new branch of industry in the Netherlands was of an unprecedented rapidity and its newness and technological complexity was no serious obstacle to potential investors. An analysis of the social backgrounds supports the idea that a stimulating enthusiasm of a few appealed to family and group solidarity. Several strategies were used to optimize production. By 1909 the country's largest refinery started to buy sugar factories in order to be partly self supporting in its raw material. The role of technical innovations in the development of the raw sugar industry cannot be separated from non technical elements. Technology transfer from abroad and experienced workers were necessary. The chemical knowledge about the production process was of great help in judging the value of new inventions. ESA

88 SPACE SCIENCES (GENERAL)

N89-29276# Technische Univ., Berlin (Germany, F.R.). Inst. fuer Astronomie und Astrophysik.
[ACTIVITIES REPORT OF THE INSTITUTE OF ASTRONOMY AND ASTROPHYSICS] Annual Report, 1987 [INSTITUT FUER ASTRONOMIE UND ASTROPHYSIK: JAHRESBEREICH FUER DAS JAHR 1987]
E. Sedlmayr 1988 8 p In GERMAN
(Mitt-9; ETN-89-94419) Avail: NTIS HC A02/MF A01

In the research field of stars and interstellar matter, mutual coverages of the planet Pluto and its moon Charon were observed; striation effects in B-stars (poor as well as rich in He) were studied; cataclysmic variables and X-ray double stars were investigated; and the chemistry of interstellar dust formation, dust shells and dust-driven winds were studied. In the field of stellar, dynamic models for elliptical galaxies, synchrotron radiation from galaxies, galactic clusters, and X-ray sources detected by EXOSAT were investigated. ESA

N89-29277# Max-Planck-Inst. fuer Physik und Astrophysik, Garching (Germany, F.R.). Inst. fuer Extraterestriche Physik.
[ACTIVITIES REPORT OF THE INSTITUTE FOR EXTRATERRESTRIAL PHYSICS] Annual Report, 1988 [TAETIGKEITSBERICHT, 1988]
Jan. 1989 137 p In GERMAN Original contains color illustrations
(MPE-212; ETN-89-94606) Avail: NTIS HC A07/MF A01

The interstellar matter in external galaxies, galactic clusters as astronomical X-ray sources, and the observation of gamma ray bursts of non-natural origin, are reviewed. Plasma physics experiments were conducted in the near-earth cosmic space. Energetic ions and electrons in the magnetosphere and the interplanetary space were investigated, and several theoretical subjects were studied. In the fields of IR- and submillimeter as well as X-ray astronomy, observations were made, theoretical activities were conducted, and instruments were developed. In the field of gamma ray astronomy, flow and burst phenomena were measured, low- and high-energy astronomical measurements were made, and the acceleration of particles in shear flow as well as bremsstahlung in a relativistic plasma were theoretically studied. ESA

89 ASTRONOMY

Includes radio, gamma-ray, and infrared astronomy, and astrometry.

N89-29278# Arizona Univ., Tucson.
A DEEP OPTICAL INFRARED SURVEY Final Report, 1 Feb. 1985 - 31 Jul. 1988
Marcia J. Lebofsky 7 Mar. 1989 3 p
(Grant AF-AFOSR-0101-85; AF Proj. 2311)
(AD-A207930; AFOSR-89-0435TR) Avail: NTIS HC A02/MF A01 CSCL 03/1

This grant was awarded to develop the necessary hardware to carry out a deep sky survey at the near-infrared wavelength of 2 microns. The grant was also to cover an initial operating period after which funding would be sought from other sources to finish the survey. The survey strategy consists of placing a near-infrared array with a silicon charged coupled readout (CCD) at the focus of a transit telescope on Kitt Peak, Arizona. DOE

N89-29279# Astronomische Rechen-Inst., Heidelberg (Germany, F.R.).
[ACTIVITIES REPORT OF THE HEIDELBURG ASTRONOMICAL INSTITUTE OF COMPUTATION (GERMANY, F.R.)] Progress Report, 1987 [TAETIGKEITSBERICHT DES ASTRONOMISCHEN RECHEN-INSTITUTS IN HEIDELBERG FUER DAS JAHR 1987]
R. Wielen 1987 16 p In GERMAN
(ETN-89-94429) Avail: NTIS HC A03/MF A01

In the field of astrometry, research activities were conducted for the European astrometry satellite HIPPARCOS, for the completion of a new fundamental catalog for the FK5-stars, and for the establishment of an astronomical data base. In the field of the structure, kinematics, dynamics and development of stellar systems, near-sun star, star clusters, milky ways and galaxies, and galactic clusters were investigated. In the field of celestial

mechanics, eigen elements were determined for asteroids of the HILDA group, and dynamic topology model calculations were performed. ESA

N89-29280# Max-Planck-Inst. fuer Physik und Astrophysik, Garching (Germany, F.R.). Inst. fuer Extraterrestrische Physik.
DEVELOPMENT OF A POSTDISPERSION SYSTEM FOR ASTRONOMICAL INFRARED OBSERVATIONS WITH FOURIER SPECTROMETERS AND ITS APPLICATION IN THE STUDY OF THE CO FUNDAMENTAL BANDS IN F, G AND K STARS
Thesis
Guenter Wiedemann Mar. 1989 130 p
(MPE-214; ISSN-0178-0719; ETN-89-95339) Copyright Avail: NTIS HC A07/MF A01

The upper layers of the atmospheres of late-ype stars is investigated. The study is based on the observation and analysis of carbon monoxide (CO) fundamental (delta v = 1) spectra at 4.7 microns. CO fundamental spectra provide an alternative way for the study of cool stellar atmospheres. A postdispersion system for astronomical Fourier spectrometers is developed. This is achieved in the constructed instrument by using a liquid helium-cooled grating monochromator as a narrowband filter. The theoretical basis for the quantitative evaluation of observed CO spectra in a number of cool stars is provided. Boundary temperatures and thermal profiles of stellar atmospheres were determined from the observation of a number of stars and semi-empirical models derived. The comparison of the observed temperatures with theoretical predictions based on radiative equilibrium (RE) models yields good agreement for several cool stars including Arcturus and Aldebaran. The CO models are incompatible with homogeneous chromospheres (hot, non-classical regions), as derived for some of the stars from conventional diagnostics by other groups. A second group of stars (epsilon Vir, beta Draco, beta Corvi, beta Gem) shows boundary temperatures considerably higher than predicted from RE-models. A strong discrepancy between CO-based and chromospheric model is still obvious in beta Gem, but cannot be claimed for beta Draco. ESA

N89-29281# European Southern Observatory, Garching (Germany, F.R.).
[ACTIVITIES REPORT IN INTERNATIONAL ASTRONOMY]
Annual Report, 1988
H. vanderLaan 1988 116 p In ENGLISH, FRENCH and GERMAN Original contains color illustrations
(ETN-89-95333) Avail: NTIS HC A06/MF A01

The European Southern Observatory annual report, 1988, is presented. The research papers are focused on the following subjects: the European coordination facility for the space telescope, the research with Chilean institutes, image processing, and sky survey. The considered equipment and instrument facilities are: telescopes, optical and infrared instrumentation, seeing improvement, computer equipment, and high resolution imaging and interferometry. Financial and organizational matters are discussed. The use of telescopes, the study programs, the publications, the 1989 council and committee members are listed. ESA

90 ASTROPHYSICS

Includes cosmology; celestial mechanics; space plasmas; and interstellar and interplanetary gases and dust.
For related information see also *75 Plasma Physics*.

N89-29282*# Stanford Univ., CA. Center for Space Science and Astrophysics.
STATISTICAL AND PHYSICAL EVOLUTION OF QSO'S
David Caditz and Vahe Petrosian Sep. 1989 41 p
(Contract NCC2-322; NGR-05-020-668)
(NASA-CR-185869; NAS 1.26:185869; CSSA-ASTRO-89-15)
Avail: NTIS HC A03/MF A01 CSCL 03B

The relationship between the physical evolution of discrete extragalactic sources, the statistical evolution of the observed population of sources, and the cosmological model is discussed. Three simple forms of statistical evolution: pure luminosity evolution (PLE), pure density evolution (PDE), and generalized luminosity evolution (GLE), are considered in detail together with what these forms imply about the physical evolution of individual sources. Two methods are used to analyze the statistical evolution of the observed distribution of QSO's (quasars) from combined flux limited samples. It is shown that both PLE and PDE are inconsistent with the data over the redshift range 0 less than z less than 2.2, and that a more complicated form of evolution such as GLE is required, independent of the cosmological model. This result is important for physical models of AGN, and in particular, for the accretion disk model which recent results show may be inconsistent with PLE. Author

N89-29283# California Univ., Berkeley. Lawrence Berkeley Lab. Theoretical Physics Group.
COSMIC RELICS FROM THE BIG BANG
Lawrence J. Hall (California Univ., Berkeley.) 6 Dec. 1988 19 p Presented at the 16th Annual SLAC Summer Institute on Particles Physics, Stanford, CA, 18 Jul. 1988
(Contract DE-AC03-76SF-00098; NSF PHY-85-15857)
(DE89-013268; LBL-26210; UCB-PTH-88/26; CONF-880747-7)
Avail: NTIS HC A03/MF A01

A brief introduction to the big bang picture of the early universe is given. Dark matter is discussed; particularly its implications for elementary particle physics. A classification scheme for dark matter relics is given. DOE

N89-29284 Max-Planck-Inst. fuer Physik und Astrophysik, Garching (Germany, F.R.). Inst. fuer Extraterrestrische Physik.
THE ORIGIN AND EVOLUTION OF X-RAY BINARIES AND LOW-MAGNETIC FIELD RADIO PULSARS
Frank Verbunt Feb. 1989 43 p Presented at the NATO Advanced Study Institute Conference on Neutron Stars: Their Birth, Evolution, Radiation and Winds, Erice, Italy, 5-7 Sep. 1988 Submitted for publication
(MPE-Preprint-145; ETN-89-95340) Copyright Avail: Fachinformationszentrum Karlsruhe, 7514
Eggenstein-Leopoldshafen 2, Fed. Republic of Germany

The theory of the formation and evolution of X-ray binaries and binary or low-magnetic-field radio pulsars is discussed. The simple semi-analytical description is emphasized. Massive X-ray binaries, low-mass X-ray binaries, and X-ray binaries in globular clusters, as well as the transformation of some of these into millisecond radio pulsars, are studied. ESA

N89-29285 Max-Planck-Inst. fuer Physik und Astrophysik, Garching (Germany, F.R.). Inst. fuer Extraterrestrische Physik.
EVOLUTION OF WIDE BINARY MILLISECOND PULSARS IN GLOBULAR CLUSTERS
S. Rappaport (Massachusetts Inst. of Tech., Cambridge.), A. Putney, and Frank Verbunt Apr. 1989 37 p Submitted for publication
(MPE-Preprint-148; ETN-89-95342) Copyright Avail: Fachinformationszentrum Karlsruhe, 7514
Eggenstein-Leopoldshafen 2, Fed. Republic of Germany

The evolution of wide binary millisecond radio pulsars, in a globular cluster environment, is investigated. Through an extensive series of numerical scattering experiments, the study of encounters between a binary radio pulsar (consisting of a neutron star and a low-mass degenerate companion) and passing cluster field stars is effectuated. Initial binary orbital periods from 3 to 1000 days are considered. Globular cluster star densities and distributions of stellar masses and velocities are taken from two models to represent moderately condensed (omega Cen) and highly condensed (47 Tuc) cluster cores. The scattering cross sections are derived for three scattering processes which can liberate the neutron star, including exchange and ionization reactions as well as direct collisions between stars. They are computed for inducing orbital eccentricities into binary radio pulsars with initially circular orbits and applied to the known pulsars in globular clusters. The measured orbital eccentricity of the PSR 1620-26 system in M4 is

only marginally consistent with its spin-down age, and that the PSR 0021-72B system in 47 Tuc is expected to have a significant eccentricity (approximately higher than 0.1) if its orbital period is near the upper end of its presently allowed period range and its age exceeds 10 to the 9th power years; and that the single millisecond pulsar PSR 2127+12 in M15 may be liberated from a wide binary via an encounter with a cluster star, whereas such a process is not likely to have produced the single millisecond pulsar PSR 1821-24 in M28. The calculations made for wide binary millisecond radio pulsars, have implications for other wide binaries in globular clusters. ESA

N89-29286 Max-Planck-Inst. fuer Physik und Astrophysik, Garching (Germany, F.R.). Inst. fuer Extraterrestrische Physik.
EVIDENCE FOR TWO CHARGED PARTICLE POPULATIONS IN THE CRAB NEBULA
Thomas Bork Mar. 1989 7 p Submitted for publication (MPE-Preprint-147; ETN-89-95341) Copyright Avail: Fachinformationszentrum Karlsruhe, 7514
Eggennstein-Leopoldshafen 2, Fed. Republic of Germany

A comparison between the measured soft X-ray brightness distribution of the Crab nebula and simulated data is made, in order to understand the conversion of the Crab pulsar's rotational energy into synchrotron radiation. Data is obtained from the High Resolution Imager on board the Einstein observatory. A 3-D model based on Rees and Gunn, and Aschenbach and Brinkmann theories is applied. The model suggests a torus shaped emission region. The analysis shows that this region, when viewed from the earth, has an angular extent of 0.24 radians and ellipticity of 5.5. Data from radio, optical, soft- and hard X-ray frequencies allowed to infer the existence of two spatially separated charged particle populations in the Crab pulsar environment. ESA

N89-29287 Max-Planck-Inst. fuer Physik und Astrophysik, Garching (Germany, F.R.). Inst. fuer Extraterrestrische Physik.
TOWARDS A THEORY OF STAR FORMATION
Hans Zinnecker Apr. 1989 18 p Submitted for publication (MPE-Preprint-150; ETN-89-95344) Avail: Fachinformationszentrum Karlsruhe, 7514
Eggenstein-Leopoldshafen 2, Fed. Republic of Germany

Some key elements towards a theory of star formation are discussed. Local and global star formation processes are included. The role of molecules and dust as well as spatial and temporal variations of the initial conditions are emphasized. Globally, the energy input from massive stars seems to regulate gas-rich galactic systems. Massive stars can cause negative or positive feedback on star formation, leading to a steady star formation rate or starbursts, respectively. On the molecular cloud scale, fragmentation is influenced by the effects of the tidal field and the magnetic field inside the clouds, with the possibility of a spatial segregation of high mass and low mass bound fragments. Locally, starbursts, respectively. On the molecular cloud scale, fragmentation is influenced by the effects of the tidal field and protostellar fragments where magnetic support breaks down. When collapse is triggered by an increase in external pressure or by radiative implosion, magnetic support is less effective and a larger fraction of the mass of each fragment will end up as stellar mass. The relation between fragment mass and stellar mass determines the slope of the Initial Mass Function that is derived from the fragment mass spectrum. For triggered star formation this relation should differ from that for spontaneous star formation which may explain why the slope of the Initial Mass Function in starburst systems is flatter than in the solar neighborhood. ESA

N89-29288 Max-Planck-Inst. fuer Physik und Astrophysik, Garching (Germany, F.R.). Inst. fuer Extraterrestrische Physik.
MEASUREMENT OF THE VELA PULSAR'S PROPER MOTION AND DETECTION OF THE OPTICAL COUNTERPART OF ITS COMPACT X-RAY NEBULA
Hakki Oegelman, Lydie Koch-Miramond, and Michel Auriere (Observatoire du Pic-du-Midi, Bagneres de Bigorre, France) Apr. 1989 18 p Submitted for publication
(Contract DFG-Mo-416/3-3) (MPE-Preprint-151; ETN-89-95345) Copyright Avail: Fachinformationszentrum Karlsruhe, 7514
Eggenstein-Leopoldshafen 2, Fed. Republic of Germany

The results of optical astrometry and photometry in the Vela pulsar field are reported. The proper motion of the pulsar and the optical counterpart of the approximately 2 minutes diameter compact nebula seen in X-rays, are investigated. The relative position measurements are fitted with previous published data yield of mu (alfa) = -0.026 (+ or -) 0.006 (1 sigma) seconds/year and mu (delta) = 0.028 (+ or -) 0.006 (1 sigma) seconds/year as the proper motion of the pulsar. The implied transverse velocity of the pulsar at an assumed distance of 500 parsec is approximately 90 (+ or -) 15 km/s, in the northwest direction. After a star detection algorithm is used to detect and subtract the stellar contribution, a diffuse nebula centered around the pulsar is clearly distinguishable in the V and B band exposures; several whisp-like structures can be recognized in the images. The optical size of the compact nebula, 2 to 6 x 10(17) cm, is comparable to that in X-rays, and the optical intensity can be connected to the X-ray points by a power-law type emission with photon number index gamma approximately 2. With this spectrum, the total luminosity of the compact nebula extending from optical to X-rays is about 10(33) power erg/s. Possible origins of this compact nebula are discussed. ESA

N89-29289# Tata Inst. of Fundamental Research, Bombay (India).
IMPLICATIONS OF THE CORRELATION BETWEEN THE RADIO CONTINUUM AND FAR-INFRARED LUMINOSITIES OF SPIRAL GALAXIES
T. N. Rengarajan and K. V. K. Iyengar 1989 15 p
Avail: NTIS HC A03/MF A01

The correlation observed between the radio continuum and the far-infrared (far-IR) luminosities for spiral galaxies was extended to lower frequency by using the 408 MHz data of Harnett (1982). The correlation was also studied as a function of radio spectral index between 2.8 cm and 6.3 cm and was found to be independent of it. The tighter correlation between the radio and the far-IR luminosities as compared to those between the blue and the radio, the blue and the far-IR, is evidence that the electrons responsible for the radio emission mostly originate in young massive stars. The dispersion observed for the far-IR radio correlation was used to set limits on the variation of several parameters like the star formation rate, the slope of the initial mass function, the relative frequency of supernovae of type I and type II, the frequency of supernovae as a function of the morphological type of the galaxy, the magnetic field in the galaxies, and the residence time of energetic electrons. Author

N89-29290# Geneva Observatory (Switzerland).
RED GIANTS IN OPEN CLUSTERS. 1: BINARITY AND STELLAR EVOLUTION IN FIVE HYADES-GENERATION CLUSTERS, NGC 2447, 2539, 2632, 6633 AND 6940
J.-C. Mermilliod (Lausanne Univ., Switzerland) and M. Mayor 1989 21 p Submitted for publication Sponsored by the Swiss National Foundation for Scientific Research
(Ser-C-Prepubl-Fasc-37-Pt-1; ETN-89-95176) Avail: NTIS HC A03/MF A01

The coravel radial velocity observations of 62 red giant stars in five Hyades-like open clusters (NGC 2447, 2539, 2632, 6633 and 6940) are analyzed for membership determination and binary detection. Fourteen spectroscopic binaries are discovered and four more are suspected, (a binary percentage equal to 25 to 30 percent). Twelve orbits are determined, including one for KW 428 in Praesepe, and two triple systems identified. At least nine of the ten stars found in the Hertz-sprung gap are composite binaries of the (gK+dA) type. Seven nonmember stars are detected. The radial velocity dispersion is close to the value expected from the virial theorem. The composite color magnitude diagram of the 55 members shows a very clean isochronous curve: the clump loop and the asymptotic branch are well defined. All bright giants appear to be in the latter phase. A second concentration of red giants

located at about 0.2 maximum available gain fainter than the clump is discovered. ESA

N89-29291# Geneva Observatory (Switzerland).
RED GIANTS IN OPEN CLUSTERS. 2: ORBITS OF TEN SPECTROSCOPIC BINARIES IN NGC 2360, 2437, 2447, 5822, 5823, 6475
J.-C. Mermelliod, M. Mayor, J. Anderson, B. Nordstrom, H. Lindgren, and A. Duquennoy 1989 14 p Submitted for publication
Sponsored by the European Southern Observatory, the Danish Board for Astronomical Research and the Swiss National Fund for Scientific Research
(Ser-C-Prepubl-Fasc-38-Pt-2; ETN-89-95177) Avail: NTIS HC A03/MF A01

The results of a systematic program to detect spectroscopic binaries in open clusters and determine their orbits are given, based on radial velocity observations made with the CORAVEL scanners in both hemispheres. Orbits for ten (single-lined) spectroscopic binaries in six southern clusters (NGC 2360, 2437, 2447, 5822, 5823, and 6475) are presented. The orbital periods range from 65 to 1370 days, and the velocity semi-amplitudes from 4.4 km/s to 26.0 km/s. All the binaries are confirmed cluster members except that in NGC 5823. The star NGC 2360-0051 has an eccentric despite its 98-day period. NGC 6475-0134 has a circular orbit with a 217-day period. For cluster giants, the cutoff period for eccentric orbits decreases with age. ESA

91 LUNAR AND PLANETARY EXPLORATION

Includes planetology; and manned and unmanned flights.
For spacecraft design or space stations see *18 Spacecraft Design, Testing and Performance.*

N89-29292*# Martin Marietta Aerospace, Denver, CO. Planetary Science Branch.
STUDY OF SAMPLING SYSTEMS FOR COMETS AND MARS Final Report
R. J. Amundsen and B. C. Clark Mar. 1987 196 p
(Contract NAS9-17511)
(NASA-CR-185514; NAS 1.26:185514; MCR-86-654) Avail: NTIS HC A09/MF A01 CSCL 03B

Several aspects of the techniques that can be applied to acquisition and preservation of samples from Mars and a cometary nucleus were examined. Scientific approaches to sampling, grounded in proven engineering methods are the key to achieving the maximum science value from the sample return mission. If development of these approaches for collecting and preserving does not preceed mission definition, it is likely that only suboptimal techniques will be available because of the constraints of formal schedule timelines and the normal pressure to select only the most conservative and least sophisticated approaches when development has lagged the mission milestones. With a reasonable investment now, before the final mission definition, the sampling approach can become highly developed, ready for implementation, and mature enough to help set the requirements for the mission hardware and its performance. Author

N89-28532# Joint Publications Research Service, Arlington, VA.
METHOD FOR RESEARCH ON PLANET VENUS USING FLOATING BALLOON STATIONS: MATHEMATICAL MODEL
V. A. Vorontsov, V. A. Deryugin, V. P. Karyagin, R. S. Kremnev, V. V. Kuznetsov, V. M. Linkin, K. M. Pichkhadze, G. N. Rogovskiy, and A. V. Terterashvili *In its* JPRS Report: Science and Technology. USSR Report: Life Sciences 15 Mar. 1989 p 49-50 Transl. into ENGLISH from Kosmicheskiye Issledovaniya (Moscow, USSR), v. 26 no. 3, May-Jun. 1988 p 430-433 (For primary document see N89-28527 23-12)
Avail: NTIS HC A05/MF A01

92 SOLAR PHYSICS

Includes solar activity, solar flares, solar radiation and sunspots.
For related information see *93 Space Radiation.*

N89-29293 Institut d'Aeronomie Spatiale de Belgique, Brussels.
SOLAR ULTRAVIOLET RADIATION WITHIN THE MIDDLE ATMOSPHERE
Paul C. Simon and Didier Gillotay 1989 20 p Presented at the International Radiation Symposium, Lille, France, 18-24 Aug. 1988 Submitted for publication
(Aeronomica-Acta-A-337-1989; ISSN-0065-3713; ETN-89-95187)
Avail: Institut d'Aeronomie Spatiale de Belgique, 3 Avenue Circulaire, B-1180 Brussels, Belgium

The analysis of the observations of solar ultraviolet irradiance, above Lyman alfa wevelength during phase of solar cycle 21, is performed. Important discrepancies (up to 40 percent) between the observations are present below 200 nm. Above this wavelength the agreement between the two space shuttle observations is good. Ultraviolet irradiance values with accuracies between 3.5 and 5.2 per cent are obtained. Variabilities related to the 27-day rotation period and the 11-year cycle are revised on the basis of the recent analysis of the solar backscatter ultraviolet and solar mesophere explorer observations. ESA

N89-29294 Institut d'Aeronomie Spatiale de Belgique, Brussels.
SOLAR SPECTRAL IRRADIANCES WITH THEIR DIVERSITY BETWEEN 120 AND 900 NM
Marcel Nicolet 1989 90 p Submitted for publication
(Aeronomica-Acta-A-338-1989; ISSN-0065-3713; ETN-89-95188)
Avail: Institut d'Aeronomie Spatiale de Belgique, 3 Avenue Circulaire, B-1180 Brussels, Belgium

The representative observations of the recent solar spectral irradiance measurements are reported. The observations are performed by means of satellites, rockets and balloons, in addition to ground level and aircraft measurements. It is shown that simultaneous and continuous measurements are needed to reduce the systematic differences between the various observed spectral irradiances. It is important to reduce the multiple random errors in order to permit meaningful studies of the variability of the solar fluxes. Permanent support by space agencies is required for the acquisition of a reliable data base of accurate spectral solar irradiances. ESA

N89-29295# European Space Agency, Paris (France).
KEY DATA ON PARTICIPATING PROJECTS. THE SOLAR-TERRESTRIAL SCIENCE PROJECT OF THE INTER-AGENCY CONSULTATIVE GROUP FOR SPACE SCIENCE (IACG)
R. Reinhard, comp. and B. Battrick, comp. Nov. 1988 118 p
(ESA-SP-1107; ISSN-0379-6566; ETN-89-95010) Copyright
Avail: NTIS HC A06/MF A01; ESA Publications Div., ESTEC, Noordwijk, Netherlands, 40 Dutch guilders

The planning includes 24 projects involving a total of 36 spacecraft. A summary of the scientific objectives, the payload, the key spacecraft and mission/orbit of each project are presented together with a drawing of the spacecraft and a plot of the orbit. ESA

93 SPACE RADIATION

Includes cosmic radiation; and inner and outer earth's radiation belts.
For biological effects of radiation see *52 Aerospace Medicine.* For theory see *73 Nuclear and High-Energy Physics.*

N89-29296# California Univ., Berkeley. Lawrence Berkeley Lab.
SPECTRAL MEASUREMENTS OF THE COSMIC MICROWAVE BACKGROUND Ph.D. Thesis

Alan J. Kogut Apr. 1989 195 p
(Contract DE-AC03-76SF-00098)
(DE89-014895; LBL-27233) Avail: NTIS HC A09/MF A01

Three experiments measured the intensity of the Cosmic Microwave Background (CMB) at wavelengths 4.0, 3.0, and 0.21 cm. The measurement at 4.0 cm used a direct-gain total-power radiometer to measure the difference in power between the zenith sky and a large cryogenic reference target. Foreground signals are measured with the same instrument and subtracted from the zenith signal, leaving the CMB as the residual. The reference target consists of a large open-mouth cryostat with a microwave absorber submerged in liquid helium; thin windows block the radiative heat load and prevent condensation atmospheric gases within the cryostat. The thermodynamic temperature of the CMB at 4.0 cm is 2.59 + or - 0.07 K. The measurement at 3.0 cm used a superheterodyne Dicke-switched radiometer with a similar reference target to measure the zenith sky temperature. A rotating mirror allowed one of the antenna beams to be redirected to a series of zenith angles, permitting automated atmospheric measurements without moving the radiometer. A weighted average of 5 years of data provided the thermodynamic temperature of the CMB at 3.0 cm of 2.62 + or - 0.06 K. The measurement at 0.21 cm used Very Large Array observations of interstellar ortho-formaldehyde to determine the CMB intensity in molecular clouds toward the giant HII region W51A (G49.5-0.4). Solutions of the radiative transfer problem in the context of a large velocity gradient model provided estimates of the CMB temperature within the foreground clouds. Collisional excitation from neutral hydrogen molecules within the clouds limited the precision of the result. The thermodynamic temperature of the CMB at 0.21 cm is 3.2 + or - 0.9 K. DOE

N89-29297# Ballistic Research Labs., Aberdeen Proving Ground, MD.
QUANTIZATION BY COSMIC BACKGROUND RADIATION
James T. Dehn May 1989 27 p
(AD-A208103; BRL-TR-2991) Avail: NTIS HC A03/MF A01
CSCL 20/10

It is suggested that various modes in the cosmic background radiation field may account for the discrete properties exhibited by small systems. In particular, this view is applied to the 1, 2-, and 3-D oscillators and the hydrogen atom, systems which were treated by Schrodinger in his first papers on quantum mechanics. The usual energy formulas for the above systems are derived using this point of view, together with some indication of how transition probabilities might also be calculated. A connection between de Broglie's associated wave and a free mass moving in the cosmic background is also discussed. Analogs of the uncertainty and correspondence principles are briefly mentioned as are some of the implications this view might have for interpreting quantum theory. In this view particles and waves are separate, interacting entities and not complementary aspects of the same thing. GRA

N89-29298* Max-Planck-Inst. fuer Physik und Astrophysik, Garching (Germany, F.R.). Inst. fuer Extraterrestrische Physik.
MILLISECOND RADIO PULSARS IN GLOBULAR CLUSTERS
Frank Verbunt, Walter H. G. Lewin, and Jan vanParadijs (Nationaal Inst. voor Kernfysica en Hoge Energiefysica, Amsterdam, Netherlands) Apr. 1989 10 p Sponsored in part by the Netherlands Organization for Scientific Research
(Grants NAG8-571; NAG8-674; NsG-7643; NATO-RG-331/88)
(NASA-CR-185909; NAS 1.26:185909; MPE-Preprint-149;
ETN-89-95343) Copyright Avail: Fachinformationszentrum Karlsruhe, 7514 Eggenstein-Leopoldshafen 2, Fed. Republic of Germany CSCL 03B

It is shown that the number of millisecond radio pulsars, in globular clusters, should be larger than 100, applying the standard scenario that all the pulsars descend from low-mass X-ray binaries. Moreover, most of the pulsars are located in a small number of clusters. The prediction that Teran 5 and Liller 1 contain at least about a dozen millisecond radio pulsars each is made. The observations of millisecond radio pulsars in globular clusters to date, in particular the discovery of two millisecond radio pulsars in 47 Tuc, are in agreement with the standard scenario, in which the neutron star is spun up during the mass transfer phase. ESA

N89-29163*# Washington State Univ., Pullman. Dept. of Physics.
ELECTROMAGNETIC INTERACTIONS OF COSMIC RAYS WITH NUCLEI
John W. Norbury *In its* Photonuclear Absorption Cross Sections 22 p(SEE N89-29159 23-72) 15 Aug. 1989 Submitted for publication (For primary document see N89-29159 23-72)
Avail: NTIS HC A07/MF A01 CSCL 03B

99 GENERAL

N89-29299# Office National d'Etudes et de Recherches Aerospatiales, Paris (France).
LA RECHERCHE AEROSPATIALE, BIMONTHLY BULLETIN, NUMBER 1988-4
ESA Jun. 1989 63 p Transl. into ENGLISH of La Recherche Aerospatiale, Bulletin Bimestriel (Paris, France), no. 1988-4, 1988
(ESA-TT-1161; ETN-89-95391) Avail: NTIS HC A04/MF A01

The model of a parallel shared memory computer and two classes of parallel multi-instruction multiple-data machines; the laminar stability theory applied to two-dimensional boundary layers in compressible flow over an adiabatic wall; an implicit finite-volume method for solving the two-dimensional and three-dimensional time-dependent Navier-Stokes equations; the applications of infrared absorption spectrometry by diode laser to the analysis of gases of combustion; and the aerodynamic visualization for impulsively started airfoils are discussed. ESA

N89-29300# Office National d'Etudes et de Recherches Aerospatiales, Paris (France).
LA RECHERCHE AEROSPATIALE, BIMONTHLY BULLETIN, NUMBER 1988-5
ESA Jun. 1989 62 p Transl. into ENGLISH of La Recherche Aerospatiale, Bulletin Bimestriel (Paris, France), no. 1988-5, 1988
(ESA-TT-1162; ETN-89-95392) Avail: NTIS HC A04/MF A01

The use of electromagnetic waves in the fabrication of composite materials; the optimization of the inputs and outputs of a secondary memory in multiprocessor architecture; the model of nonlinear combustion instability with nonlinear pressure coupling in solid propellant rocket motors; the tension-torsion testing machine operating at high temperature (1000 C); and the possibilities of millimetric waves for local, contactless measurement of temperature and humidity are discussed. ESA

N89-29301# Office National d'Etudes et de Recherches Aerospatiales, Paris (France).
LA RECHERCHE AEROSPATIALE, BIMONTHLY BULLETIN, NUMBER 1988-6
ESA Jun. 1989 55 p Transl. into ENGLISH of La Recherche Aerospatiale, Bulletin Bimestriel (Paris, France), no. 1988-6, 1988
(ESA-TT-1165; ETN-89-95393) Avail: NTIS HC A04/MF A01

Topics discussed include: (1) the solution of Euler equations, applied to supersonic flows, using a finite element method; (2) the language designed to provide a synthetic specification of the architecture/algorithm/mapping system; (3) the concept of the chemical laser emission in the visible range; (4) the generalization of the Roe scheme for computing flows by solution of the Euler equations, in the case of a mixture of inviscid gases with variable concentrations; and (5) the numerical simulation of an incompressible two-dimensional mixing layer at high Reynolds number, using a finite-difference method. ESA

N89-29302# European Space Agency, Paris (France).
[ACTIVITIES REPORT OF ESA] Annual Report, 1988
Norman Longdon, ed. and James Hunt, ed. 1989 222 p Original

contains color illustrations
(ISSN-0258-025X; ETN-89-94989) Copyright Avail: NTIS HC A10/MF A01

The described activities include, scientific programs, Earth observation program, microgravity program, telecommunications program, space transportation systems, space stations and platforms, technological research and development, scientific research, satellite operations, data handling and archiving, ground facilities for space systems, and technical infrastructure. ESA

Typical Subject Index Listing

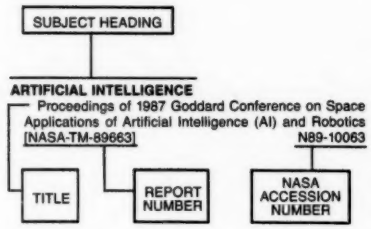

The subject heading is a key to the subject content of the document. Titles, report numbers, and accession numbers of pertinent documents are provided under each subject heading. When the title is insufficiently descriptive of the document content, a title extension has been added, separated from the title by three hyphens. The report number helps to indicate the type of document cited (e.g., NASA report, NASA translation, NASA contractor report). The NASA accession number is the number by which the document abstracts are arranged in this journal and by which the document is sold or requested. The titles, with title extensions if present, are arranged under each subject heading in ascending accession number order. The subject headings have been selected from the latest revision of the *NASA Thesaurus* (NASA SP-7064).

A

A-10 AIRCRAFT
Operational test plan concept for evaluation of close air support alternative aircraft
[AD-A208185] N89-28513

ABILITIES
Sleep deprivation and its effect on combat effectiveness
[AD-A207970] N89-29013

ABSORBERS (MATERIALS)
A method for assisting in decision-making for multilayer radar absorbent coverings --- manufacture
[ONERA-NT-1989-2] N89-28703
Development of a carbonaceous selective absorber for solar thermal energy collection and process for its formation
[DE89-008587] N89-28949

ABSORPTION CROSS SECTIONS
Absorption cross section of alternative chlorofluoroethanes and potential effects on the ozone layer
[AERONOMICA-ACTA-A-340-1989] N89-28968
Aeronomic problems of molecular oxygen photodissociation. 5: Predissociation in the Schumman-Runge Bands of Oxygen
[AERONOMICA-ACTA-A-341-1989-5] N89-28980
Photonuclear absorption cross sections
[NASA-CR-185488] N89-29159
Calculation of two-neutron multiplicity in photonuclear reactions N89-29160

ABSORPTION SPECTRA
Modelling the in situ infrared reflection-absorption spectra of the diffuse layer
[AD-A209347] N89-28598
Improvements of the efficiency of solid state lasers by spectral conversion of the excitation lamp's output
[ETN-89-94425] N89-28822

ACCELERATED LIFE TESTS
Accelerated life evaluation of valve-regulated lead-acid batteries
[DE89-012429] N89-28710

ACCESS CONTROL
Appraisal of security of data handling systems and products: A tutorial and discussion document --- civil domain
[NPL-DITC-141/89] N89-29092

ACCESS TIME
Near-neighbor algorithms for processing bearing data
[AD-A207935] N89-29053

ACCURACY
Sea gravimetry and Eotvos correction
[REPT-88.3] N89-29006
Solar spectral irradiances with their diversity between 120 and 900 nm
[AERONOMICA-ACTA-A-338-1989] N89-29294

ACID RAIN
Materials aerometric database for use in developing materials damage functions
[PB89-181259] N89-28572

ACOUSTIC EMISSION
A comprehensive guide to the literature on acoustic emission from composites, supplement 2
[DE89-013524] N89-28573
Acoustic emission technology for space applications
[DE89-014449] N89-28861

ACOUSTIC MEASUREMENT
Acoustic tests on a new motor generator system for the minuteman launch control centers in Hill engineering test facilities 1 and 2, Hill AFB, Utah
[AD-A209598] N89-28717
Acoustical tracking of fast maneuvering aircraft by distributed sensors
[REPT-6-88] N89-29156
The measurement of SEA loss factors on a fully assembled structure
[ISVR-TR-150] N89-29157
The acoustic calibration of aircraft fuselage structures, part 1
[ISVR-TR-169-PT-1] N89-29158
Helium bottle pressure measurement by portable ultrasonic technique
[AD-A208994] N89-29188

ACOUSTIC MICROSCOPES
Nondestructive characterization of simple interfaces using volume sound waves
[ETCA-89-R-015] N89-28854

ACOUSTIC SCATTERING
The inverse scattering problem for acoustic and electromagnetic waves
[AD-A209202] N89-28681

ACOUSTICAL HOLOGRAPHY
Nearfield acoustic holography: Review and perspectives
[ISVR-TR-179] N89-28807

ACOUSTICS
Acoustic tests on a new motor generator system for the minuteman launch control centers in Hill engineering test facilities 1 and 2, Hill AFB, Utah
[AD-A209598] N89-28717

ACOUSTO-OPTICS
Acousto-optic and linear electro-optic properties of organic polymeric materials
[AD-A207974] N89-28646
Acousto-optical vector matrix product processor: Implementation issues
[AD-A207933] N89-28722

ACTIVATION ENERGY
The analysis of solvent effects on the kinetics of simple heterogeneous electron transfer reactions
[AD-A210078] N89-28602

ACTIVE CONTROL
Active damping of vibration in large space structures using a Karhunen-Loeve reduced order model
[AD-A208183] N89-28558
Optimization of structures with passive damping and active controls
[AD-A208937] N89-28862

ADAPTATION
Adaptive detection and parameter estimation for multidimensional signal models
[AD-A208971] N89-28678

ADAPTIVE CONTROL
An approximation formula to evaluate the coefficient update rate of partially adaptive antennas
[REPT-5-88] N89-28844
On constrained multivariable adaptive control
[LAAS-89.093] N89-29101

ADAPTIVE FILTERS
Detection of target formations in infrared imagery
[ETCA-88-R-070] N89-29198

ADHESION
Monolayers of 11-trichlorosilylundecyl thioacetate: A system that promotes adhesion between silicon dioxide and evaporated gold
[AD-A208266] N89-28637
Pull-out and push-out tests for rubber-to-metal adhesion
[AD-A208100] N89-28647
Comparison of peel and lap shear bond strengths for elastic joints with and without residual stresses
[AD-A208102] N89-28867
Chemical effects of Ne(+) bombardment on the MoS2(0001) surface studied by high-resolution photoelectron spectroscopy
[AD-A207734] N89-29247

ADHESION TESTS
Nondestructive characterization of simple interfaces using volume sound waves
[ETCA-89-R-015] N89-28854

ADHESIVE BONDING
Nondestructive characterization of simple interfaces using volume sound waves
[ETCA-89-R-015] N89-28854

ADHESIVES
Damping properties of various materials
[AD-A209071] N89-28642
High temperature adhesive systems
[AD-A209166] N89-28643

ADIABATIC CONDITIONS
Adiabatic shear bands in one dimension
[AD-A208105] N89-28868

ADJOINTS
On adjoints and dual matroids
[MEMO-767] N89-29146

ADMIXTURES
Interpretation of remote sensing data from eastern areas of the Baltic Sea N89-28898

ADSORPTION
Formation of monolayers by the coadsorption of thiols on gold: Variation in the length of the head group, tail group and solvent
[AD-A208919] N89-28594

ADVECTION
Difference techniques for solving the advection equation
[WISS-BER-8] N89-28991
A numerical study of a mesoscale eddy interaction with an ocean front in the marginal ice zone
[AD-A209192] N89-29002

AERIAL PHOTOGRAPHY
Zeiss Digital Mapping: A new hardware and software system concept from Kombinat VEB Carl Zeiss JENA N89-28891
National report of Polish Society of Photogrammetry and Remote Sensing N89-28895
A survey of aerial image quality assessment methods N89-28916
Determining the location of an observer with respect to aerial photographs
[AD-A207791] N89-28929

AERIAL RECONNAISSANCE
Airborne FLIR (Forward Looking Infrared) detection of surface targets
[AD-A209250] N89-29189

AEROACOUSTICS
Acoustical tracking of fast maneuvering aircraft by distributed sensors
[REPT-6-88] N89-29156

AERODYNAMIC CHARACTERISTICS
The angles of the Kolibrie rotor tipvanes on the rods and on the blades
[IW-R515] N89-28499
Aerodynamic model tests of exhaust augmentors for F/A-18 engine run-up facility at RAAF Williamtown
[AD-A208110] N89-28518
One-degree-of-freedom motion induced by modeled vortex shedding
[NASA-TM-101038] N89-28870
AERODYNAMIC COEFFICIENTS
Application of computational fluid dynamics to the analysis of the aerodynamics of a railgun projectile
[AD-A207758] N89-28758
AERODYNAMIC CONFIGURATIONS
Low-speed static and dynamic force tests of a generic supersonic cruise fighter configuration
[NASA-TM-4138] N89-28486
AERODYNAMIC FORCES
Comparison between two different techniques of computing the axial induction for horizontal axis wind turbines in a locally deformed flow field
[FFA-TN-1986-56] N89-28959
AERODYNAMIC LOADS
Correlation of Puma airloads: Evaluation of CFD prediction methods
[NASA-TM-102226] N89-28498
AERODYNAMIC NOISE
The acoustic calibration of aircraft fuselage structures, part 1
[ISVR-TR-169-PT-1] N89-29158
AERODYNAMIC STABILITY
Application of computational fluid dynamics to the analysis of the aerodynamics of a railgun projectile
[AD-A207758] N89-28758
AERODYNAMIC STALLING
Three-dimensional airfoil performance measurements on a rotating wing
[DE89-009443] N89-28487
AERODYNAMICS
Small scale model tests in small wind and water tunnels at high incidence and pitch rates. Volume 1: Test program and discussion of results
[AD-A208647] N89-28488
AERONOMY
Aeronomic problems of molecular oxygen photodissociation. 5: Predissociation in the Schumman-Runge Bands of Oxygen
[AERONOMICA-ACTA-A-341-1989-5] N89-28980
Aeronomic problems of molecular oxygen photodissociation. 6: Photodissociation frequency and transmittance in the spectral range of the Schumman-Runge bands
[AERONOMICA-ACTA-A-342-1989-6] N89-28981
AEROSOLS
The aggregated state of matter: Elucidating transitions from the gas to the condensed phase and the formation of aerocolloids
[AD-A209080] N89-28595
Hazards of explosives dusts
[DE89-014554] N89-28669
Dense heavy metal aerosol monitoring by direct X-ray fluorescence
[AD-A209077] N89-28966
Activities report in meteorology in Sweden
[AR-87-88] N89-28999
The coagulation and dispersion of nonspherical, aerosol particles in a turbulent atmosphere
[AD-A208064] N89-29150
AEROSPACE ENGINEERING
Activities report in aerospace research in Germany, F.R.
[ISSN-0070-3966] N89-28485
JPRS report: Science and technology. USSR report: Life sciences
[JPRS-USP-89-005] N89-28527
Activities report of the Institute of Space Research
[ILR-1986/87] N89-28536
La Recherche Aerospatiale, bimontly bulletin, number 1988-3
[ESA-TT-1137] N89-28781
Patent abstracts bibliography: A continuing bibliography. Section 2: Indexes (supplement 35)
[NASA-SP-7039(35)-SECT-2] N89-29264
AEROSPACE PLANES
High temperature adhesive systems
[AD-A209166] N89-28643
AEROSPACE SAFETY
General-purpose heat source development: Extended series test program SRB fragment/fuselage tests
[DE89-014389] N89-29180
AEROSPACE SCIENCES
Activities report of the Institute of Space Research
[ILR-1986/87] N89-28536
NASA thesaurus supplement. A four part cumulative supplement to the 1988 edition of the NASA thesaurus
[NASA-SP-7064-SUPPL-1] N89-29262
NASA thesaurus supplement: A four part cumulative supplement to the 1988 edition (supplement 2)
[NASA-SP-7064-SUPPL-2] N89-29269
Key data on participating projects. The solar-terrestrial science project of the Inter-Agency Consultative Group for Space Science (IACG)
[ESA-SP-1107] N89-29295
AEROSPACE SYSTEMS
Intelligent multi-sensor integrations
[NASA-CR-185846] N89-28562
Acoustic emission technology for space applications
[DE89-014449] N89-28861
AEROTHERMODYNAMICS
Physical phenomenology and mathematical models of hypersonic motion
[ETN-89-95201] N89-28560
Hypersonic vehicle environment simulation, phase 1
[AD-A209030] N89-28754
AGE FACTOR
Thermoregulatory competence during exercise transients in a group of heat-acclimated young and middle-aged men is influenced more distinctly by maximal aerobic power than age
[AD-A209753] N89-29009
AGGREGATES
Microcellular foams from rigid-rod polymers in solutions: Effect of aggregation characteristics on foam properties
[AD-A209024] N89-28640
AGING (BIOLOGY)
Thermoregulatory competence during exercise transients in a group of heat-acclimated young and middle-aged men is influenced more distinctly by maximal aerobic power than age
[AD-A209753] N89-29009
AGING (MATERIALS)
Investigation of ambient and high temperature aging of PETN (Pentaerythritol Tetranitrate) by laser induced fluorescence and ultraviolet absorption spectroscopies
[DE89-013740] N89-28813
AGING (METALLURGY)
Metallurgical evaluation of 17-4 PH stainless steel castings
[PB89-193262] N89-28615
AIR DEFENSE
Operational test plan concept for evaluation of close air support alternative aircraft
[AD-A208185] N89-28513
A methodology for modeling radar detection range in air combat simulation
[AD-A209153] N89-28679
A comparison and analysis of strategic defense transition stability models
[AD-A208033] N89-29144
AIR POLLUTION
Ozone trends within a large metropolitan area: The Los Angeles Basin
[PB89-145965] N89-28960
Adequacy of forestry data in assessing the impact of ozone: A national perspective
[DE89-012359] N89-28962
A combined air and water pollution control system
[NASA-CASE-NST-00007-1] N89-28967
AIR QUALITY
Materials aerometric database for use in developing materials damage functions
[PB89-181259] N89-28572
AIR TO SURFACE MISSILES
Helium bottle pressure measurement by portable ultrasonic technique
[AD-A208994] N89-29188
AIR TRAFFIC
Competition and safety in air traffic
[TUB-DISS-PAPER-128] N89-28508
AIR TRAFFIC CONTROL
Collision avoidance operational concept
[WP-88W00418] N89-28509
AIR WATER INTERACTIONS
Ocean remote sensing and modeling
[AD-A208406] N89-28927
A numerical study of a mesoscale eddy interaction with an ocean front in the marginal ice zone
[AD-A209192] N89-29002
AIRBORNE EQUIPMENT
Optical properties and error sources of an airborne radiometer
[MITT-60] N89-28799
KRAS: A Danish high resolution airborne SAR N89-28882
Simulation of ERS-1/OPS by the use of airborne spectroradiometer N89-28912
The use of expert systems for preprocessing image data
[NLR-MP-88009-U] N89-28934
Atmospheric influence on microwave remote sensing at different frequencies: Results of the 1st September 1987 DUSCAT flight
[BCRS-89-07] N89-28941
AIRBORNE SURVEILLANCE RADAR
The airborne pulse Doppler radar: An introduction to the basic principles — surveillance radar analysis
[BAE-WAA-RP-GEN-RAD-584] N89-28696
Airborne pulse Doppler radar. Part 3: Performance estimation — surveillance radar analysis
[BAE-WAA-RP-GEN-RAD-645-PT-3] N89-28697
AIRCRAFT ACCIDENT INVESTIGATION
Aircraft accident/incident summary reports: Belleville, Illinois, August 22, 1987; Pensacola, Florida, December 27, 1987
[PB89-910405] N89-28507
AIRCRAFT CONFIGURATIONS
Low-speed static and dynamic force tests of a generic supersonic cruise fighter configuration
[NASA-TM-4138] N89-28486
Operational test plan concept for evaluation of close air support alternative aircraft
[AD-A208185] N89-28513
Composite material repair and reliability
[AD-A209150] N89-28574
AIRCRAFT CONSTRUCTION MATERIALS
Aluminum alloy
[NASA-CASE-LAR-13924-1-CU] N89-28621
AIRCRAFT CONTROL
Low-speed static and dynamic force tests of a generic supersonic cruise fighter configuration
[NASA-TM-4138] N89-28486
AIRCRAFT DETECTION
Acoustical tracking of fast maneuvering aircraft by distributed sensors
[REPT-6-88] N89-29156
AIRCRAFT ENGINES
Statistics on aircraft gas turbine engine rotor failures that occurred in US commercial aviation during 1984
[NAPC-PE-185] N89-28516
Statistics on aircraft gas turbine engine rotor failures that occurred in US commercial aviation during 1985
[NAPC-PE-188] N89-28517
AIRCRAFT EQUIPMENT
High temperature adhesive systems
[AD-A209166] N89-28643
AIRCRAFT MAINTENANCE
Prevention, reduction, and measurement of combat stress reactions: A bibliography
[AD-A209375] N89-29019
AIRCRAFT MANEUVERS
Acoustical tracking of fast maneuvering aircraft by distributed sensors
[REPT-6-88] N89-29156
AIRCRAFT NOISE
Airport noise measuring data collction system
[NLR-MP-87006-U] N89-28526
Noise produced by turbulent flow into a rotor: Users manual for noise calculation
[NASA-CR-181790] N89-29152
Noise produced by turbulent flow into a rotor: Users manual for atmospheric turbulence prediction and mean flow and turbulence contraction prediction
[NASA-CR-181791] N89-29154
AIRCRAFT PILOTS
Risk management for air ambulance helicopters operators
[DOT/FAA/DS-88/7] N89-28506
Towards a physiologically based HUD (Head-Up Display) symbology
[AD-A207748] N89-28515
AIRCRAFT SAFETY
Competition and safety in air traffic
[TUB-DISS-PAPER-128] N89-28508
An experimental optical coupling device for an airborne digital redundant system
[NAL-TR-1003] N89-28514
AIRCRAFT SPECIFICATIONS
Specifications and measurement procedures and aircraft transparencies
[AD-A209396] N89-28511
AIRCRAFT STRUCTURES
Specifications and measurement procedures and aircraft transparencies
[AD-A209396] N89-28511
AIRFOIL PROFILES
Profile-vortex interactions
[ISL-R-125/87] N89-28495
The angles of the Kolibrie rotor tipvanes on the rods and on the blades
[IW-R515] N89-28499
Wind tunnel tests of 16 percent thick airfoil with 30 percent trailing edge flap at high angles of attack and with flap angles
[FFA-TN-1985-58] N89-28500

AIRFOILS
Finite element analysis of incompressible viscous flows around single and multi-element aerofoils in high Reynolds number region
[NAL-TR-1010T] N89-28765
AIRFRAMES
Composite material repair and reliability
[AD-A209150] N89-28574
AIRPORTS
Airport noise measuring data collction system
[NLR-MP-87006-U] N89-28526
ALGAE
Fuels from microalgae
[DE88-001192] N89-28657
ALGEBRA
New infinite-dimensional algebras, sine brackets, and SU (infinity)
[DE89-013178] N89-29108
ALGORITHMS
Multitarget tracking by single sensor analysis of the main approaches developed in this area
[ONERA-NT-1988-10] N89-28702
Systolic VLSI array for implementing the Kalman filter algorithm
[NASA-CASE-NPO-17108-1-CU] N89-28713
A space marching algorithm for the thin-layer Navier-Stokes equations N89-28767
Development and implementation of an on-line multivariable control algorithm for the force control of an industrial robot
[OUEL-1748/88] N89-28848
A simple numerical algorithm for elastohydrodynamic lubrication, based on a dynamic variation principle
[MEMO-761] N89-28850
User's guide to the complex terrain dispersion model plus algorithms for unstable situations (CTDMPLUS). Volume 1: Model description and user instructions
[PB89-181424] N89-28963
Application of special sensor microwave/imager data for analysis of cyclonic storms in midlatitudes over the sea
[AD-A207675] N89-28975
Critical problems in very large scale computer systems
[AD-A208070] N89-29035
A microprogramming support tool for pipelined architectures
[AD-A208090] N89-29036
Chaotic behavior in a new class of parallel optimization algorithms
[DE89-014069] N89-29040
Bit rate recovery using digital ladder networks
[AD-A209865] N89-29043
A model of parallel performance
[AD-A207792] N89-29049
BM/C(3) algorithm mapping onto concurrent processors
[AD-A207877] N89-29052
Near-neighbor algorithms for processing bearing data
[AD-A207935] N89-29053
Maximum-likelihood parameter estimation of a generalized gumbel distribution
[AD-A207994] N89-29055
A heterogeneous multiprocessor graphics system using processor-enhanced memories
[AD-A208089] N89-29058
An algorithm for smooth interpolation to scattered data in R2
[MEMO-748] N89-29066
Chapter on distributed computing
[AD-A208996] N89-29084
Information requirements and the implications for parallel computation
[AD-A207802] N89-29088
Row-oriented direct solving of linear algebraic equations: Row orthogonalization method
[REPT-88-82] N89-29105
Application of Cholesky-like matrix decomposition methods to the evaluation of atomic orbital integrals and integral derivatives
[AD-A209682] N89-29112
Interpolating polynomials from their values
[AD-A210102] N89-29114
The problem of selecting the shape functions for a p-type finite element
[AD-A207798] N89-29117
Conditional dependence
[AD-A207881] N89-29120
Least-squares best-fit geometric elements
[NPL-DITC-140/89] N89-29125
On the shape of mathematical arguments
[ETN-89-95465] N89-29133
An improved algorithm for labeling connected components in a binary image
[AD-A210100] N89-29190
Detection of target formations in infrared imagery
[ETCA-88-R-070] N89-29198
Evaluation of functionality in distributed systems
[AD-A209167] N89-29258
Method bases: A new tool for applied information system design
[NLR-MP-88002-U] N89-29271
ALIGNMENT
Space module assembly apparatus with docking alignment flexibility and restraint
[NASA-CASE-MSC-21211-1] N89-28553
New layout of Amsterdam pulse stretcher
[NIKHEF-K/APS/88-01A-REV] N89-29182
Orbit correction scheme for the new ring --- Amsterdam electron accelerator
[NIKHEF-K/APS/88-04] N89-29184
Updated OC scheme --- electron orbit correction
[NIKHEF-K/APS/88-04A] N89-29185
ALKALINE EARTH METALS
Evaporation thermodynamics of monotellurides of selected rare Earth and alkaline Earth elements, and an attempt to systematic correlation between the standard enthalpies of formation
[ETN-89-94655] N89-29257
ALKANES
Formation of monolayers by the coadsorption of thiols on gold: Variation in the length of the head group, tail group and solvent
[AD-A208919] N89-28594
Oxidative addition of C-H bonds in organic molecules to transition metal centers
[DE89-012991] N89-28616
ALPINE METEOROLOGY
Experimental investigation of the pressure drag in the Alps
[WISS-BER-9] N89-28992
ALPS MOUNTAINS (EUROPE)
Experimental investigation of the pressure drag in the Alps
[WISS-BER-9] N89-28992
ALTITUDE
Orbits containing arcs of minimum altitude variation
[AD-A209206] N89-28539
ALUMINUM
Comparative analysis of ultrasonic inspection procedures for Kaman K747 root end fittings
[AD-A207762] N89-28512
Fundamental studies of grain boundary structure and properties in ICB aluminum
[DE89-014884] N89-28619
The Bauschinger effect in 6-6-2 titanium alloy and its influence on advanced artillery projectiles
[AD-A209355] N89-28623
ALUMINUM ALLOYS
Sulfidation/oxidation properties of iron-based alloys containing niobium and aluminum
[DE89-013766] N89-28617
Aluminum alloy
[NASA-CASE-LAR-13924-1-CU] N89-28621
An investigation of the workability of Al-8.5 percent Mg alloys
[AD-A209451] N89-28624
Fatigue crack growth-microstructural relationship of Ti-6Al-4V
[AD-A208107] N89-28626
In-situ anodising of aluminium alloys --- Airbus corrosion prevention requirements
[BAE/WMD/AR/GEN/00666] N89-28630
ALUMINUM GALLIUM ARSENIDES
AlGaAs phased array laser for optical communications
[NASA-CR-181869] N89-28820
ALUMINUM NITRIDES
Highly oriented fiber reinforced ceramic composites
[AD-A208119] N89-28578
ALUMINUM OXIDES
Infrared study of carbon deposits on catalysts
[DE89-013310] N89-28634
Ultrasonic imaging of textured alumina
[NASA-TM-101478] N89-28853
The amorphous to gamma transformation in ion implanted Al2O3
[DE89-014797] N89-29226
AMAZON REGION (SOUTH AMERICA)
Daytime turbulent exchange between the Amazon forest and the atmosphere
[NASA-CR-185487] N89-28961
AMBULANCES
Risk management for air ambulance helicopters operators
[DOT/FAA/DS-88/7] N89-28506
AMINO ACIDS
Capillary zone electrophoresis-mass spectrometry of peptides and proteins
[DE89-014466] N89-28592
AMMONIA
Ion-molecule chemistry within doubly charged ammonia clusters
[AD-A207764] N89-28608
Ion-molecule chemistry within triply charged ammonia clusters
[AD-A207766] N89-28609
Analysis of flow boiling of ammonia and R-114 in a matrix heat exchanger
[DE89-012427] N89-28752
AMMONIUM COMPOUNDS
Effect of hydraulic fluid on hydroxylammonium nitrate based liquid propellant formulations
[AD-A208061] N89-28663
AMORPHOUS MATERIALS
The amorphous to gamma transformation in ion implanted Al2O3
[DE89-014797] N89-29226
AMPLIFICATION
Quality factor and statistics for radiation patterns of shipboard HF antennas
[AD-A207931] N89-28690
Development of a novel silicon detector with internal amplification
[MPI-PAE/EXP.EL-197] N89-28798
ANALOG CIRCUITS
Electrical characterization of signal processing microcircuit
[AD-A209078] N89-28714
Picosecond electrooptic investigations of integrated circuits
[AD-A209134] N89-28863
ANALOGIES
BM/C(3) algorithm mapping onto concurrent processors
[AD-A207877] N89-29052
ANALYSIS (MATHEMATICS)
An a priori approach to the evaluation of signature analysis efficiency
[IMAG-RR-746-I] N89-29140
ANALYTIC GEOMETRY
Least-squares best-fit geometric elements
[NPL-DITC-140/89] N89-29125
ANECHOIC CHAMBERS
Almond test body --- for microwave anechoic chambers
[NASA-CASE-LAR-13747-1-CU] N89-28672
ANGLE OF ATTACK
Wind tunnel tests of 16 percent thick airfoil with 30 percent trailing edge flap at high angles of attack and with flap angles
[FFA-TN-1985-58] N89-28500
ANGLES (GEOMETRY)
Universal precision sine bar attachment
[NASA-CASE-MFS-28253-1] N89-28831
ANGULAR CORRELATION
Photon-ion angular correlation measurements on the system He(+) + Ne: Determination of the spin inversion
[ETN-89-94435] N89-29175
ANGULAR DISTRIBUTION
Energy and angular distributions of electrons emitted from gases and thin foils during light ion bombardment
[DE89-014445] N89-29147
Photon-ion angular correlation measurements on the system He(+) + Ne: Determination of the spin inversion
[ETN-89-94435] N89-29175
ANGULAR RESOLUTION
Investigation of optoelectronic angle measuring systems and their use in a diffraction-optical strain measurement and a photoelectric two-coordinate autocollimator
[PTB-F-5] N89-29199
ANILINE
Vibrational dynamics of aniline (Ar)1 and aniline (CH4)1 clusters
[AD-A209560] N89-28605
ANIMALS
ELF (Extremely Low Frequency) communications system ecological monitoring program
[AD-A208198] N89-28691
A robot that walks: Emergent behaviors from a carefully evolved network
[AD-A207958] N89-29026
ANISOTROPIC FLUIDS
The anisotropy of the friction pressure of dipolar fluids
[ETN-89-94438] N89-28771
ANISOTROPIC MEDIA
Exact image theory for uniaxially anisotropic dielectric half space
[PB89-146450] N89-28671
ANISOTROPY
Thermal conductivity anisotropy in single crystal YBa2Cu3O7-x
[DE89-009643] N89-29220
ANNIHILATION REACTIONS
Proceedings of the Antiproton Technology Workshop held in Upton, New York on 10 May 1989
[AD-A210045] N89-29170

Measurement of electroweak effects and topological branching conditions in the reaction e(+)e(-) yields tau(+)tau(-) in the storage ring PETRA
[MPI-PAE/EXP.EL-195] N89-29173

ANNULAR FLOW
Numerical studies of convective heat transfer in an inclined semiannular enclosure
[NASA-TM-102011] N89-28666

ANNULI
Stresses and strains in a cold-worked annulus
[AR-005-548] N89-28871

ANODIZING
In-situ anodising of aluminium alloys — Airbus corrosion prevention requirements
[BAE/WMD/AR/GEN/00666] N89-28630

ANTARCTIC REGIONS
The first large balloon launch from Antarctica
[AD-A207735] N89-28491
The possibilities of application of satellite data for monitoring ice condition in the Antarctic region
N89-28907
The 1988 Antarctic ozone monitoring Nimbus-7 TOMS data atlas
[NASA-RP-1225] N89-28983

ANTENNA DESIGN
Antenna fundamentals: A tutorial paper
[BAE-WAA-R-GEN-RAD-533] N89-28695
Contribution to the generation of circular polarization of high purity using planar wire antenna structures
[ETN-89-94659] N89-28872

ANTENNA RADIATION PATTERNS
Near-field testing of the 15-meter hoop-column antenna
[NASA-TM-4073] N89-28550
Quality factor and statistics for radiation patterns of shipboard HF antennas
[AD-A207931] N89-28690
Antenna fundamentals: A tutorial paper
[BAE-WAA-R-GEN-RAD-533] N89-28695
Contribution to the generation of circular polarization of high purity using planar wire antenna structures
[ETN-89-94659] N89-28872

ANTENNAS
The relationship between ground permittivity and the input impedance of a horizontal dipole near ground
[AD-A207746] N89-28668

ANTHROPOMETRY
Anthropometric survey of US Army personnel: Summary statistics
[AD-A209600] N89-29025

ANTIMISSILE DEFENSE
SDI (Strategic Defense Initiative): Shield or sword?
[AD-A209777] N89-29141
SDS (Strategic Defense System) software testing and evaluation: A review of the state-of-the-art in software testing and evaluation with recommended R and D tasks
[AD-A209447] N89-29142
Ground-Based Radar (GBR): Environmental assessment
[AD-A207654] N89-29143
A comparison and analysis of strategic defense transition stability models
[AD-A208033] N89-29144
Strategic defense system distributed operating system R and D review and recommendations
[AD-A208034] N89-29145

ANTIMONY ALLOYS
Effective masses and g factors for 2-D light holes in InSb
[DE89-014899] N89-29230

ANTIPROTONS
Proceedings of the Antiproton Technology Workshop held in Upton, New York on 10 May 1989
[AD-A210045] N89-29170
Proceedings of a RAND Workshop on Antiproton Science and Technology
[AD-A208168] N89-29172

APERTURES
Apertures of ring quadrupoles and sextupoles
[NIKHEF-K/APS/88-03] N89-29183

APL (PROGRAMMING LANGUAGE)
APL conversion software
[MEMO-INF-88-21] N89-29062

APPLICATIONS PROGRAMS (COMPUTERS)
Numerical simulation of the simultaneous detonation of two identical, fully contained explosions
[DE89-014844] N89-28660
A simple numerical algorithm for elastohydrodynamic lubrication, based on a dynamic variation principle
[MEMO-761] N89-28850
Damage predictions for wind turbine components using the LIFE2 computer code
[DE89-013813] N89-28952
WINDROSE: A program for IBM-compatible personal computers, documentation
[PB89-167423] N89-29039
Backward analysis
[MEMO-INF-89-14] N89-29080
Method bases: A new tool for applied information system design
[NLR-MP-88002-U] N89-29271

APPROPRIATIONS
Departments of Veterans Affairs and Housing and Urban Development and independent agencies appropriations for 1990. Part 6: National Aeronautics and Space Administration
[GPO-99-598] N89-29273

APPROXIMATION
Model simplification based on the concept of equivalent dead time
[NAL-TM-SE-8802] N89-28521
Solution of Euler equations by a discontinuous Galerkin method obtained from a variational formulation of entropy
[CERT-1/332400/DERI] N89-28775
A dynamic variation principle for elastic-fluid contacts, applied to elastohydrodynamic lubrication theory
[MEMO-746] N89-28782
An approximation formula to evaluate the coefficient update rate of partially adaptive antennas
[REPT-5-88] N89-28844
Linear algebra support modules for approximation and other software
[NPL-DITC-142/89] N89-29126
Approximation methods for scattering from rough surfaces
[AD-A209482] N89-29192

ARCHITECTURE
Exploring virtual worlds with head-mounted displays
[AD-A208088] N89-28797
Walkthrough-exploring virtual worlds
[AD-A208087] N89-29057

ARCHITECTURE (COMPUTERS)
Photonic architectures for performing perfect shuffle on a time-division multiplexed signal
[PB89-184352] N89-28674
Two-dimensional signal processing and storage and theory and applications of electromagnetic measurements
[AD-A207827] N89-28689
Nonfilm radiography at the Oak Ridge Y-12 Plant
[DE89-014523] N89-28852
Digital optical computing with fibers and directional couplers
[PB89-184378] N89-29030
Fault-tolerant computer architecture modeling and analysis
[AD-A209364] N89-29034
Critical problems in very large scale computer systems
[AD-A208070] N89-29035
A microprogramming support tool for pipelined architectures
[AD-A208090] N89-29036
Software technology to support real-time embedded artificial intelligence-based applications, phase 1
[AD-A209133] N89-29042
A heterogeneous multiprocessor graphics system using processor-enhanced memories
[AD-A208089] N89-29058
Parallel language constructs for tensor product computations on loosely coupled architectures
[NASA-CR-181900] N89-29061
An optoelectronic multi-Gb/s packet switching network
[PB89-184345] N89-29081
A reconfigurable arithmetic processor — for MIMD computer
[AD-A208323] N89-29082
Northeast artificial intelligence consortium. Volume 1: Executive summary
[AD-A209395] N89-29094
Northeast artificial intelligence consortium annual report 1987. Volume 9: Computer architectures for very large knowledge bases
[AD-A209454] N89-29096
Signed-digit high speed transcendental function processor architecture
[AD-A209199] N89-29110
SDS (Strategic Defense System) software testing and evaluation: A review of the state-of-the-art in software testing and evaluation with recommended R and D tasks
[AD-A209447] N89-29142
Implementation of a distributed object-oriented database management system
[AD-A209437] N89-29265
La Recherche Aerospatiale, bimonthly bulletin, number 1988-6
[ESA-TT-1165] N89-29301

ARCTIC REGIONS
The possibilities of application of satellite data for monitoring ice condition in the Antarctic region
N89-28907

ARITHMETIC AND LOGIC UNITS
A reconfigurable arithmetic processor — for MIMD computer
[AD-A208323] N89-29082

ARMATURES
Plasma properties of a large-bore, arc-armature railgun
[AD-A209550] N89-28548

ARMED FORCES (UNITED STATES)
The Bauschinger effect in 6-6-2 titanium alloy and its influence on advanced artillery projectiles
[AD-A209355] N89-28623
Advanced robotics for Air Force operations
[AD-A210098] N89-28840
Sleep deprivation and its effect on combat effectiveness
[AD-A207970] N89-29013
Prevention, reduction, and measurement of combat stress reactions: A bibliography
[AD-A209375] N89-29019
Anthropometric survey of US Army personnel: Summary statistics
[AD-A209600] N89-29025
United States Air Force Research Initiation Program for 1987, volume 2
[AD-A209727] N89-29259

ARRAYS
Piezoelectric foils as sensors in experimental flow mechanics
[ILR-MITT-214] N89-28800

ARTIFICIAL INTELLIGENCE
Intelligent multi-sensor integrations
[NASA-CR-185846] N89-28562
A study of the thermal profiles during autogenous arc welding
[AD-A209440] N89-28843
Residual vibration reduction in computer controlled machines
[AD-A208074] N89-28866
Software technology to support real-time embedded artificial intelligence-based applications, phase 1
[AD-A209133] N89-29042
Northeast artificial intelligence consortium. Volume 1: Executive summary
[AD-A209395] N89-29094
Northeast artificial intelligence consortium annual report 1987. Volume 8: Knowledge base maintenance using logic programming methodologies
[AD-A209453] N89-29095
Northeast artificial intelligence consortium annual report 1987. Volume 9: Computer architectures for very large knowledge bases
[AD-A209454] N89-29096
The performance of a mechanical design Compiler
[AD-A209540] N89-29097

ARTIFICIAL SATELLITES
COLD-SAT: Cryogenic On-Orbit Liquid Depot-Storage, Acquisition and Transfer
[NASA-TM-102308] N89-28535

ARTILLERY
The Bauschinger effect in 6-6-2 titanium alloy and its influence on advanced artillery projectiles
[AD-A209355] N89-28623

ASCENT TRAJECTORIES
Wind models for the NSTS ascent trajectory biasing for wind load alleviation
[NASA-TM-100375] N89-28551

ASSESSMENTS
The influence of structure and alloying on the cold-formability of ferritic steels and the utility of uniaxial tensile testing in its assessment
[ISBN-952-90044-3-5] N89-28632

ASTROMETRY
Activities report of the Heidelburg Astronomical Institute of Computation (Germany, F.R.)
[ETN-89-94429] N89-29279
Measurement of the Vela pulsar's proper motion and detection of the optical counterpart of its compact X-ray nebula
[MPE-PREPRINT-151] N89-29288

ASTRONAUT TRAINING
Spacecraft flight simulation: A human factors investigation into the man-machine interface between an astronaut and a spacecraft performing docking maneuvers and other proximity operations
[NASA-CR-177502] N89-29020

ASTRONOMICAL CATALOGS
Activities report of the Heidelburg Astronomical Institute of Computation (Germany, F.R.)
[ETN-89-94429] N89-29279

ASTRONOMICAL MODELS
Cosmic relics from the big bang
[DE89-013268] N89-29283

ASTRONOMICAL PHOTOMETRY
Measurement of the Vela pulsar's proper motion and detection of the optical counterpart of its compact X-ray nebula
[MPE-PREPRINT-151] N89-29288
ASTRONOMY
Activities report of the Institute of Astronomy and Astrophysics
[MITT-9] N89-29276
ASTROPHYSICS
Activities report of the Max-Planck Institute of Nuclear Physics
[ETN-89-94398] N89-29174
The origin and evolution of X-ray binaries and low-magnetic field radio pulsars
[MPE-PREPRINT-145] N89-29284
ASYMPTOTIC METHODS
Composite damaging: Methodological approach
[ETN-89-94866] N89-28582
ASYMPTOTIC PROPERTIES
A torus bifurcation theorem with symmetry
[NASA-CR-185907] N89-29135
ASYMPTOTIC SERIES
Fast-algorithm development for large-eddy simulation of circular-jet turbulence
[AD-A207928] N89-28760
Modelling, information, processing, and control
[AD-A207810] N89-28865
Stein's Lemma: A large deviations approach
[AD-A209090] N89-29137
ATLANTIC OCEAN
Satellite-derived moisture-bogusing profiles for the North Atlantic Ocean
[AD-A207829] N89-28930
Results of Seasat altimeter data processing for the northeast Atlantic
[BCRS-89-05] N89-28940
ATMOSPHERIC ATTENUATION
Atmospheric influence on microwave remote sensing at different frequencies: Results of the 1st September 1987 DUSCAT flight
[BCRS-89-07] N89-28941
ATMOSPHERIC BOUNDARY LAYER
Analysis of turbulent transport phenomena in the maritime atmospheric boundary layer
[WISS-BER-10] N89-28978
Application of similarity methods to the turbulent diffusion in the convective and stable boundary layer
[WISS-BER-12] N89-28979
The boundary layer wind regime of a representative tropical African region, central Sudan
[KNMI-WR-88-04] N89-28982
ATMOSPHERIC CHEMISTRY
Hypersonic vehicle environment simulation, phase 1
[AD-A209030] N89-28754
Activities report in meteorology in Sweden
[AR-87-88] N89-28999
ATMOSPHERIC CIRCULATION
Daytime turbulent exchange between the Amazon forest and the atmosphere
[NASA-CR-185487] N89-28961
The boundary layer wind regime of a representative tropical African region, central Sudan
[KNMI-WR-88-04] N89-28982
Propagation and saturation of nonlinear inertia-gravity waves in the atmosphere
[AD-A207871] N89-28989
A numerical study of a mesoscale eddy interaction with an ocean front in the marginal ice zone
[AD-A209192] N89-29002
Entrainment and homogenization of a passive tracer in a numerical model gyre
[AD-A208020] N89-29005
ATMOSPHERIC COMPOSITION
A high-resolution atlas of the infrared spectrum of the sun and the earth atmosphere from space. A compilation of ATMOS spectra of the region from 650 to 4800 cm-1 (2.3 to 16 microns). Volume 2: Stratosphere and mesosphere, 650 to 3350 cm-1
[NASA-RP-1224-VOL-2] N89-28969
Activities report in meteorology in Sweden
[AR-87-88] N89-28999
ATMOSPHERIC GENERAL CIRCULATION MODELS
Propagation and saturation of nonlinear inertia-gravity waves in the atmosphere
[AD-A207871] N89-28989
ATMOSPHERIC MODELS
Satellite-derived moisture-bogusing profiles for the North Atlantic Ocean
[AD-A207829] N89-28930
Parameterization of ice and water clouds and their radiation transport characteristics for large scale atmospheric models
[MITT-58] N89-28977
The boundary layer wind regime of a representative tropical African region, central Sudan
[KNMI-WR-88-04] N89-28982
Activities report in meteorology in Sweden
[AR-87-88] N89-28999
ATMOSPHERIC MOISTURE
Satellite enhanced numerical weather prediction
[AD-A210108] N89-28987
ATMOSPHERIC OPTICS
Achievement of the optimum performance from laser interferometer systems when applied to precision length measurement in the free atmosphere
[NPL-MOM-92] N89-28825
ATMOSPHERIC PHYSICS
The Strategic High-Altitude Atmospheric Radiation Code (SHARC) user instructions
[AD-A207667] N89-28974
Activities report in meteorology in Sweden
[AR-87-88] N89-28999
ATMOSPHERIC RADIATION
The Strategic High-Altitude Atmospheric Radiation Code (SHARC) user instructions
[AD-A207667] N89-28974
ATMOSPHERIC SOUNDING
Satellite-derived moisture-bogusing profiles for the North Atlantic Ocean
[AD-A207829] N89-28930
Engineering and instrumentation support of the AFGL (Air Force Geophysics Laboratory) Research Balloon Program
[AD-A209107] N89-28971
Satellite enhanced numerical weather prediction
[AD-A210108] N89-28987
ATMOSPHERIC TURBULENCE
Analysis of turbulent transport phenomena in the maritime atmospheric boundary layer
[WISS-BER-10] N89-28978
Noise produced by turbulent flow into a rotor: Users manual for atmospheric turbulence prediction and mean flow and turbulence contraction prediction
[NASA-CR-181791] N89-29154
ATOMIC ENERGY LEVELS
Electron energy levels in a quantum well within an in-plane magnetic field
[AD-A209351] N89-29256
ATOMIC EXCITATIONS
Quantitative investigation of the kinetics of a laser-pumped barium vapor
[ETN-89-94434] N89-28823
ATOMIC PHYSICS
Activities report of the Max-Planck Institute of Nuclear Physics
[ETN-89-94398] N89-29174
ATOMIC STRUCTURE
Initial stages of metal/semiconductor interface formation: Au and AgON Si(111)
[AD-A209490] N89-29245
ATTENTION
Towards a physiologically based HUD (Head-Up Display) symbology
[AD-A207748] N89-28515
ATTENUATION
Ultrasonic attenuation in heavy fermion superconductors
[DE89-014937] N89-29231
ATTITUDE CONTROL
Towards a physiologically based HUD (Head-Up Display) symbology
[AD-A207748] N89-28515
ATTITUDE INDICATORS
Towards a physiologically based HUD (Head-Up Display) symbology
[AD-A207748] N89-28515
AUDIOMETRY
A study of the effect of stimulus upon the reflex response as elicited and recorded by the tympanic membrane displacement measurement device
[ISVR-TR-177] N89-29018
AUDITORY STIMULI
A study of the effect of stimulus upon the reflex response as elicited and recorded by the tympanic membrane displacement measurement device
[ISVR-TR-177] N89-29018
AUGER SPECTROSCOPY
Simultaneous secondary ion and Auger electron analysis, illustrated by examples from microelectronics research and technology
[ETN-89-94431] N89-28611
AUTOMATA THEORY
Three dimensional cellular automata for subpixel target detection
[AD-A208163] N89-29100
AUTOMATIC CONTROL
Northeast artificial intelligence consortium. Volume 1: Executive summary
[AD-A209395] N89-29094
AUTOMATIC FLIGHT CONTROL
Designers' commentary on Buran flight control system N89-28530
AUTOMATIC GAIN CONTROL
Development of an integrated AM shortwave upconversion receiver front-end
[ETN-89-95455] N89-28699
AUTOMATIC PILOTS
The effect of autopilot configuration on missile response
[AD-A207822] N89-28520
AUTOMATIC TEST EQUIPMENT
A fully automated, single-connection tester for T/R modules
[DE89-013155] N89-28786
AUTOREGRESSIVE PROCESSES
Modelling orientation parameters of sensor platforms N89-28881
AXIAL FLOW
Measurements of mean-flow and turbulence characteristics in a turbojet exhaust using a laser velocimeter
[ISL-CO-226/88] N89-28519
AXIAL LOADS
Steel fatigue under combined loads
[ETN-89-94864] N89-28629
New set of buckling parameters for monosymmetric beam-columns/tie beams
[PB89-191639] N89-28858
AXISYMMETRIC BODIES
Laser velocimetry in the close wake of an axisymmetric rear body
[ISL-R-114/87] N89-28774
AXISYMMETRIC FLOW
Measurements of mean-flow and turbulence characteristics in a turbojet exhaust using a laser velocimeter
[ISL-CO-226/88] N89-28519
Theoretical model of gravitational perturbation of current collector axisymmetric flow field
[AD-A209499] N89-28756
Numerical determination of guaranteed Rayleigh numbers and the pertaining flow forms in steady, axisymmetric convection in cylinders
[ETN-89-94432] N89-28769

B

BACKGROUND RADIATION
Spectral measurements of the cosmic microwave background
[DE89-014895] N89-29296
Quantization by cosmic background radiation
[AD-A208103] N89-29297
BACKWARD DIFFERENCING
Backward analysis
[MEMO-INF-89-14] N89-29080
BALL BEARINGS
Ion implantation of ceramic bearings
[AD-A209770] N89-28644
Turbomachinery rotor support with damping
[NASA-CASE-MFS-28345-1] N89-28841
BALLOON FLIGHT
The first large balloon launch from Antarctica
[AD-A207735] N89-28491
Engineering and instrumentation support of the AFGL (Air Force Geophysics Laboratory) Research Balloon Program
[AD-A209107] N89-28971
BALLOONS
Method for research on planet Venus using floating balloon stations: Mathematical model N89-28532
BALTIC SEA
Interpretation of remote sensing data from eastern areas of the Baltic Sea N89-28898
BAND STRUCTURE OF SOLIDS
Electronic-structure study of the Ni-Ga and Ni-In intermetallic compounds using X-ray photoemission spectroscopy
[AD-A209696] N89-28601
BANDWIDTH
Picosecond electrooptic investigations of integrated circuits
[AD-A209134] N89-28863
A reconfigurable arithmetic processor — for MIMD computer
[AD-A208323] N89-29082
BARIUM
Quantitative investigation of the kinetics of a laser-pumped barium vapor
[ETN-89-94434] N89-28823
BARIUM COMPOUNDS
Thermal conductivity anisotropy in single crystal YBa2Cu3O7-x
[DE89-009643] N89-29220

BARIUM OXIDES
Metallic bonding to high-temperature superconducting ceramics
[DE89-014668] N89-28635
Non-uniform transition conductivity of superconducting ceramic
[NASA-TM-102133] N89-28851

BARIUM TITANATES
Holographic modulator arrays
[AD-A209387] N89-28792

BATCH PROCESSING
Design and development of a user interface and user manual for a system dynamics model of software management
[AD-A209486] N89-29048

BAUSCHINGER EFFECT
The Bauschinger effect in 6-6-2 titanium alloy and its influence on advanced artillery projectiles
[AD-A209355] N89-28623

BAYES THEOREM
Multitarget tracking by single sensor analysis of the main approaches developed in this area
[ONERA-NT-1988-10] N89-28702

BEAM CURRENTS
Full consistent analysis of high beta steady state tokamaks sustained by beam driven and bootstrap currents
[IPPJ-912] N89-29212

BEAM INJECTION
High-brightness electron injectors: A review
[DE89-014244] N89-28711
Updated OC scheme — electron orbit correction
[NIKHEF-K/APS/88-04A] N89-29185
Improved confinement in high density ohmic discharge
[IPPJ-913] N89-29213

BEAMS (SUPPORTS)
Out-of-plane buckling formulae for beam-columns/tie beams
[PB89-191613] N89-28857
New set of buckling parameters for monosymmetric beam-columns/tie beams
[PB89-191639] N89-28858
Flexural-torsional buckling of monosymmetric beam-columns/tie beams
[PB89-191654] N89-28859

BEARINGS
Superconducting Meissner effect bearings for cryogenic turbomachines, phase 1
[AD-A209875] N89-28839

BEHAVIOR
A robot that walks: Emergent behaviors from a carefully evolved network
[AD-A207958] N89-29026

BENDING FATIGUE
Survey of test procedures for high performance ceramic materials and their fundamentals
[JUEL-SPEZ-470] N89-28653

BENZENE
A study of non-rigid aromatic molecules by supersonic molecular jet spectroscopy: Observation and spectroscopic analysis of the stable conformations of various alkylbenzenes
[AD-A209561] N89-29171

BIAS
Wind models for the NSTS ascent trajectory biasing for wind load alleviation
[NASA-TM-100375] N89-28551
Laser Doppler anemometry in supersonic flows: Problems of seeding and angular bias N89-28740

BIBLIOGRAPHIES
A comprehensive guide to the literature on acoustic emission from composites, supplement 2
[DE89-013524] N89-28573
Bibliography of the NIST (National Institute of Standards and Technology) Electromagnetic Fields Division publications
[PB89-189211] N89-28673
Solar thermal program summary. Volume 2: Research summaries, fiscal year 1988
[DE89-000861] N89-28947
Prevention, reduction, and measurement of combat stress reactions: A bibliography
[AD-A209375] N89-29019
Patent abstracts bibliography: A continuing bibliography. Section 2: Indexes (supplement 35)
[NASA-SP-7039(35)-SECT-2] N89-29264

BIDIRECTIONAL REFLECTANCE
ISCCP CX observations during the FIRE/SRB Wisconsin Experiment from October 14 through November 2, 1986
[NASA-TM-101653] N89-28993

BIG BANG COSMOLOGY
Cosmic relics from the big bang
[DE89-013268] N89-29283

BIHARMONIC EQUATIONS
Smooth piecewise polynomials as conforming finite elements for plate bending problems
[MEMO-747] N89-28675

BINARY DATA
An improved algorithm for labeling connected components in a binary image
[AD-A210100] N89-29190

BINARY STARS
Evolution of wide binary millisecond pulsars in globular clusters
[MPE-PREPRINT-148] N89-29285
Red giants in open clusters. 1: Binarity and stellar evolution in five Hyades-generation clusters, NGC 2447, 2539, 2632, 6633 and 6940
[SER-C-PREPUBL-FASC-37-PT-1] N89-29290
Red giants in open clusters. 2: Orbits of ten spectroscopic binaries in NGC 2360, 2437, 2447, 5822, 5823, 6475
[SER-C-PREPUBL-FASC-38-PT-2] N89-29291

BIOASSAY
Energy and Technology Review — analytical cytology
[DE89-013919] N89-28954

BIOCHEMISTRY
The MIT/Marine Industry Collegium: Novel applications of marine biopolymers
[PB89-182950] N89-28633
Energy and Technology Review — analytical cytology
[DE89-013919] N89-28954

BIOCONVERSION
Biofuels technical information guide
[DE89-000894] N89-28658

BIOGEOCHEMISTRY
Activities report in meteorology in Sweden
[AR-87-88] N89-28999

BIOLOGICAL EFFECTS
Climate regulation by marine phytoplankton: A test by anthropogenic SO2 emissions
[DE89-014708] N89-28984

BIOMAGNETISM
Transient visual evoked neuromagnetic responses: Identification of multiple sources
[DE89-013438] N89-29008

BIOMASS ENERGY PRODUCTION
Biofuels technical information guide
[DE89-000894] N89-28658
Energy technology R and D: What could make a difference. A study by the staff of the Oak Ridge National Laboratory. Part 1: Synthesis report, volume 1
[DE89-014568] N89-28955

BIOPOLYMERS
The MIT/Marine Industry Collegium: Novel applications of marine biopolymers
[PB89-182950] N89-28633

BIOTECHNOLOGY
The MIT/Marine Industry Collegium: Novel applications of marine biopolymers
[PB89-182950] N89-28633
Fuels from microalgae
[DE88-001192] N89-28657

BIPOLAR TRANSISTORS
Higher order base dynamics of a bipolar transistor with nonuniform doping
[PB89-155451] N89-28704
A model for the simulation of the DC and small-signal behavior of the bipolar transistor
[ETN-89-94442] N89-28727

BISTATIC REFLECTIVITY
Evaluation of the bistatic equivalence theorem for the near and far-field radar cross section of complex targets
[AD-A209228] N89-28682

BIT ERROR RATE
Digitally modulated bit error rate measurement system for microwave component evaluation
[NASA-TP-2912] N89-28545
Bit rate recovery using digital ladder networks
[AD-A209865] N89-29043

BIVARIATE ANALYSIS
Wind models for the NSTS ascent trajectory biasing for wind load alleviation
[NASA-TM-100375] N89-28551

BLASIUS FLOW
The upper-branch stability of compressible boundary layer flows
[NASA-TM-102128] N89-28748

BLOCH BAND
Effect of an electric field on a split Bloch band
[AD-A209857] N89-29244

BLOCKS
A graph-theoretical approach to block-co-polymer complexes. Part 1: Stars
[MEMO-757-PT-1] N89-28654
A graph-theoretical approach to block-co-polymer complexes. Part 2: Tree approximation
[MEMO-758-PT-2] N89-28655

BLUNT BODIES
Three-dimensional viscous hypersonic flow over blunt bodies
[DFVLR-FB-89-09] N89-28504

BLUNT TRAILING EDGES
Experimental and numerical investigation of coherent structures in turbulent wake flows
[AD-A207866] N89-28759

BODY MEASUREMENT (BIOLOGY)
Anthropometric survey of US Army personnel: Summary statistics
[AD-A209600] N89-29025

BOILING
Analysis of flow boiling of ammonia and R-114 in a matrix heat exchanger
[DE89-012427] N89-28752

BOLOMETERS
Performance evaluation of radiofrequency, microwave, and millimeter wave power meters
[PB89-193916] N89-28707

BOLTS
Static and dynamic deflection studies of the SRM aft case-nozzle joint
[NASA-TM-100373] N89-28568

BONDING
Oxidative addition of C-H bonds in organic molecules to transition metal centers
[DE89-012991] N89-28616
Monolayers of 11-trichlorosilylundecyl thioacetate: A system that promotes adhesion between silicon dioxide and evaporated gold
[AD-A208266] N89-28637
Deeply bound orbits in picnic atoms and the optical potential
[ETN-89-95463] N89-29176

BOOLEAN FUNCTIONS
Minimization of Boolean sum of products with applications to the computation of reliability of general networks
[VTT-RR-571] N89-29136

BOREHOLES
Stresses and strains in a cold-worked annulus
[AR-005-548] N89-28871
Development of borehole scanner for underground geological survey N89-28899

BORON OXIDES
Investigation of laser-induced fluorescence detection of boron oxides in flames
[AD-A209154] N89-28596

BOTTLES
Helium bottle pressure measurement by portable ultrasonic technique
[AD-A208994] N89-29188

BOUNDARIES
Scattering representation of waveguide/cavity discontinuities using mode-matching and the least-squares boundary residual
[AD-A209571] N89-28686
A note on the communication complexity of totally unimodular matrices
[MEMO-768] N89-29131

BOUNDARY ELEMENT METHOD
Accurate and efficient modeling of global circuit behavior in VSLI layouts
[ETN-89-95459] N89-28732
Computations of optimal controls and designs for distributed systems in optics and elasticity
[AD-A207924] N89-29098

BOUNDARY LAYER COMBUSTION
Supersonic combustion at the DFVLR: Results and experiences
[DFVLR-88-044] N89-28610

BOUNDARY LAYER FLOW
A survey of measurements and measuring techniques in rapidly distorted compressible turbulent boundary layers
[AGARD-AG-315] N89-28734
Large scale motions in supersonic turbulent boundary layers N89-28736
General comments on the interpretation of data — mean flow for rapidly distorted turbulent boundarylayers N89-28742
Review of mean flow data — for compressible boundary layers N89-28743
Review of turbulence data — for turbulent compressible boundary layers N89-28744
The entries N89-28745
The upper-branch stability of compressible boundary layer flows
[NASA-TM-102128] N89-28748

BOUNDARY LAYER STABILITY
A nonlinear investigation of the stationary modes of instability of the three-dimensional compressible boundary layer due to a rotating disc
[NASA-CR-181901] N89-28766

Application of similarity methods to the turbulent diffusion in the convective and stable boundary layer
[WISS-BER-12] N89-28979
BOUNDARY LAYERS
Wake dissipation and total pressure loss in a two-dimensional compressor cascade with crenulated trailing edges
[AD-A209176] N89-28755
BOUNDARY LUBRICATION
A dynamic variation principle for elastic-fluid contacts, applied to elastohydrodynamic lubrication theory
[MEMO-746] N89-28782
A simple numerical algorithm for elastohydrodynamic lubrication, based on a dynamic variation principle
[MEMO-761] N89-28850
BOUNDARY VALUE PROBLEMS
On planar point matching under affine transformation
[AD-A210106] N89-29046
Probabilistic analysis of semilinear partial differential equations
[AD-A209903] N89-29113
Numerical solution of ill posed problems in partial differential equations
[AD-A207852] N89-29119
A hybrid perturbation-Galerkin method for differential equations containing a parameter
[NASA-CR-181891] N89-29122
The stability of the theta-methods in the numerical solution of delay differential equations
[TW-88-08] N89-29127
Approximation methods for scattering from rough surfaces
[AD-A209482] N89-29192
BRAIN
Monte Carlo analysis of localization errors in magnetoencephalography
[DE89-013221] N89-29007
Transient visual evoked neuromagnetic responses: Identification of multiple sources
[DE89-013438] N89-29008
BRAIN DAMAGE
Components of high-level vision: A cognitive neuroscience analysis and accounts of neurological syndromes
[AD-A207848] N89-29011
BRANCHING (MATHEMATICS)
Bifurcation and pattern formation in combustion
[DE89-013629] N89-28590
A torus bifurcation theorem with symmetry
[NASA-CR-185907] N89-29135
BRANCHING (PHYSICS)
Measurement of electroweak effects and topological branching conditions in the reaction e(+)e(-) yields tau(+)tau(-) in the storage ring PETRA
[MPI-PAE/EXP.EL-195] N89-29173
BRAZIL
The Brazilian experience in handling 15 years of remote sensing satellite data N89-28905
BREMSSTRAHLUNG
Compound-lens diode for HERMES 3
[DE89-013065] N89-28708
Proof of the feasibility of coherent and incoherent schemes for pumping a gamma-ray laser
[AD-A208071] N89-28819
BRIGHTNESS
High-brightness electron injectors: A review
[DE89-014244] N89-28711
BUILDINGS
Characterization of painted surfaces in the United States from the perspective of potential damage from acidic deposition
[DE89-014264] N89-28965
Walkthrough-exploring virtual worlds
[AD-A208087] N89-29057
BURNTHROUGH (FAILURE)
Laboratory investigations: Low earth orbit environment chemistry with spacecraft surfaces
[DE89-014280] N89-28533
BURSTS
Numerical simulation of the simultaneous detonation of two identical, fully contained explosions
[DE89-014844] N89-28660
BUTENES
Emerging resin characterization
[AD-A208173] N89-28649

C

C BAND
KRAS: A Danish high resolution airborne SAR N89-28882
CADMIUM SULFIDES
Materials analysis and device optimization of CuInSe2 solar cells
[DE89-009434] N89-28944
Polycrystalline cadmium telluride 3n-i-p solar cell
[DE89-009437] N89-28945
CADMIUM TELLURIDES
Polycrystalline cadmium telluride 3n-i-p solar cell
[DE89-009437] N89-28945
CALENDARS
Calendar of selected aeronautical and space meetings
[AGARD-CAL-89/2] N89-29261
CALIBRATING
Polarimetric calibration using passive corner reflectors
[DFVLR-FB-89-21] N89-28698
Hot-wire anemometry in supersonic flow N89-28738
NIST (National Institute of Standards and Technology) calibration services users guide, 1989 edition
[PB89-200216] N89-28785
KRAS: A Danish high resolution airborne SAR N89-28882
EXAS: Experiment on Autonomous SAR processor calibration N89-28890
Data processing and calibration of SAR data in Japan N89-28918
Significant improvement in IR surface-temperature measurements
[DE89-014808] N89-28926
The acoustic calibration of aircraft fuselage structures, part 1
[ISVR-TR-169-PT-1] N89-29158
CANONICAL FORMS
Canonical integration and analysis of periodic maps using non-standard analysis and Lie methods
[DE89-013369] N89-29106
CANOPIES (VEGETATION)
Daytime turbulent exchange between the Amazon forest and the atmosphere
[NASA-CR-185487] N89-28961
CAPILLARY FLOW
Capillary zone electrophoresis-mass spectrometry of peptides and proteins
[DE89-014466] N89-28592
CAPTURE EFFECT
Solution of the hydrodynamic device model using high-order non-oscillatory shock capturing algorithms
[NASA-CR-181886] N89-29123
CARBON
Infrared study of carbon deposits on catalysts
[DE89-013310] N89-28634
Solid lubrication studied by optical means
[AD-A209008] N89-28836
CARBON DIOXIDE LASERS
Laboratory investigations: Low earth orbit environment chemistry with spacecraft surfaces
[DE89-014280] N89-28533
The manufacture of blazed oblique zone plates for use at 10.6 microns
[NPL-MOM-91] N89-28827
CARBON DIOXIDE REMOVAL
Method and apparatus for bio-regenerative life support system
[NASA-CASE-MSC-21629-1] N89-29027
CARBON FIBER REINFORCED PLASTICS
Determination of moisture diffusion in carbon fiber reinforced epoxy composites by means of radioisotope tracer technique
[BMVG-FBWT-88-2] N89-28581
Composite damaging: Methodological approach
[ETN-89-94866] N89-28582
CARBON MONOXIDE
Development of a postdispersion system for astronomical infrared observations with Fourier spectrometers and its application in the study of the CO fundamental bands in F, G and K stars
[MPE-214] N89-29280
CARBON MONOXIDE LASERS
The 12C16O laser frequency tables for the 34.2 to 62.3 THz (1139 to 2079 cm-1) region
[PB89-193908] N89-28809
CARBON-CARBON COMPOSITES
Explanatory research on the protection of carbon-carbon composites against oxidation at very high temperatures (greater than 3000 F) with Engel-Brewer and other intermetallic compounds
[AD-A207907] N89-28577
CARBONACEOUS MATERIALS
Development of a carbonaceous selective absorber for solar thermal energy collection and process for its formation
[DE89-008587] N89-28949
CARBOXYLIC ACIDS
Infrared study of carbon deposits on catalysts
[DE89-013310] N89-28634
CASTINGS
Metallurgical evaluation of 17-4 PH stainless steel castings
[PB89-193262] N89-28615
CATABOLISM
A program for the study of skeletal muscle catabolism following physical trauma
[AD-A207983] N89-29014
CATALYSTS
Infrared study of carbon deposits on catalysts
[DE89-013310] N89-28634
CATHODE RAY TUBES
Human factors evaluation of color use in the Target Data Processor Release 10 (TDP R10)
[AD-A209438] N89-29023
CATIONS
Ion-molecule chemistry within doubly charged ammonia clusters
[AD-A207764] N89-28608
CAVITATION FLOW
Experimenting cavitation measuring instruments
[CERT-2305] N89-28803
Caviton dynamics in strong Langmuir turbulence
[DE89-012635] N89-29202
CAVITIES
Scattering representation of waveguide/cavity discontinuities using mode-matching and the least-squares boundary residual
[AD-A209571] N89-28686
CAVITONS
Caviton dynamics in strong Langmuir turbulence
[DE89-012635] N89-29202
CELESTIAL MECHANICS
Activities report of the Heidelburg Astronomical Institute of Computation (Germany, F.R.)
[ETN-89-94429] N89-29279
CELL ANODES
Corrosion prevention of lithium-alloy anodes in accumulators with organic electrolytic solutions
[ETN-89-94652] N89-28729
CELLS (BIOLOGY)
Controlled method of reducing electrophoretic mobility of various substances
[NASA-CASE-MFS-26049-1-NP] N89-28603
Energy and Technology Review — analytical cytology
[DE89-013919] N89-28954
CEMENTS
Joint sealants for airport pavements. Phase 1: Laboratory and field investigations
[DOT/FAA/DS-89/2-PHASE-1] N89-28523
CENTRAL PROCESSING UNITS
Experiences in implementing an expert system supported man-machine-interface for the configuration of the intelligent SAR processor N89-28889
EXAS: Experiment on Autonomous SAR processor calibration N89-28890
Performance evaluation of ERS-1 Synthetic Aperture Radar Fast Delivery Processor N89-28904
PC to mainframe connection: IBM PC 3270 emulation
[AD-A209204] N89-29033
The NOSC (Naval Ocean Systems Center) Code 911 Digital Dynamics Processor (DDP): A mildly coupled distributed-computing system
[AD-A210148] N89-29085
CENTRIFUGAL COMPRESSORS
Superconducting Meissner effect bearings for cryogenic turbomachines, phase 1
[AD-A209875] N89-28839
CENTRIFUGES
Higee Technology Development Program, phase 1
[PB89-161434] N89-28587
CERAMIC BONDING
Metallic bonding to high-temperature superconducting ceramics
[DE89-014668] N89-28635
CERAMICS
Highly oriented fiber reinforced ceramic composites
[AD-A208119] N89-28578
Synthesis and hot pressing of ZnS powders
[AD-A209602] N89-28625
Metallic bonding to high-temperature superconducting ceramics
[DE89-014668] N89-28635
Microwave sintering of ceramics
[DE89-014769] N89-28636
Ion implantation of ceramic bearings
[AD-A209770] N89-28644
Survey of test procedures for high performance ceramic materials and their fundamentals
[JUEL-SPEZ-470] N89-28653
Solid lubrication studied by optical means
[AD-A209008] N89-28836
Non-uniform transition conductivity of superconducting ceramic
[NASA-TM-102133] N89-28851
Plastic deformation of YBa2Cu3O7-x superconductor compound
[DE89-613395] N89-29221

Crystal chemistry, magnetic and electrical properties of La(sub2-x)Ba(subx)NiO4
[AD-A209376] N89-29240

CHALCOGENIDES
Preparation of compounds with the tetrahedral structure which transmit in the far infrared
[AD-A208697] N89-28593

CHANNEL FLOW
Calculation of reattaching shear layers in divergent channel with a multiple-time-scale turbulence model
[NASA-TM-102293] N89-28749
On the large-eddy simulation of transitional wall-bounded flows
[NASA-CR-181883] N89-28763

CHANNELS (DATA TRANSMISSION)
Routing channels in VLSI layout
[ISBN-90-6275-535-4] N89-28731

CHAOS
Chaotic behavior in a new class of parallel optimization algorithms
[DE89-014069] N89-29040
Caotic magnetic field line in toroidal plasmas
[IPPJ-911] N89-29211

CHARACTERIZATION
The atomic layer epitaxy growth and characterization of zinc sulfide and alkaline earth sulfide thin films for electroluminescence applications
[ISBN-952-90014-6-0] N89-28613
Emerging resin characterization
[AD-A208173] N89-28649
Apparatus and method for characterizing the transmission efficiency of a mass spectrometer
[NASA-CASE-NPO-16989-1-CU] N89-28794
The new generation SPOT satellites SPOT 4 and 5 N89-28814
Characterization, optimization and design of single-mode multistep fibers
[ETN-89-94440] N89-29197

CHARGE COUPLED DEVICES
Applied field and total dose dependence of trapped charge buildup in MOS devices
[AD-A209064] N89-29237

CHARGE DISTRIBUTION
Investigations of step distributions at Si/SiO2 interfaces using HR-SPA-LEED
[ETN-89-94437] N89-29251

CHARGE TRANSFER
Metal/metallion system in low temperature molten salts
[AD-A208025] N89-28724

CHARGED PARTICLES
The invariance of classical electromagnetism under Charge-conjugation, Parity and Time-reversal (CPT) transformations N89-29161
Applied field and total dose dependence of trapped charge buildup in MOS devices
[AD-A209064] N89-29237
Evidence for two charged particle populations in the Crab nebula
[MPE-PREPRINT-147] N89-29286

CHARTS
Suprathreshold contrast sensitivity vision test chart
[AD-A209915] N89-29010

CHEBYSHEV APPROXIMATION
Signed-digit high speed transcendental function processor architecture
[AD-A209199] N89-29110

CHEMICAL ANALYSIS
Investigation of ambient and high temperature aging of PETN (Pentaerythritol Tetranitrate) by laser induced fluorescence and ultraviolet absorption spectroscopies
[DE89-013740] N89-28813

CHEMICAL BONDS
Oxidative addition of C-H bonds in organic molecules to transition metal centers
[DE89-012991] N89-28616
Chemical effects of Ne(+) bombardment on the MoS2(0001) surface studied by high-resolution photoelectron spectroscopy
[AD-A207734] N89-29247

CHEMICAL COMPOSITION
Investigation of laser-induced fluorescence detection of boron oxides in flames
[AD-A209154] N89-28596
TGMDA/DDS type impregnating resins structural study
[SNEA-9595] N89-28650
Structural definition of synthetic fuels: Wilsonville 1
[DE89-013627] N89-28659
Effect of hydraulic fluid on hydroxylammonium nitrate based liquid propellant formulations
[AD-A208061] N89-28663
Dense heavy metal aerosol monitoring by direct X-ray fluorescence
[AD-A209077] N89-28966

CHEMICAL EFFECTS
Chemical effects of Ne(+) bombardment on the MoS2(0001) surface studied by high-resolution photoelectron spectroscopy
[AD-A207734] N89-29247

CHEMICAL EQUILIBRIUM
Stochastic processes in CHEMFETs
[AD-A208092] N89-28725

CHEMICAL LASERS
Chemical and Laser Sciences Division
[DE89-014385] N89-28811
La Recherche Aerospatiale, bimonthly bulletin, number 1988-6
[ESA-TT-1165] N89-29301

CHEMICAL REACTIONS
Modeling of hot fragment conductive ignition of solid propellants with application to melting and evaporation of solids
[AD-A207727] N89-28662
Hypersonic vehicle environment simulation, phase 1
[AD-A209030] N89-28754

CHIPS
Three dimensional cellular automata for subpixel target detection
[AD-A208163] N89-29100

CHIPS (ELECTRONICS)
Critical problems in very large scale computer systems
[AD-A208070] N89-29035
TWENTENET chip design
[MEMO-INF-88-49] N89-29090

CHIRAL DYNAMICS
Some aspects of a lattice formulation of chiral gauge theories
[NIKHEF-ITFA-88-51] N89-29151

CHLOROCARBONS
Atmospheric processes and effects on materials
[PB89-173215] N89-28964
Absorption cross section of alternative chlorofluoroethanes and potential effects on the ozone layer
[AERONOMICA-ACTA-A-340-1989] N89-28968

CHLOROPHYLLS
Interpretation of remote sensing data from eastern areas of the Baltic Sea N89-28898

CHROMIUM ALLOYS
Theoretical analysis of phase transformations in Fe-Ni Invar-type alloys
[DE89-014454] N89-28618
The influence of structure and alloying on the cold-formability of ferritic steels and the utility of uniaxial tensile testing in its assessment
[ISBN-952-90044-3-5] N89-28632

CHROMIUM STEELS
Effect of temperature and H2S content on the cracking resistance of a 13 percent chromium martensitic stainless steel in acidified NaCl
[NPL-DMA(A)-173] N89-28631

CIRCUIT DIAGRAMS
Routing channels in VLSI layout
[ISBN-90-6275-535-4] N89-28731

CIRCUIT RELIABILITY
Electrical characterization of signal processing microcircuit
[AD-A209078] N89-28714
VLSI integrated circuit contact reliability by interface spectroscopy
[AD-A207666] N89-28718

CIRCUITS
Slotted-waveguide amplifiers for millimeter waves
[AD-A207932] N89-28721
Metal/metallion system in low temperature molten salts
[AD-A208025] N89-28724
Accurate and efficient modeling of global circuit behavior in VSLI layouts
[ETN-89-95459] N89-28732
Method and circuit for controlling the evolution time interval of a laser output pulse
[NASA-CASE-LAR-13772-1] N89-28816
Method and circuit for shaping laser output pulses
[NASA-CASE-LAR-14203-1] N89-28817
Characterization of parallelism and deadlocks in distributed digital logic simulation
[AD-A207842] N89-29138

CIRCULAR POLARIZATION
Contribution to the generation of circular polarization of high purity using planar wire antenna structures
[ETN-89-94659] N89-28872

CIRRUS CLOUDS
ISCCP CX observations during the FIRE/SRB Wisconsin Experiment from October 14 through November 2, 1986
[NASA-TM-101653] N89-28993

CITIES
Ozone trends within a large metropolitan area: The Los Angeles Basin
[PB89-145965] N89-28960

CIVIL AVIATION
Status and development potential of the fly by light technology in civil aircraft
[ILR-MITT-212] N89-28522

CIVIL DEFENSE
SDI (Strategic Defense Initiative): Shield or sword?
[AD-A209777] N89-29141

CLASSICAL MECHANICS
Model reduction of linear conservative mechanical systems
[MEMO-752] N89-28845
Fifth force, sixth force and all that: A theoretical (classical) comment
[DE89-011971] N89-29254

CLASSIFICATIONS
Computer implementation and simulation of some neural networks used in pattern recognition and classification
[AD-A208112] N89-29099

CLIMATE
Climate regulation by marine phytoplankton: A test by anthropogenic SO2 emissions
[DE89-014706] N89-28984

CLIMATOLOGY
ISCCP CX observations during the FIRE/SRB Wisconsin Experiment from October 14 through November 2, 1986
[NASA-TM-101653] N89-28993
The WMO long-term plan overall policy and strategy 1988-1997: Second WMO long-term plan, part 1
[WMO-690-PT-1] N89-28994
The World Climate Program 1988-1997: Second WMO long-term plan, part 2, volume 2
[WMO-692-PT-2-VOL-2] N89-28996

CLOSED ECOLOGICAL SYSTEMS
Method and apparatus for bio-regenerative life support system
[NASA-CASE-MSC-21629-1] N89-29027

CLOSURE LAW
A preliminary compressible second-order closure model for high speed flows
[NASA-CR-181875] N89-28764

CLOUD COVER
Satellite enhanced numerical weather prediction
[AD-A210108] N89-28987

CLOUD PHYSICS
The scavenging of atmospheric pollutants by clouds and precipitation using a vertical wind tunnel, phase 1
[BPT-9/88] N89-28525
Satellite-derived moisture-bogusing profiles for the North Atlantic Ocean
[AD-A207829] N89-28930
Parameterization of ice and water clouds and their radiation transport characteristics for large scale atmospheric models
[MITT-58] N89-28977

CLOUDS (METEOROLOGY)
Parameterization of ice and water clouds and their radiation transport characteristics for large scale atmospheric models
[MITT-58] N89-28977
The sensitivity of Middle East precipitation and cloud forecasts to changes in Eastern Mediterranean Sea surface temperatures
[AD-A207864] N89-28988

COAGULATION
The coagulation and dispersion of nonspherical, aerosol particles in a turbulent atmosphere
[AD-A208064] N89-29150

COAL
Solid lubrication studied by optical means
[AD-A209008] N89-28836

COAL GASIFICATION
Sulfidation/oxidation properties of iron-based alloys containing niobium and aluminum
[DE89-013766] N89-28617

COAL LIQUEFACTION
Structural definition of synthetic fuels: Wilsonville 1
[DE89-013627] N89-28659

COAL UTILIZATION
Chemical Technology Division
[DE89-013917] N89-28591

COATING
Monolayers of 11-trichlorosilylundecyl thioacetate: A system that promotes adhesion between silicon dioxide and evaporated gold
[AD-A208266] N89-28637

COATINGS
Ion implantation of ceramic bearings
[AD-A209770] N89-28644

COBALT
High resolution electron energy loss studies of surface vibrations
[DE89-013964] N89-28589

CODE DIVISION MULTIPLE ACCESS
Packet-error probability analysis for unslotted FH-CDMA (Frequency Hopped-Code Division Multiple-Access) systems with error control coding
[AD-A207964] N89-29054
CODING
Design aspects of a system for geocoding satellite SAR images N89-28915
QuickDraw data structures for image processing
[AD-A208945] N89-29041
A code optimization package for REDUCE
[MEMO-INF-89-29] N89-29070
COEFFICIENTS
An approximation formula to evaluate the coefficient update rate of partially adaptive antennas
[REPT-5-88] N89-28844
COGNITION
Components of high-level vision: A cognitive neuroscience analysis and accounts of neurological syndromes
[AD-A207848] N89-29011
Sleep deprivation and its effect on combat effectiveness
[AD-A207970] N89-29013
COHERENT LIGHT
The copy of single beam holograms
[ISL-CO-212/88] N89-28802
COHERENT RADAR
The airborne pulse Doppler radar: An introduction to the basic principles --- surveillance radar analysis
[BAE-WAA-RP-GEN-RAD-584] N89-28696
COHESION
Cohesion and interparticle forces
[ETN-89-95454] N89-28874
COLD WORKING
The influence of structure and alloying on the cold-formability of ferritic steels and the utility of uniaxial tensile testing in its assessment
[ISBN-952-90044-3-5] N89-28632
Stresses and strains in a cold-worked annulus
[AR-005-548] N89-28871
COLLIMATORS
Investigation of optoelectronic angle measuring systems and their use in a diffraction-optical strain measurement and a photoelectric two-coordinate autocollimator
[PTB-F-5] N89-29199
COLLISION AVOIDANCE
Collision avoidance operational concept
[WP-88W00418] N89-28509
COLLISIONAL PLASMAS
Effects of magnetic and collisional viscosity on the E x B gradient drift instability
[AD-A207975] N89-29205
COLLISIONS
Collisional transfer between and quenching of the 3p 3p and 5p states of the oxygen atom
[AD-A207759] N89-28607
Collision dynamics and transition probabilities for vibrationally excited OH
[AD-A207856] N89-28976
Electric quadrupole excitations in relativistic nucleus-nucleus collisions N89-29164
COLLOIDS
The aggregated state of matter: Elucidating transitions from the gas to the condensed phase and the formation of aerocolloids
[AD-A209080] N89-28595
Dynamics of colloidal dispersions via lattice-gas models of an incompressible fluid
[DE89-013146] N89-28750
COLOR CODING
Human factors evaluation of color use in the Target Data Processor Release 10 (TDP R10)
[AD-A209438] N89-29023
COLUMBUS SPACE STATION
Key structures mechanical issues of the European Space Station and platform program Columbus
[MBB-UD-0041-88-PUB] N89-28561
COLUMNS (SUPPORTS)
Out-of-plane buckling formulae for beam-columns/tie beams
[PB89-191613] N89-28857
New set of buckling parameters for monosymmetric beam-columns/tie beams
[PB89-191639] N89-28858
Flexural-torsional buckling of monosymmetric beam-columns/tie beams
[PB89-191654] N89-28859
COMBAT
US Army role in space
[AD-A209178] N89-28534
A methodology for modeling radar detection range in air combat simulation
[AD-A209153] N89-28679
Sleep deprivation and its effect on combat effectiveness
[AD-A207970] N89-29013
Prevention, reduction, and measurement of combat stress reactions: A bibliography
[AD-A209375] N89-29019
COMBINATORIAL ANALYSIS
Methods of combinatorial optimization and their range of applicability
[MEMO-766] N89-29073
Solution of a tinned iron purchasing problem by Lagrangian relaxation
[MEMO-735] N89-29074
Language constructs and a search procedure to model and solve combinatorial problems
[MEMO-753] N89-29075
COMBINED STRESS
Steel fatigue under combined loads
[ETN-89-94864] N89-28629
COMBUSTION CHAMBERS
Vibration analyzer
[NASA-CASE-MSC-21408-1] N89-28829
COMBUSTION CONTROL
Engine combustion optimization by exhaust analysis
[PB89-195788] N89-28588
COMBUSTION EFFICIENCY
Engine combustion optimization by exhaust analysis
[PB89-195788] N89-28588
COMBUSTION PHYSICS
Microgravity combustion science: A program overview
[NASA-TM-101424] N89-28665
COMBUSTION PRODUCTS
Solid lubrication studied by optical means
[AD-A209008] N89-28836
COMBUSTION STABILITY
Bifurcation and pattern formation in combustion
[DE89-013629] N89-28590
La Recherche Aerospatiale, bimonthly bulletin, number 1988-5
[ESA-TT-1162] N89-29300
COMETS
Study of sampling systems for comets and Mars
[NASA-CR-185514] N89-29292
COMMAND AND CONTROL
Design of a command, communications, and control van (surrogate)
[AD-A207652] N89-28687
Evaluation of functionality in distributed systems
[AD-A209167] N89-29258
COMMERCIAL AIRCRAFT
Statistics on aircraft gas turbine engine rotor failures that occurred in US commercial aviation during 1984
[NAPC-PE-185] N89-28516
Statistics on aircraft gas turbine engine rotor failures that occurred in US commercial aviation during 1985
[NAPC-PE-188] N89-28517
COMMUNICATION EQUIPMENT
US Army role in space
[AD-A209178] N89-28534
Design of a command, communications, and control van (surrogate)
[AD-A207652] N89-28687
COMMUNICATION SATELLITES
Digitally modulated bit error rate measurement system for microwave component evaluation
[NASA-TP-2912] N89-28545
Design of a reliable computing system for the Petite Amateur Navy Satellite (PANSAT)
[AD-A208194] N89-28559
COMMUNICATION THEORY
The communication complexity of interval orders
[MEMO-745] N89-29102
A note on the communication complexity of totally unimodular matrices
[MEMO-768] N89-29131
COMPETITION
Competition and safety in air traffic
[TUB-DISS-PAPER-128] N89-28508
COMPILERS
The performance of a mechanical design Compiler
[AD-A209540] N89-29097
COMPLEX SYSTEMS
A graph-theoretical approach to block-co-polymer complexes. Part 1: Stars
[MEMO-757-PT-1] N89-28654
COMPLEXITY
Gradient Newton-flows for complex polynomials
[MEMO-764] N89-28779
The communication complexity of interval orders
[MEMO-745] N89-29102
A note on the communication complexity of totally unimodular matrices
[MEMO-768] N89-29131
COMPOSITE MATERIALS
A comprehensive guide to the literature on acoustic emission from composites, supplement 2
[DE89-013524] N89-28573
COMPOSITE STRUCTURES
Five year ground exposure of composite materials used on the Bell Model 206L flight service evaluation
[NASA-TM-101645] N89-28579
Delamination test apparatus and method
[NASA-CASE-LAR-13985-1] N89-28586
The structural response of unsymmetrically laminated composite cylinders
[NASA-CR-185834] N89-28856
COMPRESSIBLE BOUNDARY LAYER
A survey of measurements and measuring techniques in rapidly distorted compressible turbulent boundary layers
[AGARD-AG-315] N89-28734
Rapidly distorted compressible boundary-layers N89-28735
Fluctuating wall-pressure measurements N89-28741
General comments on the interpretation of data --- mean flow for rapidly distorted turbulent boundarylayers N89-28742
Review of mean flow data --- for compressible boundary layers N89-28743
Review of turbulence data --- for turbulent compressible boundary layers N89-28744
The entries N89-28745
A nonlinear investigation of the stationary modes of instability of the three-dimensional compressible boundary layer due to a rotating disc
[NASA-CR-181901] N89-28766
La Recherche Aerospatiale, bimonthly bulletin, number 1988-4
[ESA-TT-1161] N89-29299
COMPRESSIBLE FLOW
Skin-friction measurements by laser interferometry N89-28737
Laser Doppler anemometry N89-28739
The upper-branch stability of compressible boundary layer flows
[NASA-TM-102128] N89-28748
Discussion of the potential and limitations of direct and large-eddy simulations
[NASA-CR-181892] N89-28762
A preliminary compressible second-order closure model for high speed flows
[NASA-CR-181875] N89-28764
Heat transfer and film cooling in compressible nozzle flow
[ETN-89-94653] N89-28773
A compressible inverse design method based on an analytical approach
[CUED/A-TURBO/TR-125] N89-28778
COMPRESSING
Analysis and repair of impact damaged composites
[ARL-STRUCT-R-435] N89-28580
COMPRESSION LOADS
The structural response of unsymmetrically laminated composite cylinders
[NASA-CR-185834] N89-28856
COMPRESSION RATIO
Reciprocal perfect and asymptotically perfect periodic radar waveforms and their aperiodic properties
[AD-A208938] N89-28677
COMPRESSION TESTS
Compression tests using Hopkinson bars: Numerical simulation and experimental study
[ISL-C-208/88] N89-28873
COMPRESSOR BLADES
Wake dissipation and total pressure loss in a two-dimensional compressor cascade with crenulated trailing edges
[AD-A209176] N89-28755
COMPRESSORS
Wake dissipation and total pressure loss in a two-dimensional compressor cascade with crenulated trailing edges
[AD-A209176] N89-28755
COMPUTATION
Acousto-optical vector matrix product processor: Implementation issues
[AD-A207933] N89-28722
Implementation of nonhomogeneous Dirichlet boundary conditions in the p-version of the finite element method
[AD-A207799] N89-29118
Research program in computational physics
[DE89-013952] N89-29255
COMPUTATIONAL ASTROPHYSICS
Activities report of the Heidelburg Astronomical Institute of Computation (Germany, F.R.)
[ETN-89-94429] N89-29279

COMPUTATIONAL FLUID DYNAMICS
Study of the wing-vortex interaction in three dimensional flows (incompressible inviscid flow)
[ISL-R-123/87] N89-28494
Role of supercomputer in computational aerodynamics
[PD-CF-8925] N89-28496
Flow calculation over a delta-wing using the thin-layer Navier-Stokes equations
[PD-CF-8924] N89-28497
Correlation of Puma airloads: Evaluation of CFD prediction methods
[NASA-TM-102226] N89-28498
Hypersonic vehicle environment simulation, phase 1
[AD-A209030] N89-28754
Application of computational fluid dynamics to the analysis of the aerodynamics of a railgun projectile
[AD-A207758] N89-28758
Numerical determination of guaranteed Rayleigh numbers and the pertaining flow forms in steady, axisymmetric convection in cylinders
[ETN-89-94432] N89-28769
Solution of Euler equations by a discontinuous Galerkin method obtained from a variational formulation of entropy
[CERT-1/332400/DERI] N89-28775
Numerical grid generation in 3D Euler-flow simulation
[NLR-MP-88013-U] N89-28777
La Recherche Aerospatiale, bimontly bulletin, number 1988-3
[ESA-TT-1137] N89-28781
Effects of real gas in hypersonic expansion
[ETN-89-95200] N89-28783
La Recherche Aerospatiale, bimonthly bulletin, number 1988-6
[ESA-TT-1165] N89-29301

COMPUTATIONAL GEOMETRY
An efficiently computable metric for comparing polygonal shapes
[AD-A210105] N89-29045
On planar point matching under affine transformation
[AD-A210106] N89-29046
Three dimensional reconstruction from serial cross sections by set valued interpolation
[MEMO-754] N89-29076
Placing the largest similar copy of a convex polygon among polygonal obstacles
[AD-A210104] N89-29115

COMPUTATIONAL GRIDS
Development of an efficient solution scheme for incompressible steady-state flow
[AD-A207726] N89-28757
Numerical grid generation in 3D Euler-flow simulation
[NLR-MP-88013-U] N89-28777
Smooth piecewise polynomials as conforming finite elements for plate bending problems
[MEMO-747] N89-28875
Generalized grid files: Description and performance aspects
[MEMO-INF-88-63] N89-29272

COMPUTER AIDED DESIGN
Optimum design methods for structural sandwich panels
[AD-A209427] N89-28575
The manufacture of blazed oblique zone plates for use at 10.6 microns
[NPL-MOM-91] N89-28627
Fault-tolerant computer architecture modeling and analysis
[AD-A209364] N89-29034
A conceptual level design of a design database for the computer-aided prototyping system
[AD-A207808] N89-29050
The design of VLSI circuits
[ETN-89-94968] N89-29065
The performance of a mechanical design Compiler
[AD-A209540] N89-29097
Computer-aided group problem solving for Unified Life Cycle Engineering (ULCE)
[AD-A209446] N89-29260
Transfer of files between IE-32C PC/AT CAD system and Autotrol AD/380 graphics system
[PD-CC-8903] N89-29270
Method bases: A new tool for applied information system design
[NLR-MP-88002-U] N89-29271

COMPUTER AIDED MAPPING
Integrating satellite data with information from topographic maps: Method and applications --- SPOT
[NLR-MP-87035-U] N89-28933

COMPUTER AIDED TOMOGRAPHY
High resolution subsurface imaging with geophysical diffraction tomography
[DE89-013615] N89-28923
Three dimensional reconstruction from serial cross sections by set valued interpolation
[MEMO-754] N89-29076

COMPUTER GRAPHICS
Exploring virtual worlds with head-mounted displays
[AD-A208088] N89-28797
Walkthrough-exploring virtual worlds
[AD-A208087] N89-29057
A heterogeneous multiprocessor graphics system using processor-enhanced memories
[AD-A208099] N89-29058
Photoetched double spiral device
[PD-SE-8911] N89-29071
New dimensions from statistical graphics for GIS (Geographic Information System) analysis and interpretation
[DE89-012339] N89-29263
Transfer of files between IE-32C PC/AT CAD system and Autotrol AD/380 graphics system
[PD-CC-8903] N89-29270

COMPUTER INFORMATION SECURITY
Investigations of nonlinear streamcipher systems: Construction and evaluation methods
[ETN-89-95456] N89-29038
Appraisal of security of data handling systems and products: A tutorial and discussion document --- civil domain
[NPL-DITC-141/89] N89-29092
Strategic defense system distributed operating system R and D review and recommendations
[AD-A208034] N89-29145

COMPUTER NETWORKS
Tools for the development and usage of industrial mathematical software
[NLR-MP-87020-U] N89-29067
An optoelectronic multi-Gb/s packet switching network
[PB89-184345] N89-29081
Chapter on distributed computing
[AD-A208996] N89-29084

COMPUTER PROGRAMMING
Compression tests using Hopkinson bars: Numerical simulation and experimental study
[ISL-C-208/88] N89-28873
A conceptual level design of a design database for the computer-aided prototyping system
[AD-A207808] N89-29050
An object-oriented software reuse tool
[AD-A208018] N89-29056
Software engineering with database management systems
[AD-A208167] N89-29060
Generalized projected gradient-type iterative method for parametric and functional optimization of dynamical systems subject to constraints
[ONERA-NT-1988-9] N89-29083

COMPUTER PROGRAMS
Analysis of leading edge separation using a low order panel method
[NASA-CR-185892] N89-28493
Flow calculation over a delta-wing using the thin-layer Navier-Stokes equations
[PD-CF-8924] N89-28497
Evaluation of LDA 3-component velocity data on a 65 deg delta wing at M = 0.85 and first results of an analysis
[DFVLR-FB-89-19] N89-28505
Direct User Access Terminal (DUAT) operational concept
[WP-88W00075] N89-28524
Design of a reliable computing system for the Petite Amateur Navy Satellite (PANSAT)
[AD-A208194] N89-28559
Optimum design methods for structural sandwich panels
[AD-A209427] N89-28575
Numerical studies of convective heat transfer in an inclined semiannular enclosure
[NASA-TM-102011] N89-28666
A space marching algorithm for the thin-layer Navier-Stokes equations N89-28767
An improving multispectral recording set analysis method N89-28900
Design aspects of a system for geocoding satellite SAR images N89-28915
Engineering and instrumentation support of the AFGL (Air Force Geophysics Laboratory) Research Balloon Program
[AD-A209107] N89-28971
PC to mainframe connection: IBM PC 3270 emulation
[AD-A209204] N89-29033
Critical problems in very large scale computer systems
[AD-A208070] N89-29035
FREQ: A computational package for multivariable system loop-shaping procedures
[NASA-TM-4127] N89-29047
A conceptual level design of a design database for the computer-aided prototyping system
[AD-A207808] N89-29050
Maximum-likelihood parameter estimation of a generalized gumbel distribution
[AD-A207994] N89-29055
APL conversion software
[MEMO-INF-88-21] N89-29062
A code optimization package for REDUCE
[MEMO-INF-89-29] N89-29070
Photoetched double spiral device
[PD-SE-8911] N89-29071
The NOSC (Naval Ocean Systems Center) Code 911 Digital Dynamics Processor (DDP): A mildly coupled distributed-computing system
[AD-A210148] N89-29085
The performance of a mechanical design Compiler
[AD-A209540] N89-29097
Computations of optimal controls and designs for distributed systems in optics and elasticity
[AD-A207924] N89-29098
Linear algebra support modules for approximation and other software
[NPL-DITC-142/89] N89-29126
Minimization of Boolean sum of products with applications to the computation of reliability of general networks
[VTT-RR-571] N89-29136
New dimensions from statistical graphics for GIS (Geographic Information System) analysis and interpretation
[DE89-012339] N89-29263

COMPUTER STORAGE DEVICES
Reliability estimates for large satellite memories in low earth orbits
[DE89-007764] N89-28555
Analysis of cache invalidation patterns in multiprocessors
[AD-A207820] N89-29089

COMPUTER SYSTEMS DESIGN
Critical problems in very large scale computer systems
[AD-A208070] N89-29035
Fault-tolerant computer systems: A survey of some methods and techniques
[MEMO-INF-88-15] N89-29037
A reconfigurable arithmetic processor --- for MIMD computer
[AD-A208323] N89-29082
The NOSC (Naval Ocean Systems Center) Code 911 Digital Dynamics Processor (DDP): A mildly coupled distributed-computing system
[AD-A210148] N89-29085
Method bases: A new tool for applied information system design
[NLR-MP-88002-U] N89-29271

COMPUTER SYSTEMS PERFORMANCE
A code optimization package for REDUCE
[MEMO-INF-89-29] N89-29070
A static load distribution strategy for processor tools
[MEMO-INF-88-43] N89-29078
The performance of a mechanical design Compiler
[AD-A209540] N89-29097
Generalized grid files: Description and performance aspects
[MEMO-INF-88-63] N89-29272

COMPUTER SYSTEMS PROGRAMS
Design and development of a user interface and user manual for a system dynamics model of software management
[AD-A209486] N89-29048
A method of software development using functional programming
[MEMO-INF-88-64] N89-29069

COMPUTER TECHNIQUES
Primary research efforts on exploring the commercial possibilities of thin film growth and materials purification in space
[NASA-CR-184913] N89-28541
Electromagnetic scattering from two dimensional objects using the field feedback formulation
[AD-A209563] N89-28685
Three-dimensional computer analysis and modelling of remote sensing-structural geologic problems
[DE89-010875] N89-28924
Fault-tolerant computer architecture modeling and analysis
[AD-A209364] N89-29034
A conceptual level design of a design database for the computer-aided prototyping system
[AD-A207808] N89-29050
Maximum-likelihood parameter estimation of a generalized gumbel distribution
[AD-A207994] N89-29055
Software engineering with database management systems
[AD-A208167] N89-29060
Backward analysis
[MEMO-INF-89-14] N89-29080

Multicast communication in multiprocessor systems
[AD-A209606] N89-29086
Fundamental processes in partially ionized plasmas
[AD-A207910] N89-29204

COMPUTER VISION
Robotic grasping of unknown objects: A knowledge-based approach
[DE89-013875] N89-28833
An efficiently computable metric for comparing polygonal shapes
[AD-A210105] N89-29045
On planar point matching under affine transformation
[AD-A210106] N89-29046

COMPUTERIZED SIMULATION
Flow calculation over a delta-wing using the thin-layer Navier-Stokes equations
[PD-CF-8924] N89-28497
A detailed survey of the flow passing through an asymmetric contraction and parallel duct
[BAE-WWT-RP-RES-AXR-000194-PT-A] N89-28501
A detailed survey of the flow passing through an asymmetric contraction and parallel duct
[BAE-WWT-RP-RES-AXR-000194-PT-B] N89-28502
Numerical simulation of the simultaneous detonation of two identical, fully contained explosions
[DE89-014844] N89-28660
NEC (Numerical Electromagnetics Code), NECGS (Numerical Electromagnetics Code-Ground Screen), and MININEC (Mini-Numerical Electromagnetics Code) numerical models of LF top-hat monopole antennas
[AD-A209230] N89-28683
Polarimetric calibration using passive corner reflectors
[DFVLR-FB-89-21] N89-28698
Development of an efficient solution scheme for incompressible steady-state flow
[AD-A207726] N89-28757
Fast-algorithm development for large-eddy simulation of circular-jet turbulence
[AD-A207928] N89-28760
Discussion of the potential and limitations of direct and large-eddy simulations
[NASA-CR-181892] N89-28762
On the large-eddy simulation of transitional wall-bounded flows
[NASA-CR-181883] N89-28763
Numerical grid generation in 3D Euler-flow simulation
[NLR-MP-88013-U] N89-28777
Positioning error induced by axial sampling in positron emission tomography
[DE89-014519] N89-28791
Compression tests using Hopkinson bars: Numerical simulation and experimental study
[ISL-C-208/88] N89-28873
Investigation of the effectiveness and applications of Japanese ERS-1 stereoscopic images N89-28884
Fault-tolerant computer architecture modeling and analysis
[AD-A209364] N89-29034
Design and development of a user interface and user manual for a system dynamics model of software management
[AD-A209486] N89-29048
Computer implementation and simulation of some neural networks used in pattern recognition and classification
[AD-A208112] N89-29099
Study and simulation of an E-beam microlithography process on a multilayer resin structure. Research of an optimization
[LAAS-89.012] N89-29179
Orbit correction scheme for the new ring — Amsterdam electron accelerator
[NIKHEF-K/APS/88-04] N89-29184
Caviton dynamics in strong Langmuir turbulence
[DE89-012635] N89-29202
A three-dimensional resistive MHD simulation analysis of field reversal control in the reversed field pinch
[IPPJ-904] N89-29210

CONCENTRATION (COMPOSITION)
Investigation of laser-induced fluorescence detection of boron oxides in flames
[AD-A209154] N89-28596
Interpretation of remote sensing data from eastern areas of the Baltic Sea N89-28898
Ozone trends within a large metropolitan area: The Los Angeles Basin
[PB89-145965] N89-28960
Dense heavy metal aerosol monitoring by direct X-ray fluorescence
[AD-A209077] N89-28966

CONCRETES
Joint sealants for airport pavements. Phase 1: Laboratory and field investigations
[DOT/FAA/DS-89/2-PHASE-1] N89-28523

CONDENSED MATTER PHYSICS
The aggregated state of matter: Elucidating transitions from the gas to the condensed phase and the formation of aerocolloids
[AD-A209080] N89-28595
Proceedings of the Antiproton Technology Workshop held in Upton, New York on 10 May 1989
[AD-A210045] N89-29170

CONDITIONS
A necessary condition for B-convergence of Runge-Kutta methods
[TW-89-01] N89-29129

CONFERENCES
Training Course for Tropical Earth Resources Satellite (EARS) bridging phase
[BCRS-88-16D] N89-28938
Calendar of selected aeronautical and space meetings
[AGARD-CAL-89/2] N89-29261

CONFIGURATION INTERACTION
A graph-theoretical approach to block-co-polymer complexes. Part 1: Stars
[MEMO-757-PT-1] N89-28654

CONGRESSIONAL REPORTS
Departments of Veterans Affairs and Housing and Urban Development and independent agencies appropriations for 1990. Part 6: National Aeronautics and Space Administration
[GPO-99-598] N89-29273

CONICAL BODIES
Almond test body — for microwave anechoic chambers
[NASA-CASE-LAR-13747-1-CU] N89-28672

CONSERVATION EQUATIONS
Time- and volume-averaged conservation equations for multiphase flow
[DE89-012418] N89-28746

CONSERVATION LAWS
Solution of the hydrodynamic device model using high-order non-oscillatory shock capturing algorithms
[NASA-CR-181886] N89-29123

CONSTRAINTS
Composite damaging: Methodological approach
[ETN-89-94866] N89-28582
The application of constraints in query optimization
[MEMO-INF-88-55] N89-29079
On constrained multivariable adaptive control
[LAAS-89.093] N89-29101

CONSTRUCTION
Preliminary design of a consultation knowledge-based system for the minimization of distortion in welded structures
[AD-A208842] N89-28834

CONTAINERS
A method for evaluating structural transducers used in Type B package testing
[DE89-013591] N89-28784

CONTINUOUS WAVE LASERS
Quantitative analysis of laser interferometer waveforms obtained during oxygen reactive-ion etching of thin polymer films
[AD-A207836] N89-29248

CONTINUUM MECHANICS
Differential equations and continuum mechanics — polymers
[AD-A208637] N89-29109

CONTRAST
Suprathreshold contrast sensitivity vision test chart
[AD-A209915] N89-29010

CONTROL MOMENT GYROSCOPES
Consideration of gravity gradient stabilization for ORION
[AD-A207845] N89-28557

CONTROL SYSTEMS DESIGN
Docking mechanism for spacecraft
[NASA-CASE-MSC-21386-1] N89-28552
Spacecraft component heater control system
[NASA-CASE-MFS-28327-1] N89-28556
Method and circuit for controlling the evolution time interval of a laser output pulse
[NASA-CASE-LAR-13772-1] N89-28816
Robust high-performance control for robotic manipulators
[NASA-CASE-NPO-17785-1-CU] N89-28846
Development and implementation of an on-line multivariable control algorithm for the force control of an industrial robot
[OUEL-1748/88] N89-28848
A combined air and water pollution control system
[NASA-CASE-NST-00007-1] N89-28967
FREQ: A computational package for multivariable system loop-shaping procedures
[NASA-TM-4127] N89-29047
Real-time applications of neural nets
[DE89-014400] N89-29093
Computations of optimal controls and designs for distributed systems in optics and elasticity
[AD-A207924] N89-29098
Hamiltonian control systems: Decomposition and clamped dynamics
[MEMO-759] N89-29103

CONTROL THEORY
Robust high-performance control for robotic manipulators
[NASA-CASE-NPO-17785-1-CU] N89-28846
Application of optimal control theory for selective vibrational excitation in molecules modeled as harmonic systems
[MEMO-755] N89-29104

CONTROLLERS
The beam viewer
[LINO-160] N89-28693
Robust high-performance control for robotic manipulators
[NASA-CASE-NPO-17785-1-CU] N89-28846
FREQ: A computational package for multivariable system loop-shaping procedures
[NASA-TM-4127] N89-29047

CONVECTION
Application of special sensor microwave/imager data for analysis of cyclonic storms in midlatitudes over the sea
[AD-A207675] N89-28975
Propagation and saturation of nonlinear inertia-gravity waves in the atmosphere
[AD-A207871] N89-28989

CONVECTION CLOUDS
Daytime turbulent exchange between the Amazon forest and the atmosphere
[NASA-CR-185487] N89-28961

CONVECTIVE HEAT TRANSFER
Numerical studies of convective heat transfer in an inclined semiannular enclosure
[NASA-TM-102011] N89-28666
Enhancement of forced convection heat transfer in tubes using staged tangential flow injection
[PB89-204598] N89-28768

CONVERGENCE
The p-version of the finite element method for domains with corners and for infinite domains
[AD-A207797] N89-29116

CONVERGENT-DIVERGENT NOZZLES
Aerodynamic model tests of exhaust augmentors for F/A-18 engine run-up facility at RAAF Williamtown
[AD-A208110] N89-28518

CONVEXITY
An efficiently computable metric for comparing polygonal shapes
[AD-A210105] N89-29045
Placing the largest similar copy of a convex polygon among polygonal obstacles
[AD-A210104] N89-29115

COOL STARS
Development of a postdispersion system for astronomical infrared observations with Fourier spectrometers and its application in the study of the CO fundamental bands in F, G and K stars
[MPE-214] N89-29280

COOLING SYSTEMS
A cryocooler for high acceleration applications
[AD-A210075] N89-28670

COORDINATES
Least-squares best-fit geometric elements
[NPL-DITC-140/89] N89-29125
Grid generation using elliptic partial differential equations
[DFVLR-FB-89-15] N89-29132

COPOLYMERS
A graph-theoretical approach to block-co-polymer complexes. Part 1: Stars
[MEMO-757-PT-1] N89-28654
A graph-theoretical approach to block-co-polymer complexes. Part 2: Tree approximation
[MEMO-758-PT-2] N89-28655
On strain gages using the PVF2 piezoelectric polymer
[ISL-CO-210/88] N89-28801

COPPER
High resolution electron energy loss studies of surface vibrations
[DE89-013964] N89-28589

COPPER ALLOYS
Aluminum alloy
[NASA-CASE-LAR-13924-1-CU] N89-28621

COPPER CHLORIDES
Lineshape and lifetime studies of exciton luminescence from confined CuCl thin films
[AD-A209750] N89-29243

COPPER OXIDES
Metallic bonding to high-temperature superconducting ceramics
[DE89-014668] N89-28635

Non-uniform transition conductivity of superconducting ceramic
[NASA-TM-102133] N89-28851
CORES
A survey of self-consistency properties in cooperative game theory
[MEMO-763] N89-29072
CORNERS
The p-version of the finite element method for domains with corners and for infinite domains
[AD-A207797] N89-29116
CORRELATION
Determining the location of an observer with respect to aerial photographs
[AD-A207791] N89-28929
CORROSION PREVENTION
In-situ anodising of aluminium alloys — Airbus corrosion prevention requirements
[BAE/WMD/AR/GEN/00666] N89-28630
Corrosion prevention of lithium-alloy anodes in accumulators with organic electrolytic solutions
[ETN-89-94652] N89-28729
CORROSION RESISTANCE
Oxidation and hot corrosion of some advanced superalloys at 1300F to 2000F (740C to 1093C)
[AD-A209353] N89-28622
CORROSION TESTS
Oxidation and hot corrosion of some advanced superalloys at 1300F to 2000F (740C to 1093C)
[AD-A209353] N89-28622
COSMIC RAYS
Electromagnetic interactions of cosmic rays with nuclei N89-29163
Spectral measurements of the cosmic microwave background
[DE89-014895] N89-29296
Quantization by cosmic background radiation
[AD-A208103] N89-29297
COSMOLOGY
Statistical and physical evolution of QSO's
[NASA-CR-185869] N89-29282
Spectral measurements of the cosmic microwave background
[DE89-014895] N89-29296
COST ANALYSIS
Moving optical technology in-house
[AD-A207850] N89-29268
COST EFFECTIVENESS
Thin film photovoltaics
[DE89-009425] N89-28956
COST ESTIMATES
Higee Technology Development Program, phase 1
[PB89-161434] N89-28587
COUETTE FLOW
The anisotropy of the friction pressure of dipolar fluids
[ETN-89-94438] N89-28771
COUNTERMEASURES
Investigations of nonlinear streamcipher systems: Construction and evaluation methods
[ETN-89-95456] N89-29038
COUNTERS
The mock counter: A hybrid optical-electronic counter using fiber delay line memory
[PB89-184410] N89-29031
COUPLINGS
Docking mechanism for spacecraft
[NASA-CASE-MSC-21386-1] N89-28552
CRAB NEBULA
Evidence for two charged particle populations in the Crab nebula
[MPE-PREPRINT-147] N89-29286
CRACK PROPAGATION
A summary of the UK results for a VAMAS round robin project on delamination of composite materials — Versailles project on advanced materials and standards (VAMAS)
[NPL-DMA(A)-179] N89-28584
Fatigue crack growth-microstructural relationship of Ti-6Al-4V
[AD-A208107] N89-28626
Fatigue testing apparatus
[NASA-CASE-LEW-14124-1] N89-28806
Ultrasonic imaging of textured alumina
[NASA-TM-101478] N89-28853
Acoustic emission technology for space applications
[DE89-014449] N89-28861
Cohesion and interparticle forces
[ETN-89-95454] N89-28874
Damage predictions for wind turbine components using the LIFE2 computer code
[DE89-013813] N89-28952
CRACK TIPS
The effect of transients on crack tip stress fields during thermal fatigue loading
[AD-A210084] N89-28864
CRASH INJURIES
Canadian Forces aircrew ejection, descent, and landing injuries, 1 January 1975 - 31 December 1987
[AD-A208116] N89-29015
CREEP PROPERTIES
The interface in tungsten fiber reinforced niobium metal-matrix composites
[NASA-TM-102122] N89-28627
CRITICAL FLOW
The upper-branch stability of compressible boundary layer flows
[NASA-TM-102128] N89-28748
CRITICAL VELOCITY
Experiments on the magnetic field and neutral density limits on CIV interaction
[TRITA-EPP-88-08] N89-29216
On the spoke structure in critical velocity rotating plasmas
[TRITA-EPP-89-01] N89-29217
CROP IDENTIFICATION
Identification of irrigated areas in the Sao Francisco Valley through remote sensing data. Pilot area: Petrolina-Juazeiro
[INPE-4800-RPE/587] N89-28925
CRUSTAL FRACTURES
Three-dimensional computer analysis and modelling of remote sensing-structural geologic problems
[DE89-010875] N89-28924
CRYOGENIC COOLING
A cryocooler for high acceleration applications
[AD-A210075] N89-28670
Superconducting Meissner effect bearings for cryogenic turbomachines, phase 1
[AD-A209875] N89-28839
CRYOGENIC EQUIPMENT
A cryocooler for high acceleration applications
[AD-A210075] N89-28670
Superconducting Meissner effect bearings for cryogenic turbomachines, phase 1
[AD-A209875] N89-28839
CRYOGENIC FLUID STORAGE
COLD-SAT: Cryogenic On-Orbit Liquid Depot-Storage, Acquisition and Transfer
[NASA-TM-102308] N89-28535
CRYOGENIC FLUIDS
Heat-transfer and friction factor design data for all-metal compact heat exchangers
[AD-A208108] N89-28761
CRYOGENIC ROCKET PROPELLANTS
COLD-SAT: Cryogenic On-Orbit Liquid Depot-Storage, Acquisition and Transfer
[NASA-TM-102308] N89-28535
CRYOSTATS
A cryocooler for high acceleration applications
[AD-A210075] N89-28670
CRYPTOGRAPHY
Investigations of nonlinear streamcipher systems: Construction and evaluation methods
[ETN-89-95456] N89-29038
CRYSTAL DISLOCATIONS
Weak beam electron microscopy of dislocation splitting in TiAl: Relationship with plasticity
[ONERA-NT-1988-3] N89-29253
CRYSTAL GROWTH
Fundamental studies of grain boundary structure and properties in ICB aluminum
[DE89-014884] N89-28619
Chiral organic crystals for high power frequency conversion
[DE89-013791] N89-29224
Vertical gradient freeze GaAs: Growth and electrical properties
[DE89-014894] N89-29228
CRYSTAL LATTICES
Dynamics of colloidal dispersions via lattice-gas models of an incompressible fluid
[DE89-013146] N89-28750
Cognition and order in Langmuir-Blodgett films of a 3-hexadecyl pyrrole and ferrocene-derivatized pyrrole mixed monolayer system
[DE89-012974] N89-29223
Crystal chemistry, magnetic and electrical properties of La(sub2-x)Ba(subx)NiO4
[AD-A209376] N89-29240
CRYSTAL STRUCTURE
Thermodynamically stable conducting films of intermetallic PtGa2 on gallium arsenide
[AD-A210077] N89-28716
The amorphous to gamma transformation in ion implanted Al2O3
[DE89-014797] N89-29226
States of oxygen ordering in YBa2Cu3Oz
[DE89-014893] N89-29227
Redetermination of crystal structure of zinc thiogallate
[AD-A208931] N89-29234
CRYSTALLINITY
Digital refractometry of piezoelectric crystalline media
[AD-A209362] N89-29239
CRYSTALS
Holographic modulator arrays
[AD-A209387] N89-28792
Chiral organic crystals for high power frequency conversion
[DE89-013791] N89-29224
Morphology control of photoelectrochemically etched profiles in n-GaAs
[AD-A208991] N89-29235
Digital refractometry of piezoelectric crystalline media
[AD-A209362] N89-29239
Effect of an electric field on a split Bloch band
[AD-A209857] N89-29244
CULTURE TECHNIQUES
Hollow fiber clinostat: Technical abstract
[NASA-CASE-MFS-28370-1] N89-28793
CUMULATIVE DAMAGE
Composite damaging: Methodological approach
[ETN-89-94866] N89-28582
Damage predictions for wind turbine components using the LIFE2 computer code
[DE89-013813] N89-28952
CURIE TEMPERATURE
Pressure induced anomaly at Tc in Fe78 Mo2 B20
[NAL-TM-MT-8806] N89-28628
CURING
A new method for monitoring cure and mobility in epoxy matrix and fiber/epoxy interphases
[AD-A209428] N89-28576
CURRENT DISTRIBUTION
Higher order base dynamics of a bipolar transistor with nonuniform doping
[PB89-155451] N89-28704
Analytical solutions for the field, current density, force force density and mechanical stress distribution in toroidal coil systems
[IPP-2/294] N89-28728
Method of mass producing superconducting persistent current rings
[AD-D013968] N89-29219
CURVATURE
On the Riemannian curvature of a twistor space
[DE89-611897] N89-29107
CYCLES
Some recent results on long cycles in tough graphs
[MEMO-765] N89-29130
CYCLIC HYDROCARBONS
Emerging resin characterization
[AD-A208173] N89-28649
CYCLONES
Application of special sensor microwave/imager data for analysis of cyclonic storms in midlatitudes over the sea
[AD-A207675] N89-28975
CYCLOTRON RADIATION
Electron energy levels in a quantum well within an in-plane magnetic field
[AD-A209351] N89-29256
CYCLOTRON RESONANCE
Microwave emission from relativistic electron beams
[AD-A209653] N89-29181
CYLINDRICAL BODIES
The structural response of unsymmetrically laminated composite cylinders
[NASA-CR-185834] N89-28856
CYLINDRICAL PLASMAS
Stability of a Taylor-relaxed cylindrical plasma separated from the wall by a vacuum layer
[EUT-88-E-207] N89-29200
CYLINDRICAL SHELLS
Exact solutions for symmetric deformations of hollow bodies of ideal fluids with application to inertial stability
[DE89-014374] N89-28753
CYLINDRICAL TANKS
Oxygen storage on zeolites
[AD-A209352] N89-28599
CYTOLOGY
Energy and Technology Review — analytical cytology
[DE89-013919] N89-28954
CZOCHRALSKI METHOD
Factors affecting stress distribution and displacements in crystals 3-5 grown by Czochralski method with liquid encapsulation
[DE89-613396] N89-29222

D

DAMAGE
Characterization of painted surfaces in the United States from the perspective of potential damage from acidic deposition
[DE89-014264] N89-28965

DAMPING
Active damping of vibration in large space structures using a Karhunen-Loeve reduced order model
[AD-A208183] N89-28558
Damping properties of various materials
[AD-A209071] N89-28642
Turbomachinery rotor support with damping
[NASA-CASE-MFS-28345-1] N89-28841
Modelling, information, processing, and control
[AD-A207810] N89-28865
DARK MATTER
Cosmic relics from the big bang
[DE89-013268] N89-29283
DATA ACQUISITION
Airport noise measuring data collction system
[NLR-MP-87006-U] N89-28526
The possibilities of application of satellite data for monitoring ice condition in the Antarctic region N89-28907
Simulation of ERS-1/OPS by the use of airborne spectroradiometer N89-28912
A Compaq-286 micro-processor based high-speed high-density digital data-acquisition and recording system. Volume 1: System overview
[AD-A207429] N89-29029
Ultrasonic systems and system development at SNL Albuquerque
[DE89-013164] N89-29153
Fundamental processes in partially ionized plasmas
[AD-A207910] N89-29204
DATA BASE MANAGEMENT SYSTEMS
A conceptual level design of a design database for the computer-aided prototyping system
[AD-A207808] N89-29050
Software engineering with database management systems
[AD-A208167] N89-29060
Optical laser technology and its application to Defense Manpower Data Center's (DMDC) querry facsimile (QFAX) data base system
[AD-A207832] N89-29194
Implementation of a distributed object-oriented database management system
[AD-A209437] N89-29265
Generalized grid files: Description and performance aspects
[MEMO-INF-88-63] N89-29272
DATA BASES
Materials aerometric database for use in developing materials damage functions
[PB89-181259] N89-28572
A survey of JP-8 and JP-5 properties
[AD-A207721] N89-28661
A conceptual level design of a design database for the computer-aided prototyping system
[AD-A207808] N89-29050
A programming language supporting first-class parallel environments
[AD-A207833] N89-29051
Optical laser technology and its application to Defense Manpower Data Center's (DMDC) querry facsimile (QFAX) data base system
[AD-A207832] N89-29194
Transfer of files between IE-32C PC/AT CAD system and Autotrol AD/380 graphics system
[PD-CC-8903] N89-29270
DATA CORRELATION
Near-neighbor algorithms for processing bearing data
[AD-A207935] N89-29053
DATA MANAGEMENT
Local area network and data network for the Advanced Earth Observing Satellite, ADEOS system N89-28886
Tools for the development and usage of industrial mathematical software
[NLR-MP-87020-U] N89-29067
Analysis of cache invalidation patterns in multiprocessors
[AD-A207820] N89-29089
International technology transfer as practiced by the U.S.S.R.: Implications for US national security
[AD-A208010] N89-29274
DATA PROCESSING
Modelling, information, processing, and control
[AD-A207810] N89-28865
Local area network and data network for the Advanced Earth Observing Satellite, ADEOS system N89-28886
The Brazilian experience in handling 15 years of remote sensing satellite data N89-28905
National program for handling large volumes of satellite data N89-28910
Simulation of ERS-1/OPS by the use of airborne spectroradiometer N89-28912
Data processing and calibration of SAR data in Japan N89-28918
Study of an advanced civil earth remote sensing system: Executive summary
[PB89-163208] N89-28922
Results of Seasat altimeter data processing for the northeast Atlantic
[BCRS-89-05] N89-28940
A Compaq-286 micro-processor based high-speed high-density digital data-acquisition and recording system. Volume 1: System overview
[AD-A207429] N89-29029
A programming language supporting first-class parallel environments
[AD-A207833] N89-29051
Appraisal of security of data handling systems and products: A tutorial and discussion document --- civil domain
[NPL-DITC-141/89] N89-29092
Signed-digit high speed transcendental function processor architecture
[AD-A209199] N89-29110
DATA PROCESSING EQUIPMENT
A logic query language and its algebraic optimization for a multiprocessor database machine
[MEMO-INF-88-52] N89-29068
DATA PROCESSING TERMINALS
PC to mainframe connection: IBM PC 3270 emulation
[AD-A209204] N89-29033
DATA RECORDING
A Compaq-286 micro-processor based high-speed high-density digital data-acquisition and recording system. Volume 1: System overview
[AD-A207429] N89-29029
DATA SMOOTHING
An algorithm for smooth interpolation to scattered data in R2
[MEMO-748] N89-29066
DATA STORAGE
Two-dimensional signal processing and storage and theory and applications of electromagnetic measurements
[AD-A207827] N89-28689
A Compaq-286 micro-processor based high-speed high-density digital data-acquisition and recording system. Volume 1: System overview
[AD-A207429] N89-29029
A conceptual level design of a design database for the computer-aided prototyping system
[AD-A207808] N89-29050
Multicast communication in multiprocessor systems
[AD-A209606] N89-29086
Moving optical technology in-house
[AD-A207850] N89-29268
Generalized grid files: Description and performance aspects
[MEMO-INF-88-63] N89-29272
DATA STRUCTURES
Intelligent multi-sensor integrations
[NASA-CR-185846] N89-28562
QuickDraw data structures for image processing
[AD-A208945] N89-29041
A programming language supporting first-class parallel environments
[AD-A207833] N89-29051
DATA SYSTEMS
Appraisal of security of data handling systems and products: A tutorial and discussion document --- civil domain
[NPL-DITC-141/89] N89-29092
DATA TRANSMISSION
Digitally modulated bit error rate measurement system for microwave component evaluation
[NASA-TP-2912] N89-28545
DECAY
Lineshape and lifetime studies of exciton luminescence from confined CuCl thin films
[AD-A209750] N89-29243
DECISION MAKING
Risk management for air ambulance helicopters operators
[DOT/FAA/DS-88/7] N89-28506
A method for assisting in decision-making for multilayer radar absorbent coverings --- manufacture
[ONERA-NT-1989-2] N89-28703
Airborne FLIR (Forward Looking Infrared) detection of surface targets
[AD-A209250] N89-29189
Evaluation of functionality in distributed systems
[AD-A209167] N89-29258
DECODERS
Design, performance and test standards for flight termination receiver/decoders. Volume 1: Design and performance requirements
[AD-A209644] N89-28544
DECOMPOSITION
Theoretical analysis of phase transformations in Fe-Ni Invar-type alloys
[DE89-014454] N89-28618
Investigation of ambient and high temperature aging of PETN (Pentaerythritol Tetranitrate) by laser induced fluorescence and ultraviolet absorption spectroscopies
[DE89-013740] N89-28813
DEFENSE PROGRAM
Advanced power sources for space missions
[NASA-TM-101811] N89-28565
SDI (Strategic Defense Initiative): Shield or sword?
[AD-A209777] N89-29141
DEFLECTION
Static and dynamic deflection studies of the SRM aft case-nozzle joint
[NASA-TM-100373] N89-28568
DEFORMATION
Exact solutions for symmetric deformations of hollow bodies of ideal fluids with application to inertial stability
[DE89-014374] N89-28753
Plastic deformation of YBa2Cu3O7-x superconductor compound
[DE89-613395] N89-29221
DEGRADATION
VLSI integrated circuit contact reliability by interface spectroscopy
[AD-A207666] N89-28718
A new holographic inverse filtering method and its application to restoration of degraded remote sensing images N89-28877
DEGREES OF FREEDOM
Total Lagrangian formulation for large-displacement analysis of the triangular finite elements
[AD-A209378] N89-29111
DELAMINATING
Measurement of mode 1 and mode 2 strain energy release rates: A VAMAS round robin project on delamination of composite materials --- Versailles project on advanced materials and standards (VAMAS)
[NPL-DMA(A)-178] N89-28583
A summary of the UK results for a VAMAS round robin project on delamination of composite materials --- Versailles project on advanced materials and standards (VAMAS)
[NPL-DMA(A)-179] N89-28584
Delamination test apparatus and method
[NASA-CASE-LAR-13985-1] N89-28586
DELAY LINES (COMPUTER STORAGE)
Photonic architectures for performing perfect shuffle on a time-division multiplexed signal
[PB89-184352] N89-28674
The mock counter: A hybrid optical-electronic counter using fiber delay line memory
[PB89-184410] N89-29031
DELTA WINGS
Comparison of flow-visualised vortices with computed geometry over thin delta wings
[AD-A209083] N89-28489
Flow calculation over a delta-wing using the thin-layer Navier-Stokes equations
[PD-CF-8924] N89-28497
Evaluation of LDA 3-component velocity data on a 65 deg delta wing at M = 0.85 and first results of an analysis
[DFVLR-FB-89-19] N89-28505
DEMAGNETIZATION
The fluxgate ringcore sensor demagnetising factor and noise
[ORI-1-89] N89-28805
DEMODULATION
Digital carrier demodulator employing components working beyond normal limits
[NASA-CASE-NPO-17628-1-CU] N89-28684
DENSIFICATION
Microwave sintering of ceramics
[DE89-014769] N89-28636
DENSITY DISTRIBUTION
Maximum-likelihood parameter estimation of a generalized gumbel distribution
[AD-A207994] N89-29055
DEOXYRIBONUCLEIC ACID
Energy and Technology Review --- analytical cytology
[DE89-013919] N89-28954
DEPOSITION
Polycrystalline cadmium telluride 3n-i-p solar cell
[DE89-009437] N89-28945
DEPOSITS
Oxidation and hot corrosion of some advanced superalloys at 1300F to 2000F (740C to 1093C)
[AD-A209353] N89-28622
Infrared study of carbon deposits on catalysts
[DE89-013310] N89-28634

DEPTH
Kinematic vertical positioning using the global positioning system
[ETN-89-94804] N89-28510
Television monitor field shifter and an opto-electronic method for obtaining a stereo image of optimal depth resolution and reduced depth distortion on a single screen
[NASA-CASE-NPO-17249-1-CU] N89-28676

DESIGN ANALYSIS
Key structures mechanical issues of the European Space Station and platform program Columbus
[MBB-UD-0041-88-PUB] N89-28561
A medium resolution imaging spectrometer for the European polar orbiting platform
[ETN-89-95235] N89-28563
Higee Technology Development Program, phase 1
[PB89-161434] N89-28587
The Mark 101 flux compression generator: Development progress
[DE89-014296] N89-28712
Tactile sensing and the photoelastic tactile sensor
[OUEL-1758/89] N89-28849
A conceptual study of optical earth observation from geosynchronous orbit N89-28880
TWENTENET chip design
[MEMO-INF-88-49] N89-29090
Apertures of ring quadrupoles and sextupoles
[NIKHEF-K/APS/88-03] N89-29183
Updated OC scheme --- electron orbit correction
[NIKHEF-K/APS/88-04A] N89-29185
Detection of target formations in infrared imagery
[ETCA-88-R-070] N89-29198

DETECTION
Investigation of laser-induced fluorescence detection of boron oxides in flames
[AD-A209154] N89-28596
Adaptive detection and parameter estimation for multidimensional signal models
[AD-A208971] N89-28678
Investigation of a linear systems model for human visual detection and spatial frequency discrimination
[AD-A209397] N89-29022
Three dimensional cellular automata for subpixel target detection
[AD-A208163] N89-29100

DETERIORATION
Effect of environmental factors on pavement deterioration. Volume 1: Background and methodology
[PB89-182109] N89-28668

DETERMINANTS
An explicit separation of relativised random polynomial time and relativised deterministic polynomial time
[AD-A210103] N89-29044
Interpolating polynomials from their values
[AD-A210102] N89-29114

DETONATION
Numerical simulation of the simultaneous detonation of two identical, fully contained explosions
[DE89-014844] N89-28660

DEUTERIUM
Molecular beam experiment for the determination of differential cross sections of the reaction of deuterium atoms with vibrationally excited hydrogen molecules
[MPIS-10/1988] N89-29178

DIELECTRIC PROPERTIES
The relationship between ground permittivity and the input impedance of a horizontal dipole near ground
[AD-A207746] N89-28688

DIELECTRICS
Increase of the damage thresholds of dielectric layer systems for the Nd laser
[ETN-89-94436] N89-28824

DIFFERENCE EQUATIONS
Difference techniques for solving the advection equation
[WISS-BER-6] N89-28991

DIFFERENTIAL EQUATIONS
Formulation and numerical solution of the equations of constrained mechanical motion
[DFVLR-FB-89-06] N89-28847
Canonical integration and analysis of periodic maps using non-standard analysis and Lie methods
[DE89-013369] N89-29106
Differential equations and continuum mechanics --- polymers
[AD-A208637] N89-29109
A hybrid perturbation-Galerkin method for differential equations containing a parameter
[NASA-CR-181891] N89-29122
The stability of the theta-methods in the numerical solution of delay differential equations
[TW-88-08] N89-29127
On the solving of stochastic Ito differential equations by simulation
[ETN-89-94610] N89-29134

DIFFRACTION
High resolution subsurface imaging with geophysical diffraction tomography
[DE89-013615] N89-28923

DIFFRACTOMETERS
A new scattering formula for depth-resolving X-ray diffractometry based on a kinematic theory
[ETN-89-94430] N89-29195

DIFFUSION
Determination of moisture diffusion in carbon fiber reinforced epoxy composites by means of radioisotope tracer technique
[BMVG-FBWT-88-2] N89-28581

DIFFUSION COEFFICIENT
Use of microelectrode arrays to directly measure diffusion of ions in solid electrolytes: Proof of concept experiments involving Ag+ in a solid polymer electrolyte
[AD-A209536] N89-28604

DIFFUSION ELECTRODES
Modelling the in situ infrared reflection-absorption spectra of the diffuse layer
[AD-A209347] N89-28598
Use of microelectrode arrays to directly measure diffusion of ions in solid electrolytes: Proof of concept experiments involving Ag+ in a solid polymer electrolyte
[AD-A209536] N89-28604

DIGITAL DATA
Digitally modulated bit error rate measurement system for microwave component evaluation
[NASA-TP-2912] N89-28545
A practical method of remotely sensed digital image's resolving power N89-28879
Zeiss Digital Mapping: A new hardware and software system concept from Kombinat VEB Carl Zeiss JENA N89-28891
Development of borehole scanner for underground geological survey N89-28899
Studies on object reconstruction from space using three line scanner imagery N89-28919

DIGITAL ELECTRONICS
Digital optical computing with fibers and directional couplers
[PB89-184378] N89-29030
A real time microcomputer implementation of sensor failure detection for turbofan engines
[NASA-TM-102327] N89-29032

DIGITAL FILTERS
Digital carrier demodulator employing components working beyond normal limits
[NASA-CASE-NPO-17628-1-CU] N89-28684
Two-dimensional signal processing and storage and theory and applications of electromagnetic measurements
[AD-A207827] N89-28689

DIGITAL SIMULATION
A model for the simulation of the DC and small-signal behavior of the bipolar transistor
[ETN-89-94442] N89-28727
On the solving of stochastic Ito differential equations by simulation
[ETN-89-94610] N89-29134
Characterization of parallelism and deadlocks in distributed digital logic simulation
[AD-A207842] N89-29138

DIGITAL SYSTEMS
An experimental optical coupling device for an airborne digital redundant system
[NAL-TR-1003] N89-28514
Two-dimensional signal processing and storage and theory and applications of electromagnetic measurements
[AD-A207827] N89-28689
Investigation of a linear systems model for human visual detection and spatial frequency discrimination
[AD-A209397] N89-29022
A Compaq-286 micro-processor based high-speed high-density digital data-acquisition and recording system. Volume 1: System overview
[AD-A207429] N89-29029
Bit rate recovery using digital ladder networks
[AD-A209865] N89-29043
The NOSC (Naval Ocean Systems Center) Code 911 Digital Dynamics Processor (DDP): A mildly coupled distributed-computing system
[AD-A210148] N89-29085
Conversion of hard-copy documents to digital format utilizing optical scanners and optical storage media
[AD-A209473] N89-29266

DIGITAL TECHNIQUES
Digital carrier demodulator employing components working beyond normal limits
[NASA-CASE-NPO-17628-1-CU] N89-28684
TiME: Time and memory efficient distance transformations for parallel and pyramid machines
[FOA-C-30531-3.4] N89-29091

DIMENSIONAL MEASUREMENT
NIST (National Institute of Standards and Technology) calibration services users guide, 1989 edition
[PB89-200216] N89-28785
Achievement of the optimum performance from laser interferometer systems when applied to precision length measurement in the free atmosphere
[NPL-MOM-92] N89-28825
Anthropometric survey of US Army personnel: Summary statistics
[AD-A209600] N89-29025

DIMENSIONAL STABILITY
A torus bifurcation theorem with symmetry
[NASA-CR-185907] N89-29135

DIMETHYLHYDRAZINES
Synthesis of monomethylhydrazine
[ETN-89-94863] N89-28664

DIODES
Compound-lens diode for HERMES 3
[DE89-013065] N89-28708
An improved hibachi support structure for electron-beam diode foils
[DE89-014023] N89-28810

DIPOLE MOMENTS
The anisotropy of the friction pressure of dipolar fluids
[ETN-89-94438] N89-28771

DIRAC EQUATION
Some aspects of a lattice formulation of chiral gauge theories
[NIKHEF-ITFA-88-51] N89-29151

DIRECT CURRENT
A model for the simulation of the DC and small-signal behavior of the bipolar transistor
[ETN-89-94442] N89-28727

DIRECTIONAL CONTROL
Low-speed static and dynamic force tests of a generic supersonic cruise fighter configuration
[NASA-TM-4138] N89-28486

DIRECTIONAL COUPLERS
Photonic architectures for performing perfect shuffle on a time-division multiplexed signal
[PB89-184352] N89-28674
Digital optical computing with fibers and directional couplers
[PB89-184378] N89-29030
The mock counter: A hybrid optical-electronic counter using fiber delay line memory
[PB89-184410] N89-29031
Theoretical investigations of an integrated optics switching element with asymmetric directional couplers for switching matrices
[ETN-89-94439] N89-29196

DIRECTIONAL STABILITY
Low-speed static and dynamic force tests of a generic supersonic cruise fighter configuration
[NASA-TM-4138] N89-28486

DIRICHLET PROBLEM
Variational formulation for a nonlinear elliptic equation in a three-dimensional exterior domain
[NASA-CR-181885] N89-29028
Implementation of nonhomogeneous Dirichlet boundary conditions in the p-version of the finite element method
[AD-A207799] N89-29118

DISCRETE FUNCTIONS
Optimal error analysis of spectral methods with emphasis on non-constant coefficients and deformed geometries
[NASA-CR-181902] N89-29124

DISPENSERS
High temperature tribometer, phase 1
[AD-A209356] N89-28838

DISPERSIONS
Pressure drop and heat transfer characteristics of nearly neutrally buoyant particulate slurry for advanced energy transmission fluids
[DE89-013645] N89-28751

DISPLACEMENT
Total Lagrangian formulation for large-displacement analysis of the triangular finite elements
[AD-A209378] N89-29111
Factors affecting stress distribution and displacements in crystals 3-5 grown by Czochralski method with liquid encapsulation
[DE89-613396] N89-29222

DISPLAY DEVICES
Choice and perceived control: Implications for the design of displays
[AD-A208400] N89-29021
Human factors evaluation of color use in the Target Data Processor Release 10 (TDP R10)
[AD-A209438] N89-29023
QuickDraw data structures for image processing
[AD-A208945] N89-29041
Display characteristics of example light-valve projectors
[AD-A209580] N89-29193

DISSIPATION
Wake dissipation and total pressure loss in a two-dimensional compressor cascade with crenulated trailing edges
[AD-A209176] N89-28755
DISSOCIATION
Vibrational dynamics of aniline (Ar)1 and aniline (CH4)1 clusters
[AD-A209560] N89-28605
DISSOLVING
Molecular weight dependence of e-beam resist sensitivity
[AD-A207835] N89-28719
DISTANCE
TiME: Time and memory efficient distance transformations for parallel and pyramid machines
[FOA-C-30531-3.4] N89-29091
DISTILLATION
Structural definition of synthetic fuels: Wilsonville 1
[DE89-013627] N89-28659
DISTORTION
Preliminary design of a consultation knowledge-based system for the minimization of distortion in welded structures
[AD-A208842] N89-28834
DISTRIBUTED AMPLIFIERS
Optical gain control of GaAs microwave monolithic integrated circuit distributed amplifier
[AD-D013969] N89-28705
DISTRIBUTED PROCESSING
Intelligent multi-sensor integrations
[NASA-CR-185846] N89-28562
Parallel language constructs for tensor product computations on loosely coupled architectures
[NASA-CR-181900] N89-29061
A logic query language and its algebraic optimization for a multiprocessor database machine
[MEMO-INF-88-52] N89-29068
The application of constraints in query optimization
[MEMO-INF-88-55] N89-29079
Chapter on distributed computing
[AD-A208996] N89-29084
The NOSC (Naval Ocean Systems Center) Code 911 Digital Dynamics Processor (DDP): A mildly coupled distributed-computing system
[AD-A210148] N89-29085
Northeast artificial intelligence consortium annual report 1987. Volume 8: Knowledge base maintenance using logic programming methodologies
[AD-A209453] N89-29095
Strategic defense system distributed operating system R and D review and recommendations
[AD-A208034] N89-29145
Evaluation of functionality in distributed systems
[AD-A209167] N89-29258
Implementation of a distributed object-oriented database management system
[AD-A209437] N89-29265
DOCUMENT STORAGE
QuickDraw data structures for image processing
[AD-A208945] N89-29041
Conversion of hard-copy documents to digital format utilizing optical scanners and optical storage media
[AD-A209473] N89-29266
DOMAINS
The p-version of the finite element method for domains with corners and for infinite domains
[AD-A207797] N89-29116
DOPPLER EFFECT
The use of high-frequency pulsed laser diodes in fringe type laser Doppler anemometry
[ISL-CO-230/88] N89-28826
DOPPLER RADAR
Storm models for end-to-end TDWR (Terminal Doppler Weather Radar) signal processing simulation tests
[AD-A209384] N89-28966
DRAG REDUCTION
Glider ground effect investigation
[AD-A209152] N89-28490
DRILLS
In search of more output: Two strain gage bridge circuits revisited
[DE89-014039] N89-28787
DRYING
Freeze-dried tungsten heavy alloys
[DE89-014933] N89-28620
DUALITY THEOREM
On adjoints and dual matroids
[MEMO-767] N89-29146
DUST
Hazards of explosives dusts
[DE89-014554] N89-28669
DWARF STARS
Evolution of wide binary millisecond pulsars in globular clusters
[MPE-PREPRINT-148] N89-29285
DYNAMIC CHARACTERISTICS
Modelling orientation parameters of sensor platforms N89-28881
The sensitivity of Middle East precipitation and cloud forecasts to changes in Eastern Mediterranean Sea surface temperatures
[AD-A207864] N89-28988
Total Lagrangian formulation for large-displacement analysis of the triangular finite elements
[AD-A209378] N89-29111
Caviton dynamics in strong Langmuir turbulence
[DE89-012635] N89-29202
DYNAMIC CONTROL
Nonlinear dynamics and control of flexible structures
[AD-A208120] N89-28869
DYNAMIC LOADS
Optimization of structures with passive damping and active controls
[AD-A208937] N89-28862
DYNAMIC MODELS
Robust high-performance control for robotic manipulators
[NASA-CASE-NPO-17785-1-CU] N89-28846
Nonlinear dynamics and control of flexible structures
[AD-A208120] N89-28869
DYNAMIC PROGRAMMING
On the composition of interconnected systems by nonserial dynamic programming: Application to power systems
[LAAS-89.096] N89-29064
Hamiltonian control systems: Decomposition and clamped dynamics
[MEMO-759] N89-29103
DYNAMIC RESPONSE
FREQ: A computational package for multivariable system loop-shaping procedures
[NASA-TM-4127] N89-29047
DYNAMIC STRUCTURAL ANALYSIS
Optimization of structures with passive damping and active controls
[AD-A208937] N89-28862
DYNAMIC TESTS
Low-speed static and dynamic force tests of a generic supersonic cruise fighter configuration
[NASA-TM-4138] N89-28486
Electrical characterization of signal processing microcircuit
[AD-A209078] N89-28714
DYNAMICAL SYSTEMS
Generalized projected gradient-type iterative method for parametric and functional optimization of dynamical systems subject to constraints
[ONERA-NT-1988-9] N89-29063
Hamiltonian control systems: Decomposition and clamped dynamics
[MEMO-759] N89-29103

E

E REGION
Ionospheric variability
[AD-A209251] N89-28972
EARDRUMS
A study of the effect of stimulus upon the reflex response as elicited and recorded by the tympanic membrane displacement measurement device
[ISVR-TR-177] N89-29018
EARTH (PLANET)
Orbits containing arcs of minimum altitude variation
[AD-A209206] N89-28539
EARTH CRUST
Three-dimensional computer analysis and modelling of remote sensing-structural geologic problems
[DE89-010875] N89-28924
EARTH IONOSPHERE
Atmospheric influence on microwave remote sensing at different frequencies: Results of the 1st September 1987 DUSCAT flight
[BCRS-89-07] N89-28941
EARTH MAGNETOSPHERE
Electric fields in earth orbital space
[AD-A209542] N89-28973
EARTH OBSERVATIONS (FROM SPACE)
US Army role in space
[AD-A209178] N89-28534
A Bistatic Parasitical Radar (BIPAR) N89-28878
A conceptual study of optical earth observation from geosynchronous orbit N89-28880
Outline of MOS-1 Verification Program (MVP) N89-28883
Local area network and data network for the Advanced Earth Observing Satellite, ADEOS system N89-28886
Earth observation programs in Japan N89-28920
Activities report of ESA
[ISSN-0258-025X] N89-29302
EARTH ORBITAL ENVIRONMENTS
Laboratory investigations: Low earth orbit environment chemistry with spacecraft surfaces
[DE89-014280] N89-28533
EARTH ORBITS
Reliability estimates for large satellite memories in low earth orbits
[DE89-007764] N89-28555
Electric fields in earth orbital space
[AD-A209542] N89-28973
EARTH RADIATION BUDGET
Errors in the scene identification from satellite data. Effects on the determination of radiation budget parameters
[MITT-59] N89-28931
EARTH RADIATION BUDGET EXPERIMENT
ISCCP CX observations during the FIRE/SRB Wisconsin Experiment from October 14 through November 2, 1986
[NASA-TM-101653] N89-28993
EARTH SURFACE
The relationship between ground permittivity and the input impedance of a horizontal dipole near ground
[AD-A207746] N89-28688
ECCENTRICITY
Numerical determination of the location of critical inclinations for long term high eccentricity orbits about Mars
[AD-A209200] N89-28538
ECOLOGY
ELF (Extremely Low Frequency) communications system ecological monitoring program
[AD-A208198] N89-28691
ECONOMIC ANALYSIS
Biofuels technical information guide
[DE89-000894] N89-28658
ECOSYSTEMS
Adequacy of forestry data in assessing the impact of ozone: A national perspective
[DE89-012359] N89-28962
EDUCATION
Activities report of the Institute of Space Research
[ILR-1986/87] N89-28536
Training Course for Tropical Earth Resources Satellite (EARS) bridging phase
[BCRS-88-16D] N89-28938
Calendar of selected aeronautical and space meetings
[AGARD-CAL-89/2] N89-29261
EFFICIENCY
An evaluation of blazed zone plates for use in the 10 micron spectral region
[NPL-MOM-93] N89-28828
Materials analysis and device optimization of CuInSe2 solar cells
[DE89-009434] N89-28944
An a priori approach to the evaluation of signature analysis efficiency
[IMAG-RR-746-I] N89-29140
Experiments on the magnetic field and neutral density limits on CIV interaction
[TRITA-EPP-88-08] N89-29216
EIGENVALUES
A survey of self-consistency properties in cooperative game theory
[MEMO-763] N89-29072
EIGENVECTORS
A survey of self-consistency properties in cooperative game theory
[MEMO-763] N89-29072
EJECTION INJURIES
Canadian Forces aircrew ejection, descent, and landing injuries, 1 January 1975 - 31 December 1987
[AD-A208116] N89-29015
ELASTIC BENDING
Smooth piecewise polynomials as conforming finite elements for plate bending problems
[MEMO-747] N89-28875
ELASTIC BODIES
Total Lagrangian formulation for large-displacement analysis of the triangular finite elements
[AD-A209378] N89-29111
ELASTIC BUCKLING
Out-of-plane buckling formulae for beam-columns/tie beams
[PB89-191613] N89-28857
New set of buckling parameters for monosymmetric beam-columns/tie beams
[PB89-191639] N89-28858
Flexural-torsional buckling of monosymmetric beam-columns/tie beams
[PB89-191654] N89-28859
ELASTIC DEFORMATION
A simple numerical algorithm for elastohydrodynamic lubrication, based on a dynamic variation principle
[MEMO-761] N89-28850

Total Lagrangian formulation for large-displacement analysis of the triangular finite elements
[AD-A209378] N89-29111

ELASTIC PROPERTIES
Modelling, information, processing, and control
[AD-A207810] N89-28885
Computations of optimal controls and designs for distributed systems in optics and elasticity
[AD-A207924] N89-29098

ELASTOHYDRODYNAMICS
A dynamic variation principle for elastic-fluid contacts, applied to elastohydrodynamic lubrication theory
[MEMO-746] N89-28782
A simple numerical algorithm for elastohydrodynamic lubrication, based on a dynamic variation principle
[MEMO-761] N89-28850

ELECTRIC BATTERIES
Chemical Technology Division
[DE89-013917] N89-28591

ELECTRIC BRIDGES
In search of more output: Two strain gage bridge circuits revisited
[DE89-014039] N89-28787

ELECTRIC CONNECTORS
Laser-induced diode linking for wafer-scale integration
[AD-A207921] N89-28818

ELECTRIC DIPOLES
Electric quadrupole excitations in relativistic nucleus-nucleus collisions N89-29164
Electric quadrupole excitations in the interactions of Y-89 with relativistic nuclei N89-29165

ELECTRIC FIELD STRENGTH
Effect of an electric field on a split Bloch band
[AD-A209857] N89-29244

ELECTRIC FIELDS
On the use of the FEL to produce high transient space-charge potentials in a magnetized plasma
[DE89-014325] N89-28814
Parallel electric fields in a simulation of magnetotail reconnection and plasmoid evolution
[DE89-012622] N89-28970
Electric fields in earth orbital space
[AD-A209542] N89-28973
Analysis of the VHF-UHF electromagnetic radiation of lightning: Application to a model of the negative stepped-leader propagation
[ONERA-NT-1989-1] N89-29000
The potential and electric fields of a conducting sphere in the presence of a charged conducting plane
[AD-A209498] N89-29149
Microwave emission from relativistic electron beams
[AD-A209653] N89-29181
Caviton dynamics in strong Langmuir turbulence
[DE89-012635] N89-29202
Effect of an electric field on a split Bloch band
[AD-A209857] N89-29244

ELECTRIC GENERATORS
Acoustic tests on a new motor generator system for the minuteman launch control centers in Hill engineering test facilities 1 and 2, Hill AFB, Utah
[AD-A209596] N89-28717

ELECTRIC POWER TRANSMISSION
On the composition of interconnected systems by nonserial dynamic programming: Application to power systems
[LAAS-89.096] N89-29064

ELECTRICAL ENGINEERING
Center for Electronics and Electrical Engineering technical publication announcements: Covering Center programs, July - September 1988, with 1989 CEEE events calendar
[PB89-189302] N89-28706
Basic research in electronics (JSEP)
[AD-A208181] N89-28726

ELECTRICAL FAULTS
Experimental and theoretical study of transient behavior of varistors
[AD-A209081] N89-28715
Lubricant evaluation and performance
[AD-A208925] N89-28835

ELECTRICAL MEASUREMENT
Plasma properties of a large-bore, arc-armature railgun
[AD-A209550] N89-28548
HEMP (High-Altitude Electromagnetic Pulse) validation of FAA (Federal Aviation Administration) radio facility
[AD-A209187] N89-28680

ELECTRICAL PROPERTIES
Vertical gradient freeze GaAs: Growth and electrical properties
[DE89-014894] N89-29228
Crystal chemistry, magnetic and electrical properties of La(sub2-x)Ba(subx)NiO4
[AD-A209376] N89-29240

ELECTRICAL RESISTIVITY
Pressure induced anomaly at Tc in Fe78 Mo2 B20
[NAL-TM-MT-6806] N89-28628

ELECTRICITY
Center for Electronics and Electrical Engineering technical publication announcements: Covering Center programs, July - September 1988, with 1989 CEEE events calendar
[PB89-189302] N89-28706
Energy technology R and D: What could make a difference. A study by the staff of the Oak Ridge National Laboratory. Part 1: Synthesis report, volume 1
[DE89-014566] N89-28955
Thin film photovoltaics
[DE89-009425] N89-28956

ELECTRO-OPTICS
Acousto-optic and linear electro-optic properties of organic polymeric materials
[AD-A207974] N89-28646
Picosecond electrooptic investigations of integrated circuits
[AD-A209134] N89-28863
Investigation of a linear systems model for human visual detection and spatial frequency discrimination
[AD-A209397] N89-29022
Digital optical computing with fibers and directional couplers
[PB89-184378] N89-29030
United States Air Force Research Initiation Program for 1987, volume 2
[AD-A209727] N89-29259

ELECTROCHEMICAL CELLS
Corrosion prevention of lithium-alloy anodes in accumulators with organic electrolytic solutions
[ETN-89-94652] N89-28729

ELECTROCHEMISTRY
Modelling the in situ infrared reflection-absorption spectra of the diffuse layer
[AD-A209347] N89-28598
Stochastic processes in CHEMFETs
[AD-A208092] N89-28725

ELECTRODES
Effect of a converter electrode in a multicusp negative ion source
[IPPJ-914] N89-29214

ELECTROLUMINESCENCE
The atomic layer epitaxy growth and characterization of zinc sulfide and alkaline earth sulfide thin films for electroluminescence applications
[ISBN-952-90014-6-0] N89-28613

ELECTROLYTES
Modelling the in situ infrared reflection-absorption spectra of the diffuse layer
[AD-A209347] N89-28598
Corrosion prevention of lithium-alloy anodes in accumulators with organic electrolytic solutions
[ETN-89-94652] N89-28729
Morphology control of photoelectrochemically etched profiles in n-GaAs
[AD-A208991] N89-29235

ELECTROMAGNETIC ACCELERATION
Prototype testing for a hybrid gas-gun/railgun device
[DE89-014294] N89-28542

ELECTROMAGNETIC FIELDS
Exact image theory for uniaxially anisotropic dielectric half space
[PB89-146450] N89-28671
Bibliography of the NIST (National Institute of Standards and Technology) Electromagnetic Fields Division publications
[PB89-189211] N89-28673

ELECTROMAGNETIC INTERACTIONS
Electromagnetic interactions of cosmic rays with nuclei N89-29163
Electric quadrupole excitations in the interactions of Y-89 with relativistic nuclei N89-29165
Nucleon emission via electromagnetic excitation in relativistic nucleus-nucleus collisions: Re-analysis of the Weizsacker-Williams method N89-29166
Microwave emission from relativistic electron beams
[AD-A209653] N89-29181

ELECTROMAGNETIC INTERFERENCE
Igniter heater EMI transient test
[NASA-CR-183743] N89-28566
Adaptive detection and parameter estimation for multidimensional signal models
[AD-A208971] N89-28678
Meteor burst system communications compatibility
[PB89-191167] N89-28692
Center for Electronics and Electrical Engineering technical publication announcements: Covering Center programs, July - September 1988, with 1989 CEEE events calendar
[PB89-189302] N89-28706

ELECTROMAGNETIC MEASUREMENT
Two-dimensional signal processing and storage and theory and applications of electromagnetic measurements
[AD-A207827] N89-28689

ELECTROMAGNETIC NOISE
Segmentation of noisy images
[ETN-89-95461] N89-28701
Fluxons and order in long Josephson junctions
[AD-A207925] N89-29249

ELECTROMAGNETIC PROPULSION
Plasma properties of a large-bore, arc-armature railgun
[AD-A209550] N89-28548

ELECTROMAGNETIC PULSES
HEMP (High-Altitude Electromagnetic Pulse) validation of FAA (Federal Aviation Administration) radio facility
[AD-A209187] N89-28680

ELECTROMAGNETIC RADIATION
Near-field testing of the 15-meter hoop-column antenna
[NASA-TM-4073] N89-28550
Basic research in electronics (JSEP)
[AD-A208181] N89-28726

ELECTROMAGNETIC SCATTERING
The inverse scattering problem for acoustic and electromagnetic waves
[AD-A209202] N89-28681
Electromagnetic scattering from two dimensional objects using the field feedback formulation
[AD-A209563] N89-28685
Scattering representation of waveguide/cavity discontinuities using mode-matching and the least-squares boundary residual
[AD-A209571] N89-28686
The relationship between ground permittivity and the input impedance of a horizontal dipole near ground
[AD-A207746] N89-28688
Approximation methods for scattering from rough surfaces
[AD-A209482] N89-29192

ELECTROMAGNETIC SHIELDING
HEMP (High-Altitude Electromagnetic Pulse) validation of FAA (Federal Aviation Administration) radio facility
[AD-A209187] N89-28680

ELECTROMAGNETIC WAVE TRANSMISSION
Electromagnetic pulse propagation through a stratified ionosphere
[IRF-SR-199] N89-28700

ELECTROMAGNETISM
NEC (Numerical Electromagnetics Code), NECGS (Numerical Electromagnetics Code-Ground Screen), and MININEC (Mini-Numerical Electromagnetics Code) numerical models of LF top-hat monopole antennas
[AD-A209230] N89-28683
Photonuclear absorption cross sections
[NASA-CR-185488] N89-29159
The invariance of classical electromagnetism under Charge-conjugation, Parity and Time-reversal (CPT) transformations N89-29161

ELECTRON ACCELERATORS
Compound-lens diode for HERMES 3
[DE89-013065] N89-28708
High-brightness electron injectors: A review
[DE89-014244] N89-28711
High-power free-electron lasers driven by RF linear accelerators
[AD-A209740] N89-28815

ELECTRON ATTACHMENT
Reversal electron attachment ionizer for detection of trace species
[NASA-CASE-NPO-17596-1-CU] N89-28795

ELECTRON BEAMS
Multicomponent e-beam resists containing organometallic compounds and reactive monomers
[AD-A207716] N89-28606
The beam viewer
[LINO-160] N89-28693
Compound-lens diode for HERMES 3
[DE89-013065] N89-28708
High-brightness electron injectors: A review
[DE89-014244] N89-28711
Slotted-waveguide amplifiers for millimeter waves
[AD-A207932] N89-28721
An improved hibachi support structure for electron-beam diode foils
[DE89-014023] N89-28810
High-power free-electron lasers driven by RF linear accelerators
[AD-A209740] N89-28815
Trochoidal analysis of scattered electrons in a merged electron-ion beam geometry
[NASA-CASE-NPO-16789-1-CU] N89-29169

The influence of the shell closure on the microscopic structure of even-even Hg isotopes: A study with electron and muon beams — a study with electron and muon beams
[ETN-89-95464] N89-29177
Study and simulation of an E-beam microlithography process on a multilayer resin structure. Research of an optimization
[LAAS-89.012] N89-29179

ELECTRON CAPTURE
Solid-vapor differences of electronic stopping powers for protons
[IPPJ-901] N83-29207

ELECTRON CLOUDS
Deeply bound orbits in pionic atoms and the optical potential
[ETN-89-95463] N89-29176

ELECTRON DENSITY PROFILES
Ionospheric variability
[AD-A209251] N89-28972

ELECTRON DIFFRACTION
Investigations of step distributions at Si/SiO2 interfaces using HR-SPA-LEED
[ETN-89-94437] N89-29251

ELECTRON DISTRIBUTION
Applied field and total dose dependence of trapped charge buildup in MOS devices
[AD-A209064] N89-29237

ELECTRON EMISSION
Energy and angular distributions of electrons emitted from gases and thin foils during light ion bombardment
[DE89-014445] N89-29147

ELECTRON ENERGY
High resolution electron energy loss studies of surface vibrations
[DE89-013964] N89-28589
Effect of a converter electrode in a multicusp negative ion source
[IPPJ-914] N89-29214
Electron energy levels in a quantum well within an in-plane magnetic field
[AD-A209351] N89-29256

ELECTRON GUNS
Microwave emission from relativistic electron beams
[AD-A209653] N89-29181

ELECTRON IMPACT
Ion-molecule chemistry within doubly charged ammonia clusters
[AD-A207764] N89-28608
Ion-molecule chemistry within triply charged ammonia clusters
[AD-A207766] N89-28609
Effect of a converter electrode in a multicusp negative ion source
[IPPJ-914] N89-29214

ELECTRON IRRADIATION
Radiothermoluminescence studies of polymer solids
[AD-A209036] N89-28641

ELECTRON MICROSCOPES
Radiothermoluminescence studies of polymer solids
[AD-A209036] N89-28641

ELECTRON MICROSCOPY
Weak beam electron microscopy of dislocation splitting in TiAl: Relationship with plasticity
[ONERA-NT-1988-3] N89-29253

ELECTRON ORBITALS
Application of Cholesky-like matrix decomposition methods to the evaluation of atomic orbital integrals and integral derivatives
[AD-A209682] N89-29112
Deeply bound orbits in pionic atoms and the optical potential
[ETN-89-95463] N89-29176

ELECTRON SCATTERING
Trochoidal analysis of scattered electrons in a merged electron-ion beam geometry
[NASA-CASE-NPO-16789-1-CU] N89-29169

ELECTRON SPECTROSCOPY
Simultaneous secondary ion and Auger electron analysis, illustrated by examples from microelectronics research and technology
[ETN-89-94431] N89-28611

ELECTRON STATES
Vibrational dynamics of aniline (Ar)1 and aniline (CH4)1 clusters
[AD-A209560] N89-28605

ELECTRON TRANSFER
Solvent effects on simple electron transfer reactions. A comparison of results for homogeneous and heterogeneous systems
[AD-A209381] N89-28600
The analysis of solvent effects on the kinetics of simple heterogeneous electron transfer reactions
[AD-A210078] N89-28602

ELECTRON TRANSITIONS
Simultaneous secondary ion and Auger electron analysis, illustrated by examples from microelectronics research and technology
[ETN-89-94431] N89-28611

ELECTRONIC CONTROL
A real time microcomputer implementation of sensor failure detection for turbofan engines
[NASA-TM-102327] N89-29032

ELECTRONIC EQUIPMENT
Center for Electronics and Electrical Engineering technical publication announcements: Covering Center programs, July - September 1988, with 1989 CEEE events calendar
[PB89-189302] N89-28706
Preliminary design guide for arctic equipment
[AD-A209455] N89-29024
Multilayered electronic materials and devices based on 3-5 compounds
[AD-A208861] N89-29233

ELECTRONIC EQUIPMENT TESTS
A fully automated, single-connection tester for T/R modules
[DE89-013155] N89-28786

ELECTRONIC SPECTRA
Ion-molecule chemistry within triply charged ammonia clusters
[AD-A207766] N89-28609

ELECTRONS
Solvent effects on simple electron transfer reactions. A comparison of results for homogeneous and heterogeneous systems
[AD-A209381] N89-28600
Reversal electron attachment ionizer for detection of trace species
[NASA-CASE-NPO-17596-1-CU] N89-28795
Energy and angular distributions of electrons emitted from gases and thin foils during light ion bombardment
[DE89-014445] N89-29147

ELECTROPHORESIS
Capillary zone electrophoresis-mass spectrometry of peptides and proteins
[DE89-014466] N89-28592
Controlled method of reducing electrophoretic mobility of various substances
[NASA-CASE-MFS-26049-1-NP] N89-28603

ELECTROPHYSICS
Basic research in electronics (JSEP)
[AD-A208181] N89-28726

ELLIPSES
Variational formulation for a nonlinear elliptic equation in a three-dimensional exterior domain
[NASA-CR-181885] N89-29028

ELLIPTIC DIFFERENTIAL EQUATIONS
A user's guide to the SEVP (Stabilized Error Vector Propagation) solver: An efficient direct solver for elliptic partial differential equations
[AD-A208117] N89-29121
Grid generation using elliptic partial differential equations
[DFVLR-FB-89-15] N89-29132

ELLIPTIC FUNCTIONS
Probabilistic analysis of semilinear partial differential equations
[AD-A209903] N89-29113

EMBEDDING
Software technology to support real-time embedded artificial intelligence-based applications, phase 1
[AD-A209133] N89-29042

EMISSION SPECTRA
A new method for monitoring cure and mobility in epoxy matrix and fiber/epoxy interphases
[AD-A209428] N89-28576

EMITTERS
AlGaAs phased array laser for optical communications
[NASA-CR-181869] N89-28820

ENAMELS
Damping properties of various materials
[AD-A209071] N89-28642

ENERGETIC PARTICLES
The aggregated state of matter: Elucidating transitions from the gas to the condensed phase and the formation of aerocolloids
[AD-A209080] N89-28595

ENERGY CONVERSION
Fuel cell technology in the United States
[DE89-013430] N89-28951
Evidence for two charged particle populations in the Crab nebula
[MPE-PREPRINT-147] N89-29286

ENERGY CONVERSION EFFICIENCY
Biofuels technical information guide
[DE89-000894] N89-28658
Improvements of the efficiency of solid state lasers by spectral conversion of the excitation lamp's output
[ETN-89-94425] N89-28822
Research on stable, high-efficiency, large-area, amorphous-silicon-based submodules, task B
[DE89-009439] N89-28946
Photovoltaics advanced research and development
[DE89-000895] N89-28948
Material and fabrication challenges in the development of monolithic solid oxide fuel cells
[DE89-012422] N89-28957
Field tests of a novel inverter for photovoltaic power conditioning
[DE89-014322] N89-28958

ENERGY DISSIPATION
High resolution electron energy loss studies of surface vibrations
[DE89-013964] N89-28589
The measurement of SEA loss factors on a fully assembled structure
[ISVR-TR-150] N89-29157

ENERGY DISTRIBUTION
Energy and angular distributions of electrons emitted from gases and thin foils during light ion bombardment
[DE89-014445] N89-29147
Studies of the volume and plasma sheath properties of radio frequency discharges
[AD-A207980] N89-29206

ENERGY GAPS (SOLID STATE)
Field induced gap infrared detector
[NASA-CASE-NPO-17526-1-CU] N89-28796

ENERGY LEVELS
Electron energy levels in a quantum well within an in-plane magnetic field
[AD-A209351] N89-29256

ENERGY STORAGE
Proof of the feasibility of coherent and incoherent schemes for pumping a gamma-ray laser
[AD-A208071] N89-28819

ENERGY TECHNOLOGY
Activities report in aerospace research in Germany, F.R.
[ISSN-0070-3966] N89-28485
Advanced power sources for space missions
[NASA-TM-101811] N89-28565
Chemical Technology Division
[DE89-013917] N89-28591
Photovoltaics advanced research and development
[DE89-000895] N89-28948
Energy technology R and D: What could make a difference. A study by the staff of the Oak Ridge National Laboratory. Part 1: Synthesis report, volume 1
[DE89-014568] N89-28955
Proceedings of the Antiproton Technology Workshop held in Upton, New York on 10 May 1989
[AD-A210045] N89-29170

ENERGY TRANSFER
Time- and volume-averaged conservation equations for multiphase flow
[DE89-012418] N89-28746
Collision dynamics and transition probabilities for vibrationally excited OH
[AD-A207856] N89-28976
Experiments on the magnetic field and neutral density limits on CIV interaction
[TRITA-EPP-88-08] N89-29216

ENGINE TESTS
Technical Evaluation Motor 3 (TEM-3)
[NASA-CR-183740] N89-28567
Lubricant evaluation and performance
[AD-A208925] N89-28835
A real time microcomputer implementation of sensor failure detection for turbofan engines
[NASA-TM-102327] N89-29032

ENGINEERING MANAGEMENT
Software engineering with database management systems
[AD-A208167] N89-29060

ENTRAINMENT
Entrainment and homogenization of a passive tracer in a numerical model gyre
[AD-A208020] N89-29005

ENVIRONMENT EFFECTS
Adequacy of forestry data in assessing the impact of ozone: A national perspective
[DE89-012359] N89-28962

ENVIRONMENT POLLUTION
The WMO research and development program 1988-1997: Second WMO long-term plan, part 2, volume 3
[WMO-693-PT-2-VOL-3] N89-28997

ENVIRONMENT SIMULATION
Hypersonic vehicle environment simulation, phase 1
[AD-A209030] N89-28754

ENVIRONMENTAL TESTS
A study of the ultraviolet degradation embrittlement of polypropylene polymer
[ISBN-90-9002498-0] N89-28656

EPITAXY
The atomic layer epitaxy growth and characterization of zinc sulfide and alkaline earth sulfide thin films for electroluminescence applications
[ISBN-952-90014-6-0] N89-28613
Thermodynamically stable conducting films of intermetallic PtGa2 on gallium arsenide
[AD-A210077] N89-28716
Ion beam deposition of epitaxial germanium and gallium arsenide layers
[DE89-014044] N89-29225
Multilayered electronic materials and devices based on 3-5 compounds
[AD-A208861] N89-29233
Photoelectrochemical fabrication of gratings in SiC
[AD-A208992] N89-29236
Selective area epitaxy of gallium arsenide on silicon, phase 1
[AD-A209079] N89-29238
A bolt-on deposition source for ultra-high-vacuum growth of intermetallic compound films
[AD-A209699] N89-29242

EPOXY MATRIX COMPOSITES
A new method for monitoring cure and mobility in epoxy matrix and fiber/epoxy interphases
[AD-A209428] N89-28576
Determination of moisture diffusion in carbon fiber reinforced epoxy composites by means of radioisotope tracer technique
[BMVG-FBWT-88-2] N89-28581
Measurement of mode 1 and mode 2 strain energy release rates: A VAMAS round robin project on delamination of composite materials --- Versailles project on advanced materials and standards (VAMAS)
[NPL-DMA(A)-178] N89-28583
A summary of the UK results for a VAMAS round robin project on delamination of composite materials --- Versailles project on advanced materials and standards (VAMAS)
[NPL-DMA(A)-179] N89-28584

EPOXY RESINS
TGMDA/DDS type impregnating resins structural study
[SNEA-9595] N89-28650

EQUATIONS OF MOTION
Consideration of gravity gradient stabilization for ORION
[AD-A207845] N89-28557
Rapidly distorted compressible boundary-layers N89-28735
Formulation and numerical solution of the equations of constrained mechanical motion
[DFVLR-FB-89-08] N89-28847

EQUATIONS OF STATE
Time- and volume-averaged conservation equations for multiphase flow
[DE89-012418] N89-28745

EQUIPMENT SPECIFICATIONS
Airport noise measuring data collction system
[NLR-MP-87006-U] N89-28526
Vibration analyzer
[NASA-CASE-MSC-21406-1] N89-28829
KRAS: A Danish high resolution airborne SAR N89-28882

EQUIVALENCE
Evaluation of the bistatic equivalence theorem for the near and far-field radar cross section of complex targets
[AD-A209228] N89-28682

EQUIVALENT CIRCUITS
Studies of the volume and plasma sheath properties of radio frequency discharges
[AD-A207980] N89-29206

EROS (SATELLITES)
Training Course for Tropical Earth Resources Satellite (EARS) bridging phase
[BCRS-88-16D] N89-28938

ERROR ANALYSIS
Measurements and modelling of thin silicon dioxide films on silicon
[AD-A207853] N89-28720
Optical properties and error sources of an airborne radiometer
[MITT-60] N89-28799
Errors in the scene identification from satellite data. Effects on the determination of radiation budget parameters
[MITT-59] N89-28931
Sea gravimetry and Eotvos correction
[REPT-88.3] N89-29006
Monte Carlo analysis of localization errors in magnetoencephalography
[DE89-013221] N89-29007
A user's guide to the SEVP (Stabilized Error Vector Propagation) solver: An efficient direct solver for elliptic partial differential equations
[AD-A208117] N89-29121
Optimal error analysis of spectral methods with emphasis on non-constant coefficients and deformed geometries
[NASA-CR-181902] N89-29124

ERROR CORRECTING CODES
Packet-error probability analysis for unslotted FH-CDMA (Frequency Hopped-Code Division Multiple-Access) systems with error control coding
[AD-A207964] N89-29054

ERRORS
Positioning error induced by axial sampling in positron emission tomography
[DE89-014519] N89-28791
Packet-error probability analysis for unslotted FH-CDMA (Frequency Hopped-Code Division Multiple-Access) systems with error control coding
[AD-A207964] N89-29054

ERYTHROCYTES
Energy and Technology Review --- analytical cytology
[DE89-013919] N89-28954

ESA SATELLITES
Activities report of ESA
[ISSN-0258-025X] N89-29302

ESA SPACECRAFT
ESA's activities and plans for remote sensing data systems N89-28906

ESTIMATING
Airborne pulse Doppler radar. Part 3: Performance estimation --- surveillance radar analysis
[BAE-WAA-RP-GEN-RAD-645-PT-3] N89-28697

ETCHING
Lithography and spectroscopy of ultrathin Langmuir-Blodgett polymer films
[AD-A208970] N89-28639
Photoetched double spiral device
[PD-SE-8911] N89-29071
Morphology control of photoelectrochemically etched profiles in n-GaAs
[AD-A208991] N89-29235
Photoelectrochemical fabrication of gratings in SiC
[AD-A208992] N89-29236
Quantitative analysis of laser interferometer waveforms obtained during oxygen reactive-ion etching of thin polymer films
[AD-A207836] N89-29248

ETHANE
Absorption cross section of alternative chlorofluoroethanes and potential effects on the ozone layer
[AERONOMICA-ACTA-A-340-1989] N89-28968

EULER EQUATIONS OF MOTION
Role of supercomputer in computational aerodynamics
[PD-CF-8925] N89-28496
Solution of Euler equations by a discontinuous Galerkin method obtained from a variational formulation of entropy
[CERT-1/332400/DERI] N89-28775
La Recherche Aerospatiale, bimonthly bulletin, number 1988-6
[ESA-TT-1165] N89-29301

EUROPE
European crosswind frequencies
[AD-A209137] N89-28985

EUROPEAN AIRBUS
in-situ anodising of aluminium alloys --- Airbus corrosion prevention requirements
[BAE/WMD/AR/GEN/00666] N89-28630

EUROPEAN SPACE AGENCY
Activities report of ESA
[ISSN-0258-025X] N89-29302

EUROPEAN SPACE PROGRAMS
Key structures mechanical issues of the European Space Station and platform program Columbus
[MBB-UD-0041-88-PUB] N89-28561
Activities report of ESA
[ISSN-0258-025X] N89-29302

EVALUATION
Evaluation of LDA 3-component velocity data on a 65 deg delta wing at M = 0.85 and first results of an analysis
[DFVLR-FB-89-19] N89-28505
A survey of JP-8 and JP-5 properties
[AD-A207721] N89-28661
An a priori approach to the evaluation of signature analysis efficiency
[IMAG-RR-746-I] N89-29140

EVAPORATION
Evaporation thermodynamics of monotellurides of selected rare Earth and alkaline Earth elements, and an attempt to systematic correlation between the standard enthalpies of formation
[ETN-89-94655] N89-29257

EVAPORATORS
A bolt-on deposition source for ultra-high-vacuum growth of intermetallic compound films
[AD-A209699] N89-29242

EVEN-EVEN NUCLEI
The influence of the shell closure on the microscopic structure of even-even Hg isotopes: A study with electron and muon beams --- a study with electron and muon beams
[ETN-89-95464] N89-29177

EVOKED RESPONSE (PSYCHOPHYSIOLOGY)
Transient visual evoked neuromagnetic responses: Identification of multiple sources
[DE89-013438] N89-29008

EXAMINATION
Antenna fundamentals: A tutorial paper
[BAE-WAA-R-GEN-RAD-533] N89-28695

EXCITATION
Electric quadrupole excitations in relativistic nucleus-nucleus collisions N89-29164
Electric quadrupole excitations in the interactions of Y-89 with relativistic nuclei N89-29165
Trochoidal analysis of scattered electrons in a merged electron-ion beam geometry
[NASA-CASE-NPO-16789-1-CU] N89-29169

EXCITONS
Lineshape and lifetime studies of exciton luminescence from confined CuCl thin films
[AD-A209750] N89-29243

EXHAUST GASES
Engine combustion optimization by exhaust analysis
[PB89-195788] N89-28588

EXPERIMENT DESIGN
Microgravity combustion science: A program overview
[NASA-TM-101424] N89-28665

EXPERT SYSTEMS
Evolutionary growth for Space Station Freedom electrical power system
[NASA-TM-102339] N89-28570
Robotic grasping of unknown objects: A knowledge-based approach
[DE89-013875] N89-28833
Preliminary design of a consultation knowledge-based system for the minimization of distortion in welded structures
[AD-A208842] N89-28834
Experiences in implementing an expert system supported man-machine-interface for the configuration of the intelligent SAR processor N89-28889
An expert system for satellite image interpretation and G.I.S. based problem solving N89-28894
A study on information analysis aids for sea surface temperature image data N89-28897
The use of expert systems for preprocessing image data
[NLR-MP-88009-U] N89-28934

EXPLOSIONS
Reaction kinetics and mechanism of chain reactions and explosions via transient spectroscopy
[AD-A209169] N89-28597
Numerical simulation of the simultaneous detonation of two identical, fully contained explosions
[DE89-014844] N89-28660
Exploding metallic foils and fuses: A computational modeling update
[DE89-014033] N89-28709

EXPLOSIVES
Hazards of explosives dusts
[DE89-014554] N89-28669
The Mark 101 flux compression generator: Development progress
[DE89-014298] N89-28712
Dense heavy metal aerosol monitoring by direct X-ray fluorescence
[AD-A209077] N89-28966

EXPONENTIAL FUNCTIONS
The p-version of the finite element method for domains with corners and for infinite domains
[AD-A207797] N89-29116

EXPOSURE
Five year ground exposure of composite materials used on the Bell Model 206L flight service evaluation
[NASA-TM-101645] N89-28579

EXTRAGALACTIC RADIO SOURCES
Statistical and physical evolution of QSO's
[NASA-CR-185869] N89-29282

EXTRATERRESTRIAL RADIATION
Activities report of the Institute for Extraterrestrial Physics
[MPE-212] N89-29277

EXTREMELY LOW FREQUENCIES
ELF (Extremely Low Frequency) communications system ecological monitoring program
[AD-A208198] N89-28691

F

F REGION
Ionospheric variability
[AD-A209251] N89-28972

F-16 AIRCRAFT
Operational test plan concept for evaluation of close air support alternative aircraft
[AD-A208185] N89-28513

F-18 AIRCRAFT
Aerodynamic model tests of exhaust augmentors for F/A-18 engine run-up facility at RAAF Williamtown
[AD-A208110] N89-28518

FABRICATION
An X-ray source for lithography based on a quasi-optical maser undulator
[AD-A208522] N89-28675
Monolithic narrow-linewidth InGaAsP semiconductor laser for coherent optical communications
[NASA-CR-181870] N89-28821
The manufacture of blazed oblique zone plates for use at 10.6 microns
[NPL-MOM-91] N89-28827
An evaluation of blazed zone plates for use in the 10 micron spectral region
[NPL-MOM-93] N89-28828
Two-terminal CuInSe-based cascade cells
[DE89-009422] N89-28950
Material and fabrication challenges in the development of monolithic solid oxide fuel cells
[DE89-012422] N89-28957
High-temperature superconductor materials processing: Development of environmentally acceptable processing technologies
[DE89-014391] N89-29229
A manufacturing scheduler's perspective on semiconductor fabrication
[AD-A208372] N89-29232

FAILURE
Statistics on aircraft gas turbine engine rotor failures that occurred in US commercial aviation during 1984
[NAPC-PE-185] N89-28516
Statistics on aircraft gas turbine engine rotor failures that occurred in US commercial aviation during 1985
[NAPC-PE-188] N89-28517
Composite material repair and reliability
[AD-A209150] N89-28574

FAILURE ANALYSIS
Delamination test apparatus and method
[NASA-CASE-LAR-13985-1] N89-28586
Effect of temperature and H2S content on the cracking resistance of a 13 percent chromium martensitic stainless steel in acidified NaCl
[NPL-DMA(A)-173] N89-28631
Pull-out and push-out tests for rubber-to-metal adhesion
[AD-A208100] N89-28647
Estimation of some stochastic models used in reliability engineering
[VTT-RR-598] N89-28855
Damage predictions for wind turbine components using the LIFE2 computer code
[DE89-013813] N89-28952
A real time microcomputer implementation of sensor failure detection for turbofan engines
[NASA-TM-102327] N89-29032

FAILURE MODES
A summary of the UK results for a VAMAS round robin project on delamination of composite materials — Versailles project on advanced materials and standards (VAMAS)
[NPL-DMA(A)-179] N89-28584
Fatigue testing apparatus
[NASA-CASE-LEW-14124-1] N89-28806

FALSE ALARMS
Adaptive detection and parameter estimation for multidimensional signal models
[AD-A208971] N89-28678

FAR FIELDS
Evaluation of the bistatic equivalence theorem for the near and far-field radar cross section of complex targets
[AD-A209228] N89-28682

FAR INFRARED RADIATION
Preparation of compounds with the tetrahedral structure which transmit in the far infrared
[AD-A208697] N89-28593
Redetermination of crystal structure of zinc thiogallate
[AD-A208931] N89-29234
Implications of the correlation between the radio continuum and far-infrared luminosities of spiral galaxies
N89-29289

FASTENERS
Stresses and strains in a cold-worked annulus
[AR-005-548] N89-28871

FATIGUE (MATERIALS)
Fatigue crack growth-microstructural relationship of Ti-6Al-4V
[AD-A208107] N89-28626
Steel fatigue under combined loads
[ETN-89-94864] N89-28629
La Recherche Aerospatiale, bimonthly bulletin, number 1988-5
[ESA-TT-1162] N89-29300

FATIGUE LIFE
Damage predictions for wind turbine components using the LIFE2 computer code
[DE89-013813] N89-28952

FATIGUE TESTS
Furnace for tensile/fatigue testing
[NASA-CASE-LEW-14848-1] N89-28549
A summary of the UK results for a VAMAS round robin project on delamination of composite materials — Versailles project on advanced materials and standards (VAMAS)
[NPL-DMA(A)-179] N89-28584
A VAMAS round robin on fatigue test methods for polymer matrix composites. Part 1: Tensile and flexural tests of unidirectional material — Versailles project on advanced materials and standards (VAMAS)
[NPL-DMA(A)-180-PT-1] N89-28585
Steel fatigue under combined loads
[ETN-89-94864] N89-28629
Fatigue testing apparatus
[NASA-CASE-LEW-14124-1] N89-28806

FAULT TOLERANCE
Fault-tolerant computer architecture modeling and analysis
[AD-A209364] N89-29034
Fault-tolerant computer systems: A survey of some methods and techniques
[MEMO-INF-88-15] N89-29037
Strategic defense system distributed operating system R and D review and recommendations
[AD-A208034] N89-29145

FEASIBILITY
The manufacture of blazed oblique zone plates for use at 10.6 microns
[NPL-MOM-91] N89-28827
An evaluation of blazed zone plates for use in the 10 micron spectral region
[NPL-MOM-93] N89-28828

FEDERAL BUDGETS
Departments of Veterans Affairs and Housing and Urban Development and independent agencies appropriations for 1990. Part 6: National Aeronautics and Space Administration
[GPO-99-598] N89-29273

FEED SYSTEMS
High temperature tribometer, phase 1
[AD-A209356] N89-28838

FEEDBACK
The effect of autopilot configuration on missile response
[AD-A207822] N89-28520
Electromagnetic scattering from two dimensional objects using the field feedback formulation
[AD-A209563] N89-28685

FEEDBACK CONTROL
Development and implementation of an on-line multivariable control algorithm for the force control of an industrial robot
[OUEL-1748/88] N89-28848
Climate regulation by marine phytoplankton: A test by anthropogenic SO2 emissions
[DE89-014708] N89-28984
FREQ: A computational package for multivariable system loop-shaping procedures
[NASA-TM-4127] N89-29047
Real-time applications of neural nets
[DE89-014400] N89-29093

FERMIONS
Some aspects of a lattice formulation of chiral gauge theories
[NIKHEF-ITFA-88-51] N89-29151
Ultrasonic attenuation in heavy fermion superconductors
[DE89-014937] N89-29231

FERRITIC STAINLESS STEELS
The influence of structure and alloying on the cold-formability of ferritic steels and the utility of uniaxial tensile testing in its assessment
[ISBN-952-90044-3-5] N89-28632

FERROMAGNETIC MATERIALS
Pressure induced anomaly at Tc in Fe78 Mo2 B20
[NAL-TM-MT-8806] N89-28628

FIBER COMPOSITES
A new method for monitoring cure and mobility in epoxy matrix and fiber/epoxy interphases
[AD-A209428] N89-28576
Highly oriented fiber reinforced ceramic composites
[AD-A208119] N89-28578
A summary of the UK results for a VAMAS round robin project on delamination of composite materials — Versailles project on advanced materials and standards (VAMAS)
[NPL-DMA(A)-179] N89-28584
The interface in tungsten fiber reinforced niobium metal-matrix composites
[NASA-TM-102122] N89-28627
The structural response of unsymmetrically laminated composite cylinders
[NASA-CR-185834] N89-28856

FIBER OPTICS
Status and development potential of the fly by light technology in civil aircraft
[ILR-MITT-212] N89-28522
Fiber optic frequency transfer link
[NASA-CASE-NPO-17703-1-CU] N89-29191

FIBERS
Hollow fiber clinostat: Technical abstract
[NASA-CASE-MFS-28370-1] N89-28793

FIELD EFFECT TRANSISTORS
Optical gain control of GaAs microwave monolithic integrated circuit distributed amplifier
[AD-D013969] N89-28705
Stochastic processes in CHEMFETs
[AD-A207977] N89-28723
Stochastic processes in CHEMFETs
[AD-A208092] N89-28725

FIELD THEORY (PHYSICS)
Some aspects of a lattice formulation of chiral gauge theories
[NIKHEF-ITFA-88-51] N89-29151

FIGHTER AIRCRAFT
Composite material repair and reliability
[AD-A209150] N89-28574

FILE MAINTENANCE (COMPUTERS)
Generalized grid files: Description and performance aspects
[MEMO-INF-88-63] N89-29272

FILM COOLING
Heat transfer and film cooling in compressible nozzle flow
[ETN-89-94653] N89-28773

FINITE DIFFERENCE THEORY
A user's guide to the SEVP (Stabilized Error Vector Propagation) solver: An efficient direct solver for elliptic partial differential equations
[AD-A208117] N89-29121

FINITE ELEMENT METHOD
Composite material repair and reliability
[AD-A209150] N89-28574
Electromagnetic scattering from two dimensional objects using the field feedback formulation
[AD-A209563] N89-28685
Accurate and efficient modeling of global circuit behavior in VSLI layouts
[ETN-89-95459] N89-28732
Finite element analysis of incompressible viscous flows around single and multi-element aerofoils in high Reynolds number region
[NAL-TR-1010T] N89-28765
Smooth piecewise polynomials as conforming finite elements for plate bending problems
[MEMO-747] N89-28875
Total Lagrangian formulation for large-displacement analysis of the triangular finite elements
[AD-A209378] N89-29111
The p-version of the finite element method for domains with corners and for infinite domains
[AD-A207797] N89-29116
The problem of selecting the shape functions for a p-type finite element
[AD-A207798] N89-29117
Implementation of nonhomogeneous Dirichlet boundary conditions in the p-version of the finite element method
[AD-A207799] N89-29118
Numerical solution of ill posed problems in partial differential equations
[AD-A207852] N89-29119

FINNED BODIES
Compact heat and mass exchangers of the plate fin type in thermal sorption systems: Application in an absorption heat pump with the working pair CH3OH-LiBr/ZnBr2
[ISBN-90-370-0022-3] N89-28780

FISSION PRODUCTS
Chemical Technology Division
[DE89-013917] N89-28591

FITTING
Non-linear surface fitting of laser range images using a hypercube concurrent computer
[DE89-013720] N89-28808
Least-squares best-fit geometric elements
[NPL-DITC-140/89] N89-29125

FITTINGS
Comparative analysis of ultrasonic inspection procedures for Kaman K747 root end fittings
[AD-A207762] N89-28512
FIXED WINGS
Composite material repair and reliability
[AD-A209150] N89-28574
FLAME STABILITY
Supersonic combustion at the DFVLR: Results and experiences
[DFVLR-88-044] N89-28610
FLAMES
Investigation of laser-induced fluorescence detection of boron oxides in flames
[AD-A209154] N89-28596
FLAMMABILITY
Microgravity combustion science: A program overview
[NASA-TM-101424] N89-28665
FLEXIBILITY
Space module assembly apparatus with docking alignment flexibility and restraint
[NASA-CASE-MSC-21211-1] N89-28553
High temperature flexible seal
[NASA-CASE-LEW-14695-1] N89-28830
FLEXIBLE BODIES
Modelling, information, processing, and control
[AD-A207810] N89-28665
Nonlinear dynamics and control of flexible structures
[AD-A208120] N89-28669
FLEXING
Measurement of mode 1 and mode 2 strain energy release rates: A VAMAS round robin project on delamination of composite materials — Versailles project on advanced materials and standards (VAMAS)
[NPL-DMA(A)-178] N89-28583
A VAMAS round robin on fatigue test methods for polymer matrix composites. Part 1: Tensile and flexural tests of unidirectional material — Versailles project on advanced materials and standards (VAMAS)
[NPL-DMA(A)-180-PT-1] N89-28585
FLIGHT ALTITUDE
Glider ground effect investigation
[AD-A209152] N89-28490
FLIGHT CONTROL
An experimental optical coupling device for an airborne digital redundant system
[NAL-TR-1003] N89-28514
Towards a physiologically based HUD (Head-Up Display) symbology
[AD-A207748] N89-28515
Status and development potential of the fly by light technology in civil aircraft
[ILR-MITT-212] N89-28522
FLIGHT CREWS
Canadian Forces aircrew ejection, descent, and landing injuries, 1 January 1975 - 31 December 1987
[AD-A208116] N89-29015
FLIGHT OPTIMIZATION
Glider ground effect investigation
[AD-A209152] N89-28490
FLIGHT PATHS
Glider ground effect investigation
[AD-A209152] N89-28490
Orbit determination of sunlight illuminated objects detected by overhead platforms
[AD-A209227] N89-28540
FLIGHT PLANS
Direct User Access Terminal (DUAT) operational concept
[WP-88W00075] N89-28524
FLIGHT SAFETY
Competition and safety in air traffic
[TUB-DISS-PAPER-128] N89-28508
Collision avoidance operational concept
[WP-88W00418] N89-28509
FLIGHT SIMULATION
Glider ground effect investigation
[AD-A209152] N89-28490
The effect of autopilot configuration on missile response
[AD-A207822] N89-28520
Spacecraft flight simulation: A human factors investigation into the man-machine interface between an astronaut and a spacecraft performing docking maneuvers and other proximity operations
[NASA-CR-177502] N89-29020
FLIGHT TESTS
Glider ground effect investigation
[AD-A209152] N89-28490
Buran flight testing, capabilities discussed N89-28529
Development, testing procedures for Buran shuttle N89-28531
FLIR DETECTORS
Airborne FLIR (Forward Looking Infrared) detection of surface targets
[AD-A209250] N89-29189
FLOATING POINT ARITHMETIC
A reconfigurable arithmetic processor — for MIMD computer
[AD-A208323] N89-29082
FLOW DISTORTION
Rapidly distorted compressible boundary-layers N89-28735
General comments on the interpretation of data — mean flow for rapidly distorted turbulent boundarylayers N89-28742
FLOW DISTRIBUTION
Three-dimensional airfoil performance measurements on a rotating wing
[DE89-009443] N89-28487
Comparison of flow-visualised vortices with computed geometry over thin delta wings
[AD-A209083] N89-28489
Some computations of unsteady Navier-Stokes flow around oscillating airfoil/wing
[NAL-TR-1004T] N89-28492
Flow calculation over a delta-wing using the thin-layer Navier-Stokes equations
[PD-CF-8924] N89-28497
Correlation of Puma airloads: Evaluation of CFD prediction methods
[NASA-TM-102226] N89-28498
Measurements of mean-flow and turbulence characteristics in a turbojet exhaust using a laser velocimeter
[ISL-CO-226/88] N89-28519
Large scale motions in supersonic turbulent boundary layers N89-28736
General comments on the interpretation of data — mean flow for rapidly distorted turbulent boundarylayers N89-28742
Review of mean flow data — for compressible boundary layers N89-28743
Review of turbulence data — for turbulent compressible boundary layers N89-28744
The entries N89-28745
Hypersonic vehicle environment simulation, phase 1
[AD-A209030] N89-28754
Development of an efficient solution scheme for incompressible steady-state flow
[AD-A207726] N89-28757
Application of computational fluid dynamics to the analysis of the aerodynamics of a railgun projectile
[AD-A207758] N89-28758
A nonlinear investigation of the stationary modes of instability of the three-dimensional compressible boundary layer due to a rotating disc
[NASA-CR-181901] N89-28766
Experimental investigations of flow forces exerted on spheres in rest and in motion, in a plane Poiseville flow
[ETN-89-94433] N89-28770
A compressible inverse design method based on an analytical approach
[CUED/A-TURBO/TR-125] N89-28778
Comparison between two different techniques of computing the axial induction for horizontal axis wind turbines in a locally deformed flow field
[FFA-TN-1986-56] N89-28959
Evaluation of functionality in distributed systems
[AD-A209167] N89-29258
FLOW EQUATIONS
Hermes preparatory program. Fluid dynamics and numerical analysis. Theoretical modeling of high temperature hypersonic flows
[ANE-13/87] N89-28503
Rapidly distorted compressible boundary-layers N89-28735
The upper-branch stability of compressible boundary layer flows
[NASA-TM-102128] N89-28748
FLOW GEOMETRY
On the classification of plane graphs representing structurally stable rational Newton-flows
[MEMO-750-REV] N89-28776
FLOW MEASUREMENT
Measurements of mean-flow and turbulence characteristics in a turbojet exhaust using a laser velocimeter
[ISL-CO-226/88] N89-28519
A survey of measurements and measuring techniques in rapidly distorted compressible turbulent boundary layers
[AGARD-AG-315] N89-28734
Hot-wire anemometry in supersonic flow N89-28738
Laser Doppler anemometry N89-28739
Laser Doppler anemometry in supersonic flows: Problems of seeding and angular bias N89-28740
Fluctuating wall-pressure measurements N89-28741
General comments on the interpretation of data — mean flow for rapidly distorted turbulent boundarylayers N89-28742
Review of mean flow data — for compressible boundary layers N89-28743
Review of turbulence data — for turbulent compressible boundary layers N89-28744
The entries N89-28745
Piezoelectric foils as sensors in experimental flow mechanics
[ILR-MITT-214] N89-28800
Experimenting cavitation measuring instruments
[CERT-2305] N89-28803
FLOW STABILITY
The upper-branch stability of compressible boundary layer flows
[NASA-TM-102128] N89-28748
On the classification of plane graphs representing structurally stable rational Newton-flows
[MEMO-750-REV] N89-28776
Propagation and saturation of nonlinear inertia-gravity waves in the atmosphere
[AD-A207871] N89-28989
FLOW THEORY
Gradient Newton-flows for complex polynomials
[MEMO-764] N89-28779
FLOW VELOCITY
Measurements of mean-flow and turbulence characteristics in a turbojet exhaust using a laser velocimeter
[ISL-CO-226/88] N89-28519
FLOW VISUALIZATION
Comparison of flow-visualised vortices with computed geometry over thin delta wings
[AD-A209083] N89-28489
La Recherche Aerospatiale, bimonthly bulletin, number 1988-4
[ESA-TT-1161] N89-29299
FLUID DYNAMICS
Tolerable g-level for fluid science experiments — in space platforms
[TS-7-87] N89-28667
Fast-algorithm development for large-eddy simulation of circular-jet turbulence
[AD-A207928] N89-28760
On the large-eddy simulation of transitional wall-bounded flows
[NASA-CR-181883] N89-28763
Finite element analysis of incompressible viscous flows around single and multi-element aerofoils in high Reynolds number region
[NAL-TR-1010T] N89-28765
Activities report in meteorology in Sweden
[AR-87-88] N89-28999
Solution of the hydrodynamic device model using high-order non-oscillatory shock capturing algorithms
[NASA-CR-181886] N89-29123
Nonlinear stability in fluid and plasma dynamics
[AD-A207715] N89-29203
FLUID MANAGEMENT
COLD-SAT: Cryogenic On-Orbit Liquid Depot-Storage, Acquisition and Transfer
[NASA-TM-102308] N89-28535
FLUID MECHANICS
Ocean remote sensing and modeling
[AD-A208406] N89-28927
FLUID-SOLID INTERACTIONS
A dynamic variation principle for elastic-fluid contacts, applied to elastohydrodynamic lubrication theory
[MEMO-746] N89-28782
FLUOROCARBONS
Atmospheric processes and effects on materials
[PB89-173215] N89-28964
FLUOROHYDROCARBONS
On strain gages using the PVF2 piezoelectric polymer
[ISL-CO-210/88] N89-28801
Absorption cross section of alternative chlorofluoroethanes and potential effects on the ozone layer
[AERONOMICA-ACTA-A-340-1989] N89-28968
FOAMS
Microcellular foams from rigid-rod polymers in solutions: Effect of aggregation characteristics on foam properties
[AD-A209024] N89-28640
FOCUSING
An X-ray microprobe using focussing optics with a synchrotron radiation source
[DE89-013425] N89-28788
FOILS (MATERIALS)
Piezoelectric foils as sensors in experimental flow mechanics
[ILR-MITT-214] N89-28800

FORCE DISTRIBUTION
Analytical solutions for the field, current density, force force density and mechanical stress distribution in toroidal coil systems
[IPP-2/294] N89-28728
Experimental investigations of flow forces exerted on spheres in rest and in motion, in a plane Poiseville flow
[ETN-89-94433] N89-28770
FORCED CONVECTION
Enhancement of forced convection heat transfer in tubes using staged tangential flow injection
[PB89-204598] N89-28768
FORECASTING
The sensitivity of Middle East precipitation and cloud forecasts to changes in Eastern Mediterranean Sea surface temperatures
[AD-A207864] N89-28988
FOREST MANAGEMENT
Adequacy of forestry data in assessing the impact of ozone: A national perspective
[DE89-012359] N89-28962
FORESTS
Adequacy of forestry data in assessing the impact of ozone: A national perspective
[DE89-012359] N89-28962
FORMULAS (MATHEMATICS)
A dynamic variation principle for elastic-fluid contacts, applied to elastohydrodynamic lubrication theory
[MEMO-746] N89-28782
Out-of-plane buckling formulae for beam-columns/tie beams
[PB89-191613] N89-28857
A new scattering formula for depth-resolving X-ray diffractometry based on a kinematic theory
[ETN-89-94430] N89-29195
FORMULATIONS
Formulation and numerical solution of the equations of constrained mechanical motion
[DFVLR-FB-89-08] N89-28847
FOSSIL FUELS
Chemical Technology Division
[DE89-013917] N89-28591
FOURIER TRANSFORMATION
The Los Alamos Fourier-transform spectrometer: Applications to molecular spectroscopy
[DE89-014258] N89-28789
FOVEA
Transient visual effects of prolonged small spot foveal laser exposure
[AD-A207945] N89-29012
FRACTURE MECHANICS
High temperature adhesive systems
[AD-A209166] N89-28643
Damage predictions for wind turbine components using the LIFE2 computer code
[DE89-013813] N89-28952
FRACTURE STRENGTH
Highly oriented fiber reinforced ceramic composites
[AD-A208119] N89-28578
Effect of temperature and H2S content on the cracking resistance of a 13 percent chromium martensitic stainless steel in acidified NaCl
[NPL-DMA(A)-173] N89-28631
Survey of test procedures for high performance ceramic materials and their fundamentals
[JUEL-SPEZ-470] N89-28653
Ultrasonic imaging of textured alumina
[NASA-TM-101478] N89-28853
Comparison of peel and lap shear bond strengths for elastic joints with and without residual stresses
[AD-A208102] N89-28867
FRACTURES (MATERIALS)
Damage predictions for wind turbine components using the LIFE2 computer code
[DE89-013813] N89-28952
FRAGMENTS
Modeling of hot fragment conductive ignition of solid propellants with application to melting and evaporation of solids
[AD-A207727] N89-28662
General-purpose heat source development: Extended series test program SRB fragment/fuselage tests
[DE89-014389] N89-29180
FREE CONVECTION
Numerical determination of guaranteed Rayleigh numbers and the pertaining flow forms in steady, axisymmetric convection in cylinders
[ETN-89-94432] N89-28769
Heat transfer in free convection and forced, laminar flow in vertical tubes, considering temperature dependent medium characteristics
[ETN-89-94441] N89-28772
Application of similarity methods to the turbulent diffusion in the convective and stable boundary layer
[WISS-BER-12] N89-28979
FREE ELECTRON LASERS
High-brightness electron injectors: A review
[DE89-014244] N89-28711
Chemical and Laser Sciences Division
[DE89-014385] N89-28811
On the use of the FEL to produce high transient space-charge potentials in a magnetized plasma
[DE89-014325] N89-28814
High-power free-electron lasers driven by RF linear accelerators
[AD-A209740] N89-28815
Microwave emission from relativistic electron beams
[AD-A209653] N89-29181
FREE ENERGY
Solvent effects on simple electron transfer reactions. A comparison of results for homogeneous and heterogeneous systems
[AD-A209381] N89-28600
FREEZING
Vertical gradient freeze GaAs: Growth and electrical properties
[DE89-014894] N89-29228
FREQUENCY ASSIGNMENT
Meteor burst system communications compatibility
[PB89-191167] N89-28692
FREQUENCY CONTROL
Residual vibration reduction in computer controlled machines
[AD-A208074] N89-28866
Packet-error probability analysis for unslotted FH-CDMA (Frequency Hopped-Code Division Multiple-Access) systems with error control coding
[AD-A207964] N89-29054
FREQUENCY CONVERTERS
Chiral organic crystals for high power frequency conversion
[DE89-013791] N89-29224
FREQUENCY HOPPING
Packet-error probability analysis for unslotted FH-CDMA (Frequency Hopped-Code Division Multiple-Access) systems with error control coding
[AD-A207964] N89-29054
FREQUENCY MEASUREMENT
Electromagnetic pulse propagation through a stratified ionosphere
[IRF-SR-199] N89-28700
FREQUENCY MODULATION
Fiber optic frequency transfer link
[NASA-CASE-NPO-17703-1-CU] N89-29191
FREQUENCY SHIFT
Measurements of the dipolar velocity of superfluid 3 He-B
[PB89-155444] N89-29218
FREQUENCY STABILITY
Experimental and numerical investigation of coherent structures in turbulent wake flows
[AD-A207866] N89-28759
The 12C16O laser frequency tables for the 34.2 to 62.3 THz (1139 to 2079 cm-1) region
[PB89-193908] N89-28809
FRESNEL LENSES
The manufacture of blazed oblique zone plates for use at 10.6 microns
[NPL-MOM-91] N89-28827
An evaluation of blazed zone plates for use in the 10 micron spectral region
[NPL-MOM-93] N89-28828
FRICTION
High temperature tribometer, phase 1
[AD-A209356] N89-28838
FRICTION FACTOR
Heat-transfer and friction factor design data for all-metal compact heat exchangers
[AD-A208108] N89-28761
FRICTION MEASUREMENT
Pull-out and push-out tests for rubber-to-metal adhesion
[AD-A208100] N89-28647
Skin-friction measurements by laser interferometry N89-28737
FRICTION REDUCTION
Solid lubrication studied by optical means
[AD-A209008] N89-28836
FRONTS (METEOROLOGY)
Application of special sensor microwave/imager data for analysis of cyclonic storms in midlatitudes over the sea
[AD-A207675] N89-28975
FUEL CELLS
Chemical Technology Division
[DE89-013917] N89-28591
Fuel cell technology in the United States
[DE89-013430] N89-28951
Material and fabrication challenges in the development of monolithic solid oxide fuel cells
[DE89-012422] N89-28957
FUEL COMBUSTION
Bifurcation and pattern formation in combustion
[DE89-013829] N89-28590
Investigation of laser-induced fluorescence detection of boron oxides in flames
[AD-A209154] N89-28596
Supersonic combustion at the DFVLR: Results and experiences
[DFVLR-88-044] N89-28610
Hazards of explosives dusts
[DE89-014554] N89-28669
FUEL CONTROL
Engine combustion optimization by exhaust analysis
[PB89-195788] N89-28588
FUEL-AIR RATIO
Engine combustion optimization by exhaust analysis
[PB89-195788] N89-28588
FUNCTIONAL ANALYSIS
Backward analysis
[MEMO-INF-89-14] N89-29080
FUNCTIONAL DESIGN SPECIFICATIONS
A method of software development using functional programming
[MEMO-INF-88-64] N89-29069
Method bases: A new tool for applied information system design
[NLR-MP-88002-U] N89-29271
FURNACES
Furnace for tensile/fatigue testing
[NASA-CASE-LEW-14848-1] N89-28549
Oxidation and hot corrosion of some advanced superalloys at 1300F to 2000F (740C to 1093C)
[AD-A209353] N89-28622
FUSELAGES
The acoustic calibration of aircraft fuselage structures, part 1
[ISVR-TR-169-PT-1] N89-29158
General-purpose heat source development: Extended series test program SRB fragment/fuselage tests
[DE89-014389] N89-29180
FUZZY SETS
A method for assisting in decision-making for multilayer radar absorbent coverings — manufacture
[ONERA-NT-1989-2] N89-28703

G

GALACTIC CLUSTERS
Activities report of the Institute of Astronomy and Astrophysics
[MITT-9] N89-29276
GALACTIC EVOLUTION
Spectral measurements of the cosmic microwave background
[DE89-014895] N89-29296
GALERKIN METHOD
Active damping of vibration in large space structures using a Karhunen-Loeve reduced order model
[AD-A208183] N89-28558
Finite element analysis of incompressible viscous flows around single and multi-element aerofoils in high Reynolds number region
[NAL-TR-1010T] N89-28765
Solution of Euler equations by a discontinuous Galerkin method obtained from a variational formulation of entropy
[CERT-1/332400/DERI] N89-28775
A hybrid perturbation-Galerkin method for differential equations containing a parameter
[NASA-CR-181891] N89-29122
GALLIUM
Thermodynamically stable conducting films of intermetallic PtGa2 on gallium arsenide
[AD-A210077] N89-28716
Measurement of solar proton-proton fusion neutrinos with a Soviet-American gallium experiment
[DE89-014563] N89-29168
Redetermination of crystal structure of zinc thiogallate
[AD-A208931] N89-29234
GALLIUM ARSENIDES
Optical gain control of GaAs microwave monolithic integrated circuit distributed amplifier
[AD-D013969] N89-28705
Thermodynamically stable conducting films of intermetallic PtGa2 on gallium arsenide
[AD-A210077] N89-28716
Ion beam deposition of epitaxial germanium and gallium arsenide layers
[DE89-014044] N89-29225
Vertical gradient freeze GaAs: Growth and electrical properties
[DE89-014894] N89-29228
Multilayered electronic materials and devices based on 3-5 compounds
[AD-A208861] N89-29233

Morphology control of photoelectrochemically etched profiles in n-GaAs
[AD-A208991] N89-29235
Selective area epitaxy of gallium arsenide on silicon, phase 1
[AD-A209079] N89-29238

GALLIUM COMPOUNDS
Electronic-structure study of the Ni-Ga and Ni-In intermetallic compounds using X-ray photoemission spectroscopy
[AD-A209696] N89-28601
A study of thermodynamic phase stability of intermetallic thin films of Pt2Ga, PtGa and PtGa2 on gallium arsenide
[AD-A209698] N89-29241

GAME THEORY
A survey of self-consistency properties in cooperative game theory
[MEMO-763] N89-29072

GAMMA FUNCTION
Bit rate recovery using digital ladder networks
[AD-A209865] N89-29043

GAMMA RAY ASTRONOMY
The orbital space observatory Gamma N89-28528
Activities report of the Institute for Extraterrestrial Physics
[MPE-212] N89-29277

GAMMA RAY LASERS
Proof of the feasibility of coherent and incoherent schemes for pumping a gamma-ray laser
[AD-A208071] N89-28819

GAMMA RAY OBSERVATORY
The orbital space observatory Gamma N89-28528

GAMMA RAY TELESCOPES
The orbital space observatory Gamma N89-28528

GAMMA RAYS
The first large balloon launch from Antarctica
[AD-A207735] N89-28491

GAS DISCHARGES
Studies of the volume and plasma sheath properties of radio frequency discharges
[AD-A207980] N89-29206

GAS EXPANSION
Effects of real gas in hypersonic expansion
[ETN-89-95200] N89-28783

GAS GUNS
Prototype testing for a hybrid gas-gun/railgun device
[DE89-014294] N89-28542

GAS INJECTION
Enhancement of forced convection heat transfer in tubes using staged tangential flow injection
[PB89-204598] N89-28768

GAS IONIZATION
Reversal electron attachment ionizer for detection of trace species
[NASA-CASE-NPO-17596-1-CU] N89-28795

GAS MIXTURES
Hypersonic vehicle environment simulation, phase 1
[AD-A209030] N89-28754
La Recherche Aerospatiale, bimonthly bulletin, number 1988-6
[ESA-TT-1165] N89-29301

GAS PRESSURE
Helium bottle pressure measurement by portable ultrasonic technique
[AD-A208994] N89-29188

GAS TUNGSTEN ARC WELDING
A study of the thermal profiles during autogenous arc welding
[AD-A209440] N89-28843

GAS TURBINE ENGINES
Statistics on aircraft gas turbine engine rotor failures that occurred in US commercial aviation during 1984
[NAPC-PE-185] N89-28516
Statistics on aircraft gas turbine engine rotor failures that occurred in US commercial aviation during 1985
[NAPC-PE-188] N89-28517

GAS-SOLID INTERACTIONS
Solid-vapor differences of electronic stopping powers for protons
[IPPJ-901] N89-29207

GASEOUS FUELS
Preliminary design guide for arctic equipment
[AD-A209455] N89-29024

GASES
Energy and angular distributions of electrons emitted from gases and thin foils during light ion bombardment
[DE89-014445] N89-29147

GASKETS
O-ring gasket test fixture
[NASA-CASE-MFS-28376-1] N89-28546

GELS
Microcellular foams from rigid-rod polymers in solutions: Effect of aggregation characteristics on foam properties
[AD-A209024] N89-28640

GENETIC ENGINEERING
Fuels from microalgae
[DE88-001192] N89-28657

GEOCHEMISTRY
Chemical Technology Division
[DE89-013917] N89-28591

GEOGRAPHIC INFORMATION SYSTEMS
New dimensions from statistical graphics for GIS (Geographic Information System) analysis and interpretation
[DE89-012339] N89-29263

GEOLOGICAL SURVEYS
Development of borehole scanner for underground geological survey N89-28899
Application of aerial side-looking radar imagery in China N89-28902
Three-dimensional computer analysis and modelling of remote sensing-structural geologic problems
[DE89-010875] N89-28924

GEOMAGNETIC TAIL
Parallel electric fields in a simulation of magnetotail reconnection and plasmoid evolution
[DE89-012622] N89-28970

GEOMETRIC ACCURACY
Improvement of classification results of satellite imagery using context information from a topographic map
[NLR-MP-88020-U] N89-28935
Updating land-use information on topographic maps using satellite imagery: Combining the advantages of two accessible sources of geographic information
[NLR-MP-88030-U] N89-28936

GEOMETRIC RECTIFICATION (IMAGERY)
The problem of very high magnifications in holography
[ISL-CO-218/88] N89-28804
The processing of SPOT imagery in Brazil N89-28917
Methods for analyzing SAR images
[VTT-RR-612] N89-28932

GEOMORPHOLOGY
High resolution subsurface imaging with geophysical diffraction tomography
[DE89-013815] N89-28923

GEOPHYSICAL SATELLITES
Satellite enhanced numerical weather prediction
[AD-A210108] N89-28987

GEOPHYSICS
High resolution subsurface imaging with geophysical diffraction tomography
[DE89-013815] N89-28923
Activities report in meteorology in Sweden
[AR-87-88] N89-28999

GEOSYNCHRONOUS ORBITS
A conceptual study of optical earth observation from geosynchronous orbit N89-28880

GERMANIUM
Ion beam deposition of epitaxial germanium and gallium arsenide layers
[DE89-014044] N89-29225

GLIDERS
Glider ground effect investigation
[AD-A209152] N89-28490

GLOBAL POSITIONING SYSTEM
Kinematic vertical positioning using the global positioning system
[ETN-89-94804] N89-28510
Sea gravimetry and Eotvos correction
[REPT-88.3] N89-29006

GLOBULAR CLUSTERS
Evolution of wide binary millisecond pulsars in globular clusters
[MPE-PREPRINT-148] N89-29285
Millisecond radio pulsars in globular clusters
[NASA-CR-185909] N89-29298

GOLD
Formation of monolayers by the coadsorption of thiols on gold: Variation in the length of the head group, tail group and solvent
[AD-A208919] N89-28594
Modelling the in situ infrared reflection-absorption spectra of the diffuse layer
[AD-A209347] N89-28598
Monolayers of 11-trichlorosilylundecyl thioacetate: A system that promotes adhesion between silicon dioxide and evaporated gold
[AD-A208266] N89-28637

GOLD COATINGS
Monolayers of 11-trichlorosilylundecyl thioacetate: A system that promotes adhesion between silicon dioxide and evaporated gold
[AD-A208266] N89-28637

GOODNESS OF FIT
Least-squares best-fit geometric elements
[NPL-DITC-140/89] N89-29125

GRADIENTS
Gradient Newton-flows for complex polynomials
[MEMO-764] N89-28779
The problem of selecting the shape functions for a p-type finite element
[AD-A207798] N89-29117

GRAIN BOUNDARIES
Fundamental studies of grain boundary structure and properties in ICB aluminum
[DE89-014884] N89-28619

GRAPH THEORY
A graph-theoretical approach to block-co-polymer complexes. Part 1: Stars
[MEMO-757-PT-1] N89-28654
A graph-theoretical approach to block-co-polymer complexes. Part 2: Tree approximation
[MEMO-758-PT-2] N89-28655
On the classification of plane graphs representing structurally stable rational Newton-flows
[MEMO-750-REV] N89-28776

GRAPHIC ARTS
QuickDraw data structures for image processing
[AD-A208945] N89-29041

GRAPHITE
Laboratory investigations: Low earth orbit environment chemistry with spacecraft surfaces
[DE89-014280] N89-28533
Solid lubrication studied by optical means
[AD-A209008] N89-28836

GRAPHITE-EPOXY COMPOSITES
Analysis and repair of impact damaged composites
[ARL-STRUCT-R-435] N89-28580

GRAPHS (CHARTS)
Some recent results on long cycles in tough graphs
[MEMO-765] N89-29130

GRATINGS (SPECTRA)
Suprathreshold contrast sensitivity vision test chart
[AD-A209915] N89-29010
Morphology control of photoelectrochemically etched profiles in n-GaAs
[AD-A208991] N89-29235
Photoelectrochemical fabrication of gratings in SiC
[AD-A208992] N89-29236

GRAVIMETRY
Sea gravimetry and Eotvos correction
[REPT-88.3] N89-29006

GRAVITATION THEORY
Fifth force, sixth force and all that: A theoretical (classical) comment
[DE89-611971] N89-29254

GRAVITATIONAL EFFECTS
Tolerable g-level for fluid science experiments --- in space platforms
[TS-7-87] N89-28667
Theoretical model of gravitational perturbation of current collector axisymmetric flow field
[AD-A209499] N89-28756

GRAVITATIONAL FIELDS
Theoretical model of gravitational perturbation of current collector axisymmetric flow field
[AD-A209499] N89-28756
Fifth force, sixth force and all that: A theoretical (classical) comment
[DE89-611971] N89-29254

GRAVITY WAVES
Propagation and saturation of nonlinear inertia-gravity waves in the atmosphere
[AD-A207871] N89-28989

GREEN'S FUNCTIONS
Accurate and efficient modeling of global circuit behavior in VSLI layouts
[ETN-89-95459] N89-28732

GREENHOUSES
Method and apparatus for bio-regenerative life support system
[NASA-CASE-MSC-21629-1] N89-29027

GREENLAND
A numerical study of a mesoscale eddy interaction with an ocean front in the marginal ice zone
[AD-A209192] N89-29002

GROOVING
Morphology control of photoelectrochemically etched profiles in n-GaAs
[AD-A208991] N89-29235

GROUND BASED CONTROL
Acoustic tests on a new motor generator system for the minuteman launch control centers in Hill engineering test facilities 1 and 2, Hill AFB, Utah
[AD-A209598] N89-28717

GROUND EFFECT (AERODYNAMICS)
Glider ground effect investigation
[AD-A209152] N89-28490

GROUND STATE
Electron energy levels in a quantum well within an in-plane magnetic field
[AD-A209351] N89-29256

GROUND TRUTH
Development of a field radiometer as a ground truth equipment for the Japanese ERS-1 N89-28901

GROUND WAVE PROPAGATION
Meteor burst system communications compatibility
[PB89-191167] N89-28692
GROUP THEORY
Discussion of the potential and limitations of direct and large-eddy simulations
[NASA-CR-181892] N89-28762
New infinite-dimensional algebras, sine brackets, and SU (infinity)
[DE89-013178] N89-29108
GULF STREAM
Preliminary neural network detection of a gulf stream in images of sea surface temperature gradients, phase 1
[AD-A207801] N89-29003
Entrainment and homogenization of a passive tracer in a numerical model gyre
[AD-A208020] N89-29005
GYRES
Entrainment and homogenization of a passive tracer in a numerical model gyre
[AD-A208020] N89-29005
GYROSCOPIC STABILITY
Consideration of gravity gradient stabilization for ORION
[AD-A207845] N89-28557

H

HALF SPACES
Exact image theory for uniaxially anisotropic dielectric half space
[PB89-146450] N89-28671
HAMILTONIAN FUNCTIONS
Hamiltonian control systems: Decomposition and clamped dynamics
[MEMO-759] N89-29103
Canonical integration and analysis of periodic maps using non-standard analysis and Lie methods
[DE89-013369] N89-29106
Some recent results on long cycles in tough graphs
[MEMO-765] N89-29130
HARDENING (MATERIALS)
Metallurgical evaluation of 17-4 PH stainless steel castings
[PB89-193262] N89-28615
HARDNESS
Freeze-dried tungsten heavy alloys
[DE89-014933] N89-28620
HARMONIC EXCITATION
Application of optimal control theory for selective vibrational excitation in molecules modeled as harmonic systems
[MEMO-755] N89-29104
HARNESSES
Canadian Forces aircrew ejection, descent, and landing injuries, 1 January 1975 - 31 December 1987
[AD-A208116] N89-29015
HEAD-UP DISPLAYS
Towards a physiologically based HUD (Head-Up Display) symbology
[AD-A207748] N89-28515
Exploring virtual worlds with head-mounted displays
[AD-A208088] N89-28797
HEAT ACCLIMATIZATION
Thermoregulatory competence during exercise transients in a group of heat-acclimated young and middle-aged men is influenced more distinctly by maximal aerobic power than age
[AD-A209753] N89-29009
HEAT BUDGET
Daytime turbulent exchange between the Amazon forest and the atmosphere
[NASA-CR-185487] N89-28961
HEAT EXCHANGERS
A cryocooler for high acceleration applications
[AD-A210075] N89-28670
Analysis of flow boiling of ammonia and R-114 in a matrix heat exchanger
[DE89-012427] N89-28752
Heat-transfer and friction factor design data for all-metal compact heat exchangers
[AD-A208108] N89-28761
Compact heat and mass exchangers of the plate fin type in thermal sorption systems: Application in an absorption heat pump with the working pair CH3OH-LiBr/ZnBr2
[ISBN-90-370-0022-3] N89-28780
HEAT FLUX
Mathematical modeling and analysis of heat pipe start-up from the frozen state
[NASA-CR-185132] N89-28747
HEAT OF FORMATION
Evaporation thermodynamics of monotellurides of selected rare Earth and alkaline Earth elements, and an attempt to systematic correlation between the standard enthalpies of formation
[ETN-89-94655] N89-29257
HEAT PIPES
Mathematical modeling and analysis of heat pipe start-up from the frozen state
[NASA-CR-185132] N89-28747
HEAT PUMPS
Compact heat and mass exchangers of the plate fin type in thermal sorption systems: Application in an absorption heat pump with the working pair CH3OH-LiBr/ZnBr2
[ISBN-90-370-0022-3] N89-28780
HEAT RADIATORS
Arc-textured high emittance radiator surfaces
[NASA-CASE-LEW-14679-1] N89-28651
HEAT RESISTANT ALLOYS
Explanatory research on the protection of carbon-carbon composites against oxidation at very high temperatures (greater than 3000 F) with Engel-Brewer and other intermetallic compounds
[AD-A207907] N89-28577
Oxidation and hot corrosion of some advanced superalloys at 1300F to 2000F (740C to 1093C)
[AD-A209353] N89-28622
Study of sintered magnets of the Nd-Fe-B type
[AD-A209185] N89-29148
HEAT SOURCES
General-purpose heat source development: Extended series test program SRB fragment/fuselage tests
[DE89-014389] N89-29180
HEAT TRANSFER
Modeling of hot fragment conductive ignition of solid propellants with application to melting and evaporation of solids
[AD-A207727] N89-28662
Pressure drop and heat transfer characteristics of nearly neutrally buoyant particulate slurry for advanced energy transmission fluids
[DE89-013645] N89-28751
Analysis of flow boiling of ammonia and R-114 in a matrix heat exchanger
[DE89-012427] N89-28752
Heat transfer in free convection and forced, laminar flow in vertical tubes, considering temperature dependent medium characteristics
[ETN-89-94441] N89-28772
A study of the thermal profiles during autogenous arc welding
[AD-A209440] N89-28843
Daytime turbulent exchange between the Amazon forest and the atmosphere
[NASA-CR-185487] N89-28961
HEAT TRANSFER COEFFICIENTS
Heat-transfer and friction factor design data for all-metal compact heat exchangers
[AD-A208108] N89-28761
Enhancement of forced convection heat transfer in tubes using staged tangential flow injection
[PB89-204598] N89-28768
HEAT TREATMENT
Metallurgical evaluation of 17-4 PH stainless steel castings
[PB89-193262] N89-28615
HEATING
Furnace for tensile/fatigue testing
[NASA-CASE-LEW-14848-1] N89-28549
Modeling of hot fragment conductive ignition of solid propellants with application to melting and evaporation of solids
[AD-A207727] N89-28662
HEATING EQUIPMENT
Spacecraft component heater control system
[NASA-CASE-MFS-28327-1] N89-28556
Igniter heater EMI transient test
[NASA-CR-183743] N89-28566
HEAVY IONS
An optical model description of momentum transfer in heavy ion collisions N89-29162
Particle production results from HELIOS
[DE89-013454] N89-29167
HELICOPTER PERFORMANCE
Correlation of Puma airloads: Evaluation of CFD prediction methods
[NASA-TM-102226] N89-28498
HELICOPTERS
Five year ground exposure of composite materials used on the Bell Model 206L flight service evaluation
[NASA-TM-101645] N89-28579
Noise produced by turbulent flow into a rotor: Users manual for atmospheric turbulence prediction and mean flow and turbulence contraction prediction
[NASA-CR-181791] N89-29154
HELIOSTATS
An improved design for stretched-membrane heliostats
[DE89-013872] N89-28953
HELIUM
Helium bottle pressure measurement by portable ultrasonic technique
[AD-A208994] N89-29188
HELIUM IONS
Photon-ion angular correlation measurements on the system He(+) + Ne: Determination of the spin inversion
[ETN-89-94495] N89-29175
HELIUM ISOTOPES
Measurements of the dipolar velocity of superfluid 3 He-B
[PB89-155444] N89-29218
HERMES MANNED SPACEPLANE
Physical phenomenology and mathematical models of hypersonic motion
[ETN-89-95201] N89-28560
HETEROGENEITY
Solvent effects on simple electron transfer reactions. A comparison of results for homogeneous and heterogeneous systems
[AD-A209381] N89-28600
The analysis of solvent effects on the kinetics of simple heterogeneous electron transfer reactions
[AD-A210078] N89-28602
HETEROJUNCTIONS
Materials analysis and device optimization of CuInSe2 solar cells
[DE89-009434] N89-28944
Polycrystalline cadmium telluride 3n+p solar cell
[DE89-009437] N89-28945
Two-terminal CuInSe-based cascade cells
[DE89-009422] N89-28950
HEURISTIC METHODS
Accurate and efficient modeling of global circuit behavior in VSLI layouts
[ETN-89-95459] N89-28732
Preliminary design of a consultation knowledge-based system for the minimization of distortion in welded structures
[AD-A208842] N89-28834
HIGH ACCELERATION
A cryocooler for high acceleration applications
[AD-A210075] N89-28670
HIGH ALTITUDE
HEMP (High-Altitude Electromagnetic Pulse) validation of FAA (Federal Aviation Administration) radio facility
[AD-A209187] N89-28680
The Strategic High-Altitude Atmospheric Radiation Code (SHARC) user instructions
[AD-A207667] N89-28974
HIGH FREQUENCIES
The use of high-frequency pulsed laser diodes in fringe type laser Doppler anemometry
[ISL-CO-230/88] N89-28826
Chiral organic crystals for high power frequency conversion
[DE89-013791] N89-29224
HIGH GRAVITY ENVIRONMENTS
Higee Technology Development Program, phase 1
[PB89-161434] N89-28587
HIGH LEVEL LANGUAGES
A programming language supporting first-class parallel environments
[AD-A207833] N89-29051
HIGH POWER LASERS
High-power free-electron lasers driven by RF linear accelerators
[AD-A209740] N89-28815
Photoelectrochemical fabrication of gratings in SiC
[AD-A208992] N89-29236
HIGH PRESSURE
Investigation of laser-induced fluorescence detection of boron oxides in flames
[AD-A209154] N89-28596
HIGH PRESSURE OXYGEN
Oxygen storage on zeolites
[AD-A209352] N89-28599
HIGH RESOLUTION
The new generation SPOT satellites SPOT 4 and 5 N89-28914
HIGH STRENGTH ALLOYS
An investigation of the workability of Al-8.5 percent Mg alloys
[AD-A209451] N89-28624
HIGH TEMPERATURE
High temperature adhesive systems
[AD-A209166] N89-28643
High temperature flexible seal
[NASA-CASE-LEW-14695-1] N89-28830

HIGH TEMPERATURE FLUIDS
Hermes preparatory program. Fluid dynamics and numerical analysis. Theoretical modeling of high temperature hypersonic flows
[ANE-13/87] N89-28503
HIGH TEMPERATURE LUBRICANTS
High temperature tribometer, phase 1
[AD-A209356] N89-28838
HIGH TEMPERATURE PROPELLANTS
Modeling of hot fragment conductive ignition of solid propellants with application to melting and evaporation of solids
[AD-A207727] N89-28662
HIGH TEMPERATURE SUPERCONDUCTORS
Chemical Technology Division
[DE89-013917] N89-28591
Metallic bonding to high-temperature superconducting ceramics
[DE89-014668] N89-28635
Superconducting Meissner effect bearings for cryogenic turbomachines, phase 1
[AD-A209875] N89-28839
Non-uniform transition conductivity of superconducting ceramic
[NASA-TM-102133] N89-28851
States of oxygen ordering in YBa2Cu3Oz
[DE89-014893] N89-29227
High-temperature superconductor materials processing: Development of environmentally acceptable processing technologies
[DE89-014391] N89-29229
HIGH TEMPERATURE TESTS
Standard reference material for high temperature viscosity measurements: Results of interlaboratory comparison programme
[NPL-DMA(A)-175] N89-28612
Oxidation and hot corrosion of some advanced superalloys at 1300F to 2000F (740C to 1093C)
[AD-A209353] N89-28622
Development of damping treatment suitable for high temperature environment
[ISVR-TR-174] N89-28652
HISTORIES
Entrepreneurship and innovation: The Dutch sugar beet industry (1858-1919)
[ISBN-90-71617-11-4] N89-29275
HOLES (ELECTRON DEFICIENCIES)
Applied field and total dose dependence of trapped charge buildup in MOS devices
[AD-A209064] N89-29237
Lineshape and lifetime studies of exciton luminescence from confined CuCl thin films
[AD-A209750] N89-29243
HOLOGRAPHY
Two-dimensional signal processing and storage and theory and applications of electromagnetic measurements
[AD-A207827] N89-28689
Holographic modulator arrays
[AD-A209387] N89-28792
The copy of single beam holograms
[ISL-CO-212/88] N89-28802
The problem of very high magnifications in holography
[ISL-CO-218/88] N89-28804
A new holographic inverse filtering method and its application to restoration of degraded remote sensing images N89-28877
HOMOGENEITY
Solvent effects on simple electron transfer reactions. A comparison of results for homogeneous and heterogeneous systems
[AD-A209381] N89-28600
Entrainment and homogenization of a passive tracer in a numerical model gyre
[AD-A208020] N89-29005
HOOP COLUMN ANTENNAS
Near-field testing of the 15-meter hoop-column antenna
[NASA-TM-4073] N89-28550
HOT CORROSION
Oxidation and hot corrosion of some advanced superalloys at 1300F to 2000F (740C to 1093C)
[AD-A209353] N89-28622
HOT PRESSING
Synthesis and hot pressing of ZnS powders
[AD-A209602] N89-28625
HOT-WIRE ANEMOMETERS
Hot-wire anemometry in supersonic flow N89-28738
HUMAN BEINGS
Investigation of a linear systems model for human visual detection and spatial frequency discrimination
[AD-A209397] N89-29022
HUMAN BODY
Anthropometric survey of US Army personnel: Summary statistics
[AD-A209600] N89-29025
HUMAN FACTORS ENGINEERING
Towards a physiologically based HUD (Head-Up Display) symbology
[AD-A207748] N89-28515
Spacecraft flight simulation: A human factors investigation into the man-machine interface between an astronaut and a spacecraft performing docking maneuvers and other proximity operations
[NASA-CR-177502] N89-29020
Human factors evaluation of color use in the Target Data Processor Release 10 (TDP R10)
[AD-A209438] N89-29023
HUMAN PERFORMANCE
Choice and perceived control: Implications for the design of displays
[AD-A208400] N89-29021
HUMAN TOLERANCES
Thermoregulatory competence during exercise transients in a group of heat-acclimated young and middle-aged men is influenced more distinctly by maximal aerobic power than age
[AD-A209753] N89-29009
Suprathreshold contrast sensitivity vision test chart
[AD-A209915] N89-29010
HUMIDITY
Satellite-derived moisture-bogusing profiles for the North Atlantic Ocean
[AD-A207829] N89-28930
Satellite enhanced numerical weather prediction
[AD-A210108] N89-28987
HURRICANES
Hurricane hindcast methodology and wave statistics for Atlantic and Gulf hurricanes from 1956 - 1975
[AD-A207849] N89-29004
HYDRAULIC FLUIDS
Effect of hydraulic fluid on hydroxylammonium nitrate based liquid propellant formulations
[AD-A208061] N89-28663
HYDRAULIC TEST TUNNELS
Small scale model tests in small wind and water tunnels at high incidence and pitch rates. Volume 1: Test program and discussion of results
[AD-A208647] N89-28488
HYDROCARBON COMBUSTION
Supersonic combustion at the DFVLR: Results and experiences
[DFVLR-88-044] N89-28610
Effect of hydraulic fluid on hydroxylammonium nitrate based liquid propellant formulations
[AD-A208061] N89-28663
HYDROCRACKING
Structural definition of synthetic fuels: Wilsonville 1
[DE89-013627] N89-28659
HYDRODYNAMICS
Dynamics of colloidal dispersions via lattice-gas models of an incompressible fluid
[DE89-013146] N89-28750
HYDROGEN
Molecular beam experiment for the determination of differential cross sections of the reaction of deuterium atoms with vibrationally excited hydrogen molecules
[MPIS-10/1988] N89-29178
HYDROGEN ATOMS
Quantization by cosmic background radiation
[AD-A208103] N89-29297
HYDROGEN EMBRITTLEMENT
Comparative analysis of ultrasonic inspection procedures for Kaman K747 root end fittings
[AD-A207762] N89-28512
HYDROGEN OXYGEN FUEL CELLS
Supersonic combustion at the DFVLR: Results and experiences
[DFVLR-88-044] N89-28610
HYDROGEN SULFIDE
Effect of temperature and H2S content on the cracking resistance of a 13 percent chromium martensitic stainless steel in acidified NaCl
[NPL-DMA(A)-173] N89-28631
HYDROLOGY
Military hydrology: Assessment of shuttle imaging radar and LANDSAT imagery for ground-water exploration in arid environments
[AD-A209527] N89-28928
The WMO long-term plan overall policy and strategy 1988-1997: Second WMO long-term plan, part 1
[WMO-690-PT-1] N89-28994
HYDROMETEOROLOGY
Application of special sensor microwave/imager data for analysis of cyclonic storms in midlatitudes over the sea
[AD-A207675] N89-28975
HYDROXYL COMPOUNDS
Effect of hydraulic fluid on hydroxylammonium nitrate based liquid propellant formulations
[AD-A208061] N89-28663
HYDROXYL RADICALS
Collision dynamics and transition probabilities for vibrationally excited OH
[AD-A207856] N89-28976
HYPERBOLIC DIFFERENTIAL EQUATIONS
Difference techniques for solving the advection equation
[WISS-BER-8] N89-28991
HYPERCUBE MULTIPROCESSORS
Non-linear surface fitting of laser range images using a hypercube concurrent computer
[DE89-013720] N89-28808
Large scale function minimization
[AD-A207718] N89-29087
HYPERSONIC FLOW
Hermes preparatory program. Fluid dynamics and numerical analysis. Theoretical modeling of high temperature hypersonic flows
[ANE-13/87] N89-28503
Three-dimensional viscous hypersonic flow over blunt bodies
[DFVLR-FB-89-09] N89-28504
Physical phenomenology and mathematical models of hypersonic motion
[ETN-89-95201] N89-28560
Hypersonic vehicle environment simulation, phase 1
[AD-A209030] N89-28754
Effects of real gas in hypersonic expansion
[ETN-89-95200] N89-28783
HYPERSONIC REENTRY
Physical phenomenology and mathematical models of hypersonic motion
[ETN-89-95201] N89-28560
HYPERSONIC VEHICLES
Hypersonic vehicle environment simulation, phase 1
[AD-A209030] N89-28754
HYPERSONICS
Hermes preparatory program. Fluid dynamics and numerical analysis. Theoretical modeling of high temperature hypersonic flows
[ANE-13/87] N89-28503
HYPERVELOCITY GUNS
Prototype testing for a hybrid gas-gun/railgun device
[DE89-014294] N89-28542
Plasma properties of a large-bore, arc-armature railgun
[AD-A209550] N89-28548
HYPERVELOCITY LAUNCHERS
Prototype testing for a hybrid gas-gun/railgun device
[DE89-014294] N89-28542

I

I BEAMS
Flexural-torsional buckling of monosymmetric beam-columns/tie beams
[PB89-191654] N89-28859
ICE
A numerical study of a mesoscale eddy interaction with an ocean front in the marginal ice zone
[AD-A209192] N89-29002
ICE ENVIRONMENTS
Preliminary design guide for arctic equipment
[AD-A209455] N89-29024
ICE REPORTING
The possibilities of application of satellite data for monitoring ice condition in the Antarctic region N89-28907
IDEAL FLUIDS
Exact solutions for symmetric deformations of hollow bodies of ideal fluids with application to inertial stability
[DE89-014374] N89-28753
IGNITERS
Igniter heater EMI transient test
[NASA-CR-183743] N89-28566
IGNITION
Modeling of hot fragment conductive ignition of solid propellants with application to melting and evaporation of solids
[AD-A207727] N89-28662
Effect of hydraulic fluid on hydroxylammonium nitrate based liquid propellant formulations
[AD-A208061] N89-28663
Hazards of explosives dusts
[DE89-014554] N89-28669
IGNITION SYSTEMS
Technical Evaluation Motor 3 (TEM-3)
[NASA-CR-183740] N89-28567
ILLUMINATING
Orbit determination of sunlight illuminated objects detected by overhead platforms
[AD-A209227] N89-28540
IMAGE ANALYSIS
Segmentation of noisy images
[ETN-89-95461] N89-28701

JPRS Report: Science and Technology. USSR: Space. 16th International Congress of the International Society for Photogrammetry and Remote Sensing, volume 1
[JPRS-USP-89-002-VOL-1] N89-28876
A study on information analysis aids for sea surface temperature image data N89-28897
Development of borehole scanner for underground geological survey N89-28899
Methods for analyzing SAR images
[VTT-RR-612] N89-28932
Energy and Technology Review — analytical cytology
[DE89-013919] N89-28954
Development of a postdispersion system for astronomical infrared observations with Fourier spectrometers and its application in the study of the CO fundamental bands in F, G and K stars
[MPE-214] N89-29280

IMAGE CONTRAST
Investigation of a linear systems model for human visual detection and spatial frequency discrimination
[AD-A209397] N89-29022

IMAGE ENHANCEMENT
Segmentation of noisy images
[ETN-89-95461] N89-28701

IMAGE INTENSIFIERS
An improved algorithm for labeling connected components in a binary image
[AD-A210100] N89-29190

IMAGE PROCESSING
Video processing using the MSX computer
[LINO-163] N89-28694
Segmentation of noisy images
[ETN-89-95461] N89-28701
Positioning error induced by axial sampling in positron emission tomography
[DE89-014519] N89-28791
Exploring virtual worlds with head-mounted displays
[AD-A208088] N89-28797
Non-linear surface fitting of laser range images using a hypercube concurrent computer
[DE89-013720] N89-28808
Robotic grasping of unknown objects: A knowledge-based approach
[DE89-013875] N89-28833
Nonfilm radiography at the Oak Ridge Y-12 Plant
[DE89-014523] N89-28852
JPRS Report: Science and Technology. USSR: Space. 16th International Congress of the International Society for Photogrammetry and Remote Sensing, volume 1
[JPRS-USP-89-002-VOL-1] N89-28876
A new holographic inverse filtering method and its application to restoration of degraded remote sensing images N89-28877
A practical method of remotely sensed digital image's resolving power N89-28879
ERS-1 SAR processing with CESAR N89-28888
EXAS: Experiment on Autonomous SAR processor calibration N89-28890
Development of a field radiometer as a ground truth equipment for the Japanese ERS-1 N89-28901
JPRS Report: Science and Technology. USSR: Space. 16th International Congress of the International Society for Photogrammetry and Remote Sensing, volume 2
[JPRS-USP-89-003-VOL-2] N89-28903
Performance evaluation of ERS-1 Synthetic Aperture Radar Fast Delivery Processor N89-28904
Design aspects of a system for geocoding satellite SAR images N89-28915
The processing of SPOT imagery in Brazil N89-28917
Significant improvement in IR surface-temperature measurements
[DE89-014808] N89-28926
Satellite-derived moisture-bogusing profiles for the North Atlantic Ocean
[AD-A207829] N89-28930
The use of expert systems for preprocessing image data
[NLR-MP-88009-U] N89-28934
Preliminary neural network detection of a gulf stream in images of sea surface temperature gradients, phase 1
[AD-A207801] N89-29003
Monte Carlo analysis of localization errors in magnetoencephalography
[DE89-013221] N89-29007
Transient visual evoked neuromagnetic responses: Identification of multiple sources
[DE89-013438] N89-29008
QuickDraw data structures for image processing
[AD-A208945] N89-29041
An efficiently computable metric for comparing polygonal shapes
[AD-A210105] N89-29045
TiME: Time and memory efficient distance transformations for parallel and pyramid machines
[FOA-C-30531-3.4] N89-29091
Realtime tracking system for the wide-field-of-view telescope project
[DE89-013787] N89-29186
An improved algorithm for labeling connected components in a binary image
[AD-A210100] N89-29190

IMAGE RECONSTRUCTION
Segmentation of noisy images
[ETN-89-95461] N89-28701
Nearfield acoustic holography: Review and perspectives
[ISVR-TR-179] N89-28807
A new holographic inverse filtering method and its application to restoration of degraded remote sensing images N89-28877
Studies on object reconstruction from space using three line scanner imagery N89-28919
Three dimensional reconstruction from serial cross sections by set valued interpolation
[MEMO-754] N89-29076

IMAGE RESOLUTION
Segmentation of noisy images
[ETN-89-95461] N89-28701
The problem of very high magnifications in holography
[ISL-CO-218/88] N89-28804
A practical method of remotely sensed digital image's resolving power N89-28879
Methods for analyzing SAR images
[VTT-RR-612] N89-28932

IMAGERY
Television monitor field shifter and an opto-electronic method for obtaining a stereo image of optimal depth resolution and reduced depth distortion on a single screen
[NASA-CASE-NPO-17249-1-CU] N89-28676

IMAGES
Molecular weight dependence of e-beam resist sensitivity
[AD-A207835] N89-28719
Determining the location of an observer with respect to aerial photographs
[AD-A207791] N89-28929
An improved algorithm for labeling connected components in a binary image
[AD-A210100] N89-29190

IMAGING SPECTROMETERS
A medium resolution imaging spectrometer for the European polar orbiting platform
[ETN-89-95235] N89-28563
Estimation of the simulated JERS-1 data N89-28921

IMAGING TECHNIQUES
Investigation of the effectiveness and applications of Japanese ERS-1 stereoscopic images N89-28884
Performance evaluation of ERS-1 Synthetic Aperture Radar Fast Delivery Processor N89-28904
The Brazilian experience in handling 15 years of remote sensing satellite data N89-28905
A survey of aerial image quality assessment methods N89-28916
Studies on object reconstruction from space using three line scanner imagery N89-28919
Estimation of the simulated JERS-1 data N89-28921
High resolution subsurface imaging with geophysical diffraction tomography
[DE89-013615] N89-28923
Significant improvement in IR surface-temperature measurements
[DE89-014808] N89-28926
Energy and Technology Review — analytical cytology
[DE89-013919] N89-28954
Proceedings of the Antiproton Technology Workshop held in Upton, New York on 10 May 1989
[AD-A210045] N89-29170
United States Air Force Research Initiation Program for 1987, volume 2
[AD-A209727] N89-29259

IMPACT DAMAGE
Analysis and repair of impact damaged composites
[ARL-STRUCT-R-435] N89-28580

IMPACT TESTS
General-purpose heat source development: Extended series test program SRB fragment/fuselage tests
[DE89-014389] N89-29180

IMPEDANCE
The relationship between ground permittivity and the input impedance of a horizontal dipole near ground
[AD-A207746] N89-28688

IMPEDANCE MEASUREMENT
Stochastic processes in CHEMFETs
[AD-A207977] N89-28723

IMPELLERS
Turbomachinery shaft insert
[NASA-CASE-MFS-28345-2] N89-28842

IMPLOSIONS
Exact solutions for symmetric deformations of hollow bodies of ideal fluids with application to inertial stability
[DE89-014374] N89-28753

IMPREGNATING
TGMDA/DDS type impregnating resins structural study
[SNEA-9595] N89-28650

IMPURITIES
Vertical gradient freeze GaAs: Growth and electrical properties
[DE89-014894] N89-29228

INCOMPRESSIBLE FLOW
Development of an efficient solution scheme for incompressible steady-state flow
[AD-A207726] N89-28757
Fast-algorithm development for large-eddy simulation of circular-jet turbulence
[AD-A207928] N89-28760
Finite element analysis of incompressible viscous flows around single and multi-element aerofoils in high Reynolds number region
[NAL-TR-1010T] N89-28765

INCOMPRESSIBLE FLUIDS
Dynamics of colloidal dispersions via lattice-gas models of an incompressible fluid
[DE89-013146] N89-28750

INDEPENDENT VARIABLES
Numerical determination of the location of critical inclinations for long term high eccentricity orbits about Mars
[AD-A209200] N89-28538

INDEXES (DOCUMENTATION)
Bibliography of the NIST (National Institute of Standards and Technology) Electromagnetic Fields Division publications
[PB89-189211] N89-28673
Calendar of selected aeronautical and space meetings
[AGARD-CAL-89/2] N89-29261
NASA thesaurus supplement. A four part cumulative supplement to the 1988 edition of the NASA thesaurus
[NASA-SP-7064-SUPPL-1] N89-29262
NASA thesaurus supplement: A four part cumulative supplement to the 1988 edition (supplement 2)
[NASA-SP-7064-SUPPL-2] N89-29269

INDIA
National program for handling large volumes of satellite data N89-28910

INDIUM ALLOYS
Aluminum alloy
[NASA-CASE-LAR-13924-1-CU] N89-28621
Effective masses and g factors for 2-D light holes in InSb
[DE89-014899] N89-29230

INDIUM COMPOUNDS
Electronic-structure study of the Ni-Ga and Ni-In intermetallic compounds using X-ray photoemission spectroscopy
[AD-A209696] N89-28601

INDONESIA
Marketing and case study of satellite thematic maps and other products of satellite remote sensing
[BCRS-55-16E] N89-28939

INDUCTION (MATHEMATICS)
Probabilistic analysis of semilinear partial differential equations
[AD-A209903] N89-29113

INDUSTRIES
Entrepreneurship and innovation: The Dutch sugar beet industry (1858-1919)
[ISBN-90-71617-11-4] N89-29275

INFORMATION
Information requirements and the implications for parallel computation
[AD-A207802] N89-29088

INFORMATION DISSEMINATION
The Brazilian experience in handling 15 years of remote sensing satellite data N89-28905
ESA's activities and plans for remote sensing data systems N89-28906
National program for handling large volumes of satellite data N89-28910
International technology transfer as practiced by the U.S.S.R.: Implications for US national security
[AD-A208010] N89-29274

INFORMATION RETRIEVAL
A conceptual level design of a design database for the computer-aided prototyping system
[AD-A207808] N89-29050
NASA thesaurus supplement. A four part cumulative supplement to the 1988 edition of the NASA thesaurus
[NASA-SP-7064-SUPPL-1] N89-29262
NASA thesaurus supplement: A four part cumulative supplement to the 1988 edition (supplement 2)
[NASA-SP-7064-SUPPL-2] N89-29269

INFORMATION SYSTEMS
The use of a UNIX-based workstation in the Information Systems Laboratory
[AD-A209485] N89-29267
Moving optical technology in-house
[AD-A207850] N89-29268
Method bases: A new tool for applied information system design
[NLR-MP-88002-U] N89-29271
INFORMATION THEORY
The communication complexity of interval orders
[MEMO-745] N89-29102
A note on the communication complexity of totally unimodular matrices
[MEMO-768] N89-29131
INFRARED ASTRONOMY
Activities report of the Institute for Extraterrestrial Physics
[MPE-212] N89-29277
A deep optical infrared survey
[AD-A207930] N89-29278
INFRARED DETECTORS
Field induced gap infrared detector
[NASA-CASE-NPO-17526-1-CU] N89-28796
Significant improvement in IR surface-temperature measurements
[DE89-014808] N89-28926
INFRARED IMAGERY
Proposed concepts for a advanced optical payload for second generation Meteosat
[ETN-89-95236] N89-28564
Preliminary neural network detection of a gulf stream in images of sea surface temperature gradients, phase 1
[AD-A207801] N89-29003
Detection of target formations in infrared imagery
[ETCA-88-R-070] N89-29198
INFRARED LASERS
The 12C16O laser frequency tables for the 34.2 to 62.3 THz (1139 to 2079 cm-1) region
[PB89-193908] N89-28809
The manufacture of blazed oblique zone plates for use at 10.6 microns
[NPL-MOM-91] N89-28827
An evaluation of blazed zone plates for use in the 10 micron spectral region
[NPL-MOM-93] N89-28828
INFRARED RADIATION
Infrared study of carbon deposits on catalysts
[DE89-013310] N89-28634
The Strategic High-Altitude Atmospheric Radiation Code (SHARC) user instructions
[AD-A207667] N89-28974
Digital refractometry of piezoelectric crystalline media
[AD-A209362] N89-29239
INFRARED RADIOMETERS
Proposed concepts for a advanced optical payload for second generation Meteosat
[ETN-89-95236] N89-28564
INFRARED REFLECTION
Modelling the in situ infrared reflection-absorption spectra of the diffuse layer
[AD-A209347] N89-28598
Airborne FLIR (Forward Looking Infrared) detection of surface targets
[AD-A209250] N89-29189
INFRARED SCANNERS
Proposed concepts for a advanced optical payload for second generation Meteosat
[ETN-89-95236] N89-28564
Optical properties and error sources of an airborne radiometer
[MITT-60] N89-28799
Significant improvement in IR surface-temperature measurements
[DE89-014808] N89-28926
INFRARED SPECTRA
Modelling the in situ infrared reflection-absorption spectra of the diffuse layer
[AD-A209347] N89-28598
Infrared study of carbon deposits on catalysts
[DE89-013310] N89-28634
Estimation of the simulated JERS-1 data N89-28921
A high-resolution atlas of the infrared spectrum of the sun and the earth atmosphere from space. A compilation of ATMOS spectra of the region from 650 to 4800 cm-1 (2.3 to 16 microns). Volume 2: Stratosphere and mesosphere, 650 to 3350 cm-1
[NASA-RP-1224-VOL-2] N89-28969
INFRARED SPECTROMETERS
Proposed concepts for a advanced optical payload for second generation Meteosat
[ETN-89-95236] N89-28564
INFRARED SPECTROSCOPY
Reaction kinetics and mechanism of chain reactions and explosions via transient spectroscopy
[AD-A209169] N89-28597
Modelling the in situ infrared reflection-absorption spectra of the diffuse layer
[AD-A209347] N89-28598
A high-resolution atlas of the infrared spectrum of the sun and the earth atmosphere from space. A compilation of ATMOS spectra of the region from 650 to 4800 cm-1 (2.3 to 16 microns). Volume 2: Stratosphere and mesosphere, 650 to 3350 cm-1
[NASA-RP-1224-VOL-2] N89-28969
Development of a postdispersion system for astronomical infrared observations with Fourier spectrometers and its application in the study of the CO fundamental bands in F, G and K stars
[MPE-214] N89-29280
La Recherche Aerospatiale, bimonthly bulletin, number 1988-4
[ESA-TT-1161] N89-29299
INFRARED TELESCOPES
A deep optical infrared survey
[AD-A207930] N89-29278
INFRARED WINDOWS
Redetermination of crystal structure of zinc thiogallate
[AD-A208931] N89-29234
INJECTORS
High-brightness electron injectors: A review
[DE89-014244] N89-28711
INJURIES
A program for the study of skeletal muscle catabolism following physical trauma
[AD-A207983] N89-29014
INSERTS
Turbomachinery shaft insert
[NASA-CASE-MFS-28345-2] N89-28842
INSPECTION
Comparative analysis of ultrasonic inspection procedures for Kaman K747 root end fittings
[AD-A207762] N89-28512
A survey of JP-8 and JP-5 properties
[AD-A207721] N89-28661
INSTRUMENT APPROACH
Aircraft accident/incident summary reports: Belleville, Illinois, August 22, 1987; Pensacola, Florida, December 27, 1987
[PB89-910405] N89-28507
INSTRUMENT ERRORS
Optical properties and error sources of an airborne radiometer
[MITT-60] N89-28799
INTEGRAL EQUATIONS
Electromagnetic scattering from two dimensional objects using the field feedback formulation
[AD-A209563] N89-28685
Approximation methods for scattering from rough surfaces
[AD-A209482] N89-29192
INTEGRALS
Application of Cholesky-like matrix decomposition methods to the evaluation of atomic orbital integrals and integral derivatives
[AD-A209682] N89-29112
INTEGRATED CIRCUITS
Reactive ion etching of polymer films
[AD-A207674] N89-28645
An X-ray source for lithography based on a quasi-optical maser undulator
[AD-A208522] N89-28675
Optical gain control of GaAs microwave monolithic integrated circuit distributed amplifier
[AD-D013969] N89-28705
Electrical characterization of signal processing microcircuit
[AD-A209078] N89-28714
VLSI integrated circuit contact reliability by interface spectroscopy
[AD-A207666] N89-28718
Fundamental aspects of reactions in titanium-silicon thin films for integrated circuits
[ETN-89-95466] N89-28733
Laser-induced diode linking for wafer-scale integration
[AD-A207921] N89-28818
Picosecond electrooptic investigations of integrated circuits
[AD-A209134] N89-28863
A manufacturing scheduler's perspective on semiconductor fabrication
[AD-A208372] N89-29232
INTEGRATED MISSION CONTROL CENTER
Acoustic tests on a new motor generator system for the minuteman launch control centers in Hill engineering test facilities 1 and 2, Hill AFB, Utah
[AD-A209598] N89-28717
INTEGRATED OPTICS
Theoretical investigations of an integrated optics switching element with asymmetric directional couplers for switching matrices
[ETN-89-94439] N89-29196
INTEGRATORS
Canonical integration and analysis of periodic maps using non-standard analysis and Lie methods
[DE89-013369] N89-29106
INTERACTIONAL AERODYNAMICS
Study of the wing-vortex interaction in three dimensional flows (incompressible inviscid flow)
[ISL-R-123/87] N89-28494
Profile-vortex interactions
[ISL-R-125/87] N89-28495
INTERFACE STABILITY
A study of thermodynamic phase stability of intermetallic thin films of Pt2Ga, PtGa and PtGa2 on gallium arsenide
[AD-A209698] N89-29241
INTERFACES
Space module assembly apparatus with docking alignment flexibility and restraint
[NASA-CASE-MSC-21211-1] N89-28553
Expandable pallet for space station interface attachments
[NASA-CASE-MSC-21117-2] N89-28554
Transfer of files between IE-32C PC/AT CAD system and Autotrol AD/380 graphics system
[PD-CC-8903] N89-29270
INTERMETALLICS
Explanatory research on the protection of carbon-carbon composites against oxidation at very high temperatures (greater than 3000 F) with Engel-Brewer and other intermetallic compounds
[AD-A207907] N89-28577
Electronic-structure study of the Ni-Ga and Ni-In intermetallic compounds using X-ray photoemission spectroscopy
[AD-A209696] N89-28601
Thermodynamically stable conducting films of intermetallic PtGa2 on gallium arsenide
[AD-A210077] N89-28716
Effective masses and g factors for 2-D light holes in InSb
[DE89-014899] N89-29230
A study of thermodynamic phase stability of intermetallic thin films of Pt2Ga, PtGa and PtGa2 on gallium arsenide
[AD-A209698] N89-29241
A bolt-on deposition source for ultra-high-vacuum growth of intermetallic compound films
[AD-A209699] N89-29242
INTERNAL COMBUSTION ENGINES
Engine combustion optimization by exhaust analysis
[PB89-195788] N89-28588
INTERNATIONAL COOPERATION
Training Course for Tropical Earth Resources Satellite (EARS) bridging phase
[BCRS-88-16D] N89-28938
The WMO long-term plan overall policy and strategy 1988-1997: Second WMO long-term plan, part 1
[WMO-690-PT-1] N89-28994
The World Weather Watch Program 1988-1997: Second WMO long-term plan, part 2, volume 1
[WMO-691-PT-2-VOL-1] N89-28995
The World Climate Program 1988-1997: Second WMO long-term plan, part 2, volume 2
[WMO-692-PT-2-VOL-2] N89-28996
Activities report in international astronomy
[ETN-89-95333] N89-29281
Activities report of ESA
[ISSN-0258-025X] N89-29302
INTERPLANETARY MAGNETIC FIELDS
Electric fields in earth orbital space
[AD-A209542] N89-28973
INTERPOLATION
An algorithm for smooth interpolation to scattered data in R2
[MEMO-748] N89-29066
Three dimensional reconstruction from serial cross sections by set valued interpolation
[MEMO-754] N89-29076
Interpolating polynomials from their values
[AD-A210102] N89-29114
INTERSTELLAR MATTER
Activities report of the Institute of Astronomy and Astrophysics
[MITT-9] N89-29276
INTERVALS
The communication complexity of interval orders
[MEMO-745] N89-29102
INVARIANCE
The invariance of classical electromagnetism under Charge-conjugation, Parity and Time-reversal (CPT) transformations N89-29161
INVERSE SCATTERING
The inverse scattering problem for acoustic and electromagnetic waves
[AD-A209202] N89-28681

INVERTERS
Field tests of a novel inverter for photovoltaic power conditioning
[DE89-014322] N89-28958
ION BEAMS
Multicomponent e-beam resists containing organometallic compounds and reactive monomers
[AD-A207716] N89-28606
Reactive ion etching of polymer films
[AD-A207674] N89-28645
Trochoidal analysis of scattered electrons in a merged electron-ion beam geometry
[NASA-CASE-NPO-16789-1-CU] N89-29169
Ion beam deposition of epitaxial germanium and gallium arsenide layers
[DE89-014044] N89-29225
Quantitative analysis of laser interferometer waveforms obtained during oxygen reactive-ion etching of thin polymer films
[AD-A207836] N89-29248
ION CYCLOTRON RADIATION
High power ICRF heating experiments on the JIPP T-IIU tokamak
[IPPJ-903] N89-29209
ION DISTRIBUTION
Chemical effects of Ne(+) bombardment on the MoS2(0001) surface studied by high-resolution photoelectron spectroscopy
[AD-A207734] N89-29247
ION ENGINES
Ion optics for high power 50-cm-diam ion thrusters
[NASA-TM-102143] N89-28571
ION IMPLANTATION
Ion implantation of ceramic bearings
[AD-A209770] N89-28644
The amorphous to gamma transformation in ion implanted Al2O3
[DE89-014797] N89-29226
ION IRRADIATION
Energy and angular distributions of electrons emitted from gases and thin foils during light ion bombardment
[DE89-014445] N89-29147
Studies of the volume and plasma sheath properties of radio frequency discharges
[AD-A207980] N89-29206
Chemical effects of Ne(+) bombardment on the MoS2(0001) surface studied by high-resolution photoelectron spectroscopy
[AD-A207734] N89-29247
Quantitative analysis of laser interferometer waveforms obtained during oxygen reactive-ion etching of thin polymer films
[AD-A207836] N89-29248
ION PROPULSION
Ion optics for high power 50-cm-diam ion thrusters
[NASA-TM-102143] N89-28571
ION SOURCES
Compound-lens diode for HERMES 3
[DE89-013065] N89-28708
Effect of a converter electrode in a multicusp negative ion source
[IPPJ-914] N89-29214
ION STORAGE
Proceedings of a RAND Workshop on Antiproton Science and Technology
[AD-A208168] N89-29172
IONIC DIFFUSION
Use of microelectrode arrays to directly measure diffusion of ions in solid electrolytes: Proof of concept experiments involving Ag+ in a solid polymer electrolyte
[AD-A209536] N89-28604
IONIZATION
Ion-molecule chemistry within doubly charged ammonia clusters
[AD-A207764] N89-28608
Ion-molecule chemistry within triply charged ammonia clusters
[AD-A207766] N89-28609
Fundamental processes in partially ionized plasmas
[AD-A207910] N89-29204
Experiments on the magnetic field and neutral density limits on CIV interaction
[TRITA-EPP-88-08] N89-29216
On the spoke structure in critical velocity rotating plasmas
[TRITA-EPP-89-01] N89-29217
IONIZATION CROSS SECTIONS
Trochoidal analysis of scattered electrons in a merged electron-ion beam geometry
[NASA-CASE-NPO-16789-1-CU] N89-29169
IONIZING RADIATION
Radiothermoluminescence studies of polymer solids
[AD-A209036] N89-28641
IONOSPHERIC DISTURBANCES
Ionospheric variability
[AD-A209251] N89-28972
IONOSPHERIC PROPAGATION
Electromagnetic pulse propagation through a stratified ionosphere
[IRF-SR-199] N89-28700
IONS
Ion-molecule chemistry within doubly charged ammonia clusters
[AD-A207764] N89-28608
Ion-molecule chemistry within triply charged ammonia clusters
[AD-A207766] N89-28609
IRON ALLOYS
Sulfidation/oxidation properties of iron-based alloys containing niobium and aluminum
[DE89-013766] N89-28617
Theoretical analysis of phase transformations in Fe-Ni Invar-type alloys
[DE89-014454] N89-28618
Pressure induced anomaly at Tc in Fe78 Mo2 B20
[NAL-TM-MT-8806] N89-28628
IRRADIANCE
Solar spectral irradiances with their diversity between 120 and 900 nm
[AERONOMICA-ACTA-A-338-1989] N89-29294
IRRADIATION
Applied field and total dose dependence of trapped charge buildup in MOS devices
[AD-A209064] N89-29237
IRRIGATION
Identification of irrigated areas in the Sao Francisco Valley through remote sensing data. Pilot area: Petrolina-Juazeiro
[INPE-4800-RPE/587] N89-28925
ISOTOPIC LABELING
Determination of moisture diffusion in carbon fiber reinforced epoxy composites by means of radioisotope tracer technique
[BMVG-FBWT-88-2] N89-28581
ITERATION
The problem of selecting the shape functions for a p-type finite element
[AD-A207798] N89-29117
United States Air Force Research Initiation Program for 1987, volume 2
[AD-A209727] N89-29259
ITERATIVE SOLUTION
Generalized projected gradient-type iterative method for parametric and functional optimization of dynamical systems subject to constraints
[ONERA-NT-1988-9] N89-29063

J

JAPANESE SPACE PROGRAM
Earth observation programs in Japan N89-28920
Estimation of the simulated JERS-1 data N89-28921
JAPANESE SPACECRAFT
Outline of MOS-1 Verification Program (MVP) N89-28883
JET BOUNDARIES
Fast-algorithm development for large-eddy simulation of circular-jet turbulence
[AD-A207928] N89-28760
JET EXHAUST
Measurements of mean-flow and turbulence characteristics in a turbojet exhaust using a laser velocimeter
[ISL-CO-226/88] N89-28519
JET FLOW
Measurements of mean-flow and turbulence characteristics in a turbojet exhaust using a laser velocimeter
[ISL-CO-226/88] N89-28519
Laser velocimetry in the close wake of an axisymmetric rear body
[ISL-R-114/87] N89-28774
JOINTS (JUNCTIONS)
Static and dynamic deflection studies of the SRM aft case-nozzle joint
[NASA-TM-100373] N89-28568
JOSEPHSON JUNCTIONS
Fluxons and order in long Josephson junctions
[AD-A207925] N89-29249
Vortices in long Josephson junctions
[AD-A207936] N89-29250
Microwave detection using Josephson elements
[ETN-89-94650] N89-29252
JP-5 JET FUEL
A survey of JP-8 and JP-5 properties
[AD-A207721] N89-28661
JP-8 JET FUEL
A survey of JP-8 and JP-5 properties
[AD-A207721] N89-28661
JUDGMENTS
Risk management for air ambulance helicopters operators
[DOT/FAA/DS-88/7] N89-28506
Suprathreshold contrast sensitivity vision test chart
[AD-A209915] N89-29010

K

KALMAN FILTERS
Systolic VLSI array for implementing the Kalman filter algorithm
[NASA-CASE-NPO-17108-1-CU] N89-28713
KEPLER LAWS
Modeling of short arc orbital constraints for incorporation into photogrammetric adjustment of MEOSS data
[DFVLR-FB-89-14] N89-28943
KINEMATICS
A survey of JP-8 and JP-5 properties
[AD-A207721] N89-28661
A new scattering formula for depth-resolving X-ray diffractometry based on a kinematic theory
[ETN-89-94430] N89-29195
KINETIC ENERGY
Exact solutions for symmetric deformations of hollow bodies of ideal fluids with application to inertial stability
[DE89-014374] N89-28753
KINETICS
Synthesis and hot pressing of ZnS powders
[AD-A209602] N89-28625
Quantitative investigation of the kinetics of a laser-pumped barium vapor
[ETN-89-94434] N89-28823
KNOWLEDGE BASES (ARTIFICIAL INTELLIGENCE)
Software technology to support real-time embedded artificial intelligence-based applications, phase 1
[AD-A209133] N89-29042
Northeast artificial intelligence consortium annual report 1987. Volume 8: Knowledge base maintenance using logic programming methodologies
[AD-A209453] N89-29095
Northeast artificial intelligence consortium annual report 1987. Volume 9: Computer architectures for very large knowledge bases
[AD-A209454] N89-29096
Implementation of a distributed object-oriented database management system
[AD-A209437] N89-29265
KNUDSEN GAGES
A bolt-on deposition source for ultra-high-vacuum growth of intermetallic compound films
[AD-A209699] N89-29242
KRYPTON FLUORIDE LASERS
An improved hibachi support structure for electron-beam diode foils
[DE89-014023] N89-28810
Chemical and Laser Sciences Division
[DE89-014385] N89-28811

L

LABORATORIES
Multilayered electronic materials and devices based on 3-5 compounds
[AD-A208861] N89-29233
LAGRANGE COORDINATES
Total Lagrangian formulation for large-displacement analysis of the triangular finite elements
[AD-A209378] N89-29111
LAGRANGE MULTIPLIERS
Solution of a tinned iron purchasing problem by Lagrangian relaxation
[MEMO-735] N89-29074
LAMINAR FLOW
Finite element analysis of incompressible viscous flows around single and multi-element aerofoils in high Reynolds number region
[NAL-TR-1010T] N89-28765
Experimental investigations of flow forces exerted on spheres in rest and in motion, in a plane Poiseville flow
[ETN-89-94433] N89-28770
Heat transfer in free convection and forced, laminar flow in vertical tubes, considering temperature dependent medium characteristics
[ETN-89-94441] N89-28772
LAMINATES
Composite material repair and reliability
[AD-A209150] N89-28574
Analysis and repair of impact damaged composites
[ARL-STRUCT-R-435] N89-28580

A summary of the UK results for a VAMAS round robin project on delamination of composite materials --- Versailles project on advanced materials and standards (VAMAS)
[NPL-DMA(A)-179] N89-28584

LAND USE
Integrating satellite data with information from topographic maps: Method and applications --- SPOT
[NLR-MP-87035-U] N89-28933
Updating land-use information on topographic maps using satellite imagery: Combining the advantages of two accessible sources of geographic information
[NLR-MP-88030-U] N89-28936
Marketing and case study of satellite thematic maps and other products of satellite remote sensing
[BCRS-55-16E] N89-28939

LANDING GEAR
Aircraft accident/incident summary reports: Belleville, Illinois, August 22, 1987; Pensacola, Florida, December 27, 1987
[PB89-910405] N89-28507

LANDSAT SATELLITES
Identification of irrigated areas in the Sao Francisco Valley through remote sensing data. Pilot area: Petrolina-Juazeiro
[INPE-4800-RPE/587] N89-28925
Military hydrology: Assessment of shuttle imaging radar and LANDSAT imagery for ground-water exploration in arid environments
[AD-A209527] N89-28928

LANGUAGE PROGRAMMING
Language constructs and a search procedure to model and solve combinatorial problems
[MEMO-753] N89-29075

LAP JOINTS
Comparison of peel and lap shear bond strengths for elastic joints with and without residual stresses
[AD-A208102] N89-28867

LARGE SPACE STRUCTURES
A torsional suspension system for testing space structures
[NASA-CASE-LAR-14149-1-SB] N89-28547
Active damping of vibration in large space structures using a Karhunen-Loeve reduced order model
[AD-A208183] N89-28556

LASER ANEMOMETERS
Laser Doppler anemometry N89-28739
Laser Doppler anemometry in supersonic flows: Problems of seeding and angular bias N89-28740
Laser velocimetry in the close wake of an axisymmetric rear body
[ISL-R-114/87] N89-28774

LASER APPLICATIONS
Investigation of laser-induced fluorescence detection of boron oxides in flames
[AD-A209154] N89-28596
Chemical and Laser Sciences Division
[DE89-014385] N89-28811
Lidar measurements of sea surface waves N89-28909
Optical laser technology and its application to Defense Manpower Data Center's (DMDC) querry facsimile (QFAX) data base system
[AD-A207832] N89-29194

LASER BEAMS
Chemical and Laser Sciences Division
[DE89-014385] N89-28811
Laser-induced diode linking for wafer-scale integration
[AD-A207921] N89-28818
Unlimited acceleration of particles by a system of multi-laser beams
[IPPJ-902] N89-29206

LASER DAMAGE
Increase of the damage thresholds of dielectric layer systems for the Nd laser
[ETN-89-94436] N89-28824
Transient visual effects of prolonged small spot foveal laser exposure
[AD-A207945] N89-29012

LASER DOPPLER VELOCIMETERS
Measurements of mean-flow and turbulence characteristics in a turbojet exhaust using a laser velocimeter
[ISL-CO-226/88] N89-28519
Laser Doppler anemometry N89-28739
Laser Doppler anemometry in supersonic flows: Problems of seeding and angular bias N89-28740
Laser velocimetry in the close wake of an axisymmetric rear body
[ISL-R-114/87] N89-28774
The use of high-frequency pulsed laser diodes in fringe type laser Doppler anemometry
[ISL-CO-230/88] N89-28826
Wind profile estimation from point to point laser distortion data
[NASA-CR-185891] N89-28990

LASER INDUCED FLUORESCENCE
Investigation of laser-induced fluorescence detection of boron oxides in flames
[AD-A209154] N89-28596
Collision dynamics and transition probabilities for vibrationally excited OH
[AD-A207856] N89-28976

LASER INTERFEROMETRY
Skin-friction measurements by laser interferometry N89-28737
Achievement of the optimum performance from laser interferometer systems when applied to precision length measurement in the free atmosphere
[NPL-MOM-92] N89-28825
Quantitative analysis of laser interferometer waveforms obtained during oxygen reactive-ion etching of thin polymer films
[AD-A207836] N89-29248

LASER MATERIALS
Chiral organic crystals for high power frequency conversion
[DE89-013791] N89-29224

LASER MODE LOCKING
Method and circuit for controlling the evolution time interval of a laser output pulse
[NASA-CASE-LAR-13772-1] N89-28816

LASER OUTPUTS
Holographic modulator arrays
[AD-A209387] N89-28792
Linear theory of uncompensated thermal blooming in turbulence
[DE89-014604] N89-28812
Method and circuit for controlling the evolution time interval of a laser output pulse
[NASA-CASE-LAR-13772-1] N89-28816
Method and circuit for shaping laser output pulses
[NASA-CASE-LAR-14203-1] N89-28817
Microwave emission from relativistic electron beams
[AD-A209653] N89-29181

LASER PUMPING
Proof of the feasibility of coherent and incoherent schemes for pumping a gamma-ray laser
[AD-A208071] N89-28819
Quantitative investigation of the kinetics of a laser-pumped barium vapor
[ETN-89-94434] N89-28823

LASER SPECTROMETERS
Chemical and Laser Sciences Division
[DE89-014385] N89-28811

LASER SPECTROSCOPY
The 12C16O laser frequency tables for the 34.2 to 62.3 THz (1139 to 2079 cm-1) region
[PB89-193908] N89-28809

LASER STABILITY
The 12C16O laser frequency tables for the 34.2 to 62.3 THz (1139 to 2079 cm-1) region
[PB89-193908] N89-28809

LASERS
Non-linear surface fitting of laser range images using a hypercube concurrent computer
[DE89-013720] N89-28808
Digital refractometry of piezoelectric crystalline media
[AD-A209362] N89-29239
United States Air Force Research Initiation Program for 1987, volume 2
[AD-A209727] N89-29259

LATHES
Universal precision sine bar attachment
[NASA-CASE-MFS-28253-1] N89-28831

LATTICES (MATHEMATICS)
Some aspects of a lattice formulation of chiral gauge theories
[NIKHEF-ITFA-88-51] N89-29151

LAUNCHERS
REGGIE results for the Nunnally mass launcher
[DE89-014377] N89-28543

LAUNCHING
The first large balloon launch from Antarctica
[AD-A207735] N89-28491
REGGIE results for the Nunnally mass launcher
[DE89-014377] N89-28543
Acoustic tests on a new motor generator system for the minuteman launch control centers in Hill engineering test facilities 1 and 2, Hill AFB, Utah
[AD-A209598] N89-28717

LAUNCHING BASES
Acoustic tests on a new motor generator system for the minuteman launch control centers in Hill engineering test facilities 1 and 2, Hill AFB, Utah
[AD-A209598] N89-28717

LAYOUTS
Routing channels in VLSI layout
[ISBN-90-6275-535-4] N89-28731
Accurate and efficient modeling of global circuit behavior in VSLI layouts
[ETN-89-95459] N89-28732
New layout of Amsterdam pulse stretcher
[NIKHEF-K/APS/88-01A-REV] N89-29182
Apertures of ring quadrupoles and sextupoles
[NIKHEF-K/APS/88-03] N89-29183
Orbit correction scheme for the new ring --- Amsterdam electron accelerator
[NIKHEF-K/APS/88-04] N89-29184
Updated OC scheme --- electron orbit correction
[NIKHEF-K/APS/88-04A] N89-29185

LEAD ACID BATTERIES
Accelerated life evaluation of valve-regulated lead-acid batteries
[DE89-012429] N89-28710

LEADERSHIP
Sleep deprivation and its effect on combat effectiveness
[AD-A207970] N89-29013

LEADING EDGES
Analysis of leading edge separation using a low order panel method
[NASA-CR-185892] N89-28493

LEAKAGE
High temperature flexible seal
[NASA-CASE-LEW-14695-1] N89-28830

LEARNING
A robot that walks: Emergent behaviors from a carefully evolved network
[AD-A207958] N89-29026

LEAST SQUARES METHOD
Least-squares best-fit geometric elements
[NPL-DITC-140/89] N89-29125

LENGTH
Achievement of the optimum performance from laser interferometer systems when applied to precision length measurement in the free atmosphere
[NPL-MOM-92] N89-28825
Apertures of ring quadrupoles and sextupoles
[NIKHEF-K/APS/88-03] N89-29183

LENSES
Compound-lens diode for HERMES 3
[DE89-013065] N89-28708

LEPTONS
Measurement of electroweak effects and topological branching conditions in the reaction e(+)e(-) yields tau(+)tau(-) in the storage ring PETRA
[MPI-PAE/EXP.EL-195] N89-29173

LIFE (DURABILITY)
Arc-textured high emittance radiator surfaces
[NASA-CASE-LEW-14679-1] N89-28651

LIFT
Profile-vortex interactions
[ISL-R-125/87] N89-28495

LIGHT ALLOYS
An investigation of the workability of Al-8.5 percent Mg alloys
[AD-A209451] N89-28624

LIGHT AMPLIFIERS
Microwave emission from relativistic electron beams
[AD-A209653] N89-29181

LIGHT BEAMS
The copy of single beam holograms
[ISL-CO-212/88] N89-28802

LIGHT EMITTING DIODES
Field induced gap infrared detector
[NASA-CASE-NPO-17526-1-CU] N89-28796
The use of high-frequency pulsed laser diodes in fringe type laser Doppler anemometry
[ISL-CO-230/88] N89-28826

LIGHT MODULATION
Holographic modulator arrays
[AD-A209387] N89-28792
Display characteristics of example light-valve projectors
[AD-A209580] N89-29193

LIGHT SCATTERING
Radiative transfer in falling snow: A two-stream approximation
[AD-A208960] N89-29187

LIGHT TRANSMISSION
Fiber optic frequency transfer link
[NASA-CASE-NPO-17703-1-CU] N89-29191

LIGHTNING
HEMP (High-Altitude Electromagnetic Pulse) validation of FAA (Federal Aviation Administration) radio facility
[AD-A209187] N89-28680
Analysis of the VHF-UHF electromagnetic radiation of lightning: Application to a model of the negative stepped-leader propagation
[ONERA-NT-1989-1] N89-29000

LIMITS (MATHEMATICS)
A necessary condition for B-convergence of Runge-Kutta methods
[TW-89-01] N89-29129
Are limits of alpha-discounted optimal policies Blackwell optimal: A counterexample
[TW-88-10] N89-29139

LINEAR ACCELERATORS
High-power free-electron lasers driven by RF linear accelerators
[AD-A209740] N89-28815
Proof of the feasibility of coherent and incoherent schemes for pumping a gamma-ray laser
[AD-A208071] N89-28819
LINEAR PROGRAMMING
Residual vibration reduction in computer controlled machines
[AD-A208074] N89-28866
Chaotic behavior in a new class of parallel optimization algorithms
[DE89-014069] N89-29040
A prototype for converting Linear Programming (LP) models to structured modeling graphs
[AD-A208166] N89-29059
Methods of combinatorial optimization and their range of applicability
[MEMO-766] N89-29073
LINEAR SYSTEMS
Model reduction of linear conservative mechanical systems
[MEMO-752] N89-28845
Modelling, information, processing, and control
[AD-A207810] N89-28865
On constrained multivariable adaptive control
[LAAS-89.093] N89-29101
The problem of selecting the shape functions for a p-type finite element
[AD-A207798] N89-29117
Linear algebra support modules for approximation and other software
[NPL-DITC-142/89] N89-29126
LINEAR TRANSFORMATIONS
On planar point matching under affine transformation
[AD-A210106] N89-29046
LIPIDS
Fuels from microalgae
[DE88-001192] N89-28657
Stochastic processes in CHEMFETs
[AD-A207977] N89-28723
LIQUEFACTION
Modeling of hot fragment conductive ignition of solid propellants with application to melting and evaporation of solids
[AD-A207727] N89-28662
LIQUID BEARINGS
Turbomachinery rotor support with damping
[NASA-CASE-MFS-28345-1] N89-28841
LIQUID CHROMATOGRAPHY
Multivariate analysis of UV-spectral data for solute tracking in HPLC
[ISBN-90-6275-535-6] N89-28614
Emerging resin characterization
[AD-A208173] N89-28649
LIQUID METALS
Mathematical modeling and analysis of heat pipe start-up from the frozen state
[NASA-CR-185132] N89-28747
Theoretical model of gravitational perturbation of current collector axisymmetric flow field
[AD-A209499] N89-28756
LIQUID OXYGEN
Oxygen storage on zeolites
[AD-A209352] N89-28599
LIQUID ROCKET PROPELLANTS
Synthesis of monomethylhydrazine
[ETN-89-94863] N89-28664
LIQUID-LIQUID INTERFACES
Stochastic processes in CHEMFETs
[AD-A207977] N89-28723
LITHIUM ALLOYS
Aluminum alloy
[NASA-CASE-LAR-13924-1-CU] N89-28621
Corrosion prevention of lithium-alloy anodes in accumulators with organic electrolytic solutions
[ETN-89-94652] N89-28729
LITHIUM NIOBATES
The mock counter: A hybrid optical-electronic counter using fiber delay line memory
[PB89-184410] N89-29031
LITHOGRAPHY
Lithography and spectroscopy of ultrathin Langmuir-Blodgett polymer films
[AD-A208970] N89-28639
An X-ray source for lithography based on a quasi-optical maser undulator
[AD-A208522] N89-28675
Molecular weight dependence of e-beam resist sensitivity
[AD-A207835] N89-28719
Study and simulation of an E-beam microlithography process on a multilayer resin structure. Research of an optimization
[LAAS-89.012] N89-29179
LOAD DISTRIBUTION (FORCES)
Steel fatigue under combined loads
[ETN-89-94864] N89-28629
A static load distribution strategy for processor tools
[MEMO-INF-88-43] N89-29078
LOAD TESTING MACHINES
Delamination test apparatus and method
[NASA-CASE-LAR-13985-1] N89-28586
LOAD TESTS
A summary of the UK results for a VAMAS round robin project on delamination of composite materials — Versailles project on advanced materials and standards (VAMAS)
[NPL-DMA(A)-179] N89-28584
LOADS (FORCES)
Static and dynamic deflection studies of the SRM aft case-nozzle joint
[NASA-TM-100373] N89-28568
Analysis and repair of impact damaged composites
[ARL-STRUCT-R-435] N89-28580
Effect of environmental factors on pavement deterioration. Volume 1: Background and methodology
[PB89-182109] N89-28668
Experimental investigations of flow forces exerted on spheres in rest and in motion, in a plane Poiseville flow
[ETN-89-94433] N89-28770
In search of more output: Two strain gage bridge circuits revisited
[DE89-014039] N89-28787
Fatigue testing apparatus
[NASA-CASE-LEW-14124-1] N89-28806
Flexural-torsional buckling of monosymmetric beam-columns/tie beams
[PB89-191654] N89-28859
LOCAL AREA NETWORKS
Local area network and data network for the Advanced Earth Observing Satellite, ADEOS system N89-28886
TWENTENET chip design
[MEMO-INF-88-49] N89-29090
LOGIC CIRCUITS
The mock counter: A hybrid optical-electronic counter using fiber delay line memory
[PB89-184410] N89-29031
A reconfigurable arithmetic processor --- for MIMD computer
[AD-A208323] N89-29082
LOGIC PROGRAMMING
A logic query language and its algebraic optimization for a multiprocessor database machine
[MEMO-INF-88-52] N89-29068
Northeast artificial intelligence consortium annual report 1987. Volume 8: Knowledge base maintenance using logic programming methodologies
[AD-A209453] N89-29095
LOGICAL ELEMENTS
Characterization of parallelism and deadlocks in distributed digital logic simulation
[AD-A207842] N89-29138
LOGISTICS
Prevention, reduction, and measurement of combat stress reactions: A bibliography
[AD-A209375] N89-29019
LONG TERM EFFECTS
Five year ground exposure of composite materials used on the Bell Model 206L flight service evaluation
[NASA-TM-101645] N89-28579
LOW FREQUENCIES
Nearfield acoustic holography: Review and perspectives
[ISVR-TR-179] N89-28807
LOW PASS FILTERS
Digital carrier demodulator employing components working beyond normal limits
[NASA-CASE-NPO-17628-1-CU] N89-28684
LOW SPEED STABILITY
Low-speed static and dynamic force tests of a generic supersonic cruise fighter configuration
[NASA-TM-4138] N89-28486
LOW SPEED WIND TUNNELS
Small scale model tests in small wind and water tunnels at high incidence and pitch rates. Volume 1: Test program and discussion of results
[AD-A208647] N89-28488
LOW TEMPERATURE ENVIRONMENTS
Preliminary design guide for arctic equipment
[AD-A209455] N89-29024
LUBRICANT TESTS
Lubricant evaluation and performance
[AD-A208925] N89-28835
High temperature tribometer, phase 1
[AD-A209356] N89-28838
LUBRICATING OILS
Ion implantation of ceramic bearings
[AD-A209770] N89-28644
LUBRICATION
Solid lubrication studied by optical means
[AD-A209008] N89-28836
The tribology of undulated surfaces
[AD-A209275] N89-28837
Chemical effects of Ne(+) bombardment on the MoS2(0001) surface studied by high-resolution photoelectron spectroscopy
[AD-A207734] N89-29247
LUMINANCE
Specifications and measurement procedures and aircraft transparencies
[AD-A209396] N89-28511
LUMINESCENCE
Radiothermoluminescence studies of polymer solids
[AD-A209036] N89-28641
LYMAN ALPHA RADIATION
Solar ultraviolet radiation within the middle atmosphere
[AERONOMICA-ACTA-A-337-1989] N89-29293

M

MACHINE TOOLS
A proposal of more expedient methods of testing machine tools
[DE89-013033] N89-28832
MAGNESIUM ALLOYS
An investigation of the workability of Al-8.5 percent Mg alloys
[AD-A209451] N89-28624
MAGNET COILS
Analytical solutions for the field, current density, force force density and mechanical stress distribution in toroidal coil systems
[IPP-2/294] N89-28728
MAGNETIC COMPRESSION
Exploding metallic foils and fuses: A computational modeling update
[DE89-014033] N89-28709
The Mark 101 flux compression generator: Development progress
[DE89-014298] N89-28712
MAGNETIC FIELD RECONNECTION
Parallel electric fields in a simulation of magnetotail reconnection and plasmoid evolution
[DE89-012622] N89-28970
MAGNETIC FIELDS
Parallel electric fields in a simulation of magnetotail reconnection and plasmoid evolution
[DE89-012622] N89-28970
Monte Carlo analysis of localization errors in magnetoencephalography
[DE89-013221] N89-29007
Transient visual evoked neuromagnetic responses: Identification of multiple sources
[DE89-013438] N89-29008
Caotic magnetic field line in toroidal plasmas
[IPPJ-911] N89-29211
Electron energy levels in a quantum well within an in-plane magnetic field
[AD-A209351] N89-29256
MAGNETIC FLUX
The Mark 101 flux compression generator: Development progress
[DE89-014298] N89-28712
Analytical solutions for the field, current density, force force density and mechanical stress distribution in toroidal coil systems
[IPP-2/294] N89-28728
The fluxgate ringcore sensor demagnetising factor and noise
[ORI-1-89] N89-28805
Method of mass producing superconducting persistent current rings
[AD-D013968] N89-29219
Fluxons and order in long Josephson junctions
[AD-A207925] N89-29249
MAGNETIC LENSES
Apertures of ring quadrupoles and sextupoles
[NIKHEF-K/APS/88-03] N89-29183
MAGNETIC PERMEABILITY
Crystal chemistry, magnetic and electrical properties of La(sub2-x)Ba(subx)NiO4
[AD-A209376] N89-29240
MAGNETIZATION
Study of sintered magnets of the Nd-Fe-B type
[AD-A209185] N89-29148
MAGNETOHYDRODYNAMIC STABILITY
Stability of a Taylor-relaxed cylindrical plasma separated from the wall by a vacuum layer
[EUT-88-E-207] N89-29200
ECH plasma for different magnetic axis positions and initial ICRF plasma production experiments in CHS
[IPPJ-907] N89-29201

Nonlinear stability in fluid and plasma dynamics
[AD-A207715] N89-29203
Effects of magnetic and collisional viscosity on the E x B gradient drift instability
[AD-A207975] N89-29205
Full consistent analysis of high beta steady state tokamaks sustained by beam driven and bootstrap currents
[IPPJ-912] N89-29212

MAGNETOHYDRODYNAMICS
Parallel electric fields in a simulation of magnetotail reconnection and plasmoid evolution
[DE89-012622] N89-28970
Caotic magnetic field line in toroidal plasmas
[IPPJ-911] N89-29211

MAGNETOMETERS
The fluxgate ringcore sensor demagnetising factor and noise
[ORI-1-89] N89-28805

MAGNIFICATION
The problem of very high magnifications in holography
[ISL-CO-218/88] N89-28804

MAINTENANCE
Composite material repair and reliability
[AD-A209150] N89-28574
Analysis and repair of impact damaged composites
[ARL-STRUCT-R-435] N89-28580
A proposal of more expedient methods of testing machine tools
[DE89-013033] N89-28832

MAN MACHINE SYSTEMS
Towards a physiologically based HUD (Head-Up Display) symbology
[AD-A207748] N89-28515
JPRS Report: Science and Technology. USSR: Space. 16th International Congress of the International Society for Photogrammetry and Remote Sensing, volume 1
[JPRS-USP-89-002-VOL-1] N89-28676
Experiences in implementing an expert system supported man-machine-interface for the configuration of the intelligent SAR processor N89-28889
Spacecraft flight simulation: A human factors investigation into the man-machine interface between an astronaut and a spacecraft performing docking maneuvers and other proximity operations
[NASA-CR-177502] N89-29020
Choice and perceived control: Implications for the design of displays
[AD-A208400] N89-29021

MAN-COMPUTER INTERFACE
Experiences in implementing an expert system supported man-machine-interface for the configuration of the intelligent SAR processor N89-28889
Human factors evaluation of color use in the Target Data Processor Release 10 (TDP R10)
[AD-A209438] N89-29023
Design and development of a user interface and user manual for a system dynamics model of software management
[AD-A209486] N89-29048

MANAGEMENT
A prototype for converting Linear Programming (LP) models to structured modeling graphs
[AD-A208166] N89-29059

MANDRELS
Stresses and strains in a cold-worked annulus
[AR-005-548] N89-28871

MANGANESE OXIDES
Material and fabrication challenges in the development of monolithic solid oxide fuel cells
[DE89-012422] N89-28957

MANIPULATORS
Robotic grasping of unknown objects: A knowledge-based approach
[DE89-013875] N89-28833
Robust high-performance control for robotic manipulators
[NASA-CASE-NPO-17785-1-CU] N89-28846

MANUFACTURING
A manufacturing scheduler's perspective on semiconductor fabrication
[AD-A208372] N89-29232

MAPPING
Smooth piecewise polynomials as conforming finite elements for plate bending problems
[MEMO-747] N89-28875
Zeiss Digital Mapping: A new hardware and software system concept from Kombinat VEB Carl Zeiss JENA N89-28891
High resolution Soviet space photographs for topographic mapping N89-28892
BM/C(3) algorithm mapping onto concurrent processors
[AD-A207877] N89-29052
The p-version of the finite element method for domains with corners and for infinite domains
[AD-A207797] N89-29116

MAPS
An X-ray microprobe using focussing optics with a synchrotron radiation source
[DE89-013425] N89-28788

MARINE BIOLOGY
The MIT/Marine Industry Collegium: Novel applications of marine biopolymers
[PB89-182950] N89-28633

MARINE CHEMISTRY
The MIT/Marine Industry Collegium: Novel applications of marine biopolymers
[PB89-182950] N89-28633

MARINE METEOROLOGY
Satellite-derived moisture-bogusing profiles for the North Atlantic Ocean
[AD-A207829] N89-28930
Application of special sensor microwave/imager data for analysis of cyclonic storms in midlatitudes over the sea
[AD-A207675] N89-28975
Preliminary neural network detection of a gulf stream in images of sea surface temperature gradients, phase 1
[AD-A207801] N89-29003

MARKET RESEARCH
Competition and safety in air traffic
[TUB-DISS-PAPER-128] N89-28508
Study of an advanced civil earth remote sensing system: Executive summary
[PB89-163208] N89-28922
Marketing and case study of satellite thematic maps and other products of satellite remote sensing
[BCRS-55-16E] N89-28939

MARKETING
Competition and safety in air traffic
[TUB-DISS-PAPER-128] N89-28508
Study of an advanced civil earth remote sensing system: Executive summary
[PB89-163208] N89-28922
Marketing and case study of satellite thematic maps and other products of satellite remote sensing
[BCRS-55-16E] N89-28939

MARKOV CHAINS
On the solving of stochastic Ito differential equations by simulation
[ETN-89-94610] N89-29134
Are limits of alpha-discounted optimal policies Blackwell optimal: A counterexample
[TW-88-10] N89-29139

MARKOV PROCESSES
The sensitivity of Middle East precipitation and cloud forecasts to changes in Eastern Mediterranean Sea surface temperatures
[AD-A207864] N89-28986

MARS (PLANET)
Orbits containing arcs of minimum altitude variation
[AD-A209206] N89-28539

MARS SAMPLE RETURN MISSIONS
Study of sampling systems for comets and Mars
[NASA-CR-185514] N89-29292

MARTENSITIC STAINLESS STEELS
Effect of temperature and H2S content on the cracking resistance of a 13 percent chromium martensitic stainless steel in acidified NaCl
[NPL-DMA(A)-173] N89-28631

MASERS
An X-ray source for lithography based on a quasi-optical maser undulator
[AD-A208522] N89-28675

MASKS
Morphology control of photoelectrochemically etched profiles in n-GaAs
[AD-A208991] N89-29235

MASS
REGGIE results for the Nunnally mass launcher
[DE89-014377] N89-28543

MASS DISTRIBUTION
Evidence for two charged particle populations in the Crab nebula
[MPE-PREPRINT-147] N89-29286

MASS FLOW
Pressure drop and heat transfer characteristics of nearly neutrally buoyant particulate slurry for advanced energy transmission fluids
[DE89-013645] N89-28751

MASS SPECTROMETERS
Apparatus and method for characterizing the transmission efficiency of a mass spectrometer
[NASA-CASE-NPO-16989-1-CU] N89-28794

MASS SPECTROSCOPY
Capillary zone electrophoresis-mass spectrometry of peptides and proteins
[DE89-014466] N89-28592
Simultaneous secondary ion and Auger electron analysis, illustrated by examples from microelectronics research and technology
[ETN-89-94431] N89-28611
Chemical and Laser Sciences Division
[DE89-014385] N89-28811

MASS TRANSFER
Time- and volume-averaged conservation equations for multiphase flow
[DE89-012418] N89-28746
Compact heat and mass exchangers of the plate fin type in thermal sorption systems: Application in an absorption heat pump with the working pair CH3OH-LiBr/ZnBr2
[ISBN-90-370-0022-3] N89-28780
Daytime turbulent exchange between the Amazon forest and the atmosphere
[NASA-CR-185487] N89-28961
Millisecond radio pulsars in globular clusters
[NASA-CR-185909] N89-29298

MASSIVELY PARALLEL PROCESSORS
A heterogeneous multiprocessor graphics system using processor-enhanced memories
[AD-A208089] N89-29058

MATCHING
On planar point matching under affine transformation
[AD-A210106] N89-29046

MATERIALS RECOVERY
Higee Technology Development Program, phase 1
[PB89-161434] N89-28587

MATERIALS TESTS
Metallurgical evaluation of 17-4 PH stainless steel castings
[PB89-193262] N89-28615
Survey of test procedures for high performance ceramic materials and their fundamentals
[JUEL-SPEZ-470] N89-28653

MATHEMATICAL LOGIC
Parallel algorithms for solving systems of linear equations and their mapping on systolic arrays
[ETN-89-95457] N89-29077

MATHEMATICAL MODELS
Model simplification based on the concept of equivalent dead time
[NAL-TM-SE-8802] N89-28521
Method for research on planet Venus using floating balloon stations: Mathematical model N89-28532
Wind models for the NSTS ascent trajectory biasing for wind load alleviation
[NASA-TM-100375] N89-28551
Active damping of vibration in large space structures using a Karhunen-Loeve reduced order model
[AD-A208183] N89-28558
Bifurcation and pattern formation in combustion
[DE89-013629] N89-28590
Development of damping treatment suitable for high temperature environment
[ISVR-TR-174] N89-28652
Higher order base dynamics of a bipolar transistor with nonuniform doping
[PB89-155451] N89-28704
Exploding metallic foils and fuses: A computational modeling update
[DE89-014033] N89-28709
Time- and volume-averaged conservation equations for multiphase flow
[DE89-012418] N89-28746
Mathematical modeling and analysis of heat pipe start-up from the frozen state
[NASA-CR-185132] N89-28747
Dynamics of colloidal dispersions via lattice-gas models of an incompressible fluid
[DE89-013146] N89-28750
Analysis of flow boiling of ammonia and R-114 in a matrix heat exchanger
[DE89-012427] N89-28752
Exact solutions for symmetric deformations of hollow bodies of ideal fluids with application to inertial stability
[DE89-014374] N89-28753
Theoretical model of gravitational perturbation of current collector axisymmetric flow field
[AD-A209499] N89-28756
La Recherche Aerospatiale, bimontly bulletin, number 1988-3
[ESA-TT-1137] N89-28781
Linear theory of uncompensated thermal blooming in turbulence
[DE89-014604] N89-28812
Quantitative investigation of the kinetics of a laser-pumped barium vapor
[ETN-89-94434] N89-28823
Model reduction of linear conservative mechanical systems
[MEMO-752] N89-28845

Formulation and numerical solution of the equations of constrained mechanical motion
[DFVLR-FB-89-08] N89-28847
Development and implementation of an on-line multivariable control algorithm for the force control of an industrial robot
[OUEL-1748/88] N89-28848
Estimation of some stochastic models used in reliability engineering
[VTT-RR-598] N89-28855
One-degree-of-freedom motion induced by modeled vortex shedding
[NASA-TM-101038] N89-28870
Modelling orientation parameters of sensor platforms N89-28881
Studies on object reconstruction from space using three line scanner imagery N89-28919
Modeling of short arc orbital constraints for incorporation into photogrammetric adjustment of MEOSS data
[DFVLR-FB-89-14] N89-28943
User's guide to the complex terrain dispersion model plus algorithms for unstable situations (CTDMPLUS). Volume 1: Model description and user instructions
[PB89-181424] N89-28963
A prototype for converting Linear Programming (LP) models to structured modeling graphs
[AD-A208166] N89-29059
Language constructs and a search procedure to model and solve combinatorial problems
[MEMO-753] N89-29075
Solution of the hydrodynamic device model using high-order non-oscillatory shock capturing algorithms
[NASA-CR-181886] N89-29123
The coagulation and dispersion of nonspherical, aerosol particles in a turbulent atmosphere
[AD-A208064] N89-29150
Photonuclear absorption cross sections
[NASA-CR-185488] N89-29159
An optical model description of momentum transfer in heavy ion collisions N89-29162
Electric quadrupole excitations in relativistic nucleus-nucleus collisions N89-29164
Nucleon emission via electromagnetic excitation in relativistic nucleus-nucleus collisions: Re-analysis of the Weizsacker-Williams method N89-29166
Solid-vapor differences of electronic stopping powers for protons
[IPPJ-901] N89-29207
United States Air Force Research Initiation Program for 1987, volume 2
[AD-A209727] N89-29259

MATHEMATICAL PROGRAMMING
A logic query language and its algebraic optimization for a multiprocessor database machine
[MEMO-INF-88-52] N89-29068
A code optimization package for REDUCE
[MEMO-INF-89-29] N89-29070
On the shape of mathematical arguments
[ETN-89-95465] N89-29133

MATRICES (MATHEMATICS)
Electromagnetic scattering from two dimensional objects using the field feedback formulation
[AD-A209563] N89-28685
Acousto-optical vector matrix product processor: Implementation issues
[AD-A207933] N89-28722
Row-oriented direct solving of linear algebraic equations: Row orthogonalization method
[REPT-88-82] N89-29105
Application of Cholesky-like matrix decomposition methods to the evaluation of atomic orbital integrals and integral derivatives
[AD-A209682] N89-29112
Linear algebra support modules for approximation and other software
[NPL-DITC-142/89] N89-29126
A generalization of the numerical range of a matrix
[TW-88-09] N89-29128
A note on the communication complexity of totally unimodular matrices
[MEMO-766] N89-29131
On adjoints and dual matroids
[MEMO-767] N89-29146

MATRIX MATERIALS
A VAMAS round robin on fatigue test methods for polymer matrix composites. Part 1: Tensile and flexural tests of unidirectional material --- Versailles project on advanced materials and standards (VAMAS)
[NPL-DMA(A)-180-PT-1] N89-28585
The interface in tungsten fiber reinforced niobium metal-matrix composites
[NASA-TM-102122] N89-28627

MATRIX THEORY
A generalization of the numerical range of a matrix
[TW-88-09] N89-29128

MAXIMUM LIKELIHOOD ESTIMATES
Multitarget tracking by single sensor analysis of the main approaches developed in this area
[ONERA-NT-1988-10] N89-28702
Wind profile estimation from point to point laser distortion data
[NASA-CR-185891] N89-28990
Maximum-likelihood parameter estimation of a generalized gumbel distribution
[AD-A207994] N89-29055

MAXWELL EQUATION
The invariance of classical electromagnetism under Charge-conjugation, Parity and Time-reversal (CPT) transformations N89-29161

MEASURING INSTRUMENTS
An X-ray microprobe using focussing optics with a synchrotron radiation source
[DE89-013425] N89-28788
The PVF2 piezoelectric polymer shock stress sensor: System characterization for application under field test conditions
[DE89-014629] N89-28790
Universal precision sine bar attachment
[NASA-CASE-MFS-28253-1] N89-28831

MECHANICAL DEVICES
Nonlinear stability in fluid and plasma dynamics
[AD-A207715] N89-29203

MECHANICAL ENGINEERING
The performance of a mechanical design Compiler
[AD-A209540] N89-29097

MECHANICAL MEASUREMENT
NIST (National Institute of Standards and Technology) calibration services users guide, 1989 edition
[PB89-200216] N89-28785

MECHANICAL PROPERTIES
Furnace for tensile/fatigue testing
[NASA-CASE-LEW-14848-1] N89-28549

MEDICAL SCIENCE
Energy and Technology Review --- analytical cytology
[DE89-013919] N89-28954

MEDICAL SERVICES
Risk management for air ambulance helicopters operators
[DOT/FAA/DS-88/7] N89-28506

MEDITERRANEAN SEA
The sensitivity of Middle East precipitation and cloud forecasts to changes in Eastern Mediterranean Sea surface temperatures
[AD-A207864] N89-28988

MELTING
Modeling of hot fragment conductive ignition of solid propellants with application to melting and evaporation of solids
[AD-A207727] N89-28662

MEMBRANE STRUCTURES
An improved design for stretched-membrane heliostats
[DE89-013872] N89-28953

MEMBRANES
Stochastic processes in CHEMFETs
[AD-A207977] N89-28723

MEMORY (COMPUTERS)
The mock counter: A hybrid optical-electronic counter using fiber delay line memory
[PB89-184410] N89-29031
Parallel language constructs for tensor product computations on loosely coupled architectures
[NASA-CR-181900] N89-29061
TiME: Time and memory efficient distance transformations for parallel and pyramid machines
[FOA-C-30531-3.4] N89-29091

MENTAL PERFORMANCE
Exploring virtual worlds with head-mounted displays
[AD-A208088] N89-28797

MERCURY ISOTOPES
The influence of the shell closure on the microscopic structure of even-even Hg isotopes: A study with electron and muon beams --- a study with electron and muon beams
[ETN-89-95464] N89-29177

MESOSCALE PHENOMENA
A numerical study of a mesoscale eddy interaction with an ocean front in the marginal ice zone
[AD-A209192] N89-29002

MESOSPHERE
A high-resolution atlas of the infrared spectrum of the sun and the earth atmosphere from space. A compilation of ATMOS spectra of the region from 650 to 4800 cm-1 (2.3 to 16 microns). Volume 2: Stratosphere and mesosphere, 650 to 3350 cm-1
[NASA-RP-1224-VOL-2] N89-28969
The Strategic High-Altitude Atmospheric Radiation Code (SHARC) user instructions
[AD-A207667] N89-28974
Solar ultraviolet radiation within the middle atmosphere
[AERONOMICA-ACTA-A-337-1989] N89-29293

MESSAGE PROCESSING
Design of a reliable computing system for the Petite Amateur Navy Satellite (PANSAT)
[AD-A208194] N89-28559
BM/C(3) algorithm mapping onto concurrent processors
[AD-A207877] N89-29052

METAL BONDING
Metallic bonding to high-temperature superconducting ceramics
[DE89-014668] N89-28635
Monolayers of 11-trichlorosilylundecyl thioacetate: A system that promotes adhesion between silicon dioxide and evaporated gold
[AD-A208266] N89-28637

METAL FOILS
Exploding metallic foils and fuses: A computational modeling update
[DE89-014033] N89-28709
An improved hibachi support structure for electron-beam diode foils
[DE89-014023] N89-28810

METAL FUELS
Chemical Technology Division
[DE89-013917] N89-28591

METAL MATRIX COMPOSITES
The interface in tungsten fiber reinforced niobium metal-matrix composites
[NASA-TM-102122] N89-28627

METAL OXIDE SEMICONDUCTORS
Applied field and total dose dependence of trapped charge buildup in MOS devices
[AD-A209064] N89-29237

METAL SURFACES
Arc-textured high emittance radiator surfaces
[NASA-CASE-LEW-14679-1] N89-28651
Solid lubrication studied by optical means
[AD-A209008] N89-28836
The tribology of undulated surfaces
[AD-A209275] N89-28837
Initial stages of metal/semiconductor interface formation: Au and AgON Si(111)
[AD-A209490] N89-29245
Chemical effects of Ne(+) bombardment on the MoS2(0001) surface studied by high-resolution photoelectron spectroscopy
[AD-A207734] N89-29247

METAL VAPORS
Quantitative investigation of the kinetics of a laser-pumped barium vapor
[ETN-89-94434] N89-28823
Dense heavy metal aerosol monitoring by direct X-ray fluorescence
[AD-A209077] N89-28966

METALLIC GLASSES
Pressure induced anomaly at Tc in Fe78 Mo2 B20
[NAL-TM-MT-8806] N89-28628
Development of a carbonaceous selective absorber for solar thermal energy collection and process for its formation
[DE89-008587] N89-28949

METALLOGRAPHY
Theoretical analysis of phase transformations in Fe-Ni Invar-type alloys
[DE89-014454] N89-28618

METEOR TRAILS
Meteor burst system communications compatibility
[PB89-191167] N89-28682

METEOROLOGICAL PARAMETERS
Materials aerometric database for use in developing materials damage functions
[PB89-181259] N89-28572
User's guide to the complex terrain dispersion model plus algorithms for unstable situations (CTDMPLUS). Volume 1: Model description and user instructions
[PB89-181424] N89-28963
Satellite enhanced numerical weather prediction
[AD-A210108] N89-28987
WINDROSE: A program for IBM-compatible personal computers, documentation
[PB89-167423] N89-29039

METEOROLOGICAL RADAR
Storm models for end-to-end TDWR (Terminal Doppler Weather Radar) signal processing simulation tests
[AD-A209384] N89-28986
Satellite enhanced numerical weather prediction
[AD-A210108] N89-28987

METEOROLOGICAL SATELLITES
Satellite-derived moisture-bogusing profiles for the North Atlantic Ocean
[AD-A207829] N89-28930

Application of special sensor microwave/imager data for analysis of cyclonic storms in midlatitudes over the sea
[AD-A207675] N89-28975
Satellite enhanced numerical weather prediction
[AD-A210108] N89-28987

METEOROLOGICAL SERVICES
The World Weather Watch Program 1988-1997: Second WMO long-term plan, part 2, volume 1
[WMO-691-PT-2-VOL-1] N89-28995
The WMO applications of meteorology program 1988-1997: Second WMO long-term plan, part 2, volume 4
[WMO-694-PT-2-VOL-4] N89-28998

METEOROLOGY
The WMO long-term plan overall policy and strategy 1988-1997: Second WMO long-term plan, part 1
[WMO-690-PT-1] N89-28994
The World Climate Program 1988-1997: Second WMO long-term plan, part 2, volume 2
[WMO-692-PT-2-VOL-2] N89-28996
The WMO applications of meteorology program 1988-1997: Second WMO long-term plan, part 2, volume 4
[WMO-694-PT-2-VOL-4] N89-28998
Activities report in meteorology in Sweden
[AR-87-88] N89-28999

METEOSAT SATELLITE
Proposed concepts for a advanced optical payload for second generation Meteosat
[ETN-89-95236] N89-28564

METHYLHYDRAZINE
Synthesis of monomethylhydrazine
[ETN-89-94863] N89-28664

MICROANALYSIS
An X-ray microprobe using focussing optics with a synchrotron radiation source
[DE89-013425] N89-28788
Dense heavy metal aerosol monitoring by direct X-ray fluorescence
[AD-A209077] N89-28966

MICROBIOLOGY
Capillary zone electrophoresis-mass spectrometry of peptides and proteins
[DE89-014466] N89-28592

MICROCOMPUTERS
A real time microcomputer implementation of sensor failure detection for turbofan engines
[NASA-TM-102327] N89-29032

MICROELECTRONICS
Simultaneous secondary ion and Auger electron analysis, illustrated by examples from microelectronics research and technology
[ETN-89-94431] N89-28611
Electrical characterization of signal processing microcircuit
[AD-A209078] N89-28714
VLSI integrated circuit contact reliability by interface spectroscopy
[AD-A207666] N89-28718
Studies of the volume and plasma sheath properties of radio frequency discharges
[AD-A207980] N89-29206

MICROGRAVITY APPLICATIONS
Microgravity combustion science: A program overview
[NASA-TM-101424] N89-28665

MICROPROCESSORS
A Compaq-286 micro-processor based high-speed high-density digital data-acquisition and recording system. Volume 1: System overview
[AD-A207429] N89-29029

MICROPROGRAMMING
A microprogramming support tool for pipelined architectures
[AD-A208090] N89-29036

MICROSCOPES
Significant improvement in IR surface-temperature measurements
[DE89-014808] N89-28926

MICROSCOPY
Multicomponent e-beam resists containing organometallic compounds and reactive monomers
[AD-A207716] N89-28606

MICROSTRUCTURE
Highly oriented fiber reinforced ceramic composites
[AD-A208119] N89-28578
Theoretical analysis of phase transformations in Fe-Ni Invar-type alloys
[DE89-014454] N89-28618
Fundamental studies of grain boundary structure and properties in ICB aluminum
[DE89-014884] N89-28619
Freeze-dried tungsten heavy alloys
[DE89-014933] N89-28620
Fatigue crack growth-microstructural relationship of Ti-6Al-4V
[AD-A208107] N89-28626
The influence of structure and alloying on the cold-formability of ferritic steels and the utility of uniaxial tensile testing in its assessment
[ISBN-952-90044-3-5] N89-28632
Microwave sintering of ceramics
[DE89-014769] N89-28636
Non-uniform transition conductivity of superconducting ceramic
[NASA-TM-102133] N89-28851
A test system for thermomechanical fatigue of solder joints
[DE89-013886] N89-28860
Materials analysis and device optimization of CuInSe2 solar cells
[DE89-009434] N89-28944
The influence of the shell closure on the microscopic structure of even-even Hg isotopes: A study with electron and muon beams — a study with electron and muon beams
[ETN-89-95464] N89-29177

MICROWAVE AMPLIFIERS
Microwave emission from relativistic electron beams
[AD-A209653] N89-29181

MICROWAVE ANTENNAS
Holographic modulator arrays
[AD-A209387] N89-28792

MICROWAVE CIRCUITS
Optical gain control of GaAs microwave monolithic integrated circuit distributed amplifier
[AD-D013969] N89-28705

MICROWAVE EMISSION
Microwave emission from relativistic electron beams
[AD-A209653] N89-29181

MICROWAVE EQUIPMENT
Digitally modulated bit error rate measurement system for microwave component evaluation
[NASA-TP-2912] N89-28545

MICROWAVE FREQUENCIES
Atmospheric influence on microwave remote sensing at different frequencies: Results of the 1st September 1987 DUSCAT flight
[BCRS-89-07] N89-28941
Digital refractometry of piezoelectric crystalline media
[AD-A209362] N89-29239

MICROWAVE IMAGERY
Application of special sensor microwave/imager data for analysis of cyclonic storms in midlatitudes over the sea
[AD-A207675] N89-28975

MICROWAVE SCATTERING
Almond test body — for microwave anechoic chambers
[NASA-CASE-LAR-13747-1-CU] N89-28672
Atmospheric influence on microwave remote sensing at different frequencies: Results of the 1st September 1987 DUSCAT flight
[BCRS-89-07] N89-28941

MICROWAVE SENSORS
Application of special sensor microwave/imager data for analysis of cyclonic storms in midlatitudes over the sea
[AD-A207675] N89-28975
Microwave detection using Josephson elements
[ETN-89-94650] N89-29252

MICROWAVE SPECTROMETERS
Chemical and Laser Sciences Division
[DE89-014385] N89-28611

MICROWAVE TRANSMISSION
Atmospheric influence on microwave remote sensing at different frequencies: Results of the 1st September 1987 DUSCAT flight
[BCRS-89-07] N89-28941

MICROWAVES
Microwave sintering of ceramics
[DE89-014769] N89-28636
Performance evaluation of radiofrequency, microwave, and millimeter wave power meters
[PB89-193916] N89-28707
Picosecond electrooptic investigations of integrated circuits
[AD-A209134] N89-28863
Application of aerial side-looking radar imagery in China N89-28902
Sea spectra as determined from low-altitude SLAR images N89-28908
Spectral measurements of the cosmic microwave background
[DE89-014895] N89-29296
La Recherche Aerospatiale, bimonthly bulletin, number 1988-5
[ESA-TT-1162] N89-29300

MILITARY OPERATIONS
Advanced robotics for Air Force operations
[AD-A210098] N89-28840
Prevention, reduction, and measurement of combat stress reactions: A bibliography
[AD-A209375] N89-29019
SDI (Strategic Defense Initiative): Shield or sword?
[AD-A209777] N89-29141

MILITARY TECHNOLOGY
Advanced power sources for space missions
[NASA-TM-101811] N89-28565
Advanced robotics for Air Force operations
[AD-A210098] N89-28840
Picosecond electrooptic investigations of integrated circuits
[AD-A209134] N89-28863
SDI (Strategic Defense Initiative): Shield or sword?
[AD-A209777] N89-29141

MILLIMETER WAVES
Performance evaluation of radiofrequency, microwave, and millimeter wave power meters
[PB89-193916] N89-28707
Picosecond electrooptic investigations of integrated circuits
[AD-A209134] N89-28863
La Recherche Aerospatiale, bimonthly bulletin, number 1988-5
[ESA-TT-1162] N89-29300

MIMD (COMPUTERS)
A reconfigurable arithmetic processor — for MIMD computer
[AD-A208323] N89-29082
La Recherche Aerospatiale, bimonthly bulletin, number 1988-4
[ESA-TT-1161] N89-29299
La Recherche Aerospatiale, bimonthly bulletin, number 1988-5
[ESA-TT-1162] N89-29300

MINERAL EXPLORATION
Application of aerial side-looking radar imagery in China N89-28902

MINORITY CARRIERS
Higher order base dynamics of a bipolar transistor with nonuniform doping
[PB89-155451] N89-28704

MINUTEMAN ICBM
Acoustic tests on a new motor generator system for the minuteman launch control centers in Hill engineering test facilities 1 and 2, Hill AFB, Utah
[AD-A209598] N89-28717

MIR SPACE STATION
JPRS report: Science and technology. USSR report: Life sciences
[JPRS-USP-89-005] N89-28527

MIRRORS
An X-ray microprobe using focussing optics with a synchrotron radiation source
[DE89-013425] N89-28788
An improved design for stretched-membrane heliostats
[DE89-013872] N89-28953

MISSILE COMPONENTS
Metallurgical evaluation of 17-4 PH stainless steel castings
[PB89-193262] N89-28615

MISSILE CONFIGURATIONS
The effect of autopilot configuration on missile response
[AD-A207822] N89-28520

MISSILE DEFENSE
A comparison and analysis of strategic defense transition stability models
[AD-A208033] N89-29144

MISSILES
The effect of autopilot configuration on missile response
[AD-A207822] N89-28520

MISSION PLANNING
Study of sampling systems for comets and Mars
[NASA-CR-185514] N89-29292
Key data on participating projects. The solar-terrestrial science project of the Inter-Agency Consultative Group for Space Science (IACG)
[ESA-SP-1107] N89-29295

MIXING LAYERS (FLUIDS)
La Recherche Aerospatiale, bimonthly bulletin, number 1988-6
[ESA-TT-1165] N89-29301

MOBILE COMMUNICATION SYSTEMS
Design of a command, communications, and control van (surrogate)
[AD-A207652] N89-28687

MOBILITY
Controlled method of reducing electrophoretic mobility of various substances
[NASA-CASE-MFS-26049-1-NP] N89-28803

MODELS
A partitioning and redundancy model for wafer scale integrated circuits
[MEMO-INF-88-65] N89-28730
MODULATION
Digitally modulated bit error rate measurement system for microwave component evaluation
[NASA-TP-2912] N89-28545
MODULATION TRANSFER FUNCTION
Display characteristics of example light-valve projectors
[AD-A209580] N89-29193
MODULATORS
Holographic modulator arrays
[AD-A209387] N89-28792
MODULES
A fully automated, single-connection tester for T/R modules
[DE89-013155] N89-28786
MODULUS OF ELASTICITY
Damping properties of various materials
[AD-A209071] N89-28642
MOISTURE
Satellite-derived moisture-bogusing profiles for the North Atlantic Ocean
[AD-A207829] N89-28930
Daytime turbulent exchange between the Amazon forest and the atmosphere
[NASA-CR-185487] N89-28961
MOISTURE CONTENT
Determination of moisture diffusion in carbon fiber reinforced epoxy composites by means of radioisotope tracer technique
[BMVG-FBWT-88-2] N89-28581
MOLECULAR BEAM EPITAXY
Primary research efforts on exploring the commercial possibilities of thin film growth and materials purification in space
[NASA-CR-184913] N89-28541
MOLECULAR BEAMS
Molecular beam experiment for the determination of differential cross sections of the reaction of deuterium atoms with vibrationally excited hydrogen molecules
[MPIS-10/1988] N89-29178
MOLECULAR CHAINS
Plastic yielding of partially-crystalline polymers
[AD-A208101] N89-28648
MOLECULAR DIFFUSION
Use of microelectrode arrays to directly measure diffusion of ions in solid electrolytes: Proof of concept experiments involving Ag+ in a solid polymer electrolyte
[AD-A209536] N89-28604
MOLECULAR EXCITATION
Application of optimal control theory for selective vibrational excitation in molecules modeled as harmonic systems
[MEMO-755] N89-29104
Molecular beam experiment for the determination of differential cross sections of the reaction of deuterium atoms with vibrationally excited hydrogen molecules
[MPIS-10/1988] N89-29178
MOLECULAR OSCILLATIONS
Vibrational dynamics of aniline (Ar)1 and aniline (CH4)1 clusters
[AD-A209560] N89-28605
MOLECULAR SPECTROSCOPY
The Los Alamos Fourier-transform spectrometer: Applications to molecular spectroscopy
[DE89-014258] N89-28789
A study of non-rigid aromatic molecules by supersonic molecular jet spectroscopy: Observation and spectroscopic analysis of the stable conformations of various alkylbenzenes
[AD-A209561] N89-29171
Effect of an electric field on a split Bloch band
[AD-A209657] N89-29244
MOLECULAR STRUCTURE
The Los Alamos Fourier-transform spectrometer: Applications to molecular spectroscopy
[DE89-014258] N89-28789
Exploring virtual worlds with head-mounted displays
[AD-A208088] N89-28797
A study of non-rigid aromatic molecules by supersonic molecular jet spectroscopy: Observation and spectroscopic analysis of the stable conformations of various alkylbenzenes
[AD-A209561] N89-29171
MOLECULAR TRAJECTORIES
The sensitivity of Middle East precipitation and cloud forecasts to changes in Eastern Mediterranean Sea surface temperatures
[AD-A207864] N89-28988
MOLECULAR WEIGHT
Structural definition of synthetic fuels: Wilsonville 1
[DE89-013627] N89-28659
Molecular weight dependence of e-beam resist sensitivity
[AD-A207835] N89-28719
MOLECULES
Controlled method of reducing electrophoretic mobility of various substances
[NASA-CASE-MFS-28049-1-NP] N89-28603
Ion-molecule chemistry within doubly charged ammonia clusters
[AD-A207764] N89-28608
Ion-molecule chemistry within triply charged ammonia clusters
[AD-A207766] N89-28609
Oxidative addition of C-H bonds in organic molecules to transition metal centers
[DE89-012991] N89-28616
MOLTEN SALT ELECTROLYTES
Metal/metallion system in low temperature molten salts
[AD-A208025] N89-28724
MOLTEN SALTS
Metal/metallion system in low temperature molten salts
[AD-A208025] N89-28724
MOLYBDENUM SULFIDES
Chemical effects of Ne(+) bombardment on the MoS2(0001) surface studied by high-resolution photoelectron spectroscopy
[AD-A207734] N89-29247
MOMENTUM TRANSFER
Numerical studies of convective heat transfer in an inclined semiannular enclosure
[NASA-TM-102011] N89-28666
Time- and volume-averaged conservation equations for multiphase flow
[DE89-012418] N89-28746
Propagation and saturation of nonlinear inertia-gravity waves in the atmosphere
[AD-A207871] N89-28989
An optical model description of momentum transfer in heavy ion collisions N89-29162
MONITORS
Television monitor field shifter and an opto-electronic method for obtaining a stereo image of optimal depth resolution and reduced depth distortion on a single screen
[NASA-CASE-NPO-17249-1-CU] N89-28676
MONOPOLE ANTENNAS
NEC (Numerical Electromagnetics Code), NECGS (Numerical Electromagnetics Code-Ground Screen), and MININEC (Mini-Numerical Electromagnetics Code) numerical models of LF top-hat monopole antennas
[AD-A209230] N89-28683
MONTE CARLO METHOD
Monte Carlo analysis of localization errors in magnetoencephalography
[DE89-013221] N89-29007
Conditional dependence
[AD-A207881] N89-29120
MORPHOLOGY
Morphology control of photoelectrochemically etched profiles in n-GaAs
[AD-A208991] N89-29235
MOTION SICKNESS
Visual suppression of the vestibulo-ocular reflex during space flight
[NASA-TM-102157] N89-29017
MOTION SIMULATION
Determining the location of an observer with respect to aerial photographs
[AD-A207791] N89-28929
MOUNTING
Almond test body --- for microwave anechoic chambers
[NASA-CASE-LAR-13747-1-CU] N89-28672
MULTIPHASE FLOW
Time- and volume-averaged conservation equations for multiphase flow
[DE89-012418] N89-28746
MULTIPROCESSING (COMPUTERS)
Two-dimensional signal processing and storage and theory and applications of electromagnetic measurements
[AD-A207827] N89-28689
Fault-tolerant computer systems: A survey of some methods and techniques
[MEMO-INF-88-15] N89-29037
A heterogeneous multiprocessor graphics system using processor-enhanced memories
[AD-A208089] N89-29058
A logic query language and its algebraic optimization for a multiprocessor database machine
[MEMO-INF-88-52] N89-29068
A static load distribution strategy for processor tools
[MEMO-INF-88-43] N89-29078
A reconfigurable arithmetic processor --- for MIMD computer
[AD-A208323] N89-29082
Gauge: Its philosophy and design
[AD-A208944] N89-29083
The NOSC (Naval Ocean Systems Center) Code 911 Digital Dynamics Processor (DDP): A mildly coupled distributed-computing system
[AD-A210148] N89-29085
Multicast communication in multiprocessor systems
[AD-A209606] N89-29086
Analysis of cache invalidation patterns in multiprocessors
[AD-A207820] N89-29089
MULTISPECTRAL BAND SCANNERS
Identification of irrigated areas in the Sao Francisco Valley through remote sensing data. Pilot area: Petrolina-Juazeiro
[INPE-4800-RPE/587] N89-28925
MULTISPECTRAL RADAR
EXAS: Experiment on Autonomous SAR processor calibration N89-28890
MULTISTATIC RADAR
Evaluation of the bistatic equivalence theorem for the near and far-field radar cross section of complex targets
[AD-A209228] N89-28682
A Bistatic Parasitical Radar (BIPAR) N89-28878
MULTIVARIATE STATISTICAL ANALYSIS
Multivariate analysis of UV-spectral data for solute tracking in HPLC
[ISBN-90-6275-535-6] N89-28614
Adaptive detection and parameter estimation for multidimensional signal models
[AD-A208971] N89-28678
On constrained multivariable adaptive control
[LAAS-89.093] N89-29101
Conditional dependence
[AD-A207881] N89-29120
MUSCLES
A program for the study of skeletal muscle catabolism following physical trauma
[AD-A207983] N89-29014
MUSCULAR STRENGTH
Muscle changes with eccentric exercise: Implications on earth and in space
[NASA-TM-102227] N89-29016
MUSCULOSKELETAL SYSTEM
A program for the study of skeletal muscle catabolism following physical trauma
[AD-A207983] N89-29014
Muscle changes with eccentric exercise: Implications on earth and in space
[NASA-TM-102227] N89-29016

N

N-TYPE SEMICONDUCTORS
Morphology control of photoelectrochemically etched profiles in n-GaAs
[AD-A208991] N89-29235
NASA PROGRAMS
Patent abstracts bibliography: A continuing bibliography. Section 2: Indexes (supplement 35)
[NASA-SP-7039(35)-SECT-2] N89-29264
Departments of Veterans Affairs and Housing and Urban Development and independent agencies appropriations for 1990. Part 6: National Aeronautics and Space Administration
[GPO-99-598] N89-29273
NATIONAL AIRSPACE SYSTEM
Collision avoidance operational concept
[WP-88W00418] N89-28509
Direct User Access Terminal (DUAT) operational concept
[WP-88W00075] N89-28524
NATURAL GAS
Higee Technology Development Program, phase 1
[PB89-161434] N89-28587
Energy technology R and D: What could make a difference. A study by the staff of the Oak Ridge National Laboratory. Part 1: Synthesis report, volume 1
[DE89-014568] N89-28955
NAVIER-STOKES EQUATION
Some computations of unsteady Navier-Stokes flow around oscillating airfoil/wing
[NAL-TR-1004T] N89-28492
Role of supercomputer in computational aerodynamics
[PD-CF-8925] N89-28496
Flow calculation over a delta-wing using the thin-layer Navier-Stokes equations
[PD-CF-8924] N89-28497
Development of an efficient solution scheme for incompressible steady-state flow
[AD-A207726] N89-28757

Application of computational fluid dynamics to the analysis of the aerodynamics of a railgun projectile
[AD-A207758] N89-28758
A space marching algorithm for the thin-layer Navier-Stokes equations N89-28767
La Recherche Aerospatiale, bimonthly bulletin, number 1988-4
[ESA-TT-1161] N89-29299

NAVIGATION
Determining the location of an observer with respect to aerial photographs
[AD-A207791] N89-28929

NEAR FIELDS
Near-field testing of the 15-meter hoop-column antenna
[NASA-TM-4073] N89-28550
Evaluation of the bistatic equivalence theorem for the near and far-field radar cross section of complex targets
[AD-A209228] N89-28682
Nearfield acoustic holography: Review and perspectives
[ISVR-TR-179] N89-28807

NEAR INFRARED RADIATION
A deep optical infrared survey
[AD-A207930] N89-29278

NEAR WAKES
Laser velocimetry in the close wake of an axisymmetric rear body
[ISL-R-114/87] N89-28774

NEGATIVE IONS
Effect of a converter electrode in a multicusp negative ion source
[IPPJ-914] N89-29214

NEODYMIUM LASERS
Increase of the damage thresholds of dielectric layer systems for the Nd laser
[ETN-89-94436] N89-28824

NEON
Photon-ion angular correlation measurements on the system He(+) + Ne: Determination of the spin inversion
[ETN-89-94435] N89-29175

NETHERLANDS
Entrepreneurship and innovation: The Dutch sugar beet industry (1858-1919)
[ISBN-90-71617-11-4] N89-29275

NETWORK ANALYSIS
On the composition of interconnected systems by nonserial dynamic programming: Application to power systems
[LAAS-89.096] N89-29084
Chapter on distributed computing
[AD-A208996] N89-29084
Minimization of Boolean sum of products with applications to the computation of reliability of general networks
[VTT-RR-571] N89-29136

NEURAL NETS
Preliminary neural network detection of a gulf stream in images of sea surface temperature gradients, phase 1
[AD-A207801] N89-29003
Real-time applications of neural nets
[DE89-014400] N89-29093
Computer implementation and simulation of some neural networks used in pattern recognition and classification
[AD-A208112] N89-29099

NEUROLOGY
Transient visual evoked neuromagnetic responses: Identification of multiple sources
[DE89-013438] N89-29008
Components of high-level vision: A cognitive neuroscience analysis and accounts of neurological syndromes
[AD-A207848] N89-29011

NEUTRAL BEAMS
Chemical and Laser Sciences Division
[DE89-014385] N89-28811
Improved confinement in high density ohmic discharge
[IPPJ-913] N89-29213

NEUTRONS
Calculation of two-neutron multiplicity in photonuclear reactions N89-29160

NEWTON METHODS
On the classification of plane graphs representing structurally stable rational Newton-flows
[MEMO-750-REV] N89-28776
Gradient Newton-flows for complex polynomials
[MEMO-764] N89-28779

NICKEL
High resolution electron energy loss studies of surface vibrations
[DE89-013964] N89-28589
Electronic-structure study of the Ni-Ga and Ni-In intermetallic compounds using X-ray photoemission spectroscopy
[AD-A209696] N89-28601

NICKEL ALLOYS
Theoretical analysis of phase transformations in Fe-Ni Invar-type alloys
[DE89-014454] N89-28618

NICKEL COMPOUNDS
Electronic-structure study of the Ni-Ga and Ni-In intermetallic compounds using X-ray photoemission spectroscopy
[AD-A209696] N89-28601

NIOBIUM ALLOYS
Sulfidation/oxidation properties of iron-based alloys containing niobium and aluminum
[DE89-013766] N89-28617

NIOBIUM COMPOUNDS
Fluxons and order in long Josephson junctions
[AD-A207925] N89-29249

NITRATES
Effect of hydraulic fluid on hydroxylammonium nitrate based liquid propellant formulations
[AD-A208061] N89-28663

NITROGEN ATOMS
Collisional transfer between and quenching of the 3p 3p and 5p states of the oxygen atom
[AD-A207759] N89-28607

NITROGEN TETROXIDE
Analysis of the regenerative cooling of a rocket motor fed with monomethylhydrazine and nitrogen tetroxide
[ETN-89-94976] N89-28569

NOISE INTENSITY
Acoustic tests on a new motor generator system for the minuteman launch control centers in Hill engineering test facilities 1 and 2, Hill AFB, Utah
[AD-A209598] N89-28717
The fluxgate ringcore sensor demagnetising factor and noise
[ORI-1-89] N89-28805

NOISE MEASUREMENT
Airport noise measuring data collction system
[NLR-MP-87006-U] N89-28526
Acoustic tests on a new motor generator system for the minuteman launch control centers in Hill engineering test facilities 1 and 2, Hill AFB, Utah
[AD-A209598] N89-28717

NOISE PREDICTION (AIRCRAFT)
Noise produced by turbulent flow into a rotor: Users manual for noise calculation
[NASA-CR-181790] N89-29152
Noise produced by turbulent flow into a rotor: Users manual for atmospheric turbulence prediction and mean flow and turbulence contraction prediction
[NASA-CR-181791] N89-29154

NOISE REDUCTION
A new holographic inverse filtering method and its application to restoration of degraded remote sensing images N89-28877
JPRS Report: Science and Technology. USSR: Space. 16th International Congress of the International Society for Photogrammetry and Remote Sensing, volume 2
[JPRS-USP-89-003-VOL-2] N89-28903
Noise reduction from Synthetic Aperture Radar imagery N89-28913

NONDESTRUCTIVE TESTS
Ultrasonic imaging of textured alumina
[NASA-TM-101478] N89-28853
Nondestructive characterization of simple interfaces using volume sound waves
[ETCA-89-R-015] N89-28854
Ultrasonic systems and system development at SNL Albuquerque
[DE89-013164] N89-29153

NONLINEAR EQUATIONS
Probabilistic analysis of semilinear partial differential equations
[AD-A209903] N89-29113

NONLINEAR OPTICS
United States Air Force Research Initiation Program for 1987, volume 2
[AD-A209727] N89-29259

NONLINEAR PROGRAMMING
Methods of combinatorial optimization and their range of applicability
[MEMO-766] N89-29073

NONLINEAR SYSTEMS
Modelling, information, processing, and control
[AD-A207810] N89-28865
Nonlinear dynamics and control of flexible structures
[AD-A208120] N89-28869
One-degree-of-freedom motion induced by modeled vortex shedding
[NASA-TM-101038] N89-28870
Investigations of nonlinear streamcipher systems: Construction and evaluation methods
[ETN-89-95456] N89-29038
Numerical solution of ill posed problems in partial differential equations
[AD-A207852] N89-29119
Nonlinear stability in fluid and plasma dynamics
[AD-A207715] N89-29203

NONLINEARITY
Non-linear surface fitting of laser range images using a hypercube concurrent computer
[DE89-013720] N89-28808

NOTCH TESTS
Measurement of mode 1 and mode 2 strain energy release rates: A VAMAS round robin project on delamination of composite materials --- Versailles project on advanced materials and standards (VAMAS)
[NPL-DMA(A)-178] N89-28583
A summary of the UK results for a VAMAS round robin project on delamination of composite materials --- Versailles project on advanced materials and standards (VAMAS)
[NPL-DMA(A)-179] N89-28584

NOZZLE DESIGN
Static and dynamic deflection studies of the SRM aft case-nozzle joint
[NASA-TM-100373] N89-28568

NOZZLE FLOW
Heat transfer and film cooling in compressible nozzle flow
[ETN-89-94653] N89-28773

NUCLEAR BINDING ENERGY
Vibrational dynamics of aniline (Ar)1 and aniline (CH4)1 clusters
[AD-A209560] N89-28605

NUCLEAR FUEL REPROCESSING
Chemical Technology Division
[DE89-013917] N89-28591

NUCLEAR FUELS
Chemical Technology Division
[DE89-013917] N89-28591

NUCLEAR FUSION
Chemical Technology Division
[DE89-013917] N89-28591
Measurement of solar proton-proton fusion neutrinos with a Soviet-American gallium experiment
[DE89-014563] N89-29168
Proceedings of the Antiproton Technology Workshop held in Upton, New York on 10 May 1989
[AD-A210045] N89-29170
A new method of testing nuclear fusion in metals
[IPPJ-915] N89-29215

NUCLEAR MAGNETIC RESONANCE
Characterization of substituted phenol-formaldehyde resins using solid-state carbon-13 NMR
[AD-A208745] N89-28638
A study of the T(1) transition of Poly(Bis(trifluoroethoxy)Phosphazene) (PBFP) using solid-state nuclear magnetic resonance spectroscopy
[AD-A207719] N89-29246

NUCLEAR PHYSICS
Activities report of the Max-Planck Institute of Nuclear Physics
[ETN-89-94398] N89-29174

NUCLEAR REACTIONS
Particle production results from HELIOS
[DE89-013454] N89-29167
Activities report of the Max-Planck Institute of Nuclear Physics
[ETN-89-94398] N89-29174

NUCLEAR SCATTERING
Photonuclear absorption cross sections
[NASA-CR-185488] N89-29159

NUCLEAR STRUCTURE
The influence of the shell closure on the microscopic structure of even-even Hg isotopes: A study with electron and muon beams --- a study with electron and muon beams
[ETN-89-95464] N89-29177

NUCLEATION
The aggregated state of matter: Elucidating transitions from the gas to the condensed phase and the formation of aerocolloids
[AD-A209080] N89-28595

NUCLEI (NUCLEAR PHYSICS)
Electromagnetic interactions of cosmic rays with nuclei N89-29163

NUCLEONS
Nucleon emission via electromagnetic excitation in relativistic nucleus-nucleus collisions: Re-analysis of the Weizsacker-Williams method N89-29166

NUMBER THEORY
Interpolating polynomials from their values
[AD-A210102] N89-29114

NUMERICAL ANALYSIS
Three-dimensional viscous hypersonic flow over blunt bodies
[DFVLR-FB-89-09] N89-28504

NEC (Numerical Electromagnetics Code), NECGS (Numerical Electromagnetics Code-Ground Screen), and MININEC (Mini-Numerical Electromagnetics Code) numerical models of LF top-hat monopole antennas
[AD-A209230] N89-28683
Formulation and numerical solution of the equations of constrained mechanical motion
[DFVLR-FB-89-08] N89-28847
A numerical study of a mesoscale eddy interaction with an ocean front in the marginal ice zone
[AD-A209192] N89-29002
Near-neighbor algorithms for processing bearing data
[AD-A207935] N89-29053

NUMERICAL CONTROL
Spacecraft component heater control system
[NASA-CASE-MFS-28327-1] N89-28556
Preliminary design of a consultation knowledge-based system for the minimization of distortion in welded structures
[AD-A208842] N89-28834
Residual vibration reduction in computer controlled machines
[AD-A208074] N89-28866

NUMERICAL FLOW VISUALIZATION
La Recherche Aerospatiale, bimonthly bulletin, number 1988-6
[ESA-TT-1165] N89-29301

NUMERICAL STABILITY
The stability of the theta-methods in the numerical solution of delay differential equations
[TW-88-08] N89-29127
A necessary condition for B-convergence of Runge-Kutta methods
[TW-89-01] N89-29129

NUMERICAL WEATHER FORECASTING
Satellite enhanced numerical weather prediction
[AD-A210108] N89-28987

O

O RING SEALS
O-ring gasket test fixture
[NASA-CASE-MFS-28376-1] N89-28546

OBJECT PROGRAMS
An object-oriented software reuse tool
[AD-A208018] N89-29056
Implementation of a distributed object-oriented database management system
[AD-A209437] N89-29265

OBSERVATORIES
Activities report in international astronomy
[ETN-89-95333] N89-29281

OCEAN CURRENTS
Ocean remote sensing and modeling
[AD-A208406] N89-28927
A numerical study of a mesoscale eddy interaction with an ocean front in the marginal ice zone
[AD-A209192] N89-29002

OCEAN DATA ACQUISITIONS SYSTEMS
Sea gravimetry and Eotvos correction
[REPT-88.3] N89-29006

OCEAN MODELS
Ocean remote sensing and modeling
[AD-A208406] N89-28927
A numerical study of a mesoscale eddy interaction with an ocean front in the marginal ice zone
[AD-A209192] N89-29002

OCEAN SURFACE
Interpretation of remote sensing data from eastern areas of the Baltic Sea N89-28898
Results of Seasat altimeter data processing for the northeast Atlantic
[BCRS-89-05] N89-28940
Preliminary neural network detection of a gulf stream in images of sea surface temperature gradients, phase 1
[AD-A207801] N89-29003

OCEANOGRAPHIC PARAMETERS
A study on information analysis aids for sea surface temperature image data N89-28897
Sea spectra as determined from low-altitude SLAR images N89-28908
Ocean remote sensing and modeling
[AD-A208406] N89-28927

OCEANOGRAPHY
Results of Seasat altimeter data processing for the northeast Atlantic
[BCRS-89-05] N89-28940
The WMO applications of meteorology program 1988-1997: Second WMO long-term plan, part 2, volume 4
[WMO-694-PT-2-VOL-4] N89-28998

OCEANS
A numerical study of a mesoscale eddy interaction with an ocean front in the marginal ice zone
[AD-A209192] N89-29002

OHMIC DISSIPATION
Improved confinement in high density ohmic discharge
[IPPJ-913] N89-29213

OIL POLLUTION
The Archimedes 2a Experiment on oil slick dection over the North Sea, April 1988: Measurement Results obtained by the E-SAR System of the Aerospace Research Establishment
[DFVLR-MITT-89-08] N89-28942

OIL SLICKS
The Archimedes 2a Experiment on oil slick dection over the North Sea, April 1988: Measurement Results obtained by the E-SAR System of the Aerospace Research Establishment
[DFVLR-MITT-89-08] N89-28942

ON-LINE SYSTEMS
Development and implementation of an on-line multivariable control algorithm for the force control of an industrial robot
[OUEL-1748/88] N89-28848
ESA's activities and plans for remote sensing data systems N89-28906
Optical laser technology and its application to Defense Manpower Data Center's (DMDC) querry facsimile (QFAX) data base system
[AD-A207832] N89-29194

OPEN CLUSTERS
Red giants in open clusters. 1: Binarity and stellar evolution in five Hyades-generation clusters, NGC 2447, 2539, 2632, 6633 and 6940
[SER-C-PREPUBL-FASC-37-PT-1] N89-29290
Red giants in open clusters. 2: Orbits of ten spectroscopic binaries in NGC 2360, 2437, 2447, 5822, 5823, 6475
[SER-C-PREPUBL-FASC-38-PT-2] N89-29291

OPERATING SYSTEMS (COMPUTERS)
Strategic defense system distributed operating system R and D review and recommendations
[AD-A208034] N89-29145

OPERATIONS RESEARCH
Risk management for air ambulance helicopters operators
[DOT/FAA/DS-88/7] N89-28506
Evaluation of functionality in distributed systems
[AD-A209167] N89-29258

OPERATORS (MATHEMATICS)
A generalization of the numerical range of a matrix
[TW-88-09] N89-29128

OPTICAL COMMUNICATION
Status and development potential of the fly by light technology in civil aircraft
[ILR-MITT-212] N89-28522
Holographic modulator arrays
[AD-A209387] N89-28792
AlGaAs phased array laser for optical communications
[NASA-CR-181869] N89-28820
Monolithic narrow-linewidth InGaAsP semiconductor laser for coherent optical communications
[NASA-CR-181870] N89-28821

OPTICAL COMPUTERS
Digital optical computing with fibers and directional couplers
[PB89-184378] N89-29030
The mock counter: A hybrid optical-electronic counter using fiber delay line memory
[PB89-184410] N89-29031
An optoelectronic multi-Gb/s packet switching network
[PB89-184345] N89-29081

OPTICAL COUPLING
An experimental optical coupling device for an airborne digital redundant system
[NAL-TR-1003] N89-28514

OPTICAL DATA PROCESSING
Acousto-optical vector matrix product processor: Implementation issues
[AD-A207933] N89-28722
United States Air Force Research Initiation Program for 1987, volume 2
[AD-A209727] N89-29259
Moving optical technology in-house
[AD-A207850] N89-29268

OPTICAL FIBERS
Digital optical computing with fibers and directional couplers
[PB89-184378] N89-29030
Characterization, optimization and design of single-mode multistep fibers
[ETN-89-94440] N89-29197

OPTICAL FILTERS
A new holographic inverse filtering method and its application to restoration of degraded remote sensing images N89-28877

OPTICAL MEASURING INSTRUMENTS
Experimenting cavitation measuring instruments
[CERT-2305] N89-28803
Activities report in international astronomy
[ETN-89-95333] N89-29281

OPTICAL MEMORY (DATA STORAGE)
Optical laser technology and its application to Defense Manpower Data Center's (DMDC) querry facsimile (QFAX) data base system
[AD-A207832] N89-29194
Conversion of hard-copy documents to digital format utilizing optical scanners and optical storage media
[AD-A209473] N89-29266

OPTICAL PROPERTIES
Optical properties and error sources of an airborne radiometer
[MITT-60] N89-28799
United States Air Force Research Initiation Program for 1987, volume 2
[AD-A209727] N89-29259

OPTICAL RADAR
JPRS Report: Science and Technology. USSR: Space. 16th International Congress of the International Society for Photogrammetry and Remote Sensing, volume 2
[JPRS-USP-89-003-VOL-2] N89-28903
Lidar measurements of sea surface waves N89-28909

OPTICAL SCANNERS
Conversion of hard-copy documents to digital format utilizing optical scanners and optical storage media
[AD-A209473] N89-29266

OPTICAL SWITCHING
Photonic architectures for performing perfect shuffle on a time-division multiplexed signal
[PB89-184352] N89-28674
Digital optical computing with fibers and directional couplers
[PB89-184378] N89-29030
The mock counter: A hybrid optical-electronic counter using fiber delay line memory
[PB89-184410] N89-29031
An optoelectronic multi-Gb/s packet switching network
[PB89-184345] N89-29081
Theoretical investigations of an integrated optics switching element with asymmetric directional couplers for switching matrices
[ETN-89-94439] N89-29196

OPTICAL TRANSFER FUNCTION
Display characteristics of example light-valve projectors
[AD-A209580] N89-29193

OPTIMAL CONTROL
Generalized projected gradient-type iterative method for parametric and functional optimization of dynamical systems subject to constraints
[ONERA-NT-1988-9] N89-29063
On the composition of interconnected systems by nonserial dynamic programming: Application to power systems
[LAAS-89.096] N89-29064
Northeast artificial intelligence consortium. Volume 1: Executive summary
[AD-A209395] N89-29094
Computations of optimal controls and designs for distributed systems in optics and elasticity
[AD-A207924] N89-29098

OPTIMIZATION
Model simplification based on the concept of equivalent dead time
[NAL-TM-SE-8802] N89-28521
Multivariate analysis of UV-spectral data for solute tracking in HPLC
[ISBN-90-6275-535-6] N89-28614
A method for assisting in decision-making for multilayer radar absorbent coverings — manufacture
[ONERA-NT-1989-2] N89-28703
Model reduction of linear conservative mechanical systems
[MEMO-752] N89-28845
Optimization of structures with passive damping and active controls
[AD-A208937] N89-28862
Monte Carlo analysis of localization errors in magnetoencephalography
[DE89-013221] N89-29007
Solution of a tinned iron purchasing problem by Lagrangian relaxation
[MEMO-735] N89-29074
A static load distribution strategy for processor tools
[MEMO-INF-88-43] N89-29078
The application of constraints in query optimization
[MEMO-INF-88-55] N89-29079
Large scale function minimization
[AD-A207718] N89-29087
Three dimensional cellular automata for subpixel target detection
[AD-A208163] N89-29100

Application of optimal control theory for selective vibrational excitation in molecules modeled as harmonic systems
[MEMO-755] N89-29104
Are limits of alpha-discounted optimal policies Blackwell optimal: A counterexample
[TW-88-10] N89-29139
Study and simulation of an E-beam microlithography process on a multilayer resin structure. Research of an optimization
[LAAS-89.012] N89-29179
New layout of Amsterdam pulse stretcher
[NIKHEF-K/APS/88-01A-REV] N89-29182
Orbit correction scheme for the new ring — Amsterdam electron accelerator
[NIKHEF-K/APS/88-04] N89-29184
Characterization, optimization and design of single-mode multistep fibers
[ETN-89-94440] N89-29197

OPTOELECTRONIC DEVICES
Television monitor field shifter and an opto-electronic method for obtaining a stereo image of optimal depth resolution and reduced depth distortion on a single screen
[NASA-CASE-NPO-17249-1-CU] N89-28678
Digital optical computing with fibers and directional couplers
[PB89-184378] N89-29030
The mock counter: A hybrid optical-electronic counter using fiber delay line memory
[PB89-184410] N89-29031
An optoelectronic multi-Gb/s packet switching network
[PB89-184345] N89-29081
Investigation of optoelectronic angle measuring systems and their use in a diffraction-optical strain measurement and a photoelectric two-coordinate autocollimator
[PTB-F-5] N89-29199

ORBIT CALCULATION
Orbit determination of sunlight illuminated objects detected by overhead platforms
[AD-A209227] N89-28540

ORBIT PERTURBATION
Numerical determination of the location of critical inclinations for long term high eccentricity orbits about Mars
[AD-A209200] N89-28538
Orbits containing arcs of minimum altitude variation
[AD-A209206] N89-28539

ORBIT TRANSFER VEHICLES
Ion optics for high power 50-cm-diam ion thrusters
[NASA-TM-102143] N89-28571

ORBITAL MECHANICS
Numerical determination of the location of critical inclinations for long term high eccentricity orbits about Mars
[AD-A209200] N89-28538
Orbits containing arcs of minimum altitude variation
[AD-A209206] N89-28539
Modeling of short arc orbital constraints for incorporation into photogrammetric adjustment of MEOSS data
[DFVLR-FB-89-14] N89-28943

ORBITAL POSITION ESTIMATION
Orbit determination of sunlight illuminated objects detected by overhead platforms
[AD-A209227] N89-28540
Modeling of short arc orbital constraints for incorporation into photogrammetric adjustment of MEOSS data
[DFVLR-FB-89-14] N89-28943

ORDER-DISORDER TRANSFORMATIONS
States of oxygen ordering in YBa2Cu3Oz
[DE89-014893] N89-29227

ORGANIC COMPOUNDS
Chiral organic crystals for high power frequency conversion
[DE89-013791] N89-29224

ORGANIC MATERIALS
Acousto-optic and linear electro-optic properties of organic polymeric materials
[AD-A207974] N89-28646

ORGANIC SULFUR COMPOUNDS
Monolayers of 11-trichlorosilylundecyl thioacetate: A system that promotes adhesion between silicon dioxide and evaporated gold
[AD-A208266] N89-28637

ORGANIZATIONS
Calendar of selected aeronautical and space meetings
[AGARD-CAL-89/2] N89-29261

ORGANOMETALLIC COMPOUNDS
Multicomponent e-beam resists containing organometallic compounds and reactive monomers
[AD-A207716] N89-28606

ORTHOGONALITY
Row-oriented direct solving of linear algebraic equations: Row orthogonalization method
[REPT-88-82] N89-29105

OSCILLATORS
Quantization by cosmic background radiation
[AD-A208103] N89-29297

OVERVOLTAGE
Performance evaluation of radiofrequency, microwave, and millimeter wave power meters
[PB89-193916] N89-28707

OXIDATION
Laboratory investigations: Low earth orbit environment chemistry with spacecraft surfaces
[DE89-014280] N89-28533
Oxidative addition of C-H bonds in organic molecules to transition metal centers
[DE89-012991] N89-28616
Sulfidation/oxidation properties of iron-based alloys containing niobium and aluminum
[DE89-013766] N89-28617
Oxidation and hot corrosion of some advanced superalloys at 1300F to 2000F (740C to 1093C)
[AD-A209353] N89-28622

OXIDATION RESISTANCE
Explanatory research on the protection of carbon-carbon composites against oxidation at very high temperatures (greater than 3000 F) with Engel-Brewer and other intermetallic compounds
[AD-A207907] N89-28577
Oxidation and hot corrosion of some advanced superalloys at 1300F to 2000F (740C to 1093C)
[AD-A209353] N89-28622

OXIDES
Standard reference material for high temperature viscosity measurements: Results of interlaboratory comparison programme
[NPL-DMA(A)-175] N89-28612

OXYACETYLENE
Infrared study of carbon deposits on catalysts
[DE89-013310] N89-28634

OXYGEN
Aeronomic problems of molecular oxygen photodissociation. 5: Predissociation in the Schumman-Runge Bands of Oxygen
[AERONOMICA-ACTA-A-341-1989-5] N89-28980
Aeronomic problems of molecular oxygen photodissociation. 6: Photodissociation frequency and transmittance in the spectral range of the Schumman-Runge bands
[AERONOMICA-ACTA-A-342-1989-6] N89-28981
States of oxygen ordering in YBa2Cu3Oz
[DE89-014893] N89-29227

OXYGEN ATOMS
Collisional transfer between and quenching of the 3p 3p and 5p states of the oxygen atom
[AD-A207759] N89-28607

OXYGEN SUPPLY EQUIPMENT
Oxygen storage on zeolites
[AD-A209352] N89-28599

OZONE
Ozone trends within a large metropolitan area: The Los Angeles Basin
[PB89-145965] N89-28960
Adequacy of forestry data in assessing the impact of ozone: A national perspective
[DE89-012359] N89-28962

OZONE DEPLETION
Atmospheric processes and effects on materials
[PB89-173215] N89-28964
The 1988 Antarctic ozone monitoring Nimbus-7 TOMS data atlas
[NASA-RP-1225] N89-28983

OZONOMETRY
The 1988 Antarctic ozone monitoring Nimbus-7 TOMS data atlas
[NASA-RP-1225] N89-28983

OZONOSPHERE
Absorption cross section of alternative chlorofluoroethanes and potential effects on the ozone layer
[AERONOMICA-ACTA-A-340-1989] N89-28968

P

P-I-N JUNCTIONS
Research on stable, high-efficiency, large-area, amorphous-silicon-based submodules, task B
[DE89-009439] N89-28946

P-TYPE SEMICONDUCTORS
The problem of selecting the shape functions for a p-type finite element
[AD-A207798] N89-29117

PACIFIC OCEAN
Ocean remote sensing and modeling
[AD-A208406] N89-28927

PACKAGING
A method for evaluating structural transducers used in Type B package testing
[DE89-013591] N89-28784

PACKET SWITCHING
Photonic architectures for performing perfect shuffle on a time-division multiplexed signal
[PB89-184352] N89-28674
An optoelectronic multi-Gb/s packet switching network
[PB89-184345] N89-29081

PACKET TRANSMISSION
An optoelectronic multi-Gb/s packet switching network
[PB89-184345] N89-29081

PAINTS
Characterization of painted surfaces in the United States from the perspective of potential damage from acidic deposition
[DE89-014264] N89-28965

PAIR PRODUCTION
Measurement of electroweak effects and topological branching conditions in the reaction e(+)e(-) yields tau(+)tau(-) in the storage ring PETRA
[MPI-PAE/EXP.EL-195] N89-29173

PALLADIUM
A new method of testing nuclear fusion in metals
[IPPJ-915] N89-29215

PANEL METHOD (FLUID DYNAMICS)
Analysis of leading edge separation using a low order panel method
[NASA-CR-185892] N89-28493

PANELS
High temperature flexible seal
[NASA-CASE-LEW-14695-1] N89-28830

PARACHUTING INJURY
Canadian Forces aircrew ejection, descent, and landing injuries, 1 January 1975 - 31 December 1987
[AD-A208116] N89-29015

PARALLEL PROCESSING (COMPUTERS)
Two-dimensional signal processing and storage and theory and applications of electromagnetic measurements
[AD-A207827] N89-28689
ERS-1 SAR processing with CESAR N89-28888
Fault-tolerant computer architecture modeling and analysis
[AD-A209364] N89-29034
Chaotic behavior in a new class of parallel optimization algorithms
[DE89-014069] N89-29040
A model of parallel performance
[AD-A207792] N89-29049
BM/C(3) algorithm mapping onto concurrent processors
[AD-A207877] N89-29052
Parallel algorithms for solving systems of linear equations and their mapping on systolic arrays
[ETN-89-95457] N89-29077
Large scale function minimization
[AD-A207718] N89-29087
Information requirements and the implications for parallel computation
[AD-A207802] N89-29088
Analysis of cache invalidation patterns in multiprocessors
[AD-A207820] N89-29089
TIME: Time and memory efficient distance transformations for parallel and pyramid machines
[FOA-C-30531-3.4] N89-29091
Northeast artificial intelligence consortium annual report 1987. Volume 9: Computer architectures for very large knowledge bases
[AD-A209454] N89-29096
Three dimensional cellular automata for subpixel target detection
[AD-A208163] N89-29100
Row-oriented direct solving of linear algebraic equations: Row orthogonalization method
[REPT-88-82] N89-29105
The problem of selecting the shape functions for a p-type finite element
[AD-A207798] N89-29117

PARALLEL PROGRAMMING
A programming language supporting first-class parallel environments
[AD-A207833] N89-29051
Parallel language constructs for tensor product computations on loosely coupled architectures
[NASA-CR-181900] N89-29061
Parallel algorithms for solving systems of linear equations and their mapping on systolic arrays
[ETN-89-95457] N89-29077
La Recherche Aerospatiale, bimonthly bulletin, number 1988-6
[ESA-TT-1165] N89-29301

PARAMETER IDENTIFICATION
The design of VLSI circuits
[ETN-89-94968] N89-29065
PARAMETERIZATION
Modelling orientation parameters of sensor platforms N89-28881
An improving multispectral recording set analysis method N89-28900
Parameterization of ice and water clouds and their radiation transport characteristics for large scale atmospheric models
[MITT-58] N89-28977
Least-squares best-fit geometric elements
[NPL-DITC-140/89] N89-29125
Electromagnetic interactions of cosmic rays with nuclei N89-29163
PARITY
The invariance of classical electromagnetism under Charge-conjugation, Parity and Time-reversal (CPT) transformations N89-29161
PARTIAL DIFFERENTIAL EQUATIONS
Bifurcation and pattern formation in combustion
[DE89-013629] N89-28590
Computations of optimal controls and designs for distributed systems in optics and elasticity
[AD-A207924] N89-29098
Probabilistic analysis of semilinear partial differential equations
[AD-A209903] N89-29113
Numerical solution of ill posed problems in partial differential equations
[AD-A207852] N89-29119
Optimal error analysis of spectral methods with emphasis on non-constant coefficients and deformed geometries
[NASA-CR-181902] N89-29124
Grid generation using elliptic partial differential equations
[DFVLR-FB-89-15] N89-29132
PARTICLE ACCELERATION
Unlimited acceleration of particles by a system of multi-laser beams
[IPPJ-902] N89-29206
PARTICLE ACCELERATORS
Proceedings of a RAND Workshop on Antiproton Science and Technology
[AD-A208166] N89-29172
PARTICLE COLLISIONS
Photonuclear absorption cross sections
[NASA-CR-185488] N89-29159
An optical model description of momentum transfer in heavy ion collisions N89-29162
Nucleon emission via electromagnetic excitation in relativistic nucleus-nucleus collisions: Re-analysis of the Weizsacker-Williams method N89-29166
PARTICLE EMISSION
Photonuclear absorption cross sections
[NASA-CR-185488] N89-29159
Calculation of two-neutron multiplicity in photonuclear reactions N89-29160
Nucleon emission via electromagnetic excitation in relativistic nucleus-nucleus collisions: Re-analysis of the Weizsacker-Williams method N89-29166
PARTICLE INTERACTIONS
The coagulation and dispersion of nonspherical, aerosol particles in a turbulent atmosphere
[AD-A208064] N89-29150
Photonuclear absorption cross sections
[NASA-CR-185488] N89-29159
PARTICLE PRODUCTION
Particle production results from HELIOS
[DE89-013454] N89-29167
PARTICLE SIZE DISTRIBUTION
Freeze-dried tungsten heavy alloys
[DE89-014933] N89-28620
Synthesis and hot pressing of ZnS powders
[AD-A209602] N89-28625
Laser Doppler anemometry N89-28739
Laser Doppler anemometry in supersonic flows: Problems of seeding and angular bias N89-28740
PARTICLE THEORY
Proceedings of the Antiproton Technology Workshop held in Upton, New York on 10 May 1989
[AD-A210045] N89-29170
PARTICLE TRAJECTORIES
The invariance of classical electromagnetism under Charge-conjugation, Parity and Time-reversal (CPT) transformations N89-29161
PARTICLES
Controlled method of reducing electrophoretic mobility of various substances
[NASA-CASE-MFS-26049-1-NP] N89-28603
PARTICULATES
Pressure drop and heat transfer characteristics of nearly neutrally buoyant particulate slurry for advanced energy transmission fluids
[DE89-013645] N89-28751
PASCAL (PROGRAMMING LANGUAGE)
Airport noise measuring data collction system
[NLR-MP-87006-U] N89-28526
PASSIVITY
Metal/metallion system in low temperature molten salts
[AD-A208025] N89-28724
PATENT POLICY
Patent abstracts bibliography: A continuing bibliography. Section 2: Indexes (supplement 35)
[NASA-SP-7039(35)-SECT-2] N89-29264
PATTERN RECOGNITION
Non-linear surface fitting of laser range images using a hypercube concurrent computer
[DE89-013720] N89-28808
Robotic grasping of unknown objects: A knowledge-based approach
[DE89-013875] N89-28833
Transient visual evoked neuromagnetic responses: Identification of multiple sources
[DE89-013438] N89-29008
An efficiently computable metric for comparing polygonal shapes
[AD-A210105] N89-29045
Northeast artificial intelligence consortium annual report 1987. Volume 9: Computer architectures for very large knowledge bases
[AD-A209454] N89-29096
Computer implementation and simulation of some neural networks used in pattern recognition and classification
[AD-A208112] N89-29099
PAVEMENTS
Joint sealants for airport pavements. Phase 1: Laboratory and field investigations
[DOT/FAA/DS-89/2-PHASE-1] N89-28523
Effect of environmental factors on pavement deterioration. Volume 1: Background and methodology
[PB89-182109] N89-28668
PAYLOAD INTEGRATION
Coordination of Advanced Solar Observatory (ASO) Science Working Group (SWG) for the study of instrument accommodation and operational requirements on space station
[NASA-CR-185371] N89-28537
PAYLOADS
Proposed concepts for a advanced optical payload for second generation Meteosat
[ETN-89-95236] N89-28564
ESA's activities and plans for remote sensing data systems N89-28906
Study of sampling systems for comets and Mars
[NASA-CR-185514] N89-29292
PEELING
Comparison of peel and lap shear bond strengths for elastic joints with and without residual stresses
[AD-A208102] N89-28867
PEPTIDES
Capillary zone electrophoresis-mass spectrometry of peptides and proteins
[DE89-014466] N89-28592
PERFORMANCE PREDICTION
Analysis of leading edge separation using a low order panel method
[NASA-CR-185892] N89-28493
Correlation of Puma airloads: Evaluation of CFD prediction methods
[NASA-TM-102226] N89-28498
Effect of environmental factors on pavement deterioration. Volume 1: Background and methodology
[PB89-182109] N89-28668
Airborne pulse Doppler radar. Part 3: Performance estimation — surveillance radar analysis
[BAE-WAA-RP-GEN-RAD-645-PT-3] N89-28697
A model of parallel performance
[AD-A207792] N89-29049
PERFORMANCE TESTS
Design, performance and test standards for flight termination receiver/decoders. Volume 1: Design and performance requirements
[AD-A209644] N89-28544
O-ring gasket test fixture
[NASA-CASE-MFS-28376-1] N89-28546
A torsional suspension system for testing space structures
[NASA-CASE-LAR-14149-1-SB] N89-28547
Five year ground exposure of composite materials used on the Bell Model 206L flight service evaluation
[NASA-TM-101645] N89-28579
Accelerated life evaluation of valve-regulated lead-acid batteries
[DE89-012429] N89-28710
A proposal of more expedient methods of testing machine tools
[DE89-013033] N89-28832
Outline of MOS-1 Verification Program (MVP) N89-28883
Performance evaluation of ERS-1 Synthetic Aperture Radar Fast Delivery Processor N89-28904
PERMANENT MAGNETS
Study of sintered magnets of the Nd-Fe-B type
[AD-A209185] N89-29148
PERMITTIVITY
The relationship between ground permittivity and the input impedance of a horizontal dipole near ground
[AD-A207746] N89-28688
Lubricant evaluation and performance
[AD-A208925] N89-28835
PERSONAL COMPUTERS
Direct User Access Terminal (DUAT) operational concept
[WP-88W00075] N89-28524
A simple numerical algorithm for elastohydrodynamic lubrication, based on a dynamic variation principle
[MEMO-761] N89-28850
PC to mainframe connection: IBM PC 3270 emulation
[AD-A209204] N89-29033
PERSONNEL
Prevention, reduction, and measurement of combat stress reactions: A bibliography
[AD-A209375] N89-29019
Anthropometric survey of US Army personnel: Summary statistics
[AD-A209600] N89-29025
PERTURBATION
Theoretical model of gravitational perturbation of current collector axisymmetric flow field
[AD-A209499] N89-28756
A numerical study of a mesoscale eddy interaction with an ocean front in the marginal ice zone
[AD-A209192] N89-29002
A hybrid perturbation-Galerkin method for differential equations containing a parameter
[NASA-CR-181891] N89-29122
PERTURBATION THEORY
Grid generation using elliptic partial differential equations
[DFVLR-FB-89-15] N89-29132
PETN
Investigation of ambient and high temperature aging of PETN (Pentaerythritol Tetranitrate) by laser induced fluorescence and ultraviolet absorption spectroscopies
[DE89-013740] N89-28813
PETRI NETS
Evaluation of functionality in distributed systems
[AD-A209167] N89-29258
PETROLEUM PRODUCTS
Solid lubrication studied by optical means
[AD-A209008] N89-28836
PHASE TRANSFORMATIONS
The aggregated state of matter: Elucidating transitions from the gas to the condensed phase and the formation of aerocolloids
[AD-A209080] N89-28595
Theoretical analysis of phase transformations in Fe-Ni Invar-type alloys
[DE89-014454] N89-28618
A study of the thermal profiles during autogenous arc welding
[AD-A209440] N89-28843
The amorphous to gamma transformation in ion implanted Al2O3
[DE89-014797] N89-29226
PHASED ARRAYS
AlGaAs phased array laser for optical communications
[NASA-CR-181869] N89-28820
PHENOL FORMALDEHYDE
Characterization of substituted phenol-formaldehyde resins using solid-state carbon-13 NMR
[AD-A208745] N89-28638
PHENOLIC RESINS
Characterization of substituted phenol-formaldehyde resins using solid-state carbon-13 NMR
[AD-A208745] N89-28638
PHOSPHAZENE
A study of the T(1) transition of Poly(Bis(trifluoroethoxy)Phosphazene) (PBFP) using solid-state nuclear magnetic resonance spectroscopy
[AD-A207719] N89-29246
PHOSPHIDES
Preparation of compounds with the tetrahedral structure which transmit in the far infrared
[AD-A208697] N89-28593
PHOTOCHEMICAL REACTIONS
Reaction kinetics and mechanism of chain reactions and explosions via transient spectroscopy
[AD-A209169] N89-28597

Ozone trends within a large metropolitan area: The Los Angeles Basin
[PB89-145965] N89-28960
Photoetched double spiral device
[PD-SE-8911] N89-29071
Morphology control of photoelectrochemically etched profiles in n-GaAs
[AD-A208991] N89-29235
Photoelectrochemical fabrication of gratings in SiC
[AD-A208992] N89-29236

PHOTOCONDUCTIVITY
Lithography and spectroscopy of ultrathin Langmuir-Blodgett polymer films
[AD-A208970] N89-28639

PHOTOCONDUCTORS
Morphology control of photoelectrochemically etched profiles in n-GaAs
[AD-A208991] N89-29235

PHOTODISSOCIATION
Aeronomic problems of molecular oxygen photodissociation. 5: Predissociation in the Schumman-Runge Bands of Oxygen
[AERONOMICA-ACTA-A-341-1989-5] N89-28980
Aeronomic problems of molecular oxygen photodissociation. 6: Photodissociation frequency and transmittance in the spectral range of the Schumman-Runge bands
[AERONOMICA-ACTA-A-342-1989-6] N89-28981

PHOTOELASTIC ANALYSIS
Tactile sensing and the photoelastic tactile sensor
[OUEL-1758/89] N89-28849

PHOTOELECTRIC EMISSION
High-brightness electron injectors: A review
[DE89-014244] N89-28711

PHOTOELECTROCHEMISTRY
Photoelectrochemical fabrication of gratings in SiC
[AD-A208992] N89-29236

PHOTOELECTRON SPECTROSCOPY
Electronic-structure study of the Ni-Ga and Ni-In intermetallic compounds using X-ray photoemission spectroscopy
[AD-A209696] N89-28601
Chemical effects of Ne(+) bombardment on the MoS2(0001) surface studied by high-resolution photoelectron spectroscopy
[AD-A207734] N89-29247

PHOTOGRAMMETRY
JPRS Report: Science and Technology. USSR: Space. 16th International Congress of the International Society for Photogrammetry and Remote Sensing, volume 1
[JPRS-USP-89-002-VOL-1] N89-28876
Modelling orientation parameters of sensor platforms N89-28881
Map production and revision with satellite photographs taken by the MKF-6 camera and by the cameras KATE-140, KATE-200, and KFA-1000 N89-28893
National report of Polish Society of Photogrammetry and Remote Sensing N89-28895
A survey of aerial image quality assessment methods N89-28916
Determining the location of an observer with respect to aerial photographs
[AD-A207791] N89-28929
Modeling of short arc orbital constraints for incorporation into photogrammetric adjustment of MEOSS data
[DFVLR-FB-89-14] N89-28943

PHOTOGRAPHY
High resolution Soviet space photographs for topographic mapping N89-28892
Development of borehole scanner for underground geological survey N89-28899

PHOTOINTERPRETATION
An expert system for satellite image interpretation and G.I.S. based problem solving N89-28894
National report of Polish Society of Photogrammetry and Remote Sensing N89-28895
A survey of aerial image quality assessment methods N89-28916
Northeast artificial intelligence consortium. Volume 1: Executive summary
[AD-A209395] N89-29094
Northeast artificial intelligence consortium annual report 1987. Volume 8: Knowledge base maintenance using logic programming methodologies
[AD-A209453] N89-29095

PHOTOLITHOGRAPHY
Multicomponent e-beam resists containing organometallic compounds and reactive monomers
[AD-A207716] N89-28606
Reactive ion etching of polymer films
[AD-A207674] N89-28645
Molecular weight dependence of e-beam resist sensitivity
[AD-A207835] N89-28719
Photoetched double spiral device
[PD-SE-8911] N89-29071
Quantitative analysis of laser interferometer waveforms obtained during oxygen reactive-ion etching of thin polymer films
[AD-A207836] N89-29248

PHOTOLUMINESCENCE
Lineshape and lifetime studies of exciton luminescence from confined CuCl thin films
[AD-A209750] N89-29243

PHOTOMAPPING
Improvement of classification results of satellite imagery using context information from a topographic map
[NLR-MP-88020-U] N89-28935

PHOTONS
Photon-ion angular correlation measurements on the system He(+) + Ne: Determination of the spin inversion
[ETN-89-94435] N89-29175

PHOTONUCLEAR REACTIONS
Photonuclear absorption cross sections
[NASA-CR-185488] N89-29159
Calculation of two-neutron multiplicity in photonuclear reactions N89-29160
Electric quadrupole excitations in relativistic nucleus-nucleus collisions N89-29164

PHOTOVOLTAIC CELLS
Evolutionary growth for Space Station Freedom electrical power system
[NASA-TM-102339] N89-28570
Thin film photovoltaics
[DE89-009425] N89-28956

PHOTOVOLTAIC CONVERSION
Photovoltaics advanced research and development
[DE89-000895] N89-28948
Two-terminal CuInSe-based cascade cells
[DE89-009422] N89-28950
Thin film photovoltaics
[DE89-009425] N89-28956
Field tests of a novel inverter for photovoltaic power conditioning
[DE89-014322] N89-28958

PHYSICAL CHEMISTRY
Crystal chemistry, magnetic and electrical properties of La(sub2-x)Ba(subx)NiO4
[AD-A209376] N89-29240

PHYSICAL EXERCISE
Thermoregulatory competence during exercise transients in a group of heat-acclimated young and middle-aged men is influenced more distinctly by maximal aerobic power than age
[AD-A209753] N89-29009
Muscle changes with eccentric exercise: Implications on earth and in space
[NASA-TM-102227] N89-29016

PHYSICAL FITNESS
Thermoregulatory competence during exercise transients in a group of heat-acclimated young and middle-aged men is influenced more distinctly by maximal aerobic power than age
[AD-A209753] N89-29009

PHYSIOLOGY
Towards a physiologically based HUD (Head-Up Display) symbology
[AD-A207748] N89-28515
A program for the study of skeletal muscle catabolism following physical trauma
[AD-A207983] N89-29014

PHYTOPLANKTON
Climate regulation by marine phytoplankton: A test by anthropogenic SO2 emissions
[DE89-014706] N89-28984

PICKLING (METALLURGY)
In-situ anodising of aluminium alloys — Airbus corrosion prevention requirements
[BAE/WMD/AR/GEN/00666] N89-28630

PIEZOELECTRIC CRYSTALS
Digital refractometry of piezoelectric crystalline media
[AD-A209362] N89-29239

PIEZOELECTRIC GAGES
Piezoelectric foils as sensors in experimental flow mechanics
[ILR-MITT-214] N89-28800
On strain gages using the PVF2 piezoelectric polymer
[ISL-CO-210/88] N89-28801

PIEZOELECTRICITY
The PVF2 piezoelectric polymer shock stress sensor: System characterization for application under field test conditions
[DE89-014629] N89-28790
Digital refractometry of piezoelectric crystalline media
[AD-A209362] N89-29239

PIGMENTS
A comparison between the variability structure of the remotely sensed sea-surface temperature and pigment distributions N89-28896

PILOT PERFORMANCE
Risk management for air ambulance helicopters operators
[DOT/FAA/DS-88/7] N89-28506

PIONS
Deeply bound orbits in pionic atoms and the optical potential
[ETN-89-95463] N89-29176

PIPE FLOW
Mathematical modeling and analysis of heat pipe start-up from the frozen state
[NASA-CR-185132] N89-28747
Enhancement of forced convection heat transfer in tubes using staged tangential flow injection
[PB89-204598] N89-28768
Heat transfer in free convection and forced, laminar flow in vertical tubes, considering temperature dependent medium characteristics
[ETN-89-94441] N89-28772

PIPELINING (COMPUTERS)
ERS-1 SAR processing with CESAR N89-28888
Real time SAR processing techniques N89-28911
A microprogramming support tool for pipelined architectures
[AD-A208090] N89-29036
Parallel algorithms for solving systems of linear equations and their mapping on systolic arrays
[ETN-89-95457] N89-29077
Row-oriented direct solving of linear algebraic equations: Row orthogonalization method
[REPT-88-82] N89-29105

PIPES (TUBES)
Heat transfer in free convection and forced, laminar flow in vertical tubes, considering temperature dependent medium characteristics
[ETN-89-94441] N89-28772
In search of more output: Two strain gage bridge circuits revisited
[DE89-014039] N89-28787

PLANAR STRUCTURES
Contribution to the generation of circular polarization of high purity using planar wire antenna structures
[ETN-89-94659] N89-28872
On planar point matching under affine transformation
[AD-A210106] N89-29046

PLANE WAVES
Propagation problem and far-field patterns in a stratified finite depth ocean
[PB89-180707] N89-29001

PLANFORMS
Small scale model tests in small wind and water tunnels at high incidence and pitch rates. Volume 1: Test program and discussion of results
[AD-A208647] N89-28488

PLANKTON
A comparison between the variability structure of the remotely sensed sea-surface temperature and pigment distributions N89-28896

PLANTS (BOTANY)
ELF (Extremely Low Frequency) communications system ecological monitoring program
[AD-A208198] N89-28691

PLASMA CLOUDS
Effects of magnetic and collisional viscosity on the E x B gradient drift instability
[AD-A207975] N89-29205

PLASMA CONTROL
Stability of a Taylor-relaxed cylindrical plasma separated from the wall by a vacuum layer
[EUT-88-E-207] N89-29200
ECH plasma for different magnetic axis positions and initial ICRF plasma production experiments in CHS
[IPPJ-907] N89-29201
A three-dimensional resistive MHD simulation analysis of field reversal control in the reversed field pinch
[IPPJ-904] N89-29210
Improved confinement in high density ohmic discharge
[IPPJ-913] N89-29213

PLASMA CURRENTS
A three-dimensional resistive MHD simulation analysis of field reversal control in the reversed field pinch
[IPPJ-904] N89-29210
Full consistent analysis of high beta steady state tokamaks sustained by beam driven and bootstrap currents
[IPPJ-912] N89-29212
On the spoke structure in critical velocity rotating plasmas
[TRITA-EPP-89-01] N89-29217

PLASMA DENSITY
Improved confinement in high density ohmic discharge
[IPPJ-913] N89-29213

PLASMA DIAGNOSTICS
Plasma properties of a large-bore, arc-armature railgun
[AD-A209550] N89-28548

Trochoidal analysis of scattered electrons in a merged electron-ion beam geometry
[NASA-CASE-NPO-16789-1-CU] N89-29169
PLASMA DRIFT
Effects of magnetic and collisional viscosity on the E x B gradient drift instability
[AD-A207975] N89-29205
PLASMA DYNAMICS
Nonlinear stability in fluid and plasma dynamics
[AD-A207715] N89-29203
PLASMA EQUILIBRIUM
Effects of magnetic and collisional viscosity on the E x B gradient drift instability
[AD-A207975] N89-29205
Full consistent analysis of high beta steady state tokamaks sustained by beam driven and bootstrap currents
[IPPJ-912] N89-29212
PLASMA ETCHING
Multicomponent e-beam resists containing organometallic compounds and reactive monomers
[AD-A207716] N89-28606
Reactive ion etching of polymer films
[AD-A207674] N89-28645
PLASMA GUNS
Prototype testing for a hybrid gas-gun/railgun device
[DE89-014294] N89-28542
PLASMA HEATING
ECH plasma for different magnetic axis positions and initial ICRF plasma production experiments in CHS
[IPPJ-907] N89-29201
High power ICRF heating experiments on the JIPP T-IIU tokamak
[IPPJ-903] N89-29209
On the spoke structure in critical velocity rotating plasmas
[TRITA-EPP-89-01] N89-29217
PLASMA INTERACTION EXPERIMENT
Experiments on the magnetic field and neutral density limits on CIV interaction
[TRITA-EPP-88-08] N89-29216
PLASMA INTERACTIONS
Stability of a Taylor-relaxed cylindrical plasma separated from the wall by a vacuum layer
[EUT-88-E-207] N89-29200
PLASMA PHYSICS
Caotic magnetic field line in toroidal plasmas
[IPPJ-911] N89-29211
PLASMA POTENTIALS
On the use of the FEL to produce high transient space-charge potentials in a magnetized plasma
[DE89-014325] N89-28814
PLASMA SHEATHS
On the use of the FEL to produce high transient space-charge potentials in a magnetized plasma
[DE89-014325] N89-28814
Studies of the volume and plasma sheath properties of radio frequency discharges
[AD-A207980] N89-29206
PLASMA TORCHES
Fundamental processes in partially ionized plasmas
[AD-A207910] N89-29204
PLASMA-PARTICLE INTERACTIONS
Proceedings of the Antiproton Technology Workshop held in Upton, New York on 10 May 1989
[AD-A210045] N89-29170
PLASMAS (PHYSICS)
Plasma properties of a large-bore, arc-armature railgun
[AD-A209550] N89-28548
On the use of the FEL to produce high transient space-charge potentials in a magnetized plasma
[DE89-014325] N89-28814
Parallel electric fields in a simulation of magnetotail reconnection and plasmoid evolution
[DE89-012622] N89-28970
Fundamental processes in partially ionized plasmas
[AD-A207910] N89-29204
PLASTIC DEFORMATION
The Bauschinger effect in 6-6-2 titanium alloy and its influence on advanced artillery projectiles
[AD-A209355] N89-28623
Plastic yielding of partially-crystalline polymers
[AD-A208101] N89-28648
Plastic deformation of YBa2Cu3O7-x superconductor compound
[DE89-613395] N89-29221
Weak beam electron microscopy of dislocation splitting in TiAl: Relationship with plasticity
[ONERA-NT-1988-3] N89-29253
PLASTIC FLOW
The Bauschinger effect in 6-6-2 titanium alloy and its influence on advanced artillery projectiles
[AD-A209355] N89-28623
Stresses and strains in a cold-worked annulus
[AR-005-548] N89-28871
PLASTICS
Preliminary design guide for arctic equipment
[AD-A209455] N89-29024
PLATE THEORY
Smooth piecewise polynomials as conforming finite elements for plate bending problems
[MEMO-747] N89-28875
PLATFORMS
Expandable pallet for space station interface attachments
[NASA-CASE-MSC-21117-2] N89-28554
PLATINUM
Infrared study of carbon deposits on catalysts
[DE89-013310] N89-28634
Thermodynamically stable conducting films of intermetallic PtGa2 on gallium arsenide
[AD-A210077] N89-28716
PLATINUM COMPOUNDS
A study of thermodynamic phase stability of intermetallic thin films of Pt2Ga, PtGa and PtGa2 on gallium arsenide
[AD-A209698] N89-29241
PLOTTERS
Transfer of files between IE-32C PC/AT CAD system and Autotrol AD/380 graphics system
[PD-CC-8903] N89-29270
PLOTTING
Numerical determination of the location of critical inclinations for long term high eccentricity orbits about Mars
[AD-A209200] N89-28538
PLUMES
User's guide to the complex terrain dispersion model plus algorithms for unstable situations (CTDMPLUS). Volume 1: Model description and user instructions
[PB89-181424] N89-28963
POINTING CONTROL SYSTEMS
A satellite assisted-tracking system with real-time accommodation for maximal pointing N89-28885
POINTS (MATHEMATICS)
On planar point matching under affine transformation
[AD-A210106] N89-29046
POISSON DENSITY FUNCTIONS
Hamiltonian control systems: Decomposition and clamped dynamics
[MEMO-759] N89-29103
POLARIMETRY
Polarimetric calibration using passive corner reflectors
[DFVLR-FB-89-21] N89-28698
POLARIZATION (WAVES)
Sea spectra as determined from low-altitude SLAR images N89-28908
POLICIES
The WMO long-term plan overall policy and strategy 1988-1997: Second WMO long-term plan, part 1
[WMO-690-PT-1] N89-28994
The World Weather Watch Program 1988-1997: Second WMO long-term plan, part 2, volume 1
[WMO-691-PT-2-VOL-1] N89-28995
The World Climate Program 1988-1997: Second WMO long-term plan, part 2, volume 2
[WMO-692-PT-2-VOL-2] N89-28996
POLLUTION MONITORING
The Archimedes 2a Experiment on oil slick dection over the North Sea, April 1988: Measurement Results obtained by the E-SAR System of the Aerospace Research Establishment
[DFVLR-MITT-89-08] N89-28942
POLLUTION TRANSPORT
User's guide to the complex terrain dispersion model plus algorithms for unstable situations (CTDMPLUS). Volume 1: Model description and user instructions
[PB89-181424] N89-28963
POLYCRYSTALS
Synthesis and hot pressing of ZnS powders
[AD-A209602] N89-28625
Acousto-optic and linear electro-optic properties of organic polymeric materials
[AD-A207974] N89-28646
Plastic yielding of partially-crystalline polymers
[AD-A208101] N89-28648
Polycrystalline cadmium telluride 3n+i+p solar cell
[DE89-009437] N89-28945
POLYGONS
An efficiently computable metric for comparing polygonal shapes
[AD-A210105] N89-29045
A heterogeneous multiprocessor graphics system using processor-enhanced memories
[AD-A208089] N89-29058
Placing the largest similar copy of a convex polygon among polygonal obstacles
[AD-A210104] N89-29115
POLYMER CHEMISTRY
Microcellular foams from rigid-rod polymers in solutions: Effect of aggregation characteristics on foam properties
[AD-A209024] N89-28640
High temperature adhesive systems
[AD-A209166] N89-28643
Differential equations and continuum mechanics — polymers
[AD-A208837] N89-29109
POLYMER MATRIX COMPOSITES
A VAMAS round robin on fatigue test methods for polymer matrix composites. Part 1: Tensile and flexural tests of unidirectional material — Versailles project on advanced materials and standards (VAMAS)
[NPL-DMA(A)-180-PT-1] N89-28585
POLYMERIC FILMS
Lithography and spectroscopy of ultrathin Langmuir-Blodgett polymer films
[AD-A208970] N89-28639
Reactive ion etching of polymer films
[AD-A207674] N89-28645
Molecular weight dependence of e-beam resist sensitivity
[AD-A207835] N89-28719
On strain gages using the PVF2 piezoelectric polymer
[ISL-CO-210/88] N89-28801
Quantitative analysis of laser interferometer waveforms obtained during oxygen reactive-ion etching of thin polymer films
[AD-A207836] N89-29248
POLYMERIZATION
Stochastic processes in CHEMFETs
[AD-A208092] N89-28725
Cognition and order in Langmuir-Blodgett films of a 3-hexadecyl pyrrole and ferrocene-derivatized pyrrole mixed monolayer system
[DE89-012974] N89-29223
POLYMETHYL METHACRYLATE
Lithography and spectroscopy of ultrathin Langmuir-Blodgett polymer films
[AD-A208970] N89-28639
Molecular weight dependence of e-beam resist sensitivity
[AD-A207835] N89-28719
POLYNOMIALS
Gradient Newton-flows for complex polynomials
[MEMO-764] N89-28779
Smooth piecewise polynomials as conforming finite elements for plate bending problems
[MEMO-747] N89-28875
An explicit separation of relativised random polynomial time and relativised deterministic polynomial time
[AD-A210103] N89-29044
An algorithm for smooth interpolation to scattered data in R2
[MEMO-748] N89-29066
Signed-digit high speed transcendental function processor architecture
[AD-A209199] N89-29110
Interpolating polynomials from their values
[AD-A210102] N89-29114
POLYPROPYLENE
A study of the ultraviolet degradation embrittlement of polypropylene polymer
[ISBN-90-9002498-0] N89-28656
POLYSULFIDES
Chemical effects of Ne(+) bombardment on the MoS2(0001) surface studied by high-resolution photoelectron spectroscopy
[AD-A207734] N89-29247
POLYVINYL FLUORIDE
The PVF2 piezoelectric polymer shock stress sensor: System characterization for application under field test conditions
[DE89-014629] N89-28790
On strain gages using the PVF2 piezoelectric polymer
[ISL-CO-210/88] N89-28801
PORTABLE EQUIPMENT
Development of a field radiometer as a ground truth equipment for the Japanese ERS-1 N89-28901
Proceedings of a RAND Workshop on Antiproton Science and Technology
[AD-A208168] N89-29172
POSITION (LOCATION)
Numerical determination of the location of critical inclinations for long term high eccentricity orbits about Mars
[AD-A209200] N89-28538
Determining the location of an observer with respect to aerial photographs
[AD-A207791] N89-28929
POSITIONING
Kinematic vertical positioning using the global positioning system
[ETN-89-94804] N89-28510
Positioning error induced by axial sampling in positron emission tomography
[DE89-014519] N89-28791

POTASSIUM CHLORIDES
Morphology control of photoelectrochemically etched profiles in n-GaAs
[AD-A208991] N89-29235
POTENTIAL FIELDS
The potential and electric fields of a conducting sphere in the presence of a charged conducting plane
[AD-A209498] N89-29149
POTENTIAL FLOW
Comparison of flow-visualised vortices with computed geometry over thin delta wings
[AD-A209083] N89-28489
Analysis of leading edge separation using a low order panel method
[NASA-CR-185892] N89-28493
POWDER (PARTICLES)
Freeze-dried tungsten heavy alloys
[DE89-014933] N89-28620
Synthesis and hot pressing of ZnS powders
[AD-A209602] N89-28625
High temperature tribometer, phase 1
[AD-A209356] N89-28838
POWER CONDITIONING
Field tests of a novel inverter for photovoltaic power conditioning
[DE89-014322] N89-28958
POWER EFFICIENCY
Ion optics for high power 50-cm-diam ion thrusters
[NASA-TM-102143] N89-28571
Reciprocal perfect and asymptotically perfect periodic radar waveforms and their aperiodic properties
[AD-A208938] N89-28677
POWER SERIES
Canonical integration and analysis of periodic maps using non-standard analysis and Lie methods
[DE89-013369] N89-29106
PREAMPLIFIERS
An improved hibachi support structure for electron-beam diode foils
[DE89-014023] N89-28810
PREBURNERS
Turbomachinery shaft insert
[NASA-CASE-MFS-28345-2] N89-28842
PRECIPITATION (METEOROLOGY)
The scavenging of atmospheric pollutants by clouds and precipitation using a vertical wind tunnel, phase 1
[BPT-9/88] N89-28525
Application of special sensor microwave/imager data for analysis of cyclonic storms in midlatitudes over the sea
[AD-A207675] N89-28975
European crosswind frequencies
[AD-A209137] N89-28985
The sensitivity of Middle East precipitation and cloud forecasts to changes in Eastern Mediterranean Sea surface temperatures
[AD-A207864] N89-28988
The WMO research and development program 1988-1997: Second WMO long-term plan, part 2, volume 3
[WMO-693-PT-2-VOL-3] N89-28997
PREDICTION ANALYSIS TECHNIQUES
Fast-algorithm development for large-eddy simulation of circular-jet turbulence
[AD-A207926] N89-28760
Satellite-derived moisture-bogusing profiles for the North Atlantic Ocean
[AD-A207829] N89-28930
PREPROCESSING
The use of expert systems for preprocessing image data
[NLR-MP-88009-U] N89-28934
PRESSURE DISTRIBUTION
A compressible inverse design method based on an analytical approach
[CUED/A-TURBO/TR-125] N89-28778
PRESSURE DRAG
The anisotropy of the friction pressure of dipolar fluids
[ETN-89-94438] N89-28771
Experimental investigation of the pressure drag in the Alps
[WISS-BER-9] N89-28992
PRESSURE DROP
Pressure drop and heat transfer characteristics of nearly neutrally buoyant particulate slurry for advanced energy transmission fluids
[DE89-013645] N89-28751
PRESSURE EFFECTS
Pressure induced anomaly at Tc in Fe78 Mo2 B20
[NAL-TM-MT-8806] N89-28628
A space marching algorithm for the thin-layer Navier-Stokes equations N89-28767
PRESSURE MEASUREMENT
A survey of measurements and measuring techniques in rapidly distorted compressible turbulent boundary layers
[AGARD-AG-315] N89-28734
Fluctuating wall-pressure measurements N89-28741
Helium bottle pressure measurement by portable ultrasonic technique
[AD-A208994] N89-29188
PRESSURE OSCILLATIONS
Fluctuating wall-pressure measurements N89-28741
PRESSURE VESSELS
Helium bottle pressure measurement by portable ultrasonic technique
[AD-A208994] N89-29188
PROBABILITY DENSITY FUNCTIONS
A graph-theoretical approach to block-co-polymer complexes. Part 1: Stars
[MEMO-757-PT-1] N89-28654
A graph-theoretical approach to block-co-polymer complexes. Part 2: Tree approximation
[MEMO-758-PT-2] N89-28655
PROBABILITY DISTRIBUTION FUNCTIONS
Maximum-likelihood parameter estimation of a generalized gumbel distribution
[AD-A207994] N89-29055
PROBABILITY THEORY
Composite material repair and reliability
[AD-A209150] N89-28574
Packet-error probability analysis for unslotted FH-CDMA (Frequency Hopped-Code Division Multiple-Access) systems with error control coding
[AD-A207964] N89-29054
Probabilistic analysis of semilinear partial differential equations
[AD-A209903] N89-29113
Conditional dependence
[AD-A207881] N89-29120
PROBLEM SOLVING
An expert system for satellite image interpretation and G.I.S. based problem solving N89-28894
An explicit separation of relativised random polynomial time and relativised deterministic polynomial time
[AD-A210103] N89-29044
Generalized projected gradient-type iterative method for parametric and functional optimization of dynamical systems subject to constraints
[ONERA-NT-1988-9] N89-29063
Solution of a tinned iron purchasing problem by Lagrangian relaxation
[MEMO-735] N89-29074
Language constructs and a search procedure to model and solve combinatorial problems
[MEMO-753] N89-29075
Numerical solution of ill posed problems in partial differential equations
[AD-A207852] N89-29119
Linear algebra support modules for approximation and other software
[NPL-DITC-142/89] N89-29126
The stability of the theta-methods in the numerical solution of delay differential equations
[TW-88-08] N89-29127
A generalization of the numerical range of a matrix
[TW-88-09] N89-29128
Computer-aided group problem solving for Unified Life Cycle Engineering (ULCE)
[AD-A209446] N89-29260
PROCEDURES
A method of software development using functional programming
[MEMO-INF-88-64] N89-29069
PROCESS CONTROL (INDUSTRY)
Fundamental aspects of reactions in titanium-silicon thin films for integrated circuits
[ETN-89-95466] N89-28733
High-temperature superconductor materials processing: Development of environmentally acceptable processing technologies
[DE89-014391] N89-29229
PROCUREMENT MANAGEMENT
Solution of a tinned iron purchasing problem by Lagrangian relaxation
[MEMO-735] N89-29074
PRODUCT DEVELOPMENT
Development of a novel silicon detector with internal amplification
[MPI-PAE/EXP.EL-197] N89-28798
TWENTENET chip design
[MEMO-INF-88-49] N89-29090
Characterization, optimization and design of single-mode multistep fibers
[ETN-89-94440] N89-29197
Microwave detection using Josephson elements
[ETN-89-94650] N89-29252
PRODUCTION ENGINEERING
A manufacturing scheduler's perspective on semiconductor fabrication
[AD-A208372] N89-29232
Computer-aided group problem solving for Unified Life Cycle Engineering (ULCE)
[AD-A209446] N89-29260
PROGRAM VERIFICATION (COMPUTERS)
Gauge: Its philosophy and design
[AD-A208944] N89-29083
SDS (Strategic Defense System) software testing and evaluation: A review of the state-of-the-art in software testing and evaluation with recommended R and D tasks
[AD-A209447] N89-29142
PROGRAMMING LANGUAGES
An object-oriented software reuse tool
[AD-A208018] N89-29056
A prototype for converting Linear Programming (LP) models to structured modeling graphs
[AD-A208166] N89-29059
Parallel language constructs for tensor product computations on loosely coupled architectures
[NASA-CR-181900] N89-29061
Language constructs and a search procedure to model and solve combinatorial problems
[MEMO-753] N89-29075
La Recherche Aerospatiale, bimonthly bulletin, number 1988-6
[ESA-TT-1165] N89-29301
PROJECT PLANNING
The WMO long-term plan overall policy and strategy 1988-1997: Second WMO long-term plan, part 1
[WMO-690-PT-1] N89-28894
The World Weather Watch Program 1988-1997: Second WMO long-term plan, part 2, volume 1
[WMO-691-PT-2-VOL-1] N89-28995
The World Climate Program 1988-1997: Second WMO long-term plan, part 2, volume 2
[WMO-692-PT-2-VOL-2] N89-28996
The WMO research and development program 1988-1997: Second WMO long-term plan, part 2, volume 3
[WMO-693-PT-2-VOL-3] N89-28997
The WMO applications of meteorology program 1988-1997: Second WMO long-term plan, part 2, volume 4
[WMO-694-PT-2-VOL-4] N89-28998
PROJECTILES
REGGIE results for the Nunnally mass launcher
[DE89-014377] N89-28543
The Bauschinger effect in 6-6-2 titanium alloy and its influence on advanced artillery projectiles
[AD-A209355] N89-28623
PROJECTORS
Display characteristics of example light-valve projectors
[AD-A209580] N89-29193
PROLOG (PROGRAMMING LANGUAGE)
Northeast artificial intelligence consortium annual report 1987. Volume 8: Knowledge base maintenance using logic programming methodologies
[AD-A209453] N89-29095
PROPELLANT COMBUSTION
Supersonic combustion at the DFVLR: Results and experiences
[DFVLR-88-044] N89-28610
PROPELLANT DECOMPOSITION
Effect of hydraulic fluid on hydroxylammonium nitrate based liquid propellant formulations
[AD-A208061] N89-28663
PROPELLANT EVAPORATION
Modeling of hot fragment conductive ignition of solid propellants with application to melting and evaporation of solids
[AD-A207727] N89-28662
PROPELLANT TRANSFER
COLD-SAT: Cryogenic On-Orbit Liquid Depot-Storage, Acquisition and Transfer
[NASA-TM-102308] N89-28535
PROPELLER NOISE
Aircraft propeller induced structure-borne noise
[NASA-CR-4255] N89-29155
PROPELLERS
Experimenting cavitation measuring instruments
[CERT-2305] N89-28803
PROTECTIVE COATINGS
Laboratory investigations: Low earth orbit environment chemistry with spacecraft surfaces
[DE89-014280] N89-28533
Explanatory research on the protection of carbon-carbon composites against oxidation at very high temperatures (greater than 3000 F) with Engel-Brewer and other intermetallic compounds
[AD-A207907] N89-28577

PROTEIN METABOLISM
A program for the study of skeletal muscle catabolism following physical trauma
[AD-A207983] N89-29014
PROTEINS
Capillary zone electrophoresis-mass spectrometry of peptides and proteins
[DE89-014466] N89-28592
PROTONS
Solid-vapor differences of electronic stopping powers for protons
[IPPJ-901] N89-29207
PROVING
On the shape of mathematical arguments
[ETN-89-95465] N89-29133
PSYCHOPHYSIOLOGY
Components of high-level vision: A cognitive neuroscience analysis and accounts of neurological syndromes
[AD-A207848] N89-29011
PULSARS
The origin and evolution of X-ray binaries and low-magnetic field radio pulsars
[MPE-PREPRINT-145] N89-29284
Evolution of wide binary millisecond pulsars in globular clusters
[MPE-PREPRINT-148] N89-29285
Measurement of the Vela pulsar's proper motion and detection of the optical counterpart of its compact X-ray nebula
[MPE-PREPRINT-151] N89-29288
Millisecond radio pulsars in globular clusters
[NASA-CR-185909] N89-29298
PULSE COMPRESSION
Reciprocal perfect and asymptotically perfect periodic radar waveforms and their aperiodic properties
[AD-A208938] N89-28677
PULSE DOPPLER RADAR
The airborne pulse Doppler radar: An introduction to the basic principles --- surveillance radar analysis
[BAE-WAA-RP-GEN-RAD-584] N89-28696
Airborne pulse Doppler radar. Part 3: Performance estimation --- surveillance radar analysis
[BAE-WAA-RP-GEN-RAD-645-PT-3] N89-28697
PULSE GENERATORS
The Mark 101 flux compression generator: Development progress
[DE89-014298] N89-28712
PULSE MODULATION
Electrical characterization of signal processing microcircuit
[AD-A209078] N89-28714
PULSED LASERS
The use of high-frequency pulsed laser diodes in fringe type laser Doppler anemometry
[ISL-CO-230/88] N89-28826
PYRAMIDS
TiME: Time and memory efficient distance transformations for parallel and pyramid machines
[FOA-C-30531-3.4] N89-29091
PYROLYSIS
Modeling of hot fragment conductive ignition of solid propellants with application to melting and evaporation of solids
[AD-A207727] N89-28662
PYROTECHNICS
Dense heavy metal aerosol monitoring by direct X-ray fluorescence
[AD-A209077] N89-28966
PYRROLES
Cognition and order in Langmuir-Blodgett films of a 3-hexadecyl pyrrole and ferrocene-derivatized pyrrole mixed monolayer system
[DE89-012974] N89-29223

Q

Q FACTORS
Quality factor and statistics for radiation patterns of shipboard HF antennas
[AD-A207931] N89-28690
Q SWITCHED LASERS
Method and circuit for controlling the evolution time interval of a laser output pulse
[NASA-CASE-LAR-13772-1] N89-28816
Method and circuit for shaping laser output pulses
[NASA-CASE-LAR-14203-1] N89-28817
QUADRATIC PROGRAMMING
Active damping of vibration in large space structures using a Karhunen-Loeve reduced order model
[AD-A208183] N89-28558
QUADRUPOLES
Electric quadrupole excitations in relativistic nucleus-nucleus collisions N89-29164
QUALITY
A survey of aerial image quality assessment methods N89-28916
QUALITY CONTROL
NIST (National Institute of Standards and Technology) calibration services users guide, 1989 edition
[PB89-200216] N89-28785
QUANTITATIVE ANALYSIS
Quantitative analysis of laser interferometer waveforms obtained during oxygen reactive-ion etching of thin polymer films
[AD-A207836] N89-29248
QUANTUM CHEMISTRY
Application of Cholesky-like matrix decomposition methods to the evaluation of atomic orbital integrals and integral derivatives
[AD-A209682] N89-29112
QUANTUM CHROMODYNAMICS
Research program in computational physics
[DE89-013952] N89-29255
QUANTUM ELECTRONICS
Fluxons and order in long Josephson junctions
[AD-A207925] N89-29249
QUANTUM MECHANICS
Quantization by cosmic background radiation
[AD-A208103] N89-29297
QUANTUM THEORY
Research program in computational physics
[DE89-013952] N89-29255
Electron energy levels in a quantum well within an in-plane magnetic field
[AD-A209351] N89-29256
QUANTUM WELLS
Monolithic narrow-linewidth InGaAsP semiconductor laser for coherent optical communications
[NASA-CR-181870] N89-28821
Electron energy levels in a quantum well within an in-plane magnetic field
[AD-A209351] N89-29256
QUASARS
Statistical and physical evolution of QSO's
[NASA-CR-185869] N89-29282
QUERY LANGUAGES
A logic query language and its algebraic optimization for a multiprocessor database machine
[MEMO-INF-88-52] N89-29068
The application of constraints in query optimization
[MEMO-INF-88-55] N89-29079
QUEUEING THEORY
BM/C(3) algorithm mapping onto concurrent processors
[AD-A207877] N89-29052

R

RADAR
Reciprocal perfect and asymptotically perfect periodic radar waveforms and their aperiodic properties
[AD-A208938] N89-28677
Adaptive detection and parameter estimation for multidimensional signal models
[AD-A208971] N89-28678
A method for assisting in decision-making for multilayer radar absorbent coverings --- manufacture
[ONERA-NT-1989-2] N89-28703
Ground-Based Radar (GBR): Environmental assessment
[AD-A207654] N89-29143
RADAR ANTENNAS
An approximation formula to evaluate the coefficient update rate of partially adaptive antennas
[REPT-5-88] N89-28844
RADAR CORNER REFLECTORS
Polarimetric calibration using passive corner reflectors
[DFVLR-FB-89-21] N89-28698
RADAR CROSS SECTIONS
Almond test body --- for microwave anechoic chambers
[NASA-CASE-LAR-13747-1-CU] N89-28672
Evaluation of the bistatic equivalence theorem for the near and far-field radar cross section of complex targets
[AD-A209228] N89-28682
RADAR DETECTION
A methodology for modeling radar detection range in air combat simulation
[AD-A209153] N89-28679
Airborne pulse Doppler radar. Part 3: Performance estimation --- surveillance radar analysis
[BAE-WAA-RP-GEN-RAD-645-PT-3] N89-28697
RADAR IMAGERY
Exact image theory for uniaxially anisotropic dielectric half space
[PB89-146450] N89-28671
JPRS Report: Science and Technology. USSR: Space. 16th International Congress of the International Society for Photogrammetry and Remote Sensing, volume 1
[JPRS-USP-89-002-VOL-1] N89-28876
A Bistatic Parasitical Radar (BIPAR) N89-28878
SAR activities at Dornier N89-28887
Application of aerial side-looking radar imagery in China N89-28902
JPRS Report: Science and Technology. USSR: Space. 16th International Congress of the International Society for Photogrammetry and Remote Sensing, volume 2
[JPRS-USP-89-003-VOL-2] N89-28903
Sea spectra as determined from low-altitude SLAR images N89-28908
Real time SAR processing techniques N89-28911
Noise reduction from Synthetic Aperture Radar imagery N89-28913
Design aspects of a system for geocoding satellite SAR images N89-28915
Military hydrology: Assessment of shuttle imaging radar and LANDSAT imagery for ground-water exploration in arid environments
[AD-A209527] N89-28928
RADAR MEASUREMENT
Lidar measurements of sea surface waves N89-28909
RADAR RANGE
A methodology for modeling radar detection range in air combat simulation
[AD-A209153] N89-28679
RADAR RESOLUTION
The airborne pulse Doppler radar: An introduction to the basic principles --- surveillance radar analysis
[BAE-WAA-RP-GEN-RAD-584] N89-28696
Airborne pulse Doppler radar. Part 3: Performance estimation --- surveillance radar analysis
[BAE-WAA-RP-GEN-RAD-645-PT-3] N89-28697
RADAR TARGETS
A methodology for modeling radar detection range in air combat simulation
[AD-A209153] N89-28679
RADIAL DISTRIBUTION
On the spoke structure in critical velocity rotating plasmas
[TRITA-EPP-89-01] N89-29217
RADIAL VELOCITY
Red giants in open clusters. 2: Orbits of ten spectroscopic binaries in NGC 2360, 2437, 2447, 5822, 5823, 6475
[SER-C-PREPUBL-FASC-38-PT-2] N89-29291
RADIATION DETECTORS
The first large balloon launch from Antarctica
[AD-A207735] N89-28491
Measurement of solar proton-proton fusion neutrinos with a Soviet-American gallium experiment
[DE89-014563] N89-29168
RADIATION DOSAGE
Reliability estimates for large satellite memories in low earth orbits
[DE89-007764] N89-28555
HEMP (High-Altitude Electromagnetic Pulse) validation of FAA (Federal Aviation Administration) radio facility
[AD-A209187] N89-28680
Molecular weight dependence of e-beam resist sensitivity
[AD-A207835] N89-28719
RADIATION EFFECTS
ELF (Extremely Low Frequency) communications system ecological monitoring program
[AD-A208198] N89-28691
Atmospheric processes and effects on materials
[PB89-173215] N89-28964
RADIATION HARDENING
HEMP (High-Altitude Electromagnetic Pulse) validation of FAA (Federal Aviation Administration) radio facility
[AD-A209187] N89-28680
RADIATION MEASUREMENT
Molecular weight dependence of e-beam resist sensitivity
[AD-A207835] N89-28719
RADIATION TRANSPORT
Parameterization of ice and water clouds and their radiation transport characteristics for large scale atmospheric models
[MITT-58] N89-28977
RADIATIVE RECOMBINATION
Lineshape and lifetime studies of exciton luminescence from confined CuCl thin films
[AD-A209750] N89-29243
RADIATIVE TRANSFER
Radiative transfer in falling snow: A two-stream approximation
[AD-A208960] N89-29187

RADIO ANTENNAS
HEMP (High-Altitude Electromagnetic Pulse) validation of FAA (Federal Aviation Administration) radio facility
[AD-A209187] N89-28680
Antenna fundamentals: A tutorial paper
[BAE-WAA-R-GEN-RAD-533] N89-28695
RADIO EMISSION
Implications of the correlation between the radio continuum and far-infrared luminosities of spiral galaxies N89-29289
RADIO FREQUENCIES
Antenna fundamentals: A tutorial paper
[BAE-WAA-R-GEN-RAD-533] N89-28695
Performance evaluation of radiofrequency, microwave, and millimeter wave power meters
[PB89-193916] N89-28707
RADIO FREQUENCY DISCHARGE
Studies of the volume and plasma sheath properties of radio frequency discharges
[AD-A207980] N89-29206
RADIO FREQUENCY HEATING
ECH plasma for different magnetic axis positions and initial ICRF plasma production experiments in CHS
[IPPJ-907] N89-29201
High power ICRF heating experiments on the JIPP T-IIU tokamak
[IPPJ-903] N89-29209
RADIO RECEIVERS
Development of an integrated AM shortwave upconversion receiver front-end
[ETN-89-95455] N89-28699
RADIO SPECTRA
Implications of the correlation between the radio continuum and far-infrared luminosities of spiral galaxies N89-29289
RADIO TELEMETRY
The first large balloon launch from Antarctica
[AD-A207735] N89-28491
RADIO TRANSMISSION
Meteor burst system communications compatibility
[PB89-191167] N89-28692
RADIOACTIVE WASTES
A method for evaluating structural transducers used in Type B package testing
[DE89-013591] N89-28784
RADIOGRAPHY
Nonfilm radiography at the Oak Ridge Y-12 Plant
[DE89-014523] N89-28852
RADIOMETERS
A practical method of remotely sensed digital image's resolving power N89-28879
RAILGUN ACCELERATORS
Prototype testing for a hybrid gas-gun/railgun device
[DE89-014294] N89-28542
REGGIE results for the Nunnally mass launcher
[DE89-014377] N89-28543
Plasma properties of a large-bore, arc-armature railgun
[AD-A209550] N89-28548
Application of computational fluid dynamics to the analysis of the aerodynamics of a railgun projectile
[AD-A207758] N89-28758
RAIN FORESTS
Daytime turbulent exchange between the Amazon forest and the atmosphere
[NASA-CR-185487] N89-28961
RAINSTORMS
Application of special sensor microwave/imager data for analysis of cyclonic storms in midlatitudes over the sea
[AD-A207675] N89-28975
RAMAN SPECTRA
The Los Alamos Fourier-transform spectrometer: Applications to molecular spectroscopy
[DE89-014258] N89-28789
RAMAN SPECTROSCOPY
Modelling the in situ infrared reflection-absorption spectra of the diffuse layer
[AD-A209347] N89-28598
The Los Alamos Fourier-transform spectrometer: Applications to molecular spectroscopy
[DE89-014258] N89-28789
RAMP FUNCTIONS
A study of the effect of stimulus upon the reflex response as elicited and recorded by the tympanic membrane displacement measurement device
[ISVR-TR-177] N89-29018
RANDOM ACCESS MEMORY
A heterogeneous multiprocessor graphics system using processor-enhanced memories
[AD-A208089] N89-29058
RANDOM PROCESSES
An explicit separation of relativised random polynomial time and relativised deterministic polynomial time
[AD-A210103] N89-29044
RANGE (EXTREMES)
A generalization of the numerical range of a matrix
[TW-88-09] N89-29128
RANGE SAFETY
Design, performance and test standards for flight termination receiver/decoders. Volume 1: Design and performance requirements
[AD-A209644] N89-28544
RANGEFINDING
A methodology for modeling radar detection range in air combat simulation
[AD-A209153] N89-28679
RARE EARTH ELEMENTS
Evaporation thermodynamics of monotellurides of selected rare Earth and alkaline Earth elements, and an attempt to systematic correlation between the standard enthalpies of formation
[ETN-89-94655] N89-29257
RATIONAL FUNCTIONS
On the classification of plane graphs representing structurally stable rational Newton-flows
[MEMO-750-REV] N89-28776
RAYLEIGH NUMBER
Numerical determination of guaranteed Rayleigh numbers and the pertaining flow forms in steady, axisymmetric convection in cylinders
[ETN-89-94432] N89-28769
REACTION KINETICS
A new method for monitoring cure and mobility in epoxy matrix and fiber/epoxy interphases
[AD-A209428] N89-28576
Reaction kinetics and mechanism of chain reactions and explosions via transient spectroscopy
[AD-A209169] N89-28597
The analysis of solvent effects on the kinetics of simple heterogeneous electron transfer reactions
[AD-A210078] N89-28602
Oxidative addition of C-H bonds in organic molecules to transition metal centers
[DE89-012991] N89-28616
Modeling of hot fragment conductive ignition of solid propellants with application to melting and evaporation of solids
[AD-A207727] N89-28662
Hypersonic vehicle environment simulation, phase 1
[AD-A209030] N89-28754
Numerical solution of ill posed problems in partial differential equations
[AD-A207852] N89-29119
La Recherche Aerospatiale, bimonthly bulletin, number 1988-6
[ESA-TT-1165] N89-29301
REACTION TIME
A study of the effect of stimulus upon the reflex response as elicited and recorded by the tympanic membrane displacement measurement device
[ISVR-TR-177] N89-29018
REACTIVITY
A new method for monitoring cure and mobility in epoxy matrix and fiber/epoxy interphases
[AD-A209428] N89-28576
Multicomponent e-beam resists containing organometallic compounds and reactive monomers
[AD-A207716] N89-28606
Reactive ion etching of polymer films
[AD-A207674] N89-28645
Quantitative analysis of laser interferometer waveforms obtained during oxygen reactive-ion etching of thin polymer films
[AD-A207836] N89-29248
READ-ONLY MEMORY DEVICES
Optical laser technology and its application to Defense Manpower Data Center's (DMDC) querry facsimile (QFAX) data base system
[AD-A207832] N89-29194
Moving optical technology in-house
[AD-A207850] N89-29266
REAL GASES
Effects of real gas in hypersonic expansion
[ETN-89-95200] N89-28783
REAL TIME OPERATION
Nonfilm radiography at the Oak Ridge Y-12 Plant
[DE89-014523] N89-28852
A satellite assisted-tracking system with real-time accommodation for maximal pointing N89-28885
JPRS Report: Science and Technology. USSR: Space. 16th International Congress of the International Society for Photogrammetry and Remote Sensing, volume 2
[JPRS-USP-89-003-VOL-2] N89-28903
Real time SAR processing techniques N89-28911
A real time microcomputer implementation of sensor failure detection for turbofan engines
[NASA-TM-102327] N89-29032
Software technology to support real-time embedded artificial intelligence-based applications, phase 1
[AD-A209133] N89-29042
Walkthrough-exploring virtual worlds
[AD-A208087] N89-29057
A static load distribution strategy for processor tools
[MEMO-INF-88-43] N89-29078
Real-time applications of neural nets
[DE89-014400] N89-29093
Northeast artificial intelligence consortium annual report 1987. Volume 9: Computer architectures for very large knowledge bases
[AD-A209454] N89-29096
Strategic defense system distributed operating system R and D review and recommendations
[AD-A208034] N89-29145
Realtime tracking system for the wide-field-of-view telescope project
[DE89-013787] N89-29186
REATTACHED FLOW
Calculation of reattaching shear layers in divergent channel with a multiple-time-scale turbulence model
[NASA-TM-102293] N89-28749
RECEIVERS
Design, performance and test standards for flight termination receiver/decoders. Volume 1: Design and performance requirements
[AD-A209644] N89-28544
RECONSTRUCTION
Three dimensional reconstruction from serial cross sections by set valued interpolation
[MEMO-754] N89-29076
RECORDING
The copy of single beam holograms
[ISL-CO-212/88] N89-28802
RED GIANT STARS
Red giants in open clusters. 1: Binarity and stellar evolution in five Hyades-generation clusters, NGC 2447, 2539, 2632, 6633 and 6940
[SER-C-PREPUBL-FASC-37-PT-1] N89-29290
Red giants in open clusters. 2: Orbits of ten spectroscopic binaries in NGC 2360, 2437, 2447, 5822, 5823, 6475
[SER-C-PREPUBL-FASC-38-PT-2] N89-29291
REDUCED GRAVITY
COLD-SAT: Cryogenic On-Orbit Liquid Depot-Storage, Acquisition and Transfer
[NASA-TM-102308] N89-28535
Tolerable g-level for fluid science experiments --- in space platforms
[TS-7-87] N89-28667
Hollow fiber clinostat: Technical abstract
[NASA-CASE-MFS-28370-1] N89-28793
Muscle changes with eccentric exercise: Implications on earth and in space
[NASA-TM-102227] N89-29016
REDUNDANCY
A partitioning and redundancy model for wafer scale integrated circuits
[MEMO-INF-88-65] N89-28730
REDUNDANT COMPONENTS
An experimental optical coupling device for an airborne digital redundant system
[NAL-TR-1003] N89-28514
REFRACTIVITY
Measurements and modelling of thin silicon dioxide films on silicon
[AD-A207853] N89-28720
Wind profile estimation from point to point laser distortion data
[NASA-CR-185891] N89-28990
Propagation problem and far-field patterns in a stratified finite depth ocean
[PB89-180707] N89-29001
REGENERATION (PHYSIOLOGY)
Method and apparatus for bio-regenerative life support system
[NASA-CASE-MSC-21629-1] N89-29027
REGENERATIVE COOLING
Analysis of the regenerative cooling of a rocket motor fed with monomethylhydrazine and nitrogen tetroxide
[ETN-89-94976] N89-28569
RELATIVISTIC EFFECTS
Electric quadrupole excitations in relativistic nucleus-nucleus collisions N89-29164
Electric quadrupole excitations in the interactions of Y-89 with relativistic nuclei N89-29165
Nucleon emission via electromagnetic excitation in relativistic nucleus-nucleus collisions: Re-analysis of the Weizsacker-Williams method N89-29166
RELATIVISTIC ELECTRON BEAMS
Microwave emission from relativistic electron beams
[AD-A209653] N89-29181
RELATIVITY
Fifth force, sixth force and all that: A theoretical (classical) comment
[DE89-611971] N89-29254

RELIABILITY
Reliability estimates for large satellite memories in low earth orbits
[DE89-007764] N89-28555
Composite material repair and reliability
[AD-A209150] N89-28574
United States Air Force Research Initiation Program for 1987, volume 2
[AD-A209727] N89-29259
RELIABILITY ANALYSIS
Minimization of Boolean sum of products with applications to the computation of reliability of general networks
[VTT-RR-571] N89-29136
RELIABILITY ENGINEERING
An experimental optical coupling device for an airborne digital redundant system
[NAL-TR-1003] N89-28514
Estimation of some stochastic models used in reliability engineering
[VTT-RR-598] N89-28855
RELIC RADIATION
Cosmic relics from the big bang
[DE89-013268] N89-29283
REMOTE REGIONS
Design of a command, communications, and control van (surrogate)
[AD-A207652] N89-28687
REMOTE SENSING
A medium resolution imaging spectrometer for the European polar orbiting platform
[ETN-89-95235] N89-28563
The Brazilian experience in handling 15 years of remote sensing satellite data N89-28905
Study of an advanced civil earth remote sensing system: Executive summary
[PB89-163206] N89-28922
Three-dimensional computer analysis and modelling of remote sensing-structural geologic problems
[DE89-010875] N89-28924
Identification of irrigated areas in the Sao Francisco Valley through remote sensing data. Pilot area: Petrolina-Juazeiro
[INPE-4800-RPE/587] N89-28925
Methods for analyzing SAR images
[VTT-RR-612] N89-28932
The use of expert systems for preprocessing image data
[NLR-MP-88009-U] N89-28934
Improvement of classification results of satellite imagery using context information from a topographic map
[NLR-MP-88020-U] N89-28935
Updating land-use information on topographic maps using satellite imagery: Combining the advantages of two accessible sources of geographic information
[NLR-MP-88030-U] N89-28936
Monitoring and measuring human settlement changes by remote sensing methods
[BCRS-88-16C] N89-28937
Training Course for Tropical Earth Resources Satellite (EARS) bridging phase
[BCRS-88-16D] N89-28938
Marketing and case study of satellite thematic maps and other products of satellite remote sensing
[BCRS-55-16E] N89-28939
Atmospheric influence on microwave remote sensing at different frequencies: Results of the 1st September 1987 DUSCAT flight
[BCRS-89-07] N89-28941
Wind profile estimation from point to point laser distortion data
[NASA-CR-185891] N89-28990
REMOTE SENSORS
Tactile sensing and the photoelastic tactile sensor
[OUEL-1758/89] N89-28849
ESA's activities and plans for remote sensing data systems N89-28906
Military hydrology: Assessment of shuttle imaging radar and LANDSAT imagery for ground-water exploration in arid environments
[AD-A209527] N89-28928
REPRODUCTION (COPYING)
The copy of single beam holograms
[ISL-CO-212/88] N89-28802
REQUIREMENTS
Information requirements and the implications for parallel computation
[AD-A207802] N89-29088
RESEARCH
United States Air Force Research Initiation Program for 1987, volume 2
[AD-A209727] N89-29259
RESEARCH AND DEVELOPMENT
Activities report in aerospace research in Germany, F.R.
[ISSN-0070-3966] N89-28485
Activities report of the Institute of Space Research
[ILR-1986/87] N89-28536
La Recherche Aerospatiale, bimontly bulletin, number 1988-3
[ESA-TT-1137] N89-28781
Solar thermal program summary. Volume 2: Research summaries, fiscal year 1988
[DE89-000861] N89-28947
The WMO research and development program 1988-1997: Second WMO long-term plan, part 2, volume 3
[WMO-693-PT-2-VOL-3] N89-28997
The WMO applications of meteorology program 1988-1997: Second WMO long-term plan, part 2, volume 4
[WMO-694-PT-2-VOL-4] N89-28998
Departments of Veterans Affairs and Housing and Urban Development and independent agencies appropriations for 1990. Part 6: National Aeronautics and Space Administration
[GPO-99-598] N89-29273
RESEARCH MANAGEMENT
Proceedings of a RAND Workshop on Antiproton Science and Technology
[AD-A208168] N89-29172
RESIDENTIAL AREAS
Characterization of painted surfaces in the United States from the perspective of potential damage from acidic deposition
[DE89-014264] N89-28965
RESIDUAL STRESS
On the large-eddy simulation of transitional wall-bounded flows
[NASA-CR-181883] N89-28763
Comparison of peel and lap shear bond strengths for elastic joints with and without residual stresses
[AD-A208102] N89-28867
RESIN BONDING
High temperature adhesive systems
[AD-A209166] N89-28643
RESINS
Emerging resin characterization
[AD-A208173] N89-28649
Study and simulation of an E-beam microlithography process on a multilayer resin structure. Research of an optimization
[LAAS-89.012] N89-29179
RESOLUTION
Television monitor field shifter and an opto-electronic method for obtaining a stereo image of optimal depth resolution and reduced depth distortion on a single screen
[NASA-CASE-NPO-17249-1-CU] N89-28676
RESONANT FREQUENCIES
Residual vibration reduction in computer controlled machines
[AD-A208074] N89-28866
RESONATORS
Method and circuit for shaping laser output pulses
[NASA-CASE-LAR-14203-1] N89-28817
RESOURCE ALLOCATION
BM/C(3) algorithm mapping onto concurrent processors
[AD-A207877] N89-29052
A static load distribution strategy for processor tools
[MEMO-INF-88-43] N89-29078
REUSABLE SPACECRAFT
Buran flight testing, capabilities discussed N89-28529
Development, testing procedures for Buran shuttle N89-28531
REUSE
An object-oriented software reuse tool
[AD-A208018] N89-29056
REVERSE FIELD PINCH
A three-dimensional resistive MHD simulation analysis of field reversal control in the reversed field pinch
[IPPJ-904] N89-29210
REVERSED FLOW
Reversal electron attachment ionizer for detection of trace species
[NASA-CASE-NPO-17596-1-CU] N89-28795
REYNOLDS STRESS
Rapidly distorted compressible boundary-layers N89-28735
Review of turbulence data --- for turbulent compressible boundary layers N89-28744
RHENIUM
Infrared study of carbon deposits on catalysts
[DE89-013310] N89-28634
RHEOLOGY
A graph-theoretical approach to block-co-polymer complexes. Part 1: Stars
[MEMO-757-PT-1] N89-28654
A graph-theoretical approach to block-co-polymer complexes. Part 2: Tree approximation
[MEMO-758-PT-2] N89-28655
RIEMANN MANIFOLD
On the Riemannian curvature of a twistor space
[DE89-611897] N89-29107
RING CURRENTS
Method of mass producing superconducting persistent current rings
[AD-D013968] N89-29219
RISK
Risk management for air ambulance helicopters operators
[DOT/FAA/DS-88/7] N89-28506
RITZ AVERAGING METHOD
Numerical determination of guaranteed Rayleigh numbers and the pertaining flow forms in steady, axisymmetric convection in cylinders
[ETN-89-94432] N89-28769
ROBOTICS
Intelligent multi-sensor integrations
[NASA-CR-185846] N89-28562
Robotic grasping of unknown objects: A knowledge-based approach
[DE89-013875] N89-28833
Advanced robotics for Air Force operations
[AD-A210098] N89-28840
Tactile sensing and the photoelastic tactile sensor
[OUEL-1758/89] N89-28849
ROBOTS
Robotic grasping of unknown objects: A knowledge-based approach
[DE89-013875] N89-28833
Advanced robotics for Air Force operations
[AD-A210098] N89-28840
Robust high-performance control for robotic manipulators
[NASA-CASE-NPO-17785-1-CU] N89-28846
Development and implementation of an on-line multivariable control algorithm for the force control of an industrial robot
[OUEL-1748/88] N89-28848
A robot that walks: Emergent behaviors from a carefully evolved network
[AD-A207958] N89-29026
ROCKET ENGINE CASES
Technical Evaluation Motor 3 (TEM-3)
[NASA-CR-183740] N89-28567
Static and dynamic deflection studies of the SRM aft case-nozzle joint
[NASA-TM-100373] N89-28568
ROCKET ENGINE DESIGN
Analysis of the regenerative cooling of a rocket motor fed with monomethylhydrazine and nitrogen tetroxide
[ETN-89-94976] N89-28569
ROCKET FIRING
Igniter heater EMI transient test
[NASA-CR-183743] N89-28566
ROCKET NOZZLES
Technical Evaluation Motor 3 (TEM-3)
[NASA-CR-183740] N89-28567
ROCKS
Development of borehole scanner for underground geological survey N89-28899
RODS
The angles of the Kolibrie rotor tipvanes on the rods and on the blades
[IW-R515] N89-28499
Nonlinear stability in fluid and plasma dynamics
[AD-A207715] N89-29203
ROTARY STABILITY
Nonlinear stability in fluid and plasma dynamics
[AD-A207715] N89-29203
ROTARY WINGS
Correlation of Puma airloads: Evaluation of CFD prediction methods
[NASA-TM-102226] N89-28498
Noise produced by turbulent flow into a rotor: Users manual for noise calculation
[NASA-CR-181790] N89-29152
ROTATING DISKS
A nonlinear investigation of the stationary modes of instability of the three-dimensional compressible boundary layer due to a rotating disc
[NASA-CR-181901] N89-28766
ROTATING FLUIDS
Measurements of the dipolar velocity of superfluid 3 He-B
[PB89-155444] N89-29218
ROTATING PLASMAS
Full consistent analysis of high beta steady state tokamaks sustained by beam driven and bootstrap currents
[IPPJ-912] N89-29212

On the spoke structure in critical velocity rotating plasmas
[TRITA-EPP-89-01] N89-29217
ROTATION
Hollow fiber clinostat: Technical abstract
[NASA-CASE-MFS-28370-1] N89-28793
ROTOR AERODYNAMICS
The angles of the Kolibrie rotor tipvanes on the rods and on the blades
[IW-R515] N89-28499
ROTOR BLADES
The angles of the Kolibrie rotor tipvanes on the rods and on the blades
[IW-R515] N89-28499
Statistics on aircraft gas turbine engine rotor failures that occurred in US commercial aviation during 1984
[NAPC-PE-185] N89-28516
Statistics on aircraft gas turbine engine rotor failures that occurred in US commercial aviation during 1985
[NAPC-PE-188] N89-28517
ROTOR BLADES (TURBOMACHINERY)
A compressible inverse design method based on an analytical approach
[CUED/A-TURBO/TR-125] N89-28778
ROTORS
Statistics on aircraft gas turbine engine rotor failures that occurred in US commercial aviation during 1984
[NAPC-PE-185] N89-28516
Statistics on aircraft gas turbine engine rotor failures that occurred in US commercial aviation during 1985
[NAPC-PE-188] N89-28517
Turbomachinery rotor support with damping
[NASA-CASE-MFS-28345-1] N89-28841
Noise produced by turbulent flow into a rotor: Users manual for atmospheric turbulence prediction and mean flow and turbulence contraction prediction
[NASA-CR-181791] N89-29154
RUBBER
Pull-out and push-out tests for rubber-to-metal adhesion
[AD-A208100] N89-28847
RUNGE-KUTTA METHOD
A necessary condition for B-convergence of Runge-Kutta methods
[TW-89-01] N89-29129
RUNWAYS
Joint sealants for airport pavements. Phase 1: Laboratory and field investigations
[DOT/FAA/DS-89/2-PHASE-1] N89-28523
European crosswind frequencies
[AD-A209137] N89-28985

S

SAFETY MANAGEMENT
Risk management for air ambulance helicopters operators
[DOT/FAA/DS-88/7] N89-28506
SAMARIUM COMPOUNDS
Non-uniform transition conductivity of superconducting ceramic
[NASA-TM-102133] N89-28851
SAMPLERS
Study of sampling systems for comets and Mars
[NASA-CR-185514] N89-29292
SAMPLING
Digital carrier demodulator employing components working beyond normal limits
[NASA-CASE-NPO-17628-1-CU] N89-28684
Positioning error induced by axial sampling in positron emission tomography
[DE89-014519] N89-28791
SANDWICH STRUCTURES
Optimum design methods for structural sandwich panels
[AD-A209427] N89-28575
SATELLITE ALTIMETRY
Results of Seasat altimeter data processing for the northeast Atlantic
[BCRS-89-05] N89-28940
SATELLITE ATTITUDE CONTROL
Consideration of gravity gradient stabilization for ORION
[AD-A207845] N89-28557
SATELLITE IMAGERY
JPRS Report: Science and Technology. USSR: Space. 16th International Congress of the International Society for Photogrammetry and Remote Sensing, volume 1
[JPRS-USP-89-002-VOL-1] N89-28876
High resolution Soviet space photographs for topographic mapping N89-28892
An expert system for satellite image interpretation and G.I.S. based problem solving N89-28894
National report of Polish Society of Photogrammetry and Remote Sensing N89-28895
A comparison between the variability structure of the remotely sensed sea-surface temperature and pigment distributions N89-28896
A study on information analysis aids for sea surface temperature image data N89-28897
JPRS Report: Science and Technology. USSR: Space. 16th International Congress of the International Society for Photogrammetry and Remote Sensing, volume 2
[JPRS-USP-89-003-VOL-2] N89-28903
The possibilities of application of satellite data for monitoring ice condition in the Antarctic region N89-28907
National program for handling large volumes of satellite data N89-28910
The new generation SPOT satellites SPOT 4 and 5 N89-28914
Design aspects of a system for geocoding satellite SAR images N89-28915
The processing of SPOT imagery in Brazil N89-28917
Ocean remote sensing and modeling
[AD-A208406] N89-28927
Military hydrology: Assessment of shuttle imaging radar and LANDSAT imagery for ground-water exploration in arid environments
[AD-A209527] N89-28928
Integrating satellite data with information from topographic maps: Method and applications — SPOT
[NLR-MP-87035-U] N89-28933
Improvement of classification results of satellite imagery using context information from a topographic map
[NLR-MP-88020-U] N89-28935
Monitoring and measuring human settlement changes by remote sensing methods
[BCRS-88-16C] N89-28937
Training Course for Tropical Earth Resources Satellite (EARS) bridging phase
[BCRS-88-16D] N89-28938
SATELLITE OBSERVATION
A medium resolution imaging spectrometer for the European polar orbiting platform
[ETN-89-95235] N89-28563
Investigation of the effectiveness and applications of Japanese ERS-1 stereoscopic images N89-28884
The possibilities of application of satellite data for monitoring ice condition in the Antarctic region N89-28907
Satellite-derived moisture-bogusing profiles for the North Atlantic Ocean
[AD-A207829] N89-28930
Errors in the scene identification from satellite data. Effects on the determination of radiation budget parameters
[MITT-59] N89-28931
Satellite enhanced numerical weather prediction
[AD-A210108] N89-28987
SATELLITE ORBITS
Reliability estimates for large satellite memories in low earth orbits
[DE89-007764] N89-28555
SATELLITE TRACKING
A satellite assisted-tracking system with real-time accommodation for maximal pointing N89-28885
SATELLITE-BORNE INSTRUMENTS
Outline of MOS-1 Verification Program (MVP) N89-28883
Data processing and calibration of SAR data in Japan N89-28918
Earth observation programs in Japan N89-28920
SATELLITE-BORNE PHOTOGRAPHY
Military hydrology: Assessment of shuttle imaging radar and LANDSAT imagery for ground-water exploration in arid environments
[AD-A209527] N89-28928
Preliminary neural network detection of a gulf stream in images of sea surface temperature gradients, phase 1
[AD-A207801] N89-29003
SCALE MODELS
Small scale model tests in small wind and water tunnels at high incidence and pitch rates. Volume 1: Test program and discussion of results
[AD-A208647] N89-28488
SCALING LAWS
Near-neighbor algorithms for processing bearing data
[AD-A207935] N89-29053
SCANNERS
Radiothermoluminescence studies of polymer solids
[AD-A209036] N89-28641
Studies on object reconstruction from space using three line scanner imagery N89-28919
SCATTERING
An optical model description of momentum transfer in heavy ion collisions N89-29162
SCATTERING AMPLITUDE
Approximation methods for scattering from rough surfaces
[AD-A209462] N89-29192
A new scattering formula for depth-resolving X-ray diffractometry based on a kinematic theory
[ETN-89-94430] N89-29195
SCATTERING CROSS SECTIONS
Molecular beam experiment for the determination of differential cross sections of the reaction of deuterium atoms with vibrationally excited hydrogen molecules
[MPIS-10/1988] N89-29178
Evolution of wide binary millisecond pulsars in globular clusters
[MPE-PREPRINT-148] N89-29285
SCAVENGING
The scavenging of atmospheric pollutants by clouds and precipitation using a vertical wind tunnel, phase 1
[BPT-9/88] N89-28525
SCENE ANALYSIS
Errors in the scene identification from satellite data. Effects on the determination of radiation budget parameters
[MITT-59] N89-28931
SCHEDULING
A manufacturing scheduler's perspective on semiconductor fabrication
[AD-A208372] N89-29232
Calendar of selected aeronautical and space meetings
[AGARD-CAL-89/2] N89-29261
SCHOTTKY DIODES
VLSI integrated circuit contact reliability by interface spectroscopy
[AD-A207666] N89-28718
SCHUMANN-RUNGE BANDS
Aeronomic problems of molecular oxygen photodissociation. 5: Predissociation in the Schumman-Runge Bands of Oxygen
[AERONOMICA-ACTA-A-341-1989-5] N89-28980
Aeronomic problems of molecular oxygen photodissociation. 6: Photodissociation frequency and transmittance in the spectral range of the Schumman-Runge bands
[AERONOMICA-ACTA-A-342-1989-6] N89-28981
SEA ICE
Exact image theory for uniaxially anisotropic dielectric half space
[PB89-146450] N89-28671
The possibilities of application of satellite data for monitoring ice condition in the Antarctic region N89-28907
SEA STATES
Lidar measurements of sea surface waves N89-28909
SEA SURFACE TEMPERATURE
A comparison between the variability structure of the remotely sensed sea-surface temperature and pigment distributions N89-28896
A study on information analysis aids for sea surface temperature image data N89-28897
Ocean remote sensing and modeling
[AD-A208406] N89-28927
Preliminary neural network detection of a gulf stream in images of sea surface temperature gradients, phase 1
[AD-A207801] N89-29003
SEA TRUTH
Sea gravimetry and Eotvos correction
[REPT-88.3] N89-29006
SEALERS
Joint sealants for airport pavements. Phase 1: Laboratory and field investigations
[DOT/FAA/DS-89/2-PHASE-1] N89-28523
SEALING
O-ring gasket test fixture
[NASA-CASE-MFS-28376-1] N89-28546
High temperature flexible seal
[NASA-CASE-LEW-14695-1] N89-28830
SEALS (STOPPERS)
High temperature flexible seal
[NASA-CASE-LEW-14695-1] N89-28830
Turbomachinery rotor support with damping
[NASA-CASE-MFS-28345-1] N89-28841
SEAMS (JOINTS)
Joint sealants for airport pavements. Phase 1: Laboratory and field investigations
[DOT/FAA/DS-89/2-PHASE-1] N89-28523
SEASAT PROGRAM
Results of Seasat altimeter data processing for the northeast Atlantic
[BCRS-89-05] N89-28940
SEASAT SATELLITES
Methods for analyzing SAR images
[VTT-RR-612] N89-28932

SECURITY
International technology transfer as practiced by the U.S.S.R.: Implications for US national security
[AD-A208010] N89-29274
SELECTION
Choice and perceived control: Implications for the design of displays
[AD-A208400] N89-29021
SELECTIVE SURFACES
Development of a carbonaceous selective absorber for solar thermal energy collection and process for its formation
[DE89-008587] N89-28949
SELF CONSISTENT FIELDS
A survey of self-consistency properties in cooperative game theory
[MEMO-763] N89-29072
SELF FOCUSING
Slotted-waveguide amplifiers for millimeter waves
[AD-A207932] N89-28721
SEMANTICS
The application of constraints in query optimization
[MEMO-INF-88-55] N89-29079
SEMICONDUCTING FILMS
Primary research efforts on exploring the commercial possibilities of thin film growth and materials purification in space
[NASA-CR-184913] N89-28541
Thermodynamically stable conducting films of intermetallic PtGa2 on gallium arsenide
[AD-A210077] N89-28716
Multilayered electronic materials and devices based on 3-5 compounds
[AD-A208861] N89-29233
Selective area epitaxy of gallium arsenide on silicon, phase 1
[AD-A209079] N89-29238
SEMICONDUCTOR DEVICES
A manufacturing scheduler's perspective on semiconductor fabrication
[AD-A208372] N89-29232
SEMICONDUCTOR DIODES
Laser-induced diode linking for wafer-scale integration
[AD-A207921] N89-28818
SEMICONDUCTOR LASERS
Field induced gap infrared detector
[NASA-CASE-NPO-17526-1-CU] N89-28796
AlGaAs phased array laser for optical communications
[NASA-CR-181869] N89-28820
Monolithic narrow-linewidth InGaAsP semiconductor laser for coherent optical communications
[NASA-CR-181870] N89-28821
SEMICONDUCTORS (MATERIALS)
Preparation of compounds with the tetrahedral structure which transmit in the far infrared
[AD-A208697] N89-28593
Thermodynamically stable conducting films of intermetallic PtGa2 on gallium arsenide
[AD-A210077] N89-28716
VLSI integrated circuit contact reliability by interface spectroscopy
[AD-A207666] N89-28718
Thin film photovoltaics
[DE89-009425] N89-28956
A manufacturing scheduler's perspective on semiconductor fabrication
[AD-A208372] N89-29232
Crystal chemistry, magnetic and electrical properties of La(sub2-x)Ba(subx)NiO4
[AD-A209376] N89-29240
Initial stages of metal/semiconductor interface formation: Au and AgON Si(111)
[AD-A209490] N89-29245
SENSITIVITY
Molecular weight dependence of e-beam resist sensitivity
[AD-A207835] N89-28719
SEPARATED FLOW
Analysis of leading edge separation using a low order panel method
[NASA-CR-185892] N89-28493
SEPARATORS
Higee Technology Development Program, phase 1
[PB89-161434] N89-28587
SERIES (MATHEMATICS)
Three dimensional reconstruction from serial cross sections by set valued interpolation
[MEMO-754] N89-29076
Placing the largest similar copy of a convex polygon among polygonal obstacles
[AD-A210104] N89-29115
SERVICE LIFE
Effect of environmental factors on pavement deterioration. Volume 1: Background and methodology
[PB89-182109] N89-28668
Accelerated life evaluation of valve-regulated lead-acid batteries
[DE89-012429] N89-28710
Heat-transfer and friction factor design data for all-metal compact heat exchangers
[AD-A208108] N89-28761
Damage predictions for wind turbine components using the LIFE2 computer code
[DE89-013813] N89-28952
Computer-aided group problem solving for Unified Life Cycle Engineering (ULCE)
[AD-A209446] N89-29260
SET THEORY
Three dimensional reconstruction from serial cross sections by set valued interpolation
[MEMO-754] N89-29076
The communication complexity of interval orders
[MEMO-745] N89-29102
SHAFTS (MACHINE ELEMENTS)
Turbomachinery shaft insert
[NASA-CASE-MFS-28345-2] N89-28842
SHAPE CONTROL
Method and circuit for shaping laser output pulses
[NASA-CASE-LAR-14203-1] N89-28817
SHAPES
Three dimensional reconstruction from serial cross sections by set valued interpolation
[MEMO-754] N89-29076
The problem of selecting the shape functions for a p-type finite element
[AD-A207798] N89-29117
SHEAR FLOW
Entrainment and homogenization of a passive tracer in a numerical model gyre
[AD-A208020] N89-29005
SHEAR LAYERS
Calculation of reattaching shear layers in divergent channel with a multiple-time-scale turbulence model
[NASA-TM-102293] N89-28749
Adiabatic shear bands in one dimension
[AD-A208105] N89-28868
SHEAR PROPERTIES
Adiabatic shear bands in one dimension
[AD-A208105] N89-28868
SHEAR STRAIN
A test system for thermomechanical fatigue of solder joints
[DE89-013886] N89-28860
SHEAR STRENGTH
Comparison of peel and lap shear bond strengths for elastic joints with and without residual stresses
[AD-A208102] N89-28867
SHEAR STRESS
Delamination test apparatus and method
[NASA-CASE-LAR-13985-1] N89-28586
Skin-friction measurements by laser interferometry N89-28737
General comments on the interpretation of data --- mean flow for rapidly distorted turbulent boundarylayers N89-28742
Review of turbulence data --- for turbulent compressible boundary layers N89-28744
SHOCK LOADS
On strain gages using the PVF2 piezoelectric polymer
[ISL-CO-210/88] N89-28801
SHOCK MEASURING INSTRUMENTS
On strain gages using the PVF2 piezoelectric polymer
[ISL-CO-210/88] N89-28801
SHOCK WAVE INTERACTION
Fluctuating wall-pressure measurements N89-28741
Review of mean flow data --- for compressible boundary layers N89-28743
Review of turbulence data --- for turbulent compressible boundary layers N89-28744
The entries N89-28745
SHOCK WAVES
The PVF2 piezoelectric polymer shock stress sensor: System characterization for application under field test conditions
[DE89-014629] N89-28790
Solution of the hydrodynamic device model using high-order non-oscillatory shock capturing algorithms
[NASA-CR-181886] N89-29123
SHORT WAVE RADIO TRANSMISSION
Development of an integrated AM shortwave upconversion receiver front-end
[ETN-89-95455] N89-28699
SHUTTLE IMAGING RADAR
Military hydrology: Assessment of shuttle imaging radar and LANDSAT imagery for ground-water exploration in arid environments
[AD-A209527] N89-28928
SIDE-LOOKING RADAR
Application of aerial side-looking radar imagery in China N89-28902
Sea spectra as determined from low-altitude SLAR images N89-28908
SIDELOBES
Reciprocal perfect and asymptotically perfect periodic radar waveforms and their aperiodic properties
[AD-A208938] N89-28677
SIGNAL DETECTION
Adaptive detection and parameter estimation for multidimensional signal models
[AD-A208971] N89-28678
Microwave detection using Josephson elements
[ETN-89-94650] N89-29252
SIGNAL PROCESSING
Digital carrier demodulator employing components working beyond normal limits
[NASA-CASE-NPO-17628-1-CU] N89-28684
Two-dimensional signal processing and storage and theory and applications of electromagnetic measurements
[AD-A207827] N89-28689
The airborne pulse Doppler radar: An introduction to the basic principles --- surveillance radar analysis
[BAE-WAA-RP-GEN-RAD-584] N89-28696
Multitarget tracking by single sensor analysis of the main approaches developed in this area
[ONERA-NT-1988-10] N89-28702
Electrical characterization of signal processing microcircuit
[AD-A209078] N89-28714
Optical properties and error sources of an airborne radiometer
[MITT-60] N89-28799
Nearfield acoustic holography: Review and perspectives
[ISVR-TR-179] N89-28807
Vibration analyzer
[NASA-CASE-MSC-21408-1] N89-28829
A Bistatic Parasitical Radar (BIPAR) N89-28878
Real time SAR processing techniques N89-28911
Storm models for end-to-end TDWR (Terminal Doppler Weather Radar) signal processing simulation tests
[AD-A209384] N89-28986
Bit rate recovery using digital ladder networks
[AD-A209865] N89-29043
Fiber optic frequency transfer link
[NASA-CASE-NPO-17703-1-CU] N89-29191
SIGNAL TO NOISE RATIOS
Bit rate recovery using digital ladder networks
[AD-A209865] N89-29043
SIGNATURE ANALYSIS
An a priori approach to the evaluation of signature analysis efficiency
[IMAG-RR-746-I] N89-29140
SILICON
Fundamental aspects of reactions in titanium-silicon thin films for integrated circuits
[ETN-89-95466] N89-28733
Laser-induced diode linking for wafer-scale integration
[AD-A207921] N89-28818
Investigations of step distributions at Si/SiO2 interfaces using HR-SPA-LEED
[ETN-89-94437] N89-29251
SILICON CARBIDES
Highly oriented fiber reinforced ceramic composites
[AD-A208119] N89-28578
SILICON DIOXIDE
Monolayers of 11-trichlorosilylundecyl thioacetate: A system that promotes adhesion between silicon dioxide and evaporated gold
[AD-A208266] N89-28637
Measurements and modelling of thin silicon dioxide films on silicon
[AD-A207853] N89-28720
Selective area epitaxy of gallium arsenide on silicon, phase 1
[AD-A209079] N89-29238
Investigations of step distributions at Si/SiO2 interfaces using HR-SPA-LEED
[ETN-89-94437] N89-29251
SILICON FILMS
Measurements and modelling of thin silicon dioxide films on silicon
[AD-A207853] N89-28720
SILICON NITRIDES
Ion implantation of ceramic bearings
[AD-A209770] N89-29644
SILICON OXIDES
Research on stable, high-efficiency, large-area, amorphous-silicon-based submodules, task B
[DE89-009439] N89-28946
SILICON RADIATION DETECTORS
Development of a novel silicon detector with internal amplification
[MPI-PAE/EXP.EL-197] N89-28798

SIMILARITY THEOREM
Application of similarity methods to the turbulent diffusion in the convective and stable boundary layer
[WISS-BER-12] N89-28979
SIMULATION
A methodology for modeling radar detection range in air combat simulation
[AD-A209153] N89-28679
Simulation of ERS-1/OPS by the use of airborne spectroradiometer N89-28912
Estimation of the simulated JERS-1 data N89-28921
Parallel electric fields in a simulation of magnetotail reconnection and plasmoid evolution
[DE89-012822] N89-28970
Conditional dependence
[AD-A207881] N89-29120
Aircraft propeller induced structure-borne noise
[NASA-CR-4255] N89-29155
SIMULATORS
Development of damping treatment suitable for high temperature environment
[ISVR-TR-174] N89-28652
SINGLE CRYSTALS
Thermal conductivity anisotropy in single crystal YBa2Cu3O7-x
[DE89-009643] N89-29220
Lineshape and lifetime studies of exciton luminescence from confined CuCl thin films
[AD-A209750] N89-29243
SINGLE EVENT UPSETS
Reliability estimates for large satellite memories in low earth orbits
[DE89-007764] N89-28555
SINTERING
Highly oriented fiber reinforced ceramic composites
[AD-A208119] N89-28578
Freeze-dried tungsten heavy alloys
[DE89-014933] N89-28620
Microwave sintering of ceramics
[DE89-014769] N89-28636
SISO (CONTROL SYSTEMS)
Model simplification based on the concept of equivalent dead time
[NAL-TM-SE-8802] N89-28521
SIZE DETERMINATION
A graph-theoretical approach to block-co-polymer complexes. Part 1: Stars
[MEMO-757-PT-1] N89-28654
SKIN (ANATOMY)
Thermoregulatory competence during exercise transients in a group of heat-acclimated young and middle-aged men is influenced more distinctly by maximal aerobic power than age
[AD-A209753] N89-29009
SKIN FRICTION
Skin-friction measurements by laser interferometry N89-28737
SKY SURVEYS (ASTRONOMY)
A deep optical infrared survey
[AD-A207930] N89-29278
Activities report in international astronomy
[ETN-89-95333] N89-29281
SLEEP DEPRIVATION
Sleep deprivation and its effect on combat effectiveness
[AD-A207970] N89-29013
SLIDING FRICTION
The tribology of undulated surfaces
[AD-A209275] N89-28837
SLOPES
Numerical determination of the location of critical inclinations for long term high eccentricity orbits about Mars
[AD-A209200] N89-28536
SLOTS
Slotted-waveguide amplifiers for millimeter waves
[AD-A207932] N89-28721
SLURRIES
Pressure drop and heat transfer characteristics of nearly neutrally buoyant particulate slurry for advanced energy tranamission fluids
[DE89-013645] N89-28751
SNOW
Radiative transfer in falling snow: A two-stream approximation
[AD-A208960] N89-29187
SOFTWARE ENGINEERING
Zeiss Digital Mapping: A new hardware and software system concept from Kombinat VEB Carl Zeiss JENA N89-28891
Software technology to support real-time embedded artificial intelligence-based applications, phase 1
[AD-A209133] N89-29042
FREQ: A computational package for multivariable system loop-shaping procedures
[NASA-TM-4127] N89-29047
Software engineering with database management systems
[AD-A208167] N89-29060
APL conversion software
[MEMO-INF-88-21] N89-29062
A method of software development using functional programming
[MEMO-INF-88-64] N89-29069
SOFTWARE TOOLS
A microprogramming support tool for pipelined architectures
[AD-A208090] N89-29036
An object-oriented software reuse tool
[AD-A208018] N89-29056
Tools for the development and usage of industrial mathematical software
[NLR-MP-87020-U] N89-29067
Gauge: Its philosophy and design
[AD-A208944] N89-29083
Linear algebra support modules for approximation and other software
[NPL-DITC-142/89] N89-29126
Transfer of files between IE-32C PC/AT CAD system and Autotrol AD/380 graphics system
[PD-CC-8903] N89-29270
SOLAR ARRAYS
Field tests of a novel inverter for photovoltaic power conditioning
[DE89-014322] N89-28958
SOLAR CELLS
Materials analysis and device optimization of CuInSe2 solar cells
[DE89-009434] N89-28944
Polycrystalline cadmium telluride 3n-i-p solar cell
[DE89-009437] N89-28945
Research on stable, high-efficiency, large-area, amorphous-silicon-based submodules, task B
[DE89-009439] N89-28946
Photovoltaics advanced research and development
[DE89-000895] N89-28948
Two-terminal CuInSe-based cascade cells
[DE89-009422] N89-28950
SOLAR COLLECTORS
Development of a carbonaceous selective absorber for solar thermal energy collection and process for its formation
[DE89-008587] N89-28949
SOLAR ENERGY
Energy technology R and D: What could make a difference. A study by the staff of the Oak Ridge National Laboratory. Part 1: Synthesis report, volume 1
[DE89-014568] N89-28955
SOLAR ENERGY ABSORBERS
Development of a carbonaceous selective absorber for solar thermal energy collection and process for its formation
[DE89-008587] N89-28949
SOLAR ENERGY CONVERSION
Solar thermal program summary. Volume 2: Research summaries, fiscal year 1988
[DE89-000861] N89-28947
SOLAR FLUX
Solar spectral irradiances with their diversity between 120 and 900 nm
[AERONOMICA-ACTA-A-338-1989] N89-29294
SOLAR MESOSPHERE EXPLORER
Solar ultraviolet radiation within the middle atmosphere
[AERONOMICA-ACTA-A-337-1989] N89-29293
SOLAR NEUTRINOS
Measurement of solar proton-proton fusion neutrinos with a Soviet-American gallium experiment
[DE89-014563] N89-29168
SOLAR OBSERVATORIES
Coordination of Advanced Solar Observatory (ASO) Science Working Group (SWG) for the study of instrument accommodation and operational requirements on space station
[NASA-CR-185371] N89-28537
SOLAR PHYSICS
Measurement of solar proton-proton fusion neutrinos with a Soviet-American gallium experiment
[DE89-014563] N89-29168
SOLAR RADIATION
Solar ultraviolet radiation within the middle atmosphere
[AERONOMICA-ACTA-A-337-1989] N89-29293
SOLAR SPECTRA
A high-resolution atlas of the infrared spectrum of the sun and the earth atmosphere from space. A compilation of ATMOS spectra of the region from 650 to 4800 cm-1 (2.3 to 16 microns). Volume 2: Stratosphere and mesosphere, 650 to 3350 cm-1
[NASA-RP-1224-VOL-2] N89-28969
Solar spectral irradiances with their diversity between 120 and 900 nm
[AERONOMICA-ACTA-A-338-1989] N89-29294
SOLAR SYSTEM
Activities report of the Institute for Extraterrestrial Physics
[MPE-212] N89-29277
SOLAR TERRESTRIAL INTERACTIONS
Key data on participating projects. The solar-terrestrial science project of the Inter-Agency Consultative Group for Space Science (IACG)
[ESA-SP-1107] N89-29295
SOLAR THERMAL ELECTRIC POWER PLANTS
Solar thermal program summary. Volume 2: Research summaries, fiscal year 1988
[DE89-000861] N89-28947
SOLAR WIND
Electric fields in earth orbital space
[AD-A209542] N89-28973
SOLDERED JOINTS
A test system for thermomechanical fatigue of solder joints
[DE89-013886] N89-28860
SOLDERS
A test system for thermomechanical fatigue of solder joints
[DE89-013886] N89-28860
SOLID ELECTROLYTES
Use of microelectrode arrays to directly measure diffusion of ions in solid electrolytes: Proof of concept experiments involving Ag+ in a solid polymer electrolyte
[AD-A209536] N89-28604
Material and fabrication challenges in the development of monolithic solid oxide fuel cells
[DE89-012422] N89-28957
SOLID LUBRICANTS
Ion implantation of ceramic bearings
[AD-A209770] N89-28644
Solid lubrication studied by optical means
[AD-A209008] N89-28836
SOLID PROPELLANT IGNITION
Igniter heater EMI transient test
[NASA-CR-183743] N89-28566
SOLID PROPELLANT ROCKET ENGINES
Technical Evaluation Motor 3 (TEM-3)
[NASA-CR-183740] N89-28567
Static and dynamic deflection studies of the SRM aft case-nozzle joint
[NASA-TM-100373] N89-28568
SOLID PROPELLANTS
Modeling of hot fragment conductive ignition of solid propellants with application to melting and evaporation of solids
[AD-A207727] N89-28662
SOLID STATE LASERS
Improvements of the efficiency of solid state lasers by spectral conversion of the excitation lamp's output
[ETN-89-94425] N89-28622
SOLID-SOLID INTERFACES
A study of thermodynamic phase stability of intermetallic thin films of Pt2Ga, PtGa and PtGa2 on gallium arsenide
[AD-A209698] N89-29241
Investigations of step distributions at Si/SiO2 interfaces using HR-SPA-LEED
[ETN-89-94437] N89-29251
SOLIDS
Radiothermoluminescence studies of polymer solids
[AD-A209036] N89-28641
SOLITARY WAVES
Modelling, information, processing, and control
[AD-A207810] N89-28885
SOLUTIONS
Microcellular foams from rigid-rod polymers in solutions: Effect of aggregation characteristics on foam properties
[AD-A209024] N89-28640
SOLVATION
Ion-molecule chemistry within doubly charged ammonia clusters
[AD-A207764] N89-28608
SOLVENTS
Solvent effects on simple electron transfer reactions. A comparison of results for homogeneous and heterogeneous systems
[AD-A209381] N89-28600
The analysis of solvent effects on the kinetics of simple heterogeneous electron transfer reactions
[AD-A210078] N89-28602
SONAR
Adaptive detection and parameter estimation for multidimensional signal models
[AD-A208971] N89-28678
SOUND FIELDS
Propagation problem and far-field patterns in a stratified finite depth ocean
[PB89-180707] N89-29001

SOUND GENERATORS
Acoustic tests on a new motor generator system for the minuteman launch control centers in Hill engineering test facilities 1 and 2, Hill AFB, Utah
[AD-A209598] N89-28717
SOUND PRESSURE
A study of the effect of stimulus upon the reflex response as elicited and recorded by the tympanic membrane displacement measurement device
[ISVR-TR-177] N89-29018
SOUND TRANSMISSION
Aircraft propeller induced structure-borne noise
[NASA-CR-4255] N89-29155
SOUND WAVES
The inverse scattering problem for acoustic and electromagnetic waves
[AD-A209202] N89-28681
Nondestructive characterization of simple interfaces using volume sound waves
[ETCA-89-R-015] N89-28854
The measurement of SEA loss factors on a fully assembled structure
[ISVR-TR-150] N89-29157
SOUTHERN HEMISPHERE
The 1988 Antarctic ozone monitoring Nimbus-7 TOMS data atlas
[NASA-RP-1225] N89-28983
SOVIET SATELLITES
JPRS report: Science and technology. USSR report: Life sciences
[JPRS-USP-89-005] N89-28527
SOVIET SPACECRAFT
JPRS report: Science and technology. USSR report: Life sciences
[JPRS-USP-89-005] N89-28527
Buran flight testing, capabilities discussed N89-28529
Designers' commentary on Buran flight control system N89-28530
Development, testing procedures for Buran shuttle N89-28531
SPACE ADAPTATION SYNDROME
Visual suppression of the vestibulo-ocular reflex during space flight
[NASA-TM-102157] N89-29017
SPACE BASED RADAR
SAR activities at Dornier N89-28887
SPACE CHARGE
On the use of the FEL to produce high transient space-charge potentials in a magnetized plasma
[DE89-014325] N89-28814
Microwave emission from relativistic electron beams
[AD-A209653] N89-29181
SPACE COMMUNICATION
Design of a reliable computing system for the Petite Amateur Navy Satellite (PANSAT)
[AD-A208194] N89-28559
SPACE ERECTABLE STRUCTURES
Near-field testing of the 15-meter hoop-column antenna
[NASA-TM-4073] N89-28550
SPACE FLIGHT STRESS
Visual suppression of the vestibulo-ocular reflex during space flight
[NASA-TM-102157] N89-29017
SPACE MISSIONS
Advanced power sources for space missions
[NASA-TM-101811] N89-28565
SAR activities at Dornier N89-28887
SPACE PLATFORMS
Modelling orientation parameters of sensor platforms N89-28881
SPACE PROCESSING
Primary research efforts on exploring the commercial possibilities of thin film growth and materials purification in space
[NASA-CR-184913] N89-28541
SPACE PROGRAMS
Key data on participating projects. The solar-terrestrial science project of the Inter-Agency Consultative Group for Space Science (IACG)
[ESA-SP-1107] N89-29295
SPACE SHUTTLE BOOSTERS
General-purpose heat source development: Extended series test program SRB fragment/fuselage tests
[DE89-014389] N89-29180
SPACE SHUTTLE ORBITERS
General-purpose heat source development: Extended series test program SRB fragment/fuselage tests
[DE89-014389] N89-29180
SPACE SHUTTLE PAYLOADS
Coordination of Advanced Solar Observatory (ASO) Science Working Group (SWG) for the study of instrument accommodation and operational requirements on space station
[NASA-CR-185371] N89-28537
SPACE SHUTTLES
Docking mechanism for spacecraft
[NASA-CASE-MSC-21386-1] N89-28552
Static and dynamic deflection studies of the SRM aft case-nozzle joint
[NASA-TM-100373] N89-28568
Military hydrology: Assessment of shuttle imaging radar and LANDSAT imagery for ground-water exploration in arid environments
[AD-A209527] N89-28928
Spacecraft flight simulation: A human factors investigation into the man-machine interface between an astronaut and a spacecraft performing docking maneuvers and other proximity operations
[NASA-CR-177502] N89-29020
SPACE STATION POLAR PLATFORMS
A medium resolution imaging spectrometer for the European polar orbiting platform
[ETN-89-95235] N89-28563
ESA's activities and plans for remote sensing data systems N89-28906
SPACE STATION POWER SUPPLIES
Advanced power sources for space missions
[NASA-TM-101811] N89-28565
Evolutionary growth for Space Station Freedom electrical power system
[NASA-TM-102339] N89-28570
SPACE STATION STRUCTURES
Expandable pallet for space station interface attachments
[NASA-CASE-MSC-21117-2] N89-28554
SPACE STATIONS
Coordination of Advanced Solar Observatory (ASO) Science Working Group (SWG) for the study of instrument accommodation and operational requirements on space station
[NASA-CR-185371] N89-28537
Docking mechanism for spacecraft
[NASA-CASE-MSC-21386-1] N89-28552
Evolutionary growth for Space Station Freedom electrical power system
[NASA-TM-102339] N89-28570
Departments of Veterans Affairs and Housing and Urban Development and independent agencies appropriations for 1990. Part 6: National Aeronautics and Space Administration
[GPO-99-598] N89-29273
SPACE TRANSPORTATION SYSTEM
Departments of Veterans Affairs and Housing and Urban Development and independent agencies appropriations for 1990. Part 6: National Aeronautics and Space Administration
[GPO-99-598] N89-29273
SPACE WEAPONS
Advanced power sources for space missions
[NASA-TM-101811] N89-28565
SPACEBORNE ASTRONOMY
The orbital space observatory Gamma N89-28528
Solar spectral irradiances with their diversity between 120 and 900 nm
[AERONOMICA-ACTA-A-338-1989] N89-29294
SPACEBORNE EXPERIMENTS
Tolerable g-level for fluid science experiments --- in space platforms
[TS-7-87] N89-28667
SPACEBORNE PHOTOGRAPHY
Map production and revision with satellite photographs taken by the MKF-6 camera and by the cameras KATE-140, KATE-200, and KFA-1000 N89-28893
SPACEBORNE TELESCOPES
The orbital space observatory Gamma N89-28528
A conceptual study of optical earth observation from geosynchronous orbit N89-28880
SPACECRAFT COMPONENTS
Spacecraft component heater control system
[NASA-CASE-MFS-28327-1] N89-28556
SPACECRAFT CONSTRUCTION MATERIALS
Aluminum alloy
[NASA-CASE-LAR-13924-1-CU] N89-28621
Acoustic emission technology for space applications
[DE89-014449] N89-28861
SPACECRAFT CONTAMINATION
Laboratory investigations: Low earth orbit environment chemistry with spacecraft surfaces
[DE89-014280] N89-28533
SPACECRAFT CONTROL
Designers' commentary on Buran flight control system N89-28530
Active damping of vibration in large space structures using a Karhunen-Loeve reduced order model
[AD-A208183] N89-28558
SPACECRAFT DESIGN
Development, testing procedures for Buran shuttle N89-28531
Key structures mechanical issues of the European Space Station and platform program Columbus
[MBB-UD-0041-88-PUB] N89-28561
Evolutionary growth for Space Station Freedom electrical power system
[NASA-TM-102339] N89-28570
SPACECRAFT DOCKING
Docking mechanism for spacecraft
[NASA-CASE-MSC-21386-1] N89-28552
Space module assembly apparatus with docking alignment flexibility and restraint
[NASA-CASE-MSC-21211-1] N89-28553
Spacecraft flight simulation: A human factors investigation into the man-machine interface between an astronaut and a spacecraft performing docking maneuvers and other proximity operations
[NASA-CR-177502] N89-29020
SPACECRAFT LANDING
Designers' commentary on Buran flight control system N89-28530
SPACECRAFT POWER SUPPLIES
General-purpose heat source development: Extended series test program SRB fragment/fuselage tests
[DE89-014389] N89-29180
SPACECRAFT PROPULSION
Ion optics for high power 50-cm-diam ion thrusters
[NASA-TM-102143] N89-28571
SPACECRAFT STRUCTURES
Active damping of vibration in large space structures using a Karhunen-Loeve reduced order model
[AD-A208183] N89-28558
SPATIAL DISTRIBUTION
Components of high-level vision: A cognitive neuroscience analysis and accounts of neurological syndromes
[AD-A207848] N89-29011
New dimensions from statistical graphics for GIS (Geographic Information System) analysis and interpretation
[DE89-012339] N89-29263
SPATIAL FILTERING
Noise reduction from Synthetic Aperture Radar imagery N89-28913
SPATIAL MARCHING
A space marching algorithm for the thin-layer Navier-Stokes equations N89-28787
SPATIAL RESOLUTION
A new scattering formula for depth-resolving X-ray diffractometry based on a kinematic theory
[ETN-89-94430] N89-29195
SPECIMEN GEOMETRY
Compression tests using Hopkinson bars: Numerical simulation and experimental study
[ISL-C-208/88] N89-28873
SPECKLE PATTERNS
Noise reduction from Synthetic Aperture Radar imagery N89-28913
SPECTRAL METHODS
Optimal error analysis of spectral methods with emphasis on non-constant coefficients and deformed geometries
[NASA-CR-181902] N89-29124
SPECTRAL RESOLUTION
A medium resolution imaging spectrometer for the European polar orbiting platform
[ETN-89-95235] N89-28563
SPECTRAL SIGNATURES
An improving multispectral recording set analysis method N89-28900
SPECTROMETERS
The Los Alamos Fourier-transform spectrometer: Applications to molecular spectroscopy
[DE89-014258] N89-28789
SPECTROPHOTOMETRY
Development of a postdispersion system for astronomical infrared observations with Fourier spectrometers and its application in the study of the CO fundamental bands in F, G and K stars
[MPE-214] N89-29280
SPECTRORADIOMETERS
Development of a field radiometer as a ground truth equipment for the Japanese ERS-1 N89-28901
Simulation of ERS-1/OPS by the use of airborne spectroradiometer N89-28912
SPECTROSCOPIC ANALYSIS
Simultaneous secondary ion and Auger electron analysis, illustrated by examples from microelectronics research and technology
[ETN-89-94431] N89-28611
A study of non-rigid aromatic molecules by supersonic molecular jet spectroscopy: Observation and spectroscopic analysis of the stable conformations of various alkylbenzenes
[AD-A209561] N89-29171

SPECTROSCOPY
Lithography and spectroscopy of ultrathin Langmuir-Blodgett polymer films
[AD-A206970] N89-28639
VLSI integrated circuit contact reliability by interface spectroscopy
[AD-A207666] N89-28718
A study of non-rigid aromatic molecules by supersonic molecular jet spectroscopy: Observation and spectroscopic analysis of the stable conformations of various alkylbenzenes
[AD-A209581] N89-29171
A study of the T(1) transition of Poly(Bis(trifluoroethoxy)Phosphazene) (PBFP) using solid-state nuclear magnetic resonance spectroscopy
[AD-A207719] N89-29246

SPECTRUM ANALYSIS
Method and circuit for controlling the evolution time interval of a laser output pulse
[NASA-CASE-LAR-13772-1] N89-28816
A comparison between the variability structure of the remotely sensed sea-surface temperature and pigment distributions N89-28896
An improving multispectral recording set analysis method N89-28900
Spectral measurements of the cosmic microwave background
[DE89-014895] N89-29296

SPEECH RECOGNITION
Computer implementation and simulation of some neural networks used in pattern recognition and classification
[AD-A206112] N89-29099

SPENT FUELS
A method for evaluating structural transducers used in Type B package testing
[DE89-013591] N89-28784

SPERMATOZOA
Energy and Technology Review — analytical cytology
[DE89-013919] N89-28954

SPHERES
Experimental investigations of flow forces exerted on spheres in rest and in motion, in a plane Poiseville flow
[ETN-89-94433] N89-28770
The potential and electric fields of a conducting sphere in the presence of a charged conducting plane
[AD-A209498] N89-29149

SPHERICAL SHELLS
Exact solutions for symmetric deformations of hollow bodies of ideal fluids with application to inertial stability
[DE89-014374] N89-28753

SPIN-ORBIT INTERACTIONS
Photon-ion angular correlation measurements on the system He(+) + Ne: Determination of the spin inversion
[ETN-89-94435] N89-29175

SPIRAL ANTENNAS
Contribution to the generation of circular polarization of high purity using planar wire antenna structures
[ETN-89-94659] N89-28872

SPIRAL GALAXIES
Implications of the correlation between the radio continuum and far-infrared luminosities of spiral galaxies N89-29289

SPLINE FUNCTIONS
Smooth piecewise polynomials as conforming finite elements for plate bending problems
[MEMO-747] N89-28875

SPOT (FRENCH SATELLITE)
The new generation SPOT satellites SPOT 4 and 5 N89-28914
The processing of SPOT imagery in Brazil N89-28917
Integrating satellite data with information from topographic maps: Method and applications — SPOT
[NLR-MP-87035-U] N89-28933
Monitoring and measuring human settlement changes by remote sensing methods
[BCRS-88-16C] N89-28937
Training Course for Tropical Earth Resources Satellite (EARS) bridging phase
[BCRS-88-16D] N89-28938

STABILITY
A comparison and analysis of strategic defense transition stability models
[AD-A208033] N89-29144

STABLE OSCILLATIONS
Experimental and numerical investigation of coherent structures in turbulent wake flows
[AD-A207666] N89-28759

STAINLESS STEELS
Metallurgical evaluation of 17-4 PH stainless steel castings
[PB89-193262] N89-28615

STANDARDS
Standard reference material for high temperature viscosity measurements: Results of interlaboratory comparison programme
[NPL-DMA(A)-175] N89-28612
NIST (National Institute of Standards and Technology) calibration services users guide, 1989 edition
[PB89-200216] N89-28785

STAR FORMATION
Towards a theory of star formation
[MPE-PREPRINT-150] N89-29287
Millisecond radio pulsars in globular clusters
[NASA-CR-185909] N89-29298

STARS (MATHEMATICS)
A graph-theoretical approach to block-co-polymer complexes. Part 1: Stars
[MEMO-757-PT-1] N89-28654

STARTING
Mathematical modeling and analysis of heat pipe start-up from the frozen state
[NASA-CR-185132] N89-28747

STATIC CHARACTERISTICS
Static and dynamic deflection studies of the SRM aft case-nozzle joint
[NASA-TM-100373] N89-28568

STATIC LOADS
A static load distribution strategy for processor tools
[MEMO-INF-88-43] N89-29078

STATIC TESTS
Low-speed static and dynamic force tests of a generic supersonic cruise fighter configuration
[NASA-TM-4138] N89-28486

STATISTICAL ANALYSIS
Statistics on aircraft gas turbine engine rotor failures that occurred in US commercial aviation during 1984
[NAPC-PE-185] N89-28516
Statistics on aircraft gas turbine engine rotor failures that occurred in US commercial aviation during 1985
[NAPC-PE-188] N89-28517
Solvent effects on simple electron transfer reactions. A comparison of results for homogeneous and heterogeneous systems
[AD-A209381] N89-28600
Quality factor and statistics for radiation patterns of shipboard HF antennas
[AD-A207931] N89-28690
Development of a field radiometer as a ground truth equipment for the Japanese ERS-1 N89-28901
Sea spectra as determined from low-altitude SLAR images N89-28908
Hurricane hindcast methodology and wave statistics for Atlantic and Gulf hurricanes from 1956 - 1975
[AD-A207849] N89-29004
The measurement of SEA loss factors on a fully assembled structure
[ISVR-TR-150] N89-29157
New dimensions from statistical graphics for GIS (Geographic Information System) analysis and interpretation
[DE89-012339] N89-29263
Statistical and physical evolution of QSO's
[NASA-CR-185869] N89-29282

STATISTICAL TESTS
Stein's Lemma: A large deviations approach
[AD-A209090] N89-29137

STATORS
Turbomachinery rotor support with damping
[NASA-CASE-MFS-28345-1] N89-28841

STEADY FLOW
Development of an efficient solution scheme for incompressible steady-state flow
[AD-A207726] N89-28757
Numerical determination of guaranteed Rayleigh numbers and the pertaining flow forms in steady, axisymmetric convection in cylinders
[ETN-89-94432] N89-28769

STEADY STATE
Development of an efficient solution scheme for incompressible steady-state flow
[AD-A207726] N89-28757

STEELS
Steel fatigue under combined loads
[ETN-89-94864] N89-28629
Pull-out and push-out tests for rubber-to-metal adhesion
[AD-A208100] N89-28647

STELLAR ATMOSPHERES
Development of a postdispersion system for astronomical infrared observations with Fourier spectrometers and its application in the study of the CO fundamental bands in F, G and K stars
[MPE-214] N89-29280

STELLAR EVOLUTION
The origin and evolution of X-ray binaries and low-magnetic field radio pulsars
[MPE-PREPRINT-145] N89-29284
Evolution of wide binary millisecond pulsars in globular clusters
[MPE-PREPRINT-148] N89-29285
Red giants in open clusters. 1: Binarity and stellar evolution in five Hyades-generation clusters, NGC 2447, 2539, 2632, 6633 and 6940
[SER-C-PREPUBL-FASC-37-PT-1] N89-29290

STELLAR LUMINOSITY
Implications of the correlation between the radio continuum and far-infrared luminosities of spiral galaxies N89-29289

STELLAR MAGNETIC FIELDS
The origin and evolution of X-ray binaries and low-magnetic field radio pulsars
[MPE-PREPRINT-145] N89-29284

STELLAR MASS ACCRETION
Statistical and physical evolution of QSO's
[NASA-CR-185869] N89-29282
Towards a theory of star formation
[MPE-PREPRINT-150] N89-29287

STELLAR MODELS
Activities report of the Institute of Astronomy and Astrophysics
[MITT-9] N89-29276

STELLAR ORBITS
Red giants in open clusters. 2: Orbits of ten spectroscopic binaries in NGC 2360, 2437, 2447, 5822, 5823, 6475
[SER-C-PREPUBL-FASC-38-PT-2] N89-29291

STELLAR PHYSICS
Activities report of the Institute of Astronomy and Astrophysics
[MITT-9] N89-29276
Towards a theory of star formation
[MPE-PREPRINT-150] N89-29287

STELLAR ROTATION
Evidence for two charged particle populations in the Crab nebula
[MPE-PREPRINT-147] N89-29286

STELLAR SYSTEMS
Activities report of the Institute of Astronomy and Astrophysics
[MITT-9] N89-29276
Activities report of the Heidelburg Astronomical Institute of Computation (Germany, F.R.)
[ETN-89-94429] N89-29279

STEREOSCOPIC VISION
Television monitor field shifter and an opto-electronic method for obtaining a stereo image of optimal depth resolution and reduced depth distortion on a single screen
[NASA-CASE-NPO-17249-1-CU] N89-28676
Investigation of the effectiveness and applications of Japanese ERS-1 stereoscopic images N89-28884

STEREOSCOPY
JPRS Report: Science and Technology. USSR: Space. 16th International Congress of the International Society for Photogrammetry and Remote Sensing, volume 1
[JPRS-USP-89-002-VOL-1] N89-28878
Investigation of the effectiveness and applications of Japanese ERS-1 stereoscopic images N89-28884

STIFFNESS
Optimum design methods for structural sandwich panels
[AD-A209427] N89-28575

STIMULATION
A program for the study of skeletal muscle catabolism following physical trauma
[AD-A207983] N89-29014

STOCHASTIC PROCESSES
Stochastic processes in CHEMFETs
[AD-A207977] N89-28723
Stochastic processes in CHEMFETs
[AD-A208092] N89-28725
Estimation of some stochastic models used in reliability engineering
[VTT-RR-598] N89-28855
Modelling orientation parameters of sensor platforms N89-28881
Caotic magnetic field line in toroidal plasmas
[IPPJ-911] N89-29211

STOICHIOMETRY
Crystal chemistry, magnetic and electrical properties of La(sub2-x)Ba(subx)NiO4
[AD-A209376] N89-29240

STORAGE RINGS (PARTICLE ACCELERATORS)
Measurement of electroweak effects and topological branching conditions in the reaction e(+)e(-) yields tau(+)tau(-) in the storage ring PETRA
[MPI-PAE/EXP.EL-195] N89-29173
New layout of Amsterdam pulse stretcher
[NIKHEF-K/APS/88-01A-REV] N89-29182
Orbit correction scheme for the new ring — Amsterdam electron accelerator
[NIKHEF-K/APS/88-04] N89-29184

STORMS (METEOROLOGY)
Storm models for end-to-end TDWR (Terminal Doppler Weather Radar) signal processing simulation tests
[AD-A209384] N89-28986
STRAIN ENERGY RELEASE RATE
Measurement of mode 1 and mode 2 strain energy release rates: A VAMAS round robin project on delamination of composite materials --- Versailles project on advanced materials and standards (VAMAS)
[NPL-DMA(A)-178] N89-28583
STRAIN GAGES
In search of more output: Two strain gage bridge circuits revisited
[DE89-014039] N89-28787
On strain gages using the PVF2 piezoelectric polymer
[ISL-CO-210/88] N89-28801
STRAIN MEASUREMENT
Investigation of optoelectronic angle measuring systems and their use in a diffraction-optical strain measurement and a photoelectric two-coordinate autocollimator
[PTB-F-5] N89-29199
STRATA
Electromagnetic pulse propagation through a stratified ionosphere
[IRF-SR-199] N89-28700
STRATEGY
SDI (Strategic Defense Initiative): Shield or sword?
[AD-A209777] N89-29141
Ground-Based Radar (GBR): Environmental assessment
[AD-A207654] N89-29143
STRATOSPHERE
Atmospheric processes and effects on materials
[PB89-173215] N89-28964
A high-resolution atlas of the infrared spectrum of the sun and the earth atmosphere from space. A compilation of ATMOS spectra of the region from 650 to 4800 cm-1 (2.3 to 16 microns). Volume 2: Stratosphere and mesosphere, 650 to 3350 cm-1
[NASA-RP-1224-VOL-2] N89-28969
STRESS (PSYCHOLOGY)
Prevention, reduction, and measurement of combat stress reactions: A bibliography
[AD-A209375] N89-29019
STRESS ANALYSIS
Composite damaging: Methodological approach
[ETN-89-94866] N89-28582
STRESS CONCENTRATION
Stresses and strains in a cold-worked annulus
[AR-005-548] N89-28871
STRESS CORROSION
Comparative analysis of ultrasonic inspection procedures for Kaman K747 root end fittings
[AD-A207762] N89-28512
STRESS CORROSION CRACKING
Effect of temperature and H2S content on the cracking resistance of a 13 percent chromium martensitic stainless steel in acidified NaCl
[NPL-DMA(A)-173] N89-28631
STRESS DISTRIBUTION
Analytical solutions for the field, current density, force force density and mechanical stress distribution in toroidal coil systems
[IPP-2/294] N89-28728
The effect of transients on crack tip stress fields during thermal fatigue loading
[AD-A210084] N89-28864
Factors affecting stress distribution and displacements in crystals 3-5 grown by Czochralski method with liquid encapsulation
[DE89-013396] N89-29222
STRESS MEASUREMENT
Experimental and numerical investigation of coherent structures in turbulent wake flows
[AD-A207866] N89-28759
STRESS WAVES
Numerical simulation of the simultaneous detonation of two identical, fully contained explosions
[DE89-014844] N89-28660
STRESS-STRAIN RELATIONSHIPS
Plastic yielding of partially-crystalline polymers
[AD-A208101] N89-28648
Adiabatic shear bands in one dimension
[AD-A208105] N89-28868
STRESSES
The PVF2 piezoelectric polymer shock stress sensor: System characterization for application under field test conditions
[DE89-014629] N89-28790
Stresses and strains in a cold-worked annulus
[AR-005-548] N89-28871
STRUCTURAL ANALYSIS
Active damping of vibration in large space structures using a Karhunen-Loeve reduced order model
[AD-A208183] N89-28558
Static and dynamic deflection studies of the SRM aft case-nozzle joint
[NASA-TM-100373] N89-28568
The structural response of unsymmetrically laminated composite cylinders
[NASA-CR-185834] N89-28856
Out-of-plane buckling formulae for beam-columns/tie beams
[PB89-191613] N89-28857
Flexural-torsional buckling of monosymmetric beam-columns/tie beams
[PB89-191654] N89-28859
STRUCTURAL DESIGN
An improved design for stretched-membrane heliostats
[DE89-013872] N89-28953
Study of sampling systems for comets and Mars
[NASA-CR-185514] N89-29292
STRUCTURAL DESIGN CRITERIA
Flexural-torsional buckling of monosymmetric beam-columns/tie beams
[PB89-191654] N89-28859
STRUCTURAL ENGINEERING
Preliminary design of a consultation knowledge-based system for the minimization of distortion in welded structures
[AD-A208842] N89-28834
STRUCTURAL FAILURE
Out-of-plane buckling formulae for beam-columns/tie beams
[PB89-191613] N89-28857
New set of buckling parameters for monosymmetric beam-columns/tie beams
[PB89-191639] N89-28858
Flexural-torsional buckling of monosymmetric beam-columns/tie beams
[PB89-191654] N89-28859
STRUCTURAL STABILITY
New set of buckling parameters for monosymmetric beam-columns/tie beams
[PB89-191639] N89-28858
STRUCTURAL VIBRATION
Active damping of vibration in large space structures using a Karhunen-Loeve reduced order model
[AD-A208183] N89-28558
Acoustic tests on a new motor generator system for the minuteman launch control centers in Hill engineering test facilities 1 and 2, Hill AFB, Utah
[AD-A209598] N89-28717
Optimization of structures with passive damping and active controls
[AD-A208937] N89-28862
Aircraft propeller induced structure-borne noise
[NASA-CR-4255] N89-29155
STRUCTURAL WEIGHT
Optimum design methods for structural sandwich panels
[AD-A209427] N89-28575
SUBMERGED BODIES
Propagation problem and far-field patterns in a stratified finite depth ocean
[PB89-180707] N89-29001
SUBROUTINE LIBRARIES (COMPUTERS)
Linear algebra support modules for approximation and other software
[NPL-DITC-142/89] N89-29126
SUBROUTINES
A user's guide to the SEVP (Stabilized Error Vector Propagation) solver: An efficient direct solver for elliptic partial differential equations
[AD-A208117] N89-29121
SUBSONIC FLOW
Measurements of mean-flow and turbulence characteristics in a turbojet exhaust using a laser velocimeter
[ISL-CO-226/88] N89-28519
SUBSTRATES
High resolution electron energy loss studies of surface vibrations
[DE89-013964] N89-28589
Monolayers of 11-trichlorosilylundecyl thioacetate: A system that promotes adhesion between silicon dioxide and evaporated gold
[AD-A208266] N89-28637
SUDAN
The boundary layer wind regime of a representative tropical African region, central Sudan
[KNMI-WR-88-04] N89-28982
SUGAR BEETS
Entrepreneurship and innovation: The Dutch sugar beet industry (1858-1919)
[ISBN-90-71617-11-4] N89-29275
SULFIDATION
Sulfidation/oxidation properties of iron-based alloys containing niobium and aluminum
[DE89-013766] N89-28617
SULFIDES
The atomic layer epitaxy growth and characterization of zinc sulfide and alkaline earth sulfide thin films for electroluminescence applications
[ISBN-952-90014-6-0] N89-28613
SULFUR DIOXIDES
Climate regulation by marine phytoplankton: A test by anthropogenic SO2 emissions
[DE89-014708] N89-28984
SUN
Key data on participating projects. The solar-terrestrial science project of the Inter-Agency Consultative Group for Space Science (IACG)
[ESA-SP-1107] N89-29295
SUPERCOMPUTERS
Role of supercomputer in computational aerodynamics
[PD-CF-8925] N89-28496
Tools for the development and usage of industrial mathematical software
[NLR-MP-87020-U] N89-29067
La Recherche Aerospatiale, bimonthly bulletin, number 1988-4
[ESA-TT-1161] N89-29299
SUPERCONDUCTING FILMS
Primary research efforts on exploring the commercial possibilities of thin film growth and materials purification in space
[NASA-CR-184913] N89-28541
SUPERCONDUCTIVITY
Superconducting Meissner effect bearings for cryogenic turbomachines, phase 1
[AD-A209875] N89-28839
Non-uniform transition conductivity of superconducting ceramic
[NASA-TM-102133] N89-28851
Plastic deformation of YBa2Cu3O7-x superconductor compound
[DE89-013395] N89-29221
Ultrasonic attenuation in heavy fermion superconductors
[DE89-014937] N89-29231
Fluxons and order in long Josephson junctions
[AD-A207925] N89-29249
SUPERCONDUCTORS
Method of mass producing superconducting persistent current rings
[AD-D013968] N89-29219
Thermal conductivity anisotropy in single crystal YBa2Cu3O7-x
[DE89-009643] N89-29220
Plastic deformation of YBa2Cu3O7-x superconductor compound
[DE89-013395] N89-29221
Ultrasonic attenuation in heavy fermion superconductors
[DE89-014937] N89-29231
Vortices in long Josephson junctions
[AD-A207936] N89-29250
United States Air Force Research Initiation Program for 1987, volume 2
[AD-A209727] N89-29259
SUPERFLUIDITY
Measurements of the dipolar velocity of superfluid 3 He-B
[PB89-155444] N89-29218
SUPERLATTICES
Effective masses and g factors for 2-D light holes in InSb
[DE89-014899] N89-29230
SUPERNOVA REMNANTS
Measurement of the Vela pulsar's proper motion and detection of the optical counterpart of its compact X-ray nebula
[MPE-PREPRINT-151] N89-29288
SUPERNOVAE
The first large balloon launch from Antarctica
[AD-A207735] N89-28491
SUPERSONIC BOUNDARY LAYERS
Rapidly distorted compressible boundary-layers N89-28735
Large scale motions in supersonic turbulent boundary layers N89-28736
Skin-friction measurements by laser interferometry N89-28737
Fluctuating wall-pressure measurements N89-28741
SUPERSONIC COMBUSTION
Supersonic combustion at the DFVLR: Results and experiences
[DFVLR-88-044] N89-28610
SUPERSONIC COMBUSTION RAMJET ENGINES
Supersonic combustion at the DFVLR: Results and experiences
[DFVLR-88-044] N89-28610

SUPERSONIC CRUISE AIRCRAFT RESEARCH
Low-speed static and dynamic force tests of a generic supersonic cruise fighter configuration
[NASA-TM-4138] N89-28486
SUPERSONIC FLOW
A survey of measurements and measuring techniques in rapidly distorted compressible turbulent boundary layers
[AGARD-AG-315] N89-28734
Hot-wire anemometry in supersonic flow N89-28738
Laser Doppler anemometry in supersonic flows: Problems of seeding and angular bias N89-28740
SUPERSYMMETRY
New infinite-dimensional algebras, sine brackets, and SU (infinity)
[DE89-013178] N89-29108
SUPPORTS
Almond test body --- for microwave anechoic chambers
[NASA-CASE-LAR-13747-1-CU] N89-28672
Turbomachinery rotor support with damping
[NASA-CASE-MFS-28345-1] N89-28841
SUPPRESSORS
Optimization of structures with passive damping and active controls
[AD-A208937] N89-28862
SURFACE LAYERS
Formation of monolayers by the coadsorption of thiols on gold: Variation in the length of the head group, tail group and solvent
[AD-A208919] N89-28594
Initial stages of metal/semiconductor interface formation: Au and AgON Si(111)
[AD-A209490] N89-29245
SURFACE REACTIONS
Laboratory investigations: Low earth orbit environment chemistry with spacecraft surfaces
[DE89-014280] N89-28533
Arc-textured high emittance radiator surfaces
[NASA-CASE-LEW-14679-1] N89-28651
Chemical effects of Ne(+) bombardment on the MoS2(0001) surface studied by high-resolution photoelectron spectroscopy
[AD-A207734] N89-29247
SURFACE ROUGHNESS
Approximation methods for scattering from rough surfaces
[AD-A209482] N89-29192
Investigations of step distributions at Si/SiO2 interfaces using HR-SPA-LEED
[ETN-89-94437] N89-29251
SURFACE TEMPERATURE
Significant improvement in IR surface-temperature measurements
[DE89-014808] N89-28926
SURGES
Experimental and theoretical study of transient behavior of varistors
[AD-A209081] N89-28715
SURVEILLANCE
US Army role in space
[AD-A209178] N89-28534
SURVEYS
Anthropometric survey of US Army personnel: Summary statistics
[AD-A209600] N89-29025
SUSPENDING (HANGING)
A torsional suspension system for testing space structures
[NASA-CASE-LAR-14149-1-SB] N89-28547
SWEAT
Thermoregulatory competence during exercise transients in a group of heat-acclimated young and middle-aged men is influenced more distinctly by maximal aerobic power than age
[AD-A209753] N89-29009
SWEAT COOLING
Thermoregulatory competence during exercise transients in a group of heat-acclimated young and middle-aged men is influenced more distinctly by maximal aerobic power than age
[AD-A209753] N89-29009
SWITCHES
Photonic architectures for performing perfect shuffle on a time-division multiplexed signal
[PB89-184352] N89-28674
Electrical characterization of signal processing microcircuit
[AD-A209078] N89-28714
The mock counter: A hybrid optical-electronic counter using fiber delay line memory
[PB89-184410] N89-29031
SWITCHING CIRCUITS
A reconfigurable arithmetic processor --- for MIMD computer
[AD-A208323] N89-29082
Theoretical investigations of an integrated optics switching element with asymmetric directional couplers for switching matrices
[ETN-89-94439] N89-29196
SYMBOLS
Towards a physiologically based HUD (Head-Up Display) symbology
[AD-A207748] N89-28515
SYMMETRY
Experimental and numerical investigation of coherent structures in turbulent wake flows
[AD-A207866] N89-28759
Conditional dependence
[AD-A207881] N89-29120
A torus bifurcation theorem with symmetry
[NASA-CR-185907] N89-29135
SYMPATHETIC NERVOUS SYSTEM
A program for the study of skeletal muscle catabolism following physical trauma
[AD-A207983] N89-29014
SYNCHRONISM
Analysis of cache invalidation patterns in multiprocessors
[AD-A207820] N89-29089
SYNCHROTRON RADIATION
Evidence for two charged particle populations in the Crab nebula
[MPE-PREPRINT-147] N89-29286
SYNCHROTRONS
Proceedings of the Antiproton Technology Workshop held in Upton, New York on 10 May 1989
[AD-A210045] N89-29170
SYNTHESIS (CHEMISTRY)
Oxidative addition of C-H bonds in organic molecules to transition metal centers
[DE89-012991] N89-28616
Synthesis and hot pressing of ZnS powders
[AD-A209602] N89-28625
Synthesis of monomethylhydrazine
[ETN-89-94863] N89-28684
Differential equations and continuum mechanics --- polymers
[AD-A208637] N89-29109
Vertical gradient freeze GaAs: Growth and electrical properties
[DE89-014894] N89-29228
SYNTHETIC APERTURE RADAR
JPRS Report: Science and Technology. USSR: Space. 16th International Congress of the International Society for Photogrammetry and Remote Sensing, volume 1
[JPRS-USP-89-002-VOL-1] N89-28876
KRAS: A Danish high resolution airborne SAR N89-28882
SAR activities at Dornier N89-28887
ERS-1 SAR processing with CESAR N89-28888
Experiences in implementing an expert system supported man-machine-interface for the configuration of the intelligent SAR processor N89-28889
EXAS: Experiment on Autonomous SAR processor calibration N89-28890
JPRS Report: Science and Technology. USSR: Space. 16th International Congress of the International Society for Photogrammetry and Remote Sensing, volume 2
[JPRS-USP-89-003-VOL-2] N89-28903
Performance evaluation of ERS-1 Synthetic Aperture Radar Fast Delivery Processor N89-28904
National program for handling large volumes of satellite data N89-28910
Real time SAR processing techniques N89-28911
Design aspects of a system for geocoding satellite SAR images N89-28915
Data processing and calibration of SAR data in Japan N89-28918
Methods for analyzing SAR images
[VTT-RR-612] N89-28932
The Archimedes 2a Experiment on oil slick dection over the North Sea, April 1988: Measurement Results obtained by the E-SAR System of the Aerospace Research Establishment
[DFVLR-MITT-89-08] N89-28942
SYNTHETIC FUELS
Fuels from microalgae
[DE88-001192] N89-28657
Structural definition of synthetic fuels: Wilsonville 1
[DE89-013627] N89-28659
SYSTEM EFFECTIVENESS
Operational test plan concept for evaluation of close air support alternative aircraft
[AD-A208185] N89-28513
SYSTEM GENERATED ELECTROMAGNETIC PULSES
Application of optimal control theory for selective vibrational excitation in molecules modeled as harmonic systems
[MEMO-755] N89-29104
SYSTEMS ANALYSIS
Design of a reliable computing system for the Petite Amateur Navy Satellite (PANSAT)
[AD-A208194] N89-28559
Gauge: Its philosophy and design
[AD-A208944] N89-29083
Hamiltonian control systems: Decomposition and clamped dynamics
[MEMO-759] N89-29103
SYSTEMS ENGINEERING
Design of a reliable computing system for the Petite Amateur Navy Satellite (PANSAT)
[AD-A208194] N89-28559
Design aspects of a system for geocoding satellite SAR images N89-28915
Ultrasonic systems and system development at SNL Albuquerque
[DE89-013164] N89-29153
New layout of Amsterdam pulse stretcher
[NIKHEF-K/APS/88-01A-REV] N89-29182
Study of sampling systems for comets and Mars
[NASA-CR-185514] N89-29292
SYSTEMS MANAGEMENT
Optical laser technology and its application to Defense Manpower Data Center's (DMDC) querry facsimile (QFAX) data base system
[AD-A207832] N89-29194
SYSTOLIC ARRAYS
Systolic VLSI array for implementing the Kalman filter algorithm
[NASA-CASE-NPO-17108-1-CU] N89-28713
Parallel algorithms for solving systems of linear equations and their mapping on systolic arrays
[ETN-89-95457] N89-29077
Application of Cholesky-like matrix decomposition methods to the evaluation of atomic orbital integrals and integral derivatives
[AD-A209682] N89-29112

T

TACTILE DISCRIMINATION
Tactile sensing and the photoelastic tactile sensor
[OUEL-1758/89] N89-28849
TARGET ACQUISITION
Airborne pulse Doppler radar. Part 3: Performance estimation --- surveillance radar analysis
[BAE-WAA-RP-GEN-RAD-645-PT-3] N89-28697
Three dimensional cellular automata for subpixel target detection
[AD-A208163] N89-29100
Airborne FLIR (Forward Looking Infrared) detection of surface targets
[AD-A209250] N89-29189
TARGET RECOGNITION
Adaptive detection and parameter estimation for multidimensional signal models
[AD-A208971] N89-28678
Three dimensional cellular automata for subpixel target detection
[AD-A208163] N89-29100
Airborne FLIR (Forward Looking Infrared) detection of surface targets
[AD-A209250] N89-29189
Detection of target formations in infrared imagery
[ETCA-88-R-070] N89-29198
TARGETS
Orbit determination of sunlight illuminated objects detected by overhead platforms
[AD-A209227] N89-28540
TASKS
Choice and perceived control: Implications for the design of displays
[AD-A208400] N89-29021
TAYLOR INSTABILITY
Stability of a Taylor-relaxed cylindrical plasma separated from the wall by a vacuum layer
[EUT-88-E-207] N89-29200
TEARING MODES (PLASMAS)
A three-dimensional resistive MHD simulation analysis of field reversal control in the reversed field pinch
[IPPJ-904] N89-29210
TECHNOLOGY ASSESSMENT
Status and development potential of the fly by light technology in civil aircraft
[ILR-MITT-212] N89-28522
Advanced robotics for Air Force operations
[AD-A210098] N89-28840
Solar thermal program summary. Volume 2: Research summaries, fiscal year 1988
[DE89-000861] N89-28947
Fuel cell technology in the United States
[DE89-013430] N89-28951

Energy technology R and D: What could make a difference. A study by the staff of the Oak Ridge National Laboratory. Part 1: Synthesis report, volume 1
[DE89-014568] N89-28955
Thin film photovoltaics
[DE89-009425] N89-28956

TECHNOLOGY TRANSFER
International technology transfer as practiced by the U.S.S.R.: Implications for US national security
[AD-A208010] N89-29274

TECHNOLOGY UTILIZATION
Acoustic emission technology for space applications
[DE89-014449] N89-28861
Proceedings of the Antiproton Technology Workshop held in Upton, New York on 10 May 1989
[AD-A210045] N89-29170

TELECOMMUNICATION
US Army role in space
[AD-A209178] N89-28534
ELF (Extremely Low Frequency) communications system ecological monitoring program
[AD-A208198] N89-28691
Multicast communication in multiprocessor systems
[AD-A209606] N89-29086
Information requirements and the implications for parallel computation
[AD-A207802] N89-29088
Northeast artificial intelligence consortium. Volume 1: Executive summary
[AD-A209395] N89-29094
Activities report of ESA
[ISSN-0258-025X] N89-29302

TELEMETRY
Engineering and instrumentation support of the AFGL (Air Force Geophysics Laboratory) Research Balloon Program
[AD-A209107] N89-28971

TELEPHONY
Design of a command, communications, and control van (surrogate)
[AD-A207652] N89-28687

TELESCOPES
Realtime tracking system for the wide-field-of-view telescope project
[DE89-013787] N89-29186
Activities report in international astronomy
[ETN-89-95333] N89-29281

TELEVISION SYSTEMS
The beam viewer
[LINO-160] N89-28693
Video processing using the MSX computer
[LINO-163] N89-28694

TELLURIDES
Evaporation thermodynamics of monotellurides of selected rare Earth and alkaline Earth elements, and an attempt to systematic correlation between the standard enthalpies of formation
[ETN-89-94655] N89-29257

TEMPERATURE DEPENDENCE
Heat transfer in free convection and forced, laminar flow in vertical tubes, considering temperature dependent medium characteristics
[ETN-89-94441] N89-28772

TEMPERATURE DISTRIBUTION
A comparison between the variability structure of the remotely sensed sea-surface temperature and pigment distributions N89-28896

TEMPERATURE EFFECTS
Effect of temperature and H2S content on the cracking resistance of a 13 percent chromium martensitic stainless steel in acidified NaCl
[NPL-DMA(A)-173] N89-28631
Investigation of ambient and high temperature aging of PETN (Pentaerythritol Tetranitrate) by laser induced fluorescence and ultraviolet absorption spectroscopies
[DE89-013740] N89-28813
The structural response of unsymmetrically laminated composite cylinders
[NASA-CR-185834] N89-28856

TEMPERATURE GRADIENTS
Preliminary neural network detection of a gulf stream in images of sea surface temperature gradients, phase 1
[AD-A207801] N89-29003

TEMPERATURE MEASUREMENT
Significant improvement in IR surface-temperature measurements
[DE89-014808] N89-28926
A new method of testing nuclear fusion in metals
[IPPJ-915] N89-29215

TEMPERATURE PROFILES
A study of the thermal profiles during autogenous arc welding
[AD-A209440] N89-28843

TEMPORAL DISTRIBUTION
New dimensions from statistical graphics for GIS (Geographic Information System) analysis and interpretation
[DE89-012339] N89-29263

TENSILE PROPERTIES
Cohesion and interparticle forces
[ETN-89-95454] N89-28874

TENSILE STRESS
Plastic yielding of partially-crystalline polymers
[AD-A208101] N89-28648

TENSILE TESTS
Furnace for tensile/fatigue testing
[NASA-CASE-LEW-14848-1] N89-28549
A VAMAS round robin on fatigue test methods for polymer matrix composites. Part 1: Tensile and flexural tests of unidirectional material --- Versailles project on advanced materials and standards (VAMAS)
[NPL-DMA(A)-180-PT-1] N89-28585
The influence of structure and alloying on the cold-formability of ferritic steels and the utility of uniaxial tensile testing in its assessment
[ISBN-952-90044-3-5] N89-28632

TERMINOLOGY
NASA thesaurus supplement. A four part cumulative supplement to the 1988 edition of the NASA thesaurus
[NASA-SP-7064-SUPPL-1] N89-29262
NASA thesaurus supplement: A four part cumulative supplement to the 1988 edition (supplement 2)
[NASA-SP-7064-SUPPL-2] N89-29269

TERRAIN
Towards a physiologically based HUD (Head-Up Display) symbology
[AD-A207748] N89-28515
A robot that walks: Emergent behaviors from a carefully evolved network
[AD-A207958] N89-29026

TERRAIN ANALYSIS
User's guide to the complex terrain dispersion model plus algorithms for unstable situations (CTDMPLUS). Volume 1: Model description and user instructions
[PB89-181424] N89-28963

TERRESTRIAL RADIATION
ISCCP CX observations during the FIRE/SRB Wisconsin Experiment from October 14 through November 2, 1986
[NASA-TM-101653] N89-28993

TETRAHEDRONS
Preparation of compounds with the tetrahedral structure which transmit in the far infrared
[AD-A208697] N89-28593

THEMATIC MAPPERS (LANDSAT)
Methods for analyzing SAR images
[VTT-RR-612] N89-28932
Improvement of classification results of satellite imagery using context information from a topographic map
[NLR-MP-88020-U] N89-28935
Updating land-use information on topographic maps using satellite imagery: Combining the advantages of two accessible sources of geographic information
[NLR-MP-88030-U] N89-28936
Training Course for Tropical Earth Resources Satellite (EARS) bridging phase
[BCRS-88-16D] N89-28938

THEMATIC MAPPING
Map production and revision with satellite photographs taken by the MKF-6 camera and by the cameras KATE-140, KATE-200, and KFA-1000 N89-28893
An expert system for satellite image interpretation and G.I.S. based problem solving N89-28894
Identification of irrigated areas in the Sao Francisco Valley through remote sensing data. Pilot area: Petrolina-Juazeiro
[INPE-4800-RPE/587] N89-28925
Marketing and case study of satellite thematic maps and other products of satellite remote sensing
[BCRS-55-16E] N89-28939

THEOREM PROVING
Variational formulation for a nonlinear elliptic equation in a three-dimensional exterior domain
[NASA-CR-181885] N89-29028

THEOREMS
Evaluation of the bistatic equivalence theorem for the near and far-field radar cross section of complex targets
[AD-A209228] N89-28682
A torus bifurcation theorem with symmetry
[NASA-CR-185907] N89-29135
Stein's Lemma: A large deviations approach
[AD-A209090] N89-29137

THEORETICAL PHYSICS
Towards a theory of star formation
[MPE-PREPRINT-150] N89-29287

THERMAL BLOOMING
Linear theory of uncompensated thermal blooming in turbulence
[DE89-014604] N89-28812

THERMAL CONDUCTIVITY
Thermal conductivity anisotropy in single crystal YBa2Cu3O7-x
[DE89-009643] N89-29220

THERMAL CYCLING TESTS
The effect of transients on crack tip stress fields during thermal fatigue loading
[AD-A210084] N89-28864

THERMAL EMISSION
Arc-textured high emittance radiator surfaces
[NASA-CASE-LEW-14679-1] N89-28651

THERMAL FATIGUE
A test system for thermomechanical fatigue of solder joints
[DE89-013886] N89-28860
The effect of transients on crack tip stress fields during thermal fatigue loading
[AD-A210084] N89-28864

THERMAL MAPPING
Proposed concepts for a advanced optical payload for second generation Meteosat
[ETN-89-95236] N89-28564

THERMAL STABILITY
A study of thermodynamic phase stability of intermetallic thin films of Pt2Ga, PtGa and PtGa2 on gallium arsenide
[AD-A209698] N89-29241

THERMAL STRESSES
The effect of transients on crack tip stress fields during thermal fatigue loading
[AD-A210084] N89-28864

THERMOCHEMISTRY
Applied field and total dose dependence of trapped charge buildup in MOS devices
[AD-A209064] N89-29237

THERMODYNAMIC PROPERTIES
A study of the thermal profiles during autogenous arc welding
[AD-A209440] N89-28843
Airborne FLIR (Forward Looking Infrared) detection of surface targets
[AD-A209250] N89-29189

THERMODYNAMICS
Heat-transfer and friction factor design data for all-metal compact heat exchangers
[AD-A208108] N89-28761
A test system for thermomechanical fatigue of solder joints
[DE89-013886] N89-28860
Daytime turbulent exchange between the Amazon forest and the atmosphere
[NASA-CR-185487] N89-28961
Evaporation thermodynamics of monotellurides of selected rare Earth and alkaline Earth elements, and an attempt to systematic correlation between the standard enthalpies of formation
[ETN-89-94655] N89-29257

THERMOGRAPHY
A study of the thermal profiles during autogenous arc welding
[AD-A209440] N89-28843

THERMOPLASTIC RESINS
Radiothermoluminescence studies of polymer solids
[AD-A209036] N89-28641

THERMOREGULATION
Thermoregulatory competence during exercise transients in a group of heat-acclimated young and middle-aged men is influenced more distinctly by maximal aerobic power than age
[AD-A209753] N89-29009

THERMOSPHERE
The Strategic High-Altitude Atmospheric Radiation Code (SHARC) user instructions
[AD-A207667] N89-28974

THESAURI
NASA thesaurus supplement. A four part cumulative supplement to the 1988 edition of the NASA thesaurus
[NASA-SP-7064-SUPPL-1] N89-29262
NASA thesaurus supplement: A four part cumulative supplement to the 1988 edition (supplement 2)
[NASA-SP-7064-SUPPL-2] N89-29269

THIN FILMS
High resolution electron energy loss studies of surface vibrations
[DE89-013964] N89-28589
Simultaneous secondary ion and Auger electron analysis, illustrated by examples from microelectronics research and technology
[ETN-89-94431] N89-28611
The atomic layer epitaxy growth and characterization of zinc sulfide and alkaline earth sulfide thin films for electroluminescence applications
[ISBN-952-90014-6-0] N89-28613
Fundamental studies of grain boundary structure and properties in ICB aluminum
[DE89-014884] N89-28619

Lithography and spectroscopy of ultrathin Langmuir-Blodgett polymer films
[AD-A208970] N89-28639
Thermodynamically stable conducting films of intermetallic PtGa2 on gallium arsenide
[AD-A210077] N89-28716
Measurements and modelling of thin silicon dioxide films on silicon
[AD-A207853] N89-28720
Fundamental aspects of reactions in titanium-silicon thin films for integrated circuits
[ETN-89-95466] N89-28733
Materials analysis and device optimization of CuInSe2 solar cells
[DE89-009434] N89-28944
Polycrystalline cadmium telluride 3n-i-p solar cell
[DE89-009437] N89-28945
Photovoltaics advanced research and development
[DE89-000895] N89-28948
Two-terminal CuInSe-based cascade cells
[DE89-009422] N89-28950
Thin film photovoltaics
[DE89-009425] N89-28956
Energy and angular distributions of electrons emitted from gases and thin foils during light ion bombardment
[DE89-014445] N89-29147
Cognition and order in Langmuir-Blodgett films of a 3-hexadecyl pyrrole and ferrocene-derivatized pyrrole mixed monolayer system
[DE89-012974] N89-29223
Ion beam deposition of epitaxial germanium and gallium arsenide layers
[DE89-014044] N89-29225
A study of thermodynamic phase stability of intermetallic thin films of Pt2Ga, PtGa and PtGa2 on gallium arsenide
[AD-A209698] N89-29241
A bolt-on deposition source for ultra-high-vacuum growth of intermetallic compound films
[AD-A209599] N89-29242
Lineshape and lifetime studies of exciton luminescence from confined CuCl thin films
[AD-A209750] N89-29243
Quantitative analysis of laser interferometer waveforms obtained during oxygen reactive-ion etching of thin polymer films
[AD-A207836] N89-29248

THIN PLATES
The manufacture of blazed oblique zone plates for use at 10.6 microns
[NPL-MOM-91] N89-28827
An evaluation of blazed zone plates for use in the 10 micron spectral region
[NPL-MOM-93] N89-28828

THIN WINGS
Comparison of flow-visualised vortices with computed geometry over thin delta wings
[AD-A209083] N89-28489

THIOLS
Formation of monolayers by the coadsorption of thiols on gold: Variation in the length of the head group, tail group and solvent
[AD-A208919] N89-28594
Monolayers of 11-trichlorosilylundecyl thioacetate: A system that promotes adhesion between silicon dioxide and evaporated gold
[AD-A208266] N89-28637

THREE AXIS STABILIZATION
Consideration of gravity gradient stabilization for ORION
[AD-A207845] N89-28557

THREE DIMENSIONAL BODIES
Three dimensional reconstruction from serial cross sections by set valued interpolation
[MEMO-754] N89-29076

THREE DIMENSIONAL BOUNDARY LAYER
A nonlinear investigation of the stationary modes of instability of the three-dimensional compressible boundary layer due to a rotating disc
[NASA-CR-181901] N89-28766

THREE DIMENSIONAL FLOW
Study of the wing-vortex interaction in three dimensional flows (incompressible inviscid flow)
[ISL-R-123/87] N89-28494
Fast-algorithm development for large-eddy simulation of circular-jet turbulence
[AD-A207928] N89-28760
Numerical grid generation in 3D Euler-flow simulation
[NLR-MP-88013-U] N89-28777
Comparison between two different techniques of computing the axial induction for horizontal axis wind turbines in a locally deformed flow field
[FFA-TN-1986-56] N89-28959

THREE DIMENSIONAL MODELS
Walkthrough-exploring virtual worlds
[AD-A208087] N89-29057

THRESHOLDS (PERCEPTION)
Suprathreshold contrast sensitivity vision test chart
[AD-A209915] N89-29010

THRUST AUGMENTATION
Aerodynamic model tests of exhaust augmentors for F/A-18 engine run-up facility at RAAF Williamtown
[AD-A208110] N89-28518

TIME
TIME: Time and memory efficient distance transformations for parallel and pyramid machines
[FOA-C-30531-3.4] N89-29091

TIME DEPENDENCE
Experimental and theoretical study of transient behavior of varistors
[AD-A209081] N89-28715

TIME DIVISION MULTIPLE ACCESS
Digitally modulated bit error rate measurement system for microwave component evaluation
[NASA-TP-2912] N89-28545

TIME DIVISION MULTIPLEXING
Photonic architectures for performing perfect shuffle on a time-division multiplexed signal
[PB89-184352] N89-28674

TIME LAG
Model simplification based on the concept of equivalent dead time
[NAL-TM-SE-8802] N89-28521
Higher order base dynamics of a bipolar transistor with nonuniform doping
[PB89-155451] N89-28704

TIME SHARING
Gauge: Its philosophy and design
[AD-A208944] N89-29083

TIP VANES
The angles of the Kollibrie rotor tipvanes on the rods and on the blades
[IW-R515] N89-28499

TISSUES (BIOLOGY)
A program for the study of skeletal muscle catabolism following physical trauma
[AD-A207983] N89-29014

TITANIUM
Fundamental aspects of reactions in titanium-silicon thin films for integrated circuits
[ETN-89-95466] N89-28733
A new method of testing nuclear fusion in metals
[IPPJ-915] N89-29215

TITANIUM ALLOYS
The Bauschinger effect in 6-6-2 titanium alloy and its influence on advanced artillery projectiles
[AD-A209355] N89-28623
Fatigue crack growth-microstructural relationship of Ti-6Al-4V
[AD-A208107] N89-28626
Weak beam electron microscopy of dislocation splitting in TiAl: Relationship with plasticity
[ONERA-NT-1988-3] N89-29253

TITANIUM OXIDES
Research on stable, high-efficiency, large-area, amorphous-silicon-based submodules, task B
[DE89-009439] N89-28946

TOKAMAK DEVICES
High power ICRF heating experiments on the JIPP T-IIU tokamak
[IPPJ-903] N89-29209
Caotic magnetic field line in toroidal plasmas
[IPPJ-911] N89-29211
Full consistent analysis of high beta steady state tokamaks sustained by beam driven and bootstrap currents
[IPPJ-912] N89-29212

TOLERANCES (PHYSIOLOGY)
Transient visual effects of prolonged small spot foveal laser exposure
[AD-A207945] N89-29012

TOMOGRAPHY
Positioning error induced by axial sampling in positron emission tomography
[DE89-014519] N89-28791
High resolution subsurface imaging with geophysical diffraction tomography
[DE89-013615] N89-28923

TOPOGRAPHY
Smooth piecewise polynomials as conforming finite elements for plate bending problems
[MEMO-747] N89-28875
JPRS Report: Science and Technology. USSR: Space. 16th International Congress of the International Society for Photogrammetry and Remote Sensing, volume 1
[JPRS-USP-89-002-VOL-1] N89-28876
High resolution Soviet space photographs for topographic mapping N89-28892
Map production and revision with satellite photographs taken by the MKF-6 camera and by the cameras KATE-140, KATE-200, and KFA-1000 N89-28893
National report of Polish Society of Photogrammetry and Remote Sensing N89-28895
Three-dimensional computer analysis and modelling of remote sensing-structural geologic problems
[DE89-010875] N89-28924
Integrating satellite data with information from topographic maps: Method and applications — SPOT
[NLR-MP-87035-U] N89-28933
Improvement of classification results of satellite imagery using context information from a topographic map
[NLR-MP-88020-U] N89-28935
Updating land-use information on topographic maps using satellite imagery: Combining the advantages of two accessible sources of geographic information
[NLR-MP-88030-U] N89-28936

TOPOLOGY
Numerical grid generation in 3D Euler-flow simulation
[NLR-MP-88013-U] N89-28777

TOROIDAL PLASMAS
Caotic magnetic field line in toroidal plasmas
[IPPJ-911] N89-29211

TOROIDAL SHELLS
Analytical solutions for the field, current density, force force density and mechanical stress distribution in toroidal coil systems
[IPP-2/294] N89-28726

TORQUE
Consideration of gravity gradient stabilization for ORION
[AD-A207845] N89-28557

TORSION
A torsional suspension system for testing space structures
[NASA-CASE-LAR-14149-1-SB] N89-28547
Flexural-torsional buckling of monosymmetric beam-columns/tie beams
[PB89-191654] N89-28859

TORUSES
A torus bifurcation theorem with symmetry
[NASA-CR-185907] N89-29135

TOUGHNESS
Measurement of mode 1 and mode 2 strain energy release rates: A VAMAS round robin project on delamination of composite materials — Versailles project on advanced materials and standards (VAMAS)
[NPL-DMA(A)-178] N89-28583
Some recent results on long cycles in tough graphs
[MEMO-765] N89-29130

TRACE CONTAMINANTS
The scavenging of atmospheric pollutants by clouds and precipitation using a vertical wind tunnel, phase 1
[BPT-9/88] N89-28525

TRACE ELEMENTS
Reversal electron attachment ionizer for detection of trace species
[NASA-CASE-NPO-17596-1-CU] N89-28795

TRACKING (POSITION)
Multitarget tracking by single sensor analysis of the main approaches developed in this area
[ONERA-NT-1988-10] N89-28702
Exploring virtual worlds with head-mounted displays
[AD-A208088] N89-28797
Near-neighbor algorithms for processing bearing data
[AD-A207935] N89-29053
Acoustical tracking of fast maneuvering aircraft by distributed sensors
[REPT-6-88] N89-29156
Realtime tracking system for the wide-field-of-view telescope project
[DE89-013787] N89-29186

TRAILING EDGE FLAPS
Wind tunnel tests of 16 percent thick airfoil with 30 percent trailing edge flap at high angles of attack and with flap angles
[FFA-TN-1985-58] N89-28500
Experimental and numerical investigation of coherent structures in turbulent wake flows
[AD-A207866] N89-28759

TRAILING EDGES
Wake dissipation and total pressure loss in a two-dimensional compressor cascade with crenulated trailing edges
[AD-A209176] N89-28755

TRAJECTORIES
Numerical determination of the location of critical inclinations for long term high eccentricity orbits about Mars
[AD-A209200] N89-28538
Orbit determination of sunlight illuminated objects detected by overhead platforms
[AD-A209227] N89-28540
Application of computational fluid dynamics to the analysis of the aerodynamics of a railgun projectile
[AD-A207758] N89-28758

TRANSCENDENTAL FUNCTIONS
Signed-digit high speed transcendental function processor architecture
[AD-A209199] N89-29110
TRANSDUCERS
A method for evaluating structural transducers used in Type B package testing
[DE89-013591] N89-28784
The PVF2 piezoelectric polymer shock stress sensor: System characterization for application under field test conditions
[DE89-014629] N89-28790
Helium bottle pressure measurement by portable ultrasonic technique
[AD-A208994] N89-29188
TRANSFER FUNCTIONS
Model simplification based on the concept of equivalent dead time
[NAL-TM-SE-8802] N89-28521
TRANSFERRING
Collisional transfer between and quenching of the 3p 3p and 5p states of the oxygen atom
[AD-A207759] N89-28607
Transfer of files between IE-32C PC/AT CAD system and Autotrol AD/380 graphics system
[PD-CC-8903] N89-29270
TRANSFORMATIONS (MATHEMATICS)
TIME: Time and memory efficient distance transformations for parallel and pyramid machines
[FOA-C-30531-3.4] N89-29091
TRANSIENT LOADS
The effect of transients on crack tip stress fields during thermal fatigue loading
[AD-A210064] N89-28864
TRANSISTORS
Electrical characterization of signal processing microcircuit
[AD-A209078] N89-28714
Vortices in long Josephson junctions
[AD-A207936] N89-29250
TRANSITION METALS
Oxidative addition of C-H bonds in organic molecules to transition metal centers
[DE89-012991] N89-28616
TRANSITION PROBABILITIES
Collision dynamics and transition probabilities for vibrationally excited OH
[AD-A207856] N89-28976
TRANSITION TEMPERATURE
States of oxygen ordering in YBa2Cu3Oz
[DE89-014893] N89-29227
TRANSMISSION
The relationship between ground permittivity and the input impedance of a horizontal dipole near ground
[AD-A207746] N89-28688
TRANSMISSION EFFICIENCY
Apparatus and method for characterizing the transmission efficiency of a mass spectrometer
[NASA-CASE-NPO-16989-1-CU] N89-28794
A satellite assisted-tracking system with real-time accommodation for maximal pointing N89-28885
TRANSMISSION FLUIDS
Pressure drop and heat transfer characteristics of nearly neutrally buoyant particulate slurry for advanced energy transmission fluids
[DE89-013645] N89-28751
TRANSMITTANCE
The Strategic High-Altitude Atmospheric Radiation Code (SHARC) user instructions
[AD-A207667] N89-28974
Aeronomic problems of molecular oxygen photodissociation. 6: Photodissociation frequency and transmittance in the spectral range of the Schumman-Runge bands
[AERONOMICA-ACTA-A-342-1989-6] N89-28981
Radiative transfer in falling snow: A two-stream approximation
[AD-A208960] N89-29187
TRANSMITTER RECEIVERS
A fully automated, single-connection tester for T/R modules
[DE89-013155] N89-28786
TRANSONIC FLOW
Role of supercomputer in computational aerodynamics
[PD-CF-8925] N89-28496
A detailed survey of the flow passing through an asymmetric contraction and parallel duct
[BAE-WWT-RP-RES-AXR-000194-PT-A] N89-28501
A detailed survey of the flow passing through an asymmetric contraction and parallel duct
[BAE-WWT-RP-RES-AXR-000194-PT-B] N89-28502
TRANSONIC FLUTTER
Some computations of unsteady Navier-Stokes flow around oscillating airfoil/wing
[NAL-TR-1004T] N89-28492
TRANSONIC WIND TUNNELS
A detailed survey of the flow passing through an asymmetric contraction and parallel duct
[BAE-WWT-RP-RES-AXR-000194-PT-A] N89-28501
A detailed survey of the flow passing through an asymmetric contraction and parallel duct
[BAE-WWT-RP-RES-AXR-000194-PT-B] N89-28502
TRANSPARENCE
Specifications and measurement procedures and aircraft transparencies
[AD-A209396] N89-28511
TRANSPORT PROPERTIES
Analysis of the regenerative cooling of a rocket motor fed with monomethylhydrazine and nitrogen tetroxide
[ETN-89-94976] N89-28569
Hypersonic vehicle environment simulation, phase 1
[AD-A209030] N89-28754
Differential equations and continuum mechanics --- polymers
[AD-A208637] N89-29109
TRAPPED MAGNETIC FIELDS
Method of mass producing superconducting persistent current rings
[AD-D013968] N89-29219
TRAPPED PARTICLES
Unlimited acceleration of particles by a system of multi-laser beams
[IPPJ-902] N89-29208
Applied field and total dose dependence of trapped charge buildup in MOS devices
[AD-A209064] N89-29237
TRAVELING WAVE TUBES
Study of sintered magnets of the Nd-Fe-B type
[AD-A209185] N89-29148
TREES (MATHEMATICS)
A graph-theoretical approach to block-co-polymer complexes. Part 2: Tree approximation
[MEMO-758-PT-2] N89-28655
TRIANGULATION
National report of Polish Society of Photogrammetry and Remote Sensing N89-28895
An algorithm for smooth interpolation to scattered data in R2
[MEMO-748] N89-29066
Total Lagrangian formulation for large-displacement analysis of the triangular finite elements
[AD-A209378] N89-29111
Placing the largest similar copy of a convex polygon among polygonal obstacles
[AD-A210104] N89-29115
TRIBOLOGY
The tribology of undulated surfaces
[AD-A209275] N89-28837
High temperature tribometer, phase 1
[AD-A209356] N89-28838
TRIGONOMETRIC FUNCTIONS
New infinite-dimensional algebras, sine brackets, and SU (infinity)
[DE89-013178] N89-29108
TRITIUM
Determination of moisture diffusion in carbon fiber reinforced epoxy composites by means of radioisotope tracer technique
[BMVG-FBWT-88-2] N89-28581
TROPICAL METEOROLOGY
The WMO research and development program 1988-1997: Second WMO long-term plan, part 2, volume 3
[WMO-693-PT-2-VOL-3] N89-28997
TROPICAL REGIONS
Training Course for Tropical Earth Resources Satellite (EARS) bridging phase
[BCRS-88-16D] N89-28938
TUMORS
Energy and Technology Review --- analytical cytology
[DE89-013919] N89-28954
TUNGSTEN ALLOYS
Freeze-dried tungsten heavy alloys
[DE89-014933] N89-28620
TUNING
Field induced gap infrared detector
[NASA-CASE-NPO-17526-1-CU] N89-28796
TURBINE BLADES
Three-dimensional airfoil performance measurements on a rotating wing
[DE89-009443] N89-28487
TURBINES
Superconducting Meissner effect bearings for cryogenic turbomachines, phase 1
[AD-A209875] N89-28839
TURBOFAN ENGINES
Aerodynamic model tests of exhaust augmentors for F/A-18 engine run-up facility at RAAF Williamtown
[AD-A208110] N89-28518
A real time microcomputer implementation of sensor failure detection for turbofan engines
[NASA-TM-102327] N89-29032
TURBOJET ENGINE CONTROL
A real time microcomputer implementation of sensor failure detection for turbofan engines
[NASA-TM-102327] N89-29032
TURBOMACHINERY
Superconducting Meissner effect bearings for cryogenic turbomachines, phase 1
[AD-A209875] N89-28839
Turbomachinery shaft insert
[NASA-CASE-MFS-28345-2] N89-28842
TURBULENCE
Measurements of mean-flow and turbulence characteristics in a turbojet exhaust using a laser velocimeter
[ISL-CO-226/88] N89-28519
Fast-algorithm development for large-eddy simulation of circular-jet turbulence
[AD-A207928] N89-28760
Linear theory of uncompensated thermal blooming in turbulence
[DE89-014604] N89-28812
The coagulation and dispersion of nonspherical, aerosol particles in a turbulent atmosphere
[AD-A208064] N89-29150
Caviton dynamics in strong Langmuir turbulence
[DE89-012635] N89-29202
TURBULENCE MODELS
Large scale motions in supersonic turbulent boundary layers N89-28736
Calculation of reattaching shear layers in divergent channel with a multiple-time-scale turbulence model
[NASA-TM-102293] N89-28749
Discussion of the potential and limitations of direct and large-eddy simulations
[NASA-CR-181892] N89-28762
A preliminary compressible second-order closure model for high speed flows
[NASA-CR-181875] N89-28764
Noise produced by turbulent flow into a rotor: Users manual for noise calculation
[NASA-CR-181790] N89-29152
United States Air Force Research Initiation Program for 1987, volume 2
[AD-A209727] N89-29259
TURBULENT BOUNDARY LAYER
A survey of measurements and measuring techniques in rapidly distorted compressible turbulent boundary layers
[AGARD-AG-315] N89-28734
Large scale motions in supersonic turbulent boundary layers N89-28736
Fluctuating wall-pressure measurements N89-28741
General comments on the interpretation of data --- mean flow for rapidly distorted turbulent boundarylayers N89-28742
Review of mean flow data --- for compressible boundary layers N89-28743
Review of turbulence data --- for turbulent compressible boundary layers N89-28744
The entries N89-28745
TURBULENT DIFFUSION
A preliminary compressible second-order closure model for high speed flows
[NASA-CR-181875] N89-28764
Application of similarity methods to the turbulent diffusion in the convective and stable boundary layer
[WISS-BER-12] N89-28979
TURBULENT FLOW
Rapidly distorted compressible boundary-layers N89-28735
Calculation of reattaching shear layers in divergent channel with a multiple-time-scale turbulence model
[NASA-TM-102293] N89-28749
Experimental and numerical investigation of coherent structures in turbulent wake flows
[AD-A207866] N89-28759
Discussion of the potential and limitations of direct and large-eddy simulations
[NASA-CR-181892] N89-28762
On the large-eddy simulation of transitional wall-bounded flows
[NASA-CR-181883] N89-28763
A preliminary compressible second-order closure model for high speed flows
[NASA-CR-181875] N89-28764
Analysis of turbulent transport phenomena in the maritime atmospheric boundary layer
[WISS-BER-10] N89-28978
Noise produced by turbulent flow into a rotor: Users manual for noise calculation
[NASA-CR-181790] N89-29152

Noise produced by turbulent flow into a rotor: Users manual for atmospheric turbulence prediction and mean flow and turbulence contraction prediction
[NASA-CR-181791] N89-29154

TURBULENT HEAT TRANSFER
Heat transfer and film cooling in compressible nozzle flow
[ETN-89-94653] N89-28773

TWO DIMENSIONAL FLOW
Profile-vortex interactions
[ISL-R-125/87] N89-28495
Wake dissipation and total pressure loss in a two-dimensional compressor cascade with crenulated trailing edges
[AD-A209176] N89-28755
Fast-algorithm development for large-eddy simulation of circular-jet turbulence
[AD-A207926] N89-28760
Finite element analysis of incompressible viscous flows around single and multi-element aerofoils in high Reynolds number region
[NAL-TR-1010T] N89-28765
Comparison between two different techniques of computing the axial induction for horizontal axis wind turbines in a locally deformed flow field
[FFA-TN-1988-56] N89-28959

TWO PHASE FLOW
Pressure drop and heat transfer characteristics of nearly neutrally buoyant particulate slurry for advanced energy transmission fluids
[DE89-013645] N89-28751
Analysis of flow boiling of ammonia and R-114 in a matrix heat exchanger
[DE89-012427] N89-28752

U

U.S.S.R.
International technology transfer as practiced by the U.S.S.R.: Implications for US national security
[AD-A208010] N89-29274

U.S.S.R. SPACE PROGRAM
JPRS report: Science and technology. USSR report: Life sciences
[JPRS-USP-89-005] N89-28527
Development, testing procedures for Buran shuttle N89-28531

ULTRAHIGH FREQUENCIES
Analysis of the VHF-UHF electromagnetic radiation of lightning: Application to a model of the negative stepped-leader propagation
[ONERA-NT-1989-1] N89-29000

ULTRAHIGH VACUUM
A bolt-on deposition source for ultra-high-vacuum growth of intermetallic compound films
[AD-A209699] N89-29242

ULTRASONIC TESTS
Comparative analysis of ultrasonic inspection procedures for Kaman K747 root end fittings
[AD-A207762] N89-28512
Helium bottle pressure measurement by portable ultrasonic technique
[AD-A208994] N89-29188

ULTRASONICS
Ultrasonic imaging of textured alumina
[NASA-TM-101478] N89-28853
Ultrasonic systems and system development at SNL Albuquerque
[DE89-013164] N89-29153
Helium bottle pressure measurement by portable ultrasonic technique
[AD-A208994] N89-29188
Ultrasonic attenuation in heavy fermion superconductors
[DE89-014937] N89-29231

ULTRAVIOLET ABSORPTION
Absorption cross section of alternative chlorofluoroethanes and potential effects on the ozone layer
[AERONOMICA-ACTA-A-340-1989] N89-28968

ULTRAVIOLET RADIATION
A study of the ultraviolet degradation embrittlement of polypropylene polymer
[ISBN-90-9002498-0] N89-28656
Atmospheric processes and effects on materials
[PB89-173215] N89-28964

ULTRAVIOLET SPECTRA
Multivariate analysis of UV-spectral data for solute tracking in HPLC
[ISBN-90-6275-535-6] N89-28614

UNITED STATES
Fuel cell technology in the United States
[DE89-013430] N89-28951

UNIVERSE
Cosmic relics from the big bang
[DE89-013268] N89-29283

UNIX (OPERATING SYSTEM)
Design aspects of a system for geocoding satellite SAR images N89-28915
The use of a UNIX-based workstation in the Information Systems Laboratory
[AD-A209485] N89-29267

UNMANNED SPACECRAFT
Development, testing procedures for Buran shuttle N89-28531

UNSTEADY FLOW
Some computations of unsteady Navier-Stokes flow around oscillating airfoil/wing
[NAL-TR-1004T] N89-28492

UP-CONVERTERS
Development of an integrated AM shortwave upconversion receiver front-end
[ETN-89-95455] N89-28699

UPPER ATMOSPHERE
Hypersonic vehicle environment simulation, phase 1
[AD-A209030] N89-28754

URBAN DEVELOPMENT
Monitoring and measuring human settlement changes by remote sensing methods
[BCRS-88-16C] N89-28937

USER MANUALS (COMPUTER PROGRAMS)
User's guide to the complex terrain dispersion model plus algorithms for unstable situations (CTDMPLUS). Volume 1: Model description and user instructions
[PB89-181424] N89-28963
PC to mainframe connection: IBM PC 3270 emulation
[AD-A209204] N89-29033
Design and development of a user interface and user manual for a system dynamics model of software management
[AD-A209486] N89-29048
A user's guide to the SEVP (Stabilized Error Vector Propagation) solver: An efficient direct solver for elliptic partial differential equations
[AD-A208117] N89-29121
Noise produced by turbulent flow into a rotor: Users manual for noise calculation
[NASA-CR-181790] N89-29152
Noise produced by turbulent flow into a rotor: Users manual for atmospheric turbulence prediction and mean flow and turbulence contraction prediction
[NASA-CR-181791] N89-29154
The use of a UNIX-based workstation in the Information Systems Laboratory
[AD-A209485] N89-29267

USER REQUIREMENTS
Direct User Access Terminal (DUAT) operational concept
[WP-88W00075] N89-28524
The use of expert systems for preprocessing image data
[NLR-MP-88009-U] N89-28934
Design and development of a user interface and user manual for a system dynamics model of software management
[AD-A209486] N89-29048
Tools for the development and usage of industrial mathematical software
[NLR-MP-87020-U] N89-29067
Information requirements and the implications for parallel computation
[AD-A207802] N89-29088

UTILIZATION
Methods of combinatorial optimization and their range of applicability
[MEMO-766] N89-29073

V

VACUUM DEPOSITION
Ion beam deposition of epitaxial germanium and gallium arsenide layers
[DE89-014044] N89-29225
A bolt-on deposition source for ultra-high-vacuum growth of intermetallic compound films
[AD-A209699] N89-29242

VALIDITY
On the shape of mathematical arguments
[ETN-89-95465] N89-29133

VANADIUM
The Bauschinger effect in 6-6-2 titanium alloy and its influence on advanced artillery projectiles
[AD-A209355] N89-28623

VANADIUM ALLOYS
Fatigue crack growth-microstructural relationship of Ti-6Al-4V
[AD-A208107] N89-28626

VAPOR DEPOSITION
Fundamental studies of grain boundary structure and properties in ICB aluminum
[DE89-014884] N89-28619
Monolithic narrow-linewidth InGaAsP semiconductor laser for coherent optical communications
[NASA-CR-181870] N89-28821
Multilayered electronic materials and devices based on 3-5 compounds
[AD-A208861] N89-29233
Photoelectrochemical fabrication of gratings in SiC
[AD-A208992] N89-29236
Selective area epitaxy of gallium arsenide on silicon, phase 1
[AD-A209079] N89-29238

VAPOR PHASES
The aggregated state of matter: Elucidating transitions from the gas to the condensed phase and the formation of aerocolloids
[AD-A209080] N89-28595

VARIATIONAL PRINCIPLES
Solution of Euler equations by a discontinuous Galerkin method obtained from a variational formulation of entropy
[CERT-1/332400/DERI] N89-28775
A dynamic variation principle for elastic-fluid contacts, applied to elastohydrodynamic lubrication theory
[MEMO-746] N89-28782
Variational formulation for a nonlinear elliptic equation in a three-dimensional exterior domain
[NASA-CR-181885] N89-29028

VARISTORS
Experimental and theoretical study of transient behavior of varistors
[AD-A209081] N89-28715

VECTOR ANALYSIS
QuickDraw data structures for image processing
[AD-A208945] N89-29041
Signed-digit high speed transcendental function processor architecture
[AD-A209199] N89-29110

VECTOR PROCESSING (COMPUTERS)
ERS-1 SAR processing with CESAR N89-28888

VECTORS (MATHEMATICS)
Acousto-optical vector matrix product processor: Implementation issues
[AD-A207933] N89-28722

VELOCITY COUPLING
Bifurcation and pattern formation in combustion
[DE89-013629] N89-28590

VELOCITY MEASUREMENT
Evaluation of LDA 3-component velocity data on a 65 deg delta wing at M = 0.85 and first results of an analysis
[DFVLR-FB-89-19] N89-28505
A survey of measurements and measuring techniques in rapidly distorted compressible turbulent boundary layers
[AGARD-AG-315] N89-28734
Hot-wire anemometry in supersonic flow N89-28738
Laser Doppler anemometry N89-28739
Laser Doppler anemometry in supersonic flows: Problems of seeding and angular bias N89-28740
The use of high-frequency pulsed laser diodes in fringe type laser Doppler anemometry
[ISL-CO-230/88] N89-28826

VENUS (PLANET)
Method for research on planet Venus using floating balloon stations: Mathematical model N89-28532

VENUS PROBES
Method for research on planet Venus using floating balloon stations: Mathematical model N89-28532

VERTICAL ORIENTATION
Kinematic vertical positioning using the global positioning system
[ETN-89-94804] N89-28510

VERY HIGH FREQUENCIES
Meteor burst system communications compatibility
[PB89-191167] N89-28692
Analysis of the VHF-UHF electromagnetic radiation of lightning: Application to a model of the negative stepped-leader propagation
[ONERA-NT-1989-1] N89-29000

VERY LARGE SCALE INTEGRATION
Systolic VLSI array for implementing the Kalman filter algorithm
[NASA-CASE-NPO-17108-1-CU] N89-28713
VLSI integrated circuit contact reliability by interface spectroscopy
[AD-A207666] N89-28718
A partitioning and redundancy model for wafer scale integrated circuits
[MEMO-INF-88-65] N89-28730
Routing channels in VLSI layout
[ISBN-90-6275-535-4] N89-28731

Accurate and efficient modeling of global circuit behavior in VSLI layouts
[ETN-89-95459] N89-28732
The design of VLSI circuits
[ETN-89-94968] N89-29065
TWENTENET chip design
[MEMO-INF-88-49] N89-29090
Three dimensional cellular automata for subpixel target detection
[AD-A208163] N89-29100
Study and simulation of an E-beam microlithography process on a multilayer resin structure. Research of an optimization
[LAAS-89.012] N89-29179

VERY LOW FREQUENCIES
NEC (Numerical Electromagnetics Code), NECGS (Numerical Electromagnetics Code-Ground Screen), and MININEC (Mini-Numerical Electromagnetics Code) numerical models of LF top-hat monopole antennas
[AD-A209230] N89-28683

VESTIBULAR NYSTAGMUS
Visual suppression of the vestibulo-ocular reflex during space flight
[NASA-TM-102157] N89-29017

VIBRATION
High resolution electron energy loss studies of surface vibrations
[DE89-013964] N89-28589
Vibrational dynamics of aniline (Ar)1 and aniline (CH4)1 clusters
[AD-A209560] N89-28605
Vibration analyzer
[NASA-CASE-MSC-21408-1] N89-28829

VIBRATION DAMPING
Development of damping treatment suitable for high temperature environment
[ISVR-TR-174] N89-28652
Optimization of structures with passive damping and active controls
[AD-A208937] N89-28862
Residual vibration reduction in computer controlled machines
[AD-A208074] N89-28866
Nonlinear dynamics and control of flexible structures
[AD-A208120] N89-28869

VIBRATION EFFECTS
Application of optimal control theory for selective vibrational excitation in molecules modeled as harmonic systems
[MEMO-755] N89-29104

VIBRATIONAL SPECTRA
The Los Alamos Fourier-transform spectrometer: Applications to molecular spectroscopy
[DE89-014258] N89-28789
Residual vibration reduction in computer controlled machines
[AD-A208074] N89-28866
Collision dynamics and transition probabilities for vibrationally excited OH
[AD-A207856] N89-28976

VIDEO DISKS
Conversion of hard-copy documents to digital format utilizing optical scanners and optical storage media
[AD-A209473] N89-29266

VIDEO SIGNALS
Video processing using the MSX computer
[LINO-163] N89-28694

VIEWING
The beam viewer
[LINO-160] N89-28693

VINYL RADICAL
Reaction kinetics and mechanism of chain reactions and explosions via transient spectroscopy
[AD-A209169] N89-28597

VIRTUAL MEMORY SYSTEMS
Walkthrough-exploring virtual worlds
[AD-A208087] N89-29057

VISCOMETERS
Standard reference material for high temperature viscosity measurements: Results of interlaboratory comparison programme
[NPL-DMA(A)-175] N89-28612

VISCOMETRY
Standard reference material for high temperature viscosity measurements: Results of interlaboratory comparison programme
[NPL-DMA(A)-175] N89-28612

VISCOSITY
Standard reference material for high temperature viscosity measurements: Results of interlaboratory comparison programme
[NPL-DMA(A)-175] N89-28612
A graph-theoretical approach to block-co-polymer complexes. Part 1: Stars
[MEMO-757-PT-1] N89-28654
A graph-theoretical approach to block-co-polymer complexes. Part 2: Tree approximation
[MEMO-758-PT-2] N89-28655
Lubricant evaluation and performance
[AD-A208925] N89-28835

VISCOUS DRAG
The anisotropy of the friction pressure of dipolar fluids
[ETN-89-94438] N89-28771

VISCOUS FLOW
Three-dimensional viscous hypersonic flow over blunt bodies
[DFVLR-FB-89-09] N89-28504
Hypersonic vehicle environment simulation, phase 1
[AD-A209030] N89-28754
Application of computational fluid dynamics to the analysis of the aerodynamics of a railgun projectile
[AD-A207758] N89-28758
Finite element analysis of incompressible viscous flows around single and multi-element aerofoils in high Reynolds number region
[NAL-TR-1010T] N89-28765

VISION
Components of high-level vision: A cognitive neuroscience analysis and accounts of neurological syndromes
[AD-A207848] N89-29011

VISUAL ACUITY
Components of high-level vision: A cognitive neuroscience analysis and accounts of neurological syndromes
[AD-A207848] N89-29011
Transient visual effects of prolonged small spot foveal laser exposure
[AD-A207945] N89-29012

VISUAL DISCRIMINATION
Investigation of a linear systems model for human visual detection and spatial frequency discrimination
[AD-A209397] N89-29022

VISUAL PERCEPTION
Towards a physiologically based HUD (Head-Up Display) symbology
[AD-A207748] N89-28515
Exploring virtual worlds with head-mounted displays
[AD-A208088] N89-28797
Suprathreshold contrast sensitivity vision test chart
[AD-A209915] N89-29010
Visual suppression of the vestibulo-ocular reflex during space flight
[NASA-TM-102157] N89-29017
Investigation of a linear systems model for human visual detection and spatial frequency discrimination
[AD-A209397] N89-29022

VISUAL SIGNALS
Towards a physiologically based HUD (Head-Up Display) symbology
[AD-A207748] N89-28515

VOLTAGE REGULATORS
Optical gain control of GaAs microwave monolithic integrated circuit distributed amplifier
[AD-D013969] N89-28705

VOLUME
Three dimensional reconstruction from serial cross sections by set valued interpolation
[MEMO-754] N89-29076

VORTEX SHEDDING
One-degree-of-freedom motion induced by modeled vortex shedding
[NASA-TM-101038] N89-28870

VORTICES
Comparison of flow-visualised vortices with computed geometry over thin delta wings
[AD-A209083] N89-28489
Study of the wing-vortex interaction in three dimensional flows (incompressible inviscid flow)
[ISL-R-123/87] N89-28494
Profile-vortex interactions
[ISL-R-125/87] N89-28495
A detailed survey of the flow passing through an asymmetric contraction and parallel duct
[BAE-WWT-RP-RES-AXR-000194-PT-A] N89-28501
A detailed survey of the flow passing through an asymmetric contraction and parallel duct
[BAE-WWT-RP-RES-AXR-000194-PT-B] N89-28502
Wake dissipation and total pressure loss in a two-dimensional compressor cascade with crenulated trailing edges
[AD-A209176] N89-28755
Fast-algorithm development for large-eddy simulation of circular-jet turbulence
[AD-A207928] N89-28760
Discussion of the potential and limitations of direct and large-eddy simulations
[NASA-CR-181892] N89-28762
Entrainment and homogenization of a passive tracer in a numerical model gyre
[AD-A208020] N89-29005
Aircraft propeller induced structure-borne noise
[NASA-CR-4255] N89-29155
Vortices in long Josephson junctions
[AD-A207936] N89-29250

VORTICITY
A compressible inverse design method based on an analytical approach
[CUED/A-TURBO/TR-125] N89-28778

VULNERABILITY
Operational test plan concept for evaluation of close air support alternative aircraft
[AD-A208185] N89-28513

W

WAFERS
A partitioning and redundancy model for wafer scale integrated circuits
[MEMO-INF-88-65] N89-28730
Laser-induced diode linking for wafer-scale integration
[AD-A207921] N89-28818
A manufacturing scheduler's perspective on semiconductor fabrication
[AD-A208372] N89-29232
Multilayered electronic materials and devices based on 3-5 compounds
[AD-A208861] N89-29233
Selective area epitaxy of gallium arsenide on silicon, phase 1
[AD-A209079] N89-29238

WAKES
Wake dissipation and total pressure loss in a two-dimensional compressor cascade with crenulated trailing edges
[AD-A209176] N89-28755

WALKING MACHINES
A robot that walks: Emergent behaviors from a carefully evolved network
[AD-A207958] N89-29026

WALL FLOW
On the large-eddy simulation of transitional wall-bounded flows
[NASA-CR-181883] N89-28763
A nonlinear investigation of the stationary modes of instability of the three-dimensional compressible boundary layer due to a rotating disc
[NASA-CR-181901] N89-28766

WALL PRESSURE
Fluctuating wall-pressure measurements N89-28741

WARFARE
Sleep deprivation and its effect on combat effectiveness
[AD-A207970] N89-29013

WARNING SYSTEMS
Collision avoidance operational concept
[WP-88W00418] N89-28509

WASTE DISPOSAL
High-temperature superconductor materials processing: Development of environmentally acceptable processing technologies
[DE89-014391] N89-29229

WASTE TREATMENT
Method and apparatus for bio-regenerative life support system
[NASA-CASE-MSC-21629-1] N89-29027

WASTE UTILIZATION
Chemical Technology Division
[DE89-013917] N89-28591

WASTE WATER
A combined air and water pollution control system
[NASA-CASE-NST-00007-1] N89-28967

WATER POLLUTION
A combined air and water pollution control system
[NASA-CASE-NST-00007-1] N89-28967

WATER RESOURCES
Military hydrology: Assessment of shuttle imaging radar and LANDSAT imagery for ground-water exploration in arid environments
[AD-A209527] N89-28928

WATER TREATMENT
A combined air and water pollution control system
[NASA-CASE-NST-00007-1] N89-28967
Method and apparatus for bio-regenerative life support system
[NASA-CASE-MSC-21629-1] N89-29027

WATER TUNNEL TESTS
Small scale model tests in small wind and water tunnels at high incidence and pitch rates. Volume 1: Test program and discussion of results
[AD-A208647] N89-28488

WATER VAPOR
Application of special sensor microwave/imager data for analysis of cyclonic storms in midlatitudes over the sea
[AD-A207675] N89-28975

WATER WAVES
Lidar measurements of sea surface waves
N89-28909
Hurricane hindcast methodology and wave statistics for Atlantic and Gulf hurricanes from 1956 - 1975
[AD-A207849] N89-29004
WAVE EQUATIONS
Linear theory of uncompensated thermal blooming in turbulence
[DE89-014604] N89-28812
Signed-digit high speed transcendental function processor architecture
[AD-A209199] N89-29110
WAVE FUNCTIONS
The inverse scattering problem for acoustic and electromagnetic waves
[AD-A209202] N89-28881
Electron energy levels in a quantum well within an in-plane magnetic field
[AD-A209351] N89-29256
WAVE PACKETS
Electromagnetic pulse propagation through a stratified ionosphere
[IRF-SR-199] N89-28700
WAVE PROPAGATION
Numerical simulation of the simultaneous detonation of two identical, fully contained explosions
[DE89-014844] N89-28660
Linear theory of uncompensated thermal blooming in turbulence
[DE89-014604] N89-28812
Propagation and saturation of nonlinear inertia-gravity waves in the atmosphere
[AD-A207871] N89-28989
Propagation problem and far-field patterns in a stratified finite depth ocean
[PB89-180707] N89-29001
WAVE REFLECTION
Exact image theory for uniaxially anisotropic dielectric half space
[PB89-146450] N89-28671
WAVEFORMS
Reciprocal perfect and asymptotically perfect periodic radar waveforms and their aperiodic properties
[AD-A208936] N89-28677
WAVEGUIDES
Scattering representation of waveguide/cavity discontinuities using mode-matching and the least-squares boundary residual
[AD-A209571] N89-28686
Slotted-waveguide amplifiers for millimeter waves
[AD-A207932] N89-28721
Monolithic narrow-linewidth InGaAsP semiconductor laser for coherent optical communications
[NASA-CR-181870] N89-28821
WAVELENGTHS
Field induced gap infrared detector
[NASA-CASE-NPO-17526-1-CU] N89-28796
WEAK INTERACTIONS (FIELD THEORY)
Measurement of electroweak effects and topological branching conditions in the reaction e(+)e(-) yields tau(+)tau(-) in the storage ring PETRA
[MPI-PAE/EXP.EL-195] N89-29173
Research program in computational physics
[DE89-013952] N89-29255
WEAPON SYSTEMS
Computer-aided group problem solving for Unified Life Cycle Engineering (ULCE)
[AD-A209446] N89-29260
WEAR TESTS
A study of the ultraviolet degradation embrittlement of polypropylene polymer
[ISBN-90-9002498-0] N89-28656
Lubricant evaluation and performance
[AD-A208925] N89-28835
High temperature tribometer, phase 1
[AD-A209356] N89-28838
WEATHER
Application of special sensor microwave/imager data for analysis of cyclonic storms in midlatitudes over the sea
[AD-A207675] N89-28975
Storm models for end-to-end TDWR (Terminal Doppler Weather Radar) signal processing simulation tests
[AD-A209384] N89-28986
The WMO long-term plan overall policy and strategy 1988-1997: Second WMO long-term plan, part 1
[WMO-690-PT-1] N89-28994
WEATHER FORECASTING
Satellite-derived moisture-bogusing profiles for the North Atlantic Ocean
[AD-A207829] N89-28930
The World Weather Watch Program 1988-1997: Second WMO long-term plan, part 2, volume 1
[WMO-691-PT-2-VOL-1] N89-28995
The WMO research and development program 1988-1997: Second WMO long-term plan, part 2, volume 3
[WMO-693-PT-2-VOL-3] N89-28997
Hurricane hindcast methodology and wave statistics for Atlantic and Gulf hurricanes from 1956 - 1975
[AD-A207849] N89-29004
WEATHERING
Five year ground exposure of composite materials used on the Bell Model 206L flight service evaluation
[NASA-TM-101645] N89-28579
A study of the ultraviolet degradation embrittlement of polypropylene polymer
[ISBN-90-9002498-0] N89-28656
Characterization of painted surfaces in the United States from the perspective of potential damage from acidic deposition
[DE89-014264] N89-28965
WEIGHTLESSNESS
Muscle changes with eccentric exercise: Implications on earth and in space
[NASA-TM-102227] N89-29016
WEIGHTLESSNESS SIMULATION
Hollow fiber clinostat: Technical abstract
[NASA-CASE-MFS-28370-1] N89-28793
WELDED STRUCTURES
Preliminary design of a consultation knowledge-based system for the minimization of distortion in welded structures
[AD-A208842] N89-28834
WELDING
Preliminary design of a consultation knowledge-based system for the minimization of distortion in welded structures
[AD-A208842] N89-28834
An improved design for stretched-membrane heliostats
[DE89-013872] N89-28953
WEST GERMANY
Activities report in aerospace research in Germany, F.R.
[ISSN-0070-3966] N89-28485
WHEEL BRAKES
Aircraft accident/incident summary reports: Belleville, Illinois, August 22, 1987; Pensacola, Florida, December 27, 1987
[PB89-910405] N89-28507
WICKS
Mathematical modeling and analysis of heat pipe start-up from the frozen state
[NASA-CR-185132] N89-28747
WIDE ANGLE LENSES
Realtime tracking system for the wide-field-of-view telescope project
[DE89-013787] N89-29186
WIND (METEOROLOGY)
Daytime turbulent exchange between the Amazon forest and the atmosphere
[NASA-CR-185487] N89-28961
Application of special sensor microwave/imager data for analysis of cyclonic storms in midlatitudes over the sea
[AD-A207675] N89-28975
European crosswind frequencies
[AD-A209137] N89-28985
The WMO research and development program 1988-1997: Second WMO long-term plan, part 2, volume 3
[WMO-693-PT-2-VOL-3] N89-28997
WIND DIRECTION
European crosswind frequencies
[AD-A209137] N89-28985
WINDROSE: A program for IBM-compatible personal computers, documentation
[PB89-167423] N89-29039
WIND MEASUREMENT
The boundary layer wind regime of a representative tropical African region, central Sudan
[KNMI-WR-88-04] N89-28982
WINDROSE: A program for IBM-compatible personal computers, documentation
[PB89-167423] N89-29039
WIND PRESSURE
Three-dimensional airfoil performance measurements on a rotating wing
[DE89-009443] N89-28487
Wind models for the NSTS ascent trajectory biasing for wind load alleviation
[NASA-TM-100375] N89-28551
Canadian Forces aircrew ejection, descent, and landing injuries, 1 January 1975 - 31 December 1987
[AD-A208116] N89-29015
WIND PROFILES
Wind models for the NSTS ascent trajectory biasing for wind load alleviation
[NASA-TM-100375] N89-28551
Wind profile estimation from point to point laser distortion data
[NASA-CR-185891] N89-28990
WIND SHEAR
Storm models for end-to-end TDWR (Terminal Doppler Weather Radar) signal processing simulation tests
[AD-A209384] N89-28986
Wind profile estimation from point to point laser distortion data
[NASA-CR-185891] N89-28990
WIND TUNNEL MODELS
Small scale model tests in small wind and water tunnels at high incidence and pitch rates. Volume 1: Test program and discussion of results
[AD-A208647] N89-28488
WIND TUNNEL TESTS
Small scale model tests in small wind and water tunnels at high incidence and pitch rates. Volume 1: Test program and discussion of results
[AD-A208647] N89-28488
Wind tunnel tests of 16 percent thick airfoil with 30 percent trailing edge flap at high angles of attack and with flap angles
[FFA-TN-1985-58] N89-28500
A detailed survey of the flow passing through an asymmetric contraction and parallel duct
[BAE-WWT-RP-RES-AXR-000194-PT-A] N89-28501
A detailed survey of the flow passing through an asymmetric contraction and parallel duct
[BAE-WWT-RP-RES-AXR-000194-PT-B] N89-28502
WIND TUNNELS
Small scale model tests in small wind and water tunnels at high incidence and pitch rates. Volume 1: Test program and discussion of results
[AD-A208647] N89-28488
The scavenging of atmospheric pollutants by clouds and precipitation using a vertical wind tunnel, phase 1
[BPT-9/88] N89-28525
WIND TURBINES
Three-dimensional airfoil performance measurements on a rotating wing
[DE89-009443] N89-28487
Damage predictions for wind turbine components using the LIFE2 computer code
[DE89-013813] N89-28952
Comparison between two different techniques of computing the axial induction for horizontal axis wind turbines in a locally deformed flow field
[FFA-TN-1986-56] N89-28959
WIND VELOCITY
European crosswind frequencies
[AD-A209137] N89-28985
WINDROSE: A program for IBM-compatible personal computers, documentation
[PB89-167423] N89-29039
WINDPOWER UTILIZATION
Three-dimensional airfoil performance measurements on a rotating wing
[DE89-009443] N89-28487
WINDSHIELDS
Specifications and measurement procedures and aircraft transparencies
[AD-A209396] N89-28511
WING OSCILLATIONS
Some computations of unsteady Navier-Stokes flow around oscillating airfoil/wing
[NAL-TR-1004T] N89-28492
WING PROFILES
Study of the wing-vortex interaction in three dimensional flows (incompressible inviscid flow)
[ISL-R-123/87] N89-28494
WORK FUNCTIONS
Stochastic processes in CHEMFETs
[AD-A208092] N89-28725
WORKING FLUIDS
Mathematical modeling and analysis of heat pipe start-up from the frozen state
[NASA-CR-185132] N89-28747
Pressure drop and heat transfer characteristics of nearly neutrally buoyant particulate slurry for advanced energy transmission fluids
[DE89-013645] N89-28751
WORKSTATIONS
The use of a UNIX-based workstation in the Information Systems Laboratory
[AD-A209485] N89-29267
WORLD METEOROLOGICAL ORGANIZATION
The WMO long-term plan overall policy and strategy 1988-1997: Second WMO long-term plan, part 1
[WMO-690-PT-1] N89-28994
The World Weather Watch Program 1988-1997: Second WMO long-term plan, part 2, volume 1
[WMO-691-PT-2-VOL-1] N89-28995
The World Climate Program 1988-1997: Second WMO long-term plan, part 2, volume 2
[WMO-692-PT-2-VOL-2] N89-28996

The WMO research and development program 1988-1997: Second WMO long-term plan, part 2, volume 3
[WMO-693-PT-2-VOL-3] N89-28997
The WMO applications of meteorology program 1988-1997: Second WMO long-term plan, part 2, volume 4
[WMO-694-PT-2-VOL-4] N89-28998

X

X RAY ASTRONOMY
Activities report of the Institute for Extraterrestrial Physics
[MPE-212] N89-29277
X RAY BINARIES
The origin and evolution of X-ray binaries and low-magnetic field radio pulsars
[MPE-PREPRINT-145] N89-29284
Millisecond radio pulsars in globular clusters
[NASA-CR-185909] N89-29298
X RAY DIFFRACTION
A new scattering formula for depth-resolving X-ray diffractometry based on a kinematic theory
[ETN-89-94430] N89-29195
X RAY FLUORESCENCE
Dense heavy metal aerosol monitoring by direct X-ray fluorescence
[AD-A209077] N89-28966
X RAY SOURCES
An X-ray source for lithography based on a quasi-optical maser undulator
[AD-A208522] N89-28675
Measurement of the Vela pulsar's proper motion and detection of the optical counterpart of its compact X-ray nebula
[MPE-PREPRINT-151] N89-29288
X RAY SPECTROSCOPY
Electronic-structure study of the Ni-Ga and Ni-In intermetallic compounds using X-ray photoemission spectroscopy
[AD-A209696] N89-28601
X RAYS
An X-ray microprobe using focussing optics with a synchrotron radiation source
[DE89-013425] N89-28788
XENON
Ion optics for high power 50-cm-diam ion thrusters
[NASA-TM-102143] N89-28571

Y

YAWING MOMENTS
Consideration of gravity gradient stabilization for ORION
[AD-A207845] N89-28557
YIELD POINT
Increase of the damage thresholds of dielectric layer systems for the Nd laser
[ETN-89-94436] N89-28824
YIELD STRENGTH
Optimum design methods for structural sandwich panels
[AD-A209427] N89-28575
Plastic yielding of partially-crystalline polymers
[AD-A208101] N89-28648
YTTRIUM COMPOUNDS
Thermal conductivity anisotropy in single crystal YBa2Cu3O7-x
[DE89-009643] N89-29220
YTTRIUM ISOTOPES
Electric quadrupole excitations in the interactions of Y-89 with relativistic nuclei N89-29165
YTTRIUM OXIDES
Metallic bonding to high-temperature superconducting ceramics
[DE89-014668] N89-28635
Microwave sintering of ceramics
[DE89-014769] N89-28636
States of oxygen ordering in YBa2Cu3Oz
[DE89-014893] N89-29227

Z

ZEOLITES
Oxygen storage on zeolites
[AD-A209352] N89-28599
ZINC
Redetermination of crystal structure of zinc thiogallate
[AD-A208931] N89-29234
ZINC OXIDES
Experimental and theoretical study of transient behavior of varistors
[AD-A209081] N89-28715
Materials analysis and device optimization of CuInSe2 solar cells
[DE89-009434] N89-28944
ZINC SULFIDES
Synthesis and hot pressing of ZnS powders
[AD-A209602] N89-28625
ZINC TELLURIDES
Polycrystalline cadmium telluride 3n-i-p solar cell
[DE89-009437] N89-28945
ZIRCONIUM OXIDES
Material and fabrication challenges in the development of monolithic solid oxide fuel cells
[DE89-012422] N89-28957

Typical Personal Author Index Listing

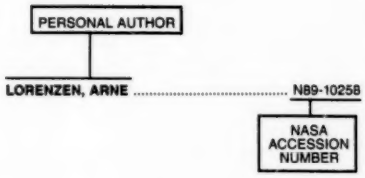

Listings in this index are arranged alphabetically by personal author. The NASA accession number denotes the number by which the citation is identified.

A

ABDEL-FATTAH, A. M. N89-28518
ABE, YOSHIHIKO N89-29211
ABEL, CHARLES E. N89-29004
ABEL, JOHN F. N89-28869
ABUBAKR, EIMAN HASSAN N89-28982
ACHARYA, P. K. N89-26974
ADAIR, ROBERT T. N89-28707
ADAMS, LUCY H. N89-28963
ADAMS, RICH N89-28506
ADAMS, RICHARD R. N89-28550
ADATI, K. N89-29213
ADELFANG, S. I. N89-28551
AGARWAL, ANANT N89-29035
AGUIRRE, JOSE LUIZ DEBARROS N89-28885
AINE, CHERYL N89-29007
N89-29008
AIREY, JOHN M. N89-29057
AKINC, MUFIT N89-28625
AKIYAMA, R. N89-29209
ALAVI, BARAKAT N89-28601
ALBRECHT, W. N89-28581
ALFTER, M. N89-29146
AMANO, T. N89-29210
AMIET, R. K. N89-29152
AMUNDSEN, R. J. N89-29292
ANDERSEN, CARL M. N89-29122
ANDERSON, CLINTON T. N89-29013
ANDERSON, J. N89-29291
ANDO, A. N89-29213
ANDO, R. N89-29209
ANDREWS, J. W. N89-28720
ANGSTEN, G. N89-28643
AOYAGI, YOSHINOBU N89-29243
APERS, PETER M. G. N89-29068
ARAI, KOHEI N89-28886
N89-28921
ARATOW, MICHAEL N89-29016
ARKIN, ESTHER M. N89-29045
ARMINI, A. J. N89-28644
ARMSTRONG, ERNEST S. N89-29047
ARNAUD, MICHEL N89-28914
ASHCROFT, K. B. N89-29029
ASHIDA, H. N89-29210
AUERBACH, STANLEY I. N89-28955
AUGENSTEIN, BRUNO W. N89-29172
AUKERMAN, L. W. N89-29237
AULD, B. A. N89-28863
AUMASSON, CLAUDE N89-29063
AURIERE, MICHEL N89-29268
AUSTIN, AMY BETH N89-29240
AXELROD, TIMOTHY S. N89-29186
AXNAS, I. N89-29216
AZIZ, T. LUKMAN N89-28937

B

BABUSKA, IVO N89-29116
N89-29117
N89-29118
BACHTEL, FREDERICK D. N89-28556
BAI, X. N89-29232
BAILEY, M. C. N89-28550
BAILEY, V. L. N89-28708
BAIN, COLIN D. N89-28594
BAKER, DONALD J. N89-28579
BAKKER, MARTIJN STEVEN COEN N89-29275
BALACHANDRAN, U. N89-28957
BANKS, BRUCE A. N89-28651
BARBOSA, MARCIO NOGUEIRA N89-28905
BARBOSA, PAULO CESAR REGO N89-28917
BARLOW, P. MICHAEL N89-28572
BARNES, NORMAN P. N89-28816
N89-28817
BASS, ARTHUR N89-28922
BASSANO, EDMONDO N89-28783
BASTIERE, ANNIE N89-28703
BATCHELOR, CHERYL L. N89-29019
BATTRICK, B. N89-29295
BATTS, G. W. N89-28551
BAUCHE, BERND N89-28799
BAUER, D. N89-29130
BAUER, F. N89-28801
BAYLESS, R. A. N89-28588
BAYLISS, A. N89-28590
BEAMAN, JOSEPH J. N89-28599
BECKER, HARRY N89-28780
BEKEFI, GEORGE N89-29181
BELL, KEN L. N89-28993
BELL, ZANE W. N89-28852
BELVIN, W. KEITH N89-28550
BENDRIEM, BERNARD N89-28791
BENINGA, KELLY N89-28953
BENNETT, GLORIA A. N89-28926
BENNETT, PHILIP G. N89-28512
BERGMAN, ROBERT G. N89-28616
BERNARDI, CHRISTINE N89-29028
BERNER, C. N89-28774
BERNER, STEVEN N89-28922
BERNIUS, MARK T. N89-28795
BERNSTEIN, E. R. N89-28605
N89-29171
BERNSTEIN, L. S. N89-28974
BERRA, P. BRUCE N89-29096
BERZ, MARTIN N89-29106
BEUMEE, J. G. B. N89-29104
BEUSEKAMP, MARTIN N89-28730
BEYER, JAMES B. N89-29250
BEZERRA, JOLLO CESAR LIMA N89-28917
BEZIAT, JEAN-PAUL N89-29101
BEZY, J. L. N89-28563
N89-28564
BHATTI, IFTEKHAR N89-28975
BIEBUYCK, HANS N89-28637
BIRKMIRE, R. W. N89-28944
N89-28950
BIRN, JOACHIM N89-28970
BISSCHOP, J. J. N89-29075
BLACKBURN, LINDA B. N89-28621
BLANKEN, HENK N89-29272
BLECHINGER, F. N89-28564
BLOOM, D. M. N89-28863
BLUM, FRANK D. N89-28638
BOBERG, ANDERS N89-28916
BOCK, R. DARRELL N89-29120
BODIS-WOLLNER, I. N89-29008
BOERSTOEL, J. W. N89-28777
BOESCHE, D. N89-28581
BORDUSELU, CONSTANTIN N89-28900
BORGEAUD, MAURICE N89-28698
BORGEFORS, GUNILLA N89-29091
BORIS, J. P. N89-29053
BORK, THOMAS N89-29286
BOURDEL, F. N89-28775
BOWDEN, J. N. N89-28661
BOWEN, KENNETH A. N89-29095
BOWER, WARD N89-28958
BOYD, FRANK W. N89-28557
BOYLE, MICHAEL E. N89-28646
BOZEMAN, RICHARD J., JR. N89-28829
BRACKEN, JEROME N89-29144
BRADTMILLER, BRUCE N89-29025
BRASSEUR, GUY N89-28968
BRAUN, HANS MARTIN N89-28878
N89-28887
BREEN, P. J. N89-29171
BRENNER, STEPHEN N89-28988
BRENNING, NILS N89-29216
N89-29217
BRIDENBAUGH, JOHN C. N89-28511
BRILES, SCOTT D. N89-28926
BRINDLE, C. N89-28630
BRINDLEY, PAMELA K. N89-28549
BRODY, ADAM R. N89-29020
BRONOWSKI, DAVID R. N89-28784
BROOKS, F. P. N89-28797
N89-29057
BROOKS, RODNEY A. N89-29026
BROWN, MARK K. N89-29194
BROWN, SAMUEL H. N89-28756
BROWNING, J. S. N89-28555
BRUINING, A. N89-28499
BRULE, JAMES F. N89-29094
BRYKCZYNSKI, BILL R. N89-29142
BUCKLEY, CRIST, JR. N89-28641
BUCKLIN, R. W. N89-28587
BUDINGER, JAMES M. N89-28545
BUECHNER, EUGEN-WALTER N89-28770
BUELOW, HENNING N89-29196
BUERGEL, ERICH N89-28769
BUETEFISCH, KARL-ALOYS N89-28505
BUFALINI, J. J. N89-28964
BUNKER, S. N. N89-28644
BURDEN, HENRY S. N89-28548
BURGHARDT, ANDREAS JEF CORNELIS N89-29177
BURKES, TOMMY R. N89-28565
BURNS, DONNA J. N89-28963
BUSHLOW, TODD N89-28488
BUTLER, BARRY N89-28953
BUTLER, CHARLES S. N89-29141
BUTLER, DAVID H. N89-28550
BUTLER, T. A. N89-28856
BUTTERFIELD, C. P. N89-28487
BUZZARD, ROBERT J. N89-28806
BYRD, GREGORY T. N89-29086

C

CABRAL, OSVALDO M. R. N89-28961
CADITZ, DAVID N89-29282
CAI, HONG N89-28731
CAIN, CHRISTINA L. N89-28539
N89-28761
CALDAS, OSVALDO N89-28917
CAMERON, ALEC N89-28849
CAMMARATA, VINCE N89-28604
CAMPBELL, THOMAS G. N89-28550
CANTER, J. M. N89-28818
CAO, HAISHENG N89-28877
CAPLIN, B. N89-29154
CAPPUCCI, MARIETTA R. N89-28624
CARIGNAN, FOREST J. N89-28838
CARLSON, N. W. N89-28820
CARMONA, EDWARD A. N89-29049
CARPENTER, DEAN E. N89-28962
CARPENTER, G. B. N89-29234
CARRABBA, MICHAEL M. N89-29235
N89-29236
CASPI, P. N89-29140
CASTAN, S. N89-28894
CASTLEMAN, A. WELFORD, JR. N89-28595
CATSIFF, E. H. N89-28643
CAULFIELD, H. J. N89-28792
CELIKKAYA, AHMET N89-28625
CHA, JONG W. N89-28596
CHAI, AN-TI N89-28666
CHAMBERS, D. H. N89-28812
CHAMPAGNE, FRANK H. N89-28759
CHANG, F. N89-28768
CHANG, JAW J. N89-28713
CHANG, WON SOON N89-28747
CHANG, XIANGQIAN N89-28877
CHAO, B. T. N89-28746
CHAPMAN, G. H. N89-28818
CHAPMAN, G. T. N89-28870
CHARATAN, ROBERT M. N89-29245

CHATELLIER, J. Y. N89-28654
CHEN, GOONG N89-29098
CHERRY, M. L. N89-29168
CHEW, L. P. N89-29045
N89-29115
CHOI, SANG-IL N89-28715
CHOI, U. S. N89-28751
CHONGSAWANGVIROD, S. N89-28720
CHOW, L. C. N89-28652
CHRISTENSEN, ERIK LINTZ N89-28882
CHRISTIAN, DAVID C. N89-28568
CHUNG, JAMES C. N89-28797
CHUNG, KAI LAI N89-29113
CHURCHILL, THOMAS N89-29025
CHUTJIAN, ARA N89-28795
N89-29169
CIESLIK, S. N89-28980
CLARK, B. C. N89-29292
CLARK, BRENT C. N89-28828
CLAUSER, CHARLES E. N89-29025
CLOUGH, S. N89-29223
COBURN, ALLEN N89-28922
COCKERHAM, KENNETH E. N89-28520
COFFEY, LIAM N89-29231
COHEN, DAVID N89-28692
COHEN, DONALD S. N89-29109
COHEN, S. S. N89-28818
COLE, J. W. N89-28748
COLELLA, NICHOLAS J. N89-29186
COLLETT, EDWARD N89-29239
COLLINS, CARL B. N89-28819
COLTON, DAVID N89-28681
COLVIN, MICHAEL E. N89-29186
COOK, M. N89-28566
COOLBAUGH, M. T. N89-28608
N89-28609
COPELAND, RICHARD A. N89-28976
CORSMEIER, ULRICH N89-28978
COUFAL, H. N89-29220
COWIE, RALPH N89-28491
COX, M. G. N89-29126
COZZENS, ROBERT F. N89-28646
CRAMER, P. G. N89-28812
CRANE, ALAN T. N89-28955
CREMEAN, S. P. N89-28588
CREWS, JOHN H., JR. N89-28586
CROOKS, RICHARD M. N89-28604
CROSS, JON B. N89-28533
CULIOLI, J. C. N89-29040
CULL, THERESA A. N89-29180
CULLINGFORD, HATICE S. N89-29027
CUNNINGHAM, ATLEE M., JR. N89-28488
CUNNINGHAM, S. E. N89-28864
CUTTER, M. A. N89-28563
N89-28564

D

DAGDIGIAN, PAUL J. N89-28607
DAHMEN, U. N89-28619
DALEY, RICHARD S. N89-29245
DALGE, ANTONIO JOSE FERREIRA N89-28917
DALLAS, KENNETH N89-28491
DALLY, WILLIAM J. N89-29035
DANIEL, RON N89-28849
DARRAH, RODNEY C. N89-29259
DASANNACHARYA, B. S. N89-29071
DAVIDOV, JOHANN N89-29107
DAVIS, LAURA E. N89-29224
DAWSON, L. R. N89-29230
DEABREUSA, LEONARDO D. N89-28961
DEB, SOMANTH N89-29052
DEBIEVE, J. F. N89-28735
DEBORD, P. N89-28894
DECKER, MADELYN M. N89-28663
DECKERT, J. C. N89-29034
DEEKSHATULU, B. L. N89-28910
DEFONTAINE, D. N89-29227
DEGRAZIA, GERVASIO ANNES N89-28979
DEHN, JAMES T. N89-29297
DEJONG, F. J. N89-28754
DEKKER, E. N89-29105
DEKKER, L. N89-29105
DELAAT, JOHN C. N89-29032
DELAGI, BRUCE A. N89-29086
DELAHOY, A. E. N89-28946
DELUCA, W. H. N89-28710
DELUCIA, R. A. N89-28516
N89-28517
DEMEDEIROS, VALDER MATOS N89-28885
DEMS, B. C. N89-28606
N89-28645
N89-28719
N89-29248
DENNIS, MICHAEL G. N89-28963
DERYUGIN, V. A. N89-28532
DESACHY, J. N89-28894
DESANTO, JOHN A. N89-29192
DESOPPER, ANDRE N89-28498
DEVADAS, SRINIVAS. N89-29035
DEVAN, J. H. N89-28617
DEVRIES, D. B. N89-29090
DEWEY, STEPHEN L. N89-28791
DEZERT, JEAN N89-28702
DHIR, V. K. N89-28768
DICKERSON, ART N89-28958
DIEKMANN, FRANK-JUERGEN N89-28931
DIEROLF, DAVID A. N89-29260
DINER, DANIEL B. N89-28676
DINGUS, MICHAEL L. N89-28670
DOIRON, SCOTT D. N89-28983
DOLLING, D. S. N89-28741
DOMINEK, ALLEN K. N89-28672
DOMMERMUTH, F. N89-29156
DONAHUE, FRANCIS M. N89-28724
DOPHEIDE, D. N89-28826
DORHOUT, B. N89-29074
DORRIS, S. E. N89-28957
DOSSER, LARRY R. N89-28813
DOUGHERTY, T. K. N89-28643
DOUGLAS, BRYANT S. N89-29050
DOWNS, M. J. N89-28825
DRAKE, MICHAEL L. N89-28642
DRIESSEN, THEO S. H. N89-29072
DROUILLARD, THOMAS F. N89-28573
DUBOIS, DON N89-29202
DUFF, J. W. N89-28974
DUMONTET, H. N89-28582
DUNHAM, S. R. N89-29034
DUNKERTON, TIMOTHY J. N89-28989
DUPEROUX, J. P. N89-28774
DUQUENNOY, A. N89-29291
DURAND, DENIS F. N89-28538
DURRANT-WHYTE, HUGH N89-28849
DUSSAUGE, J. P. N89-28734
N89-28735
N89-28738
N89-28741
DWIGHT, K. N89-28593
DYNES, PAUL J. N89-28649

E

EBEL, A. N89-28799
N89-28931
N89-28977
EBNER, HEINRICH N89-28919
EDDINGTON, LEE W. N89-28930
EDNEY, E. O. N89-28964
EGOLF, C. G. N89-29152
EIKENBROEK, JOHANNES WILHELMUS THEODORUS
N89-28699
EIMERL, DAVID N89-29224
EISCHENS, R. P. N89-28634
ELENA, M. N89-28740
ELIAS, W. E. N89-28643
ELIASON, JAY R. N89-28924
ELLIOTT, C. THOMAS N89-28796
ELLIOTT, S. J. N89-28807
ELLSWORTH, DAVID N89-29058
ELLUL, J. P. N89-28720
ELOSEGUI, PAUL N89-28848
ENGLISH, ROBERT E. N89-28565
ENSTROM, R. E. N89-28821
EPHREMIDES, A. N89-29054
ERNIE, D. W. N89-29206
ESILVA, MACHADO N89-28917
EVALL, JOE N89-28594
EVANS, E. P. N89-28555
EVANS, H. N89-28718
EVANS, J. E. N89-28986
EVENSON, K. M. N89-28809
EYLES, JOHN N89-29058

F

FABER, M. N89-28826
FAGHRI, AMIR N89-28747
FAGUYR, P. W. N89-28598
FAHY, F. J. N89-28807
N89-29158
FAIGLE, ULRICH N89-29102
N89-29131
FAIRLIE, D. B. N89-29108
FAIRMAN, TERRY M. N89-28717
FARMER, CROFTON B. N89-28969
FATEMI, EMAD N89-29123
FAWCETT, W. RONALD N89-28598
N89-28600
N89-28602
FAYETTE, DANIEL F. N89-28714
FENTON, B. C. N89-28516
N89-28517
FERNHOLZ, H. H. N89-28734
N89-28742
N89-28743
N89-28744
N89-28745
FERRANTE, JOSE ERNESTO TELLES N89-28925
FERRIOL, M. N89-28664
FILHO, MARIO VALERIO N89-28925
FINLEY, MICHAEL N89-28808
FINLEY, P. J. N89-28734
N89-28742
N89-28743
N89-28744
N89-28745
FISHBACK, JEROME N89-28687
FISHER, S. A. N89-28518
FISKE, JAMES ALEXANDER STUART N89-29082
FITZJARRALD, DAVID R. N89-28961
FLANIGAN, MICHAEL J. N89-29003
FLEISCHAUER, PAUL D. N89-29247
FLOKSTRA, JAN N89-29068
FLOREK, RYSZARD N89-28895
FLYNN, E. N89-29008
FLYNN, EDWARD R. N89-29007
FORBES, ALISTAIR B. N89-29125
FORCH, BRAD E. N89-28607
FOREST, ETIENNE N89-29106
FORSYTHE, K. M. N89-28678
FOSS, C. A., JR. N89-28602
FOSS, COLBY A., JR. N89-28600
FOWLER, C. M. N89-28712
FOWLER, R. N89-28587
FRAISSE, P. N89-28854
FRANCE, BRUCE E., SR. N89-29268
FRANK, C. W. N89-28639
FREAR, D. R. N89-28860
FREEMAN, B. L. N89-28712
FREEMAN, J. L. N89-28863
FREEMAN, JOHN R. N89-28543
FRENKEL, DAAN N89-28750
FRIDEN, JAN N89-29016
FRIESEL, M. A. N89-28861
FRITZ, I. J. N89-29230
FROUSTEY, CATHERINE N89-28629
FUCHS, HENRY N89-28797
N89-29058
FUEHRER, CLAUS N89-28847
FUJITA, J. N89-29209
FUJIWARA, M. N89-29201
FULKERSON, WILLIAM N89-28955

G

GAJJAR, J. S. B. N89-28748
GALIANO, MARIA LUCIE N89-29228
GALLILY, ISAIAH N89-29150
GAO, Y. M. N89-28593
N89-29234
GARECHT, DIANE N89-28567
GARGIULO, AL. N89-28922
GARNER, F. A. N89-28618
GARRISON, JOHN D. N89-28949
GARVEY, JAMES F. N89-28608
N89-28609
GATES, B. L. N89-29070
GAUTESEN, A. K. N89-28812
GAUZE, F. N89-29150
GAVIN, JOSEPH G., JR. N89-28565
GAZEAUD, G. N89-28873
GAZEY, S. N89-28561
GEER, JAMES F. N89-29122
GENERAZIO, EDWARD R. N89-29851
N89-28853
GENT, A. N. N89-28647
N89-28648
N89-28867
GEORGE, J. N89-29008
GEORGE, THOMAS F. N89-29256
GERBRANDS, JAN JACOB N89-28701
GERGELY, PETER N89-28869
GERLACH, KARL N89-28677
GERSHWIN, S. B. N89-29232
GEURTS, BERNARD J. N89-28654
N89-28655
GIAUQUE, R. D. N89-28788
GIBBONS, ROBERT D. N89-29120
GIBSON, KATHRYN A. N89-28673
GIBSON, LORNA J. N89-28575
GIBSON, WARREN C. N89-28862
GIESY, DANIEL P. N89-29047
GILBERT, R. P. N89-29001
GILLOTAY, DIDIER N89-28968
N89-29293

GILREATH, MELVIN C. N89-28672
GIMENEZ, JOSE LUIS N89-29064
GINSBURG, ARTHUR P. N89-29010
GIRAULT, VIVETTE N89-29028
GIUDICE, M. N89-28664
GLOVER, JOSEPH N89-29113
GMELIGMEYLING, R. H. J. N89-28875
N89-29066
N89-29076
GODAI, TOMIFUMI N89-28920
GODLOVE, T. F. N89-28815
GOLD, RONALD R. N89-28547
GOLDFEATHER, JACK N89-29058
GOLUBITSKY, M. N89-29135
GONZALEZ, RICHARD R. N89-29009
GORDON, CLAIRE C. N89-29025
GORDON, KAREN D. N89-29142
N89-29145
GORLICK, M. M. N89-29083
GRADY, DENNIS E. N89-28753
GRAHAM, R. A. N89-28801
GRANT, NICHOLAS J. N89-28565
GRANT, WILLIAM N89-28692
GRASSIAN, V. H. N89-29171
GREENE, FRANCIS A. N89-28767
GREENWOLL, J. I. N89-28790
GREER, TREY N89-29058
GRIEBEL, M. N89-29117
GRIFFIN, J. H. N89-28864
GRIFFIN, RICHARD D. N89-28722
GROBSTEIN, TONI L. N89-28627
GROGAN, TERENCE M. N89-28558
GROMOV, G. N89-28530
GROUND, JOHN N89-28491
GRUNINGER, J. H. N89-28974
GUIGNARD, J. P. N89-28904
GUIMARAES, PATRICIA T. N89-28983
GUIRAUD, A. N89-28582
GUO, B. N89-29118
GUPTA, ANOOP N89-29089
N89-29138
GURALNIK, G. S. N89-29255
GURWELL, W. E. N89-28620

H

HACHEY, JOHN P. N89-29236
HAERTIG, J. N89-28495
HAFIZI, B. N89-28675
HAFNER, THOMAS N89-28992
HAGAN, CHARLES W., JR. N89-28955
HAGUE, DOUGLAS C. N89-28635
HAHNE, DAVID E. N89-28486
HAKIM, D. MUHALLY N89-28937
HAKONEN, P. J. N89-29218
HAKONSEN, T. E. N89-29229
HALBLEIB, J. A. N89-28708
HALL, CHARLES E., JR. N89-29055
HALL, LAWRENCE J. N89-29283
HALLORAN, JOHN N89-28578
HALPERN, LAURENCE N89-29026
HAMADA, Y. N89-29209
N89-29213
HANDOROM., SAPTOMO N89-28937
HARGENS, ALAN R. N89-29016
HARGIS, K. M. N89-29229
HARMEYER, E. N89-28728
HARRIS, MARK R. N89-28797
HARRISON, W. A. N89-29231
HARTL, PHILIPP N89-28878
HASAN, P. N89-28904
HATORI, TADATSUGU N89-29211
HAUSCHILDT, HERMAN W. N89-28832
HAYNES, T. E. N89-29225
HECKER, W. N89-28581
HEDEKER, DONALD N89-29120
HEEREMA, F. J. N89-29067
HEPP, ALOYSIUS F. N89-28851
HERCZFELD, PETER R. N89-28705
HERLAND, EINAR-ARNE N89-28888
HERNANDO, B. N89-28805
HESSE, MICHAEL N89-28970
HETTLAGE, E. N89-28564
HICHO, GEORGE E. N89-28615
HIDEKUMA, S. N89-29213
HILL, C. K. N89-28551
HILL, DAVID S. N89-29059
HILLS, MALINA M. N89-29247
HIROKURA, S. N89-29209
HIRONAKA, M. C. N89-28523
HISER, JAMES K. N89-28559
HJALMARSON, H. P. N89-29230
HOBBEL, ERIK FLOOR N89-28874
HODGDON, M. L. N89-28712
HODGE, JAMES D. N89-28578
HOELTZENER-DOUARIN, B. N89-29198
HOFFMAN, R. N. N89-28987
HOLDER, J. DARRYL N89-28687
HOLLAND, JEFFREY P. N89-28757
HOLTHAM, P. M. N89-29029
HOLTKAMP, D. B. N89-28555
HOMMA, KOHZO N89-28880
N89-28897
HOPCROFT, JOHN E. N89-29046
HORDIJK, ARIE N89-29139
HORN, RALF N89-28942
HORNY, P. N89-28650
HOSOKAWA, M. N89-29201
HOUTSMA, MAURICE A. W. N89-29068
HOWARD, CELESTE M. N89-29193
HOWELL, M. N89-28617
HSIEH, K. C. N89-28662
HSIEH, W. H. N89-28662
HSU, H. S. N89-28617
HSU, LISHING N89-28601
HUANG, JUDY H. N89-29245
HUBA, J. D. N89-29205
HUG, GILLES N89-29253
HUGELMANN, C. P. N89-28991
HUGHES, H. G. N89-29189
HUIE, ROBERT M. N89-28622
HULSHOF, B. J. A. N89-29070
HUNT, JAMES N89-29302
HUOVINEN, TAPIO N89-28855
HURD, WILLIAM J. N89-28684
HUSSAINI, M. Y. N89-28762
N89-28763
HUTLEY, M. C. N89-28827
N89-28828
HUTTENLOCHER, DANIEL P. N89-29045
N89-29046
HUTTON, P. H. N89-28861
HYER, M. W. N89-28856

I

IANNELLO, VICTOR N89-28839
IDA, K. N89-29201
N89-29209
N89-29213
IDEI, H. N89-29201
IGUCHI, H. N89-29201
IHE, CENDEKIA JASA N89-28939
INABA, C. M. N89-28523
INAGAKI, T. N89-29223
INSLEY, ELIZABETH M. N89-28963
IRENE, E. A. N89-28720
IRIE, HARUYUKI N89-29211
ISAACS, R. N89-28987
ISMAIL, SHAIK N89-28521
ISMULLAH, ISHAK H. N89-28937
ISRAEL, LAURA N89-29058
ITOH, NORIAKI N89-29215
IYENGAR, K. V. K. N89-29289

J

JACAK, BARBARA N89-29167
JACHIMSKI, JOZEF N89-28895
JACKSON, C. L. N89-28640
JAGANNATHAN, SURESH N89-29051
JAHN, R. K. N89-28588
JAIN, RAMESH N89-28562
JAIN, VINOD K. N89-28835
JAINANDUNSING, K. N89-29077
JAMISON, KEITH A. N89-28548
JANARDHAN, S. N89-29270
JANATA, JIRI N89-28723
N89-28725
JANG, JONG HOON N89-28747
JANSEN, CORNELIS JOHANNES ADRIANUS
N89-29038
JARRELL, LAMONT N89-28967
JENNINGS, D. A. N89-28809
JENSEN, ROBERT A. N89-29004
JEROME, JOSEPH N89-29123
JESSBERGER, E. K. N89-29174
JOHE, CH. N89-28495
JOHNSON, DENNIS A. N89-28739
JONES, ALAN N89-28498
JONES, NATHAN H. N89-28490
JONES, R. N89-28580
JONGEN, H. TH. N89-28776
JONKER, P. N89-28776
N89-28779
JOOSTEN, S. M. M. N89-29069
JORDAN, HARRY F. N89-28674
N89-29030
JOST, G. S. N89-28871
JUPPENLATZ, M. N89-28937

K

KAANG, S. Y. N89-28647
KACZYNSKI, ROMUALD N89-28892
N89-28895
KADOTA, K. N89-29209
KAHRU, MATI N89-28896
KAKIMOTO, I. N89-28921
KALINOWSKI, JOHN N89-28787
KALLENBACH, ARNE N89-28823
KALNITSKY, A. N89-28720
KAMIYA, IZUMI N89-28879
KAMPAS, F. J. N89-28946
KANEKO, TOSHIAKI N89-29207
KANG, M. N89-28810
KARAGOZIAN, A. R. N89-28768
KARAM, N. H. N89-29238
KARATASIOS, LABROS G. N89-29060
KARR, T. J. N89-28812
KARYAGIN, V. P. N89-28532
KASH, DON E. N89-28955
KASTNER, M. P. N89-29034
KASZA, K. E. N89-28751
KATSAROS, KRISTINA B. N89-28975
KAUFFMAN, ROBERT E. N89-28835
KAUPP, VERNE H. N89-28928
KAWAHATA, K. N89-29213
KEDEM, KLARA N89-29045
N89-29115
KELLER, MICHAEL A. N89-28835
KELLEY, D. F. N89-28605
KELLEY, MICHAEL T. N89-28797
KELLY, E. J. N89-28678
KENNES, ROBERT N89-28980
N89-28981
KERN, W. N89-29073
N89-29131
N89-29146
KERSHAW, P. W. N89-28593
KERSTEN, MARTIN L. N89-29068
KESMODEL, L. L. N89-28589
KESSELMAN, C. F. N89-29083
KESSLER, HANS-JOCHEN N89-28772
KHAIDAR, MOHAMED H. N89-29099
KHAN, F. N89-29162
KHANDELWAL, G. S. N89-29162
KIM, DEW E. N89-28837
KIM, K.-S. N89-28737
KIM, S.-W. N89-28749
KIM, YOUNG K. N89-28716
N89-29241
N89-29242
KING, W. CHRIS N89-28923
KINOSHITA, KIM N89-28951
KIRILLOV-UGRYUMOV, V. G. N89-28528
KITIPORNCHAI, S. N89-28857
N89-28858
N89-28859
KLAPDOR, H. V. N89-29174
KNAUSS, W. G. N89-28643
KNIGHT, THOMAS F., JR. N89-29035
KNOTH, BRUCE H. N89-28838
KNOTHE, K. N89-28536
KOBEWKA, K. M. N89-29029
KOCH-MIRAMOND, LYDIE N89-29288
KOELLE, H. H. N89-28536
KOGUT, ALAN J. N89-29296
KOH, GARY N89-29187
KOHNO, I. N89-28921
KOIDE, S. N89-29210
KOLLENBERG, WOLFGANG N89-28653
KOMAI, JIRO N89-28884
KOMENDA, PETER N89-28729
KONIECZNY, JAN N89-28892
KONJACK, R. N89-28889
KOS, LAWRENCE D. N89-28568
KOSBAR, L. L. N89-28639
KOSHIISHI, HAJIME N89-28880
N89-28897
KOSMANN, D. N89-28915
KOSSLYN, STEPHEN M. N89-29011
KOZIARZ, NANCY A. N89-28714
KOZMINCHUK, BRIAN W. N89-29043
KRAEMER, JOACHIM N89-28893
KRAFT, ULRICH RALF N89-28872
KRAMER, L. C. N89-29034
KRANTZ, R. J. N89-29237
KRASICKY, P. D. N89-29248
KRASNOPOLER, A. A. N89-28719
KREMMLING, HORST N89-28822
KREMNEV, R. S. N89-28532
KRETSCHMER, FRANK F., JR. N89-28677
KRISHNAMURTHY, L. N89-28760

KRUEGER, ARLIN J. N89-28983
KRUEGER, ROLF N89-29199
KRUGER, C. H. N89-29204
KRUL, L. N89-28941
KUAN, S. W. N89-28639
KUBO, S. N89-29201
KUHL, LAWRENCE E. N89-29043
KULCINSKI, GERALD L. N89-28565
KUMAR, ANAND N89-28496
N89-28497
KUMAR, N. N89-29270
KUNHARDT, ERICH E. N89-28726
KUNKEL, B. N89-28564
KUO, K. K. N89-28662
KUSANO, JUN-ICHI N89-29243
KUTUFA, NICCOLA N89-28569
KUZNETSOV, V. V. N89-28532

L

LACH, E. N89-28873
LADD, ANTHONY J. C. N89-28750
LALOR, N. N89-29157
LAMBRAKOS, S. G. N89-29053
LAMMERTS, J. J. M. N89-28510
LAMPORT, LESLIE N89-29084
LAMPRECHT, D. G. N89-28587
LANDIECH, PHILIPPE N89-29063
LANGE, GREGORY A. N89-28552
LAPOTIN, PERRY J. N89-29041
LAPUMA, PETER T. N89-28511
LARKIN, TIMOTHY H. N89-28926
LARKO, DAVID E. N89-28983
LARSON, B. C. N89-29225
LASSERRE, SERGE N89-28629
LAUER, JAMES L. N89-28836
LEBOFSKY, MARCIA J. N89-29278
LECROY, STUART R. N89-28993
LEDEBUHR, ARNO G. N89-29186
LEE, D. J. N89-28588
LEE, H. R. N89-29256
LEE, JOHN N. N89-28722
LEE, L. M. N89-28801
LEE, RAN-RONG N89-28578
LEE, RONG-TAY N89-29052
LEHNIGK, SIEGFRIED H. N89-29055
LEIGHTON, F. THOMSON N89-29035
LEIMKUHLER, BENEDICT N89-28847
LEISERSON, CHARLES E. N89-29035
LEKSONO, BAMBANG EDHI N89-28937
LELAND, ROBERT N89-28990
LEMON, D. K. N89-28861
LENFERINK, H. W. J. N89-29128
LEPERA, M. E. N89-28661
LEROY, MARC N89-28914
LEUPOLD, HERBERT A. N89-29219
LEVINE, HOWARD A. N89-29119
LEVY, MILTON N89-28622
LEWIN, WALTER H. G. N89-29298
LEWIS, PAUL S. N89-29007
LI, JIANGUO N89-29235
N89-29236
LI, S. T. N89-28690
LICHTENBERGER, A. N89-28673
LIECHTI, K. M. N89-28643
LIN, C. W. N89-28867
LINCE, JEFFREY R. N89-29247
LINDELL, ISMO V. N89-28671
LINDEMUTH, IRVIN R. N89-28709
LINDENBERGER, JOACHIM N89-28881
LINDGREN, H. N89-29291
LINKIN, V. M. N89-28532
LINN, CATHY J. N89-29145
LIPFERT, F. W. N89-28965
LIU, K. V. N89-28751
LIU, M. Z. N89-29127
LIVINGSTON, ELEANOR M. N89-28707
LOBB, D. R. N89-28563
N89-28564
LOEVE, W. N89-29067
LOKK, J. N89-28898
LONGDON, NORMAN N89-29302
LONGEWAY, P. A. N89-28821
LOO, JOSEPH A. N89-28592
LOUIS, J. F. N89-28987
LUDWIGS, JOHANNES N89-29257
LUH, PETER B. N89-29052
LUM, DAMON NEAL N89-28679
LUMPKIN, RUTLEDGE P. N89-29002
LUNDBORG, BENGT N89-28700
LUTES, GEORGE N89-29191
LYNCH, NANCY N89-29084

M

MAAS, R. N89-29182
N89-29183
MACDONALD, HAROLD C. N89-28928
MACLAREN, L. D. N89-28489
MADALA, RANGARAO V. N89-29121
MADAN, S. N89-28648
MADAY, YVON N89-29124
MADSEN, MARCELLA M. N89-28764
MADSEN, SOREN NORVANG N89-28882
MAEDA, KOREHIRO N89-28883
N89-28918
MAGILL, JOSEPH H. N89-29246
MAGRADZE, O. V. N89-29218
MAGSOOD, NAWIM N89-29012
MAHEFKEY, EDWARD T. N89-28747
MAIER, CHRISTIAN N89-28727
MAJIDI-AHY, R. N89-28863
MAKO, F. N89-28675
MALHOTRA, S. N89-28606
MAMAN, SHMUEL N89-28574
MANCINI, SARA N89-28724
MANN, FRANKLIN D. N89-28831
MANN, JOHN D. N89-29033
MANN, R. C. N89-29040
MANZI, ANTONIO O. N89-28961
MARCHBANKS, R. J. N89-29018
MARELLI, LIVIO N89-28906
MARIENHOFF, PETER N89-29251
MARONI, V. A. N89-28635
MARSDEN, JERROLD E. N89-29203
MARSHALL, BRUCE B. N89-28852
MARSHALL, JEFFREY S. N89-28839
MARSHALL, MATTHEW F. N89-28570
MARTIN, A. M. N89-29018
MARTIN, P. S. N89-28639
MASAHARU, HIROSHI N89-28943
MASAI, K. N89-29201
N89-29209
N89-29213
MASON, J. M. N89-29158
MASSELI, KLAUS N89-28611
MATKOWSKY, B. J. N89-28590
MATSUMOTO, KOHTARO N89-28897
MATSUMOTO, YOSHITAKA N89-28899
MATSUMURA, SATSUKI N89-28897
MATSUOKA, K. N89-29201
MAY, A. T. N89-28631
MAYALL, BRIAN H. N89-28954
MAYOR, M. N89-29290
N89-29291
MAZET, P.-A. N89-28775
MCCALLUM, J. C. N89-29226
MCCANDLESS, B. E. N89-28950
MCCLUNEY, D. SCOTT N89-28546
MCCONVILLE, JOHN T. N89-29025
MCCORD, R. A. N89-29263
MCCULLOUGH, S. N89-28598
MCDONALD, H. N89-28754
MCDOWELL, ROBIN S. N89-28789
MCGUIRE, TERRY N89-28960
MCHARGUE, C. J. N89-29226
MCKIM, HARLAN L. N89-29041
MCLALLIN, KERRY L. N89-28570
MCMANAMEN, JOHN P. N89-28552
MCPHEETERS, C. C. N89-28957
MEDVICK, PATRICIA A. N89-29007
N89-29008
MEESON, REGINALD N. N89-29142
MEHROTRA, PIYUSH N89-29061
MEIER, H. N89-28581
MEIJER, P. G. N89-28936
MEISER, JOHN H. N89-28635
MENSON, HEINRICH N89-28522
MERCER, JOHN R. N89-28488
MERKEL, HAROLD S. N89-29022
MERMELLIOD, J.-C. N89-29291
MERMILLIOD, J.-C. N89-29290
MERRILL, WALTER C. N89-29032
MESLIN, BRAD N89-28922
MEYERS, P. V. N89-28945
MICKELSON, M. N89-28987
MIERZWA, WLADYSLAW N89-28895
MIKKELSON, K. A. N89-28708
MILDRUM, HERBERT F. N89-29148
MILLER, DOUGLAS N89-28975
MILLER, J. F. N89-28710
MILLER, JUDITH N89-28498
MILLER, TERESA Y. N89-28793
MILLIS, MARC G. N89-28571
MILLS, K. C. N89-28612
MILLS, MICHAEL TE. N89-28963
MINH, N. Q. N89-28957
MINKOFF, M. N89-28590
MITCHELL, JOSEPH S. N89-29045
MIZIOLEK, ANDRZEJ W. N89-28607
MOCK, R. N89-28708
MOLINELLI, EUGENE J. N89-29003
MOLNAR, STEVEN N89-29036
N89-29058
MONEGAN, MICHAEL D. N89-29056
MONEY, M. W. N89-28583
N89-28584
MONK, PETER N89-28681
MONKELIEN, KYLE N89-29039
MONTY, RICHARD A. N89-29021
MOON, FRANCIS C. N89-28869
MOORE, JOHN, JR. N89-28633
MOORE, KATHLEEN E. N89-28961
MOORE, THOMAS P. N89-29017
MOREIRA, ALBERTO N89-28942
MORENO, JOSE E. N89-29221
MORENODELACUEVAS, V. N89-28827
MORGOWNIK, A. F. J. N89-28564
MORI, NOBUHIKO N89-28884
MORITA, S. N89-29201
MORRIS, J. R. N89-28812
MORRISON, CLYDE A. N89-29149
MORSE, JAMES S. N89-29024
MOSCA, EUGENE P. N89-28722
MOSS, S. M. N89-29018
MOY, RUSSELL N89-28724
MUCCINI N89-29065
MUELLER, BERNHARD N89-28504
MUIRHEAD, D. N89-28708
MULLER, FRANZ N89-28919
MULLIN, JEROME P. N89-28565
MURAI, SHUNJI N89-28884
N89-28899
MURPHY, S. P. N89-29085
MURRELL, THOMAS L. N89-29039
MURTHY, UMA R. N89-29270
MUSKAROV, OLEG N89-29107

N

NAGATA, A. N89-29210
NAGATA, KOJI N89-28899
NAITOU, H. N89-29212
NAKA, MASAO N89-28897
NAKAMICHI, JIRO N89-28492
NAMASTE, Y. M. N. N89-28606
N89-28645
N89-28719
NAMBA, SUSUMU N89-29243
NAPOLITANO, LUIGI G. N89-28503
NASH, STEPHEN G. N89-29087
NEHRKORN, T. N89-28987
NEUBAUER, F. M. N89-28931
N89-28977
NEUBAUER, M. N89-28799
NEVALAINEN, SEPPO J. N89-29136
NIAMATHULLAH, S. K. N89-29111
NICOLET, MARCEL N89-28980
N89-28981
N89-29294
NIELSEN, O. V. N89-28805
NIEUWENHUIS, L. J. M. N89-29037
NIEUWENKAMP, H. N89-28693
NIMLOS, M. R. N89-28605
NING, ZHEN-QIU N89-28732
NITSCHE, WOLFGANG N89-28800
NIU, QIAN N89-29244
NOACK, W. N89-28889
N89-28890
NORBURY, JOHN W. N89-29159
N89-29160
N89-29161
N89-29162
N89-29163
N89-29164
N89-29165
N89-29166
NORDLEY, GERALD D. N89-29170
NORDMAN, JAMES E. N89-29250
NORDSTROM, B. N89-29291
NORTON, ROBERT H. N89-28969
NOVINSON, T. N89-28523
NOWLAND, JOSEPH R. N89-28534
NOYES, ROGER P. N89-28787
NUMMILA, K. K. N89-29218

O

OBENDORF, S. K. N89-28606
N89-28645
N89-28719
OCHS, R. L. N89-28681

OCONNOR, DANIEL N89-28638
ODERMAN, MARK N89-28922
OEGELMAN, HAKKI N89-29288
OELOFF, J. E. N89-28845
OELRICH, IVAN N89-29144
OGAWA, Y. N89-29209
N89-29212
OH, H. G. N89-29256
Orl, HAE-SOO N89-29116
OKADA, YOSHIHIRO N89-28897
OKAMOTO, KEN-ICHI N89-28897
OKAMOTO, Y. N89-29223
OKAMURA, S. N89-29201
OKANO, K. N89-29212
OKTAY, TURKER N89-28837
OLDEHAMPSINK, B. G. M. N89-29090
OLLILAINEN, VESA N89-28632
OLSEN, LARRY C. N89-29233
OLSON, ALDEN N89-29188
OLSON, R. J. N89-29263
OMONGAIN, E. N89-28564
ONEAL, DOUGLAS W. N89-29112
OPRESCU, NICOLAE N89-28900
OPSAL, JON N89-29220
ORDONEZ, GUSTAVO N89-28668
OSANAI, T. N89-28912
OSEDACZ, RICHARD P. N89-28540
OSHER, STANLEY N89-29123
OSKAM, D. N89-28940
OSKAM, H. J. N89-29206
OTT, K. C. N89-29229
OVERFELT, P. L. N89-28686
OWEN, JAMES W. N89-28556

P

PADMOSUTOYO, SLAMET SUHARSA N89-28683
PAINE, ROBERT J. N89-28963
PALFREY, S. L. N89-28821
PALMER, BYRON A. N89-28789
PANCHAL, C. B. N89-28752
PANDOLF, KENT B. N89-29009
PAOLELLA, ARTHUR N89-28705
PAPIERNIK, STEFAN N89-28895
PARAZYNSKI, SCOTT N89-29016
PARIS, D. T. N89-28689
PARK, HYE-SOOK N89-29186
PARKER, D. S. N89-29083
PARKER, JERALD V. N89-28542
PARKINSON, W. J. N89-29229
PASSMAN, STEPHEN L. N89-28753
PATTIPATI, KRISHNA R. N89-29034
N89-29052
PAUL, ADOLF K. N89-28972
PAUL, J. N89-28580
PEASE, R. F. N89-28639
PEDDICORD, K. LEE N89-28565
PEIFER, WILLIAM R. N89-28608
N89-28609
PELEVIN, V. N89-28898
PENFIELD, PAUL, JR. N89-29035
PENN, LANNING M. N89-28983
PENNYCOOK, S. J. N89-29225
PEREIRA, SERGIO DEPAULA N89-28905
PEREZMATZUMOTO, A. E. N89-28807
PERLMUTER, LAWRENCE C. N89-29021
PERRY, ALFRED M. BUD N89-28955
PERRY, M. B. N89-28659
PERRY, STEVEN G. N89-28963
PETERSEN, J. R. N89-28805
PETERSON, E. J. N89-29229
PETERSON, ROBERT ALAN N89-29110
PETH, P. N89-28799
PETIT-BOURDELLE, EMMANUELLE N89-29179
PETITDAMAGE, V. N89-28774
PETROSIAN, VAHE N89-29282
PETTIT, FRED N89-28622
PETTY, GRANT W. N89-28975
PFEIFER, H. J. N89-28826
PFEIFFER, HELMUT N89-29175
PFITZER, K. A. N89-28973
PFLUGER, P. R. N89-29066
PHILLIPS, J. E. N89-28944
N89-28950
PHILLIPS, N. E. N89-29231
PICCIOLO, J. J. N89-28957
PICHKHADZE, K. M. N89-28532
PICKART, ROBERT S. N89-29005
PICONE, J. M. N89-29053
PINNINGTON, R. J. N89-28652
PINTO, SERGIO DOSANJOS FERREIRA N89-28925
PIOMELLI, UGO N89-28763
PIOTROWSKI, J. N89-29140
PITKARANTA, J. N89-29117
POEPPEL, R. B. N89-28957
POERBO, HASSAN N89-28937
POGGIO, ANDREW J. N89-28954
POLLE, V. F. L. N89-28937
POOL, SAM L. N89-29017
POPELLA, A. N89-28889
N89-28890
POST, R. F. N89-28814
POSTHUMA, H. G. N89-29062
POUKEY, J. W. N89-28708
POULTON, JOHN N89-29058
POWELL, JOHN D. N89-28548
PRESTON, KENDALL, JR. N89-29100
PREUSS, RYSZARD N89-28895
PREVIC, FRED H. N89-28515
PRICE, W. L. N89-29092
PRIMAS, LORI N89-29191
PRIMDAHL, F. N89-28805
PROCHNOW N89-28536
PROTOPOPESCU, V. N89-29040
PRUPPACHER, H. R. N89-28525
PUGLIA, G. P. N89-29223
PURSEL, FRANK P. N89-28722
PURVIS, CAROLYN K. N89-28565
PUTNEY, A. N89-29285

R

RAAIJMAKERS, IVO JOHANNES MECHTILDIS MARIA N89-28733
RABITZ, H. N89-29104
RAHMAN, A. K. M. N89-29223
RAINWATER, GREGORY L. N89-28928
RAMAER, M. N89-29080
RAMANAN, SRINIVASAN N89-28674
RAMANATHAN, R. V. N89-28587
RAMESH, T. G. N89-28628
RAMON, Y. N89-28563
RAMOS, HENRY J. N89-29214
RANGANATHAN, D. N89-29270
RAPPAPORT, S. N89-29285
RASCHKE, E. N89-28799
N89-28931
N89-28977
RASHIDNIA, NASSER N89-28666
RATIER, G. N89-28563
N89-28564
RAUH, R. D. N89-29235
N89-29236
RAUSCH, GERHARD HANS N89-28887
RAUSTE, YRJO N89-28932
RAWLIN, VINCENT K. N89-28571
RAY, HEMEN N89-28623
RECAMI, ERASMO N89-29254
REDD, MARVIN D., SR. N89-29274
REED, R. P. N89-28790
REED, WILMER H., III N89-28547
REEDER, JAMES R. N89-28586
REGIS, PATRICK JEAN N89-28834
REIDY, ANNE M. N89-28673
REINHARD, R. N89-29295
REINOVSKY, ROBERT E. N89-28709
REISTER, DAVID B. N89-28955
RENGARAJAN, T. N. N89-29289
RESHOTKO, E. N89-28734
RHODES, PERCY H. N89-28793
RICE, MICHAEL D. N89-29049
RICHTER, KAREN J. N89-29260
RICKEL, D. G. N89-28712
RIDDER, SVEN-OLOF N89-28500
RIEDELBAUCH, STEFAN N89-28504
RIEGER, MARTIN N89-29252
RIEKEN, ERIC R. N89-28924
RISTAU, DETLEV N89-28824
ROBERTSON, D. C. N89-28974
ROBERTSON, J. C. N89-28695
N89-28696
N89-28697
ROBINS, DAVID O. N89-29012
ROCKEL, BURKHARDT N89-28977
RODRIGUEZ, F. N89-28606
N89-28645
N89-28719
N89-29248
RODWELL, M. J. W. N89-28863
ROESKE, S. B. N89-28555
ROGOVSKIY, G. N. N89-28532
RONQUIST, EINAR M. N89-29124
RONSTEN, GOERAN N89-28959
ROSE, E. A. N89-28810
ROSE, HARVEY A. N89-29202
ROSENCWAIG, ALLAN N89-29220
ROSSOW, WILLIAM B. N89-28993
ROTH, A. N89-28915
ROTH, DON J. N89-28851
ROY, WALTER N. N89-28512
ROYER, H. N89-28802
N89-28804
RUES, DIETRICH N89-28504
RUNGE, H. N89-28890
RUSSELL, DAVID N89-29202
RUSSELL, DAVID L. N89-28865
RUSSELL, KENNETH C. N89-28618

S

SABA, COSTANDY S. N89-28835
SABNIS, J. S. N89-28754
SADR, RAMIN N89-28684
SADWICK, LARRY P. N89-28716
N89-29241
SAKA, NANNAJI N89-28837
SAKAMOTO, K. N89-29213
SALASIN, JOHN N89-29142
SALEM, JONATHAN A. N89-28853
SALVINO, J. T. N89-28516
N89-28517
SAMARA, G. N89-28801
SAMARASEKERA, I. N89-29222
SAMUELSON, L. N89-29223
SANDERS, STEPHEN C. N89-28680
SANDLIN, DORAL R. N89-28493
SANDUBRAE, JEFF N89-28953
SANFORD, T. W. L. N89-28708
SANTOSOD., BOBBY N89-28937
SARAIYA, NAKUL P. N89-29086
SARJEANT, W. JAMES N89-28565
SARKAR, SUTANU N89-28764
SASAO, MAMIKO N89-29214
SASHEGYI, KEITH D. N89-29121
SATO, HIDEO N89-28883
N89-28918
SATO, ISAO N89-28901
SATO, K. I. N89-29210
SATO, K. N. N89-29213
SATYANARAYANA, P. N89-29205
SAUER, J. R. N89-29081
SAUGIERCOHEN-ADAD, M. T. N89-28664
SAVINO, RAFFAELE N89-28560
SCHAEFER, H. J. N89-28519
SCHAFER, R. W. N89-28689
SCHAFFAR, M. N89-28494
N89-28495
SCHALLES, FRANK N89-28958
SCHENKEL, FRANZ N89-29134
SCHIRBER, J. E. N89-29230
SCHLIESING, JOHN A. N89-28552
SCHLYER, DAVID J. N89-28791
SCHMALE, D. T. N89-28860
SCHMEICHEL, E. N89-29130
SCHMIDLY, CLAUDIA J. N89-29023
SCHMIDT, C. E. N89-28659
SCHNEID, J. N89-29129
SCHNEIDER, M. N89-28809
SCHOOLENBERG, G. E. N89-28656
SCHOTTER, ROLAND N89-28911
SCHRADER, RAINER N89-29102
SCHREIER, G. N89-28915
SCHROEDER, LYLE C. N89-28550
SCHUETTE, RALPH N89-28522
SCHUSTER, KARL-FRIEDRICH N89-28798
SCHUTZBERG, FRANCES N89-28578
SCHUURMAN, J. J. N89-29271
SCHUURMANN, W. N89-29200
SCHVEZOV, C. E. N89-29222
SCHWARTZ, STEPHEN E. N89-28984
SCHWARZL, JOSEF FRIEDRICH N89-28771
SCHWOERKE, STEVE N. N89-28488
SCOLAR, JOSE N89-28961
SEAGRAVES, SQUIRE B. N89-28971
SECOR, H. V. N89-29171
SEDDOUGUI, SHARON O. N89-28766
SEDLMAYR, E. N89-29276
SEEMAN, J. I. N89-29171
SEERING, WARREN P. N89-29097
SEGAWA, YUSABURO N89-29243
SEIBOLD, R. W. N89-28643
SELISKAR, CARL J. N89-28813
SENLIN, ZHANG N89-28919
SERAJI, HOMAYOUN N89-28846
SESHADRI, S. N. N89-28505
SETTLES, G. S. N89-28737
SHA, W. T. N89-28746
SHABANA, A. A. N89-29111
SHAFARMAN, W. N. N89-28944
SHAH, SAMIR N89-29052
SHALKHAUSER, MARY JO W. N89-28545
SHARMA, MEERA N89-28509
SHAW, M. T. N89-28640
SHEFFIELD, RICHARD L. N89-28711
SHELTON, R. N. N89-29231

SHERIDAN, T. N89-28708
SHIELDS, THOMAS E. N89-29042
SHIGEMI, MASASHI N89-28765
SHIMABUKURO, S. N89-28643
SHIMADA, MASANOBU N89-28883
SHRINER, DAVID S. N89-28962
SHUBHA, V. N89-28628
SHUH, DAVID K. N89-28601
N89-28716
N89-29241
N89-29242
N89-29243
SHURTLEFF, WILLIAM W. N89-29153
SHVYRKOV, N. N. N89-28907
SIHVOLA, ARI H. N89-28671
SILVER, MARVIN N89-28715
SIMMONS, JOE D. N89-28785
SIMON, PAUL C. N89-28968
N89-29293
SIMONICH, J. C. N89-29152
N89-29154
SIMONS, JACK N89-29112
SIMONS, JAMES M. N89-28786
SIMONSEN, LEIF N89-28724
SIMPSON, JAMES J. N89-28927
SIMS, G. D. N89-28585
SINGER, NEIL C. N89-28866
SINHA, BRIJNARESH R. N89-28638
SIPILA, MARKKU N89-28704
SIQUEIRA, FRANCISCO BEZERRA N89-28925
SIRKIA, OLLI N89-28913
SIROCKY, PAUL J. N89-28830
SITEK, ZBIGNIEW N89-28895
SKLAD, P. S. N89-29226
SKORPIK, J. R. N89-28861
SKOTHEIM, T. A. N89-29223
SKOU, NIELS N89-28882
SLOAN, GEORGE R. N89-28786
SMELSER, S. C. N89-28587
SMIT, J. H. M. N89-29006
SMIT, JAN N89-29151
SMITH, CHARLOTTE V. N89-29267
SMITH, HOOVER A. N89-28835
SMITH, JOHN H. N89-28615
SMITH, O. E. N89-28551
SMITH, RICHARD D. N89-28592
SMITH, S. T. N89-28721
SMITS, A. J. N89-28734
N89-28735
N89-28736
N89-28738
SMITS, T. W. N89-29075
SNOEIJ, P. N89-28941
SNYDER, ROBERT S. N89-28793
SNYDER, W. B. N89-28636
SOLBRIG, C. M. N89-28645
SOLNTSEV, M. V. N89-28909
SOLOMAKHA, V. N89-28898
SONAR, THOMAS N89-29132
SONDERGAARD, NEAL A. N89-28756
SOO, S. L. N89-28746
SOULE, LARRY N89-29138
SOWERS, R. N89-29137
SPEARS, JOHN H. N89-28688
SPENCE, P. W. N89-28708
SPENCER, J. E. N89-29093
SPETH, P. N89-28931
N89-28977
SPEZIALE, CHARLES G. N89-28762
N89-28763
N89-28764
SPICZAK, GEORGE R. N89-29141
SPIEKSMA, FLOS N89-29139
SPIJKER, M. N. N89-29127
N89-29128
SPRANGLE, P. N89-28675
N89-28815
SPRINGEN, A. L. N89-28524
SRIVASYTAVA, SANTASH N89-28794
STACY, W. D. N89-28839
STAHN, A. N89-28809
STANG, DAVID B. N89-28853
STANSFIELD, S. A. N89-28833
STARKE, EDGAR A., JR. N89-28621
STEELE, FRANCIS N89-28692
STEINETZ, BRUCE M. N89-28830
STENBERG, DUANE R. N89-28784
STEVENS, R. F. N89-28828
STEWART, THOMAS B. N89-29247
STICKLAND, M. T. N89-28501
N89-28502
STODDARD, G. B. N89-28555
STOETZER, MATTHIAS-WOLFGANG N89-28508
STOLL, JOACHIM N89-28773
STPIERRE, GEORGE N89-28577
STRASTERS, JOOST KAREL N89-28614
STRAWN, ROGER C. N89-28498
STRENG, M. N89-28779
STRIMAITIS, DAVID G. N89-28963
STRNAT, KARL J. N89-29148
STUEVE, J. M. N89-29034
STURGEON, WAYNE R. N89-29015
SUBRAMANIAN, N. R. N89-28496
SUGIHARA, RYO N89-29208
SUMARTO, IRAWAN N89-28937
SUNDBERG, R. L. N89-28974
SUNG, C. S. P. N89-28576
SUPEK, S. N89-29008
SURI, MANIL N89-29118
SURLES, MARK C. N89-29036
SUTHERLAND, HERBERT J. N89-28952
SWART, P. J. F. N89-28941
SWIATKIEWICZ, ANDRZEJ N89-28895
SWINDELL, DANIEL W. N89-29048
SWORSKI, THOMAS J. N89-28852
SYDNOR, RICHARD N89-29191
SYMKO, OREST G. N89-29249
SZADY, M. N89-28870

T

TAAL, ARIE N89-29176
TABER, BRADLEY M., III N89-28512
TAKAHASHI, HIDEO N89-28897
TAKAOKA, HIDETOSHI N89-28884
TAKEMURA, T. N89-28921
TALEB-IBRAHIMI, AMINA N89-29247
TALHAM, DANIEL R. N89-28604
TAMEISHI, HIDEO N89-28897
TAMMENMAA, MARKKU N89-28613
TANG, RUEN-TAI N89-28572
TANIMOTO, CHIKAOSA N89-28899
TARASOV, ANDREY N89-28531
TARR, J. A. N89-29054
TASAKI, KAZUYUKI N89-28883
TAUDIERE, ISABELLE N89-29000
TAUX, G. N89-28826
TAY, S. P. N89-28720
TAYLOR, B. C. N89-28564
TAYLOR, DOUG S. N89-28928
TAYLOR, ROBERT R. N89-29266
TEBBETS, ILSE N89-29025
TEBBS, BRICE N89-29058
TERTERASHVILI, A. V. N89-28532
THIESSEN, RICHARD L. N89-28924
THIONNET, A. N89-28582
THOMPSON, A. C. N89-28788
THOMPSON, JACK N89-28506
THOMPSON, STEVEN R. N89-28626
THOMSON, GEORGE M. N89-28966
THORN, WILLARD F. N89-28491
THORNTON, WILLIAM E. N89-29017
THORP, JAMES S. N89-28869
THOWLESS, E. A. N89-28690
TIAN, HONG N89-28837
TIGGES, C. P. N89-29230
TOBUREN, L. H. N89-29147
TOI, K. N89-29213
TONIN-ZANCHIN, VILSON N89-29254
TONOIKE, KUNISHIGE N89-28884
N89-28921
TORRES, ISAIAS N89-28568
TORRESVILLASENOR, GABRIEL N89-29221
TOULOUSE, G. N89-28803
TOWNSEND, LAWRENCE W. N89-29160
N89-29162
TRACY, BARBARA A. N89-29004
TRENT, BRUCE C. N89-28660
TRIPATHY, S. N89-29223
TRYON, GARY H. N89-28985
TUNG, V. X. N89-28768
TURAN, GYORGY N89-29102
TURK, GREG N89-29058
TURNBULL, A. N89-28631
TURNER, JAMES ERIC N89-28546
TWILT, F. N89-28776
N89-28779

U

UCHANSKI, JACEK N89-28895
UDSETH, HAROLD R. N89-28592
UHLMANN, J. N89-29053
ULE, ROBERT L. N89-28843
ULLAL, H. S. N89-28956
UM, C. I. N89-29256
UNAL, A. N89-28870
UNCAPHER, WILLIAM L. N89-28784
UNDERWOOD, J. H. N89-28788
UNRUH, JAMES F. N89-29155
URATA, KAZUHIRO N89-29211
URBAN, W. N89-28809
URI, JOHN J. N89-29017

V

V.D.MOEZEL, B. N89-28934
VACHON, D. J. N89-28643
VALLIS, GEOFFREY K. N89-28927
VALRAUD, FRANCOIS RENE HENRI N89-29258
VANALSTINE, JAMES M. N89-28603
VANDAMME, RUUD N89-28654
N89-28655
VANDENAKKER, BERT N89-29272
VANDERLAAN, F. B. N89-28933
N89-28935
N89-28936
VANDERLAAN, H. N89-29281
VANDERSCHAFT, A. J. N89-28845
N89-29103
VANDEVENDER, J. PACE N89-28565
VANE, L. M. N89-28606
VANEK, M. D. N89-28809
VANGASTEREN, ANTONETTA JOHANNA MARIA
N89-29133
VANGELDORP, G. H. M. N89-28940
VANGILS, S. A. N89-29135
VANGROESEN, E. N89-28782
VANHEERWAARDEN, M. C. N89-29070
VANHULZEN, J. A. N89-29070
VANHULZEN, J. J. P. N89-29067
N89-29271
VANKUIJK, HENDRICUS J. A. N89-29068
N89-29079
VANPARADIJS, JAN N89-29298
VANROSENDALE, JOHN N89-29061
VANVLIET, G. J. N89-28693
N89-28694
VAUCHER, MARC N89-28922
VEESART, JANET LYLE N89-28755
VELAZCO, R. N89-29140
VELDMAN, H. J. N89-29130
VELSKO, STEPHAN P. N89-29224
VERBUNT, FRANK N89-29284
N89-29285
N89-29298
VERSTAPPEN, R. N89-28782
N89-28850
VERSTEEG, M. H. J. B. N89-28526
VIECELLI, J. A. N89-28812
VIITANEN, ARI J. N89-28671
VINCENT, C. L. N89-29004
VINSON, TED S. N89-28668
VISWANATH, GUTTALU R. N89-29055
VODEGEL, M. N89-29178
VOLIAK, K. I. N89-28909
VOLIAK, KONSTANTIN N89-28908
VOLZ, RICHARD A. N89-28562
VONPRAGENAU, GEORGE L. N89-28841
N89-28842
VORONTSOV, V. A. N89-28532

W

WADA, MOTOI N89-29214
WAITE, WILLIAM P. N89-28928
WAKABAYASHI, HIROYUKI N89-28883
WAKAIRO, KAORU N89-28514
WAKKER, K. F. N89-28940
WALCOTT, KERRY N89-28953
WALDRUFF, PAUL N89-28572
WALKER, JOHN S. N89-28756
WALKER, ROBERT A. N89-29025
WALLS, CHARLES G. N89-28682
WALLWITZ, WOLFGANG N89-28891
WALSH, MICHAEL R. N89-29024
WALTER, JOHN W. N89-28868
WALTERS, E. J. N89-28706
WANG, C. M. N89-28857
N89-28858
N89-28859
WANG, KANG L. N89-28716
N89-29241
WANG, LIANKE N89-28902
WANG, LIN-WEN N89-28666
WANG, Y. N89-29236
WANGEN, L. E. N89-29229
WANKA, A. N89-29146
WARD, ALLEN C. N89-29097
WASSERMAN, STEPHEN R. N89-28637
WATANABE, AKIRA N89-28514
WATANABE, H. N89-28912
WATARI, T. N89-29209
WATMUFF, J. H. N89-28736

WATSON, CRIS A. N89-28663
WEBER, WOLF-DIETRICH N89-29089
WEENINK, M. P. H. N89-29200
WEI, WEN-CHENG J. N89-28578
WEINACHT, PAUL N89-28758
WEINBERG, F. N89-29222
WEINGARTEN, K. J. N89-28863
WEINSTEIN, B. N89-28810
WEISS, VOLKER N89-29094
WEITZ, ERIC N89-28597
WELCH, THADDEUS B., III N89-28685
WELLS, J. S. N89-28809
WESSELSKI, CLARENCE J. N89-28554
WESTBROOK, S. R. N89-28661
WESTMACOTT, K. H. N89-28619
WEYMOUTH, TERRY N89-28562
WHALEY, T. W. N89-29229
WHITAKER, WILLIE D. N89-28553
WHITE, C. M. N89-28659
WHITE, C. W. N89-29226
WHITE, G. D. N89-28620
WHITE, JACOB K. N89-29035
WHITE, WARREN B. N89-28927
WHITESIDES, GEORGE M. N89-28594
N89-28637
WHITLOCK, CHARLES H. N89-28993
WIEDEMANN, GUENTER N89-29280
WIEDENMANN, WERNER N89-29173
WIEDER, THOMAS N89-29195
WIELEN, R. N89-29279
WIESELTHIER, J. E. N89-29054
WILLENBORG, D. L. N89-29220
WILLIAMS, R. STANLEY N89-28601
N89-28716
N89-29241
N89-29242
N89-29243
N89-29245
WILMORE, DOUGLAS W. N89-29014
WILSON, J. W. N89-29162
WILSON, S. J. N89-28828
WILSON, TIM A. N89-28488
WINKELHOFF, E. N89-28561
WINTERFELD, G. N89-28610
WITTEN, ALAN J. N89-28923
WOLD, A. N89-28593
N89-29234
WOLFE, JILL D. N89-28929
WOLVERTON, BILLY C. N89-28967
WOOD, RICHARD M. N89-28672
WORCESTER, PETER N89-28926
WORLEY, PATRICK H. N89-29088
WORMS, J. N89-28844
WRIGHT, THOMAS W. N89-28868
WRIGHTON, MARK S. N89-28604
WU, P. N89-29234
WU, S. T. N89-28537
WU, Y. N89-28788
WU, Y. Y. N89-29182
N89-29183
N89-29184
N89-29185
WYATT, JOHN L., JR. N89-29035
WYATT, P. W. N89-28818
WYRICK, LYNN A. N89-29265

X

XU, Y. N89-28582
XU, YONGZHI N89-29001

Y

YADLOWSKY, ANN B. N89-29031
YAGOW, C. E. N89-28708
YAMAGUCHI, YASUSHI N89-28901
YAMAMOTO, HIROMICHI N89-28897
YAMAOKA, HITOSHI N89-29214
YAMARTINO, ROBERT J. N89-28963
YANG, E. S. N89-28718
YANG, PINGHE N89-28902
YANG, RISHENG N89-29197
YANG, X. Q. N89-29223
YANG, XUE D. N89-29190
YARMOFF, JORY A. N89-29247
YATES, L. A. N89-28870
YEH, HEN-GEUL N89-28713
YOUNG, M. A. N89-28605
YOUNG, SCOTT G. N89-29246
YOUNGBLUT, CHRISTINE N89-29142
YUNG, CHAIN-NAN N89-28666

Z

ZACHOS, C. K. N89-29108
ZALESAK, S. T. N89-29205
ZANG, THOMAS A. N89-28762
N89-28763
ZANGENEH, M. N89-28778
ZAPOTOSKY, JOHN E. N89-28691
ZEITLER, G. N89-28581
ZEITLOW, T. C. N89-29237
ZERNIC, MICHAEL J. N89-28570
ZHOU, F. N89-28768
ZHOU, JIANXIN N89-29098
ZIJSLING, T. P. N89-28934
ZIMMERHACKL, E. N89-28581
ZINNECKER, HANS N89-29287
ZIPPEL, RICHARD N89-29044
N89-29114
ZONDAG, E. G. N89-29078
ZUHR, R. A. N89-29225
ZUNIGA, M. N89-29053
ZWEIBEL, K. N89-28956
ZWICK, HARRY N89-29012

Typical Corporate Source Index Listing

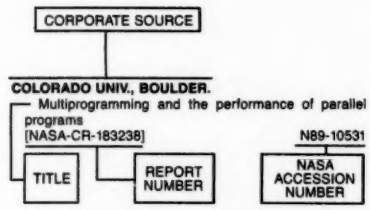

Listings in this index are arranged alphabetically by corporate source. The title of the document provides the user with a brief description of the subject matter. The report number helps to indicate the type of document cited (e.g., NASA report, translation, NASA contractor report). The NASA accession number denotes the number by which the citation is identified. The titles are arranged under each corporate source in ascending accession number order.

A

ADVANCED AVIATION CONCEPTS, JUPITER, FL.
Risk management for air ambulance helicopters operators
[DOT/FAA/DS-88/7] N89-28506

ADVANCED MECHANICAL TECHNOLOGY, INC., NEWTON, MA.
High temperature tribometer, phase 1
[AD-A209356] N89-28838

ADVISORY GROUP FOR AEROSPACE RESEARCH AND DEVELOPMENT, NEUILLY-SUR-SEINE (FRANCE).
A survey of measurements and measuring techniques in rapidly distorted compressible turbulent boundary layers
[AGARD-AG-315] N89-28734
Calendar of selected aeronautical and space meetings
[AGARD-CAL-89/2] N89-29261

AERITALIA S.P.A., NAPLES (ITALY).
Numerical grid generation in 3D Euler-flow simulation
[NLR-MP-88013-U] N89-28777

AERONAUTICAL RESEARCH INST. OF SWEDEN, STOCKHOLM.
Wind tunnel tests of 16 percent thick airfoil with 30 percent trailing edge flap at high angles of attack and with flap angles
[FFA-TN-1985-58] N89-28500
Comparison between two different techniques of computing the axial induction for horizontal axis wind turbines in a locally deformed flow field
[FFA-TN-1986-56] N89-28959

AERONAUTICAL RESEARCH LABS., MELBOURNE (AUSTRALIA).
Comparison of flow-visualised vortices with computed geometry over thin delta wings
[AD-A209083] N89-28489
Aerodynamic model tests of exhaust augmentors for F/A-18 engine run-up facility at RAAF Williamtown
[AD-A208110] N89-28518
Analysis and repair of impact damaged composites
[ARL-STRUCT-R-435] N89-28580
Stresses and strains in a cold-worked annulus
[AR-005-548] N89-28871

AEROSPACE CORP., EL SEGUNDO, CA.
Gauge: Its philosophy and design
[AD-A208944] N89-29083
Applied field and total dose dependence of trapped charge buildup in MOS devices
[AD-A209064] N89-29237
Chemical effects of Ne(+) bombardment on the MoS2(0001) surface studied by high-resolution photoelectron spectroscopy
[AD-A207734] N89-29247

AEROSPACE MEDICAL RESEARCH LABS., WRIGHT-PATTERSON AFB, OH.
Specifications and measurement procedures and aircraft transparencies
[AD-A209396] N89-28511
Investigation of a linear systems model for human visual detection and spatial frequency discrimination
[AD-A209397] N89-29022

AEROSPATIALE USINES DE TOULOUSE (FRANCE).
Composite damaging: Methodological approach
[ETN-89-94866] N89-28582

AIR FORCE ENVIRONMENTAL TECHNICAL APPLICATIONS CENTER, SCOTT AFB, IL.
European crosswind frequencies
[AD-A209137] N89-28985

AIR FORCE GEOPHYSICS LAB., HANSCOM AFB, MA.
The first large balloon launch from Antarctica
[AD-A207735] N89-28491

AIR FORCE HUMAN RESOURCES LAB., BROOKS AFB, TX.
Prevention, reduction, and measurement of combat stress reactions: A bibliography
[AD-A209375] N89-29019

AIR FORCE INST. OF TECH., WRIGHT-PATTERSON AFB, OH.
Glider ground effect investigation
[AD-A209152] N89-28490
Numerical determination of the location of critical inclinations for long term high eccentricity orbits about Mars
[AD-A209200] N89-28538
Orbits containing arcs of minimum altitude variation
[AD-A209206] N89-28539
Orbit determination of sunlight illuminated objects detected by overhead platforms
[AD-A209227] N89-28540
Investigation of laser-induced fluorescence detection of boron oxides in flames
[AD-A209154] N89-28596
A methodology for modeling radar detection range in air combat simulation
[AD-A209153] N89-28679
Evaluation of the bistatic equivalence theorem for the near and far-field radar cross section of complex targets
[AD-A209228] N89-28682
Wake dissipation and total pressure loss in a two-dimensional compressor cascade with crenulated trailing edges
[AD-A209176] N89-28755
Signed-digit high speed transcendental function processor architecture
[AD-A209199] N89-29110

AIR FORCE OCCUPATIONAL AND ENVIRONMENTAL HEALTH LAB., KELLY AFB, TX.
Acoustic tests on a new motor generator system for the minuteman launch control centers in Hill engineering test facilities 1 and 2, Hill AFB, Utah
[AD-A209598] N89-28717

AIR FORCE SYSTEMS COMMAND, EDWARDS AFB, CA.
Proceedings of the Antiproton Technology Workshop held in Upton, New York on 10 May 1989
[AD-A210045] N89-29170

AIR FORCE WEAPONS LAB., KIRTLAND AFB, NM.
A model of parallel performance
[AD-A207792] N89-29049

AIR FORCE WRIGHT AERONAUTICAL LABS., WRIGHT-PATTERSON AFB, OH.
Fatigue crack growth-microstructural relationship of Ti-6Al-4V
[AD-A208107] N89-28626
Heat-transfer and friction factor design data for all-metal compact heat exchangers
[AD-A208108] N89-28761

AIX-MARSEILLES UNIV. (FRANCE).
Rapidly distorted compressible boundary-layers
N89-28735
Laser Doppler anemometry in supersonic flows: Problems of seeding and angular bias N89-28740

AKRON UNIV., OH.
Pull-out and push-out tests for rubber-to-metal adhesion
[AD-A208100] N89-28647
Plastic yielding of partially-crystalline polymers
[AD-A208101] N89-28648
Comparison of peel and lap shear bond strengths for elastic joints with and without residual stresses
[AD-A208102] N89-28867

ALABAMA CRYOGENIC ENGINEERING, INC., HUNTSVILLE.
A cryocooler for high acceleration applications
[AD-A210075] N89-28670

ALABAMA UNIV., HUNTSVILLE.
Coordination of Advanced Solar Observatory (ASO) Science Working Group (SWG) for the study of instrument accommodation and operational requirements on space station
[NASA-CR-185371] N89-28537

ALPHATECH, INC., BURLINGTON, MA.
Fault-tolerant computer architecture modeling and analysis
[AD-A209364] N89-29034

AMETEK, INC., HARLEYSVILLE, PA.
Polycrystalline cadmium telluride 3n-i-p solar cell
[DE89-009437] N89-28945

AMSTERDAM UNIV. (NETHERLANDS).
The influence of the shell closure on the microscopic structure of even-even Hg isotopes: A study with electron and muon beams
[ETN-89-95464] N89-29177

ANALYTIC SCIENCES CORP., READING, MA.
Study of an advanced civil earth remote sensing system: Executive summary
[PB89-163208] N89-28922

ANTHROPOLOGY RESEARCH PROJECT, YELLOW SPRINGS, OH.
Anthropometric survey of US Army personnel: Summary statistics
[AD-A209600] N89-29025

ARGONNE NATIONAL LAB., IL.
Chemical Technology Division
[DE89-013917] N89-28591
Accelerated life evaluation of valve-regulated lead-acid batteries
[DE89-012429] N89-28710
Time- and volume-averaged conservation equations for multiphase flow
[DE89-012418] N89-28746
Pressure drop and heat transfer characteristics of nearly neutrally buoyant particulate slurry for advanced energy transmission fluids
[DE89-013645] N89-28751
Analysis of flow boiling of ammonia and R-114 in a matrix heat exchanger
[DE89-012427] N89-28752
Material and fabrication challenges in the development of monolithic solid oxide fuel cells
[DE89-012422] N89-28957
New infinite-dimensional algebras, sine brackets, and SU (infinity)
[DE89-013178] N89-29108

ARIZONA UNIV., TUCSON.
Experimental and numerical investigation of coherent structures in turbulent wake flows
[AD-A207866] N89-28759
A deep optical infrared survey
[AD-A207930] N89-29278

ARKANSAS UNIV., FAYETTEVILLE.
Military hydrology: Assessment of shuttle imaging radar and LANDSAT imagery for ground-water exploration in arid environments
[AD-A209527] N89-28928

ARMY COLD REGIONS RESEARCH AND ENGINEERING LAB., HANOVER, NH.
Preliminary design guide for arctic equipment
[AD-A209455] N89-29024
QuickDraw data structures for image processing
[AD-A208945] N89-29041
Radiative transfer in falling snow: A two-stream approximation
[AD-A208960] N89-29187

ARMY COMMAND AND GENERAL STAFF COLL., FORT LEAVENWORTH, KANSAS.
Sleep deprivation and its effect on combat effectiveness
[AD-A207970] N89-29013
ARMY CONSTRUCTION ENGINEERING RESEARCH LAB., CHAMPAIGN, IL.
The relationship between ground permittivity and the input impedance of a horizontal dipole near ground
[AD-A207746] N89-28688
ARMY ENGINEER WATERWAYS EXPERIMENT STATION, VICKSBURG, MS.
Development of an efficient solution scheme for incompressible steady-state flow
[AD-A207726] N89-28757
ARMY LAB. COMMAND, WATERTOWN, MA.
Comparative analysis of ultrasonic inspection procedures for Kaman K747 root end fittings
[AD-A207762] N89-28512
Oxidation and hot corrosion of some advanced superalloys at 1300F to 2000F (740C to 1093C)
[AD-A209353] N89-28622
The Bauschinger effect in 6-6-2 titanium alloy and its influence on advanced artillery projectiles
[AD-A209355] N89-28623
Crystal chemistry, magnetic and electrical properties of La(sub2-x)Ba(subx)NiO4
[AD-A209376] N89-29240
ARMY LAB. COMMAND, WHITE SANDS MISSILE RANGE, NM.
An investigation of the workability of Al-8.5 percent Mg alloys
[AD-A209451] N89-28624
ARMY MISSILE COMMAND, REDSTONE ARSENAL, AL.
Design of a command, communications, and control van (surrogate)
[AD-A207652] N89-28687
Maximum-likelihood parameter estimation of a generalized gumbel distribution
[AD-A207994] N89-29055
ARMY RESEARCH INST. OF ENVIRONMENTAL MEDICINE, NATICK, MA.
Thermoregulatory competence during exercise transients in a group of heat-acclimated young and middle-aged men is influenced more distinctly by maximal aerobic power than age
[AD-A209753] N89-29009
ARMY STATEGIC DEFENSE COMMAND, HUNTSVILLE, AL.
Ground-Based Radar (GBR): Environmental assessment
[AD-A207654] N89-29143
ARMY WAR COLL., CARLISLE BARRACKS, PA.
US Army role in space
[AD-A209178] N89-28534
SDI (Strategic Defense Initiative): Shield or sword?
[AD-A209777] N89-29141
International technology transfer as practiced by the U.S.S.R.: Implications for US national security
[AD-A206010] N89-29274
ASSOCIACAO LATINO-AMERICANA DE METALURGIA E MATERIAIS, RIO DE JANEIRO (BRAZIL).
Plastic deformation of YBa2Cu3O7-x superconductor compound
[DE89-613395] N89-29221
Factors affecting stress distribution and displacements in crystals 3-5 grown by Czochralski method with liquid encapsulation
[DE89-613396] N89-29222
ASTRONOMISCHE RECHEN-INST., HEIDELBERG (GERMANY, F.R.).
Activities report of the Heidelburg Astronomical Institute of Computation (Germany, F.R.)
[ETN-89-94429] N89-29279
ATMOSPHERIC AND ENVIRONMENTAL RESEARCH, INC., CAMBRIDGE, MA.
Satellite enhanced numerical weather prediction
[AD-A210108] N89-28987

B

BAILEY CONTROLS CO., WICKLIFFE, OH.
Engine combustion optimization by exhaust analysis
[PB89-195788] N89-28588
BALLISTIC RESEARCH LABS., ABERDEEN PROVING GROUND, MD.
Plasma properties of a large-bore, arc-armature railgun
[AD-A209550] N89-28548
Collisional transfer between and quenching of the 3p 3p and 5p states of the oxygen atom
[AD-A207759] N89-28607
Effect of hydraulic fluid on hydroxylammonium nitrate based liquid propellant formulations
[AD-A208061] N89-28663
Application of computational fluid dynamics to the analysis of the aerodynamics of a railgun projectile
[AD-A207758] N89-28758
Adiabatic shear bands in one dimension
[AD-A208105] N89-28868
Dense heavy metal aerosol monitoring by direct X-ray fluorescence
[AD-A209077] N89-28966
Quantization by cosmic background radiation
[AD-A208103] N89-29297
BELEIDSCOMMIE REMOTE SENSING, DELFT (NETHERLANDS).
Training Course for Tropical Earth Resources Satellite (EARS) bridging phase
[BCRS-88-16D] N89-28938
Marketing and case study of satellite thematic maps and other products of satellite remote sensing
[BCRS-55-16E] N89-28939
BOEING AEROSPACE CO., SEATTLE, WA.
Helium bottle pressure measurement by portable ultrasonic technique
[AD-A208994] N89-29188
BRIGHAM AND WOMEN'S HOSPITAL, BOSTON, MA.
A program for the study of skeletal muscle catabolism following physical trauma
[AD-A207983] N89-29014
BRITISH AEROSPACE PUBLIC LTD. CO., PRESTON (ENGLAND).
A detailed survey of the flow passing through an asymmetric contraction and parallel duct
[BAE-WWT-RP-RES-AXR-000194-PT-A] N89-28501
A detailed survey of the flow passing through an asymmetric contraction and parallel duct
[BAE-WWT-RP-RES-AXR-000194-PT-B] N89-28502
In-situ anodising of aluminium alloys
[BAE/WMD/AR/GEN/00666] N89-28630
Antenna fundamentals: A tutorial paper
[BAE-WAA-R-GEN-RAD-533] N89-28695
The airborne pulse Doppler radar: An introduction to the basic principles
[BAE-WAA-RP-GEN-RAD-584] N89-28696
Airborne pulse Doppler radar. Part 3: Performance estimation
[BAE-WAA-RP-GEN-RAD-645-PT-3] N89-28697
BROOKHAVEN NATIONAL LAB., UPTON, NY.
Positioning error induced by axial sampling in positron emission tomography
[DE89-014519] N89-28791
Characterization of painted surfaces in the United States from the perspective of potential damage from acidic deposition
[DE89-014264] N89-28965
Climate regulation by marine phytoplankton: A test by anthropogenic SO2 emissions
[DE89-014708] N89-28984
Chemical effects of Ne(+) bombardment on the MoS2(0001) surface studied by high-resolution photoelectron spectroscopy
[AD-A207734] N89-29247
BROWN UNIV., PROVIDENCE, RI.
Preparation of compounds with the tetrahedral structure which transmit in the far infrared
[AD-A208697] N89-28593
Redetermination of crystal structure of zinc thiogallate
[AD-A208931] N89-29234
Research program in computational physics
[DE89-013952] N89-29255
BUREAU OF MINES, PITTSBURGH, PA.
Hazards of explosives dusts
[DE89-014554] N89-28669

C

CALIFORNIA INST. OF TECH., PASADENA.
Differential equations and continuum mechanics
[AD-A208637] N89-29109
CALIFORNIA POLYTECHNIC STATE UNIV., SAN LUIS OBISPO.
Analysis of leading edge separation using a low order panel method
[NASA-CR-185892] N89-28493
CALIFORNIA STATE AIR RESOURCES BOARD, SACRAMENTO.
Ozone trends within a large metropolitan area: The Los Angeles Basin
[PB89-145965] N89-28960
CALIFORNIA UNIV., BERKELEY.
Nonlinear stability in fluid and plasma dynamics
[AD-A207715] N89-29203
States of oxygen ordering in YBa2Cu3Oz
[DE89-014893] N89-29227
Vertical gradient freeze GaAs: Growth and electrical properties
[DE89-014894] N89-29228
CALIFORNIA UNIV., BERKELEY. LAWRENCE BERKELEY LAB.
Oxidative addition of C-H bonds in organic molecules to transition metal centers
[DE89-012991] N89-28616
Fundamental studies of grain boundary structure and properties in ICB aluminum
[DE89-014884] N89-28619
An X-ray microprobe using focussing optics with a synchrotron radiation source
[DE89-013425] N89-28788
Fuel cell technology in the United States
[DE89-013430] N89-28951
Canonical integration and analysis of periodic maps using non-standard analysis and Lie methods
[DE89-013389] N89-29106
States of oxygen ordering in YBa2Cu3Oz
[DE89-014893] N89-29227
Vertical gradient freeze GaAs: Growth and electrical properties
[DE89-014894] N89-29228
Cosmic relics from the big bang
[DE89-013268] N89-29283
Spectral measurements of the cosmic microwave background
[DE89-014895] N89-29296
CALIFORNIA UNIV., DAVIS.
Modelling the in situ infrared reflection-absorption spectra of the diffuse layer
[AD-A209347] N89-28598
Solvent effects on simple electron transfer reactions. A comparison of results for homogeneous and heterogeneous systems
[AD-A209381] N89-28600
The analysis of solvent effects on the kinetics of simple heterogeneous electron transfer reactions
[AD-A210078] N89-28602
CALIFORNIA UNIV., LOS ANGELES.
Electronic-structure study of the Ni-Ga and Ni-In intermetallic compounds using X-ray photoemission spectroscopy
[AD-A209696] N89-28601
Thermodynamically stable conducting films of intermetallic PtGa2 on gallium arsenide
[AD-A210077] N89-28716
Enhancement of forced convection heat transfer in tubes using staged tangential flow injection
[PB89-204598] N89-28768
Wind profile estimation from point to point laser distortion data
[NASA-CR-185891] N89-28990
A study of thermodynamic phase stability of intermetallic thin films of Pt2Ga, PtGa and PtGa2 on gallium arsenide
[AD-A209698] N89-29241
A bolt-on deposition source for ultra-high-vacuum growth of intermetallic compound films
[AD-A209699] N89-29242
Lineshape and lifetime studies of exciton luminescence from confined CuCl thin films
[AD-A209750] N89-29243
Initial stages of metal/semiconductor interface formation: Au and AgON Si(111)
[AD-A209490] N89-29245
CALIFORNIA UNIV., SANTA BARBARA.
Effect of an electric field on a split Bloch band
[AD-A209857] N89-29244
CAMBRIDGE UNIV. (ENGLAND).
A compressible inverse design method based on an analytical approach
[CUED/A-TURBO/TR-125] N89-28778
CARNEGIE-MELLON UNIV., PITTSBURGH, PA.
The effect of transients on crack tip stress fields during thermal fatigue loading
[AD-A210084] N89-28864
CENTRE D'ETUDES ET DE RECHERCHES, TOULOUSE (FRANCE).
Solution of Euler equations by a discontinuous Galerkin method obtained from a variational formulation of entropy
[CERT-1/332400/DERI] N89-28775
Experimenting cavitation measuring instruments
[CERT-2305] N89-28803
CENTRO STUDI E LABORATORI TELECOMUNICAZIONI, TURIN (ITALY).
The design of VLSI circuits
[ETN-89-94968] N89-29065
CERAMIC PROCESS SYSTEMS CORP., CAMBRIDGE, MA.
Highly oriented fiber reinforced ceramic composites
[AD-A208119] N89-28578
CHRONAR CORP., PRINCETON, NJ.
Research on stable, high-efficiency, large-area, amorphous-silicon-based submodules, task B
[DE89-009439] N89-28946

COASTAL ENGINEERING RESEARCH CENTER, VICKSBURG, MS.
Hurricane hindcast methodology and wave statistics for Atlantic and Gulf hurricanes from 1956 - 1975
[AD-A207849] N89-29004
COLOGNE UNIV. (GERMANY, F.R.).
Optical properties and error sources of an airborne radiometer
[MITT-60] N89-28799
Errors in the scene identification from satellite data. Effects on the determination of radiation budget parameters
[MITT-59] N89-28931
Parameterization of ice and water clouds and their radiation transport characteristics for large scale atmospheric models
[MITT-58] N89-28977
COLORADO SCHOOL OF MINES, GOLDEN.
Approximation methods for scattering from rough surfaces
[AD-A209482] N89-29192
COLORADO STATE UNIV., FORT COLLINS.
Vibrational dynamics of aniline (Ar)1 and aniline (CH4)1 clusters
[AD-A209560] N89-28605
Photonic architectures for performing perfect shuffle on a time-division multiplexed signal
[PB89-184352] N89-28674
Digital optical computing with fibers and directional couplers
[PB89-184378] N89-29030
The mock counter: A hybrid optical-electronic counter using fiber delay line memory
[PB89-184410] N89-29031
An optoelectronic multi-Gb/s packet switching network
[PB89-184345] N89-29081
A study of non-rigid aromatic molecules by supersonic molecular jet spectroscopy: Observation and spectroscopic analysis of the stable conformations of various alkylbenzenes
[AD-A209561] N89-29171
COLORADO UNIV., BOULDER.
Photonic architectures for performing perfect shuffle on a time-division multiplexed signal
[PB89-184352] N89-28674
Digital optical computing with fibers and directional couplers
[PB89-184378] N89-29030
The mock counter: A hybrid optical-electronic counter using fiber delay line memory
[PB89-184410] N89-29031
An optoelectronic multi-Gb/s packet switching network
[PB89-184345] N89-29081
COLUMBIA UNIV., NEW YORK, NY.
VLSI integrated circuit contact reliability by interface spectroscopy
[AD-A207666] N89-28718
COMMITTEE ON APPROPRIATIONS (U.S. HOUSE).
Departments of Veterans Affairs and Housing and Urban Development and independent agencies appropriations for 1990. Part 6: National Aeronautics and Space Administration
[GPO-99-598] N89-29273
COMPUTER SCIENCES CORP., RESEARCH TRIANGLE PARK, NC.
Materials aerometric database for use in developing materials damage functions
[PB89-181259] N89-28572
CONNECTICUT UNIV., STORRS.
A new method for monitoring cure and mobility in epoxy matrix and fiber/epoxy interphases
[AD-A209428] N89-28576
Microcellular foams from rigid-rod polymers in solutions: Effect of aggregation characteristics on foam properties
[AD-A209024] N89-28640
BM/C(3) algorithm mapping onto concurrent processors
[AD-A207877] N89-29052
CORNELL UNIV., ITHACA, NY.
Multicomponent e-beam resists containing organometallic compounds and reactive monomers
[AD-A207716] N89-28606
Reactive ion etching of polymer films
[AD-A207674] N89-28645
Molecular weight dependence of e-beam resist sensitivity
[AD-A207835] N89-28719
Nonlinear dynamics and control of flexible structures
[AD-A208120] N89-28869
An explicit separation of relativised random polynomial time and relativised deterministic polynomial time
[AD-A210103] N89-29044
An efficiently computable metric for comparing polygonal shapes
[AD-A210105] N89-29045
On planar point matching under affine transformation
[AD-A210106] N89-29046
Interpolating polynomials from their values
[AD-A210102] N89-29114
Placing the largest similar copy of a convex polygon among polygonal obstacles
[AD-A210104] N89-29115
An improved algorithm for labeling connected components in a binary image
[AD-A210100] N89-29190
Quantitative analysis of laser interferometer waveforms obtained during oxygen reactive-ion etching of thin polymer films
[AD-A207836] N89-29248
CREARE, INC., HANOVER, NH.
Superconducting Meissner effect bearings for cryogenic turbomachines, phase 1
[AD-A209875] N89-28839
CSA ENGINEERING, INC., PALO ALTO, CA.
Optimization of structures with passive damping and active controls
[AD-A208937] N89-28862

D

DANISH SPACE RESEARCH INST., LYNGBY.
The fluxgate ringcore sensor demagnetising factor and noise
[ORI-1-89] N89-28805
DAVID SARNOFF RESEARCH CENTER, PRINCETON, NJ.
AlGaAs phased array laser for optical communications
[NASA-CR-181869] N89-28820
Monolithic narrow-linewidth InGaAsP semiconductor laser for coherent optical communications
[NASA-CR-181870] N89-28821
DAYTON UNIV., OH.
Damping properties of various materials
[AD-A209071] N89-28642
Emerging resin characterization
[AD-A208173] N89-28649
Fast-algorithm development for large-eddy simulation of circular-jet turbulence
[AD-A207928] N89-28760
Lubricant evaluation and performance
[AD-A208925] N89-28835
Study of sintered magnets of the Nd-Fe-B type
[AD-A209185] N89-29148
Display characteristics of example light-valve projectors
[AD-A209580] N89-29193
DEFENCE AND CIVIL INST. OF ENVIRONMENTAL MEDICINE, DOWNSVIEW (ONTARIO).
Canadian Forces aircrew ejection, descent, and landing injuries, 1 January 1975 - 31 December 1987
[AD-A208116] N89-29015
DEFENCE RESEARCH ESTABLISHMENT, OTTAWA (ONTARIO).
Bit rate recovery using digital ladder networks
[AD-A209865] N89-29043
DEFENCE RESEARCH ESTABLISHMENT PACIFIC, VICTORIA (BRITISH COLUMBIA).
A Compaq-286 micro-processor based high-speed high-density digital data-acquisition and recording system. Volume 1: System overview
[AD-A207429] N89-29029
DELAWARE UNIV., NEWARK.
The inverse scattering problem for acoustic and electromagnetic waves
[AD-A209202] N89-28681
Materials analysis and device optimization of CuInSe2 solar cells
[DE89-009434] N89-28944
Propagation problem and far-field patterns in a stratified finite depth ocean
[PB89-180707] N89-29001
DEPARTMENT OF THE ARMY, WASHINGTON, DC.
Optical gain control of GaAs microwave monolithic integrated circuit distributed amplifier
[AD-D013969] N89-28705
Method of mass producing superconducting persistent current rings
[AD-D013968] N89-29219
DEUTSCHE FORSCHUNGS- UND VERSUCHSANSTALT FUER LUFT- UND RAUMFAHRT, BRUNSWICK (GERMANY, F.R.).
Grid generation using elliptic partial differential equations
[DFVLR-FB-89-15] N89-29132
DEUTSCHE FORSCHUNGS- UND VERSUCHSANSTALT FUER LUFT- UND RAUMFAHRT, COLOGNE (GERMANY, F.R.).
Activities report in aerospace research in Germany, F.R.
[ISSN-0070-3966] N89-28485
Supersonic combustion at the DFVLR: Results and experiences
[DFVLR-88-044] N89-28610
DEUTSCHE FORSCHUNGS- UND VERSUCHSANSTALT FUER LUFT- UND RAUMFAHRT, GOETTINGEN (GERMANY, F.R.).
Three-dimensional viscous hypersonic flow over blunt bodies
[DFVLR-FB-89-09] N89-28504
Evaluation of LDA 3-component velocity data on a 65 deg delta wing at M = 0.85 and first results of an analysis
[DFVLR-FB-89-19] N89-28505
DEUTSCHE FORSCHUNGS- UND VERSUCHSANSTALT FUER LUFT- UND RAUMFAHRT, OBERPFAFFENHOFEN (WEST GERMANY).
Polarimetric calibration using passive corner reflectors
[DFVLR-FB-89-21] N89-28698
Formulation and numerical solution of the equations of constrained mechanical motion
[DFVLR-FB-89-08] N89-28847
The Archimedes 2a Experiment on oil slick dection over the North Sea, April 1988: Measurement Results obtained by the E-SAR System of the Aerospace Research Establishment
[DFVLR-MITT-89-08] N89-28942
Modeling of short arc orbital constraints for incorporation into photogrammetric adjustment of MEOSS data
[DFVLR-FB-89-14] N89-28943
DHV RAADGEVEND INGENIEURSBUREAU B.V., AMERSFOORT (NETHERLANDS).
Marketing and case study of satellite thematic maps and other products of satellite remote sensing
[BCRS-55-16E] N89-28939

E

ECOLE NATIONALE SUPERIEURE DES ARTS ET METIERS, BORDEAUX (FRANCE).
Steel fatigue under combined loads
[ETN-89-94864] N89-28629
EG AND G ENERGY MEASUREMENTS, INC., LAS VEGAS, NV.
In search of more output: Two strain gage bridge circuits revisited
[DE89-014039] N89-28787
EIC, INC., NORWOOD, MA.
Morphology control of photoelectrochemically etched profiles in n-GaAs
[AD-A208991] N89-29235
Photoelectrochemical fabrication of gratings in SiC
[AD-A208992] N89-29236
ENVIRONMENTAL PROTECTION AGENCY, RESEARCH TRIANGLE PARK, NC.
User's guide to the complex terrain dispersion model plus algorithms for unstable situations (CTDMPLUS). Volume 1: Model description and user instructions
[PB89-181424] N89-28963
Atmospheric processes and effects on materials
[PB89-173215] N89-28964
ETABLISSEMENT TECHNIQUE CENTRAL DE L'ARMEMENT, ARCUEIL (FRANCE).
Nondestructive characterization of simple interfaces using volume sound waves
[ETCA-89-R-015] N89-28654
Detection of target formations in infrared imagery
[ETCA-88-R-070] N89-29198
EUROCONSULT B.V., ARNHEM (NETHERLANDS).
Training Course for Tropical Earth Resources Satellite (EARS) bridging phase
[BCRS-88-16D] N89-28938
EUROPEAN SOUTHERN OBSERVATORY, GARCHING (GERMANY, F.R.).
Activities report in international astronomy
[ETN-89-95333] N89-29281
EUROPEAN SPACE AGENCY, PARIS (FRANCE).
Key data on participating projects. The solar-terrestrial science project of the Inter-Agency Consultative Group for Space Science (IACG)
[ESA-SP-1107] N89-29295
Activities report of ESA
[ISSN-0258-025X] N89-29302
EXETER UNIV. (ENGLAND).
The upper-branch stability of compressible boundary layer flows
[NASA-TM-102128] N89-28748

F

FLORIDA UNIV., GAINESVILLE.
Probabilistic analysis of semilinear partial differential equations
[AD-A209903] N89-29113
FLUOR TECHNOLOGY, INC., IRVINE, CA.
Higee Technology Development Program, phase 1
[PB89-161434] N89-28587
FOKKER B.V., AMSTERDAM (NETHERLANDS).
Numerical grid generation in 3D Euler-flow simulation
[NLR-MP-88013-U] N89-28777
FORSCHUNGSINSTITUT FUER HOCHFREQUENZPHYSIK, WERTHHOVEN (GERMANY, F.R.).
An approximation formula to evaluate the coefficient update rate of partially adaptive antennas
[REPT-5-88] N89-28844
Acoustical tracking of fast maneuvering aircraft by distributed sensors
[REPT-6-88] N89-29156

G

GENERAL DYNAMICS CORP., FORT WORTH, TX.
Small scale model tests in small wind and water tunnels at high incidence and pitch rates. Volume 1: Test program and discussion of results
[AD-A208647] N89-28488
GENEVA OBSERVATORY (SWITZERLAND).
Red giants in open clusters. 1: Binarity and stellar evolution in five Hyades-generation clusters, NGC 2447, 2539, 2632, 6633 and 6940
[SER-C-PREPUBL-FASC-37-PT-1] N89-29290
Red giants in open clusters. 2: Orbits of ten spectroscopic binaries in NGC 2360, 2437, 2447, 5822, 5823, 6475
[SER-C-PREPUBL-FASC-38-PT-2] N89-29291
GEORGIA INST. OF TECH., ATLANTA.
Two-dimensional signal processing and storage and theory and applications of electromagnetic measurements
[AD-A207827] N89-28689
Holographic modulator arrays
[AD-A209387] N89-28792
GESAMTHOCHSCHULE, KASSEL (GERMANY, F.R.).
Simultaneous secondary ion and Auger electron analysis, illustrated by examples from microelectronics research and technology
[ETN-89-94431] N89-28611
A new scattering formula for depth-resolving X-ray diffractometry based on a kinematic theory
[ETN-89-94430] N89-29195
GRENOBLE-1 UNIV. (FRANCE).
An a priori approach to the evaluation of signature analysis efficiency
[IMAG-RR-746-I] N89-29140

H

HARRY DIAMOND LABS., ADELPHI, MD.
HEMP (High-Altitude Electromagnetic Pulse) validation of FAA (Federal Aviation Administration) radio facility
[AD-A209187] N89-28680
The potential and electric fields of a conducting sphere in the presence of a charged conducting plane
[AD-A209498] N89-29149
HARVARD UNIV., CAMBRIDGE, MA.
Formation of monolayers by the coadsorption of thiols on gold: Variation in the length of the head group, tail group and solvent
[AD-A208919] N89-28594
Monolayers of 11-trichlorosilylundecyl thioacetate: A system that promotes adhesion between silicon dioxide and evaporated gold
[AD-A208266] N89-28637
Components of high-level vision: A cognitive neuroscience analysis and accounts of neurological syndromes
[AD-A207848] N89-29011
HEBREW UNIV., JERUSALEM (ISRAEL).
The coagulation and dispersion of nonspherical, aerosol particles in a turbulent atmosphere
[AD-A208064] N89-29150
HELSINKI UNIV. OF TECHNOLOGY, ESPOO (FINLAND).
The atomic layer epitaxy growth and characterization of zinc sulfide and alkaline earth sulfide thin films for electroluminescence applications
[ISBN-952-90014-6-0] N89-28613
The influence of structure and alloying on the cold-formability of ferritic steels and the utility of uniaxial tensile testing in its assessment
[ISBN-952-90044-3-5] N89-28632
Exact image theory for uniaxially anisotropic dielectric half space
[PB89-146450] N89-28671
Higher order base dynamics of a bipolar transistor with nonuniform doping
[PB89-155451] N89-28704
The problem of selecting the shape functions for a p-type finite element
[AD-A207798] N89-29117
Measurements of the dipolar velocity of superfluid 3 He-B
[PB89-155444] N89-29218
HERAEUS (W. C.) G.M.B.H., HANAU (GERMANY, F.R.).
Improvements of the efficiency of solid state lasers by spectral conversion of the excitation lamp's output
[ETN-89-94425] N89-28822
HOUSTON UNIV., TX.
Primary research efforts on exploring the commercial possibilities of thin film growth and materials purification in space
[NASA-CR-184913] N89-28541
HUGHES AIRCRAFT CO., EL SEGUNDO, CA.
High temperature adhesive systems
[AD-A209166] N89-28643
HUMAN ENGINEERING LABS., ABERDEEN PROVING GROUND, MD.
Choice and perceived control: Implications for the design of displays
[AD-A208400] N89-29021

I

IIT RESEARCH INST., CHICAGO, IL.
ELF (Extremely Low Frequency) communications system ecological monitoring program
[AD-A206198] N89-28691
ILLINOIS UNIV., CHICAGO.
Conditional dependence
[AD-A207881] N89-29120
ILLINOIS UNIV., URBANA.
Theoretical model of gravitational perturbation of current collector axisymmetric flow field
[AD-A209499] N89-28756
Total Lagrangian formulation for large-displacement analysis of the triangular finite elements
[AD-A209378] N89-29111
IMPERIAL COLL. OF SCIENCE AND TECHNOLOGY, LONDON (ENGLAND).
General comments on the interpretation of data
N89-28742
IMPLANT SCIENCES CORP., DANVERS, MA.
Ion implantation of ceramic bearings
[AD-A209770] N89-28644
INDIANA UNIV., BLOOMINGTON.
High resolution electron energy loss studies of surface vibrations
[DE89-013964] N89-28589
INSTITUT D'AERONOMIE SPATIALE DE BELGIQUE, BRUSSELS.
Absorption cross section of alternative chlorofluoroethanes and potential effects on the ozone layer
[AERONOMICA-ACTA-A-340-1989] N89-28968
Aeronomic problems of molecular oxygen photodissociation. 5: Predissociation in the Schumman-Runge Bands of Oxygen
[AERONOMICA-ACTA-A-341-1989-5] N89-28980
Aeronomic problems of molecular oxygen photodissociation. 6: Photodissociation frequency and transmittance in the spectral range of the Schumman-Runge bands
[AERONOMICA-ACTA-A-342-1989-6] N89-28981
Solar ultraviolet radiation within the middle atmosphere
[AERONOMICA-ACTA-A-337-1989] N89-29293
Solar spectral irradiances with their diversity between 120 and 900 nm
[AERONOMICA-ACTA-A-338-1989] N89-29294
INSTITUT FRANCO-ALLEMAND DE RECHERCHES, SAINT-LOUIS (FRANCE).
Study of the wing-vortex interaction in three dimensional flows (incompressible inviscid flow)
[ISL-R-123/87] N89-28494
Profile-vortex interactions
[ISL-R-125/87] N89-28495
Measurements of mean-flow and turbulence characteristics in a turbojet exhaust using a laser velocimeter
[ISL-CO-226/88] N89-28519
Laser velocimetry in the close wake of an axisymmetric rear body
[ISL-R-114/87] N89-28774
On strain gages using the PVF2 piezoelectric polymer
[ISL-CO-210/88] N89-28801
The copy of single beam holograms
[ISL-CO-212/88] N89-28802
The problem of very high magnifications in holography
[ISL-CO-218/88] N89-28804
The use of high-frequency pulsed laser diodes in fringe type laser Doppler anemometry
[ISL-CO-230/88] N89-28826
Compression tests using Hopkinson bars: Numerical simulation and experimental study
[ISL-C-208/88] N89-28873
INSTITUTE FOR COMPUTER APPLICATIONS IN SCIENCE AND ENGINEERING, HAMPTON, VA.
A preliminary compressible second-order closure model for high speed flows
[NASA-CR-181875] N89-28764
A nonlinear investigation of the stationary modes of instability of the three-dimensional compressible boundary layer due to a rotating disc
[NASA-CR-181901] N89-28766
Variational formulation for a nonlinear elliptic equation in a three-dimensional exterior domain
[NASA-CR-181885] N89-29028
Parallel language constructs for tensor product computations on loosely coupled architectures
[NASA-CR-181900] N89-29061
A hybrid perturbation-Galerkin method for differential equations containing a parameter
[NASA-CR-181891] N89-29122
Solution of the hydrodynamic device model using high-order non-oscillatory shock capturing algorithms
[NASA-CR-181886] N89-29123
Optimal error analysis of spectral methods with emphasis on non-constant coefficients and deformed geometries
[NASA-CR-181902] N89-29124
INSTITUTE FOR DEFENSE ANALYSES, ALEXANDRIA, VA.
SDS (Strategic Defense System) software testing and evaluation: A review of the state-of-the-art in software testing and evaluation with recommended R and D tasks
[AD-A209447] N89-29142
A comparison and analysis of strategic defense transition stability models
[AD-A208033] N89-29144
Strategic defense system distributed operating system R and D review and recommendations
[AD-A208034] N89-29145
Computer-aided group problem solving for Unified Life Cycle Engineering (ULCE)
[AD-A209446] N89-29260
INSTITUTO DE PESQUISAS ESPACIAIS, SAO JOSE DOS CAMPOS (BRAZIL).
Identification of irrigated areas in the Sao Francisco Valley through remote sensing data. Pilot area: Petrolina-Juazeiro
[INPE-4800-RPE/587] N89-28925
INTERNATIONAL CENTRE FOR THEORETICAL PHYSICS, TRIESTE (ITALY).
On the Riemannian curvature of a twistor space
[DE89-611897] N89-29107
INTERNATIONAL INST. FOR AERIAL SURVEY AND EARTH SCIENCES, ENSCHEDE (NETHERLANDS).
Monitoring and measuring human settlement changes by remote sensing methods
[BCRS-88-16C] N89-28937
INTERNATIONAL METEOROLOGICAL INST., STOCKHOLM (SWEDEN).
Activities report in meteorology in Sweden
[AR-87-88] N89-28999
IOWA STATE UNIV. OF SCIENCE AND TECHNOLOGY, AMES.
Synthesis and hot pressing of ZnS powders
[AD-A209602] N89-28625
Numerical solution of ill posed problems in partial differential equations
[AD-A207852] N89-29119
ISRAEL OCEANOGRAPHIC AND LIMNOLOGICAL RESEARCH LTD., HAIFA.
The sensitivity of Middle East precipitation and cloud forecasts to changes in Eastern Mediterranean Sea surface temperatures
[AD-A207864] N89-28988

J

JET PROPULSION LAB., CALIFORNIA INST. OF TECH., PASADENA.
Television monitor field shifter and an opto-electronic method for obtaining a stereo image of optimal depth resolution and reduced depth distortion on a single screen
[NASA-CASE-NPO-17249-1-CU] N89-28676
Systolic VLSI array for implementing the Kalman filter algorithm
[NASA-CASE-NPO-17108-1-CU] N89-28713

Robust high-performance control for robotic manipulators
[NASA-CASE-NPO-17785-1-CU] N89-28846
A high-resolution atlas of the infrared spectrum of the sun and the earth atmosphere from space. A compilation of ATMOS spectra of the region from 650 to 4800 cm-1 (2.3 to 16 microns). Volume 2: Stratosphere and mesosphere, 650 to 3350 cm-1
[NASA-RP-1224-VOL-2] N89-28969
Trochoidal analysis of scattered electrons in a merged electron-ion beam geometry
[NASA-CASE-NPO-16789-1-CU] N89-29169

JOHNS HOPKINS UNIV., BALTIMORE, MD.
Large scale function minimization
[AD-A207718] N89-29087

JOINT PUBLICATIONS RESEARCH SERVICE, ARLINGTON, VA.
JPRS report: Science and technology. USSR report: Life sciences
[JPRS-USP-89-005] N89-28527
The orbital space observatory Gamma N89-28528
Buran flight testing, capabilities discussed N89-28529
Designers' commentary on Buran flight control system N89-28530
Development, testing procedures for Buran shuttle N89-28531
Method for research on planet Venus using floating balloon stations: Mathematical model N89-28532
JPRS Report: Science and Technology. USSR: Space. 16th International Congress of the International Society for Photogrammetry and Remote Sensing, volume 1
[JPRS-USP-89-002-VOL-1] N89-28876
A new holographic inverse filtering method and its application to restoration of degraded remote sensing images N89-28877
A Bistatic Parasitical Radar (BIPAR) N89-28878
A practical method of remotely sensed digital image's resolving power N89-28879
A conceptual study of optical earth observation from geosynchronous orbit N89-28880
Modelling orientation parameters of sensor platforms N89-28881
KRAS: A Danish high resolution airborne SAR N89-28882
Outline of MOS-1 Verification Program (MVP) N89-28883
Investigation of the effectiveness and applications of Japanese ERS-1 stereoscopic images N89-28884
A satellite assisted-tracking system with real-time accommodation for maximal pointing N89-28885
Local area network and data network for the Advanced Earth Observing Satellite, ADEOS system N89-28886
SAR activities at Dornier N89-28887
ERS-1 SAR processing with CESAR N89-28888
Experiences in implementing an expert system supported man-machine-interface for the configuration of the intelligent SAR processor N89-28889
EXAS: Experiment on Autonomous SAR processor calibration N89-28890
Zeiss Digital Mapping: A new hardware and software system concept from Kombinat VEB Carl Zeiss JENA N89-28891
High resolution Soviet space photographs for topographic mapping N89-28892
Map production and revision with satellite photographs taken by the MKF-6 camera and by the cameras KATE-140, KATE-200, and KFA-1000 N89-28893
An expert system for satellite image interpretation and G.I.S. based problem solving N89-28894
National report of Polish Society of Photogrammetry and Remote Sensing N89-28895
A comparison between the variability structure of the remotely sensed sea-surface temperature and pigment distributions N89-28896
A study on information analysis aids for sea surface temperature image data N89-28897
Interpretation of remote sensing data from eastern areas of the Baltic Sea N89-28898
Development of borehole scanner for underground geological survey N89-28899
An improving multispectral recording set analysis method N89-28900
Development of a field radiometer as a ground truth equipment for the Japanese ERS-1 N89-28901
Application of aerial side-looking radar imagery in China N89-28902
JPRS Report: Science and Technology. USSR: Space. 16th International Congress of the International Society for Photogrammetry and Remote Sensing, volume 2
[JPRS-USP-89-003-VOL-2] N89-28903
Performance evaluation of ERS-1 Synthetic Aperture Radar Fast Delivery Processor N89-28904
The Brazilian experience in handling 15 years of remote sensing satellite data N89-28905
ESA's activities and plans for remote sensing data systems N89-28906
The possibilities of application of satellite data for monitoring ice condition in the Antarctic region N89-28907
Sea spectra as determined from low-altitude SLAR images N89-28908
Lidar measurements of sea surface waves N89-28909
National program for handling large volumes of satellite data N89-28910
Real time SAR processing techniques N89-28911
Simulation of ERS-1/OPS by the use of airborne spectroradiometer N89-28912
Noise reduction from Synthetic Aperture Radar imagery N89-28913
The new generation SPOT satellites SPOT 4 and 5 N89-28914
Design aspects of a system for geocoding satellite SAR images N89-28915
A survey of aerial image quality assessment methods N89-28916
The processing of SPOT imagery in Brazil N89-28917
Data processing and calibration of SAR data in Japan N89-28918
Studies on object reconstruction from space using three line scanner imagery N89-28919
Earth observation programs in Japan N89-28920
Estimation of the simulated JERS-1 data N89-28921

K

KARLSRUHE UNIV. (GERMANY, F.R.).
Experimental investigations of flow forces exerted on spheres in rest and in motion, in a plane Poiseville flow
[ETN-89-94433] N89-28770
Analysis of turbulent transport phenomena in the maritime atmospheric boundary layer
[WISS-BER-10] N89-28978
Application of similarity methods to the turbulent diffusion in the convective and stable boundary layer
[WISS-BER-12] N89-28979
Difference techniques for solving the advection equation
[WISS-BER-8] N89-28991
Experimental investigation of the pressure drag in the Alps
[WISS-BER-9] N89-28992

KENSAL CONSULTING, TUCSON, AZ.
Three dimensional cellular automata for subpixel target detection
[AD-A208163] N89-29100

KERNFORSCHUNGSANLAGE, JUELICH (GERMANY, F.R.).
Survey of test procedures for high performance ceramic materials and their fundamentals
[JUEL-SPEZ-470] N89-28653

L

LABORATOIRE D'AUTOMATIQUE ET D'ANALYSE DES SYSTEMES, TOULOUSE (FRANCE).
On the composition of interconnected systems by nonserial dynamic programming: Application to power systems
[LAAS-89.096] N89-29064
On constrained multivariable adaptive control
[LAAS-89.093] N89-29101
Study and simulation of an E-beam microlithography process on a multilayer resin structure. Research of an optimization
[LAAS-89.012] N89-29179

LAWRENCE LIVERMORE NATIONAL LAB., CA.
Dynamics of colloidal dispersions via lattice-gas models of an incompressible fluid
[DE89-013146] N89-28750
Linear theory of uncompensated thermal blooming in turbulence
[DE89-014604] N89-28812
On the use of the FEL to produce high transient space-charge potentials in a magnetized plasma
[DE89-014325] N89-28814
A proposal of more expedient methods of testing machine tools
[DE89-013033] N89-28832
Energy and Technology Review
[DE89-013919] N89-28954
Realtime tracking system for the wide-field-of-view telescope project
[DE89-013787] N89-29186
Chiral organic crystals for high power frequency conversion
[DE89-013791] N89-29224

LEHIGH UNIV., BETHLEHEM, PA.
Infrared study of carbon deposits on catalysts
[DE89-013310] N89-28634

LEIDEN UNIV. (NETHERLANDS).
The stability of the theta-methods in the numerical solution of delay differential equations
[TW-88-08] N89-29127
A generalization of the numerical range of a matrix
[TW-88-09] N89-29128
A necessary condition for B-convergence of Runge-Kutta methods
[TW-89-01] N89-29129
Are limits of alpha-discounted optimal policies Blackwell optimal: A counterexample
[TW-88-10] N89-29139

LETTERMAN ARMY INST. OF RESEARCH, SAN FRANCISCO, CA.
Transient visual effects of prolonged small spot foveal laser exposure
[AD-A207945] N89-29012

LOS ALAMOS NATIONAL LAB., NM.
Laboratory investigations: Low earth orbit environment chemistry with spacecraft surfaces
[DE89-014280] N89-28533
Prototype testing for a hybrid gas-gun/railgun device
[DE89-014294] N89-28542
Reliability estimates for large satellite memories in low earth orbits
[DE89-007764] N89-28555
Numerical simulation of the simultaneous detonation of two identical, fully contained explosions
[DE89-014844] N89-28660
Exploding metallic foils and fuses: A computational modeling update
[DE89-014033] N89-28709
High-brightness electron injectors: A review
[DE89-014244] N89-28711
The Mark 101 flux compression generator: Development progress
[DE89-014298] N89-28712
The Los Alamos Fourier-transform spectrometer: Applications to molecular spectroscopy
[DE89-014258] N89-28789
An improved hibachi support structure for electron-beam diode foils
[DE89-014023] N89-28810
Chemical and Laser Sciences Division
[DE89-014385] N89-28811
Significant improvement in IR surface-temperature measurements
[DE89-014808] N89-28926
Parallel electric fields in a simulation of magnetotail reconnection and plasmoid evolution
[DE89-012622] N89-28970
Monte Carlo analysis of localization errors in magnetoencephalography
[DE89-013221] N89-29007
Transient visual evoked neuromagnetic responses: Identification of multiple sources
[DE89-013438] N89-29008
Particle production results from HELIOS
[DE89-013454] N89-29167
General-purpose heat source development: Extended series test program SRB fragment/fuselage tests
[DE89-014389] N89-29180
Caviton dynamics in strong Langmuir turbulence
[DE89-012635] N89-29202
High-temperature superconductor materials processing: Development of environmentally acceptable processing technologies
[DE89-014391] N89-29229

LOUISIANA STATE UNIV., BATON ROUGE.
Measurement of solar proton-proton fusion neutrinos with a Soviet-American gallium experiment
[DE89-014563] N89-29168

LOWELL UNIV., MA.
Cognition and order in Langmuir-Blodgett films of a 3-hexadecyl pyrrole and ferrocene-derivatized pyrrole mixed monolayer system
[DE89-012974] N89-29223

LYON-1 UNIV., VILLEURBANNE (FRANCE).
Synthesis of monomethylhydrazine
[ETN-89-94863] N89-28664

M

MAINZ UNIV. (GERMANY, F.R.).
The scavenging of atmospheric pollutants by clouds and precipitation using a vertical wind tunnel, phase 1
[BPT-9/88] N89-28525

MARTIN MARIETTA AEROSPACE, DENVER, CO.
Study of sampling systems for comets and Mars
[NASA-CR-185514] N89-29292

MARYLAND UNIV., COLLEGE PARK.
The structural response of unsymmetrically laminated composite cylinders
[NASA-CR-185834] N89-28856
The p-version of the finite element method for domains with corners and for infinite domains
[AD-A207797] N89-29116
The problem of selecting the shape functions for a p-type finite element
[AD-A207798] N89-29117
Implementation of nonhomogeneous Dirichlet boundary conditions in the p-version of the finite element method
[AD-A207799] N89-29118
MASSACHUSETTS INST. OF TECH., CAMBRIDGE.
Optimum design methods for structural sandwich panels
[AD-A209427] N89-28575
Use of microelectrode arrays to directly measure diffusion of ions in solid electrolytes: Proof of concept experiments involving Ag+ in a solid polymer electrolyte
[AD-A209536] N89-28604
Theoretical analysis of phase transformations in Fe-Ni invar-type alloys
[DE89-014454] N89-28618
The MIT/Marine Industry Collegium: Novel applications of marine biopolymers
[PB89-182950] N89-28633
Preliminary design of a consultation knowledge-based system for the minimization of distortion in welded structures
[AD-A208842] N89-28634
The tribology of undulated surfaces
[AD-A209275] N89-28637
Residual vibration reduction in computer controlled machines
[AD-A208074] N89-28866
Spacecraft flight simulation: A human factors investigation into the man-machine interface between an astronaut and a spacecraft performing docking maneuvers and other proximity operations
[NASA-CR-177502] N89-29020
A robot that walks: Emergent behaviors from a carefully evolved network
[AD-A207958] N89-29026
Critical problems in very large scale computer systems
[AD-A208070] N89-29035
A programming language supporting first-class parallel environments
[AD-A207833] N89-29051
An object-oriented software reuse tool
[AD-A208018] N89-29056
A reconfigurable arithmetic processor
[AD-A208323] N89-29062
Chapter on distributed computing
[AD-A208996] N89-29084
The performance of a mechanical design Compiler
[AD-A209540] N89-29097
Microwave emission from relativistic electron beams
[AD-A209653] N89-29181
A manufacturing scheduler's perspective on semiconductor fabrication
[AD-A208372] N89-29232
Evaluation of functionality in distributed systems
[AD-A209167] N89-29258
MASSACHUSETTS INST. OF TECH., LEXINGTON.
Adaptive detection and parameter estimation for multidimensional signal models
[AD-A208971] N89-28678
Laser-induced diode linking for wafer-scale integration
[AD-A207921] N89-28818
Storm models for end-to-end TDWR (Terminal Doppler Weather Radar) signal processing simulation tests
[AD-A209384] N89-28986
MAX-PLANCK-INST. FUER KERNPHYSIK, HEIDELBERG (GERMANY, F.R.).
Activities report of the Max-Planck Institute of Nuclear Physics
[ETN-89-94398] N89-29174
MAX-PLANCK-INST. FUER PHYSIK UND ASTROPHYSIK, GARCHING (GERMANY, F.R.).
Activities report of the Institute for Extraterrestrial Physics
[MPE-212] N89-29277
Development of a postdiapersion system for astronomical infrared observations with Fourier spectrometers and its application in the study of the CO fundamental bands in F, G and K stars
[MPE-214] N89-29280
The origin and evolution of X-ray binaries and low-magnetic field radio pulsars
[MPE-PREPRINT-145] N89-29284
Evolution of wide binary millisecond pulsars in globular clusters
[MPE-PREPRINT-148] N89-29285
Evidence for two charged particle populations in the Crab nebula
[MPE-PREPRINT-147] N89-29286
Towards a theory of star formation
[MPE-PREPRINT-150] N89-29287
Measurement of the Vela pulsar's proper motion and detection of the optical counterpart of its compact X-ray nebula
[MPE-PREPRINT-151] N89-29288
Millisecond radio pulsars in globular clusters
[NASA-CR-185909] N89-29298
MAX-PLANCK-INST. FUER PHYSIK UND ASTROPHYSIK, MUNICH (GERMANY, F.R.).
Development of a novel silicon detector with internal amplification
[MPI-PAE/EXP.EL-197] N89-28798
Measurement of electroweak effects and topological branching conditions in the reaction e(+)e(-) yields tau(+)tau(-) in the storage ring PETRA
[MPI-PAE/EXP.EL-195] N89-29173
MAX-PLANCK-INST. FUER PLASMAPHYSIK, GARCHING (GERMANY, F.R.).
Analytical solutions for the field, current density, force force density and mechanical stress distribution in toroidal coil systems
[IPP-2/294] N89-28728
MAX-PLANCK-INSTITUT FUER STROEMUNGSFORSCHUNG, GOETTINGEN (GERMANY, F.R.).
Molecular beam experiment for the determination of differential cross sections of the reaction of deuterium atoms with vibrationally excited hydrogen molecules
[MPIS-10/1988] N89-29178
MCDONNELL-DOUGLAS ASTRONAUTICS CO., HUNTINGTON BEACH, CA.
Electric fields in earth orbital space
[AD-A209542] N89-28973
MEASUREMENT CONCEPTS CORP., COLTS NECK, NJ.
Digital refractometry of piezoelectric crystalline media
[AD-A209362] N89-29239
MESSERSCHMITT-BOELKOW-BLOHM G.M.B.H., BREMEN (GERMANY, F.R.).
Key structures mechanical issues of the European Space Station and platform program Columbus
[MBB-UD-0041-88-PUB] N89-28561
MESSERSCHMITT-BOELKOW-BLOHM G.M.B.H., OTTOBRUNN (GERMANY, F.R.).
Proposed concepts for a advanced optical payload for second generation Meteosat
[ETN-89-95236] N89-28564
MICHIGAN UNIV., ANN ARBOR.
Metal/metallion system in low temperature molten salts
[AD-A208025] N89-28724
MIDWEST RESEARCH INST., GOLDEN, CO.
Three-dimensional airfoil performance measurements on a rotating wing
[DE89-009443] N89-28487
Fuels from microalgae
[DE88-001192] N89-28657
Biofuels technical information guide
[DE89-000894] N89-28658
Materials analysis and device optimization of CuInSe2 solar cells
[DE89-009434] N89-28944
Polycrystalline cadmium telluride 3n-i-p solar cell
[DE89-009437] N89-28945
Research on stable, high-efficiency, large-area, amorphous-silicon-based submodules, task B
[DE89-009439] N89-28946
Solar thermal program summary. Volume 2: Research summaries, fiscal year 1988
[DE89-000661] N89-28947
Photovoltaics advanced research and development
[DE89-000895] N89-28948
Two-terminal CuInSe-based cascade cells
[DE89-009422] N89-28950
Thin film photovoltaics
[DE89-009425] N89-28956
MINERALS MANAGEMENT SERVICE, ANCHORAGE, AK.
WINDROSE: A program for IBM-compatible personal computers, documentation
[PB89-167423] N89-29039
MINNESOTA UNIV., MINNEAPOLIS.
Studies of the volume and plasma sheath properties of radio frequency discharges
[AD-A207980] N89-29206
MISSOURI UNIV., ROLLA.
Characterization of substituted phenol-formaldehyde resins using solid-state carbon-13 NMR
[AD-A208745] N89-28638
MITRE CORP., MCLEAN, VA.
Collision avoidance operational concept
[WP-88W00418] N89-28509
Direct User Access Terminal (DUAT) operational concept
[WP-88W00075] N89-28524
MORTON THIOKOL, BRIGHAM CITY, UT.
Igniter heater EMI transient test
[NASA-CR-183743] N89-28566
MOUND LAB., MIAMISBURG, OH.
Investigation of ambient and high temperature aging of PETN (Pentaerythritol Tetranitrate) by laser induced fluorescence and ultraviolet absorption spectroscopies
[DE89-013740] N89-28813

N

NAGOYA UNIV. (JAPAN).
ECH plasma for different magnetic axis positions and initial ICRF plasma production experiments in CHS
[IPPJ-907] N89-29201
Solid-vapor differences of electronic stopping powers for protons
[IPPJ-901] N89-29207
Unlimited acceleration of particles by a system of multi-laser beams
[IPPJ-902] N89-29208
High power ICRF heating experiments on the JIPP T-IIU tokamak
[IPPJ-903] N89-29209
A three-dimensional resistive MHD simulation analysis of field reversal control in the reversed field pinch
[IPPJ-904] N89-29210
Caotic magnetic field line in toroidal plasmas
[IPPJ-911] N89-29211
Full consistent analysis of high beta steady state tokamaks sustained by beam driven and bootstrap currents
[IPPJ-912] N89-29212
Improved confinement in high density ohmic discharge
[IPPJ-913] N89-29213
Effect of a converter electrode in a multicusp negative ion source
[IPPJ-914] N89-29214
A new method of testing nuclear fusion in metals
[IPPJ-915] N89-29215
NAPLES UNIV. (ITALY).
Hermes preparatory program. Fluid dynamics and numerical analysis. Theoretical modeling of high temperature hypersonic flows
[ANE-13/87] N89-28503
Physical phenomenology and mathematical models of hypersonic motion
[ETN-89-95201] N89-28560
Effects of real gas in hypersonic expansion
[ETN-89-95200] N89-28783
NATIONAAL INST. VOOR KERNFYSICA EN HOGE ENERGIEFYSICA, AMSTERDAM (NETHERLANDS).
The beam viewer
[LINO-160] N89-28693
Video processing using the MSX computer
[LINO-163] N89-28694
Some aspects of a lattice formulation of chiral gauge theories
[NIKHEF-ITFA-88-51] N89-29151
New layout of Amsterdam pulse stretcher
[NIKHEF-K/APS/88-01A-REV] N89-29182
Apertures of ring quadrupoles and sextupoles
[NIKHEF-K/APS/88-03] N89-29183
Orbit correction scheme for the new ring
[NIKHEF-K/APS/88-04] N89-29184
Updated OC scheme
[NIKHEF-K/APS/88-04A] N89-29185
NATIONAL ACADEMY OF SCIENCES - NATIONAL RESEARCH COUNCIL, WASHINGTON, DC.
Advanced power sources for space missions
[NASA-TM-101811] N89-28565
Advanced robotics for Air Force operations
[AD-A210098] N89-28840
NATIONAL AERONAUTICAL LAB., BANGALORE (INDIA).
Role of supercomputer in computational aerodynamics
[PD-CF-8925] N89-28496
Flow calculation over a delta-wing using the thin-layer Navier-Stokes equations
[PD-CF-8924] N89-28497
Model simplification based on the concept of equivalent dead time
[NAL-TM-SE-8802] N89-28521
Pressure induced anomaly at Tc in Fe78 Mo2 B20
[NAL-TM-MT-8806] N89-28628
Photoetched double spiral device
[PD-SE-8911] N89-29071
Transfer of files between IE-32C PC/AT CAD system and Autotrol AD/380 graphics system
[PD-CC-8903] N89-29270

NATIONAL AERONAUTICS AND SPACE ADMINISTRATION, WASHINGTON, DC.
NASA thesaurus supplement. A four part cumulative supplement to the 1988 edition of the NASA thesaurus
[NASA-SP-7064-SUPPL-1] N89-29262
Patent abstracts bibliography: A continuing bibliography. Section 2: Indexes (supplement 35)
[NASA-SP-7039(35)-SECT-2] N89-29264
NASA thesaurus supplement: A four part cumulative supplement to the 1988 edition (supplement 2)
[NASA-SP-7064-SUPPL-2] N89-29269

NATIONAL AERONAUTICS AND SPACE ADMINISTRATION. AMES RESEARCH CENTER, MOFFETT FIELD, CA.
Correlation of Puma airloads: Evaluation of CFD prediction methods
[NASA-TM-102226] N89-28498
Laser Doppler anemometry N89-28739
One-degree-of-freedom motion induced by modeled vortex shedding
[NASA-TM-101038] N89-28870
Muscle changes with eccentric exercise: Implications on earth and in space
[NASA-TM-102227] N89-29016

NATIONAL AERONAUTICS AND SPACE ADMINISTRATION. GODDARD SPACE FLIGHT CENTER, GREENBELT, MD.
The 1988 Antarctic ozone monitoring Nimbus-7 TOMS data atlas
[NASA-RP-1225] N89-28983

NATIONAL AERONAUTICS AND SPACE ADMINISTRATION. JOHN C. STENNIS SPACE CENTER, BAY SAINT LOUIS, MS.
A combined air and water pollution control system
[NASA-CASE-NST-00007-1] N89-28967

NATIONAL AERONAUTICS AND SPACE ADMINISTRATION. LYNDON B. JOHNSON SPACE CENTER, HOUSTON, TX.
Docking mechanism for spacecraft
[NASA-CASE-MSC-21386-1] N89-28552
Space module assembly apparatus with docking alignment flexibility and restraint
[NASA-CASE-MSC-21211-1] N89-28553
Expandable pallet for space station interface attachments
[NASA-CASE-MSC-21117-2] N89-28554
Vibration analyzer
[NASA-CASE-MSC-21408-1] N89-28829
Visual suppression of the vestibulo-ocular reflex during space flight
[NASA-TM-102157] N89-29017
Method and apparatus for bio-regenerative life support system
[NASA-CASE-MSC-21629-1] N89-29027

NATIONAL AERONAUTICS AND SPACE ADMINISTRATION. LANGLEY RESEARCH CENTER, HAMPTON, VA.
Low-speed static and dynamic force tests of a generic supersonic cruise fighter configuration
[NASA-TM-4138] N89-28486
A torsional suspension system for testing space structures
[NASA-CASE-LAR-14149-1-SB] N89-28547
Near-field testing of the 15-meter hoop-column antenna
[NASA-TM-4073] N89-28550
Five year ground exposure of composite materials used on the Bell Model 206L flight service evaluation
[NASA-TM-101645] N89-28579
Delamination test apparatus and method
[NASA-CASE-LAR-13985-1] N89-28586
Aluminum alloy
[NASA-CASE-LAR-13924-1-CU] N89-28621
Almond test body
[NASA-CASE-LAR-13747-1-CU] N89-28672
Discussion of the potential and limitations of direct and large-eddy simulations
[NASA-CR-181892] N89-28762
On the large-eddy simulation of transitional wall-bounded flows
[NASA-CR-181883] N89-28763
Method and circuit for controlling the evolution time interval of a laser output pulse
[NASA-CASE-LAR-13772-1] N89-28816
Method and circuit for shaping laser output pulses
[NASA-CASE-LAR-14203-1] N89-28817
ISCCP CX observations during the FIRE/SRB Wisconsin Experiment from October 14 through November 2, 1986
[NASA-TM-101653] N89-28993
FREQ: A computational package for multivariable system loop-shaping procedures
[NASA-TM-4127] N89-29047
Calculation of two-neutron multiplicity in photonuclear reactions N89-29160
An optical model description of momentum transfer in heavy ion collisions N89-29162

NATIONAL AERONAUTICS AND SPACE ADMINISTRATION. LEWIS RESEARCH CENTER, CLEVELAND, OH.
COLD-SAT: Cryogenic On-Orbit Liquid Depot-Storage, Acquisition and Transfer
[NASA-TM-102308] N89-28535
Digitally modulated bit error rate measurement system for microwave component evaluation
[NASA-TP-2912] N89-28545
Furnace for tensile/fatigue testing
[NASA-CASE-LEW-14848-1] N89-28549
Evolutionary growth for Space Station Freedom electrical power system
[NASA-TM-102339] N89-28570
Ion optics for high power 50-cm-diam ion thrusters
[NASA-TM-102143] N89-28571
The interface in tungsten fiber reinforced niobium metal-matrix composites
[NASA-TM-102122] N89-28627
Arc-textured high emittance radiator surfaces
[NASA-CASE-LEW-14679-1] N89-28651
Microgravity combustion science: A program overview
[NASA-TM-101424] N89-28665
Numerical studies of convective heat transfer in an inclined semiannular enclosure
[NASA-TM-102011] N89-28666
The upper-branch stability of compressible boundary layer flows
[NASA-TM-102128] N89-28748
Calculation of reattaching shear layers in divergent channel with a multiple-time-scale turbulence model
[NASA-TM-102293] N89-28749
Fatigue testing apparatus
[NASA-CASE-LEW-14124-1] N89-28806
High temperature flexible seal
[NASA-CASE-LEW-14695-1] N89-28830
Non-uniform transition conductivity of superconducting ceramic
[NASA-TM-102133] N89-28851
Ultrasonic imaging of textured alumina
[NASA-TM-101478] N89-28853
A real time microcomputer implementation of sensor failure detection for turbofan engines
[NASA-TM-102327] N89-29032

NATIONAL AERONAUTICS AND SPACE ADMINISTRATION. MARSHALL SPACE FLIGHT CENTER, HUNTSVILLE, AL.
O-ring gasket test fixture
[NASA-CASE-MFS-28376-1] N89-28546
Wind models for the NSTS ascent trajectory biasing for wind load alleviation
[NASA-TM-100375] N89-28551
Spacecraft component heater control system
[NASA-CASE-MFS-28327-1] N89-28556
Static and dynamic deflection studies of the SRM aft case-nozzle joint
[NASA-TM-100373] N89-28568
Controlled method of reducing electrophoretic mobility of various substances
[NASA-CASE-MFS-26049-1-NP] N89-28603
Hollow fiber clinostat: Technical abstract
[NASA-CASE-MFS-28370-1] N89-28793
Universal precision sine bar attachment
[NASA-CASE-MFS-28253-1] N89-28831
Turbomachinery rotor support with damping
[NASA-CASE-MFS-28345-1] N89-28841
Turbomachinery shaft insert
[NASA-CASE-MFS-28345-2] N89-28842

NATIONAL AERONAUTICS AND SPACE ADMINISTRATION. PASADENA OFFICE, CA.
Television monitor field shifter and an opto-electronic method for obtaining a stereo image of optimal depth resolution and reduced depth distortion on a single screen
[NASA-CASE-NPO-17249-1-CU] N89-28676
Digital carrier demodulator employing components working beyond normal limits
[NASA-CASE-NPO-17628-1-CU] N89-28684
Systolic VLSI array for implementing the Kalman filter algorithm
[NASA-CASE-NPO-17108-1-CU] N89-28713
Apparatus and method for characterizing the transmission efficiency of a mass spectrometer
[NASA-CASE-NPO-16989-1-CU] N89-28794
Reversal electron attachment ionizer for detection of trace species
[NASA-CASE-NPO-17596-1-CU] N89-28795
Field induced gap infrared detector
[NASA-CASE-NPO-17526-1-CU] N89-28796
Robust high-performance control for robotic manipulators
[NASA-CASE-NPO-17785-1-CU] N89-28846
Trochoidal analysis of scattered electrons in a merged electron-ion beam geometry
[NASA-CASE-NPO-16789-1-CU] N89-29169
Fiber optic frequency transfer link
[NASA-CASE-NPO-17703-1-CU] N89-29191

NATIONAL AEROSPACE LAB., AMSTERDAM (NETHERLANDS).
Airport noise measuring data collction system
[NLR-MP-87006-U] N89-28526
Numerical grid generation in 3D Euler-flow simulation
[NLR-MP-88013-U] N89-28777
Integrating satellite data with information from topographic maps: Method and applications
[NLR-MP-87035-U] N89-28933
The use of expert systems for preprocessing image data
[NLR-MP-88009-U] N89-28934
Improvement of classification results of satellite imagery using context information from a topographic map
[NLR-MP-88020-U] N89-28935
Updating land-use information on topographic maps using satellite imagery: Combining the advantages of two accessible sources of geographic information
[NLR-MP-88030-U] N89-28936
Tools for the development and usage of industrial mathematical software
[NLR-MP-87020-U] N89-29067
Method bases: A new tool for applied information system design
[NLR-MP-88002-U] N89-29271

NATIONAL AEROSPACE LAB., TOKYO (JAPAN).
Some computations of unsteady Navier-Stokes flow around oscillating airfoil/wing
[NAL-TR-1004T] N89-28492
An experimental optical coupling device for an airborne digital redundant system
[NAL-TR-1003] N89-28514
Finite element analysis of incompressible viscous flows around single and multi-element aerofoils in high Reynolds number region
[NAL-TR-1010T] N89-28765

NATIONAL BUREAU OF STANDARDS, BOULDER, CO.
The 12C16O laser frequency tables for the 34.2 to 62.3 THz (1139 to 2079 cm-1) region
[PB89-193908] N89-28809

NATIONAL INST. OF STANDARDS AND TECHNOLOGY, BOULDER, CO.
Bibliography of the NIST (National Institute of Standards and Technology) Electromagnetic Fields Division publications
[PB89-189211] N89-28673
Performance evaluation of radiofrequency, microwave, and millimeter wave power meters
[PB89-193916] N89-28707

NATIONAL INST. OF STANDARDS AND TECHNOLOGY, GAITHERSBURG, MD.
Metallurgical evaluation of 17-4 PH stainless steel castings
[PB89-193262] N89-28615
Center for Electronics and Electrical Engineering technical publication announcements: Covering Center programs, July - September 1988, with 1989 CEEE events calendar
[PB89-189302] N89-28706
NIST (National Institute of Standards and Technology) calibration services users guide, 1989 edition
[PB89-200216] N89-28785

NATIONAL PHYSICAL LAB., TEDDINGTON (ENGLAND).
Measurement of mode 1 and mode 2 strain energy release rates: A VAMAS round robin project on delamination of composite materials
[NPL-DMA(A)-178] N89-28583
A summary of the UK results for a VAMAS round robin project on delamination of composite materials
[NPL-DMA(A)-179] N89-28584
A VAMAS round robin on fatigue test methods for polymer matrix composites. Part 1: Tensile and flexural tests of unidirectional material
[NPL-DMA(A)-180-PT-1] N89-28585
Standard reference material for high temperature viscosity measurements: Results of interlaboratory comparison programme
[NPL-DMA(A)-175] N89-28612
Effect of temperature and H2S content on the cracking resistance of a 13 percent chromium martensitic stainless steel in acidified NaCl
[NPL-DMA(A)-173] N89-28631
Achievement of the optimum performance from laser interferometer systems when applied to precision length measurement in the free atmosphere
[NPL-MOM-92] N89-28825
An evaluation of blazed zone plates for use in the 10 micron spectral region
[NPL-MOM-93] N89-28828
Appraisal of security of data handling systems and products: A tutorial and discussion document
[NPL-DITC-141/89] N89-29092
Least-squares best-fit geometric elements
[NPL-DITC-140/89] N89-29125

Linear algebra support modules for approximation and other software
[NPL-DITC-142/89] N89-29126
NATIONAL TELECOMMUNICATIONS AND INFORMATION ADMINISTRATION, ANNAPOLIS, MD.
Meteor burst system communications compatibility
[PB89-191167] N89-28692
NATIONAL TRANSPORTATION SAFETY BOARD, WASHINGTON, DC.
Aircraft accident/incident summary reports: Belleville, Illinois, August 22, 1987; Pensacola, Florida, December 27, 1987
[PB89-910405] N89-28507
NAVAL AIR PROPULSION TEST CENTER, TRENTON, NJ.
Statistics on aircraft gas turbine engine rotor failures that occurred in US commercial aviation during 1984
[NAPC-PE-185] N89-28516
Statistics on aircraft gas turbine engine rotor failures that occurred in US commercial aviation during 1985
[NAPC-PE-188] N89-28517
NAVAL CIVIL ENGINEERING LAB., PORT HUENEME, CA.
Joint sealants for airport pavements. Phase 1: Laboratory and field investigations
[DOT/FAA/DS-89/2-PHASE-1] N89-28523
NAVAL OCEAN SYSTEMS CENTER, SAN DIEGO, CA.
Quality factor and statistics for radiation patterns of shipboard HF antennas
[AD-A207931] N89-28690
Ionospheric variability
[AD-A209251] N89-28972
The NOSC (Naval Ocean Systems Center) Code 911 Digital Dynamics Processor (DDP): A mildly coupled distributed-computing system
[AD-A210148] N89-29085
Airborne FLIR (Forward Looking Infrared) detection of surface targets
[AD-A209250] N89-29189
NAVAL POSTGRADUATE SCHOOL, MONTEREY, CA.
The effect of autopilot configuration on missile response
[AD-A207822] N89-28520
Consideration of gravity gradient stabilization for ORION
[AD-A207845] N89-28557
Active damping of vibration in large space structures using a Karhunen-Loeve reduced order model
[AD-A208183] N89-28558
Design of a reliable computing system for the Petite Amateur Navy Satellite (PANSAT)
[AD-A208194] N89-28559
Composite material repair and reliability
[AD-A209150] N89-28574
NEC (Numerical Electromagnetics Code), NECGS (Numerical Electromagnetics Code-Ground Screen), and MININEC (Mini-Numerical Electromagnetics Code) numerical models of LF top-hat monopole antennas
[AD-A209230] N89-28683
Electromagnetic scattering from two dimensional objects using the field feedback formulation
[AD-A209563] N89-28685
A study of the thermal profiles during autogenous arc welding
[AD-A209440] N89-28843
Determining the location of an observer with respect to aerial photographs
[AD-A207791] N89-28929
A numerical study of a mesoscale eddy interaction with an ocean front in the marginal ice zone
[AD-A209192] N89-29002
Human factors evaluation of color use in the Target Data Processor Release 10 (TDP R10)
[AD-A209438] N89-29023
PC to mainframe connection: IBM PC 3270 emulation
[AD-A209204] N89-29033
Design and development of a user interface and user manual for a system dynamics model of software management
[AD-A209486] N89-29048
A conceptual level design of a design database for the computer-aided prototyping system
[AD-A207808] N89-29050
A prototype for converting Linear Programming (LP) models to structured modeling graphs
[AD-A208166] N89-29059
Software engineering with database management systems
[AD-A208167] N89-29060
Computer implementation and simulation of some neural networks used in pattern recognition and classification
[AD-A208112] N89-29099
Optical laser technology and its application to Defense Manpower Data Center's (DMDC) querry facsimile (QFAX) data base system
[AD-A207832] N89-29194
Implementation of a distributed object-oriented database management system
[AD-A209437] N89-29265
Conversion of hard-copy documents to digital format utilizing optical scanners and optical storage media
[AD-A209473] N89-29266
The use of a UNIX-based workstation in the Information Systems Laboratory
[AD-A209485] N89-29267
Moving optical technology in-house
[AD-A207850] N89-29268
NAVAL RESEARCH LAB., WASHINGTON, DC.
Acousto-optic and linear electro-optic properties of organic polymeric materials
[AD-A207974] N89-28646
An X-ray source for lithography based on a quasi-optical maser undulator
[AD-A208522] N89-28675
Reciprocal perfect and asymptotically perfect periodic radar waveforms and their aperiodic properties
[AD-A208938] N89-28677
Slotted-waveguide amplifiers for millimeter waves
[AD-A207932] N89-28721
Acousto-optical vector matrix product processor: Implementation issues
[AD-A207933] N89-28722
High-power free-electron lasers driven by RF linear accelerators
[AD-A209740] N89-28815
Near-neighbor algorithms for processing bearing data
[AD-A207935] N89-29053
Packet-error probability analysis for unslotted FH-CDMA (Frequency Hopped-Code Division Multiple-Access) systems with error control coding
[AD-A207964] N89-29054
A user's guide to the SEVP (Stabilized Error Vector Propagation) solver: An efficient direct solver for elliptic partial differential equations
[AD-A208117] N89-29121
Stein's Lemma: A large deviations approach
[AD-A209090] N89-29137
Effects of magnetic and collisional viscosity on the E x B gradient drift instability
[AD-A207975] N89-29205
NAVAL SHIP RESEARCH AND DEVELOPMENT CENTER, BETHESDA, MD.
Theoretical model of gravitational perturbation of current collector axisymmetric flow field
[AD-A209499] N89-28756
NAVAL WEAPONS CENTER, CHINA LAKE, CA.
Scattering representation of waveguide/cavity discontinuities using mode-matching and the least-squares boundary residual
[AD-A209571] N89-28686
NEW MEXICO STATE UNIV., LAS CRUCES.
Engineering and instrumentation support of the AFGL (Air Force Geophysics Laboratory) Research Balloon Program
[AD-A209107] N89-28971
NORTH CAROLINA STATE UNIV., RALEIGH.
A space marching algorithm for the thin-layer Navier-Stokes equations N89-28767
NORTH CAROLINA UNIV., CHAPEL HILL.
Experimental and theoretical study of transient behavior of varistors
[AD-A209081] N89-28715
Exploring virtual worlds with head-mounted displays
[AD-A208088] N89-28797
A microprogramming support tool for pipelined architectures
[AD-A208090] N89-29036
Walkthrough-exploring virtual worlds
[AD-A208087] N89-29057
A heterogeneous multiprocessor graphics system using processor-enhanced memories
[AD-A208089] N89-29058
NORTHEAST ARTIFICIAL INTELLIGENCE CONSORTIUM, SYRACUSE, NY.
Northeast artificial intelligence consortium. Volume 1: Executive summary
[AD-A209395] N89-29094
Northeast artificial intelligence consortium annual report 1987. Volume 8: Knowledge base maintenance using logic programming methodologies
[AD-A209453] N89-29095
Northeast artificial intelligence consortium annual report 1987. Volume 9: Computer architectures for very large knowledge bases
[AD-A209454] N89-29096
NORTHERN TELECOM ELECTRONICS LTD., OTTAWA (ONTARIO).
Measurements and modelling of thin silicon dioxide films on silicon
[AD-A207853] N89-28720
NORTHROP CORP., HAWTHORNE, CA.
Emerging resin characterization
[AD-A208173] N89-28649
NORTHWEST RESEARCH ASSOCIATES, INC., BELLEVUE, WA.
Propagation and saturation of nonlinear inertia-gravity waves in the atmosphere
[AD-A207871] N89-28989
NORTHWESTERN UNIV., EVANSTON, IL.
Bifurcation and pattern formation in combustion
[DE89-013629] N89-28590
Reaction kinetics and mechanism of chain reactions and explosions via transient spectroscopy
[AD-A209169] N89-28597
Radiothermoluminescence studies of polymer solids
[AD-A209036] N89-28641

O

OAK RIDGE NATIONAL LAB., TN.
Sulfidation/oxidation properties of iron-based alloys containing niobium and aluminum
[DE89-013786] N89-28617
Microwave sintering of ceramics
[DE89-014769] N89-28636
Non-linear surface fitting of laser range images using a hypercube concurrent computer
[DE89-013720] N89-28808
Nonfilm radiography at the Oak Ridge Y-12 Plant
[DE89-014523] N89-28852
High resolution subsurface imaging with geophysical diffraction tomography
[DE89-013615] N89-28923
Energy technology R and D: What could make a difference. A study by the staff of the Oak Ridge National Laboratory. Part 1: Synthesis report, volume 1
[DE89-014568] N89-28955
Adequacy of forestry data in assessing the impact of ozone: A national perspective
[DE89-012359] N89-28962
Chaotic behavior in a new class of parallel optimization algorithms
[DE89-014089] N89-29040
Ion beam deposition of epitaxial germanium and gallium arsenide layers
[DE89-014044] N89-29225
The amorphous to gamma transformation in ion implanted Al2O3
[DE89-014797] N89-29226
New dimensions from statistical graphics for GIS (Geographic Information System) analysis and interpretation
[DE89-012339] N89-29263
OFFICE NATIONAL D'ETUDES ET DE RECHERCHES AEROSPATIALES, PARIS (FRANCE).
Multitarget tracking by single sensor analysis of the main approaches developed in this area
[ONERA-NT-1988-10] N89-28702
A method for assisting in decision-making for multilayer radar absorbent coverings
[ONERA-NT-1989-2] N89-28703
La Recherche Aerospatiale, bimontly bulletin, number 1988-3
[ESA-TT-1137] N89-28781
Analysis of the VHF-UHF electromagnetic radiation of lightning: Application to a model of the negative stepped-leader propagation
[ONERA-NT-1989-1] N89-29000
Generalized projected gradient-type iterative method for parametric and functional optimization of dynamical systems subject to constraints
[ONERA-NT-1988-9] N89-29063
Weak beam electron microscopy of dislocation splitting in TiAl: Relationship with plasticity
[ONERA-NT-1988-3] N89-29253
La Recherche Aerospatiale, bimonthly bulletin, number 1988-4
[ESA-TT-1161] N89-29299
La Recherche Aerospatiale, bimonthly bulletin, number 1988-5
[ESA-TT-1162] N89-29300
La Recherche Aerospatiale, bimonthly bulletin, number 1988-6
[ESA-TT-1165] N89-29301
OFFICE OF NAVAL RESEARCH, ARLINGTON, VA.
Preliminary neural network detection of a gulf stream in images of sea surface temperature gradients, phase 1
[AD-A207801] N89-29003
OFFICE OF THE SECRETARY OF DEFENSE, WASHINGTON, DC.
Operational test plan concept for evaluation of close air support alternative aircraft
[AD-A208185] N89-28513

OHIO STATE UNIV., COLUMBUS.
Explanatory research on the protection of carbon-carbon composites against oxidation at very high temperatures (greater than 3000 F) with Engel-Brewer and other intermetallic compounds
[AD-A207907] N89-28577
Ultrasonic attenuation in heavy fermion superconductors
[DE89-014937] N89-29231

OREGON STATE UNIV., CORVALLIS.
Effect of environmental factors on pavement deterioration. Volume 1: Background and methodology
[PB89-182109] N89-28668

OXFORD UNIV. (ENGLAND).
Development and implementation of an on-line multivariable control algorithm for the force control of an industrial robot
[OUEL-1748/88] N89-28848
Tactile sensing and the photoelastic tactile sensor
[OUEL-1758/89] N89-28849

P

PACIFIC MISSILE TEST CENTER, POINT MUGU, CA.
Satellite-derived moisture-bogusing profiles for the North Atlantic Ocean
[AD-A207829] N89-28930

PACIFIC NORTHWEST LABS., RICHLAND, WA.
Capillary zone electrophoresis-mass spectrometry of peptides and proteins
[DE89-014466] N89-28592
Freeze-dried tungsten heavy alloys
[DE89-014933] N89-28620
Acoustic emission technology for space applications
[DE89-014449] N89-28861
Energy and angular distributions of electrons emitted from gases and thin foils during light ion bombardment
[DE89-014445] N89-29147

PARIS VI UNIV. (FRANCE).
Composite damaging: Methodological approach
[ETN-89-94866] N89-28582

PENNSYLVANIA STATE UNIV., UNIVERSITY PARK.
The aggregated state of matter: Elucidating transitions from the gas to the condensed phase and the formation of aerocolloids
[AD-A209080] N89-28595
Modeling of hot fragment conductive ignition of solid propellants with application to melting and evaporation of solids
[AD-A207727] N89-28662
Skin-friction measurements by laser interferometry N89-28737

PHILIPS INTERNATIONAL B.V., EINDHOVEN (NETHERLANDS).
A logic query language and its algebraic optimization for a multiprocessor database machine
[MEMO-INF-88-52] N89-29068

PHYSIKALISCH-TECHNISCHE BUNDESANSTALT, BRUNSWICK (GERMANY, F.R.).
Investigation of optoelectronic angle measuring systems and their use in a diffraction-optical strain measurement and a photoelectric two-coordinate autocollimator
[PTB-F-5] N89-29199

PISA UNIV. (ITALY).
Analysis of the regenerative cooling of a rocket motor fed with monomethylhydrazine and nitrogen tetroxide
[ETN-89-94976] N89-28569

PITTSBURGH ENERGY TECHNOLOGY CENTER, PA.
Structural definition of synthetic fuels: Wilsonville 1
[DE89-013627] N89-28659

PITTSBURGH UNIV., PA.
A study of the T(1) transition of Poly(Bis(trifluoroethoxy)Phosphazene) (PBFP) using solid-state nuclear magnetic resonance spectroscopy
[AD-A207719] N89-29246

PLANNING SYSTEMS, INC., MCLEAN, VA.
Preliminary neural network detection of a gulf stream in images of sea surface temperature gradients, phase 1
[AD-A207801] N89-29003

POLYTECHNIC UNIV., FARMINGDALE, NY.
Basic research in electronics (JSEP)
[AD-A208181] N89-28726

PRINCETON UNIV., NJ.
Large scale motions in supersonic turbulent boundary layers N89-28736
Hot-wire anemometry in supersonic flow N89-28738

Q

QUEENSLAND UNIV., BRISBANE (AUSTRALIA).
Out-of-plane buckling formulae for beam-columns/tie beams
[PB89-191613] N89-28857
New set of buckling parameters for monosymmetric beam-columns/tie beams
[PB89-191639] N89-28858
Flexural-torsional buckling of monosymmetric beam-columns/tie beams
[PB89-191654] N89-28859

R

RAND CORP., SANTA MONICA, CA.
Proceedings of a RAND Workshop on Antiproton Science and Technology
[AD-A208168] N89-29172

RANGE COMMANDERS COUNCIL, WHITE SANDS MISSILE RANGE, NM.
Design, performance and test standards for flight termination receiver/decoders. Volume 1: Design and performance requirements
[AD-A209644] N89-28544

RENSSELAER POLYTECHNIC INST., TROY, NY.
Solid lubrication studied by optical means
[AD-A209008] N89-28836

RIDER COLL., LAWRENCEVILLE, NJ.
Electric quadrupole excitations in the interactions of Y-89 with relativistic nuclei N89-29165

ROCKWELL INTERNATIONAL CORP., GOLDEN, CO.
A comprehensive guide to the literature on acoustic emission from composites, supplement 2
[DE89-013524] N89-28573

ROME AIR DEVELOPMENT CENTER, GRIFFISS AFB, NY.
Electrical characterization of signal processing microcircuit
[AD-A209078] N89-28714

ROYAL INST. OF TECH., STOCKHOLM (SWEDEN).
Experiments on the magnetic field and neutral density limits on CIV interaction
[TRITA-EPP-88-08] N89-29216
On the spoke structure in critical velocity rotating plasmas
[TRITA-EPP-89-01] N89-29217

ROYAL NETHERLANDS METEOROLOGICAL INST., DE BILT.
The boundary layer wind regime of a representative tropical African region, central Sudan
[KNMI-WR-88-04] N89-28982

S

SAN DIEGO STATE UNIV., CA.
Development of a carbonaceous selective absorber for solar thermal energy collection and process for its formation
[DE89-008587] N89-28949

SANDIA LABS., ALBUQUERQUE, NM.
Ultrasonic systems and system development at SNL Albuquerque
[DE89-013164] N89-29153

SANDIA NATIONAL LABS., ALBUQUERQUE, NM.
REGGIE results for the Nunnally mass launcher
[DE89-014377] N89-28543
Compound-lens diode for HERMES 3
[DE89-013065] N89-28708
Exact solutions for symmetric deformations of hollow bodies of ideal fluids with application to inertial stability
[DE89-014374] N89-28753
A method for evaluating structural transducers used in Type B package testing
[DE89-013591] N89-28784
A fully automated, single-connection tester for T/R modules
[DE89-013155] N89-28786
The PVF2 piezoelectric polymer shock stress sensor: System characterization for application under field test conditions
[DE89-014629] N89-28790
Robotic grasping of unknown objects: A knowledge-based approach
[DE89-013875] N89-28833
A test system for thermomechanical fatigue of solder joints
[DE89-013886] N89-28860
Damage predictions for wind turbine components using the LIFE2 computer code
[DE89-013813] N89-28952
Field tests of a novel inverter for photovoltaic power conditioning
[DE89-014322] N89-28958
Effective masses and g factors for 2-D light holes in InSb
[DE89-014899] N89-29230

SANTIAGO UNIV., COMPOSTELA (SPAIN).
The manufacture of blazed oblique zone plates for use at 10.6 microns
[NPL-MOM-91] N89-28827

SCHOOL OF AEROSPACE MEDICINE, BROOKS AFB, TX.
Towards a physiologically based HUD (Head-Up Display) symbology
[AD-A207748] N89-28515

SCIENCE APPLICATIONS INTERNATIONAL CORP., SAN DIEGO, CA.
An improved design for stretched-membrane heliostats
[DE89-013872] N89-28953

SCIENTIFIC RESEARCH ASSOCIATES, INC., GLASTONBURY, CT.
Hypersonic vehicle environment simulation, phase 1
[AD-A209030] N89-28754

SCRIPPS INSTITUTION OF OCEANOGRAPHY, LA JOLLA, CA.
Ocean remote sensing and modeling
[AD-A208406] N89-28927

SIRA INST. LTD., CHISLEHURST (ENGLAND).
A medium resolution imaging spectrometer for the European polar orbiting platform
[ETN-89-95235] N89-28563

SOCIETE NATIONALE ELF ACQUITAINE, PARIS (FRANCE).
TGMDA/DDS type impregnating resins structural study
[SNEA-9595] N89-28650

SOFTWARE ARCHITECTURE AND ENGINEERING, INC., ARLINGTON, VA.
Software technology to support real-time embedded artificial intelligence-based applications, phase 1
[AD-A209133] N89-29042

SOUTHAMPTON UNIV. (ENGLAND).
Development of damping treatment suitable for high temperature environment
[ISVR-TR-174] N89-28652
Nearfield acoustic holography: Review and perspectives
[ISVR-TR-179] N89-28807
A study of the effect of stimulus upon the reflex response as elicited and recorded by the tympanic membrane displacement measurement device
[ISVR-TR-177] N89-29018
The measurement of SEA loss factors on a fully assembled structure
[ISVR-TR-150] N89-29157
The acoustic calibration of aircraft fuselage structures, part 1
[ISVR-TR-169-PT-1] N89-29158

SOUTHWEST RESEARCH INST., SAN ANTONIO, TX.
A survey of JP-8 and JP-5 properties
[AD-A207721] N89-28661
Aircraft propeller induced structure-borne noise
[NASA-CR-4255] N89-29155

SPECTRAL SCIENCES, INC., BURLINGTON, MA.
The Strategic High-Altitude Atmospheric Radiation Code (SHARC) user instructions
[AD-A207667] N89-28974

SPIRE CORP., BEDFORD, MA.
Selective area epitaxy of gallium arsenide on silicon, phase 1
[AD-A209079] N89-29238

SRI INTERNATIONAL CORP., MENLO PARK, CA.
Collision dynamics and transition probabilities for vibrationally excited OH
[AD-A207856] N89-28976

STAATLICHES FORSCHUNGSINSTITUT FUER GEOCHEMIE, BAMBERG (GERMANY, F.R.).
Determination of moisture diffusion in carbon fiber reinforced epoxy composites by means of radioisotope tracer technique
[BMVG-FBWT-88-2] N89-28581

STANFORD LINEAR ACCELERATOR CENTER, CA.
Real-time applications of neural nets
[DE89-014400] N89-29093

STANFORD UNIV., CA.
Lithography and spectroscopy of ultrathin Langmuir-Blodgett polymer films
[AD-A208970] N89-28639
Picosecond electrooptic investigations of integrated circuits
[AD-A209134] N89-28863
Multicast communication in multiprocessor systems
[AD-A209606] N89-29086
Information requirements and the implications for parallel computation
[AD-A207802] N89-29088
Analysis of cache invalidation patterns in multiprocessors
[AD-A207820] N89-29089

Characterization of parallelism and deadlocks in distributed digital logic simulation
[AD-A207842] N89-29138
Fundamental processes in partially ionized plasmas
[AD-A207910] N89-29204
Statistical and physical evolution of QSO's
[NASA-CR-185869] N89-29282

STATE UNIV. OF NEW YORK, ALBANY.
Daytime turbulent exchange between the Amazon forest and the atmosphere
[NASA-CR-185487] N89-28961

STATE UNIV. OF NEW YORK, BUFFALO.
Ion-molecule chemistry within doubly charged ammonia clusters
[AD-A207764] N89-28608
Ion-molecule chemistry within triply charged ammonia clusters
[AD-A207766] N89-28609
Electron energy levels in a quantum well within an in-plane magnetic field
[AD-A209351] N89-29256

SWEDISH DEFENCE RESEARCH ESTABLISHMENT, LINKOEPING.
TiME: Time and memory efficient distance transformations for parallel and pyramid machines
[FOA-C-30531-3.4] N89-29091

SWEDISH INST. OF SPACE PHYSICS, UPPSALA.
Electromagnetic pulse propagation through a stratified ionosphere
[IRF-SR-199] N89-28700

SYRACUSE RESEARCH CORP., NY.
Characterization of painted surfaces in the United States from the perspective of potential damage from acidic deposition
[DE89-014264] N89-28965

SYRACUSE UNIV., NY.
Northeast artificial intelligence consortium. Volume 1: Executive summary
[AD-A209395] N89-29094
Northeast artificial intelligence consortium annual report 1987. Volume 8: Knowledge base maintenance using logic programming methodologies
[AD-A209453] N89-29095
Northeast artificial intelligence consortium annual report 1987. Volume 9: Computer architectures for very large knowledge bases
[AD-A209454] N89-29096

SYSTEMS CONTROL TECHNOLOGY, INC., ARLINGTON, VA.
Risk management for air ambulance helicopters operators
[DOT/FAA/DS-88/7] N89-28506

T

TABRIZ UNIV. (IRAN).
ECH plasma for different magnetic axis positions and initial ICRF plasma production experiments in CHS
[IPPJ-907] N89-29201

TATA INST. OF FUNDAMENTAL RESEARCH, BOMBAY (INDIA).
Implications of the correlation between the radio continuum and far-infrared luminosities of spiral galaxies N89-29289

TECHNICAL RESEARCH CENTRE OF FINLAND, ESPOO.
Estimation of some stochastic models used in reliability engineering
[VTT-RR-598] N89-28855
Methods for analyzing SAR images
[VTT-RR-612] N89-28932
Minimization of Boolean sum of products with applications to the computation of reliability of general networks
[VTT-RR-571] N89-29136

TECHNISCHE UNIV., BERLIN (GERMANY, F.R.).
Competition and safety in air traffic
[TUB-DISS-PAPER-128] N89-28508
Status and development potential of the fly by light technology in civil aircraft
[ILR-MITT-212] N89-28522
Activities report of the Institute of Space Research
[ILR-1986/87] N89-28536
Review of mean flow data N89-28743
Review of turbulence data N89-28744
The entries N89-28745
The anisotropy of the friction pressure of dipolar fluids
[ETN-89-94438] N89-28771
Piezoelectric foils as sensors in experimental flow mechanics
[ILR-MITT-214] N89-28800
Contribution to the generation of circular polarization of high purity using planar wire antenna structures
[ETN-89-94659] N89-28872
Theoretical investigations of an integrated optics switching element with asymmetric directional couplers for switching matrices
[ETN-89-94439] N89-29196
Activities report of the Institute of Astronomy and Astrophysics
[MITT-9] N89-29276

TECHNISCHE UNIV., BRUNSWICK (GERMANY, F.R.).
A model for the simulation of the DC and small-signal behavior of the bipolar transistor
[ETN-89-94442] N89-28727
Heat transfer in free convection and forced, laminar flow in vertical tubes, considering temperature dependent medium characteristics
[ETN-89-94441] N89-28772
Characterization, optimization and design of single-mode multistep fibers
[ETN-89-94440] N89-29197

TECHNISCHE UNIV., CLAUSTHAL-ZELLERFELD (GERMANY, F.R.).
Numerical determination of guaranteed Rayleigh numbers and the pertaining flow forms in steady, axisymmetric convection in cylinders
[ETN-89-94432] N89-28769

TECHNISCHE UNIV., DELFT (NETHERLANDS).
The angles of the Kolibrie rotor tipvanes on the rods and on the blades
[IW-R515] N89-28499
Kinematic vertical positioning using the global positioning system
[ETN-89-94804] N89-28510
Multivariate analysis of UV-spectral data for solute tracking in HPLC
[ISBN-90-6275-535-6] N89-28614
A study of the ultraviolet degradation embrittlement of polypropylene polymer
[ISBN-90-9002498-0] N89-28656
Development of an integrated AM shortwave upconversion receiver front-end
[ETN-89-95455] N89-28699
Segmentation of noisy images
[ETN-89-95461] N89-28701
Routing channels in VLSI layout
[ISBN-90-6275-535-4] N89-28731
Accurate and efficient modeling of global circuit behavior in VSLI layouts
[ETN-89-95459] N89-28732
Compact heat and mass exchangers of the plate fin type in thermal sorption systems: Application in an absorption heat pump with the working pair CH3OH-LiBr/ZnBr2
[ISBN-90-370-0022-3] N89-28780
Cohesion and interparticle forces
[ETN-89-95454] N89-28874
Results of Seasat altimeter data processing for the northeast Atlantic
[BCRS-89-05] N89-28940
Atmospheric influence on microwave remote sensing at different frequencies: Results of the 1st September 1987 DUSCAT flight
[BCRS-89-07] N89-28941
Sea gravimetry and Eotvos correction
[REPT-88.3] N89-29006
Investigations of nonlinear streamcipher systems: Construction and evaluation methods
[ETN-89-95458] N89-29038
Parallel algorithms for solving systems of linear equations and their mapping on systolic arrays
[ETN-89-95457] N89-29077
Row-oriented direct solving of linear algebraic equations: Row orthogonalization method
[REPT-88-82] N89-29105
Deeply bound orbits in pionic atoms and the optical potential
[ETN-89-95463] N89-29176

TECHNISCHE UNIV., EINDHOVEN (NETHERLANDS).
Fundamental aspects of reactions in titanium-silicon thin films for integrated circuits
[ETN-89-95466] N89-28733
The boundary layer wind regime of a representative tropical African region, central Sudan
[KNMI-WR-88-04] N89-28982
On the shape of mathematical arguments
[ETN-89-95465] N89-29133
Stability of a Taylor-relaxed cylindrical plasma separated from the wall by a vacuum layer
[EUT-88-E-207] N89-29200
Entrepreneurship and innovation: The Dutch sugar beet industry (1858-1919)
[ISBN-90-71617-11-4] N89-29275

TECHNISCHE UNIV., HANOVER (GERMANY, F.R.).
Quantitative investigation of the kinetics of a laser-pumped barium vapor
[ETN-89-94434] N89-28823
Increase of the damage thresholds of dielectric layer systems for the Nd laser
[ETN-89-94436] N89-28824
Photon-ion angular correlation measurements on the system He(+) + Ne: Determination of the spin inversion
[ETN-89-94435] N89-29175
Investigations of step distributions at Si/SiO2 interfaces using HR-SPA-LEED
[ETN-89-94437] N89-29251

TECHNISCHE UNIV., MUNICH (GERMANY, F.R.).
Corrosion prevention of lithium-alloy anodes in accumulators with organic electrolytic solutions
[ETN-89-94652] N89-28729
Heat transfer and film cooling in compressible nozzle flow
[ETN-89-94653] N89-28773
Microwave detection using Josephson elements
[ETN-89-94650] N89-29252

TECHNO SYSTEM DEVELOPMENTS, NAPLES (ITALY).
Tolerable g-level for fluid science experiments
[TS-7-87] N89-28667

TEXAS A&M UNIV., COLLEGE STATION.
Intelligent multi-sensor integrations
[NASA-CR-185846] N89-28562
Computations of optimal controls and designs for distributed systems in optics and elasticity
[AD-A207924] N89-29098

TEXAS UNIV., AUSTIN.
Oxygen storage on zeolites
[AD-A209352] N89-28599
Fluctuating wall-pressure measurements N89-28741

TEXAS UNIV. AT DALLAS, RICHARDSON.
Proof of the feasibility of coherent and incoherent schemes for pumping a gamma-ray laser
[AD-A208071] N89-28819

THERMA-WAVE, INC., FREEMONT, CA.
Thermal conductivity anisotropy in single crystal YBa2Cu3O7-x
[DE89-009643] N89-29220

THIOKOL CORP., BRIGHAM CITY, UT.
Technical Evaluation Motor 3 (TEM-3)
[NASA-CR-183740] N89-28567

TULSA UNIV., OK.
Metallic bonding to high-temperature superconducting ceramics
[DE89-014668] N89-28635

U

UNITED TECHNOLOGIES RESEARCH CENTER, EAST HARTFORD, CT.
Noise produced by turbulent flow into a rotor: Users manual for noise calculation
[NASA-CR-181790] N89-29152
Noise produced by turbulent flow into a rotor: Users manual for atmospheric turbulence prediction and mean flow and turbulence contraction prediction
[NASA-CR-181791] N89-29154

UNIVERSAL ENERGY SYSTEMS, INC., DAYTON, OH.
United States Air Force Research Initiation Program for 1987, volume 2
[AD-A209727] N89-29259

UNIVERSIDADE ESTADUAL DE CAMPINAS (BRAZIL).
Fifth force, sixth force and all that: A theoretical (classical) comment
[DE89-611971] N89-29254

UNIVERSITAET DER BUNDESWEHR, NEUBIBERG (GERMANY, F.R.).
On the solving of stochastic Ito differential equations by simulation
[ETN-89-94610] N89-29134
Evaporation thermodynamics of monotellurides of selected rare Earth and alkaline Earth elements, and an attempt to systematic correlation between the standard enthalpies of formation
[ETN-89-94655] N89-29257

UNIVERSITEIT TWENTE, ENSCHEDE (NETHERLANDS).
A graph-theoretical approach to block-co-polymer complexes. Part 1: Stars
[MEMO-757-PT-1] N89-28654
A graph-theoretical approach to block-co-polymer complexes. Part 2: Tree approximation
[MEMO-758-PT-2] N89-28655
A partitioning and redundancy model for wafer scale integrated circuits
[MEMO-INF-88-65] N89-28730
On the classification of plane graphs representing structurally stable rational Newton-flows
[MEMO-750-REV] N89-28776
Gradient Newton-flows for complex polynomials
[MEMO-764] N89-28779
A dynamic variation principle for elastic-fluid contacts, applied to elastohydrodynamic lubrication theory
[MEMO-746] N89-28782

Model reduction of linear conservative mechanical systems
[MEMO-752] N89-28845
A simple numerical algorithm for elastohydrodynamic lubrication, based on a dynamic variation principle
[MEMO-761] N89-28850
Smooth piecewise polynomials as conforming finite elements for plate bending problems
[MEMO-747] N89-28875
Fault-tolerant computer systems: A survey of some methods and techniques
[MEMO-INF-88-15] N89-29037
APL conversion software
[MEMO-INF-88-21] N89-29062
An algorithm for smooth interpolation to scattered data in R2
[MEMO-748] N89-29066
A logic query language and its algebraic optimization for a multiprocessor database machine
[MEMO-INF-88-52] N89-29068
A method of software development using functional programming
[MEMO-INF-88-64] N89-29069
A code optimization package for REDUCE
[MEMO-INF-89-29] N89-29070
A survey of self-consistency properties in cooperative game theory
[MEMO-763] N89-29072
Methods of combinatorial optimization and their range of applicability
[MEMO-766] N89-29073
Solution of a tinned iron purchasing problem by Lagrangian relaxation
[MEMO-735] N89-29074
Language constructs and a search procedure to model and solve combinatorial problems
[MEMO-753] N89-29075
Three dimensional reconstruction from serial cross sections by set valued interpolation
[MEMO-754] N89-29076
A static load distribution strategy for processor tools
[MEMO-INF-88-43] N89-29078
The application of constraints in query optimization
[MEMO-INF-88-55] N89-29079
Backward analysis
[MEMO-INF-89-14] N89-29080
TWENTENET chip design
[MEMO-INF-88-49] N89-29090
The communication complexity of interval orders
[MEMO-745] N89-29102
Hamiltonian control systems: Decomposition and clamped dynamics
[MEMO-759] N89-29103
Application of optimal control theory for selective vibrational excitation in molecules modeled as harmonic systems
[MEMO-755] N89-29104
Some recent results on long cycles in tough graphs
[MEMO-765] N89-29130
A note on the communication complexity of totally unimodular matrices
[MEMO-768] N89-29131
A torus bifurcation theorem with symmetry
[NASA-CR-185907] N89-29135
On adjoints and dual matroids
[MEMO-767] N89-29146
Generalized grid files: Description and performance aspects
[MEMO-INF-88-63] N89-29272

UTAH UNIV., SALT LAKE CITY.
Stochastic processes in CHEMFETs
[AD-A207977] N89-28723
Stochastic processes in CHEMFETs
[AD-A208092] N89-28725
Application of Cholesky-like matrix decomposition methods to the evaluation of atomic orbital integrals and integral derivatives
[AD-A209682] N89-29112
Fluxons and order in long Josephson junctions
[AD-A207925] N89-29249

V

VISION SCIENCES RESEARCH CORP., SAN RAMON, CA.
Suprathreshold contrast sensitivity vision test chart
[AD-A209915] N89-29010

W

WASHINGTON STATE UNIV., PULLMAN.
Three-dimensional computer analysis and modelling of remote sensing-structural geologic problems
[DE89-010875] N89-28924
Photonuclear absorption cross sections
[NASA-CR-185488] N89-29159
The invariance of classical electromagnetism under Charge-conjugation, Parity and Time-reversal (CPT) transformations N89-29161
Electromagnetic interactions of cosmic rays with nuclei N89-29163
Electric quadrupole excitations in relativistic nucleus-nucleus collisions N89-29164
Electric quadrupole excitations in the interactions of Y-89 with relativistic nuclei N89-29165
Nucleon emission via electromagnetic excitation in relativistic nucleus-nucleus collisions: Re-analysis of the Weizsacker-Williams method N89-29166

WASHINGTON UNIV., SEATTLE.
Application of special sensor microwave/imager data for analysis of cyclonic storms in midlatitudes over the sea
[AD-A207675] N89-28975
Multilayered electronic materials and devices based on 3-5 compounds
[AD-A208861] N89-29233

WISCONSIN UNIV., MADISON.
Modelling, information, processing, and control
[AD-A207810] N89-28865
Vortices in long Josephson junctions
[AD-A207936] N89-29250

WOODS HOLE OCEANOGRAPHIC INSTITUTION, MA.
Entrainment and homogenization of a passive tracer in a numerical model gyre
[AD-A208020] N89-29005

WORLD METEOROLOGICAL ORGANIZATION, GENEVA (SWITZERLAND).
The WMO long-term plan overall policy and strategy 1988-1997: Second WMO long-term plan, part 1
[WMO-690-PT-1] N89-28994
The World Weather Watch Program 1988-1997: Second WMO long-term plan, part 2, volume 1
[WMO-691-PT-2-VOL-1] N89-28995
The World Climate Program 1988-1997: Second WMO long-term plan, part 2, volume 2
[WMO-692-PT-2-VOL-2] N89-28996
The WMO research and development program 1988-1997: Second WMO long-term plan, part 2, volume 3
[WMO-693-PT-2-VOL-3] N89-28997
The WMO applications of meteorology program 1988-1997: Second WMO long-term plan, part 2, volume 4
[WMO-694-PT-2-VOL-4] N89-28998

WRIGHT STATE UNIV., DAYTON, OH.
Mathematical modeling and analysis of heat pipe start-up from the frozen state
[NASA-CR-185132] N89-28747

Typical Contract Number Index Listing

Listings in this index are arranged alphanumerically by contract number. Under each contract number the NASA accession numbers denoting documents that have been produced as a result of research done under that contract are arranged in ascending order. The NASA accession number denotes the number by which the citation is identified.

AF PROJ. 2301 ..... N89-28988
N89-29181
AF PROJ. 2302 ..... N89-28864
AF PROJ. 2303 ..... N89-28724
AF PROJ. 2304 ..... N89-28681
N89-28865
N89-29087
N89-29098
N89-29109
N89-29113
N89-29119
N89-29203
AF PROJ. 2305 ..... N89-29250
AF PROJ. 2306 ..... N89-28718
AF PROJ. 2307 ..... N89-28759
AF PROJ. 2311 ..... N89-29278
AF PROJ. 2313 ..... N89-29011
AF PROJ. 2917 ..... N89-29204
N89-29233
AF PROJ. 3005 ..... N89-28578
AF PROJ. 80402 ..... N89-28985
AF-AFOSR-0012-88 ..... N89-29011
AF-AFOSR-0020-86 ..... N89-29249
AF-AFOSR-0025-86 ..... N89-29250
AF-AFOSR-0026-84 ..... N89-29181
AF-AFOSR-0034-87 ..... N89-29233
AF-AFOSR-0066-87 ..... N89-28988
AF-AFOSR-0079-88 ..... N89-28724
AF-AFOSR-0087-86 ..... N89-28681
AF-AFOSR-0091-88 ..... N89-29098
AF-AFOSR-0101-85 ..... N89-29278
AF-AFOSR-0112-86 ..... N89-28741
AF-AFOSR-0142-86 ..... N89-28864
AF-AFOSR-0146-85 ..... N89-28759
AF-AFOSR-0222-85 ..... N89-29087
AF-AFOSR-0225-86 ..... N89-29204
AF-AFOSR-0252-84 ..... N89-29119
AF-AFOSR-0263-85 ..... N89-28865
AF-AFOSR-0270-87 ..... N89-29109
AF-AFOSR-0322-85 ..... N89-29118
AF-AFOSR-0330-85 ..... N89-29113
ARGS-510 ..... N89-28857
BCRS-PROJ-3104/TO-1.4 ..... N89-28940
BCRS-PROJ-4451/TE-1.8 ..... N89-28941
BCRS-PROJ-4533/TO-3.13 ..... N89-28938
N89-28939
BMFT-FKZ-070-4580-6 ..... N89-28525
BMFT-01-QS-1138 ..... N89-28799
BMFT-07-KF-111 ..... N89-28977
BMFT-13-EU-0027/0 ..... N89-28822
BMVG-T/RF-31/G-0022/G-1312 ..... N89-29156
BMVG-T/RF-31E-0020/E-1317 ..... N89-28844
BMVG-T/RF52/80025/81524 ..... N89-28581
DA PROJ. 1L1-61102-AH-42 ..... N89-29240
DA PROJ. 1L1-61102-BW-57 ..... N89-29150
DA PROJ. 1L1-61102-H-4702 ..... N89-29148
DA PROJ. 1L1-62105-AH-84 ..... N89-28622
DA PROJ. 1L2-63001-D-150 ..... N89-28661
DA PROJ. 4A7-62719-AT-40 ..... N89-28926
DA PROJ. 351-62772-A-874 ..... N89-29014
DAAG29-85-K-0055 ..... N89-28576
DAAG29-85-K-0203 ..... N89-28641
DAAG29-85-K-0215 ..... N89-28595
DAAK11-83-C-0015 ..... N89-28662
DAAK20-84-K-0458 ..... N89-29148
DAAK60-86-C-0128 ..... N89-29025
DAAK70-87-C-0043 ..... N89-28661
DAAL01-87-C-0727 ..... N89-29239
DAAL03-86-G-0036 ..... N89-28597
DAAL03-86-G-0042 ..... N89-28836
DAAL03-86-G-0061 ..... N89-28640
DAAL03-86-K-0031 ..... N89-29192
DAAL03-87-K-0005 ..... N89-28575
DAAL03-87-K-0059 ..... N89-28689
DAAL03-87-K-0124 ..... N89-29111
DAAL03-88-C-0015 ..... N89-29238
DAAL03-88-C-0028 ..... N89-28754
DAAL03-88-C-0033 ..... N89-29042
DAAL03-88-K-0028 ..... N89-28715
DACA39-85-C-0013 ..... N89-28928
DAJA45-86-C-0041 ..... N89-29150
DAMD17-86-C-6157 ..... N89-29014
DARPA ORDER 6090 ..... N89-29036
N89-29058
DE-AC02-76CH-00016 ..... N89-28791
N89-28965
N89-28984
N89-29223
N89-29247
DE-AC02-76ER-03130 ..... N89-29255
DE-AC02-83CH-10093 ..... N89-28487
N89-28657
N89-28658
N89-28944
N89-28945
N89-28946
N89-28947
N89-28948
N89-28950
N89-28956
DE-AC03-76SF-00098 ..... N89-28616
N89-28619
N89-28788
N89-28951
N89-29106
N89-29227
N89-29228
N89-29283
N89-29296
DE-AC03-76SF-00515 ..... N89-29093
DE-AC03-88ER-80652 ..... N89-29220
DE-AC04-76DP-00789 ..... N89-28543
N89-28708
N89-28753
N89-28784
N89-28786
N89-28790
N89-28833
N89-28860
N89-28952
N89-28953
N89-28958
N89-29153
N89-29230
DE-AC04-76DP-03533 ..... N89-28573
DE-AC04-88DP-43495 ..... N89-28813
DE-AC05-84OR-21400 ..... N89-28617
N89-28636
N89-28808
N89-28852
N89-28923
N89-28955
N89-28962
N89-29040
N89-29088
N89-29225
N89-29226
N89-29263
DE-AC06-76RL-01830 ..... N89-28592
N89-28618
N89-28620
N89-28861
N89-29147
DE-AC08-88NV-10617 ..... N89-28787
DE-AI01-88EH-79050 ..... N89-28669
DE-AI03-88SF-16310 ..... N89-28627
DE-FG01-88CE-15289 ..... N89-28949
DE-FG02-84ER-45147 ..... N89-28589
DE-FG02-88ER-13612 ..... N89-28634
DE-FG02-87ER-25027 ..... N89-28590
DE-FG02-88ER-45347 ..... N89-29231
DE-FG05-88ER-40481 ..... N89-29168
DE-FG06-87ER-13796 ..... N89-28924
DFG-MO-416/3-3 ..... N89-29268
DOE-1570-1579-A1 ..... N89-29040
DOT/FA71NA-AP98 ..... N89-28516
N89-28517
DRET-84-062 ..... N89-28664
DRET-85-031 ..... N89-28495
DRET-85-193 ..... N89-28801
DRET-86-443 ..... N89-28650
DRET-87-34-325-00-470-7501 ..... N89-28582
DRET-87-002-16 ..... N89-28803
DRET-87-115 ..... N89-28629
DRET-88-002-11 ..... N89-28775
DRET/ETCA/CREA-048-329 ..... N89-28854
DTFA01-83-C-10579 ..... N89-28986
DTFA01-86-1-02015 ..... N89-28523
DTFA01-87-C-0014 ..... N89-28508
DTFA01-89-C-00001 ..... N89-28509
N89-28524
EPA-68-01-7365 ..... N89-28572
ESA-R-66-525 ..... N89-28667
ESPRIT PROJ. 991 ..... N89-28732
ETCA/CREA/SP-CI-47475 ..... N89-29198
FC-85-563 ..... N89-28980
FC-86-621 ..... N89-28981
F04701-85-C-0086 ..... N89-29083
N89-29247
F04701-88-C-0089 ..... N89-29237
F19628-84-C-0039 ..... N89-28971
F19628-85-C-0002 ..... N89-28676
N89-28818
N89-28988
F19628-86-C-0141 ..... N89-28987
F19628-87-C-0130 ..... N89-28974
F19628-87-K-0043 ..... N89-28976
F30602-81-C-0169 ..... N89-29052
F30602-81-C-0185 ..... N89-28792
F30602-85-C-0008 ..... N89-29094
N89-29095
N89-29096
F30602-85-C-0012 ..... N89-29086
F30602-85-C-0072 ..... N89-28718
F30602-85-C-0261 ..... N89-29034
F33615-83-D-0603 ..... N89-28599
F33615-83-K-2340 ..... N89-29206
F33615-84-C-0066 ..... N89-29193
F33615-85-C-2507 ..... N89-28835
F33615-85-C-5040 ..... N89-28642
F33615-86-C-1126 ..... N89-28863
F33615-87-C-0012 ..... N89-29193
F33615-87-C-5223 ..... N89-28649
F33615-88-C-2820 ..... N89-28747
F33615-88-C-2857 ..... N89-28644
F33615-88-C-2871 ..... N89-28838
F33615-88-C-5451 ..... N89-28862
F34601-84-C-1068 ..... N89-29188
F34601-88-D-0987 ..... N89-29188
F49620-85-C-107 ..... N89-28585
F49620-85-C-0013 ..... N89-29259
F49620-86-C-0026 ..... N89-28989
F49620-86-C-0030 ..... N89-29172
F49620-87-C-0011 ..... N89-28869
F49620-87-C-0118 ..... N89-29203
F49620-88-C-0040 ..... N89-28760
F49620-88-C-0075 ..... N89-28726
F49620-88-C-0083 ..... N89-29010
F49620-88-C-0104 ..... N89-28578
F49620-88-C-0137 ..... N89-28839
GRI-5083-231-0956 ..... N89-28588
GRI-5084-222-1063 ..... N89-28587
GRI-5087-260-1535 ..... N89-28768
HDL PROJ. E247E4 ..... N89-28680
HPR-5263 ..... N89-28668
IDA-10-00008 ..... N89-29061
JPL-958066 ..... N89-28562

MANE-8-4002 ..... N89-28922
MDA903-84-C-0031 ..... N89-29142
N89-29145
N89-29260
MDA972-88-K-0008 ..... N89-29232
MIPR-86-526 ..... N89-29205
MIT PROJ. A-1 ..... N89-28633
NAGW-21 ..... N89-29020
NAG1-665 ..... N89-28856
NAG1-692 ..... N89-28961
NAG1-797 ..... N89-29159
NAG2-350 ..... N89-28562
NAG2-432 ..... N89-29135
NAG3-527 ..... N89-28737
NAG8-571 ..... N89-29298
NAG8-674 ..... N89-29298
NAG8-682 ..... N89-28537
NAL PROJ. CC-9-000 ..... N89-29270
NASA ORDER C-99068-G N89-28749
NAS1-17783 ..... N89-29152
N89-29154
NAS1-17921 ..... N89-29155
NAS1-18525 ..... N89-28820
NAS1-18539 ..... N89-28821
NAS1-18605 ..... N89-28762
N89-28763
N89-28764
N89-28766
N89-29028
N89-29061
N89-29122
N89-29123
N89-29124
NAS5-29375 ..... N89-28983
NAS7-918 ..... N89-28676
N89-28684
N89-28713
N89-28794
N89-28795
N89-28796
N89-28969
N89-29169
N89-29191
NAS8-30490 ..... N89-28566
N89-28567
NAS9-17511 ..... N89-29292
NATO-RG-331/88 ..... N89-29298
NA86AA-D-SG040 ..... N89-29001
NA86AA-D-SG089 ..... N89-28633
NCC2-226 ..... N89-28493
NCC2-322 ..... N89-29282
NCC2-374 ..... N89-28990
NGR-05-020-668 ..... N89-29282
NIH-AM-25501 ..... N89-29016
NIVR-0604N N89-28777
NR PROJ. R35-82 ..... N89-28975
NR PROJ. 358-856 ..... N89-28637
NR PROJ. 372-160 ..... N89-29244
NSF ASC-85-16364 ..... N89-29070
NSF CCR-86-09588 ..... N89-29057
NSF CDR-88-22236 ..... N89-28674
N89-29030
N89-29031
N89-29081
NSF DCI-86-01152 ..... N89-29058
NSF DCM-86-17355 ..... N89-29046
NSF DMR-86-16789 ..... N89-28638
NSF DMR-87-03434 ..... N89-29244
NSF DMS-85-16191 ..... N89-29116
N89-29118
NSF DMS-86-17355 ..... N89-29044
N89-29114
N89-29115
N89-29190
NSF DMS-87-00897 ..... N89-29135
NSF DMS-87-01543 ..... N89-28590
NSF ECSE-88-57642 ..... N89-29045
NSF IRI-86-16644 ..... N89-29056
NSF IRI-87-10858 ..... N89-29045
NSF MIP-86-01552 ..... N89-29036
NSF PHY-85-15857 ..... N89-29283
NSG-7643 ..... N89-29298
N00014-75-C-1132 ..... N89-29088
N00014-76-C-0197 ..... N89-29005
N00014-79-C-0647 ..... N89-28605
N89-29171
N00014-80-C-0796 ..... N89-28973
N00014-82-C-0019 ..... N89-29005
N00014-83-K-0125 ..... N89-29084
N00014-84-C-0132 ..... N89-29005
N00014-84-K-0099 ..... N89-29051
N00014-84-K-0548 ..... N89-29244
N00014-84-K-0553 ..... N89-28604
N00014-85-C-0001 ..... N89-29005
N00014-85-C-0177 ..... N89-28593
N89-29234
N00014-85-C-0419 ..... N89-28488
N00014-85-C-0881 ..... N89-28643
N00014-85-K-0124 ..... N89-28866
N89-29026
N89-29082
N00014-85-K-0168 ..... N89-29084
N00014-85-K-0169 ..... N89-29116
N89-29117
N89-29118
N00014-85-K-0213 ..... N89-29232
N00014-85-K-0222 ..... N89-28647
N89-28648
N89-28867
N00014-85-K-0358 ..... N89-29246
N00014-85-K-0474 ..... N89-28606
N89-28645
N89-28719
N89-29248
N00014-85-K-0586 ..... N89-29120
N00014-85-K-0782 ..... N89-29258
N00014-85-K-0898 ..... N89-28594
N89-28637
N89-28819
N00014-86-C-2488 ..... N89-29256
N00014-86-K-0043 ..... N89-28577
N00014-86-K-0130 ..... N89-28837
N00014-86-K-0269 ..... N89-29044
N00014-86-K-0281 ..... N89-29045
N89-29046
N89-29114
N89-29115
N89-29190
N00014-86-K-0453 ..... N89-28975
N00014-86-K-0660 ..... N89-28797
N89-29036
N89-29057
N89-29058
N00014-86-K-0685 ..... N89-28868
N89-29026
N89-29097
N00014-86-K-0752 ..... N89-28927
N00014-87-C-0408 ..... N89-29235
N89-29236
N00014-87-K-0014 ..... N89-28601
N89-28716
N89-29241
N89-29242
N89-29243
N89-29245
N00014-87-K-0060 ..... N89-28723
N89-28725
N00014-87-K-0129 ..... N89-29190
N00014-87-K-0426 ..... N89-28639
N00014-87-K-0541 ..... N89-28598
N89-28600
N89-28602
N00014-87-K-0738 ..... N89-28625
N00014-87-K-0825 ..... N89-29035
N89-29082
N00014-87-K-0828 ..... N89-29089
N89-29138
N00014-88-C-0571 ..... N89-28670
N00014-88-C-0717 ..... N89-29100
N00014-88-K-0109 ..... N89-28638
N00014-88-K-0487 ..... N89-29056
N00014-88-K-0493 ..... N89-28608
N89-28609
N00014-88-K-0591 ..... N89-29044
N89-29045
N89-29046
N89-29114
N89-29115
N89-29190
N00014-88-K-0738 ..... N89-29082
N00014-88-M-0106 ..... N89-29061
N00014-89-J-1178 ..... N89-28720
N00014-89-J-1497 ..... N89-29112
N00039-88-C-0065 ..... N89-28691
N00228-85-G-3262 ..... N89-28834
PHS-RR-02170-05 ..... N89-28797
RF7-65208 ..... N89-28577
SAND-33-1226 ..... N89-28953
W-31-109-ENG-38 ..... N89-28590
N89-28591
N89-28635
N89-28710
N89-28748
N89-28751
N89-28752
N89-28957
N89-29106
W-7405-ENG-36 ..... N89-28533
N89-28542
N89-28555
N89-28660
N89-28709
N89-28711
N89-28712
N89-28789
N89-28810
N89-28811
N89-28926
N89-28970
N89-29007
N89-29008
N89-29167
N89-29180
N89-29202
N89-29229
W-7405-ENG-48 ..... N89-28750
N89-28812
N89-28814
N89-28832
N89-28954
N89-29186
N89-29224
XL-7-06031-5 ..... N89-28944
ZB-7-06003-1 ..... N89-28946
073-36-00-00-72 ..... N89-29017
199-21-12-04 ..... N89-29016
474-18-00 ..... N89-28570
505-60-01 ..... N89-28870
505-61-71-07 ..... N89-28486
505-62-01 ..... N89-29032
505-62-21 ..... N89-28748
N89-28749
505-63-01-06 ..... N89-28579
505-63-51 ..... N89-29152
N89-29154
505-90-21-01 ..... N89-28762
N89-28763
N89-28764
N89-28766
N89-29028
N89-29061
N89-29122
N89-29123
N89-29124
506-42-31 ..... N89-28571
506-43-11 ..... N89-28851
506-44-21 ..... N89-28821
506-44-21-01 ..... N89-28820
506-44-21-03 ..... N89-28550
506-46-11-01 ..... N89-29047
506-47-31 ..... N89-29020
506-48-21 ..... N89-28535
535-03-11-03 ..... N89-29155
535-07-01 ..... N89-28853
554-14-21-321 ..... N89-28568
586-01-11 ..... N89-28627
586-01-21 ..... N89-28747
650-60-23 ..... N89-28545
672-22-20-70 ..... N89-28993
674-22-05 ..... N89-28665
674-25-05-08 ..... N89-28666
992-21-01 ..... N89-28498

Typical Report Number Index Listing

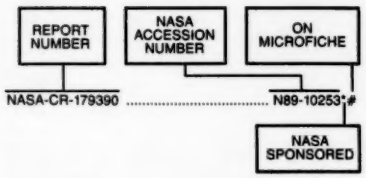

Listings in this index are arranged alphanumerically by report number. The NASA accession number denotes the number by which the citation is identified. An asterisk (*) indicates that the item is a NASA report. A pound sign (#) indicates that the item is available on microfiche.

A-88302 ..... N89-28870* #
A-89223 ..... N89-28498* #
A-89224 ..... N89-29016* #

AAMRL-TR-88-058 ..... N89-28511 #
AAMRL-TR-88-061 ..... N89-29022 #

AD-A207429 ..... N89-29029 #
AD-A207652 ..... N89-28687 #
AD-A207654 ..... N89-29143 #
AD-A207666 ..... N89-28718 #
AD-A207667 ..... N89-28974 #
AD-A207674 ..... N89-28645 #
AD-A207675 ..... N89-28975 #
AD-A207715 ..... N89-29203 #
AD-A207716 ..... N89-28606 #
AD-A207718 ..... N89-29087 #
AD-A207719 ..... N89-29246 #
AD-A207721 ..... N89-28661 #
AD-A207726 ..... N89-28757 #
AD-A207727 ..... N89-28662 #
AD-A207734 ..... N89-29247 #
AD-A207735 ..... N89-28491 #
AD-A207746 ..... N89-28688 #
AD-A207748 ..... N89-28515 #
AD-A207758 ..... N89-28758 #
AD-A207759 ..... N89-28607 #
AD-A207762 ..... N89-28512 #
AD-A207764 ..... N89-28608 #
AD-A207766 ..... N89-28609 #
AD-A207791 ..... N89-28929 #
AD-A207792 ..... N89-29049 #
AD-A207797 ..... N89-29116 #
AD-A207798 ..... N89-29117 #
AD-A207799 ..... N89-29118 #
AD-A207801 ..... N89-29003 #
AD-A207802 ..... N89-29088 #
AD-A207808 ..... N89-29050 #
AD-A207810 ..... N89-28865 #
AD-A207820 ..... N89-29089 #
AD-A207822 ..... N89-28520 #
AD-A207827 ..... N89-28689 #
AD-A207829 ..... N89-28930 #
AD-A207832 ..... N89-29194 #
AD-A207833 ..... N89-29051 #
AD-A207835 ..... N89-28719 #
AD-A207836 ..... N89-29248 #
AD-A207842 ..... N89-29138 #
AD-A207845 ..... N89-28557 #
AD-A207848 ..... N89-29011 #
AD-A207849 ..... N89-29004 #
AD-A207850 ..... N89-29268 #
AD-A207852 ..... N89-29119 #
AD-A207853 ..... N89-28720 #
AD-A207856 ..... N89-28976 #
AD-A207864 ..... N89-28988 #
AD-A207866 ..... N89-28759 #
AD-A207871 ..... N89-28989 #
AD-A207877 ..... N89-29052 #
AD-A207881 ..... N89-29120 #
AD-A207907 ..... N89-28577 #

AD-A207910 ..... N89-29204 #
AD-A207921 ..... N89-28818 #
AD-A207924 ..... N89-29098 #
AD-A207925 ..... N89-29249 #
AD-A207928 ..... N89-28760 #
AD-A207930 ..... N89-29278 #
AD-A207931 ..... N89-28690 #
AD-A207932 ..... N89-28721 #
AD-A207933 ..... N89-28722 #
AD-A207935 ..... N89-29053 #
AD-A207936 ..... N89-29250 #
AD-A207945 ..... N89-29012 #
AD-A207958 ..... N89-29026 #
AD-A207964 ..... N89-29054 #
AD-A207970 ..... N89-29013 #
AD-A207974 ..... N89-28846 #
AD-A207975 ..... N89-29205 #
AD-A207977 ..... N89-28723 #
AD-A207980 ..... N89-29206 #
AD-A207983 ..... N89-29014 #
AD-A207994 ..... N89-29055 #
AD-A208010 ..... N89-29274 #
AD-A208018 ..... N89-29056 #
AD-A208020 ..... N89-29005 #
AD-A208025 ..... N89-28724 #
AD-A208033 ..... N89-29144 #
AD-A208034 ..... N89-29145 #
AD-A208061 ..... N89-28663 #
AD-A208064 ..... N89-29150 #
AD-A208070 ..... N89-29035 #
AD-A208071 ..... N89-28819 #
AD-A208074 ..... N89-28866 #
AD-A208087 ..... N89-29057 #
AD-A208088 ..... N89-28797 #
AD-A208089 ..... N89-29058 #
AD-A208090 ..... N89-29036 #
AD-A208092 ..... N89-28725 #
AD-A208100 ..... N89-28647 #
AD-A208101 ..... N89-28648 #
AD-A208102 ..... N89-28867 #
AD-A208103 ..... N89-29297 #
AD-A208105 ..... N89-28868 #
AD-A208107 ..... N89-28626 #
AD-A208108 ..... N89-28761 #
AD-A208110 ..... N89-28518 #
AD-A208112 ..... N89-29099 #
AD-A208116 ..... N89-29015 #
AD-A208117 ..... N89-29121 #
AD-A208119 ..... N89-28578 #
AD-A208120 ..... N89-28869 #
AD-A208163 ..... N89-29100 #
AD-A208166 ..... N89-29059 #
AD-A208167 ..... N89-29060 #
AD-A208168 ..... N89-29172 #
AD-A208173 ..... N89-28649 #
AD-A208181 ..... N89-28726 #
AD-A208183 ..... N89-28558 #
AD-A208185 ..... N89-28513 #
AD-A208194 ..... N89-28559 #
AD-A208198 ..... N89-28691 #
AD-A208266 ..... N89-28637 #
AD-A208323 ..... N89-29082 #
AD-A208372 ..... N89-29232 #
AD-A208400 ..... N89-29021 #
AD-A208406 ..... N89-28927 #
AD-A208522 ..... N89-28675 #
AD-A208637 ..... N89-29109 #
AD-A208647 ..... N89-28488 #
AD-A208697 ..... N89-28593 #
AD-A208745 ..... N89-28638 #
AD-A208842 ..... N89-28834 #
AD-A208861 ..... N89-29233 #
AD-A208919 ..... N89-28594 #
AD-A208925 ..... N89-28835 #
AD-A208931 ..... N89-29234 #
AD-A208937 ..... N89-28862 #
AD-A208938 ..... N89-28677 #
AD-A208944 ..... N89-29083 #
AD-A208945 ..... N89-29041 #
AD-A208960 ..... N89-29187 #
AD-A208970 ..... N89-28639 #
AD-A208971 ..... N89-28678 #
AD-A208991 ..... N89-29235 #

AD-A208992 ..... N89-29236 #
AD-A208994 ..... N89-29188 #
AD-A208996 ..... N89-29084 #
AD-A209008 ..... N89-28836 #
AD-A209024 ..... N89-28640 #
AD-A209030 ..... N89-28754 #
AD-A209036 ..... N89-28641 #
AD-A209064 ..... N89-29237 #
AD-A209071 ..... N89-28642 #
AD-A209077 ..... N89-28966 #
AD-A209078 ..... N89-28714 #
AD-A209079 ..... N89-29238 #
AD-A209080 ..... N89-28595 #
AD-A209081 ..... N89-28715 #
AD-A209083 ..... N89-28489 #
AD-A209090 ..... N89-29137 #
AD-A209107 ..... N89-28971 #
AD-A209133 ..... N89-29042 #
AD-A209134 ..... N89-28863 #
AD-A209137 ..... N89-28985 #
AD-A209150 ..... N89-28574 #
AD-A209152 ..... N89-28490 #
AD-A209153 ..... N89-28679 #
AD-A209154 ..... N89-28596 #
AD-A209166 ..... N89-28643 #
AD-A209167 ..... N89-29258 #
AD-A209169 ..... N89-28597 #
AD-A209176 ..... N89-28755 #
AD-A209178 ..... N89-28534 #
AD-A209185 ..... N89-29148 #
AD-A209187 ..... N89-28660 #
AD-A209192 ..... N89-29002 #
AD-A209199 ..... N89-29110 #
AD-A209200 ..... N89-28538 #
AD-A209202 ..... N89-28681 #
AD-A209204 ..... N89-29033 #
AD-A209206 ..... N89-28539 #
AD-A209227 ..... N89-28540 #
AD-A209228 ..... N89-28682 #
AD-A209230 ..... N89-28683 #
AD-A209250 ..... N89-29189 #
AD-A209251 ..... N89-28972 #
AD-A209275 ..... N89-28837 #
AD-A209347 ..... N89-28598 #
AD-A209351 ..... N89-29256 #
AD-A209352 ..... N89-28599 #
AD-A209353 ..... N89-28622 #
AD-A209355 ..... N89-28623 #
AD-A209356 ..... N89-28838 #
AD-A209362 ..... N89-29239 #
AD-A209364 ..... N89-29034 #
AD-A209375 ..... N89-29019 #
AD-A209376 ..... N89-29240 #
AD-A209378 ..... N89-29111 #
AD-A209381 ..... N89-28600 #
AD-A209384 ..... N89-28986 #
AD-A209387 ..... N89-28792 #
AD-A209395 ..... N89-29094 #
AD-A209396 ..... N89-28511 #
AD-A209397 ..... N89-29022 #
AD-A209427 ..... N89-28575 #
AD-A209428 ..... N89-28576 #
AD-A209437 ..... N89-29265 #
AD-A209438 ..... N89-29023 #
AD-A209440 ..... N89-28843 #
AD-A209448 ..... N89-29260 #
AD-A209447 ..... N89-29142 #
AD-A209451 ..... N89-28624 #
AD-A209453 ..... N89-29095 #
AD-A209454 ..... N89-29096 #
AD-A209455 ..... N89-29024 #
AD-A209473 ..... N89-29266 #
AD-A209482 ..... N89-29192 #
AD-A209485 ..... N89-29267 #
AD-A209486 ..... N89-29048 #
AD-A209490 ..... N89-29245 #
AD-A209498 ..... N89-29149 #
AD-A209499 ..... N89-28756 #
AD-A209527 ..... N89-28928 #
AD-A209536 ..... N89-28604 #
AD-A209540 ..... N89-29097 #
AD-A209542 ..... N89-28973 #
AD-A209550 ..... N89-28548 #

AD-A209560 ..... N89-28605 #
AD-A209561 ..... N89-29171 #
AD-A209563 ..... N89-28685 #
AD-A209571 ..... N89-28686 #
AD-A209580 ..... N89-29193 #
AD-A209598 ..... N89-28717 #
AD-A209600 ..... N89-29025 #
AD-A209602 ..... N89-28625 #
AD-A209606 ..... N89-29086 #
AD-A209644 ..... N89-28544 #
AD-A209653 ..... N89-29181 #
AD-A209682 ..... N89-29112 #
AD-A209696 ..... N89-28601 #
AD-A209698 ..... N89-29241 #
AD-A209699 ..... N89-29242 #
AD-A209727 ..... N89-29259 #
AD-A209740 ..... N89-28815 #
AD-A209750 ..... N89-29243 #
AD-A209753 ..... N89-29009 #
AD-A209770 ..... N89-28644 #
AD-A209777 ..... N89-29141 #
AD-A209857 ..... N89-29244 #
AD-A209865 ..... N89-29043 #
AD-A209875 ..... N89-28839 #
AD-A209903 ..... N89-29113 #
AD-A209915 ..... N89-29010 #
AD-A210045 ..... N89-29170 #
AD-A210075 ..... N89-28670 #
AD-A210077 ..... N89-28716 #
AD-A210078 ..... N89-28602 #
AD-A210084 ..... N89-28864 #
AD-A210098 ..... N89-28840 #
AD-A210100 ..... N89-29190 #
AD-A210102 ..... N89-29114 #
AD-A210103 ..... N89-29044 #
AD-A210104 ..... N89-29115 #
AD-A210105 ..... N89-29045 #
AD-A210106 ..... N89-29046 #
AD-A210108 ..... N89-28987 #
AD-A210148 ..... N89-29085 #

AD-D013968 ..... N89-29219 #
AD-D013969 ..... N89-28705 #

AD-E501099 ..... N89-29144 #
AD-E501102 ..... N89-29145 #
AD-E501119 ..... N89-29142 #
AD-E501121 ..... N89-29260 #
AD-E900860 ..... N89-28548 #
AD-E900860 ..... N89-28605 #
AD-E900860 ..... N89-28685 #
AD-E900860 ..... N89-28686 #
AD-E900860 ..... N89-28973 #
AD-E900860 ..... N89-29097 #
AD-E900860 ..... N89-29171 #
AD-E951351 ..... N89-28687 #
AD-E951354 ..... N89-29014 #
AD-E951354 ..... N89-29055 #
AD-E951363 ..... N89-29141 #

AERONOMICA-ACTA-A-337-1989 ..... N89-29293
AERONOMICA-ACTA-A-338-1989 ..... N89-29294
AERONOMICA-ACTA-A-340-1989 ..... N89-28968
AERONOMICA-ACTA-A-341-1989-5 ..... N89-28980
AERONOMICA-ACTA-A-342-1989-6 ..... N89-28981

AFGL-ERP-1015 ..... N89-28491 #

AFGL-TR-88-0265 ..... N89-28491 #
AFGL-TR-89-0062 ..... N89-28974 #
AFGL-TR-89-0072 ..... N89-28976 #
AFGL-TR-89-0089 ..... N89-28971 #
AFGL-TR-89-0099 ..... N89-28987 #

AFHRL-TP-88-61 ..... N89-29019 #

AFHRL-TR-88-44 ..... N89-29193 #

AFIT/GA/ENY/89J-1 ..... N89-28539 #
AFIT/GA/ENY/89J-2 ..... N89-28538 #
AFIT/GA/ENY/89J-3 ..... N89-28540 #

AFIT/GAE/ENY/89J-2 ..... N89-28490 #
AFIT/GAE/ENY/89J-3 ..... N89-28755 #

AFIT/GCE/ENG/89J-1 ..... N89-29110 #

AFIT/GE/ENG/89J-1 ..... N89-28682 #

AFIT/GEO/ENP/89J-1 ..... N89-28596 #

AFIT/GST/ENS/89M-12 ..... N89-28679 #

AFOEHL-89-033EH0086DNA ..... N89-28717 #

AFOSR-89-0422TR ..... N89-29250 #

AFOSR-89-0435TR ..... N89-29278 #
AFOSR-89-0527TR ..... N89-28865 #
AFOSR-89-0531TR ..... N89-28578 #
AFOSR-89-0532TR ..... N89-29087 #
AFOSR-89-0533TR ..... N89-29203 #
AFOSR-89-0568TR ..... N89-28759 #
AFOSR-89-0591TR ..... N89-28760 #
AFOSR-89-0593TR ..... N89-29098 #
AFOSR-89-0595TR ..... N89-28869 #
AFOSR-89-0604TR ..... N89-29249 #
AFOSR-89-0607TR ..... N89-29119 #
AFOSR-89-0608TR ..... N89-28681 #
AFOSR-89-0613TR ..... N89-29204 #
AFOSR-89-0623TR ..... N89-28724 #
AFOSR-89-0626TR ..... N89-28989 #
AFOSR-89-0628TR ..... N89-29011 #
AFOSR-89-0684TR ..... N89-28864 #
AFOSR-89-0703TR ..... N89-29109 #
AFOSR-89-0732TR ..... N89-29233 #
AFOSR-89-0787TR ..... N89-29181 #
AFOSR-89-0806TR ..... N89-29113 #
AFOSR-89-0825TR ..... N89-28839 #
AFOSR-89-0830TR-VOL-2 ..... N89-29259 #

AFWAL-TR-88-1071 ..... N89-28863 #
AFWAL-TR-88-2103 ..... N89-29206 #
AFWAL-TR-88-3102 ..... N89-28761 #
AFWAL-TR-88-4248 ..... N89-28642 #
AFWAL-TR-88-4253 ..... N89-28862 #
AFWAL-TR-88-4254 ..... N89-28626 #
AFWAL-TR-89-2008 ..... N89-28835 #

AFWL-TR-89-01 ..... N89-29049 #

AGARD-AG-315 ..... N89-28734 #

AGARD-CAL-89/2 ..... N89-29261 #

AI-M-1091 ..... N89-29026 #
AI-M-1118 ..... N89-29056 #

AI-TR-1030 ..... N89-28866 #

AIAA-89-2717 ..... N89-28571* #

AIM-1084 ..... N89-29097 #

AL-CP-89-001 ..... N89-29170 #

AMSMI/TR-RD-DE-89-1 ..... N89-28687 #

AMSMI/TR-RD-RE-89-5 ..... N89-29055 #

AMTI-2236-1 ..... N89-28838 #

ANE-13/87 ..... N89-28503 #

ANL-HEP-CP-89-36 ..... N89-29108 #

ANL-89/15 ..... N89-28591 #

AR-87-88 ..... N89-28999 #
AR-005-548 ..... N89-28871 #
AR-005-570 ..... N89-28580 #
AR-005-583 ..... N89-28518 #

ARB/TSD-88-008 ..... N89-28960 #

ARL-AERO-PROP-TM-458 ..... N89-28518 #

ARL-FLIGHT-MECH-TM-409 ..... N89-28489 #

ARL-STRUC-R-434 ..... N89-28871 #

ARL-STRUCT-R-435 ..... N89-28580 #

ARO-22303.8-MS ..... N89-28576 #
ARO-22743.1-MS ..... N89-28641 #
ARO-22971.3-GS ..... N89-29192 #
ARO-23040.27-CH ..... N89-28595 #
ARO-23760.2-EG-F ..... N89-28836 #
ARO-23783.1-CH-F ..... N89-28597 #
ARO-23793.3-MS ..... N89-28640 #
ARO-24620.18-EG-UIR ..... N89-28575 #
ARO-25170.11-EG ..... N89-29111 #
ARO-25495.2-PH ..... N89-28715 #
ARO-25998.1-EL-SBI-PHASE-1 ..... N89-29042 #
ARO-26204.1-EL-SBI ..... N89-29238 #
ARO-26239.1-EG-SBI ..... N89-28754 #

ATC-155 ..... N89-28986 #

AVSCOM-TM-89-B-007 ..... N89-28579* #

BAE-WAA-R-GEN-RAD-533 ..... N89-28695

BAE-WAA-RP-GEN-RAD-584 ..... N89-28696
BAE-WAA-RP-GEN-RAD-645-PT-3 ..... N89-28697

BAE-WWT-RP-RES-AXR-000194-PT-A N89-28501
BAE-WWT-RP-RES-AXR-000194-PT-B N89-28502

BAE/WMD/AR/GEN/00666 ..... N89-28630

BCRS-55-16E ..... N89-28939 #
BCRS-88-16C ..... N89-28937 #
BCRS-88-16D ..... N89-28938 #
BCRS-89-05 ..... N89-28940 #
BCRS-89-07 ..... N89-28941 #

BFLRF-253 ..... N89-28661 #

BMVG-FBWT-88-2 ..... N89-28581

BMVG-RUFO-5(ALT) N89-28581

BN-1089 ..... N89-29118 #
BN-1090 ..... N89-29117 #
BN-1091 ..... N89-29116 #

BNL-42655 ..... N89-29223 #
BNL-42744 ..... N89-28984 #
BNL-42768 ..... N89-28965 #
BNL-42829 ..... N89-28791 #

BPT-9/88 ..... N89-28525 #

BRL-CR-607 ..... N89-28662 #

BRL-MR-3742 ..... N89-28758 #
BRL-MR-3759 ..... N89-28868 #

BRL-TR-2986 ..... N89-28663 #
BRL-TR-2991 ..... N89-29297 #
BRL-TR-2998 ..... N89-28607 #
BRL-TR-3003 ..... N89-28966 #
BRL-TR-3014 ..... N89-28548 #

CERC-WIS-19 ..... N89-29004 #

CERL-TM-M-89/05 ..... N89-28688 #

CERT-1/332400/DERI ..... N89-28775 #
CERT-2305 ..... N89-28803 #

CESAR-89/24 ..... N89-28808 #

CONF-880385-2 ..... N89-29263 #
CONF-880747-7 ..... N89-29283 #
CONF-881123-4 ..... N89-28751 #
CONF-890335-215 ..... N89-28711 #
CONF-890358-5 ..... N89-29186 #
CONF-890480-1 ..... N89-29227 #
CONF-890533-ABSTS ..... N89-28948 #
CONF-890545-6 ..... N89-29093 #
CONF-890621-1 ..... N89-29230 #
CONF-890631-14 ..... N89-28784 #
CONF-890665-25 ..... N89-28708 #
CONF-890665-27 ..... N89-28709 #
CONF-890665-30 ..... N89-28810 #
CONF-890674-3 ..... N89-28789 #
CONF-890692-9 ..... N89-28962 #
CONF-890710-10 ..... N89-28712 #
CONF-890710-11 ..... N89-28542 #
CONF-890717-1 ..... N89-28952 #
CONF-890717-2 ..... N89-28487 #
CONF-890718-7 ..... N89-29231 #
CONF-890723-6 ..... N89-28555 #
CONF-890754-1 ..... N89-29220 #
CONF-890768-2 ..... N89-28924 #
CONF-890789-1-SUPP-2 ..... N89-28573 #
CONF-890792-1 ..... N89-28634 #
CONF-890799-1 ..... N89-28533 #
CONF-890815-4 ..... N89-28956 #
CONF-890815-5 ..... N89-28957 #
CONF-890819-15 ..... N89-28752 #
CONF-890849-1 ..... N89-29008 #
CONF-890849-2 ..... N89-29007 #
CONF-8807172-1 ..... N89-28590 #
CONF-8807177-1 ..... N89-29106 #
CONF-8808141-13 ..... N89-28788 #
CONF-8809364-1 ..... N89-29224 #
CONF-8811214 ..... N89-29221 #
CONF-8811214 ..... N89-29222 #
CONF-8902113-1 ..... N89-28750 #
CONF-8902117-1 ..... N89-28618 #
CONF-8903128-1 ..... N89-29223 #
CONF-8903130-1 ..... N89-29108 #
CONF-8903131-1 ..... N89-28970 #
CONF-8904236-1 ..... N89-28616 #
CONF-8904238-1 ..... N89-28635 #
CONF-8904242-1 ..... N89-28791 #

CONF-8905127-4 ..... N89-28923 #
CONF-8905156-1 ..... N89-29202 #
CONF-8905158-1 ..... N89-28832 #
CONF-8905163-1 ..... N89-29167 #
CONF-8905164-1 ..... N89-28951 #
CONF-8905166-3 ..... N89-28592 #
CONF-8905175-1 ..... N89-28710 #
CONF-8905178-2 ..... N89-28861 #
CONF-8905179-1 ..... N89-29147 #
CONF-8906112-1 ..... N89-29040 #
CONF-8906119-2 ..... N89-28620 #
CONF-8906131-1 ..... N89-28746 #
CONF-8906132-1 ..... N89-28786 #
CONF-8906133-2 ..... N89-28787 #
CONF-8906133-3 ..... N89-28790 #
CONF-8906135-2 ..... N89-28636 #
CONF-8906139-1 ..... N89-29153 #
CONF-8906152-1 ..... N89-28616 #
CONF-8906154-1 ..... N89-28984 #
CONF-8906155-1 ..... N89-29226 #
CONF-8906157-1 ..... N89-29225 #
CONF-8906157-2 ..... N89-28619 #

CPS-89-004 ..... N89-28578 #

CREARE-TM-1352 ..... N89-28839 #

CRREL-SP-89-8 ..... N89-29041 #

CRREL-SR-89-13 ..... N89-29024 #

CRREL-89-6 ..... N89-29187 #

CSA-88-11-03 ..... N89-28862 #

CSSA-ASTRO-89-15 ..... N89-29282* #

CU-CSD-TR-89-963 ..... N89-29114 #
CU-CSD-TR-89-964 ..... N89-29115 #
CU-CSD-TR-89-965 ..... N89-29044 #
CU-CSD-TR-89-981 ..... N89-29190 #
CU-CSD-TR-89-986 ..... N89-29046 #
CU-CSD-TR-89-1007 ..... N89-29045 #

CUED/A-TURBO/TR-125 ..... N89-28778 #

CWP-089 ..... N89-29192 #

DCIEM-88-RR-56 ..... N89-29015 #

DEL-SG-06-89 ..... N89-29001 #

DE88-001192 ..... N89-28657 #
DE89-000861 ..... N89-28947 #
DE89-000894 ..... N89-28658 #
DE89-000895 ..... N89-28948 #
DE89-007764 ..... N89-28555 #
DE89-008587 ..... N89-28949 #
DE89-009422 ..... N89-28950 #
DE89-009425 ..... N89-28956 #
DE89-009434 ..... N89-28944 #
DE89-009437 ..... N89-28945 #
DE89-009439 ..... N89-28946 #
DE89-009443 ..... N89-28487 #
DE89-009643 ..... N89-29220 #
DE89-010875 ..... N89-28924 #
DE89-012339 ..... N89-29263 #
DE89-012359 ..... N89-28962 #
DE89-012418 ..... N89-28746 #
DE89-012422 ..... N89-28957 #
DE89-012427 ..... N89-28752 #
DE89-012429 ..... N89-28710 #
DE89-012622 ..... N89-28970 #
DE89-012635 ..... N89-29202 #
DE89-012974 ..... N89-29223 #
DE89-012991 ..... N89-28616 #
DE89-013033 ..... N89-28832 #
DE89-013065 ..... N89-28708 #
DE89-013146 ..... N89-28750 #
DE89-013155 ..... N89-28786 #
DE89-013164 ..... N89-29153 #
DE89-013178 ..... N89-29108 #
DE89-013221 ..... N89-29007 #
DE89-013268 ..... N89-29283 #
DE89-013310 ..... N89-28634 #
DE89-013369 ..... N89-29106 #
DE89-013425 ..... N89-28788 #
DE89-013430 ..... N89-28951 #
DE89-013438 ..... N89-29008 #
DE89-013454 ..... N89-29167 #
DE89-013524 ..... N89-28573 #
DE89-013591 ..... N89-28784 #
DE89-013615 ..... N89-28923 #
DE89-013627 ..... N89-28659 #
DE89-013629 ..... N89-28590 #
DE89-013645 ..... N89-28751 #
DE89-013720 ..... N89-28808 #
DE89-013740 ..... N89-28813 #
DE89-013766 ..... N89-28617 #
DE89-013787 ..... N89-29186 #
DE89-013791 ..... N89-29224 #
DE89-013813 ..... N89-28952 #
DE89-013872 ..... N89-28953 #
DE89-013875 ..... N89-28833 #
DE89-013886 ..... N89-28860 #
DE89-013917 ..... N89-28591 #
DE89-013919 ..... N89-28954 #
DE89-013952 ..... N89-29255 #
DE89-013964 ..... N89-28589 #
DE89-014023 ..... N89-28810 #
DE89-014033 ..... N89-28709 #
DE89-014039 ..... N89-28787 #
DE89-014044 ..... N89-29225 #
DE89-014069 ..... N89-29040 #
DE89-014244 ..... N89-28711 #
DE89-014258 ..... N89-28789 #
DE89-014264 ..... N89-28965 #
DE89-014280 ..... N89-28533 #
DE89-014294 ..... N89-28542 #
DE89-014298 ..... N89-28712 #
DE89-014322 ..... N89-28958 #
DE89-014325 ..... N89-28814 #
DE89-014374 ..... N89-28753 #
DE89-014377 ..... N89-28543 #
DE89-014385 ..... N89-28811 #
DE89-014389 ..... N89-29180 #
DE89-014391 ..... N89-29229 #
DE89-014400 ..... N89-29093 #
DE89-014445 ..... N89-29147 #
DE89-014449 ..... N89-28861 #
DE89-014454 ..... N89-28618 #
DE89-014466 ..... N89-28592 #
DE89-014519 ..... N89-28791 #
DE89-014523 ..... N89-28852 #
DE89-014554 ..... N89-28669 #
DE89-014563 ..... N89-29168 #
DE89-014568 ..... N89-28955 #
DE89-014604 ..... N89-28812 #
DE89-014629 ..... N89-28790 #
DE89-014668 ..... N89-28635 #
DE89-014708 ..... N89-28984 #
DE89-014769 ..... N89-28636 #
DE89-014797 ..... N89-29226 #
DE89-014808 ..... N89-28926 #
DE89-014844 ..... N89-28660 #
DE89-014884 ..... N89-28619 #
DE89-014893 ..... N89-29227 #
DE89-014894 ..... N89-29228 #
DE89-014895 ..... N89-29296 #
DE89-014899 ..... N89-29230 #
DE89-014933 ..... N89-28620 #
DE89-014937 ..... N89-29231 #
DE89-611897 ..... N89-29107 #
DE89-611971 ..... N89-29254 #
DE89-613395 ..... N89-29221 #
DE89-613396 ..... N89-29222 #

DFVLR-FB-89-08 ..... N89-28847 #
DFVLR-FB-89-09 ..... N89-28504 #
DFVLR-FB-89-14 ..... N89-28943 #
DFVLR-FB-89-15 ..... N89-29132 #
DFVLR-FB-89-19 ..... N89-28505 #
DFVLR-FB-89-21 ..... N89-28698 #

DFVLR-MITT-89-08 ..... N89-28942 #

DFVLR-88-044 ..... N89-28610 #

DOE/CE-15289/T1 ..... N89-28949 #

DOE/CH-10093/46 ..... N89-28947 #

DOE/EH-79050/T1 ..... N89-28669 #

DOE/ER-03130/3 ..... N89-29255 #
DOE/ER-13796/2 ..... N89-28924 #
DOE/ER-40481/2 ..... N89-29168 #
DOE/ER-45147/4 ..... N89-28589 #
DOE/ER-45347/13 ..... N89-29231 #

DOE/NASA/16310-10 ..... N89-28627* #

DOE/PETC-TR/89/6 ..... N89-28659 #

DOI/SW/DK-89/005A ..... N89-29039 #

DOT/FAA/CT-89/6 ..... N89-28516 #
DOT/FAA/CT-89/7 ..... N89-28517 #

DOT/FAA/DS-88/7 ..... N89-28506 #
DOT/FAA/DS-89/2-PHASE-1 ..... N89-28523 #
DOT/FAA/DS-89/27 ..... N89-28509 #

DOT/FAA/DS-89/28 ..... N89-28524 #

DOT/FAA/PM-87/37 ..... N89-28986 #

DR-5-3 ..... N89-28567* #

DREO-TN-89-1 ..... N89-29043 #

DREP-TM-88-23-VOL-1 ..... N89-29029 #

DTRC-89/004 ..... N89-28756 #

E-4456 ..... N89-28545* #
E-4524 ..... N89-28665* #
E-4600 ..... N89-28853* #
E-4723 ..... N89-28666* #
E-4754 ..... N89-28627* #
E-4916 ..... N89-28748* #
E-4928 ..... N89-28851* #
E-4938 ..... N89-28571* #
E-4965 ..... N89-28749* #
E-4997 ..... N89-28535* #
E-5028 ..... N89-28747* #
E-5029 ..... N89-29032* #
E-5047 ..... N89-28570* #

ECS-SS-1858 ..... N89-28567* #

EGG-10617-1033 ..... N89-28787 #

EPA/600/D-89/001 ..... N89-28964 #
EPA/600/3-89/031 ..... N89-28572 #
EPA/600/8-89/041-VOL-1 ..... N89-28963 #

ESA-SP-1107 ..... N89-29295 #

ESA-TT-1137 ..... N89-28781 #
ESA-TT-1161 ..... N89-29299 #
ESA-TT-1162 ..... N89-29300 #
ESA-TT-1165 ..... N89-29301 #

ESD-TR-88-224 ..... N89-28818 #
ESD-TR-88-333 ..... N89-28678 #

ESG-46 ..... N89-29106 #

ETCA-88-R-070 ..... N89-29198 #
ETCA-89-R-015 ..... N89-28854 #

ETN-89-94312 ..... N89-28500 #
ETN-89-94381 ..... N89-28610 #
ETN-89-94382 ..... N89-28485 #
ETN-89-94388 ..... N89-29173 #
ETN-89-94389 ..... N89-28798 #
ETN-89-94398 ..... N89-29174 #
ETN-89-94400 ..... N89-28844
ETN-89-94401 ..... N89-29156
ETN-89-94412 ..... N89-28581
ETN-89-94413 ..... N89-28977 #
ETN-89-94414 ..... N89-28931 #
ETN-89-94415 ..... N89-28799 #
ETN-89-94416 ..... N89-28991
ETN-89-94417 ..... N89-28992
ETN-89-94418 ..... N89-28978
ETN-89-94419 ..... N89-29276 #
ETN-89-94420 ..... N89-28536 #
ETN-89-94421 ..... N89-28508 #
ETN-89-94423 ..... N89-28525 #
ETN-89-94425 ..... N89-28822 #
ETN-89-94429 ..... N89-29279 #
ETN-89-94430 ..... N89-29195 #
ETN-89-94431 ..... N89-28611 #
ETN-89-94432 ..... N89-28769 #
ETN-89-94433 ..... N89-28770 #
ETN-89-94434 ..... N89-28823
ETN-89-94435 ..... N89-29175
ETN-89-94436 ..... N89-28824
ETN-89-94437 ..... N89-29251
ETN-89-94438 ..... N89-28771 #
ETN-89-94439 ..... N89-29196 #
ETN-89-94440 ..... N89-29197 #
ETN-89-94441 ..... N89-28772 #
ETN-89-94442 ..... N89-28727 #
ETN-89-94446 ..... N89-28781 #
ETN-89-94562 ..... N89-28522 #
ETN-89-94563 ..... N89-28800 #
ETN-89-94567 ..... N89-29178 #
ETN-89-94596 ..... N89-28653 #
ETN-89-94603 ..... N89-28979
ETN-89-94606 ..... N89-29277 #
ETN-89-94608 ..... N89-28728
ETN-89-94610 ..... N89-29134 #
ETN-89-94650 ..... N89-29252 #
ETN-89-94652 ..... N89-28729 #
ETN-89-94653 ..... N89-28773 #
ETN-89-94655 ..... N89-29257 #

ETN-89-94659 ..... N89-28872 #
ETN-89-94750 ..... N89-29037 #
ETN-89-94753 ..... N89-29062 #
ETN-89-94787 ..... N89-29090 #
ETN-89-94795 ..... N89-29200 #
ETN-89-94804 ..... N89-28510 #
ETN-89-94815 ..... N89-29253 #
ETN-89-94848 ..... N89-28873 #
ETN-89-94850 ..... N89-28801 #
ETN-89-94851 ..... N89-28802 #
ETN-89-94855 ..... N89-28774 #
ETN-89-94856 ..... N89-28494 #
ETN-89-94858 ..... N89-28495 #
ETN-89-94860 ..... N89-29063 #
ETN-89-94861 ..... N89-29198 #
ETN-89-94862 ..... N89-28854 #
ETN-89-94863 ..... N89-28664 #
ETN-89-94864 ..... N89-28629 #
ETN-89-94865 ..... N89-28650 #
ETN-89-94866 ..... N89-28582 #
ETN-89-94867 ..... N89-28775 #
ETN-89-94868 ..... N89-28803 #
ETN-89-94870 ..... N89-29101 #
ETN-89-94871 ..... N89-29064 #
ETN-89-94873 ..... N89-29275 #
ETN-89-94911 ..... N89-29105 #
ETN-89-94920 ..... N89-28693 #
ETN-89-94921 ..... N89-28694 #
ETN-89-94929 ..... N89-28994 #
ETN-89-94930 ..... N89-28995 #
ETN-89-94931 ..... N89-28996 #
ETN-89-94932 ..... N89-28997 #
ETN-89-94933 ..... N89-28998 #
ETN-89-94939 ..... N89-28999 #
ETN-89-94943 ..... N89-28959 #
ETN-89-94958 ..... N89-28501
ETN-89-94959 ..... N89-28502
ETN-89-94960 ..... N89-29157 #
ETN-89-94961 ..... N89-29158 #
ETN-89-94962 ..... N89-28652 #
ETN-89-94966 ..... N89-28825
ETN-89-94968 ..... N89-29065 #
ETN-89-94976 ..... N89-28569 #
ETN-89-94986 ..... N89-29199 #
ETN-89-94989 ..... N89-29302 #
ETN-89-95010 ..... N89-29295 #
ETN-89-95031 ..... N89-28804 #
ETN-89-95033 ..... N89-28519 #
ETN-89-95034 ..... N89-28826 #
ETN-89-95058 ..... N89-29072 #
ETN-89-95059 ..... N89-28779 #
ETN-89-95060 ..... N89-29130 #
ETN-89-95061 ..... N89-29073 #
ETN-89-95062 ..... N89-29146 #
ETN-89-95063 ..... N89-29131 #
ETN-89-95064 ..... N89-29078 #
ETN-89-95065 ..... N89-29079 #
ETN-89-95066 ..... N89-29080 #
ETN-89-95112 ..... N89-29074 #
ETN-89-95113 ..... N89-29102 #
ETN-89-95114 ..... N89-28782 #
ETN-89-95115 ..... N89-28875 #
ETN-89-95116 ..... N89-29086 #
ETN-89-95117 ..... N89-28776 #
ETN-89-95118 ..... N89-28845 #
ETN-89-95119 ..... N89-29075 #
ETN-89-95120 ..... N89-29076 #
ETN-89-95121 ..... N89-29104 #
ETN-89-95122 ..... N89-28654 #
ETN-89-95123 ..... N89-28655 #
ETN-89-95124 ..... N89-29103 #
ETN-89-95125 ..... N89-29135* #
ETN-89-95126 ..... N89-28850 #
ETN-89-95144 ..... N89-28827
ETN-89-95145 ..... N89-28828
ETN-89-95146 ..... N89-28583
ETN-89-95147 ..... N89-29216 #
ETN-89-95150 ..... N89-29217 #
ETN-89-95162 ..... N89-28700 #
ETN-89-95176 ..... N89-29290 #
ETN-89-95177 ..... N89-29291 #
ETN-89-95179 ..... N89-28613 #
ETN-89-95180 ..... N89-28632 #
ETN-89-95182 ..... N89-29136 #
ETN-89-95183 ..... N89-28855 #
ETN-89-95185 ..... N89-28932 #
ETN-89-95187 ..... N89-29293
ETN-89-95188 ..... N89-29294
ETN-89-95189 ..... N89-28968
ETN-89-95190 ..... N89-28980
ETN-89-95191 ..... N89-28981
ETN-89-95194 ..... N89-29091 #
ETN-89-95197 ..... N89-28667 #
ETN-89-95199 ..... N89-28503 #
ETN-89-95200 ..... N89-28783 #
ETN-89-95201 ..... N89-28560 #
ETN-89-95221 ..... N89-28630
ETN-89-95222 ..... N89-28695
ETN-89-95223 ..... N89-28696
ETN-89-95225 ..... N89-28697
ETN-89-95235 ..... N89-28563 #
ETN-89-95236 ..... N89-28564 #
ETN-89-95250 ..... N89-29125
ETN-89-95251 ..... N89-29092
ETN-89-95252 ..... N89-29126
ETN-89-95253 ..... N89-28631
ETN-89-95254 ..... N89-28612
ETN-89-95255 ..... N89-28584
ETN-89-95256 ..... N89-28585
ETN-89-95257 ..... N89-29179 #
ETN-89-95292 ..... N89-28702 #
ETN-89-95293 ..... N89-29000 #
ETN-89-95294 ..... N89-28703 #
ETN-89-95299 ..... N89-28942 #
ETN-89-95305 ..... N89-28847 #
ETN-89-95306 ..... N89-28504 #
ETN-89-95310 ..... N89-28943 #
ETN-89-95311 ..... N89-29132 #
ETN-89-95314 ..... N89-28505 #
ETN-89-95316 ..... N89-28698 #
ETN-89-95333 ..... N89-29281 #
ETN-89-95334 ..... N89-28561 #
ETN-89-95339 ..... N89-29280 #
ETN-89-95340 ..... N89-29284
ETN-89-95341 ..... N89-29286
ETN-89-95342 ..... N89-29285
ETN-89-95343 ..... N89-29298*
ETN-89-95344 ..... N89-29287
ETN-89-95345 ..... N89-29288
ETN-89-95391 ..... N89-29299 #
ETN-89-95392 ..... N89-29300 #
ETN-89-95393 ..... N89-29301 #
ETN-89-95394 ..... N89-29127 #
ETN-89-95395 ..... N89-29128 #
ETN-89-95396 ..... N89-29139 #
ETN-89-95397 ..... N89-29129 #
ETN-89-95398 ..... N89-29182 #
ETN-89-95399 ..... N89-29183 #
ETN-89-95400 ..... N89-29184 #
ETN-89-95401 ..... N89-29185 #
ETN-89-95403 ..... N89-29151 #
ETN-89-95410 ..... N89-28526 #
ETN-89-95411 ..... N89-29067 #
ETN-89-95412 ..... N89-28933 #
ETN-89-95414 ..... N89-29271 #
ETN-89-95415 ..... N89-28934 #
ETN-89-95416 ..... N89-28777 #
ETN-89-95417 ..... N89-28935 #
ETN-89-95420 ..... N89-28936 #
ETN-89-95421 ..... N89-29068 #
ETN-89-95422 ..... N89-29272 #
ETN-89-95423 ..... N89-29069 #
ETN-89-95424 ..... N89-28730 #
ETN-89-95427 ..... N89-29070 #
ETN-89-95428 ..... N89-28499 #
ETN-89-95429 ..... N89-29006 #
ETN-89-95453 ..... N89-28780
ETN-89-95454 ..... N89-28874 #
ETN-89-95455 ..... N89-28699 #
ETN-89-95456 ..... N89-29038
ETN-89-95457 ..... N89-29077 #
ETN-89-95458 ..... N89-28656 #
ETN-89-95459 ..... N89-28732 #
ETN-89-95460 ..... N89-28614
ETN-89-95461 ..... N89-28701 #
ETN-89-95462 ..... N89-28731
ETN-89-95463 ..... N89-29176 #
ETN-89-95464 ..... N89-29177 #
ETN-89-95465 ..... N89-29133 #
ETN-89-95466 ..... N89-28733 #
ETN-89-95467 ..... N89-28982 #
ETN-89-95475 ..... N89-28937 #
ETN-89-95476 ..... N89-28938 #
ETN-89-95477 ..... N89-28939 #
ETN-89-95486 ..... N89-28940 #
ETN-89-95487 ..... N89-28941 #
ETN-89-95489 ..... N89-29140 #
ETN-89-95531 ..... N89-29018 #
ETN-89-95532 ..... N89-28807 #
ETN-89-95536 ..... N89-28848 #
ETN-89-95537 ..... N89-28849 #
EUT-88-E-207 ..... N89-29200 #
FFA-TN-1985-58 ..... N89-28500 #
FFA-TN-1986-56 ..... N89-28959 #
FHWA-OR-RD-89-04A-VOL-1 ..... N89-28668 #
FIP-12/10 ..... N89-28800 #
FOA-C-30531-3.4 ..... N89-29091 #
FR-60112 ..... N89-29238 #
GL-TR-89-0106 ..... N89-28988 #
GPO-99-596 ..... N89-29273 #
GRI-88/0312 ..... N89-28588 #
GRI-89/0002 ..... N89-28587 #
GRI-89/0020 ..... N89-28768 #
GRL/8804 ..... N89-28819 #
HAC-REF-F7896-F ..... N89-28643 #
HDL-TM-89-5 ..... N89-28680 #
HDL-TR-2161 ..... N89-29149 #
HEL-TN-5-89 ..... N89-29021 #
IC-88/414 ..... N89-29107 #
ICASE-IR-8 ..... N89-28764* #
ICASE-89-41 ..... N89-29061* #
ICASE-89-48 ..... N89-29028* #
ICASE-89-49 ..... N89-29122* #
ICASE-89-50 ..... N89-28766* #
ICASE-89-52 ..... N89-29123* #
ICASE-89-55 ..... N89-28763* #
ICASE-89-56 ..... N89-29124* #
ICASE-89-61 ..... N89-28762* #
ICOMP-89-15 ..... N89-28748* #
ICOMP-89-18 ..... N89-28749* #
IDA-P-2132 ..... N89-29142 #
IDA-P-2142 ..... N89-29145 #
IDA-P-2145 ..... N89-29144 #
IDA-P-2149 ..... N89-29260 #
IDA/HQ-88-33599 ..... N89-29142 #
IDA/HQ-88-33701 ..... N89-29145 #
IDA/HQ-88-33716 ..... N89-29144 #
IDA/HQ-88-33815 ..... N89-29260 #
IIT-E06595-3 ..... N89-28691 #
ILR-MITT-212 ..... N89-28522 #
ILR-MITT-214 ..... N89-28800 #
ILR-1986/87 ..... N89-28536 #
IMAG-RR-746-I ..... N89-29140 #
INIS-BR-1531 ..... N89-29221 #
INIS-BR-1533 ..... N89-29222 #
INPE-4800-RPE/587 ..... N89-28925 #
IPP-2/294 ..... N89-28726
IPPJ-901 ..... N89-29207 #
IPPJ-902 ..... N89-29208 #
IPPJ-903 ..... N89-29209 #
IPPJ-904 ..... N89-29210 #
IPPJ-907 ..... N89-29201 #
IPPJ-911 ..... N89-29211 #
IPPJ-912 ..... N89-29212 #
IPPJ-913 ..... N89-29213 #
IPPJ-914 ..... N89-29214 #
IPPJ-915 ..... N89-29215 #
IRF-SR-199 ..... N89-28700 #
ISBN-0-309-03999-1 ..... N89-28565* #
ISBN-0-86776-311-6 ..... N89-28858 #
ISBN-0-86776-312-4 ..... N89-28857 #
ISBN-0-86776-314-0 ..... N89-28859 #
ISBN-3-88314-867-9 ..... N89-29199 #
ISBN-90-265-236-5 ..... N89-29068 #
ISBN-90-365-0153-9 ..... N89-29037 #
ISBN-90-365-0239-X ..... N89-29069 #
ISBN-90-365-0242-X ..... N89-29078 #
ISBN-90-370-0022-3 ..... N89-28780
ISBN-90-627-5496-1 ..... N89-28499 #
ISBN-90-6144-207-9 ..... N89-29200 #
ISBN-90-6275-535-4 ..... N89-28731
ISBN-90-6275-535-6 ..... N89-28614
ISBN-90-71617-11-4 ..... N89-29275 #
ISBN-90-9002498-0 ..... N89-28656 #
ISBN-92-63-10690-8 ..... N89-28994 #
ISBN-92-63-10691-6 ..... N89-28995 #
ISBN-92-63-10692-4 ..... N89-28996 #
ISBN-92-63-10693-2 ..... N89-28997 #
ISBN-92-63-10694-0 ..... N89-28998 #

ISBN-92-835-0506-9 ..... N89-28734 #
ISBN-92-835-0520-4 ..... N89-29261 #
ISBN-951-38-3298-8 ..... N89-29136 #
ISBN-951-38-3332-1 ..... N89-28855 #
ISBN-951-38-3434-4 ..... N89-28932 #
ISBN-951-754-665-3 ..... N89-29218 #
ISBN-951-754-692-0 ..... N89-28671 #
ISBN-951-754-726-9 ..... N89-28704 #
ISBN-952-90014-6-0 ..... N89-28613 #
ISBN-952-90044-3-5 ..... N89-28632 #

ISL-C-208/88 ..... N89-28873 #

ISL-CO-210/88 ..... N89-28801 #
ISL-CO-212/88 ..... N89-28802 #
ISL-CO-218/88 ..... N89-28804 #
ISL-CO-226/88 ..... N89-28519 #
ISL-CO-230/88 ..... N89-28826 #

ISL-R-114/87 ..... N89-28774 #
ISL-R-123/87 ..... N89-28494 #
ISL-R-125/87 ..... N89-28495 #

ISSN-0065-3713 ..... N89-28968
ISSN-0065-3713 ..... N89-28980
ISSN-0065-3713 ..... N89-28981
ISSN-0065-3713 ..... N89-29293
ISSN-0065-3713 ..... N89-29294
ISSN-0069-5882 ..... N89-28799 #
ISSN-0069-5882 ..... N89-28931 #
ISSN-0069-5882 ..... N89-28977 #
ISSN-0070-3966 ..... N89-28485 #
ISSN-0078-3781 ..... N89-28702 #
ISSN-0078-3781 ..... N89-28703 #
ISSN-0078-3781 ..... N89-29000 #
ISSN-0078-3781 ..... N89-29063 #
ISSN-0078-3781 ..... N89-29253 #
ISSN-0109-6605 ..... N89-28805 #
ISSN-0143-7313 ..... N89-28583
ISSN-0143-7313 ..... N89-28584
ISSN-0143-7313 ..... N89-28585
ISSN-0143-7313 ..... N89-28612
ISSN-0143-7313 ..... N89-28631
ISSN-0167-9708 ..... N89-29200 #
ISSN-0169-2690 ..... N89-28654 #
ISSN-0169-2690 ..... N89-28655 #
ISSN-0169-2690 ..... N89-28776 #
ISSN-0169-2690 ..... N89-28779 #
ISSN-0169-2690 ..... N89-28782 #
ISSN-0169-2690 ..... N89-28845 #
ISSN-0169-2690 ..... N89-28850 #
ISSN-0169-2690 ..... N89-28875 #
ISSN-0169-2690 ..... N89-29066 #
ISSN-0169-2690 ..... N89-29072 #
ISSN-0169-2690 ..... N89-29073 #
ISSN-0169-2690 ..... N89-29074 #
ISSN-0169-2690 ..... N89-29075 #
ISSN-0169-2690 ..... N89-29076 #
ISSN-0169-2690 ..... N89-29102 #
ISSN-0169-2690 ..... N89-29103 #
ISSN-0169-2690 ..... N89-29104 #
ISSN-0169-2690 ..... N89-29130 #
ISSN-0169-2690 ..... N89-29131 #
ISSN-0169-2690 ..... N89-29135* #
ISSN-0169-2690 ..... N89-29146 #
ISSN-0171-1342 ..... N89-28504 #
ISSN-0171-1342 ..... N89-28505 #
ISSN-0171-1342 ..... N89-28698 #
ISSN-0171-1342 ..... N89-28847 #
ISSN-0171-1342 ..... N89-28943 #
ISSN-0171-1342 ..... N89-29132 #
ISSN-0176-0777 ..... N89-28525 #
ISSN-0176-7739 ..... N89-28942 #
ISSN-0178-0719 ..... N89-29280 #
ISSN-0179-0609 ..... N89-29199 #
ISSN-0179-5619 ..... N89-28978
ISSN-0179-5619 ..... N89-28979
ISSN-0179-5619 ..... N89-28991
ISSN-0179-5619 ..... N89-28992
ISSN-0258-025X ..... N89-29302 #
ISSN-0262-5369 ..... N89-29125
ISSN-0262-5369 ..... N89-29126
ISSN-0284-1703 ..... N89-28700 #
ISSN-0309-3069 ..... N89-28825
ISSN-0309-3069 ..... N89-28827
ISSN-0309-3069 ..... N89-28828
ISSN-0309-6521 ..... N89-28778 #
ISSN-0343-7639 ..... N89-28653 #
ISSN-0347-3708 ..... N89-29091 #
ISSN-0348-7539 ..... N89-29216 #
ISSN-0348-7539 ..... N89-29217 #
ISSN-0349-0068 ..... N89-28999 #
ISSN-0358-5077 ..... N89-28855 #
ISSN-0358-5077 ..... N89-28932 #
ISSN-0358-5077 ..... N89-29136 #
ISSN-0379-6566 ..... N89-29295 #
ISSN-0389-4010 ..... N89-28492 #
ISSN-0389-4010 ..... N89-28514 #
ISSN-0389-4010 ..... N89-28765 #
ISSN-0436-1199 ..... N89-29178 #
ISSN-0469-4732 ..... N89-29212 #
ISSN-0469-4732 ..... N89-29213 #
ISSN-0469-4732 ..... N89-29214 #
ISSN-0469-4732 ..... N89-29215 #
ISSN-0922-5641 ..... N89-29105 #
ISSN-0923-1714 ..... N89-28730 #
ISSN-0923-1714 ..... N89-29070 #
ISSN-0923-1714 ..... N89-29079 #
ISSN-0923-1714 ..... N89-29272 #

ISVR-TR-150 ..... N89-29157 #
ISVR-TR-169-PT-1 ..... N89-29158 #
ISVR-TR-174 ..... N89-28652 #
ISVR-TR-177 ..... N89-29018 #
ISVR-TR-179 ..... N89-28807 #

IW-R515 ..... N89-28499 #

JPL-400-370-VOL-2 ..... N89-28969* #

JPRS-USP-89-002-VOL-1 ..... N89-28876 #
JPRS-USP-89-003-VOL-2 ..... N89-28903 #
JPRS-USP-89-005 ..... N89-28527 #

JUEL-SPEZ-470 ..... N89-28653 #

KNMI-WR-88-04 ..... N89-28982 #

KSC-TR-88-006 ..... N89-29100 #

KSL-88-81 ..... N89-29086 #

L-16410 ..... N89-28550* #
L-16566 ..... N89-29047* #
L-16599 ..... N89-28486*

LA-UR-89-489 ..... N89-28555 #
LA-UR-89-965 ..... N89-28711 #
LA-UR-89-1579 ..... N89-29007 #
LA-UR-89-1592 ..... N89-28970 #
LA-UR-89-1649 ..... N89-29167 #
LA-UR-89-1729 ..... N89-29008 #
LA-UR-89-1848 ..... N89-29202 #
LA-UR-89-1932 ..... N89-28810 #
LA-UR-89-1951 ..... N89-28789 #
LA-UR-89-1990 ..... N89-28709 #
LA-UR-89-2080 ..... N89-28712 #
LA-UR-89-2138 ..... N89-28542 #
LA-UR-89-2168 ..... N89-28533 #

LA-11294-MS ..... N89-28660 #
LA-11525-MS ..... N89-28926 #
LA-11574 ..... N89-29180 #
LA-11600-PR ..... N89-28811 #
LA-11613-MS ..... N89-29229 #

LAAS-89.012 ..... N89-29179 #
LAAS-89.093 ..... N89-29101 #
LAAS-89.096 ..... N89-29084 #

LAIR-373 ..... N89-29012 #

LBL-25609 ..... N89-29106 #
LBL-26210 ..... N89-29283 #
LBL-26662 ..... N89-28788 #
LBL-27082 ..... N89-28951 #
LBL-27164 ..... N89-28616 #
LBL-27187 ..... N89-28619 #
LBL-27233 ..... N89-29296 #
LBL-27267 ..... N89-29227 #
LBL-27271 ..... N89-29228 #

LC-88-63907 ..... N89-28565* #
LC-89-600203 ..... N89-28969* #

LFD-274 ..... N89-28844
LFD-275 ..... N89-29156

LIDS-R-1868 ..... N89-29258 #

LINC-160 ..... N89-28693 #
LINC-163 ..... N89-28694 #

LMP-88-004 ..... N89-29232 #

MBB-UD-0041-88-PUB ..... N89-28561 #

MCR-86-654 ..... N89-29292* #

MD88-32-IB ..... N89-29118 #
MD88-36-IB-MG-JP ..... N89-29117 #

MEMO-INF-88-15 ..... N89-29037 #
MEMO-INF-88-21 ..... N89-29062 #
MEMO-INF-88-43 ..... N89-29078 #
MEMO-INF-88-49 ..... N89-29090 #
MEMO-INF-88-52 ..... N89-29068 #
MEMO-INF-88-55 ..... N89-29079 #
MEMO-INF-88-63 ..... N89-29272 #
MEMO-INF-88-64 ..... N89-29069 #
MEMO-INF-88-65 ..... N89-28730 #
MEMO-INF-89-14 ..... N89-29080 #
MEMO-INF-89-29 ..... N89-29070 #

MEMO-645-REV ..... N89-28776 #
MEMO-735 ..... N89-29074 #
MEMO-745 ..... N89-29102 #
MEMO-746 ..... N89-28782 #
MEMO-747 ..... N89-28875 #
MEMO-748 ..... N89-29068 #
MEMO-750-REV ..... N89-28776 #
MEMO-752 ..... N89-28845 #
MEMO-753 ..... N89-29075 #
MEMO-754 ..... N89-29076 #
MEMO-755 ..... N89-29104 #
MEMO-757-PT-1 ..... N89-28654 #
MEMO-758-PT-2 ..... N89-28655 #
MEMO-759 ..... N89-29103 #
MEMO-760 ..... N89-29135* #
MEMO-761 ..... N89-28850 #
MEMO-763 ..... N89-29072 #
MEMO-764 ..... N89-28779 #
MEMO-765 ..... N89-29130 #
MEMO-766 ..... N89-29073 #
MEMO-767 ..... N89-29146 #
MEMO-768 ..... N89-29131 #

MIT/LCS/TM-384 ..... N89-29084 #

MIT/LCS/TR-434 ..... N89-29051 #

MITSG-89-7 ..... N89-28633 #

MITT-9 ..... N89-29276 #
MITT-58 ..... N89-28977 #
MITT-59 ..... N89-28931 #
MITT-60 ..... N89-28799 #

MLM-3590 ..... N89-28813 #

MPE-PREPRINT-145 ..... N89-29284
MPE-PREPRINT-147 ..... N89-29286
MPE-PREPRINT-148 ..... N89-29285
MPE-PREPRINT-149 ..... N89-29298*
MPE-PREPRINT-150 ..... N89-29287
MPE-PREPRINT-151 ..... N89-29288

MPE-212 ..... N89-29277 #
MPE-214 ..... N89-29280 #

MPI-PAE/EXP.EL-195 ..... N89-29173 #
MPI-PAE/EXP.EL-197 ..... N89-28798 #

MPIS-10/1988 ..... N89-29178 #

MTL-TR-89-10 ..... N89-29240 #
MTL-TR-89-26 ..... N89-28622 #
MTL-TR-89-27 ..... N89-28512 #
MTL-TR-89-33 ..... N89-29624 #
MTL-TR-89-39 ..... N89-29623 #

NAL-TM-MT-8806 ..... N89-28628 #

NAL-TM-SE-8802 ..... N89-28521 #

NAL-TR-1003 ..... N89-28514 #
NAL-TR-1004T ..... N89-28492 #
NAL-TR-1010T ..... N89-28765 #

NAPC-PE-185 ..... N89-28516 #
NAPC-PE-188 ..... N89-28517 #

NAS 1.15:4073 ..... N89-28550* #
NAS 1.15:4127 ..... N89-29047* #
NAS 1.15:4138 ..... N89-28486*
NAS 1.15:100373 ..... N89-28566* #
NAS 1.15:100375 ..... N89-28551* #
NAS 1.15:101038 ..... N89-28670* #
NAS 1.15:101424 ..... N89-28665* #
NAS 1.15:101478 ..... N89-28653* #
NAS 1.15:101645 ..... N89-28579* #
NAS 1.15:101653 ..... N89-28993* #
NAS 1.15:101811 ..... N89-28565* #
NAS 1.15:102011 ..... N89-28666* #
NAS 1.15:102122 ..... N89-28627* #
NAS 1.15:102126 ..... N89-28748* #
NAS 1.15:102133 ..... N89-28851* #
NAS 1.15:102143 ..... N89-28571* #

NAS 1.15:102157 ..... N89-29017* #
NAS 1.15:102226 ..... N89-28498* #
NAS 1.15:102227 ..... N89-29016* #
NAS 1.15:102293 ..... N89-28749* #
NAS 1.15:102308 ..... N89-28535* #
NAS 1.15:102327 ..... N89-29032* #
NAS 1.15:102339 ..... N89-28570* #
NAS 1.21:7039(35)-SECT-2 ..... N89-29264*
NAS 1.21:7064-SUPPL-1 ..... N89-29262* #
NAS 1.21:7064-SUPPL-2 ..... N89-29269* #
NAS 1.26:4255 ..... N89-29155* #
NAS 1.26:177502 ..... N89-29020* #
NAS 1.26:181790 ..... N89-29152* #
NAS 1.26:181791 ..... N89-29154* #
NAS 1.26:181869 ..... N89-28820* #
NAS 1.26:181870 ..... N89-28821* #
NAS 1.26:181875 ..... N89-28764* #
NAS 1.26:181883 ..... N89-28763* #
NAS 1.26:181885 ..... N89-29028* #
NAS 1.26:181886 ..... N89-29123* #
NAS 1.26:181891 ..... N89-29122* #
NAS 1.26:181892 ..... N89-28762* #
NAS 1.26:181900 ..... N89-29061* #
NAS 1.26:181901 ..... N89-28766* #
NAS 1.26:181902 ..... N89-29124* #
NAS 1.26:183740 ..... N89-28567* #
NAS 1.26:183743 ..... N89-28566* #
NAS 1.26:184913 ..... N89-28541* #
NAS 1.26:185132 ..... N89-28747* #
NAS 1.26:185371 ..... N89-28537* #
NAS 1.26:185487 ..... N89-28961* #
NAS 1.26:185488 ..... N89-29159* #
NAS 1.26:185514 ..... N89-29292* #
NAS 1.26:185834 ..... N89-28856* #
NAS 1.26:185846 ..... N89-28562* #
NAS 1.26:185869 ..... N89-29282* #
NAS 1.26:185891 ..... N89-28990* #
NAS 1.26:185892 ..... N89-28493* #
NAS 1.26:185907 ..... N89-29135* #
NAS 1.26:185909 ..... N89-29298*
NAS 1.60:2912 ..... N89-28545* #
NAS 1.61:1224-VOL-2 ..... N89-28969* #
NAS 1.61:1225 ..... N89-28983* #
NAS 1.71:LAR-13772-1 ..... N89-28816* #
NAS 1.71:LAR-13985-1 ..... N89-28586* #
NAS 1.71:LAR-14149-1-SB ..... N89-28547* #
NAS 1.71:LAR-14203-1 ..... N89-28817* #
NAS 1.71:LEW-14124-1 ..... N89-28806* #
NAS 1.71:LEW-14679-1 ..... N89-28651* #
NAS 1.71:LEW-14695-1 ..... N89-28830* #
NAS 1.71:LEW-14848-1 ..... N89-28549* #
NAS 1.71:MFS-28049-1-NP ..... N89-28603* #
NAS 1.71:MFS-28327-1 ..... N89-28556* #
NAS 1.71:MFS-28345-1 ..... N89-28841* #
NAS 1.71:MFS-28345-2 ..... N89-28842* #
NAS 1.71:MFS-28370-1 ..... N89-28793* #
NAS 1.71:MFS-28376-1 ..... N89-28546* #
NAS 1.71:MSC-21386-1 ..... N89-28552* #
NAS 1.71:MSC-21408-1 ..... N89-28829* #
NAS 1.71:MSC-21629-1 ..... N89-29027* #
NAS 1.71:NPO-16989-1-CU ..... N89-28794* #
NAS 1.71:NPO-17526-1-CU ..... N89-28796* #
NAS 1.71:NPO-17596-1-CU ..... N89-28795* #
NAS 1.71:NPO-17628-1-CU ..... N89-28684* #
NAS 1.71:NPO-17703-1-CU ..... N89-29191* #
NAS 1.71:NPO-17785-1-CU ..... N89-28846* #
NAS 1.71:NST-00007-1 ..... N89-28967* #

NAS-SR-DUAT ..... N89-28524 #

NAS-SR-1325 ..... N89-28509 #

NASA-CASE-LAR-13747-1-CU N89-28672*
NASA-CASE-LAR-13772-1 ..... N89-28816* #
NASA-CASE-LAR-13924-1-CU N89-28621*
NASA-CASE-LAR-13985-1 ..... N89-28586* #
NASA-CASE-LAR-14149-1-SB ..... N89-28547* #
NASA-CASE-LAR-14203-1 ..... N89-28817* #

NASA-CASE-LEW-14124-1 ..... N89-28806* #
NASA-CASE-LEW-14679-1 ..... N89-28651* #
NASA-CASE-LEW-14695-1 ..... N89-28830* #
NASA-CASE-LEW-14848-1 ..... N89-28549* #

NASA-CASE-MFS-28049-1-NP ..... N89-28603* #
NASA-CASE-MFS-28253-1 ..... N89-28831*
NASA-CASE-MFS-28327-1 ..... N89-28556* #
NASA-CASE-MFS-28345-1 ..... N89-28841* #
NASA-CASE-MFS-28345-2 ..... N89-28842* #
NASA-CASE-MFS-28370-1 ..... N89-28793* #
NASA-CASE-MFS-28376-1 ..... N89-28546* #

NASA-CASE-MSC-21117-2 ..... N89-28554* #
NASA-CASE-MSC-21211-1 ..... N89-28553*
NASA-CASE-MSC-21386-1 ..... N89-28552* #
NASA-CASE-MSC-21408-1 ..... N89-28829* #

NASA-CASE-MSC-21629-1 ..... N89-29027* #

NASA-CASE-NPO-16789-1-CU N89-29169*
NASA-CASE-NPO-16989-1-CU ..... N89-28794* #
NASA-CASE-NPO-17108-1-CU N89-28713*
NASA-CASE-NPO-17249-1-CU N89-28676*
NASA-CASE-NPO-17526-1-CU ..... N89-28796* #
NASA-CASE-NPO-17596-1-CU ..... N89-28795* #
NASA-CASE-NPO-17628-1-CU ..... N89-28684* #
NASA-CASE-NPO-17703-1-CU ..... N89-29191* #
NASA-CASE-NPO-17785-1-CU ..... N89-28846* #

NASA-CASE-NST-00007-1 ..... N89-28967* #

NASA-CR-4255 ..... N89-29155* #
NASA-CR-177502 ..... N89-29020* #
NASA-CR-181790 ..... N89-29152* #
NASA-CR-181791 ..... N89-29154* #
NASA-CR-181869 ..... N89-28820* #
NASA-CR-181870 ..... N89-28821* #
NASA-CR-181875 ..... N89-28764* #
NASA-CR-181883 ..... N89-28763* #
NASA-CR-181885 ..... N89-29028* #
NASA-CR-181886 ..... N89-29123* #
NASA-CR-181891 ..... N89-29122* #
NASA-CR-181892 ..... N89-28762* #
NASA-CR-181900 ..... N89-29061* #
NASA-CR-181901 ..... N89-28766* #
NASA-CR-181902 ..... N89-29124* #
NASA-CR-183740 ..... N89-28567* #
NASA-CR-183743 ..... N89-28566* #
NASA-CR-184913 ..... N89-28541* #
NASA-CR-185132 ..... N89-28747* #
NASA-CR-185371 ..... N89-28537* #
NASA-CR-185487 ..... N89-28961* #
NASA-CR-185488 ..... N89-29159* #
NASA-CR-185514 ..... N89-29292* #
NASA-CR-185834 ..... N89-28856* #
NASA-CR-185846 ..... N89-28562* #
NASA-CR-185869 ..... N89-29282* #
NASA-CR-185891 ..... N89-28990* #
NASA-CR-185892 ..... N89-28493* #
NASA-CR-185907 ..... N89-29135* #
NASA-CR-185909 ..... N89-29298*

NASA-RP-1224-VOL-2 ..... N89-28969* #
NASA-RP-1225 ..... N89-28983* #

NASA-SP-7039(35)-SECT-2 ..... N89-29264*
NASA-SP-7064-SUPPL-1 ..... N89-29262* #
NASA-SP-7064-SUPPL-2 ..... N89-29269* #

NASA-TM-4073 ..... N89-28550* #
NASA-TM-4127 ..... N89-29047* #
NASA-TM-4138 ..... N89-28486*
NASA-TM-100373 ..... N89-28568* #
NASA-TM-100375 ..... N89-28551* #
NASA-TM-101038 ..... N89-28870* #
NASA-TM-101424 ..... N89-28665* #
NASA-TM-101478 ..... N89-28853* #
NASA-TM-101645 ..... N89-28579* #
NASA-TM-101653 ..... N89-28993* #
NASA-TM-101811 ..... N89-28565* #
NASA-TM-102011 ..... N89-28666* #
NASA-TM-102122 ..... N89-28627* #
NASA-TM-102128 ..... N89-28748* #
NASA-TM-102133 ..... N89-28851* #
NASA-TM-102143 ..... N89-28571* #
NASA-TM-102157 ..... N89-29017* #
NASA-TM-102226 ..... N89-28498* #
NASA-TM-102227 ..... N89-29016* #
NASA-TM-102293 ..... N89-28749* #
NASA-TM-102308 ..... N89-28535* #
NASA-TM-102327 ..... N89-29032* #
NASA-TM-102339 ..... N89-28570* #

NASA-TP-2912 ..... N89-28545* #

NATICK-TR-89/027 ..... N89-29025 #

NBS/TN-1321 ..... N89-28809 #

NEPRF-CR-89-02 ..... N89-28975 #
NEPRF-CR-89-03 ..... N89-28930 #

NIKHEF-ITFA-88-51 ..... N89-29151 #

NIKHEF-K/APS/88-01A-REV ..... N89-29182 #
NIKHEF-K/APS/88-03 ..... N89-29183 #
NIKHEF-K/APS/88-04 ..... N89-29184 #
NIKHEF-K/APS/88-04A ..... N89-29185 #

NIST/SP-250 ..... N89-28785 #

NIST/TN-1310 ..... N89-28707 #

NISTIR-88/3900 ..... N89-28673 #
NISTIR-89/4067 ..... N89-28706 #
NISTIR-89/4075 ..... N89-28615 #

NLR-MP-87006-U ..... N89-28526 #
NLR-MP-87020-U ..... N89-29067 #
NLR-MP-87035-U ..... N89-28933 #
NLR-MP-88002-U ..... N89-29271 #
NLR-MP-88009-U ..... N89-28934 #
NLR-MP-88013-U ..... N89-28777 #
NLR-MP-88020-U ..... N89-28935 #
NLR-MP-88030-U ..... N89-28936 #

NOAA-NESDIS-89/01 ..... N89-28922 #

NONP-SUPPL-DK-89-223860 ..... N89-28734 #

NOSC/TD-1453 ..... N89-28690 #
NOSC/TD-1538 ..... N89-29085 #

NOSC/TR-1275 ..... N89-29189 #
NOSC/TR-1277 ..... N89-28972 #

NPL-DITC-140/89 ..... N89-29125
NPL-DITC-141/89 ..... N89-29092
NPL-DITC-142/89 ..... N89-29126

NPL-DMA(A)-173 ..... N89-28631
NPL-DMA(A)-175 ..... N89-28612
NPL-DMA(A)-178 ..... N89-28583
NPL-DMA(A)-179 ..... N89-28584
NPL-DMA(A)-180-PT-1 ..... N89-28585

NPL-MOM-91 ..... N89-28827
NPL-MOM-92 ..... N89-28825
NPL-MOM-93 ..... N89-28828

NRL-MR-6274 ..... N89-28675 #
NRL-MR-6372 ..... N89-28722 #
NRL-MR-6423 ..... N89-28721 #
NRL-MR-6438 ..... N89-29205 #
NRL-MR-6450 ..... N89-29121 #
NRL-MR-6454 ..... N89-28646 #
NRL-MR-6456 ..... N89-29053 #
NRL-MR-6463 ..... N89-28815 #

NRL-9059 ..... N89-28677 #
NRL-9185 ..... N89-29137 #
NRL-9192 ..... N89-29054 #

NTIA-TR-89-241 ..... N89-28692 #

NTSB/AAR-89/02/SUM ..... N89-28507 #

NWC-TP-6941 ..... N89-28686 #

NWRA-CR-89-R044 ..... N89-28989 #

OCS-TR-88-04 ..... N89-29031 #
OCS-TR-89-01 ..... N89-29030 #
OCS-TR-89-03 ..... N89-28674 #
OCS-TR-89-06 ..... N89-29081 #

OCS/MMS-88/0043 ..... N89-29039 #

ONERA-NT-1988-3 ..... N89-29253 #
ONERA-NT-1988-9 ..... N89-29063 #
ONERA-NT-1988-10 ..... N89-28702 #
ONERA-NT-1989-1 ..... N89-29000 #
ONERA-NT-1989-2 ..... N89-28703 #

ONR-11 ..... N89-29246 #

OPPORTUNITY-BRIEF-54 ..... N89-28633 #

ORI-1-89 ..... N89-28805 #

ORNL-6541/V1-PT-1 ..... N89-28955 #

ORNL/TM-11176 ..... N89-28617 #
ORNL/TM-11198 ..... N89-28808 #

OTN-010456 ..... N89-28561 #

OUEL-1748/88 ..... N89-28848 #
OUEL-1758/89 ..... N89-28849 #

PB89-145965 ..... N89-28960 #
PB89-146450 ..... N89-28671 #
PB89-155444 ..... N89-29218 #
PB89-155451 ..... N89-28704 #
PB89-161434 ..... N89-28587 #
PB89-163208 ..... N89-28922 #
PB89-167423 ..... N89-29039 #
PB89-173215 ..... N89-28964 #
PB89-180707 ..... N89-29001 #

PB89-181259 ..... N89-28572 #
PB89-181424 ..... N89-28963 #
PB89-182109 ..... N89-28668 #
PB89-182950 ..... N89-28633 #
PB89-184345 ..... N89-29081 #
PB89-184352 ..... N89-28674 #
PB89-184378 ..... N89-29030 #
PB89-184410 ..... N89-29031 #
PB89-189211 ..... N89-28673 #
PB89-189302 ..... N89-28706 #
PB89-191167 ..... N89-28692 #
PB89-191613 ..... N89-28857 #
PB89-191639 ..... N89-28858 #
PB89-191654 ..... N89-28859 #
PB89-193262 ..... N89-28615 #
PB89-193908 ..... N89-28809 #
PB89-193916 ..... N89-28707 #
PB89-195788 ..... N89-28588 #
PB89-200216 ..... N89-28785 #
PB89-204598 ..... N89-28768 #
PB89-910405 ..... N89-28507 #

PD-CC-8903 ..... N89-29270 #

PD-CF-8924 ..... N89-28497 #
PD-CF-8925 ..... N89-28496 #

PD-SE-8911 ..... N89-29071 #

PMTC/GSTN-145 ..... N89-28930 #

PNL-SA-16211 ..... N89-28618 #
PNL-SA-16378 ..... N89-28620 #
PNL-SA-16622 ..... N89-28592 #
PNL-SA-16890 ..... N89-29147 #
PNL-SA-16952 ..... N89-28861 #

POLY-WRI-1554-89 ..... N89-28726 #

PSI-TR-477421 ..... N89-29003 #

PTB-F-5 ..... N89-29199 #

R/D-5293-EN-01 ..... N89-29150 #

RADC-TR-88-147 ..... N89-29052 #
RADC-TR-88-284 ..... N89-28718 #
RADC-TR-88-299 ..... N89-29034 #
RADC-TR-88-324-VOL-1 ..... N89-29094 #
RADC-TR-88-324-VOL-8 ..... N89-29095 #
RADC-TR-88-324-VOL-9 ..... N89-29096 #
RADC-TR-89-53 ..... N89-28792 #
RADC-TR-89-122 ..... N89-28714 #

RAND/N-2763-AF ..... N89-29172 #

RCC/RSG-313-89-VOL-1 ..... N89-28544 #

REPT-5-88 ..... N89-28844
REPT-6 ..... N89-28704 #
REPT-6-88 ..... N89-29156
REPT-35 ..... N89-28671 #
REPT-88.3 ..... N89-29006 #
REPT-88-82 ..... N89-29105 #
REPT-89-1 ..... N89-29120 #
REPT-89B00176 ..... N89-28983* #

RFP-4297-SUPP-2 ..... N89-28573 #

RR-CE92 ..... N89-28857 #
RR-CE94 ..... N89-28858 #
RR-CE96 ..... N89-28859 #

S-598 ..... N89-29017* #

SAND-88-2974 ..... N89-28958 #
SAND-88-3057C ..... N89-28952 #
SAND-88-3360C ..... N89-28708 #
SAND-88-3383 ..... N89-28753 #
SAND-89-0324C ..... N89-29230 #
SAND-89-0521 ..... N89-28860 #
SAND-89-0560C ..... N89-28784 #
SAND-89-0927 ..... N89-28543 #
SAND-89-1087 ..... N89-28833 #
SAND-89-1192C ..... N89-28786 #
SAND-89-1406C ..... N89-29153 #
SAND-89-1594C ..... N89-28790 #
SAND-89-7027 ..... N89-28953 #

SD-TR-89-28 ..... N89-29247 #
SD-TR-89-33 ..... N89-29083 #
SD-TR-89-34 ..... N89-29237 #

SER-C-PREPUBL-FASC-37-PT-1 ..... N89-29290 #
SER-C-PREPUBL-FASC-38-PT-2 ..... N89-29291 #

SERI/CP-213-3495 ..... N89-28948 #

SERI/SP-220-3366 ..... N89-28658 #
SERI/SP-320-3396 ..... N89-28657 #

SERI/STR-211-3511 ..... N89-28950 #
SERI/STR-211-3519 ..... N89-28945 #
SERI/STR-211-3523 ..... N89-28944 #
SERI/STR-211-3528-TASK-B ..... N89-28946 #

SERI/TP-211-3501 ..... N89-28956 #
SERI/TP-217-3505 ..... N89-28487 #

SLCET-TR-84-0458-F ..... N89-29148 #
SLCET-TR-87-0727-1 ..... N89-29239 #

SNEA-9595 ..... N89-28650 #

SR-3 ..... N89-28974 #

SRAM-A-EA-87-7-1-12 ..... N89-29188 #

SRI-04-8542-1 ..... N89-29155* #

SSI-TR-152 ..... N89-28974 #

SU-SLAC-PUB-4963 ..... N89-29093 #

SU-STAN-CS-88-1212 ..... N89-29088 #
SU-STAN-CS-89-1246 ..... N89-29086 #

SUNY/DC/TR-1 ..... N89-28608 #
SUNY/DC/TR-3 ..... N89-28609 #

TKK-F-A636 ..... N89-29218 #

TNAAS-439 ..... N89-28695
TNAAS-445-PT-3 ..... N89-28697

TR-3 ..... N89-28625 #
TR-4 ..... N89-29236 #
TR-5 ..... N89-29235 #
TR-6 ..... N89-28602 #
TR-9 ..... N89-28600 #
TR-10 ..... N89-28593 #
TR-10 ..... N89-28598 #
TR-10 ..... N89-28645 #
TR-11 ..... N89-28606 #
TR-12 ..... N89-29234 #
TR-13 ..... N89-28719 #
TR-14 ..... N89-29248 #
TR-16 ..... N89-28637 #
TR-16 ..... N89-28716 #
TR-17 ..... N89-28601 #
TR-18 ..... N89-28647 #
TR-18 ..... N89-29245 #
TR-19 ..... N89-28594 #
TR-19 ..... N89-28867 #
TR-19 ..... N89-29242 #
TR-20 ..... N89-28648 #
TR-20 ..... N89-29241 #
TR-21 ..... N89-29243 #
TR-22 ..... N89-29244 #
TR-26 ..... N89-28720 #
TR-50 ..... N89-29171 #
TR-56 ..... N89-28605 #
TR-88-32 ..... N89-29118 #
TR-88-36 ..... N89-29117 #
TR-89-1 ..... N89-29011 #
TR-820 ..... N89-28818 #
TR-848 ..... N89-28678 #
TR-0086A(2920-05)-2 ..... N89-29083 #
TR-0088(3945-03)-2 ..... N89-29247 #
TR-0089(4925-07)-4 ..... N89-29237 #
TR-5629-1-ES ..... N89-28922 #

TRI-88-12-VOL-1 ..... N89-28668 #

TRITA-EPP-88-08 ..... N89-29216 #
TRITA-EPP-89-01 ..... N89-29217 #

TR89-005 ..... N89-29058 #
TR89-009 ..... N89-28797 #
TR89-012 ..... N89-29057 #

TS-7-87 ..... N89-28667 #

TUB-DISS-PAPER-128 ..... N89-28508 #

TW-88-08 ..... N89-29127 #
TW-88-09 ..... N89-29128 #
TW-88-10 ..... N89-29139 #
TW-89-01 ..... N89-29129 #

TWR-17639 ..... N89-28567* #
TWR-18915 ..... N89-28566* #

UBUFFALO/DC/89/TR-101 ..... N89-29256 #

UCB-PTH-88/26 ..... N89-29283 #

UCID-21696 ..... N89-28812 #
UCID-21734 ..... N89-28814 #

UCRL-52000-89-4 ..... N89-28954 #
UCRL-99801 ..... N89-29186 #
UCRL-100997 ..... N89-28750 #
UCRL-101023 ..... N89-29224 #
UCRL-101051 ..... N89-28832 #

UCT/DESE-TR-88-3 ..... N89-29052 #

UDR-TR-88-95 ..... N89-28835 #
UDR-TR-88-122 ..... N89-28642 #
UDR-TR-88-124 ..... N89-29193 #
UDR-TR-89-29 ..... N89-28760 #

UM-TR-89-2 ..... N89-28856* #

UMR-FDB-9 ..... N89-28638 #

UNICAMP-IMECC-RT-22/88 ..... N89-29254 #

US-PATENT-APPL-SN-032819 ..... N89-28713*
US-PATENT-APPL-SN-105841 ..... N89-28553*
US-PATENT-APPL-SN-125666 ..... N89-28676*
US-PATENT-APPL-SN-154713 ..... N89-29169*
US-PATENT-APPL-SN-165943 ..... N89-28831*
US-PATENT-APPL-SN-172102 ..... N89-28621*
US-PATENT-APPL-SN-184233 ..... N89-28554* #
US-PATENT-APPL-SN-197191 ..... N89-28672*
US-PATENT-APPL-SN-292123 ..... N89-28552* #
US-PATENT-APPL-SN-292146 ..... N89-28830* #
US-PATENT-APPL-SN-304154 ..... N89-28829* #
US-PATENT-APPL-SN-316358 ..... N89-28705 #
US-PATENT-APPL-SN-322381 ..... N89-29219 #
US-PATENT-APPL-SN-350813 ..... N89-28684* #
US-PATENT-APPL-SN-353411 ..... N89-28846* #
US-PATENT-APPL-SN-357757 ..... N89-28547* #
US-PATENT-APPL-SN-357938 ..... N89-28967* #
US-PATENT-APPL-SN-358027 ..... N89-28794* #
US-PATENT-APPL-SN-358028 ..... N89-28842* #
US-PATENT-APPL-SN-359459 ..... N89-28817* #
US-PATENT-APPL-SN-359460 ..... N89-28816* #
US-PATENT-APPL-SN-359801 ..... N89-29191* #
US-PATENT-APPL-SN-361200 ..... N89-28556* #
US-PATENT-APPL-SN-361479 ..... N89-28546* #
US-PATENT-APPL-SN-361531 ..... N89-28795* #
US-PATENT-APPL-SN-364743 ..... N89-28841* #
US-PATENT-APPL-SN-369403 ..... N89-28796* #
US-PATENT-APPL-SN-376487 ..... N89-28603* #
US-PATENT-APPL-SN-378548 ..... N89-29027* #
US-PATENT-APPL-SN-381240 ..... N89-28651* #
US-PATENT-APPL-SN-382885 ..... N89-28549* #
US-PATENT-APPL-SN-386172 ..... N89-28586* #
US-PATENT-APPL-SN-386175 ..... N89-28793* #
US-PATENT-APPL-SN-396263 ..... N89-28806* #
US-PATENT-APPL-SN-929875 ..... N89-28554* #

US-PATENT-CLASS-33-536 ..... N89-28831*
US-PATENT-CLASS-52-573 ..... N89-28554* #
US-PATENT-CLASS-52-648 ..... N89-28554* #
US-PATENT-CLASS-148-159 ..... N89-28621*
US-PATENT-CLASS-148-416 ..... N89-28621*
US-PATENT-CLASS-148-417 ..... N89-28621*
US-PATENT-CLASS-244-159 ..... N89-28553*
US-PATENT-CLASS-244-161 ..... N89-28553*
US-PATENT-CLASS-248-DIG-1 ..... N89-28554* #
US-PATENT-CLASS-250-252 ..... N89-29169*
US-PATENT-CLASS-250-397 ..... N89-29169*
US-PATENT-CLASS-285-226 ..... N89-28553*
US-PATENT-CLASS-342-1 ..... N89-28672*
US-PATENT-CLASS-342-5 ..... N89-28672*
US-PATENT-CLASS-342-165 ..... N89-28672*
US-PATENT-CLASS-358-88 ..... N89-28676*
US-PATENT-CLASS-358-91 ..... N89-28676*
US-PATENT-CLASS-358-92 ..... N89-28676*
US-PATENT-CLASS-364-724.01 ..... N89-28713*
US-PATENT-CLASS-364-724.05 ..... N89-28713*
US-PATENT-CLASS-364-735 ..... N89-28713*
US-PATENT-CLASS-364-754 ..... N89-28713*
US-PATENT-CLASS-403-4 ..... N89-28554* #
US-PATENT-CLASS-403-30 ..... N89-28554* #
US-PATENT-CLASS-403-51 ..... N89-28553*
US-PATENT-CLASS-420-529 ..... N89-28621*
US-PATENT-CLASS-420-533 ..... N89-28621*

US-PATENT-4,805,368 ..... N89-28554* #
US-PATENT-4,809,003 ..... N89-28672*
US-PATENT-4,809,441 ..... N89-28831*
US-PATENT-4,809,936 ..... N89-28553*
US-PATENT-4,818,868 ..... N89-29169*
US-PATENT-4,819,064 ..... N89-28676*

US-PATENT-4,820,488 ..... N89-28621*
US-PATENT-4,823,299 ..... N89-28713*

USAAVSCOM-TM-89-A-001 ..... N89-28498* #

USAFETAC/PR-89/001 ..... N89-28985 #

USAFSAM-TR-88-25 ..... N89-28515 #
USAFSAM-TR-88-26 ..... N89-28589 #

USARIEM-M48-89 ..... N89-29009 #

VLSI-MEMO-89-518 ..... N89-29232 #
VLSI-MEMO-89-521 ..... N89-29062 #

VTT-RR-571 ..... N89-29136 #
VTT-RR-586 ..... N89-28855 #
VTT-RR-612 ..... N89-28932 #

WBS-HQ601-20-10 ..... N89-28567* #

WES/MP/EL-79-6-16 ..... N89-28926 #

WES/TR/HL-89-8 ..... N89-28757 #

WHOI-CONTRIB-6517 ..... N89-29005 #

WISS-BER-8 ..... N89-28991
WISS-BER-9 ..... N89-28992
WISS-BER-10 ..... N89-28978
WISS-BER-12 ..... N89-28979

WMO-690-PT-1 ..... N89-28994 #
WMO-691-PT-2-VOL-1 ..... N89-28995 #
WMO-692-PT-2-VOL-2 ..... N89-28996 #
WMO-693-PT-2-VOL-3 ..... N89-28997 #
WMO-694-PT-2-VOL-4 ..... N89-28998 #

WP-88W00075 ..... N89-28524 #
WP-88W00418 ..... N89-28509 #

WRDC-TR-89-2068 ..... N89-28644 #
WRDC-TR-89-2095 ..... N89-28838 #
WRDC-TR-89-4016 ..... N89-28649 #

Y/DW-763/R1 ..... N89-28852 #

☆ U.S. GOVERNMENT PRINTING OFFICE: 1989— 261 - 275 / 00114

FEDERAL REGIONAL DEPOSITORY LIBRARIES

ALABAMA

AUBURN UNIV. AT MONTGOMERY LIBRARY
Documents Department
Montgomery, AL 36193
(205) 271-9650

UNIV. OF ALABAMA LIBRARY
Documents Dept.-Box S
University, AL 35486
(205) 348-6046

ARIZONA

DEPT. OF LIBRARY, ARCHIVES AND PUBLIC RECORDS
Third Floor—State Cap.
1700 West Washington
Phoenix, AZ 85007
(602) 255-4121

UNIVERSITY OF ARIZONA LIB.
Government Documents Dept.
Tucson, AZ 85721
(602) 621-6433

ARKANSAS

ARKANSAS STATE LIBRARY
One Capitol Mall
Little Rock, AR 72201
(501) 371-2326

CALIFORNIA

CALIFORNIA STATE LIBRARY
Govt. Publications Section
P.O. Box 2037
Sacramento, CA 95809
(916) 324-4863

COLORADO

UNIV OF COLORADO LIB.
Government Pub. Division
Campus Box 184
Boulder, CO 80309
(303) 492-8834

DENVER PUBLIC LIBRARY
Govt. Pub. Department
1357 Broadway
Denver, CO 80203
(303) 571-2131

CONNECTICUT

CONNECTICUT STATE LIBRARY
Government Documents Unit
231 Capitol Avenue
Hartford, CT 06106
(203) 566-7029

FLORIDA

UNIV. OF FLORIDA LIBRARIES
Library West
Documents Department
Gainesville, FL 32611
(904) 392-0367

GEORGIA

UNIV. OF GEORGIA LIBRARIES
Government Reference Dept.
Athens, GA 30602
(404) 542-8949

HAWAII

UNIV. OF HAWAII LIBRARY
Govt. Documents Collection
2550 The Mall
Honolulu, HI 96822
(808) 948-8230

IDAHO

UNIV. OF IDAHO LIBRARY
Documents Section
Moscow, ID 83843
(208) 885-6344

ILLINOIS

ILLINOIS STATE LIBRARY
Information Services Branch
Centennial Building
Springfield, IL 62756
(217) 782-5185

INDIANA

INDIANA STATE LIBRARY
Serials Documents Section
140 North Senate Avenue
Indianapolis, IN 46204
(317) 232-3686

IOWA

UNIV. OF IOWA LIBRARIES
Govt. Documents Department
Iowa City, IA 52242
(319) 353-3318

KANSAS

UNIVERSITY OF KANSAS
Doc. Collect—Spencer Lib.
Lawrence, KS 66045-2800
(913) 864-4662

KENTUCKY

UNIV. OF KENTUCKY LIBRARIES
Govt. Pub. Department
Lexington, KY 40506-0039
(606) 257-3139

LOUISIANA

LOUISIANA STATE UNIVERSITY
Middleton Library
Govt. Docs. Dept.
Baton Rouge, LA 70803
(504) 388-2570

LOUISIANA TECHNICAL UNIV. LIBRARY
Documents Department
Ruston, LA 71272-0046
(318) 257-4962

MAINE

UNIVERSITY OF MAINE
Raymond H. Fogler Library
Tri-State Regional Documents Depository
Orono, ME 04469
(207) 581-1680

MARYLAND

UNIVERSITY OF MARYLAND
McKeldin Lib.—Doc. Div.
College Park, MD 20742
(301) 454-3034

MASSACHUSETTS

BOSTON PUBLIC LIBRARY
Government Docs. Dept.
Boston, MA 02117
(617) 536-5400 ext.226

MICHIGAN

DETROIT PUBLIC LIBRARY
Sociology Department
5201 Woodward Avenue
Detroit, MI 48202-4093
(313) 833-1409

MICHIGAN STATE LIBRARY
P.O. Box 30007
Lansing, MI 48909
(517) 373-1593

MINNESOTA

UNIVERSITY OF MINNESOTA
Government Pubs. Division
409 Wilson Library
309 19th Avenue South
Minneapolis, MN 55455
(612) 373-7870

MISSISSIPPI

UNIV. OF MISSISSIPPI LIB.
Documents Department
University, MS 38677
(601) 232-5857

MONTANA

UNIV. OF MONTANA
Mansfield Library
Documents Division
Missoula, MT 59812
(406) 243-6700

NEBRASKA

UNIVERSITY OF NEBRASKA - LINCOLN
Love Library
Documents Department
Lincoln, NE 68588-0410
(402) 472-2562

NEVADA

UNIVERSITY OF NEVADA LIB.
Govt. Pub. Department
Reno, NV 89557-0044
(702) 784-6579

NEW JERSEY

NEWARK PUBLIC LIBRARY
5 Washington Street
Newark, NJ 07101-0630
(201) 733-7812

NEW MEXICO

UNIVERSITY OF NEW MEXICO
Zimmerman Library
Government Pub. Dept.
Albuquerque, NM 87131
(505) 277-5441

NEW MEXICO STATE LIBRARY
Reference Department
325 Don Gaspar Avenue
Santa Fe, NM 87503
(505) 827-3826

NEW YORK

NEW YORK STATE LIBRARY
Empire State Plaza
Albany, NY 12230
(518) 474-5563

NORTH CAROLINA

UNIVERSITY OF NORTH CAROLINA AT CHAPEL HILL
Davis Library
BA/SS Documents Division
Chapel Hill, NC 27515
(919) 962-1151

NORTH DAKOTA

UNIVERSITY OF NORTH DAKOTA
Chester Fritz Library
Documents Department
Grand Forks, ND 58202
(701) 777-4629
In cooperation with North Dakota State Univ. Library

OHIO

STATE LIBRARY OF OHIO
Documents Department
65 South Front Street
Columbus, OH 43266-0334
(614) 462-7051

OKLAHOMA

OKLAHOMA DEPT. OF LIB.
Government Documents
200 NE 18th Street
Oklahoma City, OK 73105
(405) 521-2502, ext. 252

OKLAHOMA STATE UNIV. LIB.
Documents Department
Stillwater, OK 74078
(405) 624-6546

OREGON

PORTLAND STATE UNIV. LIB.
Documents Department
P.O. Box 1151
Portland, OR 97207
(503) 229-3673

PENNSYLVANIA

STATE LIBRARY OF PENN.
Government Pub. Section
P.O. Box 1601
Harrisburg, PA 17105
(717) 787-3752

TEXAS

TEXAS STATE LIBRARY
Public Services Department
P.O. Box 12927—Cap. Sta.
Austin, TX 78711
(512) 475-2996

TEXAS TECH. UNIV. LIBRARY
Govt. Documents Department
Lubbock, TX 79409
(806) 742-2268

UTAH

UTAH STATE UNIVERSITY
Merrill Library, U.M.C. 30
Logan, UT 84322
(801) 750-2682

VIRGINIA

UNIVERSITY OF VIRGINIA
Alderman Lib.—Public Doc.
Charlottesville, VA 22903-2498
(804) 924-3133

WASHINGTON

WASHINGTON STATE LIBRARY
Documents Section
Olympia, WA 98504
(206) 753-4027

WEST VIRGINIA

WEST VIRGINIA UNIV. LIB.
Documents Department
Morgantown, WV 26506-6069
(304) 293-3640

WISCONSIN

MILWAUKEE PUBLIC LIBRARY
814 West Wisconsin Avenue
Milwaukee, WI 53233
(414) 278-3065

ST. HIST LIB. OF WISCONSIN
Government Pub. Section
816 State Street
Madison, WI 53706
(608) 262-4347

WYOMING

WYOMING STATE LIBRARY
Supreme Ct. & Library Bld.
Cheyenne, WY 82002
(307) 777-5919

National Aeronautics and
Space Administration
Code NTT-4
Washington, D.C.
20546

Official Business

Penalty for Private Use, $300

SPECIAL FOURTH-CLASS RATE
POSTAGE & FEES PAID
NASA
PERMIT No. G 27

NASA

POSTMASTER: If Undeliverable (Section 158
Postal Manual) Do Not Return